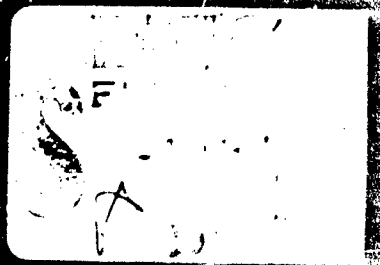


AD-A182 275

(2)



THE BOSTON HERALD

This image appears to be a scan of a heavily damaged or overexposed document page. The left side features several thick, dark horizontal bands, possibly representing redacted text or severely faded print. The right side is dominated by a dark, grainy texture with some lighter, scattered noise. A small, bright, irregular shape is visible near the bottom center, which could be a piece of tape or a hole punch mark.

20030128000

Ad-A182275

SECURITY CLASSIFICATION OF THIS PAGE

Form Approved
OMB No 0704-0188
Exp Date Jun 30, 1986

REPORT DOCUMENTATION PAGE

1a. REPORT SECURITY CLASSIFICATION Unclassified		1b. RESTRICTIVE MARKINGS	
2a. SECURITY CLASSIFICATION AUTHORITY		3. DISTRIBUTION/AVAILABILITY OF REPORT Approved for public release; distribution unlimited	
2b. DECLASSIFICATION/DOWNGRADING SCHEDULE		5. MONITORING ORGANIZATION REPORT NUMBER(S)	
4. PERFORMING ORGANIZATION REPORT NUMBER(S) <i>(DIL)</i> C-50075		7a. NAME OF MONITORING ORGANIZATION U.S. Army Biomedical Research and Development Laboratory	
6a. NAME OF PERFORMING ORGANIZATION Arthur D. Little, Inc.	6b. OFFICE SYMBOL (If applicable)	7b. ADDRESS (City, State, and ZIP Code) Fort Detrick Frederick, Maryland 21701-5010	
8a. NAME OF FUNDING/SPONSORING ORGANIZATION U.S. Army Medical Research & Development Command	8b. OFFICE SYMBOL (If applicable)	9. PROCUREMENT INSTRUMENT IDENTIFICATION NUMBER DAMD17-83-C-3274	
8c. ADDRESS (City, State, and ZIP Code) Fort Detrick Frederick, Maryland 21701-5012		10. SOURCE OF FUNDING NUMBERS	
		PROGRAM ELEMENT NO. 62720A	PROJECT NO 3E1- 62720A835 TASK NO AA WORK UNIT ACCESSION NO 021
11. TITLE (Include Security Classification) Methods for Estimating Physicochemical Properties of Inorganic Chemicals of Environmental Concern (Volume 1)			
12. PERSONAL AUTHOR(S) (See reverse)			
13a. TYPE OF REPORT Final Report	13b. TIME COVERED FROM 83/09/30 TO 87/3/31	14. DATE OF REPORT (Year, Month, Day) 1987 March	15. PAGE COUNT 676
16. SUPPLEMENTARY NOTATION A slightly revised version of this report will be published by the Society of Environmental Toxicology and Chemistry in cooperation with Pergamon Press. A Phase I problem definition report on this project was submitted in June 1984.			
17. COSATI CODES	18. SUBJECT TERMS (Continue on reverse if necessary and identify by block number) Inorganic and organometallic chemicals; Environmentally important properties; Property estimation; Environmental fate models; Uptake by biota; Speciation in water; (Con't)		
FIELD 07 08	GROUP 02 04		
19. ABSTRACT (Continue on reverse if necessary and identify by block number) This report provides information on environmentally important physicochemical properties of inorganic and organometallic chemicals. Part I provides generic descriptions of sixteen properties or processes including, where available, estimation methods for the properties along with example calculations. Part I also discusses uptake of inorganic pollutants by biota and mathematical (computerized) models for predicting speciation in water and environmental transport. Part II of the report presents environmentally important property data for several groups of elements or compounds. The data include, for example, precalculated speciation diagrams (vs pH and/or pe), complexation and solubility product constants, soil sorption constants, and several other items. Appendices provide information on background concentrations (in air, water and soil) of metals and other inorganics, federal standards and criteria for inorganic pollutants, and the properties of soils that affect the mobility of inorganic pollutants. Volume I includes the following five sections:			
20. DISTRIBUTION/AVAILABILITY OF ABSTRACT <input type="checkbox"/> UNCLASSIFIED/UNLIMITED <input type="checkbox"/> SAME AS RPT <input type="checkbox"/> DTIC USERS		21. ABSTRACT SECURITY CLASSIFICATION Unclassified	
22a. NAME OF RESPONSIBLE INDIVIDUAL Mrs. Virginia M. Miller		22b. TELEPHONE (Include Area Code) 301/663-7325	22c. OFFICE SYMBOL SGRD-RMI-S

12. Personal Author(s)

James D. Birkett, Ph.D.
Itamar Bodek, Ph.D.
Marc Bonazountas, Ph.D.
Aviva Brecher, Ph.D.
Sara E. Bysshe
Deborah L. Cerundolo
Susan F. Coons
Daniel J. Ehnholt, Ph.D.
Elizabeth D. Gibson
Anita E. Glazer
Clark F. Grain
Janice W. Green

Denise Hayes
Abraham Lerman, Ph.D.
Northwestern University
Evanston, IL
Donald B. Lindsay
Independent consultant
Lexington, MA
Christopher P. Loreti
Warren J. Lyman, Ph.D.
Madeline F. McComish
Joo Hooi Ong
Jan Shim
Robert G. Vranka, Ph.D.

Editors: Warren J. Lyman, Ph.D.

Itamar Bodek, Ph.D.
William F. Reehl
David H. Rosenblatt, Ph.D., USAMBRDL

18. Subject Terms (Con't)

Reaction Kinetics; Environmental Data; Ambient Concentrations; Criteria and Standards.

AD

(2)

METHODS FOR ESTIMATING PHYSICOCHEMICAL PROPERTIES OF INORGANIC CHEMICALS OF ENVIRONMENTAL CONCERN

FINAL REPORT
Volume 1 (of 2)

by

Warren J. Lyman, Ph.D.
Itamar Bodek, Ph.D.
William F. Reehl
and other contributors

of Arthur D. Little, Inc.

DTIC
ELECTED
S JUL 14 1987 D
D

and

David H. Rosenblatt, Ph.D.
(Contracting Officer's Representative)
US Army Biomedical Research and Development Laboratory
Fort Detrick, Frederick, MD 21701-5010

March 1987

Supported by

US Army Medical Research and Development Command
Fort Detrick, Frederick, MD 21701-5012

Contract No. DAMD 17-83-C-3274

Arthur D. Little, Inc.
Cambridge, Massachusetts 02140

Approved for public release; distribution unlimited.

The findings in this report are not to be construed as an official Department
of the Army position unless so designated by other authorized documents.

EXECUTIVE SUMMARY

The primary purpose of this project was to compile, in one report, information on environmentally important physicochemical properties of inorganic chemicals for use by environmental scientists and managers. This report, in a sense, is a companion document to the report we previously prepared for environmentally important properties of organic chemicals, and which was subsequently published under the title: *Handbook of Chemical Property Estimation Methods* (McGraw-Hill Book Co., 1982). Like the "organics" report, this "inorganics" report describes available estimation methods for various properties. Such information supports one of our primary objectives, which is to assist environmental scientists and managers (many of whom may not have a detailed knowledge or understanding of inorganic environmental chemistry) in overcoming the common problem of property data gaps and in developing timely responses to environmental problems.

In marked contrast to the "organics" report, however, this "inorganics" report is not limited to a presentation of selected estimation methods for estimable properties. Because so few properties are easily estimable, it was decided to cover environmentally important properties, without regard to estimability, and to present not only a generic discussion of these properties, but also a summary of environmentally important data for the most common elements and pollutants.

Table 1 summarizes the contents of the report, which is composed of two parts. (A more detailed outline is given in the Table of Contents.) Part I provides a generic description of properties and processes with special focus on those listed in Table 2. To the extent possible, it gives specific instructions to assist in estimating (or selecting) property values and/or assessing the importance of a particular property or process for a specific site or pollutant. Where even this kind of assistance is difficult or impossible, tabulated data, illustrations, and examples are presented to demonstrate the range of possible values or behavior. Part I also contains major sections on uptake by biota and environmental fate models.

Part II of the report presents environmentally important property data for several groups of elements or compounds: (a) major elements and anions in the earth's crust and surface waters; (b) pollutant metals; (c) pollutant ligands; (d) radionuclides; and (e) selected chemical classes, including organometallics. In each case, data are provided for specific elements, ligands or compounds along with text describing, where pertinent, how these chemicals generally behave in the environment.

Accession For	
NTIS CRA&I	<input checked="" type="checkbox"/>
DTIC TAB	<input type="checkbox"/>
Unpublished	<input type="checkbox"/>
Justification	
By	
Date Entered	
Availability Status	
Dist	
A-1	

TABLE 1

Summary of Contents

Part I	Generic Description of Properties and Processes
1	Introduction
2	Description of Individual Processes
3	Kinetics of Selected Processes
4	Uptake by Biota
5	Mathematical Environmental Fate Modeling
Part II	Information on Specific Chemicals
6	Matrix Elements and Ligands
7	Trace Metals
8	Pollutant/Trace Ligands
9	Radionuclides
10	Commercial Compounds
Appendices	
A	Notations and Symbols
B	Chemical Composition of the Environment
C	Classification and Properties of Soils
D	Pollutant Criteria and Standards
E	Recommendations for Future Research

TABLE 2

Properties and Processes Covered^a

Vapor Pressure	Electron Transfer Reactions ^b
Photolysis in Air	Solubility and Precipitation ^b
Gas Adsorption on Solids	Attenuation on Soils
Atmospheric Deposition	Photolysis in Water
Activity Coefficient	Integration of Aqueous Processes
Acid/Base Equilibria	Microbial Transformations
Polymerization	Diffusion Coefficient
Complexation ^b	Radioactive Processes and Properties

a. Generic discussion of these processes and properties, including available estimation methods, are provided in Chapter 2. Where applicable, equilibrium conditions are assumed.

b. Chapter 3 of the report describes the kinetics of these processes. (Complexation is discussed in terms of ligand exchange.)

ACKNOWLEDGEMENTS

This report is the result of a project undertaken by Arthur D. Little, Inc., under contract to the U.S. Army Medical Research and Development Command. The Army's willingness to support this work indicates a real concern for environmental protection.

The need for a handbook on inorganic environmental chemistry was originally perceived by our Project Officer, Dr. David H. Rosenblatt of the U.S. Army Biomedical Research and Development Laboratory (USABRDL), Fort Detrick, Frederick, Maryland. His initiative, guidance, and subsequent assistance in preparation of the handbook — especially as an editor — were essential to the successful completion of the project. Mr. Jesse Barkley (USABRDL), who was also very supportive and encouraging, was instrumental in obtaining funding for this project.

The U.S. Army Medical Research and Development Command funded both Phase I of this program, a preliminary problem definition study, and a major portion of Phase II, the writing of the handbook. Financial support for Phase II was also provided by the U.S. Environmental Protection Agency's Office of Toxic Substances (Washington, DC).

The names of the authors of complete chapters are shown on the first page of those chapters. These and other contributors with specific subsection responsibilities are listed on the following pages. Special credit should be given to Dr. Itamar Bodek, who provided invaluable help as Assistant Project Manager, and to William F. Reehl, who served as both a technical and style editor for each chapter. Dr. Brian Barnett contributed significantly in the early planning phase of this project and reviewed several major sections in the writing phase.

All of the chapters in this book were reviewed by one or more extramural reviewers selected from various universities, research and consulting firms, and government offices and laboratories. A list of reviewers is provided on the following pages.

**Warren J. Lyman
Program Manager
Arthur D. Little, Inc.**

CONTRIBUTORS

Except as noted, all contributors are present or former employees of Arthur D. Little, Inc.

James D. Birkett:	2.16 Diffusion Coefficient
Itamar Bodek:	2.7 Acid/Base Equilibria; 2.9 Complexation; 2.10 Electron Transfer Reactions; 3.2 Ligand Exchange Kinetics; 3.3 Kinetics of Electron Transfer (Redox) Reactions; 10.1 Organometallics
Marc Bonazountas:	Overview responsibility for: 5. Mathematical Environmental Fate Modeling plus: 5.1 Introduction; 5.2 Background; 5.4 Terrestrial Modeling; 5.5 Aquatic Modeling
Aviva Brecher:	5.6 Radionuclide Migration Modeling
Sara E. Bysshe:	4. Uptake by Biota
Deborah L. Cerundolo:	6.4 Calcium; 6.5 Magnesium
Susan F. C. Jones:	6.2 Sodium; 6.3 Potassium
Daniel J. Ehntholt:	10.1 Organometallics
Elizabeth D. Gibeon:	6.6 Silicon; 6.7 Aluminum; 6.8 Iron
Anita E. Glazer:	2.8 Polymerization; 10.2 Acids; 10.3 Bases (Hydroxides); 10.4 Salts; 10.5 Oxides; 10.6 Gases; 10.7 Sulfur-Containing Compounds; 10.9 Boron-Containing Compounds; 10.10 Silicon-Containing Compounds; 10.11 Carbonyls; 10.12 Carbides; 10.13 Cyanides; 10.14 Hydrides; 10.16 Peroxides; Appendix D: Pollutant Criteria and Standards
Clark F. Grain:	2.2 Vapor Pressure; 2.3 Photolysis in Air; 2.4 Gas Adsorption on Solids; 2.14 Photolysis in Water
Janice W. Green:	Appendix C: Classification and Properties of Soils
Denise Hayes:	2.15 Microbial Transformations
Abraham Leiman: Northwestern University, Evanston, Illinois	2.11 Solubility and Precipitation Equilibria; 2.13 Integration and Analysis of Aqueous Processes; 3.4 Kinetics of Dissolution, Precipitation and Crystallization

Donald B. Lindsay: 2.17 Radioactive Processes; 9. Radionuclides;
Independent Consultant
Lexington,
Massachusetts

Christopher P. Loretz: 2.5 Atmospheric Deposition; 6.9 Hydrogen and
Hydroxide Ion; 6.10 Chloride; 6.11 Sulfate;
6.12 Carbonates; 10.8 Phosphorus-Containing
Compounds; 10.15 Hypochlorites and Chlorates;
Appendix B: Chemical Composition of the
Environment

Warren J. Lyman: 1. Introduction; 10.1 Organometallics

Madeline F. McComish: 7.3 Barium; 7.5 Cadmium; 7.6 Chromium;
7.9 Manganese; 7.12 Selenium; 7.14 Thallium;
7.15 Zinc

Joo Hooi Ong: 2.12 Attenuation on Soils; 7.1 Antimony; 7.2 Arsenic;
7.4 Beryllium; 7.7 Copper; 7.8 Lead; 7.10 Mercury;
7.11 Nickel; 7.13 Silver

Jan Shim: Preliminary drafts of portions of Chapter 10

Robert G. Vranka: 5.3 Air Modeling

REVIEWERS

Dr. Marc Anderson, University of Wisconsin, Madison, WI

Dr. Robert Boethling, U.S. EPA, Washington, DC

Dr. Fred C. Brinckman, National Bureau of Standards, Gaithersburg, MD

Dr. Rufus Chaney, U.S. Department of Agriculture, Beltsville, MD

Dr. Jim Dragun, E.C. Jordan Co., Smithfield, MI

Dr. Stephen C. Hern, U.S. EPA, Las Vegas, NV

Dr. Donald Langmuir, Colorado School of Mines, Golden, CO

Dr. Henry Lee, U.S. EPA, Newport, OR

Dr. Asa Leifer, U.S. EPA, Washington, DC

Dr. Abraham Lerman, Northwestern University, Evanston, IL

Dr. Donald Mackay, University of Toronto, Toronto, Ontario

Dr. Constantine Maletskos, consultant, Gloucester, MA

Dr. Theodore Mill, SRI International, Menlo Park, CA

Dr. Darrell Nelson, University of Nebraska, Lincoln, NE

Dr. Albert Page, University of California, Riverside, CA

Dr. David Ryan, New England Aquarium, Boston, MA

Dr. Gary Thom, U.S. EPA, Washington, DC

Dr. Marvin Wesely, Argonne National Laboratory, Argonne, IL

Mr. William Wood, U.S. EPA, Washington, DC

SUMMARY TABLE OF CONTENTS

(A detailed Table of Contents, followed by a List of Tables and List of Figures, is given at the beginning of each Chapter and each Appendix.)

	Page
EXECUTIVE SUMMARY	iii
ACKNOWLEDGEMENTS	
<i>CONT'D</i>	
1. INTRODUCTION	
1.1 Overview	1-1
1.2 Background	1-2
1.3 The Need for Guidance	1-7
1.4 Objectives	1-8
1.5 Using the Handbook	1-9
2. DESCRIPTION OF INDIVIDUAL PROCESSES	
2.1 Introduction	2.1-1
2.2 Vapor Pressure	2.2-1
2.3 Photolysis in Air	2.3-1
2.4 Gas Adsorption on Solids	2.4-1
2.5 Atmospheric Deposition	2.5-1
2.6 Activity Coefficient	2.6-1
2.7 Acid/Base Equilibria	2.7-1
2.8 Polymerization	2.8-1
2.9 Complexation	2.9-1
2.10 Electron Transfer Reactions	2.10-1
2.11 Solubility and Precipitation Equilibria	2.11-1
2.12 Attenuation on Soils	2.12-1
2.13 Integration and Analysis of Aqueous Processes	2.13-1
2.14 Photolysis in Water	2.14-1
2.15 Microbial Transformations	2.15-1
2.16 Diffusion Coefficients	2.16-1
2.17 Radioactive Processes and Properties	2.17-1

Cont'd

3. KINETICS OF SELECTED PROCESSES

3.1	Introduction	3.1-1
3.2	Ligand Exchange Kinetics	3.2-1
3.3	Kinetics of Electron Transfer (Redox) Reactions	3.3-1
3.4	Kinetics of Dissolution, Precipitation and Crystallization	3.4-1

4. UPTAKE BY BIOTA; AND

4.1	Introduction	4.1-1
4.2	Biological Uptake Processes and Problems	4.2-1
4.3	Uptake by Terrestrial Vegetation	4.3-1
4.4	Uptake by Marine Biota	4.4-1
4.5	Uptake by Freshwater Biota	4.5-1
4.6	Literature Cited	4.6-1

5. MATHEMATICAL ENVIRONMENTAL FATE MODELING

5.1	Introduction	5.1-1
5.2	Background	5.2-1
5.3	Air Modeling	5.3-1
5.4	Terrestrial Modeling	5.4-1
5.5	Aquatic Modeling	5.5-1
5.6	Radionuclide Migration Modeling	5.6-1

6. MATRIX ELEMENTS AND LIGANDS

6.1	Introduction	6.1-1
6.2	Sodium (Na)	6.2-1
6.3	Potassium (K)	6.3-1
6.4	Calcium (Ca)	6.4-1
6.5	Magnesium (Mg)	6.5-1
6.6	Silicon (Si)	6.6-1
6.7	Aluminum (Al)	6.7-1
6.8	Iron (Fe)	6.8-1
6.9	Hydrogen and Hydroxide Ion (H^+ , OH^-)	6.9-1
6.10	Chloride (Cl^-)	6.10-1
6.11	Sulfate (SO_4^{2-})	6.11-1
6.12	Carbonates (HCO_3^- , CO_3^{2-} , etc.)	6.12-1

7. TRACE METALS

Introduction	7-1
7.1 Antimony (Sb)	7.1-1
7.2 Arsenic (As)	7.2-1
7.3 Barium (Ba)	7.3-1
7.4 Beryllium (Be)	7.4-1
7.5 Cadmium (Cd)	7.5-1
7.6 Chromium (Cr)	7.6-1
7.7 Copper (Cu)	7.7-1
7.8 Lead (Pb)	7.8-1
7.9 Manganese (Mn)	7.9-1
7.10 Mercury (Hg)	7.10-1
7.11 Nickel (Ni)	7.11-1
7.12 Selenium (Se)	7.12-1
7.13 Silver (Ag)	7.13-1
7.14 Thallium (Tl)	7.14-1
7.15 Zinc (Zn)	7.15-1

8. POLLUTANT/TRACE LIGANDS

Introduction	8-1
8.1 Nitrogen (N)	8.1-1
8.2 Sulfur (S)	8.2-1
8.3 Phosphorus (P)	8.3-1
8.4 Fluorine (F)	8.4-1

9. RADIONUCLIDES

9.1 Introduction: General Considerations	9.1-1
9.2 Properties of Selected Radionuclides	9.2-1
9.3 Literature Cited	9.3-1

10. CHEMICAL CLASSES

Introduction	10.0-1
10.1 Organometallics	10.1-1
10.2 Acids	10.2-1
10.3 Bases (Hydroxides)	10.3-1
10.4 Salts	10.4-1
10.5 Oxides	10.5-1
10.6 Gases	10.6-1
10.7 Sulfur-Containing Compounds	10.7-1
10.8 Phosphorus-Containing Compounds	10.8-1

10.9	Boron-Containing Compounds	10.9-1
10.10	Silicon-Containing Compounds	10.10-1
10.11	Carbonyls	10.11-1
10.12	Carbides	10.12-1
10.13	Cyanides	10.13-1
10.14	Hydrides	10.14-1
10.15	Hypochlorites and Chlorates	10.15-1
10.16	Peroxides	10.16-1

APPENDIX A

Notation and Symbols	A-1
-----------------------------	------------

APPENDIX B

Chemical Composition of the Environment	B-1
--	------------

APPENDIX C

Classification and Properties of Soils	C-1
---	------------

APPENDIX D

Pollutant Criteria and Standards	D-1
---	------------

1. INTRODUCTION

Warren J. Lyman

	Page
1.1 OVERVIEW	1-1
1.1.1 Content of Part I	1-1
1.1.2 Content of Part II	1-4
1.1.3 Content of Appendices	1-6
1.2 BACKGROUND	1-6
1.3 THE NEED FOR GUIDANCE	1-7
1.4 OBJECTIVES	1-8
1.5 USING THE HANDBOOK	1-9

LIST OF TABLES

1-1 Summary of Contents	1-2
1-2 Properties and Processes Covered	1-3
1-3 Chemicals Covered in Part II of Report	1-5

LIST OF FIGURES

1-1 Approach for Evaluating Situations Involving Inorganic Pollutants	1-10
---	------

1.1 OVERVIEW

This report provides basic information on important processes and properties relating to the environmental fate, transformation and mobility of inorganic and organometallic chemicals. The general style and organization of the report is that of a handbook, in order to provide easy access to specific information, data and instructions. The report is divided into two major parts. Part I provides a generic description and discussion of several environmentally important processes, while Part II provides data and information for a variety of inorganic species. The contents are summarized in Table 1-1.

1.1.1 Content of Part I

Table 1-2 lists the processes covered in Part I. The rationale for the selection of these processes, as well as the overall organization and content of the report, evolved from a preliminary problem definition study conducted for the U.S. Army.¹ The sections that describe these processes, which are primarily in Chapters 2 and 3, give specific instructions to assist in estimating (or selecting) property values and/or assessing the importance of a particular process for a specific pollutant or set of environmental conditions. For some processes, it is impractical or impossible to provide such assistance here; in those cases, tabulated data, illustrations, and examples are presented to demonstrate the range of possible values or behaviors.

A major focus of Chapter 2, which covers 15 properties or processes, is on equilibrium conditions. For example, there is significant coverage of acid/base, complexation, redox, and solubility equilibria and of equilibrium sorption on soils. The distribution coefficients or equilibrium constants corresponding to these equilibria can, in several instances, be estimated using the information provided in this report. In many cases the estimates may appear to have a large uncertainty (e.g., an order of magnitude), but this may be quite acceptable in preliminary assessments of pollution problems.

One section of Chapter 2 (§ 2.13) describes how the consideration of various aquatic speciation processes, such as complexation, redox, acid/base and precipitation reactions, can be integrated to evaluate their simultaneous effect on the distribution of species present in the system. While it is convenient in many environmental assessments to assume equilibrium conditions, it should be realized that many reactions may approach equilibrium only very slowly relative to the time scale of interest (e.g., minutes to a few years) and that erroneous conclusions could result from such an assumption.

Chapter 3 focuses on process kinetics, i.e., the rates at which reactions approach equilibrium. Due in part to project limitations, as well as to a lack of available

1. W.J. Lyman and B.M. Barnett, "Methods for Estimating Physicochemical Properties of Inorganic Chemicals of Environmental Concern," Final Report, Phase I, Contract No. DAMD17-83-C-3274 U.S. Army Medical Research and Development Command, Fort Detrick, Frederick, Md. (1984).

TABLE 1-1
Summary of Contents

PART I	GENERIC DESCRIPTION OF PROPERTIES AND PROCESSES
1	Introduction
2	Description of Individual Processes
3	Kinetics of Selected Processes
4	Uptake by Biota
5	Mathematical Environmental Fate Modeling
PART II	INFORMATION ON SPECIFIC CHEMICALS
6	Matrix Elements and Ligands
7	Trace Metals
8	Pollutant/Trace Ligands
9	Radionuclides
10	Commercial Compounds
APPENDICES	
A	Notations and Symbols
B	Chemical Composition of the Environment
C	Classification and Properties of Soils
D	Pollutant Criteria and Standards
E	Recommendations for Future Research
SUBJECT INDEX	

information on the kinetics of some reactions, only three processes are treated in detail: (1) ligand exchange, (2) oxidation and reduction, and (3) dissolution, precipitation and crystallization. (Some information on process kinetics is also provided in Chapter 2, principally in the sections on Atmospheric Deposition, Photolysis in Air, Photolysis in Water, Diffusion Coefficient, and Radioactive Processes).

The mathematical treatment of the kinetics of these processes focuses on the rate constant and methods for estimating its approximate value. Even when the rates can only be roughly estimated, they are helpful in assessing the importance of reaction kinetics for a specific environmental scenario. For example, if a reaction is very fast relative to the time scale of a scenario (e.g., discharge and dilution of a wastewater stream in a river), a detailed evaluation of the kinetics would not be warranted, and only the equilibrium reaction products need be considered.

TABLE 1-2
Properties and Processes Covered^a

Vapor Pressure	Attenuation on Soils
Photolysis in Air	Aqueous Photolysis
Gas Adsorption on Solids	Integration of Aqueous Processes
Atmospheric Deposition	Microbial Transformations
Activity Coefficient	Diffusion of Ions
Polymerization	Radioactive Processes and Properties
Complexation ^b	Uptake by Biota ^c
Electron Transfer Reactions ^b	
Solubility and Precipitation ^b	

a. Generic discussions of these processes and properties, including available estimation methods, are provided in Chapter 2.

b. Chapter 3 of the report describes the kinetics of these processes. (Complexation is discussed in terms of ligand exchange.)

c. Covered in Chapter 4.

Chapter 4 of Part I describes the uptake of inorganic chemicals by biota, particularly biotic groups of importance in the human food chain (terrestrial plants and freshwater and saltwater fish), and gives special attention to the uptake of selected heavy metals by these groups. Although detailed coverage of other biotic groups and chemical classes was not possible within the scope of this project, uptake and loss processes are discussed in sufficient detail to permit appropriate questions to be asked and some answers to be inferred.

There are no generally applicable mathematical techniques for estimating the extent of bioaccumulation of inorganics; their development awaits further research on chemical speciation in the (aquatic) environment and mechanisms and rates of uptake and loss for specific chemical species. In the absence of these estimation methods, Chapter 4 describes a "decision process" that may help the reader to choose an appropriate focus for more detailed review and use of the scientific literature, or to structure an appropriately inclusive laboratory or field experiment to investigate a potential uptake problem.

Chapter 5 provides a non-mathematical description of available environmental fate models that can predict the equilibrium speciation of many elements in aquatic environments and the transport and (generalized) fate of individual pollutants in air, water and soil media. Its primary objectives are to help readers in (1) understanding the complexities of modeling, (2) selecting specific modeling packages for their own use, and (3) evaluating other people's modeling results when, for example, that information is part of a permit application for a plant site and is used in the design of waste treatment, storage or disposal facilities.

A background section in Chapter 5 (§ 5.2) includes a general discussion of environmental pathways (for both transport and fate) to guide environmental managers in the preliminary identification and assessment of those that are potentially important in a given scenario. This is followed by descriptions of modeling transport and fate in the air, soil/groundwater, and surface water compartments (subsections 5.3, 5.4, and 5.5, respectively). A final section (§ 5.6) is devoted to the highly specialized subject of modeling the transport and fate of radionuclides in the soil/groundwater system.

1.1.2 Content of Part II

Part II presents environmentally important data and information for several groups of elements or compounds. These have been separated into chapters that focus on: (1) major elements and anions in the earth's crust and surface waters, (2) pollutant metals and metalloids, (3) pollutant ligands, (4) radionuclides, and (5) selected classes of commercial chemicals, including organometallics.

A detailed list of the chemicals and species discussed in Part II is given in Table 1-3. The specific chemicals covered in this report were selected because of their importance as environmental pollutants, workplace hazards, hazardous chemicals used in industry, and/or chemicals that might affect (e.g., through complexation) the aquatic speciation and, thus, the behavior of trace pollutants. Further details of the selection process are provided in the introductions to the various sections and in the preliminary problem definition report footnoted earlier.

Chapters 6 and 7 typically contain information under the following headings:

- Occurrence, Production, and Uses
- Speciation Reactions in Water
 - Acid/Base Dissociation
 - Complexation
 - Redox Reactions
 - Solubility and Precipitation
- Sorption on Soils and Sediments
- Biotransformation (where appropriate)
- Volatilization (where appropriate)

Chapter 8, which addresses compounds containing N, S, P and F, provides information similar to that in Chapters 6 and 7 plus a discussion of the environmental cycles for these elements and the species of environmental importance.

The coverage of radionuclides in Chapter 9 (like that of radioactive processes and properties in § 2.17 and radionuclide migration modeling in § 5.6) is limited. Understanding of the environmental fate and transport of radionuclides has advanced significantly in recent years, not only as a result of early studies of

TABLE 1-3
Chemicals and Species Covered in Part II

Chapter	Coverage	
6	Na, K, Ca, Mg, Si, Al, Fe H^+ / OH^- , Cl^- , SO_4^{2-} , HCO_3^- / CO_3^{2-}	
7	Sb, As, Ba, Be, Cd, Cr, Cu, Pb, Mn, Hg, Ni, Se, Ag, Tl, Zn	
8	Compounds of: N, S, P, F	
9	3H , ^{14}C , ^{32}P , ^{35}S , ^{40}K , ^{50}V , ^{51}Cr , ^{87}Rb , $^{99m}{^{99}Tc}$, ^{115}In , $^{125/129/131}I$, ^{133}Xe , ^{137}Cs , ^{147}Pm , ^{154}Eu , ^{176}Lu , ^{187}Re , ^{201}Tl , $^{210/214}Pb$, $^{210/214}Bi$, $^{210/214/218}Po$, $^{220/222}Rn$, ^{226}Ra , $^{232/234}Th$, ^{234}Pa , $^{235/238}U$, ^{239}Pu , ^{241}Am	
10	Organometallics Acids Bases (Hydroxides) Salts Oxides Gases Hydrides Peroxides	Sulfur-containing Compounds Phosphorus-containing Compounds Boron-containing Compounds Silicon-containing Compounds Carbonyls Carbides Cyanides Hypochlorites and Chlorates

radioactive fallout, but also due to extensive analyses of potential problems associated with the disposal of radioactive wastes from commercial products, industrial wastes, and nuclear power plants. Due to the availability of detailed books on this subject, Chapter 9 is primarily designed to provide an introduction to the problem and present some data on radiation emission and environmental behavior.

The discussion of chemical classes in Chapter 10 focuses on specific chemicals of commercial or environmental importance. Their major commercial uses and the physical and chemical properties that govern their fate in the environment are described. Information is also provided on the processes and transformations that chemicals in each class are likely to undergo under environmental conditions, such as (1) volatilization, (2) reaction with air (i.e., oxidation), (3) dissolution in and/or reaction with water (solubility, acid-base dissociation, hydrolysis), (4) aqueous reactions (complexation, oxidation/reduction, polymerization), and (5) mobility and degradation in soils.

Organometallics (§ 10.1) are covered more extensively than any of the other classes in Chapter 10. Although their inclusion is somewhat out of keeping with the primary focus on inorganics in this report, it reflects an awareness of their growing commercial and environmental importance.

1.1.3 Content of Appendices

This report concludes with five appendices and a subject index. Appendix A is a list of commonly used notations and symbols. Background concentrations of the elements and a few other chemical species in air, water, soil and sediments are tabulated in Appendix B. Because the amount of this data is limited, the values should be interpreted with caution; however readers should be able to estimate the approximate extent of pollution by comparing data from a polluted site with the listed values.

Appendix C is a primer on the classification and properties of soils, focusing on those properties that affect the movement of water and pollutants through the soil/groundwater system. Appendix D summarizes federal pollutant criteria and standards for inorganic chemicals, such as the EPA's ambient water quality standards (for the protection of aquatic life) and drinking water standards (for protection of human health). Recommendations for future research are briefly outlined in Appendix E.

1.2 BACKGROUND

The last 15 years have brought an ever-growing awareness in this country of the need for environmental protection, especially where the use of chemicals is involved. The decade of the 1970s was especially important in the United States for the passage of key government acts or actions that mandate a minimum level of protection. Included were the following:

- National Environmental Policy Act (1969)
- Creation of the U.S. Environmental Protection Agency (1970)
- Occupational Safety and Health Act (1970)
- Clean Water Act Amendments (1972)
- Marine Protection Research and Sanctuaries Act (1972)
- Safe Drinking Water Act (1973)
- Toxic Substances Control Act (1976)
- Resource Conservation and Recovery Act (1976)
- EPA/NRDC Settlement Agreement on Toxics ("Priority Pollutants") (1976)
- Clean Water Act Amendments ("Toxics" added) (1977)
- Comprehensive Emergency Response, Compensation and Liability Act (Superfund) (1980)

More recently, much of the regulatory activity at the federal level has been geared to amending these acts; at the state and local levels, it has been geared to implementing state acts, regulations and standards as required or suggested by the federal legislation.

The heightened concern and regulatory activity have, of necessity, created a multitude of environmental scientists and managers that may number in the several tens of thousands. This army of specialists is responsible for the development and implementation of regulations, for research into control technologies, for the operation of pollution control facilities and other related activities; it is these people to whom this report is directed.

1.3 THE NEED FOR GUIDANCE

There is a real need today for a wide variety of guidance manuals directed toward environmental scientists and managers in government, industry and universities. These individuals come to their positions with varied training (e.g., a B.S. in Biology, an M.S. in Civil Engineering, or a 20-year job as a chemical process engineer), little of which helps them to make timely decisions related to environmental protection where toxic chemicals are involved.

Manuals are now available for designing wastewater treatment plants, cleaning up oil spills, monitoring stack gas emissions, and preparing river management plans, for example; however, there is virtually no guidance on how to assess the very complex problems that relate more directly to the fate and transport of chemicals in the environment. What are needed are: (a) guidance in assessing what physicochemical properties and processes are environmentally important, (b) advice on how to use the properties to maximum advantage, and (c) some actual values of these properties. In 1982 we prepared a Handbook² designed to fill part of this need by providing a compilation of carefully described estimation methods for environmentally important properties of organic chemicals. The need for estimation methods was described in the introduction to this "organics" Handbook as follows:

"Over the past decade, the chemical contamination of our environment has justifiably aroused growing concern. A proper assessment of the risk — to man and the environment — created by exposure to these chemicals generally includes attempts to measure or predict the concentrations in various environmental compartments in conjunction with toxicological data. Frequently, however, neither the concentration data nor the toxicological data are adequate for any realistic assessment. In addition, basic physical and chemical data are often unavailable, especially for new organic chemicals being considered for bulk manufacture. If, however, the most important physical and chemical properties of these chemicals could be estimated, their transport and fate in the environment could be better understood — even modeled in some cases — and the environmental concentrations might be estimated."

2. W.J. Lyman, W.F. Reehl and D.H. Rosenblatt (eds.), *Handbook of Chemical Property Estimation Methods: Environmental Behavior of Organic Chemicals*, McGraw-Hill Book Co., New York (1982).

It was clear at the time the above Handbook was prepared that a separate program, and perhaps quite a different handbook, would also be required for the coverage of inorganic chemicals and special classes such as organometallics. The current program was instituted to address this need.

As noted above, the preparation of this report was preceded by a problem definition study in which the needs of environmental scientists and managers were considered in conjunction with the available information on inorganic environmental chemistry (Lyman and Barnett, *op. cit.*). Many individuals contributed to the preliminary study, and the outline and format of the present report reflect their collective wisdom.

1.4 OBJECTIVES

The primary purpose of this project was to compile, in one report, information on environmentally important physicochemical properties of inorganic chemicals for use by environmental scientists and managers. In sense, the report complements the "organics" Handbook; like that document, it describes available estimation methods for various properties. This information supports one of our primary objectives, which is to assist environmental scientists and managers (many of whom may not have a detailed knowledge or understanding of inorganic environmental chemistry) in overcoming the common problem of property data gaps and developing timely responses to environmental problems.

In marked contrast to the "organics" report, however, this "inorganics" report is not limited to the description of estimation methods. Because so few properties of inorganic species are easily estimable, the authors decided to cover environmentally important properties without regard to estimability, and to present not only a generic discussion of these properties but also a summary of environmentally important data for the most common elements and pollutants.

With this report as guidance, environmental scientists and managers should be able to undertake preliminary environmental assessments of the fate and transport of inorganic and organometallic compounds for such situations or scenarios as the following:

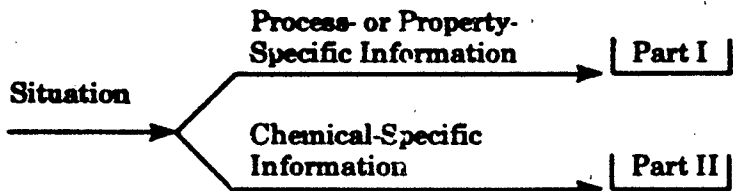
- NPDES, FIFRA, RCRA (etc.) permit applications
- R&D for wastewater treatment (e.g., metal removal)
- Modeling or assessment of chemical spills
- Modeling or assessment of soil/groundwater contamination
- Modeling the speciation and fate of metals in water
- Assessment of the consequences of agricultural use of various chemicals
- Assessment of land treatment of hazardous wastes or land application of municipal wastes or sewage sludge

- Assessment of environmental releases of pollutants to all media
- Remedial action at old chemical dump sites
- Premanufacture Notice (PMN) review
- Assessment of potential food contamination incidents
- Utilization of wastes
- Migration of food additives
- Ocean disposal
- Coal combustion
- Assessing impacts of acid rain.

Each case may present a variety of naturally occurring and pollutant chemical species to contend with, several fate and transport pathways to consider, and a host of environmental variables (e.g., temperature, pH, Eh, solid types) with which to contend. Where can the scientist or manager turn to for help today? Little reliable guidance is easily and quickly available, and research or field studies to obtain specific answers are both costly and time-consuming. This report was prepared to help meet that need.

1.5 USING THE HANDBOOK

As discussed earlier, this report is divided into (1) a generic discussion of properties and processes and (2) information on specific chemicals and chemical classes. Thus, for any given environmental scenario, an initial choice of process- (or property-) specific versus chemical-specific sections is available:



For example, to evaluate a metal-contaminated sediment, the reader can go to Part I to obtain a basic understanding of the processes that may be important (speciation in water, sediment sorption, diffusion of ions in water-filled pores of sediment, etc.). Then he can go to Part II to obtain some of the speciation and sorption information (measured constants) for the specific chemicals of concern and to determine the applicability of the data to the situation at hand. If data are not available in this report or in other readily available sources, the reader can return to Part I to estimate missing constants (or their reasonable limits) and/or modify literature values to take into account situation-specific factors such as temperature, species concentration, pH and ionic strength. A significant amount of chemical-specific information is also available in Part I; this may be found by referring to the Table of Contents or Subject Index, or by a perusal of the section of interest.

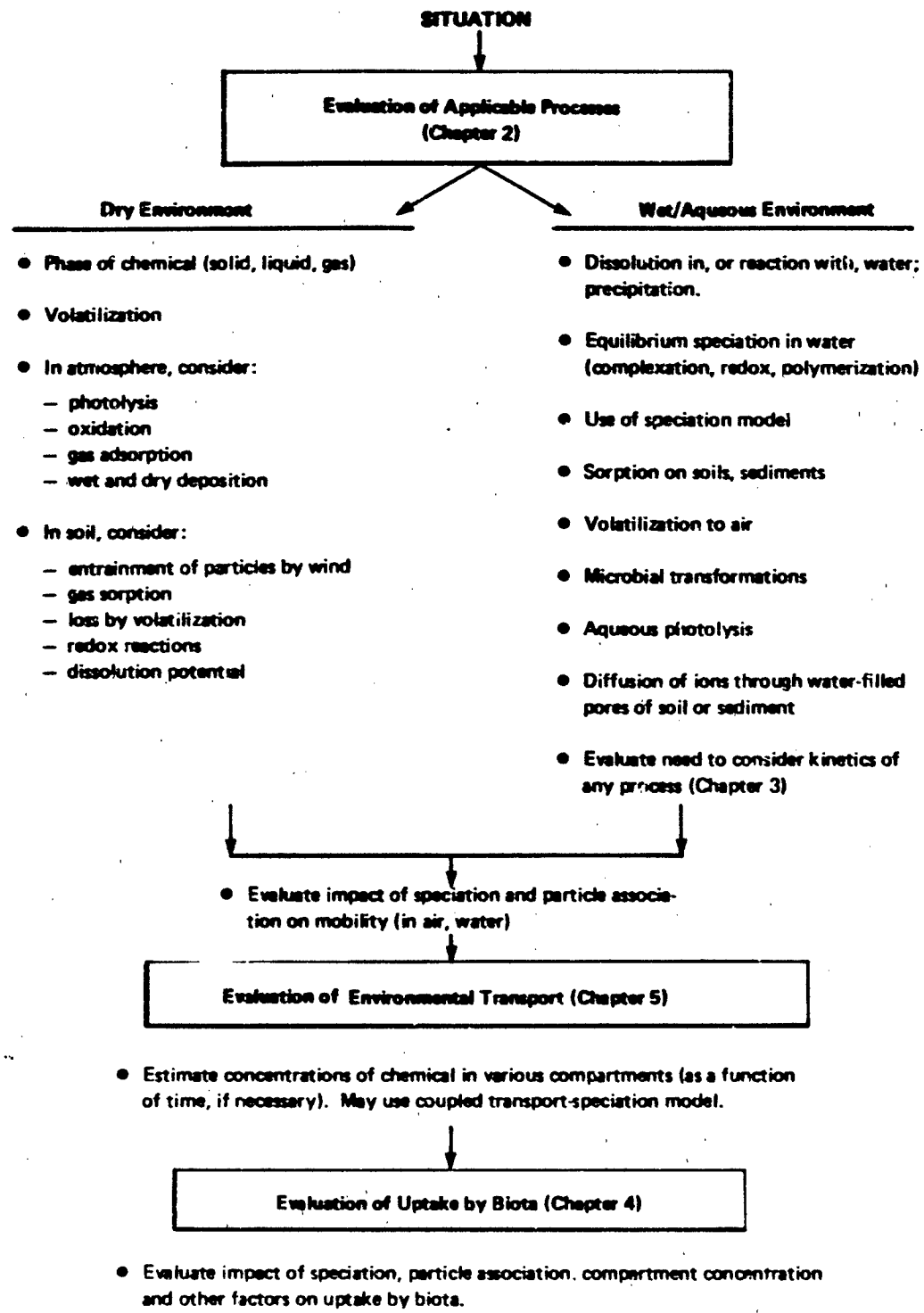


FIGURE 1-1 Approach for Evaluating Situations Involving Inorganic Pollutants

Deciding or determining what processes are important requires some work by the reader, as each pollutant and each scenario may entail consideration of a different set of processes. Figure 1-1 outlines an approach that may be helpful. It is essential to distinguish between dry and wet environments; only in the latter is it necessary to consider aqueous speciation reactions and sorption processes, which take up a major portion of Chapter 2. The introduction to Chapter 3 (§ 3.1) will help evaluate the need to consider reaction kinetics for selected aqueous processes.

Section 2.13 describes (with examples) ways to consider the net effect of several processes (e.g., complexation, redox reaction and precipitation) on a specified environmental system. The approach is practical only for simple systems (i.e., a small number of species and processes); computerized speciation models (described in sections 5.4 and 5.5) must be used for complex systems.

The individual sections of Chapters 2 and 3 typically describe the influence of key environmental variables such as temperature, pH, chemical concentration, and ionic strength on a given process. In general, however, extreme environments (e.g., very high temperatures or pressures) are not considered. The reader should be aware of the controlling variables and, where possible, specifically account for them by modifying the equilibrium and rate constants used.

The general goal of all such assessments is to evaluate the persistence, mobility and bioavailability of a chemical. The answers clearly require knowledge of the speciation of the chemical and of the biological species present.

Before evaluating uptake potential, one may have to evaluate the transport of the chemical over the relevant intervals of time and space. These can range from minutes to decades and meters to hundreds of kilometers, respectively. Transport models provide approximate concentrations of the pollutant as a function of location — usually, the distance from the source — and (possibly) time. The selection of a model, or the evaluation of model results presented by others, is aided by the material in Chapter 5.

However, sophisticated models can be misleading. They can provide the illusion of power over complexity and, for all but the most expert, can easily mask unwarranted or inappropriate assumptions, poor input data, and errors in calculation. This puts an added burden on the user (or reviewer) to understand the model's weaknesses and, if necessary, to support the results by independent assessments and hand calculations (perhaps only order-of-magnitude calculations) of the most fundamental processes or rate-limiting factors.

This report is severely limited in some aspects, largely as a result of the attempt to cover so many subjects within a given budget, scope and report size. It will clearly not be adequate for detailed investigations in which time and money allow more specific and thorough literature searches, and possibly laboratory and field experiments. In many cases, the information was obtained principally from secondary sources; this limitation on literature review and citation may disappoint those who hope to find references to the latest journal articles on a particular process, property or pollutant. We hope that such omissions will be corrected in subsequent revisions.

2. DESCRIPTION OF INDIVIDUAL PROCESSES

*James D. Birkett, Itamar Bodek, Anita E. Glazer, Clark F. Grain, Denise Hayes,
Abraham Lerman, Donald B. Lindsay, Christopher P. Loretz, Joo Hooi Ong*

	Page
2.1 INTRODUCTION	2.1-1
2.2 VAPOR PRESSURE	
2.2.1 Introduction	2.2-1
2.2.2 Experimental Determination	2.2-2
2.2.3 Estimation Methods	2.2-2
2.2.4 Recommended Methods	2.2-4
- Liquids and Solids ($T < T_b$)	2.2-4
- Gases and Vapors ($T > T_b$)	2.2-6
2.2.5 Method Error	2.2-6
2.2.6 Sample Calculations	2.2-9
2.2.7 Literature Cited	2.2-11
2.3 PHOTOLYSIS IN AIR	
2.3.1 Introduction	2.3-1
2.3.2 Units for Rate Constants and Concentrations	2.3-2
2.3.3 Solar Irradiance and Absorption Rates	2.3-2
2.3.4 Photochemical Mechanisms	2.3-8
2.3.5 Literature Cited	2.3-11
2.4 GAS ADSORPTION ON SOLIDS	
2.4.1 Introduction	2.4-1
2.4.2 Data Values	2.4-2
2.4.3 Estimating Methods	2.4-2
- Gases and Vapors ($T > T_b$)	2.4-5
- Vapors ($T < T_b$)	2.4-8
2.4.4 Method Error	2.4-9
2.4.5 Sample Calculations	2.4-9
2.4.6 Literature Cited	2.4-11
2.5 ATMOSPHERIC DEPOSITION	
2.5.1 Introduction	2.5-1
2.5.2 Dry Deposition	2.5-1
- Deposition of Particulates	2.5-1
- Dry Deposition of Gases	2.5-14
2.5.3 Wet Deposition	2.5-22
- Particle Scavenging	2.5-23
- Gas Scavenging	2.5-26

2.5.4	Deposition Velocity Data	2.5-26
2.5.5	Literature Cited	2.5-30
2.6	ACTIVITY COEFFICIENT	
2.6.1	Introduction	2.6-1
2.6.2	Description of Activity Coefficient	2.6-2
-	Definition	2.6-2
-	Conventions	2.6-3
•	The Infinite Dilution Scale	2.6-3
•	The Ionic Medium Scale	2.6-4
-	Single Ion Activity and Mean Ion Activity Coefficients	2.6-5
-	Free Activity and Total Coefficients	2.6-6
-	Importance in Environmental Calculations	2.6-6
-	Variables Affecting the Value of Activity Coefficients	2.6-7
2.6.3	Estimation Methods	2.6-9
-	Debye-Hückel Method	2.6-10
-	Extended Debye-Hückel Method	2.6-12
-	Güntelberg Method	2.6-13
-	Davies Method	2.6-14
-	Method of Pitzer <i>et al.</i>	2.6-14
-	Method of Meissner <i>et al.</i>	2.6-15
-	Other Methods	2.6-22
-	Neutral Species	2.6-22
2.6.4	Literature Cited	2.6-22
2.7	ACID/BASE EQUILIBRIA	
2.7.1	Introduction	2.7-1
2.7.2	Description of Property	2.7-1
2.7.3	Environmental Importance	2.7-3
2.7.4	Mathematical and Graphical Representation	2.7-4
2.7.5	Effect of Temperature on Acidity Constants	2.7-9
2.7.6	Values and Estimation Methods for Acid Dissociation Constants	2.7-11
-	Estimation by the Ricci Formula	2.7-13
-	Estimation by the Thermodynamic Cycle Method	2.7-14
-	Calculation from Estimated or Experimentally Derived Hydroxide Complexation Constants	2.7-16
-	Estimation by the Bayless Equations	2.7-16
2.7.7	Literature Cited	2.7-18
2.8	POLYMERIZATION	
2.8.1	Introduction	2.8-1
2.8.2	Hydroxo- and Oxo-Bridged Metal Polymers	2.8-1
2.8.3	Polysulfides	2.8-3

2.8.4 Polyphosphates	2.8-9
2.8.5 Literature Cited	2.8-13
2.9 COMPLEXATION	
2.9.1 Environmental Importance	2.9-1
2.9.2 Description of Property	2.9-1
2.9.3 Values of Complexation Equilibrium Constants	2.9-3
2.9.4 Estimation of Complexation Equilibrium Constants	2.9-7
- Outer-Sphere Association Constants	2.9-7
- Inner-Sphere Complexation Constants (Hancock and Marsicano Approach)	2.9-9
• Monodentate Ligands	2.9-9
• Polydentate Ligands Containing Nitrogen Donor Atoms	2.9-14
• Aminocarboxylate Chelating Ligands	2.9-15
- Tanaka Equations for Overall Formation Constants of ML_2 and MAL Complexes	2.9-16
2.9.5 Qualitative Trends for Complexation of Ions	2.9-21
2.9.6 Literature Cited	2.9-22
2.10 ELECTRON TRANSFER REACTIONS	
2.10.1 Introduction	2.10-1
2.10.2 Environmental Importance	2.10-1
2.10.3 Mechanisms of Redox Reactions	2.10-1
2.10.4 Mathematical Representation of Redox Equilibria	2.10-5
- Equilibrium Constant, Free Energies, Electrode Potential and Electron Activity	2.10-5
- Stability Field Diagrams	2.10-12
2.10.5 Redox in Environmental Systems	2.10-19
- Important Redox Processes	2.10-19
- Applicability of Eh (or pe) Measurements	2.10-21
- Eh and pe Values Encountered in Various Environments	2.10-22
- Other Indicators of Redox Conditions	2.10-27
2.10.6 Estimation of Equilibrium Parameters for Redox Reactions	2.10-30
- Estimation of K for Redox When No Further Reaction Takes Place	2.10-31
- Estimation of K for a Redox Reaction with Subsequent Reactions	2.10-33
- Estimation of E for the Half Reaction of a Complexed Ion	2.10-35
2.10.7 Sources of Redox Data	2.10-37
2.10.8 Literature Cited	2.10-39

	Page
2.11 SOLUBILITY AND PRECIPITATION EQUILIBRIA	
2.11.1 Introduction	2.11-1
2.11.2 Description of Property	2.11-2
- Solubility Product (K_{sp})	2.11-2
- Equilibrium Constant (K)	2.11-3
- Conditions of Equilibrium	2.11-4
- Concentrations of Dissolved Species from K_{sp}	2.11-5
- Degree of Saturation	2.11-7
- Effect of Temperature on Solubility	2.11-8
- Effect of Pressure on Solubility	2.11-9
- Effect of Particle Size on Solubility	2.11-11
- Effects of Some Solution Properties on Solubility	2.11-15
• Solubility in the Presence of Complexing Ions	2.11-15
• The pH and Solubility of Oxides	2.11-17
2.11.3 Estimation of Equilibrium Constant K and Solubility	2.11-19
- Introduction	2.11-19
- Estimation of K from the Gibbs Free Energies of Formation	2.11-21
- Estimation of K and Solubility from Correlations with Crystal Properties	2.11-24
• Correlation between Solubilities and Lattice Energies	2.11-24
• Correlation between Solubilities and Cation Electronegativities	2.11-30
• Correlation between Solubilities and Crystal Ionic Radii	2.11-32
• Correlation of Solubilities with the Ionization Potentials	2.11-34
2.11.4 Summary	2.11-35
2.11.5 Sources of Information	2.11-38
2.11.6 Literature Cited	2.11-39
2.12 ATTENUATION ON SOILS	
2.12.1 Introduction	2.12-1
2.12.2 Attenuation Mechanisms	2.12-2
2.12.3 Factors Affecting Attenuation	2.12-5
2.12.4 Measurement of Attenuation	2.12-12
2.12.5 Mathematical Representations	2.12-13
- Theoretical Models	2.12-13
- Kinetic Models	2.12-14
- Empirical Models	2.12-15

2.12.6 Adsorption Isotherms	2.12-15
- Distribution Coefficient	2.12-25
- Langmuir Isotherm	2.12-26
- Freundlich Isotherm	2.12-30
2.12.7 Soil Column Studies by Fuller and Co-workers	2.12-32
2.12.8 Estimation of Attenuation in an Environmental System	2.12-38
2.12.9 Summary	2.12-41
2.12.10 Literature Cited	2.12-41
2.13 INTEGRATION AND ANALYSIS OF AQUEOUS PROCESSES	
2.13.1 Introduction	2.13-1
2.13.2 Chemical Speciation in Solution	2.13-1
- Free Ions and 1:1 Complexes	2.13-3
- Free Ions and Multiligand Complexes	2.13-4
- Large Excess of One Component	2.13-4
- Mathematical Solutions of the General Cases	2.13-6
- Methods and Steps in Integration of Chemical Processes in Solution	2.13-6
2.13.3 Case Study of an Aqueous System	2.13-9
- Description of the Aqueous System	2.13-9
- Oxidation State of Iron in Solution	2.13-11
- Chemical Speciation of Major Components	2.13-13
- Most Abundant Species of Iron and Nickel	2.13-15
- Complexation of Phosphorus	2.13-16
- Degree of Saturation of the Aqueous System	2.13-17
• Barium Sulfate: Barite, BaSO ₄ (s)	2.13-17
• Ferric Hydroxide: Amorphous Solid, Fe(OH) ₃ (s)	2.13-18
• Ferric Phosphate, Strengite, FePO ₄ · 2H ₂ O(s)	2.13-19
- Effect of Humic Acids on Complexation of Metals	2.13-19
2.13.4 Summary	2.13-21
2.13.5 Literature Cited	2.13-22
2.14 PHOTOLYSIS IN WATER	
2.14.1 Introduction	2.14-1
2.14.2 Units	2.14-1
2.14.3 Solar Irradiance and Absorption Rates	2.14-1
2.14.4 Direct Photolysis	2.14-6
2.14.5 Indirect Photolysis - Homogeneous	2.14-8
2.14.6 Indirect Photolysis - Heterogeneous	2.14-9
2.14.7 Literature Cited	2.14-12
2.15 MICROBIAL TRANSFORMATIONS	
2.15.1 General Considerations	2.15-1
2.15.2 Oxidation and Reduction	2.15-2
2.15.3 Methylation	2.15-4

2.15.4	Dealkylation	2.15-8
2.15.5	Literature Cited	2.15-9
2.15.6	Other Sources of Information	2.15-11
2.16 DIFFUSION COEFFICIENTS		
2.16.1	Introduction	2.16-1
2.16.2	Description of Property	2.16-1
2.16.3	Environmental Importance	2.16-5
2.16.4	Estimation Methods	2.16-6
2.16.5	Literature Cited	2.16-10
2.17 RADIOACTIVE PROCESSES AND PROPERTIES		
2.17.1	Creation of New Chemical Species	2.17-1
-	Single Transmutations	2.17-1
-	Multiple Sequential Decay	2.17-2
2.17.2	Recoil Transport	2.17-7
2.17.3	Special Properties of "Tracers"	2.17-13
2.17.4	Literature Cited	2.17-17

LIST OF TABLES

VAPOR PRESSURE

2.2-1	Analytical Expressions for ΔH_v and Integrated Forms of Equation 1	2.2-3
2.2-2	Values of a and b for Equation 6	2.2-5
2.2-3	Experimental vs. Calculated Vapor Pressures	2.2-7
2.2-4	Average Method Errors as a Function of Pressure	2.2-9

PHOTOLYSIS IN AIR

2.3-1	Conversion Factors	2.3-2
2.3-2	Estimated Solar Irradiance, $W(\lambda)$, in the Lower Atmosphere	2.3-3
2.3-3	Absorption Coefficients, $\epsilon(\lambda)$, at Various Wavelengths	2.3-7
2.3-4	Calculated Rates of Absorption of Solar Radiation by SO_2	2.3-7
2.3-5	Calculated Rates of Absorption of Solar Radiation by NO_2	2.3-7
2.3-6	Initial Concentrations and Rate Constants	2.3-10

GAS ADSORPTION ON SOLIDS

2.4-1	Adsorption of Gases on Charcoal	2.4-4
2.4-2	Experimental vs. Estimated Adsorption on Charcoal	2.4-8

ATMOSPHERIC DEPOSITION

2.5-1	Turner Classes	2.5-16
2.5-2	Dry Deposition Velocities for Particles	2.5-26
2.5-3	Dry Deposition Velocities for Gases	2.5-29

ACTIVITY COEFFICIENT

2.6-1	Summary of Methods for Estimating Activity Coefficients	2.6-11
2.6-2	Values of the Parameter "a" for Some Ions	2.6-13
2.6-3	Parameters β^0 , β^1 and c^ϕ for Some Inorganic Compounds	2.6-16
2.6-4	Average Values of the Parameter 'q' for Selected Electrolytes	2.6-19
2.6-5	Comparison of Pitzer <i>et al.</i> and Meissner <i>et al.</i> Methods for High Ionic Strength Solutions	2.6-21

ACID/BASE EQUILIBRIA

2.7-1	Equations Used to Calculate f_i , the Ratio of Concentrations of a Particular Species to the Total Present in Acid/Base Equilibria	2.7-5
2.7-2	Temperature Effects on Acid/Base Reaction Equilibria	2.7-10
2.7-3	Values of Acid Dissociation Constants for a Variety of Inorganic Species	2.7-12

POLYMERIZATION

2.8-1	Formation Quotients for Polynuclear Metal Hydrolysis Products at 25°C, Corrected to Zero Ionic Strength	2.8-3
2.8-2	Equilibrium Constants for the Formation of Polysulfide Ions	2.8-5
2.8-3	Free Energy of Formation Values for Species Involved in Aqueous Polysulfide Equilibria	2.8-8

COMPLEXATION

2.9-1	Logarithms of Complexation Equilibrium Constants (K) and Overall Stability Constants (β_2) for Metals with Commonly Occurring Ligands	2.9-4
2.9-2	Logarithms of Complexation Equilibrium Constants (K) for Metals with Sequestering Agents of Commercial Interest	2.9-5
2.9-3	Experimental Coordination Numbers of Various Ions in Aqueous Media	2.9-6
2.9-4	Experimental Values of Ion Pair Association Constants at 25°C	2.9-6
2.9-5	Initial Estimates of Parameter "a"	2.9-8
2.9-6	Outer-sphere Formation Constants Calculated by Eigen/Fuoss Equation	2.9-10
2.9-7	Values of Empirical Parameters E_A , C_A , and D_A for Cations	2.9-12
2.9-8	Values for Empirical Parameters for E_B , C_B , and D_B for Ligands	2.9-13

ELECTRON TRANSFER REACTIONS

2.10-1	Redox Half-Reactions Considered in WATEQF	2.10-20
2.10-2	Microbially Mediated Oxidation and Reduction Reactions	2.10-22
2.10-3	Redox Characteristics and Eh Measurements for Various Aqueous Environments	2.10-26
2.10-4	Redox Classification Scheme Proposed by Berner	2.10-29
2.10-5	Electrode Potentials of Redox Half-Reactions	2.10-37

SOLUBILITY AND PRECIPITATION EQUILIBRIA

2.11-1	Interfacial Energy Values for Oxides and Hydroxides in Aqueous Solutions	2.11-14
2.11-2	Standard State (25°C, 1 atm total pressure) Values of the Gibbs Free Energy of Formation (ΔG_f°) and the Enthalpy of Formation (ΔH_f°) for Selected Solids, Liquids, and Aqueous Ions	2.11-23
2.11-3	Solubilities in Water and Crystal Properties of Alkali Fluorides and Chlorides	2.11-25
2.11-4	Solubility and Lattice Energy Values for Some Solid-Phase Selenites and Selenates	2.11-27
2.11-5	Solubilities and Ionization Potentials Per Unit Radius of Some Alkaline-Earth Fluorides and Heavy-Metal Fluorides	2.11-37

ATTENUATION ON SOILS

2.12-1	Physical and Chemical Properties of Soil, Soil Solution, and Solute that Affect Attenuation	2.12-6
2.12-2	Relation of Sediment-Water Partition Coefficient of Trace Metals to the Organic Carbon in Sediments	2.12-7
2.12-3	Summary of Empirical Models of Sorption	2.12-16
2.12-4	Distribution Coefficients for Some Metals	2.12-18
2.12-5	Langmuir Constants for Some Metals	2.12-19
2.12-6	Freundlich Constants for Some Metals	2.12-22
2.12-7	Empirical Parameters for Calculating the Propagation Velocity of Cadmium by Equation 17	2.12-34
2.12-8	Empirical Parameters for Calculating the Propagation Velocity of Nickel by Equation 18	2.12-35
2.12-9	Empirical Parameters for Calculating the Propagation Velocity of Zinc by Equation 19	2.12-36

INTEGRATION AND ANALYSIS OF AQUEOUS PROCESSES

2.13-1	Methods and Steps in Determination of Chemical Speciation in an Aqueous System	2.13-7
2.13-2	Chemical Analysis of Water from a Screened Piezometer at a Coal Fly-Ash Disposal Site	2.13-10
2.13-3	Stability Constants of Aqueous Ion-Complexes	2.13-14

PHOTOLYSIS IN WATER

2.14-1	L _x Values for Latitude 40°N	2.14-5
2.14-2	Examples of Direct Photolysis Involving Inorganic or Organometallic Complexes	2.14-7
2.14-3	Data Needed to Evaluate the Rate of Direct Photolysis in Example 1	2.14-8

MICROBIAL TRANSFORMATIONS

2.15-1	Elements Affected by Microbial Transformation Processes	2.15-1
--------	---	--------

DIFFUSION COEFFICIENTS

2.16-1	Measured Diffusion Coefficients of Dilute Aqueous Electrolyte Solutions	2.16-3
2.16-2	Measured Diffusion Coefficients of Concentrated Aqueous Electrolyte Solutions at 25°C	2.16-4
2.16-3	Limiting Ionic Conductance in Water at 25°C	2.16-7
2.16-4	Water Viscosity as a Function of Temperature	2.16-8
2.16-5	Viscosity A and B Coefficients for Some Common Electrolytes	2.16-9

RADIOACTIVE PROCESSES AND PROPERTIES

2.17-1	Principal Naturally Occurring and Transuranic Alpha Emitters	2.17-8
2.17-2	Daughter-Nuclides of 238-Uranium	2.17-15

LIST OF FIGURES

PHOTOLYSIS IN AIR

2.3-1	Absorption Rates for Three Inorganic Pollutants	2.3-5
2.3-2	Concentration of Reacting Species vs. Time	2.3-11

GAS ADSORPTION ON SOLIDS

2.4-1	Adsorption Isotherms for SO ₂ on Silica Gel	2.4-3
2.4-2	Adsorption of Various Gases as a Function of their Normal Boiling Points	2.4-5
2.4-3	Amount Adsorbed vs. Saturated Vapor Pressures of Various Gases	2.4-6
2.4-4	Experimental vs. Calculated Adsorption Isotherms for CO ₂ on Charcoal	2.4-9

ATMOSPHERIC DEPOSITION

2.5-1	Schematic Representation of Processes Likely to Influence the Rate of Dry Deposition of Gases and Particles	2.5-2
2.5-2	Grossly Simplified View of Break-up of a Pollutant Plume by a Turbulent Eddy, Causing the Mixing of Pollutants with "Clean" Air	2.5-3
2.5-3	Diurnal Variation of Wind Profiles (Schematic) for the Same Day	2.5-7
2.5-4	Roughness Lengths, z_0 , for Various Terrain Types	2.5-9
2.5-5	Predicted Particulate Deposition Velocities at 1 Meter, K_{1-m} , for a Friction Velocity, u_* , of 30 cm/s and Various Particle Densities	2.5-10
2.5-6	Declination of the Sun over the Year	2.5-
2.5-7	$1/L$ as a Function of Turner Class and z_0	2.5-
2.5-8	Resistance Analogue of Dry Deposition of SO_2 to a Wheat Canopy	2.5-18
2.5-9	Wet Deposition Scavenging Sequence	2.5-18
2.5-10	Theoretical Mass Scavenging Coefficients Normalized to Rainfall Rate, Based on a Typical Frontal Raindrop Size Spectrum	2.5-20 2.5-24

ACTIVITY COEFFICIENT

2.6-1	Relationship of Reduced Activity Coefficient to Ionic Strength	2.5-25 2.6-18
-------	--	------------------

ACID/BASE EQUILIBRIA

2.7-1	Effect of pK Values on Calculated Distribution of Zn(II) Species with pH	2.7-7
2.7-2	Thermodynamic Cycle which Includes Aqueous Acid Dissociation	2.7-15

POLYMERIZATION

2.8-1	Distribution of Dissolved Sulfur Species in the System $\text{H}_2\text{S}-\text{S}_8$ (colloid)- H_2O as a Function of pH for $\Sigma[\text{S}] = 10^{-3}\text{ mol/kg}$ with 0.7 M NaCl at 298 K	2.8-7
2.8-2	Time Dependence of Polysulfide Formation in Aqueous Solution with an Initial Total S(II) Concentration of $3.0 \times 10^{-3} \text{ M}$, and $p(\text{O}_2) = 1 \text{ atm}$	2.8-10
2.8-3	Apparent First-order Rate Constants for the Hydrolytic Degradation of Sodium Polyphosphates at 60°C	2.8-12

ELECTRON TRANSFER REACTIONS

2.10-1	Summary of Elements That Can Undergo Redox Reactions and Their Valence States	2.10-2
2.10-2	Sample Redox Mechanism: Outer-Sphere Electron Transfer Reaction Between Fe^{+3} and V^{+2}	2.10-3
2.10-3	Sample Redox Mechanism: Inner-Sphere Electron Transfer Reaction Between Fe^{+3} and $\text{Co}(\text{NH}_3)_5\text{NTA}$	2.10-4
2.10-4	Sample Redox Mechanism: Inner-Sphere Electron Transfer Reaction Between Cr^{+2} and $\text{Co}(\text{NH}_3)_5\text{Cl}$	2.10-4
2.10-5	Theoretical Distribution of $\text{Fe}(\text{II})$ and $\text{Fe}(\text{III})$ at Various pe Values	2.10-8
2.10-6	Variation in Concentration of Arsenic(III) and Arsenic(V) with pe at pH Values of 6, 7 and 8	2.10-8
2.10-7	pe Versus pH Diagram for the Oxygen/Water Half Reaction at Various Partial Pressures of Oxygen	2.10-9
2.10-8	Eh Versus pH for the $\text{Fe}-\text{H}_2\text{O}$ System: Diagram for Step 5	2.10-14
2.10-9	Eh Versus pH for the $\text{Fe}-\text{H}_2\text{O}$ System: Diagram for Steps 7 and 9	2.10-16
2.10-10	Eh Versus pH for the $\text{Fe}-\text{H}_2\text{O}$ System: Diagram for Steps 11 to 13	2.10-18
2.10-11	Eh Versus pH for the $\text{Fe}-\text{H}_2\text{O}$ System: Final Diagram	2.10-19
2.10-12	Comparison of Measured and Computed Eh Versus pH in 30 Groundwater Systems	2.10-24
2.10-13	Approximate Relative Position of Eh and pH for Natural Environments	2.10-25
2.10-14	Eh Versus $\text{p}(\text{Sulfide})$ in Natural Sediment Environments and Polysulfide Solutions	2.10-28
2.10-15	Classification of Sediment Environments	2.10-28
2.10-16	Variation in Concentration with Depth for Various Redox Active Species in a Fjord	2.10-30

SOLUBILITY AND PRECIPITATION EQUILIBRIA

2.11-1	Solubilities of BaSeO_4 and PbSeO_4 as a Function of Temperature	2.11-10
2.11-2	Correlation of Interfacial Tension of Solids in Solution with their Solubility	2.11-13
2.11-3	Free Metal-ion Concentration in Equilibrium with Solid Oxides or Hydroxides	2.11-19
2.11-4	Solubilities of Metal Oxides and Hydroxides as a Function of the Solution pH	2.11-20
2.11-5	Solubilities as a Function of the Lattice Energy of Alkali Fluorides and Chlorides	2.11-26
2.11-6	Correlation Between the Square Root of Solubility and the Lattice Energy for Selected Selenites and Selenates	2.11-28

2.11-7	Solubilities of Metal Hydroxides Plotted Against the Cation Electronegativities at 25°C	2.11-29
2.11-8	Dissociation Constants of Singly and Doubly Charged Hydroxide Complexes in Aqueous Solutions at 25°C Plotted Against Cation Electronegativities	2.11-29
2.11-9	Solubilities of Divalent-Metal Arsenates, $M_3(AsO_4)_2$, in Water at Room Temperatures	2.11-31
2.11-10	Equilibrium Solubility Constants (25°C) for Divalent Metal Sulfates Plotted Against the Crystal Radii of the Cations for Sixfold Coordination	2.11-33
2.11-11	Solubility Products of Uranyl Arsenates as a Function of the Ionic Radius of the Other Cation	2.11-34
2.11-12	Solubilities of Divalent-Metal Fluorides Plotted Against the Quotient of Ionization Potential and Cation Radius	2.11-36

ATTENUATION ON SOILS

2.12-1	Relationship Between pK_a and pH at the Point of Maximum Sorption	2.12-8
2.12-2	Sorption of Cu(II) from Artificial River Water on Illite as a Function of pH	2.12-9
2.12-3	Effect of pH and Ionic Strength on Sorption of Lead and Cadmium	2.12-10
2.12-4	Adsorption Isotherm of Cu on $Fe(OH)_3$ in Seawater	2.12-24
2.12-5	Relative Mobility of Cation-Forming Elements in Soil	2.12-37
2.12-6	Relative Mobility of Anion-Forming Elements in Soil	2.12-37

PHOTOLYSIS IN WATER

2.14-1	Diagram of Passage of a Beam of Sunlight Through Atmosphere into Water Body	2.14-2
2.14-2	Variations in $\log Z_\lambda$ and $\log W_\lambda$ with Wavelength for 2 Seasons	2.14-4
2.14-3	Kinetic Data for Catalytically Oxidized Species	2.14-11

MICROBIAL TRANSFORMATIONS

2.15-1	Hypothetical Model for the Conversion of Mercury in the Aquatic Environment	2.15-4
2.15-2	The Biological Cycle for Mercury	2.15-5
2.15-3	The Biological Cycle for Arsenic	2.15-7

RADIOACTIVE PROCESSES AND PROPERTIES

2.17-1	Equilibria in Multiple Sequential Decay Processes	2.17-4
2.17-2	Growth of Activity of Individual Short-lived Decay Products in Constant Source of Radon Having Unit Activity	2.17-6
2.17-3	Radioactive Decay Without Equilibrium	2.17-7
2.17-4	Schematic Diagram of Radon Emanation Processes	2.17-11
2.17-5	Percentage Escape of 222-Radon from Soils and Minerals	2.17-12

2.1 INTRODUCTION

Chapter 2 provides detailed information on 15 physicochemical properties or processes that are the chief determinants of the speciation, fate and transport of inorganic chemicals in the environment. (The properties covered were listed in Table 1-2.) The chapter is, in a sense, the keystone of the whole report, as it deals with the major subject — the description of fundamental (environmentally important) properties and available estimation methods.

With information and tools such as those provided here, we expect that preliminary environmental assessments can be made in a timely fashion without the delays and expense of detailed literature searches, or of laboratory and field studies that may not represent the exact (or changing) environmental conditions at the problem site. The assessments described in this report require the user to identify the fundamental processes that may be acting on the pollutant(s) of interest (e.g., dissolution in water, complexation, photolytic degradation), and then use the guidance provided on those processes to obtain (usually) quantitative evaluations of their importance in the form of species abundance, extent of sorption, rates of photolysis, etc.

It should be emphasized that the numbers generated, especially estimates, can have high uncertainties associated with them. However, they should at least be adequate to bracket the probable environmental behavior of the pollutant so that reasonable upper or lower limits on mobility, concentrations, and bioavailability can be set and used in preliminary exposure and risk assessments.

A major focus of Chapter 2 is on equilibrium conditions. For example, there is significant coverage of acid/base, complexation, redox and solubility equilibria and of equilibrium sorption on soils. The distribution coefficients or equilibrium constants corresponding to these equilibria can, in several instances, be estimated with the information provided in this report. Section 2.13 describes how the simultaneous action of several such speciation equilibria can be evaluated to determine the ultimate distribution of species present in the system. For complex situations, the computerized speciation models described in Chapter 5 would be required. The kinetics of several of the most important speciation reactions (complexation, oxidation/reduction, and dissolution/precipitation) are covered in Chapter 3.

In addition to the above, Chapter 2 also covers other physicochemical processes that cannot be treated as equilibrium processes. Included, for example, are photolytic degradation (in both water and air), atmospheric deposition, diffusion of ions in water, and radioactive decay along with the (sometimes important) recoil of alpha-emitting radionuclides. Biologically mediated processes, especially the microbial methylation of heavy metals, are also covered in § 2.15. (A detailed discussion of uptake of inorganic pollutants by biota is provided in Chapter 4.)

Each section of Chapter 2 is somewhat different in content; however, most provide: (1) a description of the property, including its environmental importance, range of values, units, and sensitivity to environmental variables such as temperature and

ionic strength; (2) a description of the mathematical and/or graphical representation of the property; (3) tabulated data (e.g., complexation constants); (4) a description of selected available estimation methods; (5) worked-out examples of various calculations; and (6) a bibliography of literature cited.

2.2 VAPOR PRESSURE

2.2.1 Introduction

The evaporative loss of a chemical, volatilization, depends on its vapor pressure, heat of vaporization, and on environmental conditions that influence diffusion from a surface. Volatilization is an important source of material for airborne transport and may lead to its distribution over areas far removed from the point of release. Vapor pressure values provide indications of the tendency of pure materials to vaporize in an unperturbed situation. For example, knowledge of vapor pressure and solubility (or, more precisely, activity coefficient) permits calculations of evaporation rates of dissolved species from water using Henry's Law constants, as discussed by Thomas [16]. Similarly, estimation of the transport of species from soils into the air can be made if data on soil adsorption coefficients is available [17].

The vapor pressure of a chemical determines the maximum concentration of the chemical that can be present in the air phase. In evaporation from water, an important parameter is the ratio of the concentration in the atmosphere to that in water, Henry's Law constant, H, which may be defined as the product of vapor pressure P (atm) and activity coefficient γ (mole fraction). For low solubilities, H is approximated as the ratio of P to concentration C (mol/m^3). Compounds of high H tend to partition predominantly into the atmosphere. For low-H materials, partitioning is predominantly into the water, and the evaporation rate tends to be controlled by the concentration in the air-water boundary layer.

Whereas volatilization is an extremely important transport pathway for many organic chemicals, the majority of inorganic materials have relatively high solubilities (salts) or extremely low vapor pressures, so that volatilization is unlikely to play a significant role in their transport. Organometallics, however, exhibit more of the properties of organic materials (e.g., low water solubility and non-ionic character) and probably would be transported like them through the environment. These materials are of increasing commercial importance, particularly in the semiconductor industry, where they are used as precursors in the preparation of semiconductive thin films. They are also used as catalysts in a variety of manufacturing processes. The bioalkylation of heavy metals by bacteria under aerobic conditions has been recognized as a significant environmental source of organometallics such as $\text{Hg}(\text{CH}_3)_2$.

2.2.2 Experimental Determination

Vapor pressure can be expressed in a variety of units. The most common are mm Hg, atmospheres (1 atm = 760 mm Hg), and pascals, defined as newtons per square meter (N/m^2). One mm Hg is equal to 133.3 pascals.

The experimental method used to measure vapor pressure depends on the range involved. For values exceeding 1 mm Hg, the isoteniscope can be used; the procedure is described as ANSI/ASTM Method D-2879-75. [15]

For low-vapor-pressure materials (10^{-9} to 10^{-1} mm Hg) the gas saturation method is widely used. Details of the method are described by Ambrose [2] and in the *Federal Register* [18]. While the method is straightforward, meticulous experimental technique is required; the flow rates of carrier gas through the sample of interest must be measured with great care. Moreover, the equipment is expensive, and the collection of enough material for analysis can take days if the material has a very low vapor pressure.

Many inorganic solids have high boiling points and melting points; hence, their vapor pressures at environmental temperatures can range from 10^{-9} mm to 10^{-17} mm. If such a solid is a salt, its solubility in water would be high relative to that of organic materials, and volatilization would generally not be a significant transport mechanism. However, a substantial number of inorganic solids and liquids, such as MoF_6 , AsBr_3 , $\text{Fe}(\text{CO})_5$, and TiCl_4 , have appreciable vapor pressures at environmental temperatures.

2.2.3 Estimation Methods

All of the equations used to represent and estimate vapor pressure begin with the Clausius-Clapeyron equation:

$$\frac{d \ln P}{dT} = \frac{\Delta H_v}{RT^2} \quad (1)$$

where P = vapor pressure, mm Hg
 ΔH_v = heat of vaporization, cal/mol
 T = temperature, K
 R = gas constant = 1.987 cal/mol K

To obtain an equation relating vapor pressure to temperature, one can assume an analytical form for ΔH_v and integrate equation 1. Table 2.2-1 lists a few analytical expressions (eqs. 2-5) for ΔH_v and the resulting integrated forms of equation 1.

For any of these equations to be useful, the empirical constants must be related to some readily accessible molecular property. Quite often, this property is ΔH_{vb} , the heat of vaporization at the normal boiling point (T_b). Equation 2 is of limited use for liquids and solids, being valid only below 50°C; for gases, however, it may be used if a reasonable estimate of ΔH_v can be made. Mackay [10] has successfully used equation 3 to predict the vapor pressures of organic hydrocarbons and halogenated hydrocarbons, both liquid and solid, but the correlation is not applicable to other molecules (alcohols, ketones, etc.). Equation 4 is useful only in fitting data, as the number of constants is too great for predictive purposes. Equation 5 is the recommended predictive equation, as all of the parameters can be related to structural properties of materials.

TABLE 2.2-1

Analytical Expressions for ΔH_v and Integrated Forms of Equation 1

Analytical Form for ΔH_v	Integrated Form of Eq. 1	Eq.	Reference
$\Delta H_v = \text{constant } A$	$\ln P = \frac{1}{R} \left[-\frac{A}{T} + K \right]$	(2)	[1]
$\Delta H_v = H_{vb} [1 + B(1 - T_p)]$	$\ln P = \frac{\Delta H_{vb}}{R} \left[1 + B \left(\frac{1}{T_p} - 1 \right) + B \ln T_p \right]$	(3)	[10]
$\Delta H_v = C + DT + ET^2$	$\ln P = \frac{1}{R} \left[-\frac{C}{T} + D \ln T + ET + K \right]$	(4)	[12]
$\Delta H_v = \Delta H_{vb} (3 - 2 T_p)^m$	$\ln P \approx \frac{\Delta H_{vb}}{RT_b \Delta Z_b} \left[1 - \frac{(3 - 2 T_p)^m}{T_p} - 2m (3 - 2 T_p)^{m-1} \ln T_p \right]$	(5)	[6]

A, B, C, D, E = empirical constants**K = constant of integration, empirically determined** **ΔH_{vb} = heat of vaporization at the normal boiling point** **$T_p = T/T_b$** **T_b = normal boiling point** **$m = f(T_p)$ (See text below.)** **ΔZ_b = compressibility factor**

2.2.4 Recommended Methods

LIQUIDS AND SOLIDS ($T < T_b$)

Grain [7] has related the heat of vaporization at constant values of F and T to structural parameters for organic chemicals as follows:

$$\frac{\Delta H_v}{RT} = \ln RT - a[\exp(bP)] \ln P \quad (6)$$

where P is in atmospheres and 'exp' implies the exponential, base e. This relationship is also applicable to inorganic and organometallic materials. The values of a and b are related to the structure and polarity of the material, as shown in Table 2.2-2. When $T = T_b$ (the boiling point), $\ln P$ becomes zero, and all of the structural information contained in the values of a and b is lost; hence, a reference temperature and pressure must be chosen. A reference temperature $T_1 = 0.99 T_b$ was arbitrarily chosen. At this temperature the vapor pressure can vary from about 700 mm to 650 mm, depending upon the structure of the material; an intermediate value of 680 mm was used as a fixed reference pressure (P_1). Combining equations 5 and 6 and substituting $T_1 = 0.99 T_b$, one obtains for liquids:

$$\ln P_\ell = \frac{(\ln RT_1 - a \exp(bP_1) \ln P_1)}{\Delta Z_b} \left[\frac{1 - (3 - 2T_{\rho_1})^m}{T_{\rho_1}} - 2m(3 - 2T_{\rho_1})^{m-1} \ln T_{\rho_1} \right] + \ln P_1 \quad (7)$$

where	P_ℓ	= liquid vapor pressure (atm)
	ΔZ_b	= compressibility factor = 0.97
	T_1	= reference temperature (K) = $0.99 T_b$
	P_1	= reference pressure = 0.895 atm
	T_{ρ_1}	= T/T_1
	T	= system temperature (K)
	m	= $0.4133 - 0.2575 T_{\rho_1}$
	R	= gas constant = 82.05 cc/atm/K
	a,b	= adjustable parameters (see Table 2.2-2)

Equation 7 works equally well for any reduced boiling point datum (T_2, P_2) using the same values of a and b. Thus, if a normal boiling point is given, then $T_1 = 0.99 T_b$ and $P_1 = 680 \text{ mm} = 0.895 \text{ atm}$. If a reduced boiling point is given, T_2 and P_2 may be substituted directly for T_1 and P_1 .

For solids, another term is added to equation 7 such that

$$\ln P_s = \ln P_\ell + \ln \Delta P_s \quad (8)$$

TABLE 2.2-2
Values of a and b for Equation 6

	a	b
Liquids ($T < T_b$)		
Metallic elements	0.80	0
Nonmetallic elements, Inorganic Compounds	1.00	0
Organometallics	1.67	3.50
Gases ($T > T_b$)		
Elements	1.00	0
Other Gases	1.00	2.45 ^(a)

a. Default value. If the molar refraction, R_D , is known or can be estimated, then b is expressed as follows:

$$b = 4.9 - 0.37 R_D \quad (R_D < 13)$$

$$b = 0 \quad (R_D > 13)$$

The additional term, which results in a decrease of vapor pressure as compared to the liquid, is defined as

$$\ln \Delta P_s = \ln(RT_m)(1 - 1/T_{\rho m}) \quad (9)$$

where

- P_s = solid vapor pressure (atm)
- ΔP_s = decrease in solid vapor pressure vs that of supercooled liquid (atm)
- R = gas constant = 1.987 cal/mol K
- T_m = melting point (K)
- $T_{\rho m}$ = T/T_m

For solids, two cases must be considered if a reduced vapor pressure datum (i.e., reduced boiling point) is to be used as input. If $T_1 > T_m$, $\ln \Delta P_s$ is given by equation 9 and

$$\ln P_s = \ln P_\varrho [eq. 7] + \ln \Delta P_s [eq. 9] \quad (10)$$

If $T_1 < T_m$, $\ln \Delta P_s$ is given by

$$\ln \Delta P_s = \ln (RT_m) (T_m/T_1 - T_m/T) \quad (11)$$

and

$$\ln P_s = \ln P_\varrho [eq. 7] + \ln \Delta P_s [eq. 11] \quad (12)$$

GASES AND VAPORS ($T > T_b$)

When the chemical is a gas or vapor (i.e., when the temperature of interest is greater than the normal boiling point), equation 2 coupled with the procedure for estimating ΔH_v (eq. 6) is adequate for estimating vapor pressures above 1 atmosphere. The estimation equation becomes

$$\ln P_g = \frac{(\ln RT_1 - a \exp(bP_1) \ln P_1)}{\Delta Z_b} \left(1 - \frac{1}{T_{p1}}\right) + \ln P_1 \quad (13)$$

where the symbols have the same meaning as in equation 7. Values of a and b for gases were listed in Table 2.2-2.

If neither a reduced datum nor normal boiling point is available, a hypothetical boiling point must be estimated. (This is a frequent problem with organometallics, because they generally decompose or sublime before boiling.) Banks [3] gives a simple correlation between the normal boiling point and the molecular weight, M :

$$\log T_b = 3 - 4/\sqrt{M} \quad (14)$$

Equation 14 is reasonably good for materials with molecular weights greater than 150 and should be especially suited for high-molecular-weight organometallics. For example, it yields an estimated boiling point of 600 K for aluminum acetyl acetonate, which is only 2% above the measured value of 588 K [14].

2.2.5 Method Error

Table 2.2-3 compares estimated vapor pressures with literature values. Measured vapor pressures are listed when available. However, when data had to be extrapolated, care was taken to ascertain that the extrapolation was valid. (For example, extrapolated data on solids were used only if the extrapolation was from higher temperature measurements in the solid region, not the liquid region.) In some instances normal boiling points were estimated using equation 14; these are noted in the table. Table 2.2-4 gives average method errors as a function of vapor pressure range.

The errors listed in Table 2.2-4 were correlated with $\ln P$ in an attempt to determine the errors to be expected for a given pressure range. This was done separately for gases, liquids, and solids. The correlations were not particularly good, indicating essentially random scattering; however, they were useful in at least determining the average error to be expected.

TABLE 2.2-3
Experimental vs Calculated Vapor Pressures
(temperatures are deg. K and pressures are mm Hg)

Compound	T _b	T _m	T	T ₁	θ	P ₂	P _v (exper)	P _v (calc)	% Error	Ref
Inorganic Liquids*										
POCl ₃	378	—	—	—	—	—	40.0	38.8	- 3.0	[19]
MoF ₆	309	—	290	—	—	—	400.0	377.2	- 6.7	[19]
PSCl ₃	397	—	289	—	—	—	10.0	9.3	- 7.0	[19]
SiCl ₄	330	—	278	—	—	—	100.0	86.5	- 4.5	[19]
SiH ₂ I ₂	423	—	291	—	—	—	10.0	3.2	- 67.9	[19]
SiHBr ₃	385	—	303	—	—	—	40.0	33.9	- 15.2	[19]
SnCl ₄	386	—	283	—	—	—	10.0	10.6	+ 6.0	[19]
TiCl ₄	409	—	294	—	—	—	10.0	7.3	- 26.8	[19]
BB ₃	365	—	287	—	—	—	40.0	33.9	- 15.2	[19]
VOCl ₃	400	—	285	—	—	—	10.0	6.3	- 37.0	[19]
SOCl ₂	348	—	294	—	—	—	100.0	88.3	- 1.7	[19]
S ₂ Cl ₂	411	—	301	—	—	—	10.0	10.1	+ 1.0	[19]
CrO ₂ Cl ₂	390	—	287	—	—	—	10.0	11.3	+ 13.0	[19]
PCl ₃	347	—	275	—	—	—	40.0	38.9	- 2.8	[19]
SbCl ₅	—	—	296	387	100	—	1.0	1.4	+ 40.0	[19]
Br ₂	331	—	282	—	—	—	100.0	112.0	+ 12.0	[19]
CSSe	358	—	301	—	—	—	100.0	90.6	- 9.4	[19]
Hg	—	—	293	399	1.0	1.2x10 ⁻³	1.6x10 ⁻³	+ 29.6	[19]	
CCl ₄ NO ₂	385	—	281	—	—	—	10.0	9.7	- 3.0	[19]
Fe(CO) ₅	382	—	278	—	—	—	10.0	9.2	- 8.0	[19]
SOBr ₂	413	—	304	—	—	—	10.0	11.3	+ 13.0	[19]

(Continued)

TABLE 2.2-3 (Continued)

Compound	T _b	T _m	T	T ₁	Θ	P ₁	P _v (exper)	P _v (calc)	% Error	Ref
Inorganic Solids^a										
AsBr ₃	529	371	354	—	—	—	1.0	1.2	+ 20.0	[19]
NH ₄ N ₃	433	302	407 ^b	760	1.0	1.0	0	0	0	[19]
NH ₄ CO ₂ NH ₂	333 ^b	300	331	760	100.0	125.8	+ 28.8	[19]		
SbBr ₃	370	323	403	4.2	1.9x10 ⁻²	2.2x10 ⁻²	+ 16.8	[8]		
TaCl ₅	494	288	473	193	3.8x10 ⁻⁴	6.9x10 ⁻⁴	+ 80.6	[5]		
F ₃ B ₂ N ₃ H ₃	385 ^b	293	385 ^b	760	1.6	2.5	+ 54.2	[9]		
Cl ₃ B ₃ N ₃ H ₃	458	357	302	—	2.9x10 ⁻¹	4.2x10 ⁻¹	+ 44.0	[9]		
Organometallics^c										
Ge(CH ₃) ₄	320	—	301	—	—	389.1	380	—	- 2.3	[13]
Ge(C ₂ H ₅) ₄	439	—	337	—	—	21.4	21.4	0	0	[13]
Ge(C ₃ H ₇) ₄	439	—	—	—	—	2.0	2.3	+ 17.0	[13]	
Ge(C ₅ H ₁₁) ₄	—	—	390	498	676	19.5	23.5	+ 20.0	[13]	
Fe(Ac-Ac) ₃	613 (est) ^d	452	374	—	—	2.0x10 ⁻³	4.4x10 ⁻³	+119.0	[14]	
Al(Ac-Ac) ₃	588	462	389	—	—	4.1x10 ⁻²	3.1x10 ⁻²	- 23.8	[14]	
Zn(Ac-Ac) ₂	567 (est)	411	338	—	—	4.0x10 ⁻³	2.2x10 ⁻³	- 45.9	[14]	
U(thd) ₄	720 (est)	498	372	—	—	6.8x10 ⁻⁶	5.3x10 ⁻⁶	- 22.8	[4]	
Th(Ac-Ac) ₄	679 (est)	445	373	—	—	3.2x10 ⁻⁴	6.9x10 ⁻⁵	- 78.6	[11]	

a. At environmental temperatures and pressures

b. Sublimes

c. Ac-Ac = acetylacetone; thd = tetrakis (2,2,6,6-tetramethylheptane-3,5-dionato)

d. est = estimated via equation 14

TABLE 2.2-4
Average Method Errors as a Function of Pressure

Pressure Range	No. Cpd's	Average Error (%)
1 atm-40 atm	2	5
>10 mm - 760 mm	13	8
>1 mm - 10 mm	12	20
>10 ⁻³ mm - 1 mm	6	40
10 ⁻⁶ mm - 10 ⁻³ mm	3	60

2.2.6 Sample Calculations

Example 1 Estimate the vapor pressure of POCl_3 at 27°C. The normal boiling point is 105°C.

$$\begin{aligned} T_b &= 105 + 273 = 378 \text{ K} \\ T &= 27 + 273 = 300 \text{ K} \end{aligned}$$

From Table 2.2-2, $a = 1.0$, $b = 0$

$$\begin{aligned} T_1 &= 0.99 \times T_b = 374.2 \text{ K} \\ P_1 &= 680 \text{ mm} = 0.895 \text{ atm} \end{aligned}$$

Substituting in eq. 6 gives:

$$\begin{aligned} \frac{\Delta H_v}{RT_1} &= \ln RT_1 - ae^{bP_1} \ln P_1 \\ &= \ln (82.05 \times 374.2) - 1 \times e^{0 \times 0.895} \times \ln (0.895) \\ &= 10.33 + 0.11 = 10.44 \\ T_{p1} &= T/T_1 = 0.802 \\ m &= 0.4133 - 0.2575 T_{p1} = 0.207 \\ (3 - 2T_{p1}) &= 1.396 \end{aligned}$$

From eq. 7:

$$\begin{aligned} \ln P &= \frac{10.44}{0.97} \left[1 - \frac{(1.396)^{0.207}}{0.802} - 2(0.207) \times (1.396)^{-0.793} \ln (0.802) \right] + \ln (0.895) \\ &= -2.973 \end{aligned}$$

$$P = \text{antiln} (-2.973) = 0.0512 \text{ atm (38.9 mm)}$$

Since the literature value is 40 mm, the error is -2.8%.

Example 2 Estimate the vapor pressure of solid SbBr₃ at 323 K, given that P₂ = 4.2 mm at 403 K and that T_m = 370 K.

$$P_2 = 4.2/760 = 5.53 \times 10^{-3} \text{ atm}$$

From Table 2.2-2: a = 1.0, b = 0

$$\begin{aligned}\frac{\Delta H_{v2}}{RT_2} &= \ln RT_2 - a e^{bP_2} \ln P_2 \\ &= \ln (82.05 \times 403) - \ln (5.53 \times 10^{-3}) \\ &= 10.41 + 5.20 = 15.61 \\ T_{p2} &= 323/403 = 0.801 \\ m &= 0.4133 - 0.2575(0.801) = 0.207 \\ (3 - 2T_{p2}) &= 1.397\end{aligned}$$

From eq. 7:

$$\begin{aligned}\ln P_2 &= \frac{15.61}{0.97} \left[1 - \frac{(1.397)^{0.207}}{0.801} - 2(0.207) \times (1.397)^{-0.793} \ln(0.801) \right] + \ln(5.53 \times 10^{-3}) \\ &= -4.29 - 5.20 = -9.49\end{aligned}$$

As SbBr₃ is a solid at the temperature of interest and T₂ > T_m, we must use eq. 9 and add the result to ln P₂:

$$T_{pm} = 323/370 = 0.873$$

$$\begin{aligned}\text{From eq. 9: } \ln \Delta P_s &= \ln (1.987 \times 370) (1 - 1/0.873) \\ &= 6.60 (-0.146) = -0.960\end{aligned}$$

$$\text{From eq. 8: } \ln P_s = -9.49 - 0.960 = -10.450$$

$$\begin{aligned}P_s &= \text{antiln}(-10.454) \\ &= 2.89 \times 10^{-6} \text{ atm} \\ &= 2.20 \times 10^{-2} \text{ mm}\end{aligned}$$

Since the literature value is 1.9 × 10⁻² mm, the error is +16%

Example 3 Estimate the vapor pressure of NH₃ at 352 K (79°C). The normal boiling point is 239 K.

$$\begin{aligned}T_1 &= 0.99 T_b = 237 \text{ K} \\ P_1 &= 0.895 \text{ atm} \\ T_{p1} &= 352/237 = 1.49\end{aligned}$$

The molar refraction of NH₃ is 5.54. From Table 2.2-2, a = 1 and b = 4.9 - 0.37(5.54) = 2.84.

Substituting in eq. 13:

$$\ln P_g = \frac{\ln(82.05 \times 237) - 1 \exp(2.84 \times 0.895) \ln(0.895)}{0.97} \times (1 - 1/1.49) + \ln(0.895)$$

$$= 3.694$$

$$P_g = \text{antiln } 3.694 = 40.2 \text{ atm}$$

The literature value is 40 atm, indicating an error of 0.5%.

2.2.7 Literature Cited

1. Adam, N.K., *Physical Chemistry*, Oxford Univ. Press, London, 234 (1958) or any other standard text on physical chemistry.
2. Ambrose, D., "Vapor Pressures," *Chemical Thermodynamics*, 1, 218 (1973).
3. Banks, W.H., "Considerations of a Vapour Pressure Temperature Equation, and Their Relation to Burnop's Boiling Point Function," *J. Chem. Soc.*, 1939, 292 (1939).
4. Belford, R. and E. Huss, "The Vapor Pressure of Tetrakis (2,2,6,6-tetramethyl-heptane-3,5, dianato) Uranium," *J. Chem. Eng. Data*, 22, 239 (1977).
5. Brink, T.M. and F. Stevenson, "Vapor Pressure of Tantalum Pentachloride," *J. Chem. Eng. Data*, 17, 143 (1972).
6. Grain, C.F., "Vapor Pressure" in *Handbook of Chemical Property Estimation Methods*, W.J. Lyman, W.F. Reehl and D.H. Rosenblatt (eds.), McGraw-Hill Book Co., New York (1982).
7. Grain, C.F. and W.J. Lyman, "Enhancements to CHEMEST Program: Vapor Pressure," Interim Report, EPA Contract No. 68-01-6271 (October 7, 1983).
8. Gray, G.A. and R. Sime, "Vapor Pressure of Antimony (III) Bromide," *J. Chem. Eng. Data*, 17, 176 (1972).
9. Laubengayer, A.W. and C. Scaife, "The Vapor Pressures and Some Thermodynamic Functions of B-Trifluoro, B-Trichloro, and B-Tribromoborazine," *J. Chem. Eng. Data*, 11, 172 (1966).
10. Mackay, D., A. Bobra, D. Chen, and W. Shiu, "Vapor Pressure Correlations for Low Volatility Environmental Chemicals," *Environ. Sci. Technol.*, 16, 645 (1982).
11. MacKenzie Chemical Works, "Metal Acetylacetones," Technical Data Bulletin, Central Islip, NY (undated).
12. Miller, D.G., "Estimating Vapor Pressures — A Comparison of Equations," *Ind. Eng. Chem.*, 56, 46 (March 1964).
13. Mogul, P.H., M. Hochberg, R. Michiel, G. Nestei, B. Warmsley and S. Coren, "Physical Properties of Tetra-n-alkylgermanes (C₁ - C₆)," *J. Chem. Eng. Data*, 19, 4 (1974).

14. Sachindis, J. and J.O. Hill, "A Re-evaluation of the Enthalpy of Sublimation of Some Metal Acetylacetone Complexes," *Thermochim. Acta*, **35**, 59 (1980).
15. "Standard Test Method for Vapor Pressure-Temperature Relationship and Initial Decomposition Temperature of Liquids by Isoteniscope," *Annual Book of ASTM Standards*, Sec. 5, V 5.02, 747 (1983).
16. Thomas, R.G., "Volatilization from Soil" in *Handbook of Chemical Property Estimation Methods*, W.J. Lyman, W.F. Reehl and D.H. Rosenblatt (eds.), McGraw-Hill Book Co., New York (1982).
17. Thomas, R.G., "Volatilization from Water," *ibid.*
18. "Vapor Pressure," *Fed. Reg.*, **145**, 77345 (Nov. 21, 1980).
19. Weast, R.C. (ed.), *CRC Handbook of Chemistry and Physics*, 58th ed., CRC Press, Inc., Boca Raton, FL, D-182 (1977-1978).

2.3 PHOTOLYSIS IN AIR

2.3.1 Introduction

This section provides an overall view of some of the complexities associated with the formation or transformation of atmospheric pollutants by photolysis. The evaluation of inorganic gaseous species with respect to their potential photolysis rate is explained, and reaction mechanisms leading to the generation of additional pollutants are qualitatively described.

It has long been recognized that certain air pollution smogs are caused by photochemical reactions among pollutants from automobile exhaust [9]. The direct photolysis of NO_2 is a major source of other oxidants in the atmosphere [6, 7]. "Direct photolysis" refers to the process in which a molecule absorbs solar radiation and is either dissociated or is promoted to an excited electronic state amenable to further reactions with other species present in the atmosphere. "Sensitized photolysis," in which energy is transferred from some other species in the atmosphere, is not known as an important source of pollutants.

While the direct photolysis of NO_2 is one of the most important photolytic sources of pollutants, other inorganic species subject to direct photolysis include SO_2 , O_3 , H_2O_2 and HONO . We shall attempt to assess the relative importance of these additional species as sources of pollutant molecules.

Photochemical reactions begin with the absorption of light radiation. The immediate product is an excited state of the absorbing molecule, with energy in excess of the normal state equal to the energy of the absorbed radiation. Light that produces only rotational or vibrational changes is chemically inactive in the atmosphere; only when the light absorbed produces electronic transitions leading to dissociation will a photochemical reaction occur. As most vibrational and rotational spectra lie in the infrared and most electronic spectra in the visible and ultraviolet, it is the latter regions which are of photochemical importance.

A photochemical primary process may yield stable molecules directly, or it may yield unstable products that undergo secondary reactions. In many instances the primary process consists of dissociation of the absorbing molecule into free radicals or atoms, which then take part in secondary reactions.

For environmental assessment purposes, the following information is required with respect to the photochemical process: (1) an understanding of the intensity and spectral distribution of the incident radiation, (2) the absorption characteristics of the molecular species, (3) the kinetics of the primary and secondary processes, and (4) transport mechanisms of products of the primary and secondary processes.

We have restricted our discussion to photolysis in the lower atmosphere. This is not meant to diminish the importance of upper-atmosphere photolysis, particularly as it relates to the preservation of the ozone protective layer, but simply to reflect the general concern with respect to air quality in the lower atmosphere.

2.3.2 Units for Rate Constants and Concentrations

Current practice expresses incident solar radiation in terms of photons $\cdot \text{cm}^{-2} \cdot \text{s}^{-1}$. (10 nm) $^{-1}$. The absorption coefficients of gaseous species are generally expressed in terms of liters $\cdot \text{mole}^{-1} \cdot \text{cm}^{-1}$. In studies of polluted air, it has become customary to express concentrations in terms of ppm (parts per million) or sometimes pphm (parts per hundred million). Table 2.3-1 lists factors for converting air concentrations ($\text{moles} \cdot \text{l}^{-1}$) and rate constants.

TABLE 2.3-1

Conversion Factors
(Relative to air at 1 atm, 25°C)

CONCENTRATIONS:

$$\text{mole} \cdot \text{l}^{-1} \times 2.445 \times 10^7 = \text{ppm}$$

$$\text{mole} \cdot \text{l}^{-1} \times 2.445 \times 10^9 = \text{pphm}$$

RATE CONSTANTS

Bimolecular

$$1 \cdot \text{mole}^{-1} \cdot \text{s}^{-1} \times 2.45 \times 10^{-6} = \text{ppm}^{-1} \cdot \text{min}^{-1}$$

$$1 \cdot \text{mole}^{-1} \cdot \text{s}^{-1} \times 1.47 \times 10^{-6} = \text{pphm}^{-1} \cdot \text{hr}^{-1}$$

Termolecular

$$1^2 \cdot \text{mole}^{-2} \cdot \text{s}^{-1} \times 1.005 \times 10^{-13} = \text{ppm}^{-2} \cdot \text{min}^{-1}$$

$$1^2 \cdot \text{mole}^{-2} \cdot \text{s}^{-1} \times 6.03 \times 10^{-16} = \text{pphm}^{-2} \cdot \text{hr}^{-1}$$

2.3.3 Solar Irradiance and Absorption Rates

The lower atmosphere receives solar radiation not only directly from the sun but also from the sky via scattering, and in the ultraviolet the latter may be the more important of the two. Estimating the intensity of incident solar radiation involves consideration of several factors, including the spectral irradiance outside the atmosphere, the solar zenith angle, the nature and amount of scattering, diffusion and absorption of radiation by the atmosphere, and the albedo of the earth's surface. Leighton [9] has discussed these factors at length; Table 2.3-2 (from Leighton's book) lists estimated values of solar irradiance at midday, $W(\lambda)$, in the lower atmosphere after all of the factors listed above have been accounted for. An updated and presumably more accurate listing is given by Dermerjian *et al.* [3]. (See § 2.14.3 for additional discussion of solar irradiance.)

TABLE 2.3-2

Estimated Solar Irradiance, $W(\lambda)$, in the Lower Atmosphere^a
 $(\times 10^{15} \text{ photon} \cdot \text{cm}^{-2} \cdot \text{s}^{-1} \cdot (10 \text{ nm})^{-1})$

Wavelength $\lambda(\text{nm})$	Solar Zenith Angle, Z				
	0°	20°	40°	60°	80°
290	0.0014	0.0009	0.0002	—	—
300	0.12	0.10	0.05	0.01	—
310	0.65	0.80	0.43	0.13	0.01
320	1.17	1.10	0.91	0.53	0.10
330	1.83	1.75	1.48	0.98	0.26
340	1.88	1.82	1.55	1.05	0.32
350	2.06	1.98	1.72	1.18	0.36
360	2.10	2.02	1.77	1.24	0.38
370	2.48	2.40	2.11	1.50	0.46
380	2.36	2.28	2.02	1.45	0.44
390	2.20	2.13	1.90	1.38	0.42
400	3.10	3.01	2.70	2.00	0.62
410	4.01	3.90	3.51	2.63	0.82
420	4.06	3.95	3.57	2.71	0.86
430	3.88	3.76	3.42	2.62	0.85
440	4.50	4.39	4.02	3.11	1.03
450	5.00	4.88	4.48	3.51	1.19
460	5.00	4.89	4.50	3.58	1.22
470	5.13	5.02	4.64	3.68	1.30
480	5.20	5.11	4.72	3.79	1.38
490	4.88	4.78	4.44	3.59	1.33
500	4.95	4.85	4.51	3.68	1.40
525	5.14	5.05	4.73	3.91	1.56
550	5.30	5.21	4.90	4.09	1.69
575	5.32	5.23	4.92	4.44	1.75
600	5.32	5.24	4.95	4.21	1.86
625	5.27	5.19	4.94	4.25	2.01
650	5.22	5.16	4.92	4.30	2.16
675	5.16	5.10	4.89	4.32	2.29
700	5.05	5.00	4.82	4.29	2.38
750	4.80	4.75	4.59	4.10	2.47
800	4.55	4.51	4.37	3.98	2.47

Source: Leighton [9]. (Copyright 1961, Academic Press. Reprinted with permission.)

Any discussion of a photochemical primary process must begin with a determination of the species that exhibit absorption in the region of interest. Of the inorganic species present in the lower atmosphere, just oxygen, ozone, nitrogen dioxide, sulfur dioxide, nitric and nitrous acids and hydrogen peroxide absorb to any measurable degree. To date, these species are the only ones that have been of any interest in the determination of photolysis mechanisms for inorganics. The organic gases or vapors that are of some importance include aldehydes, ketones, peroxides and various organic nitrogen compounds.

To assess the photodegradation potential of a species, we must have some means of determining its average absorption rate. The usual starting point is the Lambert-Beer law: if a surface layer of height h contains an absorbing substance at concentration c , with an absorption coefficient ϵ , then the average rate of absorption per unit value for direct and sky radiation is

$$I_a(\lambda) = \frac{I_d(\lambda) (1 - 10^{-\epsilon(\lambda)c} h \sec Z) + I_s(\lambda) (1 - 10^{-\epsilon(\lambda)c} i h)}{h} \quad (1)$$

where	$I_a(\lambda)$	=	average absorption rate ($\text{photons} \cdot \text{cm}^{-2} \cdot \text{s}^{-1}$)
	$I_d(\lambda)$	=	direct irradiance ($\text{photons} \cdot \text{cm}^{-2} \cdot \text{s}^{-1}$)
	$I_s(\lambda)$	=	sky radiance ($\text{photons} \cdot \text{cm}^{-2} \cdot \text{s}^{-1}$)
	$\epsilon(\lambda)$	=	molar absorptivity ($\text{l} \cdot \text{mol}^{-1} \cdot \text{cm}^{-1}$)
	c	=	concentration of absorbing species ($\text{mol} \cdot \text{l}^{-1}$)
	h	=	height of absorbing layer (cm)
	Z	=	solar zenith angle
	i	=	constant = 2

As c is low (typically $10^{-14} \text{ mol} \cdot \text{l}^{-1}$), equation 1 is reduced to

$$I_a(\lambda) = 2.303 c \epsilon(\lambda) [I_d(\lambda) \sec Z + I_s(\lambda) i] \quad (2)$$

The specific rate constant, $k_a(\lambda)$, is then given by

$$k_a(\lambda) = \frac{I_a(\lambda)}{jc} \quad (3)$$

where j is a conversion factor for concentration in $\text{l} \cdot \text{mol}^{-1}$, numerically equal to Avogadro's number $\times 10^{-3} = 6.023 \times 10^{20}$.

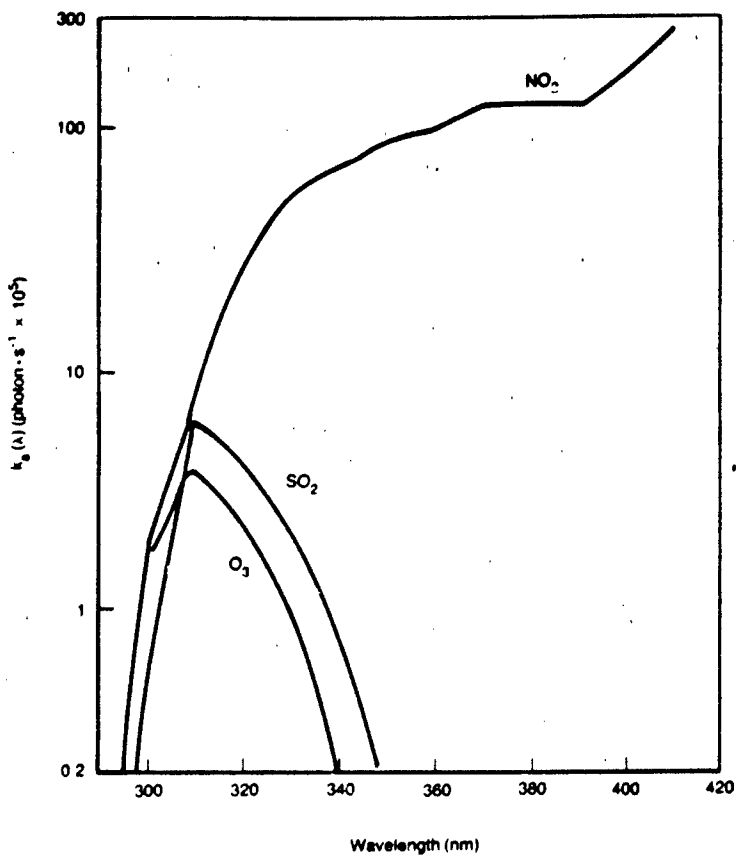
The average absorption rate $I_a(\lambda)$ is related to $W(\lambda)$, the total solar irradiance in the lower atmosphere (Table 2.3-2), through the relationship

$$I_a(\lambda) = 2.303 \epsilon(\lambda)c W(\lambda) \quad (4)$$

Hence,

$$k_a(\lambda) = \frac{2.303 \epsilon(\lambda) W(\lambda)}{j} \quad (5)$$

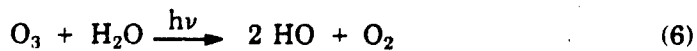
Thus, by multiplying the extinction coefficient by the estimated solar irradiance at each wavelength, we obtain the rate constant $k_a(\lambda)$ of a species as a function of λ . Figure 2.3-1 shows absorption rate constants calculated from equation 5 for three of the absorbers mentioned earlier. Clearly, NO_2 is the most significant absorber of the three and a major inorganic species to consider with respect to primary photochemical processes.



Source: Leighton [9]. (Copyright 1961, Academic Press. Reprinted with permission.)

FIGURE 2.3-1 Absorption Rates for Three Inorganic Pollutants

Formation and reaction of hydroxy radicals are also important in oxidant formation processes. The species that are photolyzed to yield HO radicals are O_3 and H_2O_2 , through the following reactions:



The absorption of solar radiation in the lower atmosphere by O_3 and H_2O_2 is low, but rates of HO formation can be significant if the initial concentrations are high enough. We shall now examine how these rates can be estimated.

The efficiency of any primary photochemical process is expressed in terms of the quantum yield, ϕ , which may be defined as the ratio of the number of molecules reacting through a primary process to the number of quanta absorbed. The maximum possible value for ϕ is unity, as the number of molecules reacting cannot exceed the number of quanta absorbed. The rate of product formation is then given by:

$$\text{Rate} = \phi c \sum_{\lambda} k_a(\lambda) \quad (8)$$

Before considering possible mechanisms for a photochemical reaction, one can assess the probability that a species will undergo photolysis and the relative importance of this process as a source of pollution. Examples 1 and 2 below show how this is done. The minimum information required is (1) the free energy of bond formation or dissociation, (2) the light absorption characteristics of the material, and (3) its approximate concentration. A useful relationship between the wavelength λ (nm) and the energy E (kcal mol^{-1}) of a photon that may cause bond dissociation is $E \cdot \lambda = 2.9 \times 10^4$.

Example 1 What is the likelihood that photolysis of sulfur dioxide would generate products that could enhance the parent compound's pollution potential?

The bond dissociation energy for the reaction $\text{SO}_2 \rightarrow \text{SO} + \text{O}$ is $-135 \text{ kcal} \cdot \text{mol}^{-1}$ [9]. The wavelength equivalent of this energy is 218 nm. As this is considerably shorter than ultraviolet wavelengths, we can immediately conclude that sunlight will not cause bond dissociation of SO_2 . However, it might generate excited states that could undergo secondary reactions. The rate of absorption of solar radiation can be estimated from equation 5 using data from Tables 2.3-2 and -3; Table 2.3-4 shows the results of this calculation for various wavelengths.

The rate of product formation is equal to $\phi k_a(\lambda)c$, where ϕ is the quantum yield for the primary photochemical process. For SO_2 , ϕ has been estimated to range from 1.0×10^{-2} to 0.3 [9]. Based on the average value of $k_a(\lambda)$ from Table 2.3-4 ($1.7 \times 10^{-4} \text{ photon} \cdot \text{s}^{-1}$) and an assumed concentration (c) of 1 ppm, the approximate rate of product formation is found to be 6.0×10^{-3} to $0.2 \text{ ppm} \cdot \text{hr}^{-1}$. Coupled with the knowledge that photolysis cannot produce bond dissociation of SO_2 but only excited states that could be quenched, the calculated rate indicates that photolysis of SO_2 plays a minor role in the generation of other pollutants.

Example 2 Is the photolysis of NO_2 a significant source of oxidizing pollutants?

The dissociation energy of NO_2 is $72 \text{ kcal} \cdot \text{mol}^{-1}$ [9]. This is equivalent to light with a wavelength of 400 nm, which is well within the portion of solar spectrum that penetrates the atmosphere. Estimates of the rate of absorption for NO_2 in the range of 290-400 nm are listed in Table 2.3-5. The average $k_a(\lambda)$ is $5.0 \times 10^{-3} \text{ photon} \cdot \text{s}^{-1}$, which is 29 times that of SO_2 ; this, plus the fact that the photolysis of NO_2 causes its dissociation into active products, suggests that the process could be a significant source of pollutants. The

TABLE 2.3-3

Absorption Coefficients, $\epsilon(\lambda)$, at Various Wavelengths
($l \cdot mol^{-1} \cdot cm^{-1}$)

$\lambda(nm)$	$\epsilon(\lambda)$			
	SO_2	NO_2	O_3	H_2O_2
290	156.0	20.0	384.0	3.9
300	121.0	37.0	102.0	2.6
310	46.0	57.0	28.0	1.8
320	13.0	78.0	7.4	1.3
330	3.7	98.0	0.5	1.0
340	1.1	119.0		0.8
350		136.0		0.5
360		149.0		0.3
370		158.0		0.2
380		163.0		
390		167.0		
400		171.0		

Bond Dissociation Energy (kcal/mol)	135	72	25 ^a	51 ^b
-------------------------------------	-----	----	-----------------	-----------------

a. Third body required. For comparison, value for O_2 is 119 kcal/mol [14].

b. For O-O bond in H_2O_2 [14].

Source: Leighton [9]

TABLE 2.3-4

Calculated Rates of Absorption of Solar Radiation by SO_2
(at $Z = 40^\circ$)

$\lambda(nm)$	$k_a(\lambda)$ (photon $\cdot s^{-1}$)
290	1.2×10^{-7}
300	2.3×10^{-5}
310	7.6×10^{-5}
320	4.6×10^{-5}
330	2.1×10^{-5}
340	6.4×10^{-6}

$$k_a = \sum k_a(\lambda) = 1.7 \times 10^{-4} \text{ photon} \cdot s^{-1}$$

TABLE 2.3-5

Calculated Rates of Absorption of Solar Radiation by NO_2
(at $Z = 40^\circ$)

$\lambda(nm)$	$k_a(\lambda)$ (photon $\cdot s^{-1}$)
290	2.0×10^{-8}
320	2.7×10^{-4}
340	7.1×10^{-4}
360	8.9×10^{-4}
380	1.3×10^{-3}
400	1.8×10^{-3}

$$k_a = \sum k_a(\lambda) = 5.0 \times 10^{-3} \text{ photon} \cdot s^{-1}$$

quantum yield has been estimated at $\phi = 0.9$ [9]; using the same value of c as in Example 1,

$$\begin{aligned}\text{Rate of product formation} &= \phi k_a(\lambda)c \\ &= (0.9)(5.0 \times 10^{-3})(1) \\ &= 4.5 \times 10^{-3} \text{ ppm} \cdot \text{s}^{-1} \\ &= 16.2 \text{ ppm} \cdot \text{hr}^{-1}\end{aligned}$$

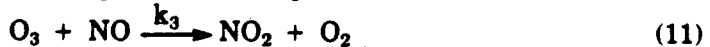
Similar reasoning, assuming $\phi = 0.9$ and the same conditions as in the preceding examples, leads to estimating product yields of $0.7 \text{ ppm} \cdot \text{hr}^{-1}$ for O_3 and $0.2 \text{ ppm} \cdot \text{hr}^{-1}$ for H_2O_2 .

We thus see that some reasonable conclusions can be drawn as to whether a given material should be considered a possible source of pollutants through a primary photochemical process. These conclusions were based on some elementary considerations of the energy requirements for dissociation by light and the absorption characteristics of the species.

2.3.4 Photochemical Mechanisms

The oxidant found in the largest quantity as a result of photolysis is ozone. Although oxygen is photolyzed in the upper atmosphere, the short wavelengths required do not reach the lower atmosphere. Therefore, photochemical generation of the observed amounts of ozone [7] must take place by some process other than direct photolysis of oxygen.

Comparison of the absorption characteristics of the major inorganic pollutants (Figure 2.3-1) indicates that NO_2 is the most efficient absorber of the ultraviolet portion of sunlight that reaches the lower atmosphere. The absorption of UV light (300-400 nm) initiates the following reactions:



In equation 10, M is a third body (air). k_1 , k_2 and k_3 are reaction rate constants, with $k_1 = \phi k_a$.

where ϕ = quantum yield
 k_a = average rate of absorption = $\sum k_a(\lambda)$

The rate equations resulting from these reactions are:

$$\frac{d(\text{NO}_2)}{dt} = k_3[\text{O}_3][\text{NO}] - \phi k_a[\text{NO}_2] \quad (12)$$

$$-\frac{d(\text{NO})}{dt} = \phi k_a[\text{NO}_2] - k_3[\text{O}_3][\text{NO}] \quad (13)$$

$$\frac{d(O_3)}{dt} = k_2[O][O_2][G] - k_3[O_3][NO] \quad (14)$$

If we assume the steady state for these rates, the ozone and oxygen atom concentrations are given by

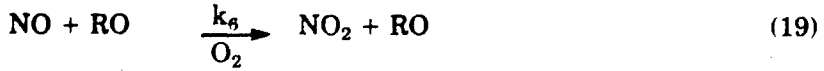
$$[O_3] = \frac{\phi k_a}{k_3} \frac{[NO_2]}{[NO]} \quad (15)$$

$$[O] = \frac{\phi k_a}{k_2} \frac{[NO_2]}{[O_2][G]} \quad (16)$$

The NO_2 photolytic cycle explains the initial formation of ozone in polluted atmospheres; however, it cannot account for the relatively high concentrations of O_3 that have been measured. At steady state, O_3 and NO would be formed and consumed in equal quantities, and there would be no O_3 accumulation. Laboratory data and atmospheric measurements indicate that hydrocarbons are involved [6, 7]. Certain hydrocarbons, notably olefins and aromatics that are introduced into the atmosphere from automobile exhausts, enter into the NO_2 cycle. Apparently, oxygen atoms attack the hydrocarbons, and the resulting free radicals react with NO to form more NO_2 ; thus, O_3 and NO_2 levels increase while NO is depleted.

The mechanisms that have been suggested to account quantitatively for the myriad of observed products are quite complex. For example, the inclusion of just one hydrocarbon, propylene, into the nitrogen cycle has led to the postulation of 150 elementary reactions, of which 60 are considered important [11]. The effects can be studied only through the use of a computer, as each of the non-steady-state rate equations must be numerically integrated to yield concentration vs. time data. Another difficulty in assessing complex mechanisms is the lack of reliable data on rate constants; a recent publication by Atkinson and Lloyd [1] has helped to alleviate this problem.

A highly simplified mechanism, first introduced by Friedlander and Seinfeld [5], provides a qualitative picture of the NO_2 -hydrocarbon interaction. In this mechanism, all hydrocarbons are considered as a single species (RH). No detailed description of products is given, except that free-radical species (RO) are postulated that cause a chain reaction with initiation, propagation and terminating steps. Overall, only seven reactions are considered — the three reactions of the NO_2 cycle (equations 9-11) plus the following four:



With certain assumptions and simplifications, the final rate equations are:

$$\frac{d[NO_2]}{dt} = [NO_2][RH] \left(\frac{k_1}{k_2} k_6 k'_4 [NO] - \frac{k_1}{k_3} k'_4 [NO_2] \right) \quad (21)$$

$$\frac{d[NO]}{dt} = - \frac{k_1}{k_2} k_6 k'_4 [NO_2][RH][NO] \quad (22)$$

$$\frac{d[RH]}{dt} = - [NO_2][RH] \left(\frac{k_1}{k_2} k_4 + \frac{k_1 k_5}{k_3 [NO]} \right) \quad (23)$$

where $k'_4 = \frac{k_4}{k_6[NO] + k_7[NO_2]}$

Using the initial concentrations and rate constants listed in Table 2.3-6, one can integrate these equations numerically, yielding the results shown in Figure 2.3-2.

If quantitative information on NO_2 -hydrocarbon interaction is desired, the detailed mechanisms must be considered. These mechanisms have been recently updated by Atkinson *et al.* [2].

Attempts have been made to simplify and consolidate the reaction mechanisms without losing too much of their quantitative aspects. Notable among these are the carbon bond approach of Whitten *et al.* [15] and the counter species concept of Leone and Seinfeld [10].

TABLE 2.3-6

Initial Concentrations and Rate Constants

$[NO_2]_0$	= 0.2 ppm
$[NO]_0$	= 1.0 ppm
$[RH]_0$	= 2.0 ppm
$\frac{k_1}{k_2} k_6 k'_4$	= 0.1 $ppm^{-2} min^{-1}$
$\frac{k_1}{k_3} k'_4$	= 0.02 $ppm^{-2} min^{-1}$
$\frac{k_1}{k_2} k_4$	= $1.83 \times 10^{-3} ppm^{-1} min^{-1}$
$\frac{k_1 k_5}{k_3}$	= $2.45 \times 10^{-4} min^{-1}$

Source: Friedlander and Seinfeld [5]

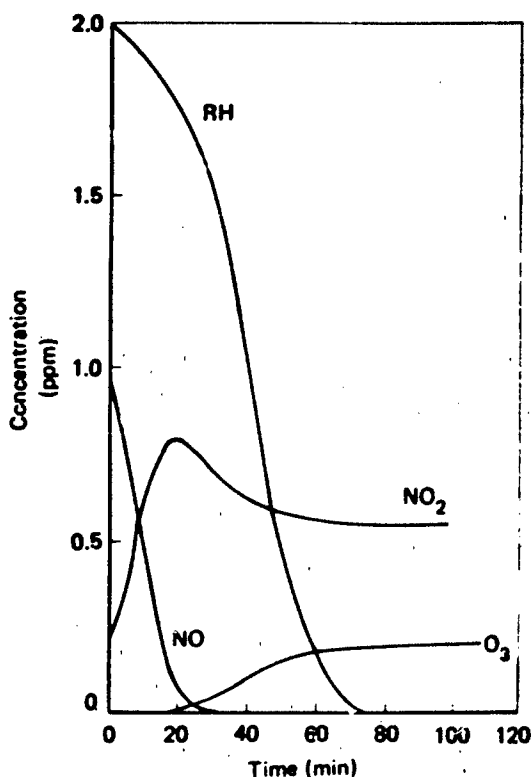


FIGURE 2.3-2 Concentration of Reacting Species vs Time

The analysis of even the most complex reaction mechanisms is only the initial step in modeling the production and transport of atmospheric pollutants resulting from photolysis. The rate equations for each species must be incorporated in a general model that describes the transport of these species over large distances.

Photochemical transport models have been reviewed by Eschenroeder and Martinez [4], Lamb and Seinfeld [8] and Seinfeld *et al.* [13]. A more recent evaluation of these models has been presented by Ruff *et al.* [12].

2.3.5 Literature Cited

1. Atkinson, R., and A. Lloyd, "Evaluation of Kinetic and Mechanistic Data for Modeling of Photochemical Smog," *J. Phys. Chem. Ref. Data*, **13**, 315 (1984).
2. Atkinson, R., A. Lloyd and L. Winges, "An Updated Chemical Mechanism for Hydrocarbon/NO_x/SO₂ Photoxidations Suitable for Inclusion in Atmospheric Simulation Models," *Atmos. Environ.*, **16**, 1341 (1982).
3. Dermerjian, K.L., K. Schere, and J. Peterson, "Theoretical Estimates of Actinic (Spherically Integrated) Flux and Photolytic Rate Constants of Atmospheric Species in the Lower Troposphere," in *Advances in Environmental Science and Technology*, **10**, pp. 369-459, Pitts, J.N., R. Metcalf and D. Grosjean (eds.), Wiley-Interscience, John Wiley & Sons, New York (1980).

4. Eschenroeder, A. and J. Martinez, "Concepts and Applications of Photochemical Smog Models," in *Photochemical Smog and Ozone Reactions*, Advances in Chemistry Series 113, American Chemical Society, Washington, D.C. (1972).
5. Friedlander, S.K. and J.H. Seinfeld, "A Dynamic Model of Photochemical Smog," *Environ. Sci. Technol.*, **3**, 1175 (1969).
6. Haagen-Smit, A.J., "Chemistry and Physiology of Los Angeles Smog," *Ind. Eng. Chem.*, **44**, 13422 (1952).
7. Haagen-Smit, A.J., C. Bradley and M. Fox, "Ozone Formation in Photochemical Oxidation of Organic Substances," *Ind. Eng. Chem.*, **45**, 2086 (1953).
8. Lamb, R.G. and J.H. Seinfeld, "Mathematical Modeling of Urban Air Pollution: General Theory," *Environ. Sci. Technol.*, **7**, 253 (1973).
9. Leighton, P.A., *Photochemistry of Air Pollution*, Academic Press, New York (1961).
10. Leone, J.A. and J. Seinfeld, "Analysis of the Characteristics of Complex Chemical Reaction Mechanisms: Application to Photochemical Smog Chemistry," *Environ. Sci. Technol.*, **18**, 280 (1984).
11. Niki, H., E. Daby and B. Weinstock, "Mechanisms of Smog Reactions," in *Photochemical Smog and Ozone Reactions*, Advances in Chemistry Series 113, American Chemical Society, Washington, D.C. (1972).
12. Ruff, R.E., K.C. Nitz, F.L. Ludwig, C.M. Bhumralkar, J.D. Shannon, C.M. Sheih, I.Y. Lee, R. Kumar and D.J. McNaughton, "Evaluation of Three Regional Air Quality Models," *Atmos. Environ.*, **19**, 1103 (1985).
13. Seinfeld, J.H., S.D. Reynolds and P.M. Roth, "Simulation of Air Pollution," in *Photochemical Smog and Ozone Reactions*, Advances in Chemistry Series 113, American Chemical Society, Washington, D.C. (1972).
14. Weast, R.C. (ed.), *CRC Handbook of Chemistry and Physics*, 54th ed., CRC Press, Cleveland (1973).
15. Whitten, C.Z., H. Hogo and J. Kills, "The Carbon Bond Mechanism: A Condensed Kinetic Mechanism for Photochemical Smog," *Environ. Sci. Technol.*, **14**, 691 (1980).

2.4 GAS ADSORPTION ON SOLIDS

2.4.1 Introduction

The extent to which a gas is adsorbed on a solid surface affects the rate at which it is released from the surface and transported to the environment. Even if it has a vapor pressure greater than 1 atmosphere under environmental conditions, a gas that is strongly adsorbed on a solid surface may remain there for some time. As the volatilization rate is related to the vapor pressure of the gas species, the "effective" vapor pressure at the soil-air interface is determined by, among other properties, the adsorption behavior of the gas. Therefore, to determine the persistence of a gas and the rate at which it is released into the atmosphere, we must be able to estimate how strongly it is adsorbed on a surface.

The association between a gas and a solid surface can be either physical or chemical in character. Physical or Van der Waals adsorption is characterized by relatively low heats of adsorption (≤ 5 kcal/mol), which are of about the same order as heats of vaporization. The equilibrium between solid and gas is reversible and is rapidly attained when the temperature or pressure changes. This form of adsorption is usually favored at low temperature.

Van der Waals adsorption occurs to some extent whenever a gas is in contact with a solid. However, when the gas and the solid can react chemically, the other type of adsorption (chemisorption) is sometimes more significant, especially at elevated temperatures. The heats of adsorption are in the range of 20-100 kcal/mol, indicating that chemical reactions are involved. Chemisorption occurs chiefly on metal surfaces. It can also occur on other surfaces, but in such cases the temperature must be elevated, because the process then requires a substantial energy input. For these reasons, a first approximation of the extent of adsorption need not consider chemisorption.

Furthermore, one can usually ignore the physical adsorption of gases that boil below 200K, since only small amounts would be adsorbed at normal temperatures and they would not persist on solid surfaces.

The environmental implications of gas and vapor adsorption are important, because high-technology industries are making increasing use of organometallic gases and low-boiling liquids, and the likelihood of their release into the environment is therefore growing.

Some of the gases and vapors now used by industry, such as PH_3 , AsH_3 , Ti(i-propoxide)_4 and SiH_4 , rapidly decompose when exposed to air, forming oxides or hydroxides. While these may cause environmental problems, gas adsorption is not involved. However, other materials such as $\text{Si(CH}_3)_4$, $\text{Sn(CH}_3)_4$ and $\text{Si(OCH}_3)_4$ may persist for finite times in the atmosphere, so an estimate of their potential adsorption might be useful in assessing their persistence.

2.4.2 Data Values

Experimentally, the amount of gas adsorbed on a given substance is determined in apparatus containing a chamber whose volume is variable and can be measured accurately. The pressure and temperature are also adjustable. A weighed sample of adsorbent is placed in the chamber, and a measured quantity of gas is introduced. The subsequent loss in volume indicates the amount of gas adsorbed. So long as there is no chemical reaction between the two components, one solid will adsorb the same amount of gas as another solid of equal surface area.

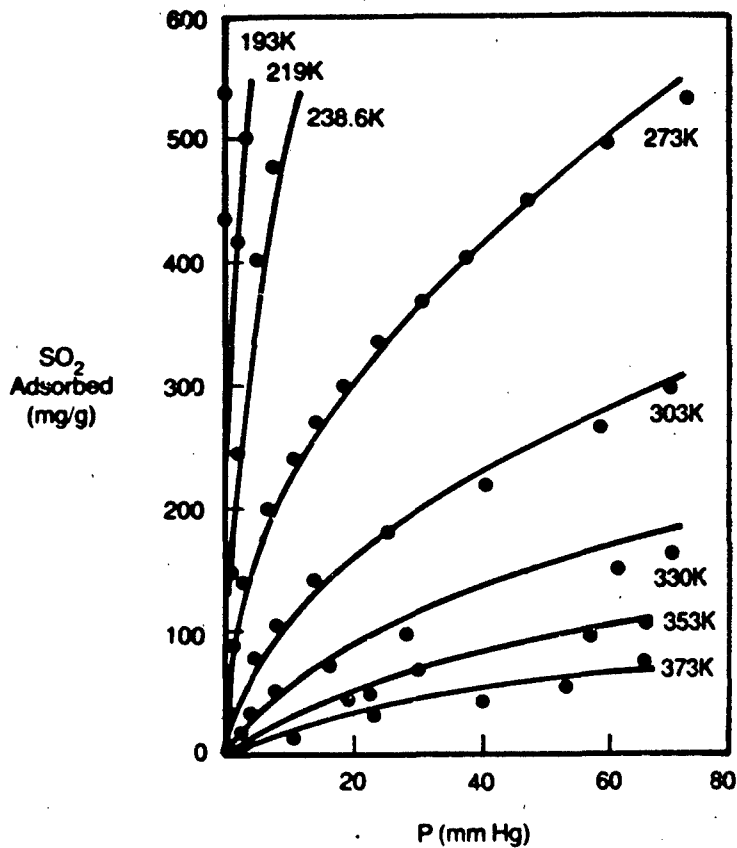
The adsorption at a given temperature (adsorption isotherm) is usually plotted as the amount adsorbed, X , vs. the relative pressure, P/P_e , where P is the system pressure and P_e is the saturated vapor pressure of the gas or vapor (atm), at the given temperature. In this discussion, P is always assumed to be 1 atmosphere. The quantity X may be expressed in units of volume (ml adsorbate/g adsorbent), weight (g adsorbate/g adsorbent), or mol adsorbate/g adsorbent. If the surface area per gram of adsorbent is known, X can be expressed in terms of weight or volume of gas per unit area, thereby facilitating estimates of adsorption on soil or some other substance. To do this, however, one must also know the unit surface area of the other substance; this is, in fact, the purpose of most adsorption measurements.

Figure 2.4-1, which shows isotherms for SO_2 on silica gel, illustrates the significant influence of temperature on the extent of adsorption. The temperature dependence of the amount adsorbed can be generally described by a function of the type $X \propto e^{-A/T}$, where A is proportional to the difference between the heat of adsorption and the latent heat of vaporization, and T is the temperature in degrees K.

Table 2.4-1 shows typical adsorption data for a variety of gases at two different temperatures. Some anomalies will be noted, in the form of an apparent decrease in adsorption at the lower temperature for some gases (N_2O , CO_2 , CO and N_2). This could be simply due to the fact that the two sets of data were obtained with nonidentical kinds of charcoal, which may have had different surface areas or surface treatments.

2.4.3 Estimating Methods

Methods of calculating the extent of physical adsorption to be expected for a given gas have not been developed; however, a way may be found to obtain at least rough estimates, such as by correlating the quantity adsorbed with other physical properties. For several organic and inorganic gases, for example, the logarithm of the volume adsorbed per gram of adsorbent varies generally in a linear fashion as a function of the normal boiling point of the gas. Figure 2.4-2 illustrates this relationship using adsorption data from Table 2.4-1; the correlation coefficient of the linear plot is 0.969.



Source: Adamson [2]. (Copyright 1960, Wiley Interscience. Reprinted with permission.)

FIGURE 2.4-1 Adsorption Isotherms for SO_2 on Silica Gel

Theoretical treatments of physical adsorption were made by Langmuir [8] and Brunauer, Emmett and Teller [5]. Langmuir derived the following relationship between the volume of gas adsorbed and the gas pressure:

$$\frac{X}{X_m} = \frac{K(P/P_0)}{1 + K(P/P_0)} \quad (1)$$

where X is the volume of gas adsorbed per weight of solid adsorbent, X_m is the volume of gas adsorbed with monolayer coverage, K is a temperature-dependent constant, and P/P_0 is the relative pressure. The equation is based on the assumptions that equilibrium has been established between the gas and the solid and that only a monomolecular layer of gas molecules has been adsorbed. These assumptions are probably valid for gases at environmental temperatures and pressures; multilayer adsorption occurs only at very low temperatures and at pressures approaching the saturated vapor pressure of the gas.

TABLE 2.41
Adsorption of Gases on Charcoal

Gas	Volume Adsorbed (ml/g)	
	25°C [2]	15°C [6]
SO ₂	98	380
Cl ₂	—	235
NH ₃	136	181
H ₂ S	—	99
HCl	—	72
N ₂ O	67	54
CO ₂	60	48
CH ₄	—	16.2
CO	14	9.3
O ₂	—	8.2
N ₂	11	8.0
H ₂	2	4.7

Brunauer, Emmett and Teller extended Langmuir's treatment to include multilayer adsorption. Their final equation takes the form

$$\frac{X}{X_m} = \frac{c(P/P_0)}{(1 - P/P_0)[1 + (c - 1)(P/P_0)]} \quad (2)$$

where c is a temperature-dependent constant and the other symbols have the same meaning as in equation 1. Equations 1 and 2 are special cases of a more generalized equation for n layers; equation 1 applies when $n = 1$, and equation 2 applies when $n = \infty$.

Equation 1 is generally applicable when environmental temperatures are above the normal boiling point of gases and vapors. Thus, we would expect only monolayer coverage for gases, particularly since the relative pressure P/P_0 rarely exceeds 0.3 for these materials. For the vapors of liquids whose normal boiling points, T_b , are near or well above environmental temperatures, we can no longer expect monolayer coverage, so equation 2 is more applicable.

As they stand, equations 1 and 2 are not very useful for estimating directly the extent to which a gas or vapor will be adsorbed on a given solid. Furthermore, in discussing estimation methods we must clearly distinguish between (a) gases and vapors with

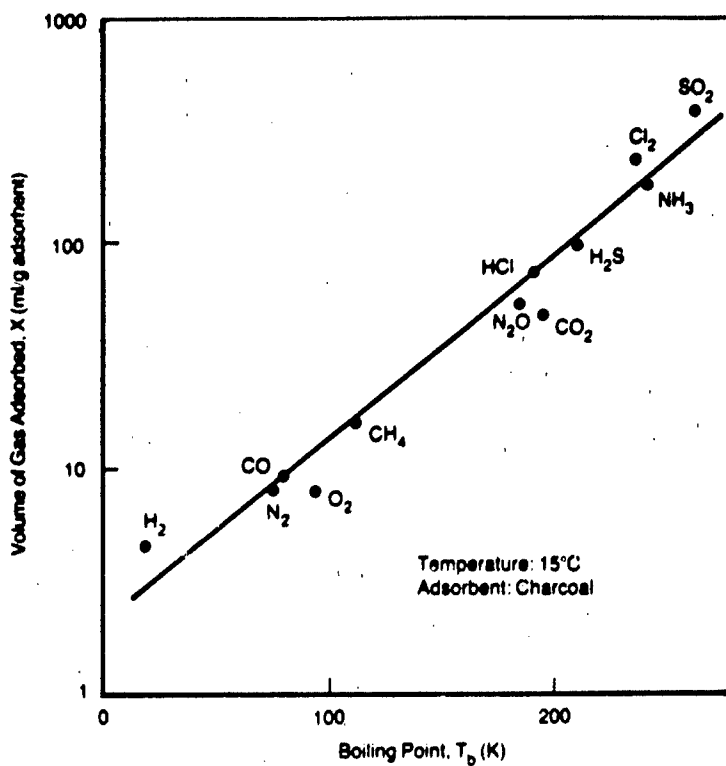


FIGURE 2.4-2 Adsorption of Various Gases as a Function of Their Normal Boiling Points

boiling points below environmental temperatures and (b) vapors whose normal boiling points are above environmental temperatures. Each of these categories is discussed below.

GASES AND VAPORS ($T > T_b$)

The correlation between X and T_b (Figure 2.4-2) implies a relationship between the extent of physical adsorption and saturated vapor pressure, P_o . Such a relationship would not be surprising, as it is natural to suppose that as a gas becomes more condensable its adsorption potential should increase. If we replot the 15°C data in Table 2.4-1 as a function of the saturated vapor pressure of each gas, we should observe a regular decrease in adsorption potential as P_o increases. Such a plot is

shown in Figure 2.4-3 as $\ln X$ vs $\ln P_o/P$. The correlation is quite good ($r^2 = 0.988$). The relationship is given by

$$\ln X = a - b \ln(P_o/P) \quad (3)$$

where X = volume adsorbed per gram of adsorbent

a = 6.62 at 288 K

b = 0.69 at 288 K

P = 1 atm

The saturated vapor pressure values were obtained via extrapolation of $\log P_o$ vs $1/T$ calculated from handbook data [12]. In some instances the extrapolated values are in

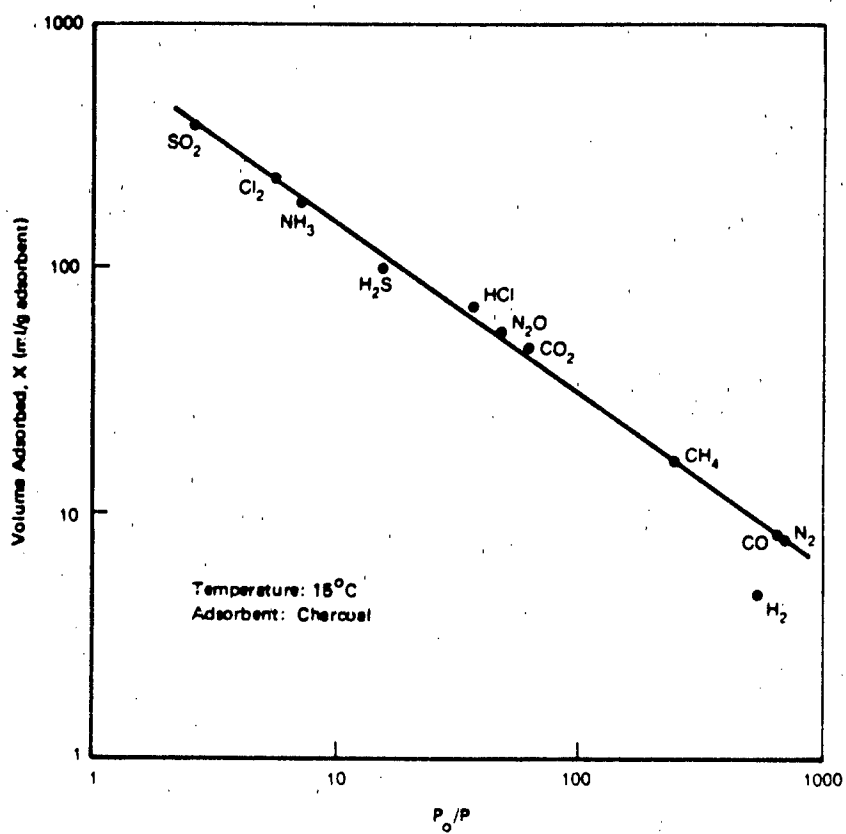


FIGURE 2.4-3 Amount Adsorbed vs Saturated Vapor Pressures of Various Gases

the supercritical region; while these are hypothetical, they are useful for estimation purposes, because they should be proportional to the tendency of the gas to condense and, hence, its adsorption potential.

Equation 3 has the same form as the Freundlich isotherm, an expression that has been found to fit isotherm data for monolayer adsorption [3]:

$$X = K(P/P_o)^{1/n} \quad (4)$$

or

$$\ln X = \ln K - (1/n) \ln (P_o/P) \quad (5)$$

In normal use, K and n are adjusted to fit the isotherm data. In the use proposed here, the values of K, n and P are fixed, so any variation in X is related to the value of P_o . Some of the temperature dependence is contained in P_o , as it is a strong function of temperature; however, we have correlated b (eq. 3) with temperature as follows:

$$b = 0.24 + (1.57 \times 10^{-3}T) \quad (6)$$

for which

$$r^2 = 0.9989$$

The task remains to obtain or estimate values of P_o as a function of temperature for the gas in question. Where possible, extrapolated experimental data should be used; if these are not available, the estimation method for gases and vapors ($T > T_b$) outlined in section 2.2 can be used.

In Table 2.4-2, experimental and estimated values of X are compared for the gases listed in Table 2.4-1. The estimates were obtained with saturated vapor pressures calculated by the method shown in section 2.2. In general, the agreement is good; the average method error is $\pm 20\%$. Similar comparisons are shown in Figure 2.4-4 for a single gas (CO_2) at three different temperatures and several values of P below atmospheric pressure.

The above correlations apply only to adsorption on clean charcoal. While the estimates have no quantitative value for other surfaces, they are useful for obtaining some indication of the relative adsorption of a gas if its boiling point is known.

Direct comparisons of the adsorption estimates obtained here with data obtained on natural surfaces (soils, clay, etc.) are complicated by the fact that interaction with these surfaces is affected by the presence of chemicals, microbes and water. For example, the uptake of SO_2 on soil surfaces has been highly correlated with soil pH and the presence of carbonate and other basic species [3]. Other studies have attributed the uptake of CO [7] and NO_2 [1] primarily to microbial action, as considerably less adsorption occurred with sterilized soil. The uptake of SO_2 and NO_2 is also enhanced by the presence of moisture [4], as these gases are quite soluble and react with water.

If we were to assume that a soil had the same unit surface area as charcoal, we would estimate its capacity for adsorbing SO_2 at 25°C to be about 800 mg/g of soil. Data

TABLE 2.4-2
Experimental vs. Estimated Adsorption on Charcoal
 $(t = 15^\circ\text{C}, P = 760 \text{ mm})$

Gas	T_b (K)	Volume Adsorbed, X (ml/g)		
		Experimental [6]	Estimated	Error (%)
SO ₂	262	380	393	+ 3
NH ₃	240	181	198	+ 9
Cl ₂	238	235	222	- 7
H ₂ S	211	99	113	+14
CO ₂	195	48	68	+42
HCl	189	72	60	-17
N ₂ O	183	54	54	0
CH ₄	109	16	13	-19
O ₂	90	8	10	+25
CO	82	9	5	-80
N ₂	63	8	8	0
H ₂	14	5	6	+20

reported by Bremner [4] yield values ranging from 0.042 mg/g to 60.1 mg/g, depending upon pH, water content, and surface area. We may be able to account for some of the large discrepancy in the data by examining the effects of surface area and water content. The typical specific surface areas of charcoals used in laboratory studies are of the order of 1000 m²/g [10]. For soils, the specific surface area can range from about 20 m²/g to 200 m²/g [9]. Thus if we assume that the actual amount of SO₂ adsorbed on soils will be proportional to the ratio of specific surface areas of soil and charcoal, we can estimate adsorption values within the range of 16 mg/g to 160 mg/g. For soils with low pH values we would expect that these estimates would be lower [3, 4]. The solubility of SO₂ in water is approximately 200 mg/g of water. If, for example, typical soils contain 5% water, we would add to the above numbers an additional 10 mg/g of soil, yielding estimated adsorption values within the range 26 mg/g to 170 mg/g. These data illustrate the difficulty of making direct comparisons between estimated values and experimental measurements.

VAPORS ($T < T_b$)

The apparent success of the correlation for gases (eq. 3) is related to the ratio P/P_∞ . Since this ratio is usually less than 0.3 at environmental temperatures and pressures, only monolayer coverage of the adsorbent has to be considered in most cases. Hence, isotherms can generally be characterized by equations similar to equation 3. For vapors of liquids whose boiling points are equal to or greater than environmental

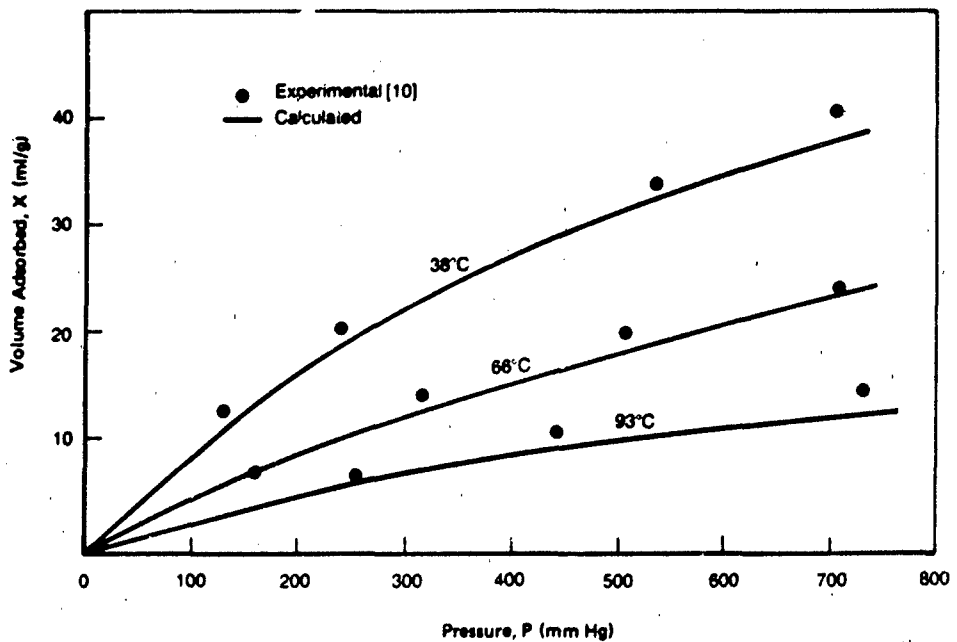


FIGURE 2.4-4 Experimental vs Calculated Adsorption Isotherms for CO₂ on Charcoal

temperatures, however, P/P_0 is 1.0 or more. This means that multilayer adsorption has occurred and the surface is saturated — i.e., liquid has condensed not only on the surface but also in any pores that may exist.

The extent to which a vapor is adsorbed depends, in fact, almost exclusively on the pore volume of the solid, because the mechanism of adsorption at the saturation pressure causes the vapor to condense within the pores of the adsorbent and fill them. Subsequent evaporation of the condensed liquid is also affected by the pores: those with narrow constrictions, for example, tend to retain the liquid longer.

Except for its vapor pressure and solubility in water, the nature of the liquid in this case is irrelevant [11].

2.4.4 Method Error

The method error is listed in Table 2.4-2. The average error for the few gases shown is $\pm 20\%$. Again, this refers only to adsorption on charcoal.

2.4.5 Sample Calculations

Example 1 Estimate the adsorption of CO₂ on charcoal at a temperature of 25°C and a pressure of 760 mm Hg. The normal boiling point of CO₂ is 195 K.

$$T_b = 195 \text{ K}$$

$$T = 25 + 273 = 298 \text{ K}$$

From section 2.2 (equation 12), the estimated saturated vapor pressure of CO₂ at 293 K is 41.5 atm.

$$P_o/P = 41.5/1 = 41.5$$

From equation 6,

$$b = 0.24 + (1.57 \times 10^{-3} \times 298) = 0.71$$

Substituting in equation 3,

$$\begin{aligned}\ln X &= 6.62 - 0.71 \ln 41.5 = 3.97 \\ X &= 53 \text{ ml/g}\end{aligned}$$

The experimental value is 60 ml/g [2], indicating an error of -12%.

The next example illustrates that even in cases of adsorption on surfaces other than charcoal, estimates to within factors considerably less than 2 can be made.

Example 2 Estimate the adsorption of SO₂ on silica gel at 273 K and a pressure of 60 mm Hg.

$$\begin{aligned}T_b &= 262 \text{ K} \\ T &= 273 \text{ K}\end{aligned}$$

The saturated vapor pressure of SO₂ at 273 K is estimated to be 1.37 atm, using the method for gases described in section 2.2 (equation 12).

$$\begin{aligned}b &= 0.24 + (1.57 \times 10^{-3} \times 273) = 0.67 \\ a &= 6.62 \\ P &= 60 \text{ mm}/760 \text{ mm} = 0.08 \text{ atm} \\ P_o/P &= 1.37/0.08 = 17.13\end{aligned}$$

From equation 3,

$$\begin{aligned}\ln X &= 6.62 - 0.67 \ln 17.13 = 4.72 \\ X &= 112 \text{ ml/g}\end{aligned}$$

The experimental value is 175 ml/g, indicating an error of -36%.

2.4.6 Literature Cited

1. Abeles, F.B., L. Cruker, L. Forence and G. Leather, "Fate of Air Pollutants: Removal of Ethylene, Sulfur Dioxide, and Nitrogen by Soil," *Science*, **173**, 914 (1972).
2. Adamson, A.N., *Physical Chemistry of Surfaces*, Interscience (Wiley), New York (1960).
3. Bohn, H.L., "Soil Adsorption of Air Pollutants," *J. Environ. Qual.*, **1**, 372 (1972).
4. Bremner, J.M., "Sorption of Pollutant Gases by Soils," Final Report to U.S. Dept. of Energy, Contract DE-AC02-79EV02530 (1981).
5. Brunauer, S., P. Emmett and E. Teller, "Adsorption of Gases in Multimolecular Layers," *J. Am. Chem. Soc.*, **60**, 309 (1938).
6. Glasstone, S., *Textbook of Physical Chemistry*, 2nd ed., D. Van Nostrand, New York (1946).
7. Inman, R.E., R. Ingersoll and E.A. Lery, "Soil: A Natural Sink for Carbon Monoxide," *Science*, **172**, 1229 (1971).
8. Langmuir, I., "The Constitution and Fundamental Properties of Solids and Liquids, Part I: Solids," *J. Am. Chem. Soc.*, **38**, 2269 (1916).
9. Puri, A.N., *Soils, Their Physics and Chemistry*, Chapter IX (p. 54), Reinhold Publishing Corp., New York (1949).
10. Ray, G. and E. Box, "Adsorption of Gases on Activated Charcoal," *Ind. Eng. Chem.*, **42**, 1315 (1950).
11. Thomas, R.G., "Volatilization from Water," in *Handbook of Chemical Property Estimation Methods*, W.J. Lyman, W.F. Reehl and D.H. Rosenblatt (eds.), McGraw-Hill Book Co., New York (1982).
12. Weast, R.C. (ed.), *CRC Handbook of Chemistry and Physics*, 58th ed., CRC Press, Cleveland (1977).

2.5 ATMOSPHERIC DEPOSITION

2.5.1 Introduction

The deposition of gaseous and particulate air pollutants, like their ambient concentration, is a determinant of their environmental effects. The ambient concentration is of primary interest for such problems as the health effects of ozone on humans; often, however, as in the effects of air pollutants on terrestrial or aquatic ecosystems, deposition may be more important.

The mechanisms by which air pollutants are deposited from the atmosphere are described below. For convenience, they have been divided into wet (i.e., occurring in precipitation) and dry deposition of gases and particulate matter. While these divisions may seem straightforward, their distinctions are often blurred. The deposition of fog droplets is considered wet deposition by some researchers but dry deposition by others. Chemical transformations also complicate the process, as in the oxidation of sulfur dioxide gas to sulfuric acid, an aerosol (particle).

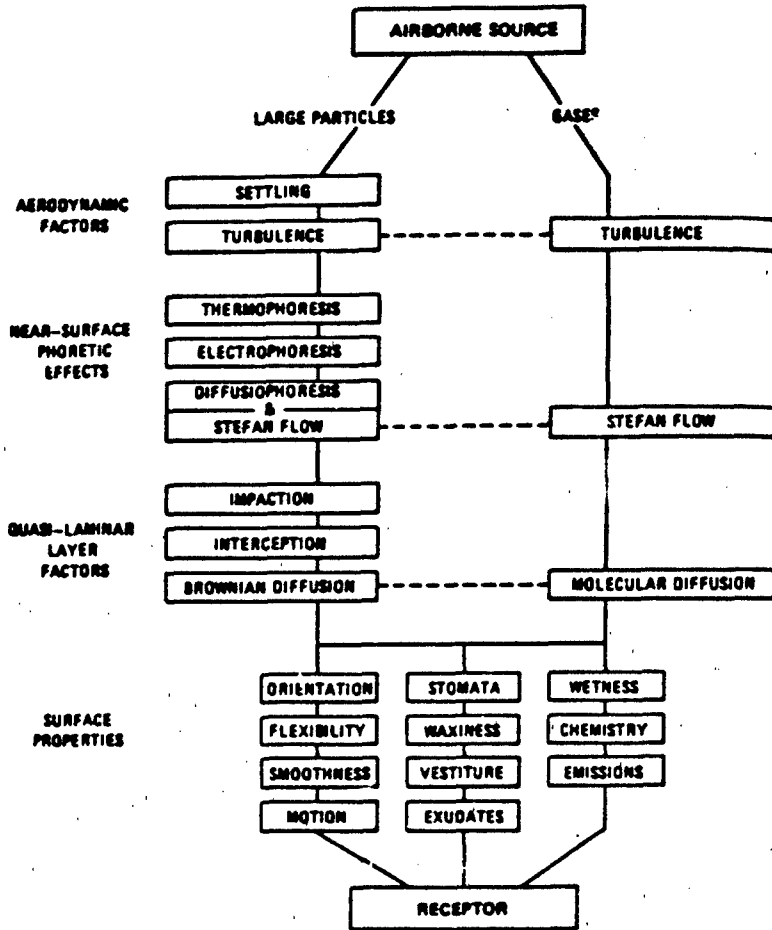
2.5.2 Dry Deposition

Dry deposition may be defined as the turbulent transfer of gaseous and particulate species from the atmosphere to the earth's surface. This includes gravitational settling but excludes deposition of gases and particles absorbed or entrained in precipitation. The deposition of pollutants with fog droplets is considered here as wet deposition.

As shown in Figure 2.5-1, many of the factors influencing the rate of dry deposition differ for gases and particles. Because of the differences between the mechanisms that most strongly affect the deposition of gases and large particles, they are described separately below. This figure emphasizes the physical factors that affect the rate of deposition rather than the chemical properties and reactions of the depositing material.

DEPOSITION OF PARTICLES

As the rate of dry deposition of particles (and gases) is extremely difficult to measure, a relationship between dry deposition and ambient concentration, which can be measured relatively easily, is often employed. The factor relating the ambient concentration to the deposition rate is known as the *deposition velocity*, since its dimensions are length/time. It is determined for a given gas or aerosol, based on a particular reference height; when multiplied by the concentration (mass/volume) at that height, the product is the deposition rate [mass/(area-time)]. Because of its importance in characterizing the removal of pollutants from the atmosphere and its use in predictive models, the deposition velocity serves as the focus of the discussion that follows. First, the processes embodied in the deposition velocity are described.



Source: National Research Council [16]

FIGURE 2.5-1 Schematic Representation of Processes Likely to Influence the Rate of Dry Deposition of Gases and Particles

Particles are transported vertically above the earth's surface by eddy diffusion (turbulence) and gravitational settling (the "aerodynamic factors" in Figure 2.5-1). Like other falling objects, particles accelerate until frictional drag forces equal the force of gravity, at which point they have reached their terminal velocity. The terminal settling velocity of falling particles (based on Stoke's law) can be expressed as [32]:

$$V_t = \frac{2a^2 \rho g}{9\mu} \quad (1)$$

where:

V_t = particle's terminal settling velocity (m/s)

ρ = particle density (kg/m^3)

g = acceleration due to gravity ($9.8 \text{ m}/\text{s}^2$)

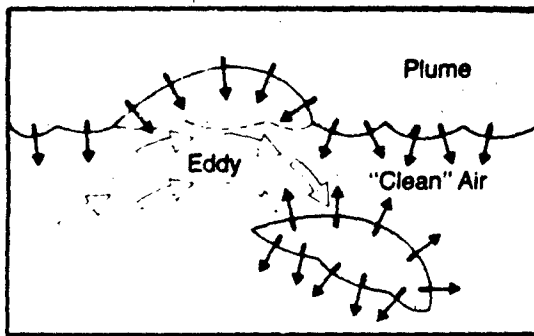
μ = viscosity of air ($1.78 \times 10^{-5} \text{ kg}/(\text{m} \cdot \text{s})$ at 18°C , 1 atm)

a = radius of the particle (m)

Equation 1 is applicable to particles having radii up to about $50 \mu\text{m}$, after which the turbulence in the wake of the falling particle must be considered [32]. It is assumed that the falling particles are solid spheres, although in reality they are often not spherical and may contain void spaces [20].

As equation 1 shows, V_t is more strongly a function of the particle's radius than its density, since the R term is squared. Furthermore, the densities of aerosol particles cover a much narrower range than their radii, varying by a factor of only 2-3 and averaging $2.25 \text{ g}/\text{cm}^3$ [32].

The other aerodynamic factor listed in Figure 2.5-1 is turbulence. Conceptually, turbulent transfer is quite simple: particles are carried towards the earth's surface with the turbulent eddies of the air. The effect a turbulent eddy has on a pollutant plume is shown in Figure 2.5-2. The mathematical description of eddy diffusion is much more complicated, however, and turbulent eddy diffusivities for mass transport may range over three orders of magnitude, depending on the height above the ground and the local hydrostatic stability of the air [13].



Source: Williamson [32]. (Copyright 1973, Addison-Wesley Publishing Co., Inc. Reprinted with permission.)

FIGURE 2.5-2 Grossly Simplified View of the Breakup of a Pollutant Plume by a Turbulent Eddy, Causing the Mixing of Pollutants with "Clean" Air

The stability of the atmosphere is indicated by the change in temperature with height. The atmosphere is said to be "neutrally stable" when the temperature decreases with height at the same rate as the adiabatic lapse rate. The adiabatic lapse rate is the decrease in temperature that a parcel of air would undergo if it were raised in the atmosphere with no heat flow to or from its surroundings (or the temperature increase it would undergo if it were lowered through the atmosphere). For dry air, the lapse rate is approximately $-9.8^{\circ}\text{C}/\text{km}$; but for warm air saturated with water vapor it may be as little as $-3.5^{\circ}\text{C}/\text{km}$; the average rate in the troposphere is about $-6.5^{\circ}\text{C}/\text{km}$ [32]. When the temperature decrease with altitude is greater than the adiabatic lapse rate, as typically occurs in the middle of a sunny day, the atmosphere is said to be "unstable," and vertical mixing is promoted. A parcel of warm air cooling at the adiabatic lapse rate will become more buoyant as it rises because the temperature difference between itself and the air surrounding it increases. (The parcel cools at the adiabatic lapse rate, but the surrounding air cools an even greater amount for a given increase in height.) Similarly, a cool, heavy parcel of air will tend to accelerate as it falls since its temperature increases at a lesser rate than the air around it.

"Stable" conditions (typical of a calm night) occur when the rate of temperature decrease with height is less than the adiabatic lapse rate. In this case, the fall of a cool parcel of air, or the rise of a warm one is inhibited, for just the opposite reasons that their motions are promoted under unstable conditions. Poor vertical mixing of the air results with the consequent decrease in the removal of air pollutants.

Near the receiving surface, various phoretic effects (i.e., transmission due to a gradient) may influence the rate of particle deposition. *Thermophoresis* refers to the tendency of a particle to be driven away from a hot surface; it can be thought of as the consequence of "hotter," more energetic air molecules hitting the side of the particle facing the hot surface [16] and therefore applies primarily to small particles (diameter $<0.03 \mu\text{m}$). For larger particles, forces due to thermal radiation can be important if a temperature gradient develops across particles that are poor heat conductors. As a rule of thumb, for particles of diameter less than $0.03 \mu\text{m}$, the thermophoretic velocity is likely to be about 0.03 cm/s , while for larger particles ($>1 \mu\text{m}$ diameter) the velocity will be only one fourth this amount [16].

Electrophoresis, as the name implies, occurs in electric fields, and serves to promote the retention as well as the deposition of particles due to the attraction of opposite electrical charges [16]. The effect of electrophoresis is greatly dependent on the particle size. Very small particles (diameter of about $0.001 \mu\text{m}$) attain a velocity of 2 cm/s per volt/cm of field strength, compared with a velocity of only 0.0003 cm/s per volt/cm for a particle of $0.1 \mu\text{m}$ diameter [6]. Since typical values of field strengths under fair-weather conditions are less than 10 volts/cm [16], electrophoresis is expected to be significant only for very small particles, which usually account for a very small fraction of the total aerosol mass.

Particles in intermixing gases undergo *diffusiophoresis*, which is the tendency to move toward the lighter of the two gases. In the atmosphere, the intermixing gases are generally water vapor and air; particles move toward the lighter of the two (water vapor), since they collide with fewer of the heavier (air) molecules on that side. A related phenomenon is *Stefan flow*, which results from the introduction into a gaseous medium of new gas molecules at an evaporating or subliming surface [16]. Since a mole of any gas occupies 22.41 liters at standard temperature and pressure, a Stefan flow velocity of 22.41 mm/s results as 18 g of water (one mole) evaporates from one square meter in one second.

While it is important to recognize the existence of phoretic effects and their significant influence on deposition rates in certain cases, often they need not be considered. Both diffusiophoresis and thermophoresis are usually small, and their effects on dry deposition can be ignored [16].

In the quasi-laminar layer (the layer less than 1 mm thick next to a surface), the mechanisms of impaction, interception, and Brownian diffusion become important. *Impaction* occurs when particles heavier than air are carried to a surface by wind or eddies. Those particles that are unable to flow around the surface, due to their inertia, will collide with it. This process is known as impaction when the particles are considered as point masses; it is important primarily for particles with diameters of between 2 and 20 μm , as larger particles tend to bounce off the surfaces and smaller ones are able to follow the air flow around them [16]. When the size of the particle is taken into account (i.e., the particle is considered larger than a point) and its trajectory relative to the surface is calculated, the process is referred to as *interception* [4].

Brownian diffusion occurs as particles are randomly struck by air molecules. The motion of smaller particles is greater than that of larger particles [32], thus increasing the possibility that the particle will be trapped by impaction. Equation 2 can be used (as described below) to estimate the Brownian diffusion coefficient [22].

$$D = \frac{kT}{6\pi\mu a} \left\{ 1 + \frac{10^{-4}}{pa} [6.32 + 2.01 \exp(-2190 pa)] \right\} \quad (2)$$

where:

- D = Brownian diffusion coefficient, cm^2/s
k = Boltzmann's constant, 1.38×10^{-16} erg/K
T = temperature, K (291 K used)
 π = 3.14159
 μ = air viscosity, g/(cm·s) [1.78×10^{-4} g/(cm·s) used]
a = particle radius, cm
p = pressure, cm Hg (76.0 cm used)

(Note that the constants within the braces have been derived such that the combined term is rendered dimensionless when p and a are employed as specified above.)

For particles with diameters of less than about $0.1 \mu\text{m}$, the gravitational settling velocity is quite low compared with the deposition velocity [21], since turbulent transfer and Brownian motion in the quasi-laminar layer are more important. For particles with diameters greater than $20 \mu\text{m}$, gravitational settling is the controlling factor in deposition; impaction is not significant with particles of this size [16]. Atmospheric sulfates, nitrates, and ammonium aerosols tend to occur in a size range of 0.1 to $2 \mu\text{m}$ diameter, and thus both gravitational settling and impaction play a role in their deposition [16]. The deposition velocity of a particle is at least as great as its terminal settling velocity, regardless of size [21], since impaction and Brownian diffusion act to enhance deposition.

Figure 2.5-1 lists a number of surface properties that influence the deposition of gases and particles. Chamberlain *et al.* [3], have shown that surface texture can have a pronounced effect on the deposition velocity for particles in the sub-micron to several micron range; the deposition velocity to filter paper was observed to be 2-3 orders of magnitude larger than that to a smooth surface. The effect of surface wetness on deposition rate was investigated by Jenkin [15], who used hygroscopic particles of 2.5 - $8.4 \mu\text{m}$ dry diameter (sodium chloride aerosol), and found a doubling of the deposition velocity when filter paper was moistened but only a 14% enhancement when artificial grass was moistened. Evaluating two models for predicting deposition to the sea, Arimoto and Duce [1] found that surface waves had little effect on the deposition rate of sodium and aluminum aerosols (mass mean diameter of approximately 2 and $10 \mu\text{m}$, respectively) while the deposition rate of lead-210 (mass mean diameter of $0.4 \mu\text{m}$) was as much as five times as great in the presence of waves, thus suggesting that the deposition of small particles may be greatly enhanced by broken water surfaces. Plant vestiture (surface covering) also affects the deposition rate; the presence of leaf hairs has been found by several researchers to enhance the deposition of small particles ($< 5 \mu\text{m}$) [16].

Ideally, all of the factors affecting the deposition rate would be easily described in mathematical terms that could be combined to give an overall equation for the deposition velocity. However, no generally accepted equation for predicting the deposition velocity of particles exists, and the actual deposition rates of particles, especially those of sub-micron diameter, remain controversial. The work of Sehmel [20, 22], Sehmel and Hodgson [23], and Slinn [26] shows relatively small deposition velocities for particles in this size range, while field studies of others, e.g., Wesely *et al.* [30] and Cadle *et al.* [2] indicate much greater values.

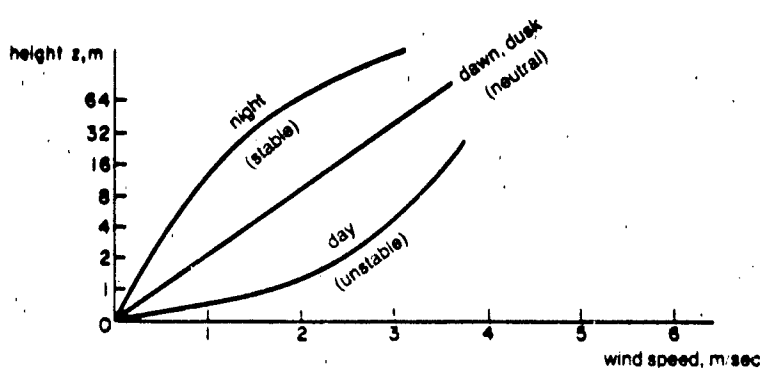
As an example of one method for predicting the deposition velocity of particles, the correlations of Sehmel [21, 22] and Sehmel and Hodgson [23] are described below. Sehmel and Hodgson's original correlation was published in 1978 [23] and was presented in graphical form in a 1980 review by Sehmel [21]. This work, which is based on wind tunnel studies, has the advantage of being in an easily usable engineering form, but as noted above, field measurements have indicated significantly higher deposition velocities for particles in the $0.1 \mu\text{m}$ to $1.0 \mu\text{m}$ diameter range. Thus the results of the correlation should not be taken as absolute, but

rather as indicative of the mechanisms affecting deposition rates. An alternative method for predicting the deposition velocities of sulfate particles (which are usually unimodally dispersed with the mode in the 0.1-1 μm range) and nitrate particles (bimodally dispersed with one mode in the same range and one in the 2-10 μm range) is described by Voldner *et al.* [28]; this method is similar to that described below for gases based on a resistance analogue, which includes a correction function for the effects of atmospheric stability.

Sehmel and Hodgson's work [23] indicates that atmospheric stability has little effect on the deposition velocity of particles, and the plots based on their correlation [21] are for stable conditions. However, Sehmel [22] notes that atmospheric stability must be considered in applying predictive equations to field situations, and others (e.g., Wesely *et al.* [30]) have observed decreased deposition velocities in the field for particles under neutral and stable conditions.

For particles of known density and diameter, two meteorological parameters known as the friction velocity (u_*) and the aerodynamic surface roughness (or roughness height, z_0) are needed to use Sehmel and Hodgson's correlation. The roughness height and friction velocity are used in describing the wind profile (wind speed as a function of height). As shown in Figure 2.5-3, under conditions of neutral atmospheric stability, wind speed is a log-linear function of height. Mathematically, this relationship can be expressed as [17]:

$$u = \ln(z/z_0) u_* / k \quad (3)$$



Source: Panofsky and Dutton [17]. (Copyright 1984, John Wiley & Sons.
Reprinted with permission.)

**FIGURE 2.5-3 Diurnal Variation of Wind Profiles
(Schematic) for the Same Day**

Here, u is the wind speed at height z , and k is the von Karman constant (dimensionless), typically taken to be 0.4. If the wind profile of interest occurs over roughness elements such as trees, houses, or crops, rather than bare soil or calm water, a displacement length, d , is employed, and the term $z - d$ is substituted for z in equation 3.

When d is small, it can be estimated from the wind profile. If the profile is measured for neutral conditions over a surface where the displacement length must be considered, the wind profile falls off sharply below the average height of the roughness elements (i.e., the plot for neutral stability in Figure 2.5-3 would drop off on the left side of the figure, below this height). To determine d , the linear portion of the profile above the height of the roughness elements is extrapolated to the ordinate (wind speed = 0); the intercept is $z_0 + d$. Over tall roughness elements such as trees or houses, a displacement length equal to 80% of the average height of the roughness elements should be assumed, rather than using the wind profile to make the estimate, since small errors in the profile can result in large errors in d [17].

Methods for determining z_0 and u_* are described below for cases where d is insignificant. (In cases where it is significant, $z - d$ is substituted for z in the equations that follow.) If the wind velocity is known at a number of heights, z_0 and u_* can be determined by plotting the wind profile (as $\ln z$ versus u). The slope of the resulting straight line is k/u_* and the intercept is $\ln z_0$.

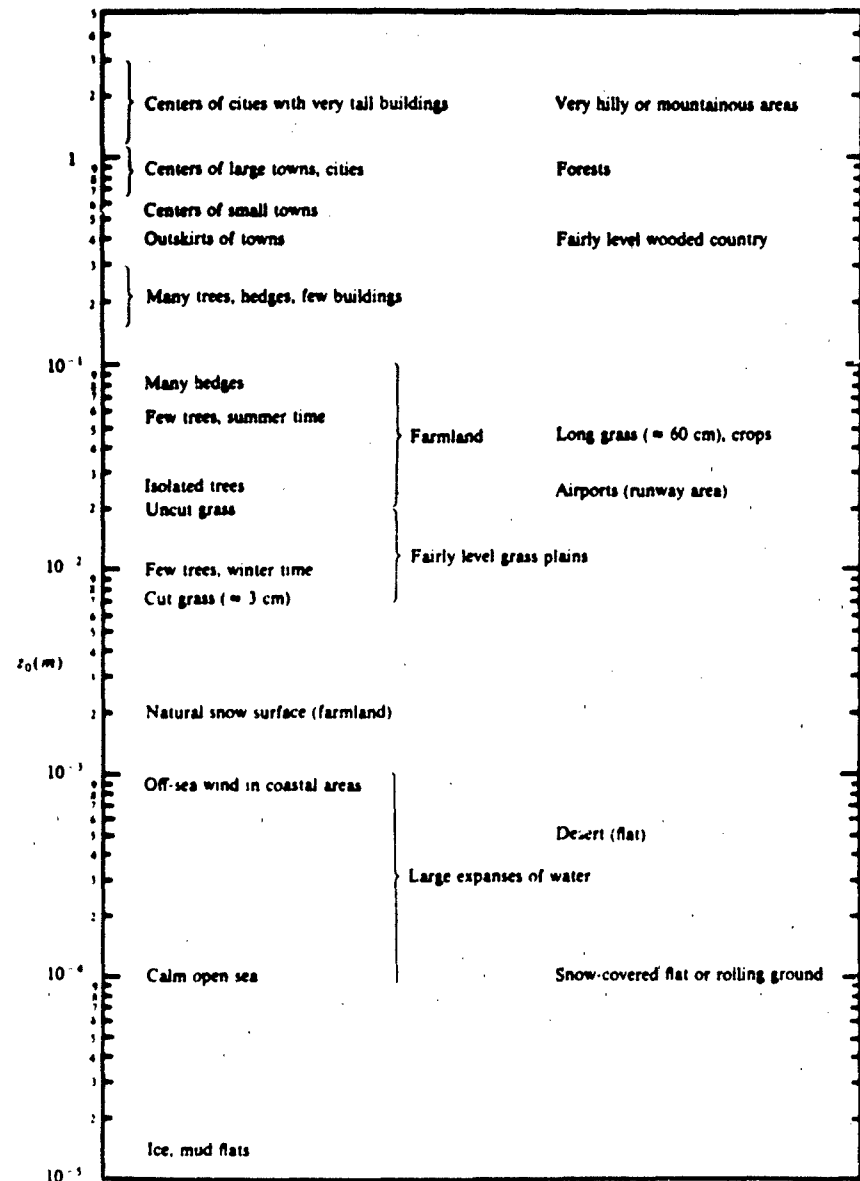
More likely, the wind speed is known only at one or two heights. If u is known at two heights, then:

$$u_* = \frac{k(u_2 - u_1)}{\ln(z_2/z_1)} \quad (4)$$

where the subscripts one and two denote the two points at which data are available. By substituting u_* calculated from equation 4 into equation 3, z_0 can be solved for with u and z data for either of the two points.

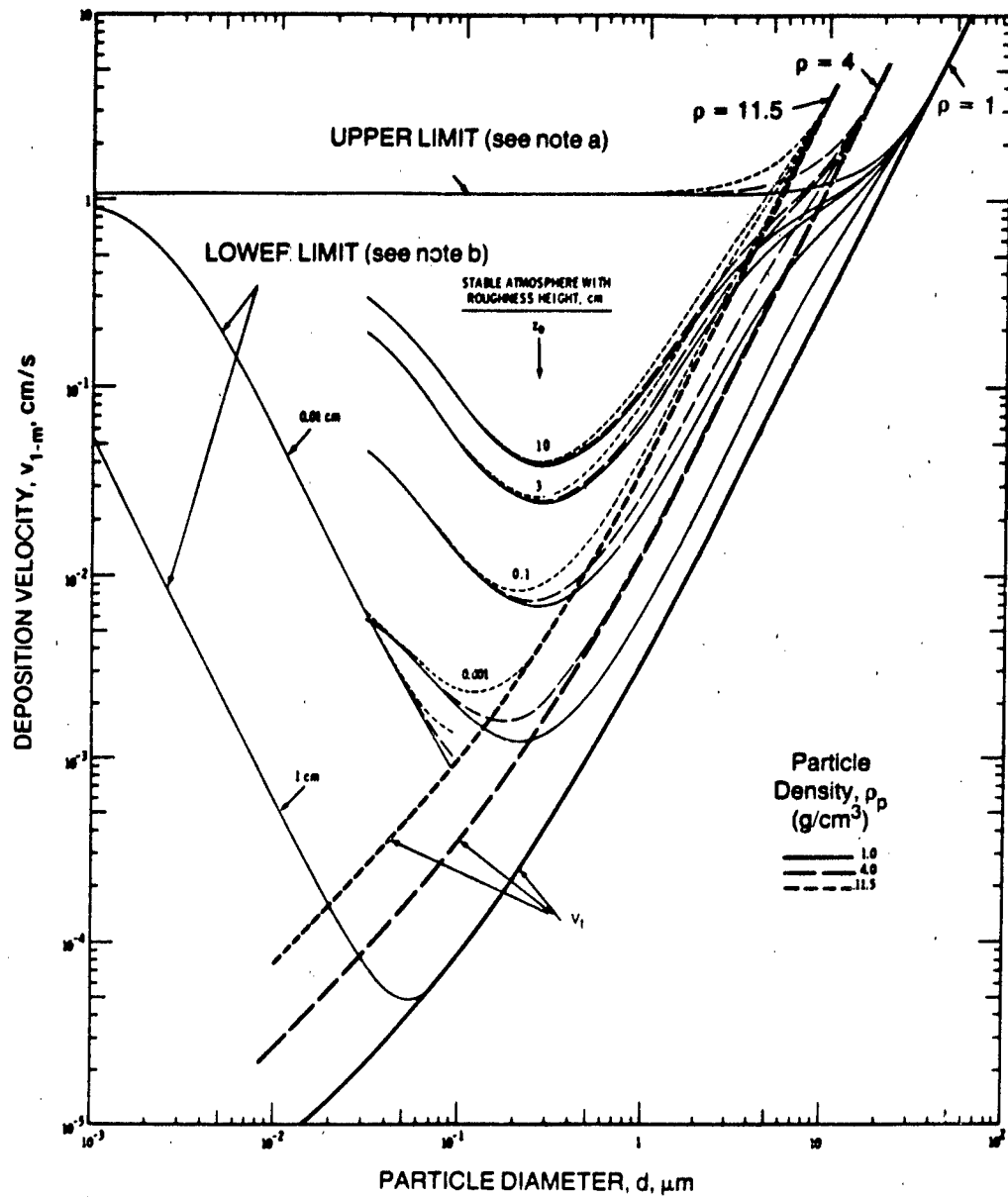
In the case where the wind velocity is known only at one height, a value of z_0 is assumed. Figure 2.5-4 lists roughness lengths for a variety of surfaces. Once the appropriate z_0 is selected, u_* is solved for with equation 3 at the known u and z .

Once u_* and z_0 are known, plots of Sehmel and Hodgson's correlation (in which the deposition velocity at a given friction velocity is plotted as a function of particle diameter for a series of roughness heights and particle densities) can be used. An example of one of these plots is shown in Figure 2.5-5 where the deposition velocity, $v_{1,m}$, is based on a reference height of 1 m. A friction velocity of 30 cm/s is used in this figure; plots for other values can be found in Sehmel's review [21].



Source: Panofsky and Dutton [17]

FIGURE 2.5-4 Roughness Lengths, z_0 , for Various Terrain Types



- a. Based on gravity settling and atmospheric diffusion between 1 cm and 1 m from the surface; no resistance to deposition assumed within 1 cm of the surface.
- b. Between the indicated height and the receiving surface, mass transfer is assumed to be caused by Brownian diffusion only; above indicated height, both turbulent and Brownian diffusion occur.

Source: Sehmel [21]. (Copyright 1980, Pergamon Press, Inc. Reprinted with permission.)

FIGURE 2.5-5 Predicted Particle Deposition Velocities at 1 meter, $v_{1\text{-m}}$, for a Friction Velocity, u_* , of 30 cm/s and Various Particle Densities

To use the plots, z_0 and u_* are determined as described above. After selecting the plot that best corresponds to this friction velocity, the appropriate curve for the particle density and the calculated z_0 is located. With the aid of this curve, the deposition velocity at one meter is read off the ordinate.

The shapes of the curves reflect the importance of gravitational settling, turbulent diffusion, and particle inertia in enhancing the deposition of larger particles ($> 1 \mu\text{m}$) and the effect of Brownian diffusion in promoting the deposition of smaller particles [21].

The lower limits of the deposition velocity are indicated by the two curves on the left side of Figure 2.5-5. Below the height indicated, only Brownian diffusion is assumed to cause mass transfer, while above the specified height, both turbulent and Brownian diffusion occur. The upper limits of deposition velocity are also shown in the figure; these assume no resistance to deposition in the 1-cm layer next to the surface and are based on gravity settling and atmospheric diffusion from 1 cm to 1 m. The three heavy curves show the deposition velocities when they are assumed to equal the terminal settling velocities, V_t .

An improved correlation based on the data used to derive the correlation illustrated in Figure 2.5-5 was published by Sehmel in 1984 [22]. This correlation is given in equation 5 based on a 1-centimeter reference height:

$$v_{1-\text{cm}} = \exp \{ 7.1108 + [\ln(\text{Sc}) \ln(d/z_0)] [0.2529 - 0.00273 \ln(d/z_0)] \\ + [\ln(\tau^*)] [0.03239 \ln(\tau^*) - 0.09177 \ln(d/z_0)] \\ - 0.14919 [\ln(d)]^2 - 4.180 \ln(d/z_0) \} \text{ in cm/s} \quad (5)$$

where:

- $v_{1-\text{cm}}$ = deposition velocity at 1 cm, cm/s
- d = particle diameter, cm
- Sc = Schmidt number, ν/D
- u_* = friction velocity, cm/s
- z_0 = aerodynamic surface roughness, cm
- ν = kinematic viscosity, μ/ρ
- ρ = air density, g/cm³ (1.2×10^{-3} g/cm³ used)
- ρ_p = particle density, g/cm³
- τ^* = dimensionless relaxation time, $(\rho_p d^2 u_*^2)/(18 \mu \nu)$

The term μ is defined after equation 2, and D , the Brownian diffusion coefficient, is calculated using that equation. The values of u_* and z_0 are determined as described above.

This new correlation gives estimates of the deposition velocity based on a 1-centimeter reference height whereas the earlier one was combined with resistances to mass transfer between one centimeter and one meter before being plotted

in Figure 2.5-5, and thus uses a 1-meter height. (The earlier correlation for a 1-centimeter reference height can be found in Sehmel and Hodgson's original publication [23].) Aerodynamic factors (settling and turbulence) become increasingly important in the transport of large particles from one meter to one centimeter, and the deposition velocities of large particles based on a 1-meter reference height are similar to their terminal settling velocities [22]. Because aerodynamic factors between one centimeter and one meter are not considered in equation 5, the estimated deposition velocity may be much greater than the terminal settling velocity for particles as large as 50 μm in diameter [22].

Although Sehmel considers the new correlation improved, except for very small particles and roughness heights greater than three centimeters, the results differ little from the earlier correlation, given the uncertainties involved; on average, the estimates of the earlier correlation are 13% higher and range from a maximum of 3.9 times as large to 0.44 as large [22]. The use of equation 5 is illustrated in example 1.

Example 1 Calculate the deposition velocity of sulfate aerosol to a field of grass 45 cm tall, where the average wind speed has been measured as 4 m/s at a height of 6 m, and the temperature is 18°C. Assume that the particle has a diameter of 0.4 μm and density of 1.5 g/cm³, and that the atmosphere has neutral stability.

To predict the deposition velocity using equation 5, the friction velocity and roughness height must be determined. Since the wind speed is known at only one height, z_0 is assumed. Figure 2.5-4 gives a value for z_0 of approximately 3.5×10^{-2} m for the surface described. A displacement length must be employed to calculate the friction velocity because the surface (tall grass) is not smooth. We will denote this displacement length as d_g . As described above, the displacement length is taken as 80% of the height of the roughness elements:

$$0.8 \times 0.45 \text{ m} = 0.36 \text{ m}$$

Equation 3 (including the term d_g) is rearranged to solve for u_* :

$$\begin{aligned} u_* &= k u / \ln [(z - d_g)/z_0] \\ &= (0.4 \times 4 \text{ m/s}) / \ln [(6 \text{ m} - 0.36 \text{ m}) / 0.035 \text{ m}] \\ &= 0.315 \text{ m/s} \end{aligned}$$

The Brownian diffusion coefficient, D, is also required to evaluate equation 5. It is determined by use of equation 2:

$$D = \frac{1.38 \times 10^{-16} \text{ erg/K} \cdot 291 \text{ K}}{6 \pi \cdot 1.78 \times 10^{-4} \text{ g/(cm s)} \cdot 2 \times 10^{-5} \text{ cm}} \left\{ 1 + \frac{10^{-4}}{p \cdot a} [6.32 + 2.01 \exp(-2190 p \cdot a)] \right\}$$

where:

$$\begin{aligned} p \cdot a &= 76.0 \text{ cm Hg} \cdot 2 \times 10^{-5} \text{ cm} \\ D &= 8.50 \times 10^{-7} \text{ cm}^2/\text{s} \end{aligned}$$

The particle deposition velocity is expressed in terms of $\ln(\text{Sc})$, $\ln(d/z_0)$, $\ln(r^+)$, and $[\ln(d)]^2$ in equation 5. Evaluating each term using the values of u_* , z_0 , and D determined above:

$$\begin{aligned}\text{Sc} &= v/D = (\mu/\rho)/D \\ &= \frac{(1.78 \times 10^{-4} \text{ g}/(\text{cm} \cdot \text{s}) / (1.2 \times 10^{-3} \text{ g}/\text{cm}^3))}{(8.50 \times 10^{-7} \text{ cm}^2/\text{s})}\end{aligned}$$

$$\ln \text{Sc} = 12.07$$

$$d/z_0 = 4 \times 10^{-5} \text{ cm} / 3.5 \text{ cm}$$

$$\ln(d/z_0) = -11.38$$

r^+ is calculated with the value of u_* determined above (31.5 cm/s)

$$r^+ = \rho_p d^2 u_*^2 / [18 \cdot (\mu v)]$$

$$\begin{aligned}r^+ &= \frac{1.5 \text{ g}/\text{cm}^3 (4 \times 10^{-5} \text{ cm})^2 (31.5 \text{ cm}/\text{s})^2}{18 (1.78 \times 10^{-4} \text{ g}/\text{cm} \cdot \text{s} \times 1.78 \times 10^{-4} \text{ g}/\text{cm} \cdot \text{s} / 1.2 \times 10^{-3} \text{ g}/\text{cm}^3)} \\ &= 5.01 \times 10^{-3}\end{aligned}$$

$$\ln(r^+) = -5.30$$

$$d = 4 \times 10^{-5} \text{ cm}$$

$$[\ln(d)]^2 = 102.55$$

Substituting these terms into equation 5 yields:

$$v_{1-\text{cm}} = 0.014 \text{ cm/s}$$

The conditions chosen for the example above were taken from a field study of particulate sulfur deposition by Wesely *et al.* [30] to illustrate the difference between the results of field studies and those obtained based on wind tunnel studies. In that study, a long term mean deposition velocity of $0.22 \pm 0.06 \text{ cm/s}$ with a day-to-day variation of over 50% was measured. This average is based on the concentration measured at 6 meters, and thus is not directly comparable to the deposition velocity obtained in this example, which is based on a 1-cm reference height. However, the value of 0.014 cm/s obtained in this example is considerably less than that found by Wesely *et al.* [30], and would be even smaller (though perhaps only slightly so) if the aerodynamic resistance to transport above 1 cm were included as it is for the 6-meter reference height.

It should be clear from the discussion above that the size of particles greatly affects the magnitude of the various processes contributing to their deposition. Particles are generally classified according to their radius (a) as giant ($a > 1.0 \mu\text{m}$), large ($0.1 < a < 1.0 \mu\text{m}$, the size range most effective for light scattering), or Aitken ($a < 0.1 \mu\text{m}$) [4,32]. Giant particles are also referred to as "coarse" and large and Aitken particles as "fine" [16]. In most aerosols over continental land masses, the concentration (on a number basis) of Aitken particles is much greater than that of large and giant particles, though they normally make up only 10-20% of the aerosol mass [32].

The size distribution of particles in the atmosphere is not static. Smaller particles may collide by any of the deposition mechanisms described above and then adhere together, a process known as coagulation. Particulates are also formed by chemical reactions such as the oxidation of gaseous SO_2 or NO_x to SO_4^{2-} or NO_3^- (either as aqueous acids or their salts), and they may grow as gases sorb to them. Large, mechanically-generated particles (e.g., dust entrained by wind or anthropogenic sources) tend to be short-lived in the troposphere, since they are removed effectively by gravity [16].

DRY DEPOSITION OF GASES

In general, the dry deposition behavior of gases is similar to that of very small particles, except that the gravitational settling of gases is insignificant. As Figure 2.5-1 shows, gases are not susceptible to thermophoretic or electrophoretic effects, because they are not distinct points and are not readily charged. Gas molecules tend to follow the movements of the air with which they are mixed; in the quasi-laminar layer, however, Brownian (molecular) diffusion becomes important, because gas molecules, like small particles, are easily bounced around by molecular collisions.

The effects of the receiving surface on gases are quite different from those on particles, primarily because of the solubility of gases in water and their aqueous-phase reactions [21]. Solubility in water is important in assessing deposition not only on bodies of water but also on surfaces wetted by rain or dew. Furthermore, the interaction of gases with vegetation can involve such processes as the dissolution of gases in leaf fluids after passing through the stomata (the tiny pores covering the surfaces of leaves through which gaseous exchange with the atmosphere occurs), or the reaction with leaf exudates.

Gases also interact with particles in the atmosphere. When sorbed onto particles, they affect both their own deposition velocities and those of the particles. (See section 2.4.) A gas sorbed onto a very small particle (diameter $< 0.1 \mu\text{m}$) has a decreased deposition velocity because the Brownian diffusion coefficient for the particle is much less than that for the gas [21].

The dry deposition of gases (and particles) is often analyzed by using an analogue to Ohm's law in which the overall resistance to deposition is equal to the inverse of the deposition velocity, v_d , and the concentration at a reference height is analogous to the electrical potential. The deposition rate (current) is equal to the concentration (potential) divided by the resistance.

The basic form of the resistance analogue is given by equation 6, where the total resistance, $1/v_d$, is equal to the sum of three resistances in series [31]:

$$1/v_d = r_a + r_s + r_c \quad (6)$$

The three resistances on the right hand side of the equation are in decreasing order of distance from the point of deposition. The aerodynamic resistance, r_a , describes the resistance to transfer between the reference height at which the concentration is measured and the quasi-laminar layer next to the receiving surface [14]. The surface resistance, r_s , is associated with the transfer across the quasi-laminar layer next to the surface [29]. The canopy resistance, r_c , is related to the adsorptivity of the surface for the gas and the opening and closing of stomata [14].

The aerodynamic resistance can be evaluated as [31]:

$$r_a = \frac{\ln(z/z_0) - \psi_c}{k u_*} \quad (7)$$

where ψ_c is a correction function for atmospheric stability, which serves to increase r_a for stable conditions and decrease it for unstable conditions. This function is employed in the study of the transfer of heat and water vapor (ψ_H and ψ_W), and ψ_c for the transfer of trace gases can be approximated by use of the same equations as for ψ_H and ψ_W [31]. The correction function ψ_M is used in the study of momentum transfer; ψ_M is subtracted from the term $\ln(z/z_0)$ in equation 3 to obtain the wind profile when the atmosphere is not neutrally stable [17]. The equations for the correction functions are [31]:

$$\psi_c = \psi_M = \psi_H = \psi_W = -5 z/L \quad (8)$$

for $0 < z/L < 1$, (stable conditions) and

$$\psi_c = \psi_H = \psi_W = \exp\{0.0598 + 0.39 \ln(-z/L) - 0.090 (\ln(-z/L))^2\} \quad (9)$$

$$\psi_M = \exp\{0.032 + 0.448 \ln(-z/L) - 0.132 (\ln(-z/L))^2\} \quad (9a)$$

for $0 > z/L > -1$ (unstable conditions)

The correction functions are expressed in terms of a stability parameter z/L , in which z is the height and L is the Obukhov scale length. The scale length can be evaluated directly by use of the equation given in Shieh *et al.* [24] and Wesely [29], for example. However, its evaluation requires such information as the latent heat flux, which usually is not available. Instead, L can be approximated by use of stability classes such as those of Pasquill [19] or Turner [27], which are based on readily available meteorological variables (airport weather observations in the case of Turner classes). Pasquill classes range from A to G and Turner classes from 1 to 7 (extremely unstable to extremely stable) with D and 4 representing neutral conditions in the respective classes. Golder [10,11] explains how to estimate L with either stability class.

Although Turner classes are less commonly used than Pasquill classes in air pollution work, they provide a better estimate of L [17]. The determination of the Turner class and the estimation of L are described below. If Pasquill classes are already known, they can be converted to Turner classes as follows (Pasquill-Turner): A→1, B→2, C→3, D→4, E→6, F→7, G→7 [11].

TABLE 2.5-1

Turner Classes

Wind Speed (knots) ^d	DAYTIME ^a				NIGHTTIME ^{b,c}		
	>60°	60°-35°	35°-15°	≤15°	Wind Speed (knots)	>4/10	≤4/10
0-1	1	1	2	3	0-3	6	7
2-3	1	2	2	3	4-5	5	5
4-5	1	2	3	4	6	5	6
6-7	2	2	3	4	7-10	4	5
8-9	2	3	3	4	≥11	4	4
10-11	3	3	4	4			
≥12	3	4	4	4			

- a. The use of the daytime table is modified as follows when the cloud cover is > 5/10 and:
 - 1) Cloud ceiling is < 7000 ft: read 2 columns to the right of the indicated column (or the rightmost column). For the special case of 10/10 cloud cover with a ceiling of < 7000 ft, use Turner class 4 regardless of wind speed.
 - 2) Cloud ceiling is from 7000 - 16,000 ft (or > 16,000 ft with 10/10 cloud cover): read 1 column to the right of the indicated column (or the rightmost column).
 - 3) Otherwise, read the table as it appears.
- b. The use of the nighttime table is modified in the following cases:
 - 1) Urban areas classified as 6 or 7 should be made class 5 because they do not become as stable in the lower layers of the atmosphere as rural areas.
 - 2) For complete cloud cover (10/10), with a ceiling of < 7000 ft, use Turner class 4 regardless of wind speed.
- c. Sunset to sunrise
- d. 1 knot = 1.151 miles/hr = 0.514 m/s
- e. Fraction of the sky covered by clouds

Source: Adapted from Turner [27].

Turner classes as a function of meteorological conditions are given in Table 2.5-1. The surface wind speed, cloud cover (fraction of the sky covered by clouds), cloud ceiling height, and solar altitude (angle of the sun above the horizon) are needed to

use this table. The solar altitude depends on the time of day, day of the year, and the line of latitude of the observer. It can be expressed mathematically as [15a]:

$$\alpha = \arcsin (\sin \phi \sin \delta + \cos \phi \cos \delta \cos h) \quad (10)$$

α = solar altitude

ϕ = latitude of the observer

δ = declination of the sun (see Figure 2.5-6)

h = hour angle of the sun

(all in degrees)

The declination of the sun reflects the seasonal change in the height of the sun in the sky, and ranges from -23.45° at the start of winter (Dec. 22) to $+23.45^\circ$ at the start of summer (June 22). It is plotted as a function of the day of the year in Figure 2.5-6.

The hour angle of the sun is a means of expressing the time of day. For the central meridian of a time zone, it can be calculated as:

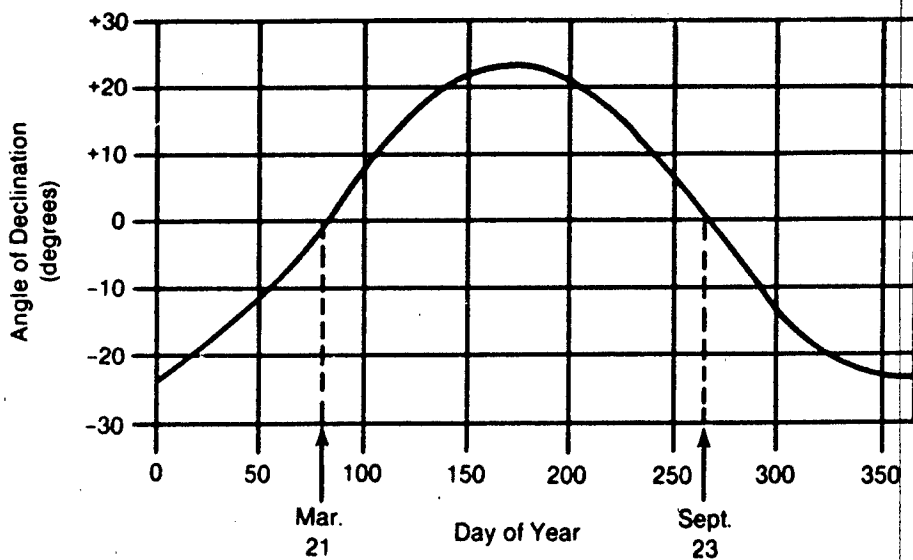
$$h = \frac{\text{hours before noon (-) or hours after noon (+)}}{24 \text{ hrs}} \cdot 360^\circ \quad (11)$$

h = hour angle of the sun, degrees

The hours before or after noon are based on local, standard time. For example, 8:15 am Eastern standard time equals -3.75 hours, but 2:30 pm Eastern daylight time equals +1.5 hours to reflect that standard time has been set ahead an hour for daylight savings. Since equation 11 is for the central meridian of the time zone, for each degree of longitude the observer lies to the east of this meridian, one degree should be added to h , and for each degree west of the meridian, one degree should be subtracted. In the United States, the central meridians for the Eastern, Central, Mountain, and Pacific time zones are 75° , 90° , 105° , and 120° W longitude, respectively.

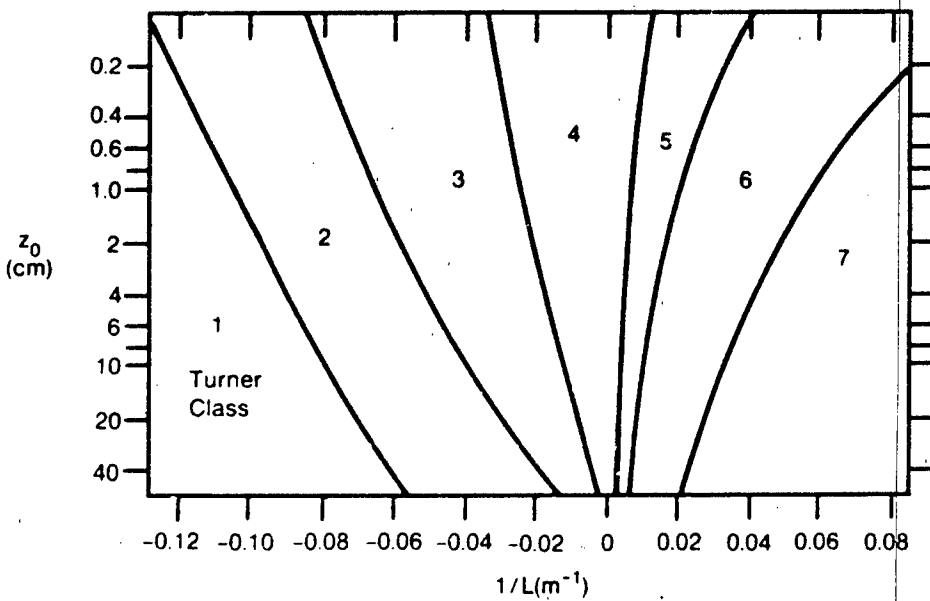
An additional correction to h has been omitted here for the sake of simplicity. Because of this, its true value may deviate from the calculated value by as much as approximately 4° , depending on the time of year. However, it should be sufficiently accurate to find the appropriate range of α for use of Table 2.5-1, since α will never deviate by more than about 4° from its true value either. The omitted correction for the mean solar time can be found in List [15a].

With ϕ , δ , and h determined, α is evaluated with equation 10 and the Turner class read from Table 2.5-1. Once the Turner class is known, $1/L$ can be approximated for a given roughness length by use of Figure 2.5-7. Once L is determined, ψ_c is calculated from either equation 8 or 9, as appropriate, and equation 7 is then evaluated. The calculation of r_a is illustrated in example 2 below, which follows the discussion of r_s and r_c .



Source: After List [15a].

FIGURE 2.5-6 Declination of the Sun Over the Year



Source: Adapted from Golder [11]. (Copyright 1972, D. Reidel Publishing Co. Reprinted with permission.)

FIGURE 2.5-7 $1/L$ as a Function of Turner Class and z_0

To evaluate the surface resistance, r_s , for deposition to vegetation, Wesely and Hicks [31], like others, use a surface transfer function, B^{-1} , where:

$$k B^{-1} = 2 (\kappa / D_c)^{2/3} \quad (12)$$

Again, k is the von Karman constant (typically 0.4); κ is the thermal diffusivity of air (e.g., $0.186 \text{ cm}^2/\text{s}$ @ 0°C , $0.213 \text{ cm}^2/\text{s}$ @ 20°C [28a]) and D_c is the molecular diffusivity for the gas of interest in air (cm^2/s). (Expressions for B^{-1} used by other researchers in various situations are described in Garland [9] and Wesely and Hicks [31].) For SO_2 and ammonia (NH_3), D_c has been measured as 0.122 and $0.198 \text{ cm}^2/\text{s}$, respectively, at 0°C and 1 atm [28a]; nitric oxide (NO), nitrogen dioxide (NO_2), and ozone (O_3) are estimated to have values of 0.175, 0.115, and $0.124 \text{ cm}^2/\text{s}$ at the same temperature and pressure. Because D_c is roughly proportional to the absolute temperature raised to the $3/2$ power, its value at some temperature T_2 can be estimated by multiplying its value at T_1 by $(T_2/T_1)^{3/2}$ (T_1 , T_2 both absolute temperatures) [28a].

The surface resistance is then expressed as:

$$r_s = B^{-1}/u_* \quad (13)$$

For transfer to smooth surfaces (small z_0 , e.g., water) Wesely [29] evaluates r_s as:

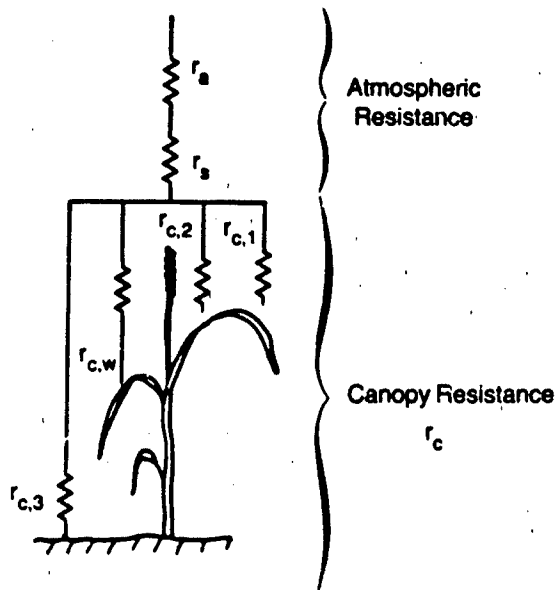
$$r_s = (u_* k)^{-1} \ln (k z_0 u_* / D_c) \quad (14)$$

where all the variables are as previously defined.

The canopy resistance, r_c , is taken as the residual resistance in field studies of deposition rates (whether a canopy of vegetation is present or not). Figure 2.5-8 shows the resistance scheme of Fowler and Unsworth [7] for SO_2 deposition to wheat. Here, the canopy resistance comprises, in parallel, the resistances to SO_2 uptake by stomata, vegetation surfaces, moisture, and soil. For the purposes of estimating the overall resistance, the total canopy resistance is more important than its individual components. Nevertheless, Figure 2.5-8 is useful for illustrating the factors affecting r_c and their temporal variations. For example, stomata close during darkness and periods of water stress (to prevent the plant from desiccation); plants may be covered with dew at night and during mornings whereby $r_{c,w}$ becomes important (e.g., of negligible value in the case of SO_2 deposition).

Wesely and Hicks [31] have suggested a minimum r_c to for SO_2 transfer to field crops at roughly 0.7 s/cm and Sheih *et al.* [22] give rough approximations of r_c for SO_2 for various land use categories and Pasquill stability classes, which serve as an indicator of the surface conditions. Wesely [29] provides equivalent estimates for ozone. Voldner *et al.* [28] give estimates of r_c for SO_2 and NO_x for various conditions, and Huebert and Robert [14] provide values for HNO_3 based on field measurements.

The dependence of r_c on the depositing gas is shown by comparing the resistances of SO_2 , O_3 and NO_x (NO and NO_2 combined) transfer to water bodies. Sulfur dioxide is estimated to have no resistance to lakes or oceans [24] whereas ozone is estimated to have a large resistance—100 s/cm to fresh water lakes and 20 s/cm to the ocean [29], while NO_x is estimated to have a resistance of 70 s/cm to fresh, open water [28].



$r_{c,1}$, $r_{c,2}$, $r_{c,3}$, and $r_{c,w}$ are the canopy resistances to stomatal uptake, deposition on the plant surface, deposition on the soil, and uptake by surface moisture, respectively; r_a is the aerodynamic resistance and r_s the surface resistance.

Source: Adapted from Fowler and Unsworth [7]. (Copyright 1979, Royal Meteorological Society.
Reprinted with permission.)

FIGURE 2.5-8 Resistance Analogue of Dry Deposition of SO_2 to a Wheat Canopy

The following example shows how the three resistances to gaseous deposition can be estimated, and then combined to give a deposition velocity.

Example 2 Estimate the deposition velocity of sulfur dioxide, SO_2 , to a large corn field, 2 meters high, near Burlington, Vermont during mid-afternoon in the second week of August if the wind speed at 10 meters is 8 miles per hour and the day is mostly sunny (cloud cover of 2/10).

The deposition velocity is solved for by use of equation 6, but first, each of the resistances r_a , r_s , and r_c must be estimated. r_a is evaluated by use of equation 7, which requires knowing the value of z_0 , the roughness length, u_* , the friction velocity, and ψ_c , the correction function. Because z_0 is not specified, a value of 5×10^{-2} m, or 5 cm, is read off of Figure 2.5-4. As in example 1, z is adjusted by a displacement length equal to 80% of the crop height. Thus z is taken as 8.4 m ($10 \text{ m} - 0.8 \cdot 2 \text{ m}$) for the rest of this example.

The correction function for atmospheric stability, ψ_c , is determined next. The procedure used here is first to calculate the solar altitude, which is needed to find the Turner class, and then to read $1/L$ from Figure 2.5-7. ψ_c can then be calculated with equation 8 or 9 as appropriate.

The variables ϕ , δ , and h are required to find the solar altitude, α , by use of equation 10. From an atlas or almanac, the position of Burlington, Vermont is found to be $44^{\circ} 28.5' N$, $73^{\circ} 12.8' W$. Thus $\phi = 44^{\circ} + 28.5'/[60('/\circ)] = 44.48^{\circ}$. The angle of declination, δ , is read off of Figure 2.5-6. Assuming "the second week in August" corresponds to August 12, the 224th day of the year, δ equals $+15^{\circ}$. Taking mid-afternoon to be 3:30 pm local time (daylight savings time) then h is evaluated by use of equation 11 as:

$$h = (+2.5 \text{ hrs}/24 \text{ hrs}) \cdot 360^{\circ} = 37.5^{\circ}$$

Since our location lies at $73^{\circ} 12.8' W$, or $1^{\circ} 47.2'$ east of the central meridian for the Eastern standard time zone, the adjustment to h is small, but is included here for illustrative purposes. Thus, $1^{\circ} 47.2'$ or 1.79° is added to h since we are east of the central meridian.

$$h = 37.5^{\circ} + 1.79^{\circ} = 39.29^{\circ}$$

The solar altitude can now be calculated with equation 10:

$$\begin{aligned} \alpha &= \arcsin(\sin 44.48^{\circ} \sin 15^{\circ} + \cos 44.48^{\circ} \cos 15^{\circ} \cos 39.29^{\circ}) \\ &= 45.6^{\circ} \end{aligned}$$

The Turner class is given as a function of wind speed and solar altitude in Table 2.5-1. A wind speed of 8 mph is equivalent to 6.95 knots (1 mph = 0.869 knots). Reading down the second column (α falls between 35° and 60°), Turner class 2 is found to correspond to this wind speed. Now, by use of Figure 2.5-7 for Turner class 2 and z_0 of $5 \times 10^{-2} \text{ m}$, $1/L$ is estimated to be -0.07 m^{-1} .

Thus, $z/L = 8.4 \text{ m} \times -0.07 \text{ m}^{-1} = -0.59$, indicating that equation 9 should be used to find ψ_c ($-1 < z/L < 0$).

$$\begin{aligned} \psi_c &= \exp(0.0598 + 0.39 \ln(0.59) - 0.090 (\ln(0.59))^2) \\ &= 0.843 \end{aligned}$$

Equation 3 is used to evaluate u_* , but first ψ_M must be subtracted from $\ln(z/z_0)$ because the atmosphere is unstable (Turner class 2); from equation 9a:

$$\begin{aligned} \psi_M &= \exp(0.032 + 0.448 \ln(0.59) - 0.132 (\ln(0.59))^2) \\ &= 0.786 \end{aligned}$$

$$\begin{aligned} u_* &= k u / [\ln(z/z_0) - \psi_M] \\ &= \frac{0.4 \times 8 \text{ mph} \times 0.4470 \text{ (m/s)/mph}}{\ln[(8.4 \text{ m})/(5 \times 10^{-2} \text{ m})] - 0.786} \\ &\approx 0.330 \text{ m/s (or } 33.0 \text{ cm/s)} \end{aligned}$$

Now, r_a can be evaluated with equation 7:

$$r_s = \frac{\ln[8.4 \text{ m}/(5 \times 10^{-2} \text{ m})] - 0.843}{0.4 \times 0.330 \text{ m/s}} \\ = 32.4 \text{ s/m (or } 0.324 \text{ s/cm)}$$

To obtain r_s , equations 12 and 13 are combined. Taking D_f for SO_2 and κ at 20°C (from the text above), $\kappa = 0.213 \text{ cm}^2/\text{s}$ and $D_c = (293 \text{ K}/273 \text{ K})^{3/2} \cdot 0.122 \text{ cm}^2/\text{s} = 0.136 \text{ cm}^2/\text{s}$.

$$r_s = \frac{2 [(0.213 \text{ cm}^2/\text{s})/(0.136 \text{ cm}^2)]^{2/3}}{0.4 \times 0.330 \text{ m/s}} \\ = 20.4 \text{ s/m (or } 0.204 \text{ s/cm)}$$

As noted in the text, 0.7 s/cm has been observed as a minimum value of r_c for SO_2 to field crops [31], and we will use that value here. Now that r_s , r_c , and r_c are known, v_d can be evaluated with equation 6.

$$1/v_d = 0.324 \text{ s/cm} + 0.204 \text{ s/cm} + 0.7 \text{ s/cm} = 1.228 \text{ s/cm} \\ v_d = 0.81 \text{ cm/s}$$

In this example it can be seen that the crop canopy, r_c , offers the greatest resistance to SO_2 transfer. Had the field been wet (from a rain shower or spray irrigation, for example) this resistance would have been taken to be zero. The total resistance would have been more than halved resulting in over a doubling of the deposition velocity.

2.5.3 Wet Deposition

Wet deposition is the removal of gaseous and particulate pollutants through such processes as rain, snow, and fog. It can account for a significant fraction of the total atmospheric deposition. For toxic metals, the mean fraction of total atmospheric deposition that occurs as wet deposition has been estimated to be between 0.4 and 0.7 [8]. At locations distant from SO_2 emitters, most of the deposited sulfur from these sources may be deposited in wet form as sulfate [16]. The effects of wet deposition can be important temporally, since precipitation is generally episodic and short lived; they can also be important spatially, because wet deposition may exceed dry deposition in rainy areas.

The wet removal of pollutants from the atmosphere by precipitation is sometimes classified into rainout and washout. *Rainout* is the removal of pollutants within a cloud by such processes as nucleation and interception, while *washout* is the removal of pollutants that occurs below the cloud base. This removal can occur as falling hydrometeors such as rain or snow, combine with gases or particles through any of the mechanisms described above for dry deposition on a surface.

Compared to dry deposition, wet deposition is relatively easy to measure experimentally, except in convective storms. For a given precipitation event, only representative precipitation samples are needed for both volume and concentration measurements. The total deposition for the precipitation event is simply the product of the precipitation volume and the concentration of the constituent in that volume. Because the measurement of wet deposition is straightforward (and because the processes leading up to the deposition are complicated and incompletely understood), the discussion that follows is brief.

Figure 2.5-9, which illustrates the scavenging sequence for atmospheric pollutants, shows the reversibility of many of the processes. "Type 1 mixing" refers to relative movement of the unmixed pollutant and condensed water (e.g., rain falling through a plume), while "Type 2 mixing" occurs as water vapor condenses in the immediate vicinity of pollutants [16]. A more complete description of the processes shown in Figure 2.5-9 is given in *Acid Deposition: Atmospheric Processes in Eastern North America* [16].

PARTICLE SCAVENGING

The removal of particles by precipitation (without considering the specific mechanisms involved) is known as *scavenging*. (This term is sometimes used to mean merely the attachment of particles to falling precipitation, whether or not the particles are actually removed from the atmosphere.) A scavenging coefficient, Λ , which represents the fractional removal of particulates (e.g., on a mass or number basis) per unit time under given precipitation conditions, is used to quantify the process. Figure 2.5-10 illustrates the effect of particle size and size distribution on the scavenging coefficient. In this figure the scavenging coefficient Λ , on a mass basis (hr^{-1}) divided by the rainfall rate, J (mm/hr), is plotted against the geometric mean radius of the particle, R_g (μm). Each curve represents a different distribution of particle sizes, as described by the geometric standard deviation of the particle radii, σ_g . For $\sigma_g = 1$, all the particles in the aerosol have the same radius. The figure is derived for a typical frontal rain storm with droplets having a geometric mean radius of 0.02 cm and a geometric standard deviation of 1.86. The use of Figure 2.5-10 is illustrated by the following example:

Example 3 Calculate the fraction of the aerosol mass concentration, m , remaining, after a three-hour frontal rainstorm if the rainfall rate, J , is 2 mm/hr and the particle geometric mean radius, a_g , is 0.20 μm with a geometric standard deviation, σ_g , of 1.75.

As shown in Figure 2.5-10, an aerosol with the characteristics described above would have a normalized washout coefficient, Λ/J , of about 0.02 mm^{-1} .

Since $J = 2 \text{ mm/hr}$, the fractional rate of aerosol removal is 0.04/hr, i.e.:

$$\frac{dm/m}{dt} = (-\Lambda/J) \cdot J = -0.02 \text{ mm}^{-1} \cdot 2 \text{ mm/hr} = -0.04 \text{ hr}^{-1}$$

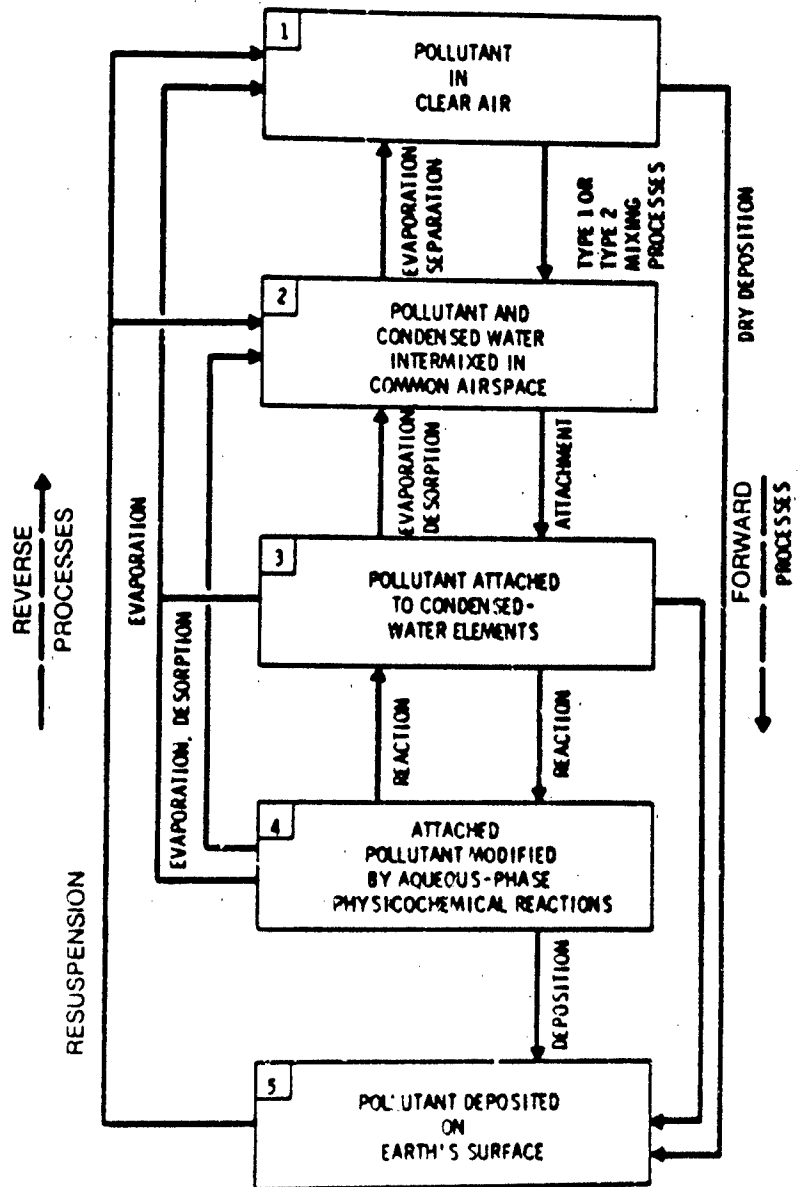
or

$$dm/m = -0.04 dt$$

Integrating this expression,

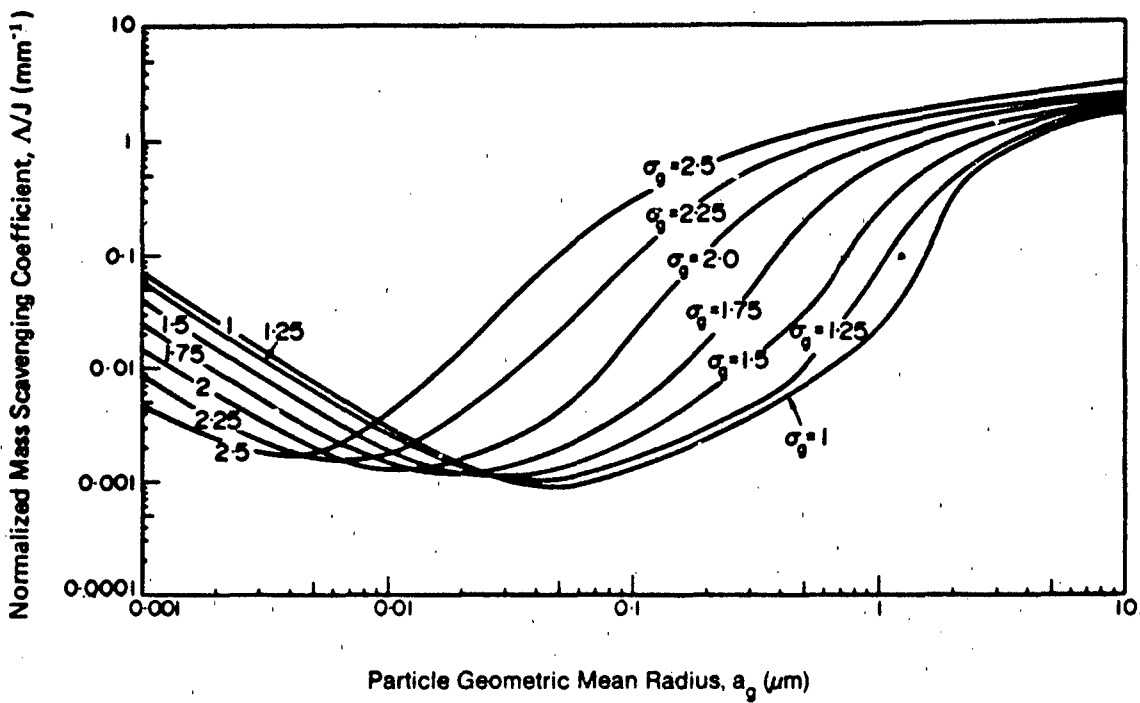
$$m/m_0 = e^{-0.04t}$$

where m_0 is the initial aerosol mass concentration and t is the time since the start of the storm, in hours. Evaluating the equation above for $t = 3$, the fraction of aerosol remaining, m/m_0 , equals 0.89 of the initial value.



Source: National Research Council [16]

FIGURE 2.5-9 Wet Deposition Scavenging Sequence



Particle density = 1 g/cm³; σ_g = geometric std. deviation of particle radii

Source: Dana and Hales[5]. (Copyright 1976, Pergamon Press, Inc. Reprinted with permission.)

FIGURE 2.5-10 Theoretical Mass Scavenging Coefficients Normalized to Rainfall Rate, Based on a Typical Frontal Raindrop Size Spectrum

For small particles (the left-hand side of Figure 2.5-10), Brownian diffusion is effective in moving them to the surface of suspended and falling droplets [16]. As discussed above, the Brownian movement of particles decreases with increasing size; this is why Λ is lower toward the center of the plots.

For large particles, inertial effects become important in scavenging, so Λ increases toward the right. Larger particles are unable to escape a falling hydrometeor by moving with the air flow around it, and thus become attached by collision. Similarly, particles moved through the air by turbulent eddies may collide with droplets in the same way they are dry-deposited on a surface.

The most notable feature of Figure 2.5-10 is the minimum in the scavenging coefficient for particles between 0.01 and 0.1 μm radius (for $\sigma_g = 1$). This region is known as the Greenfield gap and corresponds to the range of particle sizes where neither Brownian diffusion nor inertial impaction is significant [19]. Phoretic effects tend to fill the gap somewhat, but it is still pronounced.

Particles that fall within the Greenfield gap are removed from the atmosphere by other mechanisms. Particles in this size range most readily serve as cloud condensation and ice nuclei and are therefore removed from the atmosphere if cloud formation is followed by precipitation [19].

GAS SCAVENGING

For modeling purposes, it would be desirable to know the gas scavenging ratio ξ , defined as the concentration of a substance in a precipitation sample divided by its concentration in air. However, ξ is usually the result of a model calculation rather than an input [16]. While particle scavenging may be approximated by the procedure described above, gas scavenging is more complex and will not be included here. Hales [12] developed a flow chart for scavenging calculations, which has also been published by the NRC [16]. Slinn [25] has described a method for approximating the scavenging of gases by rain. Readers may consult these references for a description of gas scavenging calculations.

2.5.4 Deposition Velocity Data

Due to the difficulty of measuring and estimating deposition velocities, a value of 1 cm/s is often assumed for predicting either gaseous or particulate deposition rates [21]. Galloway *et al.* [8] have compiled data on the annual deposition quantities of trace metals and on their concentrations in precipitation. Sehmel [21] has compiled deposition velocity data for particles and gases and a variety of surfaces, and Voldner *et al.* [28] list data and experimental conditions from observations of the deposition of sulfur and nitrogen oxides. Some of these data (and those of other researchers) are given in Tables 2.5-2 and 2.5-3; since they are specific to the experimental conditions under which they were determined, caution should be used in applying them to other conditions.

TABLE 2.5-2
Dry Deposition Velocities for Particles

Depositing Material	Deposition Velocity ^a (cm/s)
Particles 0.03 - 30 μm diameter, z_0 from 0.001 - 10 cm	$10^{-3} - 40$
Pollen 20 μm diameter, to microscope slides in grassland	4.5
Sulfate to vegetation to water	0.1 (typically used) ^b 0.4 ± 0.2^c

(Continued)

TABLE 2.5-2 (Continued)
Dry Deposition Velocities for Particles

Depositing Material	Deposition Velocity ^a (cm/s)
to snow, unstable conditions, $u_* = 0.17$ m/s, 0.1 m reference height	0.10 ^c
to beech forest, summer	1.1 ^c
to loblolly pine forest, summer	0.5 ^c
to grass and crops, for both unstable and stable conditions, $u_* = 0.025, 0.30$ m/s, resp.	0.18 ^c
ZnS 5 μm mass mean diameter, to snow	0 - 31
Pb auto exhaust (aggregated) to whole leaves	0.008 - 0.12
Lead, bromine, zinc Urban St. Louis 1973 1975	2.2 \pm 1.4 1.8 \pm 0.7
Natural aerosol 1 - 10 μm diameter, to grass sward	0.8
Ag	<0.3 - 1.1
Al	0.9 - 2.7
As	<0.1 - <0.6; 0.70
Br	0.1 - 2.6; 2.3
Ca	0.4 - 1.4; 2.6
Cd	<0.4 - >8
Ce	0.5 - 1.9
Cl	0.2 - 6.3; 6.4
Co	0.3 - 1.9
Cr	0.6 - 6.8; 0.60
Cs	0.2 - 0.6
Cu	<0.6 - 1.1; 3.0
Eu	0.3 - >2
Fe	1.0 - 2.5; 0.37
I	<0.3 - <2
In	0.3 - >6
K	0.6 - 13; 2.6

(Continued)

TABLE 2.5-2 (Continued)

Depositing Material	Deposition Velocity ^a (cm/s)
La	>0.6 - 3.5
Mg	0.6 - >3
Mn	0.4 - 0.9; 0.59
Na	0.2 - 4.3
Ni	0.7 - <2; 4.0
Pb	0.38
Rb	<0.9 - 3.0
Sb	0.06 - <0.4
Sc	0.6 - 2.5
Se	0.1 - 0.6; 0.24
Sm	0.6 - 4.1
Th	0.7 - 2.2
Ti	0.7 - 2.2; 0.67
V	0.2 - <0.7; 0.24
Zn	0.4 - 4.5; 1.8
Trace elements to open bucket	0.2 - 6.4

Source: Sehmel [21], except as indicated. (Copyright 1980, Pergamon Press, Inc. Reprinted with permission.)

- a. Values following a semicolon represent those of a different researcher.
- b. From NRC [16]
- c. From Voldner, et al. [25]

TABLE 2.5-3
Dry Deposition Velocities for Gases

Depositing Material	Deposition Surface	Deposition Velocity (cm/s)	Source
Cl ₂	Alfalfa	1.8, 2.1	[21]
CO ₂	Alfalfa	0.3	[21]
Fluorides	Forage	1.9 ± 0.5	[21]
HF	Alfalfa	3.5	[21]
H ₂ S	Sandy loam soil	0.015	[21]
Iodine	Grass	7.2 ± 0.9 (upper limit)	[21]
NO _x	Pine needles (summer day)	0.4-0.8 avg.	[28]
NO _x	Crops and grassland (soybeans, summer day, unstable conditions)	0.6	[28]
HNO ₃	Crops and grassland (summer day, 1 m reference height)	2.5 0.9	[28]
O ₃	Deciduous forest (leafless, during winter day) (during winter night)	0.19-0.37 0.05	[29]
O ₃	Soybean canopy (midday, appr. 25% of soil exposed) (windy conditions)	0.85 1.2	[29]
SO ₂	Water (neutral stability, 0.2 m reference height)	0.5 ± 0.1	[28]
SO ₂	Snow (unstable conditions)	0.17	[28]
SO ₂	Forest (dry) (wet)	0.8 1.5	[28]
SO ₂	Grass and crops (unstable conditions. u _* = 0.11 — 0.26 m/s, 2 m reference height)	0.33 ± 0.30	[28]

2.5.5 Literature Cited

1. Arimoto, R. and R.A. Duce, "Dry Deposition Models and the Air/Sea Exchange of Trace Elements," *J. Geophys. Res.*, **91**, 2787-2792 (1986).
2. Cadle, S.H., J. Muhlbauer Dasch, and P.A. Mulawa, "Atmospheric Concentrations, and the Deposition Velocity to Snow of Nitric Acid, Sulfur Dioxide and Various Particulate Species," *Atmos. Environ.*, **19**, 1819-1827 (1985).
3. Chamberlain, A.C., J.A. Garland, and A.C. Wells, "Transport of Gases and Particles to Surfaces with Widely Spaced Roughness Elements," *Boundary-Layer Meteorol.*, **29**, 343-360 (1984).
4. Corn, M., "Aerosols and the Primary Air Pollutants — Nonviable Particles: Their Occurrence, Properties and Effects," in *Air Pollutants, Their Transformations and Transport*, Vol. 1 of *Air Pollution*, 3rd ed., A.C. Stern (ed.), Academic Press, New York (1976).
5. Dana, M.T. and J.M. Hales, "Statistical Aspects of the Washout of Polydisperse Aerosols," *Atmos. Environ.*, **10**, 45-50 (1976).
6. Davies, C.N., "Aerosol Properties Related to Surface Contamination," in *Surface Contamination*, B.R. Fish (ed.), Pergamon Press, New York (1967), as cited in National Research Council [16].
7. Fowler, D. and M.H. Unsworth, "Turbulent Transfer of Sulfur Dioxide to a Wheat Crop," *J. R. Meteorol. Soc.* **105**, 767-783 (1979).
8. Galloway, J.N., J.D. Thornton, S.A. Norton, H.L. Volchok, and R.A.N. McClean, "Trace Metals in Atmospheric Deposition: A Review and Assessment," *Atmos. Environ.*, **16**, 1677-1700 (1982).
9. Garland, J.A., "The Dry Deposition of Sulfur Dioxide to Land and Water Surfaces," *Proc. R. Soc. London, A.*, **354**, 245-268 (1977).
10. Golder, D.G., "A Comparison of Stability Parameters," M.S. Thesis, Department of Meteorology, The Pennsylvania State U., University Park, Pennsylvania (1970).
11. Golder, D.G., "Relations Among Stability Parameters in the Surface Layer," *Boundary-Layer Meteorol.*, **3**, 47-58 (1972).
12. Hales, J.M., "Precipitation Chemistry: Its Behavior and Calculations," in *Air Pollutants and Their Effects on the Terrestrial Ecosystem*, S.V. Krupper and A.H. Legge (eds.), John Wiley & Sons, New York (1983).
13. Hidy, G.M., "Removal Processes of Gaseous and Particulate Pollutants," in *Chemistry of the Lower Atmosphere*, S.I. Rasool (ed.), Plenum Press, New York (1973).
14. Huebert, B.J. and C.H. Robert, "The Dry Deposition of Nitric Acid to Grass," *J. Geophys. Res.*, **90**, 2085-2090 (1985).
15. Jenkin, M.E., "An Investigation into the Enhancement of Deposition of Hygroscopic Aerosols to Wet Surfaces in a Wind Tunnel," *Atmos. Environ.*, **18**, 1017-1024 (1984).
- 15a. List, R.J., *Smithsonian Meteorological Tables*, 6th revised ed., Smithsonian Institution, Washington, D.C. (1951).

16. National Research Council, *Acid Deposition: Atmospheric Processes in Eastern North America*, National Academy Press, Washington, D.C. (1983).
17. Panofsky, H.A. and J.A. Dutton, *Atmospheric Turbulence: Models and Methods for Engineering Applications*, John Wiley & Sons, New York (1984).
18. Pasquill, F., "The Estimation of the Dispersion of Windborne Material," *Meteorol. Mag.*, **3**, 47-58 (1972).
19. Pruppacher, H.R. and J.D. Klett, *Microphysics of Clouds and Precipitation*, D. Reidel Publishing Co., Dordrecht, Holland (1978).
20. Sehmel, G.A., "Particle Diffusivities and Deposition Velocities over a Horizontal Smooth Surface," *J. Colloid and Interface Sci.*, **37**, 891-906 (1971).
21. Sehmel, G.A., "Particle and Gas Dry Deposition: A Review," *Atmos. Environ.*, **14**, 983-1011 (1980).
22. Sehmel, G.A., "Dry Deposition Velocities," Paper Prepared for Presentation at the California Air Resources Board Workshop on Dry Acid Deposition, March 26, 1984, San Francisco, Calif. (March, 1984), NTIS PNL-SA-12156.
23. Sehmel, G.A. and W.H. Hodgson, "A Model for Predicting Dry Deposition of Particles and Gases to Environmental Surfaces," Battelle Pacific Northwest Laboratory, Richland, Washington, (January, 1978) PNL-SA-6721 (and in revised form October, 1979, PNL-SA-6721-REV-1).
24. Shieh, C.M., M.L. Wesely, and B.B. Hicks, "Estimated Dry Deposition Velocities of Sulfur over the Eastern United States and Surrounding Regions," *Atmos. Environ.*, **13**, 1361-1368 (1979).
25. Slinn, W.G.N., "Some Approximations for the Wet and Dry Removal of Particles and Gases from the Atmosphere," *Water Air Soil Pollut.*, **7**, 513-43 (1977).
26. Slinn, W.G.N., "Predictions for Particle Deposition to Vegetative Canopies," *Atmos. Environ.*, **16**, 1785-1794 (1982).
27. Turner, D.B., "A Diffusion Model for an Urban Area," *J. Appl. Meteorol.*, **3**, 83-91 (1964).
28. Voldner, E.C., L.A. Barrie and A. Sirois, "A Literature Review of Dry Deposition of Oxides of Sulfur and Nitrogen with Emphasis on Long-Range Transport Modelling in North America," *Atmos. Environ.*, **20**, 2101-2123 (1986).
- 28a. Welty, J.R., C.E. Wicks, and R.E. Wilson, *Fundamentals of Momentum, Heat, and Mass Transfer*, 2nd ed., John Wiley & Sons, New York (1976).
29. Wesely, M.L., "Turbulent Transport of Ozone to Surfaces Common in the Eastern Half of the United States," in *Trace Atmospheric Constituents: Properties, Transformations, and Fates*, S.E. Schwartz (ed.), John Wiley & Sons, New York (1983).
30. Wesely, M.L., D.R. Cook, R.L. Hart, and R.E. Speer, "Measurement and Parameterization of Particulate Sulfur Dry Deposition Over Grass," *J. Geophys. Res.*, **90**, 2131-2143 (1985).
31. Wesely, M.L., and B.B. Hicks, "Some Factors that Affect the Deposition Rates of Sulfur Dioxide and Similar Gases on Vegetation," *J. Air Pollut. Control Assoc.*, **27**, 1110-1116 (1977).
32. Williamson, S.J., *Fundamentals of Air Pollution*, Addison-Wesley Publishing Co., Reading, Mass. (1973).

2.6 ACTIVITY COEFFICIENT

2.6.1 Introduction

As applied to dissolved species in solution, an activity coefficient, γ , is a factor that corrects for nonideal behavior relating to chemical reactivity.¹ In an ideal solution, the components coexist with no volume effects and no interaction energies. In such ideal systems, chemical interactions are described by relationships of species concentrations. As solutions approach infinite dilution, the behavior of their components approaches this ideal behavior. However, in nonideal systems, the actual chemical "activity" of an ion is smaller than the measured concentration by a factor represented by the activity coefficient. For an ion A, we define:

$$\langle C_A \rangle = \gamma_A [C_A] \quad (1)$$

where

$\langle C_A \rangle$ = activity of ion A in solution

γ_A = activity coefficient of ion A in solution ($0 < \gamma_A \leq 1$ in most cases)

$[C_A]$ = concentration of ion A in solution

Systems found in the environment (fresh waters, seawater, concentrated saline brines, leachates) are not infinitely dilute; therefore, the dissolved species that they contain cannot be assumed to behave ideally. Activity coefficients may be needed for the calculation of equilibrium reaction constants (e.g., solubility constants) and equilibrium concentrations for such systems. The use of activity coefficients is especially important and necessary in systems that deviate significantly from ideal behavior, i.e., concentrated or high-ionic-strength solutions such as saline brines. Seawater is a unique solution of practically constant ionic composition; as a result, activity coefficients for species in seawater may be specially described in relation to this constancy.

This section covers the following topics:

- Description of the activity coefficient and its relationship to activities, concentrations and equilibrium constants;
- The importance and use of the activity coefficient in calculations for environmental systems;
- Key variables (ionic strength and temperature) that affect the value of the activity coefficient; and
- Available methods for estimating activity coefficients, their limitations and examples of their use.

1. See section 2.6.2, which discusses the alternative "activity coefficient" relating to nonideal behavior of organics in solution (i.e., nonideal with regard to phase partitioning).

2.6.2 Description of Activity Coefficient

Chemical species in solution interact in a variety of ways. Some of these interactions are strong and are considered to be "chemical reactions"; others are defined as "nonideal" effects that cause a system to depart from ideal behavior and affect the chemical reactions occurring in the solution. In dilute electrolyte mixtures (with ionic strength $I < 10^{-2} M$), deviations from ideal behavior are primarily due to long-range electrostatic interactions among ions, i.e., attractions of ions of opposite charge and repulsion of ions of like charge. In more concentrated solutions ($I > 10^{-2} M$), the deviations are due to the general electric fields of the ions, solute-water interactions and specific ionic interactions (e.g., ion-pair formation, complex formation)[19]. All these interactions on an ion serve to stabilize it and therefore decrease its chemical reactivity in the solution. The activity coefficient may be perceived as a measure of this decreased reactivity.

DEFINITION

The activity coefficient, γ_A , of ion A in solution is defined by equation 1 above or by:

$$\gamma_A = \frac{(C_A)}{[C_A]} \quad (2)$$

where

(C_A) indicates activity of species A

$[C_A]$ indicates concentration of species A

Since the activity and concentration are expressed in the same units (e.g., molar or molal), the activity coefficient is a dimensionless factor.

For a reaction:



the activity equilibrium constant is defined as:

$$K_a = \frac{(C)^c (D)^d}{(A)^a (B)^b} \quad (4)$$

The parentheses signify the activity of each species at equilibrium. In terms of concentrations:

$$K_a = \frac{\gamma_C^c [C]^c \gamma_D^d [D]^d}{\gamma_A^a [A]^a \gamma_B^b [B]^b} = \frac{\gamma_C^c \gamma_D^d [C]^c [D]^d}{\gamma_A^a \gamma_B^b [A]^a [B]^b} = \frac{\gamma_C^c \gamma_D^d}{\gamma_A^a \gamma_B^b} K_e \quad (5)$$

where K_c is the equilibrium constant expressed in terms of equilibrium concentrations:

$$K_c = \frac{[C]^p [D]^q}{[A]^a [B]^b} \quad (6)$$

It is important to know if values of equilibrium constants reported in the literature and used in calculations are based on activities or concentrations. Values are sometimes reported as a mixture of both activities and concentrations.

In the ideal system,

$$\left. \begin{array}{l} \gamma_i = 1 \\ K_a = K_c \end{array} \right\} \quad (7)$$

and

CONVENTIONS

There are basically two conventions by which the reference state (or ideal system at which $\gamma_i = 1$ and activity equals concentration) is defined. These are the Infinite Dilution Scale and the Ionic Medium Scale. The choice of one convention over the other is primarily based on the solution under consideration.

The Infinite Dilution Scale

In this convention, the activity coefficient of species A, γ_A (equation 2), is defined such that γ_A approaches 1 as the concentration of all solutes in solution approaches 0.

$$\gamma_A \rightarrow 1 \text{ as } [C_A] + \sum_i [C_i] \rightarrow 0 \quad (8a)$$

where $[C_i]$ = concentration of all solutes in solution.

For the solvent,

$$\left. \begin{array}{l} (\text{solvent}) = \gamma_{\text{solvent}} x_{\text{solvent}} \\ \gamma_{\text{solvent}} \rightarrow 1 \text{ as } x_{\text{solvent}} \rightarrow 1 \end{array} \right\} \quad (8b)$$

where x_{solvent} = mole fraction of the solvent
 (solvent) = activity of the solvent

In dilute solutions ($I < 10^{-2} M$), e.g., in many fresh waters, the infinite dilution activity convention is used. The relationship of the equilibrium constant based on activities (K_a) to the equilibrium constant based on concentrations (K_c) has been shown above (equation 5). The activity coefficients should be calculated for the conditions of ionic strength and temperature of the solution under consideration.

The Ionic Medium Scale

In this convention, the reference state is a specified ionic medium, instead of the infinitely dilute solution above. It is useful in solutions (e.g., seawater) where there is a background concentration of inert electrolyte that provides the constant ionic medium. In this case, the activity coefficient, γ' , approaches 1 as the concentrations of all ions *other than the medium ions* approach 0; i.e.,

$$\gamma' \rightarrow 1 \text{ as } [C_A] \rightarrow 0 \quad (8c)$$

where $[C_A]$ = concentration of all ions except the major medium ions.

If the concentrations of the medium ions are more than approximately 10 times the concentration of the solute species under consideration, the activity coefficients of the species may be approximated as 1 [19].

Seawater is a solution of practically constant ionic composition. The ionic medium activity scale is thus particularly useful for equilibrium calculations in seawater systems and more concentrated solutions [19].

The value of the activity coefficient is usually greater than 0 and less than or equal to 1. In certain cases, γ may go above 1 (see below in § 2.6.3 on neutral components in solution and on very high ionic strength solutions).

The equilibrium constant for a reaction using the constant ionic medium convention is called the *apparent equilibrium constant*, K_{app} . For example, the second dissociation constant for carbonate in solution,



is written as:

$$K_{app} = \frac{(H^+) [CO_3^{2-}]_T}{[HCO_3^-]} \quad (10)$$

where the subscript T refers to the total concentration of ions, both free and associated. If the concentration of the constant medium is very high compared with that of the ions under consideration, the activity coefficients of the ions may be approximated as 1. However, the apparent equilibrium constant must be determined for the medium under consideration.

The conventions above may be contrasted with the activity coefficient for organic solute solutions (including organic solutes in water), which is defined as:

$$\gamma_A = P_A / X_A P_A^0 \quad (11)$$

where

γ_A = activity coefficient of component A

P_A = partial pressure of component A

x_A = mole fraction of component A in solution

P_A^0 = vapor pressure of pure liquid of component A

The activity coefficients for organic solute solutions range in value from 0.4 up to 10⁷ [2].

For all dilute solutions, using a standard state of pure water, the activity of water is defined as 1. In seawater, the activity of water is defined as the ratio of vapor pressure of the seawater, P_g , to that of pure water, P_{H_2O} . It is close to 1 and does not usually fall below 0.98 [19].

When a solid is in equilibrium with a solution, the pure solid phase is selected as the reference state, and its activity is set to 1. For gases in equilibrium with a solution, the activity coefficient, γ_g (or fugacity coefficient) is defined as:

$$\gamma_g = \frac{(f_g)}{P_g} \quad (12)$$

where

P_g = partial pressure of gas in atmosphere

(f_g) = fugacity of the gas (the equivalent of activity)

As the total pressure decreases, $\gamma_g \rightarrow 1$. Gases deviate from ideal behavior only at very high pressures. Reactions at atmospheric pressure are considered to occur at sufficiently low pressures for the assumption of ideal behavior, and the activity of a gas is estimated by its partial pressure.

SINGLE ION ACTIVITY AND MEAN ION ACTIVITY COEFFICIENTS

The single ion activity coefficient, also known as the individual ion activity coefficient, is the activity coefficient of a cation or anion by itself, without its companion anion or cation respectively. Because anions cannot be added to solutions without an equivalent number of cations (and vice versa), the single ion activity (γ_+ or γ_-) cannot be determined experimentally. Instead, the product $\gamma_+ \gamma_-$ is experimentally measured. The mean ion activity coefficient, γ_{\pm} , for a univalent symmetrical compound (e.g., KCl) is defined as:

$$\gamma_{\pm} = (\gamma_+ \gamma_-)^{1/2} \quad (13)$$

The single ion activities of the ions of a univalent symmetrical compound are approximately equal to each other and to the mean ion activity coefficient:

$$\gamma_+ \approx \gamma_- \approx \gamma_{\pm} \quad (14)$$

Stumm and Morgan [19] have provided relationships between single and mean ion activity coefficients for other types of compounds.

FREE ACTIVITY AND TOTAL ACTIVITY COEFFICIENTS

Many ions, particularly major anions such as SO_4^{2-} , HCO_3^- and CO_3^{2-} , often exist in solution both as free ions and associated with other ions in complexes or ion pairs. It is difficult to establish unambiguously the types of interactions that occur with these ions; therefore, a total activity coefficient, γ_A^T , has been defined:

$$\gamma_A^T = \frac{(C_A)}{[C_A]_T} \quad (15)$$

where

(C_A) = activity of A in solution

$[C_A]_T$ = total (free and associated) ion concentration of A in solution

The free activity coefficient, γ_A^F , is defined as:

$$\gamma_A^F = \frac{(C_A)}{[C_{A\text{ free}}]} \quad (16)$$

where "free" represents aquo-associated ions of SO_4^{2-} , CO_3^{2-} , etc.

Total activity coefficients are dependent on the ionic composition of the system. The use of total activity coefficients is particularly appropriate for seawater because of the constancy in ionic composition and the elimination of ion pair formation constants from the calculations. Also, the total activity coefficient is more amenable to experimental measurement than individual ion pair or complex formation constants.

IMPORTANCE IN ENVIRONMENTAL CALCULATIONS

The activity coefficient is important in equilibrium calculations for environmental systems, because natural systems are rarely ideal. Corrections from concentrations to the lower activity values may sometimes be smaller than the errors associated with use of equilibrium constants from the literature, where it is not unusual to find cited values that span orders of magnitude.

Example 1 Determine the error in the calculated solubility of CaF_2 in a solution of $I = 0.1M$, if non-ideality is ignored. At this ionic strength, $\gamma_{\text{Ca}^{+2}} = 0.38$ and $\gamma_{\text{F}^-} = 0.79$ (using the Davies method described in § 2.6.3).

The activity equilibrium solubility constant, $K = 10^{-10.41}$ (mole/liter)³ [7]

$$K_s = (\text{Ca}^{+2})(\text{F}^-)^2 = \gamma_{\text{Ca}^{+2}} \gamma_{\text{F}^-}^2 [\text{Ca}^{+2}][\text{F}^-]^2 \quad (17)$$

If we assume ideal solutions and all $\gamma = 1$,

$$K_c = [\text{Ca}^{+2}] [\text{F}^-]^2 = 10^{-10.41} \quad (18)$$

which gives solution concentrations in equilibrium with $\text{CaF}_2(s)$ as follows:

$$\begin{aligned} [\text{Ca}^{+2}] &= 2 \times 10^{-4} M \\ [\text{F}^-] &= 4 \times 10^{-4} M \end{aligned}$$

If the activity coefficients were considered,

$$\begin{aligned} K &= \gamma_{\text{Ca}^{+2}} [\text{Ca}^{+2}] \gamma_{\text{F}^-}^2 [\text{F}^-]^2 \quad (19) \\ 10^{-10.41} &= (0.38) [\text{Ca}^{+2}] (0.79)^2 [\text{F}^-]^2 \\ [\text{Ca}^{+2}] [\text{F}^-]^2 &= 1.64 \times 10^{-10} \end{aligned}$$

which gives these concentrations in equilibrium with $\text{CaF}_2(s)$:

$$\begin{aligned} [\text{Ca}^{+2}] &= 3.4 \times 10^{-4} M \\ [\text{F}^-] &= 6.9 \times 10^{-4} M \end{aligned}$$

Thus, when activity coefficients are not included, the calculated saturation concentration is lower by around 40%.

VARIABLES AFFECTING THE VALUE OF ACTIVITY COEFFICIENTS

Other than those values intrinsic to the ion (e.g., charge and ion size), the key variables that affect the magnitude of the activity coefficient of an ion are solution ionic composition and concentrations (which determine the ionic strength) and temperature. Pressure affects the activity coefficient only at extremely high pressures, which are not normally encountered under environmental conditions; these effects will be neglected here. A brief discussion of pressure effects is given in Stumm and Morgan [19].

The effect of temperature, T, on the infinite dilution scale activity coefficient is described by:

$$\frac{d \ln \gamma_i}{dT} = \frac{\bar{H}_i^0 - \bar{H}_i^i}{RT^2} \quad (20)$$

where:

\bar{H}_i^i = partial molal enthalpy in actual solution

\bar{H}_i^0 = standard-state value of partial molal enthalpy

R = gas constant

An activity coefficient is defined for a particular temperature. The effect of temperature on the activity coefficients of electrolytes becomes appreciable at concentra-

tions greater than 0.1 molal, when $\bar{H}^0 - \bar{H}_1$ becomes significant [19]. In seawater, the activity coefficients of ions are significantly influenced by temperature. The magnitude and direction of the effect is dependent on the magnitude and sign of the heat of reaction as a function of temperature [19]. However, few measurements of partial molal enthalpies exist.

The ionic composition of the species in solution determines the ionic strength of the solution. The ionic strength, I , is defined by:

$$I = \frac{1}{2} \sum_i C_i Z_i^2 \quad (21)$$

where:

C_i = concentration of ionic species, i , in solution

Z_i = charge of species, i , in solution

Values of ionic strength in environmental systems range from:

Fresh water $< 0.01M$ to $< 0.1M$

Seawater $\sim 0.7M$

Saline brines $\geq 5M$

Example 2 Calculate the ionic strength of a solution containing:

$$[Na^+] = 10^{-4}M \quad [Cl^-] = 2 \times 10^{-4}M$$

$$[H^+] = 10^{-4}M \quad [HCO_3^-] = 2 \times 10^{-5}M$$

$$[Mg^{+2}] = 10^{-5}M$$

From equation 21,

$$\begin{aligned} I &= \frac{1}{2} \{ [Na^+] (1)^2 + [Cl^-] (-1)^2 + [Mg^{+2}] (2)^2 + [H^+] (1)^2 + [HCO_3^-] (-1)^2 \} \\ &= \frac{1}{2} [10^{-4} + 2 \times 10^{-4} + (4 \times 10^{-5}) + 10^{-4} + 2 \times 10^{-5}] \\ &= 2.3 \times 10^{-4}M \end{aligned}$$

In many natural waters, the ionic composition may be unknown and the ionic strength cannot be calculated by equation 21. In such cases, empirical relationships can be used to approximate the ionic strength from measured parameters. The two following relationships for natural waters, for example, are based on total dissolved solids and specific conductance [18]:

$$I = 2.5 \times 10^{-5} \times TDS \quad (22)$$

and

$$I = 1.6 \times 10^{-5} \times \text{specific conductance} \quad (23)$$

where:

I = ionic strength (M)

TDS = total dissolved solids (mg/l)

Specific conductance is in $\mu\text{mho}/\text{cm}$

Horne [4] has suggested an empirical relationship to estimate the ionic strength of seawater:

$$I = 0.0054 + 0.01840 (S\%) + 1.78 \times 10^{-5} (S\%)^2 - 3.0 \times 10^{-4} (25 - T) + 7.6 \times 10^{-6} (P) \quad (24)$$

where:

I = ionic strength in molal units (mol/kg)

S = salinity (34-36‰ in open ocean water, where
‰ = parts per thousand)

T = temperature (°C)

P = atmospheric pressure (atm)

2.6.3 Estimation Methods

Methods for estimating activity coefficients are of two basic types: those for low-ionic-strength solutions (<0.5M) and those for high-ionic-strength solutions (>1M).

Methods in the first category are based on the Debye-Hückel assumption that deviations from ideal behavior in dilute solutions are primarily caused by long-range electrostatic interactions. All these methods have the general form:

$$\log \gamma_i = - \frac{AZ_i^2 \sqrt{I}}{1 + BA_i \sqrt{I}} - b_i I \quad (25)$$

where:

γ_i = single ion activity coefficient

A, B = Debye-Hückel constants

I = ionic strength of the solution (M)

Z_i = charge of ion i

a_i = empirical parameter representing the distance of closest approach between centers of adjacent ions

b_i = adjustable parameter

Four methods based on the Debye-Hückel assumption are frequently used: Debye-Hückel, extended Debye-Hückel, Gunterberg, and Davies. These are described in many chemistry texts [11, 12, 19].

At higher ionic strengths, two methods are used. One of these is based on the Brønsted-Guggenheim specific ion interaction model, which leads to a virial equation of the general form:

$$\log \gamma_i = \log \gamma_{iDH} + \sum_j B_{ij}[j] + \sum_j \sum_k C_{ijk}[j][k] + \dots \quad (26)$$

where:

γ_i = single ion activity coefficient of ion i

γ_{iDH} = Debye-Hückel activity coefficient

$[j], [k]$ = molar concentrations of species j and k

B_{ij} = second virial coefficients for specific interactions among pairs of ions

C_{ijk} = third virial coefficients for specific interactions among three ions

Pitzer and co-workers [10] have provided expressions to calculate the virial coefficients for equation 26 for a variety of ions.

The other method applicable to high-ionic-strength solutions was developed by Kusik and Meissner [6]. It is based on experimental observations of the behavior of activity coefficients with ionic strength, which were then developed into empirical relationships.

Table 2.6-1 summarizes all of the above estimation methods and the range of their applicability. Each method is described in greater detail below.

DEBYE-HÜCKEL METHOD

The Debye-Hückel approximation is given by:

$$\log \gamma_i = -AZ_i^2 \sqrt{I} \quad (27)$$

where:

A = ion-size parameter for water (in aqueous solutions)

Z_i = ionic charge of ion i

I = ionic strength of solution (M)

The parameter A is related to the solvent dielectric constant, D, and temperature by:

$$A = 1.823 \times 10^6 / (DT^{3/2}) \quad (28)$$

where:

D = dielectric constant of solvent

T = temperature (K)

For water at 25°C, A is approximately 0.5. Values of A at other temperatures are given by Pagenkopf [12].

The Debye-Hückel estimation method is applicable to dilute solutions with ionic strength less than $5 \times 10^{-3} M$.

TABLE 2.6-1
Summary of Methods for Estimating Activity Coefficients

Method	Equation ^a	Range of I Over Which Method is Valid (M)
For low-ionic-strength solutions:		
Debye-Hückel	$\log \gamma_i = -AZ_i^2 \sqrt{I}$	$0 - 10^{-2.3}$
Extended Debye-Hückel	$\log \gamma_i = -AZ_i^2 \frac{\sqrt{I}}{1 + Ba_i \sqrt{I}}$	$0 - 10^{-1}$
Günzberg ^b	$\log \gamma_i = -AZ_i^2 \frac{\sqrt{I}}{1 + \sqrt{I}}$	$0 - 10^{-1}$
Davies	$\log \gamma_i = -AZ^2 \left(\frac{\sqrt{I}}{1 + \sqrt{I}} - 0.3I \right)$	$0 - 0.5$
For high-ionic-strength solutions:		
Pitzer et al.	Binary Solution: $\log \gamma_{\pm}(MX) = Z_M Z_X I + m(\beta^0 + I^1 \beta^1) + 1.5 m^2 c^2$ Mixed Electrolyte Solution: $\log \gamma_M = Z_M^2 I + 2 \sum m_a (B_{Ma} + EC_{Ma})$ $+ Z_M^2 \sum_c \sum_a m_c m_a B_{ca}^1 + Z_M \sum_c \sum_a m_c m_a C_{ca}$ $\log \gamma_X = Z_X^2 I + 2 \sum m_c (B_{cX} + EC_{cX})$ $+ Z_X^2 \sum_c \sum_a m_c m_a B_{ca}^1 + Z_X \sum_c \sum_a m_c m_a C_{ca}$	$0 - 6$
Meissner et al.	$\gamma_r = \gamma_{\pm}^{1/Z_1 Z_2}$ $\gamma_r = \{1 + B(1 + 0.1 I)^q - BI\} \gamma^*$ $B = 0.75 - 0.065 q$ $\log \gamma^* = \frac{-0.5107 \sqrt{I}}{1 + C \sqrt{I}}$ $C = 1 + 0.055 q \exp(-0.023 I^3)$ Mixed Electrolyte Solution: $\log \gamma_{ij} = \frac{Z_i}{Z_i + Z_j} (V_{i2} I_2 \log \gamma_{i2}^0 + V_{i4} I_4 \log \gamma_{i4}^0 + \dots) / I$ $+ \frac{Z_j}{Z_i + Z_j} (V_{j1} I_1 \log \gamma_{j1}^0 + V_{j3} I_3 \log \gamma_{j3}^0 + \dots) / I$	$0 - 100$

a. See § 2.6.3 for definitions of parameters.

b. Useful in solutions of several electrolytes.

EXTENDED DEBYE-HÜCKEL METHOD

The extended Debye-Hückel approximation is given by:

$$\log \gamma_i = -AZ_i^2 \frac{\sqrt{I}}{1 + Ba_i \sqrt{I}} \quad (29)$$

In addition to the parameters used in the Debye-Hückel approximation, two others are used in the extended Debye-Hückel:

B = parameter dependent on solvent dielectric constant and absolute temperature

a_i = empirical parameter representing distance of closest approach between centers of adjacent ions (\AA)

The parameter B is given by:

$$B = 50.3 (DT)^{-1/2} \quad (30)$$

where:

D = dielectric constant of solvent

T = temperature (K)

For water at 25°C, B is approximately 0.33.

The parameter a_i corresponds roughly to the radius of the hydrated ion, i, in angstroms and has a value between 3 and 9. Table 2.6-2 lists values of "a" for various ions.

The extended Debye-Hückel estimation method is applicable to dilute solutions with ionic strength less than 0.1 M.

Example 3 What is the activity coefficient of CO₃⁻² in lake water with an ionic strength of 0.02 M?

Using the extended Debye-Hückel method:

$$\log \gamma_i = -AZ_i^2 \frac{\sqrt{I}}{1 + Ba_i \sqrt{I}}$$

For CO₃⁻², a = 5 (see Table 2.6-2)

For water, A = 0.5, B = 0.33

TABLE 2.6-2
Values of the Parameter "a" for Some Ions

Empirical Parameter, a (Å)	Cations	Anions
3	K^+ , Ag^+ , NH_4^+ , Rb^+ , Cs^+	OH^- , F^- , Cl^- , I^- , Sr^+ , CN^- , NO_2^- , NO_3^- , ClO_3^- , ClO_4^- , MnO_4^-
4	Na^+ , Hg_2^{+2} , $CdCl^+$	HCO_3^- , $H_2PO_4^-$, HSO_3^- , $SO_4^{=2}$, $HPO_4^{=2}$, $SeO_4^{=2}$, $CrO_4^{=2}$, $PO_4^{=3}$, $H_2AsO_4^-$, $S_2O_3^{=2}$
5	Sr^{+2} , Ba^{+2} , Ra^{+2} , Cd^{+2} , Hg^{+2} , Pb^{+2}	$CO_3^{=2}$, $S^{=2}$, $S_2O_4^{=2}$, $SO_3^{=2}$, $Fe(CN)_6^{=4}$, $MoO_4^{=2}$
6	Ca^{+2} , Zn^{+2} , Cu^{+2} , Sn^{+2} , Mn^{+2} , Fe^{+2} , Ni^{+2} , Co^{+2} , Li^{+2}	
8	Mg^{+2} , Be^{+2}	
9	H^+ , Al^{+3} , Fe^{+3} , Cr^{+3} , La^{+3} , Ce^{+3} , Y^{+3}	

Source: Adapted from Stumm and Morgan [19], Pagenkopf [12] and Morel [11].

$$\log \gamma_{CO_3^{=2}} = -0.5 (-2)^2 \frac{\sqrt{0.02}}{1 + (0.33)(5) \sqrt{0.02}}$$

$$= -0.229$$

$$\gamma_{CO_3^{=2}} = 0.59$$

GÜNTELBERG METHOD

For mixtures of several electrolytes, Güntelberg proposed that a value of 3 \AA be used for the empirical parameter "a" in the extended Debye-Hückel. For water at normal temperatures, $B_a \approx 1$; this simplifies equation 29 to:

$$\log \gamma_i = -AZ_i^2 \frac{\sqrt{I}}{1 + \sqrt{I}} \quad (31)$$

The Güntelberg estimation method is applicable to dilute solutions with ionic strength less than $0.1 M$.

Example 4 What is the activity coefficient of Ca^{+2} in river water with an ionic strength of 0.01 M?

Using the Güntelberg method:

$$\begin{aligned}\log \gamma_{\text{Ca}^{+2}} &= -AZ_i^2 \frac{\sqrt{I}}{1 + \sqrt{I}} \\ &= -0.5 (2)^2 \frac{\sqrt{0.01}}{1 + \sqrt{0.01}} \\ &= -0.182 \\ \gamma_{\text{Ca}^{+2}} &= 0.66\end{aligned}$$

DAVIES METHOD

The Davies approximation is given by:

$$\log \gamma_i = -AZ^2 \left(\frac{\sqrt{I}}{1 + \sqrt{I}} - 0.3 I \right) \quad (32)$$

This empirically derived method differs from that of Güntelberg by its additional term of $0.3AZ^2I$. (Davies earlier used a coefficient of 0.2 instead of 0.3.) The method is applicable to solutions of ionic strength less than 0.5 M.

METHOD OF PITZER *et al.*

The Pitzer method is based on the specific ion interaction model (equation 26). For a binary solution of a 1-1 electrolyte, MX, the reduced activity coefficient given by the Pitzer equation is [10]:

$$\log \gamma_{\pm} (\text{MX}) = Z_M Z_X f + m (\beta^0 + f^1 \beta^1) + 1.5 m^2 c^\phi \quad (33)$$

where:

m = concentration of the cation (or anion)

f = $-0.392 [\sqrt{I}/(1 + 1.2 \sqrt{I}) + (2/1.2) \log (1 + 1.2 \sqrt{I})]$

f^1 = $(\frac{1}{2I}) [1 - \exp (-2 \sqrt{I}) (1 + 2\sqrt{I} - 2I)]$

I = ionic strength (M)

Some values of the adjustable parameters β^0 , β^1 and c^* are given in Table 2.6-3. More comprehensive listings are given by Pitzer and Mayorga [15, 16] and Pitzer [13].

For a *mixed electrolyte solution*, the single ion activity coefficients of a particular cation, M , and particular anion, X , are affected by the presence of all the other cations (c) and anions (a) in solution. The relationships are given by equations 34 and 35.

$$\log \gamma_M = Z_M^2 f + 2 \sum_a m_a (B_{Ma} + EC_{Ma}) + Z_M^2 \sum_c m_c m_a B_{ca}^1 + Z_M \sum_c \sum_a m_c m_a C_{ca} \quad (34)$$

$$\log \gamma_X = Z_X^2 f + 2 \sum_c m_c (B_{cX} + EC_{cX}) + Z_X^2 \sum_a m_c m_a B_{ca}^1 + Z_X \sum_c \sum_a m_c m_a C_{ca} \quad (35)$$

where:

m_i = concentration of cations (indicated by subscript c) or anions (subscript a), in molal units

E = the equivalent molality, defined as $E = 1/2 \sum_i m_i |Z_i|$

The second and third virial coefficients in equations 34 and 35 are:

$$\left. \begin{aligned} B_{MX} &= \beta_{MX}^0 + (\beta_{MX}^1/2I) [1 - (1 + 2\sqrt{I}) \exp(-2\sqrt{I})] \\ B_{MX}^1 &= (\beta_{MX}^1/2I^2) [-1 + (1 + 2\sqrt{I} + 2I) \exp(-2\sqrt{I})] \\ C_{MX} &= c_{MX}^*/(2|Z_M Z_X|^{1/2}) \end{aligned} \right\} \quad (36)$$

Additional terms may be added to account for interactions between like-charged ions and among triple ions [3, 14].

The Pitzer estimation method is applicable to solutions of high ionic strength (up to 6M). The deficiency of the Pitzer method lies in the general lack of parameter values for virial coefficients to calculate the activity coefficients.

METHOD OF MEISSNER *et al.*

In this method for an electrolyte that dissociates into cations of charge Z_1 and anions of charge Z_2 , Kusik and Meissner [6] used the definition:

$$\gamma_r = \gamma_{\pm}^{1/Z_1 Z_2} \quad (37)$$

where:

γ_r = reduced activity coefficient

γ_{\pm} = mean ion activity coefficient

TABLE 2.6-3
Parameters β^0 , β^1 , and c^0 for Some Inorganic Compounds

1:1 Compounds ^a				2:1 Compounds ^a				4:1 Compounds ^a			
	β^0	β^1	c^0		β^0	β^1	c^0		β^0	β^1	c^0
HCl	0.11775	0.2945	0.00080	MgCl ₂	0.4698	2.242	0.00979				
NaCl	0.0765	0.2664	0.00127	CaBr ₂	0.5068	2.151	-0.00485				
NaOH	0.0864	0.253	0.0044	Ba(ClO ₄) ₂	0.4819	2.101	-0.05894				
KF	0.06089	0.2021	0.00093	NiCl ₂	0.4639	2.108	-0.00702				
KNO ₃	-0.0816	0.0494	0.00680	Cu(NO ₃) ₂	0.4224	1.907	-0.04136				
NH ₄ Br	0.0624	0.1947	-0.00436	Zn(NO ₃) ₂	0.4641	2.255	-0.02955				
NH ₄ NO ₃	-0.0154	0.1120	-0.00023	K ₂ HAsO ₄	0.1728	2.198	-0.0336				
3:1 Compounds ^a				(3 ^{3/2} /2) c^0				8/5 β^0			
AlCl ₃	1.0490	8.767	0.0071	TlCl ₄	1.622	21.33	-0.3309				
Cr(NO ₃) ₃	1.0560	7.777	-0.1533	K ₄ P ₂ O ₇	0.977	17.88	-0.2418				
Na ₃ AsO ₄	0.3582	5.895	-0.1240	K ₄ Fe(CN) ₆	1.021	16.23	-0.5579				
K ₃ PO ₄	0.5594	5.958	-0.2255	K ₄ Mo(CN) ₆	0.854	18.53	-0.3499				
4:1 Compounds ^a				8/5 β^0				16/5 c^0			

^a The values provided for 2:1, 3:1 and 4:1 compounds are for single electrolyte solutions, and in such cases the numeric values shown are used in Equation 33 without modification. The multiplicative factors (e.g. 3/2) must be removed before the parameter values are used for solutions of mixed electrolytes.

Source: Adapted from Pitzer and Mayorga [15].

These investigators found from experimental observations that the reduced activity coefficient of a strong electrolyte is related to the ionic strength by an empirical relationship, as shown graphically in Figure 2.6-1. With a known value of γ_r , at a given ionic strength, the value at another ionic strength may be extrapolated.

Each of the curves in Figure 2.6-1 is an isotherm that can be represented by the empirical equation:

$$\gamma_r = [1 + B(1 + 0.1 I)^q - B] \gamma^* \quad (38)$$

where:

$$B = 0.75 - 0.065 q \quad (39)$$

$$\log \gamma^* = \frac{-0.5107 \sqrt{I}}{1 + C\sqrt{I}} \quad (40)$$

$$C = 1 + 0.055 q \exp(-0.023 I^3) \quad (41)$$

q = a parameter whose value is dependent on
the electrolyte and temperature

\exp = the exponent to the base e

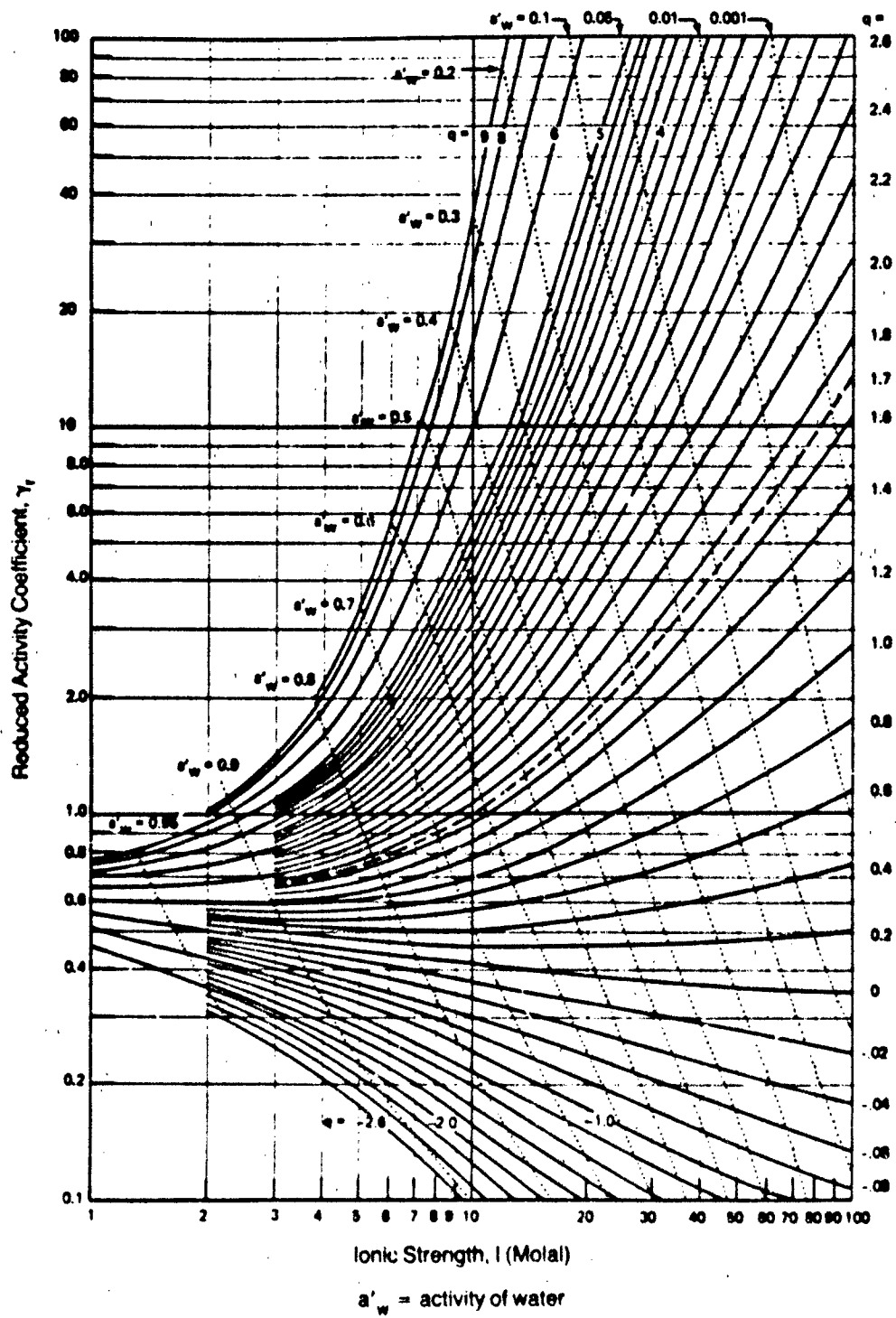
From the equations above, if γ_r for an electrolyte is known for a given ionic strength, the parameter q may be calculated. Using this calculated value of the parameter q , the γ_r at any other ionic strength may be calculated. Note that this method is based on molal units for all concentrations and ionic strengths.

Kusik and Meissner have developed values of q for various electrolytes (Table 2.6-4). To calculate γ_r for a given electrolyte, the value of q is substituted into equations 39, 41, and then 38 with the appropriate ionic strength.

Where no experimental values are available, γ_r may be estimated from data on vapor pressure lowering, as described in Kusik and Meissner[5]. Other methods by Meissner and his co-workers may also be used if there are no data on vapor pressure lowering [9].

Kusik and Meissner developed relationships to calculate γ_r at various temperatures; the reader is referred to their paper [6] for details.

An equation was also developed by Kusik and Meissner[6] to estimate the activity coefficient in a multi-component system from activity coefficients (as calculated above) for single-electrolyte aqueous solutions. This relationship is:



Source: Kusik and Meissner [6]. (Copyright 1978, American Institute of Chemical Engineers. Reprinted with permission.)

FIGURE 2.6-1 Relationship of Reduced Activity Coefficient to Ionic Strength

TABLE 2.6-4
Average Values of the Parameter "q" for Selected Electrolytes

1:1 Electrolyte	q / I	1:1 Electrolyte	q / I	Higher Electrolyte	q / I	Higher Electrolyte	q / I
AgNO ₃	-2.55 b	LiAC	2.81 a	AlCl ₃	1.92 d	Mg(ClO ₄) ₂	4.15 b
CsAC	5.59 a	LiBr	7.27 b	Al ₂ (SO ₄) ₃	0.36 d	MgI ₂	4.04 b
CsBr	-0.06 b	LiCl	5.62 b	BaBr ₂	1.92 b	Mg(NO ₃) ₂	2.32 d
CsCl	0.16 b	LiOH	-0.06 a	BaCl ₂	1.48 b	MgSO ₄	0.15 c
CsI	-0.41 a	LiNO ₃	3.80 b	Ba(ClO ₄) ₂	1.80 c	MnSO ₄	0.14 b
CsOH	7.34 u	LiTOL	0.84 b	BaI ₂	2.84 b	MnCl ₂	1.00 d
CsNO ₃	-2.62 u	NaAC	4.20 a	Ba(NO ₃) ₂	-0.52 c	Na ₂ CrO ₄	0.41 c
HCl	6.00 b	NaBr	2.98 a	CaCl ₂	2.40 d	Na ₂ FUM	0.88 b
HNO ₃	3.66 a	NaBrO ₃	-0.68 u	CaI ₂	3.27 b	Na ₂ MAL	0.12 b
KAC	5.05 a	NaCl	2.23 a	Ca(NO ₃) ₂	0.93 d	Na ₂ S ₂ O ₃	0.18 c
KBr	1.15 b	NaClO ₃	0.41 a	Cd(NO ₃) ₂	1.53 b	Na ₂ SO ₄	-0.19 c
KBrO ₃	-2.00 u	NaClO ₄	1.30 b	CdSO ₄	0.016 b	NdCl ₃	1.42 c
KCl	0.92 b	NaCNS	2.94 a	CoCl ₃	1.41 c	(NH ₄) ₂ SO ₄	-0.25 c
KClO ₃	-1.70 u	NaF	0.37 u	CoBr ₂	3.08 d	NHCl ₂	2.33 d
KCNS	0.61 b	NaFORM	1.83 a	CoCl ₂	2.25 b	NISO ₄	0.025 c
KF	2.13 a	NaHMAL	0.01 b	CoI ₂	3.87 d	Pb(ClO ₄) ₂	2.25 d
KHMAL	-0.72 b	NaHSUC	0.60 b	Co(NO ₃) ₂	2.08 d	Pb(NO ₃) ₂	-0.97 b
KH ₂ PO ₄	-2.54 a	NaH ₂ PO ₄	-1.59 a	CrCl ₃	1.72 b	PrCl ₃	1.40 c
KHSUC	0.02 b	NaI	4.06 a	Cr(NO ₃) ₃	1.51 c	Rb ₂ SO ₄	0.007 b
KI	1.62 b	NaNO ₃	-0.39 b	Cr ₂ (SO ₄) ₃	0.43 d	ScCl ₃	1.68 c
KNO ₃	-2.33 a	NaOH	3.00 a	Ca ₂ SO ₄	0.16 b	SmCl ₃	1.47 c
KOM	4.77 b	NaPROP	5.54 a	CuCl ₂	1.40 b	SrBr ₂	2.34 b
KTOL	-1.75 a	NaTOL	-0.80 a	Cu(NO ₃) ₂	1.83 d	SrCl ₂	1.96 c
		NH ₄ Cl	0.82 b	CuSO ₄	0.00 c	Sr(ClO ₄) ₂	2.84 d
		NH ₄ NO ₃	-1.15 b	EuCl ₃	1.49 c	Sm ₂	3.03 b
		RbAC	5.39 a	FeCl ₂	2.16 b	Sr(NO ₃) ₂	0.30 c
		RbBr	0.46 b	K ₂ CrO ₄	0.16 c	UO ₂ Cl ₂	2.40 b
		RbCl	0.62 b	K ₂ SO ₄	-0.25 u	UO ₂ (ClO ₄) ₂	5.84 d
		RbI	0.45 b	LaCl ₃	1.41 c	UO ₂ (NO ₃) ₂	2.90 b
		RbNO ₃	-2.49 b	Li ₂ SO ₄	0.57 c	UO ₂ SO ₄	0.066 b
		TIAC	-0.73 b	MgAC ₂	0.83 c	YCl ₃	1.55 c
				MgBr ₂	3.50 d	Zn(ClO ₄) ₂	4.30 e
				MgCl ₂	2.90 d	Zn(NO ₃) ₂	2.28 d
						ZnSO ₄	0.05 c

Legend:

AC = Acetate

PROP = Propionate

a = 3-4 Molar

FORM = Formate

SUC = Succinate

b = 4.5-6 Molar

FUM = Fumarate

TOL = p-toluene

c = 8 Molar

MAL = Maleate

sulphonate

d = 15 Molar

Source: Kusik and Metzner [6]

u = limited data

TABLE 2.6-4
Average Values of the Parameter "q" for Selected Electrolytes

1:1 Electrolyte	q / l	1:1 Electrolyte	q / l	Higher Electrolyte	q / l	Higher Electrolyte	q / l
AgNO ₃	-2.55 b	LiAC	2.81 a	AlCl ₃	1.92 d	Mg(ClO ₄) ₂	4.15 b
CaAC	5.59 a	LiBr	7.27 b	Al ₂ (SO ₄) ₃	0.36 d	MgI ₂	4.04 b
CsBr	-0.06 b	LiCl	5.62 b	BeBr ₂	1.92 b	Mg(NO ₃) ₂	2.32 d
CaCl	0.18 b	LiOH	-0.08 a	BeCl ₂	1.48 b	MgSO ₄	0.15 c
CaI	-0.41 a	LiNO ₃	3.80 b	Be(ClO ₄) ₂	1.90 c	MnSO ₄	0.14 b
CaOH	7.34 u	LiTOL	0.84 b	BeI ₂	2.84 b	MnCl ₂	1.80 d
CaNO ₃	-2.62 u	NaAC	4.20 a	Be(NO ₃) ₂	-0.52 c	Na ₂ CrO ₄	0.41 c
HCl	6.88 b	NaBr	2.98 a	CaCl ₂	2.40 d	Na ₂ FUM	0.88 b
HNO ₃	3.06 a	NaBrO ₃	-0.68 u	CaI ₂	3.27 b	Na ₂ MAL	0.12 b
KAC	5.05 a	NaCl	2.23 a	Ca(NO ₃) ₂	0.93 d	Na ₂ S ₂ O ₃	0.18 c
KBr	1.15 b	NaClO ₃	0.41 a	Ca(NO ₃) ₂	1.53 b	Na ₂ SO ₄	-0.19 c
KBrO ₃	-2.00 u	NaClO ₄	1.30 b	CdSO ₄	0.018 b	NdCl ₃	1.42 c
KCl	0.92 b	NaCNS	2.94 a	CoCl ₃	1.41 c	(NH ₄) ₂ SO ₄	-0.23 c
KClO ₃	-1.70 u	NaF	0.37 u	CoBr ₂	3.08 d	NHCl ₂	2.33 d
KCNS	0.61 b	NaFORM	1.83 a	CoCl ₂	2.25 b	NiSO ₄	0.025 c
KF	2.13 a	NaHMAL	0.01 b	CoI ₂	3.87 d	Pb(ClO ₄) ₂	2.25 d
KHMAL	-0.72 b	NaHSUC	0.60 b	Co(NO ₃) ₂	2.08 d	Pb(NO ₃) ₂	-0.97 b
KH ₂ PO ₄	-2.54 a	NaH ₂ PO ₄	-1.58 a	CrCl ₃	1.72 b	PrCl ₃	1.40 c
KHSUC	0.02 b	NaI	4.08 a	Cr(NO ₃) ₃	1.51 c	Rb ₂ SO ₄	0.007 b
KI	1.62 b	NaNO ₃	-0.39 b	Cr ₂ (SO ₄) ₃	0.43 d	ScCl ₃	1.68 c
KNO ₃	-2.33 a	NaOH	3.00 a	Ca ₂ SO ₄	0.18 b	SmCl ₃	1.47 c
KOH	4.77 b	NaPROP	5.54 a	CuCl ₂	1.40 b	SrBr ₂	2.34 b
KTOL	-1.75 a	NaTOL	-0.80 a	Cu(NO ₃) ₂	1.83 d	SrCl ₂	1.96 c
		NH ₄ Cl	0.82 b	CuSO ₄	0.00 c	Sr(ClO ₄) ₂	2.84 d
		NH ₄ NO ₃	-1.15 b	EuCl ₃	1.49 c	SrI ₂	3.03 b
		RbAC	5.39 a	FeCl ₂	2.18 b	Sr(NO ₃) ₂	0.30 c
		RbBr	0.48 b	K ₂ CrO ₄	0.18 c	UO ₂ Cl ₂	2.40 b
		RbCl	0.82 b	K ₂ SO ₄	-0.25 u	UO ₂ (ClO ₄) ₂	5.84 d
		RbI	0.45 b	LaCl ₃	1.41 c	UO ₂ (NO ₃) ₂	2.90 b
		RbNO ₃	-2.49 b	Li ₂ SO ₄	0.57 c	UO ₂ SO ₄	0.066 b
		TiAC	-0.73 b	MgAC ₂	0.83 c	YCl ₃	1.55 c
				MgBr ₂	3.50 d	Zn(ClO ₄) ₂	4.30 a
				MgCl ₂	2.90 d	Zn(NO ₃) ₂	2.28 d
						ZnSO ₄	0.05 c

Legend:

AC = Acetate

PROP = Propionate

a = 3-4 Molal

FORM = Formate

SUC = Succinate

b = 4.5-6 Molal

FUM = Fumarate

TOL = p-Toluene

c = 9 Molal

MAL = Maleate

sulphonate

d = 15 Molal

Source: Kusak and Mersener [8]

u = limited data

$$\log \gamma_{ij} = \frac{Z_i}{Z_i + Z_j} (V_{i2} I_2 \log \gamma_{i2}^0 + V_{i4} I_4 \log \gamma_{i4}^0 + \dots) / I \\ + \frac{Z_j}{Z_i + Z_j} (V_{j1} I_1 \log \gamma_{j1}^0 + V_{j3} I_3 \log \gamma_{j3}^0 + \dots) / I \quad (42)$$

where:

ij denotes the electrolyte consisting of cation i and anion j

Z_i = absolute charge on cation i

Z_j = absolute charge on anion j

γ_{ij} = reduced activity coefficient of ij in multi-component solution

γ^0 = reduced activity coefficient in single-electrolyte solution

Even subscripts denote anions in the multi-component system

Odd subscripts denote cations in the multi-component system

$V_{xy} = 0.5 (Z_x + Z_y)^2 / (Z_x Z_y)$

I_x = ionic strength of individual ion x

= $0.5 (\text{conc. of ion } x) (Z_x)^2$, molal

I = total ionic strength in solution, molal

Example 5 Calculate the mean ion activity coefficient, γ_{\pm} , of FeCl_2 in an aqueous solution of ionic strength 5 molal.

From Table 2.6-4, the value of q for FeCl_2 is 2.16. Substituting this value in equation 39,

$$B = 0.75 - 0.065 q \\ = 0.75 - 0.065 (2.16) = 0.6096$$

From equation 41,

$$C = 1 + 0.055 q \exp (-0.023 I^3) \\ = 1 + 0.055 (2.16) \exp (-0.023 \times 5^3) \\ = 1.007$$

The values of C and I are next substituted in equation 40:

$$\log \gamma^* = - \frac{0.5107 \sqrt{I}}{1 + C \sqrt{I}} \\ = - \frac{0.5107 \sqrt{5}}{1 + 1.007 (\sqrt{5})}$$

= - 0.351

$$\gamma^* = 0.445$$

The reduced activity coefficient is now calculated by equation 38:

$$\begin{aligned}\gamma_r &= [1 + B(1 + 0.1 I)^q - B] \gamma^* \\ &= [1 + 0.6096(1 + 0.1 \times 5)^{2.16} - 0.6096] 0.445 \\ &= 0.825\end{aligned}$$

According to equation 37,

$$\gamma_r = \gamma_{\pm}^{1/Z_1 Z_2} = \gamma_{\pm}^{1/2}$$

Therefore,

$$\gamma_{\pm} = 0.681$$

The Meissner *et al.* method is applicable to solutions of high ionic strength from above 1 M to very high ionic strengths (up to 100 molal).

Compared with that of Pitzer *et al.*, the method of Meissner *et al.* is superior for estimating activity coefficients in solutions of very high ionic strength (Table 2.6-5); it is also easier to use, and the necessary data are more readily available.

TABLE 2.6-5

Comparison of Pitzer *et al.* and Meissner *et al.*
Methods for High-Ionic-Strength Solutions

	Pitzer <i>et al.</i>	Meissner <i>et al.</i>
Applicability		
Ionic strength 1-6	Yes	Yes
Ionic strength 6-20	Limited	Verified for a large number of systems
Ionic strength 20-100	No	Yes
Temperature effect	No	Yes (see ref. 6)
Database for coefficients	Limited; requires extensive effort to enlarge	Limited, but easily expanded to required components
Complexity of calculation and number of parameters required (particularly with increasing number of ions in multi-component system)	Relatively high (complexity and number of parameters increase exponentially)	Relatively low (complexity and number of parameters increase linearly)

OTHER METHODS

Helgeson [8] proposed a method found to be suitable for calculating activity coefficients for ions present in low concentrations in multi-component electrolyte solutions that contain sodium chloride as the dominant component:

$$\log \gamma_i = \frac{AZ_i^2 \sqrt{I}}{1 + Ba_i \sqrt{I}} + B^0 I \quad (43)$$

The value of B^0 is 0.041 at 25°C. The Helgeson equation can be used for trace ions in sodium chloride solutions of ionic strength up to 3 M. It is appropriate for use with saline soil solutions and brines.

Additional methods for estimating activity coefficients, which are not discussed in detail here, include the following:

- Sun, Harriss and Magnuson [20] developed a modified version of the Debye-Hückel method in the form of equation 25.
- Van Luik and Jurinak [21] describe other methods by Reilly, Wood and Robinson [17] and by Glueckauf [1].

NEUTRAL SPECIES

For neutral species in solution, such as gaseous oxygen, activity coefficients can be estimated by the following empirical equation [18]:

$$\log \gamma_i = k_s I \quad (44)$$

where:

k_s = empirically determined coefficient ranging from 0.01 to 0.15
 I = ionic strength (M)

The activity coefficient of non-ionic species is approximately 1 for $M < 1$. The coefficient k_s is normally around 0.1. Equation 44 holds for solutions of ionic strength up to 5 M and solute concentrations in the range of 0.1 M to 0.5 M [12]. Methods for estimating activity coefficients for neutral organic species are discussed by Grain [2].

2.6.4 Literature Cited

1. Glueckauf, E., "Electrostatic Interactions in Electrolyte Solutions," *Proc. R. Soc. London, Ser. A*, **310**, 449-62 (1969), as cited by Van Luik and Jurinak [21].
2. Grain, C.F., "Activity Coefficient," Chap. 11 in *Handbook of Chemical Property Estimation Methods*, W.J. Lyman, W.F. Reehl and D.H. Rosenblatt (eds.), McGraw-Hill Book Co., New York (1982).

3. Harvie, C.E. and J.H. Weare, "The Prediction of Mineral Solubilities in Natural Waters: The Na-K-Mg-Cl-SO₄-H₂O System from Zero to High Concentrations at 25°C," *Geochim. Cosmochim. Acta*, **44**, 981-97 (1980).
4. Horne, R.A., *The Chemistry of Our Environment*, John Wiley & Sons, New York (1978).
5. Kusik, C.L. and H.P. Meissner, "Vapor Pressures of Water over Aqueous Solutions of Strong Electrolytes," *Ind. Eng. Chem. Process Des. Dev.*, **12**, 112-15 (1973).
6. Kusik, C.L. and H.P. Meissner, "Electrolyte Activity Coefficients in Inorganic Processing," in *Fundamental Aspects of Hydrometallurgical Processes*, T.W. Chapman, L.L. Tavlarides, G.L. Huber, and R.M. Wellek (eds.), Symposium Series 173, **74**, American Institute of Chemical Engineers, New York, 14-20 (1978).
7. Martell, A.E. and R.M. Smith, *Inorganic Complexes*, Vol. 4 of *Critical Stability Constants*, Plenum Press, New York (1976).
8. Mattigod, S.V. and G. Sposito, "Chemical Modeling of Trace Metal Equilibria in Contaminated Soil Solutions Using the Computer Program GEOCHEM," in *Chemical Modeling in Aqueous Systems*, E.A. Jenne (ed.), ACS Symposium Series 93, American Chemical Society, Washington, D.C., 837-56 (1979).
9. Meissner, H.P. and J.W. Tester, "Activity Coefficients of Strong Electrolytes in Aqueous Solutions," *Ind. Eng. Chem. Process Des. Dev.*, **11**, 128-33 (1972).
10. Millero, F.J., "The Activity of Metal Ions at High Ionic Strengths," in *Complexation of Trace Metals in Natural Waters*, C.J.M. Kramer and J.C. Duinker (eds.), Proceedings of the International Symposium, May 2-6, 1983, Texel, The Netherlands, Martinus Nijhoff/Dr. W. Junk Publishers, The Hague, 187-200 (1984).
11. Morel, F.M.M., *Principles of Aquatic Chemistry*, John Wiley & Sons, New York (1983).
12. Pagenkopf, G.K., *Introduction to Natural Water Chemistry*, Marcel Dekker, New York (1978).
13. Pitzer, K.S., "Ion Interaction Approach," in *Activity Coefficients in Electrolyte Solutions*, R.M. Pytkowicz (ed.), CRC Press, Boca Raton, Fla., 157-209 (1979).
14. Pitzer, K.S. and J.J. Kim, "Thermodynamics of Electrolytes. IV: Activity and Osmotic Coefficients for Mixed Electrolytes," *J. Am. Chem. Soc.*, **96**, 5701-707 (1974).
15. Pitzer, K.S. and G. Mayorga, "Thermodynamics of Electrolytes. II: Activity and Osmotic Coefficients for Strong Electrolytes with One or Both Ions Univalent," *J. Phys. Chem.*, **77**, 2300-308 (1973).
16. Pitzer, K.S. and G. Mayorga, "Thermodynamics of Electrolytes. III: Activity and Osmotic Coefficients for 2:2 Electrolytes," *J. Solution Chem.*, **3**, 539-46 (1974).

17. Reilly, P.J., R.H. Wood and R.A. Robinson, "The Prediction of Osmotic and Activity Coefficients in Mixed-Electrolyte Solutions," *J. Phys. Chem.*, **75**, 1305-315 (1971).
18. Snoeyink, V.L. and D. Jenkins, *Water Chemistry*, John Wiley & Sons, New York (1980).
19. Stumm, W. and J.J. Morgan, *Aquatic Chemistry*, 2nd ed., John Wiley & Sons, New York (1981).
20. Sun, M.S., D.K. Harriss and V.R. Magnuson, "Activity Corrections for Ionic Equilibria in Aqueous Solutions," *Can. J. Chem.*, **58**, 1253-57 (1980).
21. Van Luik, A.E. and J.J. Jurinak, "Equilibrium Chemistry of Heavy Metals in Concentrated Electrolyte Solution," in *Chemical Modeling in Aqueous Systems*, E.A. Jenne (ed.), ACS Symposium Series 93, American Chemical Society, Washington, D.C., 683-710 (1979).

2.7 ACID/BASE EQUILIBRIA

2.7.1 Introduction

This section addresses acid/base equilibria of inorganic substances in aqueous systems, focusing on the acid dissociation constant as the functional parameter that describes the extent of these types of equilibria. The following discussion defines the acid dissociation constant and explains how it is used, where its value can be obtained, how much it varies under different conditions, and the practicality of using an estimate. The use of the constant to calculate relative concentrations of various hydrolyzed species is also described and illustrated.

2.7.2 Description of Property

According to the definition proposed by Brønsted [3], an acid is a species that can donate a proton. Therefore, to behave as an acid, a species must be associated with a hydrogen atom that it can release to form hydronium ions (H^+_{aq}) in the aqueous solvent. Two common representations of inorganic acids are H-X , where the hydrogen atom is bonded to a single atom (e.g., HCl , H_2S), and M-X-H , where it is bonded to an atom that is, in turn, bonded to others — e.g., $[(\text{H}_2\text{O})_5\text{Fe-O-H}]^{+2}$ and $\text{H} > \text{As-O-H}$.

Species like $\text{H} > \text{As-O-H}$ are generally referred to as oxy acids.

In aqueous environmental systems, acid dissociation occurs when H_2O (acting as a base) reacts with the hydrogen ion (proton) in an acid. This results in a species that is often referred to as H^+ but in reality is a hydrated ion containing several water molecules: H_3O^+ , H_5O_2^+ , H_9O_4^+ , etc., sometimes referred to as the hydronium ion. For this reason, acid dissociation reactions are commonly written as in equation 1, where K_a is the acid dissociation equilibrium constant.



In inorganic reaction mechanism chemistry, the water reactant is commonly omitted and protonated water molecules are denoted simply as H^+ . The acid dissociation of hydrogen iodide, for example, is written as:



The subscript "aq" refers to the aqueous hydration sphere surrounding each ion in the water solvent; several H_2O molecules may be loosely associated with the central ion in this sphere as for example with I^- in the case of equation 2. It is often convenient to drop even the "aq" notation, which is understood to be present when reactions in aqueous systems are discussed. We have adopted this convention in the text that follows.

The extent of acid dissociation can be represented mathematically in terms of the activities of products and reactants of the dissociation reaction. The acid dissociation constant, K_a , for a reaction of the kind represented by equation 1 is expressed as

$$K_a = \frac{(a_{\text{MX}^-})(a_{\text{H}^+})}{(a_{\text{MXH}})} \quad (3)$$

where "a" is the activity of the component named in the subscript. Since the activity of water is essentially constant in aqueous systems, it is incorporated in the value of K_a . Activities are related to the molar concentrations of the components as follows:

$$a_i = \gamma_i [C_i] \quad (4)$$

where γ_i is the activity coefficient of component i , and $[C_i]$ is its molar concentration. (See Section 2.6 for methods of calculating activity coefficients.) Thus, equation 3 can be rewritten as

$$K_a = \frac{(\gamma_{MX^-})(\gamma_{H^+})}{(\gamma_{MXH})} \frac{[MX^-][H^+]}{[MXH]} \quad (5)$$

Dissociation constants are often quoted in the literature at an ionic strength of zero, where the γ values are 1. These data are obtained either from measurements at several ionic strengths and subsequent extrapolation to zero ionic strength or by calculation of the γ values and correction of the value of K_a measured at ionic strengths greater than zero. When K_a values are given, they are often "conditional" constants defined as:

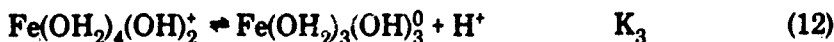
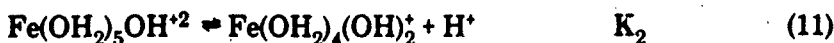
$$K_a = \frac{a_{H^+}[MX^-]}{[MXH]} \quad (6)$$

This definition arises from the experimental procedures used to determine these constants. The activity of H^+ can be directly measured (e.g., by a pH electrode), but the activities of the other components may not be known, although their concentrations can be determined. It is highly desirable that one know how a particular constant was derived before using it in calculations.

The behavior in aqueous systems of many inorganic species of environmental concern (e.g., trace metals) under a variety of pH conditions is affected by the hydroxo ($-OH$) or aquo ($-OH_2$) ligands coordinated to the central metal. In general, two or more of these ligands are bonded to the central metal; this leads to successive acid dissociation processes, each with a different dissociation constant. For example, phosphoric acid (H_3PO_4), which has three hydroxy (OH) and one oxy (O) bonded to the phosphorus (V) center, and structurally is better represented as $PO(OH)_3$ undergoes the following acid dissociation reactions:



For a trace metal ion in an aqueous environment, successive acid dissociation reactions of this kind can give rise to aquo-hydroxo species. For example, for iron (III), which is hexacoordinated with water molecules, the first three (stepwise) acid dissociation reactions are:



Acid dissociation data in the literature are commonly in the form of either K_a values or of overall (cumulative) reaction equilibrium constants (β) that are products of individual K_a values [2,17]. For example, for the aqueous iron (III) ion, the relationship of β values to the acid dissociation values is as follows:



Data are also provided in the literature in the form of base association constants, K_b :



where A^- is the conjugate base of HA, the acid. The relationship between K_a and K_b is:

$$K_a = K_w / K_b \quad (17)$$

where K_w is the dissociation constant of water ($10^{-14.0}$ at 25°C). Because K_a values tend to be very small numbers, they are most conveniently expressed in logarithmic form, $pK_a = -\log K_a$.

2.7.3 Environmental Importance

From an environmental standpoint, the acidic and basic behavior of inorganic species in solution is important for two reasons. First, the acidic (or basic) nature of major inorganic species affects the properties and pH of the solution. Second, the solution pH can play a major role in the speciation of the dissolved trace inorganic species. Modification of the solution pH (which, in turn, affects speciation of other components) is the more important of these effects when the substance is strongly acidic or basic or is relatively concentrated; the matrix impact on speciation is of greater importance when the substance is weakly acidic or basic and at low concentrations, as is the case with many trace metals. In comparison with other aqueous environmental inorganic reactions, acid dissociation reactions are usually considered to be instantaneous.

Since acid dissociation involves loss of one or more protons, the overall charge of the metal ion complex is correspondingly reduced. The dissociated ion (conjugate base) differs from the undissociated acid with regard to environmentally important properties such as solubility, soil attenuation, biological uptake, complexation, and kinetics of redox reactions. The formation of hydroxy compounds through acid dissociation is the first step in precipitation of many species from solution. The precipitates formed are often either hydroxide, oxyhydroxide, or polymeric hydroxo and oxo species.

Thus, assessment of environmental impact and mobility requires a knowledge of the speciation of the elements of interest. As noted, acid dissociation often plays a major role in this process, determining whether the prevailing ion is AsO_4^{3-} or HAsO_4^{2-} , for example. It affects the speciation of an element even in a system that contains no species (e.g., potential ligands) other than water that can react with the element. Accordingly, environmentalists must consider the extent of acid dissociation when dealing with most dissolved species that act as acids; these include dissolved gases (e.g., CO_2 , H_2S), trace metals (e.g., including transition metals) and other pollutants of environmental concern (e.g., compounds of As or Se).

The behavior of undissociated versus dissociated metal ions (i.e., M^{+x} vs. M(OH)_{y-x}^{x-y}) with regard to the extent of sorption, solubility, redox reactivity, competitive complexation, and uptake reactions is described in other sections of this report.

It should be noted that in environmental systems pH controls can be dominated by the presence of solid phases (i.e., in heterogeneous systems) or by the formulation of solid precipitates. For example, calcite (CaCO_3) can act as a base (i.e., react with H^+) to consume acidity while jarosite ($\text{KFe}_3(\text{SO}_4)_2(\text{OH})_6$) or alunite ($\text{K}_3\text{Al}_3(\text{SO}_4)_2(\text{OH})_6$) can precipitate from acidic soil pore waters when the levels of the respective ions (e.g., K^+ , Fe^{+2} , SO_4^{2-} and Al^{+3}) rise as H_2SO_4 is released during oxidation of sulfide in the soil. The presence of those solids can thus provide a long term pH control in heterogeneous environmental systems [10].

2.7.4 Mathematical and Graphical Representation

In a situation involving several interrelated equilibria, such as where several hydroxy complexes of an ion are formed by successive acid dissociation reactions, a graphical representation is useful. A graph can show the relative abundance of the various species as a function of some variable (in this case, pH) that affects which species are formed. The relative abundance of a particular hydroxy species or unprotonated form of the acid can be calculated from the acid dissociation constants and a mathematical representation of all the equilibria present in the aqueous system. In the case where dimers or polymers can be formed total concentration of the analyte is also needed.

In homogeneous reaction solution media free of ligands that might participate in further complexation equilibria or redox reactions, without gas/liquid equilibria, without precipitation/dissolution equilibria and without liquid/solid equilibria, the acid dissociation reactions (summarized in Table 2.7-1) govern the speciation of a

dissociable species. While the other equilibria are obviously important and can determine concentrations and speciation in many cases, they can sometimes be ignored; for example, if the volatility of dissolved components in the system is very low, gas/liquid equilibria may be neglected. Similarly, if concentration levels in solution are much lower than the solubility limits, it may be unnecessary to consider liquid/solid equilibria, and the presence of very weakly complexing ions (relative to that of OH⁻ ligand) may allow representation of the system by the equations given in the table.

TABLE 2.7-1

Equations Used to Calculate f_i , the Ratio of Concentrations of a Particular Species to the Total Present in Acid/Base Equilibria^a

Acid System	Equations
$\text{HL} \rightleftharpoons \text{H}^+ + \text{L}^-$, K_1	$f_L = \left[\frac{(\text{H})}{K_1} + 1 \right]^{-1}$ $f_{\text{HL}} = \left[1 + \frac{K_1}{(\text{H})} \right]^{-1}$
$\text{H}_2\text{L} \rightleftharpoons \text{HL}^- + \text{H}^+$, K_1	$f_L = \left[\frac{(\text{H})^2}{K_1 K_2} + \frac{(\text{H})}{K_2} + 1 \right]^{-1}$
$\text{HL}^- \rightleftharpoons \text{L}^{2-} + \text{H}^+$, K_2	$f_{\text{HL}} = \left[\frac{(\text{H})}{K_1} + 1 + \frac{K_2}{(\text{H})} \right]^{-1}$ $f_{\text{H}_2\text{L}} = \left[1 + \frac{K_1 K_2}{(\text{H})^2} + \frac{K_1}{(\text{H})} \right]^{-1}$
$\text{H}_3\text{L} \rightleftharpoons \text{H}_2\text{L}^- + \text{H}^+$, K_1	$f_L = \left[\frac{(\text{H})^3}{K_1 K_2 K_3} + \frac{(\text{H})^2}{K_2 K_3} + \frac{(\text{H})}{K_3} + 1 \right]^{-1}$
$\text{H}_2\text{L}^- \rightleftharpoons \text{HL}^{2-} + \text{H}^+$, K_2	$f_{\text{HL}} = \left[\frac{(\text{H})^2}{K_1 K_2} + \frac{(\text{H})}{K^2} + 1 + \frac{K_3}{(\text{H})} \right]^{-1}$
$\text{HL}^{2-} \rightleftharpoons \text{L}^{3-} + \text{H}^+$, K_3	$f_{\text{H}_2\text{L}} = \left[\frac{(\text{H})}{K_1} + 1 + \frac{K_2}{(\text{H})} + \frac{K_2 K_3}{(\text{H})^2} \right]^{-1}$ $f_{\text{H}_3\text{L}} = \left[1 + \frac{K_1}{(\text{H})} + \frac{K_1 K_2}{(\text{H})^2} + \frac{K_1 K_2 K_3}{(\text{H})^3} \right]^{-1}$

(Continued)

TABLE 2.7-1 (Continued)

Acid System	Equations
$H_4L \rightleftharpoons H_3L^+ + H^+, K_1$	$f_L = \left[\frac{(H)^4}{K_1 K_2 K_3 K_4} + \frac{(H)^3}{K_2 K_3 K_4} + \frac{(H)^2}{K_3 K_4} + \frac{(H)}{K_4} + 1 \right]^{-1}$
$H_3L^+ \rightleftharpoons H_2L^{2-} + H^+, K_2$	$f_{HL} = \left[\frac{(H)^3}{K_1 K_2 K_3} + \frac{(H)^2}{K_2 K_3} + \frac{(H)}{K_3} + 1 + \frac{K_4}{(H)} \right]^{-1}$
$H_2L^{2-} \rightleftharpoons HL^{3-} + H^+, K_3$	$f_{H_2L} = \left[\frac{(H)^2}{K_1 K_2} + \frac{(H)}{K_2} + 1 + \frac{K_3}{(H)} + \frac{K_3 K_4}{(H)^2} \right]^{-1}$
$HL^{3-} \rightleftharpoons L^{4-} + H^+, K_4$	$f_{H_3L} = \left[\frac{(H)}{K_1} + 1 + \frac{K_2}{(H)} + \frac{K_2 K_3}{(H)^2} + \frac{K_2 K_3 K_4}{(H)^3} \right]^{-1}$
	$f_{H_4L} = \left[1 + \frac{K_1}{(H)} + \frac{K_1 K_2}{(H)^2} + \frac{K_1 K_2 K_3}{(H)^3} + \frac{K_1 K_2 K_3 K_4}{(H)^4} \right]^{-1}$

a. f_i = Fraction of total concentration of acid present in the i th form. (Total concentration = sum of concentrations of all species containing central atom(s) of concern.)

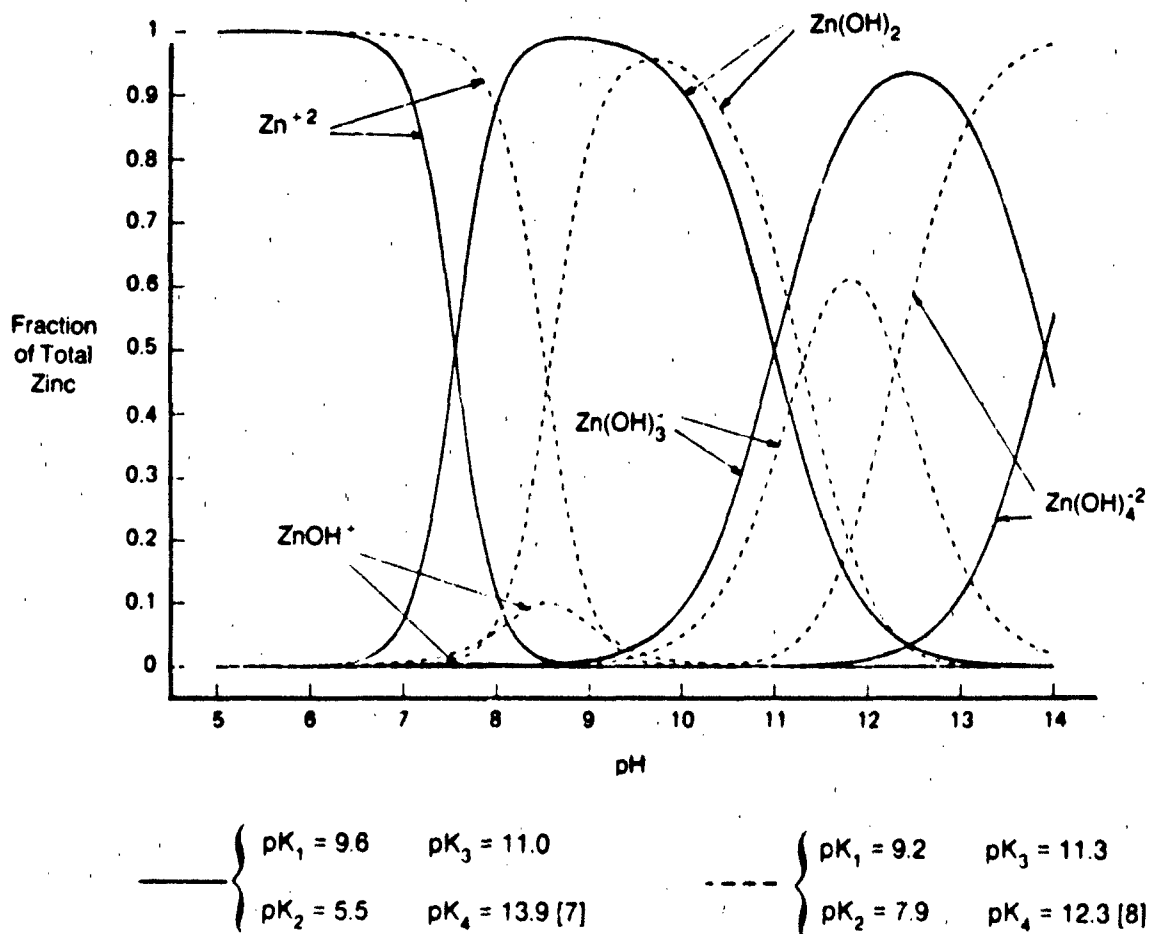
(H) = Activity of hydrogen ion

K_i = Acid dissociation constant

Activity coefficient for all species assumed to be 1.

It is often difficult to determine which of the various equilibria predominate in determining the speciation in a complex chemical system. The effect of equilibria other than acid/base equilibria on speciation is discussed in the sections of this report that deal with those processes. Computer models help in understanding which of the various equilibria are predominant.

These simple systems are generally represented by plots of fraction (f) or percent ($100 \times f$) of the ion present in the various forms (e.g., H_2L , HL^- , L^{2-}) as a function of pH. An example of this plot is given in Figure 2.7-1 for Zn^{+2} in solution, under the assumption that this ion is a tetraprotic acid [4]. Such plots can be generated from the equations in Table 2.7-1, which were derived from the definitions of each of the K_i values (e.g., $K_2 = (L^{2-})[H^+]/[HL]$ for the diprotic acid system) and an assumption that the total concentration of the various species is a constant. The fraction is then defined; for H_3L , for example, it is $f_{H_3L} = [H_3L]/[\text{Acid Total}]$. Examination of the table shows that the f values are a function of (H^+) and the respective acid dissociation constants. If we can ignore the influence of other equilibria, these plots are valid at the particular temperature and ionic strength at which the (conditional)



Source: Calculated by Arthur D. Little, Inc.

FIGURE 2.7-1 Effect of pK Values on Calculated Distribution of Zn(II) Species with pH

dissociation constants were obtained. It is somewhat unusual for a higher order pK_a (e.g., pK_1) to be less than a lower order pK_a (e.g., pK_2); yet, such is true for Zn^{+2} . This is why the concentrations of $Zn(OH)^+$ are so low. In addition, the values of the pK_a 's have a marked impact on the relative abundance of the individual hydroxy species calculated (see Figure 2.7-1).

Example 1 To illustrate how the equations in Table 2.7-1 are used, we shall calculate the fraction of sulfurous acid (H_2SO_3) present as sulfite (SO_3^{2-}) at pH 8 and ionic strength of zero. It is assumed that no other equilibria apply.

Sulfurous acid is a diprotic acid with $K_1 = 1.58 \times 10^{-2}$ ($pK_1 = 1.8$) and $K_2 = 1.58 \times 10^{-7}$ ($pK_2 = 6.8$) [3]. The fraction of acid present as sulfite is expressed as:

$$f_{SO_3^{2-}} = \left[\frac{(H^+)^2}{K_1 K_2} + \frac{(H^+)}{K_2} + 1 \right]^{-1} \quad (18)$$

Using $(H^+) = 1 \times 10^{-8} M$, $K_1 = 1.58 \times 10^{-2} M$ and $K_2 = 1.58 \times 10^{-7} M$, we obtain

$$\begin{aligned} f_{SO_3^{2-}} &= \left[\frac{(1 \times 10^{-8})(1 \times 10^{-8})}{(1.58 \times 10^{-2})(1.58 \times 10^{-7})} + \frac{(1 \times 10^{-8})}{(1.58 \times 10^{-7})} + 1 \right]^{-1} \\ &= [4.00 \times 10^{-16} + 6.33 \times 10^{-2} + 1]^{-1} = [1.063]^{-1} = 0.94 \end{aligned}$$

Thus, 94% of the sulfurous acid is present as sulfite at pH 8.

If the ionic strength is not zero, a corrected acid dissociation constant can be estimated by an equation such as the following:

$$pK' = -\log K' = pK + \frac{0.5(Z_A^2 - Z_B^2) \sqrt{I}}{1 + \sqrt{I}} \quad (19)$$

where Z_A = charge of the acid form
 Z_B = charge of the base form
 I = ionic strength (M)
 K = acidity constant at ionic strength of zero
 K' = corrected acidity constant at ionic strength I .

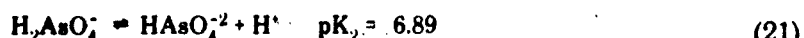
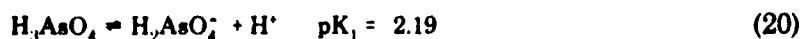
This equation utilizes the Güntelberg approximation for calculation of ion activity coefficients [19]. Other equations can be generated using the variety of approaches available for calculation of activity coefficients as discussed in section 2.6.

Equation 19 is useful for calculating ionic strength corrections up to 0.1 M . Other correction factors may be used if the activity is calculated by a different method, such as Debye-Hückel, Davies or extended Debye-Hückel. (See Section 2.6.)

The magnitude of the correction term in equation 19 ranges from 0.005 at an ionic strength of $10^{-4} M$ for a 1,0 electrolyte (e.g., $\text{H}_2\text{S} \rightleftharpoons \text{HS}^- + \text{H}^+$) to 0.60 at an ionic strength of 0.1 M for a 2,3 electrolyte (e.g., $\text{HPO}_4^{2-} \rightleftharpoons \text{PO}_4^{3-} + \text{H}^+$).¹ Use of the corrected pK' value permits calculations using concentrations for all species except H^+ , which is incorporated as activity, (H^+) [19].

Example 2 The use of equation 19 will be illustrated by calculating the effect of a 0.1 M ionic strength on the pK values of arsenic acid (H_3AsO_4) obtained at an ionic strength of $10^{-3} M$.

The acid dissociation reactions and constants for H_3AsO_4 at an ionic strength of zero [17] are:



The values of Z_A and Z_B for these reactions are:

Eq.	Z_A	Z_B
20	0	1
21	1	2
22	2	3

It can be shown by equation 19 that the pK values at $I \approx 10^{-3}$ are approximately the same as at $I = 0$. The corrected values for an ionic strength of 0.1 M are calculated as follows:

$$\text{pK}'_1 = \text{pK}_1 - 0.12 = 2.19 - 0.12 = 2.07$$

$$\text{pK}'_2 = \text{pK}_2 - 0.36 = 6.89 - 0.36 = 6.53$$

$$\text{pK}'_3 = \text{pK}_3 - 0.6 = 11.49 - 0.6 = 10.89$$

One should keep in mind, however, that the uncertainty in the magnitude of the pK values may be greater than the correction: the values reported by various sources can differ by 0.5 unit or more. The need to make the correction should be assessed on the basis of the uncertainty in the pK values and the accuracy required from the calculation. Variations in the reported pK values for Zn^{+2} and their effect on the calculated speciation are shown in Figure 2.7-1. The use of critical sources [11,12,18] of stability constants may alleviate this problem somewhat.

2.7.5 Effect of Temperature on Acidity Constants

Acid/base equilibria are affected by temperature in various ways, depending on the magnitude and sign of the enthalpy of reaction (ΔH). As Table 2.7-2 shows, the magnitude of ΔH for acid-base reaction can be either positive or negative but is seldom large, typically ranging from -15 to +15 kcal/mole. Given a reaction such as



1. "1,0" refers to $Z_A = 0$, $Z_B = \pm 1$ or vice versa; "2,3" refers to $Z_A = \pm 2$, $Z_B = \pm 3$ or vice versa.

TABLE 2.7-2
Temperature Effects on Acid/Base Reaction Equilibria^a

Reaction	$\log K(25^\circ\text{C})^b$	$\log K(t^\circ\text{C})$	$\Delta H(25^\circ\text{C})$
$\text{H}^+ + \text{CN}^- \rightleftharpoons \text{HCN}$	9.21	9.29 (15°C)	-10.1
$\text{H}^+ + \text{OH}^- \rightleftharpoons \text{H}_2\text{O}$	14.00	14.34 (15°C)	-13.48
$\text{H}^+ + \text{CO}_3^{2-} \rightleftharpoons \text{HCO}_3^-$	10.25	10.59 (0°C)	—
$\text{H}^+ + \text{HCO}_3^- \rightleftharpoons \text{H}_2\text{CO}_3$	6.35	6.29 (50°C)	—
$\text{H}^+ + \text{NO}_2^- \rightleftharpoons \text{HNO}_2$	3.14	3.22 (15°C)	-4.48
$\text{H}^+ + \text{AsO}_2^- \rightleftharpoons \text{HAsO}_2^-$	—	$9.614 - 0.0184t^c$	—
$\text{H}^+ + \text{HAsO}_2^- \rightleftharpoons \text{H}_2\text{AsO}_4^-$	—	$6.971 + 5 \times 10^{-5}(t-39.4)^2$	-0.69
$\text{H}^+ + \text{H}_2\text{AsO}_4^- \rightleftharpoons \text{H}_3\text{AsO}_4$	—	$2.014 + 5 \times 10^{-5}(t+40)^2$	2.65
$\text{H}^+ + \text{S}^{2-} \rightleftharpoons \text{HS}^-$	d	$12.9 - 0.031(t-25)$	-7.6
$\text{H}^+ + \text{HS}^- \rightleftharpoons \text{H}_2\text{S}$	—	$7.05 - 0.0125(t-25)$	-4.42
$\text{H}^+ + \text{SO}_4^{2-} \rightleftharpoons \text{HSO}_4^-$	1.99	1.80 (15°C)	5.4
$\text{H}^+ + \text{SeO}_4^{2-} \rightleftharpoons \text{HSeO}_4^-$	1.88	1.84 (15°C)	—
$\text{H}^+ + \text{Cl}^- \rightleftharpoons \text{HSO}_3^-$	7.30	7.17 (10°C)	2.9
$\text{H}^+ + \text{HSO}_3^- \rightleftharpoons \text{H}_2\text{SO}_3$	2.00	1.92 (10°C)	3.9
$\text{H}^+ + \text{F}^- \rightleftharpoons \text{HF}$	3.17	3.40 (50°C) ^e	3.20

a. All data are experimentally derived and corrected to an ionic strength of zero unless noted. K refers to reaction in column 1.

b. The relationship between K_a (as defined by equation 1) and K as written for these reactions is given by equation 25.

c. Data at ionic strength 0.1 M; $14 < t < 45^\circ\text{C}$.

d. Value of K in dispute.

e. Data at ionic strength 0.5 M.

Sources: Sillén and Martell [17], Martell and Smith [11,12] and Smith and Martell [18].

with an equilibrium constant, K, and an enthalpy change of ΔH that is independent of temperature, we can calculate the effect on the equilibrium constant of a change in temperature from T_1 to T_2 by the following equation:

$$\log K_{(T_1)} - \log K_{(T_2)} = \frac{\Delta H}{2.3R} \left(\frac{1}{T_1} - \frac{1}{T_2} \right) \quad (24)$$

where K = equilibrium constant at specified temperature
 ΔH = enthalpy of reaction (cal/mol)
 R = gas constant = 1.987 cal/mol K
 T = temperature (K)

The relationship between the pK_a of HA and K, the association equilibrium constants in Table 2.7-2 is

$$pK_a = \log K \quad (25)$$

At the highest ΔH values (about 15 kcal, assumed constant over the temperature range), equation 24 would predict a variation of 0.58 pK units over a 15-degree temperature range (283 K to 298 K).

Example 3 To illustrate the use of equation 24, we shall calculate the second acid association constant (K) of sulfurous acid (H_2SO_3) at 10°C if the value is 7.30 at 25°C.

The acid/base reaction of interest is



From Table 2.7-2, ΔH is +2.9 kcal/mole at 25°C. Assuming that the enthalpy is independent of temperature in the 10°C to 25°C range, equation 24 shows that

$$\log K_{(25\text{ C})} - \log K_{(10\text{ C})} = \frac{2900}{(2.3)(1.987)} \left(\frac{1}{298} - \frac{1}{283} \right)$$

$$7.30 - \log K_{(10\text{ C})} = 634 (-0.000178)$$

$$\log K_{(10\text{ C})} = +0.11 + 7.30 = 7.41$$

The calculated second association constant is thus $10^{7.41}$ at 10°C. Using equation 25, the value of pK_a at 10°C is 7.41.

More rigorous approaches (e.g., when ΔH is not constant but the change in heat capacity is, or when neither is constant) are available and discussed in references 5 and 19.

2.7.6 Values and Estimation Methods for Acid Dissociation Constants

Much experimental data is available on the acid dissociation constants of aqueous inorganic species. Useful compendia of these and related thermodynamic parameters are given by Sillén and Martell [17], Martell and Smith [11,12] and subsequent supplements [18] and by Perrin [14]. Table 2.7-3 lists pK_a values for a variety of inorganic substances.² The following general observations on acidity (which are not without exceptions) are suggested by the data in this table:

- For cationic species, the higher the central ion oxidation state, the higher the acidity of the first water ligand (lower pK_a value).
- 2. Because these data come from different sources than those in Table 2.7-2, some variations will be noted for corresponding species.

TABLE 2.7-3

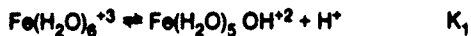
Values of Acid Dissociation Constants
for a Variety of inorganic Species

Species ^a	pK ₁	pK ₂	pK ₃	pK ₄	Ref. ^b
Ag ⁺	11.9	11.9	—	—	[14]
Al ⁺³	5.4	4.6	5.7	7.9	[14]
H ₃ AsO ₄	2.1	6.7	11.2	—	[16]
H ₃ AsO ₃	9.1	12.1	13.4	—	[16]
Ba ⁺²	13.2	—	—	—	[14]
Be ⁺²	5.7	8.2	9.9	14.0	[14]
H ₃ BO ₃	9.1	12.7	13.8	—	[6]
HCN	9.0	—	—	—	[12]
H ₂ CO ₃	6.2	10.0	—	—	[12]
H ₂ CrO ₄	0.74	6.5	—	—	[6]
Cr ⁺³	4.2	6.2	8.3	9.1	[14]
Cd ⁺²	10.3	10.3	13.2	13.1	[14]
Co ⁺²	9.9	8.9	12.7	—	[14]
Cu ⁺²	8.2	9.3	10.3	11.3	[14]
HF	2.9	—	—	—	[12]
Fe ⁺²	9.7	11.1	10.2	15.0	[14]
Fe ⁺³	2.6	3.6	3.8	11.9	[14]
Hg ⁺²	3.8	2.4	14.9	—	[14]
Mn ⁺²	10.8	11.6	12.4	13.1	[14]
Ni ⁺²	10.2	9.0	10.8	14.0	[14]
H ₃ PO ₄	2.0	6.7	11.7	—	[12]
Pb ⁺²	7.9	9.4	10.7	—	[14]
H ₂ S	7.0	12.0	—	—	[6]
H ₂ SO ₃	1.8	6.8	—	—	[6]
Sn ⁺²	3.6	3.7	9.3	—	[8]
Tl ⁺³	0.94	1.2	1.7	—	[8]
V ⁺³	2.7	3.8	7.0	—	[8]
Zn ⁺²	9.2	7.9	11.3	12.3	[8]

(Continued)

TABLE 2.7-3 (Continued)

- a. The terminology assumes an aq subscript on each species, which refers to the fact that the ion is in aqueous solution. The acid dissociation constants thus refer to loss of H⁺ from successive water molecules, e.g.,



Values are given as pK_i = -log K_i. Temperature is 20-25°C and ionic strength is 0.1 M.

- b. Data obtained from Kragten [8] was used to calculate values as follows:

$$K_1 = {}^*\beta_1, K_2 = {}^*\beta_2 / {}^*\beta_1, K_3 = {}^*\beta_3 / ({}^*\beta_1 K_2), \text{ and } K_4 = {}^*\beta_4 / ({}^*\beta_1 K_2 K_3).$$

- The magnitude of successive acid dissociation constants for a single species generally decreases (i.e., pK's generally increase).
- Small ions tend to be stronger acids than larger ions with the same charge.

Because of the diversity of inorganic species and the wealth of information available on inorganic reactions, the best sources for these constants are compilations and individual articles in the literature. In addition, five methods of estimation are described below, but all are of limited utility:

- The Ricci formula is useful only for oxy acids of a particular structure.
- The thermodynamic cycle method is complex and requires data on other reactions that may not be available. However, if a cycle can be written that includes other reactions for which data are available, the desired values can be estimated.
- Calculation from hydroxide complexation constants is possible when a procedure is available for estimating the latter constants.
- The Bayless equations apply to nonmetal hydrides and other acids.

These methods are discussed in detail below.

ESTIMATION BY THE RICCI FORMULA

The Ricci formula [15] is an empirical relationship for calculating the pK_a of an acid such as O_nM(OH)_m:

$$\text{pK}_a = 8.0 - m(9.0) + n(4.0) \quad (27)$$

where m is the formal charge on the central atom, M , and n is the number of non-hydrogenated oxygen atoms. The value of m is calculated as follows:

$$m = P.G.N. - E_u - \frac{1}{2}E_s \quad (28)$$

where P.G.N. = periodic group number of the atom
 E_u = number of unshared electrons around atom
 E_s = number of shared electrons

Example 4 To derive the first pK of arsenious acid (H_3AsO_3), for example, we first calculate m . The structure $HO-\overset{\cdot}{As}-OH$ indicates that $E_s = 6$ and $E_u = 2$. Since arsenic is in Group V,



$$m = 5 - 2 - 6/2 = 0$$

Therefore, from equation 27,

$$\begin{aligned} pK_a &= 8.0 - 0(9.0) + 0(4.0) \\ &= 8.0 \end{aligned}$$

The experimental value is 9.1.

ESTIMATION BY THE THERMODYNAMIC CYCLE METHOD

Although this procedure as described below is likely to be of little use for other chemicals of environmental concern, it provides a means of estimating the acidity of diatomic hydrogen halide acids and is therefore included here. However, where data on kinetics and on thermodynamic equilibria are available for trace elements, similar cycles could be prepared and might be useful in estimating acid dissociation and other data for trace metal complexes in aqueous systems.

The acid dissociation reaction of an acid HA is:



The equilibrium constant, K_a , is related to the free energy change of this reaction by the Gibbs Equation:

$$\Delta G_a = -RT \ln K_a \quad (30)$$

where R is the universal gas constant and T is the temperature (K). The free energy change in equation 29 at constant temperature can be calculated from the changes in enthalpy (ΔH) and entropy (ΔS) for this reaction as follows:

$$\Delta G_a = \Delta H_a - T\Delta S_a \quad (31)$$

As illustrated below, thermodynamic cycles that express the conservation of energy can be used to estimate free energy or enthalpy changes for an unknown reaction if the values for other reactions in the thermodynamic cycle are known or can be estimated.

Example 5 Figure 2.7-2 shows a thermodynamic cycle that includes the dissociation of HA [13].

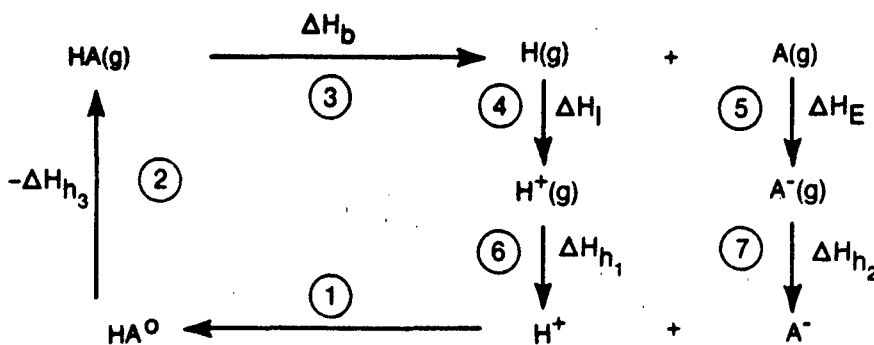


FIGURE 2.7-2 Thermodynamic Cycle which Includes Aqueous Acid Dissociation

In this cycle, 1 is the reverse of equation 23, 2 is the reverse of hydration of the neutral gas molecule, 3 is the dissociation of the gaseous molecule into atoms in the gas phase, 4 is the ionization potential of hydrogen, 5 is the enthalphy associated with the addition of an electron of the counter element (- electron affinity), 6 is the hydration of the gaseous hydrogen ion, and 7 is the hydration of the counter gaseous ion.

ΔH_a , the enthalpy change in 1, is thus:

$$\Delta H_a = \Delta H_D + \Delta H_I + H_E + \Delta H_{h_1} + \Delta H_{h_2} - \Delta H_{h_3} \quad (32)$$

ΔS_a , the entropy change in 1, is calculated as follows:

$$\Delta S_a = (S^0_{H_{aq}} + S_A - S^0_{HAaq}) - S^0_{HAAq} \quad (33)$$

This calculation requires some thermodynamic parameters that are unknown and must therefore be estimated. In the case of hydrogen halide acids, the enthalpy of hydration of undissociated HA gas (ΔH_{h_3}) can be approximated using the values for substances that are similar in size but do not ionize in solution (e.g., Ar and CH_3Cl for HCl , Kr and CH_3Br for HBr , and Xe and CH_3I for HI). ΔS^0_{HAAq} , the standard entropy of the undissociated acid, can be calculated from the standard entropy of the gas at 1 atmosphere, if the change in entropy from gas at one atmosphere to solute at unit molality is known. Values of the other parameters for the hydrogen halide acids are known [20].

Since much of the needed thermodynamic data may be unavailable for other acids (e.g., polyatomic acids), the general utility of this method is limited.

CALCULATION FROM ESTIMATED OR EXPERIMENTALLY DERIVED HYDROXIDE COMPLEXATION CONSTANTS

K_a can be calculated from K_{OH} , the equilibrium constant for reaction with hydroxide:



The acid dissociation constant, K_a , is related to K_{OH} by the following equation:

$$K_{a_i} = K_w K_{OH_i} \quad (35)$$

where K_{a_i} refers to the i th acid dissociation constant (e.g., see equations 7-9), $K_w = [H^+][OH^-] = 10^{-14.0}$ (at 25°C), and K_{OH_i} refers to the i th hydroxide equilibrium constant, which is defined as follows:



Example 6 To illustrate the use of this method, we will calculate the first acid dissociation constant of Tl^{+3}_{aq} ion (at 25°C), given a hydroxide equilibrium constant of $10^{15.4}$ [17]. From equation 35, the value of K_a is

$$K_A = 10^{-14.0} \times 10^{15.4} = 10^{1.4}$$

Thus, $pK_a = 1.4$.

Note that this value is higher than that given in Table 2.7-3 (0.94). The difference of 0.46 pK units reflects the differences due to choice in K_{OH} used. This is another example of the variation in values of acid/base equilibrium constants (and other equilibrium constants) published in the literature.

ESTIMATION BY THE BAYLESS EQUATIONS

Bayless [1] has derived an empirical relationship for calculating the aqueous pK_a of an acid in the form $[YH_{(s-g)}]^q$:

$$pK_a = 73.7 - 11.71g - 0.29gh - \frac{378.6(q-1)}{gp^2} \quad (37)$$

where

g = periodic table group number of element Y

h = number of hydrogen atoms on Y

p = period number of element Y

q = charge on the acid

Normally, hydride acids are uncharged (e.g., NH₃, HF) so q = 0, but the equation is also useful for charged species such as NH₄⁺ and SeH⁻. Reasonable agreement (average deviation of 0.4 pK_a units) was observed for a set of 17 acids [1].

Example 7 To derive the pK_a of H₂Se, we use equation 37 with the following parameter values:

$$\begin{aligned} g &= 6 \\ h &= 2 \\ p &= 4 \\ q &= 0 \end{aligned}$$

$$\text{Thus, } \text{pK}_a = 73.7 - 11.71(6) - 0.29(6)(2) - \frac{(378.6)(-1)}{(6)(4)^2} \\ = 3.90$$

The experimental value is 4.0 [1].

Bayless [1] has also extended the Ricci equation to bases of the form (HA)_nXB_m, where H represents hydrogen atoms, and A and B are atoms bonded to central atom X:

$$\text{pK}_{\text{b}} = -59.7 + 12g + 0.29gh + \frac{55.2q_a + 98.4tq_a + 225q_x}{gp^2} \quad (38)$$

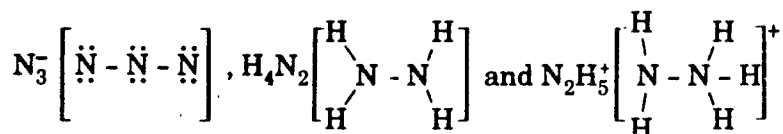
where
 g = periodic group number of atom A
 h = number of H atoms on all A atoms capable of being protonated (acting as bases)
 p = period number of atom A
 q_a = formal charge on atom A
 q_x = formal charge on atom X
 t = number of A and B atoms capable of being protonated (usually, but not always, equal to n + m).

The formal charge, q, is calculated as follows:

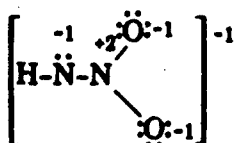
$$q = g - (\text{no. of unshared electrons}) - \frac{1}{2}(\text{no. of shared electrons}) \quad (39)$$

When using equation 38, it is helpful to draw resonance structures of the base that puts the most negative formal charge on the A and B atoms.

The equation has been tested for only a limited number of cases where A and B are nitrogen atoms, such as



Example 8 To derive the pK_b of HN_2O_2^- , we use equation 38 with the following parameter values derived from the resonance structure



$$\begin{aligned} g &= 5 \\ p &= 2 \\ h &= 1 \\ q_a &= 5 - 4 - \frac{1}{2}(4) = -1 \text{ (for N)} \text{ and } 6 - 6 - \frac{1}{2}(2) = -1 \text{ (for O)} \\ t &= 3 \text{ (the two oxygen and nitrogen atoms are considered equivalent,} \\ &\quad \text{each having the same formal charge of -1)} \\ q_x &= 5 - 0 - \frac{1}{2}(6) = 2 \end{aligned}$$

Thus,

$$pK_b = -59.7 + 12(5) + 0.29(5)(1) + \frac{55.2(-1) + 98.4(3)(-1) + 225(2)}{(5)(2)^2}$$

$$= 6.73$$

The reported value is 7.42 [1].

2.7.7 Literature Cited

1. Bayless, P.L., "Empirical pK_b and pK_a for Nonmetal Hydrides from Periodic Table Position," *J. Chem. Ed.*, **60**, 546 (1983).
2. Beck, M.T., *Chemistry of Complex Equilibrium*, Von Nostrand Reinhold Company, New York (1970).
3. Brønsted, J., *Rec. Trav. Chim.*, **42**, 718 (1923).
4. Butler, J.N., *Ionic Equilibrium, a Mathematical Approach*, Addison-Wesley Publishing Company, Reading, Mass. (1964).
5. Garrels, R.M. and C.L. Christ, *Solutions, Minerals and Equilibria*, Freeman, Cooper & Company, San Francisco, Calif. (1965).
6. Gordon, A.J. and R.A. Ford, *The Chemist's Companion*, John Wiley & Sons, New York (1972).
7. Hahne, H.C.H. and W. Kroontje, "Significance of pH and Chloride Concentration on Behavior of Heavy Metal Pollutants: Mercury (II), Cadmium (II), Zinc (II) and Lead (II)," *J. Environ. Qual.*, **2**, 444 (1973).
8. Kragten, J., *Atlas of Metal-Ligand Equilibria in Aqueous Solutions*, Halsted Press (Wiley), New York (1978).

9. Langmuir, D., *Techniques for Estimating Thermodynamic Properties for Some Aqueous Complexes of Geochemical Interest*, ACS Symposium Series No. 93, E.A. Terine (ed.), American Chemical Society (1976).
10. Lindsay, W.L., *Chemical Equilibria in Soils*, John Wiley & Sons, New York (1979).
11. Martelli, A.E. and R.M. Smith, *Critical Stability Constants, Vol. 3: Other Organic Ligands*, Plenum Press, New York (1977).
12. Martell, A.E. and R.M. Smith, *Critical Stability Constants, Vol. 5: First Supplement*, Plenum Press, New York (1982).
13. McCoubrey, J.C., "The Acid Strength of the Hydrogen Halides," *Trans. Faraday Soc.*, **51**, 743 (1955).
14. Perrin, D.D., *Ionization Constants of Inorganic Acids and Bases in Aqueous Solutions*, IUPAC Chemical Data Series, No. 29, Pergamon Press, New York (1981).
15. Ricci, J.E., "The Aqueous Ionization Constants of Inorganic Oxygen Acids," *J. Am. Chem. Soc.*, **70**, 109 (1948).
16. Ringbom, A., *Complexation in Analytical Chemistry*, Interscience (Wiley), New York (1963).
17. Sillén, L.G. and A.E. Martell, *Stability Constants of Metal-Ion Complexes*, Special Publication No. 17, The Chemical Society, Burlington House, London (1964).
18. Smith, R.M. and A.E. Martell, *Critical Stability Constants, Vol. 4: Inorganic Complexes*, Plenum Press, New York (1982).
19. Stumm, W. and J.J. Morgan, *Aquatic Chemistry*, 2nd ed., John Wiley & Sons, New York (1981).
20. Wagman, D.D., W.H. Evans, V.B. Parker, R.H. Schumm, I. Halow, S.M. Bailey, K.L. Churney and R.L. Nuttall, "The NBS Tables of Chemical Thermodynamic Properties," *J. Phys. Chem. Ref. Data*, Vol. II, Supplement No. 2 (1982).

2.8 POLYMERIZATION

2.8.1 Introduction

Polymerization is the process whereby several small molecules (monomers) react chemically with one another to form larger molecules (polymers). These polymers may be linear, linear with cross-linkages, or nonlinear.

Three types of polymers are discussed in this section: polymeric metal hydroxo complexes, polysulfides, and polyphosphates. Both metal hydroxo polymers and polysulfides can form spontaneously in aqueous systems. Polyphosphates, on the other hand, are artificially manufactured and are of environmental interest because of their degradation rather than their formation. Two additional polymerization processes, which are discussed elsewhere in this report, are the formation of polyborates (section 10.9, Boron-Containing Compounds) and the polymerization of hydrogen cyanide (section 10.2, Cyanides).

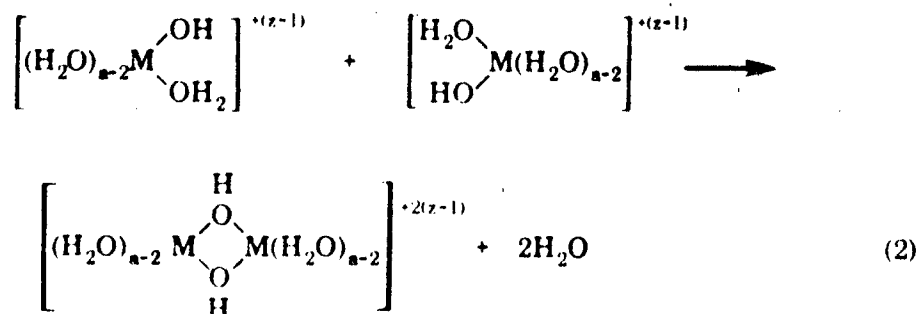
2.8.2 Hydroxo- and Oxo-Bridged Metal Polymers

When the hydroxide ion concentration of an aqueous solution containing dissolved metals is increased, the metal cations may be hydrolyzed, forming complexes with hydroxide ions. Some of the complexes formed are mononuclear — i.e., they include only one metal ion — while others, referred to as polynuclear hydroxo complexes, involve several metal ions. The formation of such polymeric species should be taken into account when one estimates the activity of various metal species in solution.

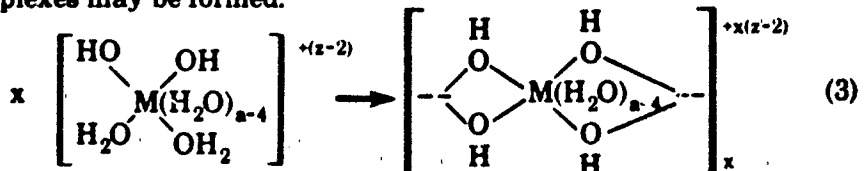
A solvated metal ion reacts with a molecule of water as follows:



Two of the resulting partially hydrolyzed species may then react, with the elimination of water, to form a dinuclear hydroxo complex:



If these hydrolysis and condensation processes are repeated, larger polynuclear hydroxo complexes may be formed:



This formation of -OH- bridges is sometimes called "olation." Under conditions of high temperature, prolonged aging and/or high pH, it may be followed by "oxolation," a process in which the -OH- bridges are converted to -O- bridges, leading eventually to the precipitation of hydrated metal oxides [6].

The linear chain structures described above are referred to as "core-plus-links" structures. They have the general formula $M[(OH)M]_{x-}^{(xz-xt+t)}$ representing a chain of $x M^{+z}$ ions in which each pair of adjacent M^{+z} ions is linked by $t OH$ -groups. The "core-plus-links" structure is in good agreement with experimental data for many metal cations [14]. However, a number of cyclic and polyhedral structures (also having hydroxide bridges connecting adjacent metal ions) have been proposed for certain polynuclear hydroxo species, and several have been confirmed by diffraction studies [1].

Formation of polynuclear hydroxo species has been reported for most metals, although in some cases the predominant species in solution is a monomer. Some metals form only dimers or trimers, while a few form much larger polynuclear species. (See Table 2.8-1.) Equilibria for the formation of simple hydrolysis species are usually established quickly, but polynuclear species are often formed more slowly. Many of these polynuclear complexes are not present under equilibrium conditions; they are often formed only under conditions of oversaturation with respect to the metal hydroxide or oxide and are kinetic intermediates in the transition from free metal ions to a solid precipitate. However, they can persist as metastable species for years and thus can be significant in natural water systems [15].

Increasing the pH of a metal ion solution, by shifting the position of the hydrolysis equilibrium (reaction 1), results in an increased concentration of hydrolyzed species $M-OH$, which in turn causes increased formation of polymeric species (as in reaction 2). Diluting a solution has two opposing effects on the formation of polymeric species:

- (1) Because dilution of acidic solutions causes a decrease in H^+ concentration (i.e., an increase in pH), it causes a shift in the hydrolysis equilibrium toward formation of hydrolyzed species.
- (2) On the other hand, dilution decreases the ratio of polynuclear to mononuclear complexes in solution. For metals that form both mononuclear and polynuclear complexes, this means that the mononuclear species predominate beyond a certain level of dilution [15].

Equilibrium constants for the formation of some polynuclear hydrolysis species are given in Table 2.8-1. An example of equilibrium calculations for the hydrolysis of iron (III), taking into account the formation of $\text{Fe}_2(\text{OH})_2^{+4}$, is given in Stumm and Morgan [15].

2.8.3 Polysulfides

Polysulfide ions, S_n^{-2} , may be formed in natural waters by the interaction of aqueous sulfide with elemental sulfur. Elemental sulfur may be formed initially either by bacterial oxidation of sulfide or by the partial oxidation of sulfide by dissolved oxygen [3]:



The reaction of hydrosulfide with sulfur then proceeds as follows [3]:



Once initiated, the formation of polysulfides from sulfur is autocatalytic, and equilibrium is attained rapidly [2].

TABLE 2.8-1

Formation Quotients for Polynuclear Metal Hydrolysis Products at 25°C,
Corrected to Zero Ionic Strength^a

$$\log K_{xy} = \log \frac{[\text{M}_x(\text{OH})_y^{+(2x-y)}][\text{H}^+]^y}{[\text{M}^{+2x}]}$$

M	M_2OH^{+2}	$\text{M}_2(\text{OH})_2^{+2}$	$\text{M}_3(\text{OH})_3^{+3}$	$\text{M}_3(\text{OH})_4^{+2}$	$\text{M}_3(\text{OH})_5^+$	$\text{M}_4(\text{OH})_6^{+4}$	$\text{M}_5(\text{OH})_8^{+4}$	$\text{M}_2(\text{OH})_y^{+(2x-y)}$
Divalent Cations								
Be^{+2}	-3.97		-8.92				-27.2	
Mg^{+2}							-39.71	
Mn^{+2}	-10.56							-23.90 [2.3]
Co^{+2}	-11.2					-30.53		
Ni^{+2}	-10.7					-27.74		
Cu^{+2}		-10.36						
Zn^{+2}	-9.0							-57.8 [2.6]
Cd^{+2}	-9.390					-32.85		
Hg^{+2}	-3.33		-6.42					
Sn^{+2}		-4.77		-6.88				
Pb^{+2}	-6.36			-23.88		-20.88	-43.61	
UO_2^{+2}		-5.62		(-11.75) ^b	-15.63			
NpO_2^{+2}		-6.39			-17.49			
PuO_2^{+2}		-8.36			-21.65			
VO^{+2}	-6.67							

(Continued)

TABLE 2.8-1 (Continued)

M	$M_2(OH)_2^{+4}$	$M_3(OH)_4^{+5}$	$M_3(OH)_5^{+4}$	$M_x(OH)^{+(3x-y)}[x,y]$
Trivalent Cations				
Al ⁺³	-7.7	-13.94		-98.73 [13,32] ^c
Sc ⁺³	-6.0		-16.34	
Y ⁺³	-14.23		-31.6	
La ⁺³	<-17.5		<-38.3	-71.2 [5,9]
Ce ⁺³	<-15.5		-33.5	
Nd ⁺³	-13.86		<-28.5	
Er ⁺³	-13.65		<-29.3	
Tl ⁺³	-3.6			
V ⁺³	-3.8			
Cr ⁺³	-5.06	-8.15		
Fe ⁺³	-2.95	-6.3		
Ga ⁺³				-139.1 [26,65] ^d
In ⁺³		-5.82 ^e		
Bi ⁺³				f
M	$M_2(OH)_2^{+6}$	$M_3(OH)_4^{+6}$	$M_3(OH)_5^{+7}$	$M_4(OH)_6^{+6}$
Tetraivalent Cations				
Zr ⁺⁴		(-0.6) ^g	(3.70) ^g	6.0
Th ⁺⁴	-6.14			-21.1 -36.76
U ⁺⁴				-17.2 ^d
M	$Sb_{12}(OH)_{64}^{-4}$	$Sb_{12}(OH)_{65}^{-5}$	$Sb_{12}(OH)_{66}^{-6}$	$Sb_{12}(OH)_{67}^{-7}$
Pentavalent Cation				
Sb ⁺⁵	20.34	16.72	11.89	6.07

(Continued)

TABLE 2.8-1 (Continued)

- a. Expressions representing the variation of these formation constants with ionic strength are given in Baes and Mesmer [1].
- b. Apparent constant which reproduces data at high chloride concentrations.
- c. The species formed is actually $\text{Al}_{13}\text{O}_4(\text{OH})_{24}^{2-}$.
- d. Approximate formula of one or more species formed.
- e. This species is consistent with the evidence, but its composition is not well established.
- f. There is evidence for the existence of $\text{Bi}_6(\text{OH})_{12}^{18}$, $\text{Bi}_9(\text{OH})_{22}^{15}$, $\text{Bi}_9(\text{OH})_{21}^{16}$, and $\text{Bi}_9(\text{OH})_{20}^{17}$, but insufficient data are available for the estimation of formation quotients.
- g. One or more of these trimeric species are believed to form. The constants are calculated from the data assuming that only one is formed.

Source: Adapted from Baes and Mesmer [1]

The equilibrium constant for reaction 5 can be written as

$$K_n = \frac{[\text{H}^+][\text{S}_n^{2-}]}{[\text{HS}^-]} \quad (6)$$

since the S(s) activity is taken as constant (unity) in a saturated solution [5]. Equilibrium constants K_n for the formation of the species S_2^{2-} through S_6^{2-} are given in Table 2.8-2. However, there is some disagreement in the literature as to which polysulfides are actually formed. Some authors consider S_5^{2-} the largest polysulfide formed [5,8], while others include S_6^{2-} as an important species [2,3,10]. Nevertheless, there is general agreement that the dominant S_n^{2-} species are those with $n \geq 4$.

TABLE 2.8-2
Equilibrium Constants for the Formation
of Polysulfide Ions

Reaction ^a		pK	
	Median ^b	Range	
$\text{S}(\text{s}) + \text{HS}^- \rightleftharpoons \text{S}_2^{2-} + \text{H}^+$	12.68	12.27-14.43	
$2 \text{S}(\text{s}) + \text{HS}^- \rightleftharpoons \text{S}_3^{2-} + \text{H}^+$	11.75	10.96-13.19	
$3 \text{S}(\text{s}) + \text{HS}^- \rightleftharpoons \text{S}_4^{2-} + \text{H}^+$	9.74	9.35-10.07	
$4 \text{S}(\text{s}) + \text{HS}^- \rightleftharpoons \text{S}_5^{2-} + \text{H}^+$	9.41	9.29-9.52	
$5 \text{S}(\text{s}) + \text{HS}^- \rightleftharpoons \text{S}_6^{2-} + \text{H}^+$	9.62	9.43-9.79	
$4 \text{S}_4^{2-} + \text{H}_2\text{O} \rightleftharpoons \text{OH}^- + \text{HS}^- + 3\text{S}_5^{2-}$	3.54	1.95-5.16	
$\text{HS}_4^- \rightleftharpoons \text{S}_4^{2-} + \text{H}^+$	7.0 ^c	—	
$\text{HS}_5^- \rightleftharpoons \text{S}_5^{2-} + \text{H}^+$	6.1 ^c	—	

(Continued)

TABLE 2.8-2 (Continued)

- a. For the reactions involving elemental sulfur (S), the sulfur activity is taken as unity and the equilibrium constant is given as $K = [S_n^{-2}] [H^+]/[HS^-]$.
- b. Except where noted, values are medians of 3 to 5 values given in cited source.
- c. Single measurements.

Source: Adapted from Boulegue & Michard [2]

This result can be demonstrated by calculating the equilibrium concentrations of the individual polysulfide species. First, the above expression for K_n can be rearranged to give the following:

$$\log [S_n^{-2}] = \log K_n + pH + \log [HS^-] \quad (7)$$

Next, using the expression for the first acid dissociation constant (K_{a1}) for H_2S and neglecting the second acid dissociation, we have

$$[HS^-] = \frac{K_{a1}[H_2S]}{[H^+]} = \frac{K_{a1}(\Sigma S^{-2} - [HS^-])}{[H^+]} \quad (8)$$

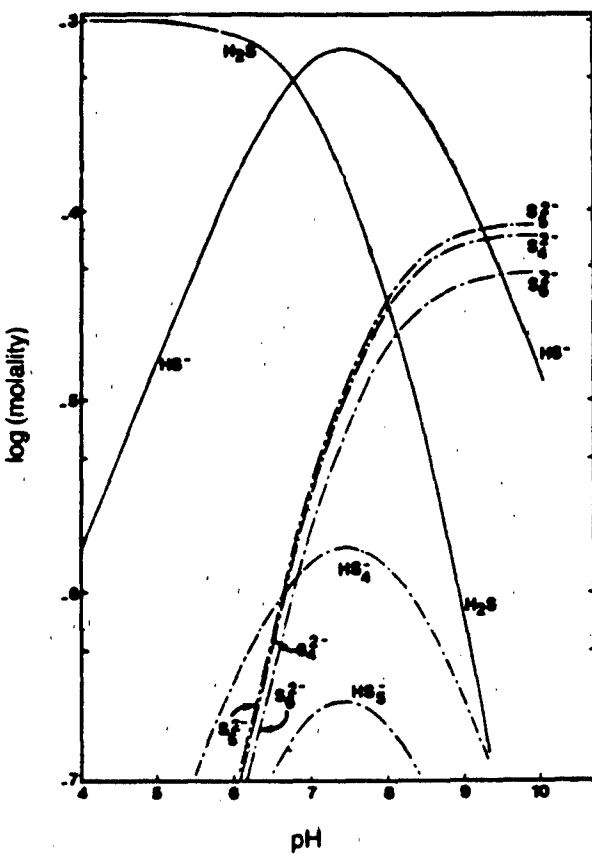
where ΣS^{-2} is the sum of the concentrations of H_2S and HS^- . Solving this equation for $[HS^-]$ and substituting into equation 7 yields an expression for the concentration of a given polysulfide species as a function of pH [5]:

$$\log [S_n^{-2}] = \log K_n + pH + \log(\Sigma S^{-2}) - \log \left(1 + \frac{[H^+]}{K_{a1}} \right) \quad (9)$$

Using the values for K_n given in Table 2.8-2, equation 9 predicts the following concentrations of polysulfide ions in a solution at pH 7 containing a total S(-II) concentration of $10^{-5} M$:

$$\begin{aligned} [S_2^{-2}] &= 1.05 \times 10^{-11} M \\ [S_3^{-2}] &= 8.91 \times 10^{-11} M \\ [S_4^{-2}] &= 9.12 \times 10^{-9} M \\ [S_5^{-2}] &= 1.95 \times 10^{-8} M \\ [S_6^{-2}] &= 1.20 \times 10^{-8} M \end{aligned}$$

By means of similar calculations (but using slightly different K_n values), Boulegue and Michard [2] plotted the distribution of sulfur species between sulfide and various polysulfides at equilibrium with colloidal elemental sulfur, as shown in Figure 2.8-1.



Source: Boulegue & Michard [3]. (Copyright 1979, American Chemical Society. Reprinted with permission.)

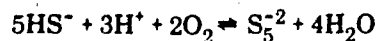
FIGURE 2.8-1 Distribution of Dissolved Sulfur Species in the System $\text{H}_2\text{S}-\text{S}_2$ (colloid) – H_2O as a Function of pH for $\Sigma[\text{S}] = 10^{-3}$ mol/kg with 0.7 M NaCl at 298 K

The above calculation is based on the assumption of a saturation concentration of elemental sulfur. Under actual reaction conditions, when sulfur must be formed by the oxidation of sulfide, polysulfide concentrations will be slightly less than the values given above. At higher pH, the formation of sulfur is not favored, so polysulfide concentrations will be much lower [5].

Table 2.8-3 gives thermodynamic data useful in calculations of equilibria involving polysulfides.

Example Is a solution containing 0.5×10^{-3} M HS^- and 0.5×10^{-3} M S_5^{2-} at pH 9.41 at equilibrium with respect to oxidation by atmospheric oxygen?

We first write the reaction of interest as



2.8-7

The equilibrium constant for this reaction can be calculated from the free energy change as follows:

$$\begin{aligned}\Delta G_r^0 &= \Delta G_f^0(S_5^{2-}) + 4\Delta G_f^0(H_2O) - 5\Delta G_f^0(HS^-) - 3\Delta G_f^0(H^+) - 2\Delta G_f^0(O_2) \\ &= 15.7 + 4(-56.69) - 5(2.88) - 0 - 0 \\ &= -225.46 \text{ kcal/mol}\end{aligned}$$

where the ΔG_f^0 values are free energies of formation of the various species from Table 2.8-3.

TABLE 2.8-3

**Free Energy of Formation Values
for Species Involved in Aqueous Polysulfide Equilibria**

Species	ΔG_f^0 (kcal/mol)
S_2^{2-}	19.0
S_3^{2-}	17.6
S_4^{2-}	16.5
S_5^{2-}	15.7
HS^-	2.88
H_2S	-6.66
$S_2O_3^{2-}$	-122.8
$H_2O(l)$	-56.687

Source: Nriagu & Hem [11] (Copyright 1978, John Wiley & Sons. Reprinted with permission.)

According to equation 6 of section 2.10.4 we can then write the following expression for the redox equilibrium constant:

$$\log K_{eq} = \frac{\Delta G_r^0}{-2.3RT} = -0.733\Delta G_r^0 = 165.26$$

The partial pressure of oxygen above this solution at equilibrium can be computed from the expression for K_{eq} together with the numerical values of the pH and concentrations of the dissolved species:

$$K_{eq} = \frac{[S_5^{2-}]}{[HS^-]^5 [H^+]^3 (pO_2)^2}$$

with $K_{eq} = 10^{165.26} M^{-7} \cdot atm^{-2}$

$$[S_5^{2-}] = 0.5 \times 10^{-3} M$$

$$[HS^-] = 0.5 \times 10^{-3} M$$

$$\text{and } [H^+] = 10^{-9.41} M$$

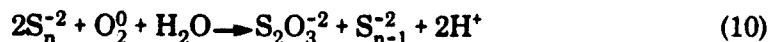
Note that since 9.41 is the pK value for the reaction of HS^- with sulfur to form S_5^{2-} , at pH 9.41 the concentrations of these two species should be approximately equal, as given above. Rearranging to solve for pO_2 , we have:

$$\begin{aligned}\text{pO}_2 &= \left(\frac{[\text{S}_5^{2-}]}{[\text{HS}^-]^5 [\text{H}^+]^3 K_{\text{eq}}} \right)^{1/2} = \left(\frac{10^{-3.3}}{(10^{-3.3})^5 (10^{-9.41})^3 10^{165.3}} \right)^{1/2} \\ &= 10^{-62} \text{ atm}\end{aligned}$$

The result shows an equilibrium partial pressure of oxygen of 10^{-62} atm, a partial pressure that is vanishingly small for all practical purposes. Oxygen pressures higher than the equilibrium value should drive the reaction to the right, producing sulfur in higher oxidation states.

A similar calculation shows that about the same pressure of oxygen is an equilibrium value for reaction 4, in which HS^- is oxidized to elemental sulfur. Thus, we see that sulfide and polysulfide are not equilibrium species in water open to the atmosphere.

As demonstrated in the preceding example, polysulfides are not stable species under aerobic conditions. However, they are sometimes found in the natural environment, especially in hydrothermal or heavily polluted water [4,11]. They are formed as intermediates in the chemical oxidation of sulfide by oxygen, as shown in equations 4 and 5. Polysulfide ions may subsequently be oxidized to thiosulfate as follows [3]:



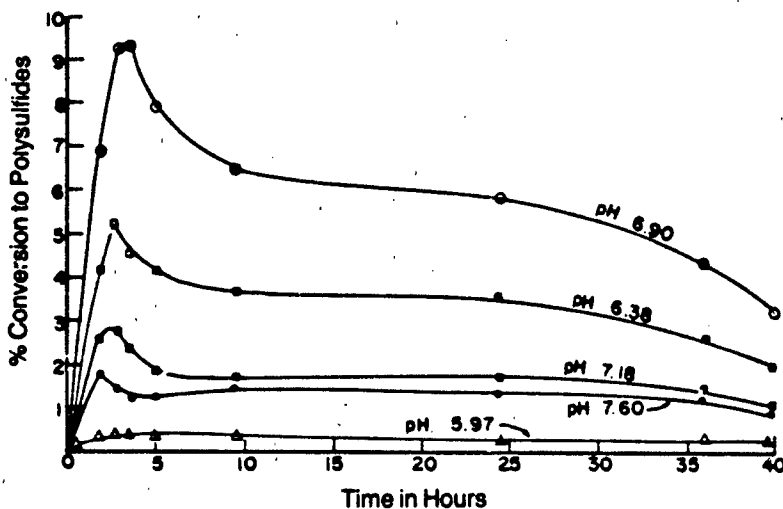
However, the oxygenation of sulfide occurs very slowly in the absence of catalysts; thus, sulfides may coexist with dissolved oxygen for long periods of time [4]. Anaerobic or reducing conditions favor the persistence of sulfides and polysulfides.

The rate of polysulfide formation, and therefore the overall rate of oxygenation of sulfide, shows a complex dependence on pH. Figure 2.8-2 shows the time dependence of polysulfide formation in dilute aqueous solution at various pH values (as determined in laboratory experiments in which sodium sulfide was added to water containing dissolved oxygen). As shown, maximum polysulfide formation occurs near pH 7. The fact that polysulfides are not formed at low pH, which is predicted by calculations of the equilibrium distribution of sulfur species (Figure 2.8-1), may be attributed to the protonation of HS^- to form H_2S . Polysulfide formation also tapers off above pH 9, presumably because elemental sulfur is not formed by the chemical oxidation of sulfide at high pH [5].

2.8.4 Polyphosphates

Polyphosphoric acids and polyphosphates consist of multiple PO_4 units. They are formed by the condensation of two or more molecules of orthophosphoric acid (H_3PO_4 , also known as simply phosphoric acid), with the loss of water. Inorganic

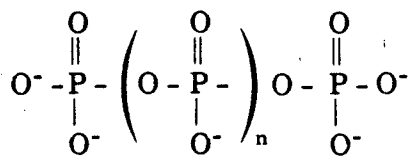
polyphosphates do not occur naturally, but they are manufactured in large quantities. They are used primarily as fertilizers, components of synthetic detergents, and water-softening agents in water treatment. They are also used in a variety of industrial processes, in the petroleum industry, in pigment manufacture, and in food processing. They are thus released to the environment both directly (e.g., as fertilizers) and in waste streams [7].



Source: Chen [4]. (Copyright 1974, Ann Arbor Science Publishers. Reprinted with permission from Butterworth Publishers, current holders of the copyright.)

FIGURE 2.8-2 Time Dependence of Polysulfide Formation in Aqueous Solution With an Initial Total S(II) Concentration of $3.0 \times 10^{-3} M$, and $p(O_2) = 1 \text{ atm}$

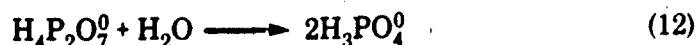
Structurally, each PO_4 unit of a polyphosphate is a phosphorus atom surrounded by a tetrahedron of four oxygen atoms; in polyphosphates, these tetrahedra are linked at their corners by shared oxygen atoms. Linear polyphosphates, with straight chains of P-O-P linkages, range from the simple diphosphate (referred to as pyrophosphate) to long-chain structures with molecular weights in the millions. The linear polyphosphate anion may be represented by the general formula



The linear polyphosphates include most commercially important phosphate salts. However, cyclic structures (known as metaphosphates), branched-chain structures (ultraporphosphates), and compounds with incompletely defined structures are also known [7].

Pyrophosphoric acid ($H_4P_2O_7$) and tripolyphosphoric acid ($H_5P_3O_{10}$) are major components of household synthetic detergents; they have the ability to complex the hardness ions Ca^{+2} and Mg^{+2} , thus preventing these ions from combining with detergent molecules. Largely as a result of their use in detergents, condensed phosphates comprise 50-60% of the phosphates in domestic wastewater [13].

Once released to the environment, however, polyphosphates are gradually hydrolyzed. Their hydrolysis ultimately yields orthophosphate, as in the following equations for the hydrolysis of tripolyphosphate and pyrophosphoric acid [13]:



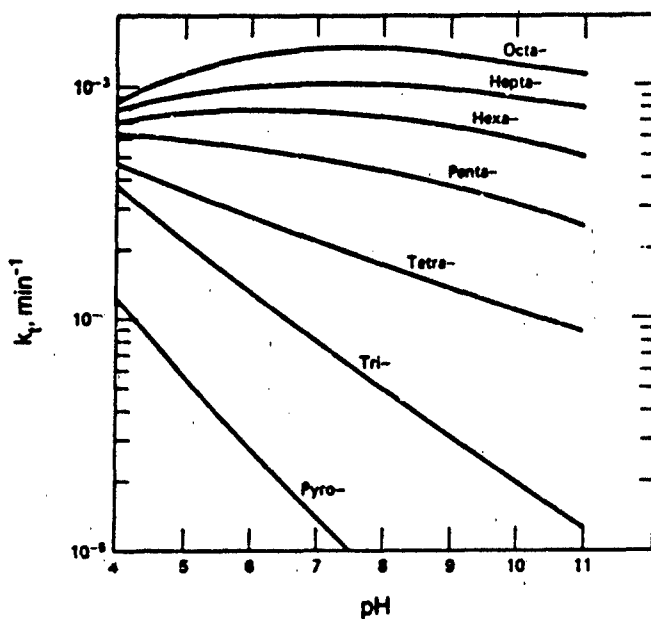
The mechanisms and initial products of hydrolysis differ for short-chain, long-chain, and cyclic polyphosphates, and the rates of hydrolysis are influenced by several factors, including pH, temperature, metal-ion catalysis, and enzymatic catalysis.

Short-chain polyphosphates (up to four phosphate units) are hydrolyzed primarily by the splitting of phosphorus-oxygen bonds at one end of the polyphosphate chain. Thus, for example, tetrapolyphosphate is converted first to tripolyphosphate, then to pyrophosphate, and finally to orthophosphate. (There is some evidence, however, that the degradation proceeds by other routes as well.) The hydrolysis reaction follows first-order kinetics in more concentrated solutions; apparent first-order degradation rate constants for sodium polyphosphates are shown in Figure 2.8-3. As shown, the hydrolysis rates for the short-chain polyphosphates increase with decreasing pH. The rates also increase with increasing temperature [12].

Long-chain polyphosphates (more than seven or eight phosphates) may be hydrolyzed by several routes: cleavage of chain-end bonds, cleavage of bonds in the interior of the chain, and splitting off of trimetaphosphate rings from either the end or the middle of the chain. Three rate constants can be calculated from experimental data: k_t , overall disappearance of a polyphosphate species; k_e , clipping of the end group to form orthophosphate; and k_m , formation of trimetaphosphate. All three rate constants follow first-order kinetics, so the degradation rate can be represented as follows:

$$-dC/dt = k_t C = (k_e + k_m)C \quad (13)$$

where C is the concentration of the polyphosphate species being studied. Variations in pH have different effects on the various hydrolysis mechanisms. The formation of orthophosphate by end-group clipping increases at low pH, while the formation of trimetaphosphate is inhibited at low pH. As a result, the ratio of orthophosphate to trimetaphosphate produced increases with decreasing pH, and the overall degradation rate reaches a maximum at pH 7. Increasing temperature results in a decrease in the ratio of orthophosphate to trimetaphosphate [12].



Source: Shen and Morgan [12]. (Copyright 1973, John Wiley & Sons.
Reprinted with permission.)

FIGURE 2.8-3 Apparent First-order Rate Constants for the Hydrolytic Degradation of Sodium Polyphosphates at 60°C.

Of the cyclic metaphosphates, the most common are tri- and tetrametaphosphates. These compounds are initially hydrolyzed to the corresponding linear polyphosphates, which are then degraded to lower phosphates. The hydrolysis to the linear polyphosphates is catalyzed by both acid and base, proceeding most slowly between pH 6 and 10 [12].

Hydrolysis of both linear polyphosphates and cyclic metaphosphates is enhanced by the presence of metal cations. In the case of long chain polyphosphates, the formation of trimetaphosphate is accelerated more than the clipping of chain ends. The degradation rate for linear polyphosphates increases with increasing chain length, approaching a limiting value for chain lengths greater than about ten [12].

Polyphosphate hydrolysis is very slow in sterile solutions. At 10°C, for example, the time required for 5% hydrolysis of a pyrophosphate solution would be about a year at pH 4, many years at pH 7, and over a century at pH 10. Hydrolysis rates are substantially increased at higher temperatures: 5% hydrolysis of a pyrophosphate solution at pH 7 would take under a month at 40°C and only a few days at 60°C [13]. However, much faster hydrolysis can result from catalysis by a number of enzymes, known as phosphatases, which are present in most microorganisms [13]. Their catalytic action is strongly affected by pH and the presence of metal ions. Such enzymes increase rates of hydrolysis by a factor of up to 10⁶ [12]. Because this

rapid hydrolysis may be catalyzed by microorganisms in raw sewage, much of the condensed phosphate in wastewater is converted to orthophosphate before it even reaches a waste treatment plant. Secondary biological treatment usually ensures the hydrolysis of all condensed phosphate in wastewater [13]. Environmental concerns related to phosphate discharges are discussed in § 8.3.2.

The direct application of polyphosphate fertilizers to the soil is another source of polyphosphates in the environment. Various cations in soil, such as Ca^{+2} and Fe^{+2} , react with liquid polyphosphate fertilizers and precipitate as complex polyphosphates [9]. However, the adsorption of polyphosphate on clay has been observed to increase its degradation rate [12]. Calculations of the equilibrium concentrations of various polyphosphate species show that pyrophosphate is unstable in soils, eventually reverting to orthophosphate. Longer-chain polyphosphates are thought to be even less stable [9].

2.8.5 Literature Cited

1. Baes, C.F., Jr. and R.E. Mesmer, *The Hydrolysis of Cations*, John Wiley & Sons, New York '1976).
2. Boulegue, J. and G. Michard, "Constantes de Formation des Ions Polysulfurés S_6^{-2} , S_5^{-5} , et S_4^{-2} en Phase Aqueuse," *J. Fr. Hydrol.*, **9**, 27-34 (1978).
3. Boulegue, J. and G. Michard, "Sulfur Speciations and Redox Processes in Reducing Environments," in *Chemical Modeling in Aqueous Systems*, E.A. Jenne (ed.), ACS Symposium Series 93, American Chemical Society, Washington, D.C. (1979).
4. Chen, K.Y., "Chemistry of Sulfur Species and Their Removal from Water Supply," in *Chemistry of Water Supply, Treatment and Distribution*, A.J. Rubin (ed.), Ann Arbor Science Publishers, Ann Arbor, Michigan (1974).
5. Chen, K.Y. and J.C. Morris, "Kinetics of Oxidation of Aqueous Sulfide by O_2 ," *Environ. Sci. Technol.*, **6**, 529-37 (1972).
6. Gimblett, F.G.R., *Inorganic Polymer Chemistry*, Butterworth and Co., London (1963).
7. Hudson, R.B. and M.J. Dolan, "Phosphoric Acid and Phosphates," in *Kirk-Othmer Encyclopedia of Chemical Technology*, 3rd ed., Vol. 17, John Wiley & Sons, New York (1982).
8. Licht, S., G. Hodes and J. Manassen, "Numerical Analysis of Aqueous Polysulfide Solutions and Its Application to Cadmium Chalcogenide/Polysulfide Photoelectrochemical Solar Cells," *Inorg. Chem.*, **25**, 2486-89 (1986).
9. Lindsay, W.L., *Chemical Equilibria in Soils*, John Wiley & Sons, New York (1979).
10. Morel, F.M.M., *Principles of Aquatic Chemistry*, John Wiley & Sons, New York (1983).

11. Nriagu, J.O. and J.D. Hem, "Chemistry of Pollutant Sulfur in Natural Waters," in *Sulfur in the Environment*, J.C. Nriagu (ed.), John Wiley & Sons, New York (1978).
12. Shen, C.Y. and F.W. Morgan, "Hydrolysis of Phosphorus Compounds," in *Environmental Phosphorus Handbook*, E.J. Griffith, A. Beeton, J.M. Spencer and D.T. Mitchell (eds.), John Wiley & Sons, New York (1973).
13. Snoeyink, V.R. and D. Jenkins, *Water Chemistry*, John Wiley & Sons, New York (1980).
14. Stumm, W., "Metal Ions in Aqueous Solutions," in *Principles and Applications of Water Chemistry; Proceedings*, S.D. Faust and J.V. Hunter (eds.), John Wiley & Sons, New York (1967).
15. Stumm, W. and J.J. Morgan, *Aquatic Chemistry: An Introduction Emphasizing Chemical Equilibria in Natural Waters*, 2nd ed., John Wiley & Sons, New York (1981).

2.9 COMPLEXATION

This section addresses the formation of aqueous complexes between metal ions and complexing agents (ligands). The various types of aqueous complexes, the importance of complexation in environmental systems and a mathematical representation (the complex formation or equilibrium constant) of the process under equilibrium conditions are presented. Values, trends, and methods for estimating the complex formation constant are provided.

2.9.1 Environmental Importance

Inorganic substances adapt to the particular aqueous chemical environments to which they are exposed, subject to kinetic limitations on the processes. Chemical environments include many potential ligands that can complex strongly or form loose ion pairs. The behavior of an aquo complexed metal ion varies considerably from that of other complexes of the same central ion in many chemical reactions. Chemical properties such as solubility, attenuation behavior on soils, bioconcentration factors and toxicity are modified through complexation.

2.9.2 Description of Property

Metal ions exist in aqueous systems in the form of complex ions, which are formed by reaction of the metal ions (e.g., Fe^{+2}) with ligands (usually neutral or anions such as H_2O or Cl^-). Ligands surround metal ions in what are termed "coordination spheres." A coordination sphere can be divided into two parts:

- The primary or inner coordination sphere consists of the ligands that are directly bonded to the metal ion.
- The secondary or outer coordination sphere consists of ligands associated (polarized or loosely coordinated) with the metal ion.

The coordination number of the metal ion (typically 6 or 4) refers to the number of ligand positions in the primary coordination sphere. Since the boundary between the secondary coordination sphere and the bulk solvent is vague, the total number of associated ligands is difficult to define and can greatly exceed the coordination number.

In aqueous systems, water molecules generally occupy most of the locations in both coordination spheres. In an aquated metal ion (designated $\text{M}^{+x}_{\text{aq}}$, with the subscript aq assumed), all the ligands are water molecules. Complexation of these "aquo ions" by other ligands refers to either of the following processes:



Equation 1 refers to substitution of one or more of the outer-sphere water molecules by a ligand (L^{-y}) to form an outer-sphere complex ion, $(M, L)^{+x-y}$. Equation 2 refers to substitution of one or more of the inner-sphere water ligands to form an inner-sphere complex, $(M-L)^{+x-y}$. The *outer-sphere or ion pair association constant* (at low ionic strength, where activity coefficients are 1), is defined as

$$K_{os} = \frac{[(M, L)^{+x-y}]}{[M^{+x}] [L^{-y}]} \quad (3)$$

where $[(M, L)^{+x-y}]$, $[M^{+x}]$, and $[L^{-y}]$ are the concentrations of the respective species. Similarly, the *inner-sphere complexation constant* is defined as:

$$K_{is} = \frac{[(M-L)^{+x-y}]}{[(M, L)^{+x-y}]} \quad (4)$$

The *complexation equilibrium constant or stability constant* as experimentally measured for many metal ions refers to the reaction:



where $K_1 = \frac{[(M-L)^{+x-y}]}{[M^{+x}] [L^{-y}]} = K_{is} K_{os}$

For many ions, the exchange between inner and outer coordination ligands is so rapid that it is not possible to distinguish between outer- and inner-sphere complexes; in this case, the measured equilibrium constant (K_1) actually refers to mixed inner and outer sphere complex formation. For other ions, the exchange between inner and outer spheres is so slow that only outer-sphere equilibria are observed.

The ligand water molecules in the inner coordination sphere of the metal ion can be successively replaced by other potential ligands. The equilibria are designated by individual equilibrium constants (called *stepwise stability constants*):



The *overall stability constant*, β , refers to the following reaction:



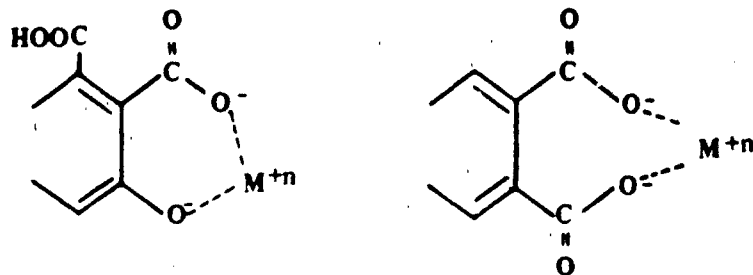
where $\beta_n = K_1 K_2 K_3 \dots K_n \quad (10)$

Ligands are often classified as to the number of donor atoms that can form a bond to the metal ion. A *monodentate* ligand (e.g., $-\text{OH}_2$, $-\text{NH}_3$) has only one atom that can coordinate to the metal; *bidentate* and *tridentate* indicate that two and three atoms of the ligand, respectively, can coordinate to the metal at two or three ligand positions (e.g., ethylenediamine and diethylenetriamine). The formation of a complex between a polydentate ligand (more than one coordinating atom) and a metal ion is referred to as a *chelate complex ion*. As chelation markedly affects chemical behavior of the central metal ion, many polydentate ligands are used commercially to "sequester," i.e., prevent precipitation.

2.9.3 Values of Complexation Equilibrium Constants

Several compilations of complexation equilibrium constants are available [11,15,22,23]. Representative values for metals with common monodentate ligands are given in Table 2.9-1. Data for polydentate ligands used in commercial applications are summarized in Table 2.9-2. It is not unusual for reported values of complexation constants to differ by 0.25 to 0.5 log units, depending on the methods by which they were calculated or experimentally derived. The coordination numbers of metal ions (Table 2.9-3) are useful in determining how many ligand equilibria should be considered when assessing their complex speciation. For many kinetically labile ions, e.g., Ag^+ , Cd^{+2} , Hg^{+2} , the coordination numbers in solution are not known [1]; for others (e.g., Ni^{+2} , V^{+3} , Fe^{+3} , Mn^{+2} , Fe^{+2} , Cu^{+2} , Ti^{+3}), spectral interpretations are consistent with a value of 6. There is some evidence [1] that rare earths have coordination numbers of 9 in solution. Values of some ion pair association constants are given in Table 2.9-4.

Naturally occurring organic compounds such as humic and fulvic acids, carbhydrates and proteinaceous material play an important role in controlling the solubilities and activities of metals in natural waters [14]. Many trace organics derived from degradation of plant and animal tissues have functional groups that can form chelates with metals. Humic and fulvic acids form quite stable complexes, especially when chelation rings such as the following can occur:



Humic acids are macromolecular materials of variable composition consisting of core units (having carboxyl, hydroxyl, carbonyl, and methoxy groups) plus hydrolyzed protein and carbohydrate fractions. Detailed complexation research is complicated by

the lack of information on the structure of the macroligands and the fact that their composition varies with the geographic location and types of systems from which they are obtained. Thus, complexation equilibria constants in the literature are useful only for the particular systems tested.

A somewhat similar situation exists for fulvic acids, which are also macromolecular-weight acids and represent the alkali-soluble degradation products of humic acids. They contain carboxyl, phenolic, and aliphatic hydroxyl groups, but their exact structures are unknown. Data for their complexation constants have been reported [6,13,19,24], but, as with humic acids, their nature varies with the sources and conditions of formation. The pH of a solution often markedly affects the extent of

TABLE 2.9-1

**Logarithms of Complexation Equilibrium Constants (K) and Overall Stability Constants (β_2) for Metals with Commonly Occurring Ligands
(at 25°C and zero ionic strength, unless noted)**

Metal	M-Cl ^a	M-Cl ₂ ^b	M-SO ₄ ^b	M-OH ^a	M(OH) ₂ ^b
Na ⁺	-1.85	--	1.06	-0.2	--
K ⁺	-0.5	--	0.96	-0.5	--
Ca ⁺²	--	--	2.31	1.15	--
Mg ⁺²	--	--	2.36	2.56	--
Ba ⁺²	-0.13 ^d	--	2.7	0.5	--
Cr ⁺³	0.6	--	3.0	10.0	18.3
Al ⁺³	--	--	--	9.0	18.7
Fe ⁺³	1.5	2.1	4.0	11.8	22.3
Mn ⁺²	0.6	--	2.3	3.4	5.8
Fe ⁺²	0.36 ^c	0.40 ^c	2.2	4.5	7.4
Co ⁺²	0.5	--	2.2	4.3	5.1
Ni ⁺²	0.6	--	2.3	4.1	9.0
Cu ⁺²	0.4	-0.4	2.4	6.5	11.8
Zn ⁺²	0.4	0.0	2.1	5.0	11.1
Pb ⁺²	1.6	1.8	2.8	6.3	10.9
Hg ⁺²	7.2	14.0	2.5	10.6	21.8
Cd ⁺²	2.0	2.6	2.3	3.9	7.6
Ag ⁺	3.3	5.3	1.3	2.0	4.0

Sources: Kotrlý and Šúcha [11]; Morel [15]; Sillén and Martell [22]

a. Refers to K values for the reaction $M + L \rightleftharpoons ML$ where $L = Cl^-$, OH^- or SO_4^{2-}

b. Refers to β_2 values for the reaction $M + 2L \rightleftharpoons ML_2$ where $L = Cl^-$ (or OH^-)

c. 2 M ionic strength

d. 18°C

complexation of an organic species with a trace metal since H^+ competes for the basic coordination site. In addition, complexation constants based on purified samples are believed to be only approximations of those for natural samples [14]. Data for humic and fulvic acids complexes of trace metals are given in Chapter 7.

TABLE 2.9-2
Logarithms of Complexation Equilibrium Constants (K) for Metals
with Sequestering Agents of Commercial Interest
(1:1 complex formation at 25°C and 0.10 M ionic strength, unless noted)

Metal	Sequestering Agent ^a					
	NTA	HIDA	EDTA	HEDTA	TPP	CIT ^b
Mg ⁺²	5.47	3.46	8.83	7.0	5.8	3.40
Ca ⁺²	6.39	4.77	10.61	8.2	5.2	3.55
Mn ⁺²	7.46	5.56	13.81	10.8	7.0	3.7
Fe ⁺²	8.82	6.77	14.27	12.2	—	4.4
Fe ⁺³	15.9	11.6	25.0	19.8	—	11.40
Co ⁺²	10.38	8.02	16.26	14.5	6.9	5.00
Ni ⁺²	11.50	9.33	18.52	17.1	6.7	5.40
Cu ⁺²	12.94	11.72	18.70	17.5	8.1	5.90
Zn ⁺²	10.66	8.45	16.44	14.6	7.3	4.98
Cd ⁺²	9.78	7.24	16.36	13.1	6.5	3.75
Hg ⁺²	14.6	5.4	21.5	20.0	—	—
Pb ⁺²	11.34	9.5	17.88	15.5	—	4.08 ^c

a. NTA = nitrilotriacetic acid, $N(CH_2COOH)_3$
HIDA = Ethanolaminodiacetic acid, $(HOCH_2CH_2)N(CH_2COOH)_2$
EDTA = ethylenediaminetetraacetic acid, $(HOOCCH_2)_2NCH_2CH_2N(CH_2COOH)_2$
HEDTA = N-(2-hydroxyethyl)-ethylene-dinitrioltriacetic acid,
 $(HOCH_2CH_2)(HOOCCH_2)NCH_2CH_2N(CH_2COOH)_2$
TPP = tripolyphosphoric acid, $(HO)_2OPOPO_2(OH)PO(OH)_2$
CIT = citric acid, $(HOOCCH_2(OH)(COOH)C(CH_2COOH)$

b. 20°C

c. 2.0 M ionic strength

Source: Martell [14]

TABLE 2.9-3
**Experimental Coordination Numbers of Various Ions
 In Aqueous Media**

Ion	Coordination Number ^a	Ion	Coordination Number ^a
Al^{+3}	6	Ni^{+2}	4 or 6
Be^{+2}	4	Sc^{+3}	5
Co^{+2}	6	Zn^{+2}	6
Ga^{+3}	6	Rh^{+3}	6
Mg^{+2}	6	Co^{+3}	6
Cr^{+3}	6	Li^{+}	4

^a Rounded to nearest integer

Sources: Basolo and Pearson [1]; Lincoln [12]

TABLE 2.9-4
Experimental Values of Ion Pair Association Constants at 25°C

Reaction	Ionic Strength (M)	K_{oe} (M^{-1})
$\text{Co}(\text{NH}_3)_5 \text{H}_2\text{O}^{+3} + \text{SCN}^- \rightleftharpoons [\text{Co}(\text{NH}_3)_5 \text{H}_2\text{O}, \text{SCN}]^{+2}$	0.5	0.65
$\text{Co}(\text{NH}_3)_5 \text{H}_2\text{O}^{+3} + \text{N}_3^- \rightleftharpoons [\text{Co}(\text{NH}_3)_5 \text{H}_2\text{O}, \text{N}_3]^{+2}$	2.0	0.26
$\text{Ni}(\text{H}_2\text{O})_6^{+2} + \text{MePO}_4^{-2} \rightleftharpoons [\text{Ni}(\text{H}_2\text{O})_6, \text{MePO}_4]$	0.1	41
$\text{Ni}(\text{H}_2\text{O})_6^{+2} + \text{NH}_3^{+2} \rightleftharpoons [\text{Ni}(\text{H}_2\text{O})_6, \text{NH}_3]^{+2}$	0.1	0.15
$\text{Cr}(\text{H}_2\text{O})_6^{+3} + \text{SCN}^- \rightleftharpoons [\text{Cr}(\text{H}_2\text{O})_6, \text{SCN}]^{+2}$	0	7
$\text{Cr}(\text{H}_2\text{O})_6^{+3} + \text{Cl}^- \rightleftharpoons [\text{Cr}(\text{H}_2\text{O})_6, \text{Cl}]^{+2}$	0	13
$\text{Co}(\text{NH}_3)_6^{+3} + \text{SO}_4^{-2} \rightleftharpoons [\text{Co}(\text{NH}_3)_6, \text{SO}_4]^+$	0	2.2×10^3

Sources: Basolo and Pearson [1]; Sillén and Martell [23]; Wilkins [27]

2.9.4 Estimation of Complexation Equilibrium Constants

Owing to the diversity of inorganic metals and complexing ions, and to the volume of experimental work that has been performed, the best sources of complexation data are individual studies and compilations. However, a few relationships have been derived to estimate these constants for a limited group of complexes. The following methods will be described:

- *Eigen-Fuoss equation* for estimation of outer-sphere (ion-pair) association constants;
- *Hancock and Marsicano approach* for estimating inner-sphere complexation constants for monodentate ligands, polydentate ligands containing nitrogen donor atoms, and aminocarboxylate ligands; and
- *Tanaka equations* for estimation of inner-sphere complexation constants for formation of ML_2 complexes and mixed complexes (two different ligands, excluding H_2O) of nickel and copper.

OUTER-SPHERE ASSOCIATION CONSTANTS

Outer-sphere (ion pair) association constants can be estimated with the following equation, which was derived independently by Eigen [3,4] and Fuoss [5]:

$$K_{os} = \frac{4\pi Na^3}{3000} \exp[-U(a)/kT] \quad (11)$$

where K_{os} = ion pair association constant for spherically symmetrical ions, i.e., all ligands identical (M^{-1})

N = Avogadro's number ($6.023 \times 10^{23}/mole$)

a = distance of closest approach between ions (cm)

e = electron charge (4.80×10^{-10} esu)

k = Boltzmann constant (1.38×10^{-16} erg/K)

T = temperature (K)

$U(a)$ = Debye-Hückel interionic potential =
 $(Z_1 Z_2 e^2 / a D) - [Z_1 Z_2 e^2 \theta / D(1 + a\theta)]$

θ = $(8\pi N e^2 l / 1000 D k T)^{1/2}$

Z_1 = charge on Ion 1

Z_2 = charge on Ion 2

D = dielectric constant of the solvent (e.g., 78.5 for H_2O at 25°C)

I = ionic strength (mol/l)

As noted by Hammes and Steinfeld [7], this method for calculating K_{os} involves many approximations, including the following:

- The distance of closest approach (a) can only be estimated.
- Only electrostatic binding forces are considered.

- A macroscopic dielectric constant (ϵ) is used at the molecular level.
- The term for calculating the Debye-Hückel interionic potential ($U(a)$) is known to become inaccurate at higher ionic strengths.

Values of K_{∞} calculated by the above method are generally regarded in the literature as accurate to within a factor of 4 [7,16].

Establishing the value of "a" is one of the chief problems in using equation 11. An approximation can be obtained by the following equation:

$$a = \frac{|Z_1 Z_2| e^2}{3 D k T} \quad (12)$$

Table 2.9-5 lists values of "a" estimated by equation 12 for various values of Z_1 and Z_2 . (Note that the tabulated values must be converted to centimeters for use in equation 11). Some investigators have used crystallographic radii or empirically derived values that fit experimentally observed results; these values of "a" typically range from 3 to 6 Å.

TABLE 2.9-5

**Initial Estimates of Parameter "a"
(using equation 12)**

Z_1	Z_2	a (Å)
+1	-1	2.4
+1	-2	4.8
+2	-2	9.5
+1	-3	7.1
+2	-3	14.3
+3	-3	21.4

Another limitation of equation 11 is that ion pairing may not always occur — i.e., in some cases where ion pairs are predicted, none have been detected. This is true, for example, of a large class of 2:1 electrolytes such as the alkaline earth halides [17].

The ion pair association constant for an unsymmetrically coordinated metal ion (one having other ligands besides H_2O) with a total coordination number of 6 can be estimated as follows [7]:

$$K'_{\infty} = S K_{\infty} \quad (13)$$

where S = steric correction factor = $n/6$
 n = number of sites occupied by water molecules
 K_{∞} = ion pair association constant for a spherically symmetrical ion

Calculated values of K_{os} are given in Table 2.9-6 for a variety of ion charges, ionic strengths and values of "a". The strong dependence of K_{os} on "a" is evident: the calculated value can change by nearly three orders of magnitude with a 2 Å variation in "a". The magnitude of the error depends on the charges of the ions. Changes in ionic strength have no effect on K_{os} if one of the ions in the pair has a zero charge, but deviations of four orders of magnitude can occur with highly charged species (+3 and -3) when the ionic strength increases from zero to 0.5 M.

Example 1 Calculate the outer-sphere association constant for the reaction between $\text{Cr}(\text{H}_2\text{O})_6^{+3}$ and Cl^- at 25°C and an ionic strength of zero. The following parameter values are used with equation 11:

$$\begin{aligned} I &= 0 \text{ M} \\ D &= 78.5 \text{ (dielectric constant of water at } 25^\circ\text{C)} \\ Z_1 &= +3 \text{ (charge on } \text{Cr}(\text{H}_2\text{O})_6^{+3}, \text{ Ion 1)} \\ Z_2 &= -1 \text{ (charge on } \text{Cl}^-, \text{ Ion 2)} \\ a &= 7.1 \times 10^{-8} \text{ cm (using equation 12)} \\ T &= 298 \text{ K} \end{aligned}$$

$$\begin{aligned} \text{Thus, } \theta &= \sqrt{\frac{8(3.14)(6.023 \times 10^{23})(4.80 \times 10^{-10})^2(0)}{1000(78.5)(138 \times 10^{-16})(298)}} \\ &= 0 \\ \text{and } U(g) &= \frac{(+3)(-1)(4.80 \times 10^{-10})^2}{(7.1 \times 10^{-8})(78.5)} - \frac{(+3)(-1)(4.80 \times 10^{-10})^2(0)}{(78.5)[1 + (7.1 \times 10^{-8})(0)]} \\ &= -1.24 \times 10^{-13} \\ \text{Therefore, } K_{\text{os}} &= \frac{4(3.14)(6.023 \times 10^{23})(7.1 \times 10^{-8})^3}{3000} \exp \left[\frac{-(-1.24 \times 10^{-13})}{(1.38 \times 10^{-16})(298)} \right] \\ &= 0.902 \exp(3.02) = 18.5 \text{ M}^{-1} \end{aligned}$$

The experimental value is 13 [1].

INNER-SPHERE COMPLEXATION CONSTANTS (HANCOCK AND MARSICANO APPROACH)

Monodentate Ligands

The approach to estimation of inner-sphere complexation equilibrium constants (formation constants) is based upon the presence of linear free energy relationships between properties of the metal and the ligand. Such relationships are observed, for example, in logarithmic plots of the formation constant of a metal with a particular ligand (K_1) versus equilibrium constant of the reaction of the ligand with another metal ion or with H^+ (K_2), according to the equation

$$\log K_1 = A \log K_2 \quad (14)$$

TABLE 2.9-6

Outer-sphere Formation Constants Calculated by Eigen-Fuoss Equation
 (In aqueous solution at 298 K; see eq. 11 for definitions of symbols)

Ion Pair	Z_1	Z_2	$K(M)$	$a(\text{\AA})$	$K_{oe}(M^{-1})$
$(M^{+x})(L^0)$	+x	0	0	3	0.068
	+x	0	0	4	0.161
	+x	0	0	5	0.315
	+x	0	0	6	0.545
	+x	0	0.5	5	0.315
$(M^{+1})(L^{-1})$	+1	-1	0	2.4	0.68
	+1	-1	0	5	1.30
	+1	-1	0.5	4	0.407
$(M^{+2})(L^{-1})$	+2	-1	0	4.8	5.45
	+2	-1	0.5	4.8	1.14
$(M^{+3})(L^{-1})$	+3	-1	0	5	22.7
	+3	-1	0	7.1	18.40
	+3	-1	0.5	5	2.58
$(M^{+2})(L^{-2})$	+2	-2	0	5	94.8
	+2	-2	0	9.5	94.8
	+2	-2	0.5	4	6.51
$(M^{+3})(L^{-2})$	+3	-2	0	5	1642
	+3	-2	0	14.3	147
	+3	-2	0.5	5	16.5
$(M^{+3})(L^{-3})$	+3	-3	0	3	1.33×10^8
	+3	-3	0.5	3	2.04×10^4
	+3	-3	0	4	1.50×10^6
	+3	-3	0.5	4	661
	+3	-3	0	5	1.19×10^5
	+3	-3	0	21.4	496

X = charge does not matter

Equation 14 is not applicable to all metals and ligands, since this would imply common behavior of all ligands with all metals (e.g., only ionic or covalent bonding and no steric or desolvation effects). Equation 14 is likely to apply to one metal with a variety of ligands of similar structure, such as Cu(II) with meta- and para-substituted pyridines.

Edwards [2] modified equation 14 to introduce the relative tendency to form ionic or covalent bonds:

$$\log K_1 = E_A E_B + C_A C_B \quad (15)$$

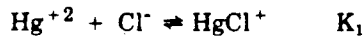
where A and B refer to the Lewis acid (metal) and Lewis base (ligand), and E_i and C_i (where $i = A$ or B) are empirically derived parameters (some initially based on physical measurements, such as the pK_a of the ligand), adjusted to give the best overall fit to stability constant data. E and C were chosen to represent the extent of ionic or covalent bonding.

A recent application of equation 15 with all parameters adjustable [9] showed that its power of prediction was unsatisfactory, unless confined to a particular class of ligands having first-row donor atoms (e.g., F^- , amines, alkyl-oxygen type ligands). This shortcoming was attributed to the neglect of specific solvation effects, such as the disruption of coordinated water molecules around the Lewis acid (metal) by the close approach of Lewis base (ligand). These solvation effects were expected to be more severe with smaller Lewis acids and larger Lewis bases, the conditions where equation 15 appeared to be less useful. Accordingly, a correction term (parameters D_A and D_B) was introduced by Hancock and Marsicano [8,9]:

$$\log K_1 = E_A E_B + C_A C_B - D_A D_B \quad (16)$$

The parameters E , C , and D are derived empirically from relationships between formation constants and by setting initial values for some parameters: the subscripts A and B refer to the Lewis acid (metal) and Lewis base (ligand), respectively. Values of E , C and D are given in Table 2.9-7 for metals and Table 2.9-8 for ligands. (See the former table for an explanation of how the values are derived). Good agreement has been observed between calculated and experimentally observed values for a variety of complexes.

Example 2 Calculate the formation constant of the monochloro complex of Hg^{+2} . The reaction of interest is:



where Hg^{+2} is the "acid" and Cl^- is the "base." The following parameter values are obtained from Tables 2.3-4-7 and -8:

$$\begin{aligned} E_A &= 1.346 \\ C_A &= 0.826 \\ D_A &= 0.0 \end{aligned}$$

TABLE 2.9-7

Values of Empirical Parameters E_A , C_A , and D_A for Cations
(for calculation of aqueous formation constants by equation 16)

Cation	E_A	C_A	D_A
Ag^+	-1.516	0.143	0.0
Al^{+3}	6.899	0.657	2.0
Bi^{+3}	5.917	0.926	0.0
Ca^{+2}	0.985	0.081	0.0
Cd^{+2}	0.993	0.300	0.6
Co^{+2}	1.198	0.276	3.0
Co^{+3}	3.299	0.875	7.0
Cr^{+3}	5.148	0.721	1.5
Cu^+	-0.559	0.43	2.5
Cu^{+2}	1.249	0.466	6.0
Fe^{+2}	1.521	0.256	2.0
Fe^{+3}	6.072	0.841	1.5
Ga^{+3}	6.060	0.788	1.5
H^+	3.067	1.099	20
Hg^{+2}	1.346	0.826	0.0
CH_3Hg^+	1.600	0.64	0.0
In^{+3}	4.498	0.714	0.5
La^{+3}	3.904	0.379	0.0
Lu^{+3}	4.572	0.454	0.0
Mg^{+2}	1.862	0.178	1.5
Mn^{+2}	1.581	0.223	1.0
Ni^{+2}	1.011	0.300	4.5
Pb^{+2}	2.763	0.413	0.0
Sc^{+3}	7.039	0.671	0.0
Sn^{+2}	5.649	0.700	0.0
Ti^{+3}	2.554	0.96	0.0
U^{+4}	7.550	0.968	3.0
UO_2^{+2}	4.948	0.589	1.0
VO_2^{+2}	3.964	0.664	3.5
Y^{+3}	2.235	0.447	0.0
Zn^{+2}	1.329	0.312	4.0

Source: Calculated from data derived by Hancock and Marsicano [9], who give values for C_A , D_A , and H_A (where $H_A = E_A/C_A$). Hancock and Marsicano used the following procedure to derive these parameters: (see next page)

TABLE 2.9-7 (Continued)

- (1) Set E_B for $F^- = 1$, C_B for $F^- = 0$, E_B for $OH^- = 0$ and C_B for $OH^- = 14$.
- (2) From Equation 15, $\log K_1(F^-) = E_A$ and $\log K_1(OH^-) = 14C_A$, which allows calculation of E_A and C_A for the metal (acid) ions. The experimentally obtained complexation constants (K) are corrected for outer-sphere contribution by the equation $\log K_{corr} = \log K - \log K_{os}$, where K_{os} is calculated by equation 11.
- (3) Rewriting equation 15 as $\frac{\log K_1}{C_A} = \frac{E_A(E_B)}{C_A} + C_B$, plot $\frac{\log K_1(NH_3)}{C_A}$ versus $\frac{E_A}{C_A}$ to derive the slope of E_B and intercept of C_B for the ligands (bases).
- (4) E_A and C_A can now be recalculated to give a better overall fit of $\log K(OH)$, $\log K(F)$ and $\log K(NH_3)$ data.
- (5) Using the revised values of E_A and C_A and rewriting equation 16 as $\frac{\log K(\text{ligand})}{C_A} = \frac{E_A(E_B)}{C_A} + C_B - \frac{D_A D_B}{C_A}$, plot values of $\frac{\log K(\text{ligand})}{C_A}$ versus E_A/C_A . E_B is then obtained from the slope and $(C_B - \frac{D_A D_B}{C_A})$ from the intercept.
- (6) Set $D_B = 1$ for Br^- .
- (7) Calculate D_A , D_B and C_B values for other metals and ligands from the results of Step 5.

TABLE 2.9-8

Values for Empirical Parameters E_B , C_B , and D_B for Ligands
(for calculation of aqueous formation constants by equation 16)

Ligand	E_B	C_B	D_B
$As(C_6H_4SO_3)_3^{-3}$	-1.93	14.3	—
Br^-	-1.54	14.2	1.0 ^a
CH_3COO^-	0.0	4.76	0.0
C_5H_5N	-0.74	7.0	0.0
Cl^-	-1.04	10.4	0.6
CN^-	-4.43	30.0	0.38
F^-	1.00 ^a	0.0 ^a	0.0
I^-	-2.43	20.0	1.7
$N=N=N^-$	-0.67	10.4	0.2
$N=C-S^-$	-1.83	14.3	1.0
$(NH_2)_2C=S$	-2.46	18.2	0.6
$(HOCH_2CH_2)_2S$	-1.36	10.1	0.6
NH_3	-1.08	12.34	0.0
SCN^-	-0.76	9.3	0.2
SO_3^{2-}	-1.94	18.2	0.4
$S_2O_3^{2-}$	-3.15	26.5	1.1
OH^-	0.0 ^a	14.00 ^a	0.0

a. Arbitrarily set

Source: Hancock and Marsicano [9]

$$\begin{aligned}E_B &= -1.04 \\C_B &= 10.4 \\D_B &= 0.6\end{aligned}$$

Substituting these values in equation 16,

$$\log K_1 = (1.346)(-1.04) + (0.826)(10.4) - (0.0)(0.6) = 7.19$$

The experimental value is 7.37 [9].

Polydentate Ligands Containing Nitrogen Donor Atoms

Equation 17 relates the complexation constants of polyamine ligands to those of ammonia, where the polyamines are of the type $\text{H}(\text{NHCH}_2\text{CH}_2)_{n-1}\text{NH}_2$.

$$\log K_1 (\text{polyamine}) = 1.152n \log K_1 (\text{ammonia}) - \left(\sum_{i=1}^{n-1} i \right) \lambda_N + (n-1)\log 55.5 \quad (17)$$

where $\log K_1 (\text{polyamine})$ = complexation constant for mono-polyamine complex
 $\log K_1 (\text{ammonia})$ = complexation constant for mono-ammonia complex
 n = defined by the structure of the ligand¹ ($n \geq 2$)
 λ_N = 0.5 (for all complexes of polyamines forming five-membered chelate rings)

As indicated by the definition of λ_N , this equation applies only to complexes with five-membered chelate rings. Complexation constants for ligands with larger chelate rings are generally less than predicted via this equation. The equation is also not valid for situations where the polydentate ligand is unable to assume the same coordination geometry as the monodentate analog. The equation thus is not well suited for linearly coordinated Hg^{+2} , tetrahedral Cd^{+2} and Zn^{+2} , and tetragonally distorted ions such as VO^{+2} , UO_2^{+2} and Cu^{+2} [8].

Example 3 Estimate the complex formation constant of Pb^{+2} with NH_3 if the complex formation constant is 10.4 for TRIEN and 10.9 for TETREN. The following parameters are used:

$$\log K_1 (\text{TRIEN}) = 10.4$$

$$n = 4$$

$$\log K_1 (\text{ammonia}) = \text{unknown}$$

$$\sum_{i=0}^{n-1} i = 1 + 2 + 3 = 6$$

$$\lambda_N = 0.5$$

Substituting in equation 17,

¹ Ethylenediamine (EN) = 2; diethylenetriamine (DIEN) = 3; triethylenetetramine (TRIEN) = 4; tetraethylenepentamine (TETREN) = 5.

$$10.4 = 1.152(4) \log K_1(\text{ammonia}) - 6(0.5) + (3) \log 55.5$$

$$\log K_1(\text{ammonia}) = (10.4 + 3.0 - 5.23)/4.6$$

$$= 1.77$$

If we had used the complex formation constant for TETREN (10.9), the corresponding calculation would have been

$$10.9 = 1.152(5) \log K_1(\text{ammonia}) - 10(0.5) + (4) \log 55.5$$

$$\log K_1(\text{ammonia}) = (10.9 + 5.0 - 6.98)/5.76$$

$$= 1.55$$

The average value calculated for the $\text{Pb}^{+2}(\text{NH}_3)$ complexation constant is thus 1.66. The value has not been determined experimentally.

Aminocarboxylate Chelating Ligands

Hancock [8] developed an equation that relates the logarithm of the complexation constant for aminocarboxylate ligands to the logarithms of the complexation constants of acetate and ammonia with various metals. The relationship is:

$$\log K_1(\text{aminocarboxylate}) = 1.152n \log K_1(\text{ammonia}) + m \log K_1(\text{acetate})$$

$$- \left(\sum_{i=0}^{n-1} i \right) \lambda_N - \left(\sum_{i=1}^m i \right) \lambda_O + (n + m - 1) \log 55.5 \quad (18)$$

where $K_1(\text{aminocarboxylate})$ = complexation constant for mono-aminocarboxylate complex formation

$K_1(\text{ammonia})$ = complexation constant for mono-ammonia complex formation

n = number of nitrogen donor groups on the aminocarboxylate ligand²

m = number of carboxylate groups on the aminocarboxylate ligand²

$K_1(\text{acetate})$ = complexation constant for monoacetate complex formation

λ_O = empirical parameter set equal to 0.26 $\log K_1(\text{acetate}) - 0.19$

λ_N = 0.5 (for all complexes containing five-membered chelate rings)

2.	Ligand	n	m
	NTA	1	3
	EDDA	2	2
	DTMA	3	1
	HEDTRA	2	3
	EDTA	2	4

EDDA = Ethylenediamine-N,N'-diacetic acid. Other abbreviations defined in footnote 1.

Example 4 Estimate the formation constant of Pb^{+2} with nitrilotriacetate (NTA).

The following parameters apply:

$$n = \text{number of nitrogen groups in NTA} = 1$$

$$m = \text{number of carboxylate groups in NTA} = 3$$

$$\log K_1(\text{ammonia}) = 1.66 \text{ (from Example 3)}$$

$$\log K_1(\text{acetate}) = 2.68 [21]$$

$$\lambda_O = 0.26 (2.68) - 0.19 = 0.51$$

$$\sum_{i=0}^{n-1} i = 0$$

$$\sum_{i=1}^m i = 1 + 2 + 3 = 6$$

$$\lambda_N = 0.5$$

Substituting in equation 18,

$$\begin{aligned}\log K_1(\text{NTA}) &= 1.152(1)(1.66) + 3(2.68) - 0(0.5) - 6(0.51) + 3(1.744) \\ &= 12.14\end{aligned}$$

Observed values are 11.34 (Table 2.9-2) and 11.8 [21].

TANAKA EQUATIONS FOR OVERALL FORMATION CONSTANTS OF ML_2 AND MAL COMPLEXES

Tanaka [25,26] derived the following equation for predicting NiL_2 complexation constants from NiL data:

$$\begin{aligned}\log K_{ML_2} &= \log K_{ML} + \Delta + \log \left(\frac{\text{No. of } H_2O \text{ in } ML}{\text{No. of } H_2O \text{ in } M} \right) + \delta_{NN} N^2 \\ &\quad + \delta_{NO} NO + \delta_{ON} ON + \delta_{OO} O^2 - \log 2\end{aligned}\quad (19)$$

where K_{ML_2} = complexation constant of ML with L

K_{ML} = complexation constant of M with L

$\Delta = \log K_{(ML,L)} - \log K_{(M,L)} =$ difference between logarithms of outer-sphere complexation constants

δ_{NN} = parameter for interaction of amine N in L with amine nitrogen in second ligand L

δ_{ON} = as above for carboxylate in L with amine nitrogen in second L

δ_{OO} = as above for carboxylate in L with carboxylate in second L

δ_{NO} = as above for amine N in L with a carboxylate in second ligand L

N = number of amine nitrogens coordinated in L

O = number of carboxylate groups coordinated in L

If L is uncharged, the value of Δ is about zero; if L is mono-anionic, $\Delta = 0.4$ at $\mu = 0.1 M$ (using $a = 5\text{\AA}$). For Ni complexes:³

$$\begin{array}{ll} \delta_{NN} = -0.25, & \delta_{NO} = 0.11 \\ \delta_{ON} = 0.11, & \delta_{OO} = -0.16 \end{array}$$

This equation and the related parameters were derived for ligands with no steric hindrance in their formation. Also note that all ligands contained only aliphatic nitrogen donor atoms.

Example 5 Calculate the second stability constant of Ni^{+2} complexation with NH_3 . The following parameters apply:

$$\begin{aligned} \log K_{\text{Ni}(\text{NH}_3)} &= 2.80 [21] \\ \text{No. of H}_2\text{O in } \text{Ni}(\text{NH}_3)^{+2} &= 5 \\ \text{No. of H}_2\text{O in } \text{Ni}^{+2} &= 6 \\ \Delta &= \log K_{\text{os}(\text{Ni}(\text{NH}_3), \text{NH}_3)} - \log K_{\text{os}(\text{Ni}, \text{NH}_3)} \approx 0 \\ N &= 1 \\ O &= 0 \end{aligned}$$

Using equation 19,

$$\begin{aligned} \log K_{\text{Ni}(\text{NH}_3)^{+2}} &= \log K_{\text{Ni}(\text{NH}_3)} + \Delta + \log \left[\frac{\text{No. of H}_2\text{O in } \text{Ni}(\text{NH}_3)}{\text{No. of H}_2\text{O in Ni}} \right] \\ &= -0.25(1)^2 + 0.11(1)(0) + 0.11(0)(1) - 0.16(0)^2 - \log 2 \\ &= 2.80 + 0 + \log(5/6) - 0.25 + 0 + 0 - 0.30 = 2.17. \end{aligned}$$

The observed value is 2.05 [22].

For predicting CuL_n and CuAL (i.e. where A is a different ligand than L) complexation constants from data available for CuL , Tanaka [24] derived the following equations:

$$\log K_{\text{CuAL}} = \log K_{\text{CuL}} + \Delta_1 + \log \left[\frac{\text{No. of H}_2\text{O in CuA}}{\text{No. of H}_2\text{O in Cu}} \right] + \sum_i \sum_j \delta_{ij} X_i(A) Y_j(L) \quad (20)$$

with $\Delta_1 = [\log K_{\text{os}(\text{CuA}, L)} - \log K_{\text{os}(\text{Cu}, L)}]$ and

$$\begin{aligned} \log K_{\text{CuL}_n} &= \log K_{\text{CuL}} + \Delta_2 + \log \left(\frac{\text{No. of H}_2\text{O in CuL}_{n-1}}{\text{No. of H}_2\text{O in Cu}} \right) \\ &\quad + \sum_i \sum_j \delta_{ij} X_i(L) Y_j(L) - \log n \end{aligned} \quad (21)$$

with $\Delta_2 = [\log K_{\text{os}(\text{CuL}_{n-1}, L)} - \log K_{\text{os}(\text{Cu}, L)}]$

3. Ligands used to derive δ_{NN} , δ_{ON} , and δ_{NO} were NH_3 , NTA, EDDA, HEDTA, EN, TETREN, GLA, and OX. Those used to derive δ_{OO} were glycine, alanine, β -alanine, sarcosine, serine, asparagine, N, N-dimethylglycine, α -amino- α -methylpropionic acid and N-ethylglycine.

where K_{CuL} = complexation constant for Cu with L
 K_{∞} = outer-sphere complexation constant of pair in ()
 δ_{ij} = empirical parameter denoting effect of donor atoms i in one ligand on donor atom j in a second ligand
 X_i = number of donor atoms i in one ligand
 Y_j = number of donor atoms j in other ligand
A = first ligand
L = second ligand
n = number of L ligands on metal

Equation 20 becomes equation 22 for a copper complex containing ligands having aromatic nitrogens [N(AR)], aliphatic nitrogen [N(AL)] and oxygen donor atoms [O] as follows (see also example 6):

$$\log K_{CuAL} = \log K_{CuL} + \Delta_1 + \log \left(\frac{\text{No. of H}_2\text{O in CuA}}{\text{No. of H}_2\text{O in Cu}} \right) \\ + \delta_{N(AL)N(AL)} \times N_{N(AL)}(A) \times N_{N(AL)}(L) + \delta_{N(AR)N(AR)} \times N_{N(AR)}(A) \times N_{N(AR)}(L) \\ + \delta_{N(AL)N(AR)} \times N_{N(AL)}(A) \times N_{N(AR)}(L) + \delta_{N(AR)O} \times N_{N(AR)}(A) \times O_o(L) \\ + \delta_{N(AL)O} \times N_{N(AL)}(A) \times O_o(L) + \delta_{O_O(\pi)} O_{\alpha(\pi)}(A) \times O_{\alpha(\pi)}(L) \\ + \delta_{O_O(\sigma)} O_{\alpha(\sigma)}(A) \times O_{\alpha(\sigma)}(L) \quad (22)$$

where

$\delta_{N(AL)N(AL)}$ = -0.35 (aliphatic N interactions)
 $\delta_{N(AR)N(AR)}$ = -0.39 (aromatic N interactions)
 $\delta_{N(AL)N(AR)}$ = -0.25 (aromatic and aliphatic N interaction)
 $\delta_{N(AR)O}$ = +0.09 (aromatic N and O interaction)
 $\delta_{N(AL)O}$ = -0.26 (aliphatic N and O interaction)
 $\delta_{O_O(\sigma)}$ = -0.29 (for O in a σ bonding system)
 $\delta_{O_O(\pi)}$ = 0.10 (for O in a π bonding system)
 N, O = number of N and O donor atoms respectively, on the ligand (A or L, as noted in parentheses); subscript notation is as defined above for the various parameters

Equation 21 similarly becomes equation 23 for Cu complexes having aromatic or aliphatic nitrogens and oxygen donor atoms in the various ligands as follows:

$$\log K_{CuL_n} = \log K_{CuL} + \Delta_2 + \log \left(\frac{\text{No. of H}_2\text{O in CuL}_{n-1}}{\text{No. of H}_2\text{O in Cu}} \right) + \delta_{N(AL)N(AL)} \times N_{N(AL)}(L) \times N_{N(AL)}(L) + \delta_{N(AR)N(AR)} \times N_{N(AR)}(L) \times N_{N(AR)}(L) + \delta_{N(AL)O} \times N_{N(AL)}(L) \times O_o(L) + \delta_{N(AR)O} \times N_{N(AR)}(L) \times O_o(L) + \delta_{N(AL)O} \times N_{N(AL)}(L) \times O_o(L) + \delta_{OO(\pi)} \times O_{o(\pi)}(L) \times O_{o(\pi)}(L) + \delta_{OO(\sigma)} \times O_{o(\sigma)}(L) \times O_{o(\sigma)}(L) \quad (23)$$

The definitions and parameter values derived for Cu(II) complexes are the same as given for equation 22. Based upon these relationships, the values of the ligand interaction terms (δ_{ij}) given above provide reasonably close estimates of formation constants of mixed and higher Cu(II) complexes. These relationships have been used for calculating complexes where at least one non-charged amine is a ligand; this reduces the term Δ to about zero, which eliminates the problem of calculating outer-sphere formation constants and the need to assume a valid interatomic distance (parameter "a") for the ion pair.

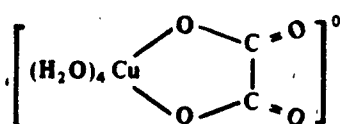
The manner in which the empirical parameters (δ_{ij}) were derived is summarized below, to indicate the kinds of ligands for which equations 22 and 23 are useful.

- $\delta_{N(AL)N(AL)}$ was derived from data for complexes containing only aliphatic nitrogen donor atoms (e.g., 1,3-diaminopropane, NH_3 , and N -n-propyl-1,2-diaminoethane).
- $\delta_{N(AR)N(AR)}$ was derived from data for complexes containing aromatic nitrogen donor atoms only (e.g., pyridine, imidazole, and 2,6 lutidine).
- $\delta_{N(AR)N(AL)}$ was estimated from data for complexes containing mixed aliphatic nitrogen and aromatic nitrogen ligands (e.g., triethylenetriamine and pyridine; 1,2-diaminoethane and bipyridine).
- $\delta_{N(AR)O}$ and $\delta_{N(AL)O}$ were estimated from complexation data for aromatic nitrogen and oxygen donor (e.g., formate, acetate, benzoate) mixed complexes and aliphatic nitrogen and oxygen donor ligands, respectively.
- δ_{OO} was derived from oxygen donor atom ligands, both for those having no pi system (e.g., formate, methoxyacetate) and those having pi system(s) directly connected to the oxygen donor (e.g., acetylacetone, salicylaldehyde).

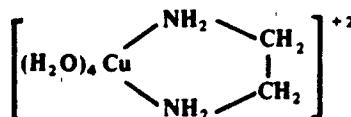
Example 6 Estimate the complexation constant for the (oxalato) (1,2-diaminoethane) copper(II) complex if the logarithm of the formation constant for the oxalato copper(II) complex is 5.7.

The structure of the oxalato ligand (L) is $O=C-O^-$, and the structure of the 1,2-diaminoethane ligand (A) is $NH_2-CH_2-CH_2-NH_2$.

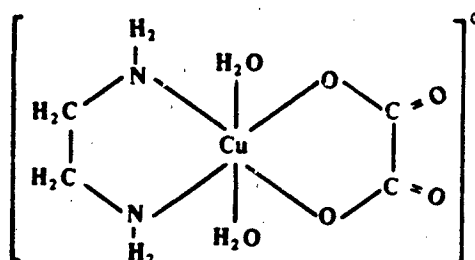
Thus, the Cu-oxalato ($Cu-L$) complex is



The Cu-1,2 diaminoethane complex is



and the mixed Cu (oxalato) (1,2-diaminoethane) complex is



We now use equation 22 with the following parameter values (which are specific to copper):

($A = 1,2$ diaminoethane, $L =$ oxalate)

$$\log K_{CuL} = 5.7$$

$\Delta_1 = 0$, since the charge product ($Z_1 Z_2$) is both +4 for CuA, L and Cu, L (A has no charge); $K_{ox(CuA,L)} \approx K_{ox(Cu,L)}$

No. of H_2O in $CuA = 4$

No. of H_2O in $Cu = 6$ (Cu exists as $Cu(H_2O)_6^{+2}$)

$$\delta_{N(AL)N(AL)} = -0.35 \text{ (interaction between aliphatic nitrogens)}$$

$$N_{N(AL)}(A) = 2 \text{ (no. of aliphatic nitrogen electrons in ligand A)}$$

$$N_{N(AL)}(L) = 0 \text{ (no. of aliphatic nitrogen atoms in ligand L)}$$

$$\delta_{N(AR)N(AR)} = -0.39 \text{ (interaction between aromatic nitrogens)}$$

$$N_{N(AR)}(A) = 0 \text{ (no. of aromatic nitrogens in ligand A)}$$

$$N_{N(AR)}(L) = 0 \text{ (no. of aromatic nitrogen atoms in ligand L)}$$

$\delta_{N(AL)N(AR)}$	= -0.25 (interaction between aliphatic and aromatic nitrogens)
$\delta_{N(AR)O}$	= 0.09 (interaction between aromatic nitrogen and oxygen)
$O_o(L)$	= 2 (no. of carboxylate groups in ligand L)
$\delta_{N(AL)O}$	= -0.26 (interaction between aliphatic nitrogen and oxygen)
$\delta_{OO(\pi)}$	= -0.10 (interaction between oxygens in a π system)
$O_{\alpha(\pi)}(A)$	= 0 (no. of oxygen atoms in a π system in ligand A)
$O_{\alpha(\pi)}(L)$	= 0 (no. of oxygen atoms in a π system in ligand L)
$\delta_{OO(\sigma)}$	= 0.10 (interaction between oxygens in a σ system)
$O_{\alpha(\sigma)}(A)$	= 0 (no. of oxygen atoms in a σ system in ligand A)
$O_{\alpha(\sigma)}(L)$	= 2 (no. of oxygen atoms in ligand L in a σ system)

Therefore,

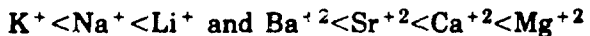
$$\begin{aligned}\log K_{CuAL} &= 5.7 + 0 + \log (4/6) + 0 + 0 + 0 + (-0.26)(2)(2) + 0 + 0 \\ &= 4.48.\end{aligned}$$

The observed value is 4.6 [23].

2.9.5 Qualitative Trends for Complexation of Ions

Studies of the complexing ability of metals by Schwarzenbach [20] and Petrucci [17] have revealed the following trends, which allow qualitative estimation of the relative magnitude of complexation constants within particular series of metals and ligand donor atoms:

- (1) For metal ions with noble gas configurations such as the alkali and alkali earth metal ions and Al^{+3} , Sc^{+3} , La^{+3} , Ti^{+4} , Zr^{+4} , Hf^{+4} , Th^{+4} , Nb^{+5} , and Ta^{+5} , purely electrostatic bonding predominates. The association constants generally are found to increase with decreasing cationic size and increasing charge for a particular ligand according to

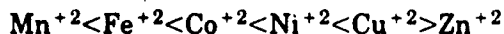


For oxyacid anions (e.g., NO_3^- , SO_4^{2-} , $S_2O_3^{2-}$), the sequence for magnitude of the stability constants is reversed. For example, complexation constants ($\log \beta_1$ at zero ionic strength) for acetate follow the sequence Ca^{+2} (1.18) > Sr^{+2} (1.14) > Ba^{+2} (1.07) [1]. The sequence for complexation by nitrate is Ba^{+2} (0.9) > Sr^{+2} (0.8) > Ca^{+2} (0.7) [1]. Ligands with F and O donor groups (e.g., OH^-) are preferred by these metal ions over N-donor groups (e.g., NH_3 , CN^-).

- (2) For metal ions with completely filled d subshells (18 electrons) such as Cu^+ , Ag^+ , Au^+ , Tl^+ , Zn^{+2} , Cd^{+2} , and Hg^{+2} , the bonding with ligands is mostly covalent. The properties that determine complexation are the electronegativity of the metal and of the ligand donor atom. An increase in the association constant

is observed with increasing electronegativity of the metal for a particular ligand. For a particular metal, an increasing association constant is observed with an increase in electron donating (decrease of electronegativity) of the ligand. The association constants thus generally decrease from S~I>Br>Cl>N>O>F. NH₃ is preferred over H₂O and CN⁻ over OH⁻.

- (3) The association constants for metal ions with incomplete subshells (such as Mn⁺², Fe⁺², Co⁺², Ni⁺², and Cu⁺²) depend on both ionization potential and ionic radii. These ions follow the Irving-Williams series [10] for a particular ligand. The order of complexing is:



with nitrogen, carbon, and sulfur ligand donor atoms. For example, the sequence for complexation constants (log β₁ at zero ionic strength) for NH₃ is Mn⁺² (1.00) < Fe⁺² (1.40) < Co⁺² (1.99) < Ni⁺² (2.72) < Cu⁺² (4.04) > Zn⁺² (2.21) [1]. Additional discussion of this series is given in Reference 18.

2.9.6 Literature Cited

1. Basolo, F. and R.G. Pearson, *Mechanisms of Inorganic Reactions*, 2nd. ed., John Wiley & Sons, New York, 37 (1967).
2. Edwards, J.O., "Correlation of Relative Rates and Equilibria with Double Basicity Scale," *J. Am. Chem. Soc.*, **76**, 1540 (1954).
3. Eigen, M., "Kinetics of High Speed Ion Reactions in Aqueous Solution," *Z. Phys. Chem.*, **1**, 176 (1954).
4. Eigen, M., "Metal Complexes and Protolytic Reactions in Aqueous Solution," *Z. Electrochem.*, **64**, 115 (1960).
5. Fuoss, R.M., "Ionic Association: III. The Equilibrium Between Ion Pairs and Free Ions," *J. Am. Chem. Soc.*, **80**, 5059 (1958).
6. Gamble, D., M. Schnitzer and I. Hoffman, "Cu(II)-Fulvic Acid Chelation Equilibrium in 0.1 M Potassium Chloride at 25°C," *Can. J. Chem.*, **48**, 3197 (1970).
7. Hammes, G.G. and J.I. Steinfeld, "Relaxation Spectra of Some Nickel(II) and Cobalt(II) Complexes," *J. Am. Chem. Soc.*, **84**, 4639 (1962).
8. Hancock, R.D. and F. Marsicano, "Parametric Correlation of Formation Constants in Aqueous Solution — Ligands with Small Donor Atoms," *Inorg. Chem.*, **17**, 560 (1978).
9. Hancock, R.D. and F. Marsicano, "Patterns in Lewis Acid-Base Interactions in Aqueous Solution," *S. Afr. J. Chem.*, **33**, 77 (1980).
10. Irving, H. and R.J.P. Williams, "The Stability of Transition Metal Complexes," *J. Chem. Soc.*, 3192 (1953).
11. Kotrlý, S. and L. Šúcha, *Handbook of Chemical Equilibria in Analytical Chemistry*, John Wiley & Sons, New York (1985).

12. Lincoln, S.F., "Solvent Coordination Numbers of Metal Ions in Solution," *Coord. Chem. Rev.*, **6**, 309 (1971).
13. Manning, P.G. and S. Ramamoorthy, "Equilibrium Studies of Metal-Ion Complexes of Interest to Natural Waters — VII," *J. Inorg. Nucl. Chem.*, **35**, 1577 (1973).
14. Martell, A.E., "The Influence of Natural and Synthetic Ligands on the Transport and Function of Metal Ions in the Environment," *Pure Appl. Chem.*, **44**, 81 (1975).
15. Morel, F.M.M., *Principles of Aquatic Chemistry*, John Wiley & Sons, New York, 242 (1983).
16. Pearson, R.G. and P. Allgen, "Rates and Mechanism of Formation of Some Nickel(II) Complexes with Methanol," *Inorg. Chem.*, **6**, 1379 (1967).
17. Petrucci, S., *Ionic Interactions*, Academic Press, New York, 147 (1971).
18. Prue, J.E., *Ionic Equilibrium*, Pergamon Press, Oxford (1966).
19. Schnitzer, M. and E.H. Hansen, "Organometallic Interactions in Soils: 8. Evaluation of Methods for the Determination of Stability Constants of Metal Fulvic Acid Complexes," *Soil Sci.*, **109**, 333 (1970).
20. Schwarzenbach, G., *Experientia Suppl.*, **5**, 162 (1956).
21. Schwarzenbach, G., G. Anderegg, W. Schneider and H. Senn, "On the Coordination Tendency of N-Substituted Iminodiacetic Acids," *Helv. Chim. Acta*, **38**, 1147 (1955).
22. Sillén, L.G. and A.E. Martell, *Stability Constants of Metal-Ion Complexes*, Special Publication No. 17, The Chemical Society, London (1964).
23. Sillén, L.G. and A.E. Martell, *Stability Constants of Metal-Ion Complexes — Supplement No. 1*, Special Publication No. 25, The Chemical Society, London, 64 (1971).
24. Stevenson, F.J., *Humus Chemistry*, Wiley-Interscience, New York, 1982.
25. Tanaka, M., "A Mechanistic Consideration of the Formation Constant of Metal Complexes with Special Reference to the Mixed Ligand Complexes of Nickel Involving Amines and Aminocarboxylates," *J. Inorg. Nucl. Chem.*, **35**, 965 (1973).
26. Tanaka, M., "The Mechanistic Consideration on the Formation Constants of Copper(II) Complexes," *J. Inorg. Nucl. Chem.*, **36**, 151 (1974).
27. Wilkins, R.G., *The Study of Kinetics and Mechanisms of Reactions of Transition Metal Complexes*, Allyn and Bacon, Boston, 183 (1974).

2.10 ELECTRON TRANSFER REACTIONS

2.10.1 Introduction

This section deals with electron transfer (redox) reactions, primarily homogeneous reactions in aqueous systems. It explains some of the parameters and graphical techniques used to represent redox equilibria and summarizes important environmental redox couples. Typical values of the redox status of various environmental waters are given in terms of parameters such as Eh and pe . Limitations on the use of experimentally determined Eh values in relation to the redox status of the solution are discussed. Finally, methods are described for calculating redox equilibria under various reaction conditions and for estimating the redox half-potential for a complexed species.

2.10.2 Environmental Importance

Many inorganic species of environmental concern can undergo electron transfer or redox reactions with species that are present naturally or as pollutants in environmental systems. The product of an electron transfer reaction is typically the reacting species in a modified oxidation state, but it can also be a product of the reaction of water (often very rapid) with the modified oxidation state species. This product species in the modified oxidation state differs greatly from the original reactant species in terms of chemical behavior. Thus, homogeneous (e.g., acid/base dissociation, complexation) and heterogeneous (e.g., solubility, attenuation) reactivity properties are modified; the result of a redox reaction is a species that differs in environmental mobility and impact from the original species.

Like other reactions, such as acidic or basic dissociation and complexation, redox reactions are fundamental to determining speciation in solution. Figure 2.10-1 summarizes the chemical identity and valence states of elements that are capable of undergoing redox reactions in the environment.

2.10.3 Mechanisms of Redox Reactions

An oxidation-reduction reaction involves a transfer of electrons between two species — the oxidizing agent (oxidant) and the reducing agent (reductant). In this transfer, the oxidant gains electrons and the reductant loses them. For example, in the reaction



the Fe(II) is oxidized to Fe(III) by loss of electrons, and the O₂ is reduced to the -2 oxidation state by gaining electrons to form H₂O. (In aqueous systems, hydronium or hydroxide ions or water may be used to balance redox reactions.) Electrons are not shown in equation 1, since free electrons usually do not exist in aqueous solution; electron transfer occurs by direct interaction of the reactants (see below) or other intermediate chemical species.

The initial reaction products are the oxidized form of the reducing agent and the reduced form of the oxidizing agent. In aqueous solution, these initial products can

1 +1
H -1

6 +2	7 +1	8 -1
C +4	N +2	O -2
-4	+3	
	+4	
	+5	
	-1	
	-2	
	-3	

14 +2	15 +3	16 +4	17 +1
Si +4	P +5	S +6	Cl +5
-4	-3	-2	+7
			-1

22 +2	23 +2	24 +2	25 +2	26 +2	27 +2	28 +2	29 +1	32 +2	33 +3	34 +4	35 +1
Tl +3	V +3	Cr +3	Mn +3	Fe +3	Co +3	Ni +3	Cu +2	Ge +4	As +5	Se +6	Br +5
+4	+4	+6	+4	+7	+7	+3	+2	+5	-3	-2	-1

41 +3	43 +4	45 +2	50 +2	51 +3	52 +4	53 +1
Nb +5	Tc +6	Pd +4	Sn +4	Sb +5	Tc +6	I +5
+7	+7			-3	-2	+7
						-1

75 +4	78 +3	77 +3	78 +2	79 +1	80 +1	81 +1	82 +2	83 +3	84 +2
Re +6	Os +4	Ir +4	Pt +4	Au +3	Hg +2	Tl +3	Pb +4	Bi +5	Po +4
+7									

Lanthanides	58 +3	62 +2	63 +2	70 +2
	Ce +4	Sm +3	Eu +3	Yb +3
Actinides	91 +5	92 +3	93 +3	94 +3
	Pa +4	U +4	Np +4	Pu +4
	+5	+5	+5	+5
	+6	+6	+6	+6

Key to Figure

Atomic Number \Rightarrow 50 +2
 Symbol \Rightarrow Sn +4 \Rightarrow Oxidation States

Elemental state has been omitted for simplification
 but is available for all elements.

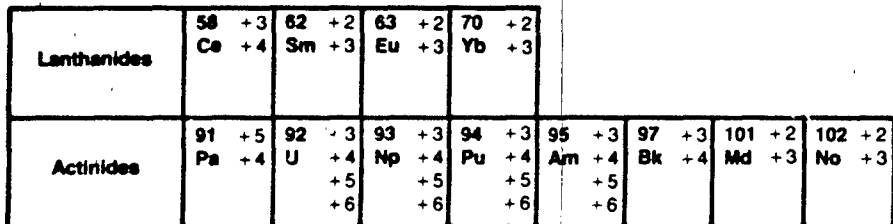
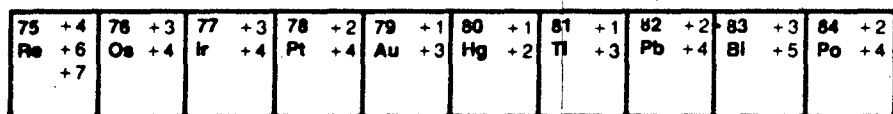
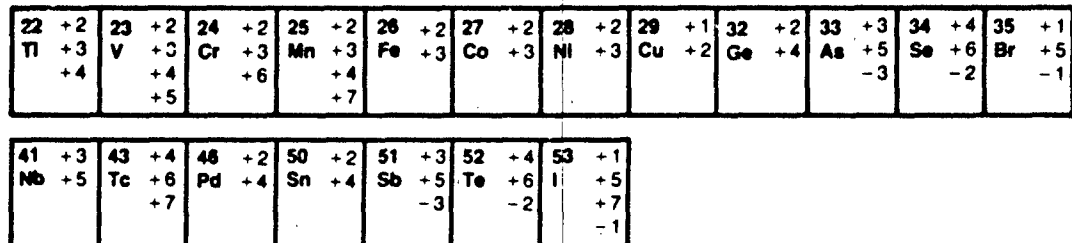
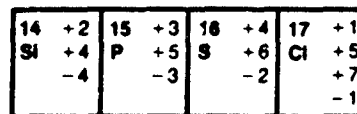
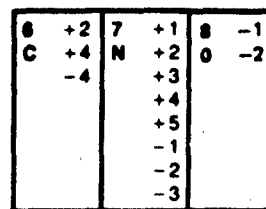


FIGURE 2.10-1 Summary of Elements That Can Undergo Redox Reactions And Their Valence States

then undergo further reactions. The latter include acid-base equilibria and dissociation of complexes with subsequent substitution of coordinated ligands by water.

The mechanism by which a redox reaction occurs is important, since it can determine the nature of the products as well as the rate of the reaction. There are two kinds of homogeneous electron transfer reactions: outer sphere and inner sphere. The reaction between Fe(III) and V(II) shown in Figure 2.10-2 is an example of an outer-sphere redox reaction [23]. In such reactions, the bonds in the primary or inner coordination sphere¹ remain intact during the transition through species I and II. (The species separated by commas are ion pairs.) The initial products of this reaction have oxidation states different from those of the reactants but have the same primary coordination spheres as the reactants. These coordination spheres may, however, be modified by subsequent rapid reactions with the aqueous environment, such as acid/base equilibria or ligand exchange.

In an inner-sphere reaction, the two reacting species are coordinated to a common "bridging" ligand in the transition state (species III and IV in Figure 2.10-3). The illustrated reaction between Fe(II) and Co(NH₃)₅NTA is an example of an inner-sphere redox reaction with NTA as the bridging ligand [5]. Electron transfer occurs in the bridged intermediate (species III). This kind of redox reaction may involve transfer of the bridging ligand from one metal center to the other, yielding a product that differs not only in oxidation state but also in composition of the primary coordination sphere. Figure 2.10-4, for example, shows an inner-sphere redox reaction between [Co(NH₃)₅Cl]⁺² and Cr⁺², in which the Cl ligand is transferred from the Co(III) metal center to the product Cr(III) center because of the kinetically inert nature of the Cr(III) and the kinetically labile nature of the Co(II) products.

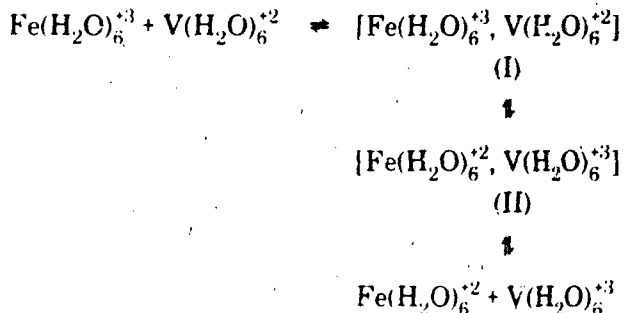


FIGURE 2.10-2 Sample Redox Mechanism: Outer-Sphere Electron Transfer Reaction Between Fe^{+3} and V^{+2}

When both products of electron transfer are kinetically labile (see section 3.2), the initial products of the electron transfer reaction will rapidly equilibrate with the aqueous environment (via ligand exchange) and form predominantly aquo complexes as well as hydroxo and other complexes resulting from acid-base equilibria. As shown in Figure 2.10-3, the product Fe(III) and Co(II) centers generated in the inner-sphere intermediate (species IV) are labile and thus exchange the ammonia and NTA ligands

1. See §2.9.2 for definition.

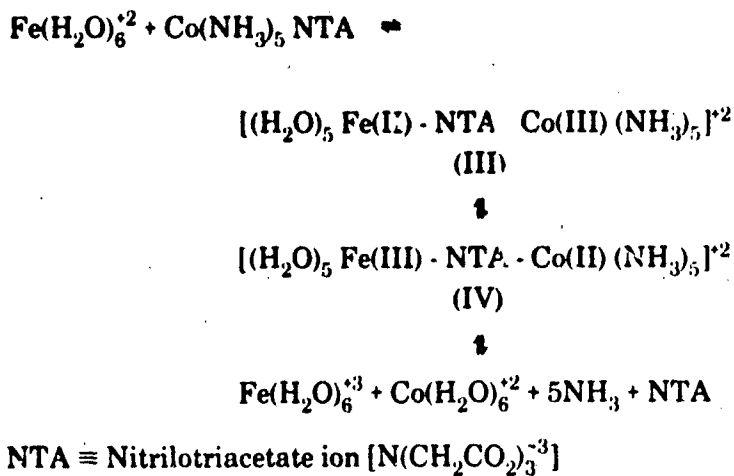


FIGURE 2.10-3 Sample Redox Mechanism: Inner-Sphere Electron Transfer Reaction Between Fe^{+2} and $\text{Co}(\text{NH}_3)_5 \text{NTA}$
(Gain or loss of free water is not shown.)

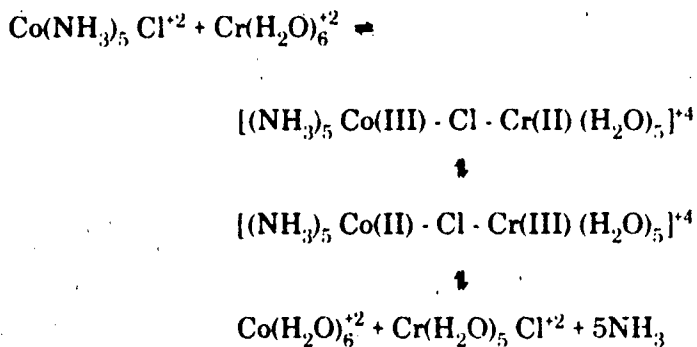


FIGURE 2.10-4 Sample Redox Mechanism: Inner-Sphere Electron Transfer Reaction Between Cr^{+2} and $\text{Co}(\text{NH}_3)_5 \text{Cl}^{+2}$
(Gain or loss of free water is not shown.)

rapidly to form aquo complexes. In Figure 2.10-4, the product Cr(III) center is inert and retains the Cl ligand, while the Co(II) center is labile and exchanges the ammonia and chloride ligands rapidly to form aquo complexes.

It is therefore necessary to distinguish between inner- and outer-sphere redox processes if one wishes to determine the rate of a reaction (see section 3.3). In addition, one must also have information about the inert or labile character of the reactant and product metal or other element centers involved (see section 3.3) and the time frame of interest to determine the final products of the reaction.

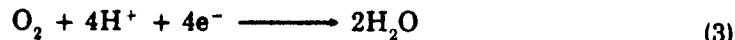
In a predominantly aqueous environment, and when the redox reaction of concern is between entirely aquated species (i.e., aquo ions), an inner-sphere redox reaction with a water-bridged intermediate that produces one inert and one labile product would cause the products to have essentially the same primary coordination spheres as those of the reactants. It would not matter if the reactants or products were kinetically labile or inert. If a water molecule were exchanged between the reactants, it would be noticed only if it were labeled (e.g., with isotopically labeled oxygen). However, an inner-sphere redox reaction leading to reaction products with inert centers may produce a bridged species similar to IV in Figure 2.10-3.

In environmental systems, electron transfer occurs only between species that are capable of donating and accepting one or more electrons. In contrast to H^+ , which can exist in finite concentrations in aqueous systems (as expressed by the pH value), the aqueous electron is not detectable under typical environmental conditions. Thus, an oxidizing agent that is added to a solution reacts directly with a reducing agent rather than with an aqueous electron. The concept of p_e , which is equal to $-\log(e^-)$, where (e^-) is the electron activity, is very useful for calculating equilibrium conditions and simplifies treatment of redox reactions in a manner analogous to that of pH [21]; nevertheless, this concept should not be interpreted as representing the mechanism of electron transfer, except in the presence of electrodes.

2.10.4 Mathematical Representation of Redox Equilibria

EQUILIBRIUM CONSTANT, FREE ENERGIES, ELECTRODE POTENTIAL AND ELECTRON ACTIVITY

The overall electron transfer reaction typified by equation 1 can be thought of as two coupled half-reactions, representing reduction and oxidation, respectively. The half-reactions for equation 1 would be as follows:



Either of these equations can be considered a "redox buffer" (analogous to a pH buffer); the activity of the electron (e^-) affects the distribution between the oxidized and reduced state, just as the activity of H^+ affects the distribution between the dissociated and undissociated forms of an acid.

Hypothetical equilibrium constants can be assigned to each half-reaction. For an oxidation reaction, the equilibrium expression would be

$$K_{red, oxid} = [\text{oxid}] [e^-] / [\text{red}] \quad (4)$$

Thus, the equilibrium constant for equation 2 would be

$$K_{Fe^{+2}, Fe^{+3}} = [Fe^{+3}] [e^-] / [Fe^{+2}] \quad (5a)$$

Similarly, for the reduction half-reaction (equation 3),

$$K_{O_2, H_2} = 1/[pO_2][H^+]^4[e^-]^4 \quad (5b)$$

These equilibrium constants are related to the free energy change of the reaction according to

$$\log K = -\Delta G^\circ/2.303 R T \quad (6)$$

where R = gas constant (1.986 cal/deg-mole)

T = absolute temperature (K)

ΔG° = free energy change (kcal/mole)

At 25°C, this relationship is

$$\Delta G^\circ = -1.364 \log K \quad (7)$$

Each half-reaction can be described by a half-cell potential, E° , referenced to the hydrogen electrode. The half-cell potential is related to the free energy change according to

$$\Delta G^\circ = -n F E^\circ = -n(23.06) E^\circ \quad (8)$$

where n = number of electrons transferred

F = Faraday constant (23.06 kcal/V-mole-equiv)

ΔG° = free energy change (kcal/mole)

E° = half-cell potential (V)

(Note that equation 8 is written based on the American sign convention for E° values which gives a positive sign to any complete reaction which goes spontaneously as written [10].)

Equations 7 and 8 allow calculation of K , ΔG° , or E° if one of these is known. Since ΔG° values are a function of temperature, the value of E° varies with temperature. This is discussed in greater detail in Section 2.11. If p_e is defined as $-\log [e^-]$, equation 4 can be written in the form

$$\begin{aligned} \log K_{red, oxid} &= \log [oxid]/[red] + \log [e^-] \\ &= \log [oxid]/[red] - p_e \end{aligned} \quad (9)$$

This relationship allows determination of the equilibrium concentrations (or ratio) of the oxidized and reduced forms of the redox couple at a given p_e value (similar to pH governing the ratio of protonated and unprotonated forms in a buffer).

Example 1 What is the relationship between pe and the ratio of oxidized and reduced forms of dissolved iron(II) and iron(III)?

For equation 2 (using equation 9),

$$\log K_{\text{Fe}^{+3}, \text{Fe}^{+2}} = \log [\text{Fe}^{+3}/[\text{Fe}^{+2}] - \text{pe} \quad (10)$$

From equations 7 and 8, with $n=1$

$$\log K_{\text{Fe}^{+3}, \text{Fe}^{+2}} = 16.91 E_{\text{Fe}^{+3}/\text{Fe}^{+2}} \quad (11)$$

Using a value of -0.771V for the half-cell potential, E^0 (see §2.10.7), we obtain

$$\log K_{\text{Fe}^{+3}, \text{Fe}^{+2}} = 16.95 (-0.771) = -13.07 \quad (12)$$

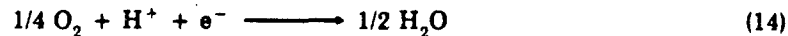
Whence from equation 10,

$$\text{pe} = 13.07 + \log [\text{Fe}^{+3}/[\text{Fe}^{+2}] \quad (13)$$

A plot of equation 13 is shown in Figure 2.10-5. Figure 2.10-6 is a plot of similar equations for arsenic(III)/arsenic(V) ratio at three pH values.

When a redox half-reaction contains H^+ or OH^- as reactants or products, the pe depends on pH. The mathematical dependence of pe on pH is a function of the reaction and of the form of the equilibrium constant. Similarly, if either a reactant or product is a gas, the pe is a function of the partial pressure of the gas. These variables are illustrated in Example 2 below. It is important to use the equilibrium constant that corresponds to the equation as written (i.e., with the same coefficients of the reactants) in the original source of the measurement. This applies to reactions where pure phases (e.g., H_2O) or gases are products or reactants. For such reactions, the values of the equilibrium constants depend on the coefficients.

Example 2 What is the dependence of pe on the pH and partial pressure of oxygen for the reduction of oxygen to water according to the following reaction?



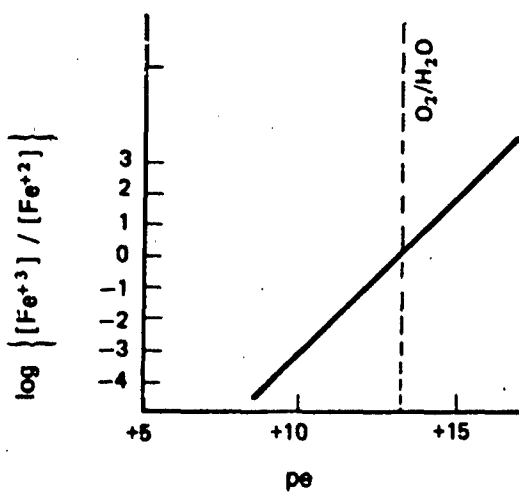
Using the convention that $[\text{H}_2\text{O}]$ is a constant, we can write the equilibrium expression for this half-reaction as

$$K_{\text{O}_2, \text{H}_2\text{O}} = \frac{1}{[\text{pO}_2]^{1/4} [\text{H}^+] [\text{e}^-]} \quad (15)$$

In terms of logarithms,

$$\log K_{\text{O}_2, \text{H}_2\text{O}} = \log 1 - 1/4 \log [\text{pO}_2] - \log [\text{H}^+] - \log [\text{e}^-] \quad (16)$$

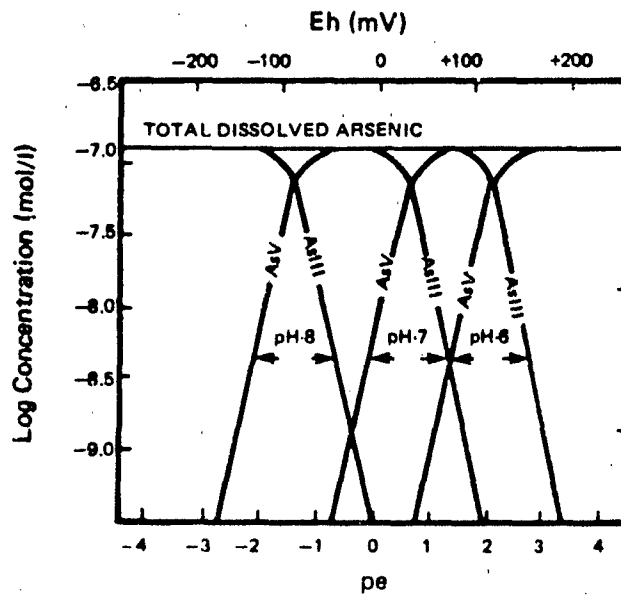
$$= -1/4 \log [\text{pO}_2] + \text{pH} + \text{pe} \quad (17)$$



Dashed line indicates position of oxygen/water couple at pH 7.5.

Source: Equation 13

FIGURE 2.10-5 Theoretical Distribution of Iron(II) and Iron(III) at Various pe Values



Source: Adapted from Cherry [7]. (Copyright 1979, New Zealand Hydrological Society. Reproduced with permission.)

FIGURE 2.10-6 Variation in Concentrations of Arsenic(III) and Arsenic(V) with pe at pH values of 6, 7 and 8. (Derived from $\text{pH} + (\frac{2}{3})\text{pe} = 6.6$ for the $\text{AsO}_4^{3-}/\text{HAsO}_4^{2-}$ Half Reaction)

The E^0 for the water/oxygen couple is 1.229 V (see §2.10.7). Since equation 14 involves one electron, $n=1$. Using these values, equations 7 and 8 yield

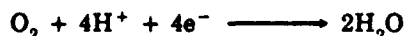
$$\log K_{O_2, H_2O} = 16.95(1.229) = 20.83 \quad (18)$$

Hence, equation 17 becomes

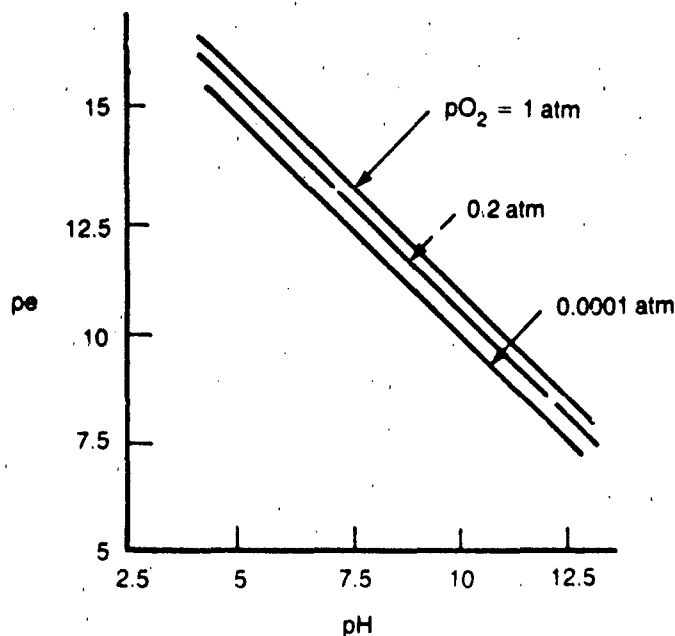
$$pe + pH = 20.83 + 1/4 \log[pO_2] \quad (19)$$

A plot of pe vs pH at various partial pressures of oxygen is shown in Figure 2.10-7.

Note that if equation 14 had been written



a different value of the equilibrium constant (four times as large) would have been used. The result would have been equivalent to equation 19 but multiplied by 4 throughout.



Source: Equation 19

FIGURE 2.10-7 pe Versus pH Diagram for the Oxygen/Water Half Reaction at Various Partial Pressures of Oxygen

The relationships described above can be used to calculate the concentration ratios between oxidized and reduced forms that would be expected under equilibrium conditions, given particular values of p_e and the other parameters. Values of p_e can be obtained experimentally, although they are subject to uncertainties and limitations (see § 2.10.5). In some cases, these values are fairly representative of redox conditions. One experimental method of determining p_e is to measure potentials with a platinum sensing electrode, using the following relationship:

$$E(Pt) = E_{Pt}^0 - B \log[e^-] = E_{Pt}^0 + B p_e \quad (20)$$

where

$E(Pt)$ = potential measured using a platinum electrode
(equal to E_h)

E_{Pt}^0 = zero by convention, so that $E_h = B p_e$

$B = 2.3RT/nF$ (0.0592 V if $n = 1$ at 25°C)

The value of $E(Pt)$ is also referred to as the value of E_h in the literature. Alternatively, we can use the following equation:

$$E_h = E^0(\text{redox couple}) + \frac{2.3 RT}{nF} \log \frac{[\text{oxid}]}{[\text{red}]} \quad (21)$$

Values of E_h are more often used when experimental data are obtained whereas p_e is convenient to use when equilibrium constant data are available and calculations are made from them. The range of E_h values in aqueous systems is approximately from -0.8 to +1.2 V (§ 2.10.5). The values of p_e are related to the values of equilibrium constants and can vary greatly.

Example 3 What is the predicted distribution between reduced and oxidized dissolved iron at an E^0 of 0.900 V (measured with a platinum electrode and a calomel reference electrode)?

Substituting $E(Pt) = 0.900\text{V}$ and $B = 0.0592$ in equation 20,

$$\begin{aligned} 0.900 &= 0.0592 p_e \\ p_e &= 15.21 \end{aligned} \quad (22)$$

From equation 13 (or Figure 2.10-5),

$$15.21 = 13.07 + \log [\text{Fe}^{+3}]/[\text{Fe}^{+2}] \quad (23)$$

Therefore,

$$\log [\text{Fe}^{+3}]/[\text{Fe}^{+2}] = 2.14$$

or

$$[\text{Fe}^{+3}]/[\text{Fe}^{+2}] = 138$$

Example 4 What is the pe of water in equilibrium with the atmosphere at pH 7?

The partial pressure of oxygen in the atmosphere is 0.21 atm. From equation 19,

$$\begin{aligned} \text{pe} &= 1/4 \log [\text{pO}_2] - \text{pH} + 20.83 \\ &= 1/4 (\log 0.21) - 7 + 20.83 \\ &= -0.17 - 7 + 20.83 \\ &= 13.66 \end{aligned} \quad (24)$$

Example 5 Calculate the expected equilibrium pe of water at pH 7.4 containing Cr(III) at 0.5 nmol/l and Cr(VI) at 0.3 nmol/l, using the ratio of the chromium species concentrations.

We first identify the species of Cr(III) and Cr(VI) that are expected to be present at pH 7.4. Using the acid dissociation constants for the aquo ions (see §7.6.2), we calculate that the dominant species are expected to be Cr(OH)_2^+ and CrO_4^{2-} . The redox reaction of concern is therefore,



Equation 25 yields the following expressions for the equilibrium constant as a function of pe and pH:

$$K = \frac{[\text{Cr(OH)}_2^+]}{[\text{CrO}_4^{2-}] [\text{H}^+]^6 [\text{e}^-]^3} \quad (26)$$

or

$$\log K = \log \{[\text{Cr(OH)}_2^+]/[\text{CrO}_4^{2-}]\} + 6 \text{pH} + 3 \text{pe} \quad (27)$$

The following values are now substituted in equation 27:

$$\begin{aligned} \log K &= 66.1 \text{ [11]} \\ \text{pH} &= 7.4 \\ [\text{Cr(OH)}_2^+] &= 0.5 \text{ nmol/l} \\ [\text{CrO}_4^{2-}] &= 0.3 \text{ nmol/l} \end{aligned}$$

$$\begin{aligned} 66.1 &= \log (0.5/0.3) + 6(7.4) + 3 \text{pe} \\ \text{pe} &= 7.16 \end{aligned}$$

The parameters K, ΔG° , E° and their relationships are applicable to the overall redox reaction



but pe is a parameter useful only in the half reactions and not for the overall reaction. Further discussions of these parameters are given in references 10 and 12.

STABILITY FIELD DIAGRAMS

Stability field diagrams are another useful method for presenting results of calculations of redox reactions under equilibrium conditions. These diagrams, which include plots of Eh (or pe) against pH for the most thermodynamically stable species, show equilibrium conditions and important chemical reactions that may dominate the behavior of an element under environmental conditions. Diagrams and procedures for their preparation have been described by several authors [8,10,11,17]. When using these diagrams to decide whether a particular phase or species is present, one should remember that they reflect the following assumptions:

- Thermodynamic equilibrium applies (i.e., kinetic limitations do not exist),
- The system is completely described (i.e., all applicable reactions are included),
- All solids are at unit activity and the activity coefficients of dissolved species are each one,
- The concentration of every dissolved species is assumed to be $10^{-6}M$ in all calculations.

For fast reactions and the existence of equilibrium, little error is introduced by using the diagrams, provided all the possible reactions have been considered. Where conditions of ionic strength are such that unit activities are not expected, the possible impact of this variation should be taken into account.

To familiarize the reader with stability field diagrams, the preparation of an Eh-pH diagram for the iron-water system is illustrated below.

Example 6 Construct the Fe-H₂O Eh-pH diagram.

The following procedure and data are adapted from Cloke[8]:

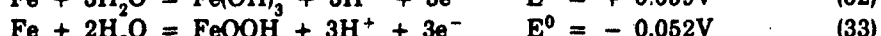
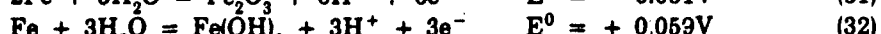
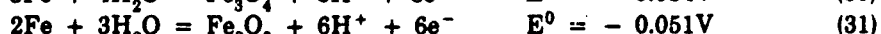
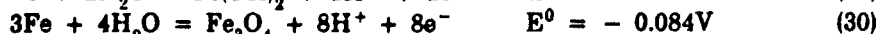
- (1) Consider all known valence states, solids and dissolved states as well as pH-dependent precipitation reactions. Scan tables that give free energies to locate compounds that can exist. Recognize that compounds that can form in a water system are those with water, OH⁻ and O⁻².

The list for iron is as follows:

Valence of Iron	Solid Substance	Dissolved Species
0	Fe	
2	FeO	
	Fe(OH) ₂	{ Fe ⁺² and Fe(II) complexes
2 and 3	Fe ₃ O ₄	
3	Fe ₂ O ₃	
	Fe(OH) ₃	{ Fe ⁺³ and Fe(III) complexes
	FeOOH	

- (2) Write balanced reactions for oxidation of the most reduced form of the substance to each of the other oxidation states given above, using only water as reactant with the most reduced form.

For the six oxidized forms of iron, one may consider the following reactions, starting with the most reduced form (Fe):



(E° values are derived or obtained using the procedure described in the next step)

- (3) Calculate E° values for each of the reactions above. (Depending on the form of the data available, equations 7 and 8 may be useful.) Write the values of E° next to the reactions, as shown above in step 2.

- (4) We can express the general reaction by means of the following equation:



for which [8]

$$Eh = E^\circ + (0.059/n)\log[C]^c[D]^d \dots / [A]^a[B]^b \dots \quad (35)$$

Write equation 35 for all of the reactions listed in step 2. In the case of reaction 28, for example, $a=1$, $b=1$, $c=2$, $d=1$, $A=[\text{Fe}]$, $B=[\text{H}_2\text{O}]$, $C=[\text{H}^+]$, $D=[\text{FeO}]$, $n=2$, and $E^\circ=-0.037$. Thus,

$$Eh = -0.037 + (0.059/2) \log [\text{H}^+]^2 [\text{FeO}]/[\text{Fe}] [\text{H}_2\text{O}] \quad (36)$$

This simplifies to the following equation:

$$Eh = -0.037 - 0.059 \text{ pH} \quad (37)$$

since the activities of the solid phases as well as of the water are defined as unity.

Similarly, for equations 29 to 33,

$$Eh = - 0.047 - 0.059 \text{ pH} \quad (38)$$

$$Eh = - 0.084 - 0.059 \text{ pH} \quad (39)$$

$$Eh = - 0.051 - 0.059 \text{ pH} \quad (40)$$

$$Eh = + 0.059 - 0.059 \text{ pH} \quad (41)$$

$$Eh = - 0.052 - 0.059 \text{ pH} \quad (42)$$

- (5) Plot equations 37 to 42 using Eh as the y axis and pH as the x axis as shown in Figure 2.10-8.

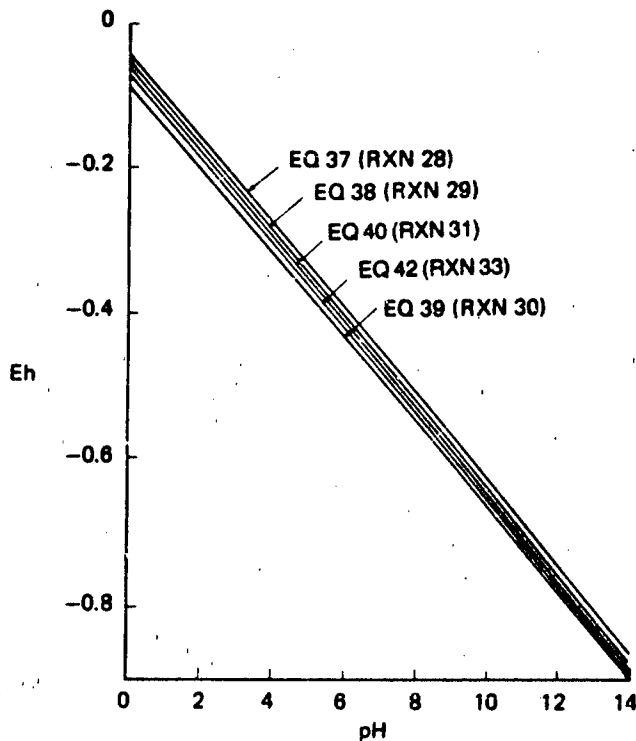


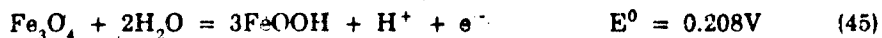
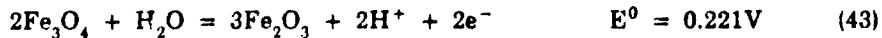
FIGURE 2.10-8 Eh Versus pH for the Fe-H₂O System: Diagram for Step 5

- (6) Use the line that is lowest (reaction 30) and disregard the others, because this line represents the reaction that uses up all the Fe and prevents any of the other reactions involving Fe from occurring.

If the lowest lines intersect, one of the lines would be used above the intersection and the other line below the intersection. The general rule is to use the line or line segment corresponding to the more negative value of Eh for a given pH. An additional line would also be drawn through the point of intersection according to an equation derived from the reaction of the two oxidized species, using only these two species and H₂O and H⁺ (not O₂, H₂ or OH⁻). Further details of this procedure are given in step 13.

- (7) Now consider oxidation to higher valences from the oxidized product of the reaction retained in step 6. The species that can be produced were identified in step 2.

For the iron system, we consider what species can result from the oxidation of Fe₃O₄:



These lead to the following three equations for the relationship between Eh and pH:

$$Eh = 0.221 - 0.059 \text{ pH} \quad (46)$$

$$Eh = 1.21 - 0.059 \text{ pH} \quad (47)$$

$$Eh = 0.208 - 0.059 \text{ pH} \quad (48)$$

When these equations are plotted, we find that the line corresponding to equation 48 is the lowest of the three, indicating that FeOOH is the product of oxidation of Fe_3O_4 at equilibrium. (See Figure 2.10-9.)

- (8) Repeat step 7 until the highest oxidation state is reached.
- (9) Draw two lines on the diagram defining the Eh-pH region where water is stable, as follows:

- For the water/oxygen half reaction,

$$Eh = 1.23 + 0.015 \log [\text{pO}_2] - 0.059 \text{ pH} \quad (49)$$

which at one atmosphere of oxygen corresponds to

$$Eh = 1.23 - 0.059 \text{ pH} \quad (50)$$

- For the hydrogen/proton couple,

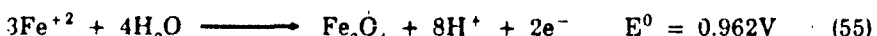
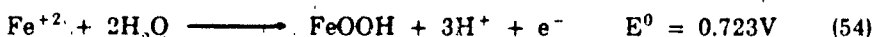
$$Eh = -0.059 \text{ pH} - 0.0295 \log [\text{pH}_2] \quad (51)$$

which at one atmosphere of hydrogen gas is

$$Eh = -0.059 \text{ pH} \quad (52)$$

Plots of equations 50 and 52 are included on Figure 2.10-9.

- (10) Discard all lines outside the area of water stability defined above — i.e., above the line for equation 50 and below the line for equation 52. Thus the plot for equation 39 is discarded, but the region between equations 52 and 48 remains a valid stability range for Fe_3O_4 .
- (11) Add lines for equilibria between solids and dissolved states of the species shown in the diagram. In this example, the following reactions are applicable:



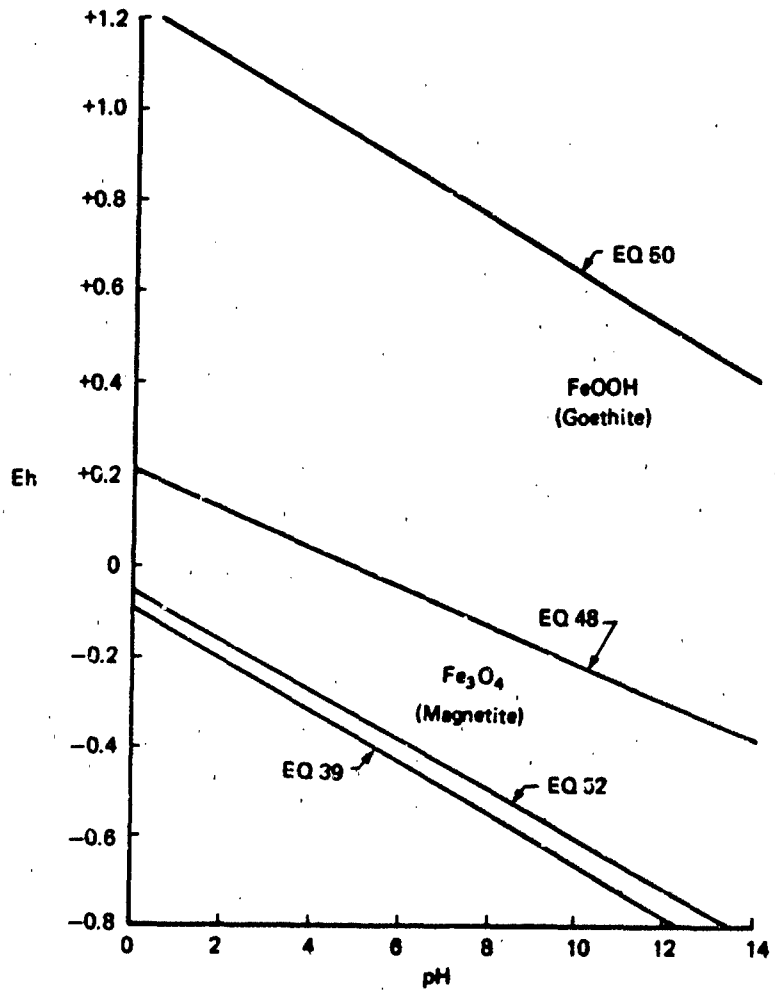


FIGURE 2.10-9 Eh Versus pH for the Fe-H₂O System: Diagram for Steps 7 and 9

For reaction 53,

$$K = [H^+]^3 / [Fe^{+3}] = 6.3 \quad (56)$$

or

$$pH = -(\log[Fe^{+3}]) / 3 = 0.268 \quad (57)$$

Since the stability field diagrams are drawn assuming a $10^{-6} M$ concentration of dissolved ions, $[Fe^{+3}] = 10^{-6} M$, and equation 57 reduces to $pH = 1.734$.

For equation 54, $E^0 = 0.723\text{V}$ and $n = 1$. Therefore, we can rewrite equation 35 as

$$Eh = 0.723 + (0.059/1) (\log[H^+]^3) - (0.059/1) (\log[Fe^{+2}]) \quad (58)$$

or

$$Eh = 0.723 - 0.177 \text{ pH} - 0.059 \log [Fe^{+2}] \quad (59)$$

For an $[Fe^{+2}] = 10^{-6}\text{M}$,

$$Eh = 1.077 - 0.177 \text{ pH} \quad (60)$$

Similarly, for equation 55,

$$Eh = 0.962 - 0.236 \text{ pH} - 0.0885 \log [Fe^{+2}] \quad (61)$$

and at $[Fe^{+2}] = 10^{-6}\text{M}$,

$$Eh = 1.493 - 0.236 \text{ pH} \quad (62)$$

Figure 2.10-10 shows the addition of lines corresponding to $\text{pH} = 1.734$ (equation 57) and equations 60 and 62 to Figure 2.10-9.

- (12) Add any redox reactions between the dissolved species. For this example, the reaction is



The redox potential for this reaction is

$$Eh = 0.771 + 0.059 \log [\text{Fe}^{+3}]/[\text{Fe}^{+2}] \quad (64)$$

At $[\text{Fe}^{+3}] = [\text{Fe}^{+2}] = 10^{-6}\text{M}$, equation 64 reduces to $Eh = 0.771\text{V}$ (referenced to hydrogen electrode). This is also plotted in Figure 2.10-10.

- (13) Erase all lines according to the following procedure. Where two lines intersect, delete the portion of each line that corresponds to the higher (more positive) Eh values at a given pH. Erase lines that no longer identify proper equilibrium reactions.

For this example, the lines to be erased are dashed in Figure 2.10-10. The portion of line for equation 57 within the Fe^{+2} area is erased because it no longer represents the proper species on either side.

The final diagram is shown in Figure 2.10-11.

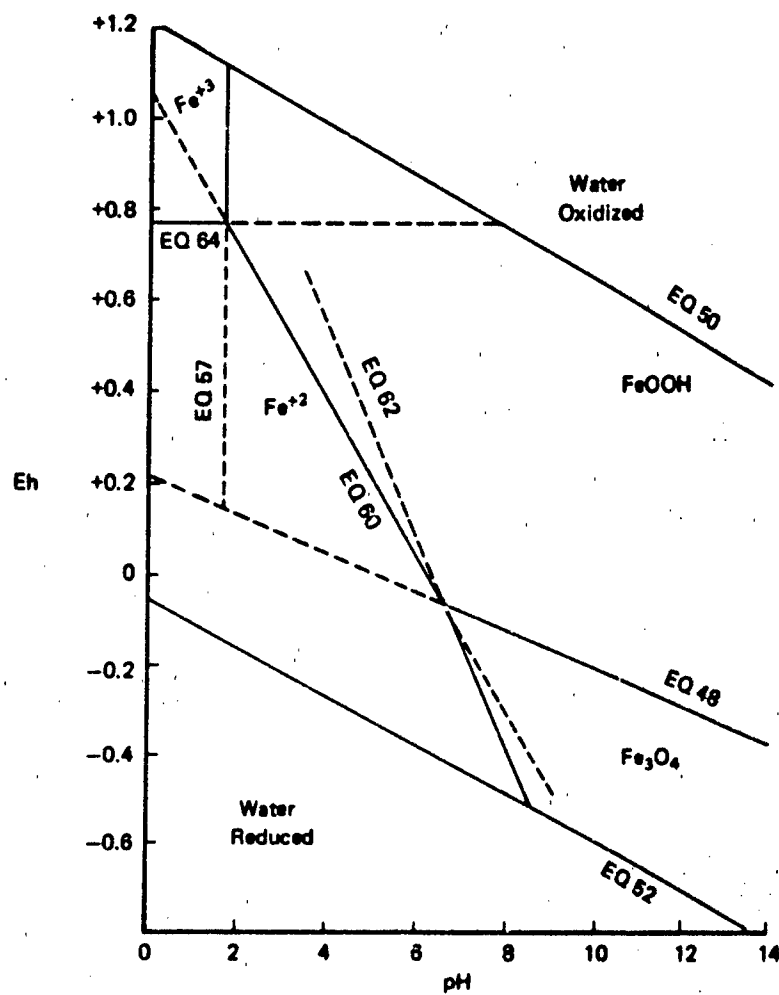


FIGURE 2.10-10 Eh Versus pH for the Fe-H₂O System: Diagram for Steps 11 to 13

The line shown on the Eh versus pH diagram for the Iron-Water System (Figure 2.10-11) separating the Fe⁺² and Fe⁺³ (at Eh = 0.77 and pH = 1) represents the conditions where the concentrations (or activities) of these two dissolved species are equal. Within the region labelled Fe⁺² this species predominates, and similarly for the Fe⁺³ region. The line separating regions of solid phases (e.g. Fe₃O₄ and FeOOH) provides the boundary where relative stability of one solid becomes greater than that of the other. A line that separates a solid phase and a dissolved species (e.g. Fe⁺³ and FeOOH at Eh = 1 and pH = 2) indicates the values of Eh and pH where the dissolved species is 10⁻⁶ M (by convention for the way this diagram was drawn). Similar diagrams could be drawn with these lines representing other dissolved ion concentrations (e.g. 10⁻⁴ or 10⁻² M). The lines that would represent higher dissolved Fe⁺³ concentrations would occur parallel to the line shown on Fig. 2.10-11 at similar Eh values but at lower pH values.

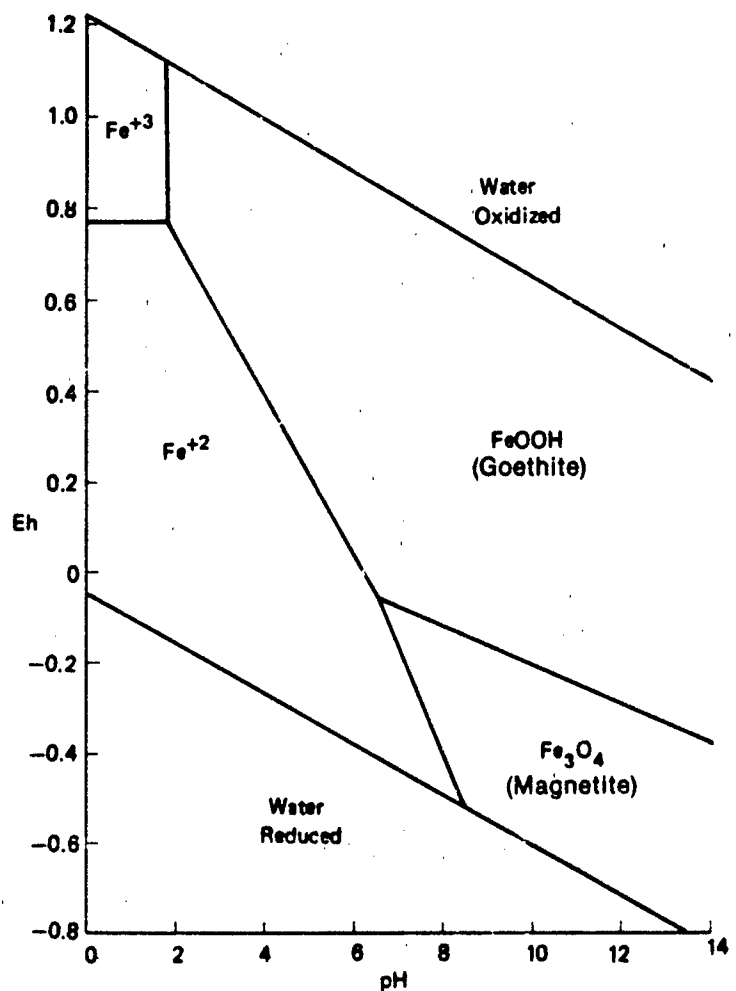


FIGURE 2.10-11 Eh Versus pH for the Fe-H₂O System: Final Diagram

2.10.5 Redox in Environmental Systems

IMPORTANT REDOX PROCESSES

Redox reactions in environmental systems can occur between species of elements that occur naturally, between pollutant species and naturally occurring species, and between pollutant species. Of the naturally occurring species, only a few commonly participate in redox processes; the typical oxidizing agents in waters (in order of decreasing oxidizing strength) are oxygen, nitrate, nitrite, ferric hydroxide, ferric phosphate, sulfate, sulfur, carbon dioxide and bicarbonate. The most important naturally occurring reducing agents in waters (in order of decreasing reducing strength) are organic substances, hydrogen sulfide, sulfur, iron sulfide, ammonium and nitrite. (This excludes kinetic considerations.)[20]

Due to kinetic limitations, local inhomogeneity, and local catalytic effects of organisms, redox equilibrium conditions may not be attained in many environmental systems, and several of the above listed species may coexist. For example, in water in equilibrium with air at pH 7 (pe = 13.6), all carbon should theoretically be present as carbon dioxide or carbonate-type species, all nitrogen as nitrate, all sulfur as sulfate, all iron as iron(III) species and all manganese as Mn(IV) species. In fact, nitrogen, reduced forms of carbon (e.g., organic matter and CH₄), sulfides, iron(II) and Mn(II) all exist under various conditions, attesting to a lack of equilibrium.

Nonequilibrium conditions usually occur when environments are isolated from the oxidizing species (e.g., oxygen) and appropriate catalyzing bacteria are present. Important redox half-reactions that are considered in the chemical equilibrium model WATEQF[16] are listed in Table 2.10-1.

All of the various forms of the naturally occurring elements (e.g. as shown in Table 2.10-1) can participate in reactions with specific species, leading to partial equilibrium (with respect to particular reactions) because of the limitations imposed on reactions with other species present. Thus, if the redox reaction and kinetics are favorable, pollutants introduced into that environment can react with these and other naturally present species.

TABLE 2.10-1
Redox Half-Reactions Considered in WATEQF

$\text{Fe}^{+2} = \text{Fe}^{+3} + e^-$	$\text{Fe}_3\text{O}_4 + 8\text{H}^+ = 3\text{Fe}^{+3} + 4\text{H}_2\text{O} + e^-$
$\text{Fe}^{+2} + \text{SO}_4^{-2} = \text{FeSO}_4^+ + e^-$	$\text{FeS}_2 + 2\text{H}^+ + 2e^- = \text{Fe}^{+2} + 2\text{HS}^-$
$\text{Fe}^{+2} + \text{Cl}^- = \text{FeCl}^{+2} + e^-$	$\text{Fe}_3\text{S}_4 + 4\text{H}^+ + 2e^- = 3\text{Fe}^{+2} + 4\text{HS}^-$
$\text{Fe}^{+2} + 2\text{Cl}^- = \text{FeCl}_2^+ + e^-$	$\text{Fe}^{+2} + \text{HFO}_4^{-2} = \text{FeHPO}_4^+ + e^-$
$\text{Fe}^{+2} + 3\text{Cl}^- = \text{FeCl}_3^0 + e^-$	$\text{Fe}^{+2} + \text{H}_2\text{PO}_4^- = \text{FeH}_2\text{PO}_4^{+2} + e^-$
$\text{SO}_4^{-2} + 10\text{H}^+ + 8e^- = \text{H}_2\text{S} + 4\text{H}_2\text{O}$	$\text{Mn}^{+2} + 4\text{H}_2\text{O} = \text{MnO}_4^- + 8\text{H}^+ + 5e^-$
$2\text{H}_2\text{O} = \text{O}_2 + 4\text{H}^+ + 4e^-$	$\text{Mn}^{+2} + 4\text{H}_2\text{O} = \text{MnO}_4^- + 8\text{H}^+ + 4e^-$
$\text{HCO}_3^- + 8e^- + 9\text{H}^+ = \text{CH}_4 + 3\text{H}_2\text{O}$	$\delta\text{-MnO}_2(\text{birnessite}) + 4\text{H}^+ + e^- = \text{Mn}^{+3} + 2\text{H}_2\text{O}$
$\text{Fe}^{+2} + 2\text{H}_2\text{O} = \text{Fe(OH)}_2^+ + 2\text{H}^+ + e^-$	$\delta\text{-MnO}_2(\text{insutite}) + 4\text{H}^+ + e^- = \text{Mn}^{+3} + 2\text{H}_2\text{O}$
$\text{Fe}^{+2} + 3\text{H}_2\text{O} = \text{Fe(OH)}_3^0 + 3\text{H}^+ + e^-$	$\text{Mn}_3\text{O}_4 + 8\text{H}^+ + 2e^- = 3\text{Mn}^{+2} + 4\text{H}_2\text{O}$
$\text{Fe}^{+2} + 4\text{H}_2\text{O} = \text{Fe(OH)}_4^- + 4\text{H}^+ + e^-$	

Source: Plummer [16]

In addition to the major elements, many trace components present in the environment can undergo redox reactions. This is important, because pollutants are generally present at very low levels, and the kinetic and redox properties of the trace substances that occur naturally may favor their reactions with the pollutants rather than with the major species such as those in Table 2.10-1. Trace elements can also catalyze redox reactions.

Some other redox species that may need consideration are shown in Figure 2.10-1. Many of these species, if present at elevated levels, would be considered pollutants.

The other category of redox interactions in environmental systems that may have to be addressed is the reaction between two or more pollutants introduced into the system. In some situations, the likelihood of a redox reaction in a mixture of two or more pollutants increases after it enters an environmental system such as groundwater or seawater. The environmental system can make the conditions for reaction more favorable or enhance the kinetics by modifying the speciation of the pollutants (e.g., by modifying the pH), or it can introduce chemical or biological species that can enhance the rate of the redox reaction. Examples of redox reactions that can be biologically mediated are given in Table 2.10-2.

APPLICABILITY OF Eh (OR pe) MEASUREMENTS

The measurement and interpretation of Eh or pe in environmental systems can be difficult [15,22]. Potentiometric measurements of Eh in environmental systems usually do not agree with those predicted by theory, due to the low concentration of redox-active species and their low exchange currents.² The most important problem in applying the Eh concept to natural waters is the lack of redox equilibrium between all the redox-active species. Reactions between the major environmentally important redox species (listed in Figure 2.10-12) often appear to be very slow; thus, for a system in disequilibrium, an Eh value that is meaningful with regard to rapid exchange between a redox couple is not expected.

Lindberg and Runnels [15] have examined data from about 30 groundwater analyses and compared the measured Eh or pe values to those predicted from calculations through the ratio of concentrations of many of the redox-active couples (iron(II)/iron(III), oxygen/water, bisulfide/sulfate, etc.) in these solutions. The expected Eh values and those calculated by use of these redox couples do not agree and vary over a wide range, as shown in Figure 2.10-12. These data show that none of the representative waters chosen for analysis exhibited equilibrium and that the computed Eh values span a wide range (as much as 1000 mV). They also suggest that indicator species (e.g., iodide/iodate or arsenic(III)/arsenic(V)) ratios may not be more representative of the redox state than the measurement using an electrode. It may be reasonably concluded that a master value of Eh or pe cannot be used to predict redox equilibria in groundwater environments and that computer models utilizing pe or Eh to calculate species ratios would most likely make erroneous predictions.

Lindberg and Runnels [15] have suggested an alternative to using measured Eh values, namely, to measure concentrations of certain redox-active species (e.g., dissolved oxygen, total sulfide species and methane) as a qualitative guide to the redox status of waters (see next section for discussion of this approach); the concentrations of the redox components of immediate interest in the water should be measured if there is a need to consider their possible redox effect on pollutants introduced into that environment.

2. The species do not readily give up or take up electrons at platinum or gold electrode surfaces.

TABLE 2.10-2
Microbially Mediated Oxidation and Reduction Reactions

Reaction	$\text{pe}^0_{\text{pH}7}$ (note a)
Oxidation	
(1) ^b $\text{CH}_2\text{O} + \text{H}_2\text{O} = \text{CO}_2(\text{g}) + 4\text{H}^+ + 4\text{e}^-$	-8.20
(2) $\text{HS}^- + 4\text{H}_2\text{O} = \text{SO}_4^{2-} + 9\text{H}^+ + 8\text{e}^-$	-3.75
(3) $\text{NH}_4^+ + 3\text{H}_2\text{O} = \text{NO}_3^- + 10\text{H}^+ + 8\text{e}^-$	+6.16
(4) ^c $\text{FeCO}_3(\text{s}) + 2\text{H}_2\text{O} = \text{FeOOH}(\text{s}) + \text{HCO}_3^{(10^{-3}M)} + 2\text{H}^+ + \text{e}^-$	-1.67
(5) ^c $\text{MnCO}_3(\text{s}) + 2\text{H}_2\text{O} = \text{MnO}_2(\text{s}) + \text{HCO}_3^{(10^{-3}M)} + 3\text{H}^+ + 2\text{e}^-$	+8.5
(1a) ^b $\text{HCOO}^- = \text{CO}_2(\text{g}) + \text{H}^+ + 2\text{e}^-$	-8.73
(1b) $\text{CH}_2\text{O} + \text{H}_2\text{O} = \text{HCOO}^- + 3\text{H}^+ + 2\text{e}^-$	-7.68
(1c) $\text{CH}_3\text{OH} = \text{CH}_2\text{O} + 2\text{H}^+ + 2\text{e}^-$	-3.01
(1d) $\text{CH}_4(\text{g}) + \text{H}_2\text{O} = \text{CH}_3\text{OH} + 2\text{H}^+ + 2\text{e}^-$	+2.88
Reduction	
(A) $\text{O}_2(\text{g}) + 4\text{H}^+ + 4\text{e}^- = 2\text{H}_2\text{O}$	+13.75
(B) ^d $2\text{NO}_3^- + 12\text{H}^+ + 10\text{e}^- = \text{N}_2(\text{g}) + 6\text{H}_2\text{O}$	+12.65
(C) $\text{NO}_3^- + 10\text{H}^+ + 8\text{e}^- = \text{NH}_4^+ + 3\text{H}_2\text{O}$	+6.16
(D) $\text{SO}_4^{2-} + 9\text{H}^+ + 8\text{e}^- = \text{HS}^- + 4\text{H}_2\text{O}$	-3.75
(E) $\text{CO}_2(\text{g}) + 8\text{H}^+ + 8\text{e}^- = \text{CH}_4(\text{g}) + 4\text{H}_2\text{O}$	-4.13
(F) ^b $\text{CH}_2\text{O} + 2\text{H}^+ + 2\text{e}^- = \text{CH}_3\text{OH}$	-3.01

(Continued)

Despite the limitations of Eh and pe, redox equilibrium models (including Eh/pH diagrams) can be valuable for interpreting observed data and identifying possible regulating mechanisms for pe buffering of a few aqueous systems [20]. The discrepancies between equilibrium calculations and experimental data can give insight as to whether the reactions are well understood and whether the systems are at equilibrium. They may also provide clues concerning which species will predominate as redox conditions change and what solid phase(s) may be expected.

Eh AND pe VALUES ENCOUNTERED IN VARIOUS ENVIRONMENTS

For waters in equilibrium with atmospheric oxygen, there is no correlation of the measured Eh and dissolved oxygen levels [6]; the water/oxygen half-reaction (equation 3) is too slow to affect the Eh value measured. The measurement of Eh is only considered valid and useful when dissolved oxygen (DO) is below the minimum detection level of 0.01 ppm. For waters where DO is above this level, measurement of dissolved oxygen is a better indication of redox conditions.

TABLE 2.10-2 (Continued)

Thermodynamic Sequence of Biologically Mediated Redox Reactions

Model 1: Excess organic material. (Water contains incipiently O_2 , NO_3^- , SO_4^{2-} , HCO_3^- .) Examples: Hypolimnetic layers of eutrophic lake, sediments; digester.

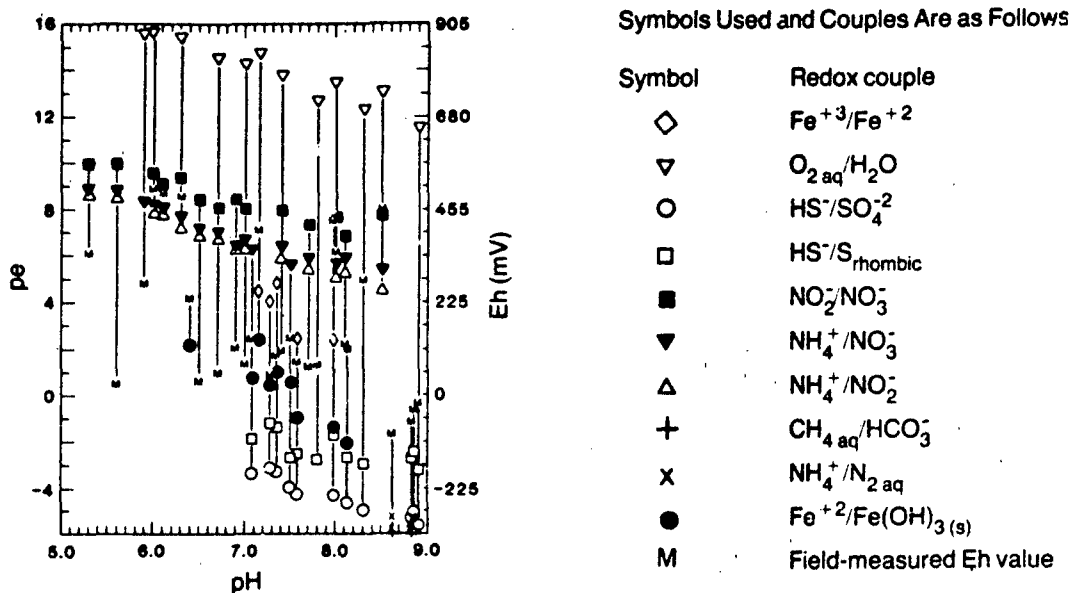
	Combination	(1/n)log K_{pH7}^0
Aerobic respiration	(1)	21.95
Dentrification ^f	(1) + (A)	20.85
Nitrate reduction	(1) + (B)	14.36
Fermentation ^{b,g}	(1b) + (F)	4.67
Sulfate reduction	(1) + (D)	4.45
Methane fermentation	(1) + (E)	4.07

Model 2: Excess O_2 . (Water contains incipiently organic material, SH^- , NH_4^+ and possibly $Fe(II)$ and $Mn(II)$.) Examples: Aerobic waste treatment, self-purification in streams; epilimnetic waters.

	Combination	(1/n)log K_{pH7}^0
Aerobic respiration	(A) + (1)	21.95
Sulfide oxidation	(A) + (2)	17.50
Nitrification ^f	(A) + (3)	7.59
Ferrous oxidation ^c	(A) + (4)	15.42
Mn(II) oxidation	(A) + (5)	5.25

- a. $p\text{e}_{pH7}^0$ is the pe if all reaction participants with exception of (H^+) are present at unit activity (for gases, partial pressure = 1). (H^+) has been set equal to 10^{-7} . $p\text{e}^0 = (1/n)\log K_{\text{reduction}}$ (n = no. of electrons). All constants given are for 25°C .
- b. CH_2O is used here as a general symbol for organic material. Examples for organic carbon with formal oxidation states of +II, 0, -II, and -IV are given in reactions 1a to 1d, respectively. $H_2(g)$ is an almost equally strong reductant as organic material and in some mediations it can be substituted for organic material: $H_2(g) = 2H^+ + 2e^-$; $p\text{e}^0_{pH7} = -7.00$.
- c. The autotrophic nature of iron and manganese bacteria is in dispute.
- d. $N_2O(g)$ may appear as an intermediate; some facultative anaerobes catalyze the reduction to NO_2 .
- e. $(1/n)\log K$ is the equilibrium constant for the combined redox reaction per electron transferred. With exception of (H^+), all reaction participants are present at unit activity. [$(H^+) = 10^{-7}$]. $(1/n)\log K$ is proportional to the free energy decrease of the redox reaction per electron transferred: $(1/n)\log K = -\Delta G^\circ_{pH7}/(nRT \ln 10)$.
- f. It has been assumed, rather arbitrarily, that the direct oxidation of NH_4^+ into N_2 is hindered. Conversion of NH_4^+ to N_2 is thus achieved by nitrification/denitrification.
- g. Fermentation is interpreted as an organic redox reaction where one organic substance is reduced by oxidizing another organic substance (e.g., alcohol fermentation). The participants in such a reaction are themselves thermodynamically unstable.

Source: Stumm [20] (Copyright 1967, Water Pollution Control Federation. Reprinted with permission.)



Source: Lindberg and Runnels [13]. (Copyright 1984, American Association for the Advancement of Science. Reprinted with permission.)

FIGURE 2.10-12 Comparison of Measured and Computed Eh Versus pH Values in 30 Groundwater Systems

The relative positions of some natural environments as functions of Eh and pH are shown in Figure 2.10-13. The validity of Eh measurement for various conditions encountered in the environment is summarized in Table 2.10-3. Reproducible and meaningful Eh values are generally obtained in well-poised systems (i.e., those that contain high concentrations of both the reduced and oxidized forms of the redox couple). This occurs in some acid mine waters that contain high levels of dissolved iron. For the other waters listed in Table 2.10-3, Eh measurements are not considered reliable because of their lack of reproducibility and stability [6].

Although, as discussed above, dissolved oxygen levels do not readily provide the redox status of oxygenated waters, concentrations of sulfide in many sediment water environments do provide an indication. This is because the Eh values of many sediments containing H_2S have been found to be controlled by the following reversible half-reactions [1]:

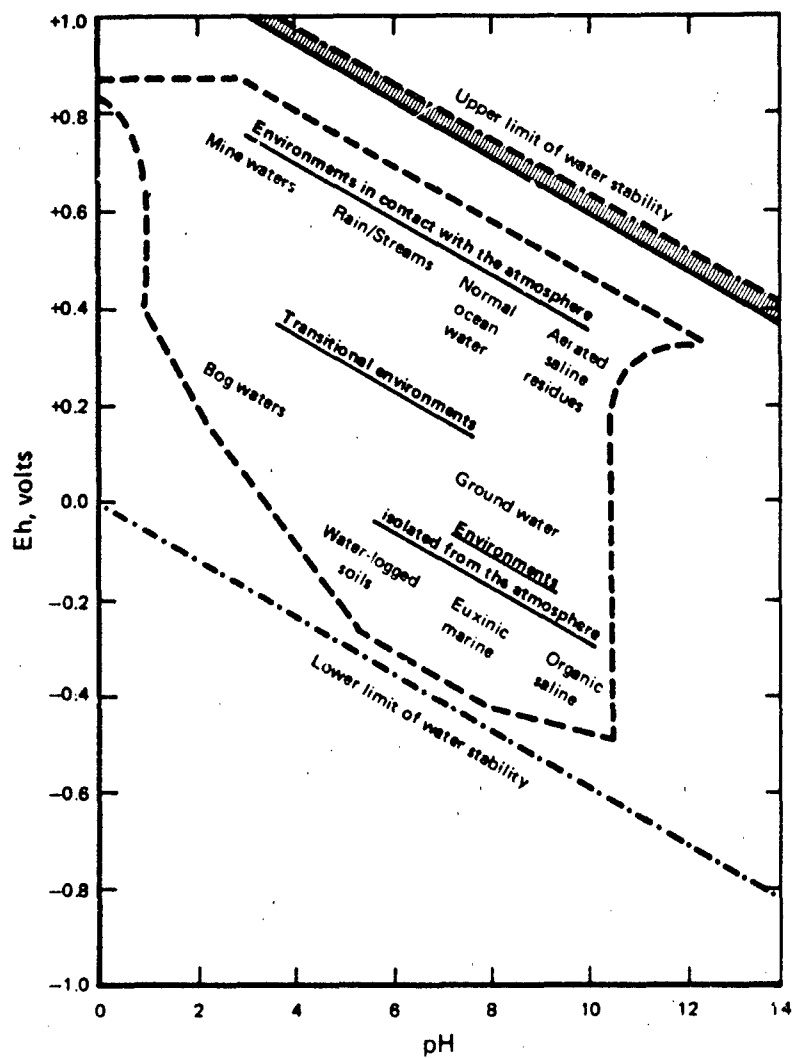


or



according to the equation (at 25°C), where

$$\text{Eh} = -0.475 + 0.0295 \text{ p}[\text{S}^{2-}] \quad (67)$$



Dashed lines represent limits of measurements in natural systems.
 Crosshatched area represents the Eh and pH of waters containing
 more than .01 ppm of oxygen, based on the oxygen/water half-reaction.

Source: Langmuir [13] (Copyright 1971, Wiley Interscience Publishers.
Reprinted with permission.)

FIGURE 2.10-13 Approximate Relative Position of Eh and pH for Natural Environments

TABLE 2.10.3
Redox Characteristics and Eh Measurements for Various Aqueous Environments

Environment	Redox Characteristics	Eh Response/Comments
Oxygenated Waters (e.g., rain, streams, some groundwater, shallow lakes)	Poorly poised, low or no concentration of electroactive species	Eh measurement drifts; D.O. levels may be more useful
Acid mine water, groundwater rich in Fe at pH below 4	May be well poised; reversible redox reaction present at significant levels	Uncommon in natural environments; Eh measurable and useful
Organic rich systems, soil waters, stagnant polluted water with low oxygen levels	Poorly poised; absence of oxidized form of redox species; mixed potentials and irreversible reactions present; biological mediation	Lowest Eh values found in these environments; drift in Eh observed
Heterogeneous environments	Variable condition	Reproducible value may not be possible

Source: Adapted from Langmuir [13]

Empirical data for values of Eh and S^{2-} correlate well with this half-reaction, as shown in Figure 2.10-14. When electrodes are inserted into these sediment environments, such measurements are rapidly attained and are stable at low Eh values, indicating a well-poised system.

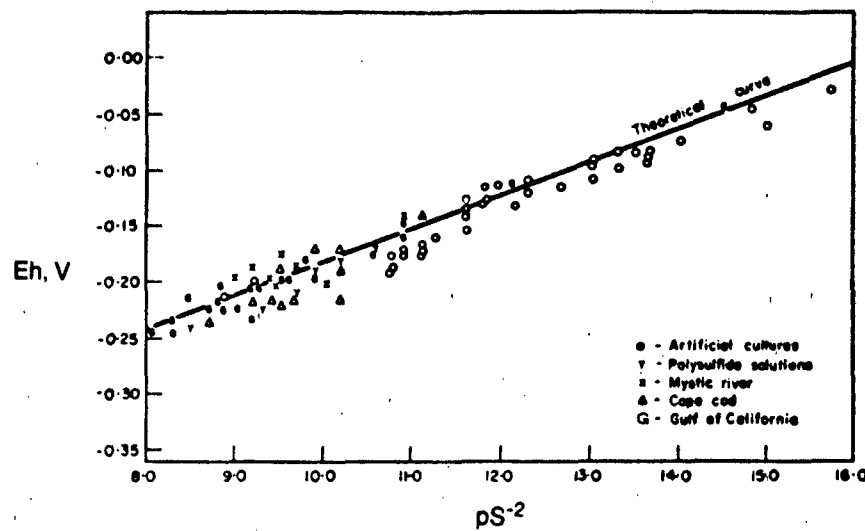
OTHER INDICATORS OF REDOX CONDITIONS

A classification of sediment redox environments proposed by Berner [2] may be more practical than the Eh approach, because it is directly related to measured concentrations. In this scheme, Eh is not considered to be a measurable quantity, owing to the difficulties described previously. The primary basis for this classification is that dissolved oxygen (DO) and total dissolved sulfide species (H_2S , HS^- , S^{2-}) are measurable and are intimately involved in redox reactions. The scheme is summarized in Figure 2.10-15, and the concentration basis for each classification is given in Table 2.10-4. The classification depends on the ability to identify naturally occurring (authigenic) Mn and Fe phases in the solids and is thus useful only for undisturbed sediment environments.

The best (but most tedious) approach to understanding redox properties of the aqueous environment and their possible impact on added pollutants is to consider the reaction of the added pollutant with each of the species present in the environment. This characterization would include determining identity, speciation, relative concentration and assessment of the rate and equilibrium position of all the possible redox reactions, and would be performed either by calculation or by experiment. The initial candidates for consideration would be the most commonly found redox active species in solution (dissolved oxygen, sulfide species, iron(II), iron(III), manganese(II) and possibly nitrite), followed by species commonly found in the solid phase (if present) — iron(II), iron (III), manganese(II) and manganese(IV).

As discussed in Section 3.3, "Kinetics of Redox Reactions," catalysis by trace species as well as biological organisms is possible; thus, after the major components are considered, possible redox reaction with trace components should be addressed. The speciation of the reactants involved will depend on the environment and the effects of the added pollutants.

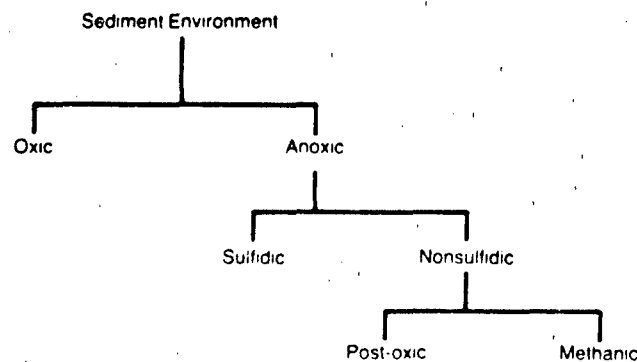
An example of the concentration profile observed for a variety of species in a pore water system that progresses from being oxic to anoxic (various depths in a sediment) is shown in Figure 2.10-16. Concentrations of many metals in the dissolved state above the interface are low (mostly existing in the solid state). Release from the solid into solution after reduction is observed below the O_2/H_2S interface.



"Theoretical Curve" represents the half-reaction $\text{sulfide} \rightleftharpoons \text{sulfur (rhomb)} + 2 e^-$

Source: Berner [1]. (Copyright 1963, Pergamon Press, Inc. Reprinted with permission.)

FIGURE 2.10-14 Eh Versus $p(\text{Sulfide})$ in Natural Sediment Environments and Polysulfide Solutions



See Table 2.10-4 for clarification of terms

Source: Berner [2]

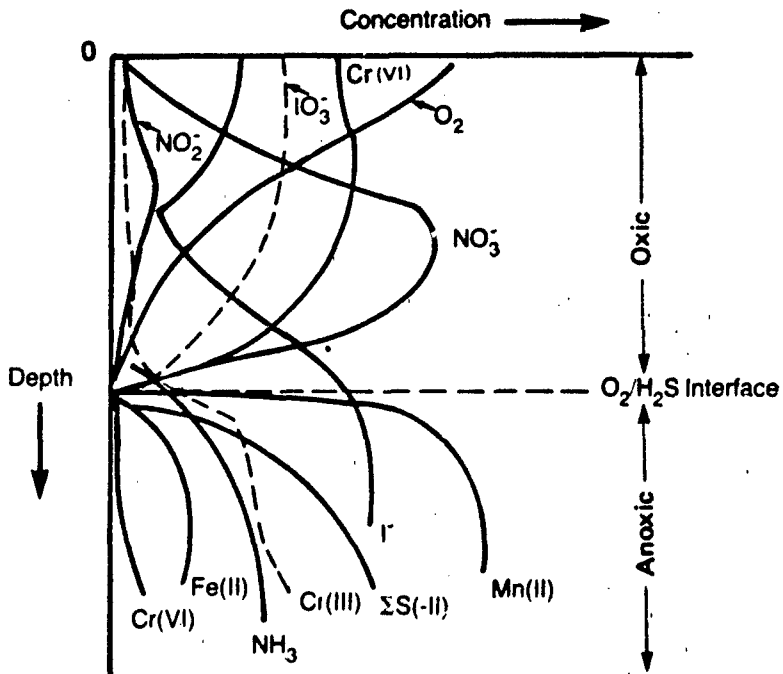
FIGURE 2.10-15 Classification of Sediment Environments

TABLE 2.10-4
Redox Classification Scheme Proposed by Berner

Environment	Class of Water/ Sediment	$[\Sigma H_2S]_{aq}$ (M)	P_{CO_2} (atm)	Characteristic Typical of Solid Phase In Equilibrium*	Other Characteristics	Progression of Biologically Mediated Organic Matter Decomposition
Oxic		$\geq 10^{-6}$	$< 10^{-6}$	$FeOOH, MnO_2, Fe_2O_3$, Relative absence of decomposable organic matter (MnO_2 is a better indicator than $Fe(III)$ solids; latter persist under anoxic conditions, since they are not reduced by any organic species)	Lack of bacteria capable of producing H_2S	Oxygen consumption
Anoxic		$< 10^{-6}$				
Sulfidic		$< 10^{-6}$	$\geq 10^{-6}$	$> 10^{-4} Fe(II)S_2, MnCO_3, Mn(II)S$	Lack of aerobic organisms and oxidized minerals	Sulfate reduction
Nonsulfidic		$< 10^{-6}$				
• Post-Oxic		$< 10^{-6}$	$< 10^{-6}$	Fe^{+2}/Fe^{+3} - containing alumino silicates, $FeCO_3, Fe_3(PO_4)_2, MnCO_3$. No sulfide minerals, minor amount of decomposable organic matter		Nitrate reduction
Methanic		$< 10^{-6}$	$< 10^{-6}$	$FeCO_3, Fe_3(PO_4)_2, MnCO_3$, Earlier formed sulfide minerals, decomposable organic matter present		Methane formation

a. $Fe(III)OOH$ = goethite; $Fe(III)_2O_3$ = hematite; FeS_2 = pyrite or marcasite; $Fe(II)CO_3$ = siderite; $Fe_3(Po_4)_2$ = ninanite; $MnCO_3$ = rhodochrosite

Source: Adapted from Berner [2]



Source: Adapted from Emerson [9]

FIGURE 2.10-16 Variation in Concentration with Depth for Various Redox Active Species in a Fjord

2.10.6 Estimation of Equilibrium Parameters for Redox Reactions

The preceding sections of this chapter have discussed methods for estimating:

- Relative concentrations of oxidized versus reduced forms of a species from p_e (or E_h) values;
- Relationship of p_e to E_h values and field measurements;
- Equilibrium constants from free energy data or redox half-reaction potentials; and
- p_e values from concentrations of other species, including dissolved oxygen and sulfide levels.

This section addresses the estimation of the equilibrium constant and the electrode potential for a half-reaction under limited conditions. The following are discussed:

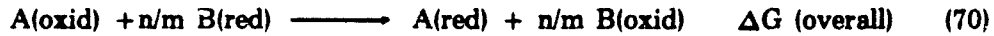
- Estimation of K for a redox reaction from E° values when no reactions after the redox reaction occur;
- Estimation of K for a redox reaction from E° and stability constants when a complex dissociation reaction occurs after redox; and
- Estimation of E° for a half-reaction of a complexed ion from that of an aquo ion and the complex stability constants.

ESTIMATION OF K FOR REDOX WHEN NO FURTHER REACTION TAKES PLACE

If the half-reaction potentials (or equilibrium constants or free energies) that together represent an overall redox reaction are known, the overall equilibrium constant for the reaction can be calculated as follows:



Taken together, equations 68 and 69 represent the overall reaction



where

$$\Delta G(\text{overall}) = \Delta G(A) - n/m \{ \Delta G(B) \} \quad (71)$$

This $\Delta G(\text{overall})$ is valid as long as A(red) and B(oxid) are the final products of the redox reaction (i.e., if no post-redox equilibria are involved).

If the data for equations 68 and 69 are given in terms of half-reaction potentials, the following expressions apply:

$$\Delta G(A) = -n F E(A) \quad (72)$$

$$\Delta G(B) = -m F E(B) \quad (73)$$

Thus,

$$\Delta G(\text{overall}) = -n F [E(A) - E(B)] = -n F E(\text{overall}) \quad (74)$$

where E(A) and E(B) are both expressed as reduction potentials.

The equilibrium constant at 25°C for reaction 70 is therefore related to the above parameters as follows:

$$\Delta G(\text{overall}) = -1.36 \log K(\text{overall}) \quad (75)$$

and

$$\Delta G(\text{overall}) = -n(23.06) E(\text{overall}) \quad (76)$$

where ΔG values are in kcal/mole and E values are in volts. The equilibrium constant at 25°C for reaction 70 is given by

$$\begin{aligned} \log K(\text{overall}) &= -\Delta G(\text{overall})/1.36 \\ &= +n(23.06/1.36) E(\text{overall}) \\ &= +n(16.96) E(\text{overall}) \end{aligned} \quad (77)$$

Example 7 Calculate the equilibrium constant for the reaction of copper(II) with bromide at 25°C according to the reaction.



The half-reactions that can represent the above reaction are



The overall E value is:

$$E(\text{overall}) = E(A) - E(B) = 0.167 - 1.066 = -0.899 \text{ V} \quad (81)$$

Using equation 77,

$$\begin{aligned} \log K(\text{overall}) &= n(16.96) E(\text{overall}) \\ &= (1)(16.96)(-0.899) \\ &= -15.25 \end{aligned}$$

Since the equilibrium constant is very small (6×10^{-16}), the reaction is highly unfavorable.

Example 8 Calculate the equilibrium constant for the reaction of tetraaquodiamminecobalt(III) ion with bromide, assuming no dissociation of the product cobalt(II) complex. (This is unrealistic, but it represents a useful hypothetical case for comparison with the more realistic Example 9.)

The reaction of interest is



The half reactions are



The overall E is

$$E(\text{overall}) = 1.22 - 1.066 = 0.154$$

Thus, according to equation 77, the equilibrium constant should be

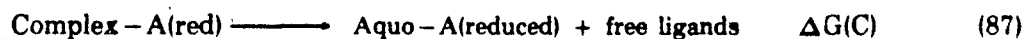
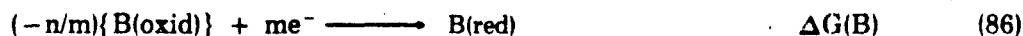
$$\begin{aligned} \log K(\text{overall}) &= +n (16.96) E(\text{overall}) \\ &= (1) (16.96) (0.154) \\ &= 2.61 \end{aligned}$$

The reaction is thus favorable, with an equilibrium constant of 4.07×10^2 .

ESTIMATION OF K FOR A REDOX REACTION WITH SUBSEQUENT REACTIONS

Many redox reactions, especially those between complexed metal ions, lead to products that can undergo subsequent dissociation or other reactions after the electron transfer. These subsequent processes can provide additional driving force for the overall reaction to occur (including the redox process).

To illustrate, we shall consider a case where the post-redox reaction is a dissociation of a labile metal complex:



Taken together, these equations represent the overall reaction



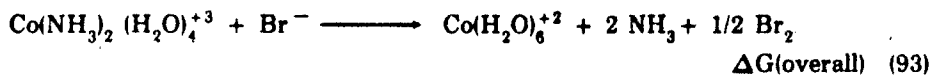
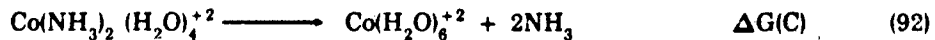
where

$$\Delta G(\text{overall}) = \Delta G(A) - n/m \{\Delta G(B)\} + \Delta G(C) \quad (89)$$

An important aspect of this follow-on reaction is that it can provide sufficient driving force for the overall reaction (equation 88) to proceed, even though the relative free energy changes for reactions 85 and 86 (or relative E° values) indicate that redox will not proceed substantially. The effect is illustrated in Example 9. When the stability constants for the oxidized metal are very large compared with those for the reduced metal, the effect can be much larger than in this example.

Example 9 Calculate the equilibrium constant for the redox reaction in Example 8 between the cobalt diammine aquo complex and bromide, including consideration of the dissociation of the cobalt(II) product into aquo cobalt(II) and NH_3 . (Assume that NH_3 does not undergo any further equilibria.)

The overall reaction is



where

$$\Delta G(\text{overall}) = \Delta G(A) - \Delta G(B) + \Delta G(C) \quad (94)$$

The value of $\Delta G(A)$ is calculated as follows, using equation 8:

$$\begin{aligned} \Delta G(A) &= -n F E(A) \\ &= -1 (23.06) (1.22) \\ &= -28.13 \text{ kcal/mole} \end{aligned}$$

Similarly, the value of $\Delta G(B)$ is:

$$\begin{aligned}\Delta G(B) &= - n F E(B) \\ &= - 1 (23.06) (1.066) \\ &= - 24.58 \text{ kcal/mole}\end{aligned}$$

The value of $\Delta G(C)$ is calculated as follows, using data obtained from Bjerrum[3] for β_2 , the stability constant for the diammine complex of cobalt(II):

$$\begin{aligned}\Delta G(C) &= - 1.36 \log K(C) \\ &= - 1.36 (1/\beta_2) \\ &= - 1.36 (1/3.62) \\ &= - 0.376 \text{ kcal/mole}\end{aligned}$$

Thus, with equation 94,

$$\begin{aligned}\Delta G(\text{overall}) &= - 28.13 + 24.58 + (-0.376) \\ &= - 3.93\end{aligned}$$

Therefore, with equation 77,

$$\begin{aligned}\log K(\text{overall}) &= - \Delta G(\text{overall})/1.36 \\ &= -(-3.93/1.36) \\ &= 2.89\end{aligned}$$

and

$$K(\text{overall}) = 7.76 \times 10^2$$

ESTIMATION OF E FOR THE HALF-REACTION OF A COMPLEXED ION

Values of the potential for a half reaction as shown for the following equation



can be calculated from the half-reaction potential for the aquo ions



according to the following equation [3]:

$$E_c = E(\text{complexed ion}) = - 0.059[\beta_n(y) - \beta_n(y-1)] + E_a \quad (97)$$

where

E_c = half-reaction potential for the complex ion

E_a = half-reaction potential for the aquo ion

$\beta_n(y)$ = stability constant for the complex ion with the overall charge on the complex of $+y$

$\beta_n(y-1)$ = stability constant for the complex ion with the overall charge on the complex of $y-1$.

The estimate of the half-reaction potential is obviously related to the accuracy of the stability constants used in the calculation.

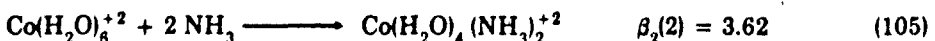
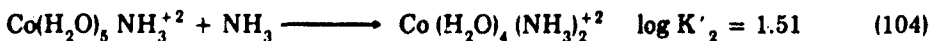
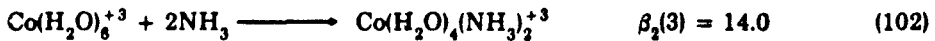
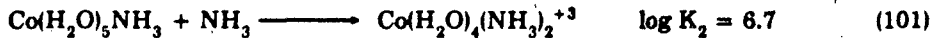
Example 10 Estimate the reduction potential of the following half reaction:



The reduction potential of the aquo ion of cobalt(III) is, according to Bjerrum[3]:



Next we obtain data for the equilibrium constants for the following reactions:



The following data are now used in equation 97:

$$\beta_n(y) = \beta_2(3) = 14.0$$

$$\beta_n(y-1) = \beta_2(2) = 3.62$$

$$E_a = 1.83 \text{ volts}$$

yielding

$$E_c(\text{cobalt}) = -0.059(14.0 - 3.62) + 1.83 \\ = 1.22 \text{ volts}$$

The value has not been experimentally determined [4].

2.10.7 Sources of Redox Data

Values of electrode potentials and equilibrium constants for redox reactions can be found in a variety of articles and compendia such as those given in References 12, 14, 18, and 19. Table 2.10-5 lists values of electrode potentials for a variety of species.

TABLE 2.10-5

Electrode Potentials of Redox Half Reactions^a

Oxidation — Reduction Reaction	$E^\circ(V)$
$\text{Ag}^{+2} + \text{e}^- \longrightarrow \text{Ag}^+$	+2.00
$\text{Ag}^{+2} + \text{e}^- \longrightarrow \text{Ag(s)}$	+0.799
$\text{Al}^{+3} + 3\text{e}^- \longrightarrow \text{Al(s)}$	-1.68
$\text{Am}^{+4} + \text{e}^- \longrightarrow \text{Am}^{+3}$	+2.40
$\text{H}_3\text{AsO}_4 + 2\text{H}^+ + 2\text{e}^- \longrightarrow \text{HAsO}_2 + \text{H}_2\text{O}$	+0.56
$\text{As(s)} + 3\text{H}^+ + 3\text{e}^- \longrightarrow \text{AsH}_3(\text{g})$	-0.61
$\text{BrO}_3^- + 3\text{H}_2\text{O} + 6\text{e}^- \longrightarrow \text{Br}^- + 6\text{OH}^-$	+0.61
$\frac{1}{2}\text{Br}_2(\text{aq}) + \text{e}^- \longrightarrow \text{Br}^-$	+1.08
$\text{Ce}^{+4} + \text{e}^- \longrightarrow \text{Ce}^{+3}$	+1.74
$\text{ClO}_3^- + 2\text{H}^+ + \text{e}^- \longrightarrow \text{ClO}_2(\text{g}) + \text{H}_2\text{O}$	+1.15
$\text{ClO}_2 + \text{e}^- \longrightarrow \text{ClO}_2^-$	+0.93
$\frac{1}{2}\text{Cl}_2(\text{aq}) + \text{e}^- \longrightarrow \text{Cl}^-$	+1.39
$\text{Co}^{+3} + \text{e}^- \longrightarrow \text{Co}^{+2}$	+1.95
$\text{HCrO}_4^- + 7\text{H}^+ + 3\text{e}^- \longrightarrow \text{Cr}^{+3} + 4\text{H}_2\text{O}$	+1.20
$\text{Cr}^{+3} + \text{e}^- \longrightarrow \text{Cr}^{+2}$	-0.41
$\text{Cu}^{+3} + \text{e}^- \longrightarrow \text{Cu}^{+2}$	+2.3
$\text{Cu}^{+2} + \text{e}^- \longrightarrow \text{Cu}^+$	+0.17
$\text{Cu}^+ + \text{e}^- \longrightarrow \text{Cu(s)}$	-0.52
$\frac{1}{2}\text{F}_2(\text{g}) + \text{e}^- \longrightarrow \text{F}^-$	+2.87
$\text{Fe}^{+3} + \text{e}^- \longrightarrow \text{Fe}^{+2}$	+0.771
$2\text{Hg}^{+2} + 2\text{e}^- \longrightarrow \text{Hg}_2^{+2}$	+0.907
$\text{Hg}_2^{+2} + 2\text{e}^- \longrightarrow 2\text{Hg(l)}$	+0.792
$\frac{1}{2}\text{I}_2(\text{aq}) + \text{e}^- \longrightarrow \text{I}^-$	+0.621
$\text{I}_3^- + 2\text{e}^- \longrightarrow 3\text{I}^-$	+0.536
$\text{MnO}_4^- + \text{e}^- \longrightarrow \text{MnO}_4^{-2}$	+0.57

(Continued)

TABLE 2.10-5
Electrode Potentials of Redox Half Reactions

Oxidation — Reduction Reaction	$E^\circ(V)$
$\text{MnO}_4^- + 4\text{H}^+ + 3\text{e}^- \longrightarrow \text{MnO}_2(\text{s}) + 2\text{H}_2\text{O}$	+1.68
$\text{MnO}_2(\text{s}) + 4\text{H}^+ + 2\text{e}^- \longrightarrow \text{Mn}^{+2} + 2\text{H}_2\text{O}$	+1.23
$\text{Mn}^{+3} + \text{e}^- \longrightarrow \text{Mn}^{+2}$	+1.488
$\text{Mn}^{+2} + 2\text{e}^- \longrightarrow \text{Mn}(\text{s})$	-1.17
$\text{Mo(VI)} + \text{e}^- \longrightarrow \text{Mo(V)}$	+0.53
$\text{NO}_3^- + 3\text{H}^+ + 2\text{e}^- \longrightarrow \text{HNO}_2 + \text{H}_2\text{O}$	+0.94
$\text{Ni}^{+2} + 2\text{e}^- \longrightarrow \text{Ni}(\text{s})$	-0.25
$\text{O}_2(\text{g}) + 4\text{H}^+ + 4\text{e}^- \longrightarrow 2\text{H}_2\text{O}$	+1.229
$\text{O}_2(\text{g}) + 2\text{H}^+ + 2\text{e}^- \longrightarrow \text{H}_2\text{O}_2$	+0.69
$\text{H}_3\text{PO}_3 + 2\text{H}^+ + 2\text{e}^- \longrightarrow \text{H}_3\text{PO}_2 + \text{H}_2\text{O}$	-0.50
$\text{Pb(IV)} + 2\text{e}^- \longrightarrow \text{Pb}^{+2}$	+1.655
$\text{Pb}^{+2} + 2\text{e}^- \longrightarrow \text{Pb}(\text{s})$	-0.126
$\text{Pu}^{+4} + \text{e}^- \longrightarrow \text{Pu}^{+3}$	+0.967
$\text{Ru}^{+3} + \text{e}^- \longrightarrow \text{Ru}^{+2}$	+0.249
$\text{SO}_4^{-2} + 4\text{H}^+ + 2\text{e}^- \longrightarrow \text{H}_2\text{SO}_3 + \text{H}_2\text{O}$	+0.17
$\text{S}(\text{s}) + 2\text{H}^+ + 2\text{e}^- \longrightarrow \text{H}_2\text{S}$	+0.141
$\text{S}(\text{s, Rhombic}) + 2\text{e}^- \longrightarrow \text{S}^{-2}$	-0.48
$2\text{S}(\text{s}) + 2\text{e}^- \longrightarrow \text{S}_2^{-2}$	-0.49
$3\text{S}(\text{s}) + 2\text{e}^- \longrightarrow \text{S}_3^{-2}$	-0.45
$4\text{S}(\text{s}) + 2\text{e}^- \longrightarrow \text{S}_4^{-2}$	-0.36
$5\text{S}(\text{s}) + 2\text{e}^- \longrightarrow \text{S}_5^{-2}$	-0.34
$6\text{S}(\text{s}) + 2\text{e}^- \longrightarrow \text{S}_6^{-2}$	-0.36
$\text{Sb(V)} + 2\text{e}^- \longrightarrow \text{Sb(III)}$	+0.75
$\text{SeO}_4^{-2} + 4\text{H}^+ + 2\text{e}^- \longrightarrow \text{H}_2\text{SeO}_3 + \text{H}_2\text{O}$	+1.15
$\text{H}_2\text{SeO}_3 + 4\text{H}^+ + 4\text{e}^- \longrightarrow \text{Se}(\text{s}) + 3\text{H}_2\text{O}$	+0.74
$\text{Se}(\text{s}) + 2\text{H}^+ + 2\text{e}^- \longrightarrow \text{H}_2\text{Se}(\text{g})$	-0.37
$\text{Sn(IV)} + 2\text{e}^- \longrightarrow \text{Sn(II)}$	+0.144
$\text{Tl(IV)} + \text{e}^- \longrightarrow \text{Tl(III)}$	+0.130
$\text{Tl}^{+3} + 2\text{e}^- \longrightarrow \text{Tl}^+$	+1.26
$\text{U}^{+4} + \text{e}^- \longrightarrow \text{U}^{+3}$	-0.609
$\text{VO}_2^+ + 2\text{H}^+ + \text{e}^- \longrightarrow \text{V}^{+3} + \text{H}_2\text{O}$	+0.34

a. Gaseous concentrations are in atmospheres.

Source: Kotrlý and Šúcha [12]

2.10.8 Literature Cited

1. Berner, R.A., "Electrode Studies of Hydrogen Sulfide in Marine Sediments," *Geochim. Cosmochim. Acta*, 27, 563-75 (1963).
2. Berner, R.A., "A New Geochemical Classification of Sedimentary Environments," *J. Sediment. Petrol.*, 51, 359 (1981).
3. Bjerrum, J., *Metal-Ammine Formation in Aqueous Solution*, P. Haase and Son, Copenhagen, 241 (1941).
4. Bodek, I., "Reactions of *cis*-Tetraaquodiamminecobalt(III) Ion in Aqueous Perchlorate Media," Ph.D. Thesis, Northeastern University (1976).
5. Cannon, R.D. and J. Gardiner, "A Binuclear Intermediate Preceding the Cobalt(III)-Iron(II) Electron Transfer Process," *J. Am. Chem. Soc.*, 92, 3800 (1970).
6. Carver, R.E., *Procedures in Sedimentary Petrology*, Wiley-Interscience, New York (1971).
7. Cherry, J.A., A.U. Shaikh, D.E. Tallman and R.V. Nicholson, "Arsenic Species as an Indicator of Redox Conditions in Groundwater," *J. Hydrol. (Amsterdam)*, 43, 373 (1979).
8. Cloke, P.L., "The Geochemical Application of Eh-pH Diagrams," *J. Geol. Educ.*, 14, 140-48 (1966).
9. Emerson, S., R.E. Cranston and P.S. Liss, "Redox Species in a Reducing Fjord: Equilibrium and Kinetic Considerations," *Deep-Sea Res.*, 26A, 859-78 (1979).
10. Garrels, R.M. and C.L. Christ, *Solutions, Minerals and Equilibria*, Freeman, Cooper & Co., San Francisco (1965).
11. Hem, J.D., "Reactions of Metal Ions at Surfaces of Hydrous Ion Oxides," *Geochim. Cosmochim. Acta*, 41, 527-38 (1977), as cited by Emerson [9].
12. Kotrlý, S. and L. Šúcha, *Handbook of Chemical Equilibria in Analytical Chemistry*, John Wiley & Sons, New York (1985).
13. Langmuir, D., "Eh-pH Determinations," Chapter 26 in Carver [6].
14. Latimer, W.M., *Oxidation Potentials*, 2nd ed., Prentice-Hall, New York (1952).
15. Lindberg, R.D. and D.D. Runnels, "Groundwater Redox Reactions: An Analysis of Equilibrium State Applied to Eh Measurements and Geochemical Modeling," *Science*, 225, 925 (1984).
16. Plummer, L.N., B.F. Jones and A.H. Truesdell, "WATEQF — A Fortran IV Version of WATEQ — A Computer Program for Calculating Chemical Equilibrium of Natural Waters," *Water-Resour. Invest. (U.S. Geol. Surv.)*, 76-13, 60 (rev. and reprinted January 1984).
17. Pourbaix, M., *Atlas of Electrochemical Equilibria in Aqueous Solutions*, Pergamon Press, Oxford, England (1966).
18. Sillén, L.G. and A.E. Martell, *Stability Constants of Metal-Ion Complexes*, Special Publication No. 17, The Chemical Society, London (1964).
19. Sillén, L.G. and A.E. Martell, *Stability Constants of Metal-Ion Complexes — Supplement No. 1*, Special Publication No. 25, The Chemical Society, London, 64 (1971).

20. Stumm, W., "Redox Potentials as an Environmental Parameter: Conceptual Significance and Operational Limitations," *Adv. Water Pollut. Res., Proc. Int. Conf. 3rd, 1966 (Munich)*, 1, 283 (1967).
21. Truesdell, A.H., "The Advantage of Using pE Rather than Eh in Redox Calculations," *J. Geol. Educ.*, 16, 17-20 (1968).
22. Whitfield, M., "Thermodynamic Limitations on the Use of the Platinum Electrode in Eh Measurements," *Limnol. Oceanogr.*, 19, 857 (1974).
23. Wilkins, R.G., *The Study of Kinetics and Mechanism of Reactions of the Transition Metal Complexes*, Allyn and Bacon, Boston (1974).

2.11 SOLUBILITY AND PRECIPITATION EQUILIBRIA

2.11.1 Introduction

In studies of environmental water quality, the question often arises as to whether a given solid is likely to dissolve and, if so, how much. Likewise, investigators often want to know if a solid phase can precipitate from a water of given composition and what the chemical consequences would be. Such questions can often be resolved through consideration of the chemical equilibria between solids and aqueous solutions.

On a macroscopic scale of observation, a solution saturated with respect to a substance neither dissolves more of the substance nor precipitates it. Put in different terms, the solution contains dissolved species in a state of thermodynamic equilibrium with the solid phase — or, at least, with some of the components of that phase. Departures from equilibrium may occur either in a direction of supersaturation or of undersaturation. Such departures may be caused by changes in the environmental characteristics of the system, as well as by a variety of internal chemical processes. When precipitation occurs in a supersaturated solution, the solution is brought towards saturation or equilibrium "from above." In contrast, dissolution may occur in an undersaturated solution that comes in contact with a particular solid phase, bringing the solute concentration towards saturation "from below." Thus, the state of a chemical thermodynamic equilibrium between a solid and an aqueous solution indicates two environmentally important quantities:

- (1) The current state of the water, with respect to its ability either to dissolve or precipitate certain solids, and
- (2) The expected limits of change in concentrations of dissolved substances, if certain solid phases were to dissolve in, or precipitate from, the water.

This chapter addresses chemical equilibria between inorganic solids and aqueous solutions. Although it is practically impossible to find an inorganic solid whose solubility in water is truly zero, not every class of inorganic solids coming in contact with waters in the environment can be considered in this chapter. Excluded from the discussion of the solid-solution equilibria are pure metals, alloys, glasses, and other industrial solids of complex composition whose chemical behavior in the environmental context usually falls outside the field of the solid-solution equilibria. The focus is on substances that can be broadly classified as ionic or partially ionic solids, such as metal oxides, hydroxides, halides, sulfides, and other compounds with anions in oxidized states (sulfates, carbonates, arsenates, selenites, selenates, and a number of silicate and aluminosilicate minerals).

The environmental importance of the classes of compounds listed above is twofold: (1) for some substances, dissolution in natural waters may never reach saturation, although they will constitute a lasting environmental load on the water systems; and (2) for others, their metallic and anionic components may enter solution from different sources to create a condition of supersaturation with respect to solids that may

eventually precipitate. The examples in this chapter deal primarily with solid-solution equilibria involving heavy-metal ions,¹ alkali metal ions, and alkaline earth ions among the cationic components of the solids.

This chapter also addresses the following issues:

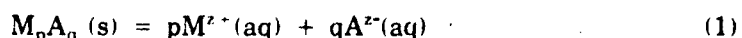
- Definitions of the solubility product, K_{sp} , and the equilibrium constant, K ;
- Establishment of either undersaturated, saturated, or supersaturated conditions by the criteria of ion-concentration product and ion-activity product;
- Effects of temperature and pressure on solubility;
- Effects of ionic strength, pH, and complexation on solubility;
- Effects of particle size on solubility; and
- Estimation of the solubility values (K_{sp} or K) from the free energy of formation, and from empirical correlations between solubilities and such crystal properties as electronegativities of the ions in the lattice, lattice energy, ionization potentials, and interfacial energies of solids.

The process of adsorption at solid-liquid interfaces is discussed in Section 2.12 (Attenuation on Soils). Other important solid precipitation processes (e.g., co-precipitation) and dissolution of impure phases (e.g., trace element leaching) are not easily described mathematically and thus their discussion has been left to books and articles which focus on them.

2.11.2 Description of Property

SOLUBILITY PRODUCT (K_{sp})

A solid made of a metal ion (M) and an anionic ligand (A) dissolves in solution and dissociates according to an overall reaction that can be written as



where (s) denotes a solid phase, (aq) denotes an aqueous species, p and q are stoichiometric coefficients, and z^+ and z^- are the positive and negative valence electrical charges. The principle of electrical neutrality of the ions in solution requires a charge balance between the positively and negatively charged species:

$$pz^+ + qz^- = 0$$

1. Heavy metals are those with atomic numbers between 21 (scandium) and 92 (uranium). Within this series, the transition elements, such as As and Se, and the heavy halogens (atomic numbers 33-36, 52-54, 85-86) are not heavy metals. Aluminum (atomic number 13), although not a heavy metal in the physical sense, is included in many environmental chemical studies of the heavy metals in water, probably because its low abundance and potential toxicity are similar to those of the trace heavy-metals.

2.10 ELECTRON TRANSFER REACTIONS

2.10.1 Introduction

This section deals with electron transfer (redox) reactions, primarily homogeneous reactions in aqueous systems. It explains some of the parameters and graphical techniques used to represent redox equilibria and summarizes important environmental redox couples. Typical values of the redox status of various environmental waters are given in terms of parameters such as Eh and pe. Limitations on the use of experimentally determined Eh values in relation to the redox status of the solution are discussed. Finally, methods are described for calculating redox equilibria under various reaction conditions and for estimating the redox half-potential for a complexed species.

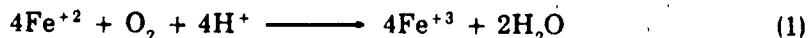
2.10.2 Environmental Importance

Many inorganic species of environmental concern can undergo electron transfer or redox reactions with species that are present naturally or as pollutants in environmental systems. The product of an electron transfer reaction is typically the reacting species in a modified oxidation state, but it can also be a product of the reaction of water (often very rapid) with the modified oxidation state species. This product species in the modified oxidation state differs greatly from the original reactant species in terms of chemical behavior. Thus, homogeneous (e.g., acid/base dissociation, complexation) and heterogeneous (e.g., solubility, attenuation) reactivity properties are modified; the result of a redox reaction is a species that differs in environmental mobility and impact from the original species.

Like other reactions, such as acidic or basic dissociation and complexation, redox reactions are fundamental to determining speciation in solution. Figure 2.10-1 summarizes the chemical identity and valence states of elements that are capable of undergoing redox reactions in the environment.

2.10.3 Mechanisms of Redox Reactions

An oxidation-reduction reaction involves a transfer of electrons between two species — the oxidizing agent (oxidant) and the reducing agent (reductant). In this transfer, the oxidant gains electrons and the reductant loses them. For example, in the reaction



the Fe(II) is oxidized to Fe(III) by loss of electrons, and the O₂ is reduced to the -2 oxidation state by gaining electrons to form H₂O. (In aqueous systems, hydronium or hydroxide ions or water may be used to balance redox reactions.) Electrons are not shown in equation 1, since free electrons usually do not exist in aqueous solution; electron transfer occurs by direct interaction of the reactants (see below) or other intermediate chemical species.

The initial reaction products are the oxidized form of the reducing agent and the reduced form of the oxidizing agent. In aqueous solution, these initial products can

1	+1
H	-1

6	+2	7	+1	8	-1
C	+4	N	+2	O	-2
-4		+3		+5	
		+4		-1	
		+5		-2	
		-1		-3	
		-2			
		-3			

14	+2	15	+3	16	+4	17	+1
Si	+4	P	+5	S	+6	Cl	+5
-4		-3		-2		+7	
						-1	

22	+2	23	+2	24	+2	25	+2	26	+2	27	+2	28	+2	29	+1	32	+2	33	+3	34	+4	35	+1	
Tl	+3	V	+3	Cr	+3	Mn	+3	Fe	+3	Co	+3	Ni	+3	Cu	+2	Ge	+4	As	+5	Se	+6	Br	+5	
+4		+4		+6		+4		+7		+3		+3		+2		+4		-3		-2		-1		
+5		+5		+7		+7																		

41	+3	43	+4	46	+2	50	+2	51	+3	52	+4	53	+1
Nb	+5	Tc	+6	Pd	+4	Sn	+4	Sb	+5	Te	+6	I	+5
+5		+6		+4		+4		+5		+6		+7	
+7								-3		-2		-1	

75	+4	78	+3	77	+3	78	+2	79	+1	80	+1	81	+1	82	+2	83	+3	84	+2
Re	+6	Os	+4	Ir	+4	Pt	+4	Au	+3	Hg	+2	Tl	+3	Pb	+4	Bi	+5	Po	+4
+7																			

Lanthanides	58	+3	62	+2	63	+2	70	+2
	Ce	+4	Sm	+3	Eu	+3	Yb	+3

Actinides	91	+5	92	+3	93	+3	94	+3	95	+3	97	+3	101	+2	102	+2
	Pa	+4	U	+4	Np	+4	Pu	+4	Am	+4	Bk	+4	Md	+3	No	+3
		+5		+5		+5		+5		+5		+6				
		+6		+6		+6		+6		+6						

Key to Figure

Atomic Number = 50 +2
Symbol = Sn +4 Oxidation States

Elemental state has been omitted for simplification
but is available for all elements.

FIGURE 2.10-1 Summary of Elements That Can Undergo Redox Reactions
And Their Valence States

then undergo further reactions. The latter include acid-base equilibria and dissociation of complexes with subsequent substitution of coordinated ligands by water.

The mechanism by which a redox reaction occurs is important, since it can determine the nature of the products as well as the rate of the reaction. There are two kinds of homogeneous electron transfer reactions: outer sphere and inner sphere. The reaction between Fe(III) and V(II) shown in Figure 2.10-2 is an example of an outer-sphere redox reaction [23]. In such reactions, the bonds in the primary or inner coordination sphere¹ remain intact during the transition through species I and II. (The species separated by commas are ion pairs.) The initial products of this reaction have oxidation states different from those of the reactants but have the same primary coordination spheres as the reactants. These coordination spheres may, however, be modified by subsequent rapid reactions with the aqueous environment, such as acid/base equilibria or ligand exchange.

In an inner-sphere reaction, the two reacting species are coordinated to a common "bridging" ligand in the transition state (species III and IV in Figure 2.10-3). The illustrated reaction between Fe(II) and Co(NH₃)₅NTA is an example of an inner-sphere redox reaction with NTA as the bridging ligand [5]. Electron transfer occurs in the bridged intermediate (species III). This kind of redox reaction may involve transfer of the bridging ligand from one metal center to the other, yielding a product that differs not only in oxidation state but also in composition of the primary coordination sphere. Figure 2.10-4, for example, shows an inner-sphere redox reaction between [Co(NH₃)₅Cl]⁺² and Cr⁺², in which the Cl ligand is transferred from the Co(III) metal center to the product Cr(III) center because of the kinetically inert nature of the Cr(III) and the kinetically labile nature of the Co(II) products.

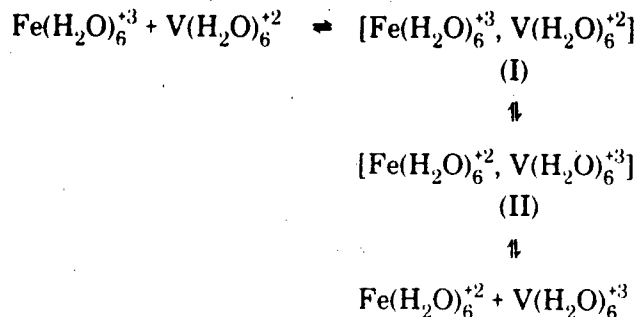


FIGURE 2.10-2 Sample Redox Mechanism: Outer-Sphere Electron Transfer Reaction Between Fe⁺³ and V⁺²

When both products of electron transfer are kinetically labile (see section 3.2), the initial products of the electron transfer reaction will rapidly equilibrate with the aqueous environment (via ligand exchange) and form predominantly aquo complexes as well as hydroxo and other complexes resulting from acid-base equilibria. As shown in Figure 2.10-3, the product Fe(III) and Co(II) centers generated in the inner-sphere intermediate (species IV) are labile and thus exchange the ammonia and NTA ligands

1. See §2.9.2 for definition.

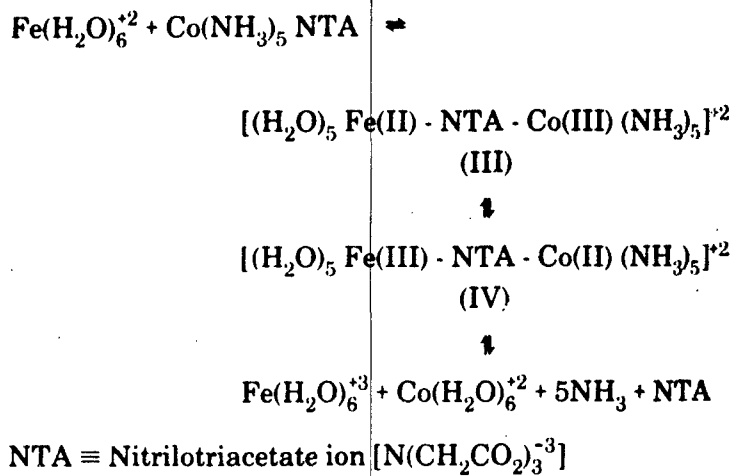


FIGURE 2.10-3 Sample Redox Mechanism: Inner-Sphere Electron Transfer Reaction Between Fe^{+2} and $\text{Co}(\text{NH}_3)_5\text{NTA}$
 (Gain or loss of free water is not shown.)

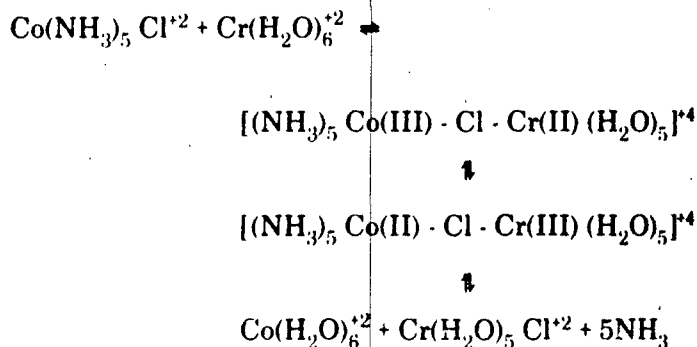


FIGURE 2.10-4 Sample Redox Mechanism: Inner-Sphere Electron Transfer Reaction Between Cr^{+2} and $\text{Co}(\text{NH}_3)_5\text{Cl}^{+2}$
(Gain or loss of free water is not shown.)

rapidly to form aquo complexes. In Figure 2.10-4, the product Cr(III) center is inert and retains the Cl ligand, while the Co(II) center is labile and exchanges the ammonia and chloride ligands rapidly to form aquo complexes.

It is therefore necessary to distinguish between inner- and outer-sphere redox processes if one wishes to determine the rate of a reaction (see section 3.3). In addition, one must also have information about the inert or labile character of the reactant and product metal or other element centers involved (see section 3.3) and the time frame of interest to determine the final products of the reaction.

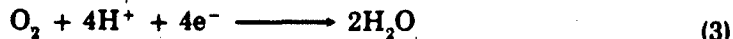
In a predominantly aqueous environment, and when the redox reaction of concern is between entirely aquated species (i.e., aquo ions), an inner-sphere redox reaction with a water-bridged intermediate that produces one inert and one labile product would cause the products to have essentially the same primary coordination spheres as those of the reactants. It would not matter if the reactants or products were kinetically labile or inert. If a water molecule were exchanged between the reactants, it would be noticed only if it were labeled (e.g., with isotopically labeled oxygen). However, an inner-sphere redox reaction leading to reaction products with inert centers may produce a bridged species similar to IV in Figure 2.10-3.

In environmental systems, electron transfer occurs only between species that are capable of donating and accepting one or more electrons. In contrast to H^+ , which can exist in finite concentrations in aqueous systems (as expressed by the pH value), the aqueous electron is not detectable under typical environmental conditions. Thus, an oxidizing agent that is added to a solution reacts directly with a reducing agent rather than with an aqueous electron. The concept of p_e , which is equal to $-\log(e^-)$, where (e^-) is the electron activity, is very useful for calculating equilibrium conditions and simplifies treatment of redox reactions in a manner analogous to that of pH [21]; nevertheless, this concept should not be interpreted as representing the mechanism of electron transfer, except in the presence of electrodes.

2.10.4 Mathematical Representation of Redox Equilibria

EQUILIBRIUM CONSTANT, FREE ENERGIES, ELECTRODE POTENTIAL AND ELECTRON ACTIVITY

The overall electron transfer reaction typified by equation 1 can be thought of as two coupled half-reactions, representing reduction and oxidation, respectively. The half-reactions for equation 1 would be as follows:



Either of these equations can be considered a "redox buffer" (analogous to a pH buffer): the activity of the electron (e^-) affects the distribution between the oxidized and reduced state, just as the activity of H^+ affects the distribution between the dissociated and undissociated forms of an acid.

Hypothetical equilibrium constants can be assigned to each half-reaction. For an oxidation reaction, the equilibrium expression would be

$$K_{red, oxid} = [oxid][e^-]/[red] \quad (4)$$

Thus, the equilibrium constant for equation 2 would be

$$K_{Fe^{+2}, Fe^{+3}} = [Fe^{+3}][e^-]/[Fe^{+2}] \quad (5a)$$

Similarly, for the reduction half-reaction (equation 3),

$$K_{O_2, H_2, 0} = 1/[pO_2][H^+]^4[e^-]^4 \quad (5b)$$

These equilibrium constants are related to the free energy change of the reaction according to

$$\log K = -\Delta G^0/2.303 R T \quad (6)$$

where R = gas constant (1.986 cal/deg-mole)

T = absolute temperature (K)

ΔG^0 = free energy change (kcal/mole)

At 25°C, this relationship is

$$\Delta G^0 = -1.364 \log K \quad (7)$$

Each half-reaction can be described by a half-cell potential, E^0 , referenced to the hydrogen electrode. The half-cell potential is related to the free energy change according to

$$\Delta G^0 = -n F E^0 = -n(23.06) E^0 \quad (8)$$

where n = number of electrons transferred

F = Faraday constant (23.06 kcal/V-mole-equiv)

ΔG^0 = free energy change (kcal/mole)

E^0 = half-cell potential (V)

(Note that equation 8 is written based on the American sign convention for E^0 values which gives a positive sign to any complete reaction which goes spontaneously as written [10].)

Equations 7 and 8 allow calculation of K , ΔG^0 , or E^0 if one of these is known. Since ΔG^0 values are a function of temperature, the value of E^0 varies with temperature. This is discussed in greater detail in Section 2.11. If p_e is defined as $-\log [e^-]$, equation 4 can be written in the form

$$\begin{aligned} \log K_{red, oxid} &= \log [oxid]/[red] + \log [e^-] \\ &= \log [oxid]/[red] - p_e \end{aligned} \quad (9)$$

This relationship allows determination of the equilibrium concentrations (or ratio) of the oxidized and reduced forms of the redox couple at a given p_e value (similar to pH governing the ratio of protonated and unprotonated forms in a buffer).

Example 1 What is the relationship between pe and the ratio of oxidized and reduced forms of dissolved iron(II) and iron(III)?

For equation 2 (using equation 9),

$$\log K_{\text{Fe}^{+2}, \text{Fe}^{+3}} = \log [\text{Fe}^{+3}/[\text{Fe}^{+2}] - \text{pe} \quad (10)$$

From equations 7 and 8, with $n=1$

$$\log K_{\text{Fe}^{+2}, \text{Fe}^{+3}} = 16.91 E_{\text{Fe}^{+3}/\text{Fe}^{+2}} \quad (11)$$

Using a value of -0.771V for the half-cell potential, E^0 (see §2.10.7), we obtain

$$\log K_{\text{Fe}^{+2}, \text{Fe}^{+3}} = 16.95 (-0.771) = -13.07 \quad (12)$$

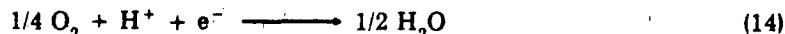
Whence from equation 10,

$$\text{pe} = 13.07 + \log [\text{Fe}^{+3}/[\text{Fe}^{+2}] \quad (13)$$

A plot of equation 13 is shown in Figure 2.10-5. Figure 2.10-6 is a plot of similar equations for arsenic(III)/arsenic(V) ratio at three pH values.

When a redox half-reaction contains H^+ or OH^- as reactants or products, the pe depends on pH. The mathematical dependence of pe on pH is a function of the reaction and of the form of the equilibrium constant. Similarly, if either a reactant or product is a gas, the pe is a function of the partial pressure of the gas. These variables are illustrated in Example 2 below. It is important to use the equilibrium constant that corresponds to the equation as written (i.e., with the same coefficients of the reactants) in the original source of the measurement. This applies to reactions where pure phases (e.g., H_2O) or gases are products or reactants. For such reactions, the values of the equilibrium constants depend on the coefficients.

Example 2 What is the dependence of pe on the pH and partial pressure of oxygen for the reduction of oxygen to water according to the following reaction?



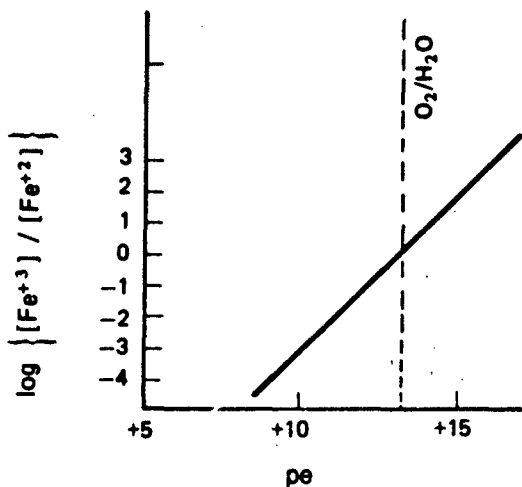
Using the convention that $[\text{H}_2\text{O}]$ is a constant, we can write the equilibrium expression for this half-reaction as

$$K_{\text{O}_2, \text{H}_2\text{O}} = \frac{1}{[\text{pO}_2]^{1/4} [\text{H}^+] [\text{e}^-]} \quad (15)$$

In terms of logarithms,

$$\log K_{\text{O}_2, \text{H}_2\text{O}} = \log 1 - 1/4 \log [\text{pO}_2] - \log [\text{H}^+] - \log [\text{e}^-] \quad (16)$$

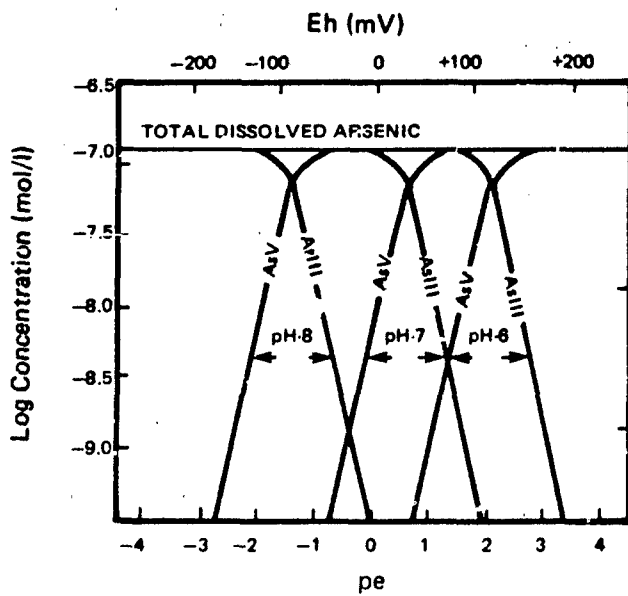
$$= -1/4 \log [\text{pO}_2] + \text{pH} + \text{pe} \quad (17)$$



Dashed line indicates position of oxygen/water couple at pH 7.5.

Source: Equation 13

FIGURE 2.10-5 Theoretical Distribution of Iron(II) and Iron(III) at Various pe Values



Source: Adapted from Cherry [7]. (Copyright 1979, New Zealand Hydrological Society. Reproduced with permission.)

FIGURE 2.10-6 Variation in Concentrations of Arsenic(III) and Arsenic(V) with pe at pH values of 6, 7 and 8. (Derived from $\text{pH} + (\frac{2}{3})\text{pe} = 6.6$ for the $\text{AsO}_4^{3-}/\text{HAsO}_4^{2-}$ Half Reaction)

The E^0 for the water/oxygen couple is 1.229 V (see §2.10.7). Since equation 14 involves one electron, $n=1$. Using these values, equations 7 and 8 yield

$$\log K_{O_2, H_2O} = 16.95(1.229) = 20.83 \quad (18)$$

Hence, equation 17 becomes

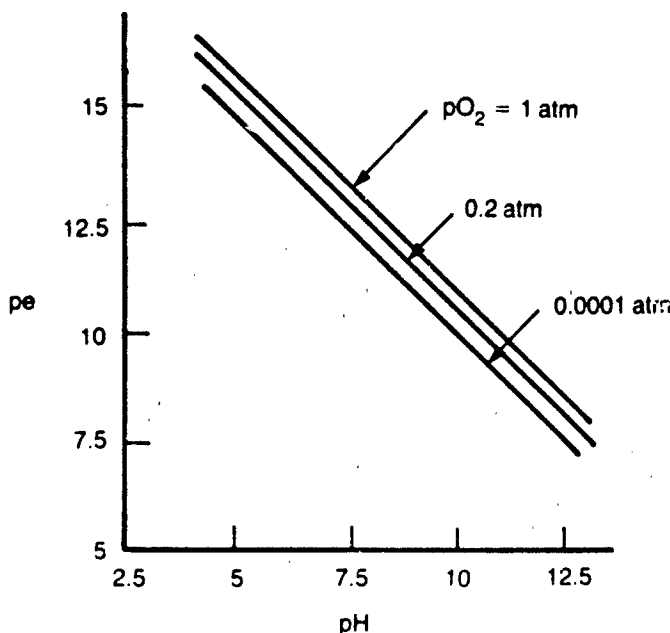
$$pe + pH = 20.83 + 1/4 \log[pO_2] \quad (19)$$

A plot of pe vs pH at various partial pressures of oxygen is shown in Figure 2.10-7.

Note that if equation 14 had been written



a different value of the equilibrium constant (four times as large) would have been used. The result would have been equivalent to equation 19 but multiplied by 4 throughout.



Source: Equation 19

FIGURE 2.10-7 pe Versus pH Diagram for the Oxygen/Water Half Reaction at Various Partial Pressures of Oxygen

The relationships described above can be used to calculate the concentration ratios between oxidized and reduced forms that would be expected under equilibrium conditions, given particular values of p_e and the other parameters. Values of p_e can be obtained experimentally, although they are subject to uncertainties and limitations (see § 2.10.5). In some cases, these values are fairly representative of redox conditions. One experimental method of determining p_e is to measure potentials with a platinum sensing electrode, using the following relationship:

$$E(Pt) = E_{Pt}^0 - B \log[e^-] = E_{Pt}^0 + B p_e \quad (20)$$

where

$E(Pt)$ = potential measured using a platinum electrode
(equal to E_h)

E_{Pt}^0 = zero by convention, so that $E_h = B p_e$

$B = 2.3RT/nF$ (0.0592 V if $n = 1$ at 25°C)

The value of $E(Pt)$ is also referred to as the value of E_h in the literature. Alternatively, we can use the following equation:

$$E_h = E^0(\text{redox couple}) + \frac{2.3 RT}{nF} \log \frac{[\text{oxid}]}{[\text{red}]} \quad (21)$$

Values of E_h are more often used when experimental data are obtained whereas p_e is convenient to use when equilibrium constant data are available and calculations are made from them. The range of E_h values in aqueous systems is approximately from -0.8 to +1.2 V (§ 2.10.5). The values of p_e are related to the values of equilibrium constants and can vary greatly.

Example 3 What is the predicted distribution between reduced and oxidized dissolved iron at an E^0 of 0.900 V (measured with a platinum electrode and a calomel reference electrode)?

Substituting $E(Pt) = 0.900\text{V}$ and $B = 0.0592$ in equation 20,

$$\begin{aligned} 0.900 &= 0.0592 p_e \\ p_e &= 15.21 \end{aligned} \quad (22)$$

From equation 13 (or Figure 2.10-5),

$$15.21 = 13.07 + \log [\text{Fe}^{+3}]/[\text{Fe}^{+2}] \quad (23)$$

Therefore,

$$\log [\text{Fe}^{+3}]/[\text{Fe}^{+2}] = 2.14$$

or

$$[\text{Fe}^{+3}]/[\text{Fe}^{+2}] = 138$$

Example 4 What is the pe of water in equilibrium with the atmosphere at pH 7?

The partial pressure of oxygen in the atmosphere is 0.21 atm. From equation 19,

$$\begin{aligned} \text{pe} &= 1/4 \log [\text{pO}_2] - \text{pH} + 20.83 \\ &= 1/4 (\log 0.21) - 7 + 20.83 \\ &= -0.17 - 7 + 20.83 \\ &= 13.66 \end{aligned} \quad (24)$$

Example 5 Calculate the expected equilibrium pe of water at pH 7.4 containing Cr(III) at 0.5 nmol/l and Cr(VI) at 0.3 nmol/l, using the ratio of the chromium species concentrations.

We first identify the species of Cr(III) and Cr(VI) that are expected to be present at pH 7.4. Using the acid dissociation constants for the aquo ions (see §7.6.2), we calculate that the dominant species are expected to be Cr(OH)_2^+ and CrO_4^{2-} . The redox reaction of concern is therefore,



Equation 25 yields the following expressions for the equilibrium constant as a function of pe and pH:

$$K = \frac{[\text{Cr(OH)}_2^+]}{[\text{CrO}_4^{2-}] [\text{H}^+]^6 [\text{e}^-]^3} \quad (26)$$

or

$$\log K = \log \{[\text{Cr(OH)}_2^+]/[\text{CrO}_4^{2-}]\} + 6 \text{pH} + 3 \text{pe} \quad (27)$$

The following values are now substituted in equation 27:

$$\begin{aligned} \log K &= 66.1 [11] \\ \text{pH} &= 7.4 \\ [\text{Cr(OH)}_2^+] &= 0.5 \text{ nmol/l} \\ [\text{CrO}_4^{2-}] &= 0.3 \text{ nmol/l} \end{aligned}$$

$$\begin{aligned} 66.1 &= \log (0.5/0.3) + 6(7.4) + 3 \text{pe} \\ \text{pe} &= 7.16 \end{aligned}$$

The parameters K, ΔG° , E° and their relationships are applicable to the overall redox reaction



but pe is a parameter useful only in the half reactions and not for the overall reaction. Further discussions of these parameters are given in references 10 and 12.

STABILITY FIELD DIAGRAMS

Stability field diagrams are another useful method for presenting results of calculations of redox reactions under equilibrium conditions. These diagrams, which include plots of Eh (or pe) against pH for the most thermodynamically stable species, show equilibrium conditions and important chemical reactions that may dominate the behavior of an element under environmental conditions. Diagrams and procedures for their preparation have been described by several authors [8,10,11,17]. When using these diagrams to decide whether a particular phase or species is present, one should remember that they reflect the following assumptions:

- Thermodynamic equilibrium applies (i.e., kinetic limitations do not exist),
- The system is completely described (i.e., all applicable reactions are included),
- All solids are at unit activity and the activity coefficients of dissolved species are each one,
- The concentration of every dissolved species is assumed to be $10^{-6}M$ in all calculations.

For fast reactions and the existence of equilibrium, little error is introduced by using the diagrams, provided all the possible reactions have been considered. Where conditions of ionic strength are such that unit activities are not expected, the possible impact of this variation should be taken into account.

To familiarize the reader with stability field diagrams, the preparation of an Eh-pH diagram for the iron-water system is illustrated below.

Example 8 Construct the $\text{Fe}-\text{H}_2\text{O}$ Eh-pH diagram.

The following procedure and data are adapted from Cloke[8]:

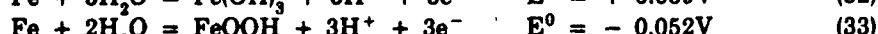
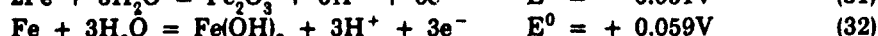
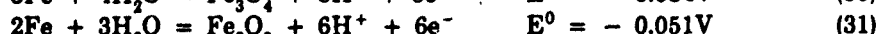
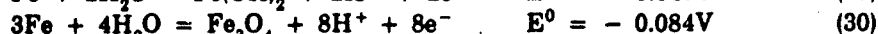
- (1) Consider all known valence states, solids and dissolved states as well as pH-dependent precipitation reactions. Scan tables that give free energies to locate compounds that can exist. Recognize that compounds that can form in a water system are those with water, OH^- and O^{2-} .

The list for iron is as follows:

Valence of Iron	Solid Substance	Dissolved Species
0	Fe	
2	FeO	
	Fe(OH)_2	Fe^{+2} and Fe(II) complexes
2 and 3	Fe_3O_4	
3	Fe_2O_3	
	Fe(OH)_3	Fe^{+3} and Fe(III) complexes
	FeOOH	

- (2) Write balanced reactions for oxidation of the most reduced form of the substance to each of the other oxidation states given above, using only water as reactant with the most reduced form.

For the six oxidized forms of iron, one may consider the following reactions, starting with the most reduced form (Fe):



(E° values are derived or obtained using the procedure described in the next step)

- (3) Calculate E° values for each of the reactions above. (Depending on the form of the data available, equations 7 and 8 may be useful.) Write the values of E° next to the reactions, as shown above in step 2.

- (4) We can express the general reaction by means of the following equation:



for which [8]

$$Eh = E^\circ + (0.059/n)\log[C]^c[D]^d \dots / [A]^a[B]^b \dots \quad (35)$$

Write equation 35 for all of the reactions listed in step 2. In the case of reaction 28, for example, $a=1$, $b=1$, $c=2$, $d=1$, $\text{A}=[\text{Fe}]$, $\text{B}=[\text{H}_2\text{O}]$, $\text{C}=[\text{H}^+]$, $\text{D}=[\text{FeO}]$, $n=2$, and $E^\circ=-0.037$. Thus,

$$Eh = -0.037 + (0.059/2) \log [\text{H}^+]^2 [\text{FeO}]/[\text{Fe}] [\text{H}_2\text{O}] \quad (36)$$

This simplifies to the following equation:

$$Eh = -0.037 - 0.059 \text{ pH} \quad (37)$$

since the activities of the solid phases as well as of the water are defined as unity.

Similarly, for equations 29 to 33,

$$Eh = -0.047 - 0.059 \text{ pH} \quad (38)$$

$$Eh = -0.084 - 0.059 \text{ pH} \quad (39)$$

$$Eh = -0.051 - 0.059 \text{ pH} \quad (40)$$

$$Eh = +0.059 - 0.059 \text{ pH} \quad (41)$$

$$Eh = -0.052 - 0.059 \text{ pH} \quad (42)$$

- (5) Plot equations 37 to 42 using Eh as the y axis and pH as the x axis as shown in Figure 2.10-8.

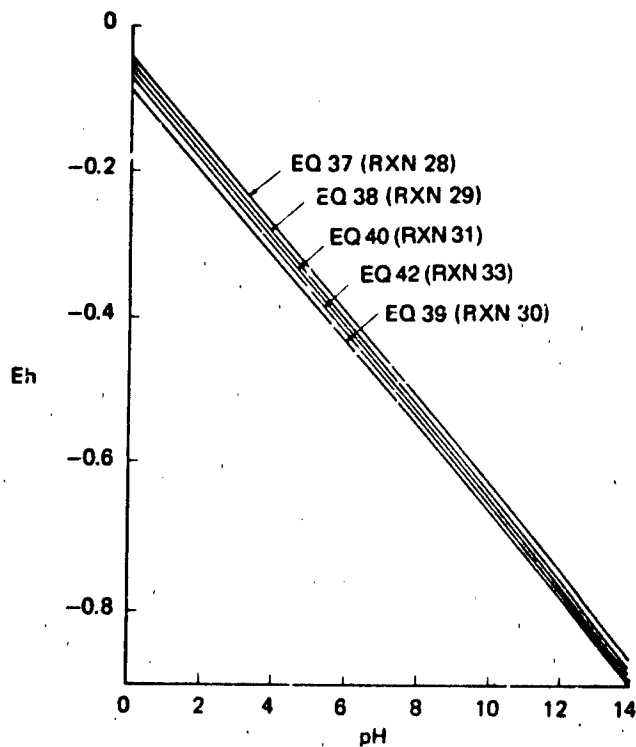


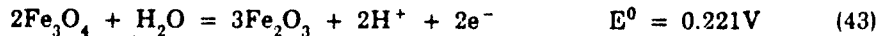
FIGURE 2.10-8 Eh Versus pH for the Fe-H₂O System: Diagram for Step 5

- (6) Use the line that is lowest (reaction 30) and disregard the others, because this line represents the reaction that uses up all the Fe and prevents any of the other reactions involving Fe from occurring.

If the lowest lines intersect, one of the lines would be used above the intersection and the other line below the intersection. The general rule is to use the line or line segment corresponding to the more negative value of Eh for a given pH. An additional line would also be drawn through the point of intersection according to an equation derived from the reaction of the two oxidized species, using only these two species and H₂O and H⁺ (not O₂, H₂ or OH⁻). Further details of this procedure are given in step 13.

- (7) Now consider oxidation to higher valences from the oxidized product of the reaction retained in step 6. The species that can be produced were identified in step 2.

For the iron system, we consider what species can result from the oxidation of Fe₃O₄:



These lead to the following three equations for the relationship between Eh and pH:

$$Eh = 0.221 - 0.059 \text{ pH} \quad (46)$$

$$Eh = 1.21 - 0.059 \text{ pH} \quad (47)$$

$$Eh = 0.208 - 0.059 \text{ pH} \quad (48)$$

When these equations are plotted, we find that the line corresponding to equation 48 is the lowest of the three, indicating that FeOOH is the product of oxidation of Fe_3O_4 at equilibrium. (See Figure 2.10-9.)

- (8) Repeat step 7 until the highest oxidation state is reached.
- (9) Draw two lines on the diagram defining the Eh-pH region where water is stable, as follows:

- For the water/oxygen half reaction,

$$Eh = 1.23 + 0.015 \log [\text{pO}_2] - 0.059 \text{ pH} \quad (49)$$

which at one atmosphere of oxygen corresponds to

$$Eh = 1.23 - 0.059 \text{ pH} \quad (50)$$

- For the hydrogen/proton couple,

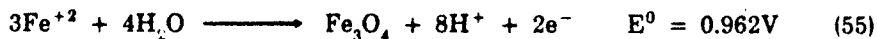
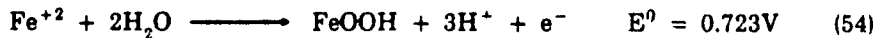
$$Eh = -0.059 \text{ pH} - 0.0295 \log [\text{pH}_2] \quad (51)$$

which at one atmosphere of hydrogen gas is

$$Eh = -0.059 \text{ pH} \quad (52)$$

Plots of equations 50 and 52 are included on Figure 2.10-9.

- (10) Discard all lines outside the area of water stability defined above — i.e., above the line for equation 50 and below the line for equation 52. Thus the plot for equation 39 is discarded, but the region between equations 52 and 48 remains a valid stability range for Fe_3O_4 .
- (11) Add lines for equilibria between solids and dissolved states of the species shown in the diagram. In this example, the following reactions are applicable:



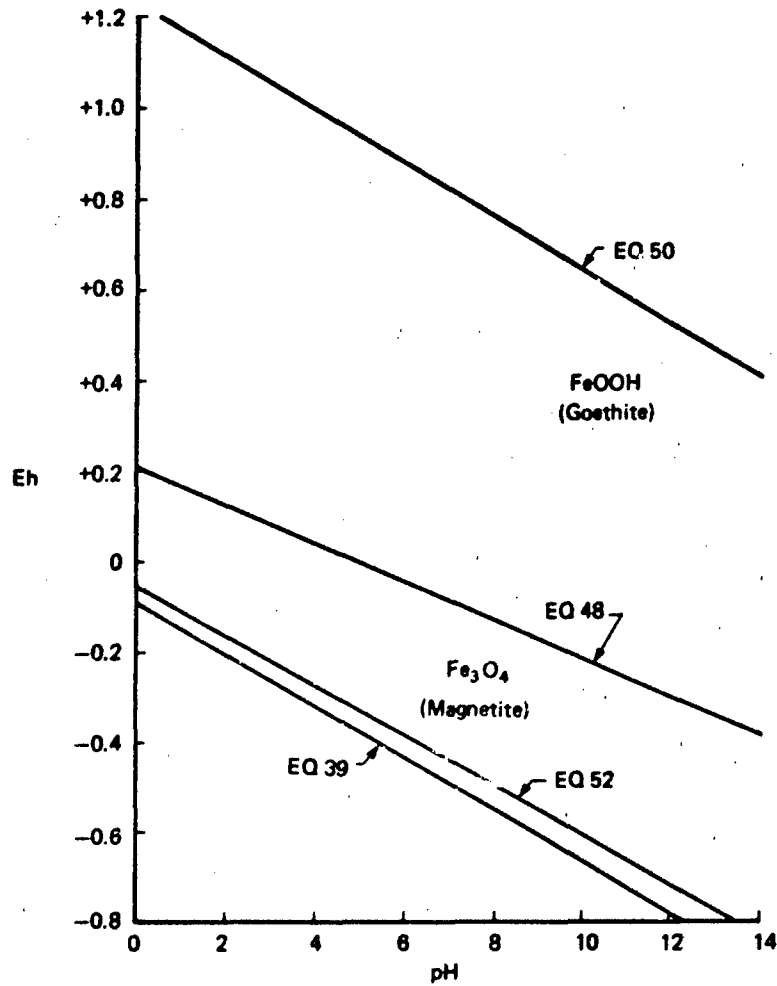


FIGURE 2.10-9 Eh Versus pH for the Fe-H₂O System: Diagram for Steps 7 and 9

For reaction 53,

$$K = [H^+]^3 / [Fe^{+3}] = 6.3 \quad (56)$$

or

$$pH = -(\log[Fe^{+3}]) / 3 = 0.266 \quad (57)$$

Since the stability field diagrams are drawn assuming a $10^{-6}M$ concentration of dissolved ions, $[Fe^{+3}] = 10^{-6}M$, and equation 57 reduces to $pH = 1.734$.

For equation 54, $E^0 = 0.723V$ and $n = 1$. Therefore, we can rewrite equation 35 as

$$Eh = 0.723 + (0.059/1) (\log[H^+]) - (0.059/1) (\log[Fe^{+2}]) \quad (58)$$

or

$$Eh = 0.723 - 0.177 pH - 0.059 \log [Fe^{+2}] \quad (59)$$

For an $[Fe^{+2}] = 10^{-6}M$,

$$Eh = 1.077 - 0.177 pH \quad (60)$$

Similarly, for equation 55,

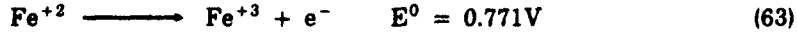
$$Eh = 0.962 - 0.236 pH - 0.0885 \log [Fe^{+2}] \quad (61)$$

and at $[Fe^{+2}] = 10^{-6}M$,

$$Eh = 1.493 - 0.236 pH \quad (62)$$

Figure 2.10-10 shows the addition of lines corresponding to $pH = 1.734$ (equation 57) and equations 60 and 62 to Figure 2.10-9.

- (12) Add any redox reactions between the dissolved species. For this example, the reaction is



The redox potential for this reaction is

$$Eh = 0.771 + 0.059 \log [Fe^{+3}]/[Fe^{+2}] \quad (64)$$

At $[Fe^{+3}] = [Fe^{+2}] = 10^{-6}M$, equation 64 reduces to $Eh = 0.771V$ (referenced to hydrogen electrode). This is also plotted in Figure 2.10-10.

- (13) Erase all lines according to the following procedure. Where two lines intersect, delete the portion of each line that corresponds to the higher (more positive) Eh values at a given pH. Erase lines that no longer identify proper equilibrium reactions.

For this example, the lines to be erased are dashed in Figure 2.10-10. The portion of line for equation 57 within the Fe^{+2} area is erased because it no longer represents the proper species on either side.

The final diagram is shown in Figure 2.10-11.

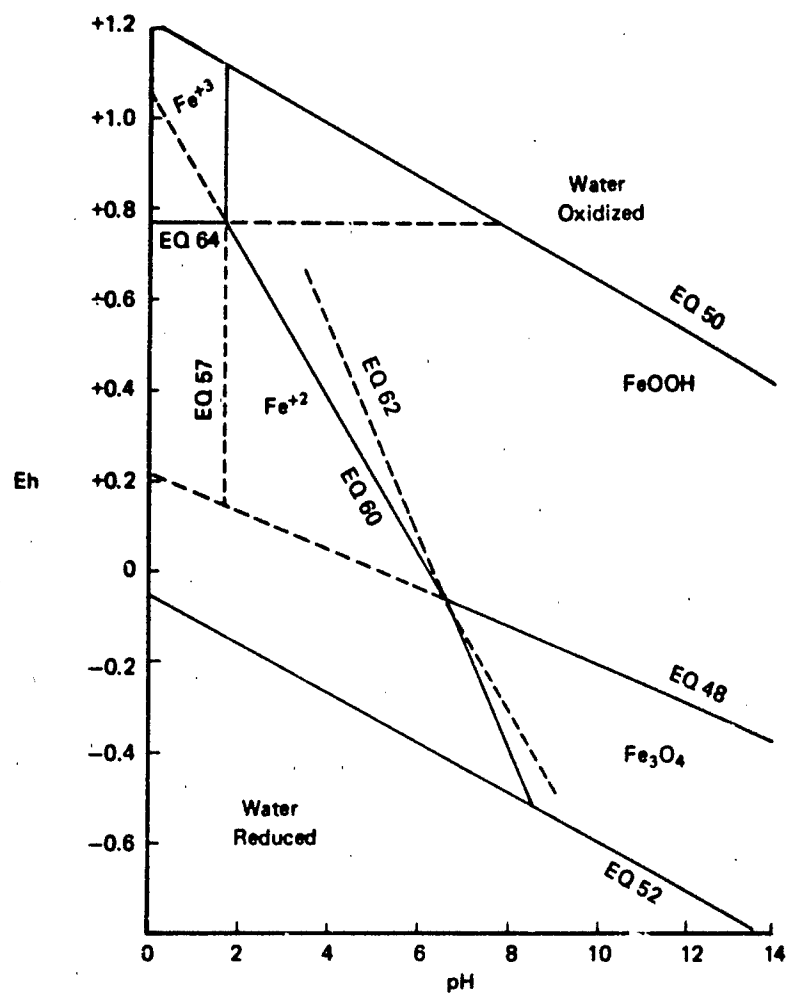


FIGURE 2 10-10 Eh Versus pH for the Fe-H₂O System: Diagram for Steps 11 to 13

The line shown on the Eh versus pH diagram for the Iron-Water System (Figure 2.10-11) separating the Fe^{+2} and Fe^{+3} (at Eh = 0.77 and pH = 1) represents the conditions where the concentrations (or activities) of these two dissolved species are equal. Within the region labelled Fe^{+2} this species predominates, and similarly for the Fe^{+3} region. The line separating regions of solid phases (e.g. Fe_3O_4 and FeOOH) provides the boundary where relative stability of one solid becomes greater than that of the other. A line that separates a solid phase and a dissolved species (e.g. Fe^{+3} and FeOOH at Eh = 1 and pH = 2) indicates the values of Eh and pH where the dissolved species is 10^{-6} M (by convention for the way this diagram was drawn). Similar diagrams could be drawn with these lines representing other dissolved ion concentrations (e.g. 10^{-4} or 10^{-2} M). The lines that would represent higher dissolved Fe^{+3} concentrations would occur parallel to the line shown on Fig. 2.10-11 at similar Eh values but at lower pH values.

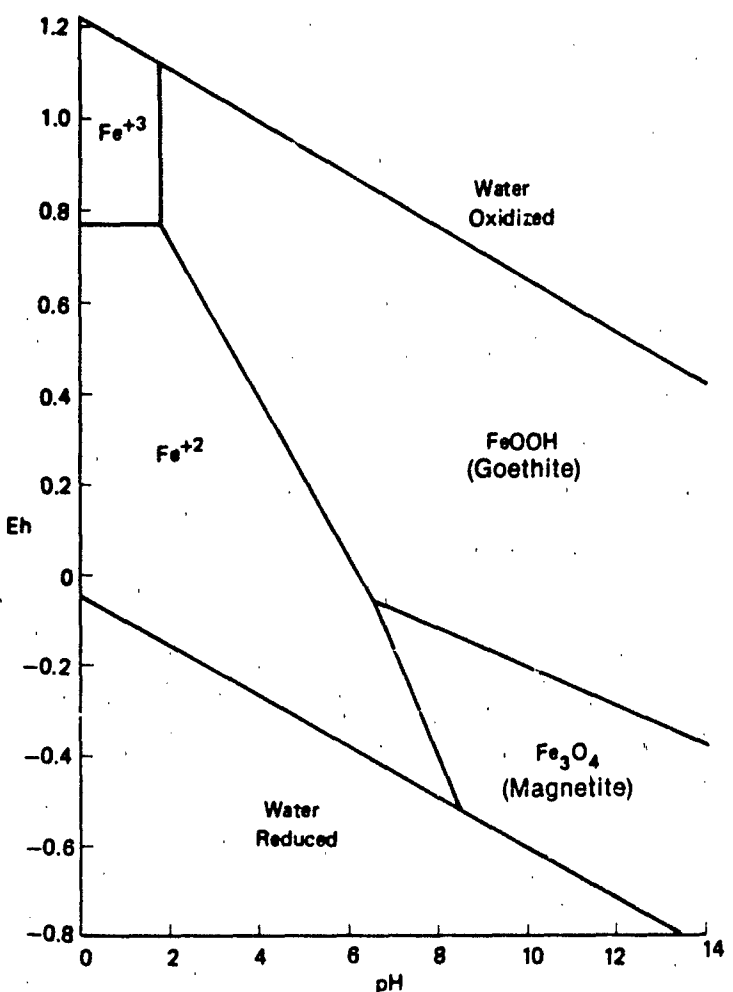


FIGURE 2.10-11 Eh Versus pH for the Fe-H₂O System: Final Diagram

2.10.5 Redox in Environmental Systems

IMPORTANT REDOX PROCESSES

Redox reactions in environmental systems can occur between species of elements that occur naturally, between pollutant species and naturally occurring species, and between pollutant species. Of the naturally occurring species, only a few commonly participate in redox processes; the typical oxidizing agents in waters (in order of decreasing oxidizing strength) are oxygen, nitrate, nitrite, ferric hydroxide, ferric phosphate, sulfate, sulfur, carbon dioxide and bicarbonate. The most important naturally occurring reducing agents in waters (in order of decreasing reducing strength) are organic substances, hydrogen sulfide, sulfur, iron sulfide, ammonium and nitrite. (This excludes kinetic considerations.)[20]

Due to kinetic limitations, local inhomogeneity, and local catalytic effects of organisms, redox equilibrium conditions may not be attained in many environmental systems, and several of the above listed species may coexist. For example, in water in equilibrium with air at pH 7 ($\text{pe} = 13.6$), all carbon should theoretically be present as carbon dioxide or carbonate-type species, all nitrogen as nitrate, all sulfur as sulfate, all iron as iron(III) species and all manganese as Mn(IV) species. In fact, nitrogen, reduced forms of carbon (e.g., organic matter and CH_4), sulfides, iron(II) and Mn(II) all exist under various conditions, attesting to a lack of equilibrium.

Nonequilibrium conditions usually occur when environments are isolated from the oxidizing species (e.g., oxygen) and appropriate catalyzing bacteria are present. Important redox half-reactions that are considered in the chemical equilibrium model WATEQF[16] are listed in Table 2.10-1.

All of the various forms of the naturally occurring elements (e.g. as shown in Table 2.10-1) can participate in reactions with specific species, leading to partial equilibrium (with respect to particular reactions) because of the limitations imposed on reactions with other species present. Thus, if the redox reaction and kinetics are favorable, pollutants introduced into that environment can react with these and other naturally present species.

TABLE 2.10-1
Redox Half-Reactions Considered in WATEQF

$\text{Fe}^{+2} = \text{Fe}^{+3} + \text{e}^-$	$\text{Fe}_3\text{O}_4 + 8\text{H}^+ = 3\text{Fe}^{+3} + 4\text{H}_2\text{O} + \text{e}^-$
$\text{Fe}^{+2} + \text{SO}_4^{-2} = \text{FeSO}_4^+ + \text{e}^-$	$\text{FeS}_2 + 2\text{H}^+ + 2\text{e}^- = \text{Fe}^{+2} + 2\text{HS}^-$
$\text{Fe}^{+2} + \text{Cl}^- = \text{FeCl}^{+2} + \text{e}^-$	$\text{Fe}_3\text{S}_4 + 4\text{H}^+ + 2\text{e}^- = 3\text{Fe}^{+2} + 4\text{HS}^-$
$\text{Fe}^{+2} + 2\text{Cl}^- = \text{FeCl}_2^+ + \text{e}^-$	$\text{Fe}^{+2} + \text{HPO}_4^{-2} = \text{FeHPO}_4^+ + \text{e}^-$
$\text{Fe}^{+2} + 3\text{Cl}^- = \text{FeCl}_3^0 + \text{e}^-$	$\text{Fe}^{+2} + \text{H}_2\text{PO}_4^- = \text{FeH}_2\text{PO}_4^{+2} + \text{e}^-$
$\text{SO}_4^{-2} + 10\text{H}^+ + 8\text{e}^- = \text{H}_2\text{S} + 4\text{H}_2\text{O}$	$\text{Mn}^{+2} + 4\text{H}_2\text{O} = \text{MnO}_4^- + 8\text{H}^+ + 5\text{e}^-$
$2\text{H}_2\text{O} = \text{O}_2 + 4\text{H}^+ + 4\text{e}^-$	$\text{Mn}^{+2} + 4\text{H}_2\text{O} = \text{MnO}_4^{-2} + 8\text{H}^+ + 4\text{e}^-$
$\text{HCO}_3^- + 8\text{e}^- + 9\text{H}^+ = \text{CH}_4 + 3\text{H}_2\text{O}$	$\delta\text{-MnO}_2(\text{birnessite}) + 4\text{H}^+ + \text{e}^- = \text{Mn}^{+3} + 2\text{H}_2\text{O}$
$\text{Fe}^{+2} + 2\text{H}_2\text{O} = \text{Fe}(\text{OH})_2^+ + 2\text{H}^+ + \text{e}^-$	$\delta\text{-MnO}_2(\text{insitite}) + 4\text{H}^+ + \text{e}^- = \text{Mn}^{+3} + 2\text{H}_2\text{O}$
$\text{Fe}^{+2} + 3\text{H}_2\text{O} = \text{Fe}(\text{OH})_3^0 + 3\text{H}^+ + \text{e}^-$	$\text{Mn}_3\text{O}_4 + 8\text{H}^+ + 2\text{e}^- = 3\text{Mn}^{+2} + 4\text{H}_2\text{O}$
$\text{Fe}^{+2} + 4\text{H}_2\text{O} = \text{Fe}(\text{OH})_4^- + 4\text{H}^+ + \text{e}^-$	

Source: Plummer [16]

In addition to the major elements, many trace components present in the environment can undergo redox reactions. This is important, because pollutants are generally present at very low levels, and the kinetic and redox properties of the trace substances that occur naturally may favor their reactions with the pollutants rather than with the major species such as those in Table 2.10-1. Trace elements can also catalyze redox reactions.

Some other redox species that may need consideration are shown in Figure 2.10-1. Many of these species, if present at elevated levels, would be considered pollutants.

The other category of redox interactions in environmental systems that may have to be addressed is the reaction between two or more pollutants introduced into the system. In some situations, the likelihood of a redox reaction in a mixture of two or more pollutants increases after it enters an environmental system such as ground-water or seawater. The environmental system can make the conditions for reaction more favorable or enhance the kinetics by modifying the speciation of the pollutants (e.g., by modifying the pH), or it can introduce chemical or biological species that can enhance the rate of the redox reaction. Examples of redox reactions that can be biologically mediated are given in Table 2.10-2.

APPLICABILITY OF Eh (OR pe) MEASUREMENTS

The measurement and interpretation of Eh or pe in environmental systems can be difficult [15,22]. Potentiometric measurements of Eh in environmental systems usually do not agree with those predicted by theory, due to the low concentration of redox-active species and their low exchange currents.² The most important problem in applying the Eh concept to natural waters is the lack of redox equilibrium between all the redox-active species. Reactions between the major environmentally important redox species (listed in Figure 2.10-12) often appear to be very slow; thus, for a system in disequilibrium, an Eh value that is meaningful with regard to rapid exchange between a redox couple is not expected.

Lindberg and Runnels [15] have examined data from about 30 groundwater analyses and compared the measured Eh or pe values to those predicted from calculations through the ratio of concentrations of many of the redox-active couples (iron(II)/iron(III), oxygen/water, bisulfide/sulfate, etc.) in these solutions. The expected Eh values and those calculated by use of these redox couples do not agree and vary over a wide range, as shown in Figure 2.10-12. These data show that none of the representative waters chosen for analysis exhibited equilibrium and that the computed Eh values span a wide range (as much as 1000 mV). They also suggest that indicator species (e.g., iodide/iodate or arsenic(III)/arsenic(V)) ratios may not be more representative of the redox state than the measurement using an electrode. It may be reasonably concluded that a master value of Eh or pe cannot be used to predict redox equilibria in groundwater environments and that computer models utilizing pe or Eh to calculate species ratios would most likely make erroneous predictions.

Lindberg and Runnels [15] have suggested an alternative to using measured Eh values, namely, to measure concentrations of certain redox-active species (e.g., dissolved oxygen, total sulfide species and methane) as a qualitative guide to the redox status of waters (see next section for discussion of this approach); the concentrations of the redox components of immediate interest in the water should be measured if there is a need to consider their possible redox effect on pollutants introduced into that environment.

2. The species do not readily give up or take up electrons at platinum or gold electrode surfaces.

TABLE 2.10-2
Microbially Mediated Oxidation and Reduction Reactions

Reaction	$\text{pe}^0_{\text{pH}7}$ (note a)
Oxidation	
(1) ^b $\text{CH}_2\text{O} + \text{H}_2\text{O} = \text{CO}_2(\text{g}) + 4\text{H}^+ + 4\text{e}^-$	-8.20
(2) $\text{HS}^- + 4\text{H}_2\text{O} = \text{SO}_4^{2-} + 9\text{H}^+ + 8\text{e}^-$	-3.75
(3) $\text{NH}_4^+ + 3\text{H}_2\text{O} = \text{NO}_3^- + 10\text{H}^+ + 8\text{e}^-$	+6.16
(4) ^c $\text{FeCO}_3(\text{s}) + 2\text{H}_2\text{O} = \text{FeOOH}(\text{s}) + \text{HCO}_3^{(10^{-3}\text{M})} + 2\text{H}^+ + \text{e}^-$	-1.67
(5) ^c $\text{MnCO}_3(\text{s}) + 2\text{H}_2\text{O} = \text{MnO}_2(\text{s}) + \text{HCO}_3^{(10^{-3}\text{M})} + 3\text{H}^+ + 2\text{e}^-$	+8.5
(1a) ^b $\text{HCOO}^- = \text{CO}_2(\text{g}) + \text{H}^+ + 2\text{e}^-$	-8.73
(1b) $\text{CH}_2\text{O} + \text{H}_2\text{O} = \text{HCOO}^- + 3\text{H}^+ + 2\text{e}^-$	-7.68
(1c) $\text{CH}_3\text{OH} = \text{CH}_2\text{O} + 2\text{H}^+ + 2\text{e}^-$	-3.01
(1d) $\text{CH}_4(\text{g}) + \text{H}_2\text{O} = \text{CH}_3\text{OH} + 2\text{H}^+ + 2\text{e}^-$	+2.88
Reduction	
(A) $\text{O}_2(\text{g}) + 4\text{H}^+ + 4\text{e}^- = 2\text{H}_2\text{O}$	+13.75
(B) ^d $2\text{NO}_3^- + 12\text{H}^+ + 10\text{e}^- = \text{N}_2(\text{g}) + 6\text{H}_2\text{O}$	+12.65
(C) $\text{NO}_3^- + 10\text{H}^+ + 8\text{e}^- = \text{NH}_4^+ + 3\text{H}_2\text{O}$	+6.16
(D) $\text{SO}_4^{2-} + 9\text{H}^+ + 8\text{e}^- = \text{HS}^- + 4\text{H}_2\text{O}$	-3.75
(E) $\text{CO}_2(\text{g}) + 8\text{H}^+ + 8\text{e}^- = \text{CH}_4(\text{g}) + 4\text{H}_2\text{O}$	-4.13
(F) ^b $\text{CH}_2\text{O} + 2\text{H}^+ + 2\text{e}^- = \text{CH}_3\text{OH}$	-3.01

(Continued)

Despite the limitations of Eh and pe, redox equilibrium models (including Eh/pH diagrams) can be valuable for interpreting observed data and identifying possible regulating mechanisms for pe buffering of a few aqueous systems [20]. The discrepancies between equilibrium calculations and experimental data can give insight as to whether the reactions are well understood and whether the systems are at equilibrium. They may also provide clues concerning which species will predominate as redox conditions change and what solid phase(s) may be expected.

Eh AND pe VALUES ENCOUNTERED IN VARIOUS ENVIRONMENTS

For waters in equilibrium with atmospheric oxygen, there is no correlation of the measured Eh and dissolved oxygen levels [6]; the water/oxygen half-reaction (equation 3) is too slow to affect the Eh value measured. The measurement of Eh is only considered valid and useful when dissolved oxygen (DO) is below the minimum detection level of 0.01 ppm. For waters where DO is above this level, measurement of dissolved oxygen is a better indication of redox conditions.

TABLE 2.10-2 (Continued)

Thermodynamic Sequence of Biologically Mediated Redox Reactions

Model 1: Excess organic material. (Water contains incipiently O_2 , NO_3^- , SO_4^{2-} , HCO_3^- .) Examples: Hypolimnetic layers of eutrophic lake, sediments; digester.

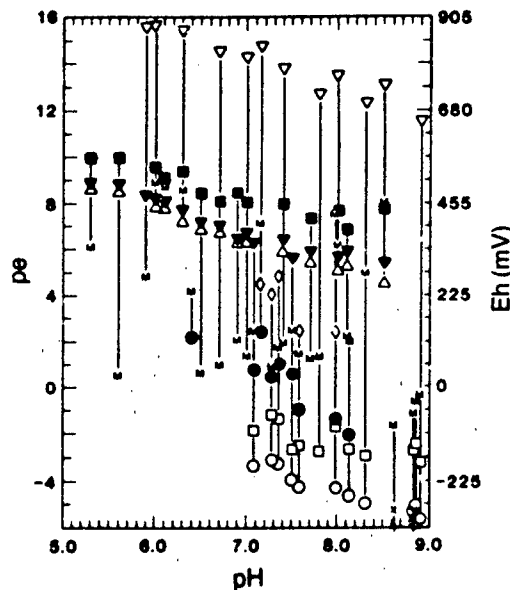
	Combination	(1/n)log K_{pH7}^*
Aerobic respiration	(1) + (A)	21.95
Dentrification ^f	(1) + (B)	20.85
Nitrate reduction	(1) + (C)	14.36
Fermentation ^{b,g}	(1b) + (F)	4.67
Sulfate reduction	(1) + (D)	4.45
Methane fermentation	(1) + (E)	4.07

Model 2: Excess O_2 . (Water contains incipiently organic material, SH^- , NH_4^+ and possibly Fe(II) and Mn(II).) Examples: Aerobic waste treatment, self-purification in streams; epilimnetic waters.

	Combination	(1/n)log K_{pH7}^*
Aerobic respiration	(A) + (1)	21.95
Sulfide oxidation	(A) + (2)	17.50
Nitrification ^f	(A) + (3)	7.59
Ferrous oxidation ^c	(A) + (4)	15.42
Mn(II) oxidation	(A) + (5)	5.25

- a. pe_{pH7}^0 is the pe if all reaction participants with exception of (H^+) are present at unit activity (for gases, partial pressure = 1). (H^+) has been set equal to 10^{-7} . $pe^0 = (1/n)\log K_{reduction}$ (n = no. of electrons). All constants given are for 25°C.
- b. CH_2O is used here as a general symbol for organic material. Examples for organic carbon with formal oxidation states of +II, 0, -II, and -IV are given in reactions 1a to 1d, respectively. $H_2(g)$ is an almost equally strong reductant as organic material and in some mediations it can be substituted for organic material: $H_2(g) = 2H^+ + 2e^-$; $pe^0_{pH7} = -7.00$.
- c. The autotrophic nature of iron and manganese bacteria is in dispute
- d. $N_2O(g)$ may appear as an intermediate; some facultative anaerobes catalyze the reduction to NO_2 .
- e. $(1/n)\log K$ is the equilibrium constant for the combined redox reaction per electron transferred. With exception of (H^+), all reaction participants are present at unit activity. $[(H^+) = 10^{-7}]$. $(1/n)\log K$ is proportional to the free energy decrease of the redox reaction per electron transferred: $(1/n)\log K = -\Delta G^\circ_{pH7}/(nRT \ln 10)$.
- f. It has been assumed, rather arbitrarily, that the direct oxidation of NH_4^+ into N_2 is hindered. Conversion of NH_4^+ to N_2 is thus achieved by nitrification/denitrification.
- g. Fermentation is interpreted as an organic redox reaction where one organic substance is reduced by oxidizing another organic substance (e.g., alcohol fermentation). The participants in such a reaction are themselves thermodynamically unstable.

Source: Stumm [20] (Copyright 1967, Water Pollution Control Federation. Reprinted with permission.)



Symbols Used and Couples Are as Follows

Symbol	Redox couple
◇	$\text{Fe}^{+3}/\text{Fe}^{+2}$
▽	$\text{O}_{2\text{aq}}/\text{H}_2\text{O}$
○	$\text{HS}^-/\text{SO}_4^{2-}$
□	$\text{HS}^-/\text{S}_{\text{rhombic}}$
■	$\text{NO}_2/\text{NO}_3^-$
▼	$\text{NH}_4^+/\text{NO}_3^-$
△	$\text{NH}_4^+/\text{NO}_2^-$
+	$\text{CH}_4\text{aq}/\text{HCO}_3^-$
×	$\text{NH}_4^+/\text{N}_2\text{aq}$
●	$\text{Fe}^{+2}/\text{Fe}(\text{OH})_3(s)$
M	Field-measured Eh value

Source: Lindberg and Runnels [13]. (Copyright 1984, American Association for the Advancement of Science. Reprinted with permission.)

FIGURE 2.10-12 Comparison of Measured and Computed Eh Versus pH Values in 30 Groundwater Systems

The relative positions of some natural environments as functions of Eh and pH are shown in Figure 2.10-13. The validity of Eh measurement for various conditions encountered in the environment is summarized in Table 2.10-3. Reproducible and meaningful Eh values are generally obtained in well-poised systems (i.e., those that contain high concentrations of both the reduced and oxidized forms of the redox couple). This occurs in some acid mine waters that contain high levels of dissolved iron. For the other waters listed in Table 2.10-3, Eh measurements are not considered reliable because of their lack of reproducibility and stability [6].

Although, as discussed above, dissolved oxygen levels do not readily provide the redox status of oxygenated waters, concentrations of sulfide in many sediment water environments do provide an indication. This is because the Eh values of many sediments containing H_2S have been found to be controlled by the following reversible half-reactions [1]:

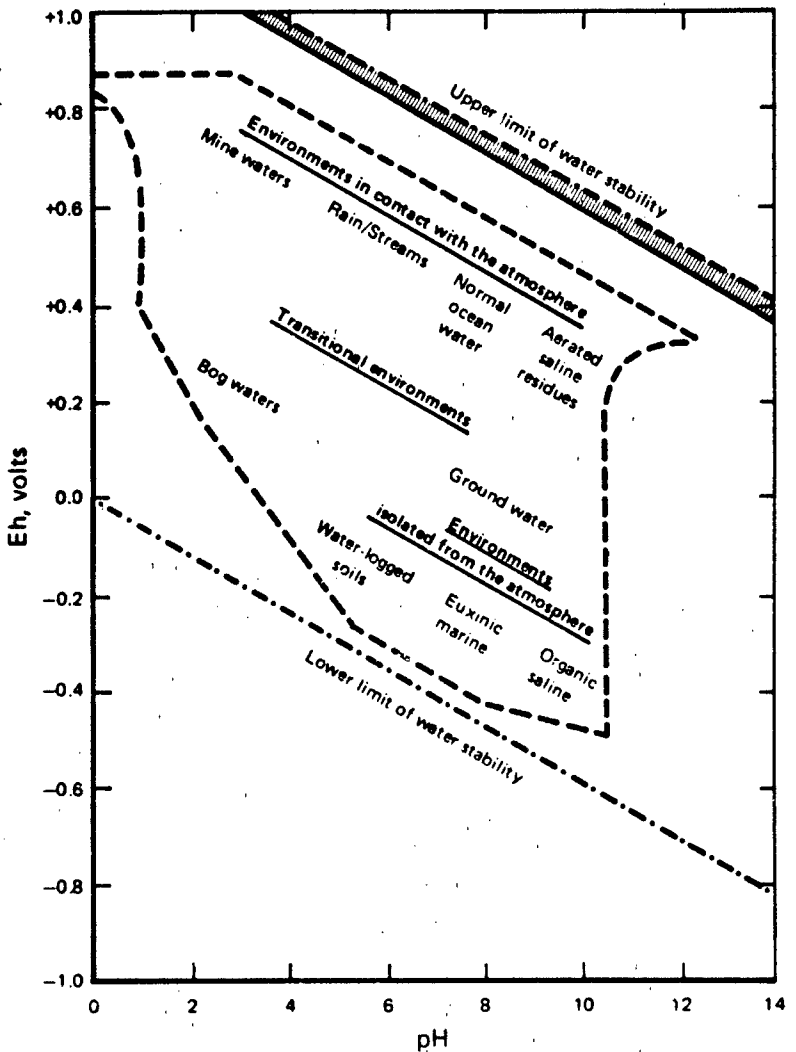


or



according to the equation (at 25°C), where

$$\text{Eh} = -0.475 + 0.0295 \text{ p}[\text{S}^{2-}] \quad (67)$$



Dashed lines represent limits of measurements in natural systems.
Crosshatched area represents the Eh and pH of waters containing
more than .01 ppm of oxygen, based on the oxygen water half-reaction.

Source: Langmuir [13] (Copyright 1971, Wiley Interscience Publishers.
Reprinted with permission.)

FIGURE 2.10-13 Approximate Relative Position of Eh and pH for Natural Environments

TABLE 2.10-3
Redox Characteristics and Eh Measurements for Various Aqueous Environments

Environment	Redox Characteristics	Eh Response/Comments
Oxygenated Waters (e.g., rain, streams, some groundwater, shallow lakes)	Poorly poised, low or no concentration of electroactive species	Eh measurement drifts; D.O. levels may be more useful
Acid mine water, groundwater rich in Fe at pH below 4	May be well poised; reversible redox reaction present at significant levels	Uncommon in natural environments; Eh measurable and useful
Organic rich systems, soil waters, stagnant polluted water with low oxygen levels	Poorly poised; absence of oxidized form of redox species; mixed potentials and irreversible reactions present; biological mediation	Lowest Eh values found in these environments; drift in Eh observed
Heterogeneous environments	Variable condition	Reproducible value may not be possible

Source: Adapted from Langmuir [13]

Empirical data for values of Eh and S^{-2} correlate well with this half-reaction, as shown in Figure 2.10-14. When electrodes are inserted into these sediment environments, such measurements are rapidly attained and are stable at low Eh values, indicating a well-poised system.

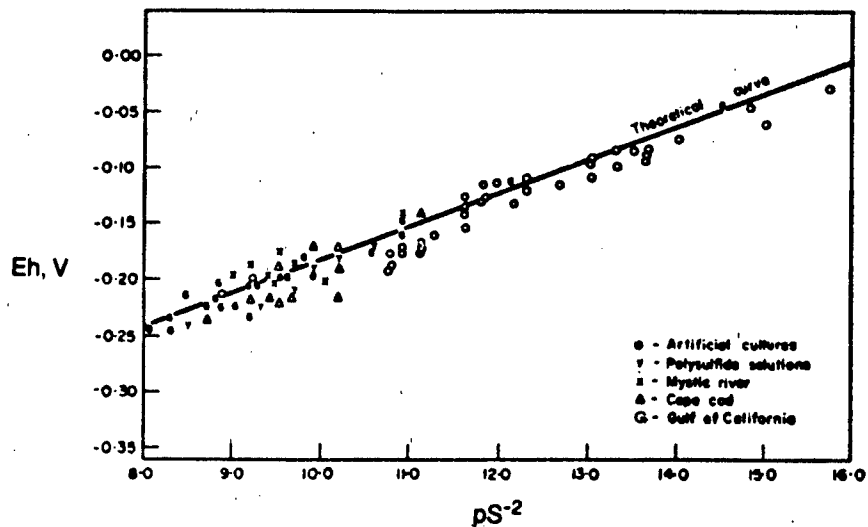
OTHER INDICATORS OF REDOX CONDITIONS

A classification of sediment redox environments proposed by Berner [2] may be more practical than the Eh approach, because it is directly related to measured concentrations. In this scheme, Eh is not considered to be a measurable quantity, owing to the difficulties described previously. The primary basis for this classification is that dissolved oxygen (DO) and total dissolved sulfide species (H_2S , HS^- , S^{2-}) are measurable and are intimately involved in redox reactions. The scheme is summarized in Figure 2.10-15, and the concentration basis for each classification is given in Table 2.10-4. The classification depends on the ability to identify naturally occurring (authigenic) Mn and Fe phases in the solids and is thus useful only for undisturbed sediment environments.

The best (but most tedious) approach to understanding redox properties of the aqueous environment and their possible impact on added pollutants is to consider the reaction of the added pollutant with each of the species present in the environment. This characterization would include determining identity, speciation, relative concentration and assessment of the rate and equilibrium position of all the possible redox reactions, and would be performed either by calculation or by experiment. The initial candidates for consideration would be the most commonly found redox active species in solution (dissolved oxygen, sulfide species, iron(II), iron(III), manganese(II) and possibly nitrite), followed by species commonly found in the solid phase (if present) — iron(II), iron (III), manganese(II) and manganese(IV).

As discussed in Section 3.3, "Kinetics of Redox Reactions," catalysis by trace species as well as biological organisms is possible; thus, after the major components are considered, possible redox reaction with trace components should be addressed. The speciation of the reactants involved will depend on the environment and the effects of the added pollutants.

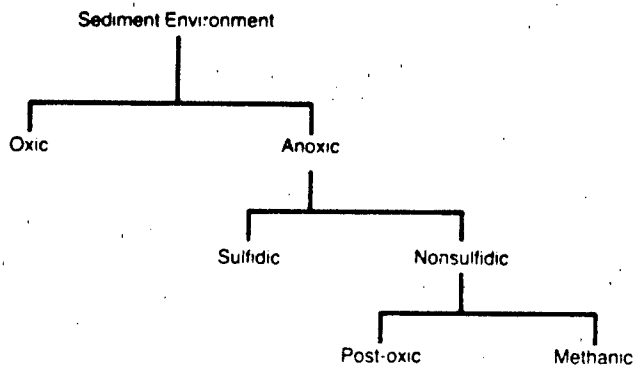
An example of the concentration profile observed for a variety of species in a pore water system that progresses from being oxic to anoxic (various depths in a sediment) is shown in Figure 2.10-16. Concentrations of many metals in the dissolved state above the interface are low (mostly existing in the solid state). Release from the solid into solution after reduction is observed below the O_2/H_2S interface.



"Theoretical Curve" represents the half-reaction sulfide ⇌ sulfur (rhomb) + 2 e⁻

Source: Berner [1]. (Copyright 1963, Pergamon Press, Inc. Reprinted with permission.)

FIGURE 2.10-14 Eh Versus p(Sulfide) in Natural Sediment Environments and Polysulfide Solutions



See Table 2.10-4 for clarification of terms

Source: Berner [2]

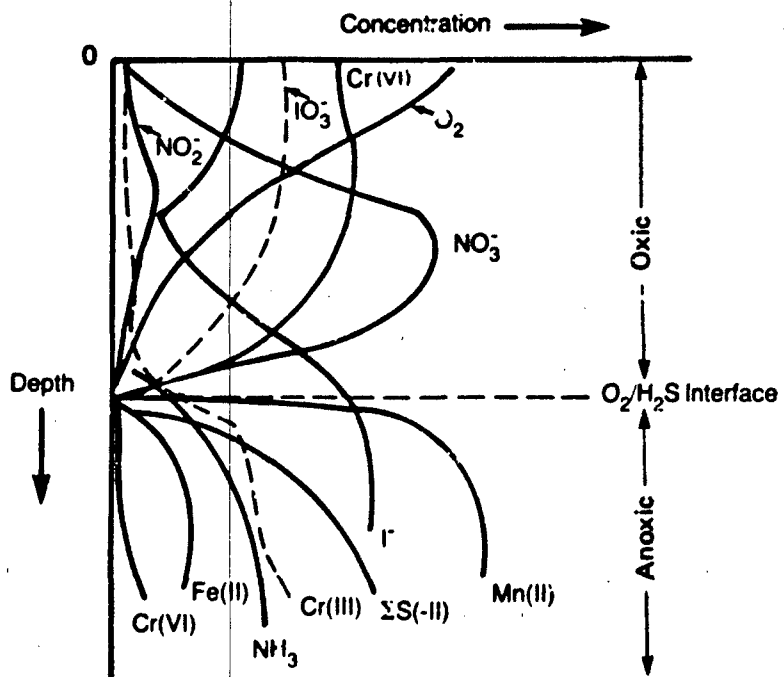
FIGURE 2.10-15 Classification of Sediment Environments

TABLE 2.10-4
Redox Classification Scheme Proposed by Berner

Environment	$[O_2]_{aq}$ (M)	$[\Sigma H_2S]_{aq}$ (M)	P_{CO_2} (atm)	Characteristic Typical of Solid Phase in Equilibrium*	Other Characteristics	Progression of Biologically Mediated Organic Matter Decomposition
Oxic	$\geq 10^{-6}$	$\leq 10^{-6}$	≤ 1	$FeOOH$, MnO_2 , Fe_2O_3 , Relative absence of decomposable organic matter (MnO_2 is a better indicator than $Fe(II)$ solids; latter persist under anoxic conditions, since they are not reduced by any organic species)	Lack of bacteria capable of producing H_2S	Oxygen consumption
Anoxic	$< 10^{-6}$					
Sulfidic	$< 10^{-6}$	$\geq 10^{-8}$	$> 10^{-4}$	$Fe(II)S_2$, $MnCO_3$, $Mn(II)S$	Lack of aerobic organisms and oxidized minerals	Sulfate reduction
Nonsulfidic	$< 10^{-6}$		$< 10^{-6}$			
• Post-Oxic	$< 10^{-6}$	$< 10^{-6}$		Fe^{+2}/Fe^{+3} containing alumino silicates, $FeCO_3$, $Fe_3(PO_4)_2$, $MnCO_3$. No sulfide minerals, minor amount of decomposable organic matter	Fe^{+2}/Fe^{+3} containing alumino silicates, $FeCO_3$, $Fe_3(PO_4)_2$, $MnCO_3$. No sulfide minerals, minor amount of decomposable organic matter	Nitrate reduction
• Methanic	$< 10^{-6}$	$< 10^{-6}$		$FeCO_3$, $Fe_3(PO_4)_2$, $MnCO_3$. Earlier formed sulfide minerals, decomposable organic matter present	$FeCO_3$, $Fe_3(PO_4)_2$, $MnCO_3$. Earlier formed sulfide minerals, decomposable organic matter present	Methane formation

a. $Fe(III)OOH$ = goethite; $Fe(III)_2O_3$ = hematite; FeS_2 = pyrite or marcasite;
 $Fe(II)CO_3$ = siderite; $Fe_3(PO_4)_2$ = ninanite; $MnCO_3$ = rhodochrosite

Source: Adapted from Berner [2]



Source: Adapted from Emerson [9]

FIGURE 2.10-16 Variation in Concentration with Depth for Various Redox Active Species in a Fjord

2.10.8 Estimation of Equilibrium Parameters for Redox Reactions

The preceding sections of this chapter have discussed methods for estimating:

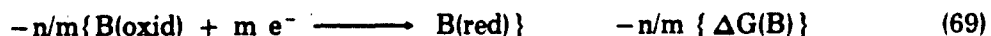
- Relative concentrations of oxidized versus reduced forms of a species from p_e (or Eh) values;
- Relationship of p_e to Eh values and field measurements;
- Equilibrium constants from free energy data or redox half-reaction potentials; and
- p_e values from concentrations of other species, including dissolved oxygen and sulfide levels.

This section addresses the estimation of the equilibrium constant and the electrode potential for a half-reaction under limited conditions. The following are discussed:

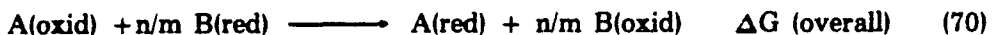
- Estimation of K for a redox reaction from E° values when no reactions after the redox reaction occur;
- Estimation of K for a redox reaction from E° and stability constants when a complex dissociation reaction occurs after redox; and
- Estimation of E° for a half-reaction of a complexed ion from that of an aquo ion and the complex stability constants.

ESTIMATION OF K FOR REDOX WHEN NO FURTHER REACTION TAKES PLACE

If the half-reaction potentials (or equilibrium constants or free energies) that together represent an overall redox reaction are known, the overall equilibrium constant for the reaction can be calculated as follows:



Taken together, equations 68 and 69 represent the overall reaction



where

$$\Delta G(\text{overall}) = \Delta G(A) - n/m \{ \Delta G(B) \} \quad (71)$$

This $\Delta G(\text{overall})$ is valid as long as A(red) and B(oxid) are the final products of the redox reaction (i.e., if no post-redox equilibria are involved).

If the data for equations 68 and 69 are given in terms of half-reaction potentials, the following expressions apply:

$$\Delta G(A) = -n F E(A) \quad (72)$$

$$\Delta G(B) = -m F E(B) \quad (73)$$

Thus,

$$\Delta G(\text{overall}) = -n F [E(A) - E(B)] = -n F E(\text{overall}) \quad (74)$$

where E(A) and E(B) are both expressed as reduction potentials.

The equilibrium constant at 25°C for reaction 70 is therefore related to the above parameters as follows:

$$\Delta G(\text{overall}) = -1.36 \log K(\text{overall}) \quad (75)$$

and

$$\Delta G(\text{overall}) = -n(23.06) E(\text{overall}) \quad (76)$$

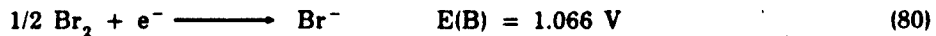
where ΔG values are in kcal/mole and E values are in volts. The equilibrium constant at 25°C for reaction 70 is given by

$$\begin{aligned} \log K(\text{overall}) &= -\Delta G(\text{overall})/1.36 \\ &= +n(23.06/1.36) E(\text{overall}) \\ &= +n(16.96) E(\text{overall}) \end{aligned} \quad (77)$$

Example 7 Calculate the equilibrium constant for the reaction of copper(II) with bromide at 25°C according to the reaction,



The half-reactions that can represent the above reaction are



The overall E value is:

$$E(\text{overall}) = E(A) - E(B) = 0.167 - 1.066 = -0.899 \text{ V} \quad (81)$$

Using equation 77,

$$\begin{aligned} \log K(\text{overall}) &= n(16.96) E(\text{overall}) \\ &= (1)(16.96)(-0.899) \\ &= -15.25 \end{aligned}$$

Since the equilibrium constant is very small (6×10^{-16}), the reaction is highly unfavorable.

Example 8 Calculate the equilibrium constant for the reaction of tetraaquodiamminecobalt(III) ion with bromide, assuming no dissociation of the product cobalt(II) complex. (This is unrealistic, but it represents a useful hypothetical case for comparison with the more realistic Example 9.)

The reaction of interest is



The half reactions are



The overall E is

$$E(\text{overall}) = 1.22 - 1.066 = 0.154$$

Thus, according to equation 77, the equilibrium constant should be

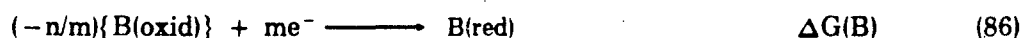
$$\begin{aligned} \log K(\text{overall}) &= +n (16.96) E(\text{overall}) \\ &= (1) (16.96) (0.154) \\ &= 2.61 \end{aligned}$$

The reaction is thus favorable, with an equilibrium constant of 4.07×10^2 .

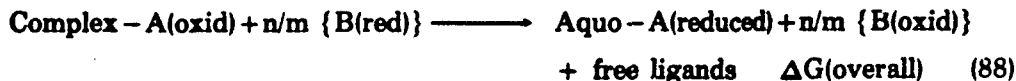
ESTIMATION OF K FOR A REDOX REACTION WITH SUBSEQUENT REACTIONS

Many redox reactions, especially those between complexed metal ions, lead to products that can undergo subsequent dissociation or other reactions after the electron transfer. These subsequent processes can provide additional driving force for the overall reaction to occur (including the redox process).

To illustrate, we shall consider a case where the post-redox reaction is a dissociation of a labile metal complex:



Taken together, these equations represent the overall reaction



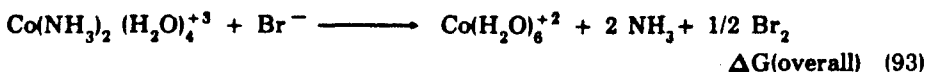
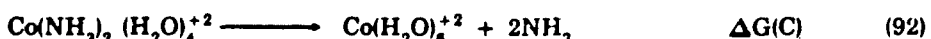
where

$$\Delta G(\text{overall}) = \Delta G(A) - n/m \{\Delta G(B)\} + \Delta G(C) \quad (89)$$

An important aspect of this follow-on reaction is that it can provide sufficient driving force for the overall reaction (equation 88) to proceed, even though the relative free energy changes for reactions 85 and 86 (or relative E° values) indicate that redox will not proceed substantially. The effect is illustrated in Example 9. When the stability constants for the oxidized metal are very large compared with those for the reduced metal, the effect can be much larger than in this example.

Example 9 Calculate the equilibrium constant for the redox reaction in Example 8 between the cobalt diammine aquo complex and bromide, including consideration of the dissociation of the cobalt(II) product into aquo cobalt(II) and NH_3 . (Assume that NH_3 does not undergo any further equilibria.)

The overall reaction is



where

$$\Delta G(\text{overall}) = \Delta G(A) - \Delta G(B) + \Delta G(C) \quad (94)$$

The value of $\Delta G(A)$ is calculated as follows, using equation 8:

$$\begin{aligned} \Delta G(A) &= -n F E(A) \\ &= -1 (23.06) (1.22) \\ &= -28.13 \text{ kcal/mole} \end{aligned}$$

Similarly, the value of $\Delta G(B)$ is:

$$\begin{aligned}\Delta G(B) &= - n F E(B) \\ &= - 1 (23.06) (1.066) \\ &= - 24.58 \text{ kcal/mole}\end{aligned}$$

The value of $\Delta G(C)$ is calculated as follows, using data obtained from Bjerrum[3] for β_2 , the stability constant for the diammine complex of cobalt(II):

$$\begin{aligned}\Delta G(C) &= - 1.36 \log K(C) \\ &= - 1.36 (1/\beta_2) \\ &= - 1.36 (1/3.62) \\ &= - 0.376 \text{ kcal/mole}\end{aligned}$$

Thus, with equation 94,

$$\begin{aligned}\Delta G(\text{overall}) &= - 28.13 + 24.58 + (-0.376) \\ &= - 3.93\end{aligned}$$

Therefore, with equation 77,

$$\begin{aligned}\log K(\text{overall}) &= - \Delta G(\text{overall})/1.36 \\ &= - (-3.93/1.36) \\ &= 2.89\end{aligned}$$

and

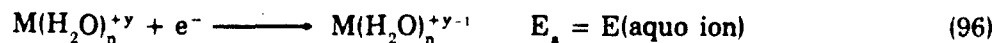
$$K(\text{overall}) = 7.76 \times 10^2$$

ESTIMATION OF E FOR THE HALF-REACTION OF A COMPLEXED ION

Values of the potential for a half reaction as shown for the following equation



can be calculated from the half-reaction potential for the aquo ions



according to the following equation [3]:

$$E_c = E(\text{complexed ion}) = - 0.059[\beta_n(y) - \beta_n(y-1)] + E_a \quad (97)$$

where

E_c = half-reaction potential for the complex ion

E_a = half-reaction potential for the aquo ion

$\beta_n(y)$ = stability constant for the complex ion with the overall charge on the complex of +y

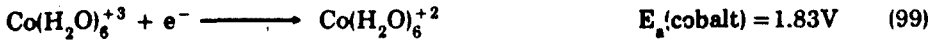
$\beta_n(y-1)$ = stability constant for the complex ion with the overall charge on the complex of y - 1.

The estimate of the half-reaction potential is obviously related to the accuracy of the stability constants used in the calculation.

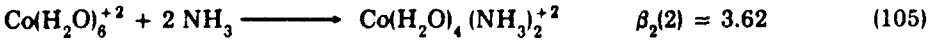
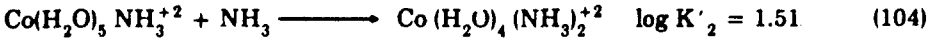
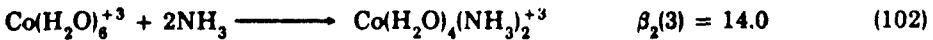
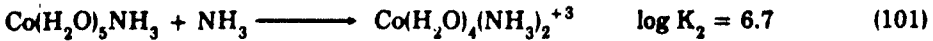
Example 10 Estimate the reduction potential of the following half reaction:



The reduction potential of the aquo ion of cobalt(III) is, according to Bjerrum[3]:



Next we obtain data for the equilibrium constants for the following reactions:



The following data are now used in equation 97:

$$\beta_n(y) = \beta_2(3) = 14.0$$

$$\beta_n(y-1) = \beta_2(2) = 3.62$$

$$E_a = 1.83 \text{ volts}$$

yielding

$$\begin{aligned} E_c(\text{cobalt}) &= -0.059(14.0 - 3.62) + 1.83 \\ &= 1.22 \text{ Volts} \end{aligned}$$

The value has not been experimentally determined [4].

2.10.7 Sources of Redox Data

Values of electrode potentials and equilibrium constants for redox reactions can be found in a variety of articles and compendia such as those given in References 12, 14, 18, and 19. Table 2.10-5 lists values of electrode potentials for a variety of species.

TABLE 2.10-5
Electrode Potentials of Redox Half Reactions*

Oxidation — Reduction Reaction	$E^{\circ}(V)$
$\text{Ag}^{+2} + \text{e}^- \longrightarrow \text{Ag}^+$	+2.00
$\text{Ag}^{+2} + \text{e}^- \longrightarrow \text{Ag(s)}$	+0.799
$\text{Al}^{+3} + 3\text{e}^- \longrightarrow \text{Al(s)}$	-1.66
$\text{Am}^{+4} + \text{e}^- \longrightarrow \text{Am}^{+3}$	+2.40
$\text{H}_3\text{AsO}_4 + 2\text{H}^+ + 2\text{e}^- \longrightarrow \text{HAsO}_2 + \text{H}_2\text{O}$	+0.56
$\text{As(s)} + 3\text{H}^+ + 3\text{e}^- \longrightarrow \text{AsH}_3(\text{g})$	-0.61
$\text{BrO}_3^- + 3\text{H}_2\text{O} + 6\text{e}^- \longrightarrow \text{Br}^- + 6\text{OH}^-$	+0.61
$\frac{1}{2}\text{Br}_2(\text{aq}) + \text{e}^- \longrightarrow \text{Br}^-$	+1.08
$\text{Ce}^{+4} + \text{e}^- \longrightarrow \text{Ce}^{+3}$	+1.74
$\text{ClO}_3^- + 2\text{H}^+ + \text{e}^- \longrightarrow \text{ClO}_2(\text{g}) + \text{H}_2\text{O}$	+1.15
$\text{ClO}_2 + \text{e}^- \longrightarrow \text{ClO}_2^-$	+0.93
$\frac{1}{2}\text{Cl}_2(\text{aq}) + \text{e}^- \longrightarrow \text{Cl}^-$	+1.39
$\text{Co}^{+3} + \text{e}^- \longrightarrow \text{Co}^{+2}$	+1.95
$\text{HCrO}_4^- + 7\text{H}^+ + 3\text{e}^- \longrightarrow \text{Cr}^{+3} + 4\text{H}_2\text{O}$	+1.20
$\text{Cr}^{+3} + \text{e}^- \longrightarrow \text{Cr}^{+2}$	-0.41
$\text{Cu}^{+3} + \text{e}^- \longrightarrow \text{Cu}^{+2}$	+2.3
$\text{Cu}^{+2} + \text{e}^- \longrightarrow \text{Cu}^+$	+0.17
$\text{Cu}^+ + \text{e}^- \longrightarrow \text{Cu(s)}$	-0.52
$\frac{1}{2}\text{F}_2(\text{g}) + \text{e}^- \longrightarrow \text{F}^-$	+2.87
$\text{Fe}^{+3} + \text{e}^- \longrightarrow \text{Fe}^{+2}$	+0.771
$2\text{Hg}^{+2} + 2\text{e}^- \longrightarrow \text{Hg}_2^{+2}$	+0.907
$\text{Hg}_2^{+2} + 2\text{e}^- \longrightarrow 2\text{Hg(l)}$	+0.792
$\frac{1}{2}\text{I}_2(\text{aq}) + \text{e}^- \longrightarrow \text{I}^-$	+0.621
$\text{I}_3^- + 2\text{e}^- \longrightarrow 3\text{I}^-$	+0.536
$\text{MnO}_4^- + \text{e}^- \longrightarrow \text{MnO}_4^{-2}$	+0.57

(Continued)

TABLE 2.10-5

Electrode Potentials of Redox Half Reactions

Oxidation — Reduction Reaction	E° (V)
$\text{MnO}_4^- + 4\text{H}^+ + 3\text{e}^- \longrightarrow \text{MnO}_2(\text{s}) + 2\text{H}_2\text{O}$	+1.68
$\text{MnO}_2(\text{s}) + 4\text{H}^+ + 2\text{e}^- \longrightarrow \text{Mn}^{+2} + 2\text{H}_2\text{O}$	+1.23
$\text{Mn}^{+3} + \text{e}^- \longrightarrow \text{Mn}^{+2}$	+1.488
$\text{Mn}^{+2} + 2\text{e}^- \longrightarrow \text{Mn}(\text{s})$	-1.17
$\text{Mo(VI)} + \text{e}^- \longrightarrow \text{Mo(V)}$	+0.53
$\text{NO}_3^- + 3\text{H}^+ + 2\text{e}^- \longrightarrow \text{HNO}_2 + \text{H}_2\text{O}$	+0.94
$\text{Ni}^{+2} + 2\text{e}^- \longrightarrow \text{Ni}(\text{s})$	-0.25
$\text{O}_2(\text{g}) + 4\text{H}^+ + 4\text{e}^- \longrightarrow 2\text{H}_2\text{O}$	+1.229
$\text{O}_2(\text{g}) + 2\text{H}^+ + 2\text{e}^- \longrightarrow \text{H}_2\text{O}_2$	+0.69
$\text{H}_3\text{PO}_3 + 2\text{H}^+ + 2\text{e}^- \longrightarrow \text{H}_3\text{PO}_2 + \text{H}_2\text{O}$	-0.50
$\text{Pb(IV)} + 2\text{e}^- \longrightarrow \text{Pb}^{+2}$	+1.655
$\text{Pb}^{+2} + 2\text{e}^- \longrightarrow \text{Pb}(\text{s})$	-0.126
$\text{Pu}^{+4} + \text{e}^- \longrightarrow \text{Pu}^{+3}$	+0.967
$\text{Ru}^{+3} + \text{e}^- \longrightarrow \text{Ru}^{+2}$	+0.249
$\text{SO}_4^{-2} + 4\text{H}^+ + 2\text{e}^- \longrightarrow \text{H}_2\text{SO}_3 + \text{H}_2\text{O}$	+0.17
$\text{S}(\text{s}) + 2\text{H}^+ + 2\text{e}^- \longrightarrow \text{H}_2\text{S}$	+0.141
$\text{S}(\text{s, Rhombic}) + 2\text{e}^- \longrightarrow \text{S}^{-2}$	-0.48
$2\text{S}(\text{s}) + 2\text{e}^- \longrightarrow \text{S}_2^{-2}$	-0.49
$3\text{S}(\text{s}) + 2\text{e}^- \longrightarrow \text{S}_3^{-2}$	-0.45
$4\text{S}(\text{s}) + 2\text{e}^- \longrightarrow \text{S}_4^{-2}$	-0.36
$5\text{S}(\text{s}) + 2\text{e}^- \longrightarrow \text{S}_5^{-2}$	-0.34
$6\text{S}(\text{s}) + 2\text{e}^- \longrightarrow \text{S}_6^{-2}$	-0.36
$\text{Sb(V)} + 2\text{e}^- \longrightarrow \text{Sb(III)}$	+0.75
$\text{SeO}_4^{-2} + 4\text{H}^+ + 2\text{e}^- \longrightarrow \text{H}_2\text{SeO}_3 + \text{H}_2\text{O}$	+1.15
$\text{H}_2\text{SeO}_3 + 4\text{H}^+ + 4\text{e}^- \longrightarrow \text{Se}(\text{s}) + 3\text{H}_2\text{O}$	+0.74
$\text{Se}(\text{s}) + 2\text{H}^+ + 2\text{e}^- \longrightarrow \text{H}_2\text{Se}(\text{g})$	-0.37
$\text{Sn(IV)} + 2\text{e}^- \longrightarrow \text{Sn(II)}$	+0.144
$\text{Ti(IV)} + \text{e}^- \longrightarrow \text{Ti(III)}$	+0.130
$\text{Ti}^{+3} + 2\text{e}^- \longrightarrow \text{Ti}^{+1}$	+1.26
$\text{U}^{+4} + \text{e}^- \longrightarrow \text{U}^{+3}$	-0.609
$\text{VO}_2^+ + 2\text{H}^+ + \text{e}^- \longrightarrow \text{V}^{+3} + \text{H}_2\text{O}$	+0.34

a. Gaseous concentrations are in atmospheres.

Source: Kotrlý and Šúcha [12]

2.10.8 Literature Cited

1. Berner, R.A., "Electrode Studies of Hydrogen Sulfide in Marine Sediments," *Geochim. Cosmochim. Acta*, **27**, 563-75 (1963).
2. Berner, R.A., "A New Geochemical Classification of Sedimentary Environments," *J. Sediment. Petrol.*, **51**, 359 (1981).
3. Bjerrum, J., *Metal-Ammine Formation in Aqueous Solution*, P. Haase and Son, Copenhagen, 241 (1941).
4. Bodek, I., "Reactions of *cis*-Tetrasquodiamminecobalt(III) Ion in Aqueous Perchlorate Media," Ph.D. Thesis, Northeastern University (1976).
5. Cannon, R.D. and J. Gardiner, "A Binuclear Intermediate Preceding the Cobalt(III)-Iron(II) Electron Transfer Process," *J. Am. Chem. Soc.*, **92**, 3800 (1970).
6. Carver, R.E., *Procedures in Sedimentary Petrology*, Wiley-Interscience, New York (1971).
7. Cherry, J.A., A.U. Shaikh, D.E. Tallman and R.V. Nicholson, "Arsenic Species as an Indicator of Redox Conditions in Groundwater," *J. Hydrol. (Amsterdam)*, **43**, 373 (1979).
8. Cloke, P.L., "The Geochemical Application of Eh-pH Diagrams," *J. Geol. Educ.*, **14**, 140-48 (1966).
9. Emerson, S., R.E. Cranston and P.S. Liss, "Redox Species in a Reducing Fjord: Equilibrium and Kinetic Considerations," *Deep-Sea Res.*, **26A**, 859-78 (1979).
10. Garrels, R.M. and C.L. Christ, *Solutions, Minerals and Equilibria*, Freeman, Cooper & Co., San Francisco (1965).
11. Hem, J.D., "Reactions of Metal Ions at Surfaces of Hydrous Ion Oxides," *Geochim. Cosmochim. Acta*, **41**, 527-38 (1977), as cited by Emerson [9].
12. Kotrlý, S. and L. Šúcha, *Handbook of Chemical Equilibria in Analytical Chemistry*, John Wiley & Sons, New York (1985).
13. Langmuir, D., "Eh-pH Determinations," Chapter 26 in Carver [6].
14. Latimer, W.M., *Oxidation Potentials*, 2nd ed., Prentice-Hall, New York (1952).
15. Lindberg, R.D. and D.D. Runnels, "Groundwater Redox Reactions: An Analysis of Equilibrium State Applied to Eh Measurements and Geochemical Modeling," *Science*, **225**, 925 (1984).
16. Plummer, L.N., B.F. Jones and A.H. Truesdell, "WATEQF — A Fortran IV Version of WATEQ — A Computer Program for Calculating Chemical Equilibrium of Natural Waters," *Water-Resour. Invest. (U.S. Geol. Surv.)*, **76-13**, 60 (rev. and reprinted January 1984).
17. Pourbaix, M., *Atlas of Electrochemical Equilibria in Aqueous Solutions*, Pergamon Press, Oxford, England (1966).
18. Sillén, L.G. and A.E. Martell, *Stability Constants of Metal-Ion Complexes*, Special Publication No. 17, The Chemical Society, London (1964).
19. Sillén, L.G. and A.E. Martell, *Stability Constants of Metal-Ion Complexes — Supplement No. 1*, Special Publication No. 25, The Chemical Society, London, 64 (1971).

20. Stumm, W., "Redox Potentials as an Environmental Parameter: Conceptual Significance and Operational Limitations," *Adv. Water Pollut. Res., Proc. Int. Conf. 3rd, 1966 (Munich)*, 1, 283 (1967).
21. Truesdell, A.H., "The Advantage of Using pE Rather than Eh in Redox Calculations," *J. Geol. Educ.*, 16, 17-20 (1968).
22. Whitfield, M., "Thermodynamic Limitations on the Use of the Platinum Electrode in Eh Measurements," *Limnol. Oceanogr.*, 19, 857 (1974).
23. Wilkins, R.G., *The Study of Kinetics and Mechanism of Reactions of the Transition Metal Complexes*, Allyn and Bacon, Boston (1974).

2.11 SOLUBILITY AND PRECIPITATION EQUILIBRIA

2.11.1 Introduction

In studies of environmental water quality, the question often arises as to whether a given solid is likely to dissolve and, if so, how much. Likewise, investigators often want to know if a solid phase can precipitate from a water of given composition and what the chemical consequences would be. Such questions can often be resolved through consideration of the chemical equilibria between solids and aqueous solutions.

On a macroscopic scale of observation, a solution saturated with respect to a substance neither dissolves more of the substance nor precipitates it. Put in different terms, the solution contains dissolved species in a state of thermodynamic equilibrium with the solid phase — or, at least, with some of the components of that phase. Departures from equilibrium may occur either in a direction of supersaturation or of undersaturation. Such departures may be caused by changes in the environmental characteristics of the system, as well as by a variety of internal chemical processes. When precipitation occurs in a supersaturated solution, the solution is brought towards saturation or equilibrium "from above." In contrast, dissolution may occur in an undersaturated solution that comes in contact with a particular solid phase, bringing the solute concentration towards saturation "from below." Thus, the state of a chemical thermodynamic equilibrium between a solid and an aqueous solution indicates two environmentally important quantities:

- (1) The current state of the water, with respect to its ability either to dissolve or precipitate certain solids, and
- (2) The expected limits of change in concentrations of dissolved substances, if certain solid phases were to dissolve in, or precipitate from, the water.

This chapter addresses chemical equilibria between inorganic solids and aqueous solutions. Although it is practically impossible to find an inorganic solid whose solubility in water is truly zero, not every class of inorganic solids coming in contact with waters in the environment can be considered in this chapter. Excluded from the discussion of the solid-solution equilibria are pure metals, alloys, glasses, and other industrial solids of complex composition whose chemical behavior in the environmental context usually falls outside the field of the solid-solution equilibria. The focus is on substances that can be broadly classified as ionic or partially ionic solids, such as metal oxides, hydroxides, halides, sulfides, and other compounds with anions in oxidized states (sulfates, carbonates, arsenates, selenites, selenates, and a number of silicate and aluminosilicate minerals).

The environmental importance of the classes of compounds listed above is twofold: (1) for some substances, dissolution in natural waters may never reach saturation, although they will constitute a lasting environmental load on the water systems; and (2) for others, their metallic and anionic components may enter solution from different sources to create a condition of supersaturation with respect to solids that may

eventually precipitate. The examples in this chapter deal primarily with solid-solution equilibria involving heavy-metal ions,¹ alkali metal ions, and alkaline earth ions among the cationic components of the solids.

This chapter also addresses the following issues:

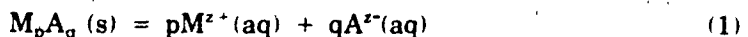
- Definitions of the solubility product, K_{sp} , and the equilibrium constant, K ;
- Establishment of either undersaturated, saturated, or supersaturated conditions by the criteria of ion-concentration product and ion-activity product;
- Effects of temperature and pressure on solubility;
- Effects of ionic strength, pH, and complexation on solubility;
- Effects of particle size on solubility; and
- Estimation of the solubility values (K_{sp} or K) from the free energy of formation, and from empirical correlations between solubilities and such crystal properties as electronegativities of the ions in the lattice, lattice energy, ionization potentials, and interfacial energies of solids.

The process of adsorption at solid-liquid interfaces is discussed in Section 2.12 (Attenuation on Soils). Other important solid precipitation processes (e.g., co-precipitation) and dissolution of impure phases (e.g., trace element leaching) are not easily described mathematically and thus their discussion has been left to books and articles which focus on them.

2.11.2 Description of Property

SOLUBILITY PRODUCT (K_{sp})

A solid made of a metal ion (M) and an anionic ligand (A) dissolves in solution and dissociates according to an overall reaction that can be written as



where (s) denotes a solid phase, (aq) denotes an aqueous species, p and q are stoichiometric coefficients, and z^+ and z^- are the positive and negative valence electrical charges. The principle of electrical neutrality of the ions in solution requires a charge balance between the positively and negatively charged species:

$$pz^+ + qz^- = 0$$

1. Heavy metals are those with atomic numbers between 21 (scandium) and 92 (uranium). Within this series, the transition elements, such as As and Se, and the heavy halogens (atomic numbers 33-36, 52-54, 85-86) are not heavy metals. Aluminum (atomic number 13), although not a heavy metal in the physical sense, is included in many environmental chemical studies of the heavy metals in water, probably because its low abundance and potential toxicity are similar to those of the trace heavy-metals.

A solution is said to be saturated with respect to the solid M_pA_q when the solubility product (K_{sp}), defined as follows, is maintained in solution:

$$K_{sp} = [M]^p[A]^q \quad (\text{mol}^{p+q}/\text{liter}^{p+q}) \quad (2)$$

where the brackets [] denote concentrations of the species in solution. In equation 2, concentrations of M and A are given in moles per liter (abbreviated M). Another unit of concentration in common use is moles per kg H_2O , known as molality. The differences between mol/liter and mol/kg H_2O can often be neglected for dilute solutions (i.e., concentrations of fractions of a mole per liter or per kg H_2O). At higher concentrations, such as in natural saline brines, the differences between molar and molal concentrations must generally be considered for accurate results.

EQUILIBRIUM CONSTANT (K)

A more accurate definition of a state of saturation or equilibrium between a chemical species in a solid phase and in an aqueous solution is based on the concept of the chemical potential and the concept of the thermodynamic activities of the reactant and product species. (The activities of aqueous and solid-phase species are defined in section 2.6.) The basic relationship between the activity of a chemical species in solution and its concentration is defined as

$$a_i = \gamma_i m_i \quad (3)$$

where subscript i denotes a chemical species, γ is its activity coefficient, and m is its molal concentration. The value of γ depends on the nature of the ion and its charge, the ionic strength of the solution, the nature of the solvent, and the temperature. Methods for computing ionic activity coefficients are outlined in section 2.6. Activities are dimensionless quantities, referred to $a=1$ in a standard state.

For reaction 1 at equilibrium, the following relationship is obeyed:

$$K = \frac{a_M^p a_A^q}{a_{M_p A_q}} \quad (4)$$

where the equilibrium constant K is defined as a quotient of the activities of the products, raised to the powers of their stoichiometric coefficients, and the activity of the reactant. The reactant, solid phase of composition M_pA_q , is a pure solid. By definition, the activity of a pure solid in a standard state (25°C, 1 atm pressure) is unity, and equation 4 can therefore be written as

$$K = a_M^p a_A^q \quad (5)$$

Thus, for a dissolution equilibrium between a pure solid and its aqueous solution, we consider only the product of the activities of the aqueous species.

The concept of a pure solid, whose activity is defined as unity in a standard state, can be briefly demonstrated by reference to a common substance, such as NaCl. In a solid

phase, NaCl is a pure solid: the proportions of the metal and the anion cannot vary. However, if some of the Cl atoms in the lattice were replaced by Br atoms, a solid of composition $\text{NaCl}_x\text{Br}_{1-x}$ would result. If the proportions of the Cl and Br atoms can vary in the crystal lattice within some limits, then the solid is not a pure solid but a *solid solution* of two components — NaCl and NaBr. In this case, the activities of the solid components are not necessarily unity. Discussion of the solubility of solid solutions is not within the scope of this chapter; for the specialized methods of evaluating the activities of the components in solid phases, texts dealing with this subject should be consulted [10, 21, 30].

Equation 5 for an equilibrium constant can be written in terms of concentrations and the activity coefficients of the species in solution, using equation 3:

$$K = [M]^p [A]^q \gamma_M^p \gamma_A^q \quad (6)$$

Finally, the equilibrium constant K for reaction 1 and the solubility product K_{sp} are interrelated as follows:

$$K = K_{sp} \gamma_M^p \gamma_A^q \quad (7)$$

The values of the activity coefficients (γ) for aqueous species in dilute solutions are usually less than unity. Therefore, K is numerically smaller than K_{sp} — sometimes much smaller, because of the exponents p and q raising the fractional values of γ to a power. Computation of the activity coefficients of aqueous species is described in section 2.6.

CONDITIONS OF EQUILIBRIUM

The conditions of a state of saturation (or equilibrium) in a solution can be defined with the aid of the relationships for K_{sp} and K .

The product of the concentrations of dissolved species on the right-hand side of equation 2 is called the *ion-concentration product* (ICP):

$$\text{ICP} = [M]^p [A]^q \quad (8)$$

In a given solution, the ICP may be less than, equal to, or greater than the value of K_{sp} for the stoichiometrically equivalent solid phase, such as shown in reaction 1. If the ICP is less than K_{sp} , the solution is undersaturated with respect to the solid, and dissolution may take place. If the two quantities are equal, the solution is saturated. If the ICP is greater than K_{sp} , the solution is supersaturated with respect to the solid phase. This can be summarized as follows:

Undersaturation:	$\text{ICP} < K_{sp}$	}
Saturation:	$\text{ICP} = K_{sp}$	
Supersaturation:	$\text{ICP} > K_{sp}$	

(9)

From the definition of K based on activities rather than concentrations (equation 5), the product of the activities of the species in solution is called the *ion-activity product* (IAP):

$$IAP = a_M^p a_A^q \quad (10)$$

Thus, the three states — undersaturation, saturation, and supersaturation — can also be defined in terms of the IAP and the equilibrium constant K as follows:

Undersaturation:	IAP < K	}
Saturation:	IAP = K	
Supersaturation:	IAP > K	

(11)

In very dilute solutions where the activity coefficients (γ_i) are close to unity, the differences between K_{sp} and K may be very small. Thus, the state of a solution with respect to saturation may be defined by either equation 10 or equation 11 without significant loss of accuracy. In more concentrated solutions, particularly in the presence of complexing agents, reliance on the IAP and K criteria should be encouraged; the values of the activity coefficients in such cases (section 2.6) assures consistency and constancy in the value of K for a reaction, whereas the solubility product K_{sp} may vary from one solution to another.

CONCENTRATIONS OF DISSOLVED SPECIES FROM K_{sp}

Solubilities of natural and man-made substances in water vary widely. For some poorly soluble substances, K_{sp} is expressed in high negative powers of 10, while highly soluble solids can have a K_{sp} higher than 10. On the lower end of the solubility scale, values smaller than 10^{-12} mol/liter are encountered; on the upper end, some strongly soluble electrolytes may be characterized by values of about 20 mol/liter.

If the value of K_{sp} for a given solid and its aqueous solution is known, concentrations of the aqueous species may be estimated. In the notation of equilibrium reaction 1, a solid of stoichiometric composition $M_p A_q$ produces in solution a total of p moles of M and q moles of A. Concentrations [M] and [A], both coming from the same solid, are interrelated as follows:

$$[M] = \frac{p}{q} [A] \quad (12)$$

$$[A] = \frac{q}{p} [M] \quad (13)$$

In terms of the anion concentration [A],

$$K_{sp} = \left(\frac{p}{q}\right)^p [A]^{p+q} \quad (14)$$

If the value of K_{sp} is known, the concentration of either the cationic or anionic species in solution at equilibrium with the solid can now be calculated from equation 14:

$$[M] = \left(\frac{p}{q} K_{sp} \right)^{1/(p+q)} \quad (15)$$

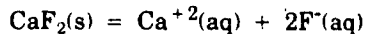
$$[A] = \left(\frac{q}{p} K_{sp} \right)^{1/(p+q)} \quad (16)$$

These equations are valid under conditions where the solutions are of low ionic strength and do not contain any of the ions of interest (i.e., there is no "common ion" effect). In real systems one needs to consider the activity as well as the presence of common ions and thus equation (5) may be more appropriate.

The preceding relationships between K_{sp} , K , and concentrations of the dissolved species are demonstrated below.

Example 1 What are the relationships between the solubility product, equilibrium constant, concentrations, and activity coefficients for fluorite (CaF_2) in pure water containing no Ca^{+2} or F^- at room temperature?

The equilibrium dissolution reaction is:



The solubility product for this reaction at 25°C, in a dilute solution, is [24]:

$$\begin{aligned} K_{sp} &= 10^{-10.31} \\ &= 5.01 \times 10^{-11} \text{ mol}^3/\text{liter}^3 \end{aligned}$$

Concentrations of Ca^{+2} and F^- in solution at equilibrium with solid CaF_2 can be estimated from equations 15 and 16, with $p = 1$ and $q = 2$:

$$\begin{aligned} [\text{Ca}^{+2}] &= 2.32 \times 10^{-4} \text{ mol/liter} \\ [\text{F}^-] &= 4.64 \times 10^{-4} \text{ mol/liter} \end{aligned}$$

For the equilibrium dissolution reaction given above, the value of K at 25°C can be computed from the tabulated data of the free energies of formation of the solid and aqueous species. Such computations are explained in section 2.11.3; here, only the value of K will be given:

$$\begin{aligned} K &= 10^{-10.5} \\ &= 3.22 \times 10^{-11} \end{aligned}$$

This value is slightly smaller than that of K_{sp} , as may be expected from equation 7. Ideally, the values of K_{sp} reported in the literature are the solubility values that were extrapolated to the value at zero ionic strength ($I = 0$), and they are, theoretically, identical to K . In practice, small differences between the reported values of K_{sp} and K often reflect differences between the measurement techniques of the investigators.

Disregarding the differences between K_{sp} and K for the fluorite-water solution equilibrium, concentrations of the calcium and fluoride ions in solution at equilibrium with CaF_2 are (using $K = 3.22 \times 10^{-11}$ in equations 15 and 16):

$$[\text{Ca}^{+2}] = 2.00 \times 10^{-4} \text{ mol/liter}$$

$$[\text{F}^-] = 4.00 \times 10^{-4} \text{ mol/liter}$$

Note that although K_{sp} is about 50% greater than K, the computed concentrations of the calcium and fluoride ions differ only by about 15% when estimated from either the K_{sp} or K values. It should be noted that in natural waters which contain both free and complexed ions, and other ions such that the ionic strength is significantly greater than zero, the calculation would be more complex (see other examples in this section).

Example 2 How would the presence of 0.1 M NaCl in a solution at equilibrium with CaF_2 affect the concentrations of Ca^{+2} and F^- calculated above?

To a good approximation, the ionic strength of the solution will be determined by the NaCl concentration: 0.1 M NaCl is much higher than the values of 10^{-4} to 10^{-3} M derived for Ca^{+2} and F^- in a pure solution. Thus, the ionic strength of the solution is, approximately, $I = 0.1 \text{ M}$. The activity coefficients of the Ca^{+2} and F^- ions at this ionic strength are (see section 2.6 on estimation of the ionic strength):

$$\gamma_{\text{Ca}} = 0.40 \text{ and } \gamma_{\text{F}} = 0.76$$

From equation 7, the solubility product is:

$$K_{sp} = \frac{3.22 \times 10^{-11}}{0.40 \times 0.76^2} = 1.39 \times 10^{-10}$$

From equations 15 and 16, the ionic concentrations of Ca^{+2} and F^- in solution are:

$$[\text{Ca}] = 3.27 \times 10^{-4} \text{ mol/liter}$$

$$[\text{F}] = 6.53 \times 10^{-4} \text{ mol/liter}$$

The results indicate that the solubility of calcium fluoride in the presence of 0.1 M NaCl will be about 40% greater than its solubility in pure water.

DEGREE OF SATURATION

The preceding two sections (equations 2, 8 and 9) showed how the conditions of either an equilibrium or a non-equilibrium were defined by means of the relationships between the solubility product K_{sp} and the ion-concentration product ICP. It is useful to introduce a parameter (Ω) defining the degree of saturation of a solution as the following quotient:

$$\Omega = \frac{\text{ICP}}{K_{sp}}$$

$$= \frac{[\text{M}]^p [\text{A}]^q}{[\text{M}]_{eq}^p [\text{A}]_{eq}^q} \quad (17)$$

where subscript eq denotes concentrations of the aqueous species in a solution at equilibrium with the solid of composition M_pA_q .

Instead of the two aqueous species in the above equation, only one can be used, if the concentration value of the other is expressed as in equation 12 or 13. Thus, the degree of saturation, written in terms of the metal-ion concentration [M], becomes

$$\Omega = \left(\frac{[M]}{[M]_{eq}} \right)^{p+q} \quad (18)$$

In an undersaturated solution, $\Omega < 1$, and at equilibrium, $\Omega = 1$; this is analogous to the definitions of undersaturation, saturation, and supersaturation in relationships 9 (for concentrations) and 11 (for activities).

EFFECT OF TEMPERATURE ON SOLUBILITY

The effect of temperature on solubility of a solid can be expressed by a relationship between the equilibrium constant, temperature, and the standard enthalpy change of the reaction. Over relatively small ranges of temperature, when the standard enthalpy of a reaction at equilibrium remains approximately constant, the dependence of K on temperature is given by the following:

$$\log \frac{K_2}{K_1} = -\frac{\Delta H_r^0}{2.3R} \left(\frac{1}{T_1} - \frac{1}{T_2} \right) \quad (19)$$

where ΔH_r^0 is the standard enthalpy of the reaction, R is the gas constant, and K_1 and K_2 are the equilibrium constants at temperatures T_1 (K) and T_2 (K), respectively.

The algebraic sign of ΔH_r^0 determines whether solubility, as expressed by the value of K, will increase or decrease if $T_2 > T_1$. To an order of magnitude, a 40°C rise in temperature increases or decreases the value of the equilibrium constant K by a factor of about 2. This approximation is based on the following considerations. For many inorganic solids, the change in the standard enthalpy of dissolution at equilibrium is of the order of a few kilocalories per mole; ± 5 kcal/mol would be a reasonable estimate. The sources of data on ΔH_r^0 are the same as those for the standard free energies of formation, as detailed in § 2.11.5. At ambient temperatures, the value of $1/T_1 - 1/T_2$ for a change of 40°C is approximately 4×10^{-4} deg⁻¹. Substitution of the above estimate of ΔH_r^0 , the reciprocal temperature difference term, and the value of the gas constant ($R \approx 2 \times 10^{-3}$ kcal mol⁻¹ deg⁻¹) in equation 19 gives

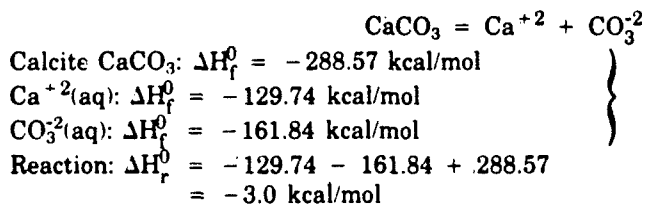
$$\log K_2/K_1 \approx \pm 0.4$$

Therefore, K_2 may range from $0.4K_1$ to $2.5K_1$.

An illustration of a use of equation 19 is given in the following example.

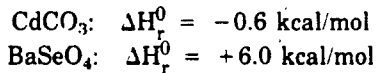
Example 3 How are temperature changes likely to affect the equilibrium solubilities of the following three solids in water: calcium carbonate (CaCO_3 , calcite), cadmium carbonate (CdCO_3), and barium selenate (BaSeO_4)?

For each of the three solids, an equilibrium dissolution reaction should be written, values of the standard enthalpies of formation (ΔH_f^0) obtained from the literature (see section 2.11.5), and the standard enthalpy change for the reaction computed. This procedure is illustrated below for CaCO_3 .



Source: Robie *et al.* [22]

Similar computations of ΔH_r^0 for the reactions at equilibrium with the two other solids, using the data from reference 22, give the following results:



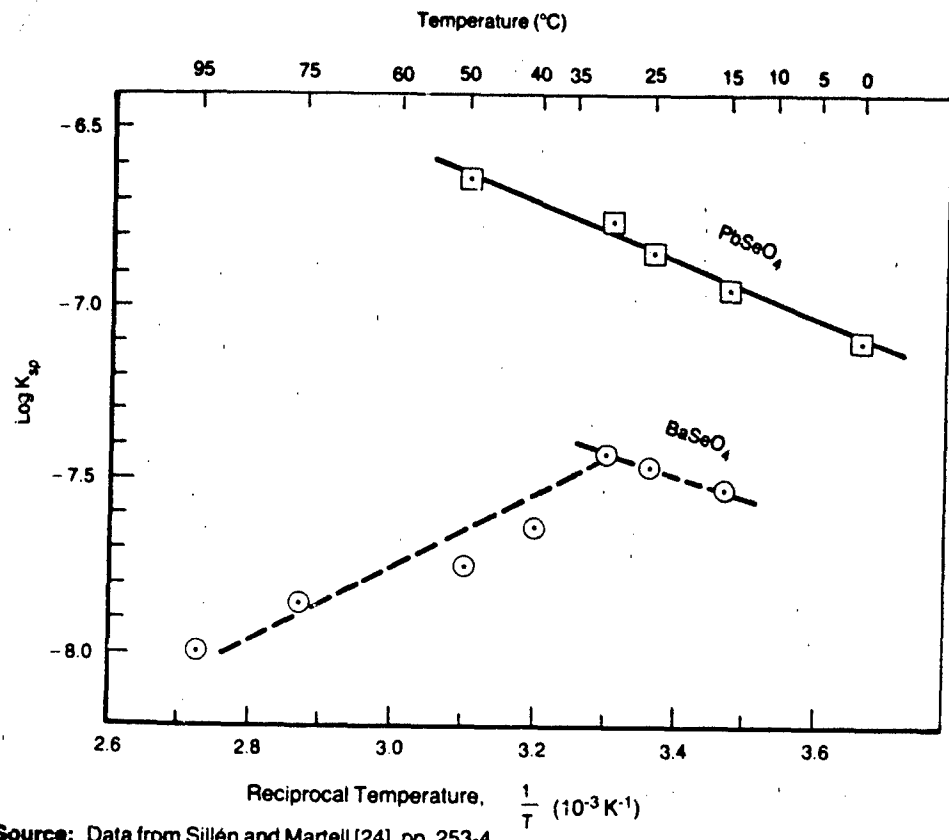
The values of the enthalpy change for the three solids should be considered in the context of the algebraic sign of the right-hand side of equation 19. The positive value of ΔH_r^0 for BaSeO_4 indicates that the solubility product will be higher at a higher temperature. For CdCO_3 , the change in ΔH_r^0 is small, so there will be only a small change in K with a changing temperature. For calcite, the negative value of ΔH_r^0 indicates that the solubility of CaCO_3 will decrease with increasing temperature.

The above statement regarding the solubility of calcite in water is confirmed by experimental data. For BaSeO_4 , experimental data (Figure 2.11-1) also affirm that its solubility increases by an amount corresponding to a value of $\Delta H_r^0 \approx +6 \text{ kcal/mol}$, but only up to 35°C. From 35° to 95°C the solubility decreases, possibly indicating a change in the reaction mechanism. The solubility of another selenate phase, PbSeO_4 , is also plotted in Figure 2.11-1; these values increase by a factor of about 2.5 with a temperature increase of 50°C.

In general, if the solubility values determined at a series of temperature points form a straight line in a graph of $\log K$ against $1/T$, it indicates that ΔH_r^0 for the reaction remains constant within the experimental accuracy of the data.

EFFECT OF PRESSURE ON SOLUBILITY

Under most environmental conditions, the pressure is around 1 atmosphere; much higher values are found in nature only far below a water surface or beneath an overburden of crustal rocks. An increase in the pressure by 1 atm is equivalent to the pressure under a column of water 10 m high or a column of rock about 3.5 m thick. Thus, the pressure at the bottom of one of the bigger lakes of the North American continent, Lake Superior, is only about 40 atm, as the maximum depth of the lake is about 400 m.



Source: Data from Sillén and Martell [24], pp. 253-4

FIGURE 2.11-1 Solubilities of $BaSeO_4$ and $PbSeO_4$ as a Function of Temperature

In general, the effect of pressure on the solubility of minerals and inorganic solids in water is small, and it is relatively much smaller than the effect of temperature within the limits of its variation in the environment. The dependence of solubility, as represented by the equilibrium constant K of a reaction, such as equation 1, is given by the following relationship:

$$\log \frac{K_2}{K_1} = - \frac{\Delta \bar{V}_r^0}{2.3RT} (P - 1) \quad (20)$$

where K_2 and K_1 are the values of the equilibrium constant at pressures P and 1 atm respectively, R is the gas constant, and T is absolute temperature. $\Delta \bar{V}_r^0$ is the standard volume change for the reaction; sources of data on the molar volumes of solids and aqueous species are given in section 2.11.5.

The relatively small effect of pressure on solubility under environmental conditions can be illustrated by the following consideration. The standard volume change in dissolution reaction at equilibrium is usually a negative quantity, typically about $-40 \text{ cm}^3/\text{mol}$ [19].

To estimate the increase in the equilibrium constant caused by an increase in pressure from 1 to 100 atm, the following values are substituted in equation 20:

$$\begin{aligned}\Delta\bar{V}^0 &\approx -40 \text{ cm}^3 \text{ mol}^{-1} \\ R &\approx 82 \text{ atm cm}^3 \text{ mol}^{-1} \text{ deg}^{-1} \\ T &\approx 300 \text{ K} \\ P &\approx 100 \text{ atm}\end{aligned}$$

The result is:

$$\log \frac{K_2}{K_1} \approx 0.07$$

or, alternatively,

$$K_2 \approx 1.17 K_1$$

This indicates an increase in the equilibrium constant K of 17%. For the individual species in solution at equilibrium with a solid, the increase in their concentrations will be even smaller, as can be estimated from equations 15 and 16.

Pressures of several tens or hundreds of atmospheres, which are very high by environmental standards, are not likely to produce any significant changes in the molar volumes of many minerals and inorganic solids. A measure of the volume change of a solid, due to pressure, is its compressibility. Near room temperature, compressibilities of the more common minerals and inorganic solids are so small that a 1% change in volume requires pressures of an order of thousands to tens of thousands of atmospheres.

Solids that formed at higher pressures are, in general, more soluble than the low-pressure phases of identical composition at the same temperature [16]. Phase transformation in the solid state at environmental temperatures may be caused by strong mechanical stresses, either natural or man-made.

EFFECT OF PARTICLE SIZE ON SOLUBILITY

Very small particles have large surface areas in relation to their volumes. The energy needed to form that surface in the process of nucleation of the particle can amount to a substantial contribution to the total free energy of formation of the small particle. Thus, in principle, very small particles are more soluble than larger ones, because the free energy of formation of the small particles is higher [29, 30].

The increase in solubility of a particle of small size, or of small diameter, relative to one whose surface has "an infinitely large" radius of curvature, is given by the following relationship:

$$\log \frac{K_r}{K} = \frac{4\sigma V}{2.3RTd} \quad (21)$$

where K = equilibrium constant for solubility of the bulk solid

K_r = equilibrium constant for the small particle

d = linear dimension of the small particle (diameter of spherical particle or edge length of a cube)

σ = interfacial energy² of small particle surface in solution, in units of energy per unit area

V = molar volume of the solid

R = gas constant

T = temperature (K)

(Units of all parameters are given in Example 4.)

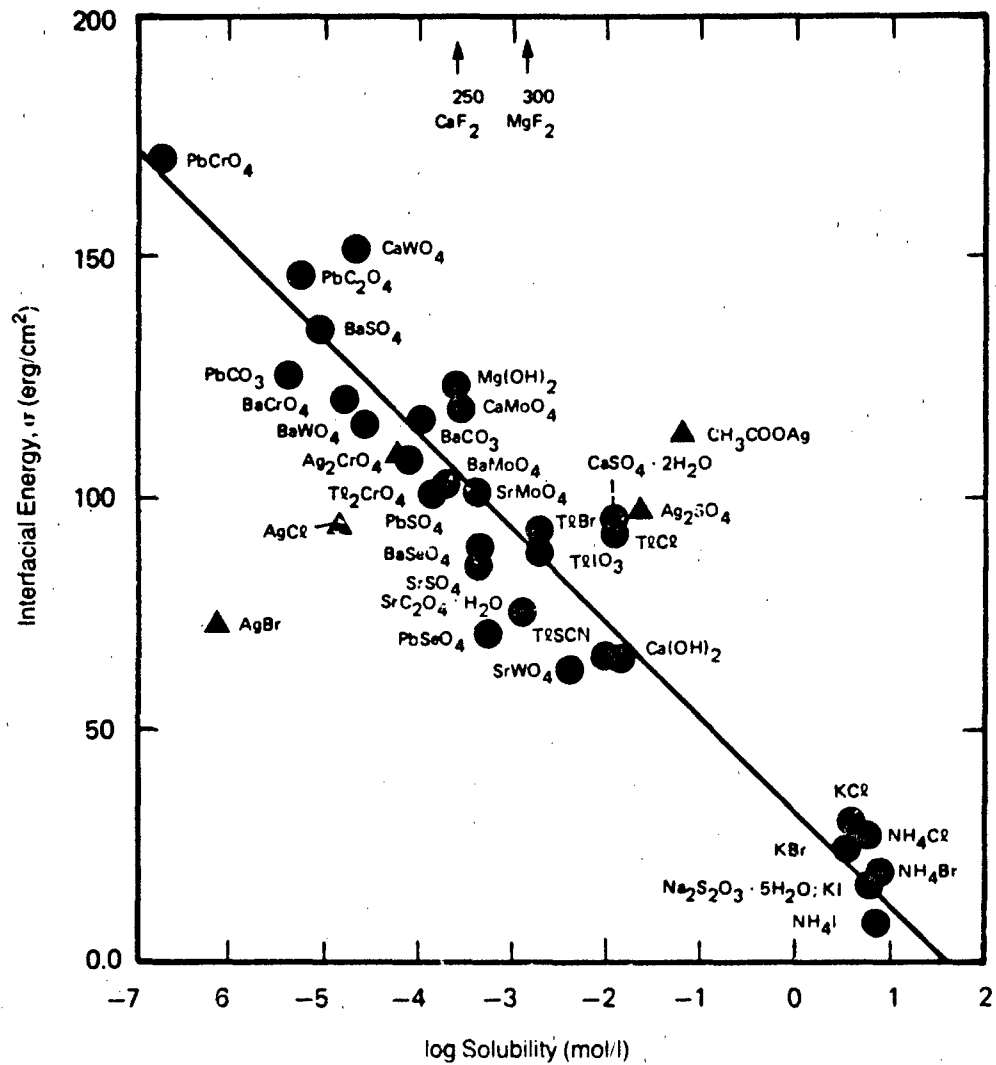
Equation 21 is valid for spheres or cubes. For other shapes, the factor 4 in the numerator will change, but the present form of the equation is adequate for many of the cases of interest, where the particle sizes are of primary concern.

Equation 21 shows that the solubility of small particles increases exponentially as the particle size and density of the solid decrease (i.e., smaller d and larger V). In general, as shown in Example 4 below, the effect of solid solubility becomes pronounced for particles smaller than about 100 Å in diameter (10^{-6} cm or 0.01 micron; for comparison, the diameters of atoms in crystal lattices are roughly 2–4 Å).

Our ability to estimate the solubility of very small particles of a given solid hinges on the availability of data on the interfacial energy (σ). Figure 2.11-2 gives this information for many minerals and inorganic solids in aqueous solutions. Note that solids of higher solubility are characterized by lower values of σ and that the limiting value of zero surface energy ($\sigma = 0$) corresponds to a solubility of 40 mol/liter.

A change in the solution composition owing to the presence of other dissolved species may affect the value of the interfacial energy reported for a solid phase in its saturated aqueous solution. For some oxides and hydroxides, errors in the measured values of the interfacial energy were reported as ±25–50% [23]. (Additional values of interfacial energies in aqueous solutions at 25° and 70°C are summarized in Table 2.11-1.) For the solids shown in Figure 2.11-2, the interfacial energies in solution cluster mostly within the range from 50 to 150 erg/cm² (equivalent to about 0.5 to 2 kcal/mol for particles of 100 Å diameter).

2. This quantity is sometimes referred to in the literature as "interfacial tension" or "surface energy."



Source: Nielsen [20]. (Copyright 1983, John Wiley & Sons. Reprinted with permission.)

FIGURE 2.11-2 Correlation of Interfacial Tension of Solids in Solution with Their Solubility

TABLE 2.11-1
Interfacial Energies of Oxides and Hydroxides in Aqueous Solutions

Solid	Solution Composition	Temperature (°C)	Interfacial Energy, σ (erg/cm ²)	Source
ZnO	0.2M NaClO ₄	25	770 ± 330	[23]
CuO			690 ± 150	
Cu(OH) ₂			410 ± 130	
α -Fe ₂ O ₃	?	70	770	Ferrier (1966), cited in [15]
α -FeOOH			1250	

Example 4 What is the maximum size of particles of barium molybdate ($BaMoO_4$) that may produce in solution a supersaturation of a factor of two?

"Supersaturation of a factor of two" means that the solubility product (or the equilibrium constant) of the small particles would be twice that of the bulk phase. Thus, we seek to determine from equation 21 the particle diameter (d) that corresponds to the following increase in solubility:

$$\frac{K_r}{K} = 2 \quad \text{or} \quad \log \frac{K_r}{K} = 0.3$$

The values of the other parameters needed are:

$$V = \text{mol.wt./density}$$

$$= \frac{297.28 \text{ g/mol}}{4.65 \text{ g/cm}^3} \quad (\text{from Weast [33]}) \\ = 63.9 \text{ cm}^3/\text{mol}$$

$$\sigma = 100 \text{ erg/cm}^2 \quad (\text{from Figure 2.11-2})$$

$$R = 8.31 \times 10^7 \text{ erg mol}^{-1} \text{ deg}^{-1}$$

$$T = 300 \text{ K} \quad (\text{assumed for this example})$$

Substitution of the above values in equation 21 gives:

$$d = \frac{4 \times 100 \times 63.9}{0.3 \times 2.3 \times 8.3 \times 10^7 \times 300} \\ = 1.49 \times 10^{-6} \text{ cm} \quad \text{or} \quad 149 \text{ Å}$$

As an approximation, concentrations of the Ba^{+2} and MoO_4^{2-} ions at equilibrium with the small particles can be estimated by equations 15 and 16, with $p = 1$ and $q = 1$. Writing $[\text{Ba}]_r$ for the barium concentration at equilibrium with the small particles and $[\text{Ba}]$ for its concentration at equilibrium with the bulk solid BaMoO_4 , we have:

$$\frac{[\text{Ba}]_r}{[\text{Ba}]} = \left(\frac{K_r}{K} \right)^{1/2}$$

$$= 2^{1/2} = 1.41$$

Thus, the concentrations of barium and molybdate in solution at equilibrium with the small particles would be about 40% higher than the concentrations at equilibrium with the bulk solid phase.

EFFECTS OF SOME SOLUTION PROPERTIES ON SOLUBILITY

Two characteristics of natural waters may have pronounced effects on the solubilities of solids: (1) the presence of complexing agents in solution, and (2) the acidity (pH) of the solution. Both of these characteristics are briefly discussed with the aid of examples in this section.

Solubility in the Presence of Complexing Ions

Inorganic and organic ions in solution tend to form a great variety of charged and neutral complexes among themselves. Manual calculation of the effect of a given complexing (or chelating) agent in solution on the solubility of a given solid can be difficult, because of the many association or dissociation equilibria that must be considered. Anyone extensively involved with the problems of chemical speciation in solution and its effects on the solubilities of different solids should acquire a familiarity with the computer methods available for solving these problems. The field is extensively covered by a number of textbooks and reference works, some of which are listed in section 2.11.5 of this chapter and others in section 2.13.

Example 5 At an equilibrium between CaF_2 and its aqueous solution, does calcium form significant concentrations of complexes with any of the negatively charged ions?

In water free of dissolved CO_2 and closed to the atmosphere, dissolution of CaF_2 is likely to produce at least the following species in solution: Ca^{+2} , H^+ , F^- , OH^- , and two ionic complexes — CaF^+ and CaOH^+ . (If the system contained dissolved CO_2 , one would include such complexes as CaHCO_3^+ and CaCO_3^0 .)

The solubility product of CaF_2 and the association constants for the complexes CaF^+ and CaOH^+ in solution are as follows:

$$[\text{Ca}^{+2}][\text{F}^-]^2 = K_{sp}; \quad K_{sp} = 5 \times 10^{-11} \quad [24] \quad (22)$$

$$\frac{[\text{CaF}^+]}{[\text{Ca}^{+2}][\text{F}^-]} = K_1; \quad K_1 = 10 \quad [3] \quad (23)$$

$$\frac{[\text{CaOH}^+]}{[\text{Ca}^{+2}][\text{OH}^-]} = K_2; \quad K_2 = 25 \quad [3] \quad (24)$$

At equilibrium between CaF_2 and its aqueous solution, a condition of electroneutrality or charge balance must be maintained for the ions in solution:

$$2[\text{Ca}^{+2}] + [\text{CaF}^+] + [\text{CaOH}^+] + [\text{H}^+] = [\text{F}^-] + [\text{OH}^-] \quad (25)$$

Having set the equation for the charge balance in solution, we have six unknowns — the concentrations of the six aqueous species above — but only four equations. A further simplification can be made: in nearly neutral solutions, the terms $[\text{H}^+]$ and $[\text{OH}^-]$ are nearly equal, so they cancel out of equation 25:

$$2[\text{Ca}^{+2}] + [\text{CaF}^+] + [\text{CaOH}^+] = [\text{F}^-] \quad (26)$$

There remain five unknowns in four equations (22, 23, 24 and 26). Consecutive substitution of equations 22-24 in equation 26 gives a final equation in terms of the fluoride-ion concentration, hydroxyl-ion concentration (or activity), and the stability constants:

$$[\text{F}^-]^3 - K_1 K_{sp}[\text{F}^-] - K_2 K_{sp}[\text{OH}^-] - 2K_{sp} = 0 \quad (27)$$

Substituting the numerical values of the solubility product and the stability constants in this equation gives

$$[\text{F}^-]^3 - 5 \times 10^{-10} [\text{F}^-] - 12.5 \times 10^{-10} [\text{OH}^-] - 1 \times 10^{-10} = 0 \quad (28)$$

The value of $[\text{OH}^-]$, usually taken as $\text{pOH} = 14 - \text{pH}$, can be measured more easily than the fluoride or calcium-ion concentration. For any reasonable value of pOH , except for the conditions of extreme alkalinity ($\text{pOH} < 2$ or $\text{pH} > 10$), the $[\text{OH}^-]$ -containing term in equation 28 is negligible in comparison with the last term, 1×10^{-10} . Thus, the equation to be solved for the unknown fluoride-ion concentration becomes:

$$[\text{F}^-]^3 - 5 \times 10^{-10} [\text{F}^-] - 1 \times 10^{-10} = 0 \quad (29)$$

A solution that reasonably satisfies this equation can be obtained by trial and error, substituting numerical values for $[\text{F}^-]$:

$$[\text{F}^-] = 4.64 \times 10^{-4} \text{ mol/liter}$$

This result is practically identical to the fluoride-ion concentration at equilibrium with CaF_2 obtained in Example 1. The fraction of the fluoride-ion in solution that is tied up in complexes must therefore be very small and, consequently, the concentration of the ion-complex CaF^+ must be very low.

As the small effects due to the ionic strength on concentrations at equilibrium in a dilute solution are disregarded in this example, concentrations of the two ionic complexes with calcium will be computed. From equation 22, the calcium-ion concentration is

$$\begin{aligned} [\text{Ca}^{+2}] &= (5 \times 10^{-11}) / (4.64 \times 10^{-4})^2 \\ &= 2.32 \times 10^{-4} \text{ mol/liter} \end{aligned}$$

The concentration of the CaF^+ complex is, from equation 23 and the preceding results,

$$\begin{aligned} [\text{CaF}^+] &= 10 \times 2.32 \times 10^{-4} \times 4.64 \times 10^{-4} \\ &= 1.08 \times 10^{-6} \text{ mol/liter} \end{aligned}$$

For the complex CaOH^+ , a value of the hydroxyl-ion concentration in solution must be known. At pH = 7, we have

$$[\text{H}^+] = [\text{OH}^-] = 10^{-7}$$

and the ion-complex concentration from equation 24 and the above value of $[\text{Ca}^{+2}]$ is

$$\begin{aligned} [\text{CaOH}^+] &= 25 \times 2.32 \times 10^{-4} \times 1 \times 10^{-7} \\ &= 5.8 \times 10^{-10} \text{ mol/liter.} \end{aligned}$$

From the preceding results, it follows that the concentration of the ion-complex CaOH^+ at a solution pH of 7 is negligibly small in comparison to the concentrations of the other species. The concentration of the other ionic complex, CaF^+ , is somewhat higher, but it also amounts to only a very small fraction of either the calcium-ion or fluoride-ion concentration: $[\text{CaF}^+]$ represents about 0.5% of the calcium ion in solution and about 0.25% of the fluoride ion.

The answer to the question posed by this example is that the aqueous complexes of the calcium and fluoride species at equilibrium with CaF_2 in a closed system are present at concentrations that are negligible for most practical purposes.

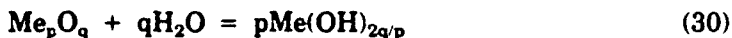
The pH and Solubility of Oxides

Hydrogen ion activity in solution is one of the more easily measurable characteristics. Therefore, chemical reactions are often studied by observing changes in rate with solution pH. Experimentally, the pH of a solution can usually be controlled by addition of acids, alkalis or buffers. Thus, in the laboratory, pH is regarded as one of the main or master environmental variables.

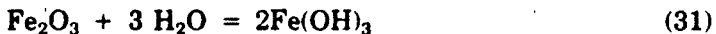
In natural systems, however, the pH of water solutions is often determined by numerous and complex reactions involving minerals and organic materials, as well as some of the atmospheric gases. Controlling the pH of a solution in a large tank, of a sludge in a large basin, or of water in a lake or stream is not as simple as in a glass vessel indoors. Moreover, the pH in an environmental system consisting of several solids and water may not be easily and simply estimated from one or more equilibrium reactions. The extensive buffering of natural water systems by chemical reactions that are not always fully understood makes one look at the pH of such systems as one of their characteristic parameters, rather than as a master variable that changes in a predictable manner, such as the temperature of the environment.

Despite these difficulties, pH is an important and useful characteristic of aqueous solutions, even if only due to our accumulated knowledge of the role of hydrogen-ion concentration in equilibrium solubility reactions.

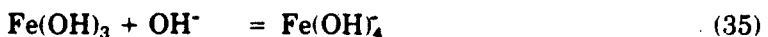
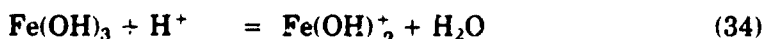
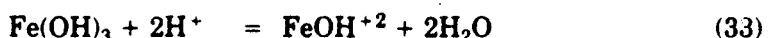
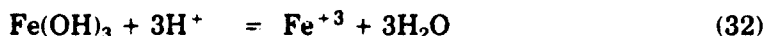
A metal oxide of general composition Me_pO_q , where p and q are the stoichiometric coefficients, can react with water to produce a solid metal-hydroxide:



Considering a Fe^{III} -oxide of composition Fe_2O_3 , the preceding general formula of a hydration reaction becomes



Dissolution of a metal hydroxide in water and establishment of equilibrium between the solid and solution involve some or all of the following types of reactions:



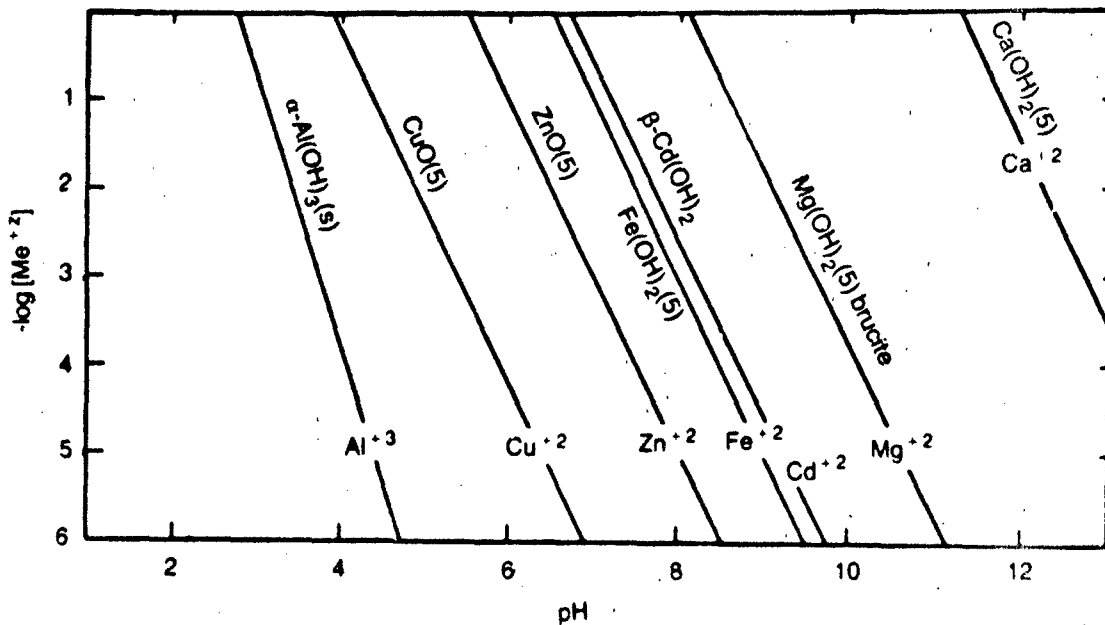
The preceding four equilibria show a dissolved species of iron as a product and the hydrogen or hydroxyl-ion as one of the reactants. From the known values of the equilibrium constants of each of the four reactions, the concentrations of ferric ion and of the other iron complexes can be estimated for various values of the pH. The same procedure applies to other metal hydroxides at equilibrium with their aqueous solutions, in the absence of any chelating agents that could form additional complexes with the dissolved iron species.

Figure 2.11-3 shows concentrations of metal ions as a function of the solution pH for reactions such as equation 32. The steeper the slope of the lines, the greater is the response of concentration to change in the pH of the solution. The response is greater for cations of higher valence.

A different representation of certain oxide and hydroxide solubilities is shown in Figure 2.11-4. The concentration of the dissolved metal as a function of the pH is high in acidic solutions, goes through a minimum in slightly acidic to mildly alkaline solutions, and increases again in strongly alkaline media.

Different sections of the solubility curves represent regions of dominance of one of the dissolved species. In acidic solutions, free ferric ion Fe^{+3} is the dominant species, but in alkaline solutions, the negatively charged Fe(OH)_4^- predominates.

The pH regions where the minima of the solubility curves occur should be noted, as they help explain the differences in the solubility and precipitation behavior of metal hydroxides in general.



Source: Stumm and Morgan [29]. (Copyright 1981, Wiley-Interscience. Reprinted with permission.)

FIGURE 2.11-3 Free Metal-Ion Concentration in Equilibrium with Solid Oxides or Hydroxides. (The occurrence of hydroxo metal complexes must be considered for evaluation of complete solubility)

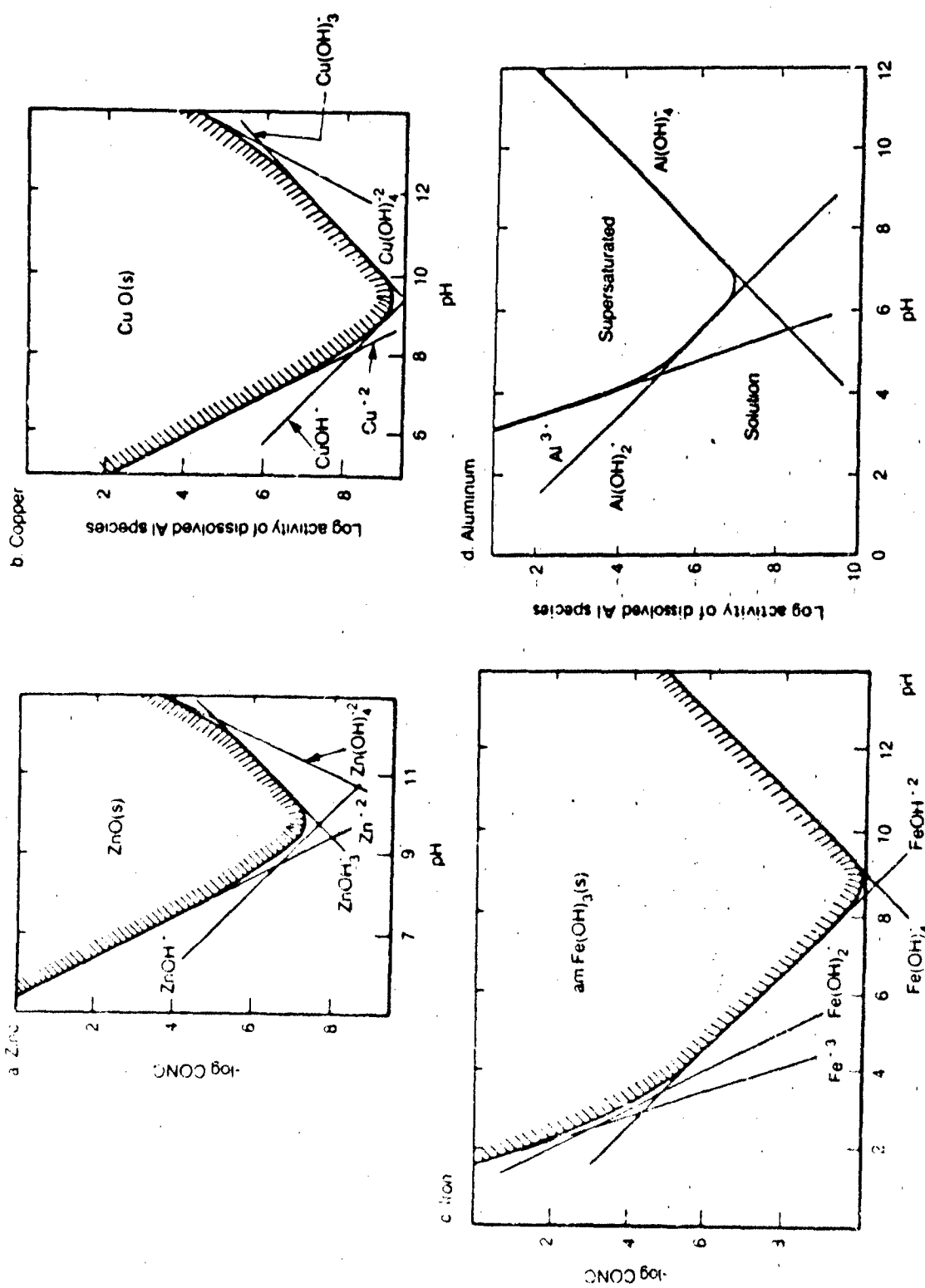
Other more complex and detailed correlations between the solubilities of metal oxides and hydroxides, and the stability constants of their aqueous complexes, are given by Stumm and Morgan [29] and by Baes and Mesmer [2].

2.11.3 Estimation of Equilibrium Constant K and Solubility

INTRODUCTION

The preceding sections of this chapter showed how the values of a solubility product K_{sp} and an equilibrium constant K can be used to estimate concentrations of the species in solution at equilibrium with a solid. For determining the solubilities of solids, K is an important parameter whose generality and usefulness are far broader than those of K_{sp} ; the latter depends on the chemical composition and the ionic strength of the solution, as shown by the relationship between K and K_{sp} in equation 7.

To reiterate briefly, the essentials of the method of estimating the solubilities of solids in water, based on the equilibrium constants of their dissolution reactions, are as follows:



Source: a, b and c from Stumm and Morgan [29]. (Copyright 1981, Wiley-Interscience. Reprinted with permission.)
d from Drever [7]. (Copyright 1982, Prentice Hall. Reprinted with permission.)

FIGURE 2.11-4 Solubilities of Metal Oxides and Hydroxides as a Function of the Solution pH

- (1) Determine the composition of the solid and write a reaction for an equilibrium between this solid and its aqueous solution;
 - (2) Determine the equilibrium constant (K) for the reaction;
 - (3) Determine the bulk chemical composition of the solution and the ionic complexes that are likely to be present;
 - (4) Calculate the ionic strength of the solution and the activity coefficients of the dissolved species;
 - (5) Calculate the concentrations of the individual species in solution, which should indicate the solubility of the solid phase.

Steps (3) through (5) were covered briefly in section 2.11.2. For solutions containing several dissolved species, these steps may require fairly extensive and iterative computations, whose complexity may depend on the chosen model of chemical speciation. More detailed treatment of chemical speciation in solutions containing several dissolved species, as well as of the solubilities of solids in them, is given in section 2.13 and in a number of textbooks [3, 7, 10, 29].

The remainder of this section describes a few simple steps for estimating the equilibrium constant K and the solubility of some classes of solids.

The estimation methods described are:

- Estimation using Gibbs free energy data;
 - Correlations with crystal properties (lattice energy and crystal ionic radii); and
 - Correlation with cation electronegatives.

Of these, the most widely useful method is that which utilizes the Gibbs free energy data. In instances where these data are not available for the species of interest, the other more empirical relationships may be useful.

ESTIMATION OF K FROM THE GIBBS FREE ENERGIES OF FORMATION

The classical textbook method of computing the equilibrium constant is based on a relationship between K and the change in the Gibbs free energy for a reaction at equilibrium, when the reactants and the products are considered in their standard states. (For definitions and discussions of the standard states of solids and aqueous solutions, see the references cited two paragraphs earlier.)

A reaction at equilibrium between a solid of composition M_pA_q and its aqueous solution containing the aqueous species $M(aq)$ and $A(aq)$ can be written as



The standard *free energy change* for this reaction (that is, at the standard state of 25°C and 1 atm of total pressure), denoted ΔG_r^0 , is the sum of the *standard free energies of formation* of the products less the sum of the *standard free energies of formation* of the reactants:

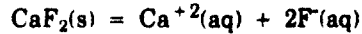
$$\Delta G_r^0 = p \Delta G_f^0(M_{aq}) + q \Delta G_f^0(A_{aq}) - \Delta G_f^0(M_p A_{q(s)}) \quad (37)$$

The equilibrium constant K for reaction 36 is related to ΔG_r^0 as follows:

$$\log K = - \frac{\Delta G_r^0}{2.3RT} \quad (38)$$

Example 6 illustrates the use of the preceding equation.

Example 6 Compute an equilibrium constant for dissolution or precipitation of fluorite (CaF_2) in water at 25°C and 1 atm total pressure. The reaction at equilibrium is:



The standard free energies of formation for the solid and aqueous species are:³

$$\text{CaF}_2: \quad \Delta G_f^0 = -281.29 \text{ kcal/mol} \quad [22]$$

$$\text{Ca}^{+2}: \quad \Delta G_f^0 = -132.30 \text{ kcal/mol} \quad [7]$$

$$\text{F}^-: \quad \Delta G_f^0 = -67.34 \text{ kcal/mol} \quad [7]$$

According to equation 37, the standard free energy change for the reaction is:

$$\begin{aligned} \Delta G_r^0 &= -132.30 + 2(-67.34) - (-281.29) \\ &= 14.31 \text{ kcal/mol} \end{aligned}$$

The equilibrium constant can now be calculated from equation 38, using the computed value of ΔG_r^0 , $R = 1.987 \times 10^{-3} \text{ kcal mol}^{-1} \text{ deg}^{-1}$, and $T = 298.15 \text{ K}$:

$$\begin{aligned} \log K &= - \frac{14.31}{1.364} = -10.49 \\ K &= 3.22 \times 10^{-11} \end{aligned}$$

This is the value used in Example 1.

Relatively small differences of about 1 kcal/mol in the values of ΔG_f^0 given by different sources may result in greater differences between the values of K computed from them. From the data listed in Table 2.11-2, an equilibrium constant for CaF_2 and its aqueous solution can be calculated as shown above:

$$\begin{aligned} \log K &= - \frac{13.42}{1.364} = -9.84 \\ K &= 14.5 \times 10^{-11} \end{aligned}$$

The latter value of K is about four times greater than the preceding.

³ Values were obtained from references noted below and differ slightly from those in Table 2.11-2.

Values of the Gibbs free energy of formation for a number of representative solids and aqueous ions are given in Table 2.11-2. Also listed in the table are enthalpies of formation at the standard state (ΔH_f^0), which can be used as in Example 3 to compute K at higher temperatures.

TABLE 2.11-2
Gibbs Free Energy of Formation (ΔG_f^0) and Enthalpy of Formation (ΔH_f^0)
for Selected Solids, Liquids, and Aqueous Ions
(at 25°C and 1 atm total pressure)

Formula	ΔG_f^0 (kcal/mol)	ΔH_f^0 (kcal/mol)
Crystalline Solids		
BaSeO ₄	-249.7	-274.0
CaF ₂	-279.0, -281.29 ^a	-291.5
Ca ₃ (AsO ₄) ₂	-732.1	-788.4
NaF	-129.902	-137.105
PbSeO ₄	-120.7	-145.6
Liquids		
D ₂ O	-58.195	-70.411
HDO	-57.817	-69.285
H ₂ O	-56.687	-68.315
H ₂ O ₂	-28.78	-44.88
Aqueous Ions		
Ba ⁺²	-134.02	-128.50
Ca ⁺²	-132.30	-129.74
CaOH ⁺	-171.7	-
H ⁺	0	0
Na ⁺	-62.593	-57.39
Pb ⁺²	-5.83	-0.4
AsO ₄ ⁻³	-155.00	-212.27
F ⁻	-66.64	-79.50
OH ⁻	-37.594	-54.970
SeO ₃ ⁻²	-88.38 ^b	-121.70 ^a
SeO ₄ ⁻²	-105.47 ^b	-143.19 ^a

a. From Robie *et al.* [22]

b. From Wagman *et al.* [32]

Source: National Bureau of Standards data reprinted in [33] unless otherwise noted.

If the values of the standard free energy (ΔG_f^0), enthalpy (ΔH_f^0), and entropy of formation (ΔS_f^0) cannot be found in the literature, they can be estimated for certain types of compounds; methods for various classes of solid phases are described in a number of publications [27, 30, 31].

ESTIMATION OF K AND SOLUBILITY FROM CORRELATIONS WITH CRYSTAL PROPERTIES

The relationship between an equilibrium constant K and the Gibbs free energy of a reaction in a standard state, as given in equation 38, is based on a well-established theory of chemical thermodynamics. Beyond the domain of this accurate relationship, it is possible to construct a number of *empirical* correlations between the values of K for solid-solution reactions and the values of certain properties characteristic of the solid crystalline phase. Such correlations are also possible between the solubility values of certain classes of solids and some of their crystalline properties. In this section, empirical correlations and their possible use are demonstrated for the solubility or K values and for the values of such characteristics as the lattice energy of the solid, the electronegativity, ionization potential, and crystal radius of the ions that comprise the crystalline solid.

To reiterate, the correlations between the solubilities of solids and their crystal properties are strictly empirical. As will be shown, the resulting estimates of solubilities or equilibrium constants are often no better than order-of-magnitude, but they can serve an orientational purpose in the absence of more reliable measured or computed data.

Correlation between Solubilities and Lattice Energies

Energy liberated in the process of formation of an ionic solid from its gaseous ions is the *lattice energy* of the solid, ΔU_0 [6, 8, 12]. For typical ionic crystals, such as alkali halides⁴, good correlations exist between such properties as the metal-to-anion bond length and various physical properties of the solids, such as their melting and boiling points. For the fluorides and chlorides of the alkali metals, the lattice energies (Table 2.11-3) show a systematic increase from the Li-halogenide to Cs-halogenide within each group. This trend is similar to the increase in the molar volume of the solid, the latter being the result of the increase in the crystal ionic radius of the metal as one progresses from Li to Cs.

The solubilities of the alkali-metal fluorides and chlorides, also listed in Table 2.11-3, show somewhat uneven trends. A plot of solubility versus lattice energy (Figure 2.11-5) gives no useful correlation for the chlorides; a trend of increasing solubility with increasing lattice energy is clearer with the fluorides, although the correlation is anything but simple.

Another set of solubility and lattice energy values is given in Table 2.11-4. These data refer to three classes of compounds: alkali-metal selenites ($M_2^+ SeO_3$), alkali-metal selenates ($M_2^+ SeO_4$), and alkaline-earth selenates ($M^{+2} SeO_4$). In Figure 2.11-6, the data are plotted as the square root of solubility versus the lattice energy. Example 7 illustrates a possible application of these three sets of data.

4. Compounds (1:1 type) of the alkali metals Li, Na, K, Rb, and Cs with the halogens F, Cl, Br, and I.

TABLE 2.11-3
Solubilities in Water and Crystal Properties of Alkali Fluorides and Chlorides

Solid Phase	Solubility ^a (mol/kg H ₂ O)	Molar Volume ^b V (cm ³ /mol)	Lattice Energy ^c (kcal/mol)	Crystal Ionic Radius (Å) of Cation for Coordination Number: ^d	
				6	8
LiF	0.075 ± 0.025	9.83	-244	0.82	
NaF	0.99	15.7 ± 0.7	-215	1.10	1.24
KF	17.5	23.2 ± 0.2	-193	1.46	1.59
RbF	20.6 ± 8.2 (18°C)	29.4	-183	1.57	1.68
CsF	22.7 ± 1.5 (18°C)	34.9 ± 2.0	-176	1.78	1.82
LiCl	20.0	20.5	-200	(same values as above)	
NaCl	6.15	27.0	-184		
KCl	4.8	37.6	-168		
RbCl	7.8	42.9	-162		
CsCl	11.4	42.2	-153		

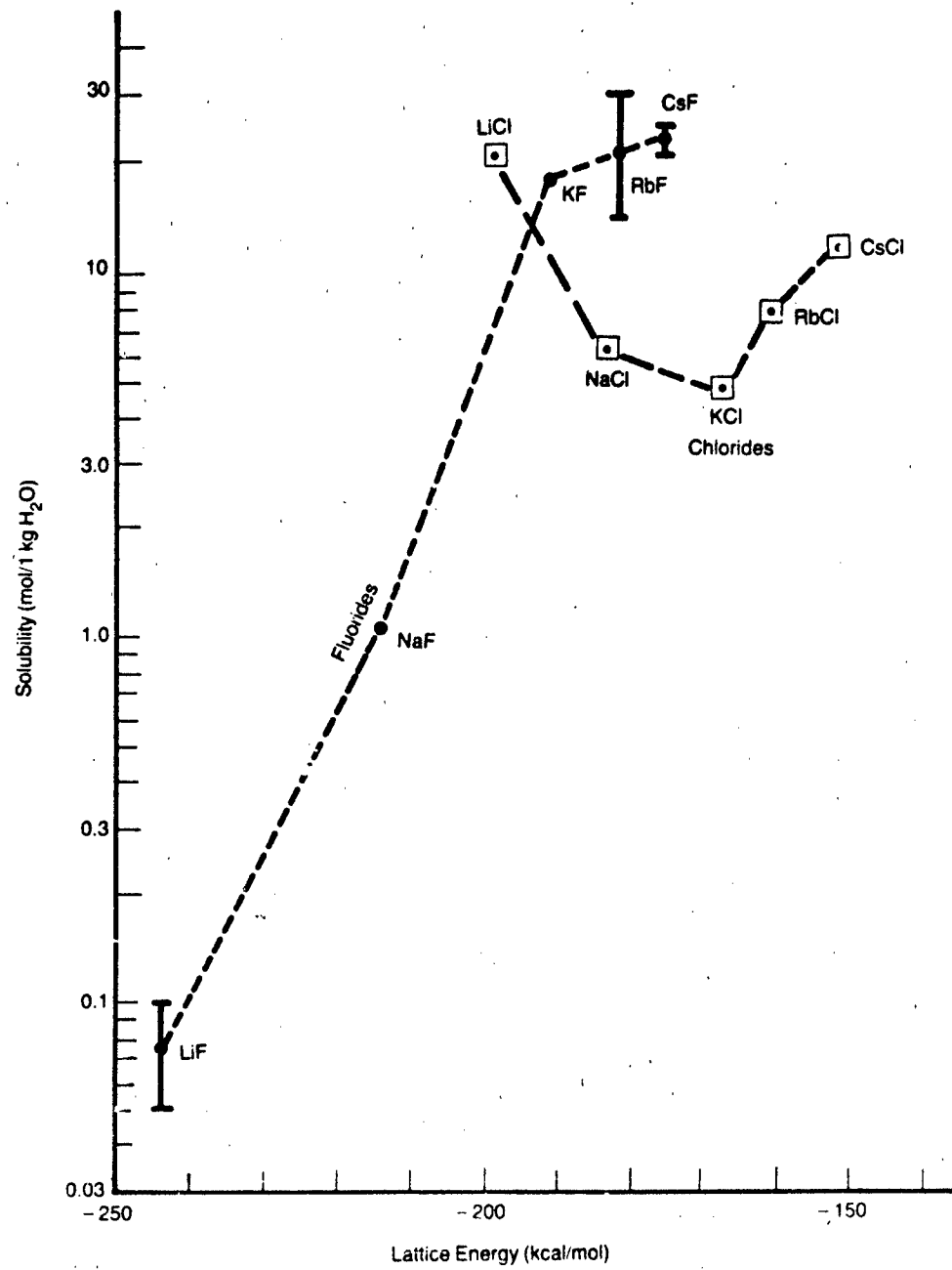
Sources:

- a. Stephen and Stephen [28]; Weast [33]. Values are at 25°C unless otherwise indicated.
- b. Computed from the molecular weights and densities of the solids [33].
- c. Evans [8], p. 48.
- d. Frye [9], p. 26.

Example 7 Figure 2.11-6 shows data points for the selenites of Li, Na and K only. Can the solubilities of two heavier members of the series, Rb₂SeO₃ and Cs₂SeO₃, be estimated from the graph?

A rough approximation of these solubilities can be obtained by extrapolating the line for the selenites beyond the point for K₂SiO₃ and finding its intersection with ordinates representing the lattice energies of the Rb and Cs selenites listed in Table 2.11-4. The solubilities of Rb₂SeO₃ and Cs₂SeO₃ are found to be about 12.5 and 15.5 mol/kg H₂O respectively. Given the empirical nature of the correlation and the data set of only three points, these estimates are not very credible. The true solubilities might deviate from the linear relationship as in the fluoride curve of Figure 2.11-5, in which case the extrapolated values would be much too high.

A similarly rough estimate of the solubility of lithium selenate (Li₂SeO₄) can be made. From the plot of the four points representing the alkali-metal selenates in Figure 2.11-6, the line is extrapolated below the point for Na₂SeO₄ to the lattice energy value $\Delta U_0 = -491$ kcal/mol that is characteristic of Li₂SeO₄ (Table 2.11-4). From the graph, the solubility value that corresponds to this point is about 0.6 mol/kg H₂O.



Source: Table 2.11-3

FIGURE 2.11-5 Solubilities as a Function of the Lattice Energy of Alkali Fluorides and Chlorides

TABLE 2.11-4
Solubility and Lattice Energy Values for Some Solid-Phase Selenites and Selenates

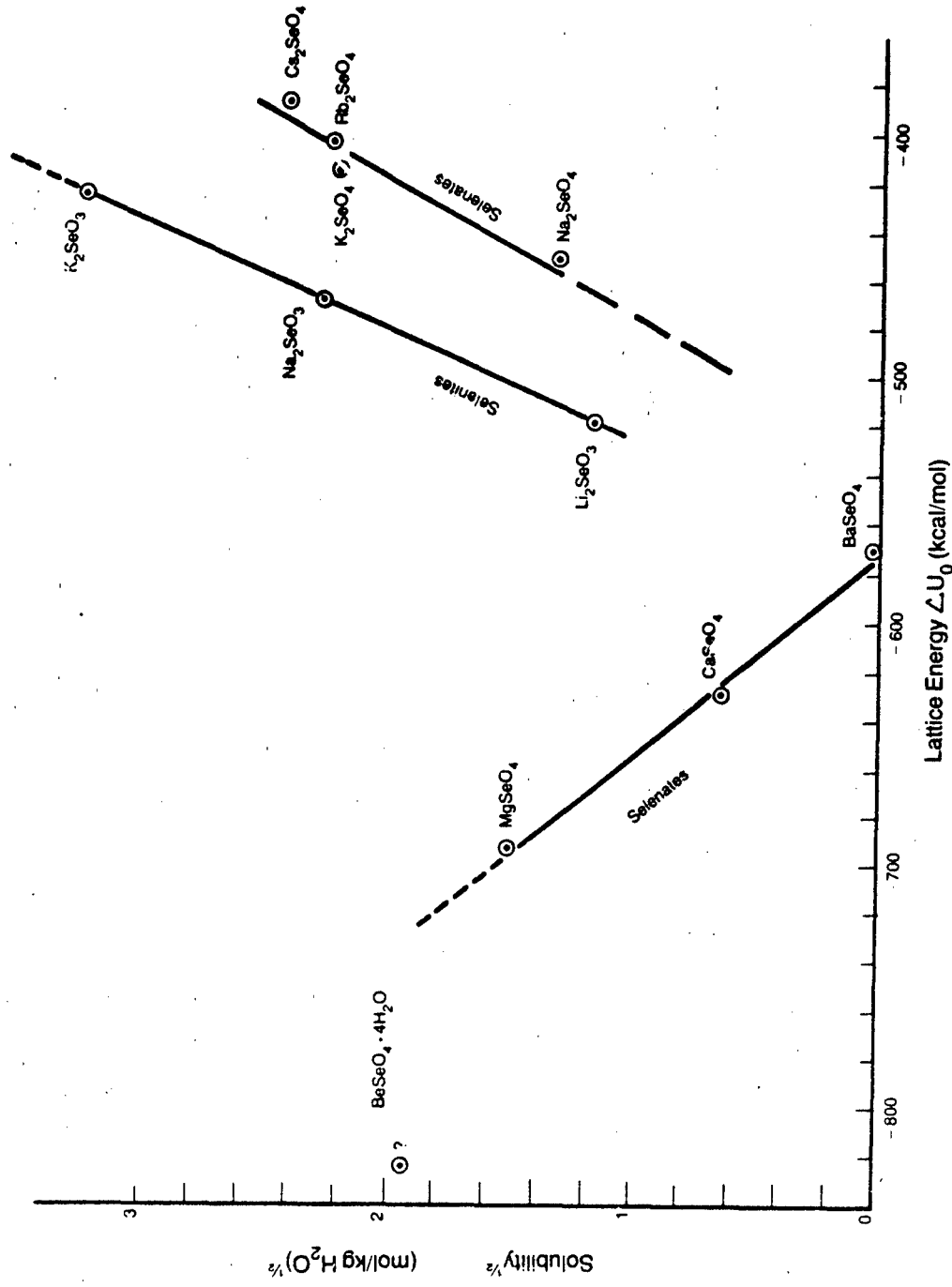
Solid	Solubility ^a (mol/kg H ₂ O)	Temperature ^a for Solubility Value (°C)	Lattice Energy ^b ΔU_0 (kcal/mol)
Li ₂ SeO ₃	1.43	24-25	-519
Na ₂ SeO ₃	5.19	24-25	-466
K ₂ SeO ₃	10.60	24-25	-424
Rb ₂ SeO ₃	—		-410
Cs ₂ SeO ₃	—		-392
Li ₂ SeO ₄	—		-491
Na ₂ SeO ₄	1.76	15	-449
K ₂ SeO ₄	4.94	12	-414
Rb ₂ SeO ₄	5.06	12	-403
Cs ₂ SeO ₄	5.99	12	-386
BeSeO ₄	3.7 ^c	25	-824
MgSeO ₄	2.27	25	-692
CaSeO ₄	0.404	25	-629
SrSeO ₄	—		-595
BaSeO ₄	2.9×10^{-4}	25	-570

a. Source: Stephen and Stephen [28]

b. Source: Jenkins [12]

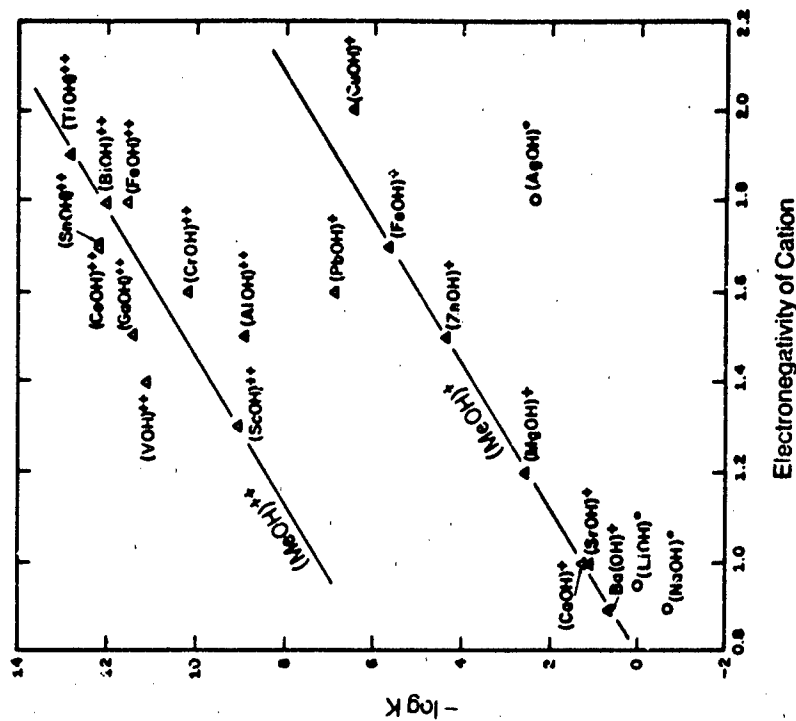
c. Hydrated phase

Finally, in the series of alkaline-earth selenates, there are solubility and lattice energy data for three solids: Mg-, Ca-, and Ba-selenate. (The given value for Be-selenate appears to be anomalous.) We may try to estimate the solubilities of the Be- and Sr-selenates by extrapolation. For Be-selenate, whose lattice energy is -824 kcal/mol, we obtain a solubility of about 9 mol/kg H₂O, in marked contrast to that of the hydrated phase (BeSeO₄ • 4H₂O), which is about 3.7 mol/kg H₂O. For Sr-selenate, the value of the lattice energy ($\Delta U_0 = -595$ kcal/mol) corresponds to a solubility of about 0.08 mol/kg H₂O. Weast [33] describes Sr-selenate as "insoluble in water", but also lists the solubility of Ba-selenate as about double the value given in Table 2.11-4. Clearly, not only the empirical correlations in Figures 2.11-5 and -6 but also some of the data behind them should not be accepted unquestioningly.

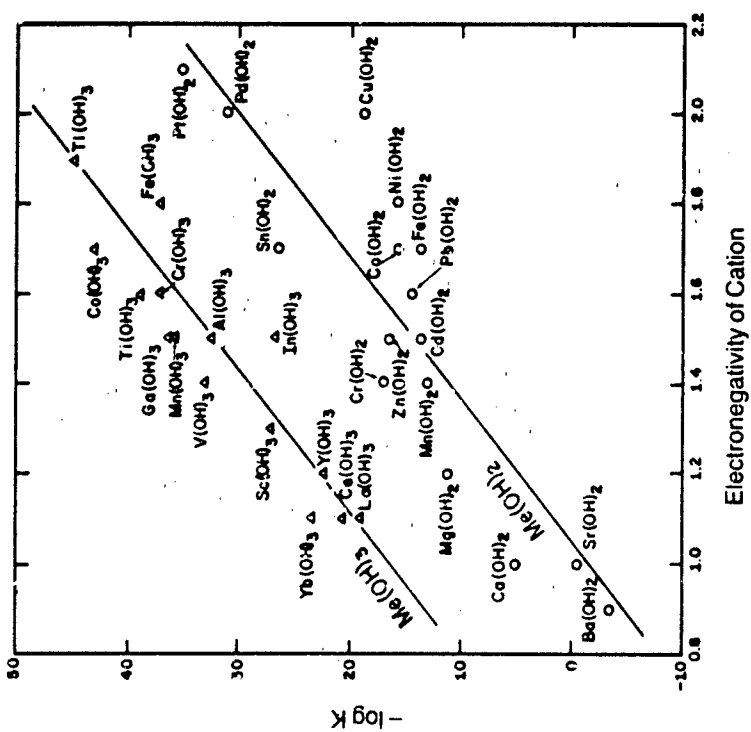


Source: Solubilities from Stephen and Stephen [28]; lattice energies from Jenkins [12]

FIGURE 2.11-6 Correlation Between the Square Root of Solubility and the Lattice Energy for Selected Selenites and Selenates



Source: Garrels and Christ [10]. (Copyright 1965, Harper and Row.
Reprinted with permission.)



Source: Garrels and Christ [10]. (Copyright 1965, Harper and Row.
Reprinted with permission.)

FIGURE 2.11-7 Solubilities of Metal Hydroxides Plotted Against the Cation Electronegativities at 25°C

FIGURE 2.11-8 Dissociation Constants of Singly and Doubly Charged Hydroxide Complexes in Aqueous Solutions at 25°C Plotted Against Cation Electronegativities

Source: Garrels and Christ [10]. (Copyright 1965, Harper and Row.
Reprinted with permission.)

Correlation between Solubilities and Cation Electronegativities

Clifford [4, 5] demonstrated and discussed a correlation between the electronegativity values of cations and the solubility values of poorly soluble solids of those cations. One such set of correlations is shown in Figure 2.11-7, a plot of the solubilities of metal hydroxides (expressed as the negative logarithms of their equilibrium constants, $-\log K$) versus the metal-cation electronegativities. Figure 2.11-8 is a similar plot for ion complexes in aqueous solution and includes some of the same metals that are considered in the hydroxide form in the preceding figure.

Figure 2.11-9 illustrates a correlation between the solubilities of divalent-metal arsenates, $(M^{+2})_3(AsO_4)_2$, and the cation electronegativity values.

For the three types of solids shown in Figures 2.11-7 and -9 — namely, divalent-metal hydroxides, trivalent-metal hydroxides, and divalent metal arsenates — the solubility generally decreases with increasing cation electronegativity. (Note the difference in the algebraic signs on the vertical axes of the two figures; the trend of the $\log K$ values as a function of the cation electronegativity is the same in both figures.)

The values on the horizontal axes of Figures 2.11-7 and -9 are the Pauling electronegativities, and their numerical values have been subject to corrections and revisions over a period of years. The plotted values stem from the 1950s. In Figure 2.11-9, two values of the cation electronegativity are shown for each metal arsenate: one from Clifford [4] and another from Evans [8]. An additional set of revised electronegativities for the elements in different valence states was produced by Allred [1].

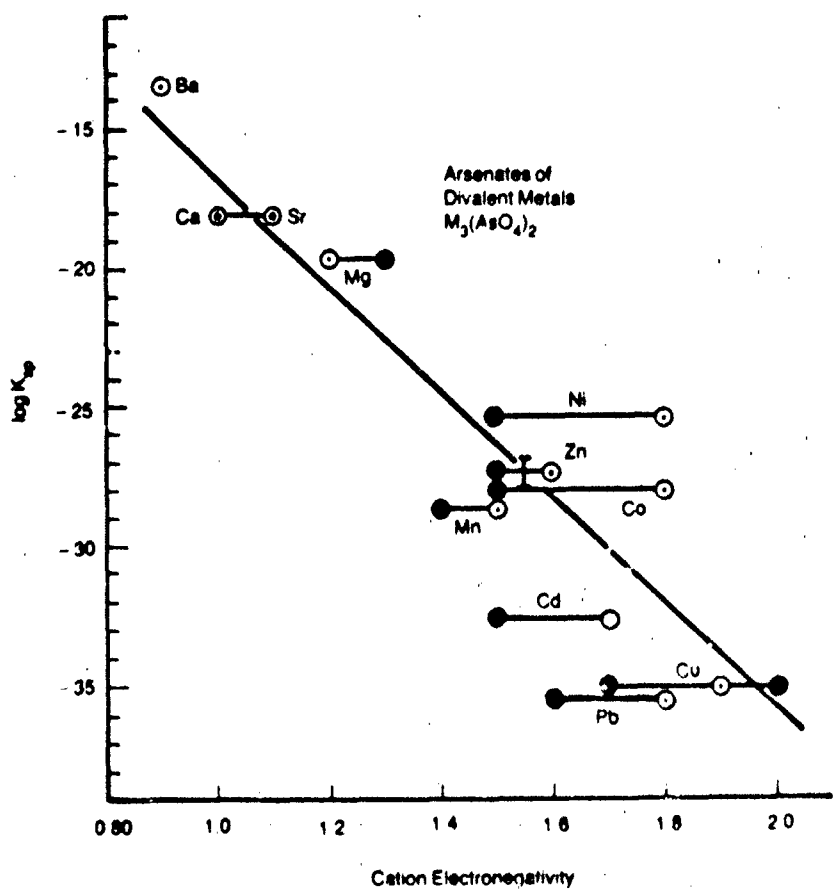
All the values of K_{sp} plotted in Figure 2.11-9 are from the tables in Sillén and Martell [24], except for that of Ba-arsenate. The solubility product for this compound was estimated from the values given in Stephen and Stephen [28] and Weast [33]: $K_{sp} \approx 10^{-13.5}$. The value given by Sillén and Martell is many orders of magnitude lower ($K_{sp} = 10^{-50.1}$), which is far removed from the trend of the other data points. The estimate of $10^{-13.5}$ fits the trend, as shown in the figure.

Some uses of the correlation between solubility and cation electronegativity are discussed in the following examples.

Example 8 What is the approximate value of the association constant of the ion-complex $CdOH^+$ in an aqueous solution at 25°C?

Among the single-charged ionic complexes shown in Figure 2.11-8, $CdOH^+$ is not given. The electronegativity value of the Cd^{+2} ion can be read off the graph in Figure 2.11-7: it is 1.5. The value of $-\log K$ for dissociation of a complex $MeOH^+$, where the cation Me^{+2} has an electronegativity of 1.5, can next be read off the graph in Figure 2.11-8: the value of $-\log K$ is similar to that of the $ZnOH^+$ complex, which is $K \approx 10^{-4}$. The association constant sought is the reciprocal of the dissociation constant. Thus, the association constant for the $CdOH^+$ complex in aqueous solution is $K \approx 10^4$.

The latter value compares well with the range of values for $CdOH^+$ association constant ($10^{3.4} - 10^{5.0}$) reported in the literature [24].



Explanatory notes: for comment on solubility of Ba-arsenate see text; electronegativities of Ca and Sr, each varies from 1.0 to 1.1; for Cu, three electronegativity values are shown.

Source: Solubilities — Sillén and Martell [24]
Electronegativity values — Evans [8],
 Clifford [4]

FIGURE 2.11-9 Solubilities of Divalent-Metal Arsenates, $M_3(AsO_4)_2$, In Water at Room Temperatures

Example 9 What is the solubility product of Cd-arsenate from the empirical correlation line drawn in Figure 2.11-9, and what error is this estimate likely to introduce in the estimated concentration of arsenic in solution?

First, using the Cd^{+2} ion electronegativity values of 1.5 and 1.7, the solubility product of Cd-arsenate (read off the straight line in Figure 2.11-9) is between $K_{sp} = 10^{-26}$ and $K_{sp} = 10^{-30}$. The difference between the K_{sp} value shown in the figure (10^{-26}) and the mean K_{sp} (10^{-28}) that corresponds to the electronegativity of 1.6 is about five orders of magnitude. We now determine the error in the arsenic concentration in solution that is introduced by this uncertainty of 10^5 in the estimated K_{sp} . Equations 15 and 16 are used, with $p = 3$ and $q = 2$, insofar as the compound $Cd_3(AsO_4)_2$ is a solid of the type M_3A_2 . In

equation 16, $[A]$ stands for concentration of the arsenate-ion AsO_4^{3-} in solution; the two estimates of $[A]$ for the two values of K_{sp} are:

$$\text{Lower estimate of } [\text{AsO}_4^{3-}] = \left(\frac{8}{27} \times 10^{-33} \right)^{1/5} = 1.97 \times 10^{-7} \text{ mol/liter}$$

$$\text{Upper estimate of } [\text{AsO}_4^{3-}] = \left(\frac{8}{27} \times 10^{-28} \right)^{1/5} = 1.96 \times 10^{-6} \text{ mol/liter}$$

The quotient of the two estimates gives:

$$\frac{\text{Lower estimate}}{\text{Upper estimate}} = (10^5)^{1/5} = 0.1$$

Thus, despite a difference of a factor of 10⁵ between the two estimates of the K_{sp} of the solid, the resulting uncertainty in the computed concentration of the arsenate ion in solution is a factor of 10. (Note, however, that in this example no complexes of cadmium and arsenate were considered and neither cadmium nor arsenate were initially present in solution.)

Correlation between Solubilities and Crystal Ionic Radii

Intuitively, it might be supposed that the size of the cation in the crystalline lattice of a solid would affect its solubility. In fact, this is the case, as shown in Figure 2.11-10 for divalent-metal sulfates. The sulfates characterized by similar values of the crystal ionic radii of the cations ($\text{Co}^{+2}, \dots, \text{Fe}^{+2}$) vary greatly in solubility; however, for the sulfates of the alkaline earths ($\text{Ca}, \dots, \text{Ra}$) and of lead, a very good correlation is found between solubility and cation crystal radius. For the aqueous complexes of some of these metal ions, either negatively charged or electrically neutral, there is no correlation between the cation radius and the dissociation constant of the complex.

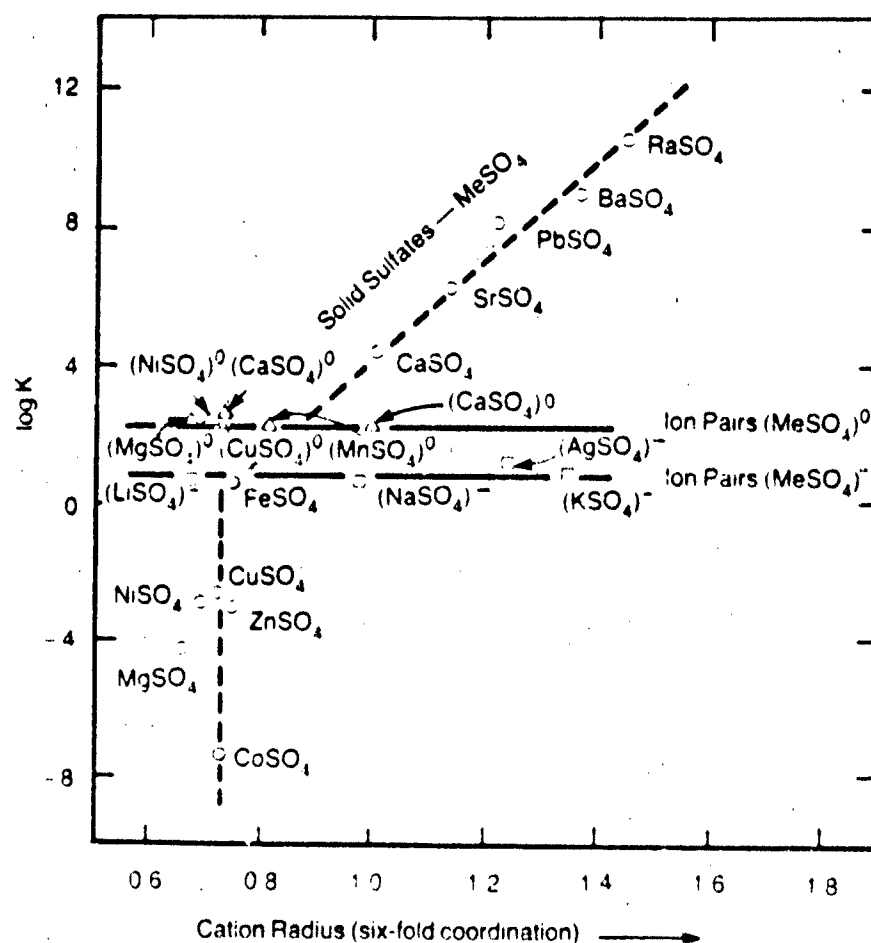
A fairly good correlation between solubility and cation radius is shown in Figure 2.11-11 for a series of solid uranyl arsenates. The variable constituent of the series is the monovalent cation: H^+ , Li^+ , Na^+ , K^+ , and NH_4^+ . An increase in the cation radius from hydrogen to ammonium correlates with a decreasing solubility of the solid at room temperature.

Example 10 Evaluate the solubility product of Na-uranyl arsenate.

The crystal ionic radius of the Na^+ ion, for a sixfold coordination, is given in Table 2.11-3: $r_{\text{Na}^+} \approx 1.10 \text{ \AA}$. In Figure 2.11-11, the value of $\log 1.10 \approx 0.04$ on the horizontal axis corresponds to a solubility product value (read off the empirical correlation line) of $K_{sp} \approx 10^{-21}$. The value for the solubility of Na-uranyl arsenate shown in this figure is $K_{sp} \approx 10^{-22}$, one order of magnitude lower.

Example 11 What would be the solubilities of Rb- and Cs-uranyl arsenates (if they exist)?

As in Examples 8 and 9 in the preceding section, this can only be a crude estimate. To illustrate the technique, the crystal ionic radii of Rb^+ and Cs^+ (Table 2.11-3) are: $r_{\text{Rb}} = 1.57 \text{ \AA}$ and $r_{\text{Cs}} = 1.78 \text{ \AA}$. Entering Figure 2.11-11 with the logarithms of these values ($\log r_{\text{Rb}} = 0.20$ and $\log r_{\text{Cs}} = 0.25$), we find the corresponding intersections with the straight line at $K_{sp} \approx 10^{-24}$ and $K_{sp} \approx 10^{-25}$. This method of estimating the solubility product assumes that uranyl arsenates exist with cations bigger than NH_4^+ , and that the trend of decrease in solubility with increasing cation radius is unchanged.

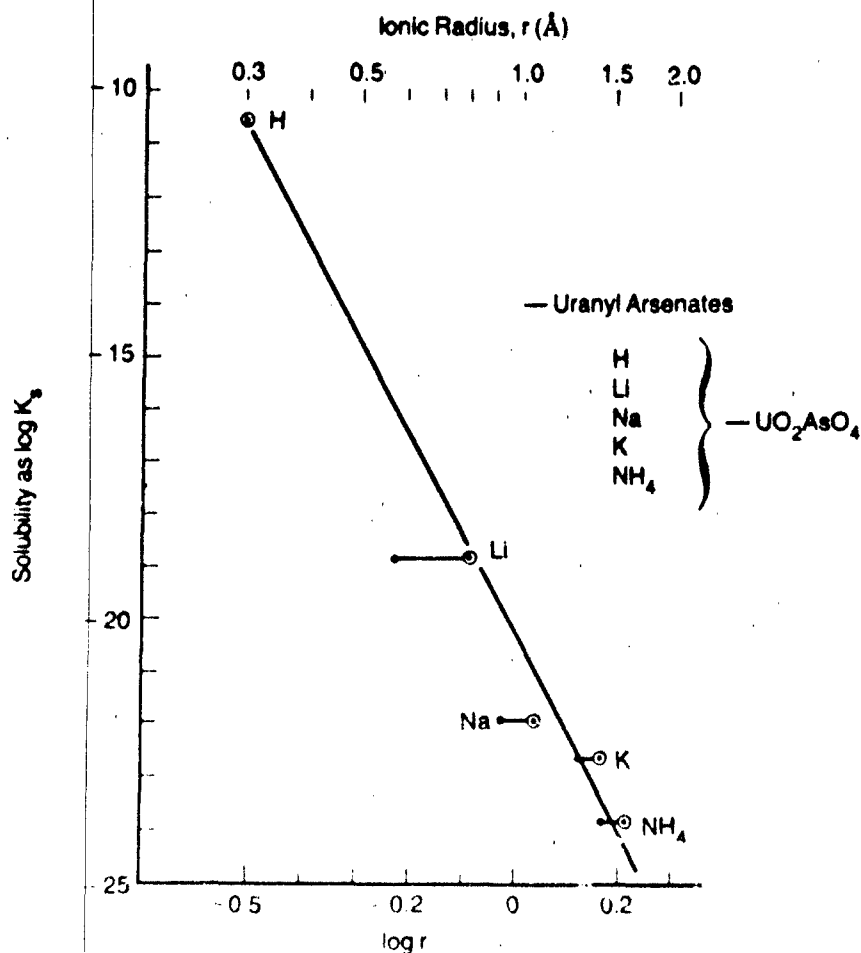


Source: Garrels and Christ [10]. (Copyright 1965, Harper and Row.
Reprinted with permission.)

FIGURE 2.11-10 Equilibrium Solubility Constants (25°C) for Divalent Metal Sulfates Plotted Against the Crystal Radii of the Cations for Sixfold Coordination

Correlation of Solubilities with Ionization Potentials

The ionization potential is a measure of the energy needed to remove an electron from an atom, making it a positively charged ion. Ionization potentials, I , are commonly given in the literature in units of electron-volts per atom. One electron-volt (eV) is a very small quantity of energy, equivalent to 1.6×10^{-12} erg or 3.83×10^{-21} calories. An ionization potential of about 20 eV may represent the energy required for removal of two electrons from a metal atom; this quantity of energy corresponds to about 460 kcal/mol, which is of the same order of magnitude as the Gibbs free energy of formation and the lattice energy of various solids.



Source: Open Circles — Frye [9]
Closed Circles — Evans [8]

FIGURE 2.11-11 Solubility Products of Uranyl Arsenates as a Function of the Ionic Radius of the Other Cation

The quotient of the ionization potential and the crystal ionic radius, I/r , has the dimensions of force (such as eV/Å, erg/cm or dyne). For two series of divalent-metal fluorides — fluorides of the alkaline earths and of other heavy metals — the relationships between the solubilities of the solid phases and the parameter I/r for the metal ion are plotted in Figure 2.11-12. The data on which the plots are based, and additional information on the molar volumes of the solids, are listed in Table 2.11-5. The plot of the alkaline-earth series in Figure 2.11-12 shows a variable relationship between solubility and the I/r value of the metal. For the heavy-metal series, however, there is a fairly consistent correlation. A use of this rough correlation is demonstrated below.

Example 12 Estimate the solubilities at room temperature of ferrous fluoride (FeF_2) and mercuric fluoride (HgF_2). Weast [33] indicates that FeF_2 is "slightly soluble" in water and HgF_2 "decomposes" in water; no solubility value for either compound is given in this source.

From Table 2.11-5,

$$\text{For } \text{Fe}^{+2}: I/r = 28.0 \text{ eV/Å}$$

$$\text{For } \text{Hg}^{+2}: I/r = 26.4 \text{ eV/Å}$$

In Figure 2.11-12, ordinates drawn at these values of I/r intersect the "heavy-metals" line at points corresponding to

$$\text{FeF}_2 \text{ solubility} \approx 6 \times 10^{-2} \text{ mol/liter}$$

$$\text{HgF}_2 \text{ solubility} \approx 4 \times 10^{-2} \text{ mol/liter}$$

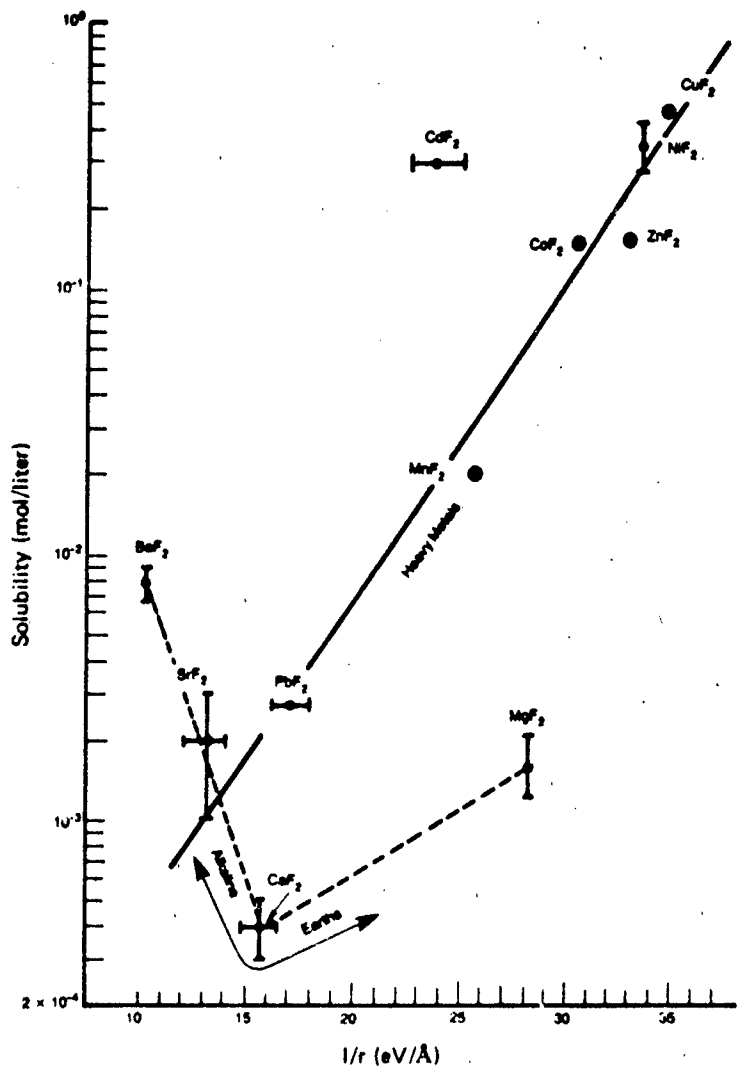
The solubility value for FeF_2 is of the same order of magnitude as that of MnF_2 (2×10^{-2} mol/liter). Although the results may be purely coincidental, Fe^{+2} and Mn^{+2} behave quite similarly in aqueous solutions.

2.11.4 Summary

Equilibria between solid phases and their aqueous solutions are defined in terms of one of the two following parameters:

- The solubility product, K_{sp} , defined as the product of the concentrations of the dissolved species at equilibrium with the solid;
- The equilibrium constant, K , defined as the quotient of the products of the thermodynamic activities of the species in solution and in the solid.

The solubility product may vary with the composition of the solution, whereas the equilibrium constant does not. Both K_{sp} and K depend on temperature and, to a much smaller degree for solids and aqueous solutions, on pressure.



Source of data: Table 2.11-5

FIGURE 2.11-12 Solubilities of Divalent-Metal Fluorides Plotted Against the Quotient of Ionization Potential and Cation Radius

Solubilities of the solids and concentrations of dissolved species at equilibrium with the solids can be estimated from either K_{sp} or K for a given set of environmental conditions, such as the temperature, composition of the aqueous solution, the pH of the solution, and the sizes of the solid particles reacting with the solution.

TABLE 2.11-5
Solubilities and Ionization Potentials Per Unit Radius of Some Alkaline-Earth Fluorides and Heavy-Metal Fluorides

Atomic Number of Metal	Composition of Solid	Molar Volume V (cm ³ /mol)	Metal ^a Crystal Radius for Coordination No. 6 r(Å)	Ionization Potential per Unit Radius		Solubility (mol/liter)
				I (eV)	U/r (eV/Å)	
Alkaline Earths						
12	MgF ₂	19.6	0.80	22.67	28.3	1.65 ± 0.45 × 10 ⁻³
20	CaF ₂	24.6	1.08	17.98	16.7	0.4 ± 0.1 × 10 ⁻³
38	SrF ₂	29.6	1.21	16.67	13.8	2.0 ± 1.0 × 10 ⁻³
56	BaF ₂	35.9	1.44	15.16	10.5	8.0 ± 1.0 × 10 ⁻³
Heavy Metals						
25	MnF ₂	23.3	0.91	23.13	25.4	0.02
26	F ₂ O ₂ F ₂	22.9	0.86	24.06	28.0	—
27	CoF ₂	21.7	0.83	25.16	30.3	0.145
28	NiF ₂	20.9	0.77	28.83	33.6	0.34 ± 0.07
29	CuF ₂	24.0	0.81	28.06	34.6	0.46
30	ZnF ₂	20.9	0.83	27.28	32.9	0.15
48	CdF ₂	22.7	1.03	25.83	25.1	0.29
80	HgF ₂	50.3	1.10	29.06	26.4	—
82	PbF ₂	29.8	1.26	22.38	17.8	0.0027

Sources:

V calculated from mol. wts. and densities listed by Weast [33].

I, r: Frye [9]; values of I are for reaction M → M⁺² + 2e⁻.

Solubilities: Stephen and Stephen [28]

Tabulations of K_{sp} and K are available in the literature for a great variety of naturally occurring and man-produced inorganic solids in aqueous solutions. It is also possible to estimate the value of K for solid-solution reactions at equilibrium, at a specified temperature and pressure. The most reliable method is to compute the values of K from the Gibbs free energies of formation of the reactants and products in a standard state (such as at 25°C and 1 atm total pressure). Additional methods for estimating the equilibrium constants for solid-solution reactions are based on empirical correlations between the solubilities of different solids and some of their solid crystal properties. Such empirical correlations between the solubility and crystal properties have been demonstrated for a number of classes of inorganic solids and for the following properties: lattice energy, cation electronegativity, crystal cation radius, and the ionization potential of the metal.

2.11.5 Sources of Information

Extensive treatment of dissolution reactions and chemical speciation in solution is given by Butler [3], Garrels and Christ [10], and Stumm and Morgan [29].

Compilations of data on the solubility of solids at various temperatures are available in *International Critical Tables* [11], Weast [33], Landolt-Börnstein [14], Linke [17, 18], and Stephen and Stephen [28].

For computations of the equilibrium constant, K, the main source of data for the Gibbs free energies of formation of the solids and aqueous species (ΔG_f^0) is Wagman *et al.* [32], who give the data for the standard state of 25°C and 1 atm total pressure. Compilations of the Gibbs free energy of formation and of other useful thermodynamic data for solids at temperatures from 25°C and up are also given by Robie *et al.* [22]. The Gibbs free energy data of Wagman and others are also compiled by Weast [33]. Some of these data, with additions that are particularly relevant to natural waters and mineral-water or rock-water systems, are also tabulated in publications by Garrels and Christ [10], Stumm and Morgan [29], and Drever [7].

The books and publications listed in the preceding paragraph also list values of the standard enthalpies of formation (ΔH_f^0) needed for estimating the temperature effect on the equilibrium constant K.

Estimation of the values of K at elevated pressures requires data on the molar volumes of the solids and aqueous species. For the solids, conveniently arranged tabulations of the molar volumes are given by Robie *et al.* [22] and Weast [33]. (The latter lists the molecular weight and the density of the solid; the molar volume is the ratio of the two.) For aqueous ions, an extensive compilation of molar volumes at temperatures of environmental interest is given by Millero [19], which also includes references to earlier works on methods of estimation of the partial molar volumes in solution.

Solubility products for solid-solution equilibria and association constants for ion-complexes in aqueous solutions are extensively tabulated by Sillén and Martell [24, 25], Smith and Martell [26], and Kotrlý and Šúcha [13]. In addition to the data on inorganic cation-anion complexes, references 13, 24 and 25 list data for metal complexes with organic ligands.

2.11.6 Literature Cited

1. Allred, A.L., "Electronegativity Values from Thermochemical Data," *J. Inorg. Nucl. Chem.*, **17**, 215 (1961).
2. Baes, C.F. and R.E. Mesmer, *The Hydrolysis of Cations*, Wiley-Interscience, New York (1976).
3. Butler, J.N., *Ionic Equilibrium*, Addison-Wesley, Reading, Mass. (1961).
4. Clifford, A.F., "The Electronegativity of Groups," *J. Phys. Chem.*, **63**, 1227 (1959).
5. Clifford, A.F., "The Prediction of Solubility Product Constant," *J. Am. Chem. Soc.*, **79**, 5404 (1957).
6. Dasent, W.E., *Inorganic Energetics*, 2nd ed., Cambridge Univ. Press (1982).
7. Drever, J.I., *The Geochemistry of Natural Waters*, Prentice-Hall, Englewood Cliffs, N.J. (1982).
8. Evans, R.C., *An Introduction to Crystal Chemistry*, 2nd ed., Cambridge Univ. Press (1964).
9. Frye, K., *Modern Mineralogy*, Prentice-Hall, Englewood Cliffs, N.J. (1974).
10. Garrels, R.M. and C.L. Christ, *Solutions, Minerals, and Equilibria*, Harper and Row, New York (1965).
11. *International Critical Tables*, 7 vols., McGraw-Hill Book Co., New York (1926-1930).
12. Jenkins, H.D.B., "Lattice Energies," in Weast [33], D-101.
13. Kotrlý, S. and L. Šúcha, *Handbook of Chemical Equilibria in Analytical Chemistry*, John Wiley & Sons, New York (1985).
14. Landolt-Börnstein, *Zahlenwerte und Funktionen. Lösungsgleichgewichte I*, Vol. 2, Part 2, Sec. B, Springer-Verlag, Heidelberg (1962).
15. Langmuir, D. and D.O. Whitemore, "Variations in the Stability of Precipitated Ferric Oxyhydroxides," *Adv. Chem. Ser.*, **106**, 209 (1971).
16. Lerman, A., *Geochemical Processes — Water and Sediment Environments*, Wiley-Interscience, New York (1979).
17. Linke, W.F., *Solubilities — Inorganic and Metal-Organic Compounds, A-Ir*, 4th ed., Vol. I, Van Nostrand, New York (1958).
18. Linke, W.F., *Solubilities — Inorganic and Metal-Organic Compounds, K-Z*, 4th ed., Vol. II, American Chemical Society, Washington, D.C. (1965).
19. Millero, F.J., "The Molal Volumes of Electrolytes," *Chem. Rev.*, **71**, 147 (1971).
20. Nielsen, A.E., "Precipitates: Formation, Coprecipitation, and Aging," in *Treatise on Analytical Chemistry*, 2nd ed., I.M. Kolthoff and P.J. Elving (eds.), Part I, Vol. 3, John Wiley & Sons, New York (1983).
21. Prigogine, I. and R. Defay, *Chemical Thermodynamics*, John Wiley & Sons, New York (1962).

22. Robie, R.A., B.S. Hemingway and J.R. Fisher, "Thermodynamic Properties of Minerals and Related Substances at 298.15 K and 1 Bar (10^5 Pascals) Pressure and at Higher Temperatures," *U.S. Geol. Surv. Bull.*, No. 1452, 1 (1978).
23. Schindler, P.W., "Heterogeneous Equilibria Involving Oxides, Hydroxides, Carbonates, and Hydroxide Carbonates," *Adv. Chem. Ser.*, **67**, 196 (1967).
24. Sillén, L.G. and A.E. Martell, *Stability Constants of Metal-Ion Complexes*, Spec. Pub. No. 17, The Chemical Society, London (1964).
25. Sillén, L.G. and A.E. Martell, *Stability Constants of Metal-Ion Complexes — Supplement No. 1*, Spec. Pub. No. 25, The Chemical Society, London (1971).
26. Smith, R.M. and A.E. Martell, *Inorganic Ligands*, Vol. 4 of *Critical Stability Constants*, Plenum Press, New York (1976).
27. Sposito, G., *The Thermodynamics of Soil Solutions*, Oxford Univ. Press (1981).
28. Stephen, H. and T. Stephen, *Solubilities of Inorganic and Organic Compounds*, Vol. 1, Part 1, Pergamon Press, Oxford (1963).
29. Stumm, W. and J.J. Morgan, *Aquatic Chemistry*, 2nd ed., Wiley-Interscience, New York (1981).
30. Swalin, R.A., *Thermodynamics of Solids*, 2nd ed., Wiley-Interscience, New York (1972).
31. Tardy, Y., "Relationships among Gibbs Energies of Formation of Compounds," *Am. J. Sci.*, **279**, 217 (1979).
32. Wagman, D.D., W.H. Evans, V.B. Parker, R.H. Schumm, I. Halow, S.M. Bailey, K.L. Churney and R.L. Nuttall, *The NBS Tables of Chemical Thermodynamic Properties*, Journal of Physical and Chemical Reference Data, **11**, Supplement 2 (1982).
33. Weast, R.C. (ed.), *Handbook of Chemistry and Physics*, 65th ed., CRC Press, Boca Raton, Fla. (1984).

2.12 ATTENUATION ON SOILS

2.12.1 Introduction

Attenuation of aqueous species via removal onto, and in the form of, solid phases is an important phenomenon in environmental systems. Attenuation reduces mobility by decreasing the concentration of species in the aqueous phase. The bioavailabilities of dissolved versus sorbed and insoluble species also differ: dissolved species are much more available to both plants and animals. Therefore, an understanding of sorption and attenuation is necessary in assessing the fate of inorganic compounds in the environment.

Although numerous experiments have been conducted using various sorbents to study the sorption of inorganics, the environmentally important sorbents include sediments, soils, and their components. This section therefore focuses on these sorbents and discusses the extent of sorption that occurs under equilibrium conditions. Although not discussed in detail, the importance of kinetics is pointed out where relevant. The emphasis of the discussion is on cations, particularly trace heavy metals, because they are the major pollutants in the environment.

The attenuation or sorption of an inorganic species is highly influenced by the environmental conditions of the system under consideration. Thus, unlike the case for most organic chemicals, *no species-unique attenuation or sorption constants can be applied to a broad range of soils and sediments*. Depending on such factors as soil texture, soil chemistry, pH, redox potential, solute and ligand concentrations in the water, a particular inorganic species may be highly mobile in one soil environment and essentially immobile in another. The effective sorption or attenuation constants for an inorganic species may differ by as much as two or three orders of magnitude. For roughly similar environments, however, the differences are usually less than one order of magnitude.

A further result of this variability (and complexity) is that *the extent of attenuation or sorption of an inorganic pollutant on a particular soil cannot be estimated, ab initio*, with the degree of accuracy and reliability usually desired for quantitative transport modeling or even for semiquantitative assessments. Computerized models of aqueous speciation do exist, and some of them include routines that represent sorption; nevertheless, there is as yet no proven methodology for using these speciation calculations, along with information on such properties as molecular structure and ionic size and charge, to predict sorption for a wide range of natural soils, sediments and minerals. The investigator is left with three general approaches for estimating the extent of attenuation of sorption in a real soil or sediment environment:¹

- (1) Rough estimates based on published data (including, for example, sorption constants, attenuation factors, and empirical correlations) for the pollutant in similar soil environments.

1. These approaches are discussed in more detail in § 2.12.6.

- (2) Rough estimates of boundaries (i.e., upper or lower limits for sorption) using calculations based on the assumption that one or more mechanisms predominate (e.g., precipitation, ion exchange, physical absorption).
- (3) Laboratory experiments.

Accordingly, this section discusses:

- attenuation mechanisms for inorganics in soils and sediments (§ 2.12.2);
- the effect of various factors (pH, Eh, ionic composition, etc.) on the attenuation of inorganics in natural environments (§ 2.12.3);
- the general procedures used to measure attenuation of pollutants in soils and sediments (§ 2.12.4);
- attempts made to model the attenuation of inorganics in natural environments (§ 2.12.5);
- empirical representations (distribution coefficient, Langmuir and Freundlich) that have been used with some success to describe the attenuation of inorganics in natural environments (§ 2.12.6);
- examples of data for parameters used in the empirical representations (§ 2.12.6);
- sample calculations of attenuation using measured data and these empirical equations (§ 2.12.6);
- soil column studies by Fuller and co-workers (§ 2.12.7);
- approaches to estimating the probable attenuation of an inorganic pollutant in a natural system (§ 2.12.8); and
- brief examples of two approaches (§ 2.12.8).

2.12.2 Attenuation Mechanisms

As used here, *sorption* refers generally to the removal of solute components from the aqueous phase of an environmental system by the *solid phase(s)* at the surface of the solid phase(s). A number of mechanisms and processes are involved. The term is often used interchangeably with *attenuation*, which is used in this section to refer to the overall increase in concentration in undissolved phases, including precipitates (and a corresponding decrease in concentration in the dissolved phase), regardless of the mechanisms.

Attenuation processes can be classified into two categories: physical and chemical. The distinction between the two is defined by the attractive forces responsible for ionic interactions between the surface and the solute. Physical adsorption is due to van der Waal's forces and is characterized by low heats of adsorption (5-10 kcal/mole) [32]. Chemical attenuation refers to chemical interactions and/or reactions with higher heats of reaction. Because of the low energy of adsorption, physical adsorption is easily reversible.

Within these two broad categories of attenuation, there are various contributing processes in natural systems. These include physical adsorption and processes involving chemical interactions: ion exchange, organic complexation, precipitation and co-precipitation, solid-state diffusion, and isomorphic substitution.

Physical adsorption, as described above, is due to long-range van der Waal's forces. It does not involve direct interaction between the sorbent surface and the solute; the forces responsible for physical adsorption are intermolecular, in contrast to the valency forces in chemical interaction. Physical adsorption occurs because the surface charges on particles attract dissolved species with opposite charges. As adsorption proceeds, the charges become neutralized, physical adsorption slows down and equilibrium is eventually reached. Also, as the surface becomes filled, fewer sites are available for adsorption. Therefore, the extent of physical adsorption is closely related to surface charge and the surface area available on the sorbent. Surface charges on minerals occur due to isomorphic substitution (see below for further discussion). Clay minerals tend to have a negative surface charge and will attract positively-charged ions.

An important chemical process responsible for the sorption of ionic species is ion exchange. In this process, the sorption of one or more ionic species is accompanied by the desorption of an amount of previously sorbed ionic species equivalent in total ionic charge [16]. When anions on the surface are replaced by dissolved anions, it is called *anion exchange*. Similarly, *cation exchange* occurs when cationic species are exchanged between the sorbent surface and the solute at the sorbent-solution interface. The cation-exchange capacity (CEC) can be calculated from a test designed to measure the amount of cations that may be exchanged by a solid phase from a solution. Similarly, an anion-exchange capacity (AEC) may be calculated. The CEC of a solid phase is specified for a particular temperature, ionic strength, pH of solution and ionic species involved; it is most frequently expressed in meq/100g or $\mu\text{eq/g}$ of solid phase [16].

The formation of complexes between dissolved and surface materials is another important sorption mechanism. Complexation in the aqueous phase has been described in section 2.9 of this report; in an analogous fashion, carboxyl, phenolic, sulphydryl and other functional groups on the surface of particles can coordinate to metal ions. The surface complexation reaction involves the loss of one or more water molecules from the inner coordination sphere of the metal ion for one or more ligand coordinating atoms on the surface of the particle. An excess of the metal over the ligand on the surface would result in metal-like coordination properties on the surface, while a ligand excess would cause ligand-like behavior of the surface toward solutes at the solid-solute interface [27]. Conceptually, on the surface of a solid, not all the coordination possibilities of the metal or the ligand atoms are satisfied [27]. The difference between this type of adsorption and aqueous complex formation is that the former occurs at heterogeneous surfaces, and the sorbed solutes are therefore no longer mobile. The process of complexation is used to model surface-solute interactions for both organic and inorganic surfaces. Mathematical equations have been used to explain and model sorption at solid-liquid interfaces [27,28,42]; these were based on the assumption that certain surface species are formed in the complexation process.

Precipitation and co-precipitation are also important processes for removing inorganics, particularly heavy metals, from solution. Precipitation is the separation of the solute as a solid from the aqueous phase under conditions of saturation; section 2.11 of this report describes these processes in greater detail. Co-precipitation, on the other hand, refers to the removal of a solute from solution via sorption onto a solid phase as the solid phase is precipitating out of solution. In natural systems, it is difficult to distinguish between precipitation and co-precipitation. The various conditions, mechanisms, and reactions involved are not easily delineated.

During the formation of clay minerals, cations may be co-precipitated in the lattice in a process called *isomorphic substitution*. Kinniburgh and Jackson [23] described nonstoichiometric isomorphic substitution in soil silicate minerals. The most common is the substitution of Al^{+3} for Si^{+4} and Mg^{+2} for Al^{+3} . Other possible substitutions include Fe^{+3} for Si^{+4} [23]. Ions that are similar to each other will have a greater tendency to substitute for each other. Arsenate, for example, may replace phosphate on surfaces of clays and amorphous hydroxides and may substitute for phosphate during precipitation of minerals [39].

One of the processes that may cause the "precipitation" of metals in natural systems is coagulation or flocculation. Most suspended particulates have a natural tendency to coagulate when placed close enough together (due to van der Waals forces). Charged particulates may repel similarly charged particles such that the relatively small distances required for van der Waals forces to become important may never be reached. These suspensions are called stable. If adsorption of oppositely charged ions occurs, interparticle repulsion may decrease and coagulation may occur. Metals associated with fine particulates (e.g., dust) suspended in water may be settled out of solution when attracted to particles with opposite surface charges. The surface charge on suspended particles may change as the pH changes. A pH value may be defined when the net surface charge of the particle equals zero, i.e., the point of zero charge (PZC). The stability of the particle-pairs thus decreases as the pH approaches its PZC value. Changes in pH could destabilize particles and cause them to coagulate. The physical adsorption of metal ions on the surface of suspended particles may also destabilize these particles and cause coagulation [16]. This process is used extensively in wastewater treatment by adding agents like alum, iron salts or polyelectrolytes to flocculate fine suspended particles.

The process of coagulation is similar to the occlusion of metals in precipitates. Freshly precipitated hydrous oxides exhibit a high degree of disorder, being frequently gelatinous and having large surface areas and high surface reactivity [23]. Metal ions are sorbed onto these surfaces and essentially become occluded or co-precipitated with the hydrous oxides. Jenne [21] suggested that the occlusion of heavy metals in growing solid phases, such as Fe and Mn oxides, is an important process for immobilizing metals in soils. At sufficiently high concentrations of a metal ion, precipitation could also occur. Kinniburgh and Jackson [23] suggested that metal hydroxides can precipitate at substoichiometric hydroxide-to-metal ratios as basic salts or as solids with a range of ill-defined stoichiometry.

A relatively minor process is that of *lattice penetration* or *solid-state diffusion*. "Holes" may occur on the surfaces of natural zeolites and other minerals, forming the "open" surface structures of these minerals [16]. Exchangeable divalent cations such as Mg, Ni, Cu, Co, and Zn may become embedded in these "holes". Upon dehydration, they become "stuck" in these holes and then diffuse into empty octahedral positions in layer silicates [9,16]. Several authors believe that this is probably not a significant process for immobilizing heavy metals [21,26]. There is little penetration (only a few atomic planes), and it occurs only at the edges and along fractures [9].

Although sorption may be measured using natural soils and sediments and natural water samples, it is difficult to determine from the data the mechanisms that are responsible. The complexity of natural systems and the diverse mechanisms of sorption and attenuation make it hard to attribute an effect to a specific mechanism. However, numerous studies of simpler, more controlled experimental systems have illuminated the individual mechanisms contributing to attenuation in natural systems. This attenuation is often found to be the result of more than one process.

The processes described above could occur as single-step reactions, parts of multi-step reactions or simultaneously with each other. As a hypothetical example, cations could be sorbed by a single-step ion exchange process on clays, and they could also be attenuated by a two-step process of physical adsorption followed by co-precipitation or precipitation. Several authors [16,19,24,45] have observed that physical adsorption probably precedes bulk precipitation, followed by dehydration and rearrangement of the precipitated phase. Similarly, nonstoichiometric isomorphic substitution usually results in a net negative surface charge, which could further result in ion exchange or other forms of sorption. Because of the heterogeneous structure of natural soils and sediments, several processes could occur simultaneously. For many heavy metals, cation exchange is important on clay minerals, co-precipitation on hydrous Fe and Mn oxides, and organic complexation on organic particles. All of these processes occur simultaneously. The attenuation of individual metals is described in Chapter 7 (Part II).

2.12.3 Factors Affecting Attenuation

The attenuation behavior of an inorganic species in soil is a complex function of the chemical form and properties of the solute, the chemical composition of the soil solution and the physical-chemical properties of the soil. Soil properties such as bulk density, compaction characteristics, and permeability influence attenuation through their effect on the rate of movement of water through the soil and the surface area of the soil exposed to the aqueous phase. Appendix C, which describes soil types and properties, includes a list (Table C-2) of the site and soil characteristics that affect the migration of inorganics. The important soil, soil solution, and solute physical-chemical properties (not including engineering properties) affecting attenuation are also listed in Table 2.12-1.

Soil composition is significant because each component differs in its ability to sorb solutes from the soil solution. Soils and sediments are heterogeneous mixtures of

TABLE 2.12-1
**Physical and Chemical Properties of Soil, Soil Solution,
 and Solute that Affect Attenuation^a**

Soil Solids	Soil Solution	Solute
Composition:	pH	Chemical identity
Hydrous oxides (Fe, Mn, Al)	Eh	Chemical behavior:
Silicates — clay content,	Temperature	Charge
type of clay	Ionic strength	Size
Organic material	Ionic composition:	Complexation chemistry
Carbonate minerals	Competing ions	Solubility
Specific area	Complexing ions	Precipitation chemistry
Cation exchange capacity (CEC)		Redox chemistry
pH (content of basic species)		(oxidation states)
Eh (content of redox active species, e.g., Fe(II), Mn(IV))		
Aeration status (saturated, unsaturated)		
Microbial type and population		
Temperature		

a. Does not include engineering properties; see Appendix C.

many different solid and dissolved phases that provide a variety of mineral and organic surfaces. The primary sorbents in natural soils and sediments are amorphous aluminosilicates, organic materials and hydrous oxides, oxyhydroxides and hydroxides of aluminum, iron and manganese [34]. Metal oxides are also important, because they often occur as coatings on other soil component surfaces [23]. Organisms, dead remains of organisms and condensed humic material provide organic surfaces in the environment; organics also exist as coatings on inorganic oxide particles [27]. Table C-11 (Appendix C) shows the ranges of organic matter content in soils. Clay minerals and other aluminosilicates provide surfaces on which other sorbents can form and are also significant sorbents in their own right. As described in Appendix C, soils from different sources contain different amounts of the various components.

Similarly, sediments contain a range of solid components that sorb solutes from aquatic systems. In one study of sediment sorption data by Pavlou and Weston [33], a statistically significant relationship was found between the sorption coefficient (K_d) of Cu, Cd and Pb (but not Zn, As or Hg) and the sediment organic carbon content. Their data are shown in Table 2.12-2. The solution pH for these equations was not specified. Other solid components may also have contributed to the sorption of these trace metals, explaining the low correlation to organic carbon.

The *specific area*, usually expressed as m^2/g of soil, is a measure of the surface area available for sorption. This property is related to the soil size distribution, pore

TABLE 2.12-2
**Relationship of Sediment-Water Partition Coefficient of Trace Metals
 to the Organic Carbon in Sediments**

Metal	Regression Equation ^a	n	r
Cu	$\log K_d = 0.33(\text{TOC}) + 3.28$	22	0.74 ^b
Zn	$\log K_d = 0.074(\text{TOC}) + 3.29$	21	0.19
As	$\log K_d = -0.05(\text{TOC}) + 2.46$	21	-0.19
Cd	$\log K_d = 0.21(\text{TOC}) + 2.34$	21	0.55 ^b
Pb	$\log K_d = 0.20(\text{TOC}) + 3.10$	22	0.47 ^b
Hg	$\log K_d = 0.05(\text{TOC}) + 1.87$	18	0.21

a. K_d = sediment/water partition coefficient

TOC = percent organic carbon in sediment

n = number of data points used to derive regression

r = correlation coefficient

b. r values indicate significant correlation.

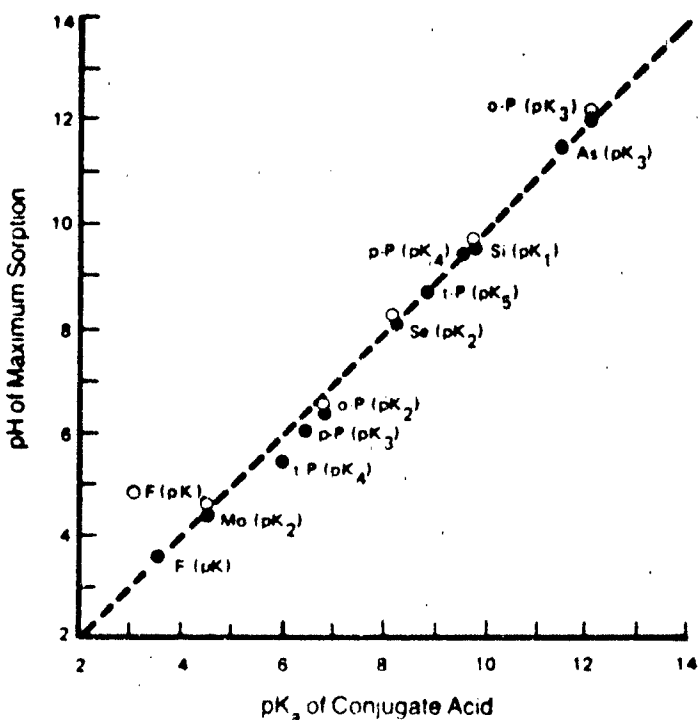
Source: Pavlou and Weston [33]

structure and pore size distribution. Normally, it is inversely proportional to the size of the soil particles. Colloidal-sized particles make up a major part of most clays (clay particles defined as < 0.002 mm in size) and present an extremely large surface area for sorption. Specific areas of three major types of clay are shown in Table C-10, which also lists their cation exchange capacities. As defined earlier, the CEC is directly related to the maximum amount of cations that may be exchanged onto the soil surface at a specified pH. The listed values range from 3-15 meq/100g for kaolinite to 80-100 meq/100g for montmorillonite. The values for some surface soils (Table C-12) range from 2.0 meq/100g dry soil for a New Jersey sand to 57.5 meq/100g for a California clay.

The pH of the soil surface is strongly related to sorption. It affects the net surface charge on amphoteric sorbents like hydrous oxides and amorphous silicates. It also affects the surface speciation and therefore the reactions on the soil surface, e.g., ion exchange, hydrolysis, complexation, and particularly the exchange of H⁺. The pH ranges in soils (as measured by mixing specified amounts of soil and water) are shown in Figure C-4. Surface pH values are normally 2 units lower than the pH of soil-water mixtures.

Solution pH is one of the primary parameters controlling solute speciation, chemical nature of protolyzable surface species and surface charge. The pH dependence of attenuation via ionic interaction is different for anions and cations. In the case of an

anion, sorption is increased with increasing pH as dissociation increases. However, with increasing pH, the sorbent surface charge of an oxide becomes increasingly negative. At pH values higher than the pK_a of the anion, sorption decreases [18]. A good correlation has been found between the pK_a values for conjugate acids and points of inflection in sorption curves reflecting maxima in sorption with varying pH; this is illustrated for FeO(OH) and Al(OH)_3 in Figure 2.12-1.



Sorbents: ● goethite (FeO(OH)), ■ gibbsite (Al(OH)_3).

Sorbates: F, fluoride; Mo, molybdate; t-P, tripolyphosphate; p-P, pyrophosphate; o-P, orthophosphate; Se, selenite; Si, silicate; As, arsenate.

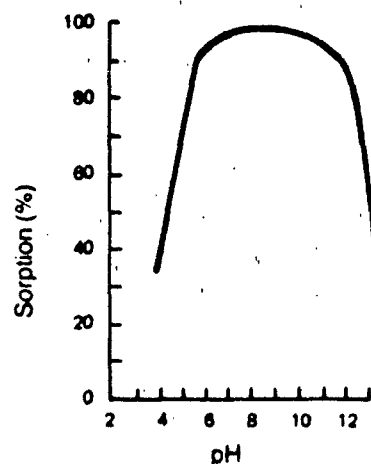
Source: Hingston [18] (Copyright 1981, Ann Arbor Science Publishers.

Reprinted with permission from M. Anderson and A. Rubin, current holders of the copyright.)

FIGURE 2.12-1 Relationship Between pK_a and pH at the Point of Maximum Sorption

The attenuation of most cations increases with increasing pH. At the point of zero charge, there is little surface ionic interaction with the cations, but as the pH increases above the PZC, the surface becomes more negatively charged and the sorption of cations increases [23,34]. Precipitation of many divalent metals also increases with pH.

Another reason for the pH-dependence of cation attenuation may be the preference of hydrolyzed species over the free ions as sorbed species [3,23]. The increase in attenuation appears to be very rapid, increasing from 0 at low pH to almost 100% with an increase of 1-2 pH units [38]. Attenuation usually reaches a plateau, and desorption occurs if the pH is increased much further; Figure 2.12-2 illustrates this behavior

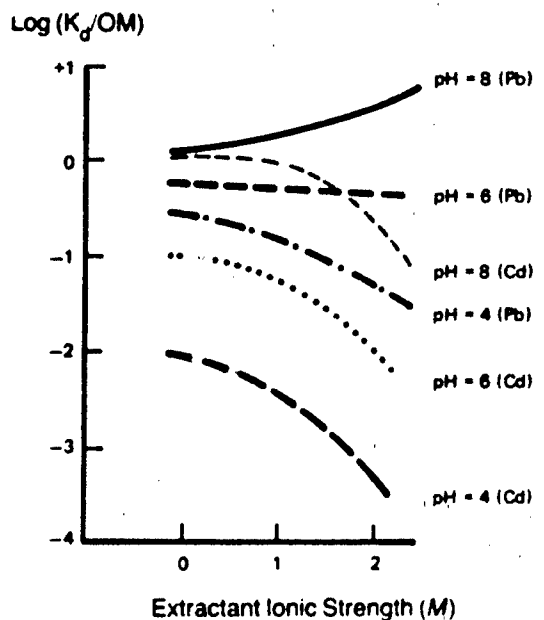


Source: O'Connor and Kester [30]. (Copyright 1975. Pergamon Press, Inc.
Reprinted with permission.)

FIGURE 2.12-2 Sorption of Cu(II) from Artificial River Water on Illite as a Function of pH

for the sorption of Cu(II) on illite. In the case of illite, the decreased sorption with increasing pH may be due to the dissolution of illite at high pH ($\text{SiO}_2(\text{s}) \rightarrow \text{H}_4\text{SiO}_9$ above pH 9). An additional example of the effect of pH (and ionic strength) on metal sorption by soils is given in Figure 2.12-3: the sorption coefficient for both cadmium and lead increases significantly as the pH rises from 4 to 8.

The redox conditions in the soil environment (e.g., as measured by the Eh) affect the speciation of the chemical constituents in the soil, which in turn affects the attenuation of the solutes present. Redox conditions also influence precipitation: under reducing conditions, sulfide precipitates of mercury, cadmium and some other heavy metals are significant species. Attenuation of these metals could be increased under reducing conditions in the presence of sulfur. Whether the soil is saturated or non-saturated with water may also affect attenuation, because changes in Eh are common in soil that is subject to repeated flooding and draining.



Plots of logarithm of the distribution coefficient expressed per unit of soil organic matter ($\log K_d/OM$) versus ionic strength. K_d (l/g) is the ratio between the concentration of the metal in the soil and in the solution, OM is in % of dry matter. Curves were derived from averaged data from studies on 20 Dutch soils.

Source: Gerritsen et al. [14]. (Copyright 1983. Reprinted with permission.)

FIGURE 2.12-3 Effect of pH and Ionic Strength on Sorption of Lead and Cadmium

The attenuation of inorganics in soil may be affected by sorption on microbial cell walls. Microorganisms may also transform inorganics into other species that differ in attenuation behavior under the soil conditions or that alter the attenuation of still other species. The transformation of SO_4^{2-} to S^{2-} by biological reduction under anaerobic conditions may cause the precipitation of metals from a soil system.

The presence of complexing species also affects the attenuation of an inorganic solute. The process may be described as a competition between surface and dissolved ligands for coordination sites on the cation [38]. The effect of complex formation on the sorption of a metal ion depends on the relative stabilities of the cation-ligand in solution and the cation-surface and on whether the surface has an affinity for the complexed form [23]. An example is the effect of Cl^- on Hg sorption: in studies with sediments, a decrease in the sorption of Hg has been found with increasing Cl^- concentration [7,36]. This is likely due to the formation of very stable Hg-Cl complexes, which are poorly sorbed [22].

Sposito [43] classified the ligand effects of metal-complexing ligands in a soil solution into five general categories:

- (1) The ligand has a high affinity for the metal, and the soluble complex formed has a high affinity for the sorbent, resulting in increased sorption;
- (2) The ligand has a high affinity for the sorbent, and the sorbed ligand has a high affinity for the metal, resulting in increased sorption;
- (3) The ligand has a high affinity for the metal, but the soluble complex formed has a low affinity for the sorbent, resulting in decreased sorption;
- (4) The ligand has a high affinity for the sorbent, but the sorbed ligand has a low affinity for the metal, resulting in decreased sorption; and
- (5) The ligand has low affinity for both metal and sorbent, resulting in little effect on sorption.

Complexing ions influence the precipitation of many metals. The complexing of metal ions effectively increases the overall solubility of the metal, as further discussed in section 2.9 of this report. In the presence of complexing ions, precipitation is less likely to occur because of the lowered concentration of the uncomplexed ion.

The relative affinity of a sorbent for different species is called its *selectivity*. This is a measure of the competitiveness among various species for surface sites on the sorbent. Kinniburgh and Jackson [23] have reported various selectivity sequences for cation sorption. Generally, divalent transition and heavy-metal cations are more strongly sorbed than alkaline-earth cations on hydrous oxides. On clays, however, there is not much difference in their selectivity. These authors state that the selectivity and competition among ions for surface sites is extremely dependent on the pH and concentration of ions present. Noting the wide separation of sorption curves between alkaline-earth cations and transition and heavy-metal ions, they suggest that Ca^+ would not be expected to interfere significantly with the sorption of these ions, even if the concentration of Ca^+ were several orders of magnitude greater.

Changes in temperature appear to affect sorption, although the relationship is not clear [23]. Sorption can result from several processes, each of which is affected by temperature changes in a different way; thus, the overall temperature dependence of the sorption process is difficult to predict for natural systems.

DiToro *et al.* [8] have investigated the effect of concentration of suspended sorbent on heavy metal sorption. In experiments with nickel and cobalt sorbed onto montmorillonite and quartz, they found that the reversible component partition coefficient was a function of particle concentration. Sorption of heavy metals does not appear to be completely reversible and is affected by the particle concentration.

2.12.4 Measurement of Attenuation

Three laboratory methods are available for measuring the extent of attenuation by soils: (1) thin-layer chromatography with soils, (2) batch tests that generate soil adsorption isotherms and (3) column tests that measure capacity and breakthrough. The EPA's Office of Toxic Substances has established some procedures for testing attenuation under the Toxic Substances Control Act [47]. These procedures are soil thin-layer chromatography and the sediment/soil adsorption isotherm (Guidelines CG-1700 and CG-1710 respectively). The Organization for Economic Cooperation and Development (OECD) has also established procedures for the testing of chemicals [30]. The procedure for determining attenuation in soils and sediments entails batch equilibrium tests and extraction, generating adsorption isotherms (Guideline No. 106). While the procedures given by both the EPA and the OECD appear to be focused on the testing of organics, they may be appropriate for inorganics with modifications. Examples of various extraction procedures to measure attenuation in soils have been described by Conway and Malloy [6]. The American Society for Testing and Materials (ASTM) has developed a new method for batch experiments to determine sorption by soils and sediments [1].

Soil thin-layer chromatography, as described by the EPA, is a qualitative screening tool for estimating the leaching potential of a chemical. This test is analogous to conventional thin-layer chromatography (TLC) but uses soil instead of adsorbents like silica gel and alumina. A slurry containing fine particles of the soil is used to produce the soil TLC plates. The plates are then spotted with the chemical and certain reference chemicals, and the movement along the TLC plate is subsequently used to estimate the relative mobility of the chemical concerned. The absolute movement on these soil TLC plates is not translatable into actual field leaching or mobility of the chemical, because natural soil systems are much more complex; however, a qualitative measure of relative leachability is provided by this test.

Data from batch equilibration tests of aqueous solutions containing environmentally realistic concentrations can be plotted to produce an "adsorption isotherm", a curve relating the concentration left in solution to the amount sorbed. EPA Guideline CG-1710 [47] uses the Freundlich isotherm (see "Empirical Models" below). A linear plot of the log of the equilibrium concentration in the solid phase (sorbed) versus the log of the equilibrium concentration in the solution phase will produce an intercept of $\log K_F$ and a slope of $1/N$. (This is true if sorption of the inorganic follows the Freundlich isotherm under the conditions of the test; other equations may be used if this isotherm is found to be unsuitable.)

Another way to measure attenuation is by the use of column studies. The approach to predicting pollutant movement suggested by Amoozegar-Fard *et al.* [2] used column studies to predict an equivalent of the relative velocity of metals in leachate through columns of soil. Samples representing a range of soil properties were packed into columns, 5.2 cm in diameter and 10 cm long. Leachates containing known initial concentrations of Cd, Ni, and Zn were perfused through the soil columns at a constant rate, and the effluent was partitioned on a fraction collector. Each fraction of the

effluent was analyzed for the metal(s) in the original leachate. The relative concentrations (concentration in effluent fraction/initial leachate concentration) were then plotted against time or pore volumes to generate breakthrough curves. Details of this procedure are given under "Empirical Models" below.

2.12.5 Mathematical Representations

Numerous models have been proposed to describe the attenuation of solutes in soils. As may be deduced from the foregoing discussion, no one mathematical representation can describe the attenuation of all solutes under different environmental conditions. The models may be divided into two types: theoretical and empirical. The theoretical models attempt to account for the specific physical and/or chemical interactions occurring between the solutes and the solid surface. The empirical models, on the other hand, are based on the overall attenuation behavior of a solute and usually assume equilibrium conditions. In this section, theoretical models will be briefly described; these are more complicated than empirical representations and are not easily applied to natural soil or sediment environments, which are very complex.

Kinetic models, which may be either theoretical or empirical, do not assume equilibrium conditions and are time-dependent. They are not discussed in detail in this section; further information on the kinetics of processes is given in Chapter 3.

THEORETICAL MODELS

Theoretical models are related to the specific processes leading to sorption in a system. They attempt to model interactions due to the occurrence of surface charges (which attract opposite charges) and also the interactions with surface species (which result in formation of surface complexes with the solutes in solution).

The Gouy-Chapman electric double-layer model is an example of a mechanistic model for the interactions of surface charges. Ravina and Gur [35] applied this model to the sorption of alkali metals onto charged surfaces from chloride solutions. It is very complicated mathematically, even for the simplest systems. Application of this theory to natural systems containing many components would be extremely difficult. Westall and Hohl [48] have shown that electrostatic models of the current generation are not necessarily more accurate than the Stern model, which makes some very simple assumptions regarding surface electrostatic interactions.

Sposito [42-44] has given excellent compilations of models that attempt to account for surface complexation; he described three surface complexation models: the Constant Capacitance Model, the Triple-Layer Model and the Objective Model. These differ generally in the hypotheses used to derive the equations in the models. For example, one of the differences between the Constant Capacitance and Triple-Layer models is that the former assumes that only inner-sphere surface complexes are formed, whereas the Triple-Layer model assumes that the proton (and/or hydroxide ions) form outer-sphere surface complexes with the sorbed species. In a surface complexation

model, the equations for complexation of ions in solution may be adapted to describe sorption on surfaces. Morel [27] illustrated the use of a surface complexation model to describe sorption in simple heterogeneous systems, such as the sorption of lead on alumina.

A primary aspect of surface complexation models is that they hypothesize the existence of one or more complexed surface species. These species are often constructs rather than real species. In simple systems (e.g., artificial laboratory systems) the surface complexation model may be applied, because equations may be derived to describe the limited number of surface complexes in such a system. In natural systems, however, numerous inorganic and organic species occur on the sorbents and the soil solution. The identities of the surface complexation species that can occur are often unknown. Also, because of the number of surface species, the set of mathematical equations is large, and their solution is complicated. Surface complexation models are therefore difficult to apply to real systems.

KINETIC MODELS

Kinniburgh and Jackson [23] reported that the sorption of cations by hydrous metal oxides is often extremely rapid; most of the sorption occurs within minutes. However, depending on the time frame under which other reactions are occurring, kinetics may become important. Cases have also been found in which more than one step is involved in the process of sorption: Jardine *et al.* [20] stated that the sorption of aluminum on kaolinite appeared to occur on two different kinds of surface sites: (1) instantaneous equilibrium sites and (2) sites following first-order reversible kinetics. It should therefore not be assumed that sorption equilibrium exists in any particular situation. The rate of desorption is very important in determining whether equilibrium can be assumed; however, there is little information on desorption.

The consideration of non-equilibrium sorption has led to the formulation of kinetic models. One of these is the Elovich equation [18,46], which is shown below in its simplest form.

$$\frac{dq}{dt} = Ae^{-Bq} \quad (1)$$

where q = fraction of sites occupied by solute at time t

A = constant relating to initial velocity of reaction

B = constant relating to activation energy for sorption

Travis and Etnier [46] reviewed a number of first-order kinetic models. Their use in environmental systems obviously requires that the values of the parameters in the equations be known. A review of the literature shows that few parameter values for sorption-desorption kinetic models are available for inorganics in soils, but several of the models have been used to describe phosphorus sorption in soils [46].

EMPIRICAL MODELS

The complexity of natural systems militates against the application of theoretical models. Individual mechanisms for attenuation are not readily or easily distinguishable, and, even if they were, modeling each mechanism could lead to complex mathematical equations containing many unknown parameters. For example, the use of any of the surface complexation models requires complexation constants for the surface complexation species for each sorbent phase. The electrostatic interaction energy between the surface and the solute must also be described.

Empirical models that ignore the mechanisms of attenuation but describe the overall behavior using simple equations are presently more appropriate and applicable to real-life conditions. The next section discusses commonly used adsorption isotherms for describing soil-solute interactions. These are the linear, Langmuir, and Freundlich isotherms. Also described is an empirical, non-equilibrium method demonstrated by Fuller and co-workers utilizing soil column studies [2,9,10].

Table 2.12-3 summarizes the empirical representations and their limitations. Tables 2.12-4, -5 and -6 show some data for the parameters; these tables by no means compile all the existing data for attenuation of inorganics, but the EPRI report on which they are based [34] includes a comprehensive review of available data for some elements. Readers should also refer to the sections on individual elements in Part II of this report for additional data. Because attenuation depends on environmental conditions, the tables include some examples of the variation in parameter values with changing environmental conditions (e.g., pH and ionic strength).

2.12.6 Adsorption Isotherms

Numerous adsorption isotherms were originally developed to describe the physical adsorption of gases onto solid surfaces. Investigators found that the experimental data fitted certain curves that were based on assumptions about the behavior of the gas molecules and the solid surface — e.g., the existence of a maximum number of uniform sites (Langmuir), or heterogeneous sites with heats of adsorption decreasing exponentially with adsorption density (Freundlich). These isotherms have been adapted to describing the attenuation of solutes in soils and sediments. Although physical adsorption is not the only mechanism that contributes to attenuation of solutes in natural environments, the isotherms are useful for describing the overall attenuation process, particularly at dilute concentrations of solutes. We will therefore use the term "adsorption isotherm" to refer to the mathematical equation describing solute sorption and attenuation in soils.

An adsorption isotherm is defined as the relationship between the amount of a substance sorbed and its concentration in solution under conditions of equilibrium and at constant temperature [23]. The shape of the isotherm curve is related to the energy of sorption and the number of sorption sites. Essentially, an adsorption isotherm is obtained by batch equilibrium experiments to obtain data points (amounts sorbed versus equilibrium concentration in solution) at increasing concentrations. An equation is then fitted to the data.

TABLE 2.12-3 Summary of Empirical Models of Sorption

Model	Equation	Definitions	Typical Units
Langmuir	$S = K_L A_m C / [1 + K_L C]$ Linear: $C/S = 1/[K_L A_m] + C/A_m$	S = mass sorbed at equilibrium per mass sorbent A_m = maximum sorption capacity of sorbent K_L = Langmuir sorption constant related to binding energy C = sorbate concentration in solution at equilibrium	mol/g mol/g liter/mol mol/liter
Freundlich	$S = K_F C^{1/N}$ Linear: $\log S = \log K_F + (1/N) \log C$	S = mass sorbed at equilibrium per mass sorbent K_F = Freundlich isotherm constant N = Freundlich isotherm constant, $N \geq 1$ C = sorbate concentration in solution at equilibrium	mol/g liter/g — mol/liter
Distribution Coefficient	$S = K_d C$	S = mass sorbed at equilibrium per mass sorbent K_d = distribution coefficient C = sorbate concentration in solution at equilibrium	mol/g liter/g mol/liter
-Ullar and Co-workers	For given $[Me]_{ss}/[Me]_i$, Cadmium: $V = (V_p/25)(a[\% clay]^{-1} + b[\% sand] + c[\% sand]^2 + d[\% FeO]^{-2} + e[\% FeO]^{-1} + f[\% TSS] + g[\% TOC])^2 + h[\% TOC] + i)$	$[Me]_i$ = initial concentration of metal in leachate $[Me]_{ss}$ = final steady state concentration of metal in leachate V = velocity for a given $[Me]_{ss}/[Me]_i$ through soil v_p = pore water velocity = v_d/b_v v_d = average water flow (Darcian velocity through soil) θ_v = porosity (water or leachate volumetric content)	mg/liter mg/liter cm/day cm/day cm/day m/m
	Nickel: $V = (V_p/25)(a[\% clay]^{-1} + b[\% sand]^{-1} + c[\% FeO]^{-1} + d[\% FeO]^{-1} + e[\% TSS] + f[\% TSS]^2 + g[\% TOC] + h[\% TOC]^2 + i)$	% clay = soil clay content; 1% = 10g/kg % sand = soil sand content; 1% = 10g/kg % silt = soil silt content; 1% = 10g/kg	— — —
Zinc:	$V = (V_p/25)(a[\% sand] + b[\% silt]^2 + c[\% FeO]^{-1} + d[\% FeO]^{-2} + e[\% TOC] + f[\% TOC]^2 + g[\% TSS] + h[\% TSS]^2 + i)$	% FeO = iron oxide content; 1% = 10g/kg % TOC = total organic carbon in leachate; 1% = 10g/liter % TSS = total soluble salts in leachate; 1% = 10g/liter a,...,i = empirical parameters, different values for each metal	— — — —

(Continued)

TABLE 2.12-3 (Continued)

Model	Variations	Applicability and Limitations	Experimental Method
Langmuir	<i>Multiple-Site:</i> $S = \sum_i K_L A_m C / (1 + K_L C)$	Empirical; does not relate to mechanism of sorption.	Batch equilibration
	Subscript i denotes site type	Equilibrium assumed. Applicable to dilute systems.	
	<i>Competitive:</i> $S_i = [A_m K_L C_i] / [1 + \sum_j n_i K_L C_j]$	Predicts saturation of monolayer; therefore, maximum implied. Sorption sites assumed uniform; no lateral interactions among sorbed species.	
	Subscript i denotes species competing with species j.		
	$n_i = A_m / A_{mi}$		
	<i>Competitive:</i> $[C_i / C_p] S = A_m / [K_L A_m] + C_i / A_m C_i$		
	<i>Sorbable and non-sorbable species of element:</i>		
	$S_a = K_{La} A_{ma} [C_m - C_n] / [1 + K_{La} (C_m - C_n)]$		
	Subscript a denotes sorbed species.		
	m denotes total and n denotes non-sorbed species.		
Freundlich	<i>Phosphate Model:</i> Above C_c : $S = aC + X_o$ linear Below C_c : $S = aC + KC^n$ Freundlich where: $X_o = KC_c^n$ $C_c = [X_o / K]^{1/n}$	Empirical; does not relate to mechanism of sorption. Equilibrium assumed. Applicable to dilute systems. Accounts for heterogeneity of surfaces; heat of sorption decreases exponentially with coverage. Extrapolation beyond data points not advisable; no maximum predicted, and sorption not linear at dilute concentrations.	Batch equilibration
Distribution Coefficient	K_d often given for a single data point, which should not be extrapolated to generate a line.	Empirical; does not relate to mechanism of sorption. Equilibrium assumed. Applicable to dilute systems. No maximum predicted.	Batch equilibration
Fuller and Co-workers	--		Column tests
			Empirical; does not relate to mechanism of sorption. Based on physically measurable soil properties. Data available for cadmium, nickel, and zinc only.

TABLE 2.12-4
Distribution Coefficients for Some Metals

Metal	Sorbent	Sorbate Conc. (M)	Electrolyte			
			Identity	Conc. (M)	pH	K_d (ml/g)
Ba	River sediment	$10^{-5.9}$	Seawater	~0.7	8	530
	River sediment	$10^{-6.4}$	River water	—	—	2,800
Cd	Montmorillonite (Na-form)	$10^{-6} - 10^{-7}$	$\text{NaNO}_3 + \text{NaOAc}$	1.0, 0.01	5.0	8
				1.0, 0.01	6.5	100
				0.01, 0.01	5.0	210
				0.01, 0.01	6.5	900
Cu	Bentonite (Ca-form) Kaolinite	$0 - 10^{-5.3}$	Seawater	~0.7	8	43
			Humic acid added	0 $\mu\text{g/l}$	6.4	43
	$\text{Fe}_2\text{O}_3 \cdot \text{H}_2\text{O}(\text{am})$ $\text{MnO}_2(\text{hydrous})$	$10^{-6.5}$	Seawater	~0.7	8	7,000
			Seawater	~0.7	8	7,300
			Seawater	~0.7	8	20,000
			Seawater	~0.7	8	59,200
	Bentonite	10^{-6}	NaNO_3	1.0	4.5	2,550,000
			$\text{Ca}(\text{NO}_3)_2$	0.01	6.7	408,000
					7.9	179,000
					8.9	119,000
Ni	Montmorillonite Fe oxide(hydrous)	$10^{-6.5}$	Seawater	~0.7	8	200
			Seawater	~0.7	8	100,000
Zn	$\delta\text{-MnO}_2$	$10^{-8} - 10^{-6}$	Seawater	~0.7	8	800,000

Definitions:

$$S = K_d C$$

where: S = mass sorbed at equilibrium per mass of sorbent ($\mu\text{mol/g}$).

K_d = distribution coefficient (ml/g)

C = sorbate concentration in solution at equilibrium ($\mu\text{mol/ml}$)

Source: Data (from various sources) adapted from Rai et al. [34]

TABLE 2.12-5
Langmuir Constants for Some Metals

Metal	Sorbent	Sorbate Conc. (M)	Electrolyte			Constants		
			Identity	Conc. (M)	pH	A_m ($\mu\text{mol/g}$)	K_L ($\log M^{-1}$)	
As	Hydroxide, $\text{Al}(\text{OH})_3$ (am)	As(V)	—	—	5	1,600	5.08	
					6	1,487	5.17	
					7	1,179	5.24	
					8	538	5.12	
					8.5	681	4.85	
Oxyhydroxide, $\text{Fe}_2\text{O}_3 \cdot \text{H}_2\text{O}$ (am)	As(III) as AsO_4^{3-} $10^{-7} - 10^{-5}$	NaNO_3	1.0	4.0	9	501	4.82	
					5.7	490	6.26	
					7.0	513	6.36	
Montmorillonite	$10^{-4} - 10^{-3}$ As(V) + $10^{-4} - 10^{-3}$ As(III)	Leachate	—	—	8.8	417	6.18	
					5	9.9 ^a	3.57 ^a	
Ba	MnO_2 (hydrous)	$10^{-5} - 10^{-3}$	NaClO_4	0.01	5	2,050	4.6	
Cd	Montmorillonite (Na-form)	$10^{-6.9} - 10^{-6}$	NaClO_4	0.01	6.5-7	0.5	7.7	
				0.03	6.5-7	0.4	7.2	
					0.05	6.5-7	0.4	6.8
					0.17	6.5-7	0.2	6.9
River sediment		$10^{-17} - 10^{-3.8}$	—	—	1.0	6.5-7	0.3	6.7
					—	~7.5	10-173	4.4-6.0
Cr	Kaolinite	$10^{-4} - 10^{-2.2}$	Leachate	—	3	3.64	—	
					4	2.5	—	
					7	0.98	—	
					3	96.3	—	
					4	283	—	

(Continued)

TABLE 2.12-5 (Continued)

Metal	Sorbent	Sorbate Conc. (M)	Electrolyte			Constants	
			Identity	Conc. (M)	pH	A_m ($\mu\text{mol/g}$)	K_L ($\log M^{-1}$)
Cu	Kaolinite	$10^{-5.8} \sim 10^{-3.8}$	CaCl ₂	0.05	5.5	1.9	4.5
	Peat	$0 \sim 10^{-3.8}$	CaCl ₂	0.05	5.5	184	5.0
	$\text{Fe}_2\text{O}_3 \cdot \text{H}_2\text{O}$ (am)	$0 \sim 10^{-4.5}$	Seawater	-0.7	8	1.120	5.3
	Montmorillonite	$10^{-4.3} \sim 10^{-2.7}$	Landfill	-0.1	5.0	$8.8(A_{m1})$ $5.38(A_{m2})$	$4.3(K_{L1})$ $2.1(K_{L2})$
Pb	Gceithite	$10^{-3} \sim 10^{-2.2}$	Leachate	-	-	85	2.9
	Mn Oxide(hydrous)	$10^{-3.5} \sim 10^{-2.8}$	KNO ₃	0.1	5.0	-	-
	Various soils	$10^{-4.6} \sim 10^{-3.3}$	-	-	6	7.000	3.7
Mn	Montmorillonite	0.0035-0.05	KCl	0.1	7	7.0-23	3.7-4.9
	Cryolite/melane ($\alpha\text{-MnO}_2$ as $\text{K}_2\text{Mn}_8\text{O}_{16}$)	$10^{-3} \sim 10^{-2.2}$	Landfill	-	-	370,610	2.7-2.8
	Clay loam	$0 \sim 10^{-2.9}$	KNO ₃	0.1	5	1,130	3.5
	Sediments	$10^{-6} \sim 10^{-4}$	Na ₂ SO ₄	0.01	5.4	14,719.3	3.4
Hg	N	2	$10^{-3} \sim 10^{-2.2}$	KNO ₃	0.1	5	690
	Se	Kaolinite	$10^{-3} \sim 10^{-4}$ Se(IV)	Landfill	-	3	4.20
				Leachate	-	5	2.93
					-	7	2.40
					-	-	3.26

(Continued)

TABLE 2.12-5 (Continued)

Metal	Sorbent	Sorbate Conc. (M)	Electrolyte			Constants	
			Identity	Cone. (M)	pH	A _m (μmol/g)	K _L (log A _m ⁻¹)
Zn	Montmorillonite	10 ^{-3.6} - 10 ^{-2.6}	Landfill Leachate	~0.1	5	29	3.0
	Ca-saturated				6	35	3.1
	Fe(OH) ₃ (am)	10 ^{-6.7} - 10 ⁻⁵	—	—	6	25	5.4
	Calcite	10 ⁻⁷ - 10 ^{-5.3}	—	—	7	170	5.9
	Clay loam	0 - 10 ^{-5.5}	CaCl ₂	—	8	440	6.7
				8.4	59	5.2	
				0.016	7.7 ^b	9.4	5.5

a. Values apply to As(V)

b. Soil pH

Definitions.

$$S = K_L A_m C [1 + K_L C]$$

where: S = mass sorbed at equilibrium per mass of sorbent (μmol/g)
A_m = maximum sorption capacity of sorbent (μmol/g)

K_L = Langmuir constant related to binding energy of sorbate (liter/μmol), given above as log [liter/mol]
C = sorbate concentration in solution at equilibrium (μmol/liter)

A_{m1}, K_{L1}, A_{m2}, K_{L2} refer to two sorption sites

Source: Data (from various sources) adapted from Rai et al. [34]

TABLE 2.12-6
Freundlich Constants for Some Metals

Metal	Sorbent	Sorbate Conc. (M)	Electrolyte Identity			pH	Constants	
			(M)	(M)	K _F (l/g)		1/M	
Cd	Montmorillonite (Na-form)	10 ^{-6.9} - 10 ⁻⁶	Na ₂ SO ₄	0.03	6.5-7	3.9	1.03	
Fe ₂ O ₃ · H ₂ O(am)	0 - 10 ^{-7.7}	NaNO ₃	0.05	6.5-7	0.74	0.78		
	10 ^{-7.7} - 10 ⁻⁴	NaNO ₃	0.075	6.5-7	0.63	0.82		
	10 ^{-7.7} - 10 ⁻⁴	NaNO ₃	0.1	6.8	1.1	1.0		
	10 ^{-7.7} - 10 ⁻⁴	NaNO ₃	0.1	6.6	0.065	0.67		
Four soils	10 ^{-7.7} - 10 ⁻⁴	NaNO ₃	0.1	6.9	0.15	0.67		
	10 ^{-8.9} - 10 ^{-5.4}	NaNO ₃	0.1	7.2	0.32	0.67		
	10 ^{-5.1} - 10 ^{-3.5}	Simulated sludge leachate	—	5.4-6.4	3.6-23.2	0.63-0.95		
Cu	Forest soil	10 ^{-6.9} - 10 ^{-4.4}	CaCl ₂	0.05	7.7	12.6, 18.8	0.33, 0.22	
Pb	Various soils	10 ⁻⁶ - 10 ^{-4.4}	CaCl ₂	—	8.2	4.3	0.22	
				—	8.6	8.9	0.18	
Mn	Bentonite	0 - 10 ⁻³	—	—	4.9	0.011	0.9	
	Illite	0 - 10 ⁻³	—	—	7.6	23	0.18	
	Kaolinite	0 - 10 ^{-2.9}	—	—	8.8	4.3	0.48	
				—	4.9	0.015	1.13	
				—	6.2	0.011	1.20	
				—	7.6	0.018	1.17	
				—	8.8	0.043	1.07	

(Continued)

TABLE 2.12-8 (Continued)

Metal	Sorbent	Sorbate Conc. (M)	Electrolytes			Constants	
			Identity	Conc. (M)	pH	K_f	$1/N$
Hg	Fe(OH) ₃ (am)	10 ⁻⁷ – 10 ⁻⁶	—	—	—	90.8	0.76
Ni	Silt loam	10 ^{-6.5} – 10 ^{-3.8}	CaCl ₂ CaCl ₂ Ca(ClO ₄) ₂ CaCl ₂	0.01 0.1 0.1 0.01	6.1 ^a 6.1 ^a 6.1 ^a 6.1 ^a	0.30 0.057 0.033 0.27	0.95 0.91 0.94 0.57
	Sandy loam	10 ^{-3.8} – 10 ^{-1.8}	CaCl ₂	0.01	6.1 ^a		
Zn	Fe ₂ O ₃ • H ₂ O(am)	10 ^{-7.5} – 10 ^{-4.0}	NaNO ₃ CaCl ₂ CaCl ₂	0.01 0.016 0.016	6.4 7.7 ^a 8.5 ^a	8.9 1.8 13	1.0 0.94 0.85
	Clay loam	0 – 10 ^{-5.5}					
	Clay	0 – 10 ^{-5.8}					

a. Soil pH
Definitions:
 $S = K_f C^{1/N}$

where: S = mass sorbed at equilibrium per mass of sorbent ($\mu\text{mol/g}$)

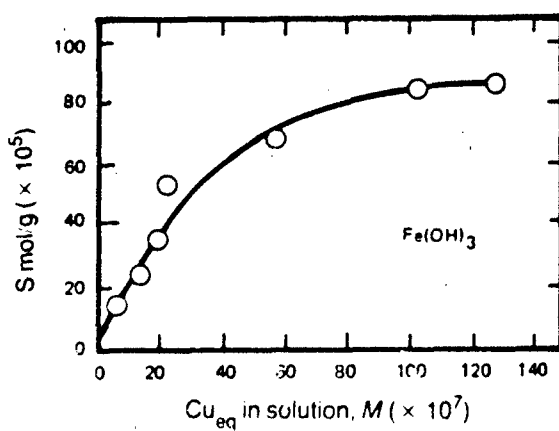
K_f = Freundlich isotherm constant (liter/g)

N = Freundlich isotherm constant; $N \geq 1$

C = sorbate concentration in solution at equilibrium ($\mu\text{mol/liter}$)

Source: Data (from various sources) adapted from Rai et al. [34]

Oakley *et al.* [29] obtained adsorption isotherms for Cu and Cd in seawater using several sorbents. Their measurements with Cu and Fe(OH)_3 in seawater are discussed below to illustrate how an adsorption isotherm is derived. Similar procedures could be used to derive adsorption isotherms for other solutes and sorbents (including soils and sediments) under different conditions. The experiments were carried out in 50-ml polyethylene centrifuge tubes containing a known amount of solid (~10 mg) and 20 ml of seawater. The required amounts of stock solution of $\text{Cu}(\text{NO}_3)_2$ were added to provide a range of initial Cu concentrations, and the pH was adjusted to 8.0 ± 0.1 with NaOH or HNO₃. The tubes were agitated for 24 hours. The solid/liquid mixtures were centrifuged to separate the dissolved and solid phases. The soluble Cu concentration was measured by atomic absorption spectrophotometry. The quantity of Cu sorbed on the Fe(OH)_3 was calculated by difference from the amount of metal added and the final soluble concentration. The adsorption isotherm (Figure 2.12-4) was obtained by plotting the concentration of dissolved Cu at equilibrium on the x-axis and the amount of Cu sorbed per gram of Fe(OH)_3 on the y-axis.



Salinity = 32 ‰, pH = 8.0, Temperature = 20°C.

Source: Oakley, Nelson and Williamson [29]. (Copyright 1981, American Chemical Society. Reprinted with permission.)

FIGURE 2.12-4 Adsorption Isotherm of Cu on Fe(OH)_3 in Seawater

Different authors have found that either the Langmuir or Freundlich isotherm would fit their experimental data. Cavallaro and McBride [5] reported that the Langmuir model described the sorption of Cu and Cd in samples of acidic and neutral silt loam soils, while Sidle and Kardos [41] found that data for Cu fitted the Freundlich isotherm better than the Langmuir in experiments with forest soil. In some cases, both models have been used to fit the same experimental data.

As Travis and Etnier have pointed out, the fit of sorption data to a particular isotherm has no bearing on the mechanism of attenuation [46]. Also, data used to generate isotherms are obtained from batch experiments in which the sorbent and solute are in prolonged contact (usually 24 hours); this may not be representative of environmental conditions.

DISTRIBUTION COEFFICIENT

The simplest mathematical representation is the linear isotherm with a distribution coefficient:

$$S = K_d C \quad (2)$$

where S = mass sorbed at equilibrium per mass of sorbent (mol/g)

K_d = distribution coefficient (l/g)

C = sorbate concentration in solution at equilibrium (mol/l)

The linear isotherm does not imply a maximum. The distribution coefficient is often given as a single point measured at a particular equilibrium concentration and defined as the mass sorbed per gram at equilibrium divided by the equilibrium concentration in mol/liter. Extrapolating this point to a different concentration could result in large errors and should not be attempted.

Example 1 How much Cd would be sorbed onto one gram of soil with a main component of montmorillonite at equilibrium concentration of $10^{-6} M$ in the liquid phase? What would the final conditions in the system be if the initial solution had a concentration of $10^{-5} M$ Cd?

Table 2.12-4 lists a K_d value of 210 ml/g for montmorillonite (Na-form) for a Cd concentration of $10^{-6} - 10^{-7} M$ using 0.01M NaNO₃ and 0.01M NaOAc as electrolyte at pH of 5.0. At an equilibrium concentration of $10^{-6} M$, $C = 1.124 \times 10^{-4}$ g/l. Therefore,

$$\begin{aligned} S &= K_d C \\ &= 0.210 \text{ l/g} \times 10^{-6} \text{ mol/l} \\ &= 0.210 \mu\text{mol/g} \end{aligned}$$

To calculate the final conditions in the system, let $Y M$ be the Cd concentration attenuated. (It is assumed that no Cd was adsorbed initially.) The Cd concentration in the final solution is then $C = (10^{-5} - Y) \text{ mol/l}$.

At equilibrium, the mass of Cd sorbed onto 1 gram of soil from 1 liter of solution is

$$S = Y \text{ mol/l} \times l/g = Y \text{ mol/g}$$

Using equation 2,

$$\begin{aligned} S &= K_d C \\ Y \text{ mol/g} &= (210 \text{ ml/g})(10^{-5} - Y) \text{ mol/l (l/1000 ml)} \\ Y &= 0.21 \times 10^{-5} - 0.21 Y \text{ mol/g} \\ 1.21 Y &= 0.21 \times 10^{-5} \text{ mol/g} \\ Y &= 1.74 \times 10^{-6} \text{ mol/g} \\ &= 1.74 \mu\text{mol Cd/g soil} \end{aligned}$$

The final solution concentration of Cd is thus

$$\begin{aligned} C &= 10^{-5} - Y \\ &= 8.3 \times 10^{-6} M \end{aligned}$$

LANGMUIR ISOTHERM

The Langmuir isotherm was first developed to describe the physical adsorption of gases by solids. It is based on the assumption that there are a finite number of sorption sites, resulting in a maximum sorption that is possible on the sorbent surface. As given by Rai *et al.* [34], the Langmuir isotherm is expressed as:

$$S = K_L A_m C / (1 + K_L C) \quad (3)$$

where: S = moles sorbed at equilibrium per mass of sorbent (mol/g)
 A_m = maximum sorption capacity of the sorbent (mol/g)
 K_L = Langmuir sorption constant, related to binding energy of the sorbate (l/mol)
 C = sorbate concentration in solution at equilibrium (mol/l)

A_m is a constant, representing the maximum number of sites on the sorbent surface. K_L is a measure of the bond strength between the sorbate and the surface site. In the Langmuir model, this bond strength is assumed to be constant. The heat of sorption is assumed to be independent of the number of occupied sites or the different types of surface sites. Essentially, there are no interactions between the sorbed molecules (or ions), and the sites on the surface are assumed to be uniform. Related to these two assumptions is that sorption is independent of the number of sites already occupied (which implies that sorption occurs on only a single layer on the sorbent surface) and that the sorption of molecules (ions) on the surface does not generate new sites on the sorbate layer.

The Langmuir isotherm may be expressed linearly in the following form [34]:

$$C/S = 1/[K_L A_m] + C/A_m \quad (4)$$

Using this equation, sorption data (C/S vs. C) are plotted to produce a line with a slope of $1/A_m$ and an intercept of $1/[K_L A_m]$.

The assumptions used in deriving the Langmuir isotherm are often not true for real systems. In soils, the sites are unlikely to be uniform because of the different types of sorbents present. As a result, K_L may not be constant. A range of different sites may be filled simultaneously. Over a large concentration range, interactions between sorbed molecules (ions) and multilayer sorption are more likely. Also, as the sorption density (fraction of occupied sites) increases, the heat of sorption changes and it becomes more difficult for subsequent molecules (ions) to become sorbed.

There are a number of ways to compensate for the imperfections of the Langmuir isotherm. Besides using another model (e.g., the Freundlich, which provides for heterogeneity of the sorbent surface), multiple-site Langmuir isotherms and the competitive Langmuir model have also been proposed and used.

The multiple-site variation of the Langmuir isotherm is based on the postulate that several energetically distinct sites are present or that different mechanisms are occurring on the same sites [34]. The total sorption arising from either of these alternatives may be represented by:

$$S = \sum_i K_{Li} A_{mi} C / [1 + K_{Li} C] \quad (5)$$

The total sorption is summed over all the possible types of sites; i.e., A_{mi} and K_{Li} are the Langmuir constants as they apply to site type i . The subscript i may also be used to denote different mechanisms, with the assumption that each of the mechanisms may be modeled using the Langmuir isotherm.

If there are two types of sites, the multiple-site variation of the Langmuir isotherm is written as:

$$S = K_{L1} A_{m1} C / [1 + K_{L1} C] + K_{L2} A_{m2} C / [1 + K_{L2} C] \quad (6)$$

In an environmental system with more than one sorbate, competition for surface sites may explain non-linearity in the Langmuir isotherm [15,17]. Rai *et al.* [34] introduced another term into the Langmuir equation to account for this factor. The sorption of the sorbate, j , in a competitive system is represented by:

$$S_j = [A_{mj} K_{Lj} C_j] / [1 + K_{Lj} C_j + \sum_i n_i K_{Li} C_i] \quad (7)$$

where i denotes the species competing with species j and $n_i = A_{mi}/A_{mj}$.

n_i compensates for the size differences of competing species. The larger the species j is, the more space it occupies compared with i . Therefore, n_i represents the ratio of the surface areas occupied by molecules (ions) j and i .

For competing species of similar size, $n = 1$. The final term in the denominator of equation 7 effectively reduces the sorption of species j in keeping with the bond

strengths of sorption and equilibrium concentrations of competing species. For two species of similar size, the equation reduces to:

$$S_j = [A_{mj}K_{Lj}C_j]/[1 + K_{Lj}C_j + K_{Li}C_i] \quad (8)$$

If C_i is assumed to be constant, equation 8 may be expressed linearly as:

$$C_j/S_j = [1 + K_{Li}C_i]/[A_{mj}K_{Lj}] + C_j/A_{mj} \quad (9)$$

If species i is present at sufficiently high concentrations compared with species j (e.g., if it is a major cation like Ca^{+2} or a major anion like Cl^- , which is present in natural environments at concentrations several orders of magnitude larger than trace metals or ligands), equation 9 will be applicable. K_{Li} will have to be determined separately under experimental conditions (pH, ionic strength, etc.) similar to those of the experiments used for the competitive system.

Boyd *et al.* [4] described the simultaneous competitive sorption of two equally charged cations by:

$$[C_j/C_i]/S = A_{mi}/[K_{Lj}A_{mj}] + C_j/A_{mi}C_i \quad (10)$$

A plot of $[C_j/C_i]/S$ against C_j/C_i generates a straight line with a slope of $1/A_{mi}$ and an intercept of $A_{mi}/[K_{Lj}A_{mj}]$.

The Langmuir isotherm can be adapted to include cases in which a solute is present in more than one form and only one form is sorbed by the sorbent [16]. For example, if the measured concentration (C_m) includes both the species that can be sorbed (C_a) and a non-sorbable species (C_n), the Langmuir model can include:

$$C_a = C_m - C_n \quad (11)$$

Therefore,

$$S_a = K_{La}A_{ma}[C_m - C_n]/[1 + K_{La}(C_m - C_n)] \quad (12)$$

Example 2 Using the Langmuir model, calculate the amount of Cd sorbed onto soil at an equilibrium concentration of $10^{-6} M$ in the liquid phase.

Sidle and Kardos [41] reported the following Langmuir constants for sorption of Cd in forest soil at a depth of 0-7.5 cm:

$$\begin{aligned} K_L &= 47.19 \text{ l/mg} \\ A_m &= 0.0024 \text{ mg/g soil} \end{aligned}$$

These values were obtained for initial Cd concentrations of 0.005-0.2 mg/l (or $10^{-7.4} - 10^{-5.8} \text{ mol/l}$).

To find S in terms of mol/g, the above constants must be converted to the proper units by applying the conversion factor of 112,400 mg/mol Cd:

$$\begin{aligned}
 K_L &= 47.19 \text{ l/mg} \times 112,400 \text{ mg/mol} \\
 &= 5.30 \times 10^6 \text{ l/mol or } 5.30 \text{ l}/\mu\text{mol} \\
 A_m &= 0.0024 \text{ mg/g} \times \text{mol}/112,400 \text{ mg} \\
 &= 2.14 \times 10^{-8} \text{ mol/g or } 0.021 \mu\text{mol/g} \\
 C &= 10^{-6} M = 1 \mu\text{mol/l}
 \end{aligned}$$

Substituting these values into equation 3, we obtain

$$\begin{aligned}
 S &= K_L A_m C / [1 + K_L C] \\
 &= \frac{5.3 \text{ l}/\mu\text{mol} \times 0.021 \mu\text{mol/g} \times 1 \mu\text{mol/l}}{1 + (5.3 \text{ l}/\mu\text{mol} \times 1 \mu\text{mol/l})} \\
 &= 0.018 \mu\text{mol/g sorbed}
 \end{aligned}$$

Example 3 Determine the final conditions in the above system if the initial solution had a concentration of $10^{-5} M$ Cd. (Assume that no Cd was sorbed initially.)

$$\begin{aligned}
 \text{Let the Cd concentration attenuated} &= Y M \\
 \text{Final concentration, } C &= \text{initial conc.} - \text{attenuated conc.} \\
 &= (10^{-5} - Y) M
 \end{aligned}$$

At equilibrium, the mass of Cd sorbed onto 1 g of soil from 1 liter of solution is

$$S = Y \text{ mol/l} \times 1/\text{g soil} = Y \text{ mol/g}$$

Then, from equation 3,

$$\begin{aligned}
 S &= K_L A_m C / [1 + K_L C] \\
 &= \frac{[5.3 \times 10^6 \text{ l/mol}] [2.14 \times 10^{-8} \text{ mol/g}] [C \text{ mol/l}]}{1 + (5.3 \times 10^6 \text{ l/mol})(C \text{ mol/l})} \\
 &= 0.113 C / [1 + 5.3 \times 10^6 C] \text{ mol/g}
 \end{aligned}$$

Substituting $C = (10^{-5} - Y) M$ and $S = Y \text{ mol/g}$,

$$\begin{aligned}
 Y &= \frac{0.113 (10^{-5} - Y)}{1 + (5.3 \times 10^6)(10^{-5} - Y)} \\
 (1.13 \times 10^{-6}) - 0.113 Y &= [54 - (5.3 \times 10^6 Y)] Y \\
 54 Y - (5.3 \times 10^6) Y^2 &= 1.13 \times 10^{-6} - 0.113 Y \\
 (5.3 \times 10^6) Y^2 - 54.11 Y + 1.13 \times 10^{-6} &= 0
 \end{aligned}$$

The two solutions to this quadratic equation are found to be:

$$Y = 1.02 \times 10^{-5} \text{ mol/g or } 2.08 \times 10^{-8} \text{ mol/g}$$

Since Y is always $\leq A_m$, the second solution is the appropriate value.

$$\begin{aligned}
 \text{Accordingly, } C &= (10^{-5} - Y) M = 10^{-5} - 2.08 \times 10^{-8} M \\
 &= 9.98 \times 10^{-6} M
 \end{aligned}$$

The final conditions are:

$$\begin{aligned}
 \text{Solution concentration} &= 9.98 \times 10^{-6} M \\
 \text{Amount attenuated} &= 0.02 \mu\text{mol/g}
 \end{aligned}$$

FREUNDLICH ISOTHERM

This isotherm attempts to account for the heterogeneity of surfaces by assuming that the heat of sorption decreases exponentially with coverage. In essence, it is assumed that the initial sites are the more favorable ones and that it becomes increasingly difficult to form a bond between the sorbate and sorbent surface as more of the surface sites are occupied. The Freundlich isotherm form is [34]:

$$S = K_F C^{1/N} \quad (13)$$

where S = moles sorbed at equilibrium per mass of sorbent (mol/g)
 K_F = Freundlich isotherm constant (l/g)
 N = Freundlich isotherm constant; $N \geq 1$
 C = sorbate concentration in solution at equilibrium (mol/l)

The Freundlich isotherm is an empirical relationship. From equation 13, it can be seen that the Freundlich does not imply a maximum sorption. At low concentrations, it generally does not become linear. Because of these two conditions, it is generally unwise to extrapolate this isotherm beyond the data points of measurement [23]. The Freundlich isotherm, having $N = 1$ becomes a linear equation with K_F equal to K_d , the distribution coefficient.

The linear form of the Freundlich isotherm is:

$$\log S = \log K_F + (1/N) \log C \quad (14)$$

A plot of $\log S$ versus $\log C$ provides a straight line with a slope of $1/N$ and an intercept of $\log K_F$.

In their study of the behavior of phosphate, Shayan and Davey [40] proposed a modified Freundlich isotherm that included a linear portion at concentrations above a critical concentration (C_c) and a modified Freundlich isotherm below this concentration. The two equations are:

$$\text{Above } C_c: S = aC + X_o \text{ (linear)} \quad (15)$$

$$\text{Below } C_c: S = aC + KC^n \text{ (Freundlich)} \quad (16)$$

At C_c , these equations are equal; therefore, $X_o = KC_c^n$ and $C_c = [X_o/K]^{1/n}$

The Freundlich isotherm successfully describes sorption at low concentrations. The Langmuir and Freundlich isotherms are sometimes indistinguishable at low concentrations and low surface coverage [16].

Example 4 Calculate the amount of Cd sorbed onto soil at an equilibrium concentration of $10^{-6} M$ in the liquid phase.

Sidle and Kardos [41] provided the following Freundlich constants for Cd in forest soil: K_F (equal to S) = 32.4 $\mu\text{g/g}$ at an equilibrium concentration of 1 $\mu\text{g/ml}$ and $1/N = 0.82$.

Substituting these parameters in equation 13,

$$32.4 \mu\text{g/g} = K_F(1)^{0.82} \mu\text{g/ml}$$
$$K_F = 32.4 \mu\text{g/g} \times \text{ml}/\mu\text{g} = 32.4 \text{ ml/g}$$

At an equilibrium concentration of $10^{-6} M$ Cd, $C = 1.124 \times 10^{-4} \text{ g/l}$. Again using equation 13,

$$S = 32.4 \text{ ml/g} (1.124 \times 10^{-4})^{0.82} \text{ g/l} (10^{-3} \text{ l/ml})$$
$$= 0.0187 \times 10^{-3} \text{ g/g}$$
$$= 18.7 \mu\text{g/g} \text{ or } 0.17 \mu\text{mol/g sorbed}$$

Example 5 Determine the final conditions in the above system if the initial solution had a concentration of $10^{-5} M$ Cd. (Assume that no Cd was sorbed initially.)

Let the Cd concentration attenuated = $Y M$

Final concentration, $C = \text{initial conc.} - \text{attenuated conc.}$

$$= (10^{-5} - Y) M$$

At equilibrium, the mass of Cd sorbed onto 1 g of soil from 1 liter of solution is

$$S = Y \text{ mol/l} \times 1 \text{ l/g soil} = Y \text{ mol/g}$$

Then, from equation 13,

$$S = K_F C^{1/N}$$
$$= 0.0324 \text{ l/g} (C \text{ mol/l})^{0.82}$$
$$= 0.0324 C^{0.82}$$

Substituting $C = (10^{-5} - Y) M$ and $S = Y \text{ mol/g}$,

$$Y = 0.0324 (10^{-5} - Y)^{0.82}$$
$$f(Y) = Y - 0.0324 (10^{-5} - Y)^{0.82} = 0$$

To solve this equation, we can use Newton's Method, which is an iterative method:

$$x_{n+1} = x_n - [f(x_n)/f'(x_n)]$$

$f'(Y)$ is the first derivative of $f(Y)$

$$f'(Y) = 1 - 0.027 (10^{-5} - Y)^{-0.18} (-1)$$
$$= 1 + 0.027 (10^{-5} - Y)^{-0.18}$$

Picking $Y_1 = 2 \times 10^{-7}$ as a first approximation and substituting it into $f(Y_1)$ and $f'(Y_1)$, we obtain:

$$\begin{aligned} Y_2 &= 2 \times 10^{-7} - [-2.33 \times 10^{-6}] / 1.215 \\ &= 2.12 \times 10^{-6} \\ Y_3 &= 2.12 \times 10^{-6} - [3.1 \times 10^{-6}] / 1.22 \\ &= 2.12 \times 10^{-6} \end{aligned}$$

The solution has converged at $Y = 2.12 \times 10^{-6}$ mol/g.

$$C = (10^{-5} - Y) = 7.88 \times 10^{-6} M$$

Thus,

$$\text{Final solution concentration} = 7.88 \times 10^{-6} M$$

$$\text{Amount attenuated} = 2.12 \mu\text{mol/g}$$

2.12.7 Soil Column Studies by Fuller and Co-workers

Simple, field-oriented regression equations have been developed to predict the movement of Cd, Ni and Zn through soils of known composition [2]. For example, the Cd equation can be used to predict the length of time it will take a given concentration of Cd to reach a particular soil depth when the initial leachate level is known. The equations can also be used to compute a concentration profile of Cd, Ni or Zn with depth of soil for periods of time after the application of a leachate containing a known quantity of the metal.

The equations were derived from data obtained in laboratory experiments with columns packed with disturbed soils that encompassed a broad spectrum of physical and chemical characteristics. The soils chosen contained little organic matter; most of the soluble organic compounds were removed by perfusion with deionized water before the leachate was applied. Leachates of known total organic carbon (TOC) and total soluble salts (TSS) content were enriched with 100 mg/l or 0.001 mol/l of Cd, Ni or Zn and were perfused through the soil columns at a constant rate. Effluent fractions were analyzed for the added metal. The data collected from these experiments were used in connection with the Lapidus and Amundson model [25] with a non-equilibrium adsorption term. This model, which provides an analytical solution to the solute flow for a step input, was used to generate the regression equations for predicting movement of the three metals through soils.

The three equations are valid only for (a) leachates that contain a single metal and have a pH of ~5.5-6.0 and (b) soils that are low in organic matter. The flux rate has little effect on the movement of Cd, Ni and Zn.

Use of these equations to calculate the propagation velocity, $V(\text{cm/day})$, for given concentrations of these metals requires determination of the following variables:

Average water flow (Darcian velocity through soil) = $v_d(\text{cm/day})$

Porosity (water or leachate volumetric content) = $\theta_v(\text{m}^3/\text{m}^3)$

Pore-water velocity = $v_p = v_3/\theta_v$ (cm/day)

Soil clay content = % clay² (mass/mass)

Soil sand content = % sand² (mass/mass)

Soil silt content = % silt² (mass/mass)

Iron oxide content (FeO) = % FeO² (mass/mass)

Total organic carbon in leachate = % TOC² (mass/volume)

Total soluble salts in leachate = % TSS² (mass/volume)

Initial concentration of metal in leachate = [Me]_i (mg/l)

Final steady-state concentration of metal in leachate = [Me]_{ss} (mg/l)

For a given $[Cd]_{ss}/[Cd]_i$, the empirical equation for Cd is:

$$V = (v_p/25) [a_{Cd}(\% \text{ clay})^{-1} + b_{Cd}(\% \text{ sand}) + c_{Cd}(\% \text{ sand})^2 + d_{Cd}(\% \text{ FeO})^2 + e_{Cd}(\% \text{ FeO})^{-1} + f_{Cd}(\% \text{ TSS}) + g_{Cd}(\% \text{ TSS})^2 + h_{Cd}(\% \text{ TOC}) + i_{Cd}] \quad (17)$$

For a given $[Ni]_{ss}/[Ni]_i$, the empirical equation for Ni is:

$$V = (v_p/25) [a_{Ni}(\% \text{ clay})^{-1} + b_{Ni}(\% \text{ sand})^{-1} + c_{Ni}(\% \text{ FeO}) + d_{Ni}(\% \text{ FeO})^{-1} + e_{Ni}(\% \text{ TSS}) + f_{Ni}(\% \text{ TSS})^2 + g_{Ni}(\% \text{ TOC}) + h_{Ni}(\% \text{ TOC})^2 + i_{Ni}] \quad (18)$$

For a given $[Zn]_{ss}/[Zn]_i$, the empirical equation for Zn is:

$$V = (v_p/25) [a_{Zn}(\% \text{ sand}) + b_{Zn}(\% \text{ silt})^2 + c_{Zn}(\% \text{ FeO})^{-1} + d_{Zn}(\% \text{ FeO})^2 + e_{Zn}(\% \text{ TOC}) + f_{Zn}(\% \text{ TOC})^2 + g_{Zn}(\% \text{ TSS}) + h_{Zn}(\% \text{ TSS})^2 + i_{Zn}] \quad (19)$$

where a_{Me} to i_{Me} are empirical parameters derived from a regression fit (analysis) of data from a variety of soils and metal concentrations of 100 mg/l or 0.001 mole/l. Values of a to i for various values of $[Me]_{ss}/[Me]_i$ are given in Table 2.12-7 (cadmium), 2.12-8 (nickel), and 2.12-9 (zinc).

For more detailed data and examples, readers should refer to several papers that describe the method used by Fuller and co-workers [9-12]. These investigators have prepared diagrams of the kind shown here as Figures 2.12-5 and -6, which portray the relative mobilities of cations and anions in various soils.

The data reported by Fuller *et al.* were obtained from column experiments, not measurements in the field. The advantage of this approach is that the data are based on physically measurable soil properties; however, detailed data are available only for Zn, Ni and Cd.

2. For clay, silt, sand, and FeO, 1% = 10 g/kg; for TSS and TOC, 1% = 10 g/liter.

TABLE 2.12-7
Empirical Parameters for Calculating the Propagation Velocity of Cadmium by Equation 17

Parameter	Ratio of $[Cd]_{14}/[Cd]_1$						
	0.1	0.2	0.3	0.4	0.5	0.6	0.7
a	32.02	31.07	30.65	29.54	29.91	29.52	29.18
b	-0.233	-0.227	-0.223	0.217	-0.217	-0.214	-0.212
c	0.00117	0.00114	0.00112	0.00109	0.00108	0.00107	0.00106
d	0.0116	0.0111	0.0106	0.00916	0.0101	0.00996	0.00970
e	9.846	9.385	9.057	8.817	8.532	8.293	8.048
f	90.83	89.19	87.32	92.20	84.13	83.06	81.63
g	-218.6	-216.4	-212.3	-234.1	-205.1	-203.1	-199.8
h	0.322	0.370	0.339	-0.148	0.442	0.494	0.511
i	-2.050	-2.015	-1.923	-2.069	-1.760	-1.702	-1.585
j ²	0.844	0.843	0.844	0.845	0.844	0.842	0.840
						0.838	0.838

Source: Amoozegar-Fard, Fuller and Warren [2]. (Copyright 1984. Reprinted with permission.)

TABLE 2.12-8
Empirical Parameters for Calculating the Propagation Velocity of Nickel by Equation 18

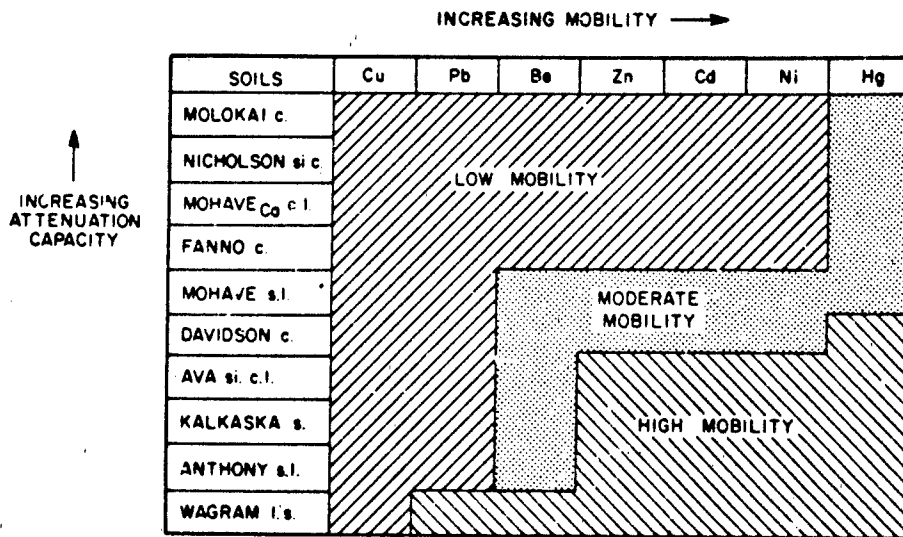
Parameter	0.1	0.2	0.3	0.4	0.5	0.6	0.7	0.8	0.9
[Ni] _{ss} /[Ni] ₀									
a	17.18	15.71	14.72	14.04	13.46	13.09	12.70	12.62	12.85
b	29.29	27.37	26.28	24.78	23.85	23.06	21.49	20.89	19.00
c	0.350	0.333	0.323	0.312	0.304	0.297	0.290	0.280	0.263
d	7.541	7.026	6.775	6.413	6.200	5.972	5.734	5.448	5.013
e	82.19	76.34	73.00	71.06	69.32	67.59	65.56	66.12	65.15
f	-266.9	-246.5	-234.4	-228.6	-222.9	-217.3	-210.0	-212.7	-210.5
g	-40.13	-37.44	-36.28	-35.63	-34.71	-34.20	-32.33	-32.19	-32.57
h	132.2	122.9	120.5	117.5	114.8	113.6	106.4	112.7	116.6
i	-6.791	-6.298	-6.052	-5.711	-5.534	-5.350	-5.195	-5.130	-4.927
j	0.908	0.905	0.907	0.892	0.885	0.874	0.861	0.839	0.795

Source: Amozagat-Fard, Fuller and Warnick [2]. (Copyright 1984. Reprinted with permission.)

TABLE 2.12-9
Empirical Parameters for Calculating the Propagation Velocity of Zinc by Equation 19

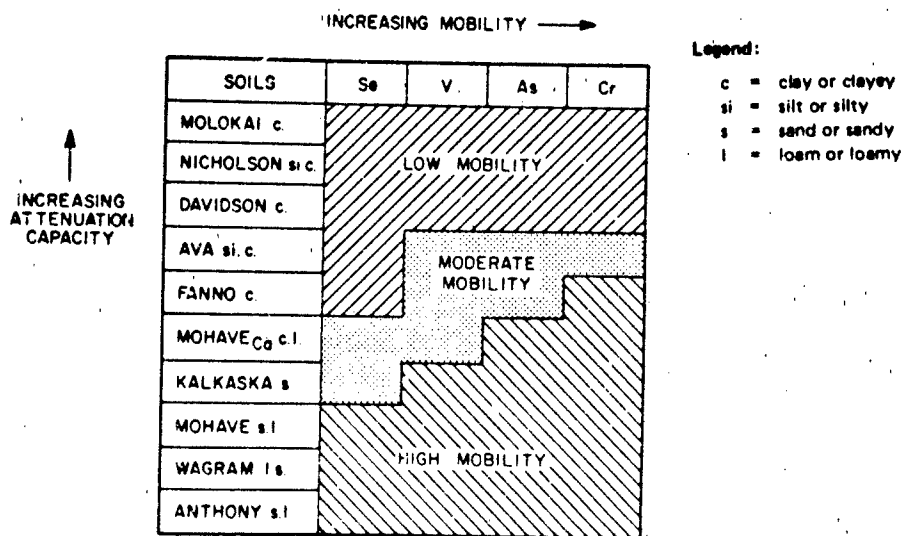
Parameter	0.1	0.2	0.3	0.4	0.5	0.6	0.7	0.8	0.9
a	0.0210	0.0173	0.0161	0.0149	0.0136	0.0111	0.00954	0.00803	0.00487
b	0.000657	0.000591	0.000570	0.000550	0.000526	0.000482	0.000466	0.000443	0.000398
c	2.784	2.747	2.697	2.660	2.637	2.638	2.660	2.648	2.698
d	0.00373	0.00336	0.00324	0.00310	0.00288	0.00255	0.00254	0.00236	0.00211
e	-15.38	-14.92	-14.86	-14.72	-14.75	-14.57	-14.76	-14.96	-15.82
f	82.37	80.25	79.18	78.42	77.79	77.12	76.71	76.57	78.93
g	67.11	60.90	58.93	56.97	54.66	51.12	51.03	49.37	46.16
h	-188.2	-167.5	-162.1	-156.3	-148.2	-135.9	-137.1	-132.3	-122.0
i	-6.44	-5.88	-5.68	-5.48	-5.27	-4.92	-4.82	-4.61	-4.22
j ²	0.841	0.844	0.846	0.848	0.847	0.848	0.848	0.848	0.846

Source: Amoozegar-Fard, Fuller and Warrick [2]. (Copyright 1984. Reprinted with permission.)



Source: Fuller [10]

FIGURE 2.12-5 Relative Mobility of Cation-Forming Elements in Soils



Source: Fuller [10]

FIGURE 2.12-6 Relative Mobility of Anion-Forming Elements in Soils

Example 6 How long will it take for a soil solution having a concentration of 3 mg/l of Cd to reach a 5-meter depth, assuming that the concentration of Cd in the leachate is 15 mg/l?³

Assume a Darcian velocity (v_d) of 0.15 cm/day and a water-filled porosity (water or leachate volumetric content) of $\theta_v = 0.1 \text{ m}^3/\text{m}^3$. The equivalent pore-water velocity is then:

$$v_p = v_d/\theta_v = 0.15/0.1 = 1.5 \text{ cm/day.}$$

For the soil and leachate, assume:

Soil	Leachate
300 g/kg (30%) clay	1100 mg/l (0.11%) TSS
200 g/kg (20%) sand	900 mg/l (0.09%) TOC
40 g/kg (4%) free FeO	

The relative concentration or attenuation factor of interest is $[Cd]_{ss}/[Cd]_i = 3/15 = 0.2$. Substituting the corresponding values for the empirical parameters from Table 2.12-7 into equation 17:

$$\begin{aligned} V_{0.2} &= (1.5/25) [(31.07/30) - (0.227)(20) + (0.00114)(20)^2 + \\ &\quad (0.0111)(4)^2 + (9.385/4) + (89.19)(0.11) - \\ &\quad (216.4)(0.11)^2 + (0.37)(0.09) - 2.015] \\ &= 0.281 \text{ cm/day} \end{aligned}$$

The time for the relative solution concentration of 0.2 to reach a depth of 5 meters is therefore 1780 days or 4.87 years under steady-state flow.

2.12.8 Estimation of Attenuation in an Environmental System

There are three approaches to estimating the attenuation of inorganic pollutants in soil: (1) direct experimentation, (2) estimation based on experiments with other soils, and (3) calculation of "boundaries" based on particular mechanisms. Except when using the direct experimental approach, one must consider each of the important factors that affect attenuation in the environment.

- **Approach 1** — Perform batch, column or field tests of attenuation, using solutions and solids that most closely resemble those of concern. (See § 2.12.4.)
- **Approach 2**
 - (a) Determine soil and soil-solution properties (physical and chemical) plus other liquor (leachate) properties that affect attenuation. (See Table 2.12-1 and Appendix C of this report.)

3. This example is taken from Amoozegar-Fard, Fuller and Warrick [2].

- (b) Determine species of interest in solution. The speciation of an element is affected by the solution equilibria; see section on each element in Part II of this report and relevant chapters in Part I.
- (c) Review literature for similar conditions, referring to section on each element in Part II of this report as a start.
- (d) Pick some values for similar conditions. Calculate attenuation that may be expected.

This approach is illustrated in more specific terms in Example 7 below.

- **Approach 3 —** Determine the boundaries of expected attenuation on the basis of calculations for the following possible contributing processes:

- (a) Precipitation equilibria (determine least soluble salt and its soluble level for the conditions of the soil environment). Refer to Part I, section 2.11.
- (b) Ion exchange capacity (for soil CEC or components of soil).
- (c) Linear, Langmuir, Freundlich, or other empirical equation.

It is also possible to assume that a single component of the soil, such as manganite, is responsible for most of the attenuation. The properties of this material as a sorbent may then be used to calculate the attenuation expected as a boundary.

Example 8 illustrates the use of Approach 3 in more specific terms.

Example 7 Estimate the attenuation of cadmium using Approach 2.

- (a) Measure soil and soil-solution properties. Refer to Table 2.12-1.
- (b) The properties and environmental behavior of Cd are discussed in section 7.5 (Part II) of this report. Refer to relevant portions of Part I for more information, particularly on complexation and solubility/precipitation, which appear to be important processes affecting attenuation of Cd.
- (c) Refer to section 7.5.4 on the attenuation of Cd in soils and sediments and the literature cited there. (Additional sources of information are available.)
- (d) If conditions are similar to those of the Pennsylvania forest soil found by Sidle and Kardos [41] as described in Examples 2-5 of section 2.12.6, Langmuir and Freundlich parameters are available. As shown in these examples, $S = 0.02 \mu\text{mol/g}$ sorbed (Langmuir) and $0.17 \mu\text{mol/g}$ sorbed (Freundlich). While the Freundlich value is 8.5 times that of the Langmuir, this range is not too great to prevent good estimates of the probable attenuation.

Example 8 Estimate the attenuation of cadmium using Approach 3.

Precipitation — Section 2.11 presents examples and calculations of precipitation equilibria.

Ion Exchange — Suppose the soil has a CEC of ~10 meq/100g of soil. For a crude estimate, assume that all the CEC is taken by the Cd ions: 0.1 meq of Cd⁺² would then be sorbed by 1 g of soil, which is equal to 50 μmol/g.

Distribution Coefficient — Ranges of distribution coefficients for soils were not found for Cd in the sources reviewed. However, for montmorillonite (Na-form) in the concentration range under consideration, values of K_d ranging from 8 to 900 ml/g have been obtained (see Table 2.12-4). Using these values for an equilibrium concentration of 10⁻⁶ M (or 1.124 × 10⁻⁴ g/l),

$$\begin{aligned}\text{Lower range: } S &= K_d C = 8 \text{ ml/g} \times 1.124 \times 10^{-4} \text{ g/l} \\ &= 8.992 \times 10^{-7} \text{ g/g or} \\ &\quad 0.9 \mu\text{g/g or } 0.008 \mu\text{mol/g}\end{aligned}$$

$$\begin{aligned}\text{Upper range: } S &= 900 \text{ ml/g} \times 1.124 \times 10^{-4} \text{ g/l} \\ &= 1011.6 \times 10^{-7} \text{ g/g or } 101.2 \mu\text{g/g or} \\ &\quad 0.9 \mu\text{mol/g}\end{aligned}$$

Langmuir — Rai *et al.* [34] reported many data values for soils using the Langmuir isotherm. Some of the data were for sorbate concentrations much higher than 10⁻⁶ M, and these may be eliminated to provide a reasonable range for our purpose. The range of Langmuir constants for Cd in soils for sorbate concentrations around 10⁻⁶ M are: A_m = 0.01 – 89 μmol/g and K_L = 10³ – 10^{7.1} l/mol or 0.001 – 12.6 l/μmol. To calculate sorption for an equilibrium soil solution concentration of 10⁻⁶ M (1 μmol/l), we use equation 3:

$$S = K_L A_m C / [1 + K_L C]$$

$$\text{Lower range: } S = [0.001 \times 0.01 \times 1] / [1 + (0.001 \times 1)] = 10^{-5} \mu\text{mol/g}$$

$$\begin{aligned}\text{Upper range: } S &= [12.6 \times 89 \times 1] / [1 + (12.6 \times 1)] \\ &= 82 \mu\text{mol/g}\end{aligned}$$

Freundlich — Garcia-Miragaya [13] reported Freundlich constants for four soils containing 0.72–16.3% organic matter and a CEC of 23.8–60 meq/100g (see Table 2.12-6). These values are K_F = 3.6 – 23.2 l/g and 1/N = 0.63 – 0.95. We now use equation 13 to calculate sorption for an equilibrium soil solution concentration of 10⁻⁶ M (1 μmol/l):

$$S = K_F C^{1/N}$$

$$\text{Lower range: } S = 3.6 \times (1)^{0.63} = 3.6 \mu\text{mol/g}$$

$$\text{Upper range: } S = 23.2 \times (1)^{0.95} = 23.2 \mu\text{mol/g}$$

Fuller and Co-workers [2] — For cadmium, equation 17 may also be used (see Example 6).

Summarizing the above results,

	Ion Exchange	Distribution Coeff.	Langmuir	Freundlich
S ($\mu\text{mol/g}$)	50	0.008-0.9	$10^{-5.82}$	3.6-23.2

The range obtained from the above calculations is very large ($82:10^{-5} = 8,200,000:1$), because wide ranges of soils, equilibrium concentrations, pHs, etc., were included in the data values selected. If only one main component of the soil is responsible for sorption, the boundaries of attenuation may be calculated using a narrower range of values for sorption constants.

2.12.9 Summary

Attenuation is a complex phenomenon consisting of many different processes and reactions within the environmental system. Estimation methods based on mechanistic considerations are extremely limited by their mathematical complexity and applicability to "real" systems. Empirical methods are more applicable to "real" systems, but there are no methods for estimating the associated parameters. The "estimation" methods consist of direct measurement, obtaining data for soil environments similar to the one under consideration, or obtaining ranges by postulating mechanisms for attenuation for the system under consideration.

2.12.10 Literature Cited

1. American Society for Testing and Materials, *Emergency Standard Method for 24-Hour Batch-Type Distribution Ratio (R_d) for Contaminant Sorption by Soils and Sediments*, ASTM ES10-85, Philadelphia, Pa. (1985).
2. Amoozegar-Fard, A., W.H. Fuller and A.W. Warrick, "An Approach to Predicting the Movement of Selected Polluting Metals in Soils," *J. Environ. Qual.*, **13**, 290-96 (1984).
3. Baes, C.F., Jr. and R.E. Mesmer, *The Hydrolysis of Cations*, John Wiley & Sons, New York (1976).
4. Boyd, G.E., J. Schubert and A.W. Adamson, "The Exchange Adsorption of Ions from Aqueous Solutions by Organic Zeolites: I: Ion Exchange Equilibria," *J. Am. Chem. Soc.*, **69**, 2818-29 (1947), as cited by Travis and Etnier [46].
5. Cavallaro, N. and M.B. McBride, "Copper and Cadmium Adsorption Characteristics of Selected Acid and Calcareous Soils," *Soil Sci. Soc. Am. J.*, **42**, 550-56 (1978).
6. Conway, R.A. and B.C. Malloy (eds.), *Hazardous Solid Waste Testing: First Conference*, A Symposium Sponsored by ASTM Committee D-34 on Waste Disposal, American Society for Testing and Materials, Ft. Lauderdale, Fla., Jan. 14-15, 1981, ASTM Special Technical Publication 760, ASTM Publication Code No. 04-760000-16, Philadelphia, Pa. (1981).

7. DeGroot, A.J., J.J.M. DeGoeij and C. Zegers, "Contents and Behavior of Mercury as Compared with Other Heavy Metals in Sediments from the Rivers Rhine and Ems," *Geol. Mijnbouw*, **50**, 393 (1971), as cited by Reimers *et al.* [37].
8. DiToro, D.M., J.D. Mahony, P.R. Kirchgraber, A.L. O'Byrne, L.R. Pasquale and D.C. Piccirilli, "Effects of Nonreversibility, Particle Concentration, and Ionic Strength on Heavy Metal Sorption," *Environ. Sci. Technol.*, **20**, 55-61 (1986).
9. Fuller, W.H., *Movement of Selected Metals, Asbestos, and Cyanide in Soil: Applications to Waste Disposal Problems*, EPA-600/2-77-020, NTIS PB 266 905, Municipal Environmental Research Laboratory, Office of Research and Development, U.S. EPA (1977).
10. Fuller, W.H., *Investigation of Landfill Leachate Pollutant Attenuation by Soils*, EPA-600/2-78-158, Municipal Environmental Research Laboratory, Office of Research and Development, U.S. EPA (1978).
11. Fuller, W.H., A. Amoozegar-Fard, E.E. Niebla and M. Boyle, "Behavior of Cd, Ni, and Zn in Single and Mixed Combinations in Landfill Leachates," in *Land Disposal: Hazardous Waste*, D. Shultz (ed.), Proc. Seventh Annual Research Symposium, EPA-600/9-81-002b, Municipal Environmental Research Laboratory, Office of Research and Development, U.S. EPA, 18-28 (1981).
12. Fuller, W.H., A. Amoozegar-Fard, E.E. Niebla and M. Boyle, "Influence of Leachate Quality on Soil Attenuation of Metals," in *Disposal of Hazardous Waste*, D. Shultz (ed.), Proc. Sixth Annual Research Symposium, EPA-600/9-80-010, Municipal Environmental Research Laboratory, Office of Research and Development, U.S. EPA, 108-17 (1980).
13. Garcia-Miragaya, J., "Specific Sorption of Trace Amounts of Cadmium by Soils," *Commun. Soil Sci. Plant Anal.*, **2**, 1157-66 (1980), as cited by Rai *et al.* [34].
14. Gerritse, R.G., W. Van Driel, K.W. Smilde and B. Van Luit, "Uptake of Heavy Metals by Crops in Relation to Their Concentration by Soil Solution," *Plant Soil*, **75**, 393-404 (1983).
15. Griffin, R.A. and A.K. Au, "Lead Adsorption by Montmorillonite Using a Competitive Langmuir Equation," *Soil Sci. Soc. Am. J.*, **41**, 880-82 (1977), as cited by Travis and Etnier [46].
16. Harmsen, K., *Behaviour of Heavy Metals in Soils*, Agricultural Research Reports 866, Center for Agricultural Publishing and Documentation, Wageningen, The Netherlands (1977).
17. Harter, R.D. and D.F. Baker, "Applications and Misapplications of the Langmuir Equation to Soil Adsorption Phenomena," *Soil Sci. Soc. Am. J.*, **41**, 1077-80 (1977), as cited by Travis and Etnier [46].
18. Hingston, F.J., "A Review of Anion Adsorption," in *Adsorption of Inorganics at Solid-Liquid Interfaces*, M.A. Anderson and A.J. Rubin (eds.), Ann Arbor Science Publishers, Ann Arbor, Mich., 51-90 (1981).
19. James, R.O. and T.W. Healy, "Adsorption of Hydrolyzable Metal Ions at the Oxide-Water Interface. I: Co(II) Adsorption on SiO₂ and TiO₂ as Model Systems," *J. Colloid Interface Sci.*, **40**, 42-52 (1972), as cited by Kinniburgh and Jackson [23].

20. Jardine, P.M., J.C. Parker and L.W. Zelazny, "Kinetics and Mechanisms of Aluminum Adsorption on Kaolinite Using a Two-Site Nonequilibrium Transport Model," *Soil Sci. Soc. Am. J.*, **49**, 867-72 (1985).
21. Jenne, E.A., "Controls on Mn, Fe, Co, Ni, Cu, and Zn Concentrations in Soils and Water: The Significant Role of Hydrous Mn and Fe Oxides," *Adv. Chem. Ser.*, **73**, 337-87 (1968), as cited by Harmsen [16].
22. Kinniburgh, D.G. and M.L. Jackson, "Adsorption of Mercury (II) by Iron Hydrous Oxide Gel," *Soil Sci. Soc. Am. J.*, **42**, 45-47 (1978), as cited by Rai *et al.* [34].
23. Kinniburgh, D.G. and M.L. Jackson, "Cation Adsorption by Hydrous Metal Oxides and Clays," in *Adsorption of Inorganics at Solid-Liquid Interfaces*, M.A. Anderson and A.J. Rubin (eds.), Ann Arbor Science Publishers, Ann Arbor, Mich., 91-160 (1981).
24. Kinniburgh, D.G., M.L. Jackson and J.K. Syers, "Adsorption of Alkaline Earth, Transition, and Heavy Metal Cations by Hydrous Oxide Gels of Iron and Aluminum," *Soil Sci. Soc. Am. J.*, **40**, 796-99 (1976), as cited by Kinniburgh and Jackson [23].
25. Lapidus, L. and N.R. Amundson, "Mathematics of Absorption in Beds. VI: The Effect of Longitudinal Diffusion in Ion Exchange and Chromatographic Columns," *J. Phys. Chem.*, **56**, 984-88 (1952), as cited by Amoozegar-Fard, Fuller and Warrick [2].
26. McBride, M.B. and M.M. Mortland, "Copper(II) Interactions with Montmorillonite: Evidence from Physical Methods," *Soil Sci. Soc. Am. Proc.*, **38**, 408-15 (1974), as cited by Harmsen [16].
27. Morel, F.M.M., *Principles of Aquatic Chemistry*, John Wiley & Sons, New York (1983).
28. Morel, F.M.M., J.C. Westall and J.G. Yeasted, "Adsorption Models: A Mathematical Analysis in the Framework of General Equilibrium Calculations," in *Adsorption of Inorganics at Solid-Liquid Interfaces*, M.A. Anderson and A.J. Rubin (eds.), Ann Arbor Science Publishers, Ann Arbor, Mich., 263-94 (1981).
29. Oakley, S.M., P.O. Nelson and K.J. Williamson, "Model of Trace-Metal Partitioning in Marine Sediments," *Environ. Sci. Technol.*, **15**, 474-80 (1981).
30. O'Connor, T.P. and D.R. Kester, "Adsorption of Copper and Cobalt from Fresh and Marine Systems," *Geochim. Cosmochim. Acta*, **39**, 1531-43 (1975).
31. Organization for Economic Co-Operation and Development, *OECD Guidelines for Testing of Chemicals*, OECD, Paris (1981).
32. Pagenkopf, G.K., *Introduction to Natural Water Chemistry*, Marcel Dekker, New York (1978).
33. Pavlou, S.P. and D.P. Weston, "Initial Evaluation of Alternatives for Development of Sediment Related Criteria for Toxic Contaminants in Marine Waters (Puget Sound). Phase II: Development and Testing of the Sediment-Water Equilibrium Partitioning Approach," Report No. EPA 910/0-83-117, U.S. EPA, Washington, D.C. (1984).

34. Rai, D., J. Zachara, A. Schwab, R. Schmidt, D. Girvin and J. Rogers, *Chemical Attenuation Rates, Coefficients, and Constants in Leachate Migration. Vol. I: A Critical Review*, Report EA-3356 to EPRI by Pacific Northwest Laboratories (Batelle Institute), Richland, Wash. (1984).
35. Ravina, L. and Y. Gur, "Application of the Electrical Double Layer Theory to Predict Ion Adsorption in Mixed Ionic Systems," *Soil Sci.*, **125**, 204-9 (1978).
36. Reimers, R.S. and P.A. Krenkel, "Kinetics of Mercury Adsorption and Desorption in Sediments," *J. Water Pollut. Control Fed.*, **46**, 352-65 (1974), as cited by Reimers *et al.* [37].
37. Reimers, R.S., P.A. Krenkel, M. Eagle and G. Tragitt, "Sorption Phenomenon in the Organics of Bottom Sediments," in *Heavy Metals in the Aquatic Environment*, P.A. Krenkel (ed.), Pergamon Press, Oxford, England, 117-29 (1975).
38. Schindler, P.W., "Surface Complexes at Oxide-Water Interfaces," in *Adsorption of Inorganics at Solid-Liquid Interfaces*, M.A. Anderson and A.J. Rubin (eds.), Ann Arbor Science Publishers, Ann Arbor, Mich., 1-49 (1981).
39. Scow, K., M. Byrne, M. Goyer, L. Nelken, J. Perwak, M. Wood and S. Young, *An Exposure and Risk Assessment for Arsenic*, Final Draft Report to U.S. Environmental Protection Agency, EPA Contract 68-01-6160, Monitoring and Data Support Division, Office of Water Regulations and Standards, Washington, D.C. (1981).
40. Shayan, A. and B.G. Davey, "A Universal Dimensionless Phosphate Adsorption Isotherm for Soil," *Soil Sci. Soc. Am. J.*, **42**, 878-82 (1978), as cited by Travis and Etnier [46].
41. Sidle, R.C. and L.T. Kardos, "Adsorption of Copper, Zinc, and Cadmium by a Forest Soil," *J. Environ. Qual.*, **6**, 313-17 (1977).
42. Sposito, G., "On the Surface Complexation Model of the Oxide-Aqueous Solution Interface," *J. Colloid Interface Sci.*, **91**, 329-40 (1983).
43. Sposito, G., *The Surface Chemistry of Soils*, Oxford University Press, New York (1984).
44. Sposito, G., "Chemical Models of Inorganic Pollutants in Soils," *CRC Crit. Rev. Environ. Control*, **15**, 1-24 (1985).
45. Tewari, P.H., A.B. Campbell and W. Lee, "Adsorption of Co^{2+} by Oxides from Aqueous Solutions," *Can. J. Chem.*, **50**, 1642-48 (1972), as cited by Kinniburgh and Jackson [23].
46. Travis, C.C. and E.L. Etnier, "A Survey of Sorption Relationships for Reactive Solutes in Soil," *J. Environ. Qual.*, **10**, 8-17 (1981).
47. U.S. Environmental Protection Agency, *Chemical Fate Test Guidelines*, EPA-560/6-82-003, Office of Pesticides and Toxic Substances, U.S. EPA (1982).
48. Westall, J. and H. Hohl, "A Comparison of Electrostatic Models for the Oxide/Solution Interface," *Advances in Colloid and Interface Science*, **12**, 265-94 (1980).

2.13 INTEGRATION AND ANALYSIS OF AQUEOUS PROCESSES

2.13.1 Introduction

A variety of chemical processes in aqueous solutions have been described individually in other sections of this chapter. This section demonstrates how some of the methods of estimation and analysis of the results for individual chemical processes can be integrated. In the case study considered here, the individual methods are integrated to permit a partial analysis of the state of an aqueous system—specifically, water from a fly ash disposal site.

As many environmental processes may affect the behavior of chemicals in an aqueous system, the first steps are to establish the nature and the kinds of the chemical species present, i.e., the chemical speciation in the system. Because of the importance of these steps in any analysis of aqueous systems, the fundamentals of chemical speciation are summarized in section 2.13.2. The theory is simplified for straightforward application, and examples are presented later.

In a typical aqueous system, several processes occur simultaneously. All of them must be considered if one is to understand the chemical state of the system under specified environmental conditions and predict how changes in that environment are likely to affect the system. This is the chief reason for attempting to integrate the methods that apply to the individual chemical processes. The results can be used to examine such aspects of aqueous species as their states of oxidation, rates of oxidation reactions, chemical speciation of the major and trace components of the solution, and the degree of saturation with respect to a number of commonly occurring solids.

2.13.2 Chemical Speciation in Solution

Chemical speciation in solution—i.e., the chemical species that exist in a solution of a given chemical composition under specified environmental conditions—is usually reported as concentrations of elements and some of the more obvious ions. For example, concentrations of sulfate and bicarbonate ions are commonly reported in analyses of water instead of, or in addition to, concentrations of the total sulfur and total carbon in solution.

The cations and anions of the components of the solution can combine to form ionic complexes (section 2.9). A cation M_i and an anion L_j can form an ionic complex M_iL_j according to a reaction of the following type:



In terms of concentrations, the equilibrium of this reaction can be expressed as:

$$K_{ij} = \frac{[M_iL_j]}{[M_i][L_j]} \quad (2)$$

where K_{ij} is the *concentration equilibrium constant* (also called the *stability constant*)

or association constant). If expressed in terms of the activities rather than the concentrations of the dissolved species, K_{ij} is called the *activity equilibrium constant* (section 2.11).

The total concentration of M_i in solution, $[M_{iT}]$, is the sum of the concentrations of the "free" species, $[M_i]$, and of all the complexes involving M_i .¹ For the case of reaction 1, representing one cation, one anion, and one 1:1 ionic complex (one metal to one ligand), the total concentrations of M_i and L_j are as follows:

$$[M_{iT}] = [M_i] + [M_i L_j] \quad (3)$$

$$[L_{iT}] = [L_j] + [M_i L_j] \quad (4)$$

The complex $M_i L_j$ can be either a positively, negatively, or uncharged species, depending on the valence charges of M_i and L_j .

The subscripts i and j are introduced for convenience, to denote each of the many cationic and anionic species in solution. In the presence of one cationic species (M_{iT}) and two different anionic ligands (L_{1T} and L_{2T}), the following equilibria hold for the two different complexes of a 1:1 type:

$$K_{11} = \frac{[M_i L_1]}{[M_i] [L_1]} \quad \text{and} \quad K_{12} = \frac{[M_i L_2]}{[M_i] [L_2]} \quad (5)$$

The case of calcium fluoride (CaF_2) in its aqueous solution, considered in section 2.11, corresponds closely to a case of one cation (Ca^{+2}) and two ligands (F^- and OH^-), with the complexes formed being CaF^+ and CaOH^+ .

A 1:1 ionic complex is the simplest variety, but complexes containing more than one stoichiometric unit of the metal (M_i) and/or the ligand (L_j) are also common (e.g., AgI_4^{3-}). In solutions of many different dissolved species, aqueous complexes may contain more than one kind of ligand in the formula (e.g., $\text{Pt}(\text{OH})_2\text{Cl}_2^{-2}$). A multiligand complex containing more than one L_j in its formula can be represented by the following reactions:

<u>REACTION</u>	<u>EQUILIBRIUM CONSTANT</u>
$M_i + L_j \rightleftharpoons M_i L_j$	$K_{ij} = \beta_{ij,1}$
$M_i L_j + L_j \rightleftharpoons M_i (L_j)_2$	$\beta_{ij,2} / \beta_{ij,1}$
•	
•	
•	
$M_i (L_j)_{p-1} + L_j \rightleftharpoons M_i (L_j)_p$	$\beta_{ij,p} / \beta_{ij,p-1}$
Overall reaction: $M_i + pL_j \rightleftharpoons M_i (L_j)_p$	$\beta_{ij,p}$

1. The term "free" species, which actually refers to the aquocomplexed monomeric ion in solution, is used throughout this section for simplicity.

From the preceding notation of the overall stability constants $\beta_{ij,p}$, it is clear that subscript p is the stoichiometric number of the ligands L_j in the formula, and $\beta_{ij,p}$ is defined from equation 7 as

$$\beta_{ij,p} = \frac{[M_i(L_j)_p]}{[M_i][L_j]^p} \quad (8)$$

The number of possible ionic complexes in an aqueous system containing only a few cationic and anionic components can be very large. In a solution containing m metal ions M_i ($i = 1, \dots, m$) and n anion-ligands L_j ($j = 1, \dots, n$), there are $m \times n$ possible ionic complexes of 1:1 type, $M_i L_j$. There are also $m \times n$ theoretically possible complexes of 1:2 type, $M_i (L_j)_2$. The total number of the 1:1, 1:2, and up to 1:p types of complexes rapidly increases to $p \times m \times n$. Computations of the concentrations of the individual species in such a system can be very time-consuming, even for a computer (see Chapter 5). Fortunately, some simple approximations make computations of chemical speciation models possible by hand, as will be demonstrated in § 2.13.3. Here, we shall simply summarize the equations for chemical speciation for three cases:

- Free ions and 1:1 complexes;
- Free ions and multiligand 1:p complexes; and
- The somewhat special case in which either the ligand or the cation concentration is much greater than those of the other species. (This case is particularly useful for computing concentrations of the major ligands with trace metals, or of the trace ligands with major cationic components of solutions.)

FREE IONS AND 1:1 COMPLEXES

Equations 3 and 4 described chemical speciation in a solution containing one metal, one anionic ligand, and one complex. A general case for 1:1 complexes can be represented by mathematically similar formulations for m cations M_i , n ligands L_j , and $m \times n$ ionic complexes of a 1:1 type, $M_i L_j$ [4]. The total concentration of each of the metals (or cations) in solution, $[M_{iT}]$, is:

$$[M_{iT}] = [M_i] \left(1 + \sum_{j=1}^n K_{ij}[L_j] \right) \quad (9)$$

where the notation of the parameters is as defined in equations 3-5. Similarly, the total concentration of each of the ligands in solution, $[L_{iT}]$, is:

$$[L_{iT}] = [L_j] \left(1 + \sum_{i=1}^m K_{ij}[M_i] \right) \quad (10)$$

If some of the metals do not form any 1:1 complexes with some of the ligands, the

corresponding terms would be zeroes in the summation series in the preceding equations.

In an aqueous system containing m metals and n ligands, there would be $m + n$ simultaneous equations like 9 and 10 above, in $m + n$ unknowns: m unknown concentrations $[M_i]$ and n unknown concentrations $[L_j]$. In general, equations 9 and 10 are nonlinear algebraic equations; methods for their solution are described later in this section under "Mathematical Solutions."

FREE IONS AND MULTILIGAND COMPLEXES

In an aqueous solution of silver iodide, the following ionic complexes and ion pairs may have to be considered: H^0 , AgI^0 , AgI_2^- , AgI_3^{2-} , and AgI_4^{3-} . In the absence of any additional information on the total concentrations of the silver and iodide, we should consider all five. The total concentrations of silver $[\text{Ag}_T]$ and iodide $[\text{I}_T]$ are then given by the following mass-balance equations:

$$[\text{Ag}_T] = [\text{Ag}^+] + [\text{AgI}^0] + [\text{AgI}_2^-] + [\text{AgI}_3^{2-}] + [\text{AgI}_4^{3-}]$$

$$[\text{I}_T] = [\text{I}^-] + [\text{HI}^0] + [\text{AgI}^0] + 2[\text{AgI}_2^-] + 3[\text{AgI}_3^{2-}] + 4[\text{AgI}_4^{3-}]$$

In this case, there are two cations (Ag^+ and H^+) and one ligand (I^-) in solution. For any number of metals (m) and ligands (n), and for any type of multiligand complex (1:p), the relationships for the total cation (metal) concentrations $[\text{M}_T]$ and total ligand concentrations $[\text{L}_T]$ become:

$$[\text{M}_T] = [\text{M}_i] \left(1 + \sum_{k=1}^p \sum_{j=1}^n K_{ij,k} [\text{L}_j]^k \right) \quad (11)$$

$$[\text{L}_T] = [\text{L}_j] \left(1 + \sum_{k=1}^p k \sum_{i=1}^m K_{ij,k} [\text{M}_i] [\text{L}_j]^{k-1} \right) \quad (12)$$

where, as in the preceding sections, i designates a metal-ion ($i = 1, \dots, m$), j designates an anionic ligand ($j = 1, \dots, n$), and k designates the number of the L_j -ligands in the stoichiometric formula of a complex $M_i(L_j)_k$, with $k = 1, \dots, p$. If some of the complexes $M_i(L_j)_k$ do not exist, the number of terms in the summation series in equations 11 and 12 is less than the total of $p \times n$ and $p \times m$, respectively.

LARGE EXCESS OF ONE COMPONENT

In the special case of aqueous systems containing trace metals as well as major metals and anions, concentrations of the trace constituents are often one or more orders of magnitude lower than those of the anionic ligands. The systems of the simultaneous equations 9-10 or 11-12 can be considerably simplified in this case, from nonlinear to linear equations, by using the following approximation: When computing the concentrations of the trace metals with a large excess of a free ligand, one may assume the concentration of the free ligand to be constant and not affected by the formation of

complexes with the trace metals; i.e.,

$$[L_j] = \text{constant } (j = 1, \dots, n) \quad (13)$$

This assumption is justified insofar as only a very small fraction of the free ligand in solution, $[L_j]$, will be taken up by the total concentrations of trace metals, $[M_{iT}]$.

However, the degree of complexation of the trace metals may be large, and the differences between the total trace-metal concentrations $[M_{iT}]$ and their free-ion concentrations $[M_i]$ may be significant. With reference to a system containing free ions and complexes of only the 1:1 type between trace metals and anionic ligands at much higher concentrations, a condition additional to equation 13 is that:

$$K_{ij}[M_i] < < 1, \text{ for all } M_i \text{ forming complexes with all } L_j$$

In this case, chemical speciation of the trace-metal complexes with a ligand L_j can be determined using a set of equations 9—one for each of the m trace metals M_i ($i = 1, \dots, m$) that form 1:1 complexes with the ligands L_j at a constant concentration:

$$[M_{iT}] = [M_i] \left(+ \sum_{j=1}^n K_{ij} [L_j] \right) \quad (14)$$

When the ligand concentrations, $[L_j]$, are practically constant and not affected by complexation of trace metals occurring at much lower concentrations, there are up to m equations of this kind. Equation 14 can be immediately solved for $[M_i]$ when the values of the total trace-metal concentration $[M_{iT}]$, ligand concentrations $[L_j]$, and stability constants of the 1:1 complexes K_{ij} are known. In this special case the equations are linear, and the unknowns are the concentrations of the free metal-ions in solution.

The preceding case of chemical speciation, summarized in equation 14, refers to an anionic ligand that forms complexes with trace metals. Similarly, the case of a metal ion forming 1:1 complexes with trace ligands L_j can be represented by the following equation:

$$[L_{iT}] = [L_j] \left(1 + \sum_{i=1}^m K_{ij} [M_i] \right) \quad (15)$$

where the condition $[M_i] = \text{constant } (i = 1, \dots, m)$ holds for the aqueous system.

A variation of this special case is when either the metal or the ligand concentration is constant, but not necessarily much greater than that of the other species. A constant low concentration of an L_j or an M_i may be maintained by a solubility equilibrium with a solid phase. In such a case, equation 14 or 15 can also be used for the aqueous system, as will be shown in the next section.

MATHEMATICAL SOLUTIONS OF THE GENERAL CASES

In the sets of the simultaneous equations 9-10 or 11-12, the unknown parameters are concentrations of the free metal-ions $[M_i]$ and free anionic ligands $[L_j]$. The values of the other parameters — the total concentrations of the metals $[M_{iT}]$ and the ligands $[L_{iT}]$, and the stability constants K_{ij} for the metal-ligand complexes — should be known. Each of the equations 9-10 or 11-12 can be written as a difference between the terms to the right of the equal sign and those to the left. This difference is some algebraic function of the known and the unknown parameters, which can be denoted $F_c(M_i, L_j)$. Thus, the solutions sought are the values of $[M_i]$ and $[L_j]$ from a set of equations

$$F_c(M_i, L_j) = 0 \quad (16)$$

where subscript c indicates the number of the equation, from 1 up to $i + j$. For example, in an aqueous system containing $m = 5$ metals ($i = 1, \dots, 5$) and $n = 3$ ligands ($j = 1, 2, 3$), computation of the free metal-ion and ligand concentrations requires solution of a system of $c = 5 + 3 = 8$ simultaneous equations.

For a dilute aqueous system, when the activity coefficients of the chemical species in solution may be taken as $\gamma \approx 1$, simultaneous nonlinear algebraic equations, such as sets of c equations 15, can be solved with the aid of standardized routines available for many types of minicomputers and mainframe computers. A computer-program library IMSL,² available for use with mainframe computers of many manufacturers, contains several routines for solutions of simultaneous nonlinear algebraic equations. One such routine, designated by the code ZSCNT in the IMSL list of programs, was used to verify some of the solutions given in § 2.13.3. (The results were practically identical with those obtained by simplified methods, as demonstrated in § 2.13.3.)

For aqueous systems at higher concentrations, particularly those involving equilibria with solid phases, there exist in the public domain highly sophisticated programs that can be used to compute concentrations of the individual chemical species in multicomponent aqueous systems, determine degrees of saturation with respect to many solid phases, and estimate changes in the chemical composition of a solution where either precipitation or dissolution of solids takes place. Some of the existing programs have been reviewed and compared by Drever [2] and in Chapter 5 of this report.

METHODS AND STEPS IN INTEGRATION OF CHEMICAL PROCESSES IN SOLUTION

Determination of the chemical speciation of an aqueous solution entails many steps, the first and most basic of which is to ascertain the bulk chemical composition of the solution. The number of steps and the amount of detail in each depend on the desired accuracy of the calculated concentrations of the individual aqueous species. Table 2.13-1 lists the steps for a relatively simple case, with additional references to background information in other sections of this report and in the case study described in section 2.13.3.

2. IMSL Library Reference Manuals, published by IMSL Inc., 7500 Bellaire Blvd., Houston, TX 77036.

TABLE 2.13-1

Methods and Steps in Determination of Chemical Speciation of an Aqueous System

Steps to Consider	Comments	Report Sections with Additional Information
① Determine bulk chemical composition of solution:		
a. Dissolved inorganic components	Results of chemical analysis commonly reported as concentrations of elements and some ionic species	
• Major components • Minor or trace components	Concentrations of major components usually 10 ² or more times higher than concentrations of minor components	Chapters 6, 7, 8, Appendix B
b. Dissolved gases	Reactive gases, such as oxygen, carbon dioxide, hydrogen sulfide, and methylated trace-metals.	6.12, 2.15, 10.6, Chapter 8
c. Dissolved organics	Results usually reported as concentrations of organic carbon, nitrogen, and, less commonly, S and P	
d. Hydrogen-ion activity	pH values should characterize the system under environmental conditions	2.7, 6.9
② First look at chemical speciation:		
a. Different oxidation states	For some elements, their different oxidation states may be reported in analysis, such as SO ₄ ⁻² and S ⁻² , Fe ⁺² and Fe ⁺³ , Cr ⁺³ and Cr ⁺⁶	2.10
b. Anionic species	For elements forming anions of polyprotic acids (H _n L), such as P or As, the main anion(s) can be determined from the acid pK _a values and solution pH.	2.7, 6.12, Chapters 7, 8, 10
③ Cation-anion complexes	List the possible complexes, using information from ① and ②	Chapters 6, 7 and 8, 2.7, 2.9, 3.2, 2.13
④ Determine the most abundant complexes	The most abundant complexes among those in ③ may be identified through use of stability constants K _{st} and the solution pH, from data in ① and ②	2.7, 2.9, 3.2, 2.13

(Continued)

TABLE 2.13-1 (Continued)

Steps to Consider	Comments	Report Sections with Additional Information
⑤ Oxidation state of ionic species: a. From Eh or pe measurements	Such measurements often give an indication of either oxidizing or reducing conditions in solution.	2.10
b. From oxidation-reduction equilibria	Computed concentrations or concentration ratios of oxidized and reduced forms of different components of solution.	2.10, 2.13.3
c. From kinetics of oxidation reactions	Results give concentrations of oxidized species, forming from reduced species, computed from reaction-rate equations.	3.3, 3.4, 2.13
⑥ Determine ionic strength of solution	Nominal ionic strength can be computed from concentrations of major ionic components, ①. The result indicates how dilute the solution is.	2.6
⑦ Calculate speciation of major components	Results are concentrations of aquo-ions and cation-anion complexes—①, ③ and ④. For dilute solutions (ionic strength not over 0.02 mol/l), concentrations may be computed by approximation methods. For more concentrated solutions, use detailed computer programs.	2.9, 2.13.3 2.13.2, 2.13.3 2.13.2, Chapter 5
⑧ Calculate speciation of minor components	Results are concentrations of aquo-ions and cation-anion complexes involving minor components. For dilute solutions (ionic strength less than about 0.02 mol/l), approximation methods can be used. For solutions of higher ionic strength, use detailed computer programs.	2.9, 7.1-7.15 2.13.2, 2.13.3 5.4

(Continued)

TABLE 2.13-1 (Continued)

Steps to Consider	Comments	Report Sections with Additional Information
(9) Determine degrees of saturation of solution with respect to solid phases	Results of such computations indicate whether solution is, or is not, supersaturated with respect to solids being considered.	2.11, 3.4, 2.13.3
(10) Estimate response of aqueous system to environmental changes	Changes in the state of the aqueous system (for example, temperature, composition of the gaseous phase, introduction of new components in solution) affect its chemical speciation. Effects of such changes may be estimated by methods listed under (7), (8), and (9).	2.13.3

2.13.3 Case Study of an Aqueous System

This section demonstrates the application of methods developed in other sections of the report to an aqueous system containing a number of major and minor dissolved components. It considers the chemical speciation of some of the main components of the solution, chemical speciation of some trace metals and nutrient elements, the degree of saturation of the aqueous system with respect to some common solids and, finally, possible effects on the system due to addition of other complexing ligands, such as humic acids.

DESCRIPTION OF THE AQUEOUS SYSTEM

The chemical composition of a sample of water taken from a coal fly-ash disposal site is summarized in Table 2.13-2. Certain characteristics of this solution should be particularly noted.

The water is of a calcium-sulfate type, as calcium and sulfate are the main dissolved components of the solution. The solution is slightly alkaline ($\text{pH} = 8.0$) and contains very little dissolved oxygen (0.7 ppm). No concentrations of dissolved carbonate species (HCO_3^- and CO_3^{2-}) are reported. Chloride and nitrate, which are common anionic constituents of natural waters, are present at very low concentrations. Among the numerous trace constituents, 14 elements are listed (alphabetically); another 10 elements are below their detection limits.

The low concentration of dissolved oxygen and the absence of reported data for the bicarbonate ion may indicate that the water was not in contact with the atmosphere.

A dilute solution such as this, at equilibrium with the atmosphere, should contain much more dissolved oxygen (between 8 and 10 ppm), and it should also contain about 10^{-3} mol HCO_3^- /liter and about 10^{-5} mol CO_3^{2-} /liter.

TABLE 2.13-2
Chemical Analysis of Water from a Screened Piezometer
at a Coal Fly-Ash Disposal Site

pH = 8.0
 Dissolved oxygen = 0.7 ppm O_2 (2.19×10^{-5} mol/l)^a at 25°C and 1 atm total pressure

Cation	ppm	mol/l ^a	Anion	ppm	mol/l ^a
Ca^{+2}	126	3.14×10^{-3}	SO_4^{2-}	320	3.33×10^{-3}
K^+	11.0	2.81×10^{-4}	Cl^-	6.8	1.92×10^{-4}
Mg^{+2}	10.5	4.32×10^{-4}	NO_3^-	1.0	1.61×10^{-5}
Na^+	5.0	2.15×10^{-4}			
Trace components at concentrations below detection limits as shown (in ppm)					
As	1.5	2.00×10^{-5}	Ag	<0.005	
B	3.7	3.40×10^{-4}	Al	<0.3	
Ba	0.37	2.69×10^{-6}	Be	<0.005	
Cr	0.01	1.92×10^{-7}	Br	<5.0	
F	0.85	4.47×10^{-5}	Cd	<0.007	
Fe	0.02	3.58×10^{-7}	Co	<0.05	
Mn	0.06	1.09×10^{-6}	Cu	<0.008	
Mo	0.90	9.38×10^{-6}	Pb	<0.05	
Ni	0.02	3.41×10^{-7}	Zn	<0.02	
P	0.60	1.94×10^{-5}	Zr	<0.05	
Se	0.003	3.80×10^{-8}			
Si	1.65	5.87×10^{-5}			
Sr	3.7	4.22×10^{-5}			
V	0.035	6.87×10^{-7}			

a. In converting ppm to mol/l, no allowance was made for the difference between 1 liter and 1 kg of solution, owing to its dilute nature.

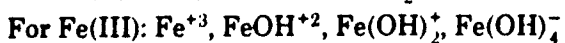
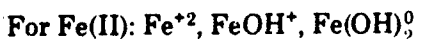
Source: Arthur D. Little, Inc. [1]

Taking the chemical analysis at face value, the nominal ionic strength of the solution (see section 2.6), computed from the listed concentrations of the cations and anions, is low: $I \approx 0.014$ mol/liter. It will be shown below that about 30% of the calcium, magnesium, and sulfate are tied up as zero-charged ion-pair complexes in solution. Thus, only the remaining 70% are free ions that contribute to the value of the ionic strength, making it somewhat lower than the preceding estimate: $I \approx 0.01$ mol/liter.

OXIDATION STATE OF IRON IN SOLUTION

The total concentration of dissolved iron is listed as 0.02 ppm. At such low concentrations, it is common to report only the total concentration, without identifying the proportions of Fe^{+2} and Fe^{+3} . The proportions of ferrous and ferric iron will be computed in this section.

Because of the tendency of Fe^{+2} and Fe^{+3} ions to hydrolyze in solution, we must first establish the most abundant species of each form of iron in solution at the pH of 8.0. The species to consider are the following (see also section 2.11.3):³

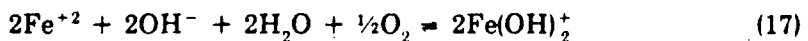


From consideration of complexation equilibria between either species of Fe and the hydroxyl ion, using the complex-stability constants listed in Tables 2.13-3 and 6.8-3, the most abundant species in the fly ash water would be Fe^{+2} for Fe(II), and Fe(OH)_2^+ for Fe(III).

To determine the main oxidation state of iron in solution, we must compute the concentration ratio of the two main species of dissolved iron:

$$\frac{[\text{Fe(OH)}_2^+]}{[\text{Fe}^{+2}]} \approx \frac{[\text{Fe (III)}]}{[\text{Fe (II)}]}$$

The following oxidation reaction at equilibrium can be used:



All the species in this reaction are aqueous species, including dissolved oxygen. From the values of the standard free energies of formation of the aqueous species [2, 6], the equilibrium constant of the reaction is found (using the methods of section 2.11.3) to be $\log K = 28.5$.

3. The zero-charged hydroxo complex, Fe(OH)_2^0 , was excluded from the calculation because of inconsistencies in the open literature on its presence and in the relevant thermodynamic data. Such inconsistencies were noted also for other metal-hydroxo species (e.g., Al(OH)_2^0). As such, many published sources do not include them in the speciation calculation although others do depending on their assessment of the validity of the available thermodynamic data. See, for example, Figure 2.11-4, page 2.11-20.

Thus, in a system at pH = 8.0 and containing dissolved oxygen at a concentration of 2.19×10^{-5} mol O₂/liter, the value of the concentration ratio [Fe (III)] / [Fe (II)] is:

$$\begin{aligned}\frac{[\text{Fe(OH)}_2^+]}{[\text{Fe}^{+2}]} &= (K [\text{OH}^-]^2 [\text{O}_2])^{1/2} \\ &= (10^{28.5} \times (10^{-6.0})^2 \times (10^{-4.66}))^{1/2} \\ &= 10^{7.1}\end{aligned}$$

The answer clearly shows that the oxidized form, Fe(OH)₂⁺, is the expected equilibrium oxidation state of iron in solution.

The preceding computation assumes that an equilibrium exists between Fe (II) and Fe (III) in the fly-ash solution. If this were not the case, and if the main form of dissolved iron were the reduced ion Fe⁺², how long would it take the Fe⁺² to oxidize?

An equation for the rate of oxidation of Fe⁺² in solution was given in section 3.4 (equation 76), in the following form:

$$-\frac{d[\text{Fe}^{+2}]}{dt} = k p\text{O}_2 [\text{OH}^-]^2 [\text{Fe}^{+2}] \quad (18)$$

This reaction-rate equation shows that higher partial pressures of oxygen and alkaline conditions increase the rate of oxidation of ferrous iron. The values of the parameters are:⁴

$$k = 2 \times 10^{13} \text{ l}^2 \cdot \text{mol}^{-2} \cdot \text{atm}^{-1} \cdot \text{min}^{-1} \quad (\text{as given in section 3.4})$$

$$p\text{O}_2 = 0.016 \text{ atm}$$

$$[\text{OH}^-] = 10^{-6.0} \quad (\text{from pH} = 8.0, \text{ given in Table 2.13-2})$$

Accordingly, equation 18 reduces to

$$-\frac{d[\text{Fe}^{+2}]}{dt} = k' [\text{Fe}^{+2}] = 0.32 [\text{Fe}^{+2}] \text{ (mol} \cdot \text{liter}^{-1} \cdot \text{min}^{-1}) \quad (19)$$

$$\text{where } k' = 2 \times 10^{13} \times 0.016 \times (10^{-5.7})^2$$

4. $p\text{O}_2$ is the partial pressure of oxygen at equilibrium with an aqueous solution containing 2.19×10^{-5} mol O₂/liter, at 25°C and 1 atm total pressure. Based on the equilibrium constant for a reaction between gaseous and aqueous O₂, $p\text{O}_2 = 10^{2.86} [\text{O}_2]$, where $p\text{O}_2$ is in atm and $[\text{O}_2]$ in mol/kg H₂O.

The half-life of the reaction can be estimated from equation 5 of section 3.2.3:

$$t_{1/2} = \frac{0.693}{k'} = \frac{0.693}{0.32 \text{ (min}^{-1}\text{)}} = 2.2 \text{ min} \quad (20)$$

This result shows that the rate of oxidation of Fe^{+2} in the fly-ash leachate is relatively fast (in the absence of complexation); this strengthens the conclusion, based on the oxidation-reduction equilibrium of equation 17, that Fe (III) is the dominant form of dissolved iron in solution.

CHEMICAL SPECIATION OF MAJOR COMPONENTS

The analytical data in Table 2.13-2 indicate that sulfate is the main anionic species in solution and calcium is the main cationic species. Concentrations of Mg^{+2} and K^+ are about equal, but Mg^{+2} has a much stronger tendency than K^+ to form ionic complexes with SO_4^{-2} . Therefore, only calcium, magnesium, and sulfate were considered in computing the concentrations of the free ions and metal-sulfate complexes in the fly-ash leachate.

The stability constants of the ionic complexes of the metals and anions dealt with in this section are summarized in Table 2.13-3. In an aqueous solution containing calcium, magnesium and sulfate as the major components, the ionic complexes to be considered are: HSO_4^- , MgSO_4^0 , CaSO_4^0 , MgOH^+ , and CaOH^+ .

From the values of the stability constants listed in Table 2.13-3, it follows that at the pH value of the solution (8.0), which is much higher than the pK_a value of HSO_4^- , the concentration of HSO_4^- can be neglected. The complexes MgOH^+ and CaOH^+ may also be neglected, for the following reason: at pH = 8.0, the concentration of the hydroxide ion is 10^{-6} mol/liter, which is much lower than the sulfate concentration of about 3×10^{-3} mol/liter (Table 2.13-2); fractions of the total Ca and Mg in solution that may be complexed by OH^- are therefore much smaller than the fractions complexed by SO_4^{-2} .

Thus, the problem at hand reduces to computing concentrations of three free ions (Ca^{+2} , Mg^{+2} , and SO_4^{-2}) and two ionic complexes (CaSO_4^0 and MgSO_4^0).

Using equations 9 and 10 and the notation of Table 2.13-3, we can express simultaneous equations for the concentration values of the three free ions:

$$[\text{Ca}_T] = [\text{Ca}^{+2}] (1 + K_{33}[\text{SO}_4^{-2}]) \quad (21)$$

$$[\text{Mg}_T] = [\text{Mg}^{+2}] (1 + K_{23}[\text{SO}_4^{-2}]) \quad (22)$$

$$[\text{SO}_{4T}] = [\text{SO}_4^{-2}] (1 + K_{23}[\text{Mg}^{+2}] + K_{33}[\text{Ca}^{+2}]) \quad (23)$$

TABLE 2.13-3

Stability Constants of Aqueous Ion-Complexes

(Tabulated values are $\log K_i$, where i designates metal ion M_i and j designates ligand L_j . Most values are for ionic strength $I=0$ and 25°C . Stability constants are for equilibrium reactions of the type $M_i + L_j \rightleftharpoons M_i L_j$, where a 1:1 complex is formed.)

i	M_i	$j = 1$	2	3
		$L_j = \text{OH}^-$	HPO_4^{2-}	SO_4^{2-}
1	H^+	14.0	7.2	2.0
2	Mg^{+2}	2.58	2.91	2.23
3	Ca^{+2}	1.30	2.74	2.31
4	Ba^{+2}	0.60	—	2.70
5	Ni^{+2}	4.10	2.08	2.32
6	Fe^{+2}	4.50	3.60	2.20
7	Fe^{+3}	11.81 ^a	8.30	4.04

a. For the reaction $\text{Fe}^{+3} + 2\text{OH}^- \rightleftharpoons \text{Fe}(\text{OH})_2^+$, $\log \beta_{712} = 22.3$ (for β_{712} see equation 8). See also footnote 3.

Source: Kotrlík and Šúcha [3]

After inserting the numerical values of the total concentrations (from Table 2.13-2) and stability constants (Table 2.13-3) in these equations, we solve equation 21 for $[\text{Ca}^{+2}]$ and equation 22 for $[\text{Mg}^{+2}]$. When the resulting expressions are substituted in equation 23, the following third-degree equation is obtained:

$$[\text{SO}_4^{2-}]^3 + 1.103 \times 10^{-2} [\text{SO}_4^{2-}]^2 + 1.355 \times 10^{-5} [\text{SO}_4^{2-}] - 9.604 \times 10^{-8} = 0 \quad (24)$$

Equation 24 can be solved by trial and error⁵, and the resulting value of $[\text{SO}_4^{2-}]$ is then substituted in equations 21 and 22 to find the concentrations of the other two species. The results of this solution are:

$$[\text{SO}_4^{2-}] = 2.23 \times 10^{-3} \text{ mol/l}; \quad 67\% \text{ free ion}$$

$$[\text{Ca}^{+2}] = 2.16 \times 10^{-3} \text{ mol/l}; \quad 69\% \text{ free ion}$$

$$[\text{Mg}^{+2}] = 3.13 \times 10^{-4} \text{ mol/l}; \quad 72\% \text{ free ion}$$

The remainder of the total calcium and magnesium is thus present as sulfate ion pairs for this solution; their respective fractions of the total concentration are 100% minus the free ion concentration:

$$[\text{CaSO}_4^0] = 31\%$$

5. That is, guessing a value of $[\text{SO}_4^{2-}]$ and subsequently adjusting it until the left-hand terms total zero.

$$[\text{MgSO}_4^0] = 28\%$$

These values lead to the following concentrations of the ion pairs:

$$[\text{CaSO}_4^0] = 0.31 (3.14 \times 10^{-3}) = 9.7 \times 10^{-4}$$

$$[\text{MgSO}_4^0] = 0.28 (4.32 \times 10^{-4}) = 1.2 \times 10^{-4}$$

MOST ABUNDANT SPECIES OF IRON AND NICKEL

The procedure used to determine the most abundant chemical species of ferric iron and nickel in the fly-ash solution is similar to that described above. The mass-balance equation for the total dissolved iron is:

$$\begin{aligned} [\text{Fe}_T] &= [\text{Fe(OH)}_2^+] + \text{FeHPO}_4^+ + \text{FeSO}_4^+ \\ &= \beta_{71.2} [\text{Fe}^{+3}] [\text{OH}^-]^2 + K_{72} [\text{Fe}^{+3}] [\text{HPO}_4^{-2}] + K_{73} [\text{Fe}^{+3}] [\text{SO}_4^{-2}] \end{aligned}$$

Using the values of $[\text{Fe}_T]$, $[\text{OH}^-]$ and $[\text{SO}_4^{-2}]$ from the preceding subsections, a value of $10^{-5.1}$ for $[\text{HPO}_4^{-2}]$ (calculated as 7.95×10^{-6} in the following subsection), and stability constants K_{ij} from Table 2.13-3, the solution of the mass-balance equation in terms of $[\text{Fe}^{+3}]$ is

$$\begin{aligned} [\text{Fe}^{+3}] &= \frac{3.58 \times 10^{-7}}{10^{22.3} (10^{-6.0})^2 + 10^{8.3} \times 10^{-5.1} + 10^{4.04} \times 10^{-2.65}} \\ &= 1.79 \times 10^{-17} \text{ mol/liter} \end{aligned}$$

Concentrations of the three iron-ligand complexes are, from the above result:

$$[\text{Fe(OH)}_2^+] = 3.58 \times 10^{-7} \text{ mol/liter}$$

$$[\text{FeHPO}_4^+] \approx 0$$

$$[\text{FeSO}_4^+] \approx 0$$

Thus, practically all of the dissolved iron occurs in the form of the hydroxide complex, Fe(OH)_2^+ .

For nickel in the fly-ash solution, the mass-balance equation can be written to include the following aqueous species (see also section 7.11):

$$\begin{aligned} [\text{Ni}_T] &= [\text{Ni}^{+2}] + [\text{NiOH}^+] + [\text{NiHPO}_4^0] + \text{NiSO}_4^0 \\ &= [\text{Ni}^{+2}] (1 + K_{51} [\text{OH}^-] + K_{52} [\text{HPO}_4^{-2}] + K_{53} [\text{SO}_4^{-2}]) \quad (25) \end{aligned}$$

This equation is now solved in terms of $[Ni^{+2}]$ as an unknown, substituting the values of the other parameters from Table 2.13-2, Table 2.13-3, and the preceding parts of this section:

$$[Ni^{+2}] = \frac{3.41 \times 10^{-7}}{1 + 10^{4.1} \times 10^{-6.0} + 10^{2.08} \times 10^{-5.1} + 10^{2.32} \times 10^{-2.65}} \quad (26)$$

$$= \frac{3.41 \times 10^{-7}}{1.48} = 2.30 \times 10^{-7} \text{ mol/liter; } 67\% \text{ of total Ni is free ion}$$

The concentrations of the three Ni-ligand complexes that appear in the mass-balance equation (25) can now be calculated:

$$[NiOH^+] = 5.74 \times 10^{-9} \text{ mol/liter; } 2\% \text{ of total Ni in solution}$$

$$[NiHPO_4^0] = 2.18 \times 10^{-10} \text{ mol/liter; } < 0.1\% \text{ of total Ni in solution}$$

$$[NiSO^0] = 1.07 \times 10^{-7} \text{ mol/liter; } 31\% \text{ of total Ni in solution}$$

Thus, the free Ni^{+2} ion is the most abundant form in the fly-ash solution, followed by the sulfate complex, with the hydroxide a distant third.

COMPLEXATION OF PHOSPHORUS

The total concentration of dissolved phosphorus in the fly-ash solution is 0.6 ppm, or 1.94×10^{-5} mol P/liter. In the absence of any further information, P will be assumed to be present as orthophosphate. At the pH value of the fly-ash solution (8.0), the main phosphate species is HPO_4^{2-} (see Figure 8.3-2, page 8.3-4). Examination of the stability constants of the metal-phosphate complexes (Table 2.13-3) shows that strong complexes exist with all the metal-ion species (except barium, for which no data were available).

A mass balance for total phosphorus in solution can be written as a sum of concentrations of the free ion $[HPO_4^{2-}]$ and of the phosphate complexes of the metals listed in Table 2.13-3:

$$[P_T] = [HPO_4^{2-}] + [CaHPO_4^0] + [MgHPO_4^0] + [NiHPO_4^0] + [FeHPO_4^+] \quad (27)$$

As shown previously, Fe^{+3} rather than Fe^{+2} is the stable form of iron in solution; therefore, the ferrous iron-phosphate complex, $FeHPO_4^0$, is not included in equation 27.

Next, examining the concentration values of the metals in solution (Table 2.13-2), it should be noted that the total phosphate concentration, 10^{-5} mol/liter, is much higher than the concentration of the free Ni^{+2} ion (10^{-7} mol/liter) and free Fe^{+3} ion (10^{-18} mol/liter) as determined in the preceding subsection. As a result, the fraction of the dissolved phosphate that may be complexed by Ni and Fe in solution would be very small in comparison to its total concentration. Thus, as an approximation, we can

ratio ICP/K (section 2.11):

$$\frac{ICP}{K} = \frac{10^{-12.45}}{10^{-17.7}} = 1.8 \times 10^5$$

The fact that ICP/K is much greater than 1 indicates that the fly-ash solution is strongly supersaturated with respect to the solid ferric hydroxide phase.⁶

Ferric Phosphate: Strengite, $\text{FePO}_4 \cdot 2\text{H}_2\text{O}$ (s)

Dissociation of ferric phosphate (mineral strengite) in an aqueous solution can be represented by the following reaction at equilibrium:



From the standard free energy of formation data [6], the equilibrium constant of this reaction is $K = 10^{-23.76}$. The ion-concentration product of the species in solution, as given in the right-hand side of equation 31, is

$$\frac{ICP}{K} = \frac{10^{-19.85}}{10^{-23.76}} = 8 \times 10^3$$

As ICP/K is much greater than 1, the solution is strongly supersaturated with respect to the hydrous ferric phosphate, as well as with respect to ferric hydroxide, dealt with in the preceding computation.

EFFECT OF HUMIC ACIDS ON COMPLEXATION OF METALS

Humic acids are organic substances of complex composition and high molecular weight that occur in soils, sediments, and in ground and surface waters. Humic acids can form strong complexes with heavy metals and with polyvalent cations in aqueous solutions. From the extensive characteristics of humic substances detailed by Stevenson [5], a few that are relevant to the complexation of metals are summarized below.

Molecular weight:	20,000 to 100,000
Carbon content (% dry basis):	50-60
Oxygen content (in COOH, CO, and OH groups; % dry basis):	30-35
Stability constants of 1:1 complexes (with Cu and Ni):	$K_{11} = 10^8$ near pH = 8; $K_{11} = 10^4$ near pH = 5

6. Although this result is somewhat surprising, extreme supersaturation of Fe(OH)_3 has been observed in laboratory systems [7]. It is also possible that the original Fe_t analysis included dispersed colloidal and dissolved iron.

Acid dissociation constants

(K_a), dilute solutions:

$$pK_a \approx 5.0 \pm 0.5$$

Although the chemical analysis of the fly ash leachate (Table 2.13-1) shows no dissolved organic carbon in the water sample, a possible effect on complexation of the trace metals in this water will be demonstrated by considering a hypothetical case of small amounts of dissolved carbon in the system. Organic carbon, in the form of humic substances, may appear in the fly-ash leachate from its contact with a soil, or from its mixing with other surface or ground waters. The large reservoir of organic matter in the soil may provide a low constant concentration of dissolved organic matter in the soil waters.

For the humic acids in the fly-ash leachate, it will be assumed that

- (a) the solution contains 1.2 mg/liter dissolved organic carbon (1×10^{-4} mol C/liter),
- (b) all the dissolved organic carbon is contained in a humic acid of molecular weight 30,000, and
- (c) the humic acid contains, by weight, 55% total C and 35% O, with all of the oxygen contained in the acidic COOH groups.

From the preceding assumptions, the concentration of dissolved organic C attributable to the complex-forming groups (COOH) of the humic acid is found as follows:

$$\text{Moles of O in humic acid} = \frac{(\text{fraction O})(\text{m.w. of humic acid})}{\text{m.w. of O}} = \frac{(0.35)(30,000)}{16} = 656$$

Moles of O in humic acid = $2 \times$ moles of -COOH in humic acid; thus,

$$\text{moles of COOH} = \frac{\text{moles of O}}{2} = \frac{656}{2} = 328$$

$$\text{Moles of total C in acid} = \frac{(\text{fraction C})(\text{m.w. humic acid})}{\text{m.w. C}} = \frac{(0.55)(30,000)}{12} = 1375$$

$$\text{Fraction of total C present as COOH} = \frac{\text{moles of COOH}}{\text{moles of total C}} = \frac{328}{1375} = 0.24$$

Concentration of COOH units in solution that can complex

$$= \text{fraction total C as COOH} \times \text{conc. total C in solution}$$

$$= 0.24 \times 1 \times 10^{-4}$$

$$= 2.4 \times 10^{-5}$$

This is the concentration of carbon as a complexing ligand, L, in the fly-ash leachate;

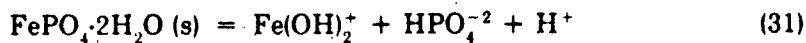
ratio ICP/K (section 2.11):

$$\frac{ICP}{K} = \frac{10^{-12.45}}{10^{-17.7}} = 1.8 \times 10^5$$

The fact that ICP/K is much greater than 1 indicates that the fly-ash solution is strongly supersaturated with respect to the solid ferric hydroxide phase.⁶

Ferric Phosphate: Strengite, $\text{FePO}_4 \cdot 2\text{H}_2\text{O}$ (s)

Dissociation of ferric phosphate (mineral strengite) in an aqueous solution can be represented by the following reaction at equilibrium:



From the standard free energy of formation data [6], the equilibrium constant of this reaction is $K = 10^{-23.76}$. The ion-concentration product of the species in solution, as given in the right-hand side of equation 31, is

$$\frac{ICP}{K} = \frac{10^{-19.85}}{10^{-23.76}} = 8 \times 10^3$$

As ICP/K is much greater than 1, the solution is strongly supersaturated with respect to the hydrous ferric phosphate, as well as with respect to ferric hydroxide, dealt with in the preceding computation.

EFFECT OF HUMIC ACIDS ON COMPLEXATION OF METALS

Humic acids are organic substances of complex composition and high molecular weight that occur in soils, sediments, and in ground and surface waters. Humic acids can form strong complexes with heavy metals and with polyvalent cations in aqueous solutions. From the extensive characteristics of humic substances detailed by Stevenson [5], a few that are relevant to the complexation of metals are summarized below.

Molecular weight:	20,000 to 100,000
Carbon content (% dry basis):	50-60
Oxygen content (in COOH, CO, and OH groups; % dry basis):	30-35
Stability constants of 1:1 complexes (with Cu and Ni):	$K_{11} \approx 10^8$ near pH = 8; $K_{11} \approx 10^4$ near pH = 5

⁶ Although this result is somewhat surprising, extreme supersaturation of Fe(OH)_3 has been observed in laboratory systems [7]. It is also possible that the original Fe_T analysis included dispersed colloidal and dissolved iron.

Acid dissociation constants

(K_a), dilute solutions:

$$pK_a = 5.0 \pm 0.5$$

Although the chemical analysis of the fly ash leachate (Table 2.13-1) shows no dissolved organic carbon in the water sample, a possible effect on complexation of the trace metals in this water will be demonstrated by considering a hypothetical case of small amounts of dissolved carbon in the system. Organic carbon, in the form of humic substances, may appear in the fly-ash leachate from its contact with a soil, or from its mixing with other surface or ground waters. The large reservoir of organic matter in the soil may provide a low constant concentration of dissolved organic matter in the soil waters.

For the humic acids in the fly-ash leachate, it will be assumed that

- (a) the solution contains 1.2 mg/liter dissolved organic carbon ($1 \times 10^{-4} \text{ mol C/liter}$),
- (b) all the dissolved organic carbon is contained in a humic acid of molecular weight 30,000, and
- (c) the humic acid contains, by weight, 55% total C and 35% O, with all of the oxygen contained in the acidic COOH groups.

From the preceding assumptions, the concentration of dissolved organic C attributable to the complex-forming groups (COOH) of the humic acid is found as follows:

$$\text{Moles of O in humic acid} = \frac{(\text{fraction O})(\text{m.w. of humic acid})}{\text{m.w. of O}} = \frac{(0.35)(30,000)}{16} = 656$$

Moles of O in humic acid = $2 \times$ moles of -COOH in humic acid; thus,

$$\text{moles of COOH} = \frac{\text{moles of O}}{2} = \frac{656}{2} = 328$$

$$\text{Moles of total C in acid} = \frac{(\text{fraction C})(\text{m.w. humic acid})}{\text{m.w. C}} = \frac{(0.55)(30,000)}{12} = 1375$$

$$\text{Fraction of total C present as COOH} = \frac{\text{moles of COOH}}{\text{moles of total C}} = \frac{328}{1375} = 0.24$$

Concentration of COOH units in solution that can complex

$$= \text{fraction total C as COOH} \times \text{conc. total C in solution}$$

$$= 0.24 \times 1 \times 10^{-4}$$

$$= 2.4 \times 10^{-5}$$

This is the concentration of carbon as a complexing ligand, L_1 , in the fly-ash leachate;

i.e., $[L_j] = 2.4 \times 10^{-5}$ mol/liter.

The effect of the humic acid ligand on the chemical speciation of a heavy metal will be computed for dissolved nickel. In equation 26 the concentration of free Ni^{+2} ion in the fly-ash leachate was computed from the total nickel concentration, $[\text{Ni}_T] = 3.41 \times 10^{-7}$ mol/liter, and concentrations of three Ni-anion complexes. To add an additional complex $[\text{NiL}_j]$, and to compute the new concentration of the free Ni^{+2} ion, only one more $K_{ij}[L_j]$ term must be added to the denominator of equation 26:

$$K_{ij}[L_j] = 10^8 \times 2.4 \times 10^{-5} = 2400, \text{ near pH} = 8$$

or

$$K_{ij}[L_j] = 10^4 \times 2.4 \times 10^{-5} = 0.24, \text{ near pH} = 5$$

(The values of the stability constants at $\text{pH} = 8$ and $\text{pH} = 5$ were given at the beginning of this section.)

Substitution of each result in equation 26 gives:

$$\text{at pH} = 8: [\text{Ni}^{+2}] = \frac{3.41 \times 10^{-7}}{1.494 + 2400} = 1.4 \times 10^{-10} \text{ mol/liter}$$

$$\text{at pH} = 5: [\text{Ni}^{+2}] = \frac{3.41 \times 10^{-7}}{1.468 + 0.24} = 2.0 \times 10^{-7} \text{ mol/liter}$$

Near the solution pH value of 8, practically all of the dissolved nickel is taken up in the Ni-humate complex. Near the value of $\text{pH} = 5$, only 42% of the total nickel concentration is complexed, mainly in $[\text{NiSO}_4^0]$ and in the nickel-humate complex (the complexes NiOH^+ and NiHPO_4^0 can be neglected at $\text{pH} = 5$). Concentrations of the Ni-sulfate and Ni-humate complexes under the more acidic conditions at $\text{pH} = 5$ are:

$$[\text{NiSO}_4^0] = 9.4 \times 10^{-8} \text{ mol/liter; } 28\% \text{ of total Ni in solution}$$

$$[\text{Ni-humate}] = 4.8 \times 10^{-8} \text{ mol/liter; } 14\% \text{ of total Ni in solution}$$

The large differences between the proportions of nickel in the nickel-humate complexes at the two pH values reflect a greater tendency of humic acids to form complexes with heavy metals under mildly alkaline conditions. Under slightly acidic conditions in the fly-ash leachate, much smaller fractions of dissolved Ni may be expected to occur as Ni-humate complexes.

2.13.4 Summary

A model analysis of an aqueous system, based on the concepts and techniques described for various processes taking place in aqueous solutions, was done on leachate from

a fly-ash site. The principal conclusions were as follows:

- (1) The leachate is a calcium-sulfate type water, of low ionic strength ($I \approx 0.01$ mol/liter), mildly alkaline ($pH = 8.0$), and low in dissolved oxygen (0.7 ppm O_2).
- (2) Iron in solution is present in an oxidized state, Fe(III), and the main aqueous species of iron is the hydroxide complex $Fe(OH)_2^+$. This conclusion is based on an assumption of an oxidation-reduction equilibrium between Fe(II) and Fe(III) in solution. However, aqueous Fe(II), if present, may be rapidly oxidized to Fe(III) at the conditions of the fly-ash site (alkaline pH and dissolved oxygen in water).
- (3) Among the three major constituents of the fly-ash leachate -- Ca^{+2} , Mg^{+2} , and SO_4^{-2} — about 70% of the total concentration of each constituent occurs as free ions, and the remaining 30% occurs as metal-sulfate complexes.
- (4) About 60% of the total dissolved phosphorus is combined in calcium-phosphate and magnesium-phosphate aqueous complexes.
- (5) The leachate is supersaturated with respect to solid $BaSO_4$, $Fe(OH)_3$, and $FePO_4 \cdot 2H_2O$.
- (6) Nickel, occurring as a trace constituent of solution (10^{-7} mol/liter), exists primarily as a free Ni^{+2} ion (about 67% of total Ni in solution). An aqueous complex of importance to the chemical speciation of Ni in the leachate is the ion-pair $NiSO_4^0$ (about 31% of total Ni).
- (7) Estimates were made of the consequences of adding small amounts of humic acids to the leachate (1×10^{-4} mol C/liter or 1.2 ppm). Under mildly acidic conditions ($pH = 5$), only about 15% of the total Ni in solution would be complexed in a Ni-humate complex. However, at an alkaline pH of 8, as in the fly-ash leachate, practically all of the dissolved Ni would be combined in the Ni-humate complex.

2.13.5 Literature Cited

1. Arthur D. Little, Inc., *Full-Scale Field Evaluation of Waste Disposal from Coal-Fired Electric Generating Plants. Appendix F (Part 4)*, EPA Contract No. 68-02-3167, Final Report to U.S. EPA, Office of Research and Development, Washington, D.C. (1984).
2. Drever, J.I., *The Geochemistry of Natural Waters*, Prentice-Hall, Englewood Cliffs, N.J. (1982).
3. Kotrlý, S. and L. Šúcha, *Handbook of Chemical Equilibria in Analytical Chemistry*, John Wiley & Sons, New York (1985).
4. Lerman, A. and C.W. Childs, "Metal-organic Complexes in Natural Waters: Control of Distribution by Thermodynamic, Kinetic and Physical Factors," in *Trace Metals and Metal-Organic Interactions in Natural Waters*, Ann Arbor Science Publishers, Ann Arbor, Mich. (1973).

5. Stevenson, F.J., *Humus Chemistry*, Wiley-Interscience, New York (1982).
6. Wagman, D.D., W.H. Evans, V.B. Parker, R.H. Schumm, I. Halow, S.M. Bailey, K.L. Churney, and R.I. Nutall, "The NBS Tables of Chemical Thermodynamic Properties," *J. Phys. Chem. Ref. Data*, 11, Supplement 2 (1982).
7. White, A.F. and A. Yee, "Aqueous Oxidation-Reduction Kinetics Associated with Coupled Electron Cation Transfer from Iron-Containing Silicates at 25°C," *Geochim. Cosmochim. Acta*, 49, 1263 (1985).

2.14 PHOTOLYSIS IN WATER

2.14.1 Introduction

This section discusses the processes involved when inorganic or organometallic species are exposed to sunlight in natural waters. The resulting photochemical degradation, which competes with other processes such as biotransformation and hydrolysis, is of two kinds:

- *Direct photolysis*, in which the species absorbs solar radiation, is promoted to an excited state, and either decomposes or undergoes secondary reactions; and
- *Indirect photolysis*, in which energy or electrons are transferred from some other photolytically sensitized species. The sensitized species may be dissolved [30] or in the form of a solid suspension [9,13,19,20].

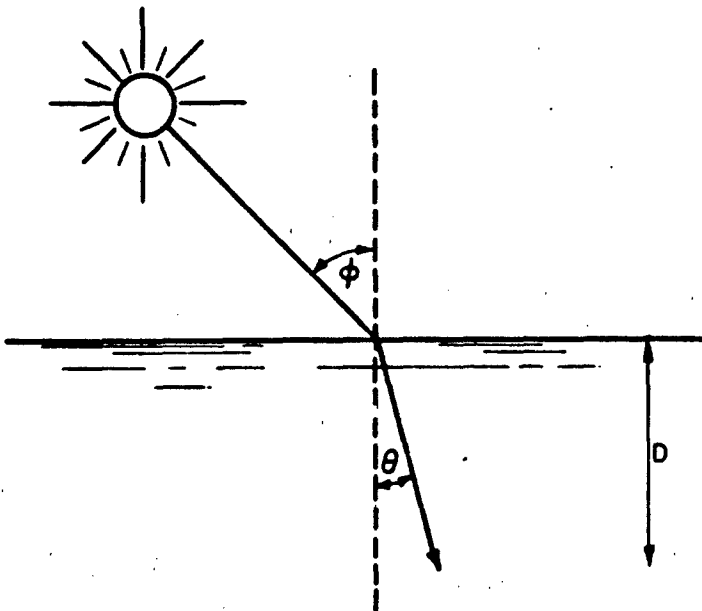
Models for predicting direct photochemical reactivity generally include methods of calculating the net rate at which the chemical absorbs light. The approach, which is discussed by Zepp and Cline [29], Harris [12] and Leighton [16], is to evaluate the degree of overlap between the ultraviolet/visible absorption spectrum of each molecule or ionic species and the solar spectrum to which it is exposed. Section 2.3 of this volume presents Leighton's method; although applied to gaseous species, it is also applicable to absorbers in solution.

2.14.2 Units

Concentrations are generally given in terms of $\text{mol} \cdot \text{l}^{-1}$ or $\text{mol} \cdot \text{cm}^{-3}$. Molar absorptivities are given in terms of $\text{l} \cdot \text{mol}^{-1} \cdot \text{cm}^{-1}$, while the decadic attenuation coefficient of water is in cm^{-1} . Linear measures are expressed in cm. The intensity of solar radiation is usually written in units of $\text{photon} \cdot \text{cm}^{-2} \cdot \text{s}^{-1}$ or in millieinsteins $\cdot \text{cm}^{-2} \cdot \text{s}^{-1}$ (1 einstein = 6.02×10^{23} photons). As described below, the symbols Z_λ , W_λ and L_λ are used to represent solar radiation intensity; each has a different definition.

2.14.3 Solar Irradiance and Absorption Rates

The lower atmosphere receives solar radiation directly from the sun and through sky reflectance. In the ultraviolet region the latter may be more important. Estimating the intensity of incident solar irradiance involves consideration of solar zenith angle, the path length of solar radiation, the amount of scattering, the absorption and diffusion of radiation by the atmosphere, and the albedo of the earth's surface. For water, one must consider additional factors, such as reflectance at the air-water interface, the pathlength of the radiation in water, and the attenuation coefficient of water (Figure 2.14-1). These topics are discussed at length in the literature [12,16,29]; hence, only the results will be given here.



ϕ = ANGLE OF INCIDENCE (Solar Zenith Angle)

θ = ANGLE OF REFRACTION

D = DEPTH OF PENETRATION

FIGURE 2.14-1 Diagram of Passage of a Beam of Sunlight through Atmosphere into Water Body

For direct photolysis, Zepp and Cline [29] derived equations relating the rate of absorption to the intensity of sunlight in the water. They considered the following two cases:

- Case 1 — Essentially all sunlight is absorbed by the system (i.e., water plus chemical).

$$k_{a\lambda} = \frac{W_\lambda \epsilon_\lambda}{jD\alpha_\lambda} \quad (1)$$

where

$k_{a\lambda}$ = rate of absorption for light of wavelength λ (s^{-1})

W_λ = $I_{d\lambda} + I_{s\lambda}$

ϵ_λ = molar absorption coefficient of absorbing species
($M^{-1} \cdot cm^{-1}$)

$I_{s\lambda}$ = intensity of solar sky radiation at midday (photon $\cdot cm^{-2} \cdot s^{-1}$)

$I_{d\lambda}$ = intensity of direct solar radiation at midday (photon · cm⁻² · s⁻¹)

j = conversion factor for concentration in
1 · mol⁻¹ = Avogadro's number × 10⁻³
= 6.023 × 10²⁰ photons · mol⁻¹

D = depth of sunlight penetration in water body (cm)

α_λ = decadic attenuation coefficient of water (cm⁻¹)
(Note that α_λ increases with decreasing water clarity. Values range from about 6 × 10⁻³ cm⁻¹ to 0.2 cm⁻¹ at a wavelength of 400 nm [29].)

Equation 1 is general, hence it is applicable to any depth where strong absorption occurs.

- Case 2 — Less than 5% of the sunlight is absorbed by the system.

$$k_{a\lambda} = \frac{2.303 \varepsilon_\lambda Z_\lambda}{j} \quad (2)$$

or

$$k_{a\lambda} = \varepsilon_\lambda L_\lambda \quad (d^{-1}) \quad (3)$$

where

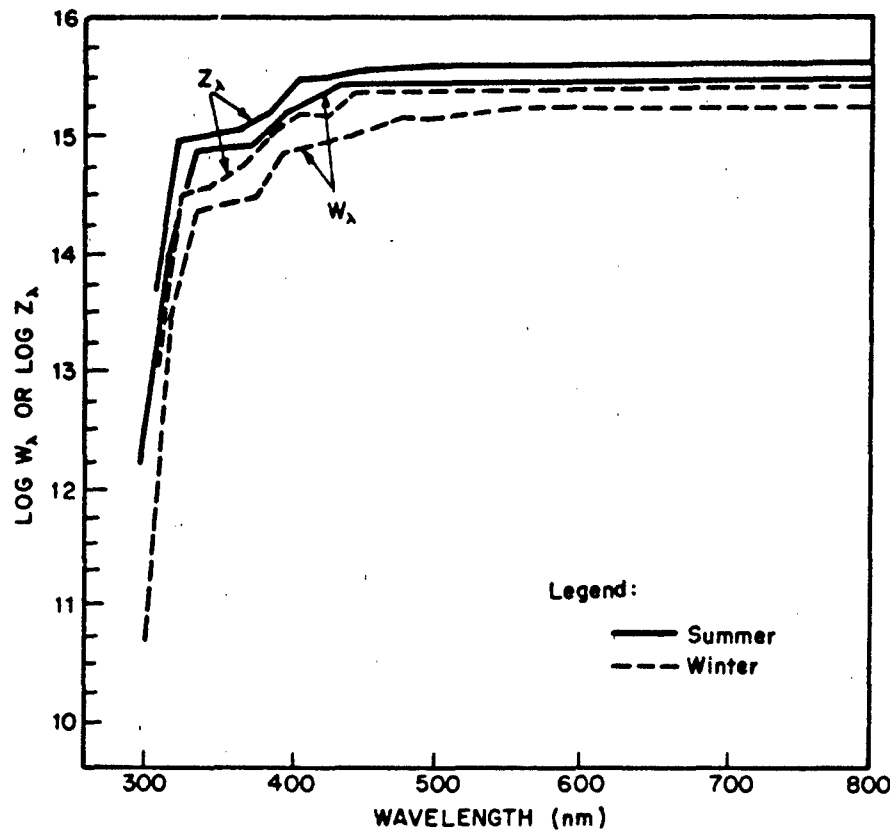
$$Z_\lambda = I_{d\lambda} \sec \theta + 1.2 I_{s\lambda} \quad (\text{photon} \cdot \text{cm}^{-2} \cdot \text{s}^{-1})$$

θ = angle of refraction (degrees)

L_λ = solar irradiance in water (10⁻³ einsteins · cm⁻² · day⁻¹) under clear sky conditions, averaged to account for diurnal fluctuations. (Note that $k_{a\lambda}$ in equation 3 is obtained with units of days⁻¹ when L_λ is in units of 10⁻³ einsteins · cm⁻² · day⁻¹ and ε_λ is in units of M⁻¹ · cm⁻¹.)

Equations 2 and 3 are applicable to shallow depths in any natural water and depths of up to 0.5 m in distilled water.

Zepp and Cline [29] have published extensive tables of W_λ and Z_λ over the wavelength range of 300 nm to 800 nm. Essentially the same tables can be found in the chapter by Harris [12]. More recent and more accurate values are given by Demerjian *et al.* [4]. Figure 2.14-2 shows the general variation of both W_λ and Z_λ with wavelength for the winter and summer seasons at 40° N latitude.



Source: Harris [12]

FIGURE 2.14-2 Variations in $\log Z_\lambda$ and $\log W_\lambda$ with Wavelength for 2 Seasons

Note that the value of the solar irradiance W_λ corresponds to the condition in which essentially all the sunlight is absorbed (by the chemical and the water) while Z_λ corresponds to very weak absorption of sunlight. Both terms correspond to the solar irradiance at midday (i.e., at noon), are a function of latitude and season of the year, and are in the units of photons \cdot cm $^{-2}$ \cdot sec $^{-1}$. While one can use Z_λ or W_λ for calculating rate constants for direct photolysis, this is not the best approach, particularly when a compound photolyzes over several days or weeks. For calculating rate constants and half-lives for direct photolysis, it is preferable to use L_λ , solar irradiance data obtained from the GCSOLAR computer program of Zepp [28]. The term L_λ corresponds to the day-averaged solar irradiance in millieinsteins \cdot cm $^{-2}$ \cdot day $^{-1}$ for shallow depths, weak absorbance, and is a function of latitude and season of the year. Tables of L_λ from the GCSOLAR program of Zepp have been published by the EPA for North latitudes 20°, 30°, 40° and 50° [8]. Those for 40° N are given here in Table 2.14-1.

TABLE 2.14-1
 L_{λ} Values for Latitude 40° N^a

λ_{center} (nm)	$\Delta\lambda$ (nm) ^b	L_{λ} $10^{-3} \text{ einsteins cm}^{-2} \text{ day}^{-1}$			
		Spring	Summer	Fall	Winter
297.5	2.5	1.85(-5)	6.17(-5)	7.83(-6)	5.49(-7)
300.0	2.5	1.06(-4)	2.70(-4)	4.76(-5)	5.13(-6)
302.5	2.5	3.99(-4)	8.30(-4)	1.89(-4)	3.02(-5)
305.0	2.5	1.09(-3)	1.95(-3)	5.40(-4)	1.19(-4)
307.5	2.5	2.34(-3)	3.74(-3)	1.19(-3)	3.38(-4)
310.0	2.5	4.17(-3)	6.17(-3)	2.19(-3)	7.53(-4)
312.5	2.5	6.51(-3)	9.07(-3)	3.47(-3)	1.39(-3)
315.0	2.5	9.18(-2)	1.22(-2)	4.97(-3)	2.22(-3)
317.5	2.5	1.20(-2)	1.55(-2)	6.57(-3)	3.19(-3)
320.0	2.5	1.48(-2)	1.87(-2)	8.13(-3)	4.23(-3)
323.1	3.8	2.71(-2)	3.35(-2)	1.51(-2)	8.25(-3)
330.0	10.0	9.59(-2)	1.16(-1)	5.44(-2)	3.16(-2)
340.0	10.0	1.23(-1)	1.46(-1)	7.09(-2)	4.31(-2)
350.0	10.0	1.37(-1)	1.62(-1)	8.04(-2)	4.98(-2)
360.0	10.0	1.52(-1)	1.79(-1)	9.02(-2)	5.68(-2)
370.0	10.0	1.63(-1)	1.91(-1)	9.77(-2)	6.22(-2)
380.0	10.0	1.74(-1)	2.04(-1)	1.05(-1)	6.78(-2)
390.0	10.0	1.64(-1)	1.93(-1)	9.86(-2)	6.33(-2)
400.0	10.0	2.36(-1)	2.76(-1)	1.42(-1)	9.11(-2)
410.0	10.0	3.10(-1)	3.64(-1)	1.87(-1)	1.20(-1)
420.0	10.0	3.19(-1)	3.74(-1)	1.93(-1)	1.24(-1)
430.0	10.0	3.08(-1)	3.61(-1)	1.87(-1)	1.20(-1)
440.0	10.0	3.65(-1)	4.26(-1)	2.22(-1)	1.43(-1)
450.0	10.0	4.11(-1)	4.80(-1)	2.51(-1)	1.61(-1)
460.0	10.0	4.16(-1)	4.85(-1)	2.54(-1)	1.64(-1)
470.0	10.0	4.30(-1)	5.02(-1)	2.63(-1)	1.69(-1)
480.0	10.0	4.40(-1)	5.14(-1)	2.70(-1)	1.74(-1)
490.0	10.0	4.16(-1)	4.86(-1)	2.56(-1)	1.65(-1)
500.0	10.0	4.23(-1)	4.96(-1)	2.62(-1)	1.68(-1)
525.0	25	1.12	1.31	6.93(-1)	4.45(-1)
550.0	25	1.16	1.36	7.21(-1)	4.61(-1)
575.0	25	1.17	1.37	7.22(-1)	4.61(-1)
600.0	25	1.18	1.38	7.39(-1)	4.69(-1)
625.0	25	1.20	1.40	7.50(-1)	4.82(-1)
650.0	25	1.21	1.41	7.62(-1)	4.95(-1)
675.0	25	1.22	1.41	7.68(-1)	5.03(-1)
700.0	25	1.21	1.40	7.66(-1)	5.05(-1)
750.0	50	2.33	2.69	1.48	9.84(-1)
800.0	50	2.25	2.59	1.43	9.56(-1)

a. The second number in the columns in parentheses is the power of ten by which the first number is multiplied

b. Wavelength interval

Source: Environmental Protection Agency [8]

2.14.4 Direct Photolysis

For direct photolysis, the average rate is proportional to the quantum yield, ϕ_λ , for the reaction and the absorption rate $k_{a\lambda}$. The kinetic expression for direct photolysis is:

$$-\left(\frac{d[C]}{dt}\right)_\lambda = \phi_\lambda k_{a\lambda} [C] \quad (4)$$

where $[C]$ = species concentration ($\text{mol} \cdot \text{l}^{-1}$)

Since ϕ is approximately independent of wavelength, equation 4 becomes:

$$-\frac{d[C]}{dt} = \phi k_a [C] \quad (5)$$

where $k_a = \sum_\lambda k_{a\lambda}$

For Case 1 above, the half-life of this reaction is given by:

$$t_{1/2} = \frac{j D[C_0]}{2 \phi \sum_\lambda W_\lambda} \quad (6)$$

where $[C_0]$ is the initial concentration and the other symbols are as defined earlier. For Case 2, the half-life is

$$t_{1/2} = \frac{0.693}{\phi k_a} \quad (7)$$

When L_λ solar irradiance is used, the direct photolysis rate constant in the environment, k_{dE} , is defined by the equation

$$k_{dE} = \phi \sum_\lambda \epsilon_\lambda L_\lambda, \quad (8)$$

and the half-life is given by the equation

$$t_{1/2} = 0.693/k_{dE} \quad (9)$$

These equations give the rate constant and half-life for direct photolysis in the units days⁻¹ and days, respectively.

Studies of the direct photolysis of inorganic species are rare. Furthermore, the simple inorganic components of natural waters are generally transparent to sunlight. However, nitrite and nitrate have been extensively studied; nitrogen oxides

and CH_\cdot radicals have been identified as the photoproducts [24, 27]. Nitrate has been found to be unreactive, while nitrite shows a net loss of about 10% per day. A few additional weak chromophores with known photochemistry include iodate, uranyl ion (UO_2^{+}), hydrogen peroxide (H_2O_2), and ferrous ions [1]; their environmental photochemistry has not been well studied.

Simple metal ligands such as OH^- , CO_3^{2-} , Cl^- and SO_4^{2-} generally absorb at wavelengths $< 290 \text{ nm}$. Inorganic metal complexes that do react photochemically follow one of two pathways [26]:

- Charge transfer (ligand to metal or metal to ligand)
- Ligand exchange (photodissociation).

Table 2.14-2 lists typical inorganic and organometallic complexes that undergo direct photolysis. The following example shows how one can estimate the half-life of this process.

TABLE 2.14-2

**Examples of Direct Photolysis Involving
Inorganic or Organometallic Complexes**

Species	Products	Probable Mechanism	Ref.
NO_2^-	$\text{NO} + \text{OH}$	Decomposition	[24]
MnO_2	$\text{Mn}(\text{II})$	Electron transfer to metal	[22]
$\text{Cu}(\text{II})$	$\text{Cu}(\text{I})$	Reduction; dissociation	[15]
$\text{Cu}(\text{II})$ -Organic	$\text{Cu}(\text{I})$	Reduction; dissociation	[15]
$\text{Fe}(\text{III})$ -Organic	$\text{Fe}(\text{II}) + \text{CO}_2$	Oxidation of organics; reduction of O_2 ; dissociation	[17]
$\text{Fe}(\text{III})$ -Organic	$\text{Fe}(\text{II}), \text{CO}_2$, amine	Electron transfers to metal; decomposition	[25]
Organic mercurials	Elemental Hg, Hg salts	Decomposition	[10, 32]
$\text{Fe}(\text{CN})_6^{4-}$	$\text{Fe}(\text{CN})_5^{3-} + \text{CN}^-$	Reduction; decomposition	[2]
$\text{Pb}(\text{CH}_2\text{CH}_3)_4$	Ethane and, eventually, inorganic Pb salts	Decomposition	[3]
BrO^-	$\text{Br} + \text{O}^-; \text{Br}^- + \text{O}$	Decomposition	[21a]
ClO_2	$\text{ClO} + \text{O};$ or $\text{Cl} + \text{O}_2$	Decomposition; cage recombination of photolysis products an intermediate	[16a]
ClO^-	$\text{Cl}^- + \text{O}; \text{Cl} + \text{O}^-$	Decomposition	[2a]
ClO_2^-	$\text{ClO}^- + \text{O}; \text{ClO} + \text{O}^-$	Decomposition	[2a]

Example Estimate the half-life for the direct photolysis of Chemical B (hypothetical) at shallow depths. Case 2 will be assumed. Table 2.14-3 lists the information needed for this calculation. (Values of ϵ_λ were taken from an example in reference 8.)

TABLE 2.14-3

Data Needed to Evaluate the Rate of Direct Photolysis
in Example 1

λ Center (nm)	ϵ_λ ($l \cdot mol^{-1} \cdot cm^{-1}$) ^(a)	L_λ (10^{-3} einsteins $\cdot cm^{-2} \cdot d^{-1}$) ^(b)	$\epsilon_\lambda L_\lambda$
297.5	1684	6.17(-5)	0.10
300.0	1434	2.70(-4)	0.39
302.5	1221	8.30(-4)	1.01
305.0	919	1.95(-3)	1.79
307.5	742	3.74(-3)	2.78
310.0	208	6.17(-3)	1.28
312.5	138	9.07(-3)	1.25
315.0	94	1.22(-2)	1.15
317.5	57	1.55(-2)	0.88
320.0	9	1.87(-2)	0.17
323.1	2	3.35(-2)	0.07
330.0	0	1.16(-1)	0.00
$\sum \epsilon_\lambda L_\lambda =$			10.87

a. From reference 8.

b. From Table 2.14-1.

From Table 2.14-3, $k_\alpha = \sum \epsilon_\lambda L_\lambda = 10.87 \text{ d}^{-1}$

Assuming a value of 0.1 for ϕ , we can then use equation 8 to calculate k_{dE} :

$$k_{dE} = (0.1)(10.87) = 1.08 \text{ d}^{-1}$$

and from equation 9

$$t_{1/2} = 0.693 / 1.08 = 0.64 \text{ d}$$

2.14.5 Indirect Photolysis — Homogeneous

In indirect photolysis, a reaction is initiated when light is absorbed by a chromophore (sensitizer) other than the reacting material. If the chromophore is regenerated, it plays a photocatalytic role; if it changes irreversibly, it has undergone direct photolysis itself, even while causing indirect photolysis of other materials. For dissolved chromophores the photolysis is homogeneous. The exact nature of the sensitizers is unknown, but they are believed to consist of dissolved organic materials of unidentified and variable structure [18,30]. "Humic" and "fulvic" acids apparently account for a large fraction of the sensitizers.

The known sensitized photoreactions involve initial excitation of chromophores, followed either by energy transfer or the transfer of electrons or hydrogen atoms to or from other components in the system. The energy transfer reaction was first recognized for inorganics by Joussot-Dubien and Kadiri [14], who studied the sensitized oxidation of ammonia to nitrite and nitrate ions. The mechanism of the reaction was believed to involve the photo formation of long-lived triplet states. The quantum yield of the original photolysis was approximately 0.01, representing a large flux of excited species [26]. In laboratory studies, dyes such as eosin were used as sensitizers, but the authors speculated that several aromatic species in seawater and wastewater could act as photosensitizers [14]. Among the prime candidates was riboflavin, despite its low concentration levels. The importance of photochemically generated singlet oxygen as an oxidant in natural waters was clearly demonstrated in subsequent work by Zeppe *et al.* [31].

The known homogeneous sensitizers appear to be primarily organic in nature, although there is some evidence that nitrate can be an important source of OH⁻ radicals in water [10a], and that metallo-organic complexes act as sensitizers. For example, Miles and Brezonik [17] hypothesized that free Fe[II] and a Fe[II]-humic complex are first oxidized by oxygen to free Fe[III] and a Fe[III]-humic complex respectively. The Fe[III]-humic complex was slowly reduced to Fe[II] in the dark. The reduction was significantly accelerated in the light through a ligand-to-metal charge transfer, producing CO₂ and other oxidation products. The Fe[II]-humic complex could dissociate and replace the free Fe[II] originally oxidized. The overall result was a catalytic redox cycle whereby iron and light caused the production of a half-molecule of CO₂ for every turn of the reaction cycle. The light-accelerated oxidation of other organic complexing agents such as citric acid and histidine by Fe[III] was also demonstrated.

2.14.6 Indirect Photolysis — Heterogeneous

Heterogenous solutions contain both a solution and a solid phase. The solid phase — which may consist of living or nonliving matter, mineral particles and other colloidal materials — may alter the rate of photolysis of sorbed species. Much of the evidence for the general importance of heterogeneous photolysis comes from studies showing spectral shifts, excited state quenching, variation in luminescence yields, and enhancement of electron transfer rates for sorbed species [26]. Although important, such reactions are difficult to study, and relatively little information is available on the mechanisms.

Several investigators [9,13,19,20] have reported, for example, that insoluble semiconductor materials suspended in water can catalyze the complete photolysis of halogenated hydrocarbons to CO₂ and HX and the oxidation of CN⁻ and SO₄²⁻. Notable among these catalysts are TiO₂ [9,19], ZnO [9] and, to a lesser extent, Fe₂O₃ and CdS [9]. These findings are significant, because they may lead to an important means of improving the quality of water containing small amounts of oxidizable organic and inorganic pollutants.

Those who have analyzed the data have generally approached it from the standpoint of first-order kinetics. This treatment is adequate for determining relative reactivities, but it does not clarify the mechanism of the i.e., the role of the solid catalyst and its relationship to the properties of the decomposed species. In the hope of encouraging further research into this matter, we briefly discuss the possible relationship between catalyst and reactants below.

The catalytic materials mentioned above all have semiconductive properties, as manifested by phenomena such as photoconductivity. The oxide materials (TiO_2 , ZnO , Fe_2O_3) in particular chemisorb molecular oxygen and convert it to O_2^- and O_2^{\cdot} . The kinetics of the chemisorption/desorption phenomena has been discussed at length by Halsey [11]. The hypothesis put forth leads to the conclusion that both chemisorption and desorption obey the following rate law:

$$\pm \frac{dQ}{dt} \propto \frac{1}{t} \quad (10)$$

where

$$Q \propto \pm \ln t \quad (11)$$

Q = quantity chemisorbed (+) or desorbed (-)
 t = time

The form of the rate law is a consequence of the fact that as material is chemisorbed (desorbed), the probability of further chemisorption (desorption) decreases. Equation 11 has been confirmed many times [5,6,7,23].

In the dark, if an organic molecule is adsorbed on the surface nothing will happen. Upon exposure of the sorbent to light of suitable wavelength, electron-hole pairs are generated, the holes moving toward the surface and combining with the electron trapped by oxygen molecules. With the loss of the trapped electron, oxygen is released which then reacts with the adsorbed organic species nearby.

Photoconductive measurements indicate that equation 11 is obeyed for both ZnO and TiO_2 [23], hence we would expect the oxidation kinetics of organic species near these surfaces to be linear in $\ln t$. Figure 2.14-3 shows that with the available data equation 11 is obeyed in every case. All of the data are fitted by an equation of the form

$$\frac{[C]}{[C_o]} = 1 + k \ln(t/t_o) \quad (12)$$

where

$[C]$ = concentration of unoxidized species in solution at time t (ppm)
 $[C_o]$ = initial concentration of unoxidized species in solution (ppm)

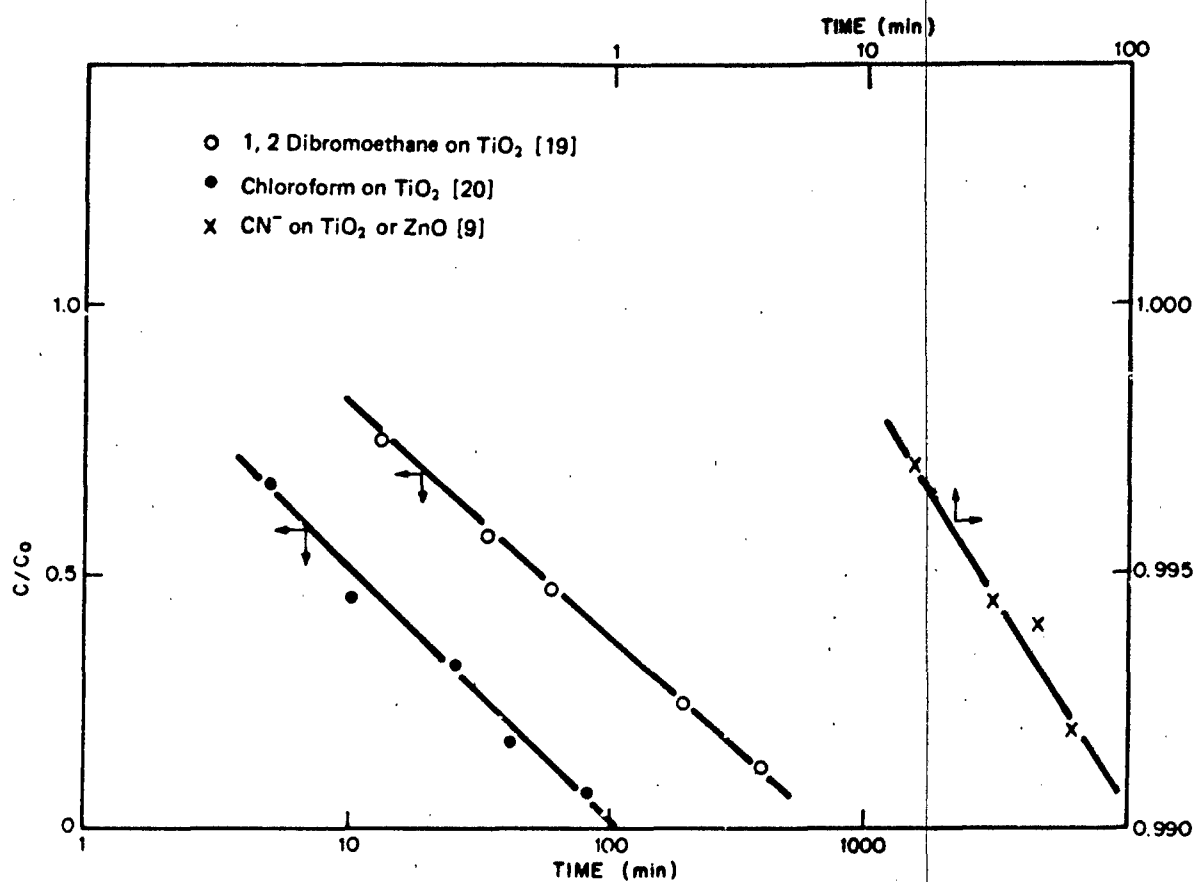


FIGURE 2.14-3 Kinetic Data for Catalytically Oxidized Species

(See text, equation 11)

t_o = characteristic time related to the nature of the reactive species (min)
 k = rate constant (dimensionless) (k is a function of light intensity)

According to Stone [21], t_o is proportional to the time interval in which no chemisorption (desorption) should occur. In gas-phase reactions, this time interval is so short as to be neglected; in a water body, however, we would expect t_o to be significant. Furthermore, we would expect t_o to be related to the ease with which the chemical species can be oxidized.

2.14.7 Literature Cited

1. Brateman, P.S., A. Cairns-Smith, R. Sloper, T. Trusealt and M. Craw, "Photoxidation of Iron(II) in Water between pH 7.5 and 4.0," *J. Chem. Soc., Dalton Trans.*, **1984**, 1441 (1984).
2. Broderios, S.J. and L.L. Smith, Jr., "Direct Photolysis of Hexacyanferrate Complexes: Proposed Applications to Aquatic Environment," Report No. EPA 600/3-80-003, U.S. Environmental Protection Agency, Washington, D.C. (1980).
- 2a. Buxton, G.V. and M.S. Subhani, "Radiation Chemistry and Photochemistry of Oxychlorine Ions," (Parts 2 and 3), *Trans. Faraday Soc. I*, **68**, 958-77 (1972).
3. Charlou, J.L., M. Caprais, G. Blanchard and G. Martin, "Degradation of TEL (Tetraethyllead) in Seawater," *Environ. Technol. Lett.*, **3**, 415-24 (1982).
4. Demerjian, K.L., K.L. Schere and J.T. Peterson, "Theoretical Estimates of Actinic (Spherically Integrated) Flux and Photolytic Rate Constants of Atmospheric Species in the Lower Troposphere," in *Advances in Environmental Science and Technology*, Volume 10, J.N. Pitts, Jr. and R.L. Metcalf (eds.), John Wiley & Sons, New York (1980).
5. Eley, D., "The Kinetics of Unimolecular Processes in Condensed Phases, Including Adsorption," *Trans. Faraday Soc.*, **49**, 643 (1953).
6. Elovich, S. and G. Zhabrova, "Mechanism of the Catalytic Hydrogenation of Ethylene on Nickel. I: Kinetics of the Process," *J. Phys. Chem. (U.S.S.R.)*, **13**, 1761-64 (1939).
7. Elovich, S. and G. Zhabrova, "Role of the Activated Adsorption of Ethylene and Hydrogen in the Hydrogenation Process: General Scheme of the Process," *J. Phys. Chem. (U.S.S.R.)*, **13**, 1775 (1939).
8. Environmental Protection Agency, "40 CFR Parts 796, 797, and 798: Toxic Substances Control Act Test Guidelines, Final Rules," *Fed. Regist.*, **50**, 39252 (September 27, 1985). (See especially § 796.3700.)
9. Frank, S. and A. Bard, "Heterogeneous Photocatalytic Oxidation of Cyanide and Sulfite in Aqueous Solutions at [sic] Semiconductor Powders," *J. Phys. Chem.*, **81**, 1484 (1977).
10. Gowenlock, B.G. and J. Trofman, "UV Absorption Spectrum of Diphenylmercury in Ethanol," *Chem. Ind. (London)*, 309 (March 13, 1954).
- 10a. Haag, W.R. and J. Hoigné, "Photo-sensitized Oxidation in Natural Water Via OH Radicals," *Chemosphere*, **14**, 1659-71 (1985).
11. Halsey, G., "The Rate of Absorption on a Nonuniform Surface," *J. Phys. Chem.*, **55**, 21 (1951).
12. Harris, J., "Rate of Aqueous Photolysis" in *Handbook of Chemical Property Estimation Methods*, W.J. Lyman, W.F. Reehl and D.H. Rosenblatt (eds.), McGraw-Hill Book Co., New York (1982).

13. Hsiao, C.Y., C. LiLee and D. Ollis, "Heterogeneous Photocatalysis: Degradation of Dilute Solutions of CH_2Cl_2 , CHCl_3 and CCl_4 with Illuminated TiO_2 Photocatalyst," *J. Catal.*, **82**, 418 (1983).
14. Joussot-Dubien, J. and A. Kadiri, "Photosensitized Oxidation of Ammonia by Singlet Oxygen in Aqueous Solution and in Seawater," *Nature*, **227**, 700 (1970).
15. Langford, C., M. Wingham and V. Sastri, "Ligand Photooxidation in Copper(II) Complexes of Nitrilotriacetic Acid," *Environ. Sci. Technol.*, **17**, 821 (1983).
16. Leighton, P.A., *Photochemistry of Air Pollution*, Academic Press, New York (1961).
- 16a. Mialocq, J.C., F. Barat, L. Gilles, B. Hickel, and B. Lesigne, "Flash Photolysis of Chlorine Dioxide in Aqueous Solution," *J. Phys. Chem.*, **77**, 742-9 (1973).
17. Miles, C. and P. Brezonik, "Oxygen Consumption in Humic-Colored Waters by a Photochemical Ferrous-Ferric Catalytic Cycle," *Environ. Sci. Technol.*, **15**, 1089 (1981).
18. Norwood, D., J. Johnson, R. Christman, J. Hass and M. Bobenrieth, "Reactions of Chlorine with Selected Aromatic Models of Aquatic Humic Material," *Environ. Sci. Technol.*, **14**, 187 (1980).
19. Ollis, D., "Contaminant Degradation in Water," *Environ. Sci. Technol.*, **19**, 480 (1985).
20. Proden, A. and D. Ollis, "Degradation of Chloroform by Photoassisted Heterogeneous Catalysis in Dilute Aqueous Suspensions of Titanium Dioxide," *Environ. Sci. Technol.*, **17**, 628 (1983).
21. Stone, F.S., *Chemistry of the Solid State*, Ch. 15, W.E. Garner (ed.), Academic Press, New York (1955).
- 21a. Subhani, M.S. and S.F. Lodhi, "A Mechanism for the Photolytic Decomposition of Hypobromite in Aqueous Solution at 365 nm, 313 nm and 253.7 nm," *Rev. Roum. Chim.*, **25**, 1567-78 (1980).
22. Sunda, W., S. Huntsman and G. Harvey, "Photoreduction of Manganese Oxides in Seawater and Its Geochemical and Biological Implications," *Nature*, **301**, 234 (1983).
23. Taylor, H. and N. Thon, "Kinetics of Chemisorption," *J. Am. Chem. Soc.*, **74**, 4169 (1952).
24. Treinin, A. and E. Hayon, "Absorption Spectra and Reaction Kinetics of NO_2 , N_2 , N_2O_3 and N_2O_5 in Aqueous Solution," *J. Am. Chem. Soc.*, **92**, 5821 (1970).
25. Trott, T., R. Henwood and C. Langford, "Sunlight Photochemistry of Ferric (NTA) Complexes," *Environ. Sci. Technol.*, **6**, 367 (1972).
26. Zafiriou, O., J. Joussot-Dubien, R. Zepp and R. Zika, "Photochemistry of Natural Waters," *Environ. Sci. Technol.*, **18**, 358 (1984).
27. Zafiriou, O.C., M. McFarland and R. Bromond, "Nitric Oxide in Seawater," *Science*, **207**, 637 (1980).

28. Zepp, R.G., Environmental Research Laboratory, U.S. Environmental Protection Agency, College Station Road, Athens, GA.
29. Zepp, R.G. and D. Cline, "Rates of Direct Photolysis in Aquatic Environment," *Environ. Sci. Technol.*, **II**(4), 359 (1977).
30. Zepp, R.G., P. Schlotzhaver and R. Sink, "Photosensitized Transformations Involving Electronic Energy Transfer in Natural Waters: Role of Humic Substances," *Environ. Sci. Technol.*, **19**, 74 (1985).
31. Zepp, R.G., N.L. Wolfe, G.L. Baughman and R.C. Hollis, "Singlet Oxygen in Natural Waters," *Nature*, **267**, 421-3 (1977).
32. Zepp, R.G., N.L. Wolfe and J. Gordon, "Photodecomposition of Phenylmercury Compounds in Sunlight," *Chemosphere*, **3**, 93 (1973).

2.15 MICROBIAL TRANSFORMATIONS

2.15.1 General Considerations

Microorganisms such as bacteria, yeast and fungi catalyze the modification of inorganics in the environment. These transformations can affect the mobility and toxicity of these substances. The high metabolic activity and versatility of diverse populations of microorganisms, combined with their rapid reproduction and mutation rates, enable them to adapt and develop enzyme systems that detoxify a variety of substances.

Microbes can be classified by their oxygen requirements: aerobes, which grow in the presence of air or oxygen, and anaerobes, which grow in the absence of air or oxygen. Facultative organisms have the ability to adapt and grow under either oxygen-containing or excluding atmospheres. Organisms in these groups may also hydrolyze, hydrate or dehydrate substances in the environment.

The rates of transformation and the transformation products are dependent on the environmental conditions and the population of microorganisms available. These transformations produce dynamic systems in the environment.

This section describes the microbial transformation of metals and metalloids and gives specific examples of reactions that can be mediated by microbes. The mechanisms involved in the transformation of one form of an element to another are important to consider, because they affect the concentration and distribution of elements in the environment. Table 2.15.1 summarizes the processes discussed in this section and the elements known to be affected by them.

TABLE 2.15.1
Elements Affected by Microbial Transformation Processes

Process	Elements Known to Be Affected
Oxidation/Reduction (Sect. 2.15.2)	Hg, As, Fe, Mn, Sb, Te, Se, S
Sulfide Precipitation (Sect. 2.15.2)	Cu, Pb, Zn, Ag, others
Methylation (Sect. 2.15.3)	Hg, As, Se, Pb, Cd, Sn, Te, Pu, Tl(?), Pt(?) Sb(?)
Dealkylation (Sect. 2.15.4)	Hg, Sn, As

2.15.2 Oxidation and Reduction

Metals and metalloids can exist in the environment in several valence forms, each of which is available for chemical and biochemical reactions. Each form may differ in its toxicity and mobility in the environment. By means of oxidative and reductive reactions, microorganisms can control the relative amount of each of the forms in the environment. Changes in temperature, pH and the composition of the microbial population may shift the equilibrium among the different forms.

For example, mercury exists in three forms shown in the following equilibrium [31]:



It has been found that bacteria and yeasts can convert HgCl_2 to elemental mercury. From a stream, Brunker and Bott [5] isolated a yeast of the genus *Cryptococcus* that was capable of reducing HgCl_2 to Hg^0 ; *Escherichia coli* and strains of *Pseudomonas* sp. were also able to catalyze this reaction [1]. Nicotinamide adenine dinucleotide, reduced form (NADH), acts as a coenzyme in this reaction [31]:

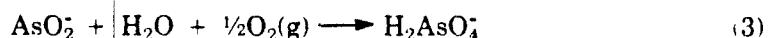


Reduced nicotinamide adenine dinucleotide phosphate (NADPH) has also been indicated as a coenzyme for similar transformations [1]. The elemental mercury formed escapes from the system due to its high volatility and shifts the equilibrium in equation 1 to the right.

A *Pseudomonas* strain was able to produce elemental mercury following incubation with phenylmercuric acetate, ethylmercuric phosphate and methylmercuric chloride [1]. The reductive dealkylation of organic mercury compounds is described in section 2.15.4.

The reverse reaction, the oxidation of Hg^0 to Hg^{+2} , has also been reported to occur in soils and sediments. Although microbes appear to mediate this reaction, the extent to which they are involved is not clear [22]. The process has important toxicologic significance, because Hg^{+2} can be methylated to form methylmercury, which is more toxic to higher organisms than elemental mercury or inorganic divalent mercury. The methylation of Hg^{+2} is described in section 2.15.3.

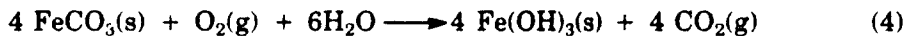
Microorganisms can also catalyze the oxidation and reduction of arsenic compounds. The oxidation of trivalent arsenite, As(III), to pentavalent arsenate, As(V), has been reported to occur in cultures of pseudomonads and in soil [1]. Quastel and Scholefield [21] suggest the following reaction to describe the oxidation of As(III) to As(V) in soil:



Pure cultures of several organisms are also able to reduce As(V) to As(III), including *Chlorella*, *Micrococcus* sp., the yeast *Pichia guillermondii* and marine bacteria [1]. McBride and Wolfe [15] described the reductive methylation of arsenate to dimethyl arsine by *Methanobacterium* in which the first step in the overall reaction was the reduction of As(V) to As(III). Reductive methylation of arsenic compounds is discussed in Section 2.15.3.

Environmental conditions are important in the interconversion of inorganic forms of arsenic. Myers *et al.* [16] showed that microbial populations in activated sludge oxidized arsenite to arsenate under aerobic conditions; under anaerobic conditions, arsenate was reduced to arsenite and to an even lower oxidation state when anaerobic incubation was continued. The form of arsenic produced is of environmental and toxicological importance, because arsenite, As(III), is generally more toxic to higher organisms than arsenate, As(V) [1]. For example, the apparent no-effect doses in rat carcinogenicity studies were 12.5 mg/kg/day and 23 mg/kg/day for sodium arsenite and sodium arsenate, respectively. In general the toxicity of the various forms of arsenic are related to their rate of clearance from the body and thus to their degree of accumulation in the tissues [23].

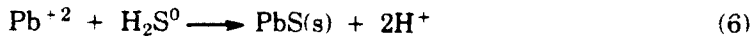
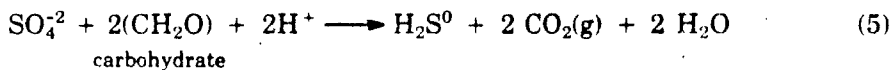
The oxidation of Fe(II) to Fe(III) is catalyzed by bacteria such as *Ferrobacillus* and *Gallionella*. The energy released in a reaction such as the following is used by the bacteria in their metabolism [9]:



Manganese is oxidized by microbes in soil, and bacterial enzymes have been reported to function in the oxidation and reduction of manganese in marine sediments. Micro-organisms also appear capable of oxidizing antimony and reducing tellurite and selenite to the metallic form [27].

Sulfide minerals of metals such as Cu, Pb, Zn and Ag are produced by the action of *Desulphovibrio desulphuricans* and other sulfate-reducing bacteria, which are found in mud, swamps and drained pools. The reactions catalyzed by these microorganisms are inhibited under aerobic and acidic conditions [1].

The first step in the formation of insoluble metal sulfides in the environment is the reduction of sulfate catalyzed by the microorganisms, followed by the precipitation of the sulfide [9]:



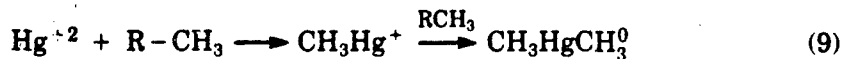
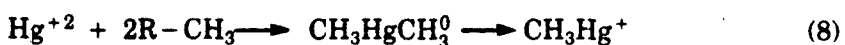
Hydrogen sulfide, H₂S, can also be formed by the cleavage of organic molecules such as proteins, polypeptides and amino acids by bacteria. An example is the transformation of cysteine to pyruvic acid:



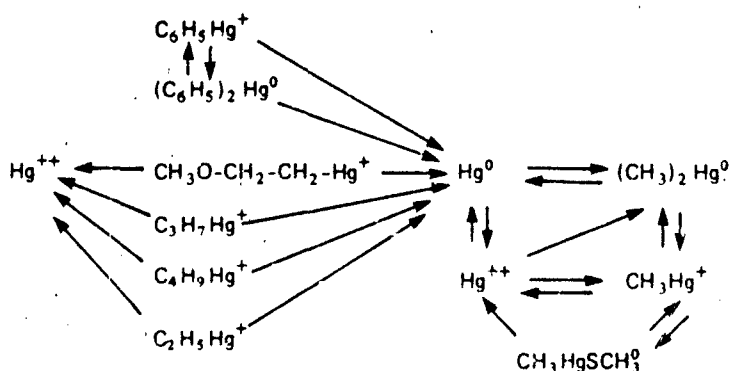
2.15.3 Methylation

Microorganisms can catalyze the methylation of inorganic metals and metalloids. This may be a detoxification mechanism for the organisms, but the methylated products formed can be more toxic to higher organisms. Investigators have reported that mercury, arsenic, selenium, lead, tin, tellurium, plutonium and cadmium can be methylated by microorganisms, and it has been suggested that thallium, antimony and platinum should undergo a similar reaction [12,22,28,31].

Mercury can be methylated by both anaerobic and aerobic microorganisms. Jensen and Jernelöv [13] reported the formation of monomethyl and dimethylmercury in the sediment of freshwater aquaria, for which they postulated the following two reactions:



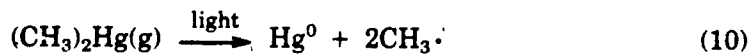
Methylation of mercury has also been detected in river and marine sediments and soil [2,3,11]. D'Itri [8] states that the mechanism involves the reaction of mercuric ion with methylcobalamin, a methylated vitamin B-12 derivative, through a combination of the reactions described in equations 8 and 9. For methylation to occur, mercury must be in the form of the divalent inorganic species. (However, HgS is not available for methylation due to its low solubility and the normally anaerobic conditions [14].) Most forms of mercury released into the environment, including elemental mercury, phenyl mercuries, alkyl mercuries and alkoxy-alkyl mercuries, can be directly or indirectly transformed into inorganic mercuric ions (Figure 2.15-1).



Source: D'Itri [8]. (Copyright 1972, CRC Press. Reprinted with permission.)

FIGURE 2.15-1 Hypothetical Model for the Conversion of Mercury in the Aquatic Environment

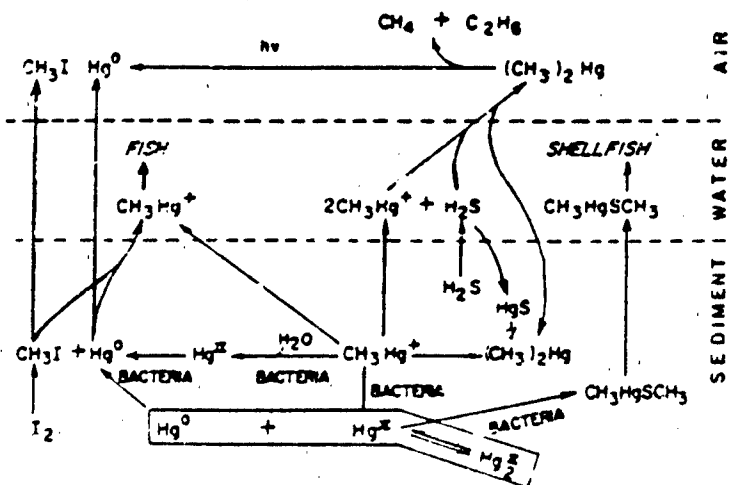
The relative amounts of mono- and dimethylmercury formed are dependent on the initial mercury concentration and the temperature and pH of the system. The formation of dimethylmercury is favored in neutral to alkaline waters and when the initial mercury concentrations are low [30]. Dimethylmercury is volatile; when released to the atmosphere, it undergoes photoysis to elemental mercury plus methyl free radicals, as shown below [8]; the methyl radicals are then reduced to methane or combine to form ethane.



Acidic pH and higher initial mercury concentrations favor the formation of monomethylmercury. Its rate of synthesis is about 6000 times faster than that of dimethylmercury [31].

Aerobic and facultative anaerobic bacterial species capable of methylating mercury include *Klebsiella pneumoniae*, *Escherichia coli* and *Clostridium cochlearum* [20].

The biological cycle for mercury suggested by Wood [32] is shown in Figure 2.15-2. Sulfide is important to volatilization and precipitation of mercury through disproportionation chemistry in the aqueous environment.

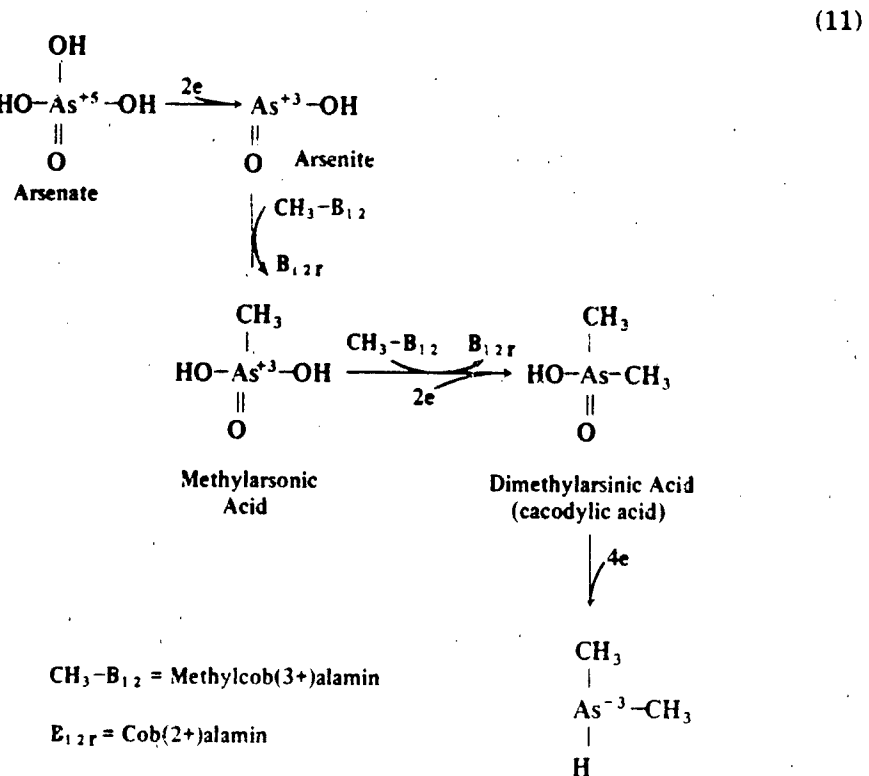


Source: Wood [32]. (Copyright 1984, Gordon and Breach Science Publishers, Inc. Reprinted with permission.)

FIGURE 2.15-2 The Biological Cycle for Mercury

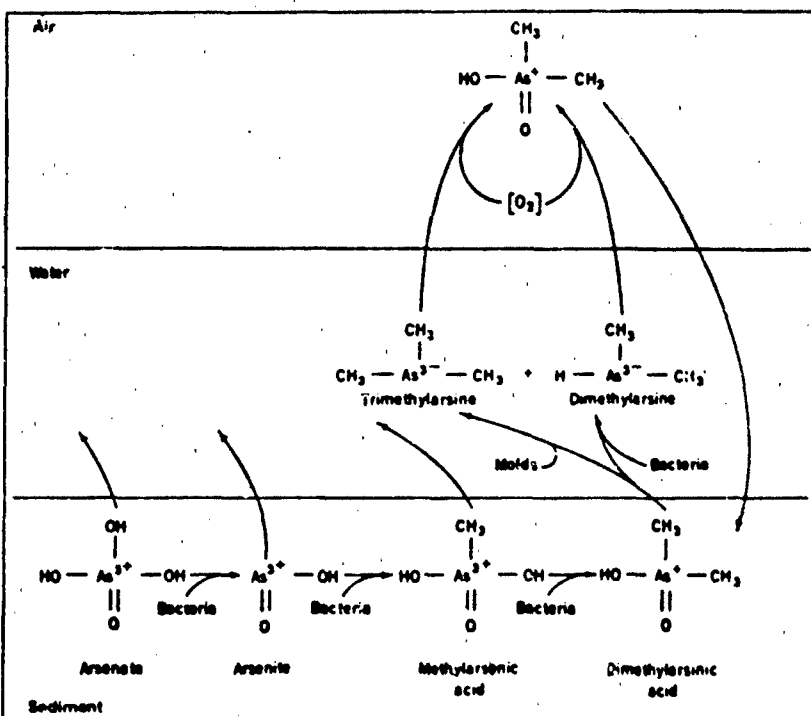
Arsenic compounds are methylated by bacteria and fungi to yield dimethyl and trimethylarsines by a mechanism that involves the replacement of substituent oxygen atoms by methyl groups [6,23]. Methylation is thought to be a detoxification mechanism for the microorganisms [4] and is important in the transfer of arsenic from the sediment to the water and atmosphere.

McBride and Wolfe [15] reported that arsenate could be reductively methylated to dimethylarsine by *Methanobacterium* under anaerobic conditions. The reaction, shown below as given by Saxena and Howard [22], involves the initial reduction of arsenate to arsenite. Methylarsonic acid, formed by the methylation of arsenite, is reductively methylated to dimethylarsinic acid, which is reduced to dimethylarsine. Methylcobalamin is the methyl-donor in the reaction:



Under acidic conditions, the sewage fungi *Candida humicola* transform arsenate to trimethylarsine. Lesser amounts of trimethylarsine are also formed by the incubation of the fungi with arsenite, methylarsonate, and dimethylarsinate. These may be intermediates in the reduction and alkylation of arsenate to trimethylarsine [7]. Fungi capable of generating trimethylarsine from the pesticides monomethylarsonate and dimethylarsine include *Candida humicola*, *Gliocladium roseum*, and a strain of *Penicillium* [1]. The rate of formation of trimethylarsine by *Candida humicola* and other molds decreases as the mold reaches its resting stage [28].

The toxic alkylarsines are volatile, with a distinct garlic-like odor, and are rapidly oxidized to less toxic products in the atmosphere. One such product, dimethylarsinic acid (cacodylic acid), has been shown to be an intermediate in the synthesis of dimethylarsine from arsenic salts [31]. The biological cycle for arsenic is shown in Figure 2.15-3.



Source: Wood [31]. (Copyright 1974, American Association for the Advancement of Science. Reproduced with permission.)

FIGURE 2.15-3 The Biological Cycle for Arsenic

Selenium can also be acted on by microorganisms to produce methylated compounds. Inorganic selenium compounds have been transformed to dimethylselenide by a strain of *Penicillium* isolated from raw sewage and by the fungus *Candida humicola* [7,10]. Methylation of selenium has also been shown to occur in soil and lake sediment [1,22]. Dimethylselenide, $(\text{CH}_3)_2\text{Se}$, dimethyldiselenide, $(\text{CH}_3)_2\text{Se}_2$, and dimethylselenone, $(\text{CH}_3)_2\text{SeO}_2$, were formed following incubation of selenium with sludge microorganisms [28].

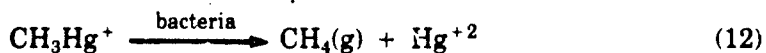
Wong *et al.* [29] have reported the transformation of inorganic and organic lead compounds into volatile tetramethyl lead by microorganisms in lake sediments under anaerobic conditions. Tetramethyl lead has been formed by the incubation of sediment with inorganic lead nitrate, lead chloride, or organic trimethyllead acetate. The

pathways for biological transformation of lead are not well understood. Species of *Pseudomonas*, *Alcaligenes*, *Acinetobacter* and *Aeromonas* isolated from lake sediment were able to convert $(CH_3)_3Pb^+$ to $(CH_3)_4Pb$ but were ineffective in methylating inorganic lead in chemically defined media; this conversion probably requires specific physical, chemical and biological conditions to proceed.

Evidence of the methylation of inorganic cadmium and tin to a volatile organic species by *Pseudomonas* sp. has also been reported [12,22]. In the presence of Sn(IV), volatile methylated forms of tin were produced. These biomethylated tin species were subsequently demonstrated to abiotically methylate Hg(II) to form methylmercury [15].

2.15.4 Dealkylation

Microbial dealkylation of alkylmercury compounds has been studied. Aerobic, anaerobic and facultative anaerobic species isolated from soil, sewage and lake sediments are capable of dealkylating methylmercury [20,24,26]. It appears that these methylmercury-resistant strains have developed enzyme systems capable of hydrolyzing the metal-carbon bond, resulting in the formation of methane and mercuric ion; the latter is then reduced to elemental mercury as described in section 2.15.2.



The high volatility of elemental mercury permits it to escape from the system [20,26].

While the rate of demethylation of mercury is reported to be much slower than that of methylation, it nevertheless helps to offset the formation of methylmercury [17,20]. Recent studies have also shown that bacteria from soil, sediment, and water were capable of dealkylating monosodium methanearsonate [25].

Dealkylation of the fungicide-slimicide phenylmercuric acetate by bacteria isolated from water and sediment samples has also been reported. Nelson *et al.* [18] isolated mercury-resistant bacteria from the Chesapeake Bay that were capable of degrading phenylmercuric acetate to benzene and metallic mercury.

Dealkylation of tributyltin oxide by several fungi has also been reported, with a dibutyltin compound the primary product in the studies [19]. Cleavage of aryltin bonds by bacteria acting on triphenyltin acetate has also been reported [12].

2.15.5 Literature Cited

1. Alexander, M., "Microbial Formation of Environmental Pollutants," *Adv. Appl. Microbiol.*, **18**, 1-73 (1974).
2. Beckert, W.F., A.A. Moghissi, F.H.F. Au, E.W. Breithauer and J.C. McFarlane, "Formation of Methylmercury in a Terrestrial Environment," *Nature*, **249**, 674-75 (1974).
3. Berdicevsky, I., H. Shoyerman and S. Yannai, "Formation of Methylmercury in the Marine Sediment," *Environ. Res.*, **20**, 325-34 (1979).
4. Braman, R.S. and C.C. Forback, "Methylated Forms of Arsenic in the Environment," *Science*, **183**, 1247-49 (1973).
5. Brunker, R.L. and T.L. Bott, "Reduction of Mercury to the Elemental State by a Yeast," *Appl. Microbiol.*, **27**, 870-73 (1974).
6. Challenger, F., "Biological Methylation," *Sci. Progress*, **35**, 396-416 (1947), as cited by Scow *et al.* [23].
7. Cox, D.P. and M. Alexander, "Effect of Phosphate and Other Anions on Trimethylarsine Formation by *Candida humicola*," *Appl. Microbiol.*, **25**, 408-13 (1973).
8. D'Itri, F.M., "Biological Methylation of Mercury in the Environment," in *The Environmental Mercury Problem*, CRC Press, Cleveland (1972).
9. Fergusson, J.E., *Inorganic Chemistry and the Earth*, Pergamon Press, Elmsford, N.Y. (1982).
10. Fleming, R.W. and M. Alexander, "Dimethylselenide and Demethyltelluride Formation by a Strain of *Penicillium*," *Appl. Microbiol.*, **24**, 424-29 (1972).
11. Hamdy, M.K and O.R. Noyes, "Formation of Methyl Mercury by Bacteria," *Appl. Microbiol.*, **30**, 424-432 (1975).
12. Iverson, W.P. and F.E. Brinckman, "Microbial Metabolism of Heavy Metals," in *Water Pollution Microbiology*, Vol. 2, Mitchell, R. (ed.), John Wiley & Sons, New York (1978).
13. Jensen, S. and A. Jernelöv, "Biological Methylation of Mercury in Aquatic Organisms," *Nature*, **223**, 753-54 (1969).
14. Lexmond, T.M., F.A.M. de Haan and M.J. Frissel, "On the Methylation of Inorganic Mercury and the Decomposition of Organo-mercury Compounds: A Review," *Neth. J. Agric. Sci.*, **24**, 79-97 (1976).
15. McBride, B.C. and R.S. Wolfe "Biosynthesis of Dimethylarsine by *Methanobacterium*," *Biochemistry*, **10**, 4312-17 (1971).
16. Myers, D.J., M.E. Heimbrook, J. Osteryoung and S.M. Morrison, "Arsenic Oxidation State in the Presence of Microorganisms. Examination by Differential Pulse Polarography," *Environ. Lett.*, **5**, 53-61 (1973).
17. National Research Council, *An Assessment of Mercury in the Environment*, National Academy of Sciences, Washington, D.C. (1977).

18. Nelson, J.D., W. Blair, F.E. Brinckman, R.R. Colwell and W.P. Iverson, "Biodegradation of Phenylmercuric Acetate by Mercury-Resistant Bacteria," *Appl. Microbiol.*, **26**, 321-26 (1973).
19. Orsler, R.J. and G.E. Holland, "Degradation of Tributyltin Oxide by Fungal Culture Filtrates," *Int. Biodeterior. Bull.*, **18**, 95-98 (1982).
20. Perwak, J., M. Goyer, L. Nelken, K. Scow, M. Wald, D. Wallace and G. Kew, "An Exposure and Risk Assessment for Mercury," Final Draft Report, U.S. Environmental Protection Agency, Office of Water Regulations and Standards (WH-553), Washington, D.C. (1980).
21. Quastel, J. H. and P.G. Scholefield, "Arsenite Oxidation in Soil," *Soil Sci.*, **75**, 279-85 (1953).
22. Saxena, J. and P.H. Howard, "Environmental Transformation of Alkylated and Inorganic Forms of Certain Metals," *Adv. Appl. Microbiol.*, **21**, 185-226 (1977).
23. Scow, K., M. Byrne, M. Goyer, L. Nelken, J. Perwak, M. Wood, S. Young, P. Cruse and S. Kroner, "An Exposure and Risk Assessment for Arsenic," Final Draft Report, U.S. Environmental Protection Agency, Office of Water Regulations and Standards (WH-553), Washington, D.C. (1981).
24. Shariat, M., A.C. Anderson and J.W. Mason, "Screening of Common Bacteria Capable of Demethylation of Methylmercuric Chloride," *Bull. Environ. Contam. Toxicol.*, **21**, 155-261 (1979).
25. Shariatpanahi, M., A.C. Anderson and A.A. Abdelghani, "Microbial Demethylation of Monosodium Methanearsononate," *Trace Subst. Environ. Health*, **15**, 383-87 (1981).
26. Spangler, W.J., J.L. Spigarelli, J.M. Rose, R.S. Flippin and H.H. Miller, "Degradation of Methylmercury by Bacteria Isolated from Environmental Samples," *Appl. Microbiol.*, **25**, 488-93 (1973).
27. Summers, A.O. and S. Silver, "Microbial Transformation of Metals," *Annu. Rev. Microbiol.*, **32**, 637-72 (1978).
28. Thayer, J.S. and F.E. Brinckman, "The Biological Methylation of Metals and Metalloids," *Adv. Organomet. Chem.*, **20**, 313-356 (1982).
29. Wong, P.T.S., Y.K. Chau and P.L. Luxon, "Methylation of Lead in the Environment," *Nature*, **253**, 263-64 (1975).
30. Wood, J.M., F.S. Kennedy and C.G. Rosen, "Synthesis of Methylmercury Compounds by Extracts of a Methanogenic Bacterium," *Nature*, **220**, 173-74 (1968).
31. Wood, J.M., "Biological Cycles for Toxic Elements in the Environment," *Science*, **183**, 1049-52 (1974).
32. Wood, J.M., "Alkylation of Metals and the Activity of Metal Alkyls," *Toxicol. Environ. Chem.*, **7**, 229-40 (1984).

2.15.6 Other Sources of Information

- Compeau, G. and R. Bartha, "Methylation and Demethylation of Mercury Under Controlled Redox, pH, and Salinity Conditions," *Appl. Environ. Microbiol.*, **48**, 1203-1207 (1984).
- Craig, P.J., "Metal Cycles and Biological Methylation," in *The Handbook of Environmental Chemistry*, Vol. I, Part A, The Natural Environment and the Biogeochemical Cycles, O. Huntzinger (ed.), Springer-Verlag (1980).
- Huey, C., F.E. Brinckman, S. Grim and W.P. Iverson, "Role of Tin in Bacterial Methylation of Mercury," *Proc. Int. Conf. Transp. Persistent Chem. Aquat. Ecosyst.*, 73-78 (1974).
- Jernelov, A. and A. Martin, "Ecological Implications of Metal Metabolism by Micro-organisms," *Annu. Rev. Microbiol.*, **29**, 61-77 (1975).
- Rapsomanikis, S. and J.H. Weber, "Environmental Implications of Methylation of Tin(II) and Methyltin(IV) Ions in the Presence of Manganese Dioxide," *Environ. Sci. Technol.*, **19**, 352-356 (1985).
- Robinson, J.B. and O.H. Tuovinen, "Mechanisms of Microbial Resistance and Detoxification of Mercury and Organomercury Compounds: Physiological, Biochemical, and Genetic Analyses," *Microbiol. Rev.*, **48**, 95-124 (1984).

2.16 DIFFUSION COEFFICIENTS

2.16.1 Introduction

The methods by which diffusion coefficients are estimated, measured and used vary considerably with both the nature of the diffusing material and the environment in which it diffuses. The diffusion of neutral and nonreactive organic species in both air and water has been comprehensively discussed in recent literature [5,7], and the approximation methods offered may be applied to neutral and nonreactive inorganic materials as well. This section focuses primarily on the diffusion in water of electrolytes, which probably include most inorganics of interest to the reader.

2.16.2 Description of Property

To describe diffusion or diffusion coefficients, one must begin by considering the motion of dissolved species in fluids. Under virtually all conditions encountered in the environment (gases at ambient pressure or liquids), a species acted upon by a force accelerates almost instantly to a limiting velocity determined by drag or viscous forces. Thus, the Newtonian approach, $f = ma$ (force equals mass times acceleration), is for practical purposes supplemented by $f = v/u$, where v is the limiting velocity and u is defined as mobility. Quite obviously, u is a rather complex function of the mobile species and, especially, of the fluid through which it moves.

From the above concept of mobility, various related but differing theories of diffusion, electrophoresis and conduction have been developed. In diffusion, the mobile species may be neutral or charged, and the acting force is a concentration gradient alone. In electrophoresis, the species is charged and the acting force is an electric field. In conduction, the species is charged, but the acting force is the concentration gradient resulting from the passage of an electric current.

Since velocity is neither easy to measure nor particularly useful, diffusion is usually defined in terms of Fick's law [6]:

$$F = -D \frac{dC}{dX} \quad (1)$$

In this equation, which is compatible with the mobility concept, F is the flux or rate of transfer of the species per unit of cross-section area, dC/dX is the concentration gradient, and D is defined as the diffusion coefficient of the species in that medium. Dimensionally, F has the units of mass (or moles) per unit time, C is mass (or moles) per unit volume, and X is unit length. Thus D must be expressed as area per unit time, usually cm^2/s . (The negative sign in equation 1 reflects the fact that diffusion takes place in the direction of decreasing concentration.¹)

1. Fick's law is analogous to Ohm's law, $I = E/R$, if we consider the current (I) to represent flux, voltage (E) to represent the driving force, and the reciprocal of resistance ($1/R$) to represent the diffusion coefficient. The mobile electron also moves with a limiting velocity, in this case the speed of light.

Up to this point, the description of diffusion appears straightforward. Regrettably, it infers several conditions that are rarely true in the real world, such as:

- there is only one diffusing species;
- the species is present only in very dilute solutions;
- no chemical interactions occur in the solution or at interfaces;
- the solution is isothermal;
- concentration and activity are considered the same; and
- the diffusion takes place in unrestricted space.

If there were only one diffusing species in very dilute solution, a simple diffusion coefficient could be used to describe its behavior. However, to be rigorous, we must use a second coefficient to describe the diffusion of the solvent into the space vacated by the solute. (Otherwise there would be net movement of the system.) If more than one solute species is present, there must be additional coefficients describing diffusion of pure components, and cross-term coefficients reflecting interaction between the components. Fortunately, however, a single value of D will usually suffice for all practical applications in dilute solutions.

When the mobile species are electrolytes, the situation is even more interesting. A highly dissociated 1:1 electrolyte, such as KCl or NaCl, can in fact be described by a single diffusion coefficient; although two separately definable ionic species are present, diffusion of one ion must be accompanied by diffusion of an ion of opposite charge in the same direction, to avoid the establishment of a charge separation in the fluid.² As might be expected, the assignment, measurement, and calculation of diffusion coefficients becomes increasingly complex with electrolytes of mixed charge, multi-component electrolytes, and partially dissociated electrolytes, and a rigorous description becomes impossible.

From the above comments, one might assume that diffusion coefficients are only of academic interest and that their measurement or estimation is impractical. However, arguments that diffusion phenomena cannot be treated rigorously should be weighed against two other points:

- Overall, diffusion coefficients do not vary greatly. (See Tables 2.16-1 and 2.) The coefficients of many simple salts generally do not change by more than a factor of 2 over a range of concentrations and temperatures, even though their conductivities vary greatly. (This is related to the fact that each diffusing ion is accompanied by a diffusing counter ion, which tends to compensate for possibly large differences in specific ion mobilities.)

2. In this respect, diffusion differs from conductance, wherein ions of opposite charge move in opposite directions and the concept of transference numbers is added to that of mobility.

TABLE 2.16-1

**Measured Diffusion Coefficients of Dilute
Aqueous Electrolyte Solutions**
(D expressed in $10^{-5}\text{cm}^2/\text{s}$, c expressed in mol/l)

Salt	Temp. (°C)	Diffusion Coefficient, D , at Indicated Concentration ^a						
		$c = 0^b$	0.001	0.002	0.003	0.005	0.007	0.010
LiCl	25	1.366	1.345	1.337	1.331	1.323	1.318	1.312
NaCl	25	1.610	1.585	1.576	1.570	1.560	1.555	1.545
KCl	20	1.763	1.739	1.729	1.722	1.708	—	1.692
KCl	25	1.993	1.964	1.954	1.945	1.934	1.925	1.917
KCl	30	2.230	—	—	2.174	2.161	2.152	2.144
RbCl	25	2.051	—	2.011	2.007	1.995	1.984	1.973
CsCl	25	2.044	2.013	2.000	1.992	1.978	1.969	1.958
LiNO ₃	25	1.336	—	—	1.296	1.289	1.283	1.276
NaNO ₃	25	1.568	—	1.535	—	1.516	1.513	1.503
KClO ₄	25	1.871	1.845	1.841	1.835	1.829	1.821	1.790
KNO ₃	25	1.928	1.899	1.884	1.879	1.866	1.857	1.846
AgNO ₃	25	1.765	—	—	1.719	1.708	1.698	—
MgCl ₂	25	1.249	1.187	1.169	1.158	—	—	—
CaCl ₂	25	1.335	1.249	1.225	1.201	1.179	—	—
		1.335	1.263	1.243	1.230	1.213	1.201	1.188
SrCl ₂	25	1.334	1.269	1.248	1.236	1.219	1.209	—
BaCl ₂	25	1.385	1.320	1.298	1.283	1.265	—	—
Li ₂ SO ₄	25	1.041	0.990	0.974	0.965	0.950	—	—
Na ₂ SO ₄	25	1.230	1.175	1.160	1.147	1.123	—	—
Cs ₂ SO ₄	25	1.568	1.489	1.454	1.437	1.420	—	—
MgSO ₄	25	0.849	0.768	0.740	0.727	0.710	0.704 ^c	—
ZnSO ₄	25	0.846	0.748	0.733	0.724	0.705	—	—
LaCl ₃	25	1.293	1.175	1.145	1.126	1.105	1.084	1.021 ^d
K ₄ Fe(CN) ₆	25	1.468	—	—	1.213	1.183	—	—

a. D values for round concentrations have been interpolated graphically from the original data.

b. Values in this column are limiting values derived from the limiting mobilities of the ions.

c. At 0.006 mol/l

d. At 0.026 mol/l

Source: Robinson and Stokes [6]. (Copyright 1959, Academic Press. Reprinted with permission.)

TABLE 2.16-2

Measured Diffusion Coefficients of Concentrated Aqueous Electrolyte Solutions at 25°C
 $(D \text{ expressed in } 10^{-5} \text{ cm}^2/\text{s}, c \text{ expressed in mol/l})$

c	HCl	HBr	LiCl	LiBr	NaCl	CsCl	NaBr	NaI	KCl	KBr	KI	NH ₄ Cl	NH ₄ NO ₃	LiNO ₃	CaCl ₂	(NH ₄) ₂ SO ₄	BaCl ₂
0 ^a	3.336	3.400	1.366	1.377	1.610	2.044	1.625	1.614	1.993	2.016	1.999	1.929	1.336	1.335	1.530	1.385	
0.05	3.07	3.15	1.28	1.30	1.507	—	1.53	1.52	1.864	1.89	1.89	—	1.788	—	1.121	0.802	1.179
0.1	3.05	3.14	1.26	1.27	1.483	1.871	1.51	1.52	1.844	1.87	1.86	1.838	1.769	1.240	1.110	0.825	1.159
0.2	3.06	3.19	1.26	1.28	1.475	1.857	1.50	1.53	1.838	1.87	1.85	1.836	1.749	1.243	1.107	0.867	1.150
0.3	3.09	3.24	1.26	1.29	1.475	1.856	1.51	1.54	1.838	1.87	1.88	1.841	1.739	1.248	1.116	0.897	1.151
0.5	3.18	3.38	1.27	1.32	1.474	1.860	1.54	1.58	1.850	1.88	1.95	1.861	1.724	1.260	1.140	0.938	1.160
0.7	3.28	3.55	1.28	1.36	1.475	1.871	1.56	1.61	1.866	1.91	2.00	1.883	1.709	1.274	1.168	0.972	1.168
1.0	3.43	3.87	1.30	1.40	1.484	1.902	1.59	1.66	1.892	1.97	2.06	1.921	1.690	1.293	1.203	1.011	1.179
1.5	3.74	—	1.33	1.47	1.495	—	1.62	1.75	1.943	2.06	2.16	1.986	1.661	1.317	1.263	1.047	1.180
2.0	4.04	—	1.36	1.54	1.516	2.029	1.66	1.84	1.999	2.13	2.25	2.051	1.633	1.332	1.307	1.069	—
2.5	4.33	—	1.39	1.59	—	—	1.70	1.92	2.057	2.19	2.34	2.113	1.605	1.336	1.306	1.088	—
3.0	4.65	—	1.43	1.65	1.565	2.175	—	1.99	2.112	2.28	2.44	2.164	1.578	1.332	1.265	1.106	—
3.5	4.92	—	1.46	1.69	—	—	—	2.160	2.35	2.53	2.203	—	—	1.195	1.122	—	
4.0	5.17	—	—	—	1.594	2.291	—	—	2.196 ^b	2.43	—	2.235	1.524	1.292	—	1.135	—
4.5	—	—	—	—	—	—	—	—	—	—	2.257	—	—	—	—	—	
5.0	—	—	—	—	—	1.590	2.364	—	—	—	—	2.264	1.472	1.238	—	—	
6.0	—	—	—	—	—	—	2.335	—	—	—	—	—	1.421	1.157	—	—	
7.0	—	—	—	—	—	—	—	—	—	—	—	—	1.370	—	—	—	

a. Limiting values
 b. At 3.9 mol/l

Source: Robinson and Stokes [6]. (Copyright 1959, Academic Press. Reprinted with permission.)

- In most practical applications involving use of the diffusion coefficient, there are much larger uncertainties and inaccuracies in the equations employed (such as those that describe the environment) than those introduced by even approximated values of the diffusion coefficients.

2.16.3 Environmental Importance

Diffusion in bulk fluids is rarely a primary factor in dispersion of materials in the environment; hydraulic flow, convection, and mechanical mixing are generally orders of magnitude more important. However, there are some special circumstances in which diffusion does assume a significant role. These include diffusion in a fluid constrained in a porous medium, diffusion very near a gas/liquid interface that limits the rate of evaporation/condensation, diffusion at a liquid/solid interface, which may limit transfer of nutrients to the roots of a plant, or the rate of dissolution of a mineral, for example. In each of these cases, either bulk flow is limited (as in the case of porous media) or a stagnant layer only a few molecules thick exists at an interface.

However, even in the case of saturated porous media, such as groundwater in an aquifer, the overall dispersion of a component has been calculated as 100 times that of the true diffusion contribution if the pore velocities exceed 0.002 cm/s (5.7 ft/day) [7]. (Slower pore velocities than this may exist in deep artesian ground waters [3].) For the case of a single non-volatile solute in a saturated porous medium, and where the ions are not adsorbed on the walls [4],

$$F = -\mathcal{D}\theta\lambda \frac{dC}{dx} \quad (2)$$

where θ is the void fraction of the medium (an effective cross-section for diffusion) and λ is a "tortuosity" or impedance factor. One can readily appreciate that in a given soil, for example, both θ and λ may vary considerably over the area involved, and that cracks, firmness, or other contributions to non-uniform diffusion or hydraulic flow can have significant impact on the observed flux. If there is interaction such as ion exchange or adsorption on the medium, an additional complex flux term (F_E) is added to account for that factor. Also, if the porous medium is not fully saturated (i.e., it has some vapor volume) and the solute is volatile, further terms must be employed to account for diffusion in the vapor space.

Thus, while a working estimate of \mathcal{D} is important for flux calculations, many uncertainties appear elsewhere in the equation; therefore, close estimates are usually not required. In bulk solution, \mathcal{D} will be found to vary with concentration, solution viscosity, temperature, and ionic strength, but in porous media these variations can often be ignored.

2.16.4 Estimation Methods

The diffusion coefficient of a neutral molecule is often described in terms of the Stokes-Einstein equation [6]:

$$\mathcal{D} = \frac{RT}{6\pi\eta r} \quad (3)$$

in which R is the universal gas constant, T is temperature (K), η is solution viscosity in centipoise (cP), and r is the effective radius of the solute. This expression is not generally useful for direct estimation of \mathcal{D} , as r is not readily known for a hydrated ion, η is rarely available, and the equation itself does not always give a good fit with experimental data. (For example, it seems empirically that η should be raised by a power of -0.45 to -0.66 to achieve the best fit, but this exponent is not predicted by theory.)

If conductance data are available, better estimates can be obtained from an equation such as the following [1]:

$$\mathcal{D}^0 = \frac{2RT}{F^2} \tau_+^0 \tau_-^0 \Lambda^0 \quad (4)$$

Equation 4 relates \mathcal{D}^0 (the diffusion coefficient at infinite dilution) to R, T, F (the Faraday), τ_+^0 and τ_-^0 (the transference numbers of the positive and negative ions at infinite dilution), and Λ^0 (the limiting specific conductance).³ While Λ^0 may be available or measured without great difficulty, τ_+ and τ_- may be more difficult to find in the literature. Therefore, the Nernst-Haskell equation [5] may be preferred:

$$\mathcal{D}^0 = \frac{RT}{F^2} \frac{1/n^+ + 1/n^-}{1/\Lambda_+^0 + 1/\Lambda_-^0} \quad (5)$$

where n^+ and n^- are the charges on the positive and negative ion, and Λ_+^0 and Λ_-^0 are the limiting specific conductances of these ions. The data in Table 2.16-3 are useful for estimating some values of Λ^0 . As can be seen by inspection of equations 4 and 5,

$$1/\Lambda^0 = (1/\Lambda_+^0 + 1/\Lambda_-^0)(\tau_+ \tau_-)(n^+ n^-)/(n^+ + n^-) \quad (6)$$

3. The equation as written applies to 1:1 or monovalent electrolytes. If a 2:1 or 1:2 salt such as CaCl₂ were under study, the equation would become:

$$\mathcal{D}^0 = \left(\frac{3}{2}\right) \frac{RT}{F^2} \tau_+^0 \tau_-^0 \Lambda^0$$

in which 3/2 is a stoichiometric factor. The generalized form of the stoichiometric factor is $(n^+ + n^-)/n^+ n^-$.

TABLE 2.16-3

Limiting Ionic Conductance^a in Water at 25°C
 [Units = A/(cm²)(V/cm)(g-equiv/cm³) = cm²/(ohm)(g-equiv)]

Cation	Λ_+^0	Anion	Λ_-^0
H ⁺	349.8	OH ⁻	197.8
Li ⁺	38.7	Cl ⁻	76.4
Na ⁺	50.1	Br ⁻	78.2
K ⁺	73.5	I ⁻	76.9
Cs ⁺	77.3	NO ₃ ⁻	71.4
NH ₄ ⁺	73.4	ClO ₄ ⁻	67.3
Ag ⁺	61.9	ClO ₃ ⁻	64.6
Tl ⁺	74.7	BrO ₃ ⁻	55.8
½Mg ⁺²	53.1	HCO ₃ ⁻	44.5
½Ca ⁺²	59.5	HCO ₂ ⁻	54.6
½Sr ⁺²	50.5	CH ₃ CO ₂ ⁻	40.9
½Ba ⁺²	63.6	ClCH ₂ CO ₂ ⁻	39.8
½Cu ⁺²	54	CNCH ₂ CO ₂ ⁻	41.8
½Zn ⁺²	53	CH ₃ CH ₂ CO ₂ ⁻	35.8
½La ⁺³	69.5	C ₆ H ₅ CO ₂ ⁻	32.3
½Ce ⁺³	69.9	HC ₂ O ₄ ⁻	40.2
		½C ₂ O ₄ ⁻²	74.2
		½SO ₄ ⁻²	80

a. When describing limiting ionic conductances, it is customary to use the convention 1/n (ion)ⁿ in naming a polyvalent ion, e.g., ½Zn⁺². This reflects the fact that the values given are calculated on a gram-equivalent, not a molar concentration basis, and so the ionic entity is described in this manner. The values of Λ^0 given here are to be used as is in equations 4, 5 and 6.

Source: Harned and Owen [2]. (Copyright 1958, Reinhold Publishing Corp. All rights reserved.)

It is often necessary to modify the calculated value of \mathcal{D}^0 for a different concentration or temperature. Diffusion coefficients at temperatures other than 25°C are usually estimated by assuming that

$$\mathcal{D}_t^0 = \mathcal{D}_{25}^0 \frac{\eta_{25}}{\eta_t} \quad (7)$$

in which \mathcal{D}_t^0 and \mathcal{D}_{25}^0 are the diffusion coefficients at temperatures t and 25°C, and η_t and η_{25} are the viscosities of the solvent (water) at these temperatures. Equation 7 is based on the Walden Rule [2], which states that the product of viscosity and limiting mobility (or conductance) is relatively constant. Table 2.16-4 lists water viscosity data that may be used for estimation by this method.

TABLE 2.16-4

Water Viscosity as a Function of Temperature

°C	η (cP)	°C	η (cP)	°C	η (cP)
0	1.787	35	0.7194	70	0.4042
5	1.519	40	0.6529	75	0.3781
10	1.307	45	0.5960	80	0.3547
15	1.139	50	0.5468	85	0.3337
20	1.002	55	0.5040	90	0.3147
25	0.8904	60	0.4665	95	0.2975
30	0.7975	65	0.4335	100	0.2818

Source: Weast [8]

Different methods are used to estimate diffusion coefficients at concentrations other than high dilution. The most general of these was developed by Falkenhagen [2]:

$$\eta_c/\eta_0 = 1 + A\sqrt{C} + BC \quad (8)$$

in which η_c and η_0 are viscosities at concentration C and for pure water respectively, and A and B are empirical constants. This viscosity ratio is then used to correct \mathcal{D}^0 in a manner analogous to equation 7 above.

$$\mathcal{D} = \mathcal{D}^0 (\eta_c/\eta_0) \quad (9)$$

Values of some A and B coefficients are shown in Table 2.16-5. (The fact that some B coefficients are positive and others negative is due to the different "structure-making and structure-breaking" characteristics of the salts in question.)

TABLE 2.16-5
Viscosity A and B Coefficients for Some Common Electrolytes
 (for use with equation 8)

Electrolyte	Coefficients		Concentration Limit (mol/l)
	A	B	
NH ₄ Cl	0.0057	-0.0144	0.2
NaCl	0.0067	0.0244	0.2
KCl	0.0052	-0.0140	0.2
KBr	0.00474	-0.0480	0.1
KNO ₃	0.0050	-0.053	0.1
KClO ₃	0.0050	-0.031	0.1
KBrO ₃	0.0058	-0.001	0.1
KMnO ₄	0.0058	-0.066	0.1
CsI	0.0039	-0.118	0.2
CsNO ₃	0.0043	-0.092	0.02
AgNO ₃	0.0063	0.045	0.1
K ₂ SO ₄	0.01406	0.194	0.1
K ₂ CrO ₄	0.0133	0.152	0.1
BaCl ₂	0.0201	0.207	0.1
LaCl ₃	0.0304	0.567	0.1
K ₄ Fe(CN) ₆	0.0370	0.366	0.1
MgSO ₄	0.0225	a	b
MnSO ₄	0.0231		
CuSO ₄	0.0229		
CdSO ₄	0.0232		
Cr ₂ (SO ₄) ₃	0.0495		
Ca ₃ [Fe(CN) ₆] ₂	0.0467		
Ca ₂ Fe(CN) ₆	0.0495		

a. B coefficients not available for these salts. n_c/n_0 must be estimated on the basis of the A coefficient alone.
 b. No concentration limits listed in source.

Source: Harned and Owen [2]. (Copyright 1958, Reinhold Publishing Corp. All rights reserved.)

Example 1 Estimate the diffusion coefficient of cesium chloride at 25°C by means of the Nernst-Haskel equation.

The following parameters apply:

$$\begin{aligned} R &= 8.31 \text{ joules/mol-deg} \\ T &= 298 \text{ K} \\ F &= 96,500 \text{ coulombs/g-equiv} \\ n^+ \\ n^- \quad \left. \right\} &= 1 \text{ for 1:1 salts} \\ \Lambda_+^0 &= 77.3 \text{ cm}^2/(\text{ohm})(\text{g-equiv}) \\ \Lambda_-^0 &= 76.3 \text{ cm}^2/(\text{ohm})(\text{g-equiv}) \end{aligned} \quad \left. \right\} \text{ from Table 2.16-3}$$

Use of the above units will yield D^0 in cm^2/s .

Substituting in equation 5,

$$\begin{aligned} D^0 &= \left(\frac{8.31 \times 298}{(96,500)^2} \right) \left(\frac{1/1 + 1/1}{1/77.3 + 1/76.3} \right) \\ &= 2.04 \times 10^{-5} \text{ cm}^2/\text{s} \end{aligned}$$

This matches the measured value listed in Table 2.16-1.

Example 2 The measured diffusion coefficient for KCl at 25°C is $1.994 \times 10^{-5} \text{ cm}^2/\text{s}$ [2]. What is the estimated value at 4°C?

In order to use equation 7, we need the viscosities (η) of water at the two temperatures. From Table 2.16-4, $\eta_{25} = 0.8904 \text{ cP}$ and η_4 (interpolated) = 1.573 cP . Substituting in equation 7,

$$\begin{aligned} D_4^0 &= 1.994 \times 10^{-5} \left(\frac{0.8904}{1.573} \right) \\ &= 1.129 \times 10^{-5} \text{ cm}^2/\text{s} \end{aligned}$$

The measured value [2] is $1.134 \times 10^{-5} \text{ cm}^2/\text{s}$.

2.16.5 Literature Cited

1. Cleary, J.G., G.E. Von Neida and W.T. Lindsay, Jr., "Diffusion and Hideout in Crevices," Report No. EPRI-NP-2979 to Electric Power Research Institute, Palo Alto, Calif. (1983).
2. Harned, H.S. and B.B. Owen, *The Physical Chemistry of Electrolyte Solutions*, 3rd ed., Reinhold Publishing Corp., New York (1958).
3. Lerman, A., *Geochemical Processes*, John Wiley & Sons, New York (1979).
4. Nye, P.H., "Diffusion of Ions and Uncharged Solutes in Soils and Soil Clays," *Adv. Agron.*, **31**, 225-69 (1979).

5. Reid, R.C., J.M. Prausnitz and T.K. Sherwood, *The Properties of Gases and Liquids*, 3rd ed., McGraw-Hill Book Co., New York (1977).
6. Robinson, R.A. and R.H. Stokes, *Electrolyte Solutions*, 2nd ed., Academic Press, New York (1959).
7. Tucker, W.A. and L.H. Nelken, "Diffusion Coefficients in Air and Water" in *Handbook of Chemical Property Estimation Methods*, W.J. Lyman, W.F. Reehl and D.H. Rosenblatt (eds.), McGraw-Hill Book Co., New York (1982).
8. Weast, R.C., M.J. Astle and W.H. Beyer (eds.), *CRC Handbook of Chemistry and Physics*, 67th ed., CRC Press, Inc., Boca Raton, FL (1986).

2.17 RADIOACTIVE PROCESSES AND PROPERTIES

Radioactive decay can affect both the transport and transformation of materials in the environment. The decay occurs spontaneously and is independent of all external physical and chemical influence. In general, the environmental effects produced are so small or so rarely encountered as to be essentially of academic interest.

In some special situations, however, radioactive decay is of practical significance in the context of this handbook. This section discusses three aspects of radioactivity that could be of importance to the reader:

- The spontaneous creation of new chemical species through radioactive decay can have troublesome consequences when the newly generated species are themselves radioactive (section 2.17.1).
- The phenomenon of nuclear recoil can transport individual atoms over unusually large distances through solid and liquid materials (section 2.17.2).
- Materials occurring at the extremely low concentrations characteristic of many radioactive materials exhibit changes in chemical properties that often result in anomalous chemical behavior (section 2.17.3).

2.17.1 Creation of New Chemical Species

Almost all types of radioactive decay lead to the formation of atoms of another element. Except in the case of spontaneous fission, in which process the large parent nucleus divides into two smaller fragments of about equal mass, the atomic number of the resulting nucleus is only one or two units different from that of the parent. Nevertheless, the chemical properties of the newly formed atoms are likely to be substantially different from those of the parent and can present special problems to users of radionuclides.

SINGLE TRANSMUTATIONS

Radioactive decay that is limited to a single transmutation results in conversion of the initial species to the product species at an exponential rate, reflecting the probabilistic nature of the process. The probability, p , that an individual atom of a particular radionuclide will decay in a time interval Δt is independent of everything except the length of that time interval and the decay constant, λ , that characterizes the disintegration probability for that nuclide. Thus, for sufficiently short time intervals, $p = \lambda \Delta t$. The probability that the atom will *not* disintegrate during the interval Δt is $1 - p$, or $1 - \lambda \Delta t$. Similarly, for any subsequent number, n , of such intervals, the probability of survival is $(1 - \lambda \Delta t)^n$. For a total time $t = n \Delta t$, $1 - p = (1 - \lambda t/n)^n$ as Δt becomes infinitely small and n approaches infinity. Because the general mathematical expression for such a process is $e^x = \lim_{n \rightarrow \infty} (1 + x/n)^n$, the substitution of λt for x gives $e^{-\lambda t}$ for the limiting value as $n \rightarrow \infty$:

$$e^{-\lambda t} = \lim_{n \rightarrow \infty} \left(1 + \frac{\lambda t}{n} \right)^n \quad (1)$$

For a large initial population, N_0 , of atoms of a given nuclide, the number of atoms remaining after time t is $N = N_0 e^{-\lambda t}$. This, of course, is similar to the rate law for any monomolecular reaction. A convenient way of expressing the decay constant λ for a given species is to show it as the time required for any given (large) number of atoms to decay to half its initial value. Thus, for $t = T_{1/2}$, $N = N_0/2$ and $\lambda = \ln 2/T_{1/2} \approx 0.693/T_{1/2}$.

Example 1 32-Phosphorus, a widely useful radiotracer, has a half-life of 14.3 days and decays by beta emission to form 32-sulfur. One micromole of ^{32}P has been made in a nuclear reactor. How much ^{32}S will be created when it decays?

The number of ^{32}P atoms in 1 micromole is

$$\frac{6.02 \times 10^{23}}{10^6} = 6.02 \times 10^{17}$$

After 14.3 days, the number of ^{32}P atoms remaining is

$$\frac{6.02 \times 10^{17}}{2} = 3.01 \times 10^{17}$$

and an equal number of ^{32}S atoms will have formed.

After 10 half-lives (143 days), the number of ^{32}P atoms remaining will have been reduced to

$$\frac{N_0}{2^{10}} = \frac{6.02 \times 10^{17}}{1024} = 5.88 \times 10^{14}$$

and the number of ^{32}P atoms will be

$$(6.02 \times 10^{17}) - (5.88 \times 10^{14}) = 6.01 \times 10^{17}$$

In the above example, as in most instances of radioactive decay, the product atom is not radioactive and is therefore stable. Furthermore, the amounts created by the process are infinitesimal in comparison with those already in the environment.

MULTIPLE SEQUENTIAL DECAY

In some instances radioactive decay produces a daughter atom that is also radioactive, with its own characteristic half-life and type of emission (alpha, beta, etc.). Occasionally, the process continues through several unstable nuclides before reaching a stable end-product. Each of the nuclides formed in this sequential decay process has a different elemental identity from its immediate parent and therefore demonstrates different chemical and physical properties. Furthermore, their radioactivity makes them potentially hazardous to human health, even in the small quantities that may be generated. For these reasons, they constitute a special problem for environmental managers.

For example, consider a composite solid waste containing an isotope such as 99-molybdenum; this isotope decays with a 67-hour half-life to form 99m-tech-

netium,¹ a metastable isotope with a 5.9-hour half-life, which in turn decays (through isomeric transition and gamma emission) to long-lived ⁹⁹Tc:



The composition of the resulting mixture varies as the parent species is depleted and its progeny accumulate and successively decay. The composition is also susceptible to change by selective chemical leaching, which can favor either technetium or molybdenum, depending on the chemical form of each element and the chemical environment to which it is exposed [7,10-12].

Although the third nuclide in this multiple-decay sequence is also radioactive, its half-life (2.12×10^5 years) is so long that it can be considered stable for purposes of illustrating two special types of equilibrium that can exist between the concentrations of the nuclides in a successive decay process.² These are called "transient equilibrium" and "secular equilibrium" and are illustrated schematically in Figure 2.17-1. (Note that values in these figures are arbitrary ones, used only for purpose of illustration.)

Figure 2.17-1a represents schematically the relationship between a longer-lived parent nuclide and a shorter-lived daughter. The ratio of numbers of parent atoms (N_1) to numbers of daughter atoms (N_2) is given by:

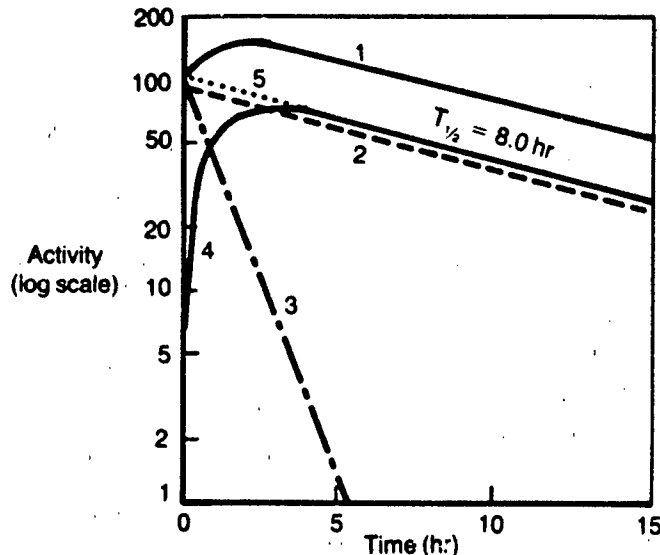
$$\frac{N_1}{N_2} = \frac{\lambda_2 - \lambda_1}{\lambda_1} \quad (2)$$

(As discussed earlier, for $t = T_{1/2}$, $\lambda = 0.693/T_{1/2}$)

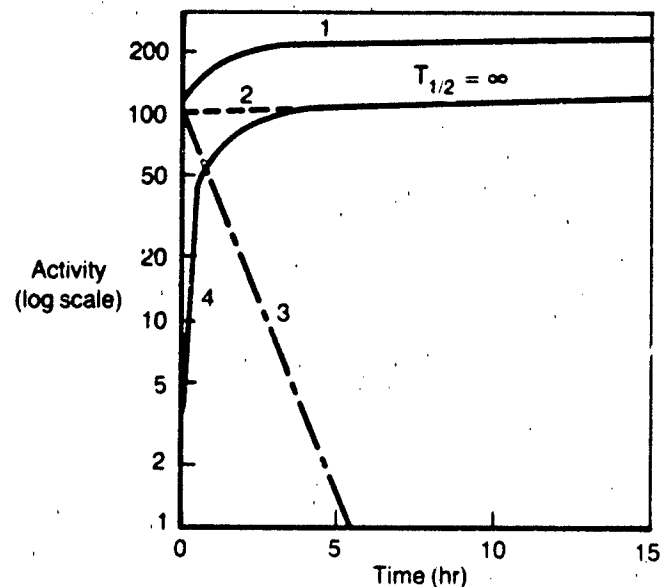
During this "transient equilibrium," the decay rate of the daughter appears to be identical with that of the parent, because a daughter atom cannot decay until it is formed. Of course, if the supply of new daughter atoms is cut off by physical removal (e.g., chemical separation) of the parent, the true decay rate of the daughter is immediately seen.

An example of transient equilibrium that has practical significance, in that the product nuclide is widely used in medical research and chemical analysis, is ^{99m}Tc. In commercial practice, ^{99m}Tc is generated in cartridges of ion-exchange resins onto which quantities of ⁹⁹Mo have been loaded. The relatively short-lived metastable technetium nuclide is allowed to grow into radioactive equilibrium with its parent nuclide, a process that requires about five times the half-life of ^{99m}Tc to exceed 95% of

1. The letter "m" following the atomic number indicates a metastable species that does not change its isotopic or elemental identity when it decays; it undergoes only a loss of energy through photon radiation. This process is known as "isomeric transition."
2. Note that this "equilibrium" is unlike chemical equilibrium, in that it refers to the relative abundances of radionuclides formed by a series of completely irreversible transformations. It is analogous to "steady state" concentrations in sequential chemical reactions.



a. Transient Equilibrium



b. Secular Equilibrium

- (1) Total activity of an initially pure parent fraction.
- (2) Activity due to parent. (In secular equilibrium this is also the total daughter activity in parent-plus-daughter fractions.)
- (3) Decay of freshly isolated daughter fraction ($T_{1/2} = 0.8 \text{ hr}$).
- (4) Daughter activity growing in freshly purified parent fraction.
- (5) Total daughter activity in parent-plus-daughter fractions. (Transient equilibrium only.)

Source: Adapted from Friedlander et al. [5]. (Copyright 1981, John Wiley & Sons.
Reprinted with permission.)

FIGURE 2.17-1 Equilibria in Multiple Sequential Decay Processes

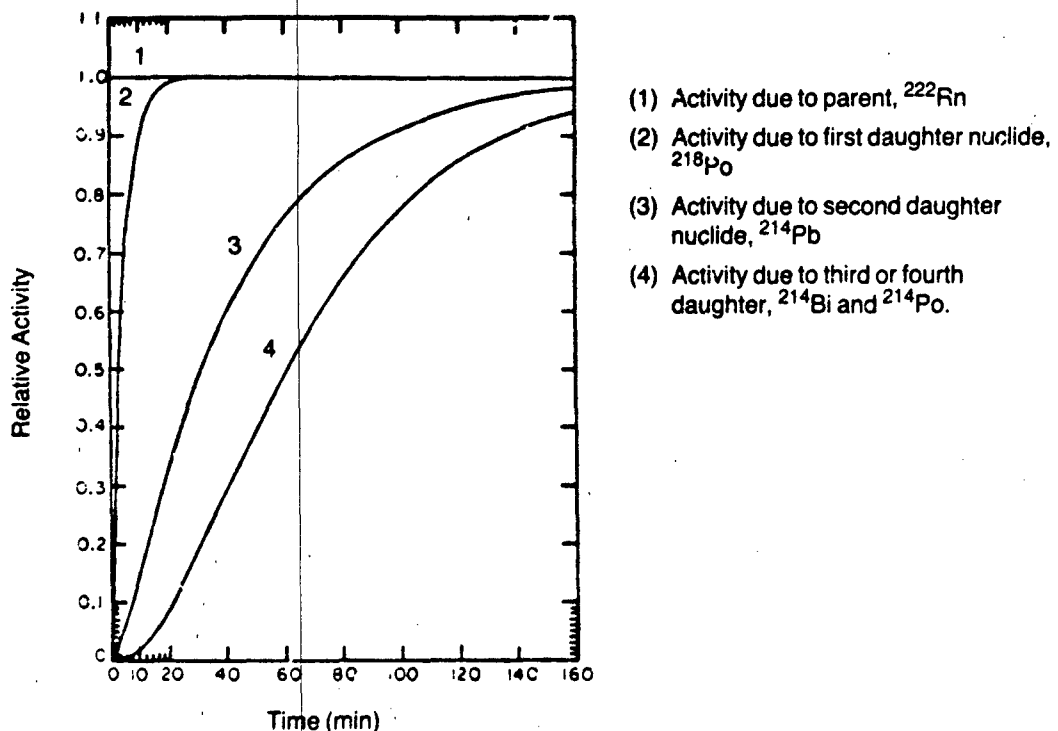
its maximum potential concentration. The desired technetium tracer may then be extracted, free of the parent molybdenum, by the ion-exchange process. The re-supply of daughter atoms proceeds constantly, governed only by the remaining supply of parent atoms, which ultimately drops to a level that is not practically useful. Meanwhile, the daughter-atoms can be repeatedly "milked" from the mixture.³

The other form of radioactive equilibrium, known as "secular equilibrium" (Figure 2.17-1b), is actually a limiting case of transient equilibrium in which the parent is so long-lived as to exhibit no measurable decrease in its activity over a time that is long compared to that of the daughter's half-life. A case in point is that of naturally occurring ^{238}U -uranium, whose half-life is 4.51×10^9 years; this element gives rise to a sequence of 17 radioactive daughter-nuclides, all shorter-lived than ^{238}U itself, leading ultimately to stable ^{206}Pb . (See Table 2.17-2.) The figure depicts a simple two-step case of secular equilibrium, representing the relationship between ^{238}U and any of its shorter-lived daughter products. When a radioactive daughter product has a much shorter half-life than that of the parent and remains physically comingled with the parent, it appears to decay at the same rate as the parent once equilibrium is attained. Only if the mixture is disturbed (such as by the separation of ^{226}Ra from the parent ^{238}U by a chemical extraction process, or by the escape of volatile ^{222}Rn to the atmosphere) is the natural balance of nuclide abundances upset.

Because gamma radiation is easily detected by remote sensors, prospectors for uranium have traditionally depended on the detection of such late decay products as ^{214}Bi and ^{214}Pb . A crucial assumption that must be made in the use of this technique is that the secular equilibrium is undisturbed by any natural or artificial process, an assumption that often proves to be invalid. Geologists have discovered that radium and thorium are sometimes displaced from each other and/or from parent uranium by natural geochemical processes [10,12,13]. The spontaneous escape of ^{222}Rn from rocks, minerals and soil removes the telltale ^{214}Bi and ^{214}Pb nuclides from their original sites and can produce environmental health hazards that would not otherwise exist.

Evans [4] has examined the problems of calculating the relative concentrations of the physiologically hazardous, short-lived daughters of ^{222}Rn . Figure 2.17-2 illustrates one way of portraying the complex radioactive equilibria created by the "grow-in" of short-lived daughters in an initially pure quantity of longer-lived ^{222}Rn ($T_{1/2} = 3.8$ days). With respect to the parent activity, the equilibria of the first four daughter nuclides is secular, because each of their half-lives is quite short compared with that of ^{222}Rn . The equilibrium between the second and third daughters, ^{214}Pb and ^{214}Bi , whose half-lives are 26.8 and 19.7 minutes respectively, is transient.

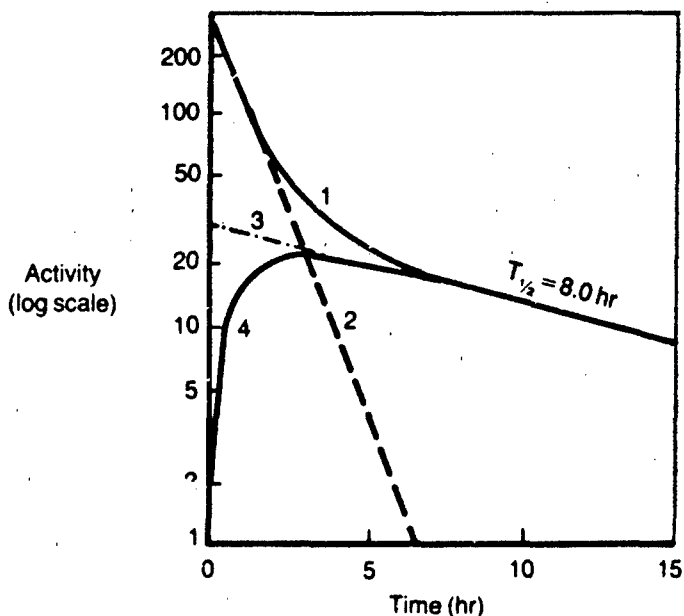
3. Technetium has no stable isotopes. Its presence in the sun has been detected, but all of the technetium on earth is man-made; some 18 isotopes of the element have been created and recognized [7].



Source: Adapted from Evans [4]. (Copyright 1969, Pergamon Press.
Reprinted with permission.)

FIGURE 2.17-2 Growth of Activity of Individual Short-lived Decay Products In Constant Source of Radon Having Unit Activity

Sequential radioactive decay need not result in either of the forms of equilibrium described above. Returning to the example of the relatively short-lived parent-daughter pair of $^{99}\text{Mo} \rightarrow ^{99\text{m}}\text{Tc}$ producing the much longer lived nuclide ^{99}Tc , it is clear that there is never a constant proportionality between the decay rates of ^{99}Mo and ^{99}Tc (ignoring, for the sake of illustration, the metastable intermediate). Figure 2.17-3 illustrates this lack of equilibrium; although, as in Figure 2.17-1, the values are only suggestive, curve 2 might represent the combined activity of the $^{99}\text{Mo} \rightarrow ^{99\text{m}}\text{Tc}$ pair and curve 4 that of the ^{99}Tc daughter. The latter eventually becomes the only activity remaining after the short-lived parent has decayed to an insignificant level. Similarly, the fifth successive decay product of ^{222}Rn is ^{210}Po , whose half-life is 138 days. Thus, a condition of "no equilibrium" exists between ^{222}Rn , together with its shorter-lived daughters, and the longer-lived ^{210}Po .



- (1) Total activity
- (2) Activity due to parent ($T_{1/2} = 0.8 \text{ hr}$)
- (3) Extrapolation of final decay curve to time zero
- (4) Daughter activity in initially pure parent

Source: Adapted from Friedlander *et al.* [5]. (Copyright 1981, John Wiley & Sons. Reprinted with permission.)

FIGURE 2.17-3 Radioactive Decay Without Equilibrium

2.17.2 Recoil Transport

Radioactive decay processes involve spontaneous losses of energy from atomic nuclei, which can occur in several ways. In most such processes there is little or no loss of mass in the parent nuclei, since the emissions are usually in the form of beta and/or gamma radiation and therefore cause a change of only one electron mass unit. (Beta decay involves a one-electron loss; gamma and x-radiation are photons and involve no mass change. A few nuclei decay by positron emission or by electron-capture, processes that result, effectively, in one-electron gains rather than losses.) Some elements, however —principally those higher than lead in the periodic table— emit an alpha particle, which consists of two neutrons and two protons; still more rarely, heavy elements in the transuranic series undergo spontaneous fission, yielding two quite massive fragments of roughly equal mass. Energies of some of the alpha-emitting radionuclides are listed in Table 2.17-1. Note that, in general, the half-life of a nuclide decreases as the energy of its alpha emission increases.

TABLE 2.17-1
Principal Naturally Occurring and Transuranic Alpha Emitters^a
(in order of increasing energy)

Energy (MeV)	Source	Half-life	Yield ^b (%)	Energy (MeV)	Source	Half-life	Yield ^b (%)
1.83	^{144}Nd	$2.1 \times 10^{15}\text{y}$	100	4.946	^{210m}Bi	$3 \times 10^6\text{y}$	58
2.14	^{152}Gd	$1.1 \times 10^{14}\text{y}$	100	5.013	^{231}Pa	$3.28 \times 10^4\text{y}$	24
2.23	^{147}Sm	$1.06 \times 10^{11}\text{y}$	100	5.028	^{231}Pa	$3.28 \times 10^4\text{y}$	23
2.50	^{174}Hf	$2 \times 10^{15}\text{y}$	100	5.058	^{231}Pa	$3.28 \times 10^4\text{y}$	11
3.18	^{190}Pt	$7 \times 10^{11}\text{y}$	100	5.105	^{239}Pu	$24,411\text{y}$	12
3.95	^{232}Th	$1.40 \times 10^{10}\text{y}$	24	5.123	^{240}Pu	6560y	24
4.011	^{232}Th	$1.40 \times 10^{10}\text{y}$	76	5.143	^{239}Pu	$24,411\text{y}$	15
4.147	^{238}U	$4.468 \times 10^9\text{y}$	25	5.156	^{239}Pu	$24,411\text{y}$	73
4.196	^{238}U	$4.468 \times 10^9\text{y}$	75	5.168	^{240}Pu	6560y	76
4.366	^{235}U	$7.04 \times 10^8\text{y}$	18	5.234	^{243}Am	$7.37 \times 10^3\text{y}$	11
4.396	^{235}U	$7.04 \times 10^8\text{y}$	57	5.276	^{243}Am	$7.37 \times 10^3\text{y}$	88
4.415	^{235}U	$7.04 \times 10^8\text{y}$	4	5.305	^{210}Po	138.4d	100
4.556	^{235}U	$7.04 \times 10^8\text{y}$	4	5.306	^{245}Cm	$8.5 \times 10^3\text{y}$	7
4.57	^{210m}Bi	$3 \times 10^6\text{y}$	6	5.342	^{246}Cm	$4.78 \times 10^3\text{y}$	19
4.597	^{235}U	$7.04 \times 10^8\text{y}$	5	5.344	^{228}Th	1.913y	28
4.599	^{226}Ra	1600y	6	5.362	^{245}Cm	$8.5 \times 10^3\text{y}$	80
4.617	^{230}Th	$7.54 \times 10^4\text{y}$	24	5.386	^{246}Cm	$4.78 \times 10^3\text{y}$	81
4.684	^{230}Th	$7.54 \times 10^4\text{y}$	76	5.42	^{249}Bk	320d	0.0015
4.722	^{234}U	$2.45 \times 10^5\text{y}$	28	5.427	^{228}Th	1.913y	71
4.733	^{231}Pa	$3.28 \times 10^4\text{y}$	11	5.443	^{241}Am	432y	13
4.765	^{237}Np	$2.14 \times 10^6\text{y}$	17	5.447	^{224}Ra	3.66d	6
4.770	^{237}Np	$2.14 \times 10^6\text{y}$	19	5.448	^{214}Bi	19.8m	0.012
4.773	^{234}U	$2.45 \times 10^5\text{y}$	72	5.456	^{238}Pu	87.74y	28
4.782	^{226}Ra	1600y	95	5.486	^{241}Am	432y	86
4.787	^{237}Np	$2.14 \times 10^6\text{y}$	51	5.490	^{222}Rn	3.823d	100
4.863	^{242}Pu	$3.76 \times 10^5\text{y}$	24	5.499	^{238}Pu	87.74y	72
4.896	^{241}Pu	14.35y	0.002	5.512	^{214}Bi	19.8m	0.008
4.903	^{242}Pu	$3.76 \times 10^5\text{y}$	76	5.52	^{247}Bk	$1.4 \times 10^3\text{y}$	58
4.909	^{210m}Bi	$3 \times 10^6\text{y}$	36	5.537	^{223}Ra	11.43d	9
4.95	^{227}Ac	21.773y	1.2	5.605	^{223}Ra	11.43d	26
4.951	^{231}Pa	$3.26 \times 10^4\text{y}$	22	5.666	^{251}Cf	900y	55

(Continued)

TABLE 2.17-1 (Continued)

Energy (MeV)	Source	Half-life	Yield ^b (%)	Energy (MeV)	Source	Half-life	Yield ^b (%)
5.68	^{247}Bk	$1.4 \times 10^3 \text{ y}$	37	6.115	^{242}Cm	163d	74
5.684	^{224}Ra	3.66d	94	6.119	^{252}Cf	2.64y	84
5.707	^{227}Th	18.72d	8	6.278	^{211}Bi	2.14m	16
5.714	^{223}Ra	11.43d	54	6.28	^{219}At	0.9m	97
5.742	^{243}Cm	28.5y	12	6.287	^{220}Rn	55.6s	100
5.745	^{223}Ra	11.43d	9	6.424	^{219}Rn	3.96s	8
5.755	^{227}Th	18.72d	20	6.551	^{219}Rn	3.96s	11
5.763	^{244}Cm	18.11y	23	6.56	^{222}Ra	38s	96
5.806	^{244}Cm	18.11y	77	6.622	^{211}Bi	2.14m	84
5.812	^{249}Cf	351y	84	6.65	^{218}At	2s	6
5.846	^{251}Cf	900y	45	6.70	^{218}At	2s	94
5.976	^{227}Th	18.72d	23	6.777	^{216}Po	0.15s	100
5.987	^{250}Cf	13.1y	17	6.818	^{219}Rn	3.96s	81
6.002	^{218}Po	3.11m	100	7.28	$^{211\text{m}}\text{Po}$	25.2s	91
6.031	^{250}Cf	13.1y	83	7.384	^{215}Po	1.78ms	100
6.037	^{227}Th	18.72d	24	7.448	^{211}Po	0.516s	99
6.051	^{212}Bi	60.6m	25	7.687	^{214}Po	$164\mu\text{s}$	100
6.071	^{242}Cm	163d	26	8.785	^{212}Po	$0.30\mu\text{s}$	100
6.076	^{252}Cf	2.64y	15	8.88	$^{211\text{m}}\text{Po}$	25.2s	7
6.090	^{212}Bi	60.6m	10	11.65	$^{212\text{m}}\text{Po}$	45s	97

a. Note: Values given in this table are subject to minor revision from time to time. Persons requiring the best and most accurate values currently available should consult an authoritative source such as the Oak Ridge Nuclear Data Project, Oak Ridge National Laboratories, Oak Ridge TN.

b. Percentage of the total decay events. Isotopes having multiple alpha emissions are listed once for each alpha-energy. If a yield of less than 100% is listed for any isotope, it indicates that other alpha emissions of that isotope also occur; when combined, the various yields total 100%.

Source: U.S. Bureau of Radiological Health [16] and *Chart of the Nuclides*, 13th ed. [17].

In the cases of alpha emission and spontaneous fission, the emission of the fragment imparts enough kinetic energy to the remaining nucleus to cause significant recoil motion. Atoms of heavy elements that undergo alpha decay are typically transported in recoil for distances of 0.1 to 0.2 mm in air at atmospheric pressure. In solids and liquids, the recoil distances are much smaller, and atoms in the bulk of such condensed phases are not sufficiently affected to produce a significant change in the system. However, atoms lying near an interface (e.g., between a host mineral and a gaseous or liquid environment such as air or water) may be transported far enough by recoil to allow them to escape from a medium in which they are relatively immobile to another in which their mobility is much greater [6]. Recoil transport distances are generally larger with spontaneous fission, because the recoil energies of fission fragments are greater and the residual nuclei are smaller [3].

These alternate recoil pathways are shown schematically in Figure 2.17-4, with ^{226}Ra used as an example. Two very fine spherical grains of solid material, 2- μm diameter, are shown in contact near B. Water is present in the stippled zone of the pore, and the open zone at the right is air-filled. Atoms of ^{226}Ra decay in the upper grain, each yielding an alpha particle (as shown at A) and a ^{222}Rn atom.

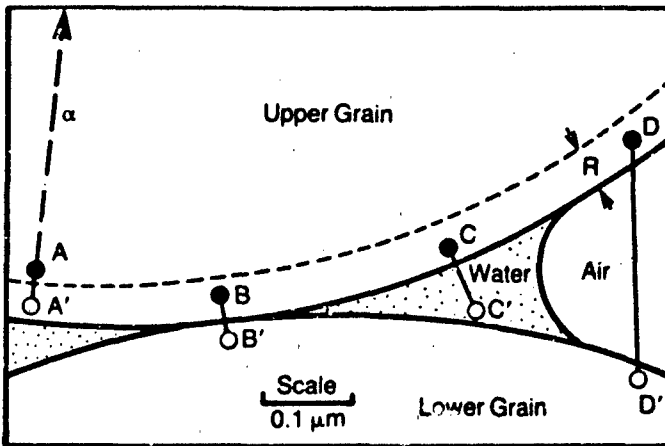
- Atom A lies at greater depth within the grain than the recoil range, R, so atom A' is contained within the grain.
- Atom B' escapes from the upper grain but buries itself in the lower grain.
- After escape from the upper grain, atom C' loses the remainder of its recoil energy in the water and is free to diffuse through the pores.
- Atom D' loses little of its recoil energy in the air and buries itself in the lower grain.

Atoms B' and D' may escape from their recoil pockets by diffusion before condensation of the excited atoms of the grain (indirect-recoil effect). Within the mean life⁴ of ^{222}Rn (5.5 days), the diffusion distance of ^{222}Rn atoms in the solid grain is less than the width of any line in the figure.

By the recoil-transport mechanism described above, radioactive isotopes like ^{222}Ra and ^{222}Rn can leave mineral grains and enter a mobile liquid or gaseous phase, creating a significant environmental hazard. This effect has been suggested as the cause of anomalously high radon emanation from soils and minerals [14,15]. The amount of ^{222}Rn that may escape from the host soil or mineral is highly variable, as shown in Figure 2.17-5.

Recent studies of environmental radiation health hazards have emphasized the importance attached by health physicists to alpha-emitting decay products of ^{222}Rn , which are a demonstrated cause of cancer of the pulmonary system. Control and amelioration of this hazard is a topic of concern to such diverse industries as underground mining, building construction and agriculture.

4. The "mean life" of a radionuclide is defined as the average time for the number of nuclei in a specified state to decrease (i.e., decay) by a factor of e (2.718 . . .).



Legend: ● = ^{226}Ra atom, ○ = ^{222}Rn atom, R = recoil range.
(Circles greatly exaggerate size of atoms). See text for discussion.

Source: Adapted from Tanner [15]

FIGURE 2.17-4 Schematic Diagram of Radon Emanation Processes

While radon emanates from rocks and soil almost everywhere, the rate at which this occurs is influenced to a remarkable extent by various environmental conditions such as atmospheric pressure and rain or snowfall [8]. The effect of such temporal influences on the true emanation rate (i.e., the process by which recoil transport of the radon nucleus across a solid-liquid or a solid-vapor interface occurs) is not well understood. As Tanner [14,15] has reported, the production rate of radon in the atmosphere over a radium-bearing soil or rocky earth appears to be significantly influenced in an otherwise unpredictable or "anomalous" manner by, among other things, the presence of an adsorbed liquid layer on the solid.

The evidence of anomalous excess radon emanation from mineral host substances is based on experimental determination of the equilibrium concentrations of ^{222}Rn from samples of crystalline rock in which (a) concentrations of the parent radioisotope ^{226}Ra have been accurately measured by special alpha-radiation detectors, (b) physical properties such as surface area and grain size are known, and (c) the homogeneity of radium distribution has been established. The migration rate of radon atoms in host crystalline substances has been determined both from basic principles and by use of parameters such as atomic radius and lattice dimensions. When all these data are combined, the predicted emanation rate of ^{222}Rn from the solid phase into the surrounding air is reduced by as much as a hundred-fold, compared with the actual production rate within the solid due to decay of ^{226}Ra . The predicted losses are attributable to various mechanisms that would be expected to account for physical entrapment of radon in the solid phase [2,8].

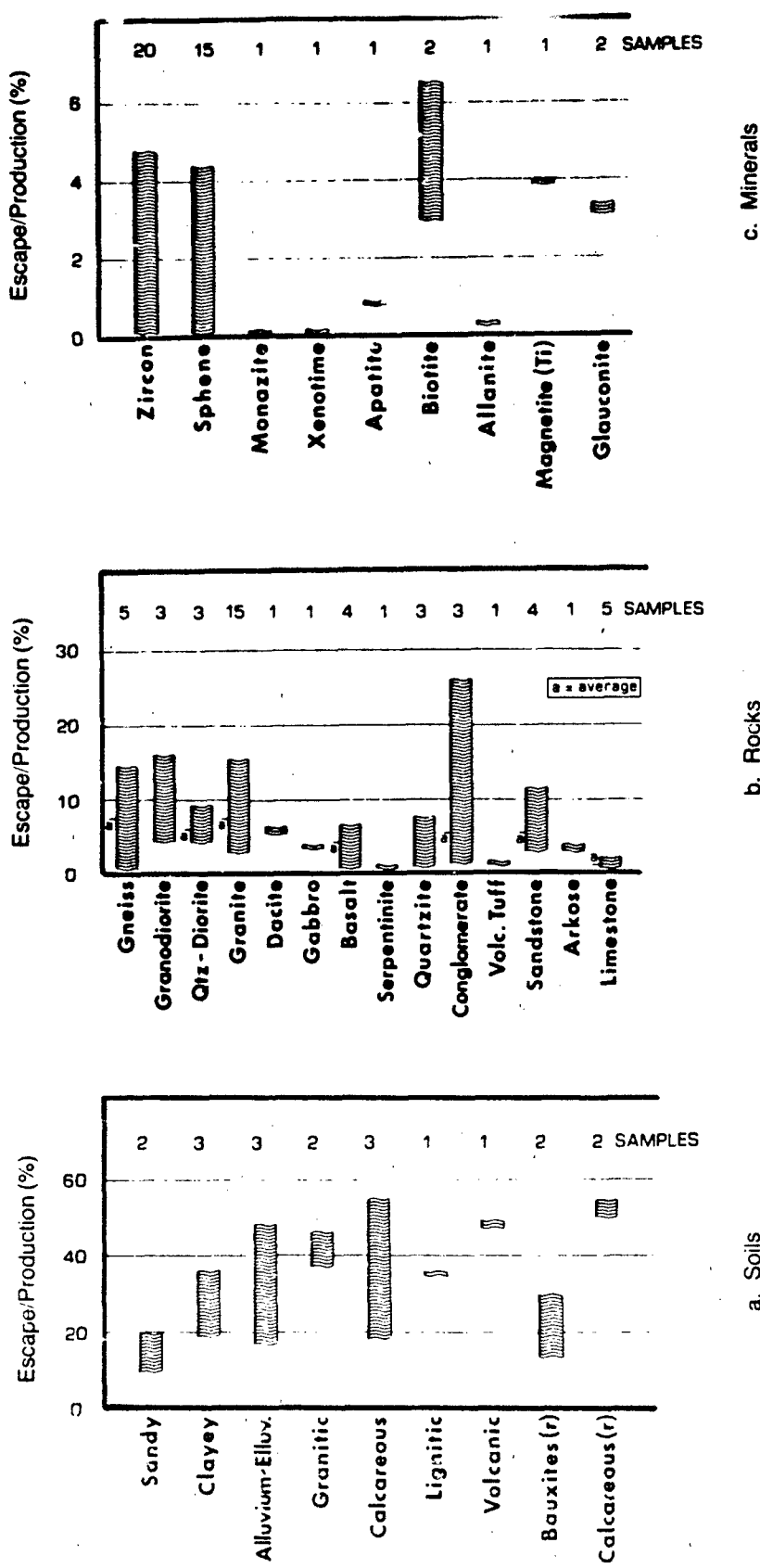


FIGURE 2.17-5 Percentage Escape of 222-Radon from Soils and Minerals

Source: Adapted from Barreto et al. [2].

In minerals of density typical of that of rocks and soil, the range of the recoiling atom is on the order of 20-70 nm; thus, only the atoms within that distance from the grain surface have any chance to escape. Moreover, in a microporous host mineral such as sandstone, most escape surfaces are close to the surfaces of adjacent grains, greatly reducing the chance of escape by "direct recoil." Experimental measurements have generally shown, however, that some compensating mechanism actually tends to restore the true emanation yield to a value closer to the actual production rate of ^{222}Rn *in situ*. Reported values for emanating fractions of ^{222}Rn have ranged from 1% to nearly 100% of the theoretical maximum, suggesting that something such as the "indirect recoil" mechanism postulated by Tanner [14,15] is operative to help explain the variation between prediction and experience. The wide range of measured values suggests that experimental variables have not been understood or controlled well enough, and also that existing theoretical models are not adequate to account for observed anomalies. A better method for estimating the emanation rate is clearly needed; this would be useful in establishing standards for the management of uranium mill tailings and other radium-bearing wastes that are important sources of $^{222}\text{-radon}$.

Recoil or alpha-emission from radioactive decay can also cause physical transport by a form of "internal sputtering" — the ejection of neighboring atoms from a solid surface into an adjacent vapor phase. This process has had significant implications for environmental pollution in the case of $^{210}\text{-polonium}$, an alpha-emitting isotope that occurs in nature primarily as a sequential decay product of $^{226}\text{-radon}$ [1]. When fabricated into metallic films for industrial purposes, ^{210}Po exhibits instability that has been attributed to such "internal sputtering," resulting in anomalously high diffusion rates through solids, escape from the surface of these solids into the air, and contamination of nearby surfaces. Even such a chemically stable alpha-emitter as $^{241}\text{-americium}$ can create a contamination hazard due to "internal sputtering" and direct alpha-particle damage when incorporated at high concentrations in metal foils and ribbons.

The energy of any spontaneous alpha emission is generally between 2 and 9 MeV (Table 2.17-1) values far greater than the energies of chemical bonds. Thus, recoil transport, combined with the massive ionization and heating of the medium resulting both from recoil and from the alpha particles themselves, is likely to produce some local disruption in any medium that contains alpha-emitters, and potential release to the environment.

2.17.3 Special Properties of "Tracers"

When radioactive substances were discovered, investigators were able to study their chemical behavior only by virtue of the radiation that they produced, because typical concentrations were many orders of magnitude smaller than could otherwise be detected. This principle was later applied in the "tracer" technique, whereby small amounts of radioactive isotopes are incorporated in materials of identical or similar chemical composition so that the "tagged" substance can be identified and measured *in situ* without difficult and laborious separations. These isotopically labeled atoms,

ions or molecules intermingle randomly with the matrix material but have essentially no effect on chemical equilibria or on any macroscopic properties such as vapor pressure, solubility or melting point.

A radioactive species may occasionally exist in isolation, unaccompanied by stable isotopes ("carriers"). Even though the quantity may be extremely small, its radioactivity can make it important — not only as a useful experimental tool, but also because of the potential health hazard. The amounts of radiation considered dangerous to human health are typically measured in picocuries. Because one picocurie (pCi) is approximately equivalent to the radioactivity of 10^{-12} gram of 226-radium, the amounts of most radionuclides needed to produce a picocurie are far too small to weigh or to measure by any conventional chemical method.

Until the late 1950s, the handling and processing of radioactive materials at "tracer" concentrations was more an art than a science, because materials in these concentrations often defy conventional mass-action principles of physics and chemistry: they adhere selectively and tenaciously to surfaces of containers, form "radiocolloids" instead of remaining freely dissolved in solutions, and respond erratically to chemical reagents that would be expected to produce complexation, precipitation, and various electrochemical and physical reactions. Moreover, no clear dividing line has yet been established between the concentrations or amounts of material whose behavior follows the rules for relatively large quantities and those that are likely to show anomalies.

The forces that govern such "anomalous" behavior are somewhat better understood now, especially since the advent of adsorption chromatography and the development of the extensive theoretical basis on which it rests. Still, the practicing environmental scientist is likely to find the behavior of ultra-trace-level radioactive materials somewhat unpredictable.

Our knowledge concerning the behavior of the decay products of 238-uranium illustrates the kinds of questions that have not been fully resolved. Table 2.17-2 lists these products, which include 222-radon and its four daughters — 218-polonium, 214-lead, 214-bismuth and 214-polonium. Until fairly recently, radon's chemical and physical behavior puzzled scientists. Although recognized to be a noble gas, its occurrence at ultra-trace-level concentrations made it appear to have unique properties: for example, it was believed to be preferentially soluble in certain natural oils. The behavior of this element has now been explained through a better understanding of adsorption science and of the equilibria in partition between immiscible liquids and between liquids and gases, much of which falls under the general category of "separation science." In fact, at very low concentrations, radon's behavior approaches theoretical ideality in sorption/desorption and partition equilibria.

The chemical behavior of the short-lived radon daughters in the environment remains unexplained, however, because present theoretical models are inadequate and laboratory experimental methods that simulate their properties under the conditions in which nature produces them have not yet been designed. The parent radon atoms are

TABLE 2.17-2

Daughter Nuclides of 238-Uranium

Nuclide ^a	Major Radiation Energies (MeV) and Intensities ^b				
	α	β		γ	
²³⁸ U 92	4.15 4.20	(25%) (75%)	---	---	---
²³⁴ Th 90	---	0.103 0.193	(21%) (79%)	0.063 0.093	(3.5%) (4%)
²³⁴ Pa ^m 91	---	2.29	(98%)	0.765 1.001	(0.30%) (0.60%)
99.87% 0.13%	---	0.51 1.13	(66%) (13%)	0.100 0.70 0.90	(50%) (24%) (70%)
²³⁴ Pa 91	4.72 4.77	(28%) (72%)	---	0.053	(0.2%)
²³⁴ U 92	4.62 4.68	(24%) (76%)	---	0.068 0.142	(0.6%) (0.07%)
²³⁰ Th 90	4.60 4.78	(6%) (95%)	---	0.186	(4%)
²²⁶ Ra 88	5.49	(100%)	---	0.510	(0.07%)
²²² Rn 86	6.00	(~100%)	0.33 (~0.019%)	---	---
²¹⁸ Po 84	6.65 6.70	(6%) (94%)	?	(~0.1%)	---
99.98% 0.02%	---	0.65 0.71 0.98	(50%) (40%) (6%)	0.295 0.352	(19%) (36%)
²¹⁴ Pb 82	6.65 6.70	(6%) (94%)	?	(~0.1%)	---
²¹⁸ At 85					

See next page

(Continued)

TABLE 2.17-2 (Continued)

Nuclide ^a	Major Radiation Energies (MeV) and Intensities ^b					
	α		β		γ	
$^{214}_{\text{Bi}}$	5.45 5.51	(0.012%) (0.008%)	1.0 1.51 3.26	(23%) (40%) (19%)	0.609 1.120 1.764	(47%) (17%) (17%)
99.98% ↓ 0.02%						
$^{214}_{\text{Po}}$	7.69	(100%)	---		0.799	(0.014%)
$^{210}_{\text{Tl}}$		---	1.3 1.9 2.3	(25%) (56%) (19%)	0.296 0.795 1.31	(80%) (100%) (21%)
$^{210}_{\text{Pb}}$	3.72	(.000002%)	0.016 0.061	(85%) (15%)	0.047	(4%)
$^{210}_{\text{Bi}}$	4.65 4.69	(.00007%) (.00005%)	1.161	(~100%)	---	
~100% ↓ 0.00013%						
$^{210}_{\text{Po}}$	5.305	(100%)	---		0.803	(0.0011%)
$^{206}_{\text{Tl}}$		---	1.571	(100%)	---	
$^{206}_{\text{Pb}}$		---	---		---	

a. See Tables 2.17-1 and 9.2-1 for half-lives of these elements.

b. Intensities refer to percentage of disintegrations of the nuclide itself,
not to original parent of series.

Source: U.S. Bureau of Radiological Health [16]

produced one at a time over periods that are long in relation to chemical reaction rates and to the lives of the daughter atoms themselves, so they and the daughters are created in extreme isolation in nature. Furthermore, each daughter atom is created in an initial state of high ionization and high chemical activity — a so-called "hot atom" — which leads to chemical and physical behavior quite unlike that associated with the corresponding element in ordinary "bulk" concentration. For example, daughter ions produced in air and in the presence of condensation nuclei or other solid and liquid surfaces tend to "plate out"; this phenomenon is widely observed but not well understood, and methods to control it are still based as much on folklore as on established scientific theory.

The potential hazards of radionuclides depend on many factors that include, for example, chemical composition and status, concentration, radiations and energies emitted, half-life, availability, etc. The popular press typically associates high environmental hazard with long radioactive half-life, the idea of persistence being assumed to be of greatest concern. To the environmental scientist, however, the anomalous behavior of some short-lived radionuclides may be of greater importance.

2.17.4 Literature Cited

1. Bagnall, K.W., "The Chemistry of Polonium," in *Advances in Inorganic Chemistry and Radiochemistry*, Vol. IV, H.N. Emeleus and A.G. Sharpe (eds.), Academic Press, New York (1962).
2. Barretto, P.M.C., R.B. Clark and J.A.S. Adams, "Physical Characteristics of Radon-222 Emanation from Rocks, Soils and Minerals: Its Relation to Temperature and Alpha Dose," in *The Natural Radiation Environment*, Vol. II (Proc. Second International Symp.), J.S. Adams, W.M. Lowder and T.F. Gesell (eds.), Houston (1972). Available from NTIS as CONF-720805-P2.
3. Evans, R.D., *The Atomic Nucleus*, McGraw-Hill Book Co., New York (1951)
4. Evans, R.D., "Engineers' Guide to the Elementary Behavior of Radon Daughters," *Health Phys.*, 17, 229-52 (1969).
5. Friedlander, G., J.W. Kennedy, E.S. Macias and J.M. Miller, *Nuclear and Radiochemistry*, 3rd ed., John Wiley & Sons, New York (1981).
6. Kigoshi, K., "Alpha-Recoil Th-234: Dissolution into Water and the U-234/U-238 Disequilibrium in Nature," *Science*, 173, 47-48 (1971)
7. Kotegov, K.V. et al., "Technetium," in *Advances in Inorganic Chemistry and Radiochemistry*, Vol. XI, H.J. Emeleus and A.G. Sharpe (eds.), Academic Press, New York (1968).
8. Kraner, H.W., G.L. Schroeder and R.D. Evans, "Measurements of the Effects of Atmospheric Variables on Radon-222 Flux and Soil Gas Concentrations," in *The Natural Radiation Environment*, J.S. Adams and W.M. Lowder (eds.), University of Chicago Press, Chicago, 191-215 (1964).

9. National Council on Radiation Protection and Measurements, "Evaluation of Occupational and Environmental Exposure to Radon and Radon Daughters in the United States," NCRP Report No. 78, Bethesda, MD (1984).
10. Rosholt, J.N. and A.J. Bartel, "Uranium, Thorium and Lead Systematics in Granite Mountains, Wyoming," *Earth Planet. Sci. Lett.*, 141-47 (1969).
11. Rosholt, J.N., B.R. Doe and M. Tatsumoto, "Evolution of the Isotopic Composition of Uranium and Thorium in Soil Profiles," *Geol. Soc. Am. Bull.*, 77, 987-1004 (1966).
12. Rosholt, J.N., R.E. Zartman and I.T. Nkono, "Lead Isotope Systematics and Uranium Depletion in the Granite Mountains, Wyoming," *Geol. Soc. Am. Bull.*, 84 (1973).
13. Stuckless, S.S. and C. Pizes Ferreira, "Labile Uranium in Granite Rocks," in *Exploration for Uranium Ore Deposits*, IAEA-SM-208/17, Vienna (1976).
14. Tanner, A.B., "Radon Migration in the Ground: A Review," in *The Natural Radiation Environment*, J.S. Adams and W.M. Lowder (eds.), University of Chicago Press, Chicago (1964).
15. Tanner, A.B., "Radon Migration in the Ground: A Supplementary Review," *Proc. 3rd Int'l. Symposium on the Natural Radiation Environment*, Houston (1978).
16. U.S. Bureau of Radiological Health, *Radiological Health Handbook*, International Atomic Energy Agency, Vienna, Austria (1970).
17. Walker, F.W., D.G. Miller and F. Feiner, *Chart of the Nuclides*, 13th ed., General Electric Co., San Jose, CA (1984).

3. KINETICS OF SELECTED PROCESSES

Itamar Bodek, Abraham Lerman

	Page
3.1 INTRODUCTION	3.1-1
3.2 LIGAND EXCHANGE KINETICS	
3.2.1 Introduction	3.2-1
3.2.2 Related Environmental Scenarios	3.2-1
3.2.3 Mathematical Representation	3.2-2
- Half-Life and Observed Rate	3.2-2
- Mechanisms and Mathematical Representation	3.2-3
3.2.4 Variables that Affect Magnitude of Observed Rate Constants (k_{obs})	
- Introduction	3.2-9
- Identity and Oxidation State of Central Metal Ion	3.2-9
- Ligands Coordinated to Metal Ion	3.2-10
- Identity of Incoming Ligand	3.2-12
- Chemical Composition of the Aqueous Environment	3.2-14
- Reaction Mechanism and Rate Law	3.2-14
- Temperature	3.2-15
- Effect of Ionic Strength on Rate Constant	3.2-19
3.2.5 Sources of Data on Rates of Ligand Substitution	3.2-21
3.2.6 Estimation of Substitution Rates	3.2-21
- Introduction	3.2-21
- Use of Water Exchange Rates	3.2-23
- Use of the Edwards Relationship	3.2-24
- Use of Derived Molecular Orbital Bond Energies	3.2-26
- Use of Linear Free Energy Relationships	3.2-27
3.2.7 Literature Cited	3.2-29
3.3 KINETICS OF ELECTRON TRANSFER (REDOX) REACTIONS	
3.3.1 Introduction	3.3-1
3.3.2 Environmental Relevance	3.3-1
- Common Redox Scenarios	3.3-1
- Rate Limiting Steps	3.3-2
3.3.3 Mathematical Representation	3.3-3
3.3.4 Mechanisms and Rate Laws for Homogeneous Redox	3.3-6
- Inner and Outer Sphere	3.3-6
- Evidence and Requirements for Inner Sphere Redox Reactions	3.3-8
- Evidence for an outer Sphere Process	3.3-12
- Other Redox Mechanisms	3.3-13

3.3.5	Examples of Rates, Rate Laws and Trends	3.3-13
-	Trends in Oxyanion Redox Reactions	3.3-13
-	Oxidation of Iron(II)	3.3-14
-	Oxidation of Manganese(II) by Oxygen	3.3-17
-	Oxidation of Sulfide by Oxygen	3.3-19
-	Environmental Reactions of Arsenic(III) and Arsenic(V)	3.3-19
-	Oxidation by Ozone	3.3-19
3.3.6	Chemical and Environmental Factors Affecting Rates	3.3-20
-	One and Two Equivalent Redox Agents	3.3-20
-	Characteristics of Ligands and Metal ions	3.3-23
•	Electronic Configuration	3.3-23
•	Substitution Inert Complexes	3.3-23
•	Presence of Non-Complexing and Complexing Ions in Solution	3.3-23
•	Redox Potential	3.3-24
-	Environmental Factors	3.3-24
3.3.7	Estimation of the Rates of Redox Reactions	3.3-24
-	Marcus Equation for Outer Sphere Reactions	3.3-26
-	Modified Marcus Equation for Inner Sphere Reactions	3.3-30
-	Edwards Equation for Inner Sphere Reactions	3.3-32
-	Inner Sphere Substitution Controlled Reactions	3.3-34
3.3.8	Sources of Data	3.3-35
3.3.9	Literature Cited	3.3-35
3.4	KINETICS OF DISSOLUTION, PRECIPITATION AND CRYSTALLIZATION	
3.4.1	Introduction	3.4-1
3.4.2	Key Variables, Information Needs and Data Sources	3.4-1
-	Environmental Conditions	3.4-1
•	Physical Conditions	3.4-1
•	Chemical Conditions	3.4-2
-	Information Needed for Dissolution and Precipitation Rates	3.4-2
-	Literature Sources of Kinetic Data	3.4-4
3.4.3	Dissolution	3.4-5
-	Description of Dissolution Processes	3.4-5
•	Congruent Dissolution	3.4-5
•	Incongruent Dissolution	3.4-5
•	Leaching or Dissolution of Minor Components	3.4-6
-	Criteria of Dissolution	3.4-7
-	Dissolution on a Global Scale	3.4-9

- Differences in Kinetics Between Closed and Open Systems	3.4-11
• Closed Systems	3.4-12
• Open Systems	3.4-12
- Dissolution Rate Laws	3.4-13
• Zeroeth Order Law	3.4-14
• First Order Law	3.4-15
• Second and Higher Order Laws	3.4-17
• Fractional Order Laws	3.4-17
• Time-dependent Laws	3.4-17
- Dissolution Rate Parameter, k	3.4-19
• Solid Surface Area and Solution Volume	3.4-19
• Dissolution Rate and Degree of Saturation	3.4-20
• Dissolution Reaction Mechanisms	3.4-22
• Porous Media	3.4-22
- Effect of Temperature on Dissolution Rates	3.4-26
- Rate of Dissolution Advance	3.4-27
• Half-life of a Reaction	3.4-27
• Time to Reach an Equilibrium	3.4-28
- Examples of Dissolution of Materials	3.4-29
• Dissolution of Silica-containing Minerals	3.4-29
- Dissolution of Pure SiO ₂ Solids	3.4-30
- Dissolution of Feldspars	3.4-32
- Dissolution Rates of Other Silicate Minerals	3.4-39
- Dissolution Rates of Calcite	3.4-42
3.4.4 Precipitation, Nucleation, Growth, and Recrystallization	3.4-45
- Rates and Example of Precipitation	3.4-45
• Precipitation of Fe(III)-hydroxide	3.4-45
• Dependence of k on Temperature and Solution Composition	3.4-46
• Sources of Fe(II)	3.4-46
• Rates of Oxygen Consumption	3.4-47
- Nucleation and Crystal Growth	3.4-48
• Homogeneous Nucleation	3.4-49
• Heterogeneous Nucleation and Crystal Growth	3.4-52
• Temperature Dependence of Growth Rate	3.4-52
• Nucleation of Calcite and Inhibition of Growth	3.4-53
- Kinetics of Recrystallization	3.4-56
• The Nature and Driving Forces of Dehydration	3.4-56
• Occurrences of Hydration and Dehydration Reactions	3.4-56
• Mechanisms and Rates of Dehydration	3.4-58
• Dehydration of CaSO ₄ -Hydrates	3.4-59
• Other Hydrates	3.4-61
3.4.5 Literature Cited	3.4-63

LIST OF TABLES

LIGAND EXCHANGE KINETICS

3.2-1	Half-Life ($t_{1/2}$) for Various Observed First-Order Rate Constants (k_{obs})	3.2-3
3.2-2	Water Exchange Rate Constants for a Variety of Metal Ions	3.2-6
3.2-3	Inert and Labile Six-coordinate Metal Centers and Complexes	3.2-10
3.2-4	Effect of Changes in Central Atom and Coordinated Ligands on Rate of Substitution Reactions	3.2-11
3.2-5	Ranking of Nucleophile Strength for Substitution Reactions	3.2-13
3.2-6	Effect of Changes in Entering Ligand on Rate of Substitution for Various Mechanisms	3.2-13
3.2-7	Rate Laws for Some Substitution Reactions	3.2-16
3.2-8	Activation Energies for Formation of Metal Complexes from Aquo Complexes in Aqueous Solution at 25°C	3.2-17
3.2-9	Electron Donor Constants and Basicity Parameters for Use in Equation 26	3.2-25
3.2-10	Binding Energies, $E(I)$, per Water Molecule in First Hydration Shell of Cations	3.2-26

KINETICS OF ELECTRON TRANSFER (REDOX) REACTIONS

3.3-1	Rate Equations and Mechanisms for Inner Sphere Reactions	3.3-9
3.3-2	Examples of Known or Suspected Inner-Sphere Redox Reactions	3.3-11
3.3-3	Examples of known or Suspected Outer-Sphere Redox Reactions	3.3-12
3.3-4	Kinetic Data on Cr(VI) Redox Reactions of Environmental Concern	3.3-16
3.3-5	Some Redox Reactions of Fe(II)	3.3-18
3.3-6	Rates of Oxidation of Sulfide by Oxygen in Natural Systems	3.3-19
3.3-7	Rate Constants for Aqueous Oxidations by Ozone	3.3-21
3.3-8	One, Two and One, Two Equivalent Oxidizing Reactants	3.3-22
3.3-9	Values of Exchange Rate Constants and Reduction Potentials	3.3-25
3.3-10	Examples of Calculated and Observed Rate Constants	3.3-28
3.3-11	Sensitivity Analysis of Marcus Equation	3.3-29
3.3-12	Donor Constants for Use with Edwards Equation	3.3-33

KINETICS OF DISSOLUTION, PRECIPITATION AND CRYSTALLIZATION

3.4-1	Mean Composition of the Rivers of the World, and Rates of Delivery to the Oceans	3.4-10
3.4-2	Values of Parabolic Dissolution Rate Parameter (k_{ps}) for Three Silicate Minerals	3.4-18

3.4-3	Linear Dissolution Rates and Solubilities of Some Moderately to Strongly Soluble Salts	3.4-21
3.4-4	Solubilities of Solid Phases and Reaction Mechanisms that Control Dissolution	3.4-23
3.4-5	Summary of the Relationships and Units for the Reaction Rate Parameters, k	3.4-25
3.4-6	Reaction Rate Parameters, Activation Energies, and Equilibrium Constants for Dissolution of Four SiO_2 Solid Phases in Water	3.4-27
3.4-7	Dissolution Rate Parameters for Feldspars in Water	3.4-34
3.4-8	Composition and Specific Surface Area of Feldspars in the Albite-Anorthite Series	3.4-36
3.4-9	Dissolution Rates of Selected Silicate Minerals in Water at 25°C, and Other Data for a Correlation of Dissolution Rates with $\Delta G^\circ/n$	3.4-41
3.4-10	Geometric Shape Factor, β , in the Homogeneous Nucleation Equation (82)	3.4-51
3.4-11	Interfacial Energy of Crystal Nuclei Against Aqueous Solutions for Spherical and Cubic Nuclei, Critical Supersaturation Ratio for Homogeneous Nucleation and Critical Diameter of Nucleus	3.4-51
3.4-12	Order of Precipitation and Crystal Growth Reactions for Equation 85	3.4-54
3.4-13	Activation Energies for Heterogeneous Nucleation in Aqueous Solutions	3.4-54
3.4-14	Effect of Inhibiting Additives on Rates of Calcite Crystallization in a Supersaturated Solution	3.4-55
3.4-15	Rate Equations for Dehydration Reactions	3.4-59
3.4-16	Kinetic Parameters for Some Dehydration Reactions of the Type $\text{Solid 1} \rightarrow \text{Solid 2} + \text{Water Vapor}$	3.4-62

LIST OF FIGURES

LIGAND EXCHANGE KINETICS

3.2-1	Second-order Rate Constants for Formation of Metal Complexes in Aqueous Solution for Aquo Ions at 25°C	3.2-8
3.2-2	Effect of Ionic Strength on Rate Constants	3.2-20
3.2-3	Kinetic Data for Reactions of Common Ligands with Various Metal Complexes at 25°C	3.2-22

KINETICS OF ELECTRON TRANSFER (REDOX) REACTIONS

3.3-1	Relative Rates of HCrO_4^- Oxidations of Various Species	3.3-15
3.3-2	Effect of Organic Complexation of Fe^{+2} on Reaction with Oxygen	3.3-18

3.3-3	Rates of Conversion of As(III) and As(V) by Different Reactants	3.3-20
-------	---	--------

KINETICS OF DISSOLUTION, PRECIPITATION AND CRYSTALLIZATION

3.4-1	Rate of a Reaction dC/dt as a Function of Distance from Saturation ($C_s - C$), for First- and Second-Order Reactions	3.4-14
3.4-2	Increase in Concentration in Solution, C, for First- and Second-Order Dissolution Reaction, as a Function of Dimensionless Parameter kt	3.4-15
3.4-3	Rate of Dissolution of Sodium-Feldspar (Albite) as a Function of pH, at a Constant Rate of Albite Dissolution	3.4-38
3.4-4	Rates of Dissolution of Some Silicates, $\log R$, Plotted Against Their Gibbs Free Energies of Formation, Normalized to the Number of Oxygen Atoms (n) in the Stoichiometric Formula of the Silicate	3.4-39
3.4-5	Rate of Calcite Dissolution as a Function of Distance from Saturation	3.4-43
3.4-6	Observed Rate Constant for Oxidation of Fe^{+2} in Water	3.4-48
3.4-7	Schematic Diagram of Crystal Growth in Solution	3.4-53
3.4-8	Progress of Dehydration Reactions Computed from Equations a,c,f, and g in Table 3.4-15	3.4-60

3.1 INTRODUCTION

The kinetics or rates of reactions are an important aspect of environmental chemistry, especially with regard to understanding the speciation of chemicals. An understanding of the relative rates of environmental processes allows calculations of speciation based upon an equilibrium model, a non-reaction model or an intermediate model where kinetics must be considered. A simple answer with regard to the kinetics (e.g., that it is either instantaneous or very slow) is useful in determining which way to proceed. Detailed kinetic information is necessary only when the rates of the processes are of the same time frame of interest in the particular environmental system. In that case, a calculation based upon equilibrium conditions may indicate limits to the range of product concentrations. However, as discussed in the following section, relative rates can sometimes affect product identity.

The kinetics of processes is discussed in several locations in this report. These include § 2.3 (Photolysis in Air), § 2.5 (Atmospheric Deposition), § 2.14 (Photolysis in Water), § 2.16 (Diffusion Coefficients) and § 2.17 (Radioactive Processes). In addition, rates are presented in other sections on particular reactions. This chapter focuses on kinetics of ligand exchange (§ 3.2), oxidation-reduction (§ 3.3), and dissolution-precipitation (§ 3.4) reactions. The information presented in this chapter, in general, concerns the following topics:

- Environmental relevance
- Mathematical representation
- Typical values of the rate, or rate constants, and correlations
- The effect of different environments on the reaction rate
- Mechanisms of the particular reaction
- Methods of estimating rates and rate constants.

Sections 3.2 and 3.3 address homogeneous reaction kinetics (i.e., between dissolved ions and dissolved gases), while § 3.4 addresses the rates of heterogeneous reactions such as dissolution, nucleation and recrystallization. The equilibrium conditions for the reactions described in this chapter are given in § 2.9 (Complexation), § 2.10 (Electron Transfer Reactions), and § 2.11 (Solubility and Precipitation Equilibria).

3.2 LIGAND EXCHANGE KINETICS

3.2.1 Introduction

This section addresses rates of substitution of coordinated ligands, especially water molecules, in the primary coordination sphere of metal ions. The principal topics considered are:

- Environmental relevance of the rate of ligand substitution;
- Mathematical representation of reaction rates and their use in estimating the time required for completion of the reaction;
- Mechanism (sequence of steps) of substitution reactions;
- Variation in rates and rate constants due to differences in metal ions, ligands and aqueous environments;
- Typical values of rate constants for substitution in a variety of complex ions; and
- Methods for estimating substitution rates from observed correlations with various properties.

Additional information on complexation can be found in section 2.9. The reading of that section prior to this one may help clarify some topics discussed below. Throughout this section a small k is used to represent a rate constant while a large K is used to represent an equilibrium constant.

3.2.2 Related Environmental Scenarios

An important aspect of environmental chemistry, especially with regard to the speciation of dissolved inorganics, is the determination of the rate and mechanism by which complexation reactions approach equilibrium. When complexation is "fast" (compared with an arbitrary or particularly relevant time frame), equilibrium conditions can be used as a basis for calculation of speciation. If the reaction is very "slow," the reactant will remain in its original form, and little or no reaction occurs. However, if the reaction is "intermediate" in rate, one must consider the reaction process in great detail to estimate the quantities of reactants and products present at various times.

The ease with which a particular complex ion (e.g., M_{aq}^{+x}) enters into reactions that entail the replacement of one or more of the existing ligands (typically H_2O in environmental systems) in the primary coordination sphere provides a means of assessing reaction rates involving such ions.¹ Taube [23] has characterized metal ions as kinetically *labile* ("fast" substitution rate occurring within time of mixing) or kinetically *inert* ("slow" or "intermediate" substitution rate).

1. The term "free" or "uncomplexed" is often used in the literature to describe the aquo complexed metal ion (i.e., $M(H_2O)_v^{+x}$ or M_{aq}^{+x}); in reality, the free or uncomplexed ion does not exist in solution.

3.2.3 Mathematical Representation

HALF-LIFE AND OBSERVED RATE

The ligand substitution reaction can be represented as follows:



where X is the leaving ligand and Y is the entering ligand on metal ion M.

The *overall* rate of this reaction is generally expressed as

$$\text{Rate} = \frac{d[M-Y]}{dt} = \frac{d[M-X]}{dt} = k_{\text{obs}} [M-X] \quad (2)$$

where k_{obs} is the *pseudo* first-order observed rate constant. These reactions are typically first-order in M-X and are conveniently studied under conditions where other reactants are essentially at constant concentrations relative to [M-X]. Equation 2 can also be written in either of the following forms:

$$-\frac{d[M-X]}{[M-X]} = -d \ln [M-X] = k_{\text{obs}} dt \quad (3)$$

or

$$\ln [M-X]_0 - \ln [M-X]_t = k_{\text{obs}} (t - t_0) \quad (4)$$

where $[M-X]_t$ and $[M-X]_0$ are the concentrations of M-X species at time t and time zero, respectively.

Thus, plots of $\ln [M-X]_0 - \ln [M-X]_t$ versus $(t - t_0)$ should yield a straight line with a slope of k_{obs} . The half-life of an irreversible chemical reaction, which represents the time for reactant M-X to reach half of its initial concentration, is given by

$$t_{1/2} = \frac{0.69315}{k_{\text{obs}}} \quad (5)$$

If homogeneous reaction conditions are assumed, the percentage of original M-X complex remaining after 1, 2, 3, and 4 half-lives have passed is 50%, 25%, 12.5%, and 6.25%, respectively. A first-order or *pseudo* first-order reaction that proceeds for over four half-lives can therefore be considered nearly complete.

To indicate what values of k_{obs} may be environmentally important, calculated half-lives corresponding to various k_{obs} values are listed in Table 3.2-1. The k_{obs} value that corresponds to $t_{1/2}$ values that begin to be important from an environmental perspective (say time of mixing) will thus be on the order of $1 - 10 \text{ min}^{-1}$ ($t_{1/2} = 4 - 40 \text{ s}$).

The values listed in Table 3.2-1 are not the *fundamental* rate constants commonly given in the literature, which refer to a single reaction step; *observed* rate constants

TABLE 3.2-1

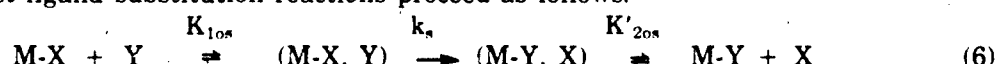
**Half-Life ($t_{1/2}$) for Various Observed
First-order Rate Constants (k_{obs})
(calculated by equation 5)**

k_{obs} (min ⁻¹)	$t_{1/2}$ (min)
6.0×10^{-7}	1.2×10^6
6.0×10^{-6}	1.2×10^5
6.0×10^{-5}	1.2×10^4
6.0×10^{-4}	1.2×10^3
6.0×10^{-3}	1.2×10^2
6.0×10^{-2}	1.2×10^1
6.0×10^{-1}	1.2
6.0	1.2×10^{-1}
6.0×10^1	1.2×10^{-2}

represent the sum of many possible reaction steps and are therefore related to the overall reaction rates, as expressed in equation 2. These values depend on the reaction mechanism, fundamental rate constants, incoming ligand concentration, pH, temperature, and other factors, as discussed later in this section. Due to the complexity of substitution mechanisms, it is easier to consider the overall reaction in terms of k_{obs} than to calculate the separate contributions of individual steps.

MECHANISMS AND MATHEMATICAL REPRESENTATION

Most ligand substitution reactions proceed as follows:



where $M-X$ is the metal ion with ligand X coordinated in the inner sphere, Y is the incoming ligand, and $(M-X, Y)$ and $(M-Y, X)$ are outer-sphere complexes or ion pairs. (The comma separates the two species in the ion pair.) K_{1os} is the ion pair formation equilibrium constant of $(M-X, Y)$, k_s is the substitution rate constant for the conversion of X from outer to inner sphere within the ion pair, and $K'_{2os} = 1/K_{2os}$, where K_{2os} is the ion pair equilibrium formation constant of $(M-Y, X)$.

The reaction step $(M-X, Y) \rightarrow (M-Y, X)$ involves substitution via interchange of ligands in the outer and inner spheres of M and is thus termed an *interchange* mechanism (I). Interchange mechanisms of ligand exchange are generally divided into two categories:

- Dissociative (I_d), where an $M-X$ bond is partially broken before the $M-Y$ bond is formed.

- Associative (I_a), where an M-Y bond is partially formed while the M-X bond is still present.

The situation where bond breaking occurs to form an intermediate of reduced coordination number (e.g., five from a six-coordinate complex) is referred to as a dissociative (D) mechanism. An intermediate of increased coordination (e.g., seven from a six-coordinate reactant) is formed by an associative (A) mechanism. For an interchange (I) mechanism, an intermediate of modified coordination number does not exist.²

The mechanism of the substitution reaction determines the mathematical relationship between k_{obs} and the fundamental rate constants available in the literature. As a rule, substitution of cationic complex ions occurs via an interchange mechanism [21]. The generally accepted view [20] is that M^{+2} ions react via I_d and M^{+3} ions via I_a mechanisms.³

Using the assumption that k_s is rate limiting, the rate law for equation 6 (I mechanisms) is as follows [24]:

$$\text{Rate} = \frac{d \ln[M-Y]}{dt} = \frac{k_s K_{1os} [Y]}{1 + K_{1os} [Y]} \quad (7)$$

When $K_{1os} (Y) \ll 1$, equation 7 can be approximated by

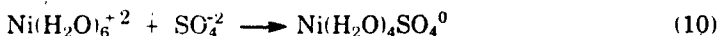
$$\text{Rate} = \frac{d \ln[M-Y]}{dt} = k_s K_{1os} [Y] \quad (8)$$

Comparison of equations 8 and 3 then gives

$$k_{obs} = k_s K_{1os} [Y] \quad (9)$$

Thus, for an I mechanism, equation 9 allows the calculation of k_{obs} from data on ion pair formation constants and rates of substitution.

Example 1 Calculate the half-life of reaction 10, given the following information and assumptions:



- Initial $\text{Ni}(\text{H}_2\text{O})_6^{+2}$ concentration is 1×10^{-5} mol/l (0.59 ppm).
- Initial SO_4^{2-} concentration is 1×10^{-3} mol/l (96 ppm).
- Ionic strength is 0.5 M.

2. A, I_a , I_d and D can be roughly conceptualized by the following terminology, which is commonly used in reaction chemistry [1]:



3. Some notable exceptions are Mn^{+2} , Co^{+3} , and Al^{+3} aquo ions. The few examples of a D mechanism involve neutral or anionic complexes, e.g., $[\text{Co}(\text{CN})_5\text{OH}_2]^{2-}$. [20.21]

- Rate of water exchange (k_s) on $\text{Ni}(\text{H}_2\text{O})_6^{+2}$ is $3 \times 10^4 \text{ s}^{-1}$.
- Assume reaction proceeds via an I_n mechanism.
- Assume that $\text{Ni}(\text{H}_2\text{O})_6^{+2}$ is the only complex that is reacting.

To estimate $t_{1/2}$ for this reaction, we first estimate the observed rate constant (k_{obs}) under the stated conditions. This requires the following:

- (1) Calculation of the outer-sphere association constant (K_{los}) for $[\text{Ni}(\text{H}_2\text{O})_6, \text{SO}_4]^0$
- (2) Value of the rate of water exchange on $\text{Ni}(\text{H}_2\text{O})_6^{+2}$
- (3) Verification that the concentration of $\text{SO}_4^{+2}([\text{Y}])$ is approximately constant during the reaction (pseudo first-order conditions.)
- (4) Verification that $K_{\text{los}}[\text{SO}_4^{+2}] = K_{\text{los}}[\text{Y}] \ll 1$ so that equation 9 can be used rather than the more complex equation 7.

We first calculate K_{los} for the $[\text{Ni}(\text{H}_2\text{O})_6, \text{SO}_4]^0$ ion pair by the procedure given in section 2.9, using the following parameters in equation 11 of that section:

$$\begin{aligned} I &= 0.5 \\ Z_1 &= +2 \\ Z_2 &= -2 \\ a &= 9.5 \text{ \AA} (\text{Table 2.9-5}) = 9.5 \times 10^{-8} \text{ cm} \end{aligned}$$

This leads to a value of $K_{\text{los}} = 5.5 M^{-1}$.

To approximate k_s for $\text{Ni}(\text{H}_2\text{O})_6^{+2}$, we can use the value of k_{ex} listed in Table 3.2-2 for Ni^{+2} , which is $3 \times 10^4 \text{ s}^{-1}$. As discussed below, k_s is usually greater than k_{ex} in this situation, but they are of the same order of magnitude.

We then compare the value of $[\text{SO}_4^{+2}]$ with that of $[\text{Ni}(\text{H}_2\text{O})_6^{+2}]$ to verify that the reaction would not markedly affect $[\text{SO}_4^{+2}]$. Since complete reaction of $1 \times 10^{-5} \text{ mol/l}$ of $\text{Ni}(\text{H}_2\text{O})_6^{+2}$ would remove an identical amount of SO_4^{+2} and this amount is much smaller than the $[\text{SO}_4^{+2}]$, which is $1 \times 10^{-3} \text{ mol/l}$, the concentration of SO_4^{+2} in solution would be essentially constant. This leads to pseudo first-order conditions.

The above values of K_{los} and $[\text{SO}_4^{+2}]$ are next multiplied together to verify that their product is much less than 1:

$$(5.5 M^{-1})(1 \times 10^{-3} M) = 5.5 \times 10^{-3} \ll 1$$

Having assumed an I_n mechanism and no other reaction paths, we can now use equation 9:

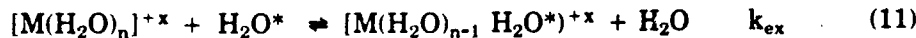
$$k_{\text{obs}} = k_s K_{\text{los}} [\text{SO}_4^{+2}] = (3 \times 10^4 \text{ s}^{-1})(5.5 M^{-1})(1 \times 10^{-3} M) = 1.65 \times 10^2 \text{ s}^{-1}$$

In accordance with equation 5, the half-life of the reaction is

$$t_{1/2} = \frac{0.693}{1.65 \times 10^2 \text{ s}^{-1}} = 4.2 \times 10^{-3} \text{ s}$$

The reaction is thus very rapid. Note that a difference of a factor of 10 in the value of k_s would not significantly alter this conclusion.

The kinetic time frame of ligand substitution reactions in general is frequently paralleled by the rate of water exchange for the aquo complexed ion species, $M(H_2O)_n^{+x}$, shown below.



where k_{ex} is the exchange rate constant and H_2O^* is an isotopically labeled (e.g., ^{18}O) water molecule. The water exchange reaction occurs continuously in aqueous media, even though the product and reactants are the same. Isotopic labeling studies allow measurement of the rate of exchange.

Values of k_{ex} for water exchange by a variety of metal ions are given in Table 3.2-2. Rates of exchange for acid dissociated species (e.g., reaction 12) are very different from those for aquo ions (reaction 11).



TABLE 3.2-2

**Water Exchange Rate Constants for
a Variety of Metal Ions**
(see equation 11)

Ion	k_{ex} (s^{-1})	Ion	k_{ex} (s^{-1})
Cr^{+2}	7×10^9	Hg^{+2}	$>10^4$
Mn^{+2}	3×10^7	Al^{+3}	~ 1
Fe^{+2}	3×10^6	Fe^{+3}	3×10^3
Co^{+2}	1×10^6	Ga^{+3}	$<10^4$
Ni^{+2}	3×10^4	Gd^{+3}	2×10^9
Cu^{+2}	8×10^9	Bi^{+3}	$>10^4$
Be^{+2}	3×10^4	Cr^{+3}	3×10^{-6}
Mg^{+2}	$>10^4$	Rh^{+3}	4×10^{-8}
Ba^{+2}	$>10^4$	VO^{+2}	5.2×10^2
Sn^{+2}	$>10^4$		

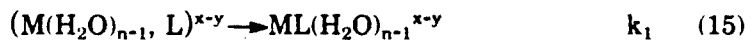
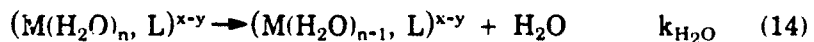
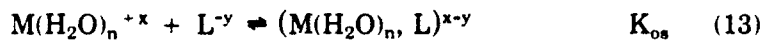
Source: Saito and Sasaki [20]; Basolo and Pearson [2].

The relationship between k_s (equation 6) and k_{ex} (equation 11) depends on the mechanism of ligand substitution and the nature of the metal ion and incoming ligand. The following general patterns have been observed [22]:

- For an I_a mechanism, when Y is more nucleophilic than H_2O toward the metal (i.e., M is a "soft" metal and Y is a "soft" ligand⁴), $k_s > k_{ex}$;
- For an I_a mechanism, when Y is less nucleophilic than H_2O toward the metal (i.e., M is a "hard" metal), $k_s \leq k_{ex}$; and
- For an I_d mechanism, $k_s \leq k_{ex}$, and k_s should be similar for a variety of different Y ligands.

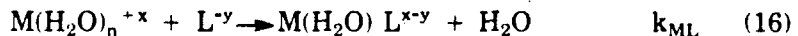
Characteristic rates of substitution for a variety of metal ions are shown in Figure 3.2-1. The similarity of these data to those of Table 3.2-2 suggest that rates of water removal from the inner coordination sphere is often the rate-determining step.

For complexation reactions where an aquo complexed metal ion (i.e., $M(H_2O)_n^{+x}$) and a monodentate⁵ ligand, L^{-y} , react, the following dissociative interchange mechanism (I_d) has been found generally applicable [8,18]:



The constants K_{os} , k_{H_2O} and k_1 refer to the equilibrium constant for outer-sphere complex formation, rate-limiting water loss and rate of conversion of outer-sphere to inner-sphere complex, respectively. The constant k_{H_2O} is a first-order rate constant for unaided metal-water bond breaking in the aquo complexed ion, and k_1 is much faster than k_{H_2O} .

Equations 13-15 can be summarized as:



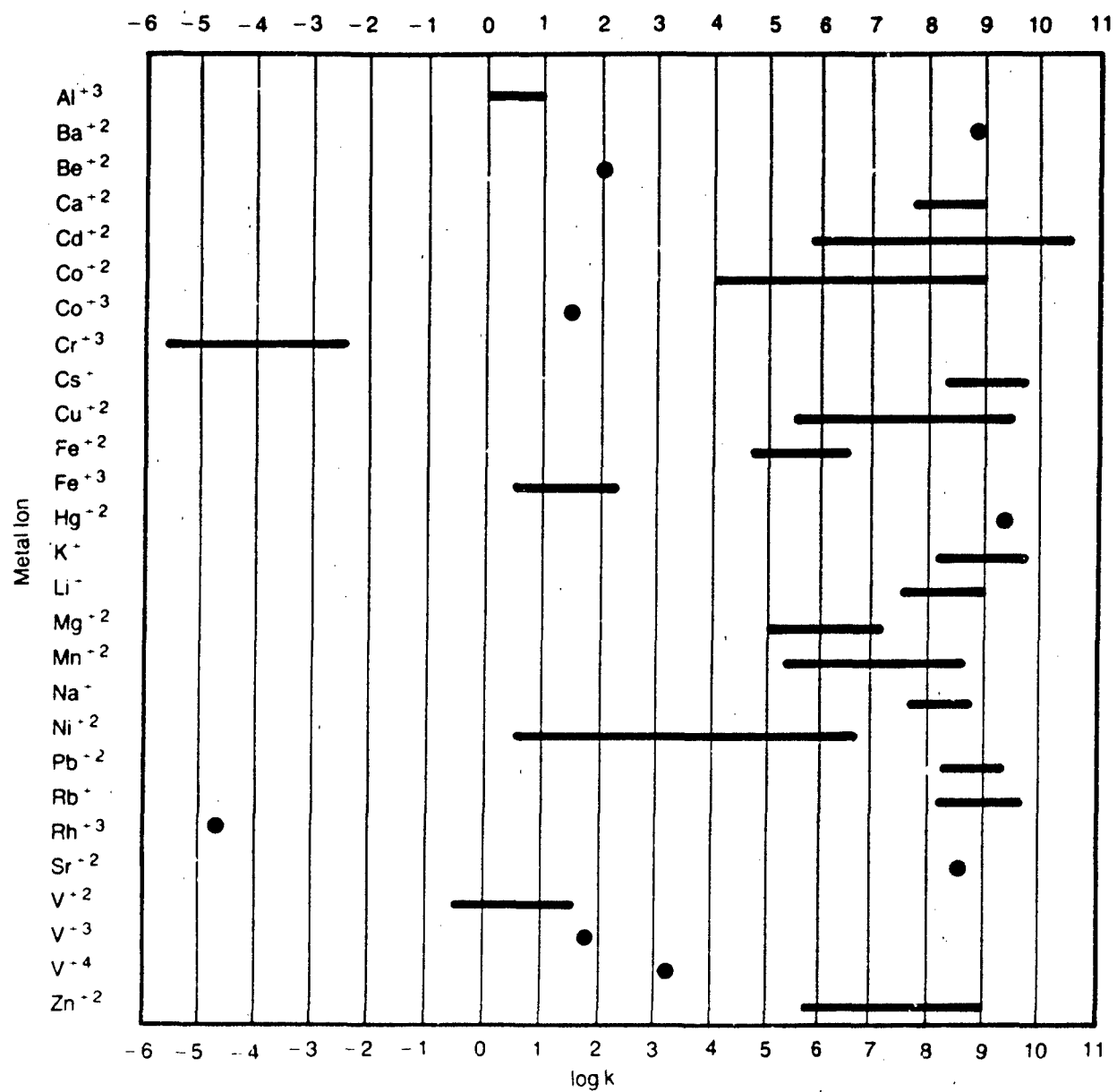
where k_{ML} is the *overall* rate constant for complex formation. The value of k_{ML} is related to K_{os} and k_{H_2O} as follows:

$$k_{ML} = K_{os} k_{H_2O} \approx K_{os} k_{ex} \quad (17)$$

Equation 17 is related to equation 9 with Y = H_2O and provides a method for estimating k_{ML} from data for k_{ex} . (See "Use of Water Exchange Rates" in §3.2.6.)

4. For definitions and classifications of "hard" and "soft," see Basolo and Pearson [2].

5. Monodentate ligands are defined in section 2.9.



Note: k is expressed in $\text{M}^{-1}\text{s}^{-1}$. Bars indicate range of values for a variety of inorganic and organic ligands, while dots give single values.

Source: Based on data in Table 1 of Eigen and Wilkins [8]

FIGURE 3.2-1 Second-order Rate Constants for Formation of Metal Complexes in Aqueous Solution for Aquo Ions at 25°C

3.2.4 Variables that Affect Magnitude of Observed Rate Constant (k_{obs})

INTRODUCTION

The utility of k_{obs} in estimating the rate of substitution was described above. To estimate k_{obs} , it is useful to understand what factors affect its value. This section discusses the following factors and their impact on the relative magnitude of k_{obs} :

- Identity and oxidation state of central metal ion,
- Identity of ligands coordinated to the metal ion,
- Identity of incoming ligand,
- Chemical composition of the aqueous environment,
- The mechanism and rate law for the substitution reaction,
- Temperature of the aqueous environment, and
- Ionic strength of the solution.

IDENTITY AND OXIDATION STATE OF CENTRAL METAL ION

The magnitude of k_{obs} is a function of k_s , the rate of water substitution on the metal ion. Significant relationships have been observed between the value of k_s and the identity and oxidation state of the central metal ion:

- High reactivity ($k_s > 10^5 \text{ s}^{-1}$) for alkali metals, alkali earth metals, rare earths (+3 oxidation state) and first transition metals of +2 oxidation state in the order Cu(II) = Cr(II) > Zn(II) > Mn(II) > Fe(II);
- Lesser reactivity ($k_s < 10^5 \text{ s}^{-1}$) for Ni(II), V(II), Fe(III), Be(II), and Al(III);
- Low reactivity ($k_s < 1 \text{ s}^{-1}$) for transition metals of +3 and +4 oxidation state with large crystal field stabilization energies [2], such as Cr(III), Co(III) and Rh(III); see Table 3.2-3.

Metal ions have also been classified as being either "kinetically inert" (reaction occurring longer than one minute at room temperature for a 0.1 M solution) or "kinetically labile" (reactions essentially complete within one minute under the same conditions) [2]. The constitution of the electronic shell of the metal and stereochemistry of the ligands (e.g., octahedral, tetrahedral, or square planar) play an important role in determining these reaction rates. For example, octahedral complexes such as Cr(III), Co(III), Fe(III), Mo(III) and Au(III) — all of which have electronic configurations of d^3 , d^4 (low spin), d^5 (low spin), or d^6 (low spin) — are essentially inert [2]. Of the metal species that have these electronic configurations, Cr(III) is particularly important from an environmental standpoint. Table 3.2-3 classifies a large number of metal ions into labile and inert categories.

Because of the electrostatic nature of the interaction of metals and ligands, substitution reactions are affected by the size of metal ions and their charge.

TABLE 3.2-3

Inert and Labile Six-coordinate Metal Centers and Complexes

Labile ^a			Inert ^a		
Mn(II)	Y(III)	Mo(V)	Co(III) ^b	V(II)	Cr(bipy) ⁺²
Fe(II)	Ti(IV)	W(V)	Rh(III)	Re(III)	Mn(CN) ₆ ⁻³
Fe(III)	Zr(IV)	Re(VI)	Ir(III)	Ru(IV)	Cr(bipy) ₃ ⁺³
Co(II)	Hf(IV)	Ti(II)	Ni(IV)	Os(V)	Mn(CN) ₆ ⁻⁴
Zn(II)	Ce(IV)	V(III)	Pd(IV)	Re(II)	Fe(CN) ₆ ⁻³
Cd(II)	Th(IV)	Nb(III)	Pt(IV)	Ru(III)	Fe(phen) ₃ ⁺³
Hg(II)	Nb(V)	Ta(III)	Cr(III)	Os(III)	Fe(bipy) ₃ ⁺³
Al(III)	Ta(V)	Mo(IV)	Mo(III)	Ir(IV)	Mn(CN) ₆ ⁻⁴
Ga(III)	Mo(VI)	W(IV)	W(III)	Ru(II)	Fe(CN) ₆ ⁻⁴
Tl(III)	W(VI)	Re(V)	Mn(IV)	Os(II)	Fe(phen) ₃ ⁺²
In(III)	Ti(III)	Ru(VI)	Re(IV)	Cr(CN) ₆ ⁻⁴	Fe(bipy) ₃ ⁺²
Sc(III)	V(IV)	Rare Earths (III)			

a. As defined in the text. No consideration has been given to the composition of the primary coordination spheres in listing these metal oxidation states. bipy = 2,2'-bipyridyl, phen = o-phenanthroline.

b. Except CoF₆⁻³

Source: Basolo and Pearson [2], pp. 143-44.

Table 3.2-4(A) shows how changes in the central metal ion's size and charge can be expected to affect the rate of substitution reactions via three different mechanisms. Since the interaction is not always purely electrostatic, these generalizations should be used with caution.

LIGANDS COORDINATED TO METAL ION

As with the central metal ion, variations in the electrostatic properties of ligands in the first coordination shell also affect the rate of substitution reactions; some useful generalizations are given in Table 3.2-4(B). Since the electrostatic model used is a simplistic representation of the interactions that occur, these generalizations again must be used cautiously.

TABLE 3.2-4
**Effect of Changes in Central Atom and Coordinated Ligands on
 Rate of Substitution Reactions^a**

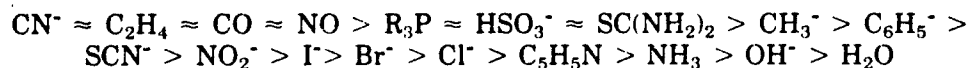
Change	Mechanism ^b		
	D	I	A
A. Central Metal Atom			
Increase in positive charge	Decrease	c	Increase
Increase in size	Increase	Increase	Increase
B. Coordinated Ligands			
Increase size of leaving group	Increase	c	Decrease
Increase negative charge of leaving group	Decrease	Decrease	Decrease
Increase negative charge of non-labile ligand	Increase	c	Decrease
Increase size of non-labile ligand	Increase	c	Decrease

- a. Charge and size effects only; type of bonding assumed to be unchanged.
- b. D = dissociative, I = interchange, A = associative
- c. Multiple effects oppose each other; therefore, the rate may be either increased or decreased to some extent.

Sources: Benson [4]; Basolo and Pearson [2]

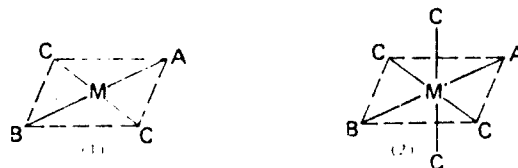
The chemical nature and position of the other coordinated ligands around the metal ion, especially those in the *trans* position,⁶ can also influence the rate of substitution. In complexes that contain a "strong" *trans* labilizing ligand, substitution may occur a million times faster than with a "weak" *trans* ligand. This effect has been largely observed in square planar complexes such as Pt(II) and Ni(II), but some instances involving reactions of octahedral complexes have also been observed [2].

In Pt(II) complexes, the strength of the *trans* labilizing effect decreases as follows [4]:



These effects occur when bond breaking (i.e., I_d or D mechanisms are in effect. Thus, for example, substitution occurs more rapidly if a ligand is *trans* to a CN⁻ rather than

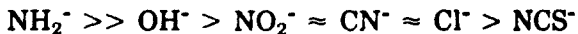
6. "Trans" and "cis" locations with respect to ligand A are at B and C, respectively, in the following schematics for square planar (1) and pseudo octahedral (2) stereochemistries:



3.2-11

a Cl^- . The strength of the *trans* effect is enhanced by the bonding ability of the ligand [1]. Ligands that are *cis* to the leaving group in a square planar complex have comparatively little effect on the rate of replacement, unless steric effects are important [2].

The position of a *trans* stabilizing ligand in the above series is greatly dependent on the chemical nature of the particular metal complex. Thus, for example, in complexes of *trans*- $\text{Co}(\text{en})_2\text{ACl}^+$ (where en is ethylenediamine and the ligand A is *trans* to Cl^- in the octahedral complex), the rate of Cl^- loss via an I_d or D mechanisms suggests that the effect of A decreases as follows:



This order is very different from that observed for square planar Pt(II) complexes. Clearly, a change in the chemical composition of the primary coordination sphere (e.g., from $\text{M}(\text{H}_2\text{O})_6^{+3}$ to $\text{M}(\text{NH}_3)_5\text{H}_2\text{O}^{+3}$) can strongly affect the rate of substitution of a leaving ligand such as H_2O .

IDENTITY OF INCOMING LIGAND

In a coordination complex, the central metal ion is referred to as the *electrophilic* reagent (acceptor of e^-) and the ligand as the *nucleophilic* agent (donor of e^-). The ease with which a ligand acts as a nucleophilic agent in $\text{S}_{\text{N}}2$ mechanisms (I , I_a or A) is determined by factors such as its Lewis basicity, polarizability, and the "alpha effect"⁷ [7]. The relative effect of these ligand properties on the rate of substitution reaction depends on the metal or atom center with which they react. The importance of polarizability of the ligand increases in a series in which the number of outer electrons increases (e.g., I^- vs. Br^-) or the net positive charge decreases, as in Fe(III) to Fe(II) and S(VI) to S(II). The "alpha effect" appears to be general.

However, as a mixed contribution from each of these properties is generally observed, a relative ranking of ligands can be made only for a particular metal. Table 3.2-5 provides examples of the ranking of ligands with regard to overall nucleophile strength for particular metals or atoms.

A later subsection (§3.2.6) presents a relative ranking of basicity and polarizability for a variety of species as values of H and E_n , respectively. The "Edwards Relationship," a method for estimating the influence of these two parameters on the rate of substitution, is also described in that subsection.

Table 3.2-6 shows the general effect of changes in the size and charge of the entering ligand on the rate of substitution, considering only electrostatic interactions. Again, these generalizations should be used cautiously.

7. An effect attributed to the presence of unshared pairs of electrons on the atom adjacent to the donor atom (bonded to the metal).

TABLE 3.2-5
Ranking of Nucleophile Strength for Substitution Reactions

Reactant Atom	Relative Nucleophile Strength	Important Property ^a
Neutral four-coordinate phosphorus	$\text{OOH}^- > \text{OH}^- \approx \text{OCl}^- > \text{NH}_2\text{OH} > \text{NO}_2^- > \text{N}_3^- > \text{H}_2\text{O}$	Basicity >> polarizability
Trigonal boron ^b	$\text{OH}^- > \text{OR}^- > \text{NH}_3^- > \text{R}_2\text{NH} \approx \text{SR}^-$	Basicity >> polarizability
Tetrahedral boron ^c	$\text{OH}^- > \text{F}^- > \text{H}_2\text{O}$	Basicity >> polarizability
Tetrahedral sulfur	$\text{OH}^- > \text{CH}_3\text{O}^- > \text{C}_6\text{H}_5\text{O}^- > \text{RNH}_2 > \text{C}_6\text{H}_5\text{NH}_2 > \text{C}_6\text{H}_5\text{S}^-$	Basicity and polarizability
Bivalent sulfur	$\text{RS}^- > \text{R}_3\text{P} > \text{C}_6\text{H}_5\text{S} \approx \text{CN}^- > \text{SO}_3^{2-} > \text{OH}^- > \text{S}_2\text{O}_3^{2-} > \text{SC}(\text{NH}_2)_2 > \text{SCN}^- > \text{Br}^- > \text{Cl}^-$	Polarizability and basicity
Trivalent nitrogen ^d	Phosphines > amines > oxygen bases	Polarizability > basicity
Oxygen (in peroxide)	$\text{SO}_3^{2-} > \text{S}_2\text{O}_3^{2-} > \text{SC}(\text{NH}_2)_2 > \text{I}^- > \text{CN}^- > \text{SCN}^- > \text{NO}_2^- > \text{OH}^- > \text{N}_3^- > \text{Br}^- > \text{NH}_3 > \text{Cl}^- > \text{C}_5\text{H}_5\text{N} > \text{H}_2\text{O}$	Polarizability >> basicity
Square planar platinum (II)	$\text{R}_3\text{P} \approx \text{thiourea} \approx \text{SCN}^- \approx \text{I}^- > \text{N}_3^- > \text{NO}_2 > \text{Py} > \text{aniline} > \text{oletin} \approx \text{NH}_3 \approx \text{Br}^- > \text{Cl}^- > \text{glycine} \approx \text{OH}^- \approx \text{H}_2\text{O} \approx \text{F}^-$	Polarizability >> basicity

a. Extent is highly compound-specific.

b. Based on R_2BX

c. Based on BF_3NH_3

d. Based on NH_2X

Source: Edwards and Pearson [7]

TABLE 3.2-6
**Effect of Changes in Entering Ligand on Rate of Substitution
for Various Mechanisms^a**

Change in Entering Ligand	Mechanism ^b		
	D	I	A
Increase negative charge	No effect	Increase	Increase
Increase size	No effect	Decrease	Decrease

a. Charge and size effects only; type of bonding assumed to be unchanged.

b. D = dissociative, I = interchange, A = associative.

Source: Benson [4].

CHEMICAL COMPOSITION OF THE AQUEOUS ENVIRONMENT

The chemical composition of the aqueous environment can influence rates of substitution by (1) altering the speciation of the metal ion and (2) introducing other ions that affect the reaction. Both of these actions allow the overall substitution process to proceed via different reaction paths, which have their own characteristic rates.

The effect of ionic strength on reaction rate is discussed later in this subsection. One of the major determinants of substitution rate is the pH of the solution. Since many complexes, especially aquo complexed metal ions, participate in acid dissociation equilibria (see section 2.7), the pH can affect the relative amounts of $M(H_2O)_n^{+x}$ and $M(H_2O)_{n-y}(OH)^{x-y}$ species. The latter (especially when $y = 1$) often reacts much faster with ligands than does the completely aquo complexed metal ion [9].

The magnitude of this effect is determined by the individual aquo-hydroxo-complex reaction rate constant and pH. The following examples illustrate the extent to which the rate constant can vary [8,9]:

Reaction	Rate Constant ($M^{-1} s^{-1}$)
$Cr(H_2O)_6^{+3} + Cl^-$	3.0×10^{-8}
$Cr(H_2O)_5OH^{+2} + Cl^-$	2.3×10^{-5}
$Fe(H_2O)_6^{+3} + SCN^-$	1.3×10^2
$Fe(H_2O)_5OH^{+2} + SCN^-$	1×10^4

Since the speciation of ligands can also be affected by pH, the rate of substitution can be modified. Ligands and other chelating agents containing oxygen and nitrogen donor atoms, such as EDTA and ethylenediamine, are especially affected through acid/base equilibria. For example [8]:

Reaction	Rate Constant ($M^{-1} s^{-1}$)
$Ni^{+2} + C_2O_4^{+2}$	7.9×10^4
$Ni^{+2} + HC_2O_4^-$	5.0×10^3

The presence of particular metal ions can promote the substitution of coordinated ligands; Hg(II) is by far the most effective in enhancing rates of removal of ligands such as Cl^- , CN^- , N_3^- and NCS^- from complexes and replacement by H_2O . Ag(I) and Tl(III) are also effective, but much less so than Hg(II). Metal ions can also accelerate the rate of removal of chelated ligands by coordinating to the freed donor atoms of the chelating ligand [24]:



REACTION MECHANISM AND RATE LAW

An understanding of the reaction mechanism and its mathematical representation (rate law) allows the rate of substitution to be defined as a function of the important variables. As previously mentioned, the interchange (I) substitution mechanism is most commonly observed for aquo complexed metal ions.

First-row transition metals with divalent oxidation states generally undergo substitution via I_a ; the I_d mechanism is more typical for cationic octahedral complexes of trivalent metals such as V(III), Mo(III), Ru(III), Cr(III), Ir(III) and Re(III), but not Co(II) [21].

Dissociative mechanisms have been proposed for oxo-metal ions of Ti(IV), V(V) and Cr(VI) (e.g., for CrO_4^{2-}), while associative mechanisms appear to operate for W(VI) and Mo(VI) (e.g., MoO_4^{2-}). An increase in rate with increasing concentration of H^+ is observed in the formation of oxo-metal complexes of Cr(VI) and Ti(IV) [20].

The mathematical representation (rate law) is determined by individual steps in the reaction mechanism. Even though the reaction may proceed predominantly along one path, the mechanism can be quite complicated if it completely describes all possible paths for substitution. The rate laws of mechanisms described previously (e.g., I_a , I_d) apply to one path for one form of the metal (e.g., aquo complexed metal ion); in reality, however, substitution can proceed through the hydroxo form of the aquo ion as described above or through catalyzed processes involving H^+ or other ions. A term in the empirically observed rate law which has an *inverse* dependence on hydrogen ion concentration (e.g., $[\text{H}^+]^{-1}$) suggests a path via hydroxo species, while a term with *direct* dependence on the concentration of hydrogen or some other ion (e.g., $[\text{H}^+]$ or $[\text{Hg}^{+2}]$) indicates a path catalyzed by that ion.

Examples of some rate laws for substitution reactions are given in Table 3.2-7. These rate expressions show the strong dependence of the observed rate and observed rate constant on the magnitude of the individual step rate constants and concentrations of other species in solution.

TEMPERATURE

Temperature nearly always affects the magnitude of the rate constants. The rate of a chemical reaction generally varies with temperature according to the empirical Arrhenius expression:

$$k = A e^{-E_a/RT} \quad (19)$$

where k = rate constant (s^{-1})
 A = Arrhenius pre-exponential factor (s^{-1})
 E_a = activation energy (cal/mole)
 R = gas constant (1.99 cal/deg-mole)
 T = temperature (K)

Equation 19 can be rearranged to give

$$\log k = \log A - \frac{E_a}{2.303 RT} \quad (20)$$

TABLE 3.2-7
Rate Laws for Some Substitution Reactions^a

Reaction	Rate Law	Source
$\text{Cr}^{+3} + \text{Br}^- \rightleftharpoons \text{CrBr}^{+2} + \text{H}_2\text{O}$	$V = [(3.0 \times 10^{-8})(\text{Br}^-) + 3.6 \times 10^{-9}(\text{Br}^-)(\text{H}^+)^{-1}] (\text{Cr}^{+3})$	[24]
$\text{Fe}^{+2} + 3 \text{bipy} \rightleftharpoons \text{Fe}(\text{bipy})_3^{+2}$	$V = [(1.4 \times 10^{13})(\text{bipy})^3](\text{Fe}^{+2})$	[24]
$\text{CrSO}_4^{+} \rightleftharpoons \text{Cr}^{+3} + \text{SO}_4^{-2}$	$V = [(6.1 \times 10^{-7}) + (1.1 \times 10^{-7})(\text{H}^+)](\text{CrSO}_4^{+})$	[24]
$\text{Fe}^{+3} + \text{Cl}^- \rightleftharpoons \text{FeCl}^{+2}$	$V = [(9.4)(\text{Cl}^-) + (1.1 \times 10^4)(\text{Cl}^-)(\text{H}^+)^{-1}] (\text{Fe}^{+3})$	[24]
$\text{HCrO}_4^{-} + X^{+n} \rightleftharpoons \text{HCrO}_3X^{1-n}$	$V = [(10^5)(X)(\text{H}^+)](\text{HCrO}_4^{-})$	[20]
$\text{MoO}_4^{-2} + \text{HC}_2\text{O}_4^{-} \rightleftharpoons \text{MoO}_4\text{HC}_2\text{O}_4^{-3}$	$V = [(4.1 \times 10^2)(\text{HC}_2\text{O}_4^{-})](\text{MoO}_4^{-2})$	[20]
$\text{VO}^{+2} + \text{SO}_4^{-2} \rightleftharpoons \text{VOSO}_4^0$	$V^b = [(1.5 \times 10^3)(\text{SO}_4^{-2})](\text{VO}^{+2})$	[20]

a. Data at 25°C unless noted. V refers to rate for product formation (e.g., $d\text{CrB}^{+2}/dt$ for the first reaction) in M/s.

Term in [] in the rate law refers to k_{obs} . X^{+n} is a variety of Lewis bases. bipy = 2,2-bipyridyl.

b. Rate given is for outer to inner sphere complex conversion.

Most studies of the effect of temperature on rate derive values of E_a from graphical representation of $\log k$ vs. $1/T$. These plots exhibit a linear dependence of $\log k$ on $1/T$ (as expected from eq. 20) over a finite temperature range with a slope of $-E_a/2.303R$ and an intercept of $\log A$. Values of E_a for some substitution reactions are summarized in Table 3.2-8. With equation 21, the value of the rate constant can be extrapolated from one temperature to another given values of E_a and k at some point in the temperature domain for which linear dependence is valid.

$$\log k_{T_1} - \log k_{T_2} = \frac{E_a}{2.3R} \left(\frac{1}{T_1} - \frac{1}{T_2} \right) \quad (21)$$

where k_{T_1} and k_{T_2} are the rate constants at temperatures T_1 and T_2 respectively (in K).

TABLE 3.2-8
Activation Energies for Formation of Metal Complexes
from Aquo Complexes in Aqueous Solutions at 25°C

Metal Ion	Ligand	E_a (kcal/mole)
V^{+2}	bipy	15
Mn^{+2}	SO_4^{-2}	6
	Cl^-	9
Fe^{+2}	H_2O^*	8
Co^{+2}	SO_4^{-2}	6
Ni^{+2}	SO_4^{-2}	8
	$C_2O_4^{-2}$	15
	SCN^-	9
	NH_3	10
	en	12
	bipy	14
Cu^{+2}	HEDTA ⁻³	8
Cr^{+3}	SO_4^{-2}	28
	SCN^-	26
	H_2O^*	27
Fe^{+3}	Cl^-	17
	SCN^-	13
$FeOH^{+2}$	N_3^-	1
$Co(EDTA)H_2O^-$	H_2O^*	25

bipy = 2,2-bipyridyl

H_2O^* = labeled water

en = ethylenediamine

HEDTA = monoprotonated
ethylenediaminetetraacetate

Source: Eigen and Wilkins [8]

Example 2 To illustrate the effect of temperature on reaction rate and the use of equation 21, consider the rate of reaction of Cr^{+3} with SO_4^{-2} to give CrSO_4^+ at 15°C. The rate constant is $2.0 \times 10^{-6} \text{ M}^{-1} \text{ s}^{-1}$ at 25°C.

The following values are substituted in equation 21:

$$\begin{aligned} T_1 &= 298\text{K} \\ T_2 &= 288\text{K} \\ E_a &= 28,000 \text{ cal/mole (Table 3.2-8)} \\ R &= 1.99 \text{ cal/deg-mole} \\ \log k_{T_1} &= \log (2.0 \times 10^{-6}) = -5.7 \end{aligned}$$

We now calculate the rate constant at 288°K to be:

$$-5.7 - \log k_{288} = \frac{-28,000 \text{ cal/mole}}{(2.3)(1.99 \text{ cal/deg-mole})} \left(\frac{1}{298} - \frac{1}{288} \right)$$

$$\begin{aligned} \log k_{288} &= -6.4 \\ k_{288} &= 4.0 \times 10^{-7} \text{ M}^{-1} \text{ s}^{-1} \end{aligned}$$

The literature often provides activation energies in the form of enthalpies of activation, ΔH^\ddagger [3], which are related to E_a by equation 22.

$$\Delta H^\ddagger = E_a - RT \quad (22)$$

The entropy of activation, ΔS^\ddagger , is related to A by equation 23.

$$\Delta S^\ddagger = 2.303 R [\log A - \log (k_B T/h)] - R \quad (23)$$

where R = gas constant ($1.99 \text{ cal deg}^{-1} \text{ mole}^{-1}$)
 A = Arrhenius pre-exponential factor (s^{-1})
 k_B = Boltzmann constant ($1.38 \times 10^{-16} \text{ erg/deg}$)
 h = Planck constant ($6.62 \times 10^{-27} \text{ erg-s}$)
 T = temperature (K)

Data for ΔH^\ddagger and ΔS^\ddagger provide an additional source for calculating E_a and evaluating the effect of temperature on the rates.

EFFECT OF IONIC STRENGTH ON RATE CONSTANT

Rate constants are often provided at zero ionic strength or at values of ionic strength different from those encountered in the environmental system of concern. Since ionic strength affects many reaction rate constants, corrections are usually necessary. The effect of ionic strength on the magnitude of a biomolecular rate constant can be estimated by the following equation [24]:

$$\log k = \log k_0 + \frac{2 \alpha Z_A Z_B \sqrt{I}}{1 + \sqrt{I}} \quad (24)$$

where k = rate constant at ionic strength I
 k_0 = rate constant at zero ionic strength
 Z_A = charge on reactant A
 Z_B = charge on reactant B
 α = constant (0.52 at 25°C)
 I = ionic strength ($= \frac{1}{2} \sum Z_i^2 M_i$, where Z_i = charge of ion i and M_i = molar concentration of i)

This equation has been used quite successfully to correlate the effect of salt concentrations on rate constants for reactions involving ions [12,14]. In contrast to the variables discussed earlier, it is not necessary to know the chemical identity of the species involved in order to model the effect of ionic strength on rates. The limitations of this equation are similar to those expected for the Gunterberg and Davies equations (§ 2.6) for calculating activity coefficients.

According to equation 24, a plot of $\log(k/k_0)$ vs. $\sqrt{I}/(1 + \sqrt{I})$ would be linear with an intercept of zero. Such a plot for a variety of $Z_A Z_B$ product values is given in Figure 3.2-2. The equation predicts an increase in rate over that at $I=0$ with an increase in ionic strength when reactants are of the same charge sign; a decrease in rate is predicted as ionic strength increases if the charges are of opposite sign.

Example 3 What is the effect of increasing ionic strength from zero (infinite dilution) to 0.1 M on the rate of reaction of $\text{Co}(\text{NH}_3)_5 \text{Br}^{+2}$ with OH^- at 25°C?

The following parameter values apply:

α	=	0.52
Z_A	=	+2
Z_B	=	-1
I	=	0.1 M
k	=	rate constant at $I = 0.1 M$
k_0	=	rate constant at $I = 0 M$

Substituting these values in equation 24, we obtain

$$\begin{aligned} \log(k/k_0) &= \frac{2 \alpha Z_A Z_B \sqrt{I}}{1 + \sqrt{I}} = \frac{2(0.52)(+2)(-1)\sqrt{0.1}}{1 + \sqrt{0.1}} \\ &= -0.5 \end{aligned}$$

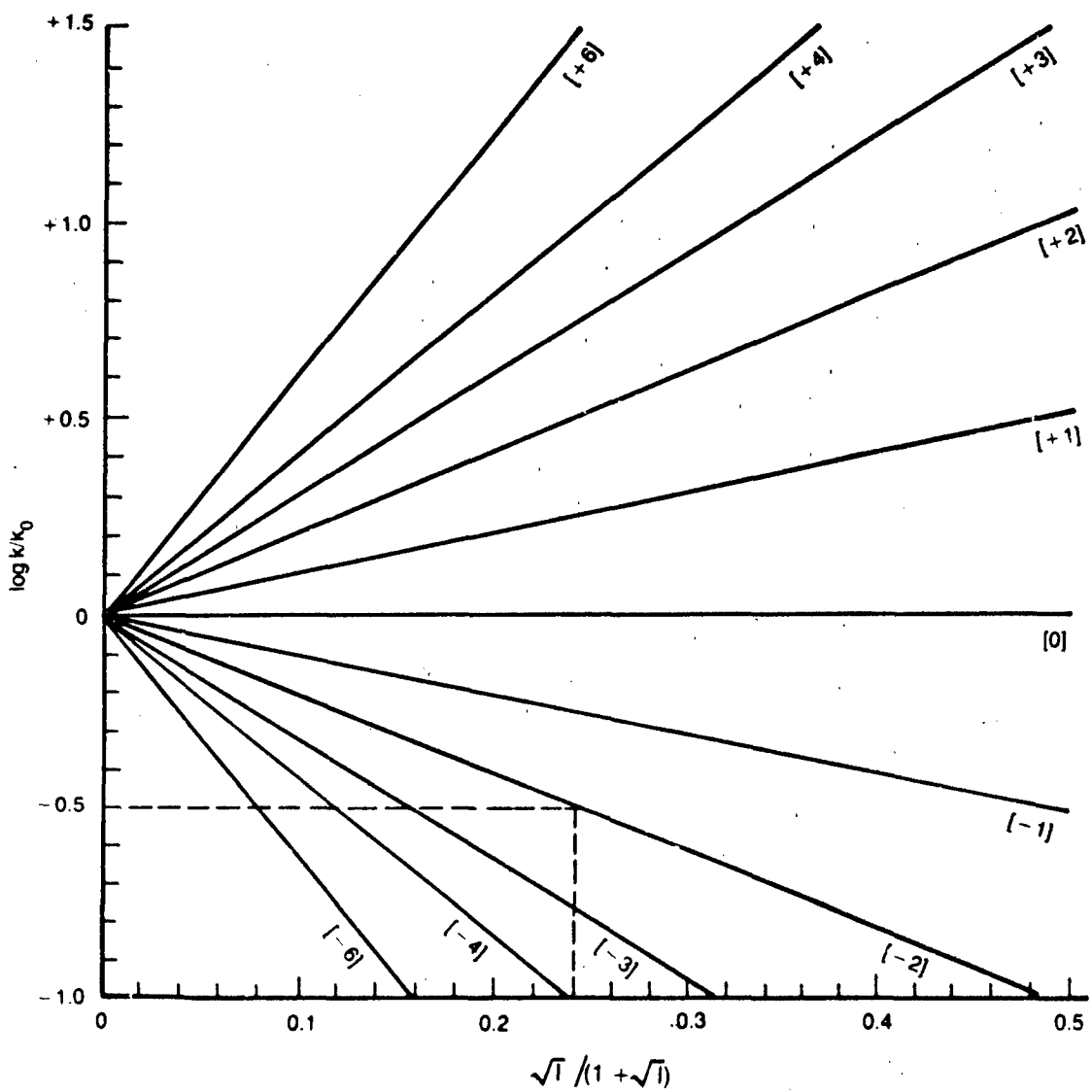
Thus, $\log k = \log k_0 - 0.5$, and $k = 0.316 k_0$.

Alternatively, we can use Figure 3.2-2 as follows:

Since $I = 0.1$, $\sqrt{I}/(1 + \sqrt{I}) = 0.24 M$

$$Z_A Z_B = (2)(-1) = -2$$

A vertical line drawn from 0.24 on the abscissa intersects the [-2] line at $\log(k/k_0) = -0.5$



k_0 is the rate constant at $I = 0$; k is the rate constant at I . Numbers in brackets are products of reactants' ionic charges $[Z_A Z_B]$.

Source: Equation 24

FIGURE 3.2-2 Effect of Ionic Strength on Rate Constants

Thus, the rate constant at $I = 0.1$ is estimated to be about one third that at $I = 0$, illustrating that even for ions of relatively low charge, the effect can be significant.

3.2.5 Sources of Data on Rates of Ligand Substitution

Kinetic data for ligand substitution reactions of metal complexes can be found in books dealing with mechanisms of inorganic reactions [2,4,24], and numerous review articles have described the reaction chemistry of a variety of metals and types of metal ion complexes [1,8,22]. In addition, journal articles that discuss reactions of particular species provide a source of specific rate constants.

The range of rates of substitution for reactions of aquo metal ions with common ligands (e.g., Cl^- , SO_4^{2-} , EDTA) was displayed in Figure 3.2-1; Figure 3.2-3 is a similar diagram for reactions of various metal ion complexes with other common ligands. As these figures show, the rates of substitution vary over a large range and are highly dependent on the chemical characteristics of the complex ion.

3.2.6 Estimation of Substitution Rates

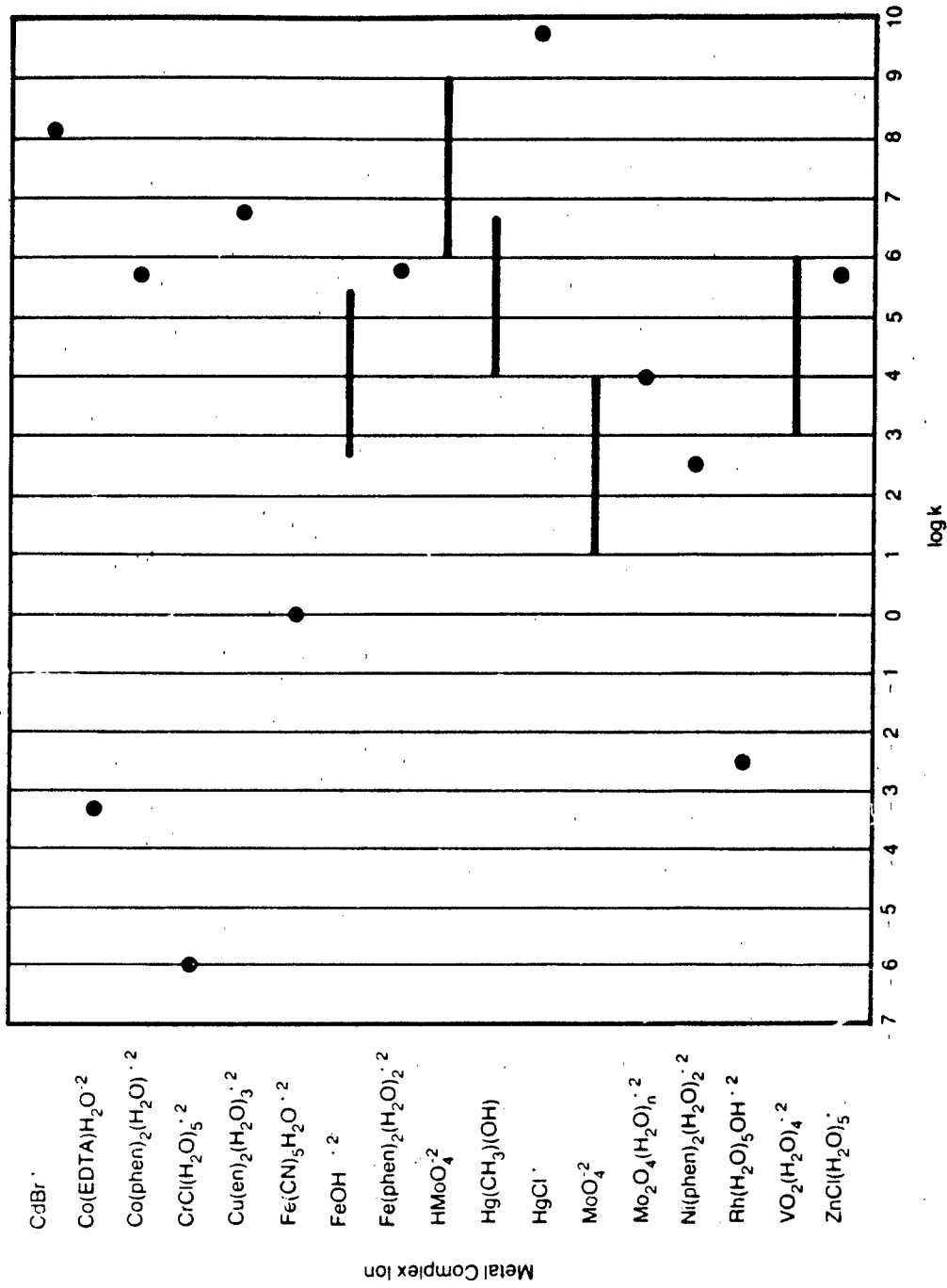
INTRODUCTION

Estimation of the rates of ligand substitution reactions is complicated by the diverse chemical behavior of metal ions, the presence of several complexes for a particular metal (speciation), the diverse properties of the incoming ligands and the variety of mechanisms by which substitution reactions can proceed. Even for a particular metal ion, generalizations are tenuous, in part because ligand substitution mechanisms can differ greatly for different complexes with the same central metal.

Nevertheless, as discussed in §3.2.2 through §3.2.5, general trends have been observed that allow qualitative estimates of rates of ligand substitution for a variety of species. The initial determination (semi-quantitative) of whether a metal ion is "inert" or "labile" was also discussed earlier; this determination allows an estimate of the need for further consideration of its behavior in a particular scenario (i.e., time frame of importance in the chemical environment of interest).

The rate constant for substitution is very specific to the particular species present under the environmental conditions, and approaches for its estimation are limited. In this section, four useful quantitative methods of estimation are described:

- (1) Use of water exchange rates (for dissociative mechanisms),
- (2) Use of the Edwards relationship (for associative reactions),
- (3) Use of derived molecular orbital bond energies, and
- (4) Use of linear free energy relationships (for an I_d ligand substitution mechanism).



Note: k is expressed in $M^{-1}s^{-1}$. Bars indicate the range of values for a variety of inorganic ligands, while dots represent a single value.

Sources: Eigen and Wilkins [8]; Saito and Sasaki [20]

FIGURE 3.2-3 Kinetic Data for Reactions of Common Ligands with Various Metal Complexes at 25°C

USE OF WATER EXCHANGE RATES

When loss of a coordinated water molecule is the rate-determining step in substitution (via the I_d mechanism, equations 13-17), the rate of formation of the product can be expressed as:

$$\frac{d[ML]}{dt} = k_{ML} [M] [L] \quad (25)$$

where

$$k_{ML} = K_{os} k_{H_2O} \text{ (equation 17)}$$

K_{os} = outer-sphere equilibrium constant for $[M, L]$ ion pair association (M^{-1})

k_{H_2O} = rate constant for metal-water bond rupture (s^{-1})

This relationship between k_{H_2O} and k_{ML} suggests that the mechanism of substitution for a series of ligands is dissociative; it can also be used as a predictive tool if the mechanism is expected to be dissociative.

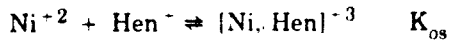
Values of k_{H_2O} (which is approximately equal to k_{ex} as defined in equation 11) are listed in Table 3.2-2 for a variety of metal ions. A method for estimating K_{os} is given in section 2.9.

Example 4 Rorabacher *et al.* [19] used equation 17 to estimate the rate of reaction of Ni^{+2} with Hen^+ (protonated ethylenediamine) at $25^\circ C$ and $I = 0.1 M$ from the rate of water exchange on Ni^{+2} as follows:

The reaction of interest is



The reaction that forms the intermediate ion pair (outer-sphere complex) is



By means of an equation similar to equation 11 in section 2.9, the value of K_{os} was calculated to be $0.038 M^{-1}$. ($Z_A = +1$, $Z_B = +2$, $a = 4.8 \text{ \AA}$ [from Table 2.9-5], $I = 0.1 M$.)

From Table 3.2-2, the value for k_{H_2O} on Ni^{+2} is $3 \times 10^4 \text{ s}^{-1}$. Thus,

$$k_{Hen^+} = K_{os} k_{H_2O} = (0.038 M^{-1}) (3 \times 10^4 \text{ s}^{-1}) = 1.1 \times 10^3 M^{-1} \text{ s}^{-1}$$

The observed experimental value is 6.3×10^2 [19].

USE OF THE EDWARDS RELATIONSHIP

Edwards [5,6] derived an equation based upon properties of metal ions and ligands which is useful for correlation of rate data for I- and I_a-type inorganic and organic reactions. The equation is:

$$\log k - \log k_0 = \alpha E_n + \beta H \quad (26)$$

where

- k = rate constant for substitution reaction of nucleophile (e.g., ligand) with electrophile (e.g., metal), $M^{-1} s^{-1}$
- k_0 = rate of substitution reaction of H_2O with electrophile (e.g., metal), $M^{-1} s^{-1}$
- α, β = empirical parameters specific to the electrophile (e.g., metal)
- E_n = electron donor constant for a specific nucleophile (e.g., ligand)
- H = basicity constant for a specific nucleophile (e.g., ligand)

Values of E_n and H for a variety of ligands and metals are given in Table 3.2-9. Thus, rates of substitution can be estimated by equation 26 based on the electrophilic and nucleophilic properties of the ligand and metal complex.

The values of H are related to pK_a as follows:

$$H = pK_a + 1.74 \quad (27)$$

and the values of E_n are related to E_o by

$$E_n = E_o + 2.70 \quad (28)$$

In the above equations, K_a is the acid dissociation constant of the protonated form of the ligand, and E_o is the electrode potential for reduction of the ligand. If values of K_a and E_o are not available, H and E_n can be estimated by empirical fitting of available kinetic data (equation 26).

Values of α and β in the Edwards relationship for electrophiles are empirically derived by fitting rate data (values of k and k_0) for reaction of a particular electrophile with a variety of nucleophiles (various values of E_n and H) to equation 26. Equation 29 is a convenient form of equation 26 that makes it easier to obtain values of α and β from a variety of rate data for different ligands.

$$(\log k - \log k_0)/E_n = \alpha + \beta(H/E_n) \quad (29)$$

TABLE 3.2-9
Electron Donor Constants and Basicity Parameters for Use in Equation 26^a

Species	E_n	H	Species	E_n	H
H_2O	0	0	$\text{C}_6\text{H}_5\text{NH}_2$	1.78	6.28
NO_3^-	0.29	0.4	SCN^-	1.83	1.00
SO_4^{2-}	0.59	3.74	NH_3	1.84	11.22
$\text{ClCH}_2\text{COO}^-$	0.79	4.54	$(\text{CH}_3\text{O})_2\text{PO}^-$	2.04	4.00
CO_3^{2-}	0.91	12.1	$\text{C}_2\text{H}_5\text{SO}_2\text{S}^-$	2.06	-5.00
CH_3COO^-	0.95	6.46	I ⁻	2.06	-9.00
$\text{C}_5\text{H}_5\text{N}$	1.20	7.04	$(\text{C}_2\text{H}_5\text{O})_2\text{PO}^-$	2.07	4.00
Cl^-	1.24	-3.00	$\text{CH}_3\text{C}_6\text{H}_4\text{SO}_2\text{S}^-$	2.11	-6.00
$\text{C}_6\text{H}_5\text{O}^-$	1.46	11.74	$\text{SC}(\text{NH}_2)_2$	2.18	0.80
Br^-	1.51	-6.00	$\text{S}_2\text{O}_3^{2-}$	2.52	3.60
N_3^-	1.58	6.46	SO_3^{2-}	2.57	9.00
OH^-	1.65	17.48	CH ⁻	2.79	10.88
NO_2^-	1.73	5.09	S ²⁻	3.08	14.66

a. Many values are empirically estimated, not calculated by equations 27 and 28.

Source: Edwards [5.6]

Example 5 Estimate the rate of reaction of Fe^{+3} with SO_4^{2-} using equation 26 with available data for reaction of Cl^- , SCN^- , and N_3^- .

Since the values of α and β for Fe^{+3} are not known for these reactions, they must be calculated from the following data, which is partly from Basalo and Pearson [2] and partly from Table 3.2-9:

Ligand	$\log k$ ($M^{-1} \text{s}^{-1}$)	E_n	H	$(\log k - \log k_o)/E_n$	H/E_n
H_2O	2.44 ⁸⁾	0	0	—	—
Cl^-	0.97	1.24	-3.00	-1.20	-2.4
SCN^-	2.10	1.83	1.00	-0.19	0.55
N_3^-	5.20	1.58	6.46	1.75	4.1

8. The value of $k_{\text{H}_2\text{O}}$ (s^{-1}) has been divided by 55.5 M (concentration of H_2O) to convert to a second-order rate constant in units of $M^{-1}\text{s}^{-1}$, like those for the other ligands.

A least-squares fit of the data for a plot of $(\log k - \log k_0)/E_n$ vs. H/E_n (eq. 29) gives values of $\alpha = -0.222$ and $\beta = 0.456$ for Fe^{+3} , with a correlation coefficient of 0.992.

We can now use these values of α and β , together with the values of E_n and H for SO_4^{2-} (Table 3.2-9), to estimate the rate of reaction of Fe^{+3} with SO_4^{2-} as follows:

$$\begin{aligned}\log k &= \alpha E_n + \beta H + \log k_0 \\ &= (-0.222)(0.59) + (0.456)(3.74) + 2.44 \\ &= 4.01 \text{ M}^{-1} \text{ s}^{-1}\end{aligned}$$

The experimental value is $3.80 \text{ M}^{-1} \text{ s}^{-1}$ [2].

USE OF DERIVED MOLECULAR ORBITAL BOND ENERGIES

Using a calculated value⁹ for the binding energy of water molecules in the first solvation sphere of cations [$E(I)$], Rode *et al.* [17] obtained the following linear correlation (with a correlation coefficient of 0.991) between the free energy of activation (ΔG^\ddagger) for rates of water exchange (k_{ex}) and values of $E(I)$ for 12 metals (see Table 3.2-10):

$$\Delta G^\ddagger = 0.118 E(I) + 1.3 \quad (30)$$

This approach illustrates the ability to calculate binding energies and, thus, rates of exchange of water.

TABLE 3.2-10

Binding Energies, $E(I)$, per Water Molecule
in First Hydration Shell of Cations^a
(kcal/mole)

Ion	Tetrahedral Coordination	Octahedral Coordination	Ion	Tetrahedral Coordination	Octahedral Coordination
Li^+	25.7	22.1	Mn^{+2}	—	63.8
Na^+	17.3	15.4	Fe^{+2}	—	69.9
K^+	14.7	14.2	Co^{+2}	—	75.2
Be^{+2}	116.1	105.4	Ni^{+2}	—	77.8
Mg^{+2}	59.4	50.5	Zn^{+2}	—	71.0
Ca^{+2}	47.1	46.9	Al^{+3}	—	134.3

a. Calculated (see footnote 9)

Source: Rode *et al.* [17]

9. Obtained by MESQUAC (Mixed Electrostatic Quantum Chemical) molecular orbital calculations [10,15-17].

Activation energy and rate are related by the "Eyring relationship":

$$k_{ex} = (k_B T/h) \exp(-\Delta G^\ddagger/RT) \quad (31)$$

Assuming that the rate of water loss is rate-determining, we can relate k_{ex} to $E(I)$ as follows:

$$k_{ex} = (k_B T/h) \exp\left(\frac{-(0.118E(I) + 1.3)}{RT}\right) \quad (32)$$

where

- k_B = Boltzmann constant (1.380×10^{-16} erg/deg)
 T = temperature (K)
 h = Planck's constant (6.62×10^{-27} erg-s)
 R = gas constant (1.987 cal/deg-mole)

Thus, at 298°K,

$$k_{ex} = (6.21 \times 10^{12}) e^{-(1.99 \times 10^{-4} E(I) + 0.0022)} \text{ s}^{-1}$$

Example 6 The value of k_{ex} for an octahedrally coordinated Al^{+3} ion at 298K can be derived using the calculated value of the binding energy of the first coordination water molecule (134.3 kcal/mole) from Table 3.2-10.

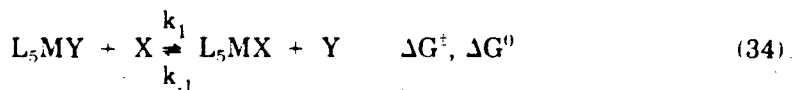
Using equation 33, we substitute 134,300 cal/mole for $E(I)$. Thus,

$$\begin{aligned} k_{ex} &= 6.21 \times 10^{12} e^{-(1.99 \times 10^{-4} (134.300) + 0.0022)} \\ &= 6.21 \times 10^{12} e^{-(26.73 + 0.0022)} \\ &= 6.21 \times 10^{12} (2.46 \times 10^{-12}) = 14.97 \text{ s}^{-1} \end{aligned}$$

The experimental value is approximately 1 s^{-1} (see Table 3.2-2).

USE OF LINEAR FREE ENERGY RELATIONSHIPS

The reaction path profile (see for example, Wilkins [24]) for an I_d ligand substitution mechanism is typified by reactions such as



where ΔG^\ddagger is the activation energy and ΔG^0 the overall free energy change for the reaction. Equation 34 suggests that for a series of different X ligands substituting the same Y ligand in L_5MY complex ion, a linear free energy relationship (LFER) applies [21], so that

$$\Delta G^\ddagger = -a \Delta G^0 + \text{constant} \quad (35)$$

where "a" is the slope of the LFER. Swaddle [21] notes that while values other than 1 have been observed for this slope, it is theoretically equal to 1 for an I_d mechanism.

Equation 35 can be used to calculate activation energies and, thus, rates for a reaction in a series if the overall free energy, ΔG^0 , is known. The consequence of $a = 1$ in this equation is that the *inverse* of reaction 34 proceeds at the same rate (k_{-1}), independent of the nature of Y. (See, for example, Haim [11].)

Equation 35 is more conveniently written as shown below, using the relationships between ΔG° and k_1 , and between ΔG° and K_1 (and recognizing that $K_0 = k_1/k_{-1}$).

$$\log k_1 = -\log K_0 + B \quad (36)$$

where

- k_1 = rate constant for reaction 34
- K_0 = equilibrium constant for reaction 34
- B = constant (equal to $\log k_{-1}$ for I_d mechanism)

This relationship is illustrated in the series of reactions of $[Co(NH_3)_5H_2O]^{+3}$ with various ligands [11,13]:



where



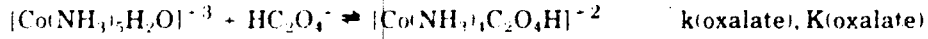
Example 7 With equation 36, the rate constant for the reaction of I^- with $[Co(NH_3)_5H_2O]^{+3}$ can be calculated using equilibrium constants and rate data for reaction of the cobalt complex with $HC_2O_4^-$.

The reaction of interest is



with $K(\text{iodide}) = 0.12 M^{-1}$ [11] and the rate constant for reaction with iodide being $k(\text{iodide})$.

The reference reaction is



with $k(\text{oxalate}) = 2.2 \times 10^{-4} \text{ s}^{-1}$ and $K(\text{oxalate}) = 35 M^{-1}$ [11].

Equation 36 can be modified to calculate $k(\text{iodide})$ as follows:¹⁰

$$\log k(\text{iodide}) = \log k(\text{oxalate}) - \log K(\text{iodide}) + \log K(\text{oxalate})$$

From the values given above,

$$\log k(\text{oxalate}) = -7.66$$

$$\log K(\text{oxalate}) = 1.54$$

$$\log K(\text{iodide}) = -0.92$$

$$\text{Thus, } \log k(\text{iodide}) = -7.66 - (-0.92) + (1.54) = -5.2$$

The observed value is -5.08 [11].

3.2.7 Literature Cited

1. Bamford, C.H. and C.F.H. Tipper (eds.), *Reactions of Metallic Salts and Complexes, and Organometallic Compounds*, Vol. VII of *Comprehensive Chemical Kinetics*, Elsevier Publishing Co., New York, 13 (1972).
2. Basolo, F. and R. Pearson, *Mechanisms of Inorganic Reactions*, John Wiley & Sons, New York (1967).
3. Bender, M.L. and L.J. Brubacher, *Catalysis and Enzyme Action*, McGraw-Hill Book Co., New York (1973).
4. Benson, D., *Mechanisms of Inorganic Reactions in Solution*, McGraw-Hill Book Co., London (1968).
5. Edwards, J.O., "Correlation of Relative Rates and Equilibria with Double Basicity Scale," *J. Am. Chem. Soc.*, **76**, 1540 (1954).
6. Edwards, J.O., "Polarizability, Basicity, and Nucleophilic Character," *J. Am. Chem. Soc.*, **78**, 1819 (1956).
7. Edwards, J.O. and R.G. Pearson, "The Factors Determining Nucleophilic Reactivities," *J. Am. Chem. Soc.*, **84**, 16 (1962).
8. Eigen, M. and R.G. Wilkins, "The Kinetics and Mechanism of Formation of Metal Complexes," in *Mechanisms of Inorganic Reactions*, R.K. Murman, R.T.M. Fraser and J. Bauman (eds.), Advances in Chemistry Series 49, American Chemical Society, Washington, D.C. (1965).
9. Espenson, J.E., "Formation Rates of Monosubstituted Chromium(III) Complexes in Aqueous Solution," *Inorg. Chem.*, **8**, 1554 (1969).
10. Fujiwara, S. and B.M. Rode, *Bull. Chem. Soc. Japan.*, **52**, 321 (1979).
11. Haim, A., "Some Comments on the Mechanism of Substitution Reactions of Cobalt(III) Complexes of the Pentaammine Class," *Inorg. Chem.*, **9**, 426 (1970).
10. The modified equation is derived by writing equation 36 for the iodide reaction and then for the oxalate reaction, subtracting the second equation from the first, and rearranging assuming the value of B is the same for both reactions.

12. Lamer, V.K., "Reaction Velocity in Ionic Systems." *Chem. Rev.*, **10**, 179 (1932).
13. Langford, C.H., "On the Acid Hydrolysis of $[Co(NH_3)_5X]^{+2}$ Ions and the Mechanism of Interchange," *Inorg. Chem.*, **4**, 265 (1965).
14. Livingston, R., "An Introduction to Chemical Catalysis in Homogeneous Systems," *J. Chem. Ed.*, **7**, 2887 (1930).
15. Rode, B.M. and G.J. Reibnegger, "MESQUAC: Mixed Electrostatic-Quantum Chemical Approach to the Description of Large Complexes," *J. Chem. Soc. Faraday Trans. 2*, **75**, 178 (1979).
16. Rode, B.M. and G.J. Reibnegger, *Monatsh. Chem.*, **110**, 813 (1979).
17. Rode, B.M., G.J. Reibnegger and S. Fujiwara, "Transition State Model for Water Exchange in the First Solvation Shell of Hydrated Cations According to Quantum Calculations," *J. Chem. Soc. Faraday Trans. 2*, **76**, 1268 (1980).
18. Rorabacher, D.B. and D.B. Moss, "Steric Effects in Chelation Kinetics: II. Role of Oxygen as a Donor Atom and the Internal Conjugate Base Effect in Cobalt(II)-Poly(amino alcohol) Reactions," *Inorg. Chem.*, **9**, 1314 (1970).
19. Rorabacher, D.B., T.S. Turan, J.A. Defever and W.G. Nickels, "Steric Effects in Chelation Kinetics: The Formation and Dissociation of Nickel (II) Complexes with Branched Poly(amino alcohols) Related to Ethylenediaminetetraacetic Acid," *Inorg. Chem.*, **8**, 1498 (1969).
20. Saito, K. and Y. Sasaki, *Substitution Reactions of Oxo Metal Complexes*, Vol. I of *Advances in Inorganic and Bioinorganic Mechanisms*, A.G. Sykes (ed.), Academic Press, New York, 182 (1982).
21. Swaddle, T.W., "Activation Parameters and Reaction Mechanism in Octahedral Substitution," *Coord. Chem. Rev.*, **14**, 217-68 (1974).
22. Swaddle, T.W., *Substitution Reactions of Divalent and Trivalent Metal Ions*, Vol. II of *Advances in Inorganic and Bioinorganic Mechanisms*, A.G. Sykes (ed.), Academic Press, New York (1983).
23. Taube, H., "Rates and Mechanisms of Substitution in Inorganic Complexes in Solution," *Chem. Rev.*, **50**, 69 (1952).
24. Wilkins, R.G., *The Study of Kinetics and Mechanism of Reactions of Transition Metal Complexes*, Allyn and Bacon, Boston (1974).

3.3 KINETICS OF ELECTRON TRANSFER (REDOX) REACTIONS

3.3.1 Introduction

The rate of electron transfer between oxidizing and reducing species is important in assessing speciation of inorganic materials in the environment. Assessing how fast a redox reaction will occur is complicated, requiring specific knowledge of the chemistry of the oxidant and reductant and the reaction mechanism, and consideration of all possible effects of the physical and chemical properties of the reaction medium. Accordingly, this section discusses the following topics:

- Exemplar scenarios involving redox reactions;
- Inner- and outer-sphere mechanisms of redox reactions and their mathematical representation;
- Exemplar rates and rate laws for some environmentally important redox reactions and species;
- Chemical and environmental factors affecting redox rates;
- Correlation and estimation of rates for particular mechanisms; and
- Sources of kinetic data.

Additional information on redox reactions, including a discussion of distribution between oxidized and reduced forms and redox mechanisms, is given in section 2.10.

3.3.2 Environmental Relevance

Differences in redox reaction rates can lead to products different from those predicted by equilibrium calculations. For example, although a particular reaction between species A and B may be thermodynamically favorable, the kinetics may be so slow that no reaction occurs in the time frame of interest. If a third species, C, is introduced into the system, reacts rapidly with A, and depletes it, the final distribution of products can be very different from that predicted by the thermodynamic calculation. In the real environment, this is illustrated by the disequilibrium conditions that are observed for many species, as discussed in section 2.10.

COMMON REDOX SCENARIOS

The following are the most common redox situations in the environment:

- a. Reactions between two dissolved components (homogeneous),
- b. Reactions between a component originally in the gas phase and a dissolved species (heterogeneous), and
- c. Reactions between a solid and a dissolved species (heterogeneous).

Examples of reactions that fall under these classifications are:

- a. Dissolved iron (II) with dissolved chromium (VI),
- b. Gaseous oxygen with dissolved iron (II), and
- c. Manganese dioxide (in soil) with dissolved chromium (III).

Although the sources of the two reactants may be in different phases (solid, liquid or gaseous), electron transfer occurs in a single phase. However, unlike reaction in a homogeneous phase, the presence of the source of the reactant as a separate phase can affect the reaction kinetics. For example, in the oxidation of sulfite by oxygen, the reaction occurs via the dissolved oxygen species, but the presence of a constant partial pressure of oxygen above the solution (together with other factors, such as the extent of turbulence) affects the level of dissolved oxygen in solution and thus the rate of the reaction. In the absence of the external source of oxygen and other dissolved ions, the reaction rate is predictable from the concentration of oxygen and sulfite present in solution. Similarly, continuous dissolution of iron (II) from a soil will affect its dissolved level and thus affect the rate of depletion of the oxidant reacting with the iron (II).

RATE-LIMITING STEPS

Various steps in redox mechanisms may control the overall reaction rate. These can be broadly characterized as relating to the availability of one of the reacting species (physical factors) or to the chemical behavior of species (chemical factors). The *physical factors* are exemplified by the following:

- Mode of contact of a solution with a gaseous reactant (such as the atmosphere);
- Availability and rate of dissolution of a reactant from a solid into a dissolved state (e.g., from wastes or soils); and
- Diffusion of dissolved reactants.

The *chemical factors* are exemplified by the following:

- Identity of the reactants [e.g., Fe (II) vs Mn (II)] as well as composition of the coordination sphere [e.g., $\text{Fe}(\text{H}_2\text{O})_6^{+2}$ vs $\text{Fe}(\text{CN})_6^{-4}$];
- Effects of the reaction medium on speciation of the reactants; and
- Mechanism of the formation of the activated complexes (i.e., the precursors to product formation, as discussed below).

An example of the balance between the chemical and physical factors that may limit rate is illustrated in the common mechanism for oxidation of dissolved metal ions, M, by oxygen as follows:

a. Dissolution of oxygen in water



b. Inner-sphere complex formation and subsequent electron transfer



When $k_1 pO_2 \gg k_2 [O_2^0][M]$, chemical kinetics control the rate; when this relationship is reversed, on the other hand, diffusion of oxygen controls the rate, and the physical geometry of the system (i.e., mode of contact) is of great importance in determining the rate.

In the following sections a greater emphasis is placed on the discussion of chemical factors and homogeneous redox reactions. The discussion is also useful for heterogeneous reactions, provided that some assumptions are made relative to the physical factors and mechanism of the reaction (e.g., that physical factors are not rate-limiting).

3.3.3 Mathematical Representation

Most commonly, redox reaction rates are characterized in the following ways:

- Half-life of the reaction ($t_{1/2}$)
- Observed rate constant (k_{obsd})
- Rate of change of concentration of a reactant or product ($d[C]/dt$)

The *half-life* of a reaction is defined as the time required for a reactant to reach half of its initial concentration. Half-life is usually used when the concentrations of all other species on which the rate depends are in large excess over that of the reactant of concern, so that pseudo first-order conditions apply, or when the reaction is actually first-order. Half-life is defined for higher order reactions but is not commonly used in those cases. In a first-order reaction, the half-life and the first-order rate constant are related by the equation $k = 0.693 t_{1/2}$ (See § 3.2 for an expanded discussion of this relationship.) A redox reaction that proceeds for over five half-lives can be considered essentially complete, as only about 3% of the original reactant remains after this time.

The *observed rate constant* is ordinarily measured under conditions in which all species that affect the rate of the redox reaction of a particular species R are defined

and their concentrations are kept constant.¹ The value of k_{obsd} is usually determined from a plot of $\ln[R]_{\text{eq}} - \ln[R]_t$ versus time, where $[R]_{\text{eq}}$ and $[R]_t$ are the concentrations of R at equilibrium and at time t, respectively. If the reaction is run under such conditions (termed pseudo-first-order), the relationship between the rate of the reaction expressed as dR/dt and the observed rate constant, k_{obsd} , is

$$d[R]_t/dt = k_{\text{obsd}} [R]_t \quad (3)$$

To determine the effect of different variables on observed rate constants, subsequent experiments such as the following can be performed:

- Variation in the concentration of the oxidant, [OX], at values above $10[R]$. A plot of the value of k_{obsd} versus [OX] then yields, for example, a function of the form $k_{\text{obsd}} = A[\text{OX}]$ when other variables are held constant.
- Variation in the concentration of $[\text{H}^+]$. A plot of the value of k_{obsd} versus $[\text{H}^+]$ could yield, for example, a function of the form: $k_{\text{obsd}} = B + C/[\text{H}^+]$ when other variables are held constant.
- Variation in the concentration of other ions in solution (such as chloride or sulfate) to determine the effect on the observed rate. A plot of the value of the observed rate constant versus chloride, for example, produces a function of the form: $k_{\text{obsd}} = D[\text{Cl}^-]$ when other variables, including acidity and concentration of oxidant, are held constant.
- Variation in the temperature to obtain activation energies; this allows calculation of the reaction rates at different temperatures and also helps to define the mechanism of the reaction.

The overall rate law can then be expressed as a function of these variables; for example,

$$d[R]_t/dt = E[\text{OX}][R]_t[\text{Cl}^-] + (F[\text{OX}][R]_t[\text{Cl}^-])/[\text{H}^+] \quad (4)$$

where the values of E and F are calculated from A, B, C and D given above.

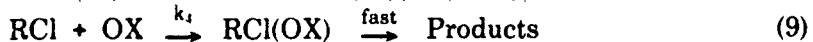
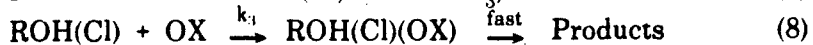
The expression for the rate law (equation 4) suggests the composition of the activated complex by which the reaction proceeds and thus is useful in postulating a reaction mechanism consistent with this rate law. Thus, equation 4 suggests that two types of activated complexes are important in determining the rate of the reaction. They are derived from each of the expressions in the rate law. As the first term in the expression contains R, OX and Cl^- , a structure consisting of all these in the activated complex is indicated, and can be represented as $[\text{R}-\text{Cl}--\text{OX}]^\ddagger$.

1. This is usually accomplished by using a buffer system or keeping the concentration of the reactant at least 10 times that of R, so that their concentrations undergo minimal change during the progress of the reaction.

Similarly, the second term in equation 4 suggests that a deprotonated form (minus the H⁺) of the above structure is also important. For example, if R is an aquo complexed metal ion, the deprotonated form is R-OH and the activated complex would be [OH-R-Cl--OX][‡]

These structures imply the reactions that must occur before the formation of the activated complex and allow us to write a stepwise mechanism for the redox reaction. For example, reactions to form R-Cl, OH-R-Cl, and R-OH are needed. Since the reactions to form the activated complex are rate-determining, we can assume that all subsequent reactions are faster.

The overall mechanism that fits the above rate law is as follows:



A proposed mechanism is said to be consistent with the observed kinetic rate law and kinetic data rather than proven, because only the structure of the activated complex is suggested and not the details of how that structure is derived from any prior reactions. Previous and subsequent reactions are generally postulated from experience.

The empirical parameters E and F in equation 4 can be expressed as a function of the rate constants in equations 5-9. For example, assuming that k₃ and k₄ are the rate-determining constants,

$$E = K_1 k_4 \quad \text{and} \quad F = K_2 K_3 k_3$$

As indicated earlier, the mathematical representation of the rate as

$$d[R]_t/dt = f(\text{concentrations})$$

can be very complex. It can be a function of the concentration of many species, including H⁺, complexing ions, reactants, intermediates and even products (where reactions are reversible), as well as physical factors such as temperature (discussed in § 3.4) and ionic strength (§ 3.2). The paths that may generate equation 4 include, for example, some involving the intermediate chloro and chloro-hydroxo complexes of the reactant R. More typically, these steps can include aquo ions, other complexes of the oxidant or reductant, products of acid or base dissociation and catalyst species.

It is noteworthy that the rate laws for one class of redox reactions are similar to those found for ligand substitution reactions (§ 3.2). This is due to the presence of a redox mechanism that is limited by the rate of substitution of one of the reactants, as discussed in § 3.3.4 and § 3.3.7.

3.3.4 Mechanisms and Rate Laws for Homogeneous Redox Reactions

INNER- AND OUTER-SPHERE REDOX MECHANISMS

To understand and predict the rate of a homogeneous redox reaction (not including one catalyzed by various ions), one should make a distinction as to whether the reaction proceeds via an inner-sphere or an outer-sphere process. (These processes are described in § 2.10.3 and illustrated in Figures 2.10-2, -3 and -4.) The particular path of electron transfer for a pair of reactants is determined by the relative ease of these two processes: if the outer-sphere path is too slow, redox will proceed via an inner-sphere process, and vice versa. In rare instances, the two processes are comparable in rate and both occur.

The general scheme proposed for a solution-phase redox reaction between a complexed metal ion (M) and a reductant (R) is as follows [7]:

(a) *Ion pair formation*



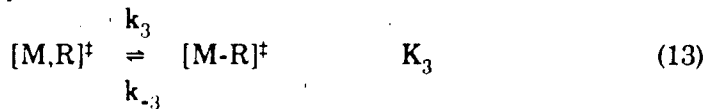
(b) *Activation of the ion pair*



(c) *Outer-sphere reaction of the activated ion pair*



(d) *Alternatively, conversion of the activated ion pair to an activated inner-sphere complex*



(e) *Electron transfer within inner-sphere activated complex and subsequent breakdown to products*



Step *a* represents a rapid equilibrium between the original reactants and an ion pair, which is activated (rearranged with respect to the metal-to-ligand bond distance) in step *b* prior to electron transfer and product formation in step *c* for an

outer-sphere process. Alternatively, the activated complex can form an inner-sphere complex in step *d*, followed by electron transfer and product formation in step *e*. An essential feature of the outer-sphere mechanism is that the first coordination spheres of both reactants and products remain intact throughout the process.

Two limiting rate laws for the outer-sphere process can be derived from the above mechanism:

- (1) If $k_{-1} \gg k_2$, the electron transfer is rate-limiting, and the rate law becomes:

$$d[M]/dt = K_0 K_1 k_2 [M][R] = k_{\text{obsd}} [M][R] \quad (15)$$

- (2) If $k_2 \gg k_{-1}$, activation of the ion pair is rate-limiting, and the rate law becomes:

$$d[M]/dt = K_0 k_1 [M][R] \quad (16)$$

In (1) above, the observed rate constant (k_{obsd}), and thus k_2 , is influenced by the overall free energy change (or equilibrium constant) of the redox reaction, and correlations between k_2 and free energy change represented in the aggregate by equations 10, 11 and 12 can be made (see § 3.3.7).

If electron transfer through an outer-sphere precursor (step *c*) is slow, the reaction may proceed through steps *a*, *b*, *d* and *e*, which represent an inner-sphere mechanism. This mechanism is possible only if one of the reactants has a ligand (e.g., Cl^- or OH^-) that can act as a bridge for electron transfer and if the accepting species is sufficiently labile. These and other aspects of the inner-sphere reaction are discussed later in this section.

Two limiting forms can be derived for this mechanism:

- (3) If $k_{-3} \gg k_4$ (indicating that electron transfer in the inner-sphere complex is rate-limiting), the rate law is

$$d[M]/dt = K_0 K_1 K_3 k_4 [M][R] \quad (17)$$

- (4) If $k_4 \gg k_{-3}$ and the rate of conversion of $[M \cdot R]^{\ddagger}$ to products is faster than dissociation of the complex, substitution can be limited by the rate of complex formation, and the rate law is

$$d[M]/dt = K_0 K_1 k_3 [M][R] \quad (18)$$

The limit corresponding to equation 18 is characterized by rate constants and activation parameters for the redox reaction with widely different reductants covering a small range of values. In addition, these rates and activation parameters are similar to those observed for substitution at the metal center. This limit is sometimes called a *substitution-controlled* redox reaction.

The rate laws given above are simplified forms of the generally observed rate laws, which typically include other terms, owing to the presence of competitive paths from species in equilibrium with the reactants; however, they are useful for understanding individual terms in rate laws. Table 3.3-1 summarizes the rate equations commonly encountered in inner-sphere redox processes for limiting situations.

EVIDENCE AND REQUIREMENTS FOR INNER-SPHERE REDOX REACTIONS

The preceding discussion suggests that one must classify the mechanism of a redox reaction in order to estimate its rate. The rates of inner-sphere reactions are chiefly a function of substitution (ligand exchange) rates, whereas rates of outer-sphere reactions are more sensitive to the overall free energy change of the reaction (e.g., differences in redox potentials between oxidant and reductant couples).

Redox reactions have been classified as *inner-sphere* processes on the basis of the following evidence [12]:

- Transfer of a ligand from one reactant to the other (see Figures 2.10-3 and -4);
- A redox reaction rate less than or equal to the rate of ligand replacement;
- The rate law is independent (i.e., zero order) in one important reactant (e.g., $[R]$ is missing from equation 18);
- The form of the rate law for the redox reaction is similar to that of substitution;
- Values of the activation energies for the redox reaction and those of substitution are similar; and/or
- Intermediate complexes are detected where the two reactants are bonded (e.g., M-R).

In addition, particular ligand properties are needed for an inner-sphere reaction to occur [14]. In the formation of the precursor to the electron transfer, a ligand bound to one of the reacting species becomes the bridge in the electron transfer step. The presence of a basic unshared pair of electrons on the bridging ligand is a necessary condition for the inner-sphere process. In general, the bridging ligand will have one or two sigma bonds and a lone pair available for electron transfer. Such is the case for M-O-H and M-S-CN. Each of these can act as a bridge for electron transfer. The unshared electron pair must be sufficiently basic to form a bond to the other reactant; thus, although the coordinated water molecule (M-H₂O) has a lone pair, it is not a good bridging ligand, because its basicity is too low. The coordinated ammonia ligand has no free lone pair and thus cannot act as a bridge. Similarly, carbon-bonded species such as M-CN have no lone pairs available on the carbon

TABLE 3.3-1
Rate Equations and Mechanisms for Inner-sphere Reactions

Mechanism	Steps	Comments	Rate Law
1	$\left\{ \begin{array}{l} MA_x \xrightleftharpoons[k_2]{k_1} MA_{x-1} + A \\ MA_{x-1} + B \xrightleftharpoons[k_4]{k_3} MA_{x-1}B \end{array} \right.$ $MA_{x-1}B \xrightarrow{k_5} \text{Products}$	Inner-sphere mechanism Dissociation of complex takes place prior to redox reaction	For k_1 rate-limiting: $\frac{d[\text{Prod}]}{dt} = k_1[MA_x]$ For k_3 rate-limiting: $\frac{d[\text{Prod}]}{dt} \approx \frac{k_1 k_3 [MA_x][B]}{k_2[A]}$ For k_5 rate-limiting: $\frac{d[\text{Prod}]}{dt} \approx \frac{k_1 k_3 k_5 [MA_x][B]}{k_2 k_4 [A]}$
2	$\left\{ \begin{array}{l} B + MA_x \xrightleftharpoons[k_1]{k_5} MA_{x-1}B + A \\ MA_{x-1}B \xrightarrow{k_5} \text{Products} \end{array} \right.$	Inner sphere Reducing agent is good nucleophile; aids in replacement of A ligand	For k_1 rate-limiting: $\frac{d[\text{Prod}]}{dt} = k_1[MA_x][B]$
3	$\left\{ \begin{array}{l} A + B \xrightleftharpoons{K_c} C \\ C \xrightleftharpoons{k_3} C^\ddagger \rightarrow \text{Products} \end{array} \right.$	Rapid precursor [C] formation Rate-limiting activation of precursor prior to electron transfer	For $[B] \gg [A]$: $\frac{-d[A_0]}{dt} = \frac{k_3 K_c [A]_0[B]}{1 + K_c[B]}$ $[A]_0 = [A] + [C]$
4	$\left\{ \begin{array}{l} MO_x^{-n} + 2H^+ \xrightleftharpoons{K_e} H_2MO_x^{2-n} \\ H_2MO_x^{2-n} + Y^- \xrightarrow{k_1} YM O_x^{-(n+1)} + H_2O \end{array} \right.$	Acid/base equilibrium of reactant Rate-determining substitution of reactant	$-d[MO_x^{-n}] = K_e k_1 [MO_x^{-n}][Y^-][H^+]^2$

Source: Edwards [12]

for direct bridging via an adjacent atom. A bridge can occur in either of the following ways:



I. Remote coordination

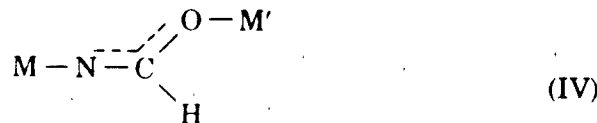


II. Adjacent coordination

Bridge formation can occur if the atom producing the bridge (e.g., B in I and A in II) has a lone pair available for bonding. However, an effective electron transfer bridge will occur only if the bridging structure is part of a conjugated system. For example, in structure III (below) remote coordination does not lead to an effective electron transfer bridge, since there is lack of conjugation between the oxygen and nitrogen after the other reactant is coordinated to the nitrogen.



In structure IV, a remote bridge is possible and effective, because conjugation is retained even after use of an electron pair on the oxygen for coordination to the other reactant.



Although the presence of a basic lone pair and conjugation are needed for inner-sphere redox, they do not necessarily guarantee it. For example, where the orbital symmetry of the donor and acceptor orbitals [14] is the same but different from that of the bridge system, conjugation is not sufficient; in this case, a stepwise process may occur in which the bridging group acquires an electron and is thus reduced, followed by transfer of the electron from the bridging group to the metal. The ability of the bridging ligand system to be reduced (or oxidized) then becomes an important parameter in determining the rate of reaction.

Some examples of known or suspected inner-sphere redox reactions are given in Table 3.3-2.

TABLE 3.3-2
Examples of Known or Suspected Inner-sphere Redox Reactions

Oxidant	Reducant(s) ^a	Oxidant	Reducant(s) ^a
$\text{Co}(\text{C}_2\text{O}_4)_3^{-3}$	Fe^{+2}	SeO_3^{-2}	I^- , ketones
$\text{P}_2\text{O}_8^{-4}$	$\text{Fe}(\text{terpy})_3^{+2}$	$\text{Mn}(\text{III})$	Various ($\text{C}_2\text{O}_4^{-2}$, N_2H_4 , HN_3 , HNO_2)
$\text{P}_2\text{O}_8^{-4}$	$\text{Fe}(\text{phen})_3^{+2}$	$\text{Fe}(\text{III})$	Various (I^- , $\text{S}_2\text{O}_3^{-2}$, N_2H_4)
$\text{P}_2\text{O}_8^{-4}$	$\text{Fe}(\text{bipy})_3^{+2}$	$\text{S}_2\text{O}_8^{-2}$	$\text{Fe}^{+2}, \text{Ag}^+$
$\text{P}_2\text{O}_8^{-4}$	$\text{VO}^{+2}, \text{Ag}^+, \text{Fe}^{+2}$	HNO_2	I^- , N_3^- , N_2H_5^+ , HSO_3^-
XO_m^{-n} ($\text{X}=\text{Cr, S, Br, Cl, N}$)	Various reducing species (e.g., I^- , Br^- , Cl^- , $\text{As}(\text{OH})_3$, SO_3^{2-})	Ti^{+3}	Br^-
HCrO_4^-	Various (I^- , Br^- , N_2H_4 , $\text{As}(\text{OH})_3$, H_3PO_2 , H_3PO_3)	H_3AsO_4	I^-
TeO_4^{-2}	Glycol	$\text{Ce}(\text{IV})$	Br^- , H_3PO_2 , Cl^- , glycols
IO_4^{-2}	Glycol	I_2	$\text{S}_2\text{O}_3^{-2}$
H_2O_2	HNO_2	Br_2	N_3^-

^a terpy = terpyridine; phen = 1,10-orthophenanthroline; bipy = bipyridyl
Source: Benson [6] and Edwards [12]

EVIDENCE FOR AN OUTER-SPHERE PROCESS

An outer-sphere redox mechanism is indicated on the following bases [6]:

- The ligands that are bonded to both reacting species and that constitute the first coordination shells are substantially inert to substitution, and the rate of the redox reaction is faster than the substitution rate on each of the species.
- The coordination shell of one reactant is rather kinetically inert to substitution, and no ligands capable of forming a bridge are present on this inert metal center.
- The rate law is first-order in each reactant (without modification of the ligands bonded to it).
- The rates of a series of related reactions are very dependent on the difference in electrode potentials between the reacting couples.

Some examples of known or suspected outer-sphere redox reactions are given in Table 3.3-3. It should be noted that the high substitution rates for many aquo metal ion complexes normally preclude assignment of mechanisms based on the rates of ligand exchange. The reactions between persulfate ($S_2O_8^{2-}$) and iron (II) complexes of N-(2-pyridylmethylene) aniline are examples of oxidations that proceed by parallel inner- and outer-sphere mechanisms [12].

TABLE 3.3-3

Examples of Known or Suspected Outer-Sphere Redox Reactions

Oxidant ^a	Reducant ^a
Co^{+3}	Fe^{+2}
Ce(IV)	$Fe(CN)_6^{-4}$
$Mo(CN)_8^{-3}$	$Fe(CN)_6^{-4}$
$IrCl_6^{-2}$	$Mo(CN)_6^{-4}$
$Co(NH_3)_6^{+3}$	$Ru(NH_3)_5^{+2}$
$Co(NH_3)_6^{+3}$	Cr^{+2}
$S_2O_8^{2-}$	$Fe(\text{terpy})_3^{+2}$
$S_2O_8^{2-}$	$Fe(\text{phen})_3^{+2}$
$S_2O_8^{2-}$	$Fe(\text{bipy})_3^{+2}$
Haloamine complexes of Pt(IV)	V^{+2}

a. phen = 1,10-o-phenanthroline; terpy = terpyridyl; bipy = bipyridyl.

Source: Benson [6] and Lappin [19].

OTHER REDOX MECHANISMS

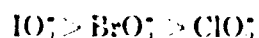
Among the less frequently encountered mechanisms of redox reactions are direct group transfer [18] and free-radical oxidation [4]. Because these are of lesser importance in transition-metal chemistry, and since methods for estimating the rates of these processes were not readily found, they are not discussed here.

3.3.5 Examples of Redox Rates, Rate Laws and Trends

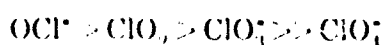
TRENDS IN OXYANION REDOX REACTIONS

Oxyanion species (XO_m^{+n}) often react via substitution of the oxygen atom. Thus, the rates of redox reactions of the various oxyanions are related to the rate of substitution of the oxygen at the central atom. A few parallels in the rate of redox by a variety of oxyanions are generally observed, and these are useful in estimating relative rates [12].

- The rate of oxidation by halates generally follows the order of:



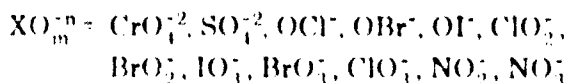
and oxychlor species,



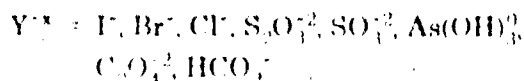
- Oxidations by perchloric, sulfuric, selenic and nitric acids in aqueous systems are generally slow, while those by chlorous, sulfurous, selenous and nitrous acids are faster.
- Within a periodic table group, for the same oxidation state, the oxyanion whose central atom has the higher atomic number generally reacts faster. For example, arsenic acid reacts more rapidly than phosphoric acid, periodate more rapidly than perchlorate, and telluric more rapidly than either sulfuric or selenic.
- Redox reactions for a large number of oxyanions follow one of the following rate laws:

(a) $\text{Rate} = k [XO_m^{+n}] [Y^{-x}] [H^+]^2$

where

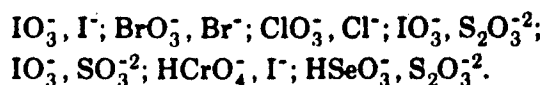


and



$$(b) \quad \text{Rate} = k [XO_m^{-n}] [Y^{+x}]^2 [H^+]^2$$

for reactions between the following pairs of species:



- Oxygen exchange reactions generally follow one of the following rate laws:

$$(a) \quad \text{Rate} = k [XO_m^{-n}] [H^+]^2$$

This equation applies, for example, to sulfate, nitrate, chlorite, bromite, carbonate and nitrite ions.

$$(b) \quad \text{Rate} = k [XO_m^{-n}] [H^+]$$

This equation applies, for example, to iodite, rhenate, hypobromite and hypochlorite ions.

There are exceptions to these trends. For example, relative rates of reduction of chromate by a variety of two-equivalent reducing agents vary widely for no obvious reason [5]. Some correlation between the rate of oxidation and the reduction potential of the reducing species has been noted for chromate (see Figure 3.3-1), but several exceptions do occur.

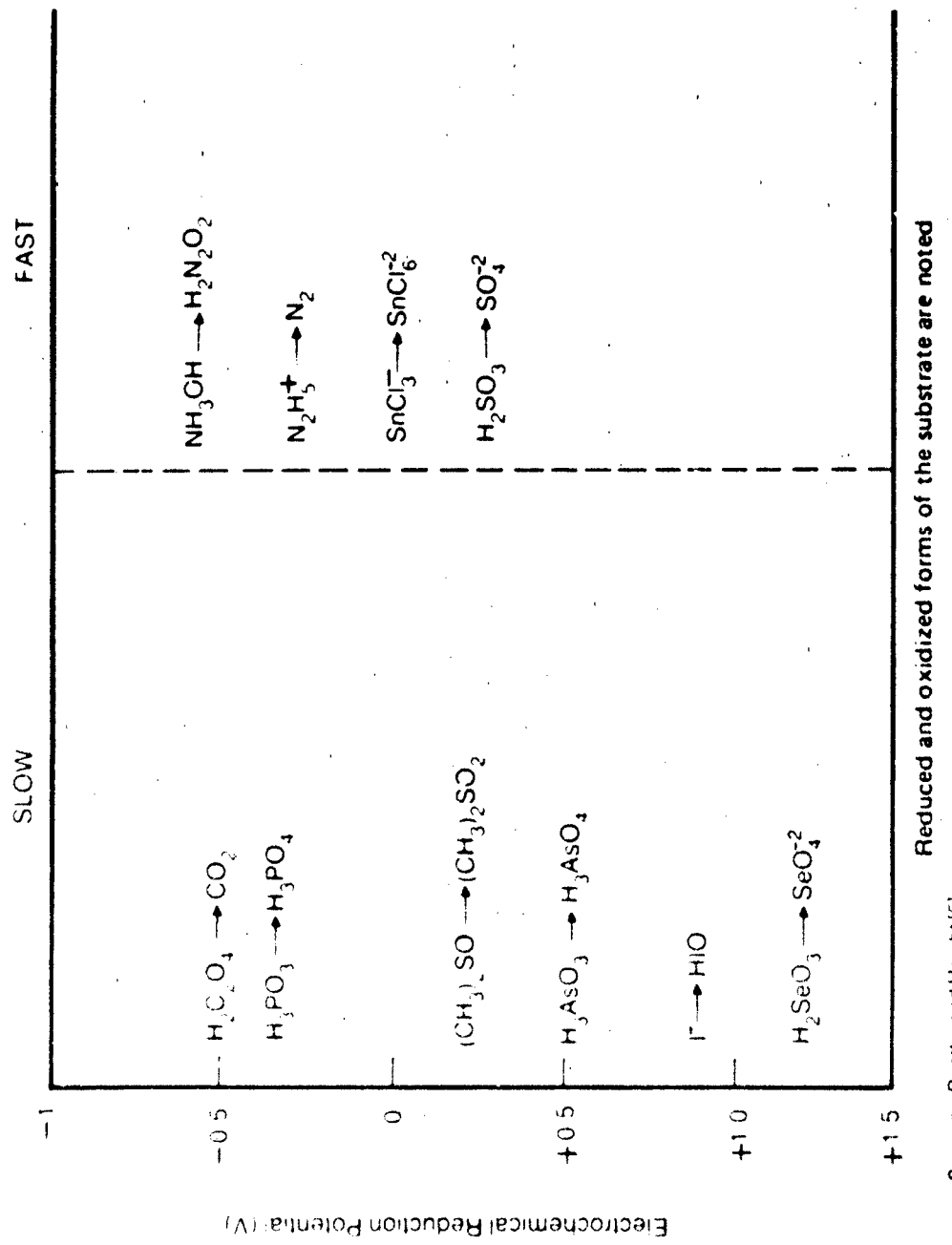
Of the oxyanions discussed above, chromate is of major environmental concern. A variety of redox processes for conversion of chromium (VI) to chromium (III) and vice versa have been noted [22, 25, 26]. These include oxidation of chromium (III) by oxygen (with or without promotion by uv light) and by manganese dioxide. Reduction of chromium (VI) by iron (II), sulfides, and sulphydryl groups in organic matter have similarly been noted. The rates of these and other environmentally relevant reactions of chromium are summarized in Table 3.3-4.

OXIDATION OF IRON(II)

Oxidation of iron(II) by oxygen at a pH of 6 - 7.5 and in the absence of catalytic or other contaminant effects obeys the following rate law [27]:

$$\text{Rate} = d[\text{Fe(II)}]/dt = k [\text{Fe(II)}] [\text{OH}^-]^2 P_{O_2} \quad (19)$$

The value of k at 20.5°C is $1.5 \times 10^{13} \text{ l}^2 \text{ mol}^{-2} \text{ atm}^{-1} \text{ min}^{-1}$. Thus, for a pH of 7.35, a partial pressure of oxygen of 0.195 atm, and a temperature of 20.5°C, the observed first-order rate constant ($k_{\text{obsd}} = k \times [\text{OH}^-]^2 P_{O_2}$) is equal to 0.147 min^{-1} , which corresponds to a half-life of 4.7 minutes. The oxidation of iron(II) by oxygen is, however, efficiently catalyzed by a variety of species, including copper(II), cobalt(II), manganese(II), manganese dioxide, zeolite and dihydrogen phosphate.



Source: Beattie and Haight [5]

FIGURE 3.3.1 Relative Rates of HCrO_4^- Oxidations of Various Species

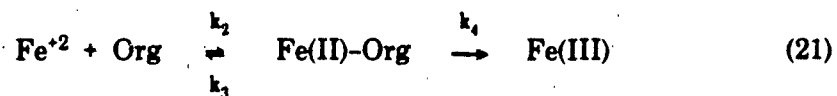
TABLE 3.3-4
Kinetic Data for Redox Reactions of Chromium

Reaction	[Cr] ^a	[Br] ^b	Temp. (°C)	pH	Buffer/Medium	Rate or Half-life	Ref.
Cr(III) + O ₂	125 $\mu\text{g/l}$		25 35	8.6 8.1	10 ⁻² M KHCO ₃ Seawater/0.02 M borate	0.09 $\mu\text{g/l/d}$ 1.2 $\mu\text{g/l/d}$	[25]
Cr(III) + O ₂	10 ⁻⁵ M	Bubbling	25	8.1	Seawater/0.02 M borate	$t_{1/2} >> 12 \text{ d}$	[22]
Cr(III) + MnO ₂	125 $\mu\text{g/l}$	25 mg/l	25	8.6	10 ⁻² M KHCO ₃	$t_{1/2} = 42 \text{ min}$	[25]
Cr(III) + MnO ₂		250 mg/l	25			$t_{1/2} = 3 \text{ min}$	[25]
Cr(III) + γ-MnOOH (with 10 ⁻³ citric acid)	10 ⁻⁵ M	500 mg/l	25	8.1	Seawater/0.02 M borate	$t_{1/2} >> 12 \text{ d}$	[22]
Cr(III) + γ-MnOOH	10 ⁻⁵ M	30 mg/l	25	8.1	Seawater/0.02 M borate	5% in 2 d	[22]
Cr(V) + Fe(II)	100 $\mu\text{g/l}$	0.4 mg/l	N.C.	7.5	10 ⁻² M	$t_{1/2} \sim 6 \text{ min}$	[25]
Cr(V) + Fe(II)		1.2 mg/l	N.C.	7.1	10 ⁻² M	$t_{1/2} \sim 2 \text{ min}$	[25]
Cr(V) + S ²⁻	100 $\mu\text{g/l}$	10 ⁻³ M	N.C.	9.1	N.C.	$t_{1/2} < 5 \text{ min}$	[25]
Cr(V) + Cysteine	100 $\mu\text{g/l}$	10 ⁻³ M	N.C.	N.C.	N.C.	$t_{1/2} \sim 20 \text{ min}$	[25]
Cr(V) + Mercapto-succinic acid	100 $\mu\text{g/l}$	10 ⁻³ M	N.C.	N.C.	N.C.	$t_{1/2} < 5 \text{ min}$	[25]
Cr(V) + Alanine	100 $\mu\text{g/l}$	10 ⁻³ M	N.C.	N.C.	N.C.	$t_{1/2} >> 1 \text{ d}$	[25]
Cr(V) + Succinic acid	100 $\mu\text{g/l}$	10 ⁻³ M	N.C.	N.C.	N.C.	$t_{1/2} >> 1 \text{ d}$	[25]
Cr(V) + Ascorbic acid	10 ⁻⁵ M	10 ⁻⁶ M	25	8.0-12	Seawater/0.02 M borate	$t_{1/2} < 72 \text{ hr}$	[22]
Cr(V) + Ascorbic acid	10 ⁻⁵ M	10 ⁻⁶ M	25	20-8	Seawater/0.02 M borate	$t_{1/2} >> 72 \text{ hr}$	[22]
Cr(V) + Humic acid	10 ⁻⁵ M	10 ⁻⁶ M	25	7.5-12	N.C.	$t_{1/2} >> 72 \text{ hr}$	[22]
Cr(V) + Humic acid	10 ⁻⁵ M	10 ⁻⁶ M	25	20-7	N.C.	$t_{1/2} < 72 \text{ hr}$	[22]
Cr(V) + Fulvic acid	1.9 × 10 ⁻⁶ M	DOC at 5.8 mg/l	25	59	Groundwater	$t_{1/2} \sim 5 \text{ d}$	[26]
Cr(V) + H ⁺ b.c.		1.9 × 10 ⁻⁶ M	0.04 M	25	< 2.0 Aqueous acid	1-10% loss per 29 days	[26]

a [Br] = concentration of second reactant c H⁺ added as HCl, H₂SO₄, or HNO₃
 b 4HCrO₄ + 16H⁺ = 4Cr³⁺ + 3CO₂ + 10H₂O NC = Not cited

ion. Also, ions that form strong complexes with iron(III) and metal ions that can react directly (via electron transfer) with iron(II) can apparently catalyze the reaction [27].

Both oxidation states of iron can be stabilized by the presence of complexing organic matter, and this can change the oxidation rate. The effect of organic species (Org) on the rate of iron(II) oxidation can be interpreted in terms of the occurrence of two parallel routes for oxidation:



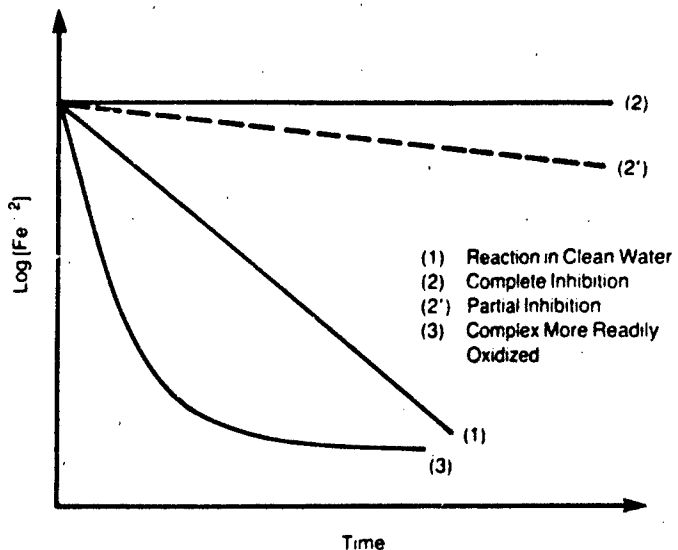
where $k_2/k_3 = K$, the formation constant for the Fe(II)-Org complex.

Limiting cases of the above mechanism (see Figure 3.3-2) explain the observed effects of a variety of organic substances on the rate of oxidation. For example, for vanillic acid, phenol, syringic acid and histidine, the value of K is small and $k_4 \ll k_1$; this results in a very small amount of iron(II) being complexed and little effect on the rate of oxidation (curve 1). When K is large and $k_4 \ll k_1$, an oxidation-resistant complex is formed; depending on the value of k_4 , total or partial inhibition of oxidation (curves 2 and 2') occurs. This condition is observed in the presence of tannic acid and glutamine. When $k_4 \gg k_1$, the complex formed is oxidized more rapidly than aquo iron(II), and an enhanced rate (curve 3) is observed.

Rates and rate laws of other redox reactions of iron(II) are given in Table 3.3-5. Reactions with mercury(II), thallium(III) and nitrite are relatively slow, while those with chlorine, cerium(IV) and vanadium(V) are fast.

OXIDATION OF MANGANESE(II) BY OXYGEN

The kinetics of oxidation of manganese(II) by oxygen in waters resembling those of natural systems has been studied [15]. At pH 9, the oxidation to Mn(IV) and subsequent precipitation is complete within minutes; the half-life is approximately 1.5 min. At a lower pH, the reaction is much slower ($t_{1/2} \approx 30$ min at pH 8.5). The reaction rate is inhibited by species that form strong complexes with manganese(II). The presence of 2000 ppm of sulfate inhibits the rate at pH 9, and a half-life of 80 min is observed. Similarly, the presence of 100 ppm of bicarbonate ions increases the half-life to 60 min at pH 9. Catalysis of the reaction by copper(II) has been reported; like the reaction of iron(II) with oxygen, this reaction is probably also catalyzed by a variety of species.



Source: Adapted from Figure 5 in Theis and Singer [29]

FIGURE 3.3-2 Effect of Organic Complexation of Fe^{+2} on Reaction with Oxygen

TABLE 3.3-5
Some Redox Reactions of $\text{Fe}(\text{II})$

Oxidant	Rate = $d[\text{Fe}(\text{II})]/dt$	Rate Constant ^a	Ionic Strength (M)	Temperature (°C)
Cl_2	$2k_1 [\text{Fe}(\text{II})] [\text{Cl}_2]$	9.1×10^2	1	30
Ce(IV)	$k_1 [\text{Fe}(\text{II})] [\text{Ce}(\text{IV})]$	5865	2	0.3
Hg(II)	$k_1 [\text{Fe}(\text{II})] [\text{Hg}(\text{II})]$	2.0×10^{-6}	c	80
Mn(III)	$k_1 [\text{Fe}(\text{II})] [\text{Mn}(\text{III})]$	1.67×10^4	1	25
NO_2^-	$\left\{ \begin{array}{l} k_1 [\text{Fe}(\text{II})] [\text{NO}_2^-] \\ k_1 [\text{H}^+] [\text{Fe}(\text{II})] [\text{NO}_2^-] \end{array} \right.$	7.8×10^{-3} 0.227^b	c	25
V(V)	$\left\{ \begin{array}{l} k_1 [\text{VO}_2^+] [\text{Fe}(\text{II})] \\ k_1 [\text{H}^+] [\text{VO}_2^{+2}] [\text{Fe}(\text{II})] \end{array} \right.$	60 3400 ^b	c	c

a. Value of k_1 in $\text{M}^{-1} \text{s}^{-1}$ unless noted

b. Units are $\text{i}^2 \text{M}^2 \text{s}^{-2}$

c. Not available

Source: Banford and Tipper [3].

OXIDATION OF SULFIDE BY OXYGEN

The rate of oxidation of sulfide has been determined in both freshwater and seawater media [1,2,8,23]. These rates are summarized in Table 3.3-6. The reaction is relatively slow. At a sulfide concentration of greater than 50 $\mu\text{mol/l}$ the reaction obeys the following rate law [1]:

$$-\frac{d[\text{S(-II)}]}{dt} = k_1 [\text{S(-II)}] [\text{O}_2^0] = k_2 [\text{S(-II)}] \quad (22)$$

where S(-II) is the sum of sulfide, hydrosulfide and dissolved hydrogen sulfide.

The value of the pseudo-first-order rate constant k_2 at room temperature and pH 8 in seawater saturated with oxygen is $3 \times 10^{-5} \text{ min}^{-1}$.

TABLE 3.3-6
Rates of Oxidation of Sulfide by Oxygen in Natural Systems^a

Aqueous Medium	$[\text{O}_2]$ (μM)	$[\text{S(-II)}]_0$ (μM)	pH	Order with Respect to $[\text{S}^{2-}]$	$t_{1/2}$ (min)	Ref.
Fresh water	5	100	> 11.0	1.0	130	[2]
Fresh water	800	100	9.4	1.34	3000	[8]
Seawater	200	50	8.0	1.0	180	[1]
Seawater	200	200	8.0	1.0	280	[1]
Seawater	200	40	8.2	1.0	24	[23]

a. Temp. = 23-25°C.

ENVIRONMENTAL REACTIONS OF ARSENIC(III) AND ARSENIC(V)

Laboratory data from experiments using redox agents typically found in natural waters, such as oxygen, hydrogen sulfide and iron(III), suggest that their reactions with dissolved arsenic species occur slowly [9] and that the rates should be considered in speciation calculations. The change in concentration of arsenic(III) and arsenic(V) with time by reaction with these species is shown in Figure 3.3-3.

OXIDATION BY OZONE

The aqueous oxidation of many species by ozone has been studied, and their rates were recently reported [17]. The reactions generally obey the following rate law:

$$\text{Rate} = k_{\text{O}_3} [\text{O}_3] [\text{Reducing Agent}] \quad (23)$$

Values of k_{O_3} for a number of inorganic reducing agents are given in Table 3.3-7.

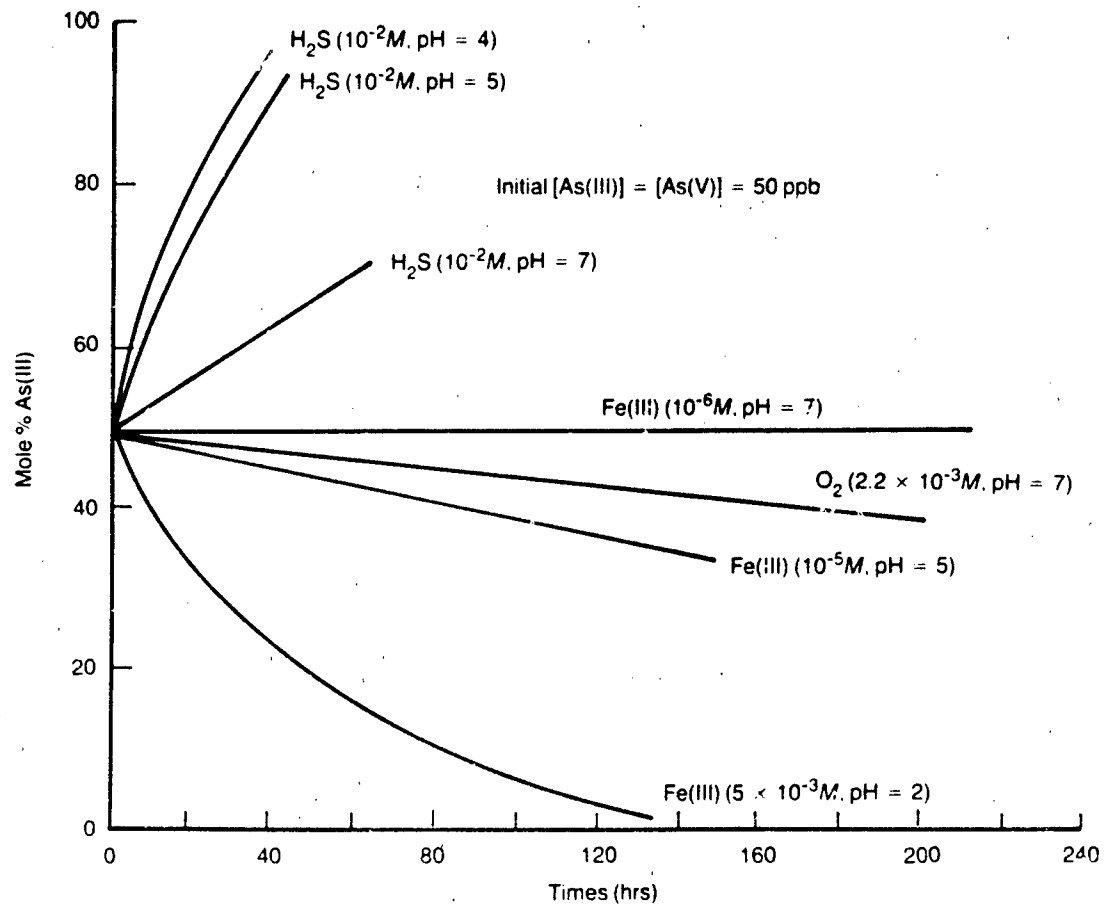
3.3.6 Chemical and Environmental Factors Affecting Rates

ONE- AND TWO-EQUIVALENT REDOX AGENTS

Oxidizing and reducing agents can be classified as one-equivalent, two-equivalent and one-two-equivalent. These refer to the following reactions:

- (a) $X(N) \longrightarrow X(N+1)$; one-equivalent process
- (b) $X(N+1) \longrightarrow X(N+2)$; one-equivalent process
- (c) $X(N) \longrightarrow X(N+2)$; two-equivalent process

where $X(N)$ is species X in the Nth oxidation state.



Source: Cherry, Shaik, Tallman and Nicholson [9]

FIGURE 3.3-3 Rates of Conversion of As(III) and As(V) by Different Reactants

TABLE 3.3-7
Rate Constants for Aqueous Oxidations by Ozone^a

Substrate	k_{O_3} (M ⁻¹ s ⁻¹)	Substrate	k_{O_3} (M ⁻¹ s ⁻¹)
Cl ⁻	~0.003	CN ⁻	$10^3 - 10^5$
Br ⁻	160	O CN ⁻	<10 ⁻²
I ⁻	>10 ⁶	HO CN	<10 ⁻²
HOCl	<0.002	HS ⁻	3×10^9
OCl ⁻	120	H ₂ S	3×10^4
HOBr	<0.01	H ₂ SO ₃	2×10^4
OB r ⁻	530	HSO ₃ ⁻	3.2×10^5
ClO ₃ ⁻	<10 ⁻⁴	SO ₃ ⁻²	1×10^9
BrO ₃ ⁻	<10 ⁻³	Fe ⁺²	>5 × 10 ⁵
IO ₃ ⁻	<10 ⁻⁴	H ₂ O ₂	<10 ⁻²
IO ₄ ⁻	<10 ⁻²	HO ₂ ⁻	5.5×10^6
NH ₃	20	Co ⁺²	0.6

a. Rate = $k_{O_3} [O_3] [\text{substrate}]$. Temperature = 20-23°C.

Source: Hoigné [17]

Species that can react via both (a) and (b) are termed one-two-equivalent agents, while those that react only via (a) are one-equivalent and only via (c) are two-equivalent agents, respectively. For example, Fe(III) produces Fe(II) when it gains one electron. Since Fe(II) is not further reduced by additional electrons, the Fe(III) is only a one-equivalent agent. The process of reducing I₂ to 2I⁻ can occur by simultaneous gain of two electrons, so I₂ is a two-equivalent agent. One-two-equivalent agents are exemplified by transition metal ions that form stable intermediate oxidation states when gaining electrons. For example, V(V) can form V(IV) by gain of one electron or V(III) by gain of two electrons and is thus a one-two-equivalent agent. Examples of other species in each of these categories are shown in Table 3.3-8.

The following general observation regarding the rates of redox reaction between species in these categories has been noted [4]:

- Redox reactions between noncomplementary reactants (i.e., a one- and a two-equivalent) are often slow compared with those between complementary reactants (i.e., a one- and a one-equivalent or a two- and a two-equivalent).

TABLE 3.3-8
One-, Two-, and One-Two-Equivalent Oxidizing Agents

One-Equivalent	Two-Equivalent	One-Two-Equivalent
Ce(IV)	I ₂	Cr ₂ O ₇ ⁻²
Co(III)	Br ₂	MnO ₄ ⁻ ^a
Fe(III)	Cl ₂	PCl ₆ ⁻²
Fe(CN) ₆ ³⁻	HBrO	VO ₂ ⁺
	HClO	
	IO ₃ ⁻	
	BrO ₃ ⁻	
	H ₂ O ₂	
	Tl(III)	

a. Complex situations can occur with manganese due to possibility of a variety of oxidation states (e.g., +7, +6, +5, +4, +3, +2)

Source: Higginson and Marshall [16]

This behavior is based on the lower probability of collision of three species and is not an inviolate rule.

It is useful to note the following observations as to what type of species undergo particular reactions [16]:

- Redox reactions between two complex metal ions usually occur in one-equivalent steps.
- Redox reactions between two species derived from non-transition elements (metals and nonmetals) usually occur in two-equivalent steps.
- Redox reactions between one species with a transition metal center and another having a non-transition element as the center may occur in one- or two-equivalent steps. The one-equivalent appears to be more common.
- For free radicals, irrespective of their origin, a one-equivalent step is more probable.

A one-two-equivalent agent can produce unstable intermediate oxidation states (e.g., X(N+1) radicals), which can lead to products such as {X(N+1)}₂ in addition to the more stable X(N+2) oxidation state [16].

CHARACTERISTICS OF LIGANDS AND METAL IONS

Several characteristics of ligands and metal ions affect the rates of redox reactions. These characteristics include the electronic configuration of the metal or central ion, its lability, the properties of the complexing ions in the medium, and the difference in electrode potential between the reactants (which affects the driving force for the redox reaction). The impact of these and other variables on the rate is discussed below.

Electronic Configuration

Activation of the ion-pair precursor to redox (e.g., equation 11) often involves changing the bond length between the metal and the ligand centers to bring it closer to that of the products. Adding or removing an electron from non-bonding orbitals is easier than from bonding or anti-bonding orbitals, since in the former case bond strength (and thus distance) is not affected. For example, for an octahedral complex (six equivalent ligands around a metal center) it is easier to remove, or add an electron to the t_{2g} orbital than the e_g orbital: the exchange reaction between ruthenium(II) (six electrons in t_{2g}) and ruthenium(III) (five electrons in t_{2g}) is much faster than that between cobalt(II) ($t_{2g}^5 e_g^2$) and cobalt(III) (t_{2g}^6) [31].

In general, the more similar the molecular geometries of the oxidized and reduced forms of the reactants, the less energy is required to bring about the activated state and the faster the reaction [4].

Substitution-Inert Complexes

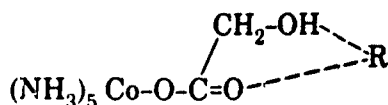
In the reaction of two metal complex ions containing ligands that are difficult to replace or that cannot act as bridges, the reaction is likely to proceed in an outer-sphere process whose rate is faster than that based on dissociation or atom transfer [4]. This is true, for example, for reactions of species such as hexacyanoiron (II) with hexacyanoiron (III), tris (o-phenanthroline) iron (II) with tris (o-phenanthroline) iron (III), hexacyanomanganese (II) with hexacyanomanganese (III), with tris (bipyridyl) chromium (II) with tris (bipyridyl) chromium (III). The electronic configuration of metal ions that results in substitution-inert complexes has been discussed in section 3.2.

Presence of Non-Complexing and Complexing Ions in Solution

The rate of a redox reaction is sensitive to the presence of other ions in solution [4]. Usually, the greatest effects are created by anions when both reactants are cationic, and by cations when both reactants are anionic. Anions enhance the rates between cations, usually by forming bridges, if substitutionally labile metal ions are involved. Other ways the rates may be affected include decreases in rate due to stabilization of the reactant oxidation state by complexation and an increase in

rate due to reduced electrostatic repulsion by complexing of the reactants and formation of lower-charged reactants (when both reactants are of same charged sign).

Some bridging ligands that can act as multidentate complexing agents enhance the rates over those that act only as monodentate ligands [28]. For example, as illustrated below, ligands of the alpha-hydroxy acid class complexed to a cobalt (III) center can chelate the reducing agent, R, and increase the redox rate over that of a ligand that can form only one bond to the other reactant.



Redox Potential

The greater the difference between the redox potentials for the half-reactions between the two reactants, the greater the probability that the reaction will proceed in an outer-sphere path. This also indicates that for a series of outer-sphere reactions, the larger the difference in electrode potentials, the greater the rate. A quantitative discussion of this relationship is provided in section 3.3.7. Table 3.3-9 lists half-reaction (reduction) potentials for some metal ion species.

ENVIRONMENTAL FACTORS

Factors such as temperature, ionic strength and the presence of other ions in solution affect the rates of redox reactions. The relationships between the rate, the temperature and the ionic strength were discussed in section 3.2. Where inner-sphere processes are involved, temperature dependence is related to the effect of temperature on the rate of substitution. As previously mentioned, a similarity of activation energies between a redox and corresponding substitution reaction is one indication that the redox reaction is proceeding via an inner-sphere mechanism. The presence of other ions may lead to stabilization of the reactants or products; in addition, they can alter the rate by introducing a new, lower-energy path (i.e., catalysis) or by altering the speciation of the reactants.

3.3.7 Methods for Estimating the Rates of Redox Reactions

To estimate the rate of a homogeneous redox reaction, one must know the mechanism by which the reaction proceeds. The estimation methods described below can be classified as those based on the Marcus equation for outer-sphere processes [21], those related to the Marcus or Edwards equations for inner-sphere processes [10, 24], and those where correlations between rates of redox of other species and the particular species of interest have been made.

TABLE 3.3-9
Values of Exchange Rate Constants and Reduction Potentials^a

Oxidant/Reducant Couple ^b	k_{11} (or k_{22}) ($M \cdot s^{-1}$)	Reduction Potential E° (V)
Fe(III)/Fe(II)	4.0	+0.73
Cr(III)/Cr(II)	$\leq 2.0 \times 10^{-5}$	-0.41
Eu(III)/Eu(II)	$\leq 1.0 \times 10^{-4}$	-0.43
V(III)/V(II)	1.0×10^{-2}	-0.21
$Fe(CN)_6^{3-}/Fe(CN)_6^{4-}$	3.0×10^2	+0.69
$W(CN)_6^{3-}/W(CN)_6^{4-}$	7.0×10^4	+0.57
$Mo(CN)_6^{3-}/Mo(CN)_6^{4-}$	3.0×10^4	+0.54
$Fe(\text{phen})_3^{+3}/Fe(\text{phen})_3^{+2}$	10^5	+1.07
$Ru(NH_3)_6^{+3}/Ru(NH_3)_6^{+2}$	3.0	-0.21
Ce(IV)/Ce(III)	4.4	+1.44
Co(III)/Co(II)	~ 5.0	+1.82
$IrCl_6^{3-}/IrCl_6^{2-}$	2.0×10^5	+1.017
$Co(NH_3)_6^{+3}/Co(NH_3)_6^{+2}$	$< 3.3 \times 10^{-12}$	+0.10

a. For use in equation 24.

b. phen = 1,10-o-phenanthroline.

Sources: Benson [6], Basolo and Pearson [4], Banford and Tipper [3], Latimer [20], Endicott and Taube [13].

The following quantitative methods are described:

- Estimation of the rate of an outer-sphere redox reaction using the Marcus equation or related equations;
- Estimation of the rate of an inner-sphere redox reaction using a Marcus-type equation;
- Estimation of the rate of a substitution-limited inner-sphere redox reaction using an Edwards-type equation; and
- Estimation of the rate of a substitution-controlled inner-sphere redox reaction from ligand exchange data.

When a reaction is known to proceed by an outer-sphere process, the Marcus equation can provide a good initial estimate of rate. For inner-sphere reactions, depending on the available data and detailed mechanism, any of the three methods given above may be applicable. When the mechanism is unknown, the approximate range can be calculated by any of several methods.

MARCUS EQUATION FOR OUTER-SPHERE REACTIONS

Outer-sphere redox reactions are simpler to treat theoretically than inner-sphere reactions because of the complexities of estimating energies for bond breaking. Marcus [21] derived the following relationship for calculating the rate of an outer-sphere electron transfer reaction:

$$k_{12} = (k_{11} k_{22} K_{12} f)^{1/2} \quad (24)$$

where

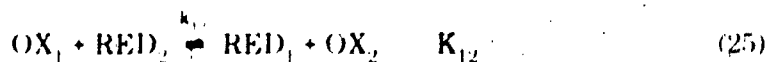
k_{12} = rate constant for equation 25

K_{12} = equilibrium constant for equation 25

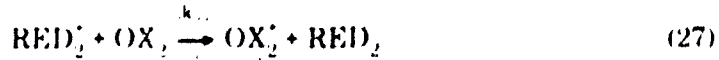
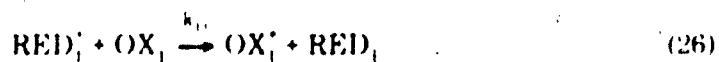
k_{11} = rate constant for equation 26

k_{22} = rate constant for equation 27

f is defined by equation 28



(OX_1 and OX_2 are the oxidized forms of species 1 and 2 respectively, and RED_1 and RED_2 are the reduced forms.)



$$\log f = \frac{(\log K_{12})^2}{4 \log(k_{11} k_{22}/Z^2)} \quad (28)$$

$$(Z = 10^{11} \text{ mol}^{-1} \cdot \text{l} \cdot \text{s}^{-1})$$

Equations 26 and 27 are termed the *related isotopic electron exchange reactions*, and the isotopic species are designated by asterisks.

Equation 24 may also be written in terms of the free energies of activation for reactions 26 and 27 and the overall free energy change for reaction 25 as follows:

$$\Delta G_{12}^{\ddagger} = 0.5 \Delta G_{11}^{\ddagger} + 0.5 \Delta G_{22}^{\ddagger} + \Delta G_{12}^0 - 1.15 RT \log f \quad (29)$$

Equation 29 predicts that a plot of $[\Delta G_{12}^{\ddagger} + 1.15 RT \log f]$ versus ΔG_{12}^0 is linear with a slope of 0.5 and an intercept of $0.5 [\Delta G_{11}^{\ddagger} + \Delta G_{22}^{\ddagger}]$.

For a series of outer sphere reactions of reactant 1 with several similar reactants 2, the value of the free energy of activation for the exchange reactions is relatively constant; thus, the intercept term would be constant.

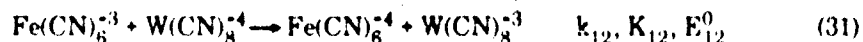
When species OX_1 and OX_2 have similar reduction potentials, the value of the f term is about 1 [31]. This leads to simplification of equation 24 to the following:

$$k_{12} = (k_{11} k_{22} K_{12})^{1/2} \quad (30)$$

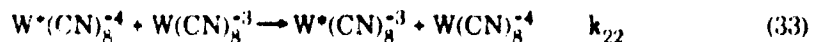
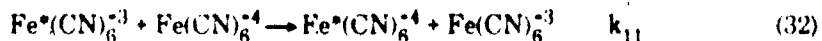
The agreement between calculated and observed k_{12} values has been used as evidence that a reaction proceeds by an outer-sphere mechanism. These equations are also useful in predicting the rates if the mechanism is considered to be outer-sphere. Their utility is limited by the available data for the exchange reactions of interest. In some cases the rates of exchange can be back-calculated by these equations if the other needed information is available.

Example 1 Estimate the rate of the outer-sphere redox reaction between hexacyanoferrate (II) and octacyanotungstate (VI).

The overall reaction of interest is



The individual exchange reactions are



From Table 3.3-9, the reduction potential for the iron-cyanide complex (E_1^0) is +0.69 V. Similarly, the reduction potential for the tungsten-cyanide complex (E_2^0) is +0.57 V. Using these reduction potentials, we can calculate the equilibrium constant for reaction 31 as follows:

$$E_{12}^0 = E_1^0 - E_2^0 = 0.69 - 0.57 = 0.12 \text{ V}$$

Using equations 7 and 8 in section 2.10 at 25°C, we calculate the equilibrium constant for reaction 31 as

$$\begin{aligned} \log K_{12} &= n (23.06) E_{12}^0 / 1.36 \\ &\approx (1) (16.96) (0.12) \\ &\approx 2.04 \end{aligned}$$

This corresponds to an equilibrium constant (K_{12}) of 1.08×10^2 .

Using equation 28 with the following parameters, we calculate the value of f:

$$\begin{aligned}
 k_{11} &= 3 \times 10^2 \text{ mol} \cdot \text{l}^{-1} \cdot \text{s}^{-1} \text{ (Table 3.3-9)} \\
 k_{22} &= 7 \times 10^4 \text{ mol} \cdot \text{l}^{-1} \cdot \text{s}^{-1} \text{ (Table 3.3-9)} \\
 K_{12} &= 108 \quad \log K_{12} = 2.04 \\
 Z &= 10^{11} \quad Z^2 = 10^{22} \\
 \log f &= \frac{(2.04)^2}{4 \log (300 \times 70,000/10^{22})} \\
 &\approx 4.16/(-58.71) \approx -0.071 \\
 f &= 0.85
 \end{aligned}$$

The rate constant for reaction 31 is now calculated from equation 24 with the above value of f:

$$\begin{aligned}
 k_{12} &= (300 \times 70,000 \times 108 \times 0.85)^{1/2} \\
 &= 4.4 \times 10^4 \text{ mol} \cdot \text{l}^{-1} \cdot \text{s}^{-1}
 \end{aligned}$$

The observed rate constant [6] is $4.3 \times 10^4 \text{ mol} \cdot \text{l}^{-1} \cdot \text{s}^{-1}$.

The close agreement shown in the example is not representative of other calculations performed using the Marcus equation, as illustrated in Table 3.3-10. The calculated values are sensitive to the equilibrium constant and rates of exchange used. Table 3.3-11 illustrates the effect on the calculated values of using slightly different electrode potentials for the reacting species. Different electrode potentials are commonly observed for species in different reaction media.

TABLE 3.3-10
Examples of Calculated and Observed Rate Constants

Reaction	Calculated ^a (M ⁻¹ · s ⁻¹)	Observed ^b (M ⁻¹ · s ⁻¹)
Ce(IV) + Fe(II)	5.9×10^6	1.3×10^6
Fe(III) + Cr(II)	$> 6.7 \times 10^5$	$\sim 8.0 \times 10^3$
Fe(III) + V(II)	1.0×10^6	$> 10^5$
Co(III) + Cr(II)	$< 1.0 \times 10^{10}$	$> 3.0 \times 10^2$
IrCl ₆ ⁻² + Fe(CN) ₆ ⁻⁴	1.9×10^6	3.8×10^5
Co(NH ₃) ₆ ⁺³ + V(II)	6.2×10^5	3.3×10^3
Co(NH ₃) ₆ ⁺³ + Ru(NH ₃) ₆ ⁺³	$< 3.6 \times 10^7$	1.6×10^{-2}

a. Using equation 24 and data in Table 3.3-9

b. Source: Banford and Tipper [3]

TABLE 3.3-11
Sensitivity Analysis of Marcus Equation

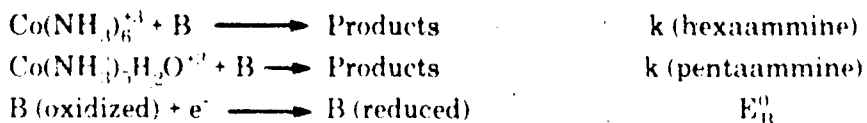
Reaction	E_1 (V)	E_2 (V)	K_{12} (calc)	$k_{12} (M^{-1} \cdot s^{-1})$	
				Calculated ^a	Observed ^b
$\text{Co}(\text{NH}_3)_6^{+3} + \text{Ru}(\text{NH}_3)_6^{+2}$	+0.10	-0.21	1.4×10^{-2}	3.6×10^{-7}	1.0×10^{-2}
		-0.20	2.0×10^{-2}	4.4×10^{-7}	
		-0.10	1.0	3.1×10^{-6}	
$\text{Ce(IV)} + \text{Fe(II)}$	+1.44	-0.73	1.1×10^{12}	5.9×10^5	1.3×10^6
	+1.54	-0.73	5.4×10^{13}	2.3×10^6	
	+1.64	-0.73	2.7×10^{15}	8.0×10^6	
$\text{IrCl}_6^{+2} + \text{Fe(CN)}_6^{+4}$	1.0	-0.69	1.8×10^5	1.9×10^6	3.8×10^5
	1.1	-0.69	8.9×10^6	8.7×10^6	
	1.0	-0.79	3.6×10^3	3.6×10^5	

a. Calculated by equation 24.

b. Source: Banford and Tipper [3].

Relationships between rates for a particular oxidant (A) and a series of reductants (B) and those for the same series with another oxidant (C) have been observed [30]. These relationships are simpler than the Marcus-type equation for outer-sphere reactions; they occur under conditions that simplify the form of the equation, such as when the ion pair equilibrium constants are very similar in the two series. Examples of such relationships are given below.

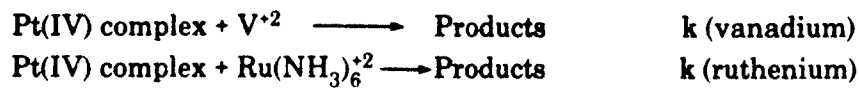
- For outer-sphere reactions of the type:



where k (hexaammine) and k (pentaammine) are the rate constants for the two oxidant series and E_B^0 is the reduction potential for the series of reducing agents. The observed relationship is

$$\log k \text{ (hexaammine)} - \log k \text{ (pentaammine)} = 1.3 E_B^0 + 2.3 \quad (34)$$

- Similarly, for a series of outer-sphere (one-electron rate-determining step) reactions of platinum(IV) haloamine complexes,



the following relationship is observed:

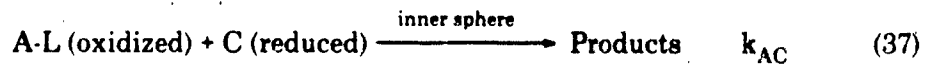
$$\log k(\text{vanadium}) = 0.89 \log k(\text{ruthenium}) - 1.68 \quad (35)$$

MODIFIED MARCUS EQUATION FOR INNER-SPHERE REACTIONS

Patel and Endicott [24] estimated the rates of an inner-sphere redox reaction of an oxidant A-L with a reductant C using data for outer-sphere reactions of the same oxidant. They used the relationship shown in equation 36, which is based on modification of that derived by Marcus (see previous section):²

$$\log k_{AC} = 0.5 \log F_{AL} + 0.5 \log k_{CC} + 8.45 E_{CC}^0 \quad (36)$$

where k_{AC} is the rate constant for the following inner-sphere reaction:



and where A-L is a metal ion with ligand L coordinated to it. E_{CC}^0 is the reduction potential for reaction 38:



where C-L is the reductant C with ligand L coordinated to it; k_{CC} is the rate of the electron exchange reaction between the reduced and oxidized forms {C (reduced) and C-L (oxidized)}, and F_{AL} is a parameter defined by the following equation:

$$\log F_{AL} = 2 \log k_{AB} - \log k_{BB} - 16.9 E_{BB}^0 \quad (39)$$

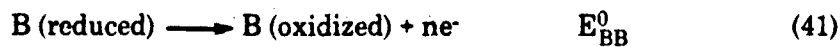
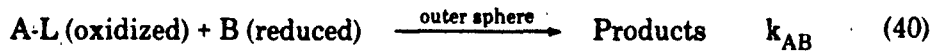
2. This equation is a variation of the following equation found elsewhere [31]:

$$k_{AB}/k_{AC} = (k_{BB} K_{AB}/k_{CC} K_{AC})^{1/2}$$

k_{AB} = rate constant for the reference outer-sphere reaction (40)

k_{BB} = rate constant for the electron exchange reaction of the reduced and oxidized forms of the outer-sphere reducing agent B

E_{BB}^0 = reduction potential for the outer-sphere reducing agent B in reaction 41

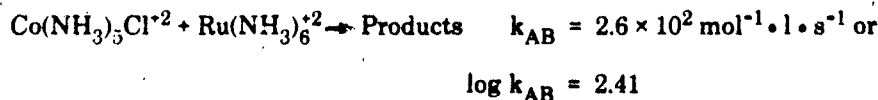


The observation that a Marcus-type equation predicts the rates for some inner-sphere reactions implies that in certain cases the activation of the oxidant center in both inner- and outer-sphere processes is similar. As this is by no means generally true, the utility of the equation is limited.

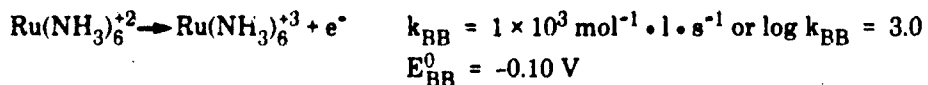
Example 2 Estimate the rate of the inner-sphere redox reaction between $\text{Co}(\text{NH}_3)_5\text{Cl}^{+2}$ and Fe^{+2} , using data available for the outer-sphere redox reaction of the cobalt complex with $\text{Ru}(\text{NH}_3)_6^{+2}$.

The following information is needed [24]:

The reference outer-sphere reaction is



The rate constant for the exchange reaction of the ruthenium (II) and ruthenium (III) complexes and the half-reaction potential are



The value of $\log F_{AL}$ for the cobalt complex is calculated by use of equation 39:

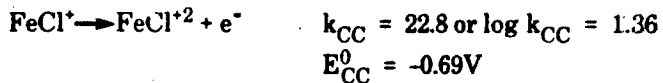
$$\begin{aligned} \log F_{AL} &= 2 \log k_{AB} - \log k_{BB} - 16.9 E_{BB}^0 \\ &= 2(2.41) - 3.0 + 1.69 \\ &= 3.51 \end{aligned}$$

The inner-sphere reaction of interest is



Here, chloride is the bridging ligand, and the iron (II) chloride complex is the initial product of the reaction. In aqueous media, the latter complex eventually dissociates to form aquo iron (II) and free chloride ions.

The appropriate exchange reaction for the reducing agent is thus [24],



(Note that values of E^0 for complexed species can be calculated from those for the aquo ions and related stability constants as given in § 2.10.)

We can now calculate the value of k_{AC} using equation 36.

$$\begin{aligned} \log k_{\text{AC}} &= 0.5 \log F_{\text{AL}} + 0.5 \log k_{\text{CC}} + 8.45 E_{\text{CC}}^0 \\ &= 0.5(3.51) + 0.5(1.36) + 8.45(-0.69) \\ &= -3.39 \end{aligned}$$

The observed value [24] is $\log k_{\text{AC}} = -2.89$

EDWARDS EQUATION FOR INNER-SPHERE REACTIONS

Edwards [10] developed a relationship for the rates of oxidation of several substrates by hydrogen peroxide. All of the related reactions appear to require initial replacement of oxygen on the hydrogen peroxide center by the reductant. The relationship is

$$\log (k_x/k_o) = \alpha E_n + \beta H \quad (42)$$

where

k_x = rate of reaction with species x

k_o = rate of reaction with water (oxygen exchange or substitution)

α, β = empirically determined oxidant constants

E_n = nucleophilic constant for electron donor (reductant)

H = basicity constant for electron donor (reductant)

Table 3.3-12 lists values of E_n and H for some species. Values of α and β are determined from data for a series of related reactions; in the case of hydrogen peroxide, for example, Edwards [10] found that $\alpha = 6.31$, $\beta = -0.394$, and $\log k_o = -16.33$.

Values of k_o , α and β were obtained from empirical fit of the available kinetic data for several reducing agents to equation 42 [10].

Example 3 Estimate the rate of reaction of hydrogen peroxide with chloride, assuming that the reaction proceeds via replacement in a manner similar to that for bromide, iodide and cyanide.

From Table 3.3-12 and values derived by Edwards [10, 11] from the related equations,

$$\begin{aligned}\alpha &= 6.31 \\ \beta &= -0.394 \\ E_n &= 1.24 \\ H &= -3.00 \\ \log k_o &= -16.33\end{aligned}$$

The rate is now calculated from equation 42:

$$\begin{aligned}\log k_x - (-16.33) &= (6.31)(1.24) + (-0.394)(-3.00) \\ \log k_x &= 7.82 + 1.13 - 16.33 \\ &= -7.33\end{aligned}$$

The value observed for reaction with chloride is $\log k_x = -6.96$.

TABLE 3.3-12
Donor Constants for Use with Edwards Equation

N	E_n	H	N	E_n	H
NO_3^-	0.29	0.40	SCN^-	1.83	1.00
SO_4^{-2}	0.59	3.74	NH_3	1.84	11.22
$\text{ClCH}_2\text{COO}^-$	0.79	4.54	$(\text{CH}_3\text{O})_2\text{POS}^-$	2.04	4.00
CH_3COO^-	0.95	6.46	$\text{C}_2\text{H}_5\text{SO}_2\text{S}^-$	2.06	-5.00
$\text{C}_5\text{H}_5\text{N}$	1.20	7.04	I^-	2.06	-9.00
Cl^-	1.24	-3.00	$(\text{C}_2\text{H}_5\text{O})_2\text{POS}^-$	2.07	4.00
$\text{C}_6\text{H}_5\text{O}^-$	1.46	11.74	$\text{CH}_3\text{C}_6\text{H}_4\text{SO}_2\text{S}^-$	2.11	-6.00
Br^-	1.51	-6.00	$\text{SC}(\text{NH}_2)_2$	2.18	0.80
N_3^-	1.58	6.46	$\text{S}_2\text{O}_3^{-2}$	2.52	3.66
OH^-	1.65	17.48	SO_3^{-2}	2.57	9.00
NO_2^-	1.73	5.09	CN^-	2.79	10.88
$\text{C}_6\text{H}_5\text{NH}_2$	1.78	6.28	S^{-2}	3.08	14.66

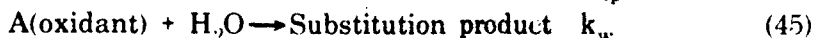
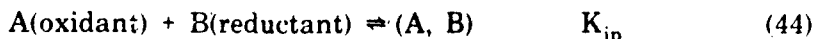
Source: Edwards [10]

INNER-SPHERE SUBSTITUTION-CONTROLLED REACTIONS

When the rate of redox reaction is limited by the substitution of a ligand at the metal center (one of the limits described in § 3.3.4), the rate can be estimated using the following equation:

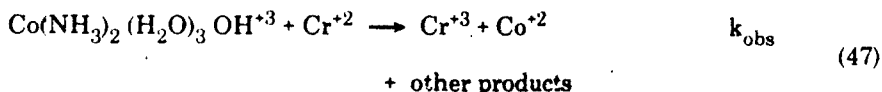
$$k_{\text{obs}} = K_{\text{ip}} k_w \quad (43)$$

where the rate and equilibrium constants refer to the following reactions:

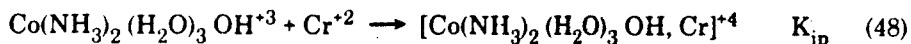


Example 4 Estimate the rate of the substitution-controlled redox reaction between the triaquohydroxodiaminecobalt (III) complex and chromium (II).

The reaction of interest is:



The ion pair formation reaction is:



The substitution rate constant, k_w , to be used in this case is that for the chromium (II) reductant, since substitution at the cobalt (II) center is much slower than at the chromium (II) center (see § 2.9). The value of K_{ip} is calculated by use of the Eigen Fuoss equation, as described in § 2.9.4; if both ionic charges are +2, $K_{\text{ip}} = 1.6 \times 10^{-3} M^{-1}$. The first-order rate constant for substitution at the chromium (II) center is about 10^9 s^{-1} [Table 3.2-2]; this indicates a second-order rate constant of $55.5 \times 10^9 \text{ mol} \cdot \text{l}^{-1}$, using a value of $55.5 \text{ mol} \cdot \text{l}^{-1}$ for the concentration of water in an aqueous system. The rate constant for redox reaction is then estimated using equation 43:

$$\begin{aligned} k_{\text{obs}} &= (1.6 \times 10^{-3})(55.5 \times 10^9) \\ &= 8.9 \times 10^7 \text{ s}^{-1} \end{aligned}$$

3.3.8 Sources of Data

The best data on the kinetics of redox reactions are usually found in journal articles that describe kinetic studies of particular reactions. Several books dealing with the mechanisms of inorganic redox reactions in inorganic chemistry include limited compilations of data; however, most of these are not directly relevant to environmental conditions, because the studies were usually done at ionic strengths and in media unlike those found in the environment. Moreover, the conditions seldom resemble those found in the environment with regard to the other species present. Nevertheless, such data help to show whether a given reaction is likely to be fast or slow and, thus, if an understanding of the kinetics is important in that particular case. Data of this kind can be found in references 3, 4, 6, 12 and 31.

3.3.9 Literature Cited

1. Almoran, T.A. and I. Hagstrom, "The Oxidation Rate of Sulfide in Sea Water," *Water Res.*, **8**, 398 (1974).
2. Avrahami, M. and R.M. Goldberg, "The Oxidation of Sulfite at Very Low Concentrations in Aqueous Solution," *J. Chem. Soc. A*, 647 (1968).
3. Banford, C.H. and C.F.H. Tipper, *Comprehensive Chemical Kinetics*, Vol. 7, Elsevier Publishing Co., New York (1972).
4. Basolo, F. and R.G. Pearson, *Mechanisms of Inorganic Reactions*, John Wiley & Sons, New York (1967).
5. Beattie, J.K. and G.P. Haight, "Chromium (VI) Oxidations of Inorganic Substrates," in *Inorganic Reaction Mechanisms*, Part II, J.O. Edwards (ed.), Interscience Publishers, New York (1972).
6. Benson, D., *Mechanisms of Inorganic Reactions in Solution*, McGraw-Hill Book Co., London (1968).
7. Bodek, I. and G. Davies, "Phenomenological Model for Redox Reactions in Solution," *Coord. Chem. Rev.*, **14**, 269 (1974).
8. Chen, K.Y. and J.C. Morris, "Kinetics of Oxidation of Aqueous Sulfide by Oxygen," *Environ. Sci. Technol.*, **6**, 529 (1972).
9. Cherry, J.A., A.U. Shaik, D.E. Tallman and R.V. Nicholson, "Arsenic as an Indicator of Redox Conditions in Groundwater," *J. Hydrol.*, **43**, 373 (1979).
10. Edwards, J.O., "Correlation of Relative Rates and Equilibria with a Double Basicity Scale," *J. Am. Chem. Soc.*, **76**, 1540 (1954).
11. Edwards, J.O., "On the Reactions of Hydrogen Peroxide with Donor Particles," *J. Phys. Chem.*, **56**, 279 (1952).
12. Edwards, J.O. (ed.), "Inorganic Reaction Mechanisms," in *Progress in Inorganic Chemistry*, Vol. 13, S. Lippard (ed.), Interscience Publishers, New York (1970).
13. Endicott, J. and H. Taube, "Studies on Oxidation-Reduction of Ruthenium Ammines," *Inorg. Chem.*, **4**, 437 (1965).

14. Haim, A., "Mechanism of Electron Transfer Reactions," in *Progress in Inorganic Chemistry*, Vol. 30, S. Lippard (ed.), Interscience Publishers, New York (1983).
15. Hem, J.D., "Chemical Equilibria and Rates of Manganese Oxidation," *U.S. Geol. Surv. Water-Supply Pap.*, 1667-A (1963).
16. Higginson, W.C.E. and J.W. Marshall, "Equivalence Changes in Oxidation Reduction Reactions in Solution: Some Aspects of Oxidation of Sulphurous Acid," *J. Chem. Soc.*, 447 (1957).
17. Hoigne, J., H. Bader, W.R. Haag and J. Staehelin, "Rate Constants of Reactions of Ozone with Organic and Inorganic Compounds in Water-III," *Water Res.*, **19**, 993 (1985).
18. Housé, D.A., "Kinetics and Mechanism of Oxidations by Peroxydisulfate," *Chem. Rev.*, **62**, 185 (1962).
19. Lappin, A.G., "Electron Transfer Reactions," in *Mechanisms of Inorganic and Organometallic Chemistry*, Vol. 1, M.V. Twigg (ed.), Plenum Press, New York (1983).
20. Latimer, W.M., *Oxidation Potentials*, 2nd ed., Prentice-Hall, New York (1952).
21. Marcus, R.A., "On the Theory of Oxidation-Reduction Reactions Involving Electron Transfer. V: Comparison and Properties of Electrochemical and Chemical Rate Constants," *J. Phys. Chem.*, **67**, 853 (1963).
22. Nakayama, E., T. Kuwamoto, S. Tsurubo and T. Fujinage, "Chemical Speciation of Chromium in Sea Water," *Anal. Chim. Acta*, **130**, 401 (1981).
23. Ostland, G.H. and J. Alexander, "Oxidation Rate of Sulfide in Sea Water," *J. Geophys. Res.*, **68**, 3995 (1963).
24. Patel, R.C. and J.F. Endicott, "Electron Transfer Reactions of Cobalt (III): Relative Rate Comparison and Free Energy Relations," *J. Am. Chem. Soc.*, **90**, 6364 (1968).
25. Schrocder, I.C. and G.F. Lee, "Potential Transformations of Chromium in Natural Waters," *Water Air Soil Pollut.*, **4**, 355 (1975).
26. Stollewerk, K.G. and D.B. Grove, "Reduction of Hexavalent Chromium in Water Samples Acidified for Preservation," *J. Environ. Qual.*, **14**, 301 (1985).
27. Stumm, W. and G.F. Lee, "Oxygenation of Ferrous Iron," *Ind. Eng. Chem.*, **53**, 143 (1961).
28. Taube, H., "Bridging Groups in Electron Transfer Reactions," in *Mechanisms of Inorganic Reactions*, Adv. Chem. Ser. No. 49, American Chemical Society, Washington, D.C. (1965).
29. Theis, T.L. and P.C. Singer, "Complexation of Iron (II) by Organic Matter and Its Effect on Iron (II) Oxygenation," *Environ. Sci. Technol.*, **8**, 569 (1974).
30. Twigg, M.V. (ed.), *Mechanisms of Inorganic and Organometallic Reactions*, Vol. 1, Plenum Press, New York (1983).
31. Wilkins, R.G., *The Study of Kinetics and Mechanism of Reactions of Transition Metal Complexes*, Allyn and Bacon, Boston (1974).

3.4 KINETICS OF DISSOLUTION, PRECIPITATION AND CRYSTALLIZATION

3.4.1 Introduction

The goal of this section is to provide the reader with the tools and methods for answering questions on the kinetics of dissolution, nucleation and precipitation of materials of environmental concern. Within this broad category of chemical kinetic processes, the more important and straightforward questions can be stated as follows:

- How fast does a solid material dissolve?
- How fast does the chemical composition or the quality of water change during dissolution?
- How fast can a state of saturation or chemical equilibrium be obtained?
- How fast does a solid precipitate and/or recrystallize?

Each of these questions can arise in an investigation or in monitoring of a great variety of systems containing solids and water. Natural systems made of rocks, soils and running waters, and any number of man-made systems ranging from simple water conduits to complex waste treatment and disposal systems, all have in common one feature: they all contain water and solids that can react with water.

The presentation in this section deals with variables needed in making environmental decisions and obtainable from experimental work, from measurements in natural situations, or from literature data.

Environmental conditions affect to a variable extent the rates of dissolution of solids in undersaturated solutions and the rates of precipitation in supersaturated solutions. As outlined below, the environmental conditions may be divided into two groups — physical and chemical.

3.4.2 Key Variables, Information Needs and Data Sources

ENVIRONMENTAL CONDITIONS

Physical Conditions

The physical conditions of a system that affect the rates of dissolution or precipitation are mainly the following:

- Temperature
- Volume of solution
- Homogeneity of the liquid phase
- Surface area of the solid

Most reactions increase in rate with an increasing temperature. The environmental temperature range of several tens of degrees centigrade makes this effect important

for many reactions. For pressure, however, its range of variation near the earth's surface is too small to be significant. Temperature also has indirect effects on dissolution or precipitation processes, such as temperature-induced changes in viscosity of solutions or changes in the rate of water evaporation from open systems.

The volume of water in a system and the surface area of the solid phase are the two physical parameters that control how much solid material will be transferred into a given volume of solution in a given time.

One speaks of a solution as homogeneous if it is well mixed. Mechanical stirring of a solution often increases the rate of dissolution of a solid because of the faster transport of material from the solid surface. In nature, water turbulence plays the role of mechanical stirring. Although methods exist to quantify degrees of turbulence in natural waters or, analogously, degrees of mixing in a stirred volume of water, their treatment usually fails in the domain of dissolution or precipitation processes in engineered systems. Such systems, where the geometric shape of the system (such as the cross-section of a pipe, a reactor, or a body of water) affects the rates of dissolution or precipitation, are outside the scope of this section.

Chemical Conditions

Rates of dissolution or precipitation are, to a large extent, determined by the chemical nature of the components of the system. For example, the rate of dissolution of a carbonate phase, such as CaCO_3 , depends on the amount of dissolved CO_2 and on the pH of the solution. In this case, the chemical composition of the solution phase includes hydrogen-ion concentration and CO_2 . In a case of dissolution of calcium sulfate, CaSO_4 , the concentration of CO_2 in water may be inconsequential and would not need to be considered. However, the presence of the SO_4^{2-} ion in solution from another dissolved salt, such as Na_2SO_4 , might control CaSO_4 dissolution by making the solution more nearly saturated with calcium sulfate.

Ionic strength, a parameter based on the concentrations of all the ionic components of the solution (section 2.6), can also affect the rates of dissolution or precipitation.

INFORMATION NEEDED FOR DISSOLUTION AND PRECIPITATION RATES

Each of the four questions in the Introduction refers to a mass of a solid or dissolved material transferred from one phase to another in a unit of time. Questions as to how fast a solid dissolves and how fast solution composition changes are answerable quantitatively, usually in such units as mass per unit time, mass per unit volume per unit time, and mass per unit area per unit time.

Basic data for computation of the rates of dissolution and of the kinetic parameters that enter in the dissolution rate equations are as follows (see also preceding section on Environmental Conditions):

Physical conditions of the system:

- Temperature
- Solution volume (in a system without flow)
- Solution volume flow rate (in a system with flow)
- Surface area of the dissolving solid

Chemical conditions of the system:

- Chemical composition of the solid, or concentrations of the components of interest in the dissolving solid
- Chemical composition of the solution, both initially and as a function of time during dissolution
- Concentrations and chemical states of other components of the system that may affect the rate of dissolution (such as dissolved gases, complexing agents or common ions).

Estimation of the rates of precipitation is often based on monitoring changes in concentration of the precipitating component in solution. In both natural and man-made systems, it is often easier to monitor a change in concentration of the solution than to measure the mass of solid precipitated over a period of time. Therefore, most of the data on rates of precipitation and crystal growth (in closed systems) are derived from measurements of rates of decrease in concentration. To relate the mass of a material removed from solution to the rate of growth of the solid crystals, it is necessary to know the surface area of the solid; this is obtainable either by direct measurements (the gas-adsorption method of solid surface-area determination) or by measuring the numbers and sizes of the crystals formed.

Recrystallization is a process taking place when precipitates age and, more generally, when phase transformations occur in solids under certain environmental conditions. A glassy or amorphous solid may sooner or later become crystalline, a very slow process under environmental conditions but one that speeds up at high temperatures. Amorphous and gelatinous precipitates often contain large proportions of water; removal of this water may result in dry amorphous or crystalline solids.

Another type of recrystallization is dehydration: a solid containing H₂O as part of its stoichiometric chemical formula and its crystal structure recrystallizes to a solid containing fewer H₂O molecules or to an anhydrous form containing none. Such reactions take place under conditions of low humidity or somewhat elevated temperatures. The basic data from which the kinetic parameters of such recrystallization reactions are derived consist of measurements of the volume of crystals of a new phase forming at the expense of the original phase.

LITERATURE SOURCES OF KINETIC DATA

Kinetic data for dissolution and precipitation of solids in aqueous solutions are, in general, more difficult to find than those on the kinetics of reactions in homogeneous or two-fluid systems. While the latter are compiled in reference volumes, one must search the current scientific and engineering literature for the water and solids of environmental concern. Some suggestions on sources of published kinetic data of environmental interest follow.

For systems containing natural waters and mineral solids, articles dealing with the kinetics of dissolution and precipitation reactions, as studied either in a laboratory or in the field, appear in such journals as *Geochimica et Cosmochimica Acta*, *Limnology and Oceanography*, *American Journal of Science*, and *Marine Chemistry*.

More specifically oriented toward soils and waters (including the kinetics of ion exchange, leaching and dissolution processes) are the journals *Proceedings of the Soil Science Society of America*, *Soil Science*, *Journal of Soil Science*, and *Water, Air and Soil Pollution*.

Kinetics of various chemical reactions of environmental concern is frequently discussed in articles in *Environmental Science and Technology*.

Experimental studies of crystal growth in systems of environmental and medical interest may be found in *Journal of Crystal Growth* and sporadically in the periodical publications of the chemical and mineralogical societies of various countries.

Professional societies, such as the American Chemical Society and the Mineralogical Society of America, occasionally publish proceedings of symposia devoted to particular aspects of the kinetics of solid-water systems.

In recent years, voluminous experimental data on adsorption and leaching kinetics of trace elements and radionuclides have been produced by concerted research supported by the U.S. Department of Energy. Many of these studies were aimed at determining the rates of either uptake or leaching of trace metals and radionuclides in systems consisting of groundwater and rocks, or groundwater and processed nuclear wastes. Experimental determinations of the rates of leaching of components of nuclear fuel waste and of metals in subsurface rocks have been conducted for a variety of materials (glasses, basaltic rocks, clays, volcanic tufts, and some of their individual mineral components) at temperatures of up to several hundred degrees centigrade and pressures of up to hundreds of atmospheres. Much of the results are available in reports published for the Department of Energy by the National Laboratories (for example, Argonne, Brookhaven, Oak Ridge, and Sandia) and by the major contractors to the D.O.E., such as Battelle-Pacific Northwest Laboratories and Rockwell Hanford Operations, both at Richland, Washington. These publications are not always available from the main clearinghouse of government technical publications in Springfield, Virginia, but can be requested either through the D.O.E. in Washington, D.C., or through the publication and distribution departments of the individual laboratories and agencies.

3.4.3 Dissolution

Dissolution is a chemical reaction that results in transfer of materials from one phase or medium to another. This definition includes a variety of processes involving transfer of chemical species between combinations of solid, liquid and gaseous phases. Thus, one may speak of dissolution of one liquid in another or in a mixture of other liquids, of a gas in other gases or in liquids, and of solids in aqueous solutions. A feature common to all these processes is transfer of the components of one phase — the *dissolving substance* — to another phase, the *solvent*. Chemical species dissolved in a solvent are generally referred to as the *solute*. A number of examples illustrating different types of dissolution are given below.

DESCRIPTION OF DISSOLUTION PROCESSES¹

Congruent Dissolution

In congruent dissolution, a solid phase produces dissolved components in the same stoichiometric proportions as in the solid. An example is the dissolution in water of sodium chloride, which occurs in nature as the mineral halite (NaCl):



where symbol (s) denotes a solid phase. As each mole of sodium chloride dissolving in water produces 1 mole each of sodium and chloride ions, reaction 1 can be written as a stoichiometrically balanced equality:



Here, the equal sign does not necessarily mean that an equilibrium or a state of saturation has been attained; it indicates a stoichiometrically balanced relationship between the reactants and products of a dissolution reaction between halite and water.

Incongruent Dissolution

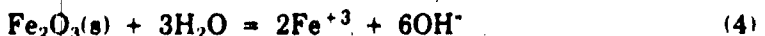
In the incongruent dissolution of a solid, the proportions of the species in solution differ from those in the solid. Such a stoichiometric imbalance can be achieved only if a new solid forms in a reaction between the original solid and the aqueous solution. An example is the dissolution of kaolinite, a common alumino-silicate mineral; the reaction takes place slowly under certain natural conditions, resulting primarily in dissolution of silica and formation of an aluminum hydroxide mineral, gibbsite:



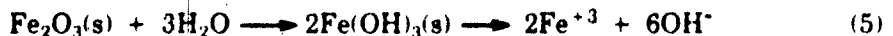
¹ See Appendix A for an explanation of the notation used to designate the states of matter.

In the preceding reaction, the equal sign refers to a stoichiometric balance between the initial reactants (kaolinite and water) and the final products (gibbsite and aqueous SiO_2). The notation does not show any of the intermediate dissolution steps, such as transfer of aluminum species to solution and their precipitation in a new hydroxide phase. Implied in the reaction is conservation of aluminum in the solid and transfer of SiO_2 to solution. Reaction 3 is a process of desilicification; under natural conditions it manifests itself in the development of aluminum hydroxide and oxyhydroxide layers on top of weathered beds of kaolinite.

The shorthand method of writing dissolution reactions as stoichiometrically balanced equations may conceal the occurrence of important compounds that form in the process of dissolution and control it. For example, the net effect of dissolution of Fe_2O_3 , occurring in nature as the mineral hematite, can be written as



In reaction 4, dissolved Fe^{+3} will be present as a number of hydrated iron species, such as FeOH^{+2} , Fe(OH)_2^+ , and Fe(OH)_3^0 . However, in the process of dissolution a hydrated mineral may form at the reaction interface. This may be represented by a sequence such as the following:



A similarity to a more obvious case of an incongruent dissolution, reaction 3, can be emphasized by a model of dissolution of Fe_2O_3 with concomitant formation of solid iron hydroxide, Fe(OH)_3 , and aqueous iron and hydroxide species.

Leaching or Dissolution of Minor Components

Leaching is an environmentally important process of dissolution of minor components from a solid matrix. Numerous examples of leaching processes occur in reactions of waters with soils, man-made solid wastes, different types of ash from power plants burning fossil fuels, and — with an eye on the possible future — in reactions of waters with nuclear fuel wastes.

For a trace component X residing in a solid matrix M, one process of dissolution may involve transfer of X from a virtually insoluble matrix. In this case, a solid MX loses component X, becoming solid M in the process:

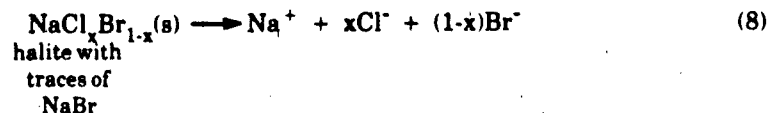


Reaction 6 is analogous to the incongruent dissolution of kaolinite, shown in reaction 3.

If both the matrix component M and the trace component X are soluble, the dissolution reaction is, schematically,



Example 1 An example of the latter reaction is dissolution of an impure sodium chloride. Natural NaCl almost always contains minor amounts of bromide, coprecipitated with sodium chloride from the original saline brine of oceanic origin. The composition of such a solid can be written as $\text{NaCl}_x\text{Br}_{1-x}$. As both NaCl and NaBr are highly soluble in water, the dissolution reaction is



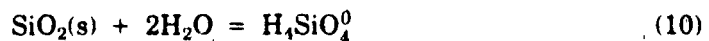
Example 2 An example of leaching of a component from a nuclear fuel waste in a form of fused glass is the reaction:



In this reaction, only plutonium leached from the glass is being monitored. Other radioactive and nonradioactive components of the glass, as well as SiO_2 dissolving from the glass, are not dealt with in this case. Compare reaction 6.

CRITERIA OF DISSOLUTION

Why do solids dissolve in water? In the language of chemical thermodynamics (see section 2.11), transfer of a component of a solid phase to solution takes place if the chemical potential of this component in the solid is greater than its chemical potential in solution. The chemical potential of a component is the driving force responsible for its transfer from a phase where the chemical potential is higher to a phase where the chemical potential is lower. Dissolution reaction of a commonly occurring form of silica (mineral quartz, SiO_2) can be represented by



or, disregarding H_2O in the stoichiometric balance for simplicity, by



Dissolution takes place if the chemical potential of SiO_2 in the solid is greater than its chemical potential in the aqueous phase, at the same temperature and pressure. The chemical potential of a component in each of the phases is commonly denoted μ , in units of kJ/mol or kcal/mol. Dissolution can occur if the following condition exists:

$$\mu_{\text{SiO}_2(\text{s})} > \mu_{\text{SiO}_2^0} \quad (12)$$

The case of saturation — that is, no net dissolution or precipitation — corresponds to an equality of the chemical potentials of the SiO_2 component in the two phases:

$$\mu_{\text{SiO}_2(\text{s})} = \mu_{\text{SiO}_2^0} \quad (13)$$

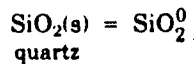
Precipitation may occur if the chemical potential of SiO_2 in the aqueous phase is greater than in the solid phase, which is the opposite of the case in dissolution:

$$\mu_{\text{SiO}_2(\text{s})} < \mu_{\text{SiO}_2}^0 \quad (14)$$

The inequality of the chemical potentials, defining the conditions of either dissolution or precipitation, does not indicate the speed of either of these processes, or even whether they proceed at all; it indicates only that dissolution or precipitation *may* take place. The following example illustrates the use of the dissolution or precipitation criterion without deriving the mathematical relationships for the chemical potentials of the aqueous and solid species. (Information on chemical potentials and their use is given in section 2.11, which discusses solubilities.)

Example 3 A river water contains 12 mg SiO_2 /liter. Will quartz dissolve in this water? Will noncrystalline silica glass dissolve in this river?

To answer these questions, we must establish which of the three criteria, equations 12 through 14, is met within the environmental conditions of the system. At the standard conditions of 25°C and 1 bar total pressure, the following relationship applies to the reaction between quartz and water:



The chemical potential is related to the chemical potential in a standard state, μ^0 , and the activity, a , of the component by the relationship

$$\mu = \mu^0 + RT \ln a \quad (15)$$

where T is temperature (K) and R is the gas constant, as given under equation 57.

Solid SiO_2 is a pure one-component phase and, by definition, the activity of SiO_2 in it is unity, $a_{\text{SiO}_2(\text{s})} = 1$. Therefore, for SiO_2 in quartz, equation 15 reduces to

$$\mu_{\text{qtz}} = \mu_{\text{qtz}}^0 \quad (16)$$

For the chemical potential of SiO_2 in quartz at a standard state, one can use the value of the Gibbs standard free energy of formation of quartz [38].

$$\mu_{\text{qtz}}^0 = \Delta G_f^0(\text{qtz}) = -856.3 \text{ kJ/mol} \quad (17)$$

For a dilute solution, activity can be replaced by concentration in molal units, giving the following form of the chemical potential:

$$\mu_{\text{SiO}_2}^0 = \mu_{\text{SiO}_2}^0 + RT \ln m_{\text{SiO}_2}^0 \quad (18)$$

The standard chemical potential of aqueous SiO_2 is

$$\mu_{\text{SiO}_2}^0 = \Delta G_f^0(\text{SiO}_2^0) = -833.72 \text{ kJ/mol} \quad (19)$$

The concentration of SiO_2 (12 mg/l) is, very nearly,

$$m = \frac{12 \times 10^{-3} \text{ g/l}}{60 \text{ g/mol}} \approx 2 \times 10^{-4} \text{ mol/kg or molal.}$$

Thus, the chemical potential of aqueous SiO_2 in river water is

$$\mu_{\text{SiO}_2}^0 = -833.72 + (0.00831)(298) \ln(2 \times 10^{-4}) \quad (20)$$
$$= -854.0 \text{ kJ/mol}$$

Comparing equations 20 and 17, we see that the chemical potential of SiO_2 in solution is greater than its chemical potential in the quartz phase ($-854.0 > -856.3$). The conclusion is that quartz will not dissolve in this river water.

For a noncrystalline, amorphous form of SiO_2 , the value of the standard chemical potential is

$$\mu_{\text{SiO}_2(\text{am})}^0 = \Delta G_f^0(\text{SiO}_2(\text{am})) = -850.56 \text{ kJ/mol} \quad (21)$$

Since this value is greater than μ_{SiO_2} in the river water,

$$\mu_{\text{SiO}_2(\text{am})} > \mu_{\text{SiO}_2}^0 \quad (22)$$

The amorphous, glass-like SiO_2 should dissolve in this river water.

DISSOLUTION ON A GLOBAL SCALE

Dissolution occurs on a global scale in the natural process of chemical weathering, which takes place when minerals in rocks react with waters, releasing some of their components to solution and also forming new minerals in the process.

The global rate of chemical weathering can be estimated quite accurately from the measured concentrations of dissolved mineral species in the rivers and groundwaters of the world. The main chemical species in river waters (Table 3.4-1) are the products of reactions between the minerals in the crustal rocks of the earth, and water and atmospheric reactive gases. Ideally, to estimate the global mass of dissolved mineral matter in the rivers of the world, one should have a very comprehensive data base of chemical analyses of the more important rivers, averaged over seasons and years. This global mass, removed from the continents in some unit of time, is a measure of the mean global rate of chemical weathering or, in the language of this section, of a mean global rate of dissolution of the earth's crust. To estimate this rate, we can think either in terms of mass removed per unit area of the land surface per unit of time, or of the thickness of a layer stripped by dissolution per unit of area and per unit of time. The rate of dissolution, R_m , in units of mass, is

$$R_m = \frac{CF}{A} (\text{g} \cdot \text{cm}^{-2} \cdot \text{yr}^{-1}) \quad (23)$$

where C = mean concentration of dissolved mineral species in rivers (g/l)

F = mean water flow rate in rivers (l/yr)

A = area of the continents drained by all the rivers (cm^2)

TABLE 3.4-1
Mean Composition of the Rivers of the World and Rates of Delivery to the Oceans

Dissolved Component	Concentration (mg/kg)				Mass Delivered by Rivers to Oceans ^e (10 ¹⁴ g/yr)
	a	b	c	d	
Na ⁺	4.3	4.8	5.15	7.2	1.93
K ⁺	2.0	2	1.3	1.4	0.49
Ca ⁺²	15.5	15	13.4	14.7	5.01
Mg ⁺²	3.9	4	3.35	3.65	1.25
Cl ⁻	3.65	5.7	5.75	8.25	2.15
SO ₄ ⁻²	11	6.7	8.25	11.5	3.09
HCO ₃ ⁻	61 ^f	23 ^g	52	53	19.5
SiO ₂ ⁰	13.3	13	10.4	10.4	3.89

a. Garrels and Mackenzie [17].

b. Holland [19].

c. Meybeck [28] (background or pristine concentrations).

d. Meybeck [28] (values include input from human activity).

e. Values in column (c) multiplied by rate of H₂O delivery to the ocean (3.74×10^{16} kg/yr). From Drever [10].

f. Includes bicarbonate formed from atmospheric CO₂.

g. Refers to bicarbonate species derived from land sources only.

Keep in mind that parts of some continents do not drain into the oceans; regions of Central Asia and Africa have only internal drainage. Similarly, on a smaller scale, internal drainage may occur in the form of a closed basin or lake within a relatively large drainage area. For the purpose of this example, however, the above parameters are [10, 28]:

$$\begin{aligned} C &= 100 \text{ mg/l} = 0.1 \text{ g/l} \\ F &= 3.74 \times 10^{16} \text{ l/yr} \\ A &= 149,000,000 \text{ km}^2 = 1.49 \times 10^{18} \text{ cm}^2 \end{aligned}$$

From these data and equation 23, the mean rate of chemical weathering is

$$R_m \approx 0.003 \text{ g} \cdot \text{cm}^{-2} \cdot \text{yr}^{-1} \quad (24)$$

In detailed studies of erosion rates of watersheds and individual stream basins, variations of as much as a factor of ten have been reported. Such large variations are caused in part by variable rainfall but, significantly, they can also reflect different kinds of rocks in different river basins. Over geologically long periods of time, calcium

sulfates, in the form of the minerals gypsum ($\text{CaSO}_4 \cdot 2\text{H}_2\text{O}$) and anhydrite (CaSO_4), dissolve in running water faster than crystalline silicate rocks. Thus, a terrain made primarily of calcium sulfate beds weathers more rapidly than a river basin where crystalline rocks are exposed.

The mean rate of dissolution or chemical weathering can also be expressed in terms of a thickness stripped from the earth's surface. In this estimate, the rate of dissolution, R_L , represents the volume of material per unit area dissolved in a unit of time:

$$R_L = \frac{CF}{A\rho} \quad (\text{cm} \cdot \text{yr}^{-1}) \quad (25)$$

where ρ is the mean density ($\text{g} \cdot \text{cm}^{-3}$) of the dissolving materials. From equations 23 and 25, the two estimates of the rate are interrelated:

$$R_L = R_m/\rho \quad (26)$$

A mean density of the crustal materials is

$$\rho = 2.7 \text{ g} \cdot \text{cm}^{-3}$$

The linear rate of dissolution is therefore

$$R_L = \frac{0.003}{2.7} \approx 0.001 \text{ cm} \cdot \text{yr}^{-1} \quad (27)$$

Recall that natural erosion of the earth's surface involves two kinds of processes: chemical weathering and physical weathering. The former can be likened to dissolution and the latter to mechanical abrasion. Rivers carry both dissolved and suspended materials, corresponding to the products of the chemical and physical denudation processes. In a later section, the slowness of the global rates will be emphasized by some much faster dissolution rates measured under laboratory conditions.

DIFFERENCES IN KINETICS BETWEEN CLOSED AND OPEN SYSTEMS

In considering the rates of dissolution of natural and environmentally important substances, one must always bear in mind the differences between closed and open systems. A closed system consists of the dissolving phase and water, without flow-through; no material is added by inflow nor removed by outflow. However, precipitation from solution can take place in a closed system, where the mass of the dissolving material is conserved. Open systems, with flow in and out, are common in natural environments, and the kinetics of dissolution in such systems is in certain fundamental aspects always different from the kinetics in closed systems.

Closed Systems

The rate of dissolution in a closed system is a measure of mass of a solid transferred to a volume of solution in a unit of time. As the solute concentration in solution rises when dissolution occurs, the rate of increase in solute concentration is

$$\left(\frac{dC}{dt} \right)_{\text{closed}} = R(C, t, \text{environmental parameters}) \quad (28)$$

which indicates that, in a general case, the rate of dissolution may depend on the solute concentration in solution and it may vary with time t ; it also depends on such environmental parameters as the temperature, pressure, ionic strength, and viscosity of the solution.

Open Systems

An open system with inflow and outflow may be receiving input of a solute from an external source through the inflow and additional input through dissolution within the system. At the same time, it may be losing solute through outflow. A general form of an equation for the rate of change in concentration within such a system is

$$\left(\frac{dC}{dt} \right)_{\text{open}} = \frac{F(t)C_{\text{in}}}{V} + R(C, t, \dots) - \frac{F(t)C}{V} \quad (29)$$

where $F(t)$ = time-dependent volume flow into or out of the system

C_{in} = solute concentration in inflow

V = solution volume in the system

$R(C, t, \dots)$ = dissolution rate, as defined in equation 28

The flushing or water-residence time of the system — i.e., the length of time needed theoretically to renew the water within the volume of the system — is equal to V/F . In equation 29, concentration in inflow, C_{in} , should not be so great as to suppress the solid dissolution, R .

Solute is removed from the system through outflow. Its concentration in the outflow is the same as throughout the well-mixed volume of the system, C .

An open system that is flushed by solute-free water (that is, no input from outside) is represented by a simpler equation:

$$\left(\frac{dC}{dt} \right)_{\text{open}} = R(C, \dots) - \frac{F(t)}{V} C \quad (30)$$

Equation 30 does not imply that the rate of dissolution in an open system is necessarily smaller than in a closed system (equation 28); the value of dC/dt in either equation depends on R , which in turn depends on concentration C . The remainder of this section will be concerned with dissolution rates in closed systems as represented by the term R in the preceding equations 28 to 30.

DISSOLUTION RATE LAWS

Empirical studies of dissolution demonstrate that the greater the undersaturation of a solution, the faster the concentration increases. Mathematically, this observation is represented by the rate law written as

$$\frac{dC}{dt} = k(C_s - C) \quad (31)$$

where k = dissolution rate parameter (time⁻¹)

C_s = concentration at saturation or equilibrium

C = concentration varying with time.

The rate equation is known as the first-order rate law, where the rate term depends on the first power of the concentration terms. If k is a constant under given environmental conditions, dissolution should be faster in an undersaturated solution, where the difference $C_s - C$ is relatively large, than near saturation, when this difference becomes small. For constant k and C_s , Figure 3.4-1 shows how dC/dt changes with concentration C , and Figure 3.4-2 shows how C changes as a function of time.

With constant k and C_s , the integrated form of equation 31 is:

$$C = C_s(1 - e^{-kt}) + C_0e^{-kt} \quad (32)$$

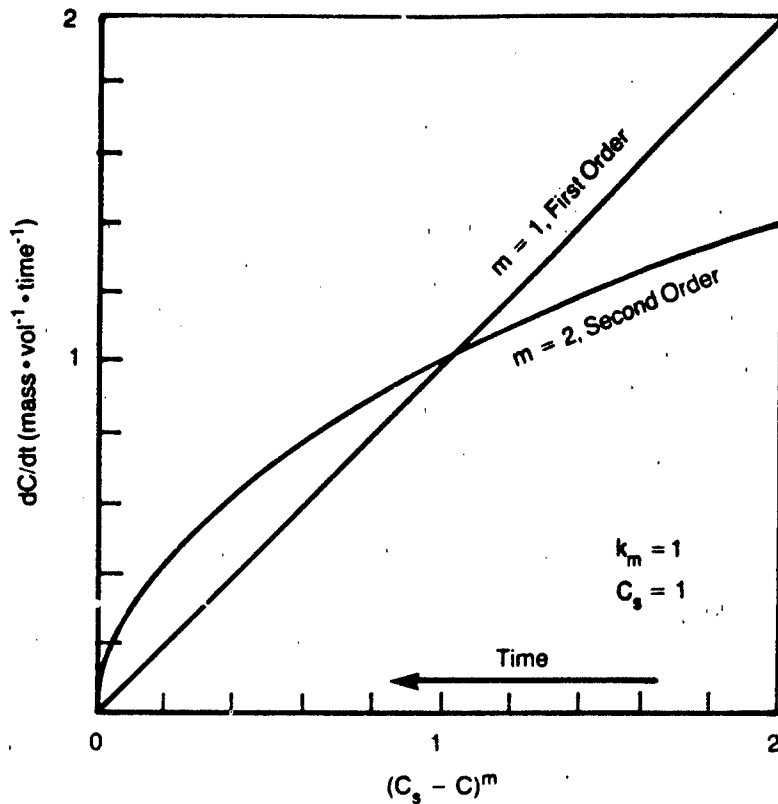
where C_0 is the initial concentration in solution at time $t = 0$.

The preceding shows that, in order to determine how concentration in solution increases with time, one has to know the value of the rate parameter k , the value of the saturation concentration C_s , and the initial concentration C_0 , which may be zero.

Alternatively, to determine the value of k , one must know the saturation concentration C_s (or how it can be obtained, see section 2.11), and a series of data on concentration C as a function of time t .

Intuitively, it is reasonable to suppose that the rate of increase in concentration dC/dt is affected by the volumes of the solid and the solution. Dissolution will in general proceed faster if the surface area of the solid is relatively large. This is reflected in the values of the solid surface area and the solution volume: a value of k in equations 31 and 32 is valid only for a certain set of physical and chemical conditions, among which the surface area of the solid and the solution volume must be known. The dependence of the rate parameter k on these and other conditions will be explained in later sections.

Equation 31 is one of the mathematical forms of dissolution rates. Other forms of dissolution rate equations are given below, and their use is illustrated in a subsequent section.



Note: As time progresses, concentration difference $C_s - C$ decreases.

FIGURE 3.4-1 Rate of a Reaction dC/dt as a Function of Distance from Saturation ($C_s - C$) for First- and Second-order Reactions

Zeroeth Order Law

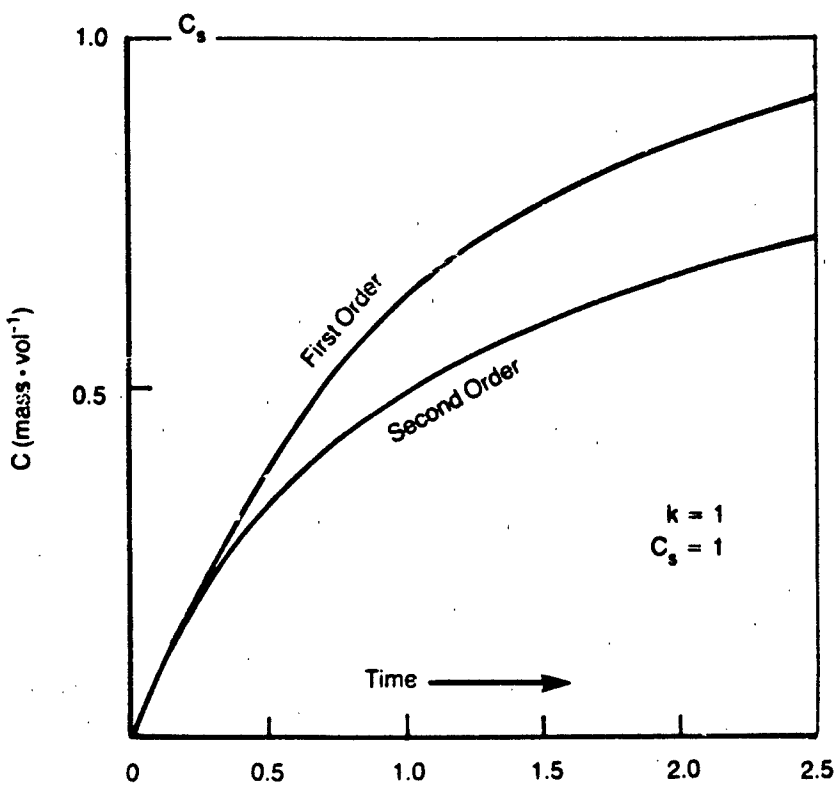
The zeroeth order represents a constant rate of dissolution:

$$\frac{dC}{dt} = k_0 \quad (\text{mol} \cdot \text{cm}^{-3} \cdot \text{s}^{-1}) \quad (33)$$

An integrated form is:

$$C = C_0 + k_0 t \quad (\text{mol} \cdot \text{cm}^{-3}) \quad (34)$$

Dissolution according to this law cannot go on indefinitely, because C cannot increase indefinitely with time. If this law is observed, it can be valid only for some limited period of the dissolution process.



$$\begin{aligned} \text{For First Order: } C &= 1 - \exp(-kt) \\ \text{For Second Order: } C &= 1 - 1/(1 + kt) \end{aligned}$$

Compare equations 32 and 39

FIGURE 3.4-2 Increase in Concentration in Solution, C , for a First- and Second-order Dissolution Reaction, as a Function of Dimensionless Parameter kt

First Order Law

The following equation, a modified form of equation 31, is a general form of the first-order dissolution process

$$\frac{dC}{dt} = k_1(C_s - C)$$

Many solids in the environment occur in the form of grains or small crystals. It is mathematically convenient to treat dissolution of single grains as if they were spherical particles. One of the problems that may have to be solved is how long the individual grains of a certain initial size can survive during dissolution under given

environmental conditions. Such questions may arise in dealing with mixtures of more or less soluble solids in wastes, mixtures of fertilizers in soils, or with the longevities of mineral grains in stream beds. For a spherical particle of radius r , dissolution can be visualized as transport of the components of the solid through a thin layer of solution at the solid surface. Where the solution and the solid are in contact, the solution is saturated at concentration C_s ; outward, concentration diminishes, and the dissolving species diffuses away from the solution-solid interface. (The model of such a dissolution process is analogous to that of either evaporation or condensation of a water droplet in air.) A first-order dissolution reaction of a spherical particle is the relationship [5, 33]:

$$-\frac{dr}{dt} = \frac{DV_m(C_s - C)}{r} \quad (35)$$

where V_m = molar volume of the solid ($\text{cm}^3 \cdot \text{mol}^{-1}$), defined in equation 46

D = diffusion coefficient of dissolved species in solution ($\text{cm}^2 \cdot \text{s}^{-1}$)

C_s = concentration at equilibrium between the solid and solution ($\text{mol} \cdot \text{cm}^{-3}$)

C = concentration in the bulk solution ($\text{mol} \cdot \text{cm}^{-3}$)

r = solid particle radius (cm)

In an environmental situation, a small amount of a solid dissolving in a large volume of water would not significantly change concentration, C . Thus the concentration-difference term, $C_s - C$, is nearly constant, and integration of equation 35 gives an explicit equation for the dissolving particle radius r as a function of time t and other parameters considered as constants (D , V_m , C_s , and C). The time to complete dissolution (t when $r = 0$) is, from integration of equation 35,

$$t = \frac{r_0^2}{2DV_m(C_s - C)} \quad (36)$$

where r_0 is the initial radius of the dissoiving particle. Application of this equation is demonstrated in Example 4. The equation may be used to estimate a lower limit of time to dissolution in dilute suspensions. Adsorption of inorganic and organic components, and other reactions on the particle surfaces may slow down the dissolution process. In thicker suspensions and in packed beds, concentration C may not be constant, thereby affecting the dissolution rate as given in equation 35.

Example 4 Estimate the time to dissolution of SiO_2 -glass particles, 1 mm in diameter, in an average river water.

The following parameters are needed to obtain t from equation 36:

Initial particle radius given: $r_0 = 0.05 \text{ cm}$

Molecular diffusion coefficient
of SiO_2 in water at 25°C
(see also § 2.16): $D = 1 \times 10^{-5} \text{ cm}^2 \cdot \text{s}^{-1}$ [21]

Molar volume of SiO_2 glass: $V_m = 27 \text{ cm}^3 \cdot \text{mol}^{-1}$ [38]

Solubility of SiO_2 glass at 25°C: $C_s = 1.9 \times 10^{-6} \text{ mol} \cdot \text{cm}^{-3}$ (Example 5)
 SiO_2^0 in river waters: $C = 0.17 \times 10^{-6} \text{ mol} \cdot \text{cm}^{-3}$ (Table 3.4-1, column d)

$$t = \frac{0.05^2}{2 \times 1 \times 10^{-6} \times 27(1.9 \times 10^{-6} - 0.17 \times 10^{-6})} = 2.68 \times 10^6 \text{ s}$$

$$\approx 31 \text{ days}$$

The time to dissolution of 31 days is a lower limit estimate for a dilute suspension of silica-glass particles. A related but different case is dealt with in Example 8.

Second and Higher Order Laws

The rate of increase in concentration in solution is some power function of the concentration of the dissolving or reacting species:

$$\frac{dC}{dt} = k_m(C_s - C)^m \quad (37)$$

where m is generally greater than unity.

The integrated form is:

$$C = C_s - \left[\frac{1}{\frac{1}{C_s - C_0} + (m-1)k_m t} \right]^{1/(m-1)} \quad (38)$$

In the case of $m = 2$, a second-order dissolution reaction, the integrated form is

$$\frac{1}{C_s - C} = \frac{1}{C_s - C_0} + k_2 t \quad (39)$$

where $C_s > C > C_0$, and the product $k_2 t$ is positive.

Fractional Order Laws

Empirical relationships describing the rates of dissolution of such stoichiometrically complex phases as bone mineral (apatites) and feldspars (sodium and potassium alumino-silicates) give the rates of dissolution in terms of fractional powers of the hydrogen-ion activity, $(a_{\text{H}})^n$, where the value of n varies over the pH range. For feldspars, some of these relationships are tabulated in a later section (Table 3.4-7).

Time-dependent Laws

Dissolution of many substances and leaching of the matrix components often follow the so-called parabolic rate law, which states that the rate of dissolution is inversely related to the square root of time:

$$\frac{dC}{dt} \propto k_p t^{-1/2} \quad (40)$$

$$C = C_0 + 2k_p t^{1/2} \quad (41)$$

As in the case of the linear dissolution rate, equation 34, the parabolic rate law cannot apply indefinitely, because C cannot increase indefinitely with time. However, the parabolic rate law is rooted in the mathematical theory of molecular diffusion, and it can be derived for a dissolution process that describes diffusional migration of a component from a solid, when migration takes place through the matrix toward the solid-solution interface. Data on parabolic rates of dissolution of silicates are given in Table 3.4-2.

TABLE 3.4-2

Values of Parabolic Dissolution Rate Parameter (k_{ps}) for Three Silicate Minerals
 $k_p = k_{ps} S/V$

(C_0 = initial concentration in solution, V = solution volume, S = solid surface area;
experimental conditions: 1.0 g solid, 1 liter solution, 25°C)

Mineral	Density ρ ($\text{g} \cdot \text{cm}^{-3}$)	Specific Surface Area, S_g ($\text{cm}^2 \cdot \text{g}^{-1}$)	Initial pH	$C_0 V/S$ ($10^{-9} \text{ mol} \cdot \text{cm}^{-2}$)		$2k_{ps}$ ($10^{-11} \text{ mol} \cdot \text{cm}^{-2} \cdot \text{s}^{-1/2}$)	
				Mg	Si	Mg	Si
Enstatite $\text{Mg}_2\text{Si}_2\text{O}_6$	3.29	576	3.2	4.9	7.3	7.8	2.4
			5.0	2.3	3.0	2.6	2.6
			7.0	0.09	0.2	1.6	1.4
			9.6	1.0	0.57	1.7	2.4
Forsterite Mg_2SiO_4	3.13	445	3.2	20.0	5.0	180.0	20.0
			5.0	9.0	2.0	61.0	3.6
			7.0	2.0	0.7	120.0	2.9
			9.6	4.0	0.6	67.0	0.3
Serpentine $\text{Mg}_3\text{Si}_2\text{O}_5(\text{OH})_4$	2.62	914	3.2	20.0	0.0	27.0	6.3
			5.0	5.8	0.0	2.2	6.8
			7.0	3.4	0.2	1.9	6.8
			9.6	1.0	0.2	1.4	0.7

Source: Luce et al. [27]

Dissolution of some solids according to the parabolic rate law may result from the fact that the solid aggregates are made of particles of different sizes, with some of the bigger particles containing overgrowths and broken edges [5]. Washing in water or acid or etching of the solid particles may produce dissolution according to the zeroth order law, equations 33-34.

To obtain a value of the rate parameter k for a parabolic rate dissolution, proceed as follows: To verify the parabolic rate law, concentration C should plot as a straight line

function of the square root of time, $t^{1/2}$. The slope of this plot is the value of $2k_p$, given in equation 41. From the numerical data of concentration as a function of time, the rate parameter k_p can be computed by using a concentration value C_1 at time t_1 and C_2 at time t_2 :

$$k_p = \frac{C_1 - C_2}{2(t_1^{1/2} - t_2^{1/2})} \quad (\text{g} \cdot \text{l}^{-1} \text{ sec}^{-1/2}) \quad (42)$$

This value of k_p can be used in equation 41 to compute and plot C as a function of t .

DISSOLUTION RATE PARAMETER, k

In the preceding sections, the dissolution rate parameter k was used in a form that was strictly applicable to homogeneous reactions. In heterogeneous reactions, such as dissolution or precipitation of solids, the reactive surface area of the solid is one of the parameters that determine the reaction rate. The aqueous phase in a thick suspension reaches a state of saturation faster than in a dilute suspension, other factors being equal.

The rate parameter k can be expressed in an internally consistent form for the homogeneous as well as heterogeneous reactions in suspensions, in systems consisting of a solution and a bulk solid, and in packed beds or porous media.

Solid Surface Area and Solution Volume

The importance of these two parameters — the surface area of the solid and the solution volume — and of their ratio will be demonstrated in this section.

Dissolution is a loss of mass by a solid in a time interval dt , which can be written as

$$-dM = k_i S dt \quad (43)$$

where dM is an increment of mass lost (mol), k_i is some intrinsic dissolution rate constant ($\text{mol} \cdot \text{cm}^{-2} \cdot \text{s}^{-1}$), S is the reactive surface area of the solid (cm^2), and dt is a time interval (s).

Division of both sides of equation 43 by V , the volume of the solution, gives an equation of a form similar to equation 33:

$$\frac{dC}{dt} = k_i \frac{S}{V} \quad (\text{mol} \cdot \text{cm}^{-3} \cdot \text{s}^{-1}) \quad (44)$$

The latter equation shows the effect of the solid surface area on the dissolution rate: the higher the surface/volume ratio in solution, the higher is the reaction rate. This is a zeroeth-order rate equation; for the higher-order rates, the rate constants can also

be expressed in terms of the intrinsic rate parameter k_i , solid surface, and solution volume. For a first-order dissolution reaction,

$$\frac{dC}{dt} = \frac{k_i SV_m}{V} (C_s - C) \quad (\text{mol} \cdot \text{cm}^{-3} \cdot \text{s}^{-1}) \quad (45)$$

where C_s and C are as defined in equation 31.

V_m , the molar volume of the solid ($\text{cm}^3 \cdot \text{mol}^{-1}$), is equal to the ratio of gram-formula weight (M , g/mol) and density (ρ , g/cm³):

$$V_m = \frac{M}{\rho} \quad (46)$$

In equations 45 and 46, the product $k_i V_m$ has the dimensions of velocity ($\text{cm} \cdot \text{s}^{-1}$); it can be interpreted as a linear rate of dissolution of a flat solid surface receding with a velocity $k_i V_m$. Measured values of such linear velocities of dissolution are listed in Table 3.4-3 for a number of salts. High dissolution rates are generally associated with high values of salt solubility; however, the values of the linear dissolution rates of strongly soluble compounds may be biased by the fact that the reactive surface area of the solid, S , is likely to change substantially during the dissolution of single crystals or agitated suspensions.

Dissolution Rate and Degree of Saturation

The rate of a dissolution reaction that proceeds according to the first-order rate law (equation 31) may be written in the following form:

$$\frac{dC}{dt} = k_i C_s \left(1 - \frac{C}{C_s}\right) \quad (47)$$

C/C_s is the ratio of concentration of a species in solution to its concentration at equilibrium with its parent solid. This ratio is closely related to the *degree of saturation* of a solution (Ω), as defined in § 2.11.2. For a solid of composition $M_p A_q$, the degree of saturation of a solution with respect to this solid, written in terms of concentration of the metal-ion species M , is

$$\Omega = \left(\frac{[M]}{[M]_{eq}}\right)^{p+q} \quad (48)$$

where $[M]$ is the concentration of M in solution, $[M]_{eq}$ is its concentration at equilibrium with solid $M_p A_q$, and p and q are stoichiometric coefficients. We may write C for $[M]$ and C_s for $[M]_{eq}$, obtaining the following form for the degree of saturation:

$$\Omega = \left(\frac{C}{C_s}\right)^{p+q}$$

TABLE 3.4-3

Linear Dissolution Rates and Solubilities of Some Moderately to Strongly Soluble Salts
(Rates of dissolution determined at 25°C, in solutions subjected to rotary stirring at 400 rpm,
with the exposed surface of the dissolving solid below the stirrer.)

Solid Phase	Solubility ^a (g/100 g H ₂ O)	Linear Dissolution Rate (cm · s ⁻¹)
KI	146.45	3.10 × 10 ⁻³
KBr	67.75	2.85 × 10 ⁻³
KCl	36.62	2.45 × 10 ⁻³
NaCl	35.92	1.75 × 10 ⁻³
BaCl ₂ · 2H ₂ O	36.9	1.60 × 10 ⁻³
K ₂ SO ₄	12.04	1.70 × 10 ⁻³
FeSO ₄ · 7H ₂ O	29.7	0.80 × 10 ⁻³
NiSO ₄ · 7H ₂ O	39.6	0.55 × 10 ⁻³
CoSO ₄ · 7H ₂ O	37.8	0.60 × 10 ⁻³
ZnSO ₄ · 7H ₂ O	57.9	0.50 × 10 ⁻³
MgSO ₄ · 7H ₂ O	38.3	0.50 × 10 ⁻³
CuSO ₄ · 5H ₂ O	22.29	0.65 × 10 ⁻³
CaSO ₄ · 2H ₂ O ^b	0.21	0.35 × 10 ⁻³

a. For hydrated phases, solubility refers to the anhydrous part of the stoichiometric formula.

b. Selenite (variety of gypsum); dissolution parallel to crystal face (010).

Source: Van Name [42]

or, alternatively, by rearrangement:

$$\frac{C}{C_s} = \Omega^{1/(p+q)} \quad (49)$$

By combining equations 47 and 49, we define the first-order dissolution rate, dC/dt, in terms of the degree of saturation:

$$\frac{dC}{dt} = k_1 C_s \left(1 - \Omega^{1/(p+q)} \right) \quad (50)$$

This expression can be generalized for the rates of dissolution of order m > 1, from equation 37:

$$\frac{dC}{dt} = k_m C_s^m \left(1 - \Omega^{1/(p+q)} \right)^m \quad (51)$$

The use of an equation of this kind is described in the later section on "Dissolution Rates of Calcite" (see equation 76).

Dissolution Reaction Mechanisms

The chemical kinetic literature draws a clear distinction between "diffusion-controlled" dissolution and "reaction-controlled" dissolution. In the latter, the state of the crustal surface, the distribution of lattice dislocations, "kinks," and "steps" determine the overall rate of the dissolution reaction. In diffusion-controlled dissolution, on the other hand, it is assumed that a thin laminar layer of solution, of the order of 10^{-3} cm in thickness, exists adjacent to the solid surface. At the base of this layer, at the interface between the solid and the solution, the solution is saturated with respect to the solid phase. Dissolved ions or molecules diffuse through the laminar layer into the bulk solution. The process of equilibration at the base of the layer is attained much faster than the transport of dissolved species away from the solid into the bulk solution. Therefore, the rate of diffusional transport controls the rate of the dissolution reaction.

In surface-controlled (reaction-controlled) dissolution, chemical reactions at the solid surface control the overall dissolution rate. The existence of surface-controlled reactions is corroborated by observations of the dissolving surfaces that show signs of non-uniform corrosion, suggestive of reactions taking place at certain preferred sites. Other evidence is of a negative kind: diffusion-controlled dissolution is believed to be confirmed by a shrinkage of the laminar surface layer when the rate of stirring in solution is increased, and by a temperature dependence of the dissolution rate similar to that of molecular diffusion in water. In practical terms, a thinner surface layer results in a shorter path of transport, such that the rate of dissolution would increase if the layer were made thinner by faster stirring. The temperature dependence of the dissolution rate is commonly expressed as the activation energy of a reaction; for a diffusion-controlled process it is expected to be between 17 and 21 kJ/mol. (A further discussion of activation energies of dissolution is given in a later section.)

Data listed in Table 3.4-4 show that, in general, mineral phases of low solubility dissolve in a reaction-controlled process, but those of higher solubilities dissolve in a diffusion-controlled reaction. (The apparently exceptional case of dissolution of AgCl has been attributed to possible photochemical effects.) Thus, the solubility of a solid is a tentative indication of its dissolution mechanism.

Porous Media

Porous media in the environment are sediments, soils, and packed beds of granular materials. In such systems the pores are generally interconnected, enabling water to pass through them. A characteristic of porous media that bears on solid dissolution rates is a high ratio of the volume of solids to the volume of solution. For example, sediments on the bottom of water reservoirs and lakes typically contain between 10% and 30% by volume of solids, the remainder of the volume being taken up by water. Under heavier loads, deep-seated sands may contain as much as 70% to 80% solids by volume, the remainder consisting of pores filled with either gas or water.

TABLE 3.4-4
Solubilities of Solid Phases and Reaction Mechanisms that Control Dissolution

Solid Phase	Solubility In Pure Water (mol/l)	Reaction Mechanism Controlling Dissolution
$\text{Ca}_5(\text{PO}_4)_3\text{OH}$	2×10^{-8}	Surface-reaction
KAISi_3O_8	3×10^{-7}	Surface-reaction
$\text{NaAlSi}_3\text{O}_8$	6×10^{-7}	Surface-reaction
BaSO_4	1×10^{-5}	Surface-reaction
AgCl	1×10^{-5}	Transport
SrCO_3	3×10^{-5}	Surface-reaction
CaCO_3	6×10^{-5}	Surface-reaction
Ag_2CrO_4	1×10^{-4}	Surface-reaction
PbSO_4	1×10^{-4}	Mixed
$\text{Ba}(\text{IO}_3)_2$	8×10^{-4}	Transport
SrSO_4	9×10^{-4}	Surface-reaction
Opaline SiC_2	2×10^{-3}	Surface-reaction
<hr/>		
$\text{CaSO}_4 \cdot 2\text{H}_2\text{O}$	5×10^{-3}	Transport
$\text{Na}_2\text{SO}_4 \cdot 10\text{H}_2\text{O}$	2×10^{-1}	Transport
$\text{MgSO}_4 \cdot 7\text{H}_2\text{O}$	3×10^0	Transport
$\text{Na}_2\text{CO}_3 \cdot 10\text{H}_2\text{O}$	3×10^0	Transport
KCl	4×10^0	Transport
NaCl	5×10^0	Transport
$\text{MgCl}_2 \cdot 6\text{H}_2\text{O}$	5×10^0	Transport

a. Note change in mechanism near solubility of 0.002 mol/l.

Source: Berner [5]. (Copyright 1981, Mineralogical Society of America. Reprinted with permission.)

In the presence of water, a bulk sediment or a bulk porous medium consists of solids and water. The fraction of a unit bulk volume occupied by water is called *porosity*, denoted by the symbol ϕ . The fraction occupied by the solids is $1 - \phi$.

A porous solid filled with an aqueous solution is a heterogeneous medium in which the rates of dissolution of the solid phases must be described by equations that take into account the surface areas of the dissolving solids and the volume of the solution occupying the pore space, analogous to equations 44 and 45. The latter two equations

apply in a fairly general way to solids undergoing dissolution. We shall now recast these relatively simple equations in terms of the parameters characteristic of porous media. In essence, this requires that the surface area of the solid (S , cm^2) and the volume of the solution (V , cm^3) be expressed in terms of the surface area and porosity of a porous medium filled with water.

The following reasoning indicates the main relationships between the parameters of a porous medium and those of a more general case of a solid and water.

The volume fraction of the solid in a unit volume of a porous medium, as defined above, is $1 - \phi$ ($\text{cm}^3 \cdot \text{cm}^{-3}$). If the solid has a density of $\rho(\text{g} \cdot \text{cm}^{-3})$, the mass of the solid contained in a unit volume of the porous medium is $\rho(1 - \phi)$ ($\text{g} \cdot \text{cm}^{-3}$).

If the solid in the porous medium is characterized by a value of the surface area S_g , in units of cm^2 per gram of solid, the surface area of the solid contained in a unit volume of the porous medium is

$$S = S_g \rho(1 - \phi) \quad (\text{cm}^2 \cdot \text{cm}^{-3}) \quad (52)$$

The volume of solution, V , filling a unit volume of the pore space of the porous solid is equal to the porosity, as defined earlier:

$$V = \phi \quad (\text{cm}^3 \cdot \text{cm}^{-3}) \quad (53)$$

Substitution of the right-hand side of equations 52 and 53 for S and V , respectively, in the dissolution rate equations 44 and 45 gives the following two relationships:

$$\begin{aligned} \text{Zeroth-order law } \frac{dC}{dt} &= k_i \frac{S_g \rho(1 - \phi)}{\phi} \\ &= k_0 \end{aligned} \quad (54)$$

$$\begin{aligned} \text{First-order law } \frac{dC}{dt} &= k_i V_m \frac{S_g \rho(1 - \phi)}{\phi} (C_s - C) \\ &= k_1 (C_s - C) \end{aligned} \quad (55)$$

The relationships for the rate constants k of dissolution reactions of different orders in porous media and in other solid-solution systems are summarized in Table 3.4-5.

Owing to the dependence of the dissolution rate dC/dt on the ratio S/V (see equations 44, 45, 54, and 55), the rate of reaction varies directly with the surface area of the solid and inversely with the volume of the solution. In porous media, the reaction rate constants k_0 and k_1 in equations 54 and 55 depend on the solid surface area, its

TABLE 3.4-5
Summary of Relationships and Units for Reaction Rate Parameters, k

Reaction Type and Order	k	Units
Homogeneous Reactions		
Zeroth Order	k_0	$\text{mol} \cdot \text{cm}^{-3} \cdot \text{s}^{-1}$
First Order	k_1	s^{-1}
Second Order	k_2	$\text{cm}^3 \cdot \text{mol}^{-1} \cdot \text{s}^{-1}$
Heterogeneous Reactions*		
Solid and Solution, Suspensions		
Zeroth Order	$k_0 = k_i S/V$	$\text{mol} \cdot \text{cm}^{-3} \cdot \text{s}^{-1}$
First Order	$k_1 = k_i S V_m / V$	s^{-1}
Porous Media, Packed Beds		
Zeroth Order	$k_0 = k_i S_g \rho (1-\phi) / \phi$	$\text{mol} \cdot \text{cm}^{-3} \cdot \text{s}^{-1}$
First Order	$k_1 = k_i V_m S_g \rho (1-\phi) / \phi$	s^{-1}

a. Definition of symbols:

k_i = rate parameter ($\text{mol} \cdot \text{cm}^{-2} \cdot \text{s}^{-1}$)
 S = surface area (cm^2 or $\text{cm}^2 \cdot \text{cm}^{-3}$)
 S_g = specific surface area ($\text{cm}^2 \cdot \text{g}^{-1}$)
 V = solution volume (cm^3 or $\text{cm}^3 \cdot \text{cm}^{-3}$)

ϕ = pore volume fraction
 V_m = solid molar volume ($\text{cm}^3 \cdot \text{mol}^{-1}$)
 ρ = solid density ($\text{g} \cdot \text{cm}^{-3}$)

density, and the porosity. Some representative values of these parameters are given below to illustrate their effect on reaction rates.

- *Suspension of fine quartz sand at a concentration of 100 mg/l:*

Surface areas of fine sands commonly range from 1 to a few square meters per gram. Thus, for quartz sand, $S_g = 1 \text{ m}^2 \cdot \text{g}^{-1} = 10^4 \text{ cm}^2 \cdot \text{g}^{-1}$, and its concentration in suspension is $10^4 \text{ g} \cdot \text{cm}^{-3}$. The ratio S/V is

$$\begin{aligned} S/V &= 10^4 \text{ cm}^2 \cdot \text{g}^{-1} \times 10^4 \text{ g} \cdot \text{cm}^{-3} \\ &= 1 \text{ cm}^2 \cdot \text{cm}^{-3} \end{aligned}$$

- *A porous medium of fine quartz sand of the same specific surface area as above and having a porosity value of 40%:*

The parameters needed for estimation of S/V (from equations 52 and 53) are:

Surface area: $S_g = 10^4 \text{ cm}^2 \cdot \text{g}^{-1}$
 Quartz density: $\rho = 2.65 \text{ g} \cdot \text{cm}^{-3}$
 Porosity: $\phi = 0.4$
 Solid fraction: $1 - \phi = 0.6$

$$\begin{aligned} S/V &= \frac{10^4 \times 2.65 \times 0.6}{0.4} \\ &= 4 \times 10^4 \text{ cm}^2 \cdot \text{cm}^{-3} \end{aligned}$$

The preceding two estimates of the ratio S/V, one for a fairly dilute suspension and the other for a packed porous medium, indicate a range of values that are encountered in the environment and the possible magnitude of their effect on the rates of dissolution.

EFFECT OF TEMPERATURE ON DISSOLUTION RATES

The dependence of dissolution rate on temperature is most often expressed through a relationship between the reaction rate parameter k and temperature, proposed by Arrhenius in 1889:

$$k = A \exp \left(-\frac{E_a}{RT} \right) \quad (56)$$

$$\ln k = \ln A - \frac{E_a}{RT} \quad (57)$$

where A = pre-exponential factor, in the same units as k

E_a = activation energy for the reaction (kJ/mol)

R = gas constant (8.314×10^{-3} kJ · deg $^{-1}$ · mol $^{-1}$)

T = temperature (K)

The parameters A and E_a are positive quantities, such that k increases with temperature.

Other types of dependence of reaction rates on temperature have been schematically illustrated, but not discussed, by Frost and Pearson [15]. Eyring and Eyring [13] pointed out that among many reactions that do not obey the Arrhenius relationship are certain adsorption reactions and enzyme-catalyzed hydrolysis.

In estimating the values of the rate parameter k at different temperatures, an explicit value of the factor A can be avoided. If k is known at some reference temperature (k_0 , T_0) and the activation energy for the reaction, E_a , is also known over some temperature range, then the value of k at some other temperature, T , can be computed from

$$\ln \frac{k}{k_0} = - \frac{E_a}{RT} \left(\frac{1}{T} - \frac{1}{T_0} \right) \quad (58)$$

For a number of dissolution and precipitation reactions, as well as some other environmentally relevant reactions, the values of E_a are given in Tables 3.4-6 and -13.

TABLE 3.4-6

**Reaction Rate Parameters, Activation Energies and Equilibrium Constants for Dissolution
of Four SiO_2 Solid Phases in Water**

Reaction Rate Parameter (k_+, $\text{mol} \cdot \text{cm}^{-2} \cdot \text{s}^{-1}$) as a Function of Temperature (°K)	
Quartz	$\log k_+ = -2.826 - 2.028 \times 10^{-3}T - 4158/T$
α -Cristobalite	$\log k_+ = -4.739 - 3586/T$
β -Cristobalite	$\log k_+ = -4.963 - 3392/T$
Amorphous SiO_2	$\log k_+ = -4.369 - 7.890 \times 10^{-4}T - 3438/T$
Activation Energy (kJ/mol)	
Quartz	$E_a = 72.0 \pm 4.6$
α -Cristobalite	$E_a = 68.7$
β -Cristobalite	$E_a = 65.0$
Amorphous SiO_2	$E_a = 62.9 \pm 2.0$
Equilibrium Constant (K) for Equation 10 as a Function of Temperature (°K)	
Quartz	$\log K = 1.881 - 2.028 \times 10^{-3}T - 1560/T$
α -Cristobalite	$\log K = -0.0321 - 988.2/T$
β -Cristobalite	$\log K = -0.2560 - 793.6/T$
Amorphous SiO_2	$\log K = 0.3380 - 7.889 \times 10^{-4}T - 840.1/T$

Source: Rimstidt and Barnes [37]

RATE OF DISSOLUTION ADVANCE

Half-life of a Reaction

From the first-order reaction rate equations 31 and 32, the half-life can be defined as the time required for concentration in solution to reach a midpoint between the initial C_0 and saturation C_s concentrations. Thus, the time at half-life, $t_{1/2}$, corresponds to the concentration $C = (C_0 + C_s)/2$. Using this value of C and $t_{1/2}$ in equation 32, the half-life is

$$t_{1/2} = \frac{\ln 2}{k_1} = \frac{0.693}{k_1} \quad (59)$$

or, for simplicity and as an approximation,

$$t_{1/2} = \frac{1}{k_1} \quad (60)$$

Similarly, from equation 45, the half-life is

$$t_{1/2} = \frac{V}{k_i SV_m} = \frac{1}{k_1} \quad (61)$$

where k_1 is defined in Table 3.4-5.

For a second-order dissolution reaction (equation 39), if k_2 is in units of $\text{cm}^3 \cdot \text{mol}^{-1} \cdot \text{s}^{-1}$, the half-life is

$$t_{1/2} = \frac{1}{k_2(C_s - C_0)} \quad (\text{s}) \quad (62)$$

If the rate parameter k' refers to a unit of area and is given as k' in units of $\text{cm}^3 \cdot \text{mol}^{-1} \cdot \text{cm}^{-2} \text{S}^{-1}$, then k_2 in equation 62 is replaced by the product of k' and the solid surface area S :

$$t_{1/2} = \frac{1}{k'S(C_s - C_0)} \quad (\text{s}) \quad (63)$$

Time to Reach an Equilibrium

In dissolution reactions obeying the first, second or a higher-integer order rate law (equations 32, 38 and 39), the time needed to attain an equilibrium concentration in solution, C_s , is mathematically infinitely long (see Figure 3.4-2). However, a convenient measure of attainment of an equilibrium is some value of concentration C that is very close to an equilibrium concentration C_s . For such a measure, one can use $C = 0.95C_s$; alternatively, one can say that an equilibrium has been effectively reached when a concentration equal to 95% of the difference between the equilibrium and the initial concentrations has been attained:

$$C - C_0 = 0.95(C_s - C_0)$$

The latter condition for attainment of equilibrium, when substituted for C in the first-order dissolution rate equation (32), corresponds to the following value of the dimensionless product, kt :

$$k_1 t = 3$$

From the preceding, the time to attain an equilibrium, as defined by the 95% level of concentration, is

$$t = \frac{3}{k_1} \quad (64)$$

For a second-order reaction (equation 39), the condition of closeness to an equilibrium given above corresponds to the following value of the dimensionless quotient $k_2 t(C_s - C_0)$:

$$k_2 t(C_s - C_0) = 19$$

Thus, the time to attain saturation in a second-order dissolution reaction is:

$$t = \frac{19}{k_2(C_s - C_0)} \quad (65)$$

The progress of first-order and second-order reactions shown in Figures 3.4-1 and -2 indicates that concentration changes as either a function of the distance from saturation (Figure 3.4-1) or as a function of the product kt (Figure 3.4-2). It should not be generalized from these graphs that the second-order dissolution is slower than the first-order; in Figure 3.4-1, this is the result of an arbitrary choice of the value of $k = 1$ and $C_s = 1$, as noted on the figure.

To summarize the preceding, the time needed to nearly reach an equilibrium in a first-order dissolution reaction can be estimated from equation 64, if the value of the rate parameter k_1 is known. For a second-order reaction, the time to reach an equilibrium is a function of the rate parameter k_2 and of the equilibrium concentration C_s , as given in equation 65. For definitions of the rate parameters k_1 and k_2 in either homogeneous or heterogeneous systems, see Table 3.4-5.

For other dissolution rate laws — the zeroeth-order law, parabolic law, and time-dependent rate laws (equations 34, 41 and 70) — concentrations in solution increase indefinitely with time, and an equilibrium is therefore theoretically unattainable. In practice, this means that such rate laws hold for certain periods of time during the dissolution process but that the approach to equilibrium is controlled by other reaction mechanisms.

EXAMPLES OF DISSOLUTION OF MATERIALS

Dissolution of Silica-containing Minerals

Oxygen, silicon and aluminum are the three most abundant elements in the Earth's crust. In many minerals of which the crust is made, they occur together and are known by the generic names of the silicates and alumino-silicates. The ubiquitous presence of the silicates and alumino-silicates in our environment — in rocks, in soils, in atmospheric dust, in suspension or as sediments in waters, and in man-made ceramic materials — makes it relevant to the context of this section to summarize briefly with a few examples the kinetics of their dissolution in water. The case studies presented in the sections that follow deal with dissolution of pure SiO_2 minerals, a group of alumino-silicate minerals known as feldspars, and a number of other commonly occurring silicate phases.

When silicates crystallize from melts (magma, if the molten rock occurs deep within the Earth's crust, and lava, if the melt is on the surface), individual minerals and groups of structurally similar minerals form within certain ranges of temperature. The sequences of crystallization of the solids from melts depend, in general, on the chemical composition of the melt and the initial and final temperatures of the cooling process.

A qualitative relationship has been observed between the temperature of formation of a silicate mineral in a cooling melt and the resistance of the mineral to weathering and dissolution under the Earth's surface conditions. In general, the higher the temperature of formation of a silicate mineral in the melt, the poorer are its survival chances in contact with waters on the surface. Over long periods of time, high-temperature minerals that become exposed to surface waters may dissolve or react to become more stable forms, whereas the minerals formed at lower temperatures in melts are often preserved in sediments deposited in water for times comparable to the age of the Earth.

As an example of this differential survival of silicates on the Earth's surface, one may consider a beach made of quartz sand. (Quartz is one of the lower-temperature minerals crystallizing from metal-silicate melts.) Such beaches are very common, but those consisting of the green-brown grains of olivine minerals are very rare. Olivines are magnesium and iron silicates, of general composition $(Mg, Fe)_2SiO_4$, that are common in basalts. Olivines form at the higher temperatures in a cooling melt, and they break down faster than quartz through weathering when exposed to water. Beaches made of fine fragments of basalt containing olivines can form in proximity to big masses of basalt or other olivine-containing rocks, such as in Hawaii, where the source rocks are geologically young and close to the shore.

Dissolution of Pure SiO₂ Solids. — The most abundant mineral form of SiO₂ in nature is quartz. The SiO₂ family of minerals, in addition to quartz, includes several polymorphs:² tridymite, cristobalite (each of the two represented by an α and a β phase), coesite, stishovite, and silica glass or amorphous silica. α -Quartz is the polymorph that is stable in our environment. Tridymite and cristobalite form at higher temperatures in volcanic and metamorphic rocks. Coesite and stishovite are dense phases that form at high pressures, such as in impact craters of meteorites. Silica glass or structurally amorphous silica occurs as precipitates from water, in skeletal shells secreted by planktonic organisms, and in volcanic rocks.

2. Polymorphs are different crystal structures of the same chemical composition. Transformation of one polymorph into another — for example, by the phase transition CaCO₃(calcite) \longrightarrow CaCO₃(aragonite) — is accomplished by changes of temperature and/or pressure. At any given temperature and pressure, only one of the polymorphs is thermodynamically stable, unless the particular temperature and pressure values happen to permit an equilibrium between the two polymorphs.

Chalcedony, agate, onyx, chert, and jasper are different microcrystalline forms of SiO_2 that contain various metal-oxide impurities. A peculiar form of SiO_2 in nature, known by the name of lechatelierite, occurs in quartz sandstones struck by lightning and in meteorite-impact craters; this fused SiO_2 underwent recrystallization at the Earth's surface and sometimes preserves the tube-shaped or bore-shaped irregular channel formed in the sandstone by a lightning discharge. Occurrences of the SiO_2 polymorphs tridymite, cristobalite and glass on the Earth's surface indicate that such phases can metastably coexist without converting to the stable form — quartz — for geologically long periods of time.

A dissolution reaction of SiO_2 in water was presented earlier as



where $\text{SiO}_2(\text{s})$ represents any one of its polymorphs. The rate of increase in concentration of dissolved silica, H_4SiO_4^0 , can be represented by the following kinetic equation:

$$\frac{dC}{dt} = \frac{S}{V} k_+ (1 - \frac{C}{K}) \quad (66)$$

where C = concentration of H_4SiO_4^0 in a dilute solution (mol/l or mol/kg H_2O)

S = surface area of the solid (cm^2)

V = solution volume or mass of water in it (l or kg H_2O)

k_+ = forward reaction rate parameter ($\text{mol} \cdot \text{cm}^{-2} \cdot \text{s}^{-1}$)

K = equilibrium constant for equation 10.

In its physical units, k_+ is identical to k_+ in equation 44. In agreement with the units of the parameters in equation 66, the equilibrium constant K is defined as the solubility of pure SiO_2 -solid in a dilute solution where the activity of water is unity, $a_{\text{H}_2\text{O}} \approx 1$:

$$K = [\text{H}_4\text{SiO}_4^0] = C_s \text{ (mol/l or mol/kg H}_2\text{O)} \quad (67)$$

Equation 66 is a simplified, practical version of a kinetic equation that was derived in great detail by Rimstidt and Barnes [37], whose data for k_+ , K , and the activation energy (E_a) of the dissolution reaction of four SiO_2 -solids are summarized in Table 3.4-6. The kinetic equation is valid for dilute solutions, when the differences between the molal and molar concentration scales can be neglected, and the activity coefficient values of the species in solution may be taken as approximately unity.

The quotient C/K in equation 66 expresses the degree of saturation of the solution with respect to the solid. (See section 2.11.2 for the definition of degree of saturation.) If $C/K < 1$, the solid should be dissolving; if $C/K > 1$, precipitation may be taking place, a process that corresponds to a negative value of dC/dt ; and at equilibrium,

$C = K$. The equilibrium constant K can also be defined as the ratio of the forward and backward reaction rate constants, k_+ and k_- :

$$K = \frac{k_+}{k_-} \quad (68)$$

Because K , k_+ and k_- are interrelated, only two of these parameters are needed in equation 66 and Table 3.4-6 to compute either dissolution or precipitation reaction rates.

Example 5 Which of two solids — quartz grains or shells of diatoms made of amorphous SiO_2 — should dissolve faster in water containing dissolved silica at a concentration of 4 mg SiO_2/l at 25°C ?

From Table 3.4-6, using $T = 298 \text{ K}$,

$$\begin{aligned} \text{Quartz: } K &= 1.1 \times 10^{-4}, \quad \log k_+ = -17.38 \\ \text{Glass: } K &= 1.92 \times 10^{-3}, \quad \log k_+ = -16.14 \end{aligned}$$

Concentration of silica in solution is

$$C = \frac{4 \times 10^{-3} \text{ g/l}}{60 \text{ g/mol}} = 6.67 \times 10^{-5} \text{ mol/liter}$$

In the absence of other information on the surface areas of the two solids, assume that they are the same, making a comparison easier. The ratio of the dissolution rates, from equation 66, is as follows:

$$\begin{aligned} \frac{(dC/dt)_{\text{glass}}}{(dC/dt)_{\text{quartz}}} &= \frac{k_+ (\text{amorphous } \text{SiO}_2)}{k_+ (\text{quartz})} \quad (69) \\ &= 10^{-16.14}/10^{-17.38} = 10^{1.24} = 17 \end{aligned}$$

Thus, under the conditions stipulated, amorphous SiO_2 is expected to dissolve about 17 times faster than quartz.

Two corollaries can be drawn from the above result:

- (1) the concentration of silica in solution during the dissolution processes will effectively be driven by the faster-dissolving phase, and
- (2) the concentration in solution may exceed the solubility values of quartz while the diatom shells continue to dissolve, although this does not necessarily indicate that quartz would be precipitating from its supersaturated solution.

Dissolution of Feldspars. — Feldspars are aluminosilicate minerals of major abundance in crustal rocks and sediments. The general formula of their chemical composition is $M^{+n}\text{Al}_x\text{Si}_{4-x}\text{O}_8$, with $n = 1$ or 2. Potassium feldspar, KAlSi_3O_8 ,

sodium feldspar, $\text{NaAlSi}_3\text{O}_8$, and solid solutions of composition ranging from $\text{NaAlSi}_3\text{O}_8$ (albite) to $\text{CaAl}_2\text{Si}_2\text{O}_8$ (anorthite) belong to the main rock-forming minerals. Under environmental conditions, it has been observed that the Ca-feldspar and Ca-rich members of the solid solution series dissolve faster than the Na and K-feldspars. Ca-feldspars generally occur in igneous rocks formed at temperatures higher than those with Na-feldspar and K-feldspar, and their faster dissolution correlates with the general phenomenon of the relative rates of weathering of alumino-silicate minerals.

In a study of the rates of dissolution of feldspars in water, at 25°C and 1 atm pressure of CO_2 , four stages of dissolution have been identified [8]:

- (1) Rapid surface exchange,
- (2) Concentration increases as some power function of time,
- (3) Parabolic dissolution rate, and
- (4) Concentration increases linearly with time (steady dissolution rate).

The time-dependence of concentrations of cations and silica in solution and the approximate duration of each of the four dissolution stages are as follows:

First stage: Surface solution, H^+ -cation exchange (<3 min)

Second stage: Concentration rises as a low-power function of time; the stage lasts up to 50 hours,

$$C = k_e t^n \quad (70)$$

Third stage: Increase in concentration obeys the parabolic rate law; duration up to 20 days following the second stage,

$$C = C_0 + 2k_p t^{1/2} \quad (71)$$

The latter equation is identical to equation 41.

Fourth stage: Concentration increases linearly with time; duration up to 30 days following the third stage,

$$C = C_0 + k_o t \quad (72)$$

Rate parameters (k_e , $2k_p$, and k_o) for individual minerals in the second through fourth dissolution stages are listed in Table 3.4-7; these values must be multiplied by γV to obtain the corresponding rate constants. During the first two stages, more ions than silica is released to solution, resulting in a cation-deficient layer at the

TABLE 3.4-7

Dissolution Rate Parameters for Feldspars in Water
(at 25°C and 1 atm total CO₂ pressure)

Mineral ^a	Power Law (Eq. 65) $k_{ds} (10^{-10} \text{ mol} \cdot \text{cm}^{-2} \cdot \text{s}^{-n})$			Parabolic (Eq. 66) $2k_{ps} (10^{-13} \text{ mol} \cdot \text{cm}^{-2} \cdot \text{s}^{-1})$			Linear (Eq. 67) $k_{0s} (10^{-16} \text{ mol} \cdot \text{cm}^{-2} \cdot \text{s}^{-1})$			
	Na	Ca	K	Na	Ca	K	Na	Ca	K	Si
Albite	11.8	0.059	0.34	2.98			9.25	25.4	4.41	
Oligoclase	n =	6.18	3.90	0.223						
n =	0.059	0.053	0.76	2.81	1.10	5.83	1.67	0.89	2.60	
Andesine	2.41	—	0.153	—	—	—	4.05	0.86	—	1.40
n =	0.030	—	0.30	1.14	—	—	—	—	—	
Labradorite	3.87	3.58	0.193	—	—	—	4.05	—	—	
n =	0.039	0.057	0.72	1.02	1.29	3.27	0.72	1.09	1.26	
Bytownite	2.31	4.41	0.057	0.84	1.34	3.38	3.47	0.54	1.29	1.07
n =	0.061	0.064	0.057	0.158	—	—	—	—	—	
Anorthite	1.43	3.63	0.093	0.96	0.34	3.36	4.01	0.32	2.18	1.32
n =	0.027	0.093	0.173	—	—	—	—	—	—	
Orthoclase	1.49	5.43	0.066	0.30	1.49	4.19	3.78	0.66	2.70	1.68
n =	0.087	0.066	0.134	—	—	—	—	—	—	
Hilgardite	1.85	5.25	0.26	1.16	2.55	3.34	0.55	1.27	1.52	
n =	0.067	0.075	0.164	—	—	—	—	—	—	

a. See Table 3.4-8 for composition and specific surface areas of these minerals.

Source: Busenberg and Clemency [8]

feldspar surface. Within the albite-anorthite series, the rate constants for the release of sodium and calcium increase with an increasing mole fraction of each cation in the solid. The faster release of cations continues during the third (parabolic-rate dissolution) stage. When dissolution is continuous, the value of C_0 at the beginning of each dissolution stage is the concentration value attained at the end of the preceding stage. A computational example of silica release during dissolution of oligoclase is given below.

Example 6 Compute SiO_2 concentration in solution in a system closed to water flow and in contact with oligoclase having a solid concentration of $50 \text{ g} \cdot \text{l}^{-1}$.

After the stage of rapid surface exchange, the solubility of silica is given by equations 70-72. For the dissolution process described by equation 70, Table 3.4-7 lists the value of k_{es} as $0.76 \times 10^{-10} \text{ mol} \cdot \text{cm}^{-2} \cdot \text{s}^{-n}$. To calculate the rate parameter k_e , k_{es} must be multiplied by S/V. From Table 3.4-8, $S_g = 1 \text{ m}^2 \cdot \text{g}^{-1} = 10^4 \text{ cm}^2 \cdot \text{g}^{-1}$; therefore,

$$k_e = (0.76 \times 10^{-10} \text{ mol} \cdot \text{cm}^{-2} \cdot \text{s}^{-n}) (10^4 \text{ cm}^2 \cdot \text{g}^{-1}) (50 \text{ g} \cdot \text{l}^{-1}) \\ = 3.8 \times 10^{-5} \text{ mol} \cdot \text{l}^{-1} \cdot \text{s}^{-n}$$

If this dissolution stage lasts 30 hr ($t = 1.08 \times 10^5 \text{ s}$), the concentration of SiO_2 at the end of this time is, by equation 70 and with the power exponent value $n = 0.153$,

$$C = 3.8 \times 10^{-5} \times (1.08 \times 10^5)^{0.153} = 2.23 \times 10^{-4} \text{ mol} \cdot \text{l}^{-1} = 13.4 \text{ mg} \cdot \text{l}^{-1}$$

This C value of $2.23 \times 10^{-4} \text{ mol} \cdot \text{l}^{-1}$ becomes the new C_0 (initial concentration) for the next dissolution stage (parabolic-rate dissolution), which is characterized by the rate constant value of $2k_p = 5.83 \times 10^{-13} \text{ mol} \cdot \text{cm}^{-2} \cdot \text{s}^{-1/2}$. As in the preceding computation, the rate constant k_p is

$$2k_p = 5.83 \times 10^{-13} \times 10^4 \times 50 = 2.92 \times 10^{-7} \text{ mol} \cdot \text{l}^{-1} \text{ s}^{-1/2}$$

Allowing the parabolic dissolution stage to last 20 days ($t = 17.28 \times 10^5 \text{ s}$), we use equation 71 with the value of initial concentration $C = 2.23 \times 10^{-4} \text{ mol} \cdot \text{l}^{-1}$, attained at the end of the preceding stage. Thus,

$$C = 2.23 \times 10^{-4} + 2.92 \times 10^{-7} \times (17.28 \times 10^5)^{1/2} \\ = 6.07 \times 10^{-4} \text{ mol} \cdot \text{l}^{-1} = 36.4 \text{ mg} \cdot \text{l}^{-1}$$

This C value becomes the new C_0 (initial concentration) for the next stage of dissolution.

In the next (linear) stage, the dissolution rate constant in Table 3.4-7 is $k_{0n} = 2.60 \times 10^{-16} \text{ mol} \cdot \text{cm}^{-2} \cdot \text{s}^{-1}$, and the rate constant k_0 is

$$k_0 = 2.60 \times 10^{-16} \times 10^4 \times 50 = 1.30 \times 10^{-10} \text{ mol} \cdot \text{l}^{-1} \cdot \text{s}^{-1}$$

Allowing the linear-rate dissolution to continue for 30 days ($25.92 \times 10^5 \text{ s}$), we use equation 72 with the initial concentration $C_0 = 6.07 \times 10^{-4} \text{ mol} \cdot \text{l}^{-1}$, from the end of the preceding stage. The new concentration value is

$$C = 6.07 \times 10^{-4} + 1.30 \times 10^{-10} \times 25.92 \times 10^5 \\ = 9.44 \times 10^{-4} \text{ mol} \cdot \text{l}^{-1} \\ = 56.6 \text{ mg} \cdot \text{l}^{-1}$$

TABLE 3.4-8
Composition and Specific Surface Area of Feldspars
In the Albite-Anorthite Series

Mineral	Composition (mol %)			Specific Surface Area, S_g ($\text{m}^2 \cdot \text{g}^{-1}$)
	$\text{NaAlSi}_3\text{O}_8$	$\text{CaAl}_2\text{Si}_2\text{O}_8$	KAISi_3O_8	
Albite	98.9	0.1	1.0	0.83
Oligoclase	69.6	24.0	6.4	1.01
Andesine	49.5	42.7	7.8	1.49
Labradorite	44.5	53.0	2.5	1.04
Bytownite	22.2	77.4	0.4	1.14
Anorthite	5.8	94.0	0.2	1.84
Orthoclase	20.3	0.2	79.5	1.52
Microcline	24.8	0	75.2	1.07

Source: Busenberg and Clemency [8]

The main cation in oligoclase is sodium. For the oligoclase of composition given in Table 3.4-7, the atomic ratio Na/Si is approximately $1/4 = 0.25$. The differences between the dissolution rates of the individual components of feldspars are responsible for the ratios in solution that differ from those of the bulk solid. For Na, using the computation procedure shown above, with the data from Table 3.4-7, the Na concentrations at the end of each dissolution stage are consecutively 6.12×10^{-4} , 7.97×10^{-4} , and 10.13×10^{-4} $\text{mol} \cdot \text{l}^{-1}$. Thus, the Na/Si ratios in solution are 2.7 (after 30 hr), 1.3 (after 21 days), and 1.07 (after 51 days). The higher ratios show that sodium is removed from the solid preferentially to silicon; although the Na/Si ratio decreases with time, even after almost two months of dissolution it is higher than in the bulk solid, reflecting the faster removal of Na from the solid surface.

Example 7 How thick is the leached surface layer of a dissolving feldspar? This question can be answered using the results of the preceding computation. Initially, 50 g of oligoclase was in contact with 1 liter of water; 50 days later, about 100 mg of dissolved solids are in solution. (The amounts of 57 mg SiO_2 and 23 mg Na were computed in Example 6, such that the mass of 100 g of total solids is an orientational figure.) Thus, the fraction of the original solid that dissolved is $0.1 \text{ g}/50 \text{ g} = 0.002$ or 0.2%. A mass balance between the material in solution, $M(\text{soln})$, in the original solid, $M(\text{orig})$, and in the residual solid, $M(\text{res})$, is

$$\begin{aligned} M(\text{soln}) &= M(\text{orig}) - M(\text{res}) \\ \frac{M(\text{soln})}{M(\text{orig})} &= 1 - \frac{M(\text{res})}{M(\text{orig})} = 0.002 \end{aligned}$$

For spherical particles dissolving at the surface, the ratio of the remaining to the original mass is equal to the ratio of the cubes of the radii: $M(\text{res})/M(\text{orig}) = r^3/r_0^3$. Thus where r is the radius of the dissolving particle, and r_0 is the initial radius.

$$r^3/r_0^3 = 0.998$$

The fractional decrease in the radius of the fresh feldspar grains is

$$1 - \frac{r}{r_0} = 0.0007 \text{ or } 0.07\%$$

For particles of radius $r_0 = 10 \mu\text{m}$, the decrease translates into a 70\AA thickness of the leached layer.

The role of hydrogen-ion concentration in the dissolution of Na-feldspar was considered in detail for the region of linear dissolution, equation 72, by Wollast and Chou [45]. Their results, shown in Figure 3.4-3, indicate that the bulk rate of dissolution goes through a minimum in the neutral pH range, increasing by a factor of 100 under acidic or alkaline conditions. An explanation of this behavior has been given in terms of the transition state theory and activated complexes forming on the mineral surface. The following empirical equation describes the rate of congruent dissolution of sodium feldspar (albite), where R is in $\text{mol} \cdot \text{cm}^{-2} \cdot \text{s}^{-1}$:

$$R = 10^{-13.69} a_{\text{H}^+}^{0.49} + 10^{-16.15} + 10^{-18.15} a_{\text{H}^+}^{-0.30} \quad (73)$$

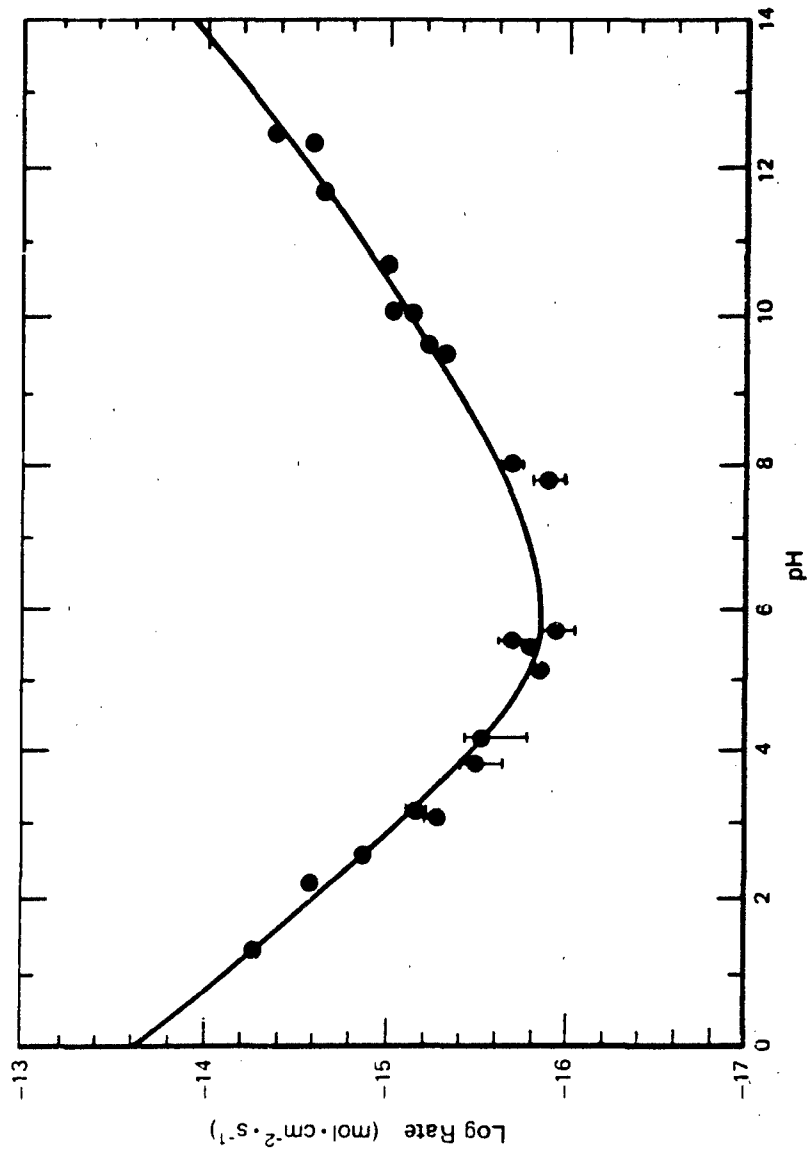
Example 3 In Example 4, the speed with which a silicate particle would dissolve in a diffusion-controlled dissolution reaction was calculated. For a spherical grain of the same diameter (1 mm), the rate of dissolution is many orders of magnitude slower when dissolution proceeds in a surface-controlled reaction. From Figure 3.4-3, the rate of dissolution near neutral pH is about $R = 2 \times 10^{-16} \text{ mol} \cdot \text{cm}^{-2} \cdot \text{s}^{-1}$. For a feldspar grain of radius $r = 0.05 \text{ cm}$ and molar volume $V_m = 100 \text{ cm}^3 \cdot \text{mol}^{-1}$, we have

$$\text{Initial dissolution rate} = RV_m = 2 \times 10^{-14} \text{ cm} \cdot \text{s}^{-1} = 6.2 \times 10^{-7} \text{ cm} \cdot \text{yr}^{-1}$$

In terms of a time scale measurable in years, the mineral grain is virtually insoluble. The rate of dissolution near $\text{pH} = 7$ translates into a linear rate (in the direction perpendicular to the grain surface) of about 60 \AA per year, in the absence of any catalytic or reaction-accelerating process. The time to complete dissolution of a spherical grain, under surface-controlled reaction conditions [21], is:

$$t = \frac{r}{RV_m} = \frac{5 \times 10^{-2} \text{ cm}}{6.2 \times 10^{-7} \text{ cm/yr}} = 80,000 \text{ years}$$

A grain ten times smaller in diameter (0.1 mm) will survive under the same conditions one-tenth as long, or 8,000 years. The order of magnitude agrees with the times of renewal or mean age of soils, 10^3 to 10^4 years [21].

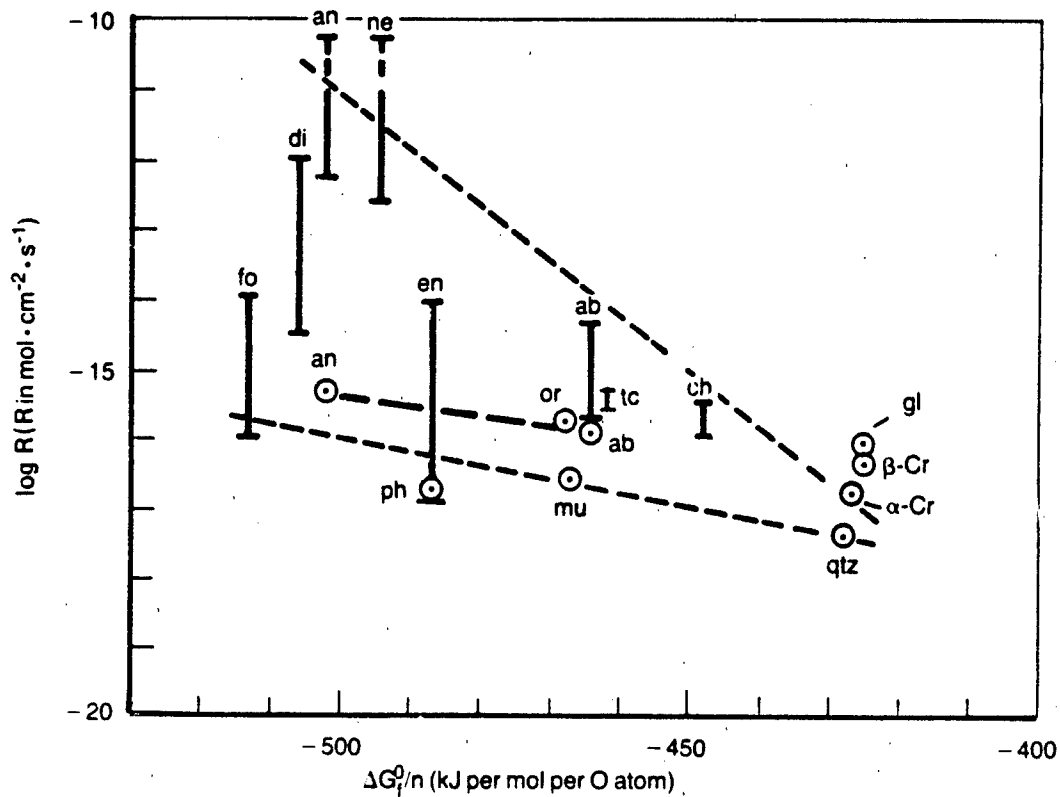


Source: Wollast and Chou [45]. (Copyright 1985, Reidel Publishing Co. Reprinted with permission.)

FIGURE 3.4-3 Rate of Dissolution of Sodium-Feldspar (Albite) as a Function of pH, at a Constant Rate of Albite Dissolution

Dissolution Rates of Other Silicate Minerals. — The preceding two sections concerned minerals made of pure SiO_2 and several members of the feldspar group. The variety of the silicate minerals extends to many other groups, such as olivines, pyroxenes, amphiboles, and micas, all of which are characterized by specific crystal structures and chemical compositions of varying complexity.

In Figure 3.4-4 are plotted the rates of dissolution at 25°C of 16 minerals, expressed as $\log R$, against their standard Gibbs free energies of formation. The data for this plot



Notations for different solids are given in Table 3.4-9. Dashed lines bracket the range of solubility rates of the common silicate minerals.

Source: See Table 3.4-9 for explanation of symbols.

FIGURE 3.4-4 Rates of Dissolution of Some Silicates, $\log R$, Plotted Against Their Gibbs Free Energies of Formation (25°C), Normalized to the Number of the Oxygen Atoms (n) in the Stoichiometric Formula of the Silicate

are summarized in Table 3.4-9, which also lists the chemical composition of each mineral and the identifying symbols used in Figure 3.4-4. The tabulated values of $\Delta G_f^0/n$ are the free energies of formation per mole, divided by the number of oxygen atoms in the stoichiometric formula of the mineral; this division helps to normalize the ΔG_f^0 values, which vary considerably with the solid compositions and complexity of the stoichiometric formulas. Figure 3.4-4 shows that the solubility rate R increases as ΔG_f^0 becomes more negative.³

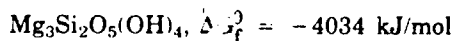
The range of the log R values plotted for several minerals reflects in many cases the dependence of the dissolution rate on pH. Some of this dependence is noted in the final column of Table 3.4-9, and the subject was also discussed earlier under "Dissolution of Feldspars."

At least some of the aluminosilicates listed in Table 3.4-9 are characterized by a dissolution behavior as a function of pH of the type shown in Figure 3.4-3: dissolution rates are high in the acidic range, then decline to a more or less clearly defined minimum in the range $5 < \text{pH} < 7$, and finally increase again through the alkaline pH range.

The following example shows how $\log k$ is obtained from the free energy values and indicates the uncertainty of this empirical estimation:

Example 9 What is the solubility rate of white asbestos (chrysotile) in water at 25°C?

Chemical composition and the standard free energy of formation of chrysotile are:



The total number of oxygen atoms in the stoichiometric formula is $n = 9$. Thus,

$$\Delta G_f^0/n = -4034/9 = -448 \text{ kcal/mol per O atom}$$

From Figure 3.4-4, the value of $\log R$ corresponding to -448 on the horizontal axis is within the range from -15.2 to -17 between the dashed lines. The midpoint of this range is $\log R \approx -16$. Experimentally determined dissolution rates of silica in chrysotile at 25°C are in the range of $\log R \approx -16$ to -15.5 over the pH range from 11 to 8 [1].

In the temperature range from about 100°C to 700°C, rates of dissolution of many silicate and aluminosilicate minerals in water indicate increasing solubility with

3. The more negative values of ΔG_f^0 do not necessarily indicate that the minerals are relatively more stable in an aquatic environment. The relative stability of a solid with respect to dissolution — or, in broader terms, its relative resistance to weathering — is determined by the free energy change for a dissolution reaction, not by the ΔG_f^0 values of the solid alone.

TABLE 3.4-9

Dissolution Rates of Selected Silicate Minerals in Water at 25°C,
and Other Data for Correlating Dissolution Rates with $\Delta G_f^0/n$

Mineral	Formula	Symbol in Figure 3.4-4	Number of O Atoms n	Free Energy of Formation ^a per O atom		Log Dissolution Rate ^b log R	pH at Source Low k High k
				$\Delta G_f^0/n$	(kJ/mol per O atom)		
Quartz	SiO_2	qtz	2	-428		-17.4	[37]
α -Cristobalite	SiO_2	$\alpha\text{-Cr}$	2	-427		-16.8	[37]
β -Cristobalite	SiO_2	$\beta\text{-Cr}$	2	-425		-16.3	[37]
SiO_2 glass	SiO_2	gl	2	-425		-16.1	[37]
Nepheline	NaAlSiO_4	ne	4	-494		-12.6 to -10.3	[41]
Forsterite	Mg_2SiO_4	fo	4	-513		-16 to -14	[1] ^c
Enstatite	$\text{Mg}_2\text{Si}_2\text{O}_6$	en	6	-487		-16.5 to -14	[1] ^c
Diopside	$\text{CaMgSi}_2\text{O}_6$	di	6	-506		-14.5 to -12	[1] ^c
K-feldspar	KAlSi_3O_8	or	8	-468		-15.8	[8]
Albite	$\text{NaAlSi}_3\text{O}_8$	ab	8	-464		-15.8 to -14.3	[45]
Anorthite	$\text{CaAl}_2\text{Si}_2\text{O}_8$	an	8	-502		-12.3 to -10.3	[14]
Albite-Anorthite series		(ab to an)	8	(-464 to -502)		-15.9 to -15.4	[8]
Chrysotile	$\text{Mg}_3\text{Si}_2\text{O}_5(\text{OH})_4$	ch	9	-448		-16.0 to -15.5	[1] ^c
Talc	$\text{Mg}_3\text{Si}_4\text{O}_{10}(\text{OH})_2$	tc	12	-461		15.4 to -15.2	[23]
Muscovite	$\text{KAl}_3\text{Si}_3\text{O}_{10}(\text{OH})_2$	mu	12	-467		-16.6	[24]
Phlogopite	$\text{KMg}_3\text{AlSi}_3\text{O}_{10}(\text{OH})_2$	ph	12	-487		-16.4	[25]

a. From Robbie et al. [38]; phlogopite from Drever [10].

b. Dissolution rate k refers to release of Si, when individual elemental components of solids are reported as having different k-values.

c. Plus other sources and own data on chrysotile.

increasing temperature. Wood and Walther [46] demonstrated this trend by application of the Arrhenius relationship (equation 57) to experimental data and summarized it in the following equation:

$$\log R = -6.85 - \frac{2900}{T} \quad (74)$$

where T is temperature (K) and the dissolution rate R is in units of gram-atoms of oxygen per square centimeter per second ($\text{g-at O} \cdot \text{cm}^{-2} \cdot \text{s}^{-1}$). Compared with some experimental values of R measured at approximately 25°C , the results of this equation are low by about a factor of 10, an uncertainty margin comparable to that of the data plotted in Figure 3.4-4.

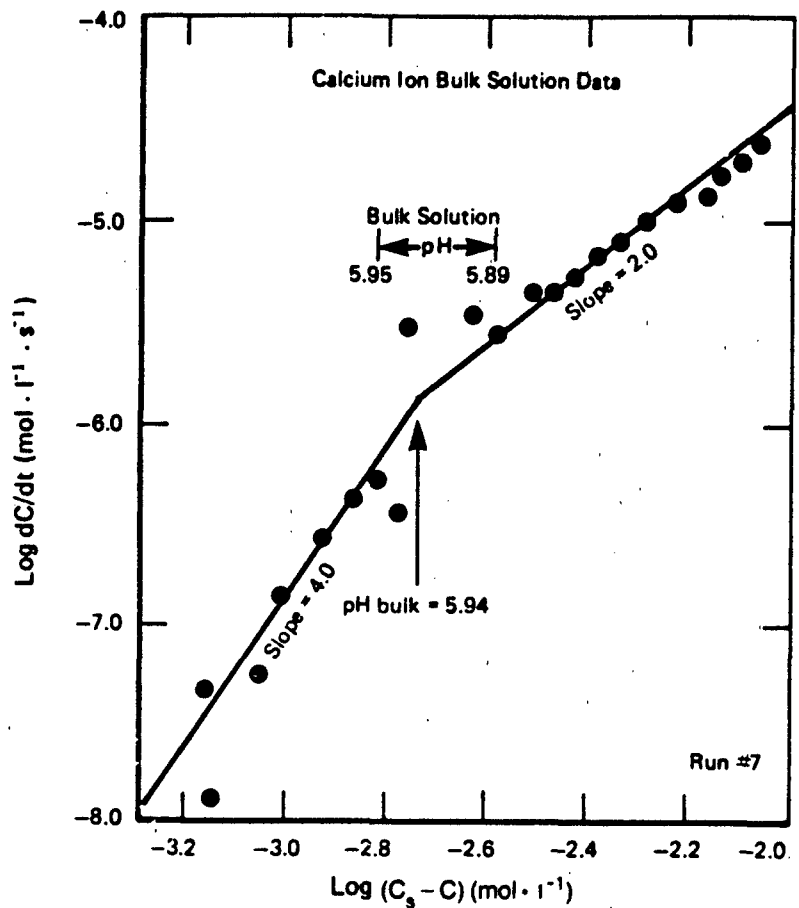
Dissolution Rates of Calcite. — Experimental study of the dissolution of calcite (CaCO_3) is a subject of considerable environmental importance, owing to the abundance of CaCO_3 as the minerals calcite and aragonite, in fresh sediments, in old sedimentary rocks, and in the deposits that form in various engineered structures in contact with water.

The rates of dissolution of calcite in natural waters show, in general, great variability that is related to the physical state of the solid, to the chemical composition of the aqueous phase, and to the pH and the partial pressure of CO_2 of the solution.

Plummer and Wigley [35], some of whose results on the dissolution rate of calcite in water are reproduced in Figure 3.4-5, have cited extensive evidence from several investigators that trace amounts of metals and other species in solution can inhibit the rate of calcite dissolution. The inhibiting effects on calcite dissolution in fresh and ocean waters have been known for trace concentrations of the ferric and chromic ions, scandium, copper, and phosphate; this is presumably due to attachment of the tracer ions to the more reactive surface sites on the solid. In natural waters, particularly in those flowing slowly through groundwater aquifers in limestones, the inhibiting effects of tracer impurities may keep the groundwater below saturation with respect to CaCO_3 for many centuries.

The main conclusions of the dissolution rate experiments of Plummer and Wigley are the following:

- (1) When the pH of the solution is below 4, dissolution is probably a diffusion-controlled process;
- (2) At a pH of about 5 and higher, dissolution is controlled by surface reactions;
- (3) Up to $\text{pH} \approx 5.94$, the rate of reaction of the Ca^{+2} -release and the consumption of H^+ ions is very nearly second-order (Figure 3.4-5);
- (4) Above $\text{pH} \approx 5.94$, the reaction rate is slower, tending to follow a fourth-order rate law.



Conditions: 25°C, CO₂ saturated solution at 1 atm, pH range approximately 4 to 6.

Source: Plummer and Wigley [35]. (Copyright 1976, Pergamon Press, Inc. Reprinted with permission.)

FIGURE 3.4-5 Rate of Calcite Dissolution as a Function of Distance from Saturation

In the region of the second-order reaction, the rate of release of the Ca^{+2} ions into solution is:

$$\frac{dC}{dt} = \frac{S}{V} - k(C_s - C)^2 \quad (\text{mol} \cdot \text{l}^{-1} \cdot \text{s}^{-1}) \quad (75)$$

where S = surface area of the solid (cm^2)

V = solution volume (cm^3)

k = reaction rate parameter ($\text{cm} \cdot \text{l} \cdot \text{mol}^{-1} \cdot \text{s}^{-1}$)

C_s = concentration of Ca^{+2} at the solid surface, at equilibrium with the solid (mol/l)

C = concentration of Ca^{+2} in solution (mol/l).

The rate parameter k is pH-dependent; for calcium-ion release, the value of k increases about linearly from 0.012 at $\text{pH} = 5.70$ to 0.034 at $\text{pH} = 5.94$. (The units of k are defined above.)

In an experimental study of the rate of dissolution of calcite at $\text{pH} = 9.8$, and in solutions containing other dissolved electrolytes, Rickard and Sjöberg [36] showed that the rate of dissolution is a function of the degree of saturation of solution with respect to calcite:

$$\frac{dC}{dt} = k_2 S (1 - \Omega^{1/2}) \quad (76)$$

where k_2 is a reaction rate parameter, S is the surface area of the solid, and Ω is the degree of saturation (see section 2.11.2), expressed as the ratio of the ion-concentration product (ICP) and the solubility product (K_{sp}):

$$\Omega = \frac{\text{ICP}}{K_{sp}} = \frac{[\text{Ca}^{+2}][\text{CO}_3^{2-}]}{K_{sp}} \quad (77)$$

Equation 76 for calcite is similar in form to equation 66 for the dissolution rates of SiO_2 minerals.

As a whole, laboratory experiments such as those cited in this section provide information on the reaction mechanisms of the calcite dissolution process, but they do not (and are not claimed to) reproduce the dissolution rates of natural environments, which are often much slower than those achieved in the laboratory.

3.4.4 Precipitation, Nucleation, Growth, and Recrystallization

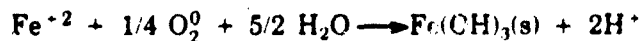
This section deals with the kinetics of the processes that are the reverse of dissolution — removal of materials from an aqueous to a solid phase.

Although a process of precipitation must begin with nucleation — formation of nuclei and submicroscopic crystals in solution — the theory and the mathematical treatment of the two are very different. Precipitation can be observed and recorded, and its rate can be measured by direct determination of a decrease of some reactant concentration in solution. The treatment and computations based on the results when applied to rates of precipitation are fairly similar to those discussed in the preceding sections on rates of dissolution; for this reason, a case study of precipitation rate will be dealt with before other processes, such as nucleation, crystal growth, and recrystallization.

RATES AND EXAMPLE OF PRECIPITATION

Precipitation of Fe(III)-hydroxide

Ferric hydroxide of composition Fe(OH)_3 is a commonly occurring substance in the environment. In aqueous solutions, oxidation of ferrous iron by dissolved oxygen leads to precipitation of ferric hydroxide according to the reaction:



The rate of removal of Fe^{+2} from solution is a measure of ferric hydroxide precipitation. The rate of removal of the ferrous iron can be written as [39]:

$$\frac{d[\text{Fe}^{+2}]}{dt} = k [\text{Fe}^{+2}] p\text{O}_2 [\text{OH}^-]^4 \quad (78)$$

where $p\text{O}_2$ is the partial pressure of oxygen (atm), and brackets denote concentrations in mol/liter.

The foregoing rate equation stipulates a dependence on the first power of O_2 , whereas a fractional stoichiometric coefficient (1/4) appears in the reaction that precedes it. The 4:1 stoichiometric ratio for Fe/O_2 has been confirmed by White and Yee [44].

At a constant partial pressure of oxygen and a constant pH, the rate equation reduces to the form of a first-order kinetic law:

$$-\frac{d[\text{Fe}^{+2}]}{dt} = k_1 [\text{Fe}^{+2}] \quad (79)$$

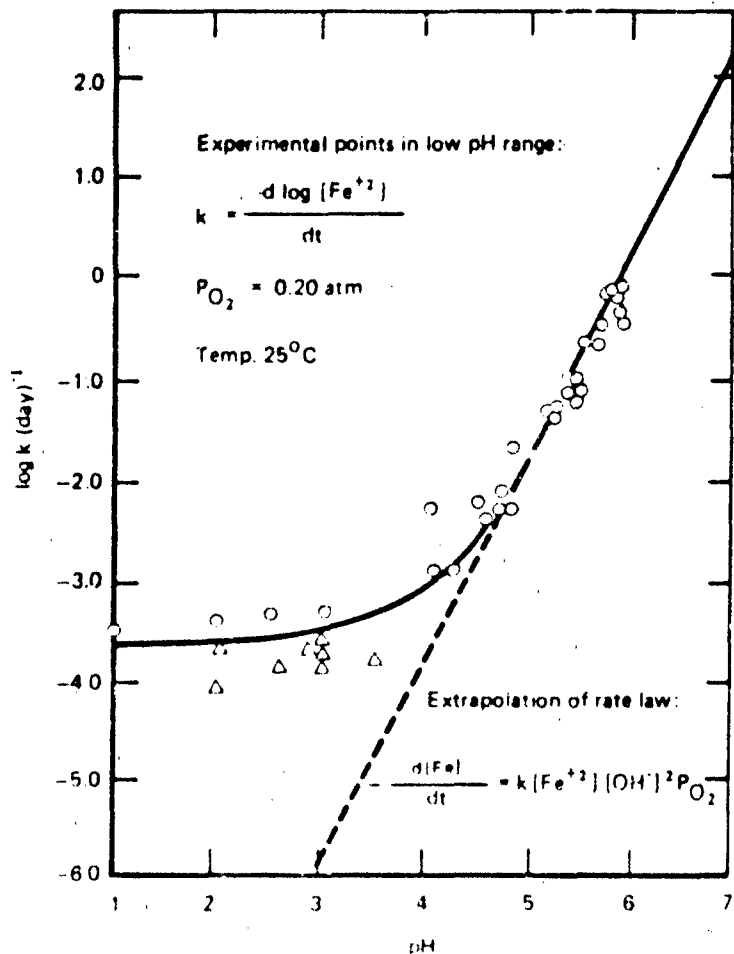
Stumm and Morgan [39] give the value for the reaction rate constant in equation 78, at 20°C, as

$$k = (8.0 \pm 2.5) \times 10^{13} \text{ l}^2 \cdot \text{mol}^{-2} \cdot \text{atm}^{-1} \cdot \text{min}^{-1}$$

From the results of many investigators who have studied Fe^{+2} oxidation in various natural waters, Davison and Seed [9] concluded that the best values of k are slightly lower:

$$k = (2 \pm 1) \times 10^{13} \text{ l}^2 \cdot \text{mol}^{-2} \cdot \text{atm}^{-1} \cdot \text{min}^{-1}$$

The variation of the rate parameter k as a function of pH is shown in Figure 3.4-6.



Source: Stumm and Morgan [39] (Copyright 1981, John Wiley & Sons. Reproduced with permission.)

FIGURE 3.4-6 Observed Rate Constant for Oxidation of Fe^{+2} in Water

Dependence of k on Temperature and Solution Composition

For the oxidation reaction of Fe^{+2} , as given in the preceding section, the dependence of k on temperature in the range from 5° to 30°C is reflected in the value of the activation energy parameter $E = 96 \text{ kJ/mol}$ [39]. This value can be used in equations 56-58 to compute the rate parameter k at temperatures below or above the value for 20°C.

Salts in solution tend to slow down the Fe(II) oxidation reaction [40] according to the relationship

$$\log k = 13.76 - 2.06 I^{1/2} \quad (80)$$

where I is the ionic strength of the solution. (For definition of I, see section 2.6.) It has also been reported [18] that in solutions of relatively high alkalinity, above an equivalent of 340 mg CaCO_3/l , k increases with alkalinity.

Sources of Fe(II)

Reduced iron occurs in many rock-forming minerals, either as the only main metal constituent or as a companion to the oxidized ferric iron, Fe(III). Purely ferrous iron minerals include both common and less abundant species, such as:

FeS_2	— pyrite, marcasite
FeCO_3	— siderite
$\text{Fe}_3(\text{PO}_4)_2 \cdot 8\text{H}_2\text{O}$	— vivianite
Fe_2SiO_4	— fayalite, an olivine
Pyroxenes	— for example, augite

Minerals with iron present in the lattice in two oxidation states are such commonly occurring species as

Fe_3O_4	— magnetite ($\text{FeO} \cdot \text{Fe}_2\text{O}_3$)
Biotite	— a mica

Ferric iron occurs in a variety of alumino-silicate minerals and in the three abundant oxides and oxy-hydroxides:

Fe_2O_3	— hematite
$\alpha\text{-FeOOH}$	— goethite
$\gamma\text{-FeOOH}$	— lepidocrocite
Fe(OH)_3	— amorphous ferric hydroxide

The solubilities of Fe(III) oxy-hydroxides are very low at near-neutral pH values, and the oxidized Fe(II) is generally removed from solution very efficiently.

In the deeper groundwaters and in the deeper parts of some lakes, the decay of organic matter consumes all the oxygen. This promotes reduction of Fe(III) to Fe(II), which (depending on the local environmental conditions) can either react with sulfide in water, forming FeS or FeS₂, or migrate into the water column. Transport of dissolved Fe(II) toward the upper oxygenated layers ultimately results in its oxidation, whereupon the iron returns to the lake bottom as precipitated Fe(OH)₃.

Rates of Oxygen Consumption

In a homogeneous Fe(II) solution, the rate of removal of Fe(II), as shown in Figure 3.4-6, translates into a rate of oxygen consumption by the Fe(II) sink.

Below pH ≈ 3, the reaction is evidently independent of hydrogen-ion concentration and takes place slowly, with a half-life of about $t_{1/2} = 1/k = 3000$ days. From equation 78, at the atmospheric value of the oxygen partial pressure $pO_2 = 0.2$ atm and for an arbitrarily chosen pH of 6.5, the reaction rate parameter k_1 is

$$k_1 = 2 \times 10^{13} \times 0.2 \times (10^{-7.5})^2 = 0.004 \text{ min}^{-1}$$

The reaction half-life is then

$$t_{1/2} = 1/k_1 = 250 \text{ min}$$

Half-lives of comparable magnitude, 10² to 10³ min, have been reported for the oxidation of iron in pyrite [39].

The oxidation reaction may be retarded through aqueous complex formation with organic materials and, as mentioned earlier, through an increase in the salt concentration in solution.

A study of the oxidation of Fe(II) on the surfaces of silicate minerals (biotite, hornblende and augite) in contact with water has shown that the rate of oxygen consumption increases with acidity: at a pH of 1.5-3.5, the rates of oxidation are significantly higher [44]. Overall, the reported half-lives of the oxygen consumption reactions are about 12 days.

NUCLEATION AND CRYSTAL GROWTH

Crystal nuclei form in supersaturated solutions by processes known as homogeneous and heterogeneous nucleation.

Homogeneous nucleation is the formation of clusters of atoms or molecules of a certain critical size from a supersaturated solution, where they continue to grow as long as the solution remains supersaturated.

In *heterogeneous nucleation*, clusters of atoms or molecules form on an existing substrate. In a supersaturated solution this substrate can consist of crystals of the same phase, such as seeds of NaCl in a solution supersaturated with respect to this mineral, or it can consist of particles of a different phase, such as flakes of mica or practically any other poorly soluble solid.

The more commonly observable nucleation events in the environment are nucleation of ice, nucleation of sulfur and other minerals from the vapor phase emanating from volcanic vents, and nucleation of some commonly occurring minerals in natural waters. In the latter group of processes, fine-grained CaCO₃ can nucleate in surface layers of freshwater lakes and oceans, forming characteristic patches of white-colored water ("whitenings") during periods of strong biological productivity. Seasonally strong growth of photosynthetic organisms reduces concentrations of dissolved CO₂ in water, which increases the pH and causes CaCO₃ crystals to appear in the surface water layers. Similarly, sodium chloride crystals can nucleate and grow in the surface layer of saline brine lakes, where evaporation may cause local supersaturation with respect to halite. These crystals may grow in a pattern of thin snowflakes and remain on the brine surface for some length of time.

Alkaline brine lakes that are rich in bicarbonate and carbonate, in arid climates, contain relatively high concentrations of dissolved SiO₂. During rainy periods, fresh-water runoff overflows the brine, causing a decrease in the pH and subsequent nucleation and precipitation of amorphous SiO₂ gel [11, 12].

Homogeneous Nucleation

The universal presence of suspended solids in natural waters makes it difficult to distinguish between homogeneous and heterogeneous nucleation. In effect, a statement that homogeneous nucleation is an important mechanism of mineral phase formation in natural waters requires proof of its correctness.

A classical theory of homogeneous nucleation in a supersaturated aqueous solution is based on a concept of the free energy change required for the formation of a molecular cluster and the formation of a surface in a supersaturated solution. Supersaturation, relative to the solubility of the bulk phase, provides the driving force needed for the formation of the cluster and the solid surface. Based on the theory of the free energy change in the process of a nucleus formation, the rate of formation of new nuclei (J , number of nuclei per unit volume of solution per unit of time) is represented as a function of temperature, volume of the molecules, interfacial energy between the crystal and solution, and the degree of supersaturation of the solution, as follows [33, 43]:

$$J = A \exp\left(-\frac{\Delta G^*}{RT}\right) \quad (81)$$

where J = rate of nucleation (cm⁻³ · s⁻¹)

A = pre-exponential factor, ranging from 10²⁵ to 10³⁰

ΔG^* = free energy of formation of a nucleus of critical size

T = temperature (K)

R = gas constant

An explicit form of the free energy term ΔG^* gives the following relationship for the nucleation rate:

$$J = A \exp \left[-\frac{\beta v^2 \sigma^3}{k^3 T^3 (n \ln s)^2} \right] \quad (82)$$

where β = nucleus shape factor (Table 3.4-10)
 v = volume of the cluster-forming molecules (cm^3)
 σ = interfacial energy ($\text{erg} \cdot \text{cm}^{-2}$, (as given in Table 3.4-11))
 n = number of atoms making up a molecule in the cluster
 s = degree of supersaturation, defined as (concentration in solution)/(concentration at saturation with bulk phase)
 k = Boltzmann constant ($1.38 \times 10^{-16} \text{ erg} \cdot \text{deg}^{-1}$)

For the rate of appearance of one nucleus, $J = 1 \text{ cm}^{-3} \cdot \text{s}^{-1}$, supersaturation can be defined as critical supersaturation, s^* . The value of s^* for this event can be derived from equation 82:

$$\ln s^* = \left(\frac{\beta v^2 \sigma^3}{k^3 T^3 n^2 \ln A} \right)^{1/2} = \frac{v \sigma}{k T n} \left(\frac{\beta \sigma}{k T \ln A} \right)^{1/2} \quad (83)$$

It is worth examining the effects of the individual parameters in equation 83 on the theoretical degree of supersaturation needed to induce homogeneous nucleation.

The molecular volume, v , is easily derived from the tabulations of densities ($\rho, \text{ g} \cdot \text{cm}^{-3}$) of molar volumes ($V_m, \text{ cm}^3 \cdot \text{mol}^{-1}$):

$$V = \text{gfw}/(\rho N) \quad (\text{cm}^3) \quad (84)$$

$$= V_m/N \quad (\text{cm}^3)$$

where gfw is the gram-formula weight of the solid and N is the Avogadro number.

For most simple oxides of metals, and for simple anhydrous halides, carbonates, and sulfates, the molar volumes fall in the range from 10 to $80 \text{ cm}^3 \cdot \text{mol}^{-1}$. This eightfold variation is also reflected in the molecular volumes v .

The cluster shape factor β , given in Table 3.4-10, varies by more than a factor of 10, depending on the cluster shape. Even for such shapes as the sphere and the cube, which are commonly used in theoretical computations of nucleation rates, there is a difference of a factor of two. The dependence of critical supersaturation s^* on the shape factor β is somewhat reduced by the power $1/2$.

The values of the interfacial energy, σ , as given in Table 3.4-11, differ from one compound to another by a factor of about two. Because of the $3/2$ power, the dependence of s^* on σ is not insignificant. The same type of dependence applies to temperature, but the range of the environmental temperatures from about 10°C to 40°C (283 to 313 K) is fairly small.

TABLE 3.4-10

Geometric Shape Factor, β , in the Homogeneous Nucleation Equation (82)

Body Shape	β
Sphere	16.7552
Icosahedron	20.2162
Dodecahedron	22.2012
Octahedron	27.7128
Cube	32.0000
Rectangular parallelepiped ($4\ell \times 2\ell \times \ell$)	50.8148
Tetrahedron	55.4256
Rod ($10\ell \times \ell \times \ell$)	109.7600
Plate ($10\ell \times 10\ell \times \ell$)	204.8000

Source: Nielsen [33]

TABLE 3.4-11

Interfacial Energy of Crystal Nuclei Against Aqueous Solutions for Spherical and Cubic Nuclei, Critical Supersaturation Ratio for Homogeneous Nucleation, and Critical Diameter of Nucleus

Solid Phase	Critical Supersaturation Ratio, s^*	Interfacial Energy, σ (erg · cm ⁻²)		Critical Diameter, d^* (Å)
		Spherical Nuclei	Cubic Nuclei	
BaSO ₄	1000; 500	116	151	11
PbSO ₄	28; 40	74	119	13
SrSO ₄	39	81	70	12
PbCO ₃	106	105		11
SrCO ₃	30	86		12
CaF ₂	80	140	140	9
MgF ₂	30	129		9
AgCl	5.5	72		15
AgBr	3.7	56		15
Ag ₂ SO ₄	19	62		14

Source: Walton [43]

The uncertainty or variation in the magnitude of the pre-exponential factor A is small, because its natural logarithm appears in equation 83: $\ln A$ varies, depending on the value of A, from 57.6 to 69.1, and the difference of 20% is reduced to 10% by the power 1/2.

Some values of critical supersaturation for homogeneous nucleation of a number of inorganic phases are listed in Table 3.4-11.

Heterogeneous Nucleation and Crystal Growth

Mathematical treatment of the initial stages of heterogeneous nucleation is fairly complex, because numerous parameters concerning the structure and energy states of the substrate surface must be known. A process of crystal growth, following the early stage of nucleation, is schematically shown in Figure 3.4-7. The rate of crystal growth in solution is amenable to a much simpler mathematical treatment if one considers growth on existing nuclei. In supersaturated solutions seeded with small crystals of the same composition, relief of the supersaturation is attained through the process of growth, either entirely or at least partly caused by heterogeneous nucleation.

An empirical relationship that applies in general to growth of crystals in solution has the form

$$-\frac{dC}{dt} = k_m S (C_s - C)^m \quad (85)$$

where C = concentration in a supersaturated solution

C_s = concentration at saturation with the bulk phase ($C_s < C$)

S = surface area of the growing crystals

k_m = rate parameter for crystal growth

m = the order of the reaction

The order of the crystal growth reaction, m , is often equal to the total number of ions in the stoichiometric formula of the crystalline phase. The reaction order values are summarized in Table 3.4-12. An exception to the rule is $Mg(OH)_2$, whose rate of growth in solution has been described as following the first-order rate law. The mechanism of growth in the early stage of nucleation and growth is considered to be surface-reaction controlled or interface controlled [30].

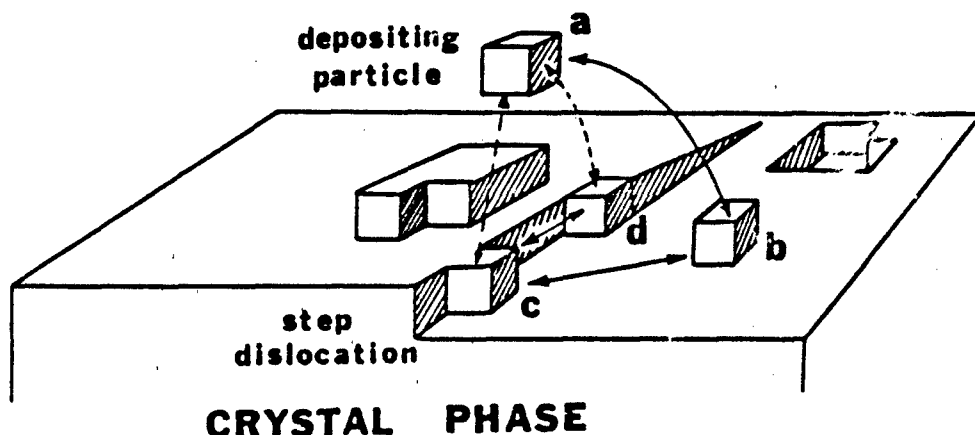
Temperature Dependence of Growth Rate

The Arrhenius type of dependence of the reaction rate parameter k_2 for second-order crystal growth reactions is written as

$$\ln k_2 = \ln A - E_a/RT \quad (57)$$

where A is a pre-exponential factor, E_a is the activation energy for new growth, and R is the gas constant.

SUPERSATURATED SOLUTION



Dissolved species (a) attaches to the crystal surface (b), and migrates by a process of surface diffusion to the face of crystal step (c). At c, the added material is bonded stronger to the crystal than at b, owing to a greater portion of its surface being in contact with the crystal faces. Diffusion from c to d stabilizes the added material further (greater area of contact), enabling it to become incorporated in the crystal lattice.

Source: Nancollas and Reddy [30]. (Copyright 1974, Ann Arbor Science Publishers. Reprinted with permission from Butterworth Publishers, current holders of the copyright.)

FIGURE 3.4-7 Schematic Diagram of Crystal Growth in Solution

The values of the activation energy listed in Table 3.4-13 may be compared with the value of $E_a \approx 20$ kJ/mol expected for diffusion-controlled reactions. The values for AgCl and BaSO₄ are similar to those for diffusion-controlled growth, but it is not a proof of a diffusion-controlled reaction. Other values are substantially below or above 20 kJ/mol.

Nucleation or Calcite and Inhibition of Growth

In the section on dissolution of calcite (CaCO₃), it was mentioned that inhibition of dissolution has been observed for a number of major and minor constituents of natural waters. Inhibition of the oxidation of Fe(II) in water has also been cited in §6.8.

Inhibition of crystal growth is a process of considerable importance in water treatment, in chemical and pharmaceutical industries, and in natural water environ-

TABLE 3.4-12
**Order of Precipitation and Crystal Growth
 Reactions for Equation 85**

Solid Phase	Reaction Order m
AgCl	2
AgI ₃	2
BaSO ₄	2
SrSO ₄	2
PbSO ₄	2
CaSO ₄ · 2H ₂ O	2
CaC ₂ O ₄ · H ₂ O	2
MgC ₂ O ₄ · 2H ₂ O	2
Ag ₂ CrO ₄	3
Mg(OH) ₂	1
SrC ₂ O ₄ · H ₂ O	1
CdC ₂ O ₄ · 3H ₂ O	1

Sources: References 16, 20, 22, 26, 29, 32, 43

TABLE 3.4-13
Activation Energies for Heterogeneous Nucleation in Aqueous Solutions

Solid Phase	E _a (kJ · mol ⁻¹)	Source
MgC ₂ O ₄ · 2H ₂ O	12.5	[22]
AgCl	20.9	[20]
BaSO ₄	20.9 ± 2.1	[32]
CaHPO ₄ · 2H ₂ O	43.9	[30]
CaC ₂ O ₄ · H ₂ O	49.0 ± 4.2	[29]
CaSO ₄ · 2H ₂ O	62.8 ± 2.1	[26]

ments. A systematic study of the inhibition of crystal growth of calcite, magnesium hydroxide, calcium sulfate dihydrate, and dicalcium phosphate dihydrate has been done by Nancollas and Reddy [30], whose data on calcite are given in Table 3.4-14.

The values of k_2 in Table 3.4-14 apply to the reaction rate parameter in the second-order reaction 85. Concentration in solution, C, as a function of time is given by an integrated form of equation 85:

$$\frac{1}{C_s - C} - \frac{1}{C_s - C_0} = k_2 St \quad (86)$$

where C_0 is the concentration of calcium at the start of the experimental measurements. In equation 86, the surface area of the growing crystals is assumed to be constant. The accuracy of this assumption can generally be either confirmed or disproved only by measurements of the surface area before and after the experiment. Concentrations of calcium (C in equation 86) obtained by measurement in the course of crystal growth over a period of about one hour are used to compute the left-hand side of equation 86, when the initial and equilibrium concentrations must also be known. A plot of the values of the left-hand side of equation 86 against time produces a straight line, indicating that the second-order reaction is obeyed.

TABLE 3.4-14

Effect of Inhibiting Additives on Rates of Calcite Crystallization in a Supersaturated Solution at 25°C

Precipitation Rate Constant, ^a k_s ($\text{cm}^6 \cdot \text{mol}^{-1} \cdot \text{cm}^{-2} \cdot \text{s}^{-1}$)	Additive Concentration		Additive ^b
	mg/l	$\mu\text{ mol/l}$	
1.52 \pm 0.35	0	0	—
1.10	0.05	0.12	ENTMP
0.70	0.08	0.18	ENTMP
0.28	0.12	0.28	ENTMP
0.15	0.50	1.2	ENTMP
0.12	2.5	5.8	ENTMP
0.028	0.5	1.0	TENTMP
0.009	2.5	5.1	TENTMP

a. $k_s = k_2 V/S$, where k_2 is the second-order reaction rate constant ($\text{cm}^3 \cdot \text{mol}^{-1} \cdot \text{s}^{-1}$), V is the solution volume (cm^3), and S is the solid surface area (cm^2).

b. ENTMP = N,N,N',N'-ethylenediaminetetra (methyleneephosphonic) acid

TENTMP = N,N,N',N'-triethylenenetetraamino-tetra (methyleneephosphonic) acid

Source: Nancollas and Reddy [30]

The inhibiting effect of the phosphonate ions, as shown in Table 3.4-14, is noticeable at low concentrations, of the order of 10^{-7} to 10^{-6} mol/l, in the presence of much higher calcium concentration in the supersaturated solution, of the order of 10^{-4} mol/l. A decrease in the growth rate by a factor of ten is accomplished by a tenfold increase in concentration of the inhibiting agent, in a low concentration range.

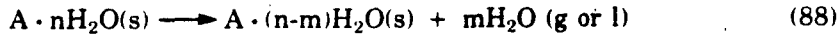
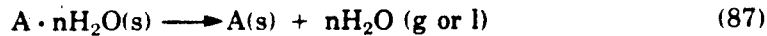
KINETICS OF RECRYSTALLIZATION

In the early part of this section, several types of recrystallization and precipitate aging processes were mentioned. For one type of recrystallization — dehydration and hydration reactions of solids — the data base seems to be more developed than for other recrystallization reactions; for this reason, the kinetics of dehydration and hydration are presented here, along with some case studies.

The Nature and Driving Forces of Dehydration

Dehydration is the removal of water molecules that form part of a crystal lattice of a solid. As such, the process clearly differs from drying or desiccation, which is the removal of water that is adsorbed on the surfaces of solids or that fills the capillary and interstitial spaces within solid materials.

A dehydration reaction can be either complete or partial, depending on whether an anhydrous phase or a hydrate with fewer water molecules in the structure is the reaction product. A general reaction balance is



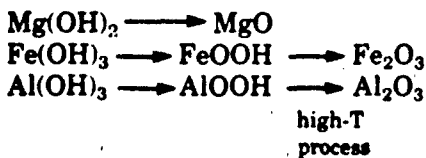
Decomposition of solids into other solids and evolving gases is a chemical problem of considerable industrial and technological concern, particularly in processes at elevated temperatures, where thermal stresses become the main driving forces of decomposition reactions.

In reactions 87 and 88, the partial pressure of water vapor or its activity (that is, relative humidity of the atmosphere) is one of the factors that determine whether dehydration will take place at the given temperature and total pressure. (For more details on the activity of water as a driving force in such reactions, see section 2.7.)

Occurrences of Hydration and Dehydration Reactions

Clay minerals and sheet-layer structured silicates of the mica group contain hydroxyls (OH) in their lattices. At elevated temperatures (see Table 3.4-16), dehydroxylation reactions take place, resulting in evolution of H_2O from the minerals. Among the hydroxides and oxy-hydroxides of simpler stoichiometric composition,

dehydration or dehydroxylation reactions can be represented by the following sequences:



Hydrated minerals, in which H_2O forms part of the crystal structure, abound in salt deposits [6]. They are formed during the evaporation of ocean and lake waters and are sometimes preserved in the subsurface, which can be mined for rocksalt and various K-, Mg- and Ca-containing minerals.

The following list gives the chemical compositions and mineral names for some hydrated phases and their anhydrous counterparts. (Those in parentheses are either rare or do not occur in nature.)

$\text{CaSO}_4 \cdot 2\text{H}_2\text{O}$	gypsum	$\text{CaHPO}_4 \cdot 2\text{H}_2\text{O}$	brushite
$(\text{CaSO}_4 \cdot 1/2 \text{H}_2\text{O})$	hemihydrate	CaHPO_4	monetite
CaSO_4	anhydrite	CaCO_3	calcite, aragonite
$\text{MgSO}_4 \cdot 7\text{H}_2\text{O}$	epsomite	$(\text{CaCO}_3 \cdot 6\text{H}_2\text{O})$	
$\text{MgSO}_4 \cdot 6\text{H}_2\text{O}$	hexahydrite	$\text{Na}_2\text{SO}_4 \cdot 10\text{H}_2\text{O}$	mirabilite
$\text{MgSO}_4 \cdot 5\text{H}_2\text{O}$	pentahydrite	Na_2SO_4	thenardite
$(\text{MgSO}_4 \cdot 4\text{H}_2\text{O})$		$\text{NaCl} \cdot 2\text{H}_2\text{O}$	hydrohalite
$(\text{MgSO}_4 \cdot 2\text{H}_2\text{O})$		NaCl	halite
$\text{MgSO}_4 \cdot \text{H}_2\text{O}$	kieserite		

Under appropriate conditions, hydrated and anhydrous phases can form independently; they are not necessarily produced by the hydration or dehydration of each other.

Hydrous sulfates of heavy metals, such as $\text{CuSO}_4 \cdot 5\text{H}_2\text{O}$, and those of Ni, Zn, and Co have often been used in laboratory studies of the rates and mechanisms of dehydration reactions. Their occurrences in nature suggest that they are formed by the oxidation of heavy-metal sulfides that are exposed to the surface or near-surface environment.

Dehydration reactions in nature often take place in saline brines, where the activity of water and, hence, its partial pressure in the vapor phase are low. A classic example of such a dehydration reaction is the transformation of gypsum (calcium sulfate dihydrate) to anhydrite (anhydrous calcium sulfate).

Mechanisms and Rates of Dehydration

During dehydration, water molecules escape from the surface of the solid and subsequently from the deeper lattice sites. There are three basic mechanisms of dehydration:

- In **nucleation**, nuclei of the anhydrous phase form according to a pattern that may vary from one solid to another and may also depend on the conditions of the experiment. Instances of spontaneous one-, two-, and three-dimensional nucleation and nucleation along certain preferred crystallographic directions have been reported.
- In **dehydration by a boundary-controlled reaction**, a chemical reaction takes place at a boundary between the hydrated and anhydrous phases. In the course of the reaction, the boundary moves deeper into the solid, as a front of an advancing anhydrous phase forming at the expense of the hydrated solid.
- In a **diffusion-controlled process**, usually associated with dehydration at higher temperatures, the progress of the reaction can be described by a parabolic kinetic law (see equations 40 and 41). Here again, diffusion in one, two or three dimensions, and either isotropic or anisotropic diffusion, may be responsible for different interpretations of the reaction mechanism and mathematically different formulations of the dehydration rates.

For determining the rates of dehydration, the concentration of a dehydrated phase in a volume containing both the hydrated reactant and dehydrated product is not a convenient parameter; instead, the fraction of the hydrated phase reacted, denoted α , is conventionally used in the mathematical formulations of dehydration reactions. For example, the parabolic rate law for a diffusion-controlled dehydration reaction is, in the notation of a reacted fraction:

$$\frac{d\alpha}{dt} = \frac{k'}{2} t^{-1/2} \quad (89)$$

and the integrated form of the kinetic equation is

$$\alpha^2 = kt \quad (90)$$

with $k = (k')^2$.

Several rate equations, with explanatory notes, are given in Table 3.4-15 for different mechanisms of dehydration reactions. Figure 3.4-8 shows the progress of dehydration reactions with time for four dehydration mechanisms.

At room temperatures and atmospheric pressure, even in dry air, dehydration reactions are very slow. Therefore, dehydration rates are commonly measured under partial vacuum and elevated temperatures. The progress of the reaction can be observed in the solid and by monitoring the pressure of the water vapor formed.

TABLE 3.4-15
Rate Equations for Dehydration Reactions

For nucleation and boundary-reaction control:

Avrami-Erofe'ev equations:

- a. $(-\ln(1-\alpha))^{1/2} = kt$
- b. $(-\ln(1-\alpha))^{1/3} = kt$
- c. $(-\ln(1-\alpha))^{1/4} = kt$
- d. Contracting area: $1 - (1-\alpha)^{1/2} = kt$
- e. Contracting volume: $1 - (1-\alpha)^{1/3} = kt$

For diffusion control:

- f. One-dimensional (parabolic) diffusion: $\alpha^2 = kt$
- g. Two-dimensional diffusion: $(1-\alpha)\ln(1-\alpha) + \alpha = kt$
- h. Three-dimensional diffusion: $[1 - (1-\alpha)^{1/3}]^2 = kt$

Explanation of symbols:

- α = volume fraction of hydrate phase reacted
 t = time
 k = reaction rate parameter (differs for each equation)

Source: Brown *et al.* [7]

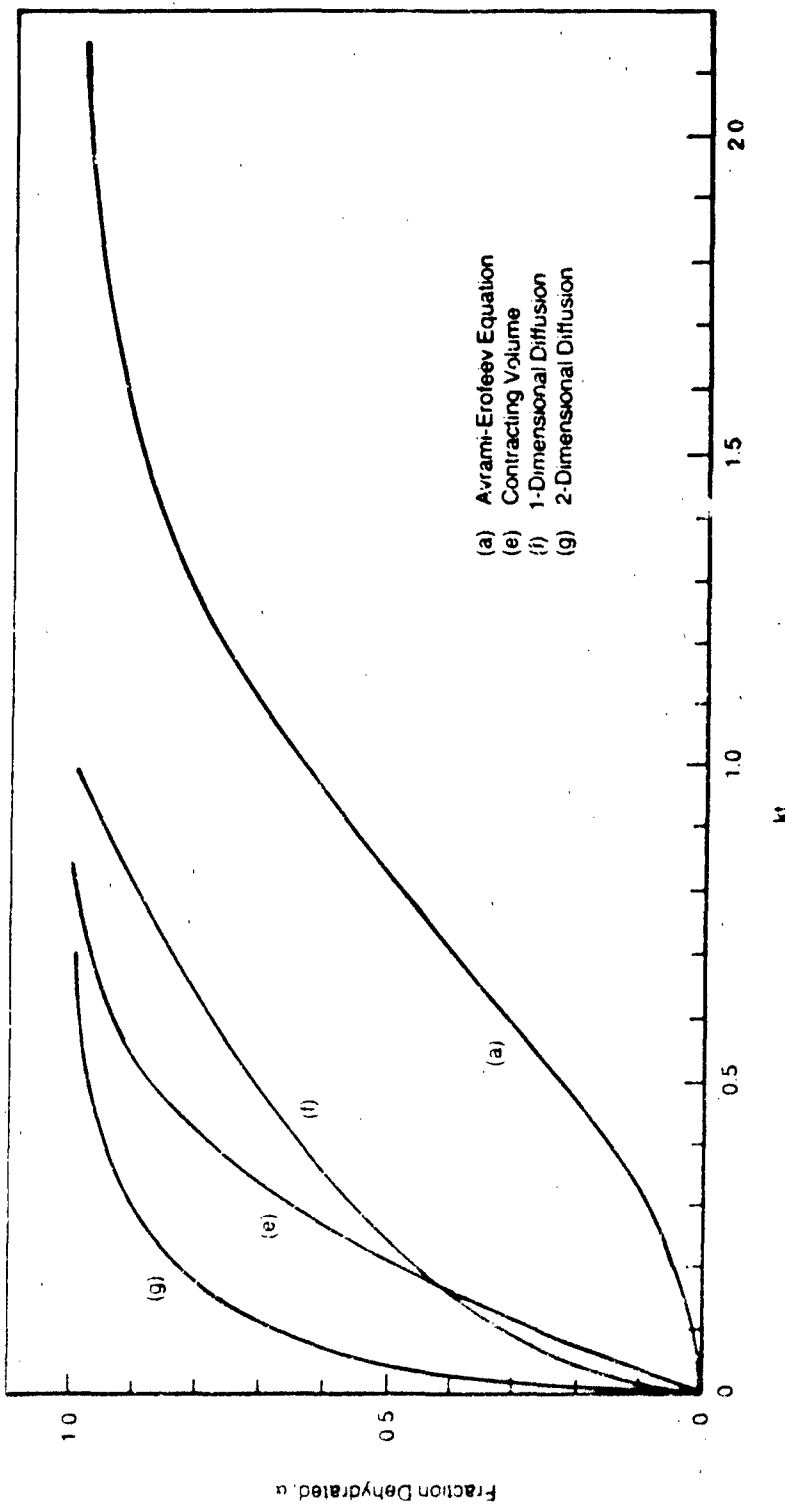
The rate of dehydration reactions, in a temperature range from about 40°C to 120°C, is of the order of 10^{-7} to 10^{-5} cm · s⁻¹. This represents the rate of advance of a dehydrated phase replacing the hydrated reactant. The two orders of magnitude range corresponds to the difference between 1 cm per day and 1 cm per year.

In general, it is doubtful that rates of dehydration reactions obtained at elevated temperatures in near vacuum (pressures of water vapor in the range of $P_{H_2O} < 1$ torr to over 100 torr, or from less than 0.001 atm to over 0.1 atm) are applicable to dehydration processes in the inorganic or organic environment.

Dehydration of CaSO_4 Hydrates

Reactions in the system CaSO_4 -- H_2O (vapor) involve three hydrated solids and two anhydrous products: $\text{CaSO}_4 \cdot 2\text{H}_2\text{O}$ (gypsum), $\alpha\text{-CaSO}_4 \cdot 1/2 \text{H}_2\text{O}$, $\beta\text{-CaSO}_4 \cdot 1/2 \text{H}_2\text{O}$, $\gamma\text{-CaSO}_4$ (known as soluble anhydrite), and $\beta\text{-CaSO}_4$ (anhydrite). Studies of the dehydration reactions in this system [2-4] have shown the following:

Dehydration of $\text{CaSO}_4 \cdot 2\text{H}_2\text{O}$ proceeds directly to the anhydrous phase when water-vapor pressure is very low, $P_{H_2O} = 10^{-5}$ torr (1 torr = 1 mm Hg = 1/760 atm). At higher water-vapor pressures, dihydrate goes to hemihydrate, which then dehydrates further to the anhydrous phase.



Below 110°C, dehydration reactions in $\text{CaSO}_4 \cdot 2\text{H}_2\text{O}$ and in $\text{CaSO}_4 \cdot 1/2 \text{H}_2\text{O}$ are controlled by a mixed mechanism of nucleation and boundary reaction. Above 110°C, the mechanism is diffusion-controlled. The activation energy of dehydration shows a dependence on the water-vapor pressure; in general, activation energies are higher for a nucleation-controlled dehydration and lower for a diffusion-controlled stage. The values of the activation energy and the rate constants for the different reactions in the calcium sulfate — water vapor system are summarized in Table 3.4-16.

Other Hydrates

There are numerous reports in the literature on the rates of dehydration of copper sulfate hydrates, $\text{CuSO}_4 \cdot 5\text{H}_2\text{O}$ and $\text{CuSO}_4 \cdot 3\text{H}_2\text{O}$. Some of the data on these reactions are shown in Table 3.4-16.

A transformation reaction for calcium oxalate trihydrate to a monohydrate in solution has been studied by Gardner [16]:



Although this can be formally considered a dehydration reaction, it involves dissolution of one phase and nucleation of another in solution (see "Nucleation and Crystal Growth" in §3.4.4). The same can be said of the dehydration reaction of $\text{CaSO}_4 \cdot 2\text{H}_2\text{O}$ in a saline brine: the crystal structures of gypsum and anhydrite are different; removal of H_2O from a hydrate phase probably involves dissolution of the reactant, and nucleation and precipitation of the anhydrous product.

TABLE 3.4-16

Kinetic Parameters for Some Dehydration Reactions of the Type Solid 1 → Solid 2 + Water Vapor

Dehydration Reaction	Temperature Range (°C)	Water Vapor Pressure (torr or mm Hg)	E_a^* (kJ/mol)	log A	$k = A \exp(-E_a/RT)$ (s ⁻¹ , unless otherwise noted)	Source
$\text{CuSO}_4 \cdot 5\text{H}_2\text{O} \rightarrow \text{CuSO}_4 \cdot 3\text{H}_2\text{O} + 2\text{H}_2\text{O}$	47-63	104 ± 10	12	10 ¹² exp(-1.25 × 10 ⁴ /T)	[31]	
$\text{CuSO}_4 \cdot 3\text{H}_2\text{O} \rightarrow \text{CuSO}_4 \cdot \text{H}_2\text{O} + 2\text{H}_2\text{O}$	70.5-86	134 ± 3	15.5	10 ^{15.5} exp(-1.61 × 10 ⁴ /T)	[31]	
$\text{BaCl}_2 \cdot 2\text{H}_2\text{O} \rightarrow \text{BaCl}_2 + 2\text{H}_2\text{O}$	40-43	142 ± 8		0.5×10^{-6} to 32×10^{-6} cm ⁻¹ s ⁻¹ , for different crystal faces	[34]	
$\text{CaSO}_4 \cdot 2\text{H}_2\text{O} \rightarrow \text{CaSO}_4 \cdot \frac{1}{2}\text{H}_2\text{O} + \frac{1}{2}\text{H}_2\text{O}$	80-152					
	< 110	4.6	247			[2]
	< 110	17	146			[2]
	< 110			92 ^a		[2]
	> 110			46 ± 4 ^b		[2]
$\alpha\text{-CaSO}_4 \cdot \frac{1}{2}\text{H}_2\text{O} \rightarrow \gamma\text{-CaSO}_4 + \frac{1}{2}\text{H}_2\text{O}$	68-270	10 ⁵	65.3	7.3	$10^{7.3} \exp(-7854/T)$	[4]
			44	151	$10^{17.7} \exp(-1.82 \times 10^4/T)$	[4]
$\beta\text{-CaSO}_4 \cdot \frac{1}{2}\text{H}_2\text{O} \rightarrow \gamma\text{-CaSO}_4 + \frac{1}{2}\text{H}_2\text{O}$	115-140	10 ⁵	26.6		3.5×10^{-4} (388°K)	[3]
			24	84.5	1.1×10^{-4} (388°K)	[3]

a. Boundary control

b. Diffusion control

3.4.5 Literature Cited

1. Bales, R.C. and J.J. Morgan, "Dissolution Kinetics of Chrysotile at pH 7 to 10," *Geochim. Cosmochim. Acta*, **49**, 2281 (1985).
2. Ball, M.C. and L.S. Norwood, "Studies in the System Calcium Sulphate—Water. Part I: Kinetics of Dehydration of Calcium Sulphate Dihydrate," *J. Chem. Soc. A*, 1633-37 (1969).
3. Ball, M.C. and L.S. Norwood, "Studies in the System Calcium Sulphate—Water. Part II: The Kinetics of Dehydration of $\beta\text{-CaSO}_4 \cdot 1/2\text{H}_2\text{O}$," *J. Chem. Soc. A*, 528-30 (1970).
4. Ball, M.C. and L.S. Norwood, "Studies in the System Calcium Sulphate—Water. Part III: Kinetics of Dehydration of $\alpha\text{-Calcium Sulphate Hemihydrate}$," *J. Chem. Soc. A*, 1476-79 (1970).
5. Berner, R.A., "Kinetics of Weathering and Diagenesis," in Lasaga, A.C. and R.J. Kirkpatrick (eds.), "Kinetics of Chemical Processes," *Rev. Mineral.*, **8**, 111-34 (1981).
6. Braitsch, O., *Salt Deposits*, Springer-Verlag, New York (1971).
7. Brown, M.E., D. Dollimore and A.K. Galwey, "Reactions in the Solid State," in Bamford, C.H. and C.F.H. Tipper (eds.), *Comprehensive Chemical Kinetics*, Vol. 22, Elsevier, New York (1980).
8. Busenberg, E. and C.V. Clemency, "The Dissolution Kinetics of Feldspars at 25°C and 1 atm CO_2 Partial Pressure," *Geochim. Cosmochim. Acta*, **40**, 41-49 (1976).
9. Davison, W. and G. Seed, "The Kinetics of the Oxidation of Ferrous Iron in Synthetic and Natural Waters," *Geochim. Cosmochim. Acta*, **47**, 67-80 (1983).
10. Drever, J.I., *The Geochemistry of Natural Waters*, Prentice-Hall, Englewood Cliffs, N.J. (1982).
11. Eugster, H.P., "Hydrous Sodium Silicates from Lake Magadi, Kenya: Precursors of Bedded Chert," *Science*, **157**, 1177-80 (1967).
12. Eugster, H.P. and L.A. Hardie, "Saline Lakes," in Lerman, A. (ed.), *Lakes: Chemistry, Geology, Physics*, Springer-Verlag, New York, 237-93 (1978).
13. Eyring, H. and E.M. Eyring, *Modern Chemical Kinetics*, Chapman and Hall, London (1963).
14. Fleer, V.M., *The Dissolution Kinetics of Anorthite ($\text{CaAl}_2\text{Si}_2\text{O}_8$) and Synthetic Strontium Feldspar ($\text{SrAl}_2\text{Si}_2\text{O}_8$) in Aqueous Solution at Temperatures Below 100°C*, Ph.D. Dissertation, Pennsylvania State University, University Park, Pa. (1982).
15. Frost, A.A. and R.G. Pearson, *Kinetics and Mechanism*, John Wiley & Sons, New York (1961).
16. Gardner, G.L., "Kinetics of the Dehydration of Calcium Oxalate Trihydrate Crystals in Aqueous Solution," *J. Colloid Interface Sci.*, **54**, 298-310 (1976).
17. Garrels, R.M. and F.T. Mackenzie, *Evolution of Sedimentary Rocks*, Norton, New York (1971).

18. Ghosh, M.M., "Oxygenation of Ferrous Iron (II) in Highly Buffered Waters," in Rubin, A.J. (ed.), *Aqueous Chemistry of Metals*, Ann Arbor Science Publishers, Ann Arbor, Mich. (1974), p. 193.
19. Holland, H.D., *The Chemistry of the Atmosphere and Oceans*, John Wiley & Sons, New York (1978).
20. Howard, J.R., G.H. Nancollas and N. Purdie, "The Precipitation of Silver Chloride from Aqueous Solutions. Part 6: Kinetics of Dissolution of Seed Crystals," *Trans. Faraday Soc.*, **56**, 278-83 (1960).
21. Lerman, A., *Geochemical Processes — Water and Sediment Environments*, John Wiley & Sons, New York (1979).
22. Lichstein, B. and F. Brescia, "The Mechanism of Precipitation of Magnesium Oxalate from Supersaturated Solutions. II: The Heat and Entropy of Activation," *J. Am. Chem. Soc.*, **79**, 1591-92 (1957).
23. Lin, F.-C. and C.V. Clemency, "The Dissolution Kinetics of Brucite, Antigorite, Talc, and Phlogopite at Room Temperature and Pressure," *Am. Mineral.*, **66**, 801 (1981).
24. Lin, F.-C. and C.V. Clemency, "The Kinetics of Dissolution of Muscovites at 25°C and 1 atm CO₂ Partial Pressure," *Geochim. Cosmochim. Acta*, **45**, 571 (1981).
25. Lin, F.-C. and C.V. Clemency, "Dissolution Kinetics of Phlogopite in a Closed System," *Clays Clay Miner.*, **29**, 101 (1981).
26. Liu, S.-T. and G.H. Nancollas, "The Kinetics of Crystal Growth of Calcium Sulfate Dihydrate," *J. Cryst. Growth*, **6**, 281-89 (1970).
27. Luce, R.W., R.W. Bartlett and G.A. Parks, "Dissolution Kinetics of Magnesium Silicates," *Geochim. Cosmochim. Acta*, **36**, 35-50 (1972).
28. Meybeck, M., "Concentrations des Eaux Fluviales en Éléments Majeurs et Apports en Solution aux Océans." *Rev. Geol. Dyn. Geogr. Phys.*, **21**, 215-46 (1979).
29. Nancollas, G.H. and G.L. Gardner, "Kinetics of Crystal Growth of Calcium Oxalate Monohydrate," *J. Cryst. Growth*, **21**, 267-76 (1974).
30. Nancollas, G.H. and M.M. Reddy, "Crystal Growth Kinetics of Minerals Encountered in Water Treatment Processes," in Rubin, A.J. (ed.), *Aqueous-Environmental Chemistry of Metals*, Ann Arbor Science Publishers, 219-53 (1974).
31. Ng, W.-L., C.-C. Ho and S.-K. Ng, "Isothermal Dehydration of Copper Sulphate Pentahydrate and Trihydrate," *J. Inorg. Nucl. Chem.*, **34**, 459-62 (1978).
32. Nielsen, A.E., "The Kinetics of Crystal Growth in Barium Sulfate Precipitation. II: Temperature Dependence and Mechanism," *Acta Chem. Scand.*, **13**, 784-802 (1959).
33. Nielsen, A.E., *Kinetics of Precipitation*, Macmillan, New York (1964).
34. Osterheld, R.K. and P.R. Bloom, "Dehydration Kinetics for Barium Chloride Dihydrate Single Crystals," *J. Phys. Chem.*, **82**, 1591-96 (1978).
35. Plummer, L.N. and T.M.L. Wigley, "The Dissolution of Calcite in CO₂-Saturated Solutions at 25°C and 1 Atmosphere Total Pressure," *Geochim. Cosmochim. Acta*, **49**, 191-202 (1976).

36. Rickard, D. and E.L. Sjöberg, "Mixed Kinetic Control of Calcite Dissolution Rates," *Am. J. Sci.*, **283**, 815 (1983).
37. Rimstidt, J.D. and H.L. Barnes, "The Kinetics of Silica-Water Reactions," *Geochim. Cosmochim. Acta*, **44**, 1683-1700 (1980).
38. Robie, R.A., B.S. Hemingway and J.R. Fisher, *Thermodynamic Properties of Minerals and Related Substances at 298.15 K and 1 bar (10⁵ Pascals) Pressure and at Higher Temperatures*, Bulletin 1452, U.S. Geological Survey, 1-456 (1978).
39. Stumm, W. and J.J. Morgan, *Aquatic Chemistry*, John Wiley & Sons, New York (1981).
40. Sung, W. and J.J. Morgan, "Kinetics and Product of Ferrous Iron Oxygenation in Aqueous Systems," *Environ. Sci. Technol.*, **14**, 561-68 (1980).
41. Tole, M.P., A.C. Lasaga, C. Pantano and W.B. White, "Factors Controlling the Kinetics of Nepheline Dissolution," *Geochim. Cosmochim. Acta*, **50**, 379-92 (1986).
42. Van Name, R.G., "The Velocity of Dissolving of Crystals in Liquids," in *International Critical Tables*. Vol. 5, McGraw-Hill Book Co., New York, 55-60 (1929).
43. Walton, A.G., *The Formation and Properties of Precipitates*, John Wiley & Sons, New York (1967).
44. White, A.F. and A. Yee, "Aqueous Oxidation-Reduction Kinetics Associated with Coupled Electron-Cation Transfer from Iron-Containing Silicates at 25°C," *Geochim. Cosmochim. Acta*, **49**, 1263-76 (1985).
45. Wollast, R. and L. Chou, "Kinetic Study of the Dissolution of Albite with a Continuous Flow-through Fluidized Bed Reactor," in Drever, J.I. (ed.), *The Chemistry of Weathering*, Reidel Publishing Company, Boston, 75-96 (1985).
46. Wood, B.J. and J.V. Walther, "Rates of Hydrothermal Reactions," *Science*, **222**, 413-15 (1983).

4. UPTAKE BY BIOTA

Sara E. Bysshe

	Page
4.1 INTRODUCTION	4.1-1
4.2 BIOLOGICAL UPTAKE PROCESSES AND PROBLEMS	
4.2.1 General Description of Uptake Processes	4.2-1
4.2.2 Methods for Investigation of Uptake	4.2-3
4.2.3 Estimation of Uptake of Inorganic Chemicals	4.2-5
4.2.4 Decision Process for Analyzing Problems Related to Uptake of Inorganic Chemicals	4.2-14
4.3 UPTAKE BY TERRESTRIAL VEGETATION	
4.3.1 Uptake and Loss Processes in Plants	4.3-1
4.3.2 Environmental Factors Influencing Uptake	4.3-2
4.3.3 Data and Criteria on Uptake Potential	4.3-5
- Macronutrients	4.3-6
- Water	4.3-6
- Acids, Bases, Salts	4.3-6
- Uptake of Trace Metal Species	4.3-6
4.3.4 Models and Predictive Techniques	4.3-11
4.4 UPTAKE BY MARINE BIOTA	
4.4.1 Introduction	4.4-1
4.4.2 Uptake Processes	4.4-2
4.4.3 Loss Processes	4.4-4
4.4.4 Data and Criteria on Uptake Potential	4.4-5
4.4.5 Models and Predictive Techniques	4.4-6
4.5 UPTAKE BY FRESH-WATER BIOTA	
4.5.1 Introduction	4.5-1
4.5.2 Uptake and Loss Processes in Fresh-Water Organisms	4.5-2
- Chemical Environmental Variables	4.5-2
- Physical Environmental Variables	4.5-5
4.5.3 Data and Criteria on Uptake Potential	4.5-6
4.5.4 Models and Predictive Techniques	4.5-6
4.6 LITERATURE CITED	4.6-1
4.7 SOME USEFUL SOURCES	4.7-1

LIST OF TABLES

BIOLOGICAL UPTAKE PROCESSES AND PROBLEMS

4.2-1	Typical Relative Bioaccumulation and Bioconcentration of Toxic Trace Metals	4.2-6
4.2-2	Relative Importance of Biomagnification and Biominification in Food Chains	4.2-7
4.2-3	Concentration Ratios of Trace Metals in Edible Tissues of Invertebrates and Fish	4.2-8
4.2-4	Criteria for Concentrations of Persistent and Bioaccumulative Inorganic Toxic Substances in a Hazardous Waste or Material	4.2-11
4.2-5	Relative Hazard to Humans from Metals Accumulated in Edible Portions of Fish and Shellfish	4.2-12
4.2-6	Examples of Criteria for Selected Trace Elements in Soils and Plants	4.2-13

UPTAKE BY TERRESTRIAL VEGETATION

4.3-1	Relative Sensitivity of Crops to Sludge-Applied Heavy Metals	4.3-4
4.3-2	Trace Metal Translocation (Root to Shoot) Capabilities	4.3-4
4.3-3	Suggested Safe Limits of Zinc for Sensitive Crops in Three Kinds of Soil Managed at Three pH Levels	4.3-5
4.3-4	Uptake and Accumulation of Selected Trace Elements in Plants	4.3-8
4.3-5	Interactions Between Major Elements and Trace Elements in Plants	4.3-11

UPTAKE BY MARINE BIOTA

4.4-1	Some General Characteristics of Trace Metal Uptake in Selected Groups of Marine Organisms	4.4-7
-------	--	-------

UPTAKE BY FRESHWATER BIOTA

4.5-1	Some General Characteristics of Trace Metal Uptake in Selected Groups of Freshwater Organisms	4.5-8
-------	--	-------

LIST OF FIGURES

BIOLOGICAL UPTAKE PROCESSES AND PROBLEMS

- | | | |
|-------|---|--------|
| 4.2-1 | Summary of Cycling/Equilibria Processes Among Environmental Components Controlling Availability of Inorganic Substances for Biological Uptake | 4.2-2 |
| 4.2-2 | Productivity in Biological Populations or Organisms as a Function of Uptake of Essential and Nonessential Substances | 4.2-3 |
| 4.2-3 | Decision Process for Analyzing Problems Related to Uptake of Inorganic Chemicals | 4.2-16 |

UPTAKE BY TERRESTRIAL VEGETATION

- | | | |
|-------|---|--------|
| 4.3-1 | Values of the Soil-to-Plant Concentration Factors B_v and B_r | 4.3-12 |
|-------|---|--------|

UPTAKE BY MARINE BIOTA

- | | | |
|-------|------------------------------------|-------|
| 4.4-1 | Effects of Introduced Contaminants | 4.4-3 |
|-------|------------------------------------|-------|

UPTAKE BY FRESHWATER BIOTA

- | | | |
|-------|---|-------|
| 4.5-1 | EPA Criteria for Freshwater Aquatic Life as a Function of Water Hardness | 4.5-3 |
| 4.5-2 | Regions in North America Containing Lakes That Are Sensitive to Acidification by Acid Precipitation | 4.5-7 |
| 4.5-3 | Weighted Annual Average pH of Precipitation in the Eastern United States | 4.5-7 |

4.1 INTRODUCTION

Investigation of inorganic species in the environment often leads to questions concerning uptake by biological organisms and the potential for accumulation. Concern over accumulation derives from the historical consequences of excessive levels of inorganics such as lead, cadmium and mercury in environmental and food sources, which have led to debilitating and even lethal effects in humans [32, 42, 47].¹

This chapter is designed to provide an overview of biological uptake of inorganics. It is intended to assist a reader facing a potential or uncertain uptake problem, or a reader seeking an introductory understanding of the subject. The discussion is divided between (a) general biological uptake processes and problems, and (b) issues specifically associated with uptake phenomena in terrestrial, marine and freshwater environments.

The first sections are intended to provide the reader with several key steps that should be followed to establish whether or not specific circumstances will result in risk due to uptake of particular inorganics. In this context, the "Decision Process" presented in § 4.2.4 may help the reader choose an appropriate focus for more detailed review and use of the scientific literature, or it may help him to structure an appropriately inclusive field measurement or laboratory experimental design for investigation of a potential uptake problem.

The latter portions of the chapter explore combinations of circumstances and environments that are likely to result in increases in availability and subsequent uptake of inorganics that could ultimately harm the environment or human consumers. The circumstances emphasized are those in the various environmental compartments that are presently understood to be at potential risk from inorganic uptake. Most of the discussion concerns uptake of trace metals, because of the inherent hazard represented by their toxicity and the fact that they have been the subject of much research. The chapter focuses on agricultural species in the terrestrial environment and on finfish and shellfish in the aquatic environment, again because so much of the concern and research has been in these areas.

Most of the experimental data reviewed for this chapter came from earlier summaries on the subject of uptake. The objective here is to indicate the range of uptake values observed, not to provide a comprehensive collection of data for the elements cited. Since a review of all of the most recently reported uptake values, summarized in this manner, would not provide a better answer for a specific problem in a specific environment, no attempt has been made to provide detailed information of this kind. Several of the references listed at the end of this chapter will be helpful to readers who wish to examine the data and further understand key processes.

1. All references cited in this chapter are grouped in section 4.6.

4.2 BIOLOGICAL UPTAKE PROCESSES AND PROBLEMS

4.2.1 General Description of Uptake Processes

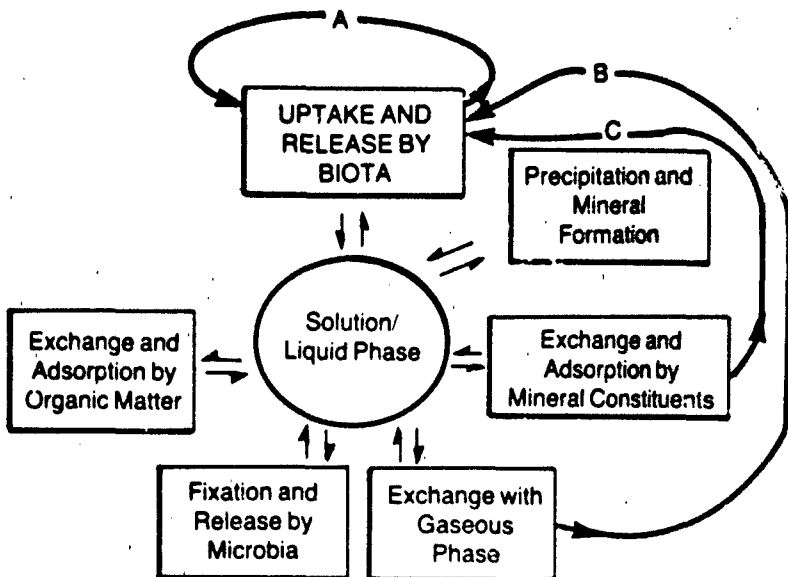
In the most general sense, the uptake of inorganic constituents by plants and animals, both terrestrial and aquatic, is a part of natural cycling processes. Living organisms play a major role in the cycling of elements such as C, O, H and N but a more minor or even incidental role with respect to many other elements. Figure 4.2-1 portrays some of these cycling processes. It can generally be assumed that uptake from soil solution through roots is the predominant uptake pathway for plants. Uptake of gaseous species from the atmosphere through the leaves is a major pathway for a few major constituents (CO_2 , O_2 , etc.) and may be a common but less widely investigated uptake pathway for other chemicals. A major exposure pathway for animals, especially aquatic ones, is that of chemicals in aqueous solution. Food chain transfer (eating other organisms) can also be an important route. Animals may take up substances through inhalation or by consuming non-food particles, but these are generally considered less significant ingestion routes for aquatic organisms. Ingestion of soil by livestock and humans can be a major transfer pathway for elements such as Pb, F, As, and Hg, among others.

Loss of inorganic constituents from tissues can result from shifts in the equilibria that hold those specific chemicals. Loss of inorganic constituents from living organisms must take place across respiratory membranes such as gills or plant surfaces, or across some other exchange surface that is part of a simple or complex organic system (e.g., digestive system, urinary system). One or many systems may be involved. The rate of loss appears to be quite variable, depending not only on the inorganic constituent involved but also probably other factors such as temperature and reproductive season.

Contributions of inorganics from industrial and agricultural activities have altered equilibria in some ecosystems. While new equilibria are ultimately established among compartments, changes in the availability of some constituents can create problems.

Figure 4.2-2 further illustrates the relationship between uptake and organism requirements. Many inorganics in the environment are required nutrients; examples include Cu, Zn, Cl, Na, and Fe, as well as O, C, N, and H. As the figure illustrates, biological productivity is diminished by deficiencies in these nutrients. On the other hand, even nutrients can be present in such excessive concentrations as to cause chronic toxicity and ultimately death. Some inorganics (e.g., Hg, Cd and Pb) are not essential for growth; at sufficiently low levels, these are not believed to be harmful, but at higher levels they can have toxic effects. Thus, uptake processes contribute directly to both normal life-cycle requirements and possible toxicity.

The term "bioconcentration" or "bioaccumulation" refers to the degree to which an organism accumulates a specific chemical from the environment. Many researchers limit the use of "bioconcentration" to uptake from water, and use "bioaccumulation"



- A. Consumption of plants or animals that have concentrated inorganic species.
- B. Uptake through inhalation.
- C. Uptake through mouthing/ingestion of non-food particles.

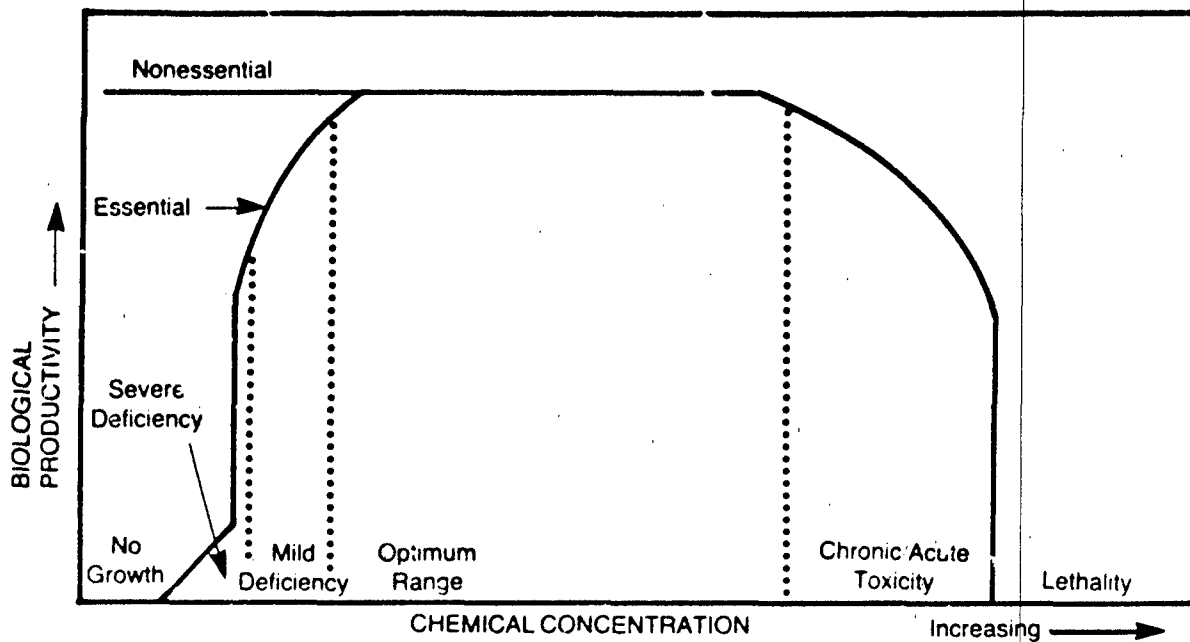
Source: Adapted from Kabata-Pendias and Pendias [20]. (Copyright 1984, CRC Press, Inc. Reproduced with permission.)

FIGURE 4.2-1 Summary of Cycling/Equilibria Processes Among Environmental Components Controlling Availability of Inorganic Substances for Biological Uptake

to refer to uptake from all possible sources. The terminology is not standardized, and numerous exceptions can be found in the literature. Bioaccumulation is usually not applied to macronutrients but to micronutrients and other substances that tend to accumulate from the environment to adverse levels. The "concentration factor," a further refinement of this terminology, may generally be defined as the degree (factor) to which an organism has concentrated a substance above environmental concentrations [32]:

$$\text{Concentration Factor} = \frac{\text{Concentration of Substance in Organism (wt/wt)}}{\text{Concentration of Substance in Soil or Water (wt/wt or wt/vol)}}$$

Organisms take up a substance at one rate and lose it at a different rate, usually a slower one. These rates are normally affected by the ambient environmental concentrations. Some time is required for a plateau or equilibrium concentration to be reached; at this point, concentrations in the organism are believed to be relatively constant for that environmental concentration and, by definition, uptake and loss



Source: Adapted from Overcash and Pal [28]

FIGURE 4.2-2 Productivity in Biological Populations or Organisms as a Function of Uptake of Essential and Nonessential Substances

rates are the same. It is at this so-called equilibrium concentration that measurements of concentration factor are considered most useful. For example, as of this writing a minimum of 28 days is considered necessary for equilibrium in laboratory-based tests to establish concentration factors in aquatic organisms [32]. In practice, as discussed below, the time required for equilibrium to be achieved has proven quite variable.

4.2.2 Methods for Investigation of Uptake

Uptake, accumulation and concentration factors are determined in various ways. For terrestrial plants, laboratory-type studies might include the addition of a measured concentration of a trace element from a soluble salt (e.g., copper sulfate, lead nitrate) to soil or other growth medium. Research has shown that results from soluble metal salts have no relation to results from tests using actual environmental media [10].

Thus, uptake studies have been developed where inorganics such as metals from contaminated soils, sludges, wastes, or as metal oxides, are introduced into the growth medium (e.g., soil), where test species are grown. These studies are considered to be more environmentally representative of exposure. Even though the latter may result in lower uptake and lower toxicity over the time of the test, and the chemical speciation may be only partially known, they are nearly always considered more realistic and thus more useful [30].

Tests may also be conducted with plants in greenhouse or field studies. The former approach permits greater control and is typically less expensive, but it also tends to result in higher uptake and toxicity than do comparable field experiments [30].

Plants are grown for a certain amount of time, with tests stopped at some particular growth stage. Concentrations of one or more forms of the added trace constituent are measured in plant parts (usually food chain tissues) or in the whole plant. Concentrations of a constituent may be measured and/or reported on a wet weight, dry weight, or ash weight basis of a specified plant tissue. Wet weights are highly irregular, being dependent on such factors as moisture content of the soil, and are not often used. Dry or ash weights can be converted to wet weights by use of the appropriate factors (moisture content, etc.). Wet weight/dry weight ratios vary from 1.1 for grain to 5-10 for roots and tubers, to 10-25 for leaf crops such as lettuce [10]. These data are used to calculate the ratios of plant concentration to medium concentration. Clearly, differences in experimental conditions (such as exposure time and the parts of the plant that are examined) may complicate comparison among different studies. And these differences illustrate the need for caution when interpreting the results from a single test, as well as when comparing results obtained under different test conditions.

The Army Corps of Engineers has developed a standard plant bioassay for uptake of soil toxic elements using yellow nutsedge (*Cyperus esculentus*), *Spartina alterniflora*, or *Distichlis spicata* in an experimental test chamber [22]. In such studies, plants are observed for phytotoxic effects, harvested for yield measurement after growth, and then plant material is analyzed for trace metal concentrations.

Aquatic tests are typically done in a tank with commonly used test species (such as *Daphnia* or bluegills). The inorganic chemical is added in a specified form to the water and is typically noted as the concentration of the ion. In such cases, the medium may be from a natural water source (ocean, lake, stream, etc.), or prepared in accordance with specified standards and free of contaminants. (Tests with marine organisms typically use filtered piped-in water.) In both cases, pH, salinity, or concentrations and characteristics of known dissolved ions of importance to uptake, such as carbonate, are usually identified. Laboratory-produced test media do not contain natural organics or natural sediments that might affect availability by forming complexes with test substances. Piped-in water from a natural source, by contrast, would not be free of dissolved organic matter.

The inorganics of concern for uptake may be added in a specific concentration, metered in at a constant rate and/or verified through monitoring for concentration or ionic activity. These different measuring procedures can make the exact levels of testing for a constituent quite variable, even when reported test concentrations are similar. Measurement and calculation of results for concentration factors are similar to the procedure described above for plants. Alternatively, field measurements can be made of uptake in naturally occurring or "caged" organisms in a contaminated aquatic environment, but the calculation of concentration factors is more difficult because exposure is not as well controlled.

The duration of the tests also varies, but regulatory preference (e.g., for a 28-day test or equilibrium conditions) helps to encourage standardization. Extended tests present difficulties, as even controls may be difficult to keep under confined conditions for 28 days or longer. Further, organisms already stressed by confined conditions may not survive (or respond typically to) experimentally altered conditions. Low control mortality is generally the only measurable indicator of success in this type of test.

Some tests require the examination of specific parts of test species if the substance in question preferentially accumulates in certain tissues. (For example, some trace elements tend to concentrate in plant roots or animal liver rather than in leaves or muscle tissue.) Examination of concentrations of an element in a whole organism thus yields an average value and may not be the optimum approach in a given circumstance. The optimum approach should be determined by the intended use of the data. For example, the average concentration may be sufficient if the entire organism is consumed, while specific tissue concentrations may be important if only those tissues are eaten. Either or both approaches may be appropriate for measuring uptake as long as care is taken to avoid inappropriate combination or comparison of results.

Field measurements of the concentrations of numerous elements in plants and animals in the various ecosystem types discussed here are increasingly common. As with laboratory tests, the results may be reported as concentrations per wet, dry, or ashed weight. The concentrations of a number of metals in agricultural crops and aquatic organisms used for human consumption are readily available from sources including: "Market Basket" studies conducted by the FDA that examine nutrient and toxic elements in food; more recent surveys by the USEPA and USDA designed to examine background levels of elements in selected crops [58,59]; a compilation of literature data on aquatic organisms uptake by Eisler [13]; a compilation of monitoring data for trace metals in food chain organisms by Jenkins [18]. Tables 4.2-1, -2, and -3 summarize some of the findings from Jenkins' review [18]. Data on uptake by plants from soil have been reviewed by Baes *et al.* [1]; some of their findings are presented in section 4.3.

However, ambient water/soil concentrations associated with the measured organism values are often unavailable, or the measurements may not be useful. For example, aquatic organisms are not stationary and have variable exposure histories. They may obtain a specific constituent from water, food, or sediments, or all three. Single or a few measurements of a constituent by grab sample at one location may or may not reflect important organism exposure concentrations. In addition to organism movement, seasonal or episodic variations in ambient water quality (e.g., storm flows, snow melt or lake stratification) can dominate the availability and uptake of inorganics.

4.2.3 Estimation of Uptake of Inorganic Chemicals

There are no generally applicable mathematical techniques for estimating the extent of biological concentrations of inorganics, even for combinations of chemicals and biological species known to result in bioaccumulation. This is primarily because the

TABLE 4.2-1
Typical Relative Bioaccumulation and Bioconcentration of Toxic Trace Metals

	Mammals, Birds and Fish	Molluscs, Crustacea, Lower Animals	Higher Plants	Mosses, Lichens and Algae
Antimony	x	x	x	x
Arsenic	xx	xxx	xxx	xx
Beryllium	x	x	x	x
Boron	x	xx	xxx	x
Cadmium	xxx	xxx	xxx	xxx
Chromium	xx	xxx	xxx	xxx
Cobalt	x	x	xxx	x
Copper	xxx	xxx	xxx	xxx
Lead	xxx	xxx	xxx	xxx
Mercury	xxx	xxx	x	x
Nickel	xx	xxx	xxx	xxx
Selenium	xx	x	xxx	x
Tin	xx	x	xxx	x
Vanadium	x	xxx	xx	xx

Bioaccumulation Scale:

- x - low or limited
- xx - moderate
- xxx - high to very high

Source: Jenkins [18]

biological uptake of inorganics is entirely situation-specific, depending on combinations of many factors that affect environmental availability and fate within the organism. In contrast to organics, for example, no single "internal fate" factor such as lipid solubility can serve as the foundation for a quantitative estimation technique for inorganics as a general group. Also, as indicated in sections 4.2.2 above and 4.3 below, previous investigation in this area has been more helpful in defining how to conduct future studies than in providing a data base for mathematical estimation techniques. Partly as a result, laboratory uptake results and field observations often disagree.

It would be easier to calculate the potential uptake of inorganics if we knew what forms or chemical species of a substance were available for uptake by biological organisms. The lack of this knowledge reflects our limited ability to identify and then measure the concentrations of the biologically available forms. This problem is exacerbated by the many chemical reactions and environmental conditions that affect chemical forms and the equilibria among them. If the available and toxic forms of inorganics in various media could be accurately measured and compared with

TABLE 4.2-2
Relative Importance of Biomagnification and Biominification^a in Food Chains

	Terrestrial			Aquatic				
	Plants		Herbivores	Carnivores	Plants		Herbivores	Carnivores
					B	B	B	M
Antimony	-	M	-	-	-	-	-	M
Arsenic	-	M	+	-	M	-	-	M
Beryllium	+	-	-	-	-	-	-	-
Boron	B	M	B	0	M	0	B	0
Cadmium	B	M	B	0	M	0	B	M
Chromium	+	M	+	M	0	-	B	-
Cobalt	M	0	M	-	M	-	M	M
Copper	M	+	M	-	M	-	M	M
Lead	B	0	M	0	M	0	-	M
Mercury	+	M	B	0	B	0	B	0
Nickel	B	M	+	0	B	-	-	-
Selenium	B	M	+	M	B	B	B	-
Tin	+	0	M	-	B	-	B	-
Vanadium	+	M	-	M	-	+ B*	B	-

a. Biomagnification is defined by Jenkins [18] as the decrease in concentration of a trace element in organisms with increasing higher trophic levels in food chains.

b. Symbols used in Table are defined as follows:

- B — biomagnification reported two or more times
- + — biomagnification reported once
- M — biomagnification reported two or more times
- - — biomagnification reported once
- 0 — no change in trace metal level
- . — tunicates

Source: Jenkins [18]

TABLE 4.2-3

**Typical Concentration Ratios of Trace Metals in Edible Tissues of Invertebrates
and Fish ($\times 10^{-3}$)^a**

	Marine		Fleshwater	
	Invertebrates	Fish	Invertebrates	Fish
Antimony	0.005	0.04	0.01	0.001
Arsenic	0.333	0.333	0.333	0.333
Beryllium	0.2	0.2	0.01	0.002
Cadmium	50.0	3.0	2.0	0.2
Chromium	2.0	0.4	0.04	0.04
Cobalt	1.0	0.1	0.2	0.02
Copper	1.67	0.667	1.0	0.2
Lead	1.0	0.3	0.1	0.3
Mercury	33.3	1.67	100.0	1.0
Nickel	0.25	0.1	0.1	0.1
Selenium	1.0	4.0	0.167	0.167
Tin	1.0	3.0	1.0	3.0
Vanadium	0.05	0.01	3.0	0.01

a. For example, for arsenic in fish, $C(\text{fish})/C(\text{water}) = 333$.

Source: Vaughn et al. [56], as adapted by Jenkins [18].

observed uptake, reliable correlations and predictions could be made more readily. Research is also being directed toward verifying fundamental models for equilibria and soil and plant uptake processes in an indirect approach to this problem [10].

Much research effort has been focused on trace metals because of their observed toxicity. Nonetheless, direct measurement of available chemical forms has been hampered by the uncertainty as to which forms should be the basis for calculating uptake concentrations and the proper way to *measure* these forms. Even the measurement of soil properties known to have an effect on the availability of trace metals for uptake is complicated by the variety of approaches and standards used by different agencies [20]. For example, soil pH measurements can give different values depending on the test method used; typical differences between common methods — relative to the simple use of a 1:1 (by volume) soil-water mix — are: (1) use of 0.01 M calcium chloride, which gives a pH of about 0.5 units lower; and (2) use of 1 N KCl, which gives a pH of about 1.0 unit lower [10].

However, the standardization of tests for these properties would not permit consistent approximations of the chemical forms available to a plant or their reliable correlation with observed uptake. For example, even so-called direct measurements of a metal in soil do not provide such information; at least six extraction procedures are used to measure plant-available metals in the soil, in addition to measurements of the "total" amount of an element [28]. It is generally conceded that a specific method can give reliable information for a specific soil-plant system [20] and can therefore be used for

monitoring at a specific site, but it cannot be used universally and may not be useful in predictions. Attempts are now being made to find more universally applicable approaches for measuring plant-available metals in the soil. (See § 4.3.2.)

In aquatic systems, the free metal ion and some hydrolyzed species are considered the ones available for uptake and toxicity [27]. According to recent versions of some of the EPA Water Quality Criteria documents, there are no ideal analytical methods for determining available toxic concentrations of many trace elements (e.g., lead) in water. This is largely due to the variety of forms in a water system and the lack of definitive information on the uptake and toxicity of each. The EPA's present approach for some metals is to measure the "active element," defined as the amount passing through a 0.45- μm membrane filter following acidification to pH 4 with nitric acid; like other extractions with a specified pH "end point," however, this method does not cover all potentially toxic forms. Methylmercury is a particularly important example [50]. Recent research (e.g., Cowan *et al.* [12]) is making use of modeled theoretical predictions of trace metal speciation in specific, measured water quality circumstances, in combination with examples of uptake under the latter circumstances, to develop correlations between specific predicted chemical species and observed uptake. This may result in a useful tool for approximating uptake potential, at least in controlled situations.

Bioavailability from sediments is not well understood from either a theoretical standpoint or the measurement of actual concentrations. Few states have developed criteria for sediments defining limits for inorganics that bioaccumulate. In California, criteria for determining the hazard of a waste of any material has been applied to contaminated sediments [39]. California (Table 4.2-4) defines the criteria threshold limits of listed inorganics as a combination of the measured water-soluble quantity and the amount available from a leaching test, in this case using sodium citrate. Bioavailability from sediments is expected to be inversely proportional to the sediment organic carbon content for several trace metals (e.g., Cu, Cd, Pb and possibly Hg) [19]; this is probably due to complexation of the metals by the acid functional groups on humic and fulvic acids in the organic matter. Redox reactions and sulfide activity can also affect availability, through the precipitation of a number of trace metal inorganics.

It is clear from the available data base that the uptake of some inorganics is likely to be more problematic than others with regard to:

- Concentration in the environment,
- Environmental bioavailability, and
- Toxicity to organisms in the food chain.

Two reviews have produced rankings of inorganics that have historically caused health problems when consumed by humans:

- (1) Table 4.2-5 compares the toxicities of some key metals and their observed tendency to accumulate in aquatic organisms. These qualitative comparisons, which are based on the data reviewed and the apparent nature of uptake for individual metal species, provide a useful indication of risk. It should be cautioned that a lower hazard rating in no way implies that such chemical species may not be present at concentrations that could be harmful.
- (2) Table 4.2-6 compares uptake levels in plants that are toxic to the plant with levels that are toxic to grazing animals. In some cases, because plants die first, accumulated metals are not passed along to consumers in high amounts, and the upper ends of the food chain are protected; in other cases, plants are more tolerant, and toxic levels can be transferred to consumers such as livestock.

While the above tables (including Tables 4.2-1, -2 and -3) are possible sources of information for assigning priority to inorganics of environmental concern, there are many site-specific exceptions. Thus, the inorganic environmental problem at a specific site can be reliably defined only through a knowledge of the uptake potential and hazard at that particular site. The following illustrate exceptions to the priorities that one might derive from the majority of evidence:

- Lead is not readily taken up by aquatic organisms except shellfish and is generally concentrated only in plant roots, yet lead poisoning has been implicated in the loss of endangered California condors due to the ingestion of lead bullets in prey [21]. A lead level of 4 mg/kg in waterfowl livers is used as a guideline by the U.S. Fish and Wildlife Service in considering restriction of use of lead shot in specific hunting areas [54]. High levels of lead in urban children have been blamed on soils contaminated by old, flaked paint and by automobile exhaust [47].
- High selenium levels in the Kesterson reservoir and associated wetlands in California have reportedly had adverse effects on wildlife and cattle. The circumstances include the release of selenium previously bound in seleniferous agricultural soils in an alkaline environment. Irrigation waters, which are drained in this area to avoid salt buildup, leach selenium from the soil. The irrigation drainage flows to the reservoir, where biological uptake has led to waterfowl mortalities and birth defects [39]. Human Se toxicity occurred in China when ash from seleniferous coal was used to fertilize cropland [60].
- The availability and subsequent uptake of heavy metals by plants from contaminated dredge material is believed to be controlled to a large extent by the degree of soil oxidation in combination with pH. Plant

TABLE 4.2-4
Criteria for Concentration of Persistent and Bioaccumulative Inorganic
Toxic Substances in a Hazardous Waste or Material
(From Section 66699, Title 22 of California Administrative Code)

Substance ^a	STLC ^b (mg/l)	TTLC (wet weight mg/kg)
Antimony and/or antimony compounds	15	500
Arsenic and/or arsenic compounds	5.0	500
Asbestos ^c	—	1.0 (as %)
Barium and/or barium compounds (excluding barite)	100	10,000
Beryllium and/or beryllium compounds	0.75	75
Cadmium and/or cadmium compounds	1.0	100
Chromium (+ 6) compounds	5	500
Chromium and/or chromium (+ 3) compounds	560	2,500
Cobalt and/or cobalt compounds	80	8,000
Copper and/or copper compounds	25	2,500
Fluoride salts	180	18,000
Lead and/or lead compounds	5.0	1,000
Mercury and/or mercury compounds	0.2	20
Molybdenum and/or molybdenum compounds	350	3,500
Nickel and/or nickel compounds	20	2,000
Selenium and/or selenium compounds	1.0	100
Silver and/or silver compounds	5	500
Thallium and/or thallium compounds	7.0	700
Vanadium and/or vanadium compounds	24	2,400
Zinc and/or zinc compounds	250	5,000

STLC = soluble threshold limit concentration; TTLC = total threshold limit concentration

- a. STLC and TTLC values are calculated on the concentrations of the elements, not the compounds. Values apply to asbestos and elemental metals only if they are in a friable, powdered, or finely divided state.
- b. STLC includes both the water-soluble and the leachable quantities using sodium citrate.
- c. Includes chrysotile, amosite, crocidolite, tremolite, anthophyllite and actinolite.

Source: California Administrative Code [9]

TABLE 4.2-5

Relative Hazard to Humans from Metals Accumulated in Edible Portions of Fish and Shellfish

Metal	Bioaccumulative Tendency											
	Toxicity to Humans from Oral Ingestion		Freshwater Fish Muscle		Marine Fish Muscle		Marine Shellfish or Crustaceans		Human Hazard Rating			
	low	high	low	high	low	high	low	high	low	med.	high	
Aluminum	x			x	x		c		x			
Arsenic		x	x			x		x			x	
Beryllium	x		x		c		c		x			
Boron	x		x		x		x		x			
Cadmium		x	x		x			x			x	
Cesium ^a	x			x	x		x				x	
Chromium	x		x		x		x		x			
Cobalt ^a		x	x		x		x		x			
Copper	x		x		x			x	x			
Iron	x			x		x		x	x			
Lead		x	x		x			x			x	
Manganese	x		x		x		x				x	
Molybdenum	x		x		x		c		x			
Mercury ^b		x		x		x		x			x	
Nickel	x		x		x		x				x	
Plutonium ^a	x		c		x		x				x	
Ruthenium ^a	x		x		x		x				x	
Selenium	x		x		x		x				x	
Silver	x		x		x			x			x	
Strontium ^a	x		x		x		x				x	
Zinc	x		x		x			x	x			

a. Radioisotope is primary form of concern.

b. Methylmercury is the species of concern.

c. Insufficient information available.

Source: Phillips and Russo [32]

TABLE 4.2-6
Examples of Criteria for Selected Trace Elements in Soils and Plants
 (all values based on dry weight)

Element	Range of Soil Background Levels ^a (ppm)	Range of Plant Background Levels ^a (ppm)	Plant Concentration Known to Be Deficient (ppm)	Excessive Level/ Toxic Threshold in Plants ^a (ppm)	Maximum Chronic Tolerated Level in Grazing Animal Diet (mg/kg)
As	0.1-50	0.01-1.7	—	3-20	50
B	0.2-130	10-200	<5-30	50-200	150
Cd	0.01-1	0.1-0.8	—	5-700	0.05
Cr	5-3000	0.01-1	—	5-30	3000
Cu	2-100	4-30	<2-5	20-50	25-300
Fe	7,000-550,000	3-300	—	—	500-3000
Hg	0.01-0.8	—	—	1-2	—
Mn	100-4000	15-300	<15-25	300-2000	400-2000
Mo	0.02-5	0.2-5	<0.1-0.3	10-100	10-100
Ni	5-5000	0.1-5	—	50-100	50-300
Pb	2-200	0.1-10	—	30-300	30
Se	0.1-38	0.01-2	—	5-100	2
Zn	10-300	8-150	<10-20	>300-1500	300-1000

a. Extreme range of values measured. Concentrations generally apply to forage crop species rather than hyperaccumulators.

Sources: Leeper [24], p. 40

Owerbach and Pal [28], p. 394

Kabata-Pendias and Pendias [20], p. 57

Chaney in Parr, Marsh and Kia [30], p. 162

Chaney [10]

bioassays have shown that cadmium and zinc availability were lowered in a flooded (reduced) environment, but increased in upland (oxidizing) conditions, which also lowered pH. The reverse was true for the plant uptake of arsenic from contaminated sediments placed in the same two types of experimental environments [22].

The point of these examples is that waste outfalls, waste disposal sites and chemical spills are not the only sources of problems related to uptake of inorganics. As described below, those who must make decisions about inorganic uptake phenomena should employ procedures sufficiently flexible to allow for unconventional sources and a range of potential influencing factors.

4.2.4 Decision Process for Analyzing Problems Related to Uptake of Inorganic Chemicals

The uptake and accumulation of inorganic species are inherently variable processes, and the data base for accurate quantitative estimation of uptake/accumulation phenomena is inadequate. Therefore, related problems are often best approached by a combination of selective literature review and original data collection or experimentation. Figure 4.2-3 illustrates in simplified form a decision process based on such a combination. This approach is modified from decision processes developed for evaluating problems in managing large-volume waste disposal [36].

Until usable approximation techniques become available, the investigator or decision-maker faced with a possible uptake/bioaccumulation problem should begin by obtaining initial information on the identity of the inorganic chemical of interest and on the characteristics of the receiving environment. If available, the following characteristics of the environment should be listed at this stage:

- (a) *Media of exposure* (air, surface water, ground water, soil, aquatic sediments, biota)
- (b) *Biological target species* (potentially exposed species that are important to man or linked to important species by the food web)
- (c) *Exposure history* (geography and chronology of any known sources and sinks of higher-than-background concentrations of the inorganic chemicals of interest, as well as any data on background concentrations)

With the above information, the investigator may conduct a preliminary literature review to determine whether a more extensive review of literature and extrapolation from historical data will adequately describe the scope and magnitude of the problem. Literature appropriate for review at this stage of the investigation would include summary texts such as this one and the references cited in section 4.6. The merits of a more comprehensive review would be uncertain until a preliminary review is completed and indicates one of the following:

- (1) The inorganic chemical has a history of causing uptake/bioaccumulation-related problems under similar circumstances;

- (2) There is conclusive evidence that the chemical cannot cause an uptake/bioaccumulation-related problem under the given circumstances; or
- (3) More information is needed to reach a defensible conclusion.

If either of the first two statements applies, it is reasonable to assume that analysis of factors a,b and c above based on a more detailed literature review will adequately define the problem and identify appropriate mitigation or response options. However, the third conclusion may well prevail if uptake of the particular inorganic in question has not been evaluated previously under sufficiently similar circumstances.

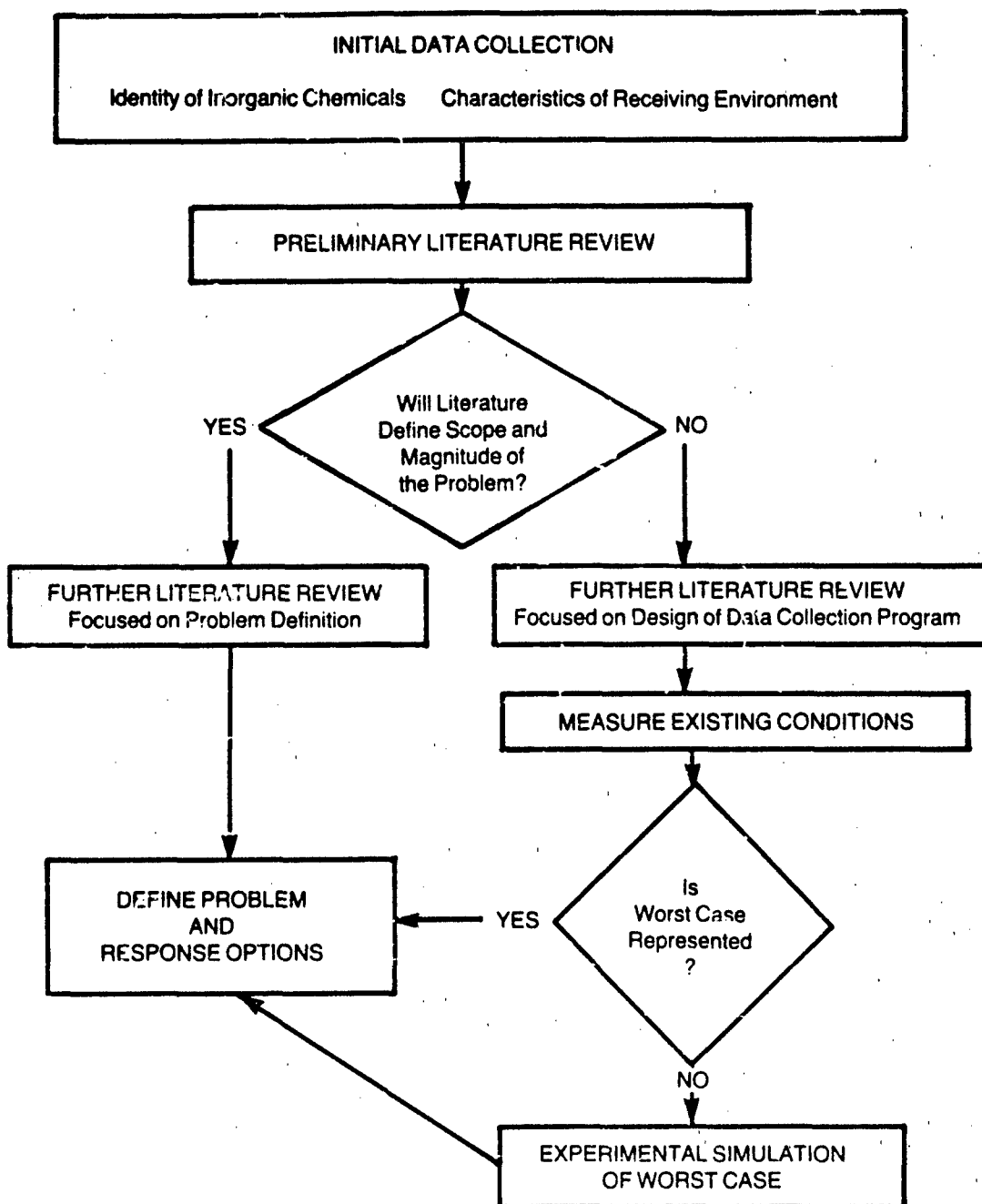
In any case, as indicated in Figure 4.2-3, the next step would be a focused search and review of the above-listed factors in the literature, extending to original research publications on field and laboratory studies of similar conditions. Numerous on-line services accessible by remote terminals provide rapid access to abstracts of articles in relevant journals.

The search and review should focus on defining the problem and finding precedents for its resolution if adequate data are already available. If, on the other hand, there is considerable uncertainty and insufficient data, the review should focus on precedents for the design and interpretation of a meaningful, valid field and/or laboratory data collection program.

If additional data collection is needed, the problem definition effort should first focus on accurate measurement and interpretation of the field situation, to determine whether those conditions represent a reasonable "worst case" for exposure and uptake of the inorganic(s) of concern. "Typical" or "boundary" conditions of interest may be defined later, as appropriate. The keys to achieving the objectives of the field research are:

- 1 Synoptic (simultaneous) measurement of the levels of the contaminant(s) and other controlling variables in the potentially important exposure media and exposed organisms; and
2. Adequate geographic coverage and duration to determine contamination gradients (including "control" conditions) and important periodic (e.g., seasonal) variations. In particular, monitoring should consider seasonal changes that control contaminant bioavailability, such as the temperature, redox and pH stratification of many temperate lakes or the seasonal water and sediment fluxes of runoff-dominated rivers or agricultural lands.

If the measurement of existing conditions suggests that a "worst case" equilibrium has not yet been achieved, it may be useful to simulate this equilibrium through further laboratory and/or field experimentation in order to assess the ultimate seriousness of the uptake-related problem. However, accurate simulation is extremely difficult and potentially costly because of the need to control the factors mentioned above. The frequently observed discrepancies between laboratory and field results for uptake of inorganics point up the difficulties of laboratory simulation; limited field-scale tests should receive at least preliminary emphasis whenever practical.



Source: C.B. Cooper, Arthur D. Little, Inc.

FIGURE 4.2-3 Decision Process for Analyzing Problems Related to Uptake of Inorganic Chemicals

4.3 UPTAKE BY TERRESTRIAL VEGETATION

4.3.1 Uptake and Loss Processes in Plants

Plants obtain nutrients through uptake of material by roots from the surrounding soil environment and, to a lesser extent, from the air through their leaves.

The soil environment may be broadly viewed as consisting of mineral matter, organic matter, soil solution, and slowly mixing gases. The relative proportions of these general components, as well as their physical and chemical makeup, are a result of geologic history, recent history and climatic influences. The site-specific characterization of soils is an important input for understanding the material available for uptake by local plant species; for example, soil pH, clay content, and organic matter strongly influence the concentrations of many elements in soil solution.

Inorganic elements that are most readily available for root uptake are those dissolved in soil solutions. They may be in the form of ions, soluble chelates or other complexed forms. Weakly adsorbed ions or species may also be bioavailable. This availability can vary with changes in soil solution chemical characteristics: cations, for example, are more available at low pH, becoming more strongly bound at high pH. The reverse is generally true for anions [20, 28, 30]. The variables that affect adsorption are further discussed in section 2.12.

Root uptake can be either passive, as in diffusion, or active. Active transport processes include transport across membranes by chelating agents or carriers [20, 28]. Such uptake applies to the movement of both macronutrients and micronutrients into a plant; it also applies to the mechanisms for uptake of non-nutrient elements and excessive accumulations of micronutrients.

Another avenue for material entry into plants is through the leaves. Aerosol materials may be deposited on leaf surfaces. Gases such as O₂ and CO₂, or even SO₂ or Hg⁰, may diffuse into leaves, where they can become dissolved. Uptake from leaf surfaces is believed to be a combination of passive (diffusion) and active transport [20]. Of course, irrespective of whether airborne materials penetrate leaf surfaces, they may be available to the food chain as the result of grazing.

Phosphorus, nitrogen, calcium and other macronutrients that enter a plant are utilized in plant metabolism. Micronutrients — typically trace element species (anions or cations) — perform a wide variety of functions within a plant system. As their name implies, they are required in small amounts. Key functions include incorporation in enzyme systems and structural materials. Many, however, are simply attached to other large molecules. Their function is unknown, although their essential nature has been established for at least some plant species [20]. (See also Mengel and Kirby [25].)

Micronutrients may be translocated from their entry points to places where they can be utilized, stored, immobilized, or accumulated. The same appears to be true for the

uptake of trace elements that have not been shown to be essential. Many such elements remain or are concentrated in fibrous root tissues. Fewer are translocated into leaves, and fewer still into tubers, fruits and seeds. Transport is believed to take place through the plant's vascular tissue (xylem and phloem) and is affected by transpiration (evapotranspiration) intensity [20]. Movement of an element into vascular tissue appears to hinge on the nature and location of chelates formed when it enters the root, and whether or not such chelates are translocated [30].

Loss processes (other than metabolic by-products) are fairly limited. Few trace elements are lost directly at leaf or root surfaces. Roots and old leaves appear to be common sites for accumulation and/or immobilization of excess or non-essential trace elements; thus, trace elements are lost through the dropping of leaves. While fewer trace elements are stored or immobilized in fruits or seeds, the seasonal loss of these structures is another loss process for the plant. If storage is in the roots, trace elements would not be "removed" from the plant until it is decomposed.

The most common (and most complex) mechanisms for removal of excess/toxic materials appear to be within the plant itself, through chemical fixation and/or physical separation within cell structures. Species of plants that are noted accumulators of certain trace elements make extensive use of these mechanisms; hence, while some chemicals may appear to remain within the plant, they are prevented from having a toxic effect on its life processes. There are also tolerant species that appear capable of excluding high levels of a microelement from uptake, a different protective mechanism against excess internal levels [30].

4.3.2 Environmental Factors Influencing Uptake

In any study of uptake in plants and the accumulation of inorganics that are considered potentially toxic, one of the major tasks is to describe the situations or circumstances that result in such adverse effects. The preceding discussion has referred to the variability inherent in interactions between soil and plant systems; some characteristics of this variability will now be outlined.

Plant species differ greatly in their need and uptake potential for various inorganic species. Studies aimed at maximizing agricultural yields have examined macro-nutrient requirements, largely from the perspective of deficiency. Differences in phosphorus and nitrogen removal from soil of up to an order of magnitude have been observed among a broad range of forage, field and forest vegetative cover [28]. Above-ground portions of field and forage crops have exhibited somewhat less than order-of-magnitude differences in levels of a number of macronutrients; for example, under normal conditions a crop such as coastal Bermuda grass removes from soil and contains relatively high phosphorus levels, while sugar cane may contain less than a third as much of this nutrient.

High levels of some macronutrients appear to cause a number of potentially adverse conditions, one of which is an imbalance in required nutrients. For example, excess

potassium can produce an imbalance in the K to (Ca + Mg) ratio in plants in some environmental circumstances. This, in turn, may result in a deficiency of magnesium and a potentially lethal disease in grazing cattle and sheep [30]. High phosphate levels in soil reduce the uptake of many trace elements that are either necessary or potentially toxic. Very high levels of a number of added macronutrients, where soil and plant assimilative/uptake capacity is exceeded, may be transported overland by surface runoff to surface water or leached into groundwater. While these are potentially significant environmental concerns, they are somewhat removed from problems directly resulting from uptake in biota.

Plant species also vary in their uptake of trace elements, both essential and non-essential, even when other environmental factors affecting availability are thought to be controlled. Species and cultivar (genetic strain) variability appears to be of two types: (1) effectiveness in excluding excessive levels of soil trace constituents, and (2) adaptations for excessive plant concentrations of trace metal species. The result is diversity in sensitivity to changes in soil concentrations of these elements. Chaney (see Table 4.3-1) has classified a number of crop species for sensitivity to heavy metals; he suggests that these crops have varying abilities to exclude the increasingly available concentrations of metals found in sludge.

In addition, however, some species can adapt to natural soils that are extremely high in one or more cations, which may or may not be micronutrients. These "hyperaccumulators" are able to adsorb extremely high concentrations, typically of one element only. Such species have been identified for Ni, Zn, Cu, Co, and Cr and Se [30]. For example, while typical species exhibit phytotoxic reactions with foliar concentrations of nickel in the 50-100 ppm range, hyperaccumulator species grow well with foliar concentrations of up to 19,000 ppm.

Another key variable in plant reactions to micronutrients is the manner and degree to which specific trace elements are translocated to other parts of the plant once they are taken up by the roots. Table 4.3-2 summarizes the results of research on trace metal translocation. Root cell sap contains constituents that have an affinity for, or chelate, trace metals to varying degrees [30].

Plant species also vary in terms of whether trace metals are translocated to seeds and fruits as well as shoots and leaves. It has been reported that some species (e.g., corn, beans, fruit trees) exclude excess concentrations from fruits and seeds, while other species (e.g., wheat, oats, soybean, and root crops) exhibit similar microelement concentrations in storage tissues and leaves [30].

Soil composition clearly plays a vital role in determining the availability of trace elements for uptake. Soil pH, organic matter, and clay content all have a strong influence in this regard. The amount of soluble zinc in the soil, for example, decreases with higher values of pH and C.E.C.; since the ability of the soil to adsorb zinc cations is thereby increased, more zinc can be safely added under these conditions (Table 4.3-3). The availability of trace elements can also be altered by chemical reactions such as precipitation with iron oxides or phosphates, microbial activity, and redox conditions.

TABLE 4.3-1
Relative Sensitivity of Crops to Sludge-Applied Heavy Metals

Very Sensitive^a	Sensitive^b	Tolerant^c	Very Tolerant^d
Chard	Mustard	Cauliflower	Corn
Lettuce	Kale	Cucumber	Sudangrass
Redbeet	Spinach	Zucchini squash	Smooth bromegrass
Carrot	Broccoli	Flatpea	'Merlin' red fescue
Turnip	Radish	Oat	
Peanut	Tomato	Orchardgrass	
Ladino clover	Marigold	Japanese bromegrass	
Alsike clover	Zigzag clover	Switchgrass	
Crown vetch	Red kura clover	Red top	
'Arc' alfalfa	Crimson clover	Buffelgrass	
White sweetclover	Alfalfa	Tall fescue	
Yellow sweetclover	Korean lespedeza	Red fescue	
Weeping lovegrass	Sericea lespedeza	Kentucky bluegrass	
Lehman lovegrass	Blue lupine		
Deertongue	Birdsfoot trefoil		
	Hairy vetch		
	Soybean		
	Snapbean		
	Timothy		
	Colonial bentgrass		
	Perennial ryegrass		
	Creeping bentgrass		

- a. Injured at 10% of a high metal sludge at pH 6.5 and at pH 5.5.
- b. Injured at 10% of a high metal sludge at pH 5.5, but not at pH 6.5.
- c. Injured at 25% high metal sludge at pH 5.5, but not at pH 6.5, and not at 10% sludge at pH 5.5 or 6.5.
- d. Not injured even at 25% sludge, pH 5.5.

TABLE 4.3-2
Trace Metal Translocation (Root to Shoot) Capabilities

Weakly Chelated/ Easily Translocated to Shoots and Leaves^a	Moderately Chelated/ Moderate Translocation	Strongly Held/ Little Translocation
Zn	Cu	Pb
Cd	Ni	Cr
Mn	Co	Hg
B		
Se		
Mo		

a. Root cell sap contains chemicals that chelate or hold different microelements to differing degrees.

Source: Chaney in Parr [30, pp 56 and 57]

TABLE 4.3-3
**Suggested Safe Limits of Zinc for Sensitive Crops in Three Kinds of Soil
 Managed at Three pH Levels**

Soil Texture	Cation Exchange Capacity	pH	Percentage of C.E.C. Safely Occupied with Zinc	Added Zinc (lb/acre)
Average	15	6.0	5	490
		6.5	10	980
		7.0	20	1,960
Clayey	30	6.0	5	980
		6.5	10	1,960
		7.0	20	3,920
Sand	3	6.0	5	100
		6.5	10	200
		7.0	20	390

Source: Leeper [24]. (Copyright 1978, Marcel Dekker. Reprinted with permission.)

4.3.3 Data and Criteria on Uptake Potential

The concern over vegetative uptake of inorganics derives from circumstances where such uptake:

- reduces crop productivity or choice of crop;
- limits soil cover, resulting in erosion or loss of topsoil or water; or
- has an undesirable effect on the food chain.

The interaction between concentrations of a constituent and yield (growth) were illustrated earlier (Figure 4.2-2). With regard to nutrients, concentrations below a threshold value inhibit growth. Above this value, each constituent exhibits a range of concentrations that are optimal for growth. If these concentrations are exceeded, however, yields and even survival are jeopardized. In this model, non-essential constituents are taken up without any effect on growth until a similar toxicity threshold is reached. When plant toxicity occurs, crop loss, soil loss and surface water/ground water effects may become environmental issues. Another issue, important whether or not plant productivity is reduced, is the potential for adverse effects of contaminated vegetation on humans or animals.

The interaction of plants with water, macronutrients, salts, ions and trace metal species all follow the general model shown in Figure 4.2-2 and can result in any of the listed environmental effects. However, the latter are not always the direct result of excessive uptake, as discussed below.

MACRONUTRIENTS

The macronutrients include species of elements such as N, P, K, Na, S, Ca and Mg. As mentioned earlier, a major problem with excess levels of these constituents is the possibility of chemical imbalance in the soil. This, in turn, can alter the proper ratio of other macronutrients within the plant and induce or (more likely) inhibit the uptake of other essential and non-essential nutrients. Long-term severe effects can be of two types: (1) food-chain impacts, resulting from a particular nutrient excess, especially on grazing animals, and (2) plant death, resulting in decreased plant cover and increased potential runoff. Even in less severe cases, many macronutrients are in highly soluble form (e.g., nitrates), and excesses tend to be leached from surface soils (to groundwater, for example).

WATER

Different soil systems have differing capacities for water assimilation before they become hydraulically overloaded. Plants require and take up water. However, when soils become waterlogged for any length of time, various adverse effects can occur: anaerobic conditions may result which, if sustained, may destroy plants and some soil macro- and microbiota; anaerobic conditions may cause chemical changes that increase soluble concentrations of some trace elements; and leaching or runoff from such sites may add contaminants to usable water in other locations.

ACIDS, BASES, SALTS

The most common soluble ions in soils are potassium, sodium, calcium, magnesium, nitrate, chloride and sulfate. Sodium and chloride, in elevated amounts, do not result in increased uptake; rather, they reduce water uptake, increase plant dehydration, and may even cause a breakdown of soil aggregation and its arable potential [28, 30]. Ultimately, the ability of soils to support vegetative cover may be reduced. Although there is a wide variability in plant salt tolerance, the surviving species might not be considered useful.

Changes in soil pH can alter the availability of numerous other constituents because of shifts in pH-dependent equilibria and chemical associations. These reactions are especially important with respect to trace metal species. The following section cites specific examples of the effects of pH on uptake.

UPTAKE OF TRACE METAL SPECIES

Agricultural concern about trace metal species is the result of lowered productivity from nutrient deficiencies as well as the more recently recognized effects of excesses. Much has been written about trace element uptake; the subjects of research cover the full range of deficiency diseases through toxicity and include the effects of many variables on such uptake. Because uptake potential is so dependent on the characteristics of the site and the species, it is impractical to present data that are other than general or explanatory in nature.

Thus, the approach here is to provide examples of the type of information that would be useful in searching out more detail, to help explain that information, and to provide sufficient overview for understanding the complexities of the soil/plant system that control uptake and its impacts. Appendix D (Pollutant Criteria and Standards) has been used as a source of reasonably conservative maximum levels; however, these criteria constantly change as new information becomes available, so those used here may already be somewhat dated.

Some ranges of values for soil and plant concentrations of selected trace elements were listed in Table 4.2-6. A recently completed survey summarizes the levels of Cd, Pb, Zn, Cu and Ni in agricultural soils in the United States [17]. The percentile distributions of metal concentrations is a useful perspective for usual soil metal levels. It should be kept in mind that concentrations within the background-level range may, under some circumstances, have deleterious effects on plants or animals through uptake. Similarly, typical plant levels may be excessive for very sensitive species.

The tabulated ranges of concentrations that are toxic to plants and animals indicate that plants provide foraging animals with some measure of protection from toxic constituents, since Zn, Cu, Ni, Mn, As, B and some others can kill plants at levels that are generally not toxic to animals. There are some notable exceptions, particularly among rare hyperaccumulator plant species. Only elements such as Zn, Cd, Mo and Se are readily available to grazing animals, because they are easily translocated to the exposed portions of plants. Many trace elements are simply held too tightly in the soil or bound in the roots (e.g., species of Fe, Pb, Hg, Al, Ti, Cr⁺³, Ag, Au, Sn, Hg, Si and Zr). Caution should be used in interpreting these generalizations, as grazing animals can also obtain heavy metals from plant surfaces and direct ingestion of soil.

Much of the research in this area has been devoted to understanding the specific circumstances that inhibit or encourage uptake of individual trace elements. Table 4.3-4 lists some of the findings for 12 selected trace-metal residues; it is not intended as a summary of this information but, rather, a collection of examples of important factors that influence uptake. The table is especially useful for pointing out what factors lead one to expect high or low concentrations of constituents in plants in a particular environment. It also indicates the importance of soil environmental factors, such as the role of pH, clay and organic matter, cation exchange capacity and other conditions that are known to help immobilize or make available the trace metal species. Recent studies have shown that roots of grass species (*Gramineae*) excrete chelating substances, "phytosiderophores," that solubilize Fe for uptake [34]. Other species appear to acidify the immediate root environment to solubilize Fe for uptake [10, 11]. It is believed that these mechanisms cannot avoid other metals in the environment. Calcium, as the major soil cation, is believed to play an important role in the control of uptake of divalent metal ions.

Documented interactions among macro and micro soil elements, without reference to levels and the nature of interaction, are summarized in Table 4.3-5. Such interactions may help to explain uptake phenomena of interest or concern, and may also shed light on some otherwise inexplicable uptake patterns that require further inquiry by the reader.

TABLE 4.3-4
Uptake and Accumulation of Selected Trace Elements In Plants

Element	Uptake Potential and Destination	Form	Factors Affecting Uptake	Other Fate
Arsenic (non-essential element)	Uptake seems to be passive, with water. Translocated to many parts of plants; most found in old leaves and roots.	Soluble forms. The very toxic sodium arsenite and arsenic dioxide are extreme examples, but there are many anionic forms of both As ⁻³ and As ⁻⁵ that are soluble, the latter being less toxic.	Promoted by: Reduction processes that liberate soluble forms from Al and Fe oxides. Restrained by: Ferrous sulfate, calcium carbonate, oxidation. Uncertain: Phosphate reduces toxicity.	Strong sorption by clays, hydroxides, Fe and Al oxides. Organic matter reduces mobility. Enrichment evident in surface soils. Microbial reactions release volatile forms from soil. Some forms behave in soil in fashion similar to phosphate. Alkylarsine can be formed under anaerobic conditions.
Boron (essential nutrient)	Deficient in some soils. Highest concentration in old leaves; low in seeds and grains. Passive sorption.	Boric acid and other soluble species.	Promoted by: Alkaline soil and high soil salinity. Restrained by: Gypsum and calcium hypophosphate; pH < 7. Uncertain: Antagonistic interaction with Cu, Cr, Mo, Mn, Fe, Si.	Can occur naturally in hazardous amounts (especially arid regions).
Cadmium (non-essential element)	Uptake by roots passive or metabolic. Highly mobile in plants — highest in roots, leafy portions, low in seeds. Soluble species highly available; can disturb enzyme activity.	Valence state in soil is Cd ⁺² . Forms complex ions and organic chelates. Absorbed by clay and organic matter.	Promoted by: Low soil pH (< 6). Restrained by: Moderately alkaline soil (above pH 7). Uncertain: Organic matter may reduce availability in acid soil, but forms precipitates in alkaline soils.	Stays in zone of incorporation, causing build-up in soil. Zn, Cu, and Se seem to reduce Cd uptake or toxicity.
Chromium (essential element to animals at least)	Concentrates in roots; very slow movement to other plant parts.	Cr ⁺⁶ highly available and toxic, but rapidly reduced to Cr ⁺³ in all soils. Little Cr ⁺³ is absorbed by roots.	Promoted by: Difficult oxidation to Cr ⁺⁶ , which is very mobile and unstable. Restrained by: Reduction of Cr ⁺⁶ to Cr ⁺³ (which is mobile only in very acid soils; almost all precipitates at pH 5.5). Reduction stimulated by organic matter, lime, and phosphate but also occurs naturally in most soils.	Precipitates in soil

(Continued)

TABLE 4.3-4 (Continued)

Element	Uptake Potential and Destination	Form	Factors Affecting Uptake	Other Fate
Copper (essential element)	Deficiency or toxicity, depending on soil concentration of available form. Uptake by roots. Uptake likely active and also passive (at least in toxic range of soluble species). Movement to leaves related to concentration (supply) in roots.	Soluble forms in soil 99% chelated: organic chelates. Products of hydrolysis, anionic hydroxy compounds or carbonates are inorganic soluble forms (some pH-dependent).	<i>Promoted by:</i> Low pH <i>Restrained by:</i> Most ions have lowest solubility at soil pH of 7 to 8. Lime, organic matter and phosphate additions to soil reduce phytotoxicity. <i>Variable uncertain:</i> Available species in soil. Interactions with Zn, Fe, Mo, Cd, Cr.	Tends to be immobile in soil because it readily interacts with minerals and also precipitates easily with soil anions.
Iron (essential nutrient in plants and animals)	Deficiency not uncommon. Uptake metabolically controlled. Transport regulated by plant to control shoot Fe.	Soluble Fe, including soluble organic complexes (small fraction of total levels).	<i>Promoted by:</i> Acid, waterlogged soils, mobile organic complexes, and chelates. <i>Restrained by:</i> Alkaline, well-aerated soils (may become deficient). <i>Uncertain:</i> Great number of nutritional and other soil factors affect uptake (e.g., antagonism by many heavy metals, P, etc.).	Iron readily precipitates as oxides, hydroxides and can be in chelated forms where organic matter is high.
Lead (non-essential element)	Absorbed by roots and concentrated there; probably passive. Little translocated to other plant parts; airborne deposition believed to contribute to leafy concentrations.	Ionic forms in soil solution. Airborne sources.	<i>Promoted by:</i> Flooding and other anaerobic conditions, low pH, low CEC, low organic levels, phosphate deficient soils (e.g., mine waste). <i>Restrained by:</i> pH above 6, lime, phosphate, organic matter. <i>Variable uncertain:</i> Toxicity of soil or plant levels uncertain.	Largely immobile in soils due to soil clays, phosphates, sulfates, carbonates, hydroxides, sesquioxides and organic matter. More toxic to rest of food chain. Accumulates in surface soils (soil half-life has been estimated in the 700 to 6000 year range). High soil levels may inhibit microbial processes and reduce decomposition (especially low-CEC soils)
Mercury (non-essential element)	Transfer to plants nearly totally as elemental vapor.	Retained in soil as slightly mobile organo-complexes.	<i>Promoted by:</i> Methylation; other organo-compounds also available, but to lesser degree. Extent of methylation in soil uncertain. <i>Uncertain:</i> Liming, sulfur compounds, or rock phosphates may reduce uptake; the effect of organic matter.	Migration processes are limited; soil build-up. Reduction to elemental form results in toxic mercury vapor.

(Continued)

TABLE 4.3-4 (Continued)

Element	Uptake Potential and Destination	Form	Factors Affecting Uptake	Other Fate
Molybdenum (essential nutrient)	Found in most tissues	Soluble forms; molybdate; adsorbed or Fe in soil.	Promoted by: High pH and saturated soils. Restrained by: pH < 5.5, humic acid (although organic soils can release it slowly); iron oxides. <i>Uncertain:</i> Availability limited by Cu, Mn, Fe.	Least soluble in acid soils. Toxic to grazing animals at levels not toxic to plants.
Nickel (essential element for some plant species)	Soluble forms readily absorbed by roots; mobile, and also accumulates in leaves and seeds. Required by some N-fixing species; may be essential at very low levels.	Possibly soluble organic chelates and possibly also adsorbed on oxides of Fe and Mn.	Promoted by: pH below 6.0. Restrained by: Lime, Fe, phosphate reduce availability to plants. <i>Variable:</i> Addition of organic matter can sometimes reduce availability.	Excess can cause iron deficiency in plants; coprecipitates with Fe and Mn in soil. Adsorbed readily by organic matter.
Selenium (uncertain role in plants; micro-nutrient in animals)	Uptake of water-soluble fraction by roots. Distributed to growing tips and seeds; concentration in roots.	Water-soluble fraction in soils is not fixed by Fe oxides, so readily available. Se-amino acids from plant residue increase available Se in soil.	Promoted by: Alkaline, well-oxidized soils. Restrained by: Acid and neutral conditions where selenides and selenites (as Fe hydroxides or oxides) are not formed.	Micronutrient in animals. Levels toxic to livestock are lower than toxic levels for plants. Methylated derivatives of microbial activity volatilize. Some plants are hyperaccumulators.
Zinc (essential element)	Deficiency in soil and plants not uncommon; high uptake potential and probability in plants if available; found in various plant parts.	Readily available as hydrated Zn ²⁺ , Zn ²⁺ with some organic chelates, and adsorbed on Fe, Mn oxides.	Promoted by: Low soil pH. Restrained by: High soil pH, high clay content, high cation exchange capacity, high phosphate. <i>Uncertain:</i> Possible antagonistic effects with Cu, Fe, Cd, As; possible Zn Cd synergism, in some proportions.	Very soluble in soil solution compared with other metals. Very mobile in acid soil.

Sources: Overcash and Pal [28] (all elements); Kabata-Pendias and Pendias [20] (all elements except Mo); Ryan *et al.* [35] (Cd only); Chaney [10].

TABLE 4.3-5
Interactions Between Major Elements and Trace Elements in Plants

Major Element	Antagonistic Elements	Synergistic Elements
Ca	Al, B, Ba, Be, Cd, Co, Cr, Cs, Cu, F, Fe, Li, Mn, Ni, Pb, Sr, Zn	Cu, Mn, Zn
Mg	Al, Be, Ba, Cr, Mn, F, Zn, Ni ^a , Co ^a , Cu ^a , Fe ^a	Al, Zn
P	Al, As, B, Be, Cd, Cr, Cu, F, Fe, Hg, Mo, Mn, Ni, Pb, Rb, Se, Si, Sr, Zn	Al, B, Cu, F, Fe, Mo, Mn, Zn
K	Al, B, Hg, Cd, Cr, F, Mo, Mn, Rb	—
S	As, Ba, Fe, Mo, Pb, Se	F ^b , Fe
N	B, F, Cu	B, Cu, Fe, Mo
Cl	Br, I	—

a. Reported for microorganisms.

b. Mutual pollution causes significant injury.

Source: Adapted from Kabata-Penias and Penias [20]. (Copyright 1984, CRC Press, Inc. Reprinted with permission.)

4.3.4 Models and Predictive Techniques

There are no models of plant uptake that are consistently useful for predicting concentrations of trace elements under a broad range of circumstances. Over the years, however, agronomists have produced much data on "optimal" doses of chemical fertilizers (particularly macronutrients) to maximize crop yields. This represents a large data base. A recent publication by Barber [2] summarizes a number of predictive models for plant uptake and soil-plant interactions affecting uptake of metals by plants.

Figure 4.3-1 presents estimates of soil-to-plant concentration factors for most of the stable elements. The two values given for each element, B_v and B_r , are defined as follows:

$$B_v = C_v/C_s \quad (1)$$

$$B_r = C_r/C_s \quad (2)$$

where

- B_v = soil-to-plant elemental transfer coefficient for *vegetative* portions of food crops and feed plants,
- B_r = soil-to-plant elemental transfer coefficient for *nonvegetative (reproductive)* portions of food crops and feed plants,

FIGURE 4.3-1 Values of the Soil-to-Plant Concentration Factors B_y and B_z

Source: Baes et al. [1]

- C_v = elemental concentration in *vegetative* portions of food crops and feed plants (dry weight) at edible maturity,
 C_r = elemental concentration in *nonvegetative (reproductive)* portions of food crops and feed plants (dry weight) at edible maturity, and
 C_s = elemental concentration in root zone soil (dry weight).

The estimates were generated by Baes *et al.* [1] for use in a computerized model (TERRA) of the terrestrial transport of radionuclides. All estimates of B_v and B_r were based on any combination of: (1) analysis of literature references; (2) correlations with other parameters; (3) elemental statistics; or (4) comparisons of observed and predicted elemental concentrations in foods. In general, no *a priori* bases or protocols were used to produce conservative values. The final values selected were estimated to two significant digits and then rounded off to the nearest 0.5 decimal place. Because of the significant variability in uptake ratios caused by environmental variables, it should be clear that the single values in Figure 4.3-1 must be used with extreme caution.

Acknowledging problems with the usefulness of any one extraction procedure in determining soil trace metal availability for plant uptake, Gerritse *et al.* [15] have found high correlations between concentrations of some trace metals (e.g., Zn, Cd and Cu, but not Pb) measured in soil solutions and uptake from a broad range of soil types. While measurement of soil solution concentrations is not necessarily a simple analytical exercise and the extraction method used is subject to choice, correlations with uptake have been an improvement over soil-extracted metal concentrations. This type of approach, which is aimed at developing generalizable principles, may ultimately lead to useful prediction techniques. The investigator faced with a potential problem of inorganic uptake in a terrestrial system may follow the steps outlined in § 4.2.4 when no better approach is available.

4.4 UPTAKE BY MARINE BIOTA

4.4.1 Introduction

The marine environment serves as the major aquatic source of food for man. It has also become a place for waste discharge and disposal. The understanding of plant uptake processes described in the section above was derived in part from agricultural science. In that instance, cause and effect relationships could sometimes be directly observed, even under field conditions. Observational understanding of inorganic uptake in the marine environment, especially in natural settings, is more difficult.

Like the terrestrial environment, the marine environment is not uniform. At the very simplest level, three general types of marine environments must be considered:

- *Estuaries*, which are characterized by a range of salinities from fresh to salt water that varies seasonally and even daily in some locations, and a degree of seasonal and even daily variation in temperature, sometimes pH, and large seasonal changes in primary productivity with associated dissolved organic matter.
- *Nearshore Areas*, which tend to have less salinity variation than estuaries but are characterized by variability in depth, and hence temperature, by major water exchanges due to seasonal phenomena, storms, and the tides.
- *Offshore Areas*, which usually vary in temperature with depth. Even with the partial exceptions of the euphotic zone near the surface and occasional periods and areas of upwelling, temperature and salinity changes tend to occur less in offshore areas than in the estuaries and nearshore areas above.

While these are simplistic descriptions, they are useful in understanding general observations about marine uptake processes.

A large number of marine species spend some or all of their life cycle in nearshore coastal or estuarine environments, primarily because the shallower and warmer waters, increased light penetration, and energy subsidies such as tides combine to generate an enormous food production capability. However, when we attempt to examine the contamination exposure history of a particular organism, the problem can be far more complex than studying the exposure of fish in a tank. For example, bivalves such as clams and oysters are essentially bottom dwellers in close contact with sediments, but they also spend their very early life floating with other plankton in nearshore/estuarine habitats. Striped bass, sometimes a nearshore fish, spawn in estuaries; during their embryo-to-juvenile life stages, they remain in the estuaries, slowly migrating downstream from brackish to salt water, and the adults move freely in and out of the estuarine and nearshore environments. Salmon migrate through estuaries to freshwater headwaters to spawn, and juveniles migrate downstream and out to sea months later. Species such as the mummichog remain in estuaries for their

entire life cycles. Planktonic species, plant and animal, are moved with tides and currents but essentially remain within one ecological regime. Rooted aquatics and marsh plants are clearly stationary while alive, but their decomposition products can be transported to nearshore or offshore environments. Birds and other terrestrial species may feed from the nearshore and estuarine areas without being directly part of them. The complexity of this exposure history is compounded by feeding behavior that may change over the course of development in some species: juveniles of a given fish species may feed on plankton, while the adults feed on other fish.

Many coastal areas, particularly the lands bordering major estuaries, are urbanized and industrialized, causing marine ecosystems to be exposed to large volumes of waste. Inland areas also contribute to this waste load as rivers emptying into estuaries carry portions of effluents and surface runoff from upstream. It is significant that these same waters, out to the edge of the continental shelf, have supported more than 90% of the American commercial seafood catch and virtually all of the recreational fishing [18]. Even fish caught offshore are dependent to some degree on the shallower estuaries and nearshore waters.

Attempts to understand uptake in marine organisms must take these facts into account. Poisonous levels of contaminants (e.g., Cd, Hg) in seafood have directly affected humans and fish-eating birds. Awareness of the potential for adverse effects from this major food resource has led to regulation of the levels of many chemicals in seafood as well as to research into uptake and loss processes.

4.4.2 Uptake Processes

Uptake of inorganic constituents varies with the nature of the organism and the constituent in question. There are a number of obvious differences between algae and fish, as well as similarities. Many trace metal species, including some of the heavy metals, are required micronutrients; they typically play a role in enzyme-mediated processes or form integral components of cell structure.

There are three major routes of uptake, only one or two of which are important to each specific group of organisms. These routes are:

- Direct absorption from water of chemically available forms of an inorganic constituent across cellular or respiratory surfaces;
- Direct absorption of chemically available constituents from sediments through filter feeding or simple contact; and
- Uptake from food containing inorganic constituents.

In contrast to lipophilic organics, where direct uptake from water is usually the most important route, uptake of inorganics may well be directly from the environment *and* from food. Unfortunately, most laboratory experiments have examined only one exposure route at a time — most often, uptake from water.

As with terrestrial plants, inorganic uptake by marine biota can be a source of required nutrients as well as of non-essential elements, and there appears to be no optimum range and/or tolerance for tissue concentrations of a particular trace element, whether it is a nutrient or not. Once certain concentrations are exceeded, however, toxic effects become evident. Figure 4.4-1 shows the relationships between observed uptake and adverse effects in aquatic species. Since the damage threshold for some species can be much lower than for others, their sensitivity to different inorganic constituents varies. Research, especially laboratory studies, has indicated that other factors such as age, size of the individual, and even the season of the year may play a role in observed variations in tolerance [4,13]. This discussion of toxicity, however, is limited to their relationship to uptake processes and effects.

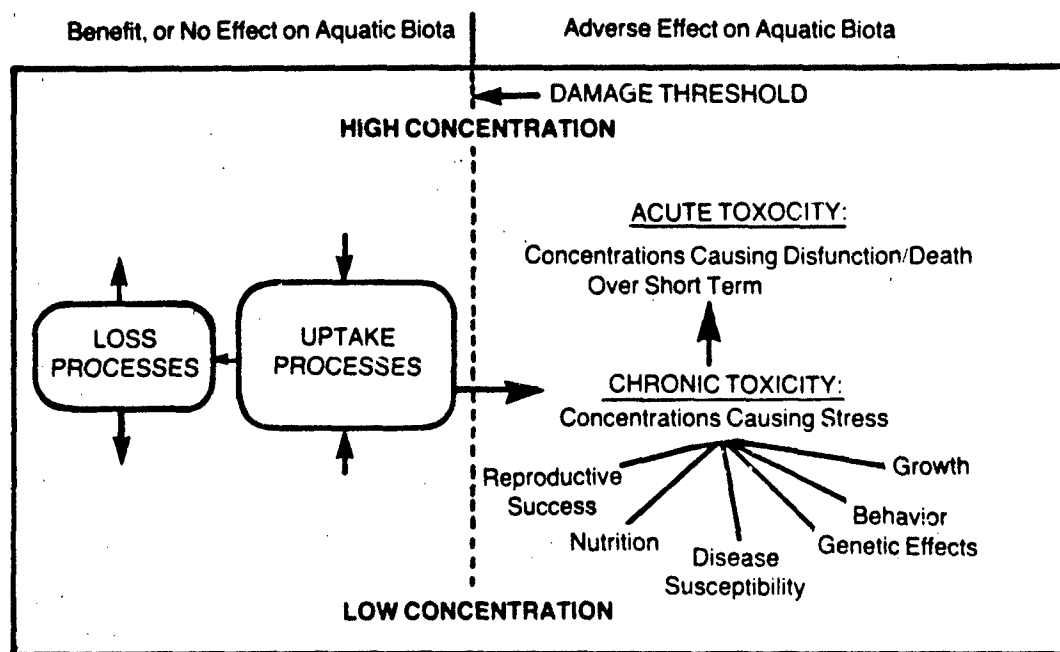


FIGURE 4.4-1 Effects of Introduced Contaminants

Recent investigations of several West Coast marine species have provided direct chemical evidence to explain the mechanisms of observed damage-threshold phenomena. For some time, researchers had noted that some trace metals measured in tissues were associated with molecules in a specific weight range [13]. Brown *et al.* [7], at the Southern California Coastal Water Research Project (SCCWRP), devised a method for examining the location and association of several heavy metal species with specific molecules in fish tissue. They identified three distinct tissue chemical pools into which specific contaminants may become partitioned:

- [ENZ] A high-molecular-weight pool that contains cellular enzyme systems and is the site of toxic action by both heavy metal species and organics.

- [MT] A medium-molecular-weight pool that has been shown to contain a metal-binding protein, metallothionein, and is considered the site of trace metal species detoxification.
- [GSH] A low-molecular-weight pool of compounds such as glutathione, considered the site of organic metabolite detoxification.

As expected, micronutrients such as Cu and Zn, which are components of enzymes (metalloenzymes), were found in the [ENZ] pool of tissues. The authors theorized that such species were not toxic until they were found in the [ENZ] pool in excess of requirements [7]. When tissues of fish from contaminated areas were examined, elevated levels of Cu and Zn were found in the metallothionein-containing fraction as well as the enzyme fraction. The non-essential element, cadmium, was almost entirely bound in the metallothionein-containing fraction. It was theorized that non-essential metal species are partitioned into the [MT] pool and, hence, are not harmful unless assimilative capacity is exceeded. Excesses of essential metal species are also partitioned into the [MT] pool and similarly rendered non-toxic.

Several additional observations concerning uptake phenomena have been made during the course of this research. Fish from Southern California offshore areas heavily polluted by outfall discharges of both heavy metal species and chlorinated hydrocarbons showed reduced metal uptake where chlorinated hydrocarbon uptake was high. Greater uptake of metal species was observed in areas less polluted by hydrocarbons, and with *lower* metal concentrations as well. Subsequent examination of this phenomenon led SCCWRP researchers to hypothesize, with evidence from biochemical examination, that oxygenated metabolites of chlorinated hydrocarbons may interfere with metal uptake in fish; this might cause adverse effects due to deficiencies in uptake of required metal species or allowing some metals to escape detoxification by "spillover" into the [ENZ] pool [5]. This latter hypothesis has come under criticism. The area studied is also heavily influenced by sewage discharges, resulting in high levels of particulate and dissolved organic matter as well as the above noted chlorinated hydrocarbons. Thus, the observed reduction in trace metal uptake could be due to the levels of organic matter in the water decreasing metal bioavailability [23].

Questions remain concerning what combined levels of metal species and organics lead to toxicity, which tissues are most sensitive to excesses, and how such observations may be related to environmental factors such as seasonal changes. Questions also remain concerning the general applicability of these observations across the broad range of marine organisms (beyond the fish, mollusks, and sea urchins studied) and across the range of inorganics other than Cu, Zn and Cd. It is essential that our understanding be advanced to the point at which we can relate such observations to damage thresholds and identifiable environmental causes.

4.4.3 Loss Processes

Keys to the ultimate tissue concentrations of a substance in marine biota are the length of time organisms are exposed to the contaminant, the environmental concen-

tration of the contaminant, the rates of uptake and loss, and often organism size. Sedentary organisms may be in relatively constant contact with contaminated sediments, while seasonal visitors may spend a short time in an area and return to cleaner environs for long periods. For many compounds, depuration rates decline with the size of the organisms: larger fish contain higher levels of a contaminant than smaller ones of the same species and exposure history.

Further, loss of an inorganic contaminant has been shown in research to be represented by a two compartment loss curve. Thus, there is an initial, relatively fast rate and a longer-term slower rate. For regulatory purposes the first order rate loss is considered an adequate initial assumption and is referred to as the "half life" of the chemical in an organism [23].

Finally, mercury may be lost from different marine species at different rates: a biological half-life for mercury in predatory fish, feeding on contaminated food, of greater than 1000 days has been reported [13], while mercury in prey fish in the same experiment exhibited a biological half-life of less than 60 days. These are potentially important contributing factors in the differences often seen in tissue concentrations of organisms taken from a similar environment.

4.4.4 Data and Criteria on Uptake Potential

A fairly large body of data exists on observed concentrations of inorganic contaminants in marine organisms, but the data base on uptake potential/accumulation factors is far smaller. For certain contaminants -- mercury, cadmium, chromium, copper, zinc, and a few others — there is much information on uptake concentrations from both field and laboratory data collections; there are significantly less data on trace metal species and other inorganics that have been less problematic or are less well-known.

Two general types of data are available on uptake in marine organisms. The first is from laboratory experiments. As a rule, organisms are placed in contact with one or more target elements for a given length of time prior to sacrifice for measurement of tissue levels of the given contaminant. Some test organisms may also be placed in clean water following exposure, to determine their degree of retention of contaminants. Laboratory experiments typically use a specific chemical form of an element, measure the duration of exposure, and may report species, size, water conditions and water concentrations of the contaminant.

Field collections of organisms may report species, size or age, and existing water or sediment conditions for a specific area. However, it is very difficult to know the exposure history that produced any observed uptake by the organisms collected. Relatively sedentary organisms, including rooted aquatics, mussels, clams and other bivalves, and a broad group of sediment dwellers such as worms or tunicates do have a reasonably constant exposure to sediments. However, they may also principally receive dissolved inorganics from overlying water concentrations that are not necessarily so constant. There is clearly even less certainty with free-swimming community members, whose exposure changes continually.

Another important variable in marine uptake literature is the tissue examined for contaminant concentrations. (See earlier discussion of this factor in § 4.2.2.) Muscle tissue levels and concentration factors for fish or crustacea that are used for human consumption are useful in assessing risk potential for humans. However, muscle tissue is frequently *not* the site of highest concentration of trace metal contaminants that are not organo-metallics. (Mercury, as an organo-mercury compound, concentrates in fish flesh; technically, this is not an exception but often appears so if it is analyzed as total mercury.)

Recent research indicates that organisms have specific sites for detoxifying at least some contaminants. Toxicity to the organism occurs when detoxification capacity is exceeded *at these sites*. Organs important to detoxification may or may not be the ones of highest concentration, but they appear to be locations where accumulation is high. Sites of threshold toxic action may also be quite specific. These latter points are not yet well defined by ongoing research, but it is clear that data on whole body concentrations and/or on tissues that represent low accumulation may be misleading if used as indicators for threshold toxicity. Unfortunately, the linkages between environmental exposure, documented uptake and accumulation, toxicity, and risk to the food chain are not yet well quantified. The particular tissues that should be used for indicators of accumulation in various species are also not yet firmly established.

Selected data on uptake of inorganics in marine organisms have been summarized for specific contaminants. Table 4.4-1 emphasizes information on the general uptake process for several phyla of marine organisms consumed by humans. The field data are taken from Eisler's extensive compilation of such numbers [10], in which the methodology is not specified. One striking generalization can be inferred from these data: uptake and toxicity increase at higher temperatures and lower salinities for all the trace metal species of toxicological concern. These conditions are most common in the nearshore areas and in estuaries; thus, the same areas required for reproductive success for many economically and ecologically important species are the marine environments with potentially highest contaminant loading and uptake. All concentration factors listed are intended to illustrate *relative* uptake potential, since uptake will vary with exposure, environmental availability and, especially, chemical speciation.

Concentration factors measured in the laboratory appear to be generally lower than those from field samples. Possible causes for this include: longer exposure duration in the field, undocumented exposure to higher than measured ambient concentrations, complexation, salinity variation, handling techniques and analysis, analysis of previously deceased rather than freshly sacrificed individuals, and both water and food as sources for uptake. Appendix D (in Part II) lists USEPA and other nationally applicable marine uptake/bioaccumulation (residue) criteria for inorganics.

4.4.5 Models and Predictive Techniques

The general constraints in § 4.2.3 apply particularly to uptake by marine biota. No generally applicable models or estimation techniques are available. One special

TABLE 4.4-1

Some General Characteristics of Trace Metal Uptake in Selected Groups of Marine Organisms

Chemical	Algae/Macrophytes	Molluscs	Crustaceans	Finfish
Arsenic (non-essential)	<ul style="list-style-type: none"> • Arsenate appears more absorbed, and with adverse effect. • Lab uptake measured, reported in 200x to 3000x range (highest in lipid fractions) • Source of organic arsenic compounds in marine food-web. 	<ul style="list-style-type: none"> • High field bivalve concentration factors reported as 1500x to 18,000x, up to 46,000x (data from Greece). • Short-term lab studies do not show significant uptake magnification. • Concentrated in lipid extracts, mostly in non-toxic form. • Loss is in two phases, with half times of 3 days and 32 days. • Increased uptake at lower salinity. 	<ul style="list-style-type: none"> • Concentrated in lipid fractions as organic arsenic likely less toxic to organism. • Salinity, temperature modify uptake rates. • Food chain accumulation. 	<ul style="list-style-type: none"> • High tissue levels (especially in lipid fractions) compared with freshwater and terrestrial organisms. • Inorganic forms converted to organic forms not toxic to organism or to terrestrial species (man). • Some evidence for reformation of toxic arsenite in fish flesh after death, becoming more toxic to consumer.
Cadmium (non-essential)	<ul style="list-style-type: none"> • Concentration factors in field samples, found to be as high as 4200x to 11,000x. • Lab study concentration factors ranged from 11x to 8300x • Release rates, in clean water, appear to be slow. • Cations in seawater (Ca, Mg, Sr) compete for uptake sites with Cd, Cu, Zn. Availability reduced with organic chelates. 	<ul style="list-style-type: none"> • Concentration factors for field samples of 10,000x were not uncommon. Highest levels in digestive gland, kidney. • Lab studies show concentration factors from 2x or 3x to 20,000x (dry weight). • Higher uptake at lower salinity. • Proteins similar to metallothioneins believed involved in detoxification. • Very slow depuration of body burden of cadmium in clean water. 	<ul style="list-style-type: none"> • Highest levels found in viscera, lowest in muscle. • Uptake values in lab were in 100x to 600x range. Half-life for loss in clean water, up to one year. • Most efficient uptake is through gills at higher concentrations, food at low concentrations. • Increased uptake at lower salinity, higher temperature. • Proteins isolated in midgut that bind to cadmium (metallothioneines). 	<ul style="list-style-type: none"> • Highest levels found in liver and other viscera; whole body range similar to molluscs-crustaceans. • Increasing age, lower temperature, high salinity reduce uptake. • Metallothionein-cadmium bonding interactions are a detoxification mechanism. Calcium in seawater may also interfere with cadmium effects. • Diet and water are indicated as important exposure pathways. • Significance of lower levels and intermittent exposure (common in ocean) not certain.
Chromium (essential element)	<ul style="list-style-type: none"> • Concentration factors of up to 8600x reported. • Short-term C. studies show uptake of 18x. • Little evidence for food chain biomagnification. 	<ul style="list-style-type: none"> • High field accumulations reported at 16,000x to 260,000x (high levels from Greek waters). • Less accumulation by heavier individuals and at high salinities. • Lab studies showed accumulation up to about 100x and 500x. • Uptake from water likely to be greater in lab; uptake from food greater in natural environment 	<ul style="list-style-type: none"> • Digestive glands and gills contained highest levels • Uptake equilibrium shown to take up to 5 days • Some studies show accumulation up to 100x 	<ul style="list-style-type: none"> • 1000-fold variation in accumulation among species from same location, same collection method. • Laboratory uptake observed in the 1x to 100x range, with higher concentration in liver, low in muscle.

(Continued)

TABLE 4.4-1 (Continued)

Chemical	Algae/Macrophytes	Molluscs	Crustaceans	Finfish
Copper (essential)	<ul style="list-style-type: none"> Accumulation range from 2000x to 20,000x in field collections. Hypothesized variation in species tolerance to very phytotoxic ion. Dead algae release soluble copper available for other uptake. Uptake increases with temperature, decreases with salinity. Chelation complexation with organic matter, iron, citrate found to reduce availability. 	<ul style="list-style-type: none"> High biomagnification in field collections from 4100x to 15,000x (high levels in Greek waters). Seasonal, sex, age differences. Uptake increases with increased temperature, decreases at higher salinity. Highest accumulation in gills, digestive tract, kidney. Accumulations in long-term lab experiments up to 20,000x. 	<ul style="list-style-type: none"> High in blood, as a component of respiratory pigments in this and other groups. Muscle contains lowest concentration. Hepatopancreas stores copper; chitin of some species absorbs copper. Small metal-binding proteins have been identified in digestive tract gland of some species. Age, developmental stage and season affect uptake. Uptake and/or toxicity greater at lower salinity and higher temperature. 	<ul style="list-style-type: none"> Concentrations in marine vertebrates lowest among marine biota. Highest fish concentrations in liver and gills, viscera. Very low in muscle. Copper-binding proteins have been isolated from some species. Age, sex, size, season may affect uptake, sensitivity. Free cupric iron is form affecting toxicity. More toxic at lower salinity. Probable increase in uptake following death. Lab study showed 5000x to 7000x concentration for viscera.
Lead (non-essential)	<ul style="list-style-type: none"> Field collections illustrate accumulation ranges from 1200x to 82,000x. Examples of lab tests show concentrations at 124x for short-term tests. 	<ul style="list-style-type: none"> Long-term lab studies show accumulations of 200x to more than 20,000x dry weight in various soft tissues. Highest accumulations in kidney, gills, and digestive gland. Younger and smaller organisms exhibit faster uptake, slower loss rate. Higher uptake levels with lower salinity. Uptake of lead in sediments by some species can be controlled by higher iron levels. Uptake may be from food or from water 	<ul style="list-style-type: none"> Radioisotope studies show uptake of about 100x in whole organism (ranged from 10x in muscle to 1 million x in hepatopancreas). Localized in exoskeleton and lost with molt. Uptake and/or toxicity greater at lower salinity, also higher temperature. 	<ul style="list-style-type: none"> Some fish shown to accumulate from water by 100x. Lead accumulates in bone, so whole fish levels relatively higher than in muscle or viscera.
Mercury (non-essential)	<ul style="list-style-type: none"> Short-term lab experiments showed uptake in the 10,000x to 75,000x range. Organomercury compounds more readily taken up, greater uptake at lower salinity, high pH. Great species differences in sensitivity. 	<ul style="list-style-type: none"> Short-term lab uptake of 100x from water. Long-term lab uptake of 2800x to about 30,000x. Uptake of inorganic forms about 1/4 that of organic forms. Methylmercury more toxic and more readily taken up. Biological processes convert a number of other forms of mercury to organic mercury compounds. Uptake greater in low salinity. Less uptake in presence of selenium. 	<ul style="list-style-type: none"> Field collections do not show exceedingly high levels except in very polluted areas. Laboratory studies have illustrated uptake factors in the 500x to more than 10,000x range in different tissues over different duration exposures. Concentrations high in gills, digestive glands. Relatively lower in muscle and blood. Bioconcentration from food demonstrated but is faster and higher from solution 	<ul style="list-style-type: none"> Field collections show accumulation in <i>edible flesh</i>. Most in flesh in organic form and higher in large, upper-level carnivores than species with short food chain. Some uptake believed to represent natural background conditions. Concentration from food sources believed by some to be greater than from water but is still argued. Fish appear to have high tolerance for mercury without obvious adverse effects.

(Continued)

TABLE 4.4-1 (Continued)

Chemical	Algae/Macrophytes	Molluscs	Crustaceans	Finfish
Mercury (non-essential, (continued)		<ul style="list-style-type: none"> Loss processes are extremely slow over 6 months and up to 3 years in clean water environments. Uptake highest among organisms with direct contact with sediments. 	<ul style="list-style-type: none"> Organomercury compounds are more toxic and more readily taken up than inorganic salts. Toxicity uptake greater at lower salinity — for inorganic salts. 	<ul style="list-style-type: none"> Concentration factors in long-term lab studies show levels from 450x to 2000x, depending upon life stage and form of mercury. Depuration rates reported from weeks to years, with loss from muscle relatively slow.
Nickel (possibly essential)	<ul style="list-style-type: none"> Reported accumulations in field samples range from 146x to above 1000x. 	<ul style="list-style-type: none"> High variability in field concentrations; one extraordinary uptake value of 120,000x. Concentration varies with season of collection. Tissue of highest concentration varies with species. Long and short-term lab studies show uptake potential from 20x to more than 500x. 	<ul style="list-style-type: none"> High variability in field collection concentrations. Lowest concentrations found in edible flesh, highest in exoskeleton. 	<ul style="list-style-type: none"> Low levels found in field collections of these species. Not accumulated in amounts of concern to human consumers.
Zinc (essential)	<ul style="list-style-type: none"> Field sample concentrations were at least several orders of magnitude above ambient water levels. Uptake inversely related to organic pesticide uptake, pH and salinity, and directly related to temperature and O₂ levels. High variability in uptake among species (even from same area). Required element. Macrophytes (especially in marshes) play role in cycling of element. 	<ul style="list-style-type: none"> Lowest concentration factor from field collections greater than 1500x. Concentration factors as high as 1.7 to 4 million x in kidney, as high as 25,000x to 100,000x in soft parts. Filter feeders are high accumulators. Highest in kidney and digestive gland. Uptake varies in some species with weight and sex; much can be bound by proteins or in organelles. Higher temperature and lower salinity increased zinc levels. Loss rates may be rapid or slow. Reported half-life of 255 days in oysters. 	<ul style="list-style-type: none"> Zn apparently not limiting in marine environment. Also accumulates beyond "needs," likely bound to an enzyme-organic fraction. Food considered more important pathway for uptake than water. Losses of internal Zn measured in months at fastest. High degree of variability in uptake with life stage of species. Uptake higher at higher temperature and lower salinity. 	<ul style="list-style-type: none"> Field concentrations generally low. Highest levels in viscera and gonad, low in muscle. Food greater source of metal than water. Age and sex of fish affect uptake. Zn-binding proteins have been identified. Uptake affected by organo-chlorine pesticides. Cd and Cu as well as temperature, salinity, and others. Uptake may increase after death.

Note: Concentration factors, where given, represent the only numbers from a small data base or upper-range. "worst case" numbers from a large data base.
 Sources: Eissler [13]; Phillips and Russo [32]

circumstance where modeling is used to trigger an "early warning" system is through the "Mussel Watch" program. Mussels are used as indicators of contamination, and are collected and analyzed on a regular basis. Its major benefit is to provide an early warning, but it works well only if samples are collected where contaminant concentrations are high. Because of the lack of uniformity typical of marine water concentrations, it is possible for pulses that are toxic to some organisms to be missed by this method. However, it remains a significant monitoring tool, even if it is not as useful for broader predictive purposes.

The Mussel Watch model, as reported by Goldberg *et al.* [16], is:

$$dM/dt = KM_{sw} - TM$$

where

- M = metal concentration in bivalve tissue
- t = age of organism
- K = constant
- T = biological half-life of metal
- M_{sw} = concentration of metal in seawater

The principal limitation of this model is the assumption that M_{sw} , remains constant for any appreciable length of time. In fact, major pulses of different concentrations are common in field exposure situations. A secondary limitation may be the assumption that the constant K can be based on linearity in the availability/uptake relationship; while linearity may prevail under some of the conditions of uptake observed to date, the extent of appropriate generalization from these observations is unclear [13].

4.5 UPTAKE BY FRESHWATER BIOTA

4.5.1 Introduction

The freshwater environment includes a wide range of water characteristics and habitats whose variations affect uptake processes. Uptake in these environments can become problematic because of their heavy use for water supply (e.g., crop irrigation) and recreational harvest of edible finfish and waterfowl. Some freshwater habitats are large, relatively deep lakes, characterized by seasonal changes in temperature, oxygen concentration and pH stratification, with subsequent turnover and mixing. Other lakes that are too small or too shallow to stratify have limited water exchange and are particularly vulnerable to contaminant buildup. Major rivers are characterized by large-volume flows and sediment loads, even with seasonal variations in input. Many small streams and headwaters regularly experience great fluctuations in flow volume, sediment load, temperature, pH and oxygen as the result of seasonal changes and storms. These characteristics can strongly influence exposure to and uptake of inorganics by adding or removing inorganics and changing their availability.

Some less readily observed characteristics can also influence the uptake of inorganic substances in fresh water:

- The nature and degree of watershed development (roads, deforestation, houses, etc.) can influence the quality and quantity of water that enters a surface freshwater system. Inputs may include organic matter such as leaf litter, or nutrients that stimulate the production of organic matter, which in turn affects uptake. Disturbed areas can contribute increased concentrations of leachable substances such as organic acids from natural soils [38]. Watersheds with agricultural and/or urban development may contribute a wide range of organic as well as inorganic substances. Such contributions may increase or decrease the potential for uptake of inorganics that are already present, as well as contributing substances directly for uptake.
- Freshwater systems show great variation in pH, water hardness and alkalinity, and the presence and concentration of a number of solid materials and dissolved constituents (e.g., phosphates and clays or silts) that can form immobilizing complexes with inorganic constituents otherwise available for uptake.

In each freshwater environment, some or all of these factors affect the equilibria among the various chemical forms of an introduced or newly mobilized inorganic substance and, hence, the amounts and chemical species available to biological organisms.

4.5.2 Uptake and Loss Processes in Freshwater Organisms

In general, the discussion of uptake and loss processes for marine biota in § 4.4.2 and § 4.4.3 applies equally to uptake by freshwater biota.

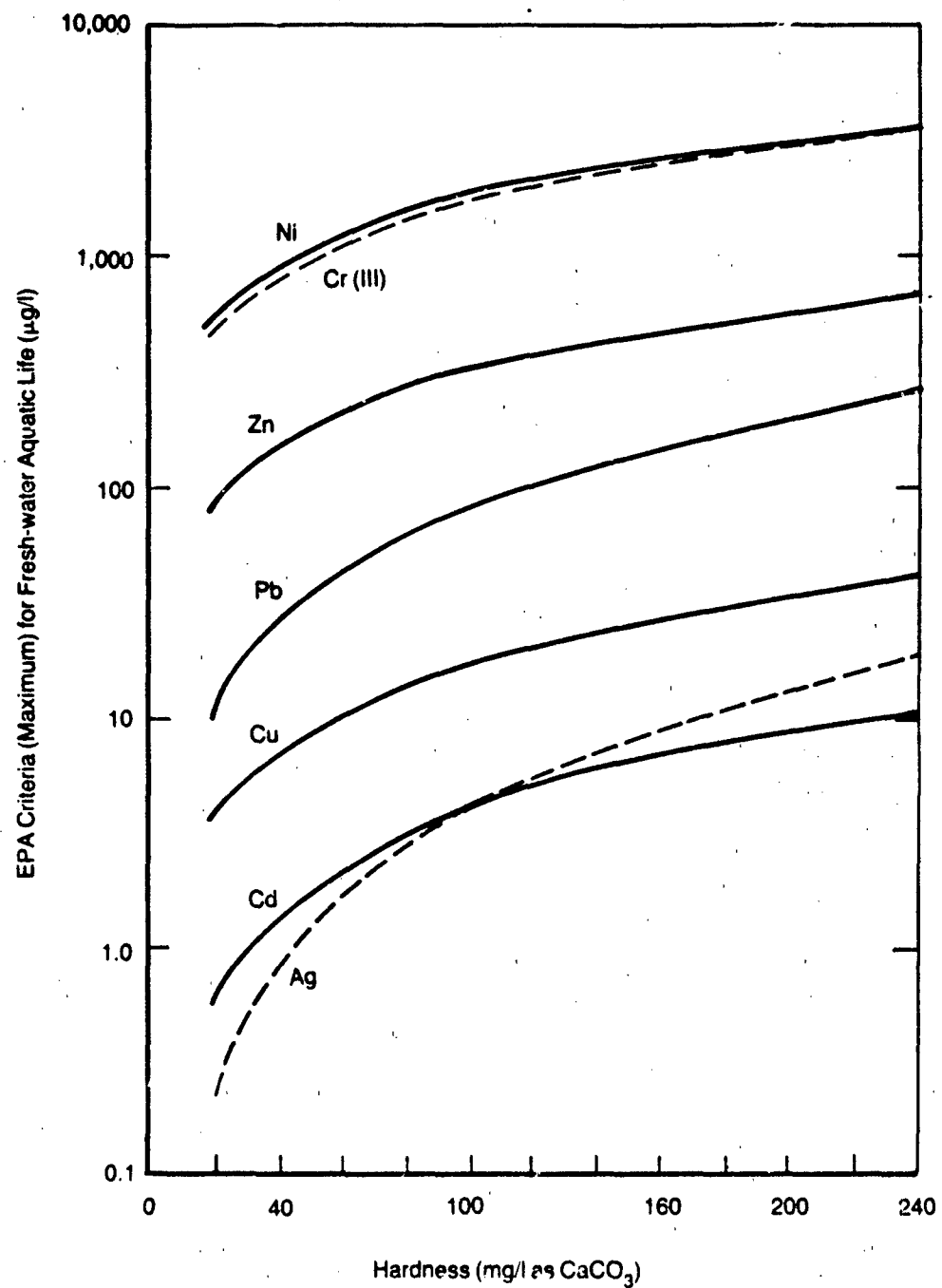
Evidence exists for binding of some heavy metals by specific metallothionein-like proteins in some freshwater fish. Such proteins apparently increase with exposure of the biota to mercury, zinc, or copper [33] or to cadmium [32]. Copper- and cadmium-specific metallothioneins have been identified in freshwater species [33]. Zinc may associate with more than one type of binding protein [32]. The data presented to date for freshwater species (*Salmonids*) do not yet indicate support for the hypothesis (discussed in § 4.4.2) that toxicity occurs when the detoxification capacity of the binding proteins is exceeded; however, they do support the potential corollary hypothesis of protection to those organisms that are preexposed, produce the detoxifying protein, and are then reexposed to otherwise toxic concentrations [33]. Numerical relationships between accumulation levels, protein binding, and toxicity to the organism are not yet defined as well by these data as they have been in the research on marine species.

CHEMICAL ENVIRONMENTAL VARIABLES

There are additional explanations for variations in inorganic metal uptake, primarily involving water chemistry. For a substance to be toxic, it must be available for uptake. A number of inorganic constituents, including many of the trace metals, exist in more than one valence state and are complexed and/or in equilibrium with other substances in the water. Several of these factors, which are known to alter the types or concentrations of ions present, have significant effects on the toxicity of many inorganic species. The ones most frequently cited in demonstrable correlations with toxicity effects are water hardness/alkalinity, pH, organic matter, and (sometimes) temperature. Because they can have such a dramatic effect on toxicity, the EPA has stipulated varying criteria for the allowed concentrations of some elements in surface waters. Figure 4.5-1 shows, for example, how the EPA's freshwater aquatic life criteria increase with increasing hardness of the water..

In fresh-water systems as a whole, these factors vary considerably from one water body to the next; thus, it is important to examine the role that they may play in the uptake of specific constituents. One should also be aware that each of these water quality factors may affect the availability/uptake of only some inorganics, and may affect them in differing degrees.

Hardness and alkalinity are related measures of water quality (carbonate and bicarbonate). They are often similarly high or low. Highly alkaline and hard waters tend to have a high pH; soft water usually has a lower pH, but not always. Where there is an effect on substance toxicity/uptake, each of these factors may act in combination or separately to influence the availability of a specific inorganic species. Examples of modes of interaction include competition for binding sites, complexation to reduce availability, and shifting of equilibria among the forms of an inorganic



Note: Curves were derived from equations given in Table D-3 of Appendix D. For Ag, Ni, and Zn, criteria are maximum concentrations not to be exceeded at any one time. For Cd, Cr, Cu and Pb, criteria are one-hour average concentrations, not to be exceeded more than once every three years on the average.

FIGURE 4.5-1 EPA Criteria for Fresh-water Aquatic Life as a Function of Water Hardness

substance present. Sometimes the interaction among these factors is understood; at other times it can only be deduced. Unfortunately, the historic body of literature has not always noted what are now considered key water quality parameters (e.g., hardness/alkalinity, pH, organic matter, temperature). Because such parameters appear to affect the availability of toxic forms of a constituent, it must also be assumed that there is some effect on uptake and subsequent accumulation.

Temperature changes affect the metabolism of aquatic biota, and there is evidence that the uptake of trace metals increases at higher temperatures [32]. Several of these interactions are described in the examples below (and are also listed in Table 4.5-1).

- Copper occurs in many forms in natural waters. Soluble cupric ions are believed to be the toxic form as well as the form most available for accumulation. Calcium ions are believed to compete for binding sites on biological surfaces, indirectly interfering with copper uptake [29]. Carbonate ions and increasing pH are thought to shift copper equilibria toward less available soluble forms; thus, copper uptake is believed to be reduced by higher alkalinity/hardness/pH [46,57].
- Cadmium, another inorganic ion that can be highly mobile and has been toxic through food-web accumulation, is precipitated from solution by carbonate and adsorbed by a number of naturally occurring substances. As pH increases, these processes become more effective, and cadmium may precipitate from the water column [42]. In a very recent study, increased calcium levels in water have been shown to reduce the uptake and accumulation of cadmium in fish [31].
- The uptake and toxicity of chromium VI was judged by the EPA to be strongly influenced by water hardness [43]. Uptake of chromate by fish increased with a shift in pH from 7.8 to 6.5, which purportedly caused greater oxidizing action by chromate ions [55].

Mathematical relationships between observed toxicity and water hardness, in those cases where regression correlations are plausible, have been formulated by the EPA for use in approximating safe water levels for some substances (such as Cd, Cu, and Zn; see Appendix D). Such correlations have not been tested/observed for accumulation of these same constituents. A qualitative relationship, similar to that observed for toxicity, is believed to occur; in fact, as noted above, cadmium uptake and accumulation by perfused gills was reduced by increased water hardness.

An additional factor that is believed to affect the uptake of some inorganic species is the presence of organic matter in the water. Loosely defined, this may include humic substances and other suspended organic matter, as well as dissolved amino acids. Different forms of a number of inorganic species found in water are adsorbed or complexed by such material. Most often, this associated material is less toxic or less available for uptake, and may often be precipitated and become associated with the sediments [8, 57]. These factors are most important in the measurement of water and sediment concentrations of a specific inorganic. For example, measurement of "total" levels of a trace metal could include chelated or adsorbed forms that may not be

available for uptake by biota. A capability for defining and then measuring available forms has remained largely elusive.

There are exceptions to the above broad generalizations. Methylation renders some inorganics more soluble and more readily available for uptake, and the resulting organometallic species may be more or less toxic than the prior form. The classic example of a more toxic, available form that bioaccumulates is methylmercury. Any mercurial compound introduced into water can apparently be converted to methylmercury. (See section 2.15, Microbial Transformations.) The conversion of methylmercury to elemental mercury can also occur but evidently is not significant unless large amounts of methylmercury exist [32]. Significantly, methylmercury does not behave like its inorganic form; it is more readily taken up, especially by fish, and is lost very slowly. Its half-life is probably 1-3 years. (See Table 4-5-1.) Further, unlike many other inorganics of potential concern to human consumers, methylmercury concentrates in muscle tissue as well as in other organs [32].

Arsenic is another example of an inorganic element that can be methylated by bacteria. In this case, however, the highly toxic methyl and dimethyl products are both highly volatile and readily oxidized. Their bioaccumulative significance is unknown [32].

Suspended or deposited sediments, including clays, can act in a similar fashion to reduce the availability of trace inorganics for uptake in freshwater as well as in terrestrial systems. While the presence of these substances has been shown to reduce the toxicity of some heavy metal species, predictive or quantifiable relationships have not been demonstrated. In view of the variety of potential complexing agents, this is not surprising.

PHYSICAL ENVIRONMENTAL VARIABLES

The above discussion points up the need to understand the environmental circumstances that are coupled with any examination of the fate of inorganic constituents. Streams, for example, usually have small dilution capacity; however, if they flow through an area that contributes large amounts of leaf litter and other organics or a fairly heavy sediment load, the uptake/toxicity potential of inorganics such as some trace metal species can be reduced. Large lakes represent another example: many become stratified during warm months, and the temperature barriers prevent mixing of water between upper and lower levels. The resultant anaerobic condition in the lower level can cause a seasonal decrease in pH, which disturbs adsorption and speciation equilibria and causes some trace metal species to be released from the sediments. During the fall turnover, when surface waters become colder and sink, there is a remixing of the water column and a resuspension of material, increasing potential uptake.

Uptake processes for inorganics are also affected by other watershed and waterbody characteristics. For example, water in areas of igneous or metamorphic bedrock tend

to have low alkalinity, while areas of sedimentary or calcareous bedrock geology and accompanying higher weathering rates tend to produce waters with higher alkalinity. (See Figure 4.5-2.) When the former circumstances are accompanied by watershed soils that are acidic and/or characterized by low buffering capacity, lakes in the region are potentially vulnerable to damage from acid precipitation [38].

Patterns of acid precipitation for the eastern United States are illustrated in Figure 4.5-3. The sufficient lowering of pH can have an adverse effect in and of itself. Moreover, such circumstances also lead to the release of otherwise bound inorganic constituents such as aluminum species through the shifting of pH-related equilibria in soils and sediments. More to the point of this discussion, low pH sometimes appears to enhance uptake and toxicity of harmful inorganics, including many trace metal species.

Finally, it is important to note that even when existing circumstances suggest low uptake potential, they may change and alter uptake risk. Annual turnover in large lakes, agricultural drainage modifications, and acid precipitation effects are examples of short- and long-term changes in environmental circumstances that alter uptake potential.

4.5.3 Data and Criteria on Uptake Potential

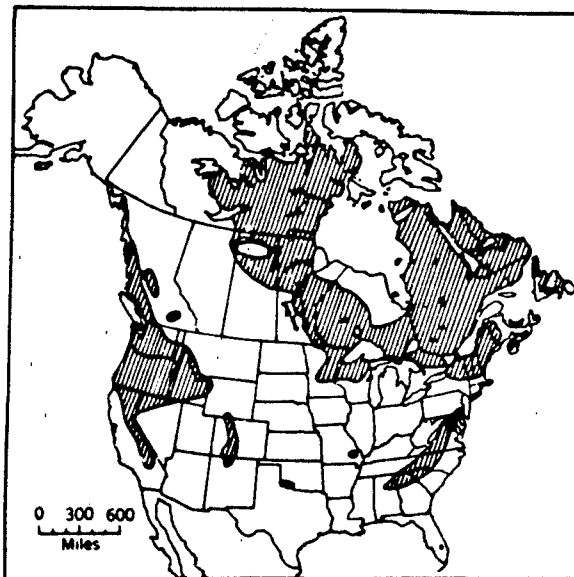
In general, the data available on uptake of inorganics by freshwater organisms are similar to that for marine organisms (§ 4.4.4.) The major difference is that a far greater volume of data exists for freshwater organisms, but, perhaps as a consequence, it has not been compiled as comprehensively or systematically as that for marine biota or terrestrial vegetation.

As in the two earlier sections, very general summaries concerning the behavior of a number of inorganics in fresh water are given in Table 4.5-1. Note that many trace elements become more available in soft, non-alkaline water but that a few are more available in alkaline situations. The high degree of environmental variability in freshwater systems makes it particularly difficult to generalize uptake rates.

Appendix D lists USEPA, FDA and other nationally applicable freshwater bioaccumulation criteria for inorganics. Table 4.2-4 in this chapter lists criteria developed by the State of California based on combined availability from dissolved and leachable sediment sources.

4.5.4 Models and Predictive Techniques

As for the other environments, no generally applicable models or predictive techniques are available for quantitative estimation of uptake or accumulation of inorganics by freshwater biota. The degree of water hardness, more specifically measured as calcium carbonate concentration, shares a demonstrated relationship with the toxicity of some of the species of heavy metals such as Cu and Zn. For these metals, there has been sufficient laboratory-demonstrated change in toxicity with

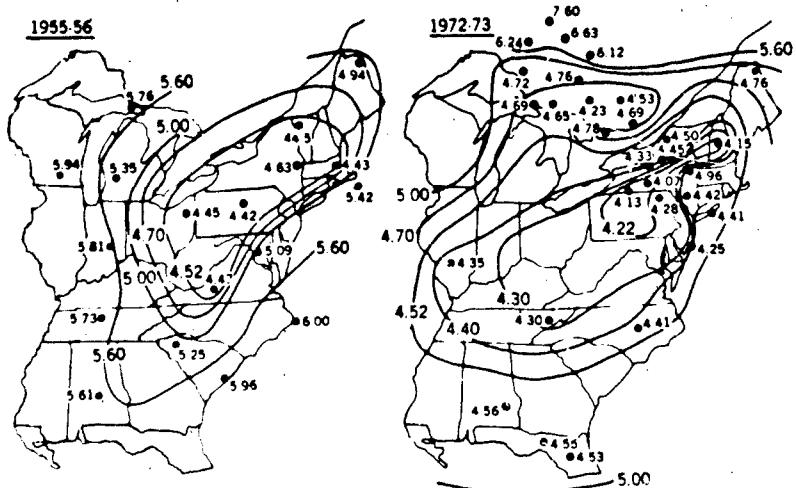


Shaded areas have igneous or metamorphic bedrock geology; unshaded areas have calcareous or sedimentary bedrock geology.

Because of the slower geological weathering rates in areas of metamorphic and igneous bedrock geology, lakes in these areas are expected to be dilute and to have low alkalinites ($<0.5 \text{ meq HCO}_3$ per liter). This hypothesis was tested by compiling lake alkalinity data from several sources; regions having lakes with low alkalinity coincided with the shaded areas.

Source: Galloway and Cowling [11]. (Copyright 1978, Air Pollution Control Association. Reprinted with permission.)

FIGURE 4.5-2 Regions in North America Containing Lakes That Are Sensitive to Acidification by Acid Precipitation



Source: Galloway and Cowling [11]. (Copyright 1978, Air Pollution Control Association. Reprinted with permission.)

FIGURE 4.5-3 Weighted Annual Average pH of Precipitation in the Eastern United States

TABLE 4.5-1

Some General Characteristics of Trace Metal Uptake In Selected Groups of Freshwater Organisms

Chemical	General Information	Uptake in Plants	Uptake in Invertebrates	Uptake in Aquatic Vertebrates	Sources
Arsenic (non-essential)	<ul style="list-style-type: none"> May be present in trivalent, pentavalent or organic complexes and other organic forms in water. Wide range of toxicity among species tested with inorganic trivalent and pentavalent forms. Water hardness seems to have little effect on toxicity. Laboratory data base limited, reflects several orders of magnitude differences in active toxicity among species tested. 	<ul style="list-style-type: none"> Data not available for freshwater aquatic species. 	<ul style="list-style-type: none"> Appears to be little difference in uptake of inorganic and several organic forms. Uptake is low at levels that are not also toxic. Less than 20x for freshwater species tested with trivalent, pentavalent and some organic arsenic forms. Fats contain more than other tissue. Does accumulate in muscles. 	<ul style="list-style-type: none"> Studies show low bioconcentration and short half-life for concentrations that are not also toxic. Less than 20x for freshwater species tested with trivalent, pentavalent and some organic arsenic forms. Fats contain more than other tissue. Does accumulate in muscles. 	[32, 40, 41]
Cadmium (non-essential)	<ul style="list-style-type: none"> Probably occurs in many forms in fresh water. Calcium carbonate (hardness) reduces toxicity, but effect of hardness on uptake not demonstrated. High organic, high pH reduce toxicity, but effect on uptake not demonstrated. Laboratory acute toxicity tests reflect over 4 orders of magnitude across species tested. Test water hardness is partly responsible for wide range. 	<ul style="list-style-type: none"> Over long time, concentration factors may be extremely high, and certainly similar to any high uptake potential in animals. (Up to and greater than 1000x.) 	<ul style="list-style-type: none"> Steady-state concentrations appear to be reached quickly in freshwater crustaceans. Data from marine molluscs indicate that some invertebrates are very high accumulators and that a long time is required for a steady-state to be reached. Existence of cadmium-binding protein demonstrated in marine molluscs (up to 3500x in freshwater invertebrates.) 	<ul style="list-style-type: none"> Very broad range of uptake values reported. Very low concentration factor shown for muscle. Highest levels from whole body analysis and viscera. Apparently takes more than 28 days for steady-state concentrations to be reached. Elimination of cadmium accumulated from water is slower than elimination of accumulations from food. Binds with metallothionein-like protein in liver and kidney (up to about 12,000x in muscle). 	[32, 42]

TABLE 4.5-1 (Continued)

Chemical	General Information	Uptake in Plants	Uptake in Invertebrates	Uptake in Aquatic Vertebrates	Sources
Chromium (essential element)	<ul style="list-style-type: none"> Hexavalent forms vary somewhat in fresh water, and toxicity does not seem affected by hardness. Trivalent forms form stable complexes with negatively charged species, so less soluble/toxic. Toxicities of the two are not widely different. Toxicity covers three orders of magnitude across species. 	<ul style="list-style-type: none"> Uptake of hexavalent form by algae community reported at 8500x. Data unavailable for trivalent form. 	<ul style="list-style-type: none"> Data not available for freshwater species; uptake in marine forms in the 80x to 200x range (not extensive data base.) 	<ul style="list-style-type: none"> Uptake in one tested species less than 5x. Relatively little accumulates in edible tissues. 	[32, 43, 44]
Copper (essential element)	<ul style="list-style-type: none"> Required micronutrient Soluble ions readily complexed by organic matter and calcium carbonate, and adsorbed by suspended solids. Higher pH decreases availability. Only water hardness presently reflected in regulatory evaluation. Other factors above reduce toxicity as well, but effect on uptake less certain. Significance of tissue residues uncertain. 	<ul style="list-style-type: none"> A value of 2000x for one species (marine values higher). 	<ul style="list-style-type: none"> Single value of about 200x for insect larvae. (Marine values higher.) 	<ul style="list-style-type: none"> Value of 300x for one fish only, 1x for fish muscle in another test. Uptake appears to begin at levels that also result in chronic effects. 	[32, 45]
Lead (non-essential)	<ul style="list-style-type: none"> Many problems encountered in analytical measurement. Precipitation of divalent cation by hydroxide, carbonate and organic matter common. Less toxic in hard water and higher pH. Up to three orders of magnitude in laboratory acute toxicity — with water hardness and species differences credited. Effect on uptake not noted. 	<ul style="list-style-type: none"> Data unavailable for freshwater species. (One saltwater value more than 700x.) 	<ul style="list-style-type: none"> Values reported from 500x to 1700x for whole-body levels. Highest concentrations in viscera 	<ul style="list-style-type: none"> Whole-body concentration factors around 50x. Mucus concentrates lead to levels much higher than organism. May "contaminate" samples. 	[32, 47, 48]

TABLE 4.5-1 (Continued)

Chemical	General Information	Uptake in Plants	Uptake in Invertebrates	Uptake in Aquatic Vertebrates	Sources
Mercury (non-essential)	<ul style="list-style-type: none"> Elemental and divalent forms can be methylated. Methylmercury is more water-soluble, many times more toxic, and has higher uptake/bioconcentration potential than many inorganic forms. Toxicity and uptake increase with increased temperature; higher uptake at lower pH. Bioconcentration is high because uptake rates are fast, loss rates slow. Depuration of methyl-mercury so slow that this form predominates in tissue even with greater exposure to inorganic forms. 	<ul style="list-style-type: none"> Short-term non-steady-state concentration factor of 29,000x reported for inorganic mercury. Short-term concentration of up to 2100x for methylmercury. 	<ul style="list-style-type: none"> Steady-state data unavailable for freshwater species. Up to 40,000x for methylmercury for saltwater bivalves. 10,000x for inorganics in saltwater at steady state. Short-term methyl-mercury uptake up to the 8000x range. 	<ul style="list-style-type: none"> Half-life of methyl-mercury in fish tissue 2 to 3 years. Mercury moves from absorbing surface to internal organs via blood, then kidney/gall bladder for recycle or elimination, and muscle for long-term storage. Uptake via gills and intestine. Selenium antagonism. Muscle and other tissue concentration similar. 5000x long-term uptake factor in fish for inorganic forms. Up to 64,000x long-term uptake factor for methylmercury. 	[32, 49, 50]
Nickel (may be essential element)	<ul style="list-style-type: none"> Toxicity reduced with increase in hardness. CaCO_3 likely reduces availability. 	<ul style="list-style-type: none"> Value of about 10x reported for fresh-water algae. 	<ul style="list-style-type: none"> Value of less than 100x reported for one freshwater fish species. 	<ul style="list-style-type: none"> Value of 100x reported for fresh-water crustacean (saltwater bivalve values 3 to 4 times higher). 	[32, 51]
Selenium (essential element)	<ul style="list-style-type: none"> Selenite (+ 6) may be less toxic than selenites (+ 4) and favored by alkaline and oxidizing conditions. Essential element in animal nutrition. Toxicity data base mostly for selenites; indicates great biological species differences. Data on effects of pH, hardness, etc. insufficient. Freshwater data unavailable for organic forms which can be formed from inorganic forms in environment. 	<ul style="list-style-type: none"> None reported for freshwater species. 	<ul style="list-style-type: none"> Uptake/concentration values for selenite in fresh-water fish up to 78x for whole body and 18x for muscle. Half-life in fish about 2 months. 	<ul style="list-style-type: none"> Values for selenite in 	[32, 52]

(Continued)

TABLE 4.5-1 (Continued)

Chemical	General Information	Uptake in Plants	Uptake in Invertebrates	Uptake in Aquatic Vertebrates	Sources
Zinc (essential element)	<ul style="list-style-type: none"> • Toxicity reduced with increasing hardness. • Required trace element in most organisms. • Occurs in many forms—dissolved, suspended, etc. 	<ul style="list-style-type: none"> • None reported for fresh-water species. (Up to 16,000x reported for marine species.) 	<ul style="list-style-type: none"> • Uptake values up to 1130x reported (up to 1600x for marine mollusc). 	<ul style="list-style-type: none"> • Uptake values up to 432x reported for fresh-water species. 	[32, 53]

(Concentration factors, where noted, represent the only numbers for a small data base OR the upper range, "worst case" numbers from a large data base.)

measured changes in calcium carbonate hardness to permit significant correlations by regression analyses. These, in turn, have been used to predict safe and potentially toxic concentrations of the associated metals in waters of varying hardness [42, 45, 53]. Unfortunately, data to date have not allowed comparably demonstrable relationships for varying uptake potential and water hardness. Similarly, reliably predictive relationships have not been broadly developed between toxicity or uptake potential and any other of the important water quality parameters, such as pH, sediment load, organic matter (other than that described by JRB [19]), redox state or temperature. For the time being, they must be discussed ad hoc or qualitatively for most inorganic chemicals. Exceptions include ammonia, where combinations of temperature and pH can be reliably used to predict the percentage of the un-ionized (toxic) form, but not necessarily its uptake pattern.

Some models, such as the EPA's EXAMS, use simplified uptake algorithms based on phenomena such as adsorption (not really uptake) by phytoplankton. These have little predictive value in problem definition for higher species and are mainly used in descriptions of the interim fate of contaminants.

Thus, the type of decision process outlined in § 4.2.4 above is recommended as the basis for identifying and resolving potential uptake-related problems in the freshwater environment.

4.6 LITERATURE CITED

1. Baes, C.F. III, R.D. Sharp, A.L. Sjoreen and R.W. Shor, "A Review and Analysis of Parameters for Assessing Transport of Environmentally Released Radionuclides Through Agriculture," Report No. ORNL-5786 prepared by Oak Ridge National Laboratory for the U.S. Environmental Protection Agency (1984). (NTIS: DE85-000287.)
2. Barber, S.A., *Soil Nutrient Bioavailability — A Mechanistic Approach*, John Wiley & Sons, New York (1984).
3. Bascom, W. (ed.), *Biennial Report, 1981-82*, Southern California Coastal Water Research Project, Long Beach, CA (1982).
4. Bascom, W. (ed.), *Biennial Report, 1983-84*, Southern California Coastal Water Research Project, Long Beach, CA (1984).
5. Brown, D.A., S.M. Bay, P. Szalay, G.P. Hershelman, C.F. Ward, A.M. Westcott and D.J. Greenstein, "Metal and Organic Detoxification/Toxicification in Fish Livers and Gonads," in Bascom [4], 195-209.
6. Brown, D.A., R.W. Gossett, G.P. Hershelman, C.F. Ward and J.N. Cross, "Metal and Organic Contaminants in Sediments and Animals," in Bascom [4], 179-93.
7. Brown, D.A., K.D. Jenkins, E.M. Perkins, R.W. Gossett and G.P. Hershelman, "Detoxification of Metals and Organic Compounds in White Croakers," in Bascom [1], 157-71.
8. Brown, V.M., T.L. Shaw and D.G. Shurben, "Aspects of Water Quality and the Toxicity of Copper to Rainbow Trout," *Water Res.*, **8**, 797-803 (1974).
9. California Administrative Code; Title 22, Division 4: Environmental Health, Article 11: "Criteria for Identification of Hazardous and Extremely Hazardous Wastes," distributed by State of California, Documents Section, P.O. Box 1015, North Highlands, CA 95660.
10. Chaney, R.L. (Beltsville, MD), personal communication to W. Lyman (Arthur D. Little, Inc.), June 1986.
11. Chaney, R.L., J.C. Smith, Jr., D.E. Baker, R. Bruins, D. Cole and R.F. Korcals, "Transfer of Sludge Applied Trace Elements to the Food Chain," draft report (unpublished) (1986).
12. Cowan, C.E., E.A. Jenne and R.R. Kinnison, *Methodology for Determining the Relationship between Toxicity and the Aqueous Speciation of a Metal*, PNL-SA-12471, CONF-8504147-1, NTIS No. DE85012442/WEP, Battelle Pacific Northwest Labs., Richland, Wash. (1985).
13. Eisler, R., *Trace Metal Concentrations in Marine Organisms*, Pergamon Press, New York (1981).
14. Galloway, J.N. and E.B. Cowling, "The Effects of Precipitation on Aquatic and Terrestrial Ecosystems: A Proposed Precipitation Chemistry Network," *J. Air Pollut. Control Assoc.*, **28**, 229-35 (1978).
15. Gerritse, R.G., W. Van Driel, K.W. Smilde and B. Van Luit, "Uptake of Heavy Metals by Crops in Relation to Their Concentration in the Soil Solution," *Plant Soil*, **75**, 393-404 (1983).

16. Goldberg, E.D., V.T. Bowen, J.W. Farrington, G. Harvey, J.H. Martin, P.L. Parker, R.W. Rosebrough, W. Robertson, E. Schneider and E. Gamble, "The Mussel Watch," *Envir. Conserv.*, 5, 101-25 (1978), in Eisler [13].
17. Holmgren, G.G.S., M.W. Meyer, R.B. Daniels, R.L. Chaney and J. Kubota, "Cadmium, Lead, Zinc, Copper and Nickel in Agricultural Soils of the United States," submitted to *J. Environ. Qual.* (1986).
18. Jenkins, D.W., "Biological Monitoring of Toxic Trace Metals: Volume I. Biological Monitoring and Surveillance," Report No. EPA-600/3-80-089, U.S. Environmental Protection Agency, Las Vegas, NV (1980).
19. JRB Associates (Bellevue, Wash.), *Initial Evaluation of Alternatives for Development of Sediment-related Criteria for Contaminants in Marine Waters (Puget Sound). Phase II: Development and Testing of the Sediment-Water Equilibrium Partition Approach*, EPA Report 910/9-83-117, U.S. Environmental Protection Agency, Washington, D.C. (1984).
20. Kabata-Pendias, A. and H. Pendias, *Trace Elements in Soils and Plants*, CRC Press, Boca Raton, Fla. (1984).
21. Ketwig, K., "Lost Condors Spark Debate; Lead Poisoning Takes Two," *Audubon Action*, 3 (Aug. 1985).
22. Lee, C.R., B.L. Folsom, Jr., and R.M. Engler, "Availability and Plant Uptake of Heavy Metals from Contaminated Dredged Material Placed in Flooded and Upland Disposal Environments," *Environ. Internat.*, 7, 65-71 (1982).
23. Lee, H. (U.S. Environmental Protection Agency, Newport, OR), personal communication to W. Lyman (Arthur D. Little, Inc.) (May 1986).
24. Leeper, G.W., *Managing the Heavy Metals on the Land*, Marcel Dekker, New York (1978).
25. Mengel, K. and E.A. Kirkly, *Principles of Plant Nutrition*, 3rd edition, International Potash Institute, Bern, Switzerland (1982).
26. National Academy of Sciences and National Academy of Engineering, *Water Quality Criteria, 1972*, EPA R3-73-033, U.S. Environmental Protection Agency, Washington, D.C. (1973).
27. O'Donnell, J.R., B.M. Kaplan and H.E. Allen, "Bioavailability of Trace Metals in Natural Waters," *Aquatic Toxicology and Hazard Assessment: Seventh Symposium*, ASTM STP 854, R.D. Cardwell, R. Purdy and R.C. Bahner (eds.), American Society for Testing and Materials, Philadelphia, 485-501 (1985).
28. Overcash, M.R. and D. Pal, *Design of Land Treatment Systems for Industrial Wastes — Theory and Practice*, Ann Arbor Science Publishers, Ann Arbor, Mich. (1979).
29. Pagenkopf, G.K., "Gill Surface Interaction Model for Trace-Metal Toxicity to Fishes: Role of Complexation, pH, and Water Hardness," *Environ. Sci. Technol.*, 17, 342-47 (1983).
30. Parr, J.F., P. B. Marsh and M. Kla, *Land Treatment of Hazardous Wastes*, Noyes Data Corp., Park Ridge, N.J. (1983).

31. Pärt, P., O. Svanberg and A. Kiessling, "The Availability of Cadmium to Perfused Rainbow Trout Gills in Different Water Qualities," *Water Res.*, **19**, 427-34 (1985).
32. Phillips, G.R. and R.C. Russo, *Metal Bioaccumulation in Fishes and Aquatic Invertebrates: A Literature Review*, EPA-600/3-78-103, U.S. Environmental Protection Agency, Environmental Research Laboratory, Duluth, Minn. (1978).
33. Roch, M., J.A. McCarter, A.T. Matheson, M.J.R. Clark and R.W. Olafson, "Hepatic Metallothionein in Rainbow Trout (*salmo gairdneri*) as an Indicator of Metal Pollution in the Campbell River System," *Can. J. Fish. Aquat. Sci.*, **39**, 1596-1601 (1982).
34. Römhild, V. and H. Marschner, "Evidence for a Specific Uptake System for Iron Phytosiderophores in Roots of Grasses," *Plant Physiol.*, **80**, 175-80 (1986).
35. Ryan, J.A., R.L. Chaney, G. Prince, A.D. Otte and J.M. Walker, "Review of the Soil Factors and the Concept of Cumulative Application Rate of Cd on Cd Content of Crops," Background Document from J.A. Ryan, USEPA, WRD, MERL to A.A. Peter, Jr., EPA, OSW (May 13, 1980).
36. Santhanam, C.J., A. Balasco, I. Bodek and C.B. Cooper, *Full-scale Field Evaluation of Waste Disposal from Coal-Fired Electric Generating Plants, Vol. II*, Report EPA-600/7-85-028b, U.S. Environmental Protection Agency, Office of Research and Development, Washington, D.C. (1985).
37. Takagi, S., K. Nomoto and T. Takemoto, "Physiological Aspect of Mugineic Acid, a Possible Phytosiderophore of Graminaceous Plants," *J. Plant Nutrition*, **7**, 469-77 (1984).
38. Talbot, R.W. and A.W. Eizerman, "Acidification of Southern Appalachian Lakes," *Environ. Sci. Technol.*, **19**, 552-57 (1985).
39. U.S. Department of the Interior, *Kesterton Reservoir Closure and Cleanup Plan*, Bureau of Reclamation, Mid-Pacific Regional Office, Sacramento, Calif. (1985).
40. U.S. Environmental Protection Agency, *Ambient Water Quality Criteria for Arsenic*, EPA 440/5-80-021, Office of Water Regulations and Standards, Criteria and Standards Division, Washington, D.C. (1980).
41. U.S. Environmental Protection Agency, "Revised Section B of Ambient Water Quality Criteria for Arsenic," Draft (Aug. 19, 1983).
42. U.S. Environmental Protection Agency, *Ambient Water Quality Criteria for Cadmium*, EPA 440/5-80-025, Office of Water Regulations and Standards, Criteria and Standards Division, Washington, D.C. (1980).
43. U.S. Environmental Protection Agency, *Ambient Water Quality Criteria for Chromium*, EPA 440/5-80-005, Office of Water Regulations and Standards, Criteria and Standards Division, Washington, D.C. (1980).
44. U.S. Environmental Protection Agency, "Revised Section B of Ambient Water Quality Criteria for Chromium," Draft (Aug. 19, 1983).
45. U.S. Environmental Protection Agency, *Ambient Water Quality Criteria for Copper*, EPA 440/5-80-036, Office of Water Regulations and Standards, Criteria and Standards Division, Washington, D.C. (1980).

46. U.S. Environmental Protection Agency, "Revised Section B of *Ambient Water Quality Criteria for Copper — Aquatic Toxicology*," Draft (Aug. 19, 1983).
47. U.S. Environmental Protection Agency, *Ambient Water Quality Criteria for Lead*, EPA 440/5-80-057, Office of Water Regulations and Standards, Criteria and Standards Division, Washington, D.C. (1980).
48. U.S. Environmental Protection Agency, "Revised Section B of *Ambient Water Quality Criteria for Lead*," Draft (Aug. 19, 1983).
49. U.S. Environmental Protection Agency, *Ambient Water Quality Criteria for Mercury*, EPA 440/5-80-058, Office of Water Regulations and Standards, Criteria and Standards Division, Washington, D.C. (1980).
50. U.S. Environmental Protection Agency, "Revised Section B of *Ambient Water Quality Criteria for Mercury*," Draft (Aug. 19, 1983).
51. U.S. Environmental Protection Agency, *Ambient Water Quality Criteria for Nickel*, EPA 440/5-80-060, Office of Water Regulations and Standards, Criteria and Standards Division, Washington, D.C. (1980).
52. U.S. Environmental Protection Agency, *Ambient Water Quality Criteria for Selenium*, EPA 440/5-80-070, Office of Water Regulations and Standards, Criteria and Standards Division, Washington, D.C. (1980).
53. U.S. Environmental Protection Agency, *Ambient Water Quality Criteria for Zinc*, EPA 440/5-80-079, Office of Water Regulations and Standards, Criteria and Standards Division, Washington, D.C. (1980).
54. U.S. Fish and Wildlife Service, *Fed. Regist.*, 50, 30849-53 (July 30, 1985).
55. Van Der Putte, I., J. Lubbers and Z. Kolar, "Effect of pH on Uptake, Tissue Distribution and Retention of Hexavalent Chromium in Rainbow Trout (*salmo gairdneri*)," *Aquat. Toxicol.*, 1, 3-18 (1981).
56. Vaughan, B.E., K.H. Abel, D.A. Cataldo, J.M. Hales, C.E. Hane, L.A. Rancitelli, R.C. Roufson, R.E. Wildung and E.G. Wolf, "Review of Potential Impact on Health and Environmental Quality from Metals Entering the Environment as a Result of Coal Utilization," Battelle Energy Prog. Rpt., Pacific Northwest Laboratory (1975).
57. Winner, R.W., "Bioaccumulation and Toxicity of Copper as Affected by Interactions between Humic Acid and Water Hardness," *Water Res.*, 19, 449-55 (1985).
58. Wolnik, K.A., F.L. Fricke, S.G. Capar, M.W. Meyer, R.D. Satzger, E. Bonnin and C.M. Gaston, "Elements in Major Raw Agricultural Crops in the United States, 3. Cadmium, Lead and Eleven other Elements in Carrots, Field Corn, Onions, Rice, Spinach, and Tomatoes," *J. Agric. Food Chem.*, 33, 807-11 (1985).
59. Wolnik, K.A., F.L. Fricke, S.G. Capar, G.I. Braude, M.W. Meyer, R.D. Salzger and E. Bonnin, "Elements in Major Raw Agricultural Crops in the United States, 1. Cadmium and Lead in Lettuce, Peanuts, Potatoes, Soybeans, Sweet Corn and Wheat," *J. Agric. Food Chem.*, 31, 1240-49 (1983).
60. Yang, G., S. Wang, R. Zhov and S. Sun, "Endemic Selenium Intoxication of Humans in China," *Am. J. Clinical Nutrition*, 37, 872-81 (1983).

4.7 SOME USEFUL SOURCES

In addition to the sources listed above, the following will also be found useful for background information:

61. Cardwell, R.D., R. Purdy and R.C. Bahner (eds.), *Aquatic Toxicology and Hazard Assessment: Seventh Symposium*, Report No. STP 854, American Society for Testing and Materials, Philadelphia, PA (1985).
62. Solomons, W. and U. Forstner, *Metals in the Hydrocycle*, Springer-Verlag, New York (1984).

Particularly useful sources for *assessment approaches* are given in references 2, 28 and 61.

Particularly useful sources of *data* are references 13, 17, 18, 20, 28, 58 and 59.

5. MATHEMATICAL ENVIRONMENTAL FATE MODELING

Marc Bonazountas, Aviva Brecher, Robert G. Vranka

	Page
5.1 INTRODUCTION	5.1-1
5.2 BACKGROUND	
5.2.1 Legal/Regulatory Issues	5.2-1
5.2.2 General Concept and Pathways	5.2-2
- Information Requirements	5.2-2
- Entry and Dynamics of Chemicals in the Environment	5.2-4
- Pathways of Pollutants	5.2-6
5.2.3 Routes of Environmental Interactions and Properties	5.2-8
- Volatilization	5.2-8
- Solubility	5.2-10
- Fast Reaction in Aqueous Media	5.2-10
- Slower Reaction in Aqueous Media	5.2-11
- Speciation	5.2-11
- Soil and Sediment Interactions	5.2-11
- Bioaccumulation	5.2-12
- Terrestrial Plants	5.2-12
5.2.4 Literature Cited	5.2-12
5.3 AIR MODELING	
5.3.1 Background	5.3-1
5.3.2 Types of Pollutant Sources	5.3-2
- Point Sources	5.3-2
- Area Sources	5.3-2
- Line Sources	5.3-3
5.3.3 Physical and Chemical Factors/Problems	5.3-3
5.3.4 Modeling Issues/Approaches, Input	5.3-3
5.3.5 Survey of Air Models	5.3-7
5.3.6 Model Application	5.3-7
5.3.7 Literature Cited	5.3-10
5.4 TERRESTRIAL MODELING	
5.4.1 Introduction	5.4-1
5.4.2 Background	5.4-1
5.4.3 Principal Processes	5.4-2
5.4.4 Models	5.4-2
5.4.5 Speciation Codes/Models	5.4-6
5.4.6 Model Applications	5.4-12

5.4.7	Example of Model Application	5.4-12
-	Statement of Problem	5.4-13
-	Field Monitoring	5.4-13
-	Model Application	5.4-13
-	Discussion of Findings	5.4-15
5.4.8	Literature Cited	5.4-19
5.5	AQUATIC MODELING	
5.5.1	Background	5.5-1
5.5.2	Modeling Issues	5.5-2
5.5.3	Modeling Limitations	5.5-3
5.5.4	Model Codes	5.5-5
-	REDEQL2	5.5-5
-	WATEQ2	5.5-8
-	MINEQL	5.5-9
-	MEXAMS	5.5-9
5.5.5	Availability/Suitability of Codes	5.5-10
5.5.6	Data Availability for Models	5.5-11
5.5.7	Issues Related to Modeling	5.5-11
-	Total Concentration of Metals and Ligands	5.5-11
-	Stability Constants	5.5-12
-	Ionic Strength	5.5-12
-	pH	5.5-13
-	pe	5.5-13
-	Suspended Solids	5.5-13
-	Organic Species	5.5-14
5.5.8	Model Applications	5.5-16
-	Modeling of Laboratory and Natural Water	5.5-16
-	Other Uses of Equilibrium Models	5.5-18
5.5.9	Example of Model Application	5.5-19
-	Problem Statement	5.5-19
-	Field Monitoring	5.5-19
-	Model Application	5.5-19
-	Discussion of Results	5.5-21
5.5.10	Conclusions	5.5-21
5.5.11	Literature Cited	5.5-24
5.6	RADIOMUCLIDE MIGRATION MODELING	
5.6.1	Introduction	5.6-1
5.6.2	Principal Processes	5.6-1
5.6.3	Radionuclide Codes	5.6-4
5.6.4	Model Applications	5.6-4
5.6.5	Literature Cited	5.6-9

LIST OF TABLES

AIR MODELING

5.3-1	Features of Selected Air Quality Models	5.3-8
-------	---	-------

TERRESTRIAL MODELLING

5.4-1	Some Well-documented Pollutant Fate Models and Their Features	5.4-5
5.4-2	Summary of Geochemical Code Capability, Adaptability Availability	5.4-9
5.4-3	Advantages and Disadvantages of Chemical Speciation Models	5.4-11
5.4-4	Chemical Composition of Soil Solutions From Untreated and Sludge-Treated Soils	5.4-14
5.4-5	Effect of Excluding Organic Ligands from Consideration by GEOCHEM on the Percentage of Free Metals in Soil Solution	5.4-16
5.4-6	Concentration and Speciation of Mn, Cu, and Ni in the Soil Solution as Affected by Rate and Frequency of Sludge Application	5.4-17
5.4-7	Concentration and Speciation of Zn and Cd in the Soil Solution as Affected by Sludge Rate and Frequency of Application	5.4-18

AQUATIC MODELING

5.5-1	Descriptive Features of REDELQ2, WATEQL, MINEQL and MEXAMS	5.5-6
5.5-2	Calculated Distribution of 18 Metals and 12 Ligands in Lake Superior Water	5.5-17
5.5-3	Trace Metals in JWPCP Sewage Outfall	5.5-20
5.5-4	Metal Distribution Among Various Species in Three Equilibrium Models of JWPCP Sewage	5.5-22

RADIONUCLIDE MIGRATION MODELING

5.6-1	Synopsis of Selected Radionuclide Transport Models for Nuclear Waste Repository Performance Assessment	5.6-2
5.6-2	Selected Radionuclide Migration Models	5.6-5
5.6-3	SWENT Model Validation Studies	5.6-8

LIST OF FIGURES

BACKGROUND

5.2-1	Schematic for Environmental Modeling	5.2-3
5.2-2	Environmental Pathways Chart	5.2-7
5.2-3	Important Mechanisms of Environmental Interactions of Inorganic Materials	5.2-9

AIR MODELING

5.3-1	Typical Plume Behavior and Ground-Level Concentrations in a Neutrally Stratified Atmosphere	5.3-4
5.3-2	Schematic of a Standard Gaussian Plume, Showing Plume Rise and Vertical and Crosswind Diffusion Patterns	5.3-5

TERRESTRIAL MODELLING

5.4-1	Schematic of Phases in a Soil System	5.4-3
5.4-2	Principal Controls on Free Trace Metal Concentrations in Soil Solutions	5.4-4
5.4-3	Evolution of Geochemical Codes	5.4-7

AQUATIC MODELING

5.5-1	Metal Solids as a Function of Dilution and Oxidation	5.5-23
--------------	---	---------------

5. MATHEMATICAL ENVIRONMENTAL FATE MODELING

5.1 INTRODUCTION

This chapter can be read as a separate document; it describes concepts, uses, and limitations of state-of-the-art mathematical environmental pollutant fate modeling for use in both environmental studies and analyses of environmental quality or human exposure.

The purpose of this chapter is to help readers understand modeling complexities, identify specific modeling packages, and select a documented mathematical model.

The text that follows is divided into five major sections:

- **Background (Section 5.2),**
- **Air Modeling (Section 5.3),**
- **Terrestrial Modeling (Section 5.4),**
- **Aquatic Modeling (Section 5.5), and**
- **Radionuclide Modeling (Section 5.6).**

The models have been categorized on the basis of the types of environmental systems they include, *not* the environmental processes involved. Aquatic and terrestrial models differ significantly in the data base (minerals considered) and mode of transport.

Each section of this chapter is fairly self-contained; it includes an introduction, a discussion of key physical and chemical issues related to each modeling category, a discussion of important environmental interactions of inorganic pollutants with the specific environment, an outline of model requirements for input data and model applications, and examples of model applications. References for each modeling category are presented at the end of the subsection for that category.

Readers of this chapter who are not familiar with a particular modeling category should first read section 5.2 and then the relevant section of this chapter (e.g., Terrestrial Modeling). The Background (section 5.2) not only refers to other chapters but also summarizes information on the use of models, general modeling concepts (e.g., multimedia modeling), pathways of pollutants in the environment, exposure assessments, states of inorganic materials, and environmental interactions and properties of materials in modeling. This information is important to a better understanding of modeling concepts, features and models, as well as the power and limitations of environmental models presented in the subsequent sections.

5.2 BACKGROUND

5.2.1 Legal/Regulatory Issues

Models are applied in a variety of ways to assist in decision-making and will be used to a greater extent in the future. Specific statutes or regulations require the use of models in certain situations. Additionally, provisions of the National Environmental Policy Act of 1969 (NEPA), as well as judicial decisions implementing NEPA and other environmental statutes, should facilitate the increased use of mathematical models [3].

There are a number of reasons for the increasingly widespread involvement of mathematical and computer models in environmental decisions. For example, Congress mandated the employment of computer models in the 1977 amendments to the Clean Air Act. Under the 1977 Amendments, models must be used in connection with the Prevention of Significant Deterioration (PSD) of air quality and for designation of nonattainment areas. Under the PSD program enacted in the 1977 Amendments, a major emitting facility in an area subject to PSD regulations must obtain a permit prior to commencing construction; this must be preceded by an analysis of air quality impacts projected for the area as a result of growth associated with such facility. The analysis must be based on air quality models specified by regulations promulgated by EPA. The 1977 Amendments also require conferences on air quality modeling every three years, to ensure that air quality models used in the PSD program reflect the current state-of-the-art in modeling [3].

The increasing use of quantitative models, particularly computer models, has placed a new burden upon the courts in their review of environmental decisions based on those models. This burden is a part of the "new era" in environmental decision-making and reflects the increasing involvement of scientific and technical issues in legal decisions. Problems in judicial review arising from the use of computer models and other quantitative methodologies in environmental decision-making are described by Case [3], whose publication is the source of a considerable amount of the information presented here.

The problems arising from the use of an environmental model in regulatory practice are twofold: first, it may actually increase the likelihood that a substantively incorrect decision will be reached. This greater probability of error generally can be traced to the inability of environmental decision-makers to deal with certain aspects of modeling in making such decisions. Second, the use of a model increases the danger that wrong environmental decisions may not be detected and corrected by the reviewing courts. Additionally, certain institutional aspects of the environmental agencies, the courts, and their mutual relationship further contribute to the difficulties of judicial review in cases relying on environmental models. Such institutional problems include the self-perceived lack of scientific expertise on the part of judges, the lack of judicial access to technical resources to assist in analyzing the issues involved, the limits on the court's ability to supplement or go outside the record, and the traditional deference that the courts give to administrative decisions.

Nevertheless, model development and application will increase in the future. Beyond any legal mandates, increasingly complicated and intractable environmental problems will compel the greater use of quantitative models by environmental decision-makers. Many experts believe in environmental fate, exposure and risk modeling, since models contribute to the scientific understanding of environmental quality. (See, for example, Swann and Eschenroeder [4].)

5.2.2 General Concepts and Pathways

INFORMATION REQUIREMENTS

Environmental pathway analysis provides the link between quantification of source emissions and assessments of receptor exposure (e.g., human exposure) through estimation of the ambient concentrations of contaminants in the various environmental media. A successful mathematical modeling effort must quantify fairly accurately the relationship between chemical releases into the environment and actual amounts of these chemicals to which the air, soil and water, as well as humans and other biota, are exposed.

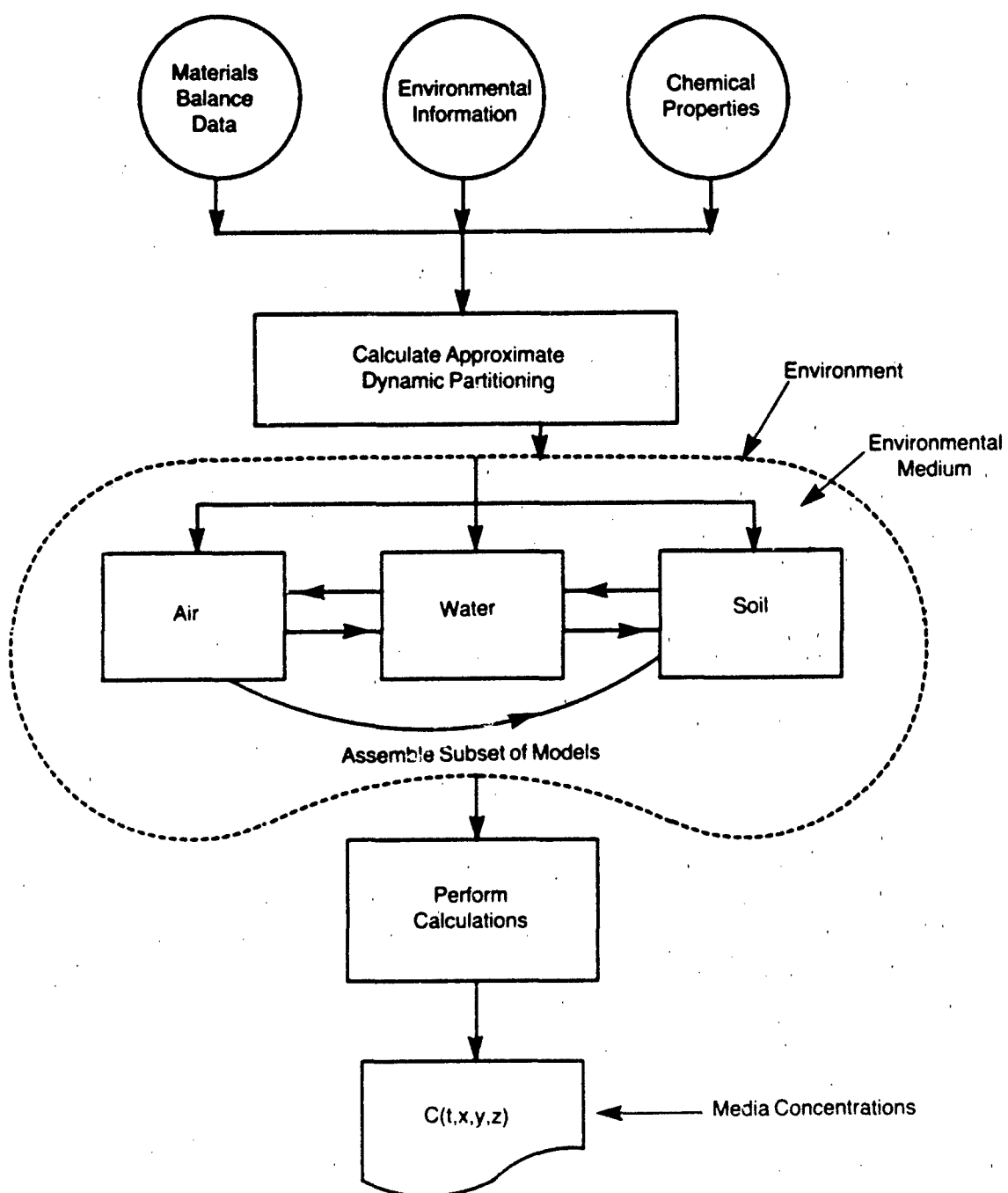
Whether the concern is for human health or environmental impact, concentrations of the chemical compounds at user-specified receptors or media of concern must be estimated. This estimation is designated as "mathematical environmental fate modeling."

Mathematical environmental fate modeling generally requires a knowledge of (1) the distribution of the releases of the material into the natural environment, (2) the environmental conditions influencing the fate (transport, transformation) of the chemical compounds, (3) the physical and chemical properties of the material, and (4) techniques (models) for analyzing the information gathered, as schematically shown in Figure 5.2-1.

Two basic techniques can be employed to investigate environmental pathways: analytic sampling programs and mathematical fate modeling. Sampling programs are costly to design and implement; therefore, computerized mathematical models of environmental processes are frequently used to generate information unavailable by other means, or to estimate data (i.e., environmental concentrations) that would otherwise be costly to obtain.

Optimal use of environmental mathematical models necessitates knowledge of the following:

- Entry and dynamics of chemicals in the environment,
- Potential pathways of pollutants,
- Exposure pathways when confronted with human and biotic exposure,
- Mathematical modeling concepts, and
- Model application, input data, monitoring and validation issues.



Source: Bonazountas and Fiksel [2]

FIGURE 5.2-1 Schematic for Environmental Modeling

ENTRY AND DYNAMICS OF CHEMICALS IN THE ENVIRONMENT

When identifying pathways and, hence, choosing models, we must consider what becomes of the pollutant as it enters the environmental media. Within any medium, three types of process (defined here as intramedia processes) govern the pollutant concentration at each point at any given time:

- *Advection* — pollutant mass movement in the medium carrying the pollutant.
- *Diffusion* — movement or spread of the pollutant, relative to the mass of the medium, and as driven by molecular or turbulence-scale dynamics.
- *Transformation* — production or consumption of the pollutant, usually driven by chemical reactions in the medium.

Superimposed on these mechanisms of change operating in the bulk volume of each medium are processes that transfer the pollutant from one medium to another. These processes are called "intermedia transfers" and, as such, are distinguished from transformation processes. (Some conceptual model frameworks lump intermedia transfers with embedded transformation processes.)

Examples of intermedia pollutant transfers are as follows:

- *Surface deposition* — rainout (liquid \rightarrow solid), washout, fallout and dry deposition
- *Evaporation* — codistillation (liquid \rightarrow gas) or volatilization
- *Adsorption* — liquid (or gas) \rightarrow solid and *desorption* (solid \rightarrow liquid (or gas))

These processes are further discussed later in this chapter.

In locating and choosing a model, one can simplify fate assessment efforts by delineating (1) the source release patterns, and (2) the dominant dynamic processes as explained here. Taking the intramedia processes first, one can address model criteria by considering the ratio of characteristic times [2]. The advection time is the principal length scale of the domain, L, divided by the average flow speed, u:

$$t_a = L/u \quad (1)$$

Typically, L may be stream reach distance and u the flow velocity.

The diffusion time is approximated by the random walk hypothesis and is given by:

$$t_d = \Delta^2/2D \quad (2)$$

where Δ is the characteristic transverse direction (e.g., stream depth) and D is the transverse diffusivity, be it turbulent or molecular.

Finally, the transformation time is approximated by:

$$t_t \approx C/\Delta C_t \quad (3)$$

where ΔC_t is the average rate of concentration change due only to transformation (typically a chemical reaction rate) and C is the average concentration in the domain.

If $t_t \ll t_a$ and $t_t \ll t_d$, there is rapid chemical change before any movement occurs. If $t_t \gg t_a$ and $t_d \ll t_a$, there is little chemical change; diffusion spreads the pollutant rapidly, making the mixture homogeneous. If $t_t \approx t_d \approx t_a$, all processes act simultaneously. Taking these cases in order, we see that the first case does not require a model (except possibly a reacting plume in the near field), the second case is approximated by a non-reactive box model, and the third calls for a full reactive diffusion model.

Source geometry, interphase transfer and time dependencies must be superimposed on the above features. For example, the advection distances would be different for point and area sources. Also, the significance of source location must be considered in light of interphase transfer efficiency. For example, a water discharge containing a pollutant of high volatility and low solubility transfers the problem immediately from one of water modeling to one of air modeling. Implicit in these environmental dynamic considerations are three general principles:

- Intramedia processes are largely assessed on the basis of environmental scenarios.
- Intermedia transfers are largely determined by the pollutant's fate properties.
- Chemical transformations can be involved in both of the above.

There are, of course, exceptions to these rules. For example, molecular diffusivity is a pollutant fate property but may control an intramedia process; similarly, rainfall history is an environmental scenario characteristic but may control an intermedia transfer.

An experienced model user can do a simplified systems-level analysis prior to model selection, based on entry characteristics and environmental dynamics of the pollutant. Experienced analysts would advise that it is better to rely on intuition and a few calculations than to construct a formal, logical decision tree for guiding this process. Inexperienced scientists must analyze source characteristics, environmental dynamics, and pollutant fate properties more carefully before proceeding with model selection and application.

There are no specific rules or procedures for approaching model selection based on entry characteristics and environmental dynamics of the pollutant. The only criteria are the model features described in the user's manual, but these are often not objectively reported. Characterization of the sources, the environment and the fate properties is prerequisite to any such procedure.

PATHWAYS OF POLLUTANTS

The two major stages of an environmental modeling pathway analysis are:

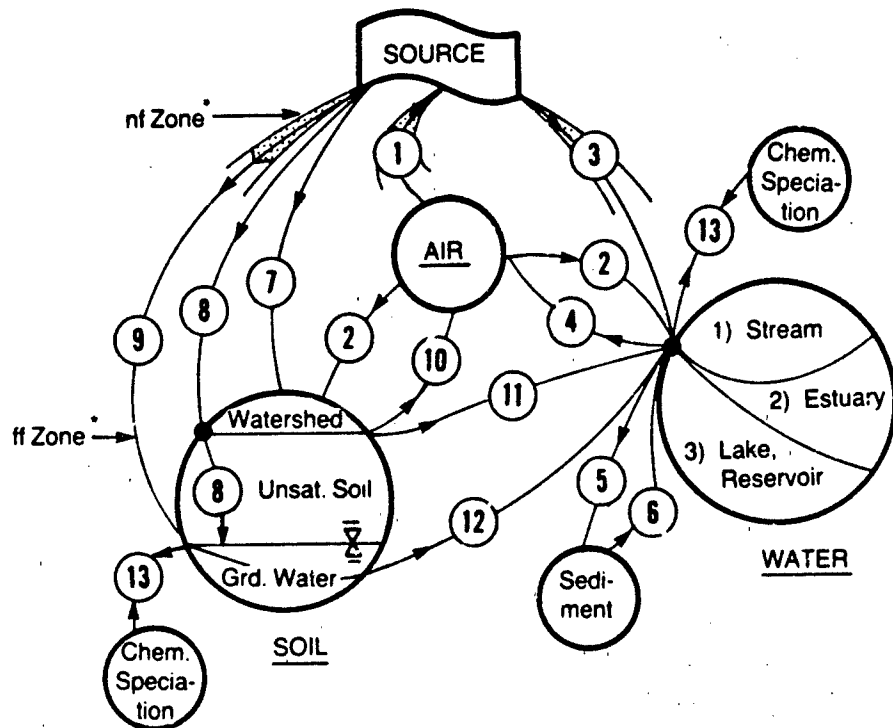
- (I) Examination of background information relevant to the environment; and
- (II) The quantitative analysis.

Stage I may amplify an initial "scan" effort to identify key factors, such as monitoring data evaluations and geographic setting evaluation, that may indicate which media (air, soil, water) must be modeled, and which pathways and media are likely to be of secondary importance. Principally, Stage I aims at (a) identifying potential (probable) pathways of species, (b) evaluating available data on the specific region or site, (c) identifying what receptors in the area might be affected or are of importance for further consideration, and (d) identifying candidate models for estimating media concentrations.

Stage II, the quantitative analysis, involves (a) collection of monitoring and other site data, (b) prioritization of the important pathways, (c) selection of models to simulate these pathways, (d) compilation of input data for the models, (e) performance of the simulations, (f) analysis of model output/results, (g) output validation (using monitoring data) whenever feasible, and (h) design and/or evaluation of control strategies (future actions) for environmental protection which may involve additional model runs.

By carefully considering the fate properties and potential receptor effects during Stage I, the user will gain an understanding of the critical environmental pathways, enabling him to establish priorities for Stage II. For example, for a chemical whose main effect is toxicity to benthic organisms, the pathway leading from the source through the air into the water and to the receptor provides the logic for selecting a model that considers the relevant pathways. Considering relative contributions of multiple release modes, amounts or dominant fate properties, certain pathways will be preferred to others among the rather large array of possible combinations. Flow charts or diagrams are useful tools for identifying and establishing the pathway connections between sources and receptors and thereby defining fate modeling approaches.

Figure 5.2-2 is a typical environmental pathway chart designed for a regional pollutant fate modeling application [2]. It shows the three major environmental media — air, soil and water — and the intermedia and intramedia pathways of pollutants originating from a source (point, area, line, other). In reference to this chart, section 5.3 describes models and pathways relevant to the air compartment of the chart, section 5.4 describes models relevant to the terrestrial (soil) compartment, section 5.5 describes models and pathways related to the aquatic (water) compartment, and section 5.6 describes radionuclide models that are related to all compartments.



Notes

- Paths 1,3,9 have near-field (nf) and far-field (ff) zones
- Degradation, transformation, and out-of-basin transfer pathways are not shown in this chart.

- #1: Source-to-Air
- #2: Air-to-Surface (i.e., wet/dry depositions)
- #3: Source-to-Water (stream, estuary, lake/reservoir; nf, ff models; overall water quality; pollutant-specific models)
- #4: Water-to-Air (e.g., volatilization, codistillation; pollutant-specific models)
- #5: Water-to-Sediment (e.g., adsorption, diffusion; pollutant-specific models)
- #6: Sediment-to-Water (e.g., desorption, dissolution, dispersion; pollutant-specific models)
- #7: Not a real pathway; rather, pollutant input modes to watershed soil models
- #8: Source-to-Soil-to-Groundwater
- #9: Source-to-Groundwater (nf, ff models)
- #10: Land-to-Air (e.g., volatilization, dust pollutant particle resuspension)
- #11: Land-to-Water (e.g., via runoff or sedimentation)
- #12: Groundwater-to-Water (e.g., via advection, diffusion)
- #13: Aquatic Equilibria (or chemical speciation for water or soil)

Source: Bonazountas and Fiksel [2]

FIGURE 5.2-2 Environmental Pathways Chart**

Figure 5.2-2 shows, for example, that a model user can proceed to either (a) separately consider each medium and select the appropriate calculation technique or model that characterizes the behavior in a medium (e.g., air), or (b) consider transfer mechanisms to other media (e.g., water via deposition) from that medium. Experience is a key factor in selecting the appropriate time and space scales for the modeling task. Preliminary half-life estimates for transfer and transformation processes and a comparison among them can provide initial indication of which fate properties are important to consider. A possible outcome is that chemical transformations or dilution may effectively terminate the pathway within a specific medium.

Aravamudan *et al.* [1] present five hypothetical examples that illustrate the thinking required to analyze and model the fate of chemicals in multimedia environments. In this chapter, however, we shall deal with modeling issues and models of only the three single medium environments of air, soil, and water and their major interactions with the adjacent environments via key processes (e.g., soil-air *via* volatilization).

5.2.3 Routes of Environmental Interaction and Properties

This section describes important routes of environmental interactions and characteristics of inorganic species with regard to these interactions. This discussion is aimed at summarizing important information about mathematical modeling, processes considered by models, and the input parameters required.

The various paths and interactions are shown schematically in Figure 5.2-3. Major mechanisms discussed below are: volatilization, solubility, fast aqueous reactions, slow aqueous reactions, speciation, soil interaction, and bioaccumulation.

VOLATILIZATION

The evaporative loss of a chemical (volatilization) depends upon the vapor pressure of the chemical and on environmental conditions that influence diffusion from a surface. Volatilization is an important source of material for airborne transport and may lead to the distribution of a chemical over wide areas far removed from the point of release. Vapor pressure values indicate the tendency of pure materials to vaporize in an unperturbed situation. Vapor pressure data combined with solubility or, more precisely, activity coefficient data permit estimation of rates of evaporation of dissolved species from water, using Henry's Law constants and other parameters.

Chemicals with relatively low vapor pressure, high adsorptivity onto solids, or high solubility are less likely to volatilize and become airborne. However, many chemicals with very low vapor pressures can volatilize at surprisingly high rates, because of their low solubilities in water (i.e., high activity coefficients) or low adsorptivity to solids.

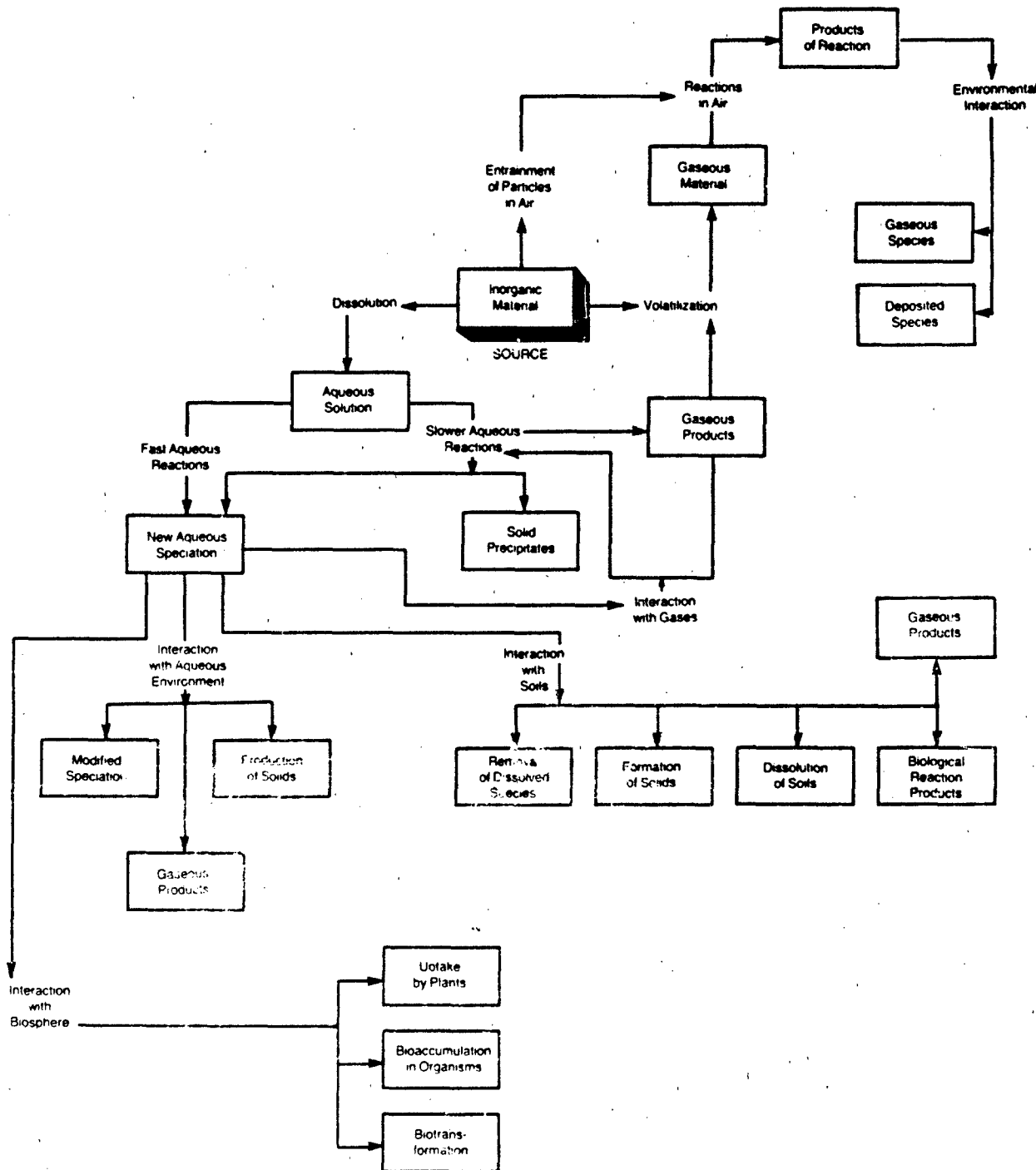


FIGURE 5.2-3 Important Mechanisms of Environmental Interactions of Inorganic Materials

SOLUBILITY

The equilibrium relationships for dissolution and dissociation of inorganic salts in aqueous solution, and other reactions, govern the chemical solubility. Solubility product constants for many species are tabulated in the literature; those that are not available may be calculated from Gibbs free energies of formation (which are tabulated in the literature) as described in section 2.11.

The aqueous solubility of a salt in the presence of a common ion (i.e., one of the ions into which the salt dissociates) may be either depressed or increased. An increase can occur when a charged complex is formed from a neutral complex by additional association, i.e., complexation (e.g., $\text{AgCl} + \text{Cl}^- \rightarrow \text{AgCl}_2^-$). When this process is not favored, the common ion effect suppresses solubility, as when sodium sulfate is dissolved in a saturated solution of calcium sulfate, causing the latter to precipitate. Complexes can also form between cations and other species (ligands). The extent to which metals form complexes varies significantly; alkali and alkaline earth metals form very weak complexes (i.e., ion pairs), while other metals can form highly stable complexes (e.g., copper ammonia complexes).

The effect of complexation (see section 2.9) on solubility can be taken into account mathematically by employing a series of equilibrium relationships written in terms of complexation equilibrium constants (stability constants). The above factors are frequently taken into account by mathematical modeling packages.

FAST REACTIONS IN AQUEOUS MEDIA

Fast reactions of inorganic dissolved species in aqueous media can be classified under the following general categories:

- Reactions with dissociation (of solvent molecules)
- Substitution reactions (with solvent or dissolved species)
- Redox reactions (with dissolved gases or other ions)

These reactions can lead to formation of new complex ions (those with different ligands in the coordination sphere and those with different oxidation state of the metal centers) and/or other ions. For details, the reader is referred to appropriate sections of Chapters 2 and 3.

The fast reactions of metal-containing species are important, because the medium in which the particular inorganic substance is dissolved largely determines the speciation of the particular metal ion. Since the extent of environmental interaction (e.g., soil attenuation, uptake by plants, toxicity) will depend on the chemical form (species) of the metal, knowledge of the behavior with regard to rapid reactions is essential.

In addition, when solutions of these metal-containing species are mixed with the environment (e.g., when leachate mixes with groundwater), chemical modification of the species will occur initially via thermodynamically favored rapid reactions and

subsequently by the possible slower reactions. Such knowledge is important when selecting and applying the aqueous equilibria or speciation models described in section 5.5.5.

SLOWER REACTIONS IN AQUEOUS MEDIA

In the category of slower reactions in aqueous media, one may consider the following:

- Ligand substitution reactions of kinetically rather inert ions;
- Electron transfer reactions (e.g., inner-sphere mechanisms for kinetically inert ions and some outer-sphere reactions);
- Reactions with dissolved gaseous species (e.g., oxidation by dissolved oxygen, H₂S formed by bacterial reduction);
- Precipitation of solids by formation of insoluble species via substitution; and
- Oxidation reactions (e.g., formation of metal hydroxides and metal sulfides).

SPECIATION

These slower reactions affect the speciation and concentration of inorganic substances in the aqueous phase and determine the type and extent of further interactions in the same manner as the fast reactions, although they take place over a different time frame. (See Chapter 3.) For the relatively inert metal centers such as Co(III) and Cr(III), immediate modification of the speciation of the ion may *not* occur upon mixing with other aqueous phases; the reaction may not proceed until the mixture has reacted with soil components.

Thus, the time frame for some reactions may indicate that characterizing the speciation in the original aqueous phase (e.g., leachate) will dictate the chemical behavior of the compound with the environment. In other cases, it will be necessary to understand the speciation under the exact conditions of environmental interaction, such as adsorption. Information on chemical speciation is provided in sections 2.6-2.13.

SOIL AND SEDIMENT INTERACTIONS

Dissolved aqueous inorganic species interact with soils. The more important mechanisms of interaction include (a) formation of precipitates, (b) adsorption of components onto soil surfaces, (c) modification of speciation by soil constituents (solid and liquid phases), and (d) reactions induced by bacteria.

The surface properties of soil particles that dictate adsorption behavior can be modified by the acid/base buffer system in contact with the soil. (See section 2.12.) Most minerals display amphoteric properties toward solutions — i.e., they behave as weak acid or bases. The buffer capacity of soil, such as that related to its CaCO₃ content,

affects the potential of soil water pH to fluctuate. Microorganisms can cause important changes in the solubility of soil minerals and other precipitates by altering solution conditions and catalyzing reactions.

Conceptual models for the adsorption of species onto soils have been developed to incorporate factors such as electrostatic energy and chemical bonding effects (e.g., van der Waals, dipole effects and covalent bonding). In particular, Langmuir adsorption isotherms consistent with this conceptual model have been generated. As previously mentioned, solution chemical equilibria modify the adsorptive behavior of the soil as well as the species present in solution and their tendencies to be adsorbed; therefore, simplified adsorption, attenuation or speciation models must be used with caution. Supported computerized packages are preferable to the simpler models.

BIOACCUMULATION

Much information is available on the effects of individual inorganic constituents on a large variety of organisms in specific environments. However, such information has generally been difficult to use in developing techniques for the estimation of effects, and no such methods relating to the effect of inorganic compounds on organisms in aquatic or terrestrial environments have yet been developed. Chapter 4 discusses this subject further.

TERRESTRIAL PLANTS

If there are exceptions to the general lack of estimation techniques and models relating inorganic chemical concentrations, biological effects and fate, they are likely to be found in agricultural theory and modeling. The application of soil amendments (fertilizers) as macronutrients (e.g., phosphates, nitrates) or micronutrients (e.g., Mn), or for improving the soil chemical environment to release nutrients (liming), is a relatively well-developed science. At the least, there is an understanding of optimum ranges of concentrations of agriculturally related chemicals for the growth of crop species. This stands in contrast to the paucity of information regarding uptake of organic soil contaminants by plants.

5.2.4 Literature Cited

1. Aravanudan, K., M. Bonazountas, A. Eschenroeder, D. Gilbert, L. Nelken, K. Scow, R. Thomas, W. Tucker and C. Unger, *An Environmental Partitioning Model for Risk Assessment of Chemicals: Part 1. Narrative Descriptions of the Methodology*, Arthur D. Little, Inc. Report to U.S. Environmental Protection Agency, Office of Toxic Substances, Contract 68-01-0387 (1979).
2. Bonazountas, M. and J. Fiksel, "Environmental Mathematical Pollutant Fate Modeling Handbook Catalogue," Draft Report prepared for U.S. Environmental Protection Agency, Office of Policy and Resource Management, Washington, D.C. (1982).

3. Case, C.D., "Problems in Judicial Review Arising from the Use of Computer Models and Other Quantitative Methodologies in Environmental Decision Making," *Environ. Aff.*, 10, 251 (1983).
4. Swann, R.L. and A. Eschenroeder, *Fate of Chemicals in the Environment: Compartmental and Multimedia Models for Prediction*, ACS Symposium Series 225, American Chemical Society, Washington, D.C. (1983).

5.3 AIR MODELING

This section describes principles of air-quality modeling and summarizes well-documented or Government-approved computerized models. Information and references on relationships between ambient concentrations and emissions for assessing the health risks of airborne carcinogens are presented by Eschenroeder *et al.* [20]. General information on mathematical modeling packages is presented by Bonazountas and Fiksel [4], Drake and Laulainen [15], Bass and Benkley [3], the U.S. Environmental Protection Agency [41], Aravamudan *et al.* [1], and others.

5.3.1 Background

Atmospheric fate modeling generally considers the transport and diffusion of pollutants from sources to receptors by the air pathway. Receptors can be defined as locations at which exposure to pollutants can take place.

Atmospheric models characterize the dispersion and deposition of pollutants during transport [37]. Generally, the output of air quality models consists of air concentrations of pollutants of interest in time and space as well as the amount of material deposited on the earth's surface by wet and dry deposition processes. The time and space aspect of these quantities depends on the characteristics of the model and how it is applied.

Models for estimating exposure levels are used to predict short-term average (acute) and long-term average (chronic) exposure to air pollutants. They vary in complexity, required input data, and form of output. If the exposure to be determined includes contact with a pollutant through inhalation, average ambient concentrations over a given time at a receptor must be combined with the inhalation rate to give an integrated exposure level. Estimation of exposure to pollutants through dermal contact requires the ambient air concentration of the pollutant at the receptor along with the rate of deposition.

The selection of a model for a given application must consider the following:

- Definition of emissions with regard to the space and time in question;
- Wind flow patterns as a function of location, topography, urban influences, surface roughness and large-scale weather patterns;
- Physical processes and chemical reactions of pollutants as they are transported and dispersed in the atmosphere; and
- Transport of pollutants from other regions that create background levels for the region in question;
- Use of data bases that are sufficient to calibrate a model and validate it for predictive purposes.

Present atmospheric models range from simple empirical kinds to very complex, time-dependent ones [18]. Simple empirical models are based on a deterministic analysis of

air quality, emissions and meteorological data [10,12]. Time-dependent models are derived from basic physical and chemical principles related to the processes of transport, diffusion, chemical transformation and removal [24,35]. Some semi-empirical models, an intermediate class, share the simplicity of empirical models but approach the predictive ability of complex, time-dependent models [28,40]; such models, which are based on the Gaussian plume approach, are considered in greater detail in this review.

Semi-empirical models provide sufficient flexibility to address exposure to inorganic pollutants in the atmosphere. Some that differ with source emission type, geographic extent and averaging time are included in the list of approved models of the EPA Users Network of Applied Models for Air Pollution (UNAMAP) [42]. Details on the use of a given model in the UNAMAP series are given in the related user's manual. Information on several of these models is reported in section 5.3.4.

5.3.2 Types of Pollutant Sources

A number of different types of pollutant sources may have to be analyzed when atmospheric pollutant concentrations and human exposure levels are calculated. A model can be selected on the basis of the type of source and receptor to be considered. Generally, the calculation of exposure levels must consider point, area and line sources, as described below.

POINT SOURCES

Point sources are the most commonly encountered release modes in air quality assessments. For an exhaust stack, the following specifications are required: stack height, gas exit velocity, exhaust temperature and emission rate of each pollutant [11,21,38,40]. Many of these parameters can be measured or can be estimated from data on a similar stack.

Emission rates can also be calculated by using either a mass balance approach or emission factors related to the process being modeled. For complex industrial facilities, a number of stacks may have to be considered. As a simple worst-case screening approach, these multiple sources can be treated either as (1) a single source, with all of the emissions assumed to originate from one stack, or (2) individually, with the relative location of each source being included in the modeling analysis [23]. Complex sources may also include low stacks and roof-top vents from which pollutants can be entrained in building wakes before being transported downwind. For some analyses, these emission characteristics must be specified, and models used to simulate their unique transport mechanisms.

AREA SOURCES

When emissions from a number of sources are spread more or less uniformly over a given area [16], a different characterization is required for modeling exposure assessment. This type of source would include emissions from residences or an

extended area of small industrial facilities. In this case, emissions are usually treated as uniform pollutant releases at a given height in units of mass per unit area. Models designed to simulate the transport of pollutants from an area source should be utilized [9,22,33,34,35].

LINE SOURCES

Transportation activities can produce a number of pollutants of concern. These releases can be treated as line sources for a given roadway; for combined roadways in a larger area, they can be treated as area sources. Emission rates are usually based on the number of vehicle miles traveled on the road segment that is modeled. Line source models should be used to characterize the transport and exposure to pollutants [8,32].

5.3.3 Physical and Chemical Factors/Problems

Transformation and removal mechanisms in the atmosphere must be considered [20] for many pollutants to appropriately characterize exposure levels. Depletion mechanisms in the atmosphere include photochemical reactions [14,31], wet deposition, dry deposition and gravitational settling.

Chemical reactions usually are treated as first-order decay with half-life terms [2,7]. Gravitational settling and deposition caused by washout or turbulent transfer to the surface can be simulated by specifying settling velocities, deposition velocities and scavenging ratios for the given pollutants [29,36,39]. A number of the models described below can simulate these processes.

5.3.4 Modeling Issues/Approaches, Input

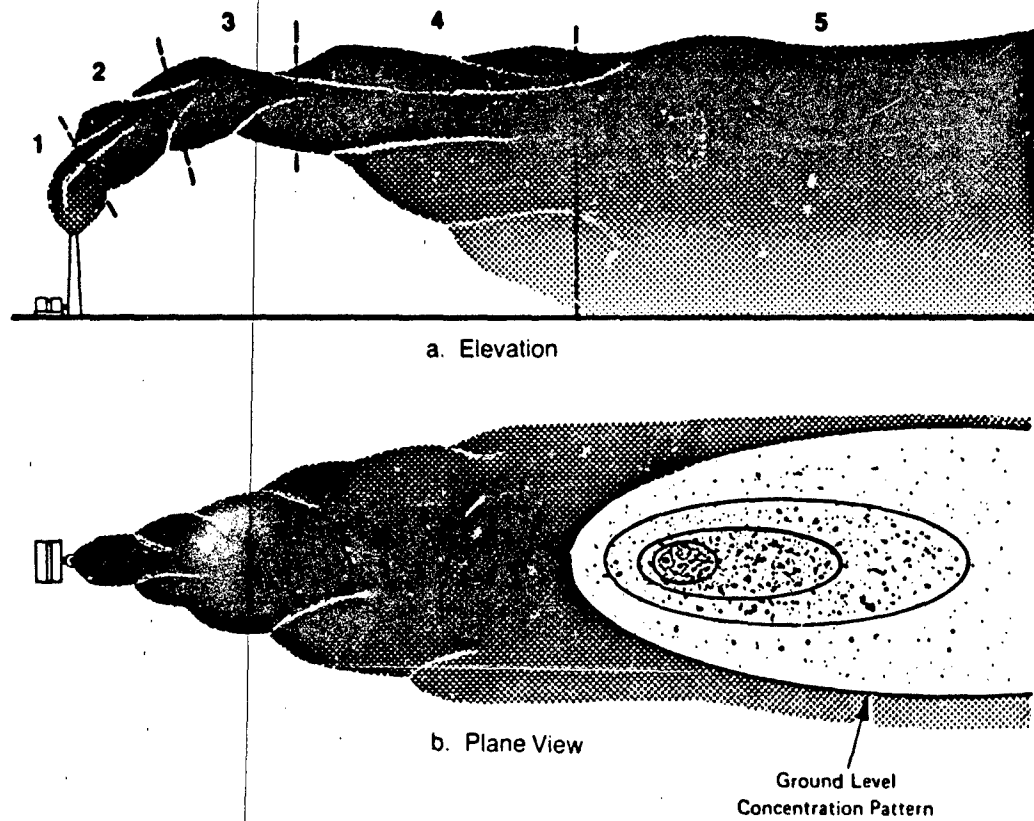
Since most models were formulated to study dispersion of stack exhausts, this section will focus on modeling this aspect. Five processes (steps) can be of importance in mathematical air modeling [13,18,19]:

- (1) Plume rise from the stack exit,
- (2) Atmospheric turbulence and dispersion mechanisms,
- (3) Chemical pollutant transformation,
- (4) Loss to surface by deposition or other mechanisms, and
- (5) Near-field dispersion versus far-field (long range) transport.

Current models and computer codes address these processes in varying degrees of completeness and detail; many do not treat one or more of these processes at all. A thorough discussion of the processes is given by Eschenroeder *et al.* [20], and Figure 5.3-1 illustrates where they occur in a typical plume.

The most used and most reliable atmospheric models involve the Gaussian plume concept (Figure 5.3-2), in which emissions and transport are assumed to be steady-state or pseudo steady-state. These models have the following properties:

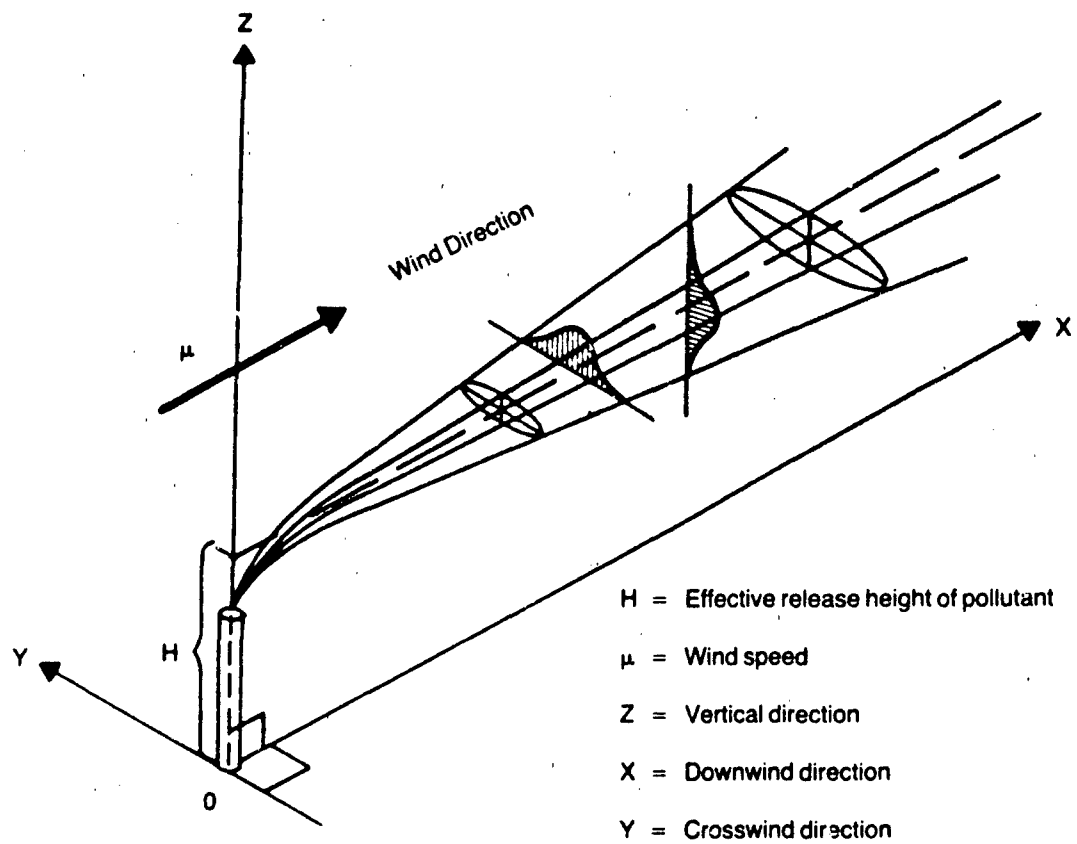
- Concentrations from a continuous, steady source vary in direct proportion to the source strength or rate of emission.



Source: Eschenroeder et al. [20]. (Copyright 1985, Electric Power Research Institute. Reprinted with permission.)

FIGURE 5.3-1 Typical Plume Behavior and Ground-level Concentrations in a Neutrally Stratified Atmosphere

- Concentrations vary inversely with the mean wind speed at the source.
- The distance from the source to the receptor and intensity of atmospheric turbulence determine the height and width of the plume at the receptor.
- Concentrations may decrease because of chemical reactions, radioactive decay and removal.
- Practical time scales are 1 to 2 hours, with adaptation for daily and monthly time averages; maximum space scales are 10 to 30 km.
- Extra provisions are made to account for complex terrain and different atmospheric stability conditions.



Source: Turner [40]

FIGURE 5.3-2 Schematic of a Standard Gaussian Plume, Showing Plume Rise and Vertical and Crosswind Diffusion Patterns

Dispersion models of this kind can provide reasonable estimates of exposure levels without great investment of time and money [2]. The basic equation for ground-level concentrations from an elevated point source is [40]:

$$X(x,y,z=0) = \frac{Q}{\pi\sigma_y\sigma_z\bar{\mu}} \exp\left[-\left(\frac{H^2}{2\sigma_z^2}\right) - \left(\frac{y^2}{2\sigma_y^2}\right)\right] \quad (4)$$

where
 X = atmospheric concentration (g/m^3)
 Q = pollutant release rate (g/s)
 σ_y, σ_z = crosswind and vertical plume concentration standard deviation (m)
 $\bar{\mu}$ = mean wind speed (m/s)
 H = effective release height of the pollutant (m)
 x, y = downwind and crosswind distances (m)
 z = vertical height (m)

Most of the models reported in a later section utilize equation 4 or derivatives of it to simulate transport and to calculate exposure levels. The parameters σ_y and σ_z can be obtained from plots of values given as a function of downwind distance from the source (x) and other parameters [40].

When using models, one must specify a number of parameters for the simulations. These parameters fall into the following three categories:

- *Meteorological Inputs:* To simulate the transport and diffusion of pollutants, an atmospheric model requires information on the meteorological variables that control these processes — wind direction, wind speed, and atmospheric stability (a parameter describing the extent of turbulence and changes in wind direction). These data, related to the specific simulation, are generally derived from measurements made at a site that is similar to the one being simulated.
- *Source Input Parameters:* In an evaluation of the exposure to a specific pollutant, the estimated emission rate or release rate can be the most critical but least known parameter. Information on emission rates for less common pollutants are generally not well documented; however, failure to properly characterize the release rate may result in large discrepancies between predicted and actual exposure levels. The most accurate data for point source emissions come from isokinetic stack sampling to measure the concentrations of gas and particulates.
Emission estimates based on empirical studies of comparable sources should be used with caution, because the conditions associated with the latter can be vastly different from those that apply to the studied source. Not only should release rates be properly characterized, but the time of day of a given release should be incorporated, because it can drastically affect the magnitude of a predicted exposure level.
- *Receptor Characteristics:* The locations of the key receptors relative to the sources to be evaluated must be specified when estimating exposure

levels. This includes specification of not only the horizontal distances and directions from the source but also the elevation of the receptors relative to the source. This is particularly important when evaluating exposure to pollutants in areas of hilly terrain. Certain models identified below have algorithms that can simulate pollutant transport in complex or hilly terrain.

The propagation of uncertainty is a major concern in air modeling estimates [30]. Consistent with the objective of assessing the accuracy of concentration estimates made by the model, it is necessary that explicit and rational treatment be given to the sources and propagation of uncertainty in those estimates. An analysis of uncertainty has been made by Eschenroeder *et al.* [20]. To the extent possible, this treatment employs standard methods of analysis of propagated error and divides the total propagated uncertainty into two components: (1) a model or method error contribution, originating from uncertainty in the algorithms and (2) errors due to uncertainty in one or more data inputs [20].

5.3.5 Survey of Air Models

The models contained in the UNAMAP Series address the wide variety of the problems identified above and have some of the analytical capabilities required to simulate pollutant transport phenomena for assessing human exposure levels. These models and their capabilities are identified in Table 5.3-1. A user's guide for each model can be obtained from the National Technical Information Service (NTIS). Typical minimum data required for using the models are: wind direction, wind speed, atmospheric stability, atmospheric mixing height data, ambient temperature, precipitation, stack characteristics, sources and receptors, terrain data, and pollutant data.

Each model identified in Table 5.3-1 can be modified to fulfill a specific, limited use. The differences between the models involve such terms as the spreading of plumes as a function of atmospheric stability [27,28], vertical mixing [26], plume rise [5,6], source configuration [25], terrain considerations [17], acute or chronic exposure, etc. Most of the models are quite different with regard to specific capabilities, and for almost any need one can find an appropriate model.

5.3.6 Model Application

A typical screening approach for evaluating peak ground-level concentrations resulting from stack emissions would include the use of the model PTPLU. This model of the EPA-UNAMAP series can calculate the maximum ground-level concentrations under a number of meteorological conditions. For a given stack with identified operating parameters, the model will cycle through a number of combinations of wind speeds and atmospheric stabilities. It will identify the maximum concentration for each wind speed/stability category and indicate the downwind distance from the stack to where the maximum occurs. The model's output covers the typical range of meteorological conditions, and it indicates the expected short-term (up to one hour) average acute exposure levels that a receptor may encounter.

TABLE 5.3-1

Features of Selected Air Quality Models

MODEL FUNCTION	APPAC-1	CDM	CRASTER	HIGHWAY-2	ISC	MPTER	PAL	PTM3	PTPLU	RAM	TCM	TEM	VALLEY	WALL	COMPLEX
Point Source	•	•	•	•	•	•	•	•	•	•	•	•	•	•	•
Area Source	•	•	•	•	•	•	•	•	•	•	•	•	•	•	•
Line Source															
Volume Source															
Short-Term	•	•	•	•	•	•	•	•	•	•	•	•	•	•	•
Long-Term															
Plume Trapping	•	•	•	•	•	•	•	•	•	•	•	•	•	•	•
Half-Life															
Gravitational Settling															
Aerodynamic Effects															
Buoyant Plume Rise															
Momentum Plume Rise															
Stack Downwash															
Turbulent Deposition															
Terrain Adjustment															
Complex Terrain															
Calibration	•														
Urban/Rural Dispersion															
Coefficient ^a	U	U	•	•	•	•	•	•	•	•	•	•	•	•	•
Background Calculated															
Street Canyon Flows															
Wind Speed Extrapolation															
Highway Generated															
Turbulence															
Emission Rates Function															
of Met. Conditions															
Emission Rate Function															
of Time of Day															

(Continued)

TABLE 5.3-1(Continued)

MODEL FUNCTION	Buoyancy Induced Dispersion	σ_y Function of Averaging	Time and Stability	Inversion Penetration	Factors	Particle Resuspension	Washout
APRAC-1	No. of Sources (Max.) ^d	1200	200 P	19	24	100 ^b	250
CDM	No. of Receptors (Max.)	2500 ^a	Un-limited	400 ^b	180	180	(PTMTP)
CSTER		625	Un-limited	50	30	25	100 A
HIGHWAY-2						(PTMTP)	300 P
ISCC						150	50 A
MPTER						2500	250
PAL						112	180
PTMAX							
PTDIS							
PTPLU							
RAM							
TECM							
VALLEY							
COMPLEX							

a. U = Urban Only, R = Rural Only

b. The maximum number of sources and receptors are interrelated: These values are reasonable estimates.

c. These capabilities are available on a version which is not part of the UNAMAP series of models.

d. P = Point, A = Area

Source: Bonazontas and Fiksel [4]

This screening analysis is useful for quickly estimating peak short-term average levels, and it can be used to determine whether a problem may exist. It generally is geared to calculate a conservative worst case. More accurate levels can be determined by using other models that utilize site-specific meteorological data and can better simulate atmospheric reactivity and atmospheric transport mechanisms such as gravitational settling, deposition and washout.

5.3.7 Literature Cited

1. Aravamudan, K., M. Bonazountas, A. Eschenroeder, D. Gilbert, L. Nelken, K. Scow, R. Thomas, W. Tucker and C. Unger, *An Environmental Partitioning Model for Risk Assessment of Chemicals: Part 1. Narrative Descriptions of the Methodology*, Arthur D. Little, Inc. Report to U.S. Environmental Protection Agency, Office of Toxic Substances, Contract 68-01-0387 (1979).
2. *Air Quality Display Model*, TRW Systems Group Manual for NAPCA, HEW, Contract No. PH-22-68-60, Washington, D.C. (1969).
3. Bass, A. and C.W. Benkley, *Development of Mesoscale Air Quality Models: Vol. 2, User's Guide to MESOPLUME (Mesoscale Plume Segment) Model*, EPA-600/7-80-059, U.S. Environmental Protection Agency, Research Triangle Park, N.C. (1980).
4. Bonazountas, M. and J. Fiksel, "Environmental Mathematical Pollutant Fate Modeling Handbook/Catalogue," draft report prepared for the U.S. Environmental Protection Agency, Office of Policy and Resource Management, Washington, D.C. (1982).
5. Briggs, G.A., "Plume Rise," USAEC Critical Review Series, TID-25075, Clearinghouse for Fed. Sci. and Tech. Info. (1969).
6. Briggs, G.A., "Plume Rise Predictions," Lectures on Air Pollution and Environmental Impact Analysis, American Meteorological Society, Boston (1975), pp. 59-111.
7. Busse, A.D. and J.R. Zimmerman, *User's Guide for the Climatological Dispersion Model*, U.S. Environmental Protection Agency, EPA-R4-73-024, Research Triangle Park, N.C. (1973).
8. Calder, K.L., "On Estimating Air Pollution Concentrations from a Highway in an Oblique Wind," *Atmos. Environ.*, 7, 863-68 (1973).
9. Calder, K.L., "Multiple-Source Plume Models of Urban Air Pollution — Their General Structure," *Atmos. Environ.*, 11, 403-14 (1977).
10. Calder, K.L. and W.S. Meisel, "Source-oriented Empirical Air Quality Models," *Proc. Conf. Environ. Modeling and Simulation*, Cincinnati, April 19-22, 1976 (1976).
11. Carson, J.E. and H. Moses, "The Validity of Several Plume Rise Formulas," *J. Air Pollut. Control Assoc.*, 19, 862-66 (1969).
12. Chang, T.Y. and B. Weinstock, "Generalized Rollback Modeling for Urban Air Pollution Control," *J. Air Pollut. Control Assoc.*, 25, 1033-37 (1975).

13. Committee on Atmospheric Turbulence and Diffusion, "Accuracy of Dispersion Models," *Bull. Am. Meteorol. Soc.*, **59**, 1025-26 (1978).
14. Demerjian, K.L., A.J. Kerr and J.G. Calvet, "The Mechanism of Photochemical Smog Formation," in *Advances in Environmental Science and Technology*, J.N. Pots and R.L. Metcalf (eds.), John Wiley & Sons, New York (1974).
15. Drake, R.L. and N.S. Laulainen, *Mathematical Models for Atmospheric Pollutants*, EPRI Report No. EA-1131 (1979).
16. Egan, B.A. and J.R. Mahoney, "Numerical Modeling of Advection and Diffusion of Urban Area Source Pollutants," *J. Appl. Meteorol.*, **11**, 312-22 (1972).
17. Egan, B.A., "Turbulent Diffusion in Complex Terrain," Lectures on Air Pollution and Environmental Impact Analysis, American Meteorological Society, Boston, 112-35 (1975).
18. Environmental Protection Agency, *Guideline on Air Quality Models (Revised)*, OAQPS Guideline Series, Research Triangle Park, N.C. (1986).
19. Environmental Protection Agency, *Summaries and Proposed Recommendations Concerning Air Quality Models*, Research Triangle Park, N.C. (1980).
20. Eschenroeder, A.Q., G.C. Magil, C.R. Woodruff, "Assessing the Health Risks of Airborne Carcinogens," Final Report EPRI EA-4021, Electric Power Research Institute, Palo Alto, Calif. (1985).
21. Gibson, L.V. and L.K. Peters, "A Short-term Air Quality Model for Sulfur Dioxide in Louisville, Kentucky," *J. Air Pollut. Control Assoc.*, **27**, 218-23 (1977).
22. Gifford, F.A., "Atmospheric Transport and Dispersion over Cities," *Nucl. Saf.*, **13**, 391-402 (1972).
23. Guzewich, D.C. and W.J.B. Pringle, "Validation of the EPA-PTMTP Short-term Gaussian Dispersion Model," *J. Air Pollut. Control Assoc.*, **27**, 540-42 (1977).
24. Liu, M.K. and J.H. Seinfeld, "On the Validity of Grid and Trajectory Models of Urban Air Pollution," *Atmos. Environ.*, **9**, 555-74 (1975).
25. Pasquill, F., "The Estimation of Windborne Material," *Meteorol. Mag.*, **90**, 33-39 (1961).
26. Pasquill, F., *The "Gaussian-Plume" Model with Limited Vertical Mixing*, U.S. Environmental Protection Agency, EPA-600 4-76-042, Research Triangle Park, N.C. (1976).
27. Pasquill, F., *Atmospheric Dispersion Parameters in Gaussian Plume Modeling: Part II. Possible Requirements for Change in the Turner Workbook Values*, U.S. Environmental Protection Agency, EPA-600 4-76-030b, Research Triangle Park, N.C. (1976).
28. Pasquill, F., *Atmospheric Diffusion*, 2nd ed., John Wiley & Sons, New York (1974).
29. Peterson, K.R., T.V. Crawford and L.A. Lawson, *CPS: A Continuous-Point-Source Computer Code for Plume Dispersion and Deposition Calculations*, UCRL-52049, Lawrence Livermore Laboratory, Livermore, Calif. (1976).

30. Ragland, K.W., "Worst-case Ambient Air Concentrations from Point Sources Using the Gaussian Plume Model," *Atmos. Environ.*, **10**, 371-74 (1976).
31. Reynolds, S.D., P.M. Roth and J.H. Seinfeld, "Mathematical Modeling of Photochemical Air Pollution: I. Formulation of the Mode," *Atmos. Environ.*, **7**, 1033-61 (1973).
32. Sharma, V. and L.O. Myrup, "Diffusion from a Line Source in an Urban Atmosphere," *Atmos. Environ.*, **9**, 907-22 (1975).
33. Sharma, V., "An Area-source Model for Urban Air-pollution Applications," *Atmos. Environ.*, **10**, 1027-32 (1976).
34. Shieh, L.J. and P.K. Halper, *Numerical Comparison of Various Model Representations for a Continuous Area Source*, IBM Scientific Center, Palo Alto, Calif. (1971).
35. Shir, C.E., "Numerical Investigation of the Atmospheric Dispersion of Stack Effluents," *IBM J. Res. Dev.*, **16**, 171-79 (1972).
36. Slade, D.H., "Deposition of Particles and Gases," in *Meteorology and Atomic Energy*, Section 5-3, U.S. Atomic Energy Commission (1977).
37. Slade, D.H. (ed.), *Meteorology and Atomic Energy*, TID-24190, Atomic Energy Commission, Washington, D.C. (1968).
38. Smith, M.E., "Recommended Guide for the Prediction of the Dispersion of Airborne Effluents," American Society of Mechanical Engineers (1968).
39. Sullivan, D.A. and B.A. Woodcock, "Gravitational Settling and Dispersion Modeling of Fugitive Dust Sources," presented at the 75th Annual Meeting of the Air Pollution Control Association, New Orleans, La. (1982).
40. Turner, D.B., "Workbook of Atmospheric Dispersion Estimates," U.S. Environmental Protection Agency, Office of Air Programs, Research Triangle Park, N.C. (1974).
41. U.S. Environmental Protection Agency, "Guideline on Air Quality Models (Revised)," Office of Air Quality Planning and Standards, Research Triangle Park, N.C. (1986). Report No. EPA/450/2-78/027R.
42. "User's Network for Applied Modeling of Air Pollution (Version 4)," National Technical Information Service (NTIS), U.S. Department of Commerce, Springfield, Va. (1982).

5.4 TERRESTRIAL MODELING

5.4.1 Introduction

This section describes principles of state-of-the-art mathematical terrestrial (land, soil, groundwater) modeling for use primarily in environmental quality studies and secondarily in environmental decision-making. Terrestrial modeling of inorganic species is complex and must deal with many uncertainties; therefore, it has not been extensively employed in decision-making.

Subsequent paragraphs provide a short background on terrestrial modeling (section 5.4.2), describe the principal processes considered by models (section 5.4.3), summarize the differences between organic and inorganic pollutant computer FORTRAN codes (section 5.4.4), list speciation codes (section 5.4.5), and illustrate applications of speciation models (section 5.4.6).

Readers should also review section 5.5, Aquatic Modeling, because of the chemical and mathematical similarities between the two modeling categories [2].

5.4.2 Background

Terrestrial chemical fate modeling has traditionally been performed for three distinct subcompartments: (1) the land surface (or watershed), (2) the unsaturated soil (or "soil") zone, and (3) the saturated (or "groundwater") zone of a region. In general, the mathematical simulation is structured around two major processes, the *hydrologic cycle* and the *pollutant cycle*, each of which is associated with a number of physicochemical processes. Land surface models also account for a third cycle, *sedimentation*.

Land surface models describe pollutant fate on land (known as watershed), the unsaturated soil zone of the region, and pollutant contribution to the water body of the area. Unsaturated soil zone models simulate both (1) soil moisture movement and (2) soil moisture and soil solid quality conditions of a soil zone profile extending between the ground surface and the groundwater table. Groundwater models describe the fate of pollutants in aquifers [3].

When used properly and with an understanding of their limitations, mathematical models can greatly assist decision-makers in determining the importance of pollutant pathways in the terrestrial environment [9,41]. For this reason, the use of models has grown dramatically over the past decade. Although the number of terrestrial model types is very large, there are only a few fundamental modeling concepts.

Soil zone modeling is highly complex, because the physical and chemical dynamics of a soil subcompartment — in contrast to those of a water or air subcompartment — are governed by external ("out-compartmental") forces such as precipitation, air temperature, and solar radiation. Water and air modeling are generally simpler, because the dynamics of these compartments are governed by "in-compartmental" forces.

Chemical modeling in soil systems provides information on the distribution of elements (e.g., metal species) within a soil matrix consisting of soil-solids, soil-moisture (in the soil zone) or soil-water (in groundwater), and soil-air (in the soil zone), as schematically shown in Figure 5.4-1 for the soil zone of a region [8]. The objective is to determine the amount of pollutants in the solid phase, aqueous phase and/or gaseous phase at a given point and time.

5.4.3 Principal Processes

An evaluation of the fate of inorganic compounds in soil and groundwater requires a detailed consideration of the physical, chemical and biological processes and reactions involved, such as complexation, adsorption, precipitation, oxidation-reduction [29], chemical speciation and biological reactions (Figure 5.4-2) to determine (for metallic species) the free metal concentration in soil solutions. These processes can affect such characteristics as species solubility, availability for biological uptake, physical transport, and corrosion potential [28,44].

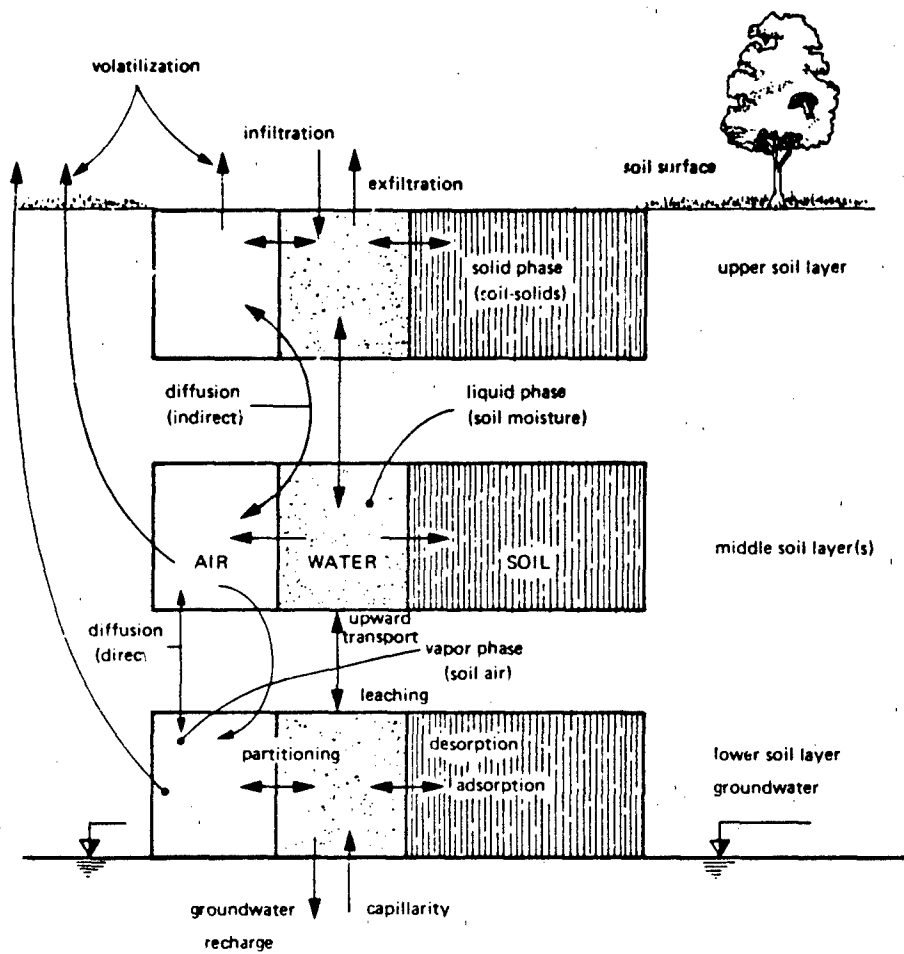
To describe the complex interactions involved [3], various kinds of models have been developed. These are, for example, "adsorption" models (which utilize mathematics involved in specific adsorption, surface complex formation and ion exchange), surface complexation models, constant-capacitance models, cation-exchange models, and overall fate-modeling packages that take into account the effects of one or more geochemical processes. One category ("equilibrium" or "speciation" models) is designed to determine the distribution of inorganic species in the soil water. Chemically based computer models of soluble trace metal speciation are being employed increasingly in decision-making, such as in studies related to sewage and effluents applied to agricultural land [45].

The transport of particular chemical species in terrestrial systems is of interest to a variety of scientists [10,11], since measurement or reporting of "total" concentration of a particular inorganic compound [15] in the soil may be misleading in many environmental management situations [13]. Toxic effects of trace metals, for example, may be affected more by their chemical form than by their total concentration [16,2]. Therefore, mathematical computer models capable of simulating the distribution of inorganic pollutant species in soil and groundwater systems are valuable tools for analyzing contaminant pathways.

5.4.4 Models

At this stage of intensive research on terrestrial chemical modeling, we can group the prevailing concepts into two major categories: (1) *geochemical* or, more appropriately, *pollutant fate* models, and (2) *speciation equilibria* models. This terminology is not standard but is employed here for convenience.

Geochemical models may be applicable for simplified overall inorganic pollutant fate estimates via adsorption processes (routine) or for many chemical and biological processes that govern the fate of the total pollutant mass from dissolved or partially

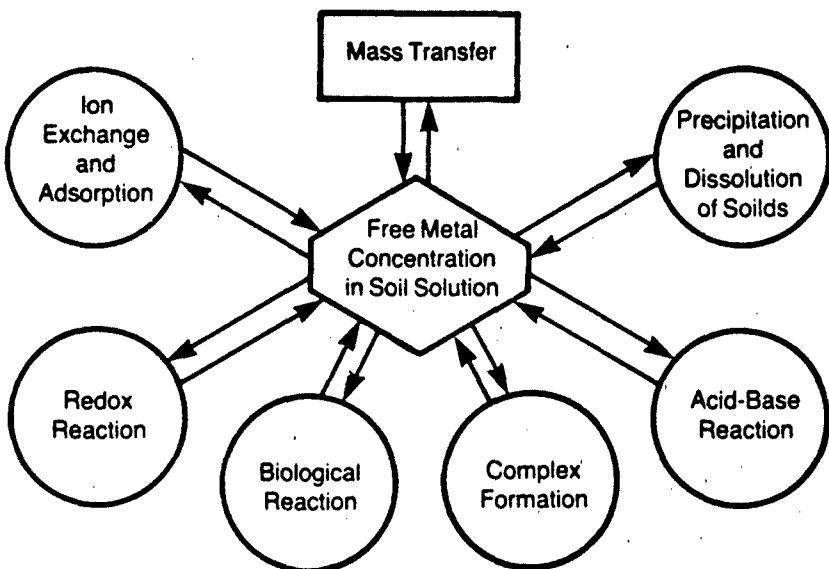


Source: Bonazountas and Wagner [7]

FIGURE 5.4-1 Schematic of Phases in a Soil System

dissolved (immiscible) fluids. Speciation models estimate the distribution of metals in various forms, but certain "speciation" codes can simulate the fate of individual dissolved pollutant species and the total mass of dissolved pollutants, since they combine fate and speciation in one package.

The variety of geochemical (pollutant fate) models has dramatically increased during the last decade. These models can be employed for both organic and inorganic pollutants, since the chemical processes are simulated via their overall equilibrium coefficients (e.g., adsorption coefficients). Information on such models is beyond the scope of this chapter and is not presented here, but some (mainly for organic pollutant models) is given by Bonazountas [9]. (See Table 5.4-1.) A study on the use and limitations of the three EPA unsaturated soil zone models SESOIL, PRZM and PESTAN of Table 5.4-1 has been conducted by Hern and Melancon [17a,17b] and others [33a].



Source: Adapted from Mattigod et al. [32]. (Copyright 1981, American Society of Agronomy. Reprinted with permission.)

FIGURE 5.4-2 Principal Controls on Free Trace Metal Concentrations in Soil Solutions

The status of geochemical speciation equilibria models for inorganic pollutants in soils is described below. Note that speciation computer codes account for additional processes — redox reaction [26], adsorption [25], complexation [23,24], and others (e.g., [18,27,37]). Speciation equilibria models are based on chemical thermodynamic principles. Some of the computer codes available for speciation calculations in soil and groundwater aqueous systems are described below.

Speciation calculations and procedures are described in sections 2.9-2.13. Steps of speciation calculations are not of concern in the following section, which focuses on integrated computerized modeling codes.

Excellent state-of-knowledge reviews of chemical equilibria codes (models) of inorganic pollutants in soils are presented by numerous investigators [19,21,22,31,34,38,42,49,52]. The following discussion has drawn on these reviews, particularly that of Sposito [49]. Readers interested in details should refer to the original publications.

TABLE 5.4-1
Some Well-documented Pollutant Fate Models and Their Features

Model Acronym	Model Type ^a	Model Formulation ^b				Mathematics ^c	Chemistry Issues ^d				User Concerns ^e	Source	
	Groundwater	Flow Module	Solute Module	TDE Approach	Compartmental		Analytical	Numerical	Organics	Inorganics	Metals	Gaseous Phase	
PESTAN	•		•	•		•		•					L L L • [15]
PRZM	•	•	•		•		•	•	•				M M M • [10a]
SCRAM	•	•	•	•			•	•	•				H H H • [1]
SESOIL	•	•	•		•	•	•	•	•	•	•	•	M M M • [7]
AT123D		•	•	•		•		•	•	•			M L M [56,57]
PATHS		•	•	•	•	•	•	•	•	•	•		L M M • [36]
MMT/VVT		•	•	•			•	•	•				H H H • [11]
FEMWASTE		•		•			•	•	•				H H H • [57]
R. WALK		•		•	•		•	•	•				H H H • [44]
USGS Models	•	•	•	•	•	•	•	•	•	•	•	•	H H H • [4]
Other Models													[22]

- a. The use of complex models (e.g., a numerical soil and groundwater package) that can handle more than one compartment is not always desirable, since generalized packages tend to be cumbersome unless especially designed.
- b. The most representative characteristics are given. The Traditional Differential Equation (TDE) approach applies to the flow and solute module. "Other" includes linear analytic system solutions, for example.
- c. The most representative characteristics are given.
- d. Almost all models can simulate organic, inorganic and metal fate, assuming that a careful calibration via an adsorption coefficient may alter the model output to predict measured monitored values. However, not all models have by design increased chemistry capabilities (e.g., cation exchange capacity, complexation); therefore, the most representative capabilities are indicated.
- e. L = low, M = medium, H = high input data requirements. In general, numerical models have higher input data requirements and calibration needs and therefore may better represent spatial resolution of a domain. Compartment models provide an optimal compromise. The level of effort is intuitively defined here.

Source: Adapted from Bonazountas [9]. (Copyright 1983, American Chemical Society. Reprinted with permission.)

5.4.5 Speciation Codes/Models

Although geochemical speciation modeling was developed relatively recently, more than a dozen comprehensive computer codes are already available. Kincaid *et al.* [22] provide an overview of the geochemical code history (up to 1983) in which they group models into four major families according to their evolutionary stage (Figure 5.4-3).

Speciation models can be grouped today into two categories: (1) "speciation" codes, which account for speciation equilibria of inorganic pollutants for a terrestrial water compartment (e.g., codes of Figure 5.4-3), and (2) "coupled speciation" codes, which can simulate both speciation equilibria and solute transport of individual species in the terrestrial (soil, groundwater) environment in both time and space.

Coupled codes are formulated by two mathematical methods, one described by Miller and Benson [34] and the other by Jennings *et al.* [21]. The former interfaces the computer code for equilibrium distributions of species (e.g., code of Figure 5.4-3) with the code for transport and performs calculations in two steps: (1) species estimation and (2) species transport. This procedure is repeated in time. Jennings' method consists of solving simultaneously a system of equations describing chemical reactions, advective-dispersive transport of reacting contaminants, and interphase mass transfer. The method of solution is irrelevant here.

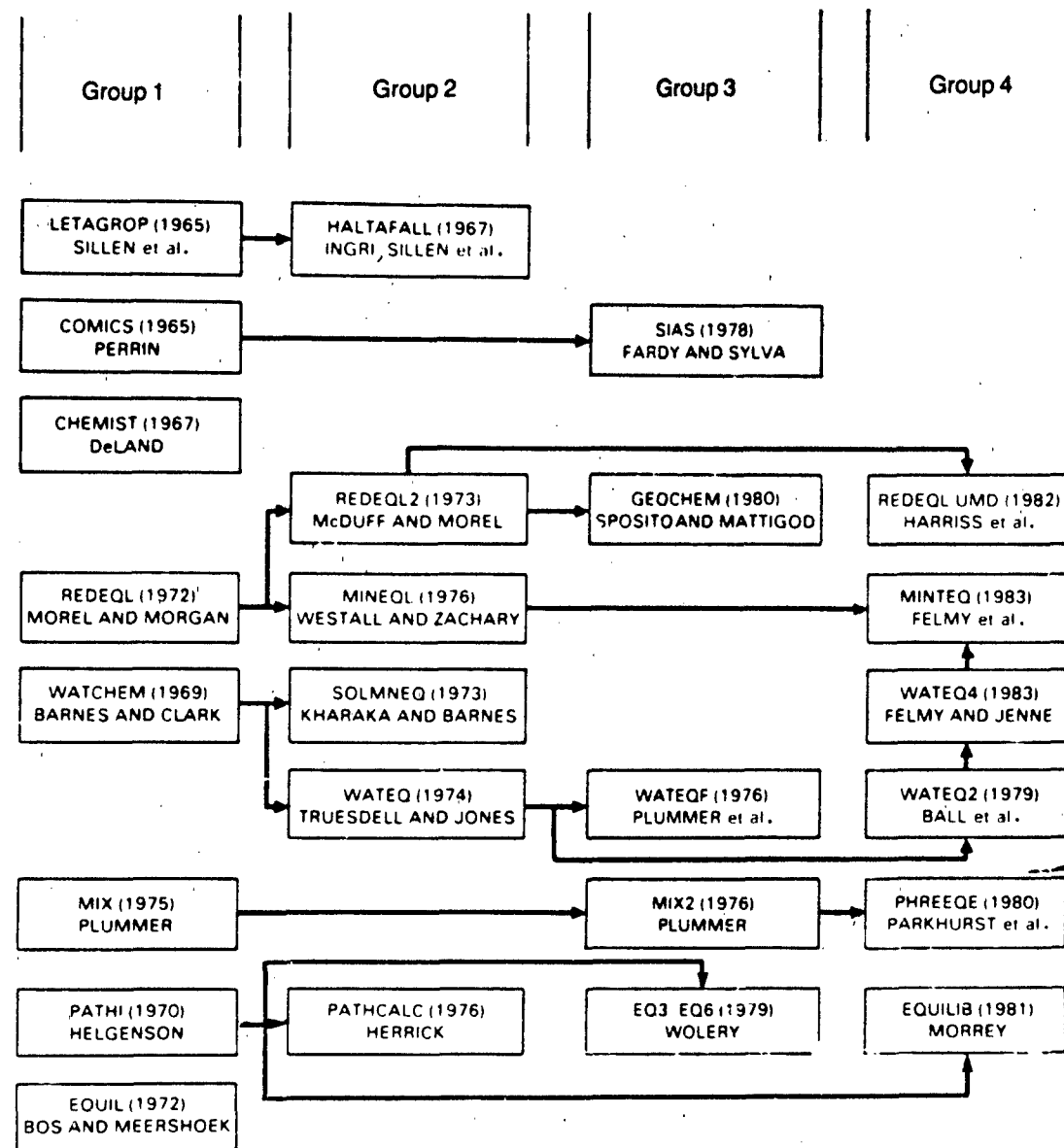
Coupled speciation codes such as FIESTA [23,52] and CHEMTRN [34] are the subject of current research, as are the extension of the speciation codes. Although coupled codes appear to be powerful tools, they are also large and require extensive input data; as a result, they are complex and frequently inefficient (in terms of input data requirements and effort) for obtaining practical solutions to problems.

Coupled codes are not further analyzed in this report; rather, emphasis is placed on speciation equilibria (geochemical simple compartment) codes, because these models have been more extensively applied and the activity coefficients have been validated by laboratory and field studies.

The significant advances made in aquatic chemistry during the past decade [50] have yielded an approach to the soil solution that is parallel to that taken for other natural waters [48]. In that respect, there are many similarities between models presented in this section and the one that follows (see § 5.5); for example, the model GEOCHEM [50] has been developed from the water bodies speciation model REDEQL2, a program created originally by Morel and Morgan and their co-workers at Caltech [33].

The basic geochemical and aquatic equilibria processes modeled by existing computer codes include adsorption/desorption, precipitation/dissolution, reduction/oxidation, ion exchange, and aqueous speciation in soil solution. Various mathematical expressions are used to model these processes.

For aqueous speciation in soil solutions, Sposito [49] reports that chemical modeling can be accomplished either by a "specific interaction" approach or an "ion-association"



Source: Adapted from Kincaid et al. [22]. (Copyright 1984, Electric Power Research Institute.
Reprinted with permission.)

FIGURE 5.4-3 Evolution of Geochemical Codes

approach. In the former, the composition of an electrolyte solution is described in terms of the total number of molalities of the stoichiometric components of neutral solutes, while the thermodynamic properties of the solution are expressed with "mean ionic" activity coefficients for neutral solutes introduced into standard chemical thermodynamic equations. In the ion-association approach, the composition of an electrolyte solution is described in terms of the molalities of molecular species presumed to exist in the solution, and the thermodynamic properties are expressed with "single-species" activity coefficients for the assumed molecular constituents. The latter approach appears to be used universally by soil chemists, despite its more tenuous relationship with rigorous thermodynamics. For additional details, the reader is referred to the original work of Sposito [49].

The geochemical data bases used are the most important features of a computer code. Data bases can provide typical values of kinetic and adsorption rates at typical temperatures. Reasonably good data bases are available for GEOCHEM and MINTEQ, among others.

Table 5.4-2 lists features of computer codes that are suitable for geochemical modeling. Of the nine codes summarized, the first six listed are very capable in the areas of aqueous speciation, adsorption/desorption and precipitation/dissolution [22]. In addition, all these codes are documented, available in the public domain in the United States, recently updated, and frequently accompanied with a sizeable data base. CHEMTRN features are not presented in Table 5.4-2 because of the limited information available during the production of this report. Table 5.4-3 provides user-related information for these codes. Many other codes in the literature (e.g., BALANCE [40]) are not reported here.

Model selection is a major issue in mathematical geochemical modeling. Factors of importance are the study objectives, the features of the model, input requirements, monitoring data available to validate prediction, model documentation, and cost for an application. As it is difficult to recommend a universal computer code that can handle all of the above factors, decision-makers must first review a number of codes that may meet project requirements and then select one that best suits their study objectives.

Two of the best known geochemical speciation codes are GEOCHEM and MINTEQ. CHEMTRN, a coupled geochemical/speciation and transport code, is also receiving increased attention. These codes are briefly described below.

- GEOCHEM is based on the computer program REDEQL2 for calculating equilibrium speciation of chemical elements in a soil solution. The component species are identified as uncomplexed metal cations, the free proton, uncomplexed ligands, and the free electron. Single species activity coefficients are calculated in the program. The model contains critical thermodynamic data for soils, a method for calculating cation exchange, and a correcting method for non-zero ionic strength up to 3 molal. Currently, the model stores thermodynamic data for 36 metals and 69 ligands, and it can handle more than 200 soluble complexes and

TABLE 5.4-2

Summary of Geochemical Code Capability, Adaptability and Availability

Criterion	GEOCHEM	REDEQL UMD	MINTEQ	PHREEQE	EQUILIB	EQ3/EG6	SIAS	SOLMINEQ	CHEMIST
Code Classification	III 36 (94)	III 3	III 32	II 19 (26)	II 26	IIR	I	II	I
Number of Elements	69/-	65/-	16/373	8/120	186	-20	10 (200)	162	
Aqueous Speciation		20	22	6	20	6	10 (200)	10	
Number of redox species	48 (60)	DA,HN	DA,SHM	ECH	HN	None	HN	169 Variable	
Activity-coefficient correction	Yes	Yes	DA	Yes	Yes	No	No	None	
Calculation of pH	N-R	N-R	N-F	N-R,C-F	Pred.	N-R	B-S	B-S	N-R
Method of iteration									
Absorption Model	J-H	Swiss	Three mdls.	Two mdls.	None	None	None	None	
Number of species	10	20	No limit	Variable	None	None	None	None	
Number of surfaces	6	5	3	NA	None	None	None	None	
Number of species	No limit	None	None	None	None	None	None	None	
Precipitation/Dissolution									
Number of minerals	~500	<500	238	24	200	250	None	158	
Quantitative mass transfer	Yes	Yes	Yes	Yes	Yes	Yes	None	No	
Automatic selection of mineral	Yes	Yes	Yes	No	Yes	Yes	None	No	
Capability for solid solutions	No	No	No	No	None	Yes	None	No	
Gas Generation									
Ammonia	No	No	No	No	Yes	Yes	No	No	
Oxygen	Yes	Yes	Yes	Yes	Yes	Yes	No	No	
Hydrogen	No	No	No	Yes	Yes	Yes	No	No	
Carbon dioxide	Yes	Yes	Yes	Yes	Yes	Yes	Yes	No	
Code Structure									
Size (32 bit words, K)	434	62	68.1	>64	20.5	363	34	30	25
Modularity	Yes	Yes	Yes	Yes	Yes	Yes	No	No	
Language	FORTRAN	FORTRAN	FORTRAN	FORTRAN	FORTRAN	FORTRAN	FORTRAN	PL/1	FORTRAN
	IVG	IV	IV	IVH	IV	4.6	H		

(Continued)

TABLE 5.4-2 (Continued)

	REDEQ	UMD	MINTEQ	PHREEQE	EQUILIB	EOS/EOS	SIAS	SOLMNEQ	CHEMIST
GEOCHEM	IBM 4314 VAX	CDC CYBER 171	UNIVAC 1144 PDP 11/70 VAX	Amdahl DEC VAX	CDC 7600 PDP VAX	CDC 7600 CDC 6600 VAX	IBM/360/65	IBM/360	IBM/360
System									
Other Criteria									
Latest documentation date	1980	1982	1980	1978	1979	1978	1973	1968	
Data Base									
Temperature range	No	No	Yes	Yes	Yes	Yes	No	Yes	
Easily modified	Yes	Yes	Yes	Yes	Yes	Yes	No	No	No

Legend: () = maximum, U-S = user supplied, J-H = James-Healy, N-R = Newton-Raphson, B-S = back substitution, Pred. = predictor/back substitution, DA = Davies, HN = Helgeson-Nigrini, SHM = Sun-Harris-Mattigod, ECH = extended Debye-Hückel, I = chemical speciation, II = I + mass transfer by precipitation or dissolution, III = II + adsorption and ion exchange, IIR and IIIIR = pseudo kinetics.

Source: Kincaid et al. [22]. (Copyright 1984, Electric Power Research Institute. Reprinted with permission.)

TABLE 5.4-3
Advantages and Disadvantages of Chemical Speciation Models

Code	Characteristics
GEOCHEM	Available in public domain. Documentation marginal. Recently updated. Models important processes. Includes adsorption. Data base probably the largest available. Modularity not yet evaluated.
REDEQL.UMD	Should be available in the public domain soon. Well documented, although not in final form. Recently updated. Models important processes. Data base and modularity not yet evaluated.
MINTEQ	Available in the public domain. Well documented. Models important processes. Includes adsorption. Modular construction. Data base is the best documented; one of largest available.
PHREEQE	Available in the public domain. Documented. Models precipitation/dissolution. Includes adsorption. Data base supplied by user. Modular construction.
EQUILIB	EPRI proprietary code. Well documented. Models precipitation, not adsorption. Data base quite extensive, reasonably well documented. Can use other data bases. Construction is modular. Method of solution involves unique elements.
EQ3/EQ6	Publicly available. Documentation available for EQ3 only. Updated version of PATHI construction. Contains precipitation, no adsorption but structured for inclusion. Contains capability to model paths of chemical changes.
SOLMNEQ	Publicly available. Documentation old. Does not contain unique characteristics. Data base not easily modifiable.
CHEMIST	Publicly available. Old and sketchy documentation. No precipitation/adsorption. No unique modeling characteristics.
CHEMCSMP	Publicly available. Old and very inadequate documentation. May have unique kinetic characteristics but tied to IBM system.
SIAS	Update of an old program. Documentation sketchy. SIAS capabilities covered in better documented, more inclusive codes.

Source: Kincaid et al. [22]. (Copyright 1984, Electric Power Research Institute. Reprinted with permission.)

solids. Adsorbed metal species are described in the model, and adsorbed ligand species will be considered in the future. A new version of GEOCHEM is being prepared [49]; therefore, interested scientists should contact its developers [50].

- MINTEQ is similar in structure to MINEQL, and both of these are similar in overall structure to GEOCHEM, since they originate from REDEQL. As shown in Figure 5.4-3, MINTEQ was formed from MINEQL and the data base of WATEQ [5,43]. The model includes ion speciation, redox equilibria, calculation of activity coefficients, solubil-

ity, adsorption, and mass transfer. The model and its large data bases are well documented, the latter containing data on more than 35 metals and 60 ligands.

As reported in a comparative analysis by Sposito [49], a principal difference between MINEQL (and consequently MINTEQ) and GEOCHEM is that MINEQL can accept the concentration of any free ionic species, soluble complex, or dissolved gas as input data to be held fixed during a calculation, whereas GEOCHEM can do this only for the activities of H^+ , e^- , $CO_2(g)$, and $N_2(g)$. Therefore, if desired, the concentration of Cu^{+2} can be specified as a fixed input datum in MINEQL, a feature that gives the code user great flexibility in speciation calculations.

- CHEMTRN is a one-dimensional geochemical transport/speciation (coupled) model for solutes in a saturated porous medium. The model includes dispersion/diffusion, advection, ion exchange, formation of complexes and speciation in the aqueous phase, and the dissociation of water. The mass action, transport, and site constraint equations are expressed in differential/algebraic form and are solved simultaneously. This coupled model is in the development stage; therefore, no data base accompanies the computer code.

5.4.6 Model Applications

Reports in the literature on the chemical forms of heavy metals in soil solutions are limited [13,29]. One reason for this is the large number of chemical forms in which metals exist and the analytical problems associated with their determination [39]; another reason is that the modeling of metal species in soil solutions has only recently become a matter of concern.

The use of chemical equilibrium models in decision-making has been described by many researchers [6,12,13,14,20,21,24,30,31,34,45,46,47,52,53,54,55] who have employed and validated models such as GEOCHEM with data from field (e.g., [6]) and laboratory [13] analyses.

5.4.7 Example of Model Application

This section illustrates the use of a model to estimate the chemical speciation of metals in a soil system. The modeling experiment was conducted by the Tennessee Valley Authority [6] and relates to land-treated sewage sludge. It is presented in four sections:

- (1) Statement of problem,
- (2) Field monitoring,
- (3) Model application, and
- (4) Discussion of findings.

STATEMENT OF PROBLEM

Anaerobically digested, air-dried sewage sludge was applied (in 1971) in plots of 3.6 by 15.0 meters and was incorporated into the soil to a depth of 15 cm. The application rates were 50, 100 and 200 tons/ha.

Cultivation of the plots began after 12 months with sweet corn (*Zea Mays L. cv. Silver Queen*). At that time, the plots were subdivided into areas of 3.6 by 7.5 meters. Half of each plot received three additional sludge applications — in that year, 12 months later, and 24 months later — at the rate used in the initial application. The other half of each plot received no additional sludge, so that residual effects from the original applications could be monitored. The sludge contained both organic and inorganic pollutants.

FIELD MONITORING

Before application, the sludge was analyzed for inorganic species and total organic carbon. A field monitoring program was conducted in 1971. The soil of the area is a Sango silt loam soil (Glossic Fragiudult) with a pH of 4.9 and a cation exchange capacity of 7 mol (NH_4^+) kg^{-1} .

The field monitoring program (collection and analysis of contaminated soils) was repeated in 1977. Soil samples were collected, air-dried, and crushed to less than 2 mm. Water was added to 150-g samples to bring the soil water potential (see Appendix C) to -0.33 bar, and the samples were then incubated for 7 days at 25°C. Soil solutions were recovered by centrifugation [17] and analyzed for total Cd, Zn, Mn, Fe, Al, Cu, Ni, Pb, Ca, Mg, Na, K, P, Cl, sulfate, organic carbon, conductivity and pH. The chemical composition of soil solutions from untreated and sludge-treated soils is shown in Table 5.4-4.

Concentrations of Zn, Cd, Mn, Ca, Mg, Na, K, $\text{PO}_4\text{-P}$, $\text{SO}_4\text{-S}$, and Cl in the soil solution tended to increase with sludge application, particularly in plots that received multiple sludge applications. Concentrations of Cu, Ni, Pb, and Fe were generally low (less than 10^{-6} M) at all sludge application rates, but soluble Cu and Ni concentrations in soil treated with sludge at 800 t ha^{-1} were markedly higher than those in soil receiving lesser amounts of sludge.

MODEL APPLICATION

An attempt was made to duplicate the above conditions and estimate species of chemicals in the soil systems via a mathematical model. The GEOCHEM model was used to predict the equilibria of the metals in solution because its data base can adequately support simulations of the species presented.

To facilitate both model use and interpretation of the data obtained, GEOCHEM calculations were performed using three sets of conditions: (a) metal-organic complexes were ignored; (b) metal-organic complexes were approximated by a mixture

TABLE 5.4-4
Chemical Composition of Soil Solutions from Untreated and Sludge-treated Soils

Parameter	Units	Sludge Applied, t ha ⁻¹					
		0	50	100	200	0	200
Zn	$\times 10^{-5} M$	0.35	7.94	10.72	16.98	0.49	11.75
Cd	$\times 10^{-6} M$	0.98	2.24	3.09	79.4	1.26	3.02
Cu	$\times 10^{-6} M$	<1.0	<1.0	<1.0	3.16	<1.0	<1.0
N	$\times 10^{-6} M$	<1.0	<1.0	<1.0	<1.0	<1.0	<1.0
Pb	$\times 10^{-6} M$	<1.0	<1.0	<1.0	<1.0	<1.0	<1.0
Mn	$\times 10^{-4} M$	3.72	3.09	3.85	3.55	3.63	5.37
Fe	$\times 10^{-6} M$	<1.0	<1.0	<1.0	<1.0	<1.0	<1.0
Al	$\times 10^{-4} M$	1.86	1.86	1.86	<1.0	1.86	1.86
Ca	$\times 10^{-3} M$	1.95	3.63	3.72	4.07	2.19	3.89
Mg	$\times 10^{-4} M$	1.20	5.89	4.07	4.37	0.95	4.37
K	$\times 10^{-4} M$	7.59	19.95	10.23	9.55	8.13	10.0
Na	$\times 10^{-3} M$	3.31	3.89	3.89	3.98	2.51	8.32
PO ₄ ³⁻ , P	$\times 10^{-6} M$	2.6	2.9	4.2	15.49	2.57	9.33
SO ₄ ²⁻ , S	$\times 10^{-3} M$	0.26	0.85	0.98	1.15	0.44	0.91
Cl ⁻	$\times 10^{-1} M$	0.60	1.55	1.29	1.23	0.51	0.72
Organic C (g m ⁻³)		160	130	160	190	170	150
Conductivity (dS m ⁻¹)		1.54	2.25	2.14	2.08	1.56	2.03
pH		4.7	4.9	5.1	5.6	4.6	5.0

a A denotes a single application in 1971. B denotes repeat applications of initial rate in 1972, 1973, and 1974.

Source Behel et al [6] (Copyright 1983, American Society of Agronomy. Reprinted with permission.)

model [31]; and (c) metal-organic complexes were modeled using stability constants obtained experimentally [48] for a sludge fulvic acid (fulvate model). It is almost always necessary to make assumptions of this kind when using a model.

The mixture sub-model of GEOCHEM predicted that less than 16% of the total (t) Cd, Zn_t, and Mn_t in solution would be complexed with organic and inorganic ligands. Therefore, it was not surprising that exclusion of the mixture model from GEOCHEM has a minor effect on the speciation of Cd, Zn, and Mn (Table 5.4-5). The results of the overall simulation are shown in Table 5.4-6.

The predominant species of Zn in the soil solutions was Zn⁺² (Table 5.4-7). Even though sludge applications increased total soluble Zn (Zn_t) from $4 \times 10^{-6} M$ to more than $1 \times 10^{-4} M$, 87-97% of the Zn_t was present as Zn⁺². For most sludge treatments, SO₄ complexes accounted for 5-8% of Zn_t. Fulvate complexes (mixture model) with Zn tended to increase with sludge applied, but the amount of Zn_t associated with soluble organic C was always less than 2%. The distribution of Zn species was essentially the same after application of 200 t ha⁻¹ in a single treatment or in four annual 50-t ha⁻¹ increments. Soluble Zn_t increased to a greater extent with the single 200-t ha⁻¹ sludge application ($1.7 \times 10^4 M$) when compared with four increments of 50 t ha⁻¹ ($1.2 \times 10^4 M$).

The activity of Zn⁺² in the soil solutions was similar to that supported by several Zn solid phases. The activity of Zn⁺² ranged from approximately 10^{-5} to $10^{-3} M$ in solutions of pH 5 to 6. Based on stability diagrams [27], the Zn⁺² in soil solution could be controlled by one or more of the following solids: (a) ZnFe₂O₄ in equilibrium with soil Fe; (b) soil Zn; and (c) Zn₂SiO₄ in equilibrium with amorphous Si. At similar pH values, Zn⁺² activities obtained from this study were greater than those previously reported for soils incubated with sewage sludge [13]. The pH range of the sludge-treated soils was too narrow to evaluate the pH dependence of Zn⁺², as predicted by the solubility of known Zn solid phases.

DISCUSSION OF FINDINGS

According to Behel *et al.* [6], GEOCHEM calculations were close to monitored values and indicated that Zn⁺² and Cd⁺² are the predominant species in the soil solution of acid soils treated with sludges of metal additions. The amount approached the maximum recommended as safe for growth of agronomic crops.

Computer modeling of trace metal equilibria can provide a useful framework for understanding the nature of the multitude of reactions that take place in a soil system. However, a field monitoring program is needed to guide model application with data and calibration parameters.

Model output validation is essential to any soil modeling effort, although this term has a broad meaning in the literature. For the purpose of this section, we can define validation as "the process that analyzes the validity of final model output," namely, the validity of the predicted pollutant concentrations or mass in the soil column (or in

TABLE 5.4-5

Effect of Excluding Organic Ligands from Consideration by GEOCHEM on the Percentage of Free Metals in Soil Solution

Sludge Applied ^a (t ha ⁻¹)	Organic Ligands Included ^b												
		A	B	A	B	A	B	A	B	A	B		
(calculated % of total present as free metal ion)													
0	0	Fulvate model		67	67	79	80	— ^c	—	—	69	73	
		Mixture model		92	91	97	96	—	—	—	98	97	
		None		94	93	98	96	—	—	—	98	97	
50	200	Fulvate model		69	72	84	84	—	—	—	80	81	
		Mixture model		85	89	94	94	—	—	—	95	95	
		None		86	90	95	95	—	—	—	96	96	
100	400	Fulvate model		66	67	80	81	—	—	—	74	78	
		Mixture model		84	83	92	91	—	—	—	95	84	
		None		86	86	94	92	—	—	—	95	93	
200	800	Fulvate model		64	63	79	78	69	69	—	72	74	76
		Mixture model		82	79	91	87	19	19	—	87	77	80
		None		86	82	93	88	93	88	—	90	94	90

a. A denotes 1 application in 1971; B denotes repeat applications of initial rate in 1972, 1973, and 1974.

b. Fulvate model — calculations based on equilibrium constants for fulvic acid extracted from sewage sludge [48]; Mixture model — mixture model for soluble fulvic acid [31].

c. Total concentrations below detection limits of analytical methods used.

Source: Behel et al. [6]. (Copyright 1983, American Society of Agronomy. Reprinted with permission.)

groundwater), as compared to available knowledge of measured pollutant concentrations from monitoring data (field sampling).

Disagreement in the absolute levels of concentration (predicted versus measured) does not necessarily indicate that either method of obtaining data (modeling, field sampling) is incorrect or that either data set should be revised. Laboratory analysis of field samples is difficult and uncertain. Field sampling approaches and modeling approaches produce two different perspectives of the same situation [9].

Field information, data, sampling and analysis are subject to temporal and spatial uncertainties. Model results are based on assumptions and utilize deterministic approaches; therefore, a disagreement of concentrations is to be expected.

TABLE 5.4-6
**Concentration and Speciation of Mn, Cu, and Ni in the Soil Solution As Affected by Rate
 and Frequency of Sludge Application**

Metal	Sludge Applied (t ha ⁻¹ y ⁻¹)	No. of Applications ^a	Total Concentration (× 10 ⁻⁵ M)	Free Metal	Metal Complexes		
					SO ₄	PO ₄	MM ^b
Mn	0	0	37	98	1.8	<0.1	0.3
		0	36	97	2.8	<0.1	0.3
	50	1	31	95	4.2	<0.1	0.3
		4	54	95	4.0	<0.1	0.4
	100	1	39	95	4.9	<0.1	0.5
		4	65	84	6.0	<0.1	9.5
	200	1	36	77	4.5	<0.1	17.9
		4	74	80	8.3	0.2	11.4
	200	1	0.32	19	1.4	<0.1	79.8
	200	4	0.63	19	2.5	<0.1	78.3
Ni	200	4	0.68	87	9.0	0.1	3.3

a. Single application in 1971; repeat applications of initial rate in 1972, 1973, and 1974.

b. MM denotes mixture model for fulvate [31].

Source: Behel et al. [6]. (Copyright 1983, American Society of Agronomy. Reprinted with permission.)

TABLE 5.4-7
**Concentration and Speciation of Zn and Cd in the Soil Solution As Affected by Sludge Rate
 and Frequency of Application**

Sludge Applied (t ha ⁻¹ y ⁻¹)	No. of Applications ^a	Total Zinc ^b				Complexed Zn ^b			Total Cadmium ^b				Complexed Cd ^b				
		Free Zn ⁺²		Complexed Zn ^b		Free Cd ⁺²		Complexed Cd ^b		Free SO ₄ ²⁻		Complexed SO ₄ ²⁻		Free Cl ⁻		Complexed Cl ⁻	
		(x 10 ⁻⁵ M)	(x 10 ⁻⁵ M)	(x 10 ⁻⁵ M)	(x 10 ⁻⁵ M)	(x 10 ⁻⁵ M)	(x 10 ⁻⁵ M)	(x 10 ⁻⁵ M)	(x 10 ⁻⁵ M)	(x 10 ⁻⁵ M)	(x 10 ⁻⁵ M)	(x 10 ⁻⁵ M)	(x 10 ⁻⁵ M)	(x 10 ⁻⁵ M)	(x 10 ⁻⁵ M)	(x 10 ⁻⁵ M)	
0	0	0.35	97	2.2	0.5	0.98	92	2.7	3.6	1.7							
	0	0.40	96	3.5	0.4	1.3	91	4.2	2.9	1.5							
50	1	7.9	94	5.3	0.4	2.2	35	6.0	7.5	1.5							
	4	11.8	94	5.0	0.7	3.0	89	5.9	3.3	1.9							
100	1	10.7	93	6.0	0.9	3.1	84	6.9	6.2	2.4							
	4	16.6	91	8.1	1.0	59	83	9.4	4.4	2.8							
200	1	17.0	91	6.7	1.7	79	82	7.7	5.6	4.6							
	4	36.3	87	11.3	1.3	144	79	13.0	4.6	3.6							

a. A single application in 1971; repeat applications of initial rate in 1972, 1973, and 1974.

b. Complexes not given represented < 0.1% of total soluble metal.

c. MM denotes mixture model for fulvate [31].

Source: Behel et al. [8]. (Copyright 1983, American Society of Agronomy. Reprinted with permission.)

5.4.8 Literature Cited

1. Adams, R.T. and Kurisu, F.M., *Simulation of Pesticide Movement in Small Agricultural Watersheds*, Final Report, Environmental Research Laboratory, U.S. Environmental Protection Agency, Athens, Ga. (1976).
2. Allen, H.E., R.H. Hall and T.D. Brishin, "Metal Speciation: Effects on Aquatic Toxicity," *Environ. Sci. Technol.*, **14**, 441-43 (1980).
3. Anderson, M.P., "Movement of Contaminants in Groundwater: Chemical Processes," in *Groundwater*, National Academy Press, Washington, D.C. (1984).
4. Appel, C.A. and J.D. Bredehoeft, *Status of Groundwater Modeling in the U.S. Geological Survey*, U.S. Department of the Interior, Washington, D.C. (1978).
5. Ball, J.W., E.A. Jenne and D.K. Nordstrom, "WATEQ2 — A Computerized Chemical Model for Trace and Major Element Speciation and Mineral Equilibria in Natural Waters," in *Chemical Modeling in Aqueous Systems: Speciation, Sorption, Solubility, and Kinetics*, E.A. Jenne (ed.), American Chemical Society, ACS Symposium Series 93, Washington, D.C. (1979).
6. Behel, D., Jr., D.W. Nelson and L.E. Sommers, "Assessment of Heavy Metal Equilibria in Sewage Sludge-treated Soil," *J. Environ. Qual.*, **12**, 181 (1983).
7. Bonazountas, M. and J. Wagner, *SESOIL: A Seasonal Soil Compartment Model*, Draft Report, EPA Contract No. 68-01-6271, Office of Toxic Substances, U.S. Environmental Protection Agency, Washington, D.C. (1984, 1981).
8. Bonazountas, M., J. Wagner, and B. Goodwin, *Evaluation of Seasonal Soil/Groundwater Pollutant Pathways via SESOIL*, Final Report, Office of Water Regulations and Standards, U.S. Environmental Protection Agency, Washington, D.C. (1981).
9. Bonazountas, M., "Soil and Groundwater Fate Modeling: A Review," in *Fate of Chemicals in the Environment: Compartmental and Multimedia Models for Predictions*, R.L. Swann and A. Eschenroeder (eds.), ACS Symposium Series No. 225, American Chemical Society, Washington, D.C. (1983).
10. Bower, C.A. and L.V. Wilcox, "Soluble Salts," in *Methods of Soil Analysis*, C.A. Black (ed.), American Society of Agronomy, Madison, Wis., 947-48 (1965).
- 10a. Carsel, R.F., C.N. Smith, L.A. Mulkey, J.D. Dean, and P.P. Jowise, "User's Manual for the Pesticide Root Zone Model (PRZM): Release 1," Report No. EPA/600/3-84/109, U.S. Environmental Protection Agency, Athens, GA (1984).
11. Cole, C.R., "Information on the MMT/VVT Model to be Obtained by the Author," Battelle Pacific Northwest Laboratory, Richland, Wash. 99352 (1980).
12. Dowdy, R.H. and V.V. Volk, "Movement of Heavy Metals in Soils," Chapter 15 in Nelson *et al.*, Special Publication No. 11, Soil Science Society of America, American Society of Agronomy, Madison, Wis. (1983).
13. Emmerich, W.E., L.J. Lund, A.L. Page and A.C. Chang, "Predicted Solution Phase Forms of Heavy Metals in Sewage Sludge-treated Soils," *J. Environ. Qual.*, **11**, 182-86 (1982).

14. Emmerich, W.E., "Chemical Forms of Heavy Metals in Sewage Sludge-amended Soils as They Relate to Movement through Soils," Ph.D. Dissertation, University of California, Riverside (1980).
15. Enfield, C.G., R.F. Carsel, S.Z. Cohen, T. Phan and D.M. Walters, "Approximating Pollutant Transport to Groundwater," USEPA, RSKERL, Ada, Okla. (unpublished paper) (1980).
16. Florence, T.M., "Trace Metal Species in Fresh Waters," *Water Res.*, **11**, 681-87 (1977).
17. Gillman, G.P., "A Centrifuge Method for Obtaining Soil Solution," Division of Soils Report No. 16, Commonwealth Scientific and Industrial Research Organization, Melbourne, Australia (1976).
- 17a. Hern, S.C. and S.M. Melancon, "Guidelines for Field Testing Soil Fate and Transport Models," Report No. EPA/600/4-86/020, U.S. Environmental Protection Agency, Las Vegas, NV (1986).
- 17b. Hern, S.C. and S.M. Melancon, *Vadose Zone Modeling of Organic Pollutants*, Lewis Publishers, Inc., Chelsea, Michigan (1986).
18. James, R.V. and J. Rubin, "Applicabilities of Local Equilibrium Assumption to Transport through Soils of Solutes Affected by Ion Exchange," in *Chemical Modeling in Aqueous Systems*, E.A. Jenne (ed.), Symposium Series No. 93, American Chemical Society, Washington, D.C. (1979).
19. Jenne, E.A., "Chemical Modeling — Goals, Problems, Approaches and Priorities," in *Chemical Modeling in Aqueous Systems*, E.A. Jenne (ed.), Symposium Series No. 93, American Chemical Society, Washington, D.C. (1979).
20. Jennings, A.A. and D.J. Kirkner, "Instantaneous Equilibrium Approximation Analysis," *J. Hydraul. Div. Am. Soc. Civ. Eng.* (1984).
21. Jennings, A.A., D.J. Kirkner and T.L. Theis, "Multicomponent Equilibrium Chemistry in Groundwater Quality Models," *Water Resour. Res.*, **18**, 1089-96 (1982).
22. Kincaid, C.T., J.R. Morrey and J.E. Rogers, *Geochemical Models for Solute Migration*, Vol. 1, "Process Description and Computer Code Selection," Report EA-3417, Electric Power Research Institute, Palo Alto, Calif. (1984).
23. Kirkner, D.J., H.W. Reeves and A.A. Jennings, "Finite Element Analysis of Multicomponent Contaminant Transport Including Precipitation-dissolution Reactions," Laible *et al.* (eds.), Proc. 5th International Conference, Burlington, Vt., Springer-Verlag, New York (1984).
24. Kirkner, D.J., T.L. Theis and A.A. Jennings, "Multicomponent Solute Transport with Sorption and Soluble Complexation," *Adv. Water Resour.*, **7**, 120 (1984).
25. Langmuir, D., "Techniques in Estimating Thermodynamic Properties for Some Aqueous Complexes of Geochemical Interest," in *Chemical Modeling in Aqueous Systems*, E.A. Jenne (ed.), Symposium Series No. 93, American Chemical Society, Washington, D.C. (1979).

26. Lindberg, R.D. and D.D. Runnels, "Groundwater Redox Reactions: An Analysis of Equilibrium State Applied to Eh — Measurements and Geochemical Modeling," *Science*, **225**, 925 (1984).
27. Lindsay, W.L., *Chemical Equilibria in Soils*, John Wiley & Sons, New York (1979).
28. Lyman, W.J., W.F. Reehl and D.H. Rosenblatt, *Handbook of Chemical Property Estimation Methods*, McGraw-Hill Book Co., New York (1982).
29. Mahier, R.J., F.T. Bingham, G. Sposito and A.L. Page, "Cadmium-enriched Sewage Sludge Application to Acid and Calcareous Soils: Relation Between Treatment, Cadmium in Saturation Extracts, and Cadmium Uptake," *J. Environ. Qual.*, **9**, 359-64 (1980).
30. Matthews, P.J., "Control of Metal Applications Rates from Sewage Sludge Utilization in Agriculture," *CRC Crit. Rev. Environ. Control*, **14**, (1984).
31. Mattigod, S.V. and G. Sposito, Chemical Modeling of Trace Metal Equilibria in Contaminated Soil Solutions Using the Computer Program GEOCHEM," in *Chemical Modeling in Aqueous Systems*, E.A. Jenne (ed.), Symposium Series No. 93, American Chemical Society, Washington, D.C. 837-56 (1979).
32. Mattigod, S.V., G. Sposito and A.L. Page, "Factors Affecting the Solubilities of Trace Metals in Soils," in *Chemistry in the Environment*, American Society of Agronomy, Soil Science Society of America, ASA Special Publication No. 40 (1981).
33. McDuff, R.E. and F.M.M. Morel, "Description and Use of the Chemical Equilibrium Program REDEQL-2," Tech. Rep. EQ-73-02, W.M. Keck Laboratory, California Institute of Technology, Pasadena, Calif. (1974).
- 33a. Melancon, S.M., J.E. Pollard and S.C. Hern, "Evaluation of SENSOIL, PRZM and PESTAN in a Laboratory Column Leaching Experiment," *Environ. Toxicol. Chem.*, **5**, 865-878 (1986).
34. Miller, C.W. and L.V. Benson, "Simulation of Solute Transport in a Chemically Reactive Heterogeneous System: Model Development and Application," *Water Resour. Res.*, **19**, 381-91 (1983).
35. Murarka, L., "Planning Workshop on Solute Migration from Utility Solid Waste," Publication EA-2415, Electric Power Research Institute, Palo Alto, Calif. (1982).
36. Nelson, R.W. and J.A. Schur, "Assessment of Effectiveness of Geologic Oscillation Systems: PATHS Groundwater Hydrologic Model," Battelle Pacific Northwest Laboratory, Richland, Wash. (1980).
37. Nelson, D.W., D.E. Elrick and K.K. Tanji (eds.), "Chemical Mobility and Reactivity in Soil Systems," Special Publication No. 11, Soil Science Society of America, American Society of Agronomy, Madison, Wis. (1983).
38. Nordstrom, D.K., L.N. Plummer, T.M.L. Wigley, T.T. Wolery, J.W. Ball, E.A. Jenne, R.L. Bassett, D.A. Crerar, T.M. Florencce, B. Fritz, M. Hoffman, G.R. Holdren, G.M. Lafon, S.V. Mattigod, R.E. McDuff, F. Morel, M.M. Reddy,

- G. Sposito and J. Threlkild, "A Comparison of Computerized Chemical Models for Equilibrium Calculations in Aqueous Systems," in *Chemical Modeling in Aqueous Systems*, E.A. Jenne (ed.), Symposium Series No. 93, American Chemical Society, Washington, D.C. (1979).
39. Norvell, W.A., "Equilibria of Metal Chelates in Soil Solution," in *Micronutrients in Agriculture*, J.J. Mortvedt, P.M. Giordano, and W.L. Lindsay (eds.), Soil Science Society of America, Madison, Wis. (1972).
 40. Parkhurst, D.L., L.N. Plummer and D.C. Thorstenson, *BALANCE — A Computer Program for Calculating Mass Transfer for Geochemical Reactions in Ground Water*, Report USGS/WRI-82-14, U.S. Geological Survey, Reston, Va. (1982).
 41. Parkhurst, D.L., D.C. Thorstenson and L.M. Plummer, "PHREEQE: A Computer Program for Geochemical Calculations," *Water-Resour. Invest. U.S. Geol. Surv.*, pp. 80-96 (1980). (NTIS Association No. PB81 167801.)
 42. Plummer, L.M., D.L. Parkhurst and D.R. Kouir, "MIX2: A Computer Program for Modeling Chemical Reactions in Natural Waters," *Water-Resour. Invest. U.S. Geol. Surv.*, pp. 61-75 (1975).
 43. Plummer, L.M., B.F. Jones and A.H. Truesdell, "WATEQF — A FORTRAN IV Version of WATEQ, A Computer Program for Calculating Equilibrium of Natural Water," *Water-Resour. Invest. U.S. Geol. Surv.*, **76** (1976).
 44. Prickett, T.A., T.G. Naymik and C.G. Lonnquist, *A Random-Walk Solute Transport Model for Selected Groundwater Quality Evaluations*, Bulletin 65, Illinois State Water Survey, Champaign, Ill. (1981).
 45. Senesi, N. and G. Sposito, "Residual Copper(II) Complexes in Purified Soil and Sewage Sludge Fulvic Acids: Electron Spin Resonance Study," *Soil Sci. Am. J.*, **48**: 1247-53 (1984).
 46. Sposito, G., F.T. Bingham, S.S. Yadav and C.A. Inouye, "Trace Metal Complexation by Fulvic Acid Extracted from Sewage Sludge: II. Development of Chemical Models," *Soil Sci. Soc. Am. J.*, **46**, 51-56 (1982).
 47. Sposito, G., K.M. Holtzclaw and C.S. LeVesque-Madore, "Trace Metal Complexation by Fulvic Acid Extracted from Sewage Sludge: I. Determination of Stability Constants and Linear Correlation Analysis," *Soil Sci. Soc. Am. J.*, **45**, 465-68 (1981).
 48. Sposito, G., *The Thermodynamics of Soil Solutions*, Clarendon Press, Oxford, England (1981).
 49. Sposito, G., "Chemical Models of Inorganic Pollutants in Soils," *CRC Crit. Rev. Environ. Control*, **15**, No. 1 (1985).
 50. Sposito, G. and S.V. Mattigod, *GEOCHEM: A Computer Program for the Calculation of Chemical Equilibria in Soil Solutions and Other Natural Water Systems*, Dept. of Soil and Environmental Sciences, University of California, Riverside, Calif. (1980).
 51. Stumm, W. and J.J. Morgan, *Aquatic Chemistry*, 2nd ed., John Wiley & Sons, New York (1981).

52. Theis, D.L., D.J. Kirkner and A.A. Jennings, *Multi-Solute Subsurface Transport Modeling for Energy and Solid Wastes*, Dept. of Civil Engineering, University of Notre Dame, Notre Dame, Ind. (1982).
53. Truesdell, A.H. and B.F. Jones, "WATEQ — A Computer Program for Calculating Chemical Equilibria of Natural Water," *J. Res. U.S. Geol. Surv.*, **2** (1974).
54. Westall, J. and H. Hohl, "A Comparison of Electrostatic Models for the Oxide/Solution Interface," *Adv. Colloid Interface Sci.*, **12**, 265-94 (1980).
55. Wolery, T.J., *Calculation of Chemical Equilibrium Between Aqueous Solution and Mineral: The EQ3/6 Software Package*, UCRL-52658, Lawrence Livermore Laboratory, Livermore, Calif. (1979).
56. Yeh, G.T. and D.S. Ward, *FEMWASTE: A Finite-element Model of Waste Transport through Saturated-Unsaturated Porous Media*, Publication No. 1462, ORNL-5601, Oak Ridge National Laboratory, Oak Ridge, Tenn. (1981).
57. Yeh, G.T. and D.S. Ward, *FEMWATER: A Finite-Element Model of Water Flow through Saturated-Unsaturated Porous Media*, ORNL-5567, Oak Ridge National Laboratory, Oak Ridge, Tenn. (1980).

5.5 AQUATIC MODELING

Until recently, virtually all modeling studies directed at examining the migration and fate of metals have neglected important chemical interactions that control their behavior in aquatic systems. For example, a study of Pb, Cd, Zn, Cu and S movement through Crooked Creek Watershed in Missouri conducted by Munro *et al.* [31] considered only metal adsorption through the use of an equilibrium partitioning coefficient [7].

The EPA is now giving states the latitude to establish site-specific standards, in recognition of the major impacts to water quality of metal species likely to harm an ecosystem. As a result, there is a growing need for more thorough investigation of the chemical reactions of inorganic species in aquatic systems and models for calculating the distribution and activities of species in aqueous regimes.

An evaluation of the fate of trace metals in surface waters (stream, lake, estuary, coastal waters) requires the consideration of speciation, adsorption, precipitation, and other chemical reactions or processes. These processes can affect the solubility, bioavailability, toxicity, physical transport, and corrosion potential of metals. Various computerized models of the complex interactions have been developed for specific applications. This section briefly describes several metal speciation models and important limitations to their usefulness.

5.5.1 Background

Computer modeling of metal speciation in aquatic environments has developed only in the last decade, and the number of available models is small. Some are quite narrow in applicability, in that their use is restricted to certain environments — e.g., anoxic sediments, seawater, and waters overlying carbonate mineralization. The historical development of terrestrial water models for metals was shown in Figure 5.4-3.

The models that consider the speciation of trace metals in waters are equilibrium models. For natural water systems, the model must be able to establish the following for various ranges of pH, pe, ionic strength and temperature:

- Equilibrium concentrations of trace metals complexed with organic and inorganic ligands,
- Adsorption and desorption equilibria,
- Precipitation and dissolution of solids, and
- Redox equilibria.

Equilibrium constants for organometallic interactions in natural systems [41,42] are not well defined; models often incorporate organic ligands such as amino acids rather than humic and fulvic acids, which in real systems may act as the major sources of complexes of organic ligands. With regard to adsorption and desorption equilibria, the

type of adsorption surface (i.e., clays or hydrous metal oxides), and extent of surface area are important aspects of the modeling of trace metal behavior in water. Computer code flexibility (e.g., pH, pe) allows more representative computation of the equilibria in well-characterized natural waters.

We shall not deal here with details of the specific reactions included in aqueous chemical modeling, since these are treated in Chapter 2 of this report. Felmy *et al.* [6] have prepared a primer on key concepts for aqueous chemistry, with special emphasis on speciation, activity, adsorption, and solid-phase reaction as modeled by a recent EPA computer code designated MEXAMS (Metals Exposure Analysis Modeling System; see Section 5.5.4).

5.5.2 Modeling Issues

A discussion of computerized chemical models for equilibrium calculations in aqueous systems is given by Nordstrom *et al.* [32], and Jenne [17] has written an excellent essay on the goals, problems, approaches, and priorities of chemical modeling. Information from the work of these researchers is included in the following paragraphs.

There are several ways to formulate aqueous models, such as the Bjerrum ion association theory [4], the Fuoss ion association theory [9] and the Reilly, Wood and Robinson mixed electrolyte theory [37]. Each theory carries a set of assumptions and restrictions.

When using an ion association theory, which is by far the most common method, one can formulate the species distribution in two distinct but thermodynamically related ways: (1) the equilibrium constant approach and (2) the Gibbs free-energy approach. As described by Nordstrom *et al.* [32], both approaches are subject to the conditions of *mass balance* and *chemical equilibrium*.

The mass balance condition requires that the computed sum of the free and derived species be equal to the given total concentration. Chemical equilibrium requires that the most stable arrangement for a given system be found, as defined by the equilibrium constants for all mass action expressions of the system, or through the use of Gibbs free energies for all of the components and derived species. In the equilibrium constant approach, the mass action expressions are substituted into the mass balance conditions, resulting in a set of nonlinear equations that must be solved simultaneously. The Gibbs free-energy approach is simply a transformation of variables through the thermodynamic relation, which allows a different numerical approach.

Most models use the equilibrium constant approach, which utilizes measured equilibrium constants for all mass action expressions of the system. The Gibbs approach uses free-energy minimization techniques, and Gibbs free-energy values are required. In both cases, the most stable condition is sought, and a solution to a set of nonlinear equations is required. The solution involves interactive procedures, several of which are discussed by Nordstrom *et al.* [32]. The use of the Gibbs free-energy minimization approach is primarily useful for simple systems because of the limited availability of

free-energy values. The equilibrium constant approach has the advantage of a larger data base and is therefore generally preferable.

The inputs required for these models include an estimated concentration of all the species considered (usually the total concentration), partial pressures of any gases to be considered, information regarding adsorbing surfaces, the solids allowed to precipitate, the pH (which can be calculated) and the redox potential, Eh (or pe , if redox equilibria are considered). Data base requirements are further discussed in section 5.5.6.

As most of the models function similarly, their outputs are generally of a similar type. They provide the final concentration of the free ion, as well as the concentrations of complexes. The extent of adsorption, cation exchange and precipitation is also indicated, if allowed in the particular run or model. Specific outputs are discussed in section 5.5.7.

Although several computerized codes are now available and are widely applied, all have significant limitations. The general limitations are described in the next section, followed by reference to specific modeling codes.

5.5.3 Modeling Limitations

Nordstrom *et al.* [32] and Jenne [17] cite a number of major factors that limit the effectiveness of models. One is that all the models assume equilibrium conditions; that is, the kinetics of precipitation, oxidation-reduction and adsorption are ignored. This may not be a valid assumption in some cases, because of kinetically unfavorable chemical processes, biological transformation, and physical transport. However, it provides a good approximation of some environments, such as the hypolimnion of a thermally stratified lake, where most of the above chemical reactions are assumed to be kinetically rapid for modeling purposes.

As the outputs of these models are strongly related to their inputs, the characterization of the situation to be modeled will directly affect the results obtained. In this respect, models are more dependably used in a descriptive way and "after the fact" (i.e., to reproduce an existing situation); they may have limited applicability if used in a predictive way (with default generalized data) for a specific future environment. In some cases, the input data are also limited by the state-of-the-art, such as in the characterization of organic matter in natural systems.

For all models/codes there can be large variation in the stability constants for the same reaction. These differences can dramatically affect the results, as shown by Nordstrom *et al.* [32] for 15 models applied to two test cases (a river water and a seawater). The authors attributed the largest source of differences between predicted and observed values to the fact that the thermodynamic data (equilibrium constants) used by the various codes varied by up to three orders of magnitude. Concerted efforts are now being made to develop consistent and documented data bases.

Most equilibrium constants are measured at 25°C, and most models are applicable only at that temperature. Other temperatures can be used in some models, but the activation energy data base required to adjust equilibrium constants is somewhat limited [13].

The calculations are valid over a specific range of ionic strength; approximations become more inexact as ionic strength increases. At high ionic strength, different approaches are needed, and various forms of the Debye-Hückel or Davies equations are used [17]. In addition, assumptions about redox conditions may not be realistic. (The user must choose which redox reactions to consider and the dominant redox potential.) Nordstrom *et al.* [32] recommend that redox reactions be analyzed separately in some cases. The total number of complexes considered by an aqueous model affects the overall output.

The modeling of adsorption is not well developed, owing to a general lack of understanding of the phenomenon. In addition, surface modifications may cause solids in natural systems to behave quite differently from pure phases [6,13]. Modeling of the adsorption process is accomplished via equilibrium constants, which are frequently estimated in the laboratory and later adjusted in real work applications.

Harris *et al.* [13] report that at very low concentrations, which may be of particular interest to the user, inaccuracies may result from computational limitations. In addition, the validity of models at high or low concentrations and in real-world applications is largely untested because of inadequate analytical capabilities for measuring dissolved species. Monitoring and model validation programs have recently been established by the EPA for the MEXAMS model [7].

Other important restrictions on the usefulness of chemical models are the limited capability to characterize organic ligands in natural waters, the scarcity of thermodynamic data, limitations in scientists' training, inadequate literature reviews, and the lack of integrated studies.

There is no general-purpose model that can be used for all applications. While there are numerous limitations to the use of equilibrium models, the general consensus is that they can provide useful results if applied correctly and with an understanding of the differences between simulated and real systems.

Users tend to employ models that are well documented, have an integrated or thorough data base, and are supported by an organization. Remarkable support for water quality modeling in the United States has been provided by the EPA's Environmental Research Laboratory in Athens, Georgia. The recently developed model MEXAMS, for example, was supported by this organization.

5.5.4 Model Codes

Nordstrom *et al.* [32] have surveyed over 30 computer codes and described the features of 14 of them. Therefore, this information is not duplicated here. Some of these codes were specifically developed for "water quality" models; others were developed to be "geochemical" (soil moisture or groundwater quality) codes.

Although certain terrestrial (geochemical) codes (e.g., GEOCHEM) can be used to simulate the speciation and fate of metals in a water body by "tailoring" the size of a model compartment (e.g., sediment) to reflect the size of the corresponding compartment of the water body, codes specifically developed for aquatic modeling should be used.

The models REDEQL2, WATEQ2, MINEQL and MEXAMS are now available and widely accepted, applied, supported, and validated. Various versions of these models exist in the literature also (e.g., [13,38]). Table 5.5-1 summarizes some major features of the four models discussed below; interested readers should refer to the original works for details.

REDEQL2

REDEQL2 is an offspring of REDEQL (see Figure 5.4-3) developed by Morel and Morgan at the California Institute of Technology [28]. The University of Minnesota in Duluth undertook modifications and improvements to the program in 1978-1982.

General Features

REDEQL2 is a multiphase, multicomponent aqueous equilibrium program that can impose metal precipitation and dissolution and simulate adsorptive behavior. It is currently able to model systems at 25°C and has an enthalpy data base to broaden this aspect of the program. According to model developers, REDEQL2 can be used for both laboratory and natural systems. Its application may handle metal speciation in algal culture media, degradation of NTA in natural waters, metal speciation in sewage oxidized and diluted by seawater, zinc speciation with regard to toxicity to fish, and metal speciation relative to changes in the Great Lakes [35].

As of May 1985, the data base for REDEQL2 included 36 metals, 65 ligands, 212 solids, 2239 complexes (of which 113 are ternary) and 22 redox reactions. To model water quality, the chemical equilibrium and redox equilibrium constants are needed at infinite dilution ($I = 0$) at 25°C. Constants are adjusted by the model for various ambient temperatures. Since most data are also measured at a higher ionic strength, the program makes certain adjustments. The University of Minnesota researchers added an ability to handle ternary complexes (M, L, L_k or M, M, L_k) in which H^+ and OH^- are not M or L , respectively. Some equilibrium constants for these complexes are not well known and must be measured. The REDEQL2 program can accommodate redox equilibria in which the reaction causes the ion to reverse charge, such as Cr^{+3} going to CrO_4^{2-} .

TABLE 5.5-1
Descriptive Features of REDEQL2, WATEQ2, MINEQL and MEXAMS

Parameter	REDEQL2 ^a	WATEQ2	MINEQL	MEXAMS ^b
Model type	Equilibrium constant	Free energy minimization	Equilibrium constant	Equilibrium constant
Metals	36	26	34	7
Ligands	65	80	57	More than 80
Organics	Amino acids	Fulvate and humates	14 Amino acids	Amino acids
Complexes	2239	220	Almost unlimited	Almost unlimited
Ternary	113	—	No	No
Minerals	$\text{Pb}_5(\text{SO}_4)_3\text{Cl}$, Chlorite, illite, Na-montmorillonite, dolomite, microcline	309-all types	Allowed as inputs	Allowed as inputs
Gases	CO_2 , N_2 , O_2 MnO_2 , $\text{Fe}(\text{OH})_3$, TiO_2 , SiO_2	CO_2 , O_2 , CH_4 No	Allowed as inputs	Allowed as inputs
Adsorption surfaces			No	Six algorithms (various surfaces)
Redox reactions	22	12	Davies	18
Activity coefficient	Magnuson or Davies	Extended Debye-Hückel or Davies	Davies	Extended Debye-Hückel
Temperature	25°C	0-100°C	25°C	25°C
Inorganic carbon	Controlled by pCO_2 , $\text{HCO}_3\text{-Alk}$ or input []	Calc. from $\text{HCO}_3\text{-Alk}$	Cc , controlled by pCO_2 , $\text{HCO}_3\text{-Alk}$ or input []	Controlled by pCO_2 , $\text{HCO}_3\text{-Alk}$, or input []
pH	Fixed or variable	Field sample pH	Fixed or variable	Fixed or variable
Solids not allowed				
To precipitate	Yes	No	Yes	Yes
Iterations	Less than 2000 (Newton-Raphson)	Less than 40 (back substitution)	Less than 2000 (Newton-Raphson)	Less than 2000 (Newton-Raphson)
Inputs	[], Redox rxns, ionic strength, solids	Complete chemical analysis of water, trace elements	Same as REDEQL2	Chemical analysis of water, pH, dissolved O_2

a. [] = "concentration(s)"

Adsorption in REDEQL2 is calculated using the James-Healy approach; the dielectric constants of the solids are important surface characteristics. The free energy of adsorption is used as the fitting parameter. SiO_2 , MnO_2 , Fe(OH)_3 and TiO_2 were chosen as sorption surfaces, because (1) with the exception of TiO_2 , all are thought to be commonly occurring sorption surfaces in soils, (2) they are available and used for laboratory work, and (3) data are available for these species.

Input parameters of REDEQL2 include the concentration or activity of each metal, ligand, and solid; the ionic strength, if it is to remain fixed; the pH, also if fixed; the redox reactions; the solids prohibited from precipitating; the adsorption surface area and adsorption surfaces; and (optionally), the pe, CO_2 , and N_2 . Some options available to the user are detailed below.

Multicase Runs

The program can handle a set number of ligands and metals per case run. Up to ten cases may be run at the same time; however, the free-ion concentrations resulting from the previous run must be used as input to the next run. To prevent dissimilar parameters between case runs, the types of metals and ligands are fixed, and non-precipitable solids, redox reactions and charge-balance ions are not permitted to change. The pe, total concentrations, gaseous partial pressure, and pH are allowed to vary.

Charge Balance at Fixed pH

The overall charge of the final solution calculated for a non-fixed pH is balanced by adjusting the hydrogen and hydroxide ion concentrations to achieve a charge-balanced solution. If the pH is kept constant, the program continues to adjust the concentrations of one or more chosen ligands until the charge of the solution is less than 0.1% of the ionic strength.

pH Calculation

The pH of the final solution may be calculated with each interaction or remain fixed throughout. The user is cautioned against the former option for waters that cannot be exactly characterized, such as natural waters. Since the pH is determined by balancing the charge of all the metals, ligands, and electrons, the exact concentration of these components must be known to obtain a meaningful pH; therefore, the calculated pH option is best used for laboratory waters only.

Inorganic Carbon

The partial pressure of CO_2 , carbonate alkalinity and total inorganic carbon are the three options available to the user to control the inorganic carbon (H_2CO_3 , HCO_3^- , and CO_3^{2-}) distribution in the program. The alkalinity case is usable only for options in which the pH is fixed and in sample runs containing no carbonate solids. The CO_2 option determines the amount of inorganic carbon dissolved in solution at a fixed pH.

One drawback of this option is that CO_2 will be drawn from the atmosphere if the solution is undersaturated with respect to CO_3^{2-} . To avoid "draining" the atmosphere of CO_2 , the concentration of CO_3^{2-} is increased by the program until the situation is alleviated.

Ionic Strength

The ionic strength of the solution, if not fixed, is calculated at the end of the program for the new concentrations of metals and ligands. If the ionic strength has changed more than 0.5% from the initial input value, the program will resume calculations using thermodynamic data adjusted to the new ionic strength.

Redox Reactions at Fixed Potential

REDEQL2 calculates the redox reactions for the specified set of reactions from potential data input as dissolved O_2 , pe, or Eh (volts). A fixed pH must accompany a fixed potential, since chemical speciation is dependent on both parameters. Again, knowledge of possible redox reactions is required in selecting redox reactions to be included in the program; typically, the program can accommodate only two or three reactions of this type, so it is best to avoid including one that is not dynamic for the given pe and pH. Accordingly, if the concentration of an ion involved in a redox reaction is less than 10^{-10} M at the pH and pe of the system, or if the redox species form a ratio of less than 10^{-8} or greater than 10^5 , the reaction should be excluded from the program.

Redox Reactions with Changing Potential

This option is usable only at a variable pH, since some reactions cause changes in both the pH and the potential. The initial redox state and concentrations of the participating redox species must be specified in order to use this option.

Minerals

REDEQL2 includes data in its thermodynamic data file for six alumino-silicate clays, which can be present in either the suspended or solid state [25].

WATEQ2

WATEQ2 is a model of the WATEQ-series [40] that evolved from WATCHEM (Figure 5.4-3) and is designed to accept water analysis with on-site values for pH, Eh, and temperature [2,3]. It is essentially a water-rock equilibrium model in which almost every conceivable ore and mineral containing a trace metal is included.

WATEQ2 is a Gibbs free-energy minimization program in which the anion concentrations are juggled until the difference in Gibbs energy between calculation steps is within 0.1% of the input concentrations. The thermodynamic data base is of substantial size and concerns solid forms of trace elements, polysulfides, metastable

solids, sparingly soluble salts and complexes of major ions. Organic ligands are incorporated as groups of molecular weight 6550 g/mole or 2000 g/mole to simulate fulvate and humate ligands. Twelve redox reactions are included.

The required inputs are standard water parameters such as conductivity, dissolved solids, dissolved organic carbon, salinity, and the following species: Fe (II and III), Mn (II), Cr (II), Zn (II), Cd (II), Pb (II), Ni (II), Ag (I), As (III, V, total), Cs (I), Rb (I), Li (I), Ba (II), Sr (II), I, Br, and dissolved O₂. The outputs are the concentration in ppm, molality, activity, and the activity coefficient. The program calculates a standard deviation from errors propagated from analytical and thermophysical data.

MINEQL

MINEQL [43] evolved from REDEQL [28], aiming to be a more compact program of greater clarity and flexibility. At present, it cannot accommodate adsorption equilibria, but a subroutine is being devised [35]. The input ligands and metals are classified according to phase and solubility, and each ion or complex is placed in one of the following classifications:

- Type I — Soluble components (e.g., metals)
- Type II — Soluble complexes (e.g., CO₃²⁻)
- Type III — Precipitated solids not allowed to dissolve (includes gases)
- Type IV — Precipitated solids that dissolve

Presently, MINEQL has 50 cations and 198 neutral and anionic ligands in its thermochemical data bank. Creation of new species or modifications of formulation constraints indicate the flexibility of the program, in that only two of the three needed parameters (species, equilibrium constant and the type of category) will prompt these changes.

MEXAMS

MEXAMS, the Metals Exposure Analysis Modeling System [6], provides an enhanced capability for assessing the impact of priority pollutant metals on aquatic systems. It allows the user to consider the complex chemistry affecting the behavior of metals in conjunction with the transport processes that affect their migration and fate. This is accomplished by linking MINTEQ, a geochemical model, with EXAMS, an aquatic exposure assessment model.

General Features

MINTEQ is a thermodynamic equilibrium model that computes aqueous speciation, adsorption, and precipitation/dissolution of solid phases [6,7]. It has a well-documented thermodynamic data base that contains equilibrium constants and other accessory data for seven priority pollutant metals: As, Cd, Cu, Pb, Ni, Ag and Zn. The model was developed by combining the best features of MINEQL and WATEQ4. EXAMS, which was designed for the rapid evaluation of organic pollutants in water bodies, was modified to achieve linkage to MINTEQ.

Applicability

MEXAMS was developed to provide EPA with a predictive tool capable of performing screening-level analyses, but it can also be used on a more site-specific basis to investigate potential impacts of different metal sources such as industrial discharges or mine drainage. An example of the former is a study by Morel *et al.* on the fate of trace metals discharged from a Los Angeles County treatment plant [7].

According to the model manual, other applications of MEXAMS relate to improving the information available from bioassays and involve the use of the model to identify what is and what is not known about the behavior of priority pollutant metals in aquatic systems.

Limitations

Despite the many capabilities that both MINTEQ and EXAMS offer, model developers report several limitations that MEXAMS users should be aware of: (1) MINTEQ's thermodynamic data base contains equilibrium constants and accessory data for only seven pollutant metals (As, Cd, Cu, Pb, Ni, Ag, Zn); (2) the data base contains no data for processes of inorganic complexation; (3) only equilibrium processes that govern the kinetics of precipitation/dissolution, oxidation/reduction, and adsorption are considered; (4) MEXAMS has been tested on only relatively simple problems.

Guidelines for Use

MEXAMS is available in an interactive mode; in fact, the user can separately employ MINTEQ or EXAMS via an interactive process. In MINTEQ, species are assigned to one of four categories: species complex, fixed species, dissolved solids subject to precipitation, and species not considered. MINTEQ contains six algorithms for calculating adsorption, and the user must provide data and algorithm selection.

The more data the user has on the water chemistry of the system, the more accurate will be the predicted results. This does not mean that the user must have data for all the components to be simulated, since the default data base may substantially facilitate operations. However, certain parameters are of greater importance and should be given special attention; these are: pH, Eh (pe), temperature, ionic strength, major anions, major cations, trace constituents (H_2S , PO_4^{3-} , F^- , Fe (II), Mg (II), Al (III), Ba (II), Sr (II), other). The MEXAMS and MINTEQ manuals provide detailed information on the above topics.

5.5.5 Availability/Suitability of Codes

Of the codes previously discussed, MEXAMS receives the strongest support (from EPA's Environmental Research Laboratory). REDEQL2 appears to have the strongest data base and to be suited for many purposes. WATEQ2 is restricted to calculating metal-ligand equilibria for overlying rock formations, while MINEQL2 appears to offer great flexibility and compactness. There is no general guidance as to which code should be used for a specific situation; the user must either review reported codes and

select the one that is suitable to the relevant metals and ligands, or he must consult an organization that supports a model and request assistance for a site-specific application.

5.5.6 Data Availability for Models

As previously mentioned, the types of reactions considered in REDEQL2 and equivalent models include metal ion hydrolysis, ligands, protonation, complexation, precipitation, redox and adsorption. Each such reaction can be described quantitatively by a stability or formation constant that relates the concentrations of reactants and products. At the computed equilibrium, all equilibrium constant expressions are satisfied simultaneously, and the sum of the individual species of metals and ligands is equal to a fixed total concentration. The input data required for this computation include: (1) total concentrations of all metals and ligands to be considered, (2) equilibrium constants for the types of reactions described above, (3) ionic strength, which may be calculated or specified, (4) pH, which also may be calculated or specified, and (5) redox potential in the case of redox reactions.

The fact that models have sometimes been used quite successfully indicates that data are available for some cases. However, most of the waters that may have to be modeled are not well characterized, making the use of models difficult in terms of calibration and validation. The following sections discuss some of the problems that may be encountered.

5.5.7 Issues Related to Modeling

TOTAL CONCENTRATION OF METALS AND LIGANDS

For any given system that the model is intended to represent, the concentrations of all ligands present in the system which can significantly complex any or all of the trace metals present must be known. A considerable body of knowledge on thermodynamic data and/or the complexes that are formed has been built up through the study of simple systems containing one metal and one ligand at concentrations higher than those ordinarily found in natural water.

However, natural systems are considerably more complex in terms of the diversity of trace metal species that may exist and the extremely low concentrations of individual species. Until recently, most workers used stability constants singly or in pairs to enable them to calculate the equilibrium concentration of a particular species. In recent reviews of trace metal speciation, however, researchers have noted that this procedure is invalid, since any natural water contains many metals capable of reacting with each ligand and many ligands that can react with each metal. The correct equilibrium concentration of any species can be computed only by simultaneously taking into account all the competing equilibria.

STABILITY CONSTANTS

The extent of complexation of trace metals in solution can be calculated if the concentration of ligands and the stability constants of the appropriate reactions are known. Unfortunately, the stability constants of all possible complexes have not been measured. Sibley and Morgan [39] cite the example of borate complexes, for which stability constants are not available, and chloro-complexes of copper and lead, which have several reported constants for the same complex.

IONIC STRENGTH

The equilibrium quotient is not constant for all concentrations when analytically measured values are used, because the behavior (concentration vs. activity) of dissolved participants in chemical reactions is not "ideal." (See section 2.6.)

Some measurement techniques serve to determine directly the activity of a particular ion. Ion-selective electrodes, for example, are available and can measure the activities of a large number of cations and anions of interest in natural water. The first of these electrodes to be developed, and still the best known, is the glass electrode, which has been used for many years to determine the hydrogen ion activity (pH) of solutions.

If direct measurement of the activity of an ion is not possible, it can be calculated by multiplying the activity coefficient by the analytically determined concentration of the ionic species. (See section 2.6.) The method commonly employed for this calculation uses some form of the Debye-Hückel equation, which involves, in turn, determination of a quantity defined as the ionic strength. The importance of this fact to the investigator concerned with modeling natural or laboratory water systems is that the required equilibrium constant data are usually specified for solutions of zero ionic strength.

In solutions containing less than 50 mg/l of dissolved ions, activity coefficients for most ions are 0.95 or more. In such dilute solutions, activity values are equal to measured concentrations (within ordinary analytical error). If concentrations are near 500 mg/l of dissolved solids, the value of the activity coefficient may be as low as 0.70 for divalent ions. At the maximum ionic strength where the Debye-Hückel equation can be accurately used, the activity coefficients for some divalent ions may be less than 0.50 [14]. For the concentration ranges of principal interest in natural water chemistry, the Debye-Hückel equation and equilibrium constants applicable at zero ionic strength provide sufficient accuracy.

However, investigators working with more highly concentrated solutions who elect to use the models in the mode in which ionic strength is specified have no choice but to use constants that are directly applicable to those solutions. As noted in the user's guide for REDEQL, the usual approach is to allow the program to calculate ionic strength (unless one is working with a solution of very constant (and well known) ionic strength, such as seawater), because ionic strength is difficult to estimate accurately without knowing the concentrations of all the species present.

pH

Like ionic strength, the pH of the solution under consideration can be either specified or calculated by the program. Also, as with ionic strength, if the pH value is specified, it must be carefully interpreted. As noted by Hem, the pH of a water sample represents the interrelated results of a number of chemical equilibria, which may be altered by the sampling operation: "A pH measurement taken at the moment of sampling may represent the original equilibrium conditions . . . satisfactorily, but if the water is put into a sample bottle and the pH is not determined until the sample is taken out for analysis some days, weeks, or months later, the measured pH may be influenced by other reactions such as oxidation of ferrous iron, and the laboratory pH can be a full unit different from the value at the time of sampling. A laboratory determination of pH can be considered as applicable only to the sample solution in the sample bottle at the time the determination is made." [14]

pe

In computations in which redox reactions are to be considered, a value for pe (the negative logarithm of the electron activity) must be specified. Field and laboratory measurements of the redox potential, Eh, from which pe is calculated are subject to misinterpretation in much the same way as are pH measurements. The redox potential of sample solutions exposed to air can be affected by atmospheric oxygen. Measurements on reducing systems, such as groundwater containing a mixture of ferrous and ferric iron, can be made to give meaningful answers only if oxygen is very carefully excluded from all parts of the sampling and measuring system [14].

SUSPENDED SOLIDS

Inorganic species such as common clay minerals, hydrous oxides of iron and manganese, silica, and sulfides present as suspended particulate matter in natural waters [4] have been shown in both laboratory [19] and field [21] studies to be able to adsorb significant quantities of trace elements from solution. Models that consider adsorption on suspended solids may allow only for simple precipitation, which does not involve occlusion or adsorption of other trace metals by the precipitate.

In some of their modeling efforts, Sibley and Morgan [39] described adsorption in terms of the James-Healey model for aqueous metals and oxide surfaces. In that approach, adsorbing surfaces are treated as ligands, and the adsorption process is described as a metal-ligand equilibrium. They concluded that significant quantities of certain metals could occur in fresh waters as adsorbed species, and that trace metal speciation is, in fact, determined primarily by competition between adsorption and complexation.

Most reports in the recent literature agree with the conclusion of Florence and Batley [8]: "In the past, the presence of soluble, stable metal-organic complexes in natural waters has been overemphasized at the expense of appreciation of the influence of colloidal particles, both organic and inorganic . . . almost nothing is known about the

concentration of organic and inorganic colloidal particles or their metal-binding ability. For these reasons the results from even the most sophisticated computer model of trace metals speciation in natural waters bear little, if any, relation to reality."

While the above statement may be overly harsh, the representation of adsorption clearly presents a stumbling block to the modeling of at least some waters.

ORGANIC SPECIES

It is now well known that a number of organic materials of both natural and anthropogenic origin are capable of complexing with several heavy metals (e.g., copper and iron) and thereby affecting environmental reactions such as bioavailability. A number of studies have investigated this phenomenon.

A statement by Jenne [17] aptly summarizes the applicability of currently available data to chemical modeling of heavy metal speciation in aquatic systems: "The information being developed in these studies has not been shown to be particularly useful to quantitative chemical modeling . . . Complexation capacity values have served to identify and dramatize the potentially important role of dissolved organic compounds as ligands capable of promoting the solubilization and hydrologic transport of trace elements. However, there seems little point in continuing these determinations, since their magnitude is now known and it is not apparent how they can be used in quantitative chemical modeling."

A similar conclusion was reached by McCrady and Chapman [24] after a study of the copper-complexing capacity of several natural waters: "The theoretical equilibrium approach for predicting free cupric ion concentrations in natural waters, utilizing REDEQL, should be used with caution, realizing that at best, quantitative results might be obtained at the higher copper concentrations. At the present time, it is not possible to quantitatively predict and model the effect of a vast array of organic interactions in natural water."

What is required for modeling efforts are measurements of the molar concentrations of the complexing organic species (in different surface waters and at different times), their stability constants for the trace metals of concern, and the effects of pH, ionic strength and temperature on these stability constants. The situation will be much simplified if it is found that there are only a few important natural organic ligands for each metal.

A number of stability constants for metal-natural organic complexes have been reported for a few metals (see below); however, the values for a particular metal can vary widely and could be expected to account only qualitatively for the complexation phenomena in a modeling effort.

- *Organic Chemicals in Surface Waters* — In surface waters free from significant amounts of man-made pollution, a large majority of the

dissolved organic carbon (DOC) is of natural origin; fulvic acid, humic acid, tannins and lignins are usually the major components [20]. The total concentration of these species (DOC) in natural waters may range from several parts per billion to several hundred parts per million [18], though a more common range is probably 2-20 mg/l. Particulate organic carbon (POC) will also contain chemicals capable of complexing or adsorbing metals. POC concentrations may in some cases be higher than DOC concentrations, but the effective surface area and adsorption capacity are lower.

Humic and fulvic acids are amorphous, yellow-brown or black, hydrophylic, polydisperse substances of wide-ranging molecular weight (<10,000 for fulvic acid, 10,000-30,000 for humic acid) [20]. Tannins and lignins are high-molecular-weight polycyclic aromatic compounds and are highly resistant to biological degradation [20]. A significant amount of this material is probably present in macromolecular or colloidal form [10]. In one study of pond waters, approximately 70% of the total organic carbon was in the filtrate fraction that passed a 0.0032 μm (nominal pore diameter) filter but was retained on a 0.0009 μm filter [11].

In surface water, without strong vertical mixing, these organics — with their complexed metals and other adsorbed pollutants — may be concentrated in the surface microlayer. Some anthropogenic (organic) pollutants may also act to bind heavy metals in waters, but no literature data support this conjecture.

- *The Complexation Process* — The most probable reaction mechanism between humic compounds and metal ions is the formation of complex bonds with carboxyl and phenolic groups [18]. Information on this subject is presented in section 2.9.
- *Stability Constants* — The literature and the data bases of models list a number of stability constants (in terms of log K) for various metal ions with humic (HA) and fulvic (FA) acids. It should be noted that many of these values were measured under acidic conditions that are seldom found in natural waters. The values of K are a function of pH and ionic strength. In general, K increases with increasing pH and decreases with increasing ionic strength [18]. Also, the values of K obtained for humic and fulvic acids are usually much smaller than those associated with man-made chelating agents such as EDTA, NTA, NEDTA and CDTA; thus the latter values should not be used as surrogates in chemical modeling.

The preceding paragraphs have described some of the limitations associated with modeling aquatic systems. While these are important considerations, they should not prevent the use and continued development of such models.

5.5.8 Model Applications

The first equilibrium models were developed for use in seawater, but their use has now expanded to many applications in fresh waters, both groundwaters and surface waters. These are briefly discussed below.

MODELING OF LABORATORY AND NATURAL WATERS

Computer equilibrium models have been used to predict the speciation of metals in natural waters in order to estimate the toxic effects of contaminants on water quality and biota (e.g., refs. 10,22). For example, Pagenkopf [33,34] used the COMICS program to determine zinc speciation in laboratory test waters; similarly, Andrew *et al.* [1] used REDEQL to determine speciation of copper in Lake Superior water.

Magnuson *et al.* [23] reevaluated the data used by Andrew *et al.* with REDEQL2 and found that the inclusion of new species, especially $\text{Cu}(\text{OH})_2^0$, greatly changed the predicted speciation, since this species then became dominant. These authors also performed a sensitivity analysis using a three-metal, three-ligand system; by varying pK by 0.05 unit, they produced concentration changes of 6-30%. Both of these studies used measured dissolved copper as the input, and no adsorption, organic complexing, or precipitation was allowed. In addition, no analytical work was conducted in conjunction with the modeling to verify the results.

Glass [12] also used REDEQL2 to model Lake Superior water, choosing citrate as a representative ligand in place of organic carbon. EDTA, NTA and cysteine were included to illustrate trace quantities of organic ligands. The author stated that these results (Table 5.5-2) agree generally with what is known about chemical speciation in Lake Superior; for example, less than 1% of total copper is measured as the free ion, as predicted by the model. Precipitation and adsorption were not considered in this study.

McCrady and Chapman [24] used RFDEQL2 to compare copper speciation in reconstituted water, well water and natural river waters. No adsorption, precipitation, or complexing with organics was allowed. A cupric ion electrode was used to determine the concentration of that species analytically. These authors found that the model predicted the concentration of the cupric ion quite well in the reconstituted water and the well water, but the concentrations predicted in river water showed poor agreement with the measured concentrations at low levels (0.1-0.5 m moles/liter); the ratio of measured copper ion to computed copper ion ranged from 0.02 to 0.26 at these levels. Agreement improved at higher copper concentrations and was better in some rivers than in others.

Hoffman and Eisenreich [15] used a modified version of REDEQL2 to determine the source of variation of iron and manganese in the hypolimnion of Lake Mendota. They included three adsorbing surfaces (SiO_2 , MnO_2 , and Fe_3O_4) and organic complexes with citrate, sulfosalicylate, glycine, phthalate, and dipyridyl. The concentrations of these organics were based on one-tenth of the DOC concentration according to the equivalents of carbon for each ligand. Numerous solids were allowed to precipitate.

TABLE 5-5-2
Calculated Distribution of 18 Metals and 12 Ligands in Lake Superior Water^a

Ligand:	H ₂ O	OH	CO ₃	Cl	SO ₄	SiO ₃	PO ₄	NO ₃	CIT	EDTA	NTA	CYST
Total —	- 1.74	- 1.74	3.058	4.442	4.438	4.350	7.490	4.784	6.00	25.0	25.0	25.0
↓	Free —	6.17	5.41	4.44	4.46	11.36	12.23	4.78	16.13	36.88	28.77	28.11
	Metal											
Ca	3.487	3.50	7.93	5.19(2)	b	5.82	b	9.18	b	6.08(3)	28.08(2)	25.29
Mg	3.959	3.97	7.40	5.63(2)	b	6.20	b	9.15	b	7.36(2)	32.06(2)	26.77
Na	4.252	4.25	b	8.55	b	8.11	b	b	b	38.50	31.74	b
K	4.889	4.89	b	b	b	8.34	b	b	b	b	b	b
Sr	6.75	6.75	11.58	b	b	b	12.74(2)	b	10.13	32.93(2)	29.84	b
Ba	7.0	7.00	12.03	b	b	b	b	b	26.78	33.98(2)	30.50	b
Fe(II)	7.268	1.861	9.30(3)	b	21.77(3)	19.20(2)	14.45	18.27	b	26.80(3)	26.15(3)	43.52
Cr(II)	7.796	11.23	11.35(5)	10.09(4)	12.83(5)	13.56	b	15.51(2)	b	7.80(3)	27.22(3)	26.72(2)
Zn	7.959	8.18	9.38(5)	8.40(2)	11.22(5)	10.51	b	13.28	b	11.35	26.37(2)	25.78
Mn(II)	8.26	8.29	10.62(2)	9.55	11.72(3)	10.61	b	12.97	b	11.07(2)	28.97(2)	29.08
Cr(III)	8.420	15.82	8.42(3)	b	19.58(2)	17.81	b	14.67	b	26.01(3)	b	b
Rb	8.47	8.90	9.83	8.91(2)	12.93(2)	11.22	b	14.27	b	9.13(3)	25.08(3)	25.79(2)
Co(II)	8.47	6.73	10.14(3)	8.84(2)	11.86(2)	10.85	b	14.01	b	26.11(2)	27.21(2)	26.32
Pb	9.015	10.88	10.79	9.03	13.58	12.80	b	b	b	11.83	27.56	27.27
Cd	9.745	10.00	12.23(6)	10.12(2)	12.30(5)	12.32	b	18.56	14.17	11.57(3)	28.18(3)	28.09
Ag	10.0	10.02	14.22(2)	b	11.41(4)	13.47	b	b	19.39	38.62(2)	b	b
Hg	10.30	19.67	10.31(5)	13.94(2)	11.81(5)	21.90(2)	b	b	37.96	32.65(3)	33.01(2)	32.85
Cr ₂ O ₇	11.30	12.35	22.65(2)	b	11.34	b	b	b	b	b	25.45	
Fractionated ligand		- 1.74	3.08(2)	b	10.13	4.35(2)	7.51	b	7.23(4)	33.46(3)	27.18(3)	25.22(3)

^a Values are the relative logarithm of the concentration (moles/liter). Values in parentheses are numbers of different complexes that contain the ligand in the total metal-ligand concentration. CIT = citrate; a representative organic ligand in place of humic acids. EDTA = ethylenediaminetetraacetic acid.

NTA = nitrilotriacetic acid. CYST = cysteine. Cr₂O₇ = mercuric oxonate, pH = 7.8.

b Stability constants for these complexes were not available.

Source: Gross [12]. Copyright 1977 New York Academy of Sciences. Reproduced with permission.

The calculated manganese concentrations agreed well with the trend in observed values. The authors concluded that the variations in total manganese concentration were due to pH-dependent dissolution of solid MnCO₃. The pH-dependent desorption from oxide surfaces was apparently of secondary importance.

OTHER USES OF EQUILIBRIUM MODELS

There have been a few, somewhat peripherally related uses of water body models. Some of these applications deal with soil quality (e.g., speciation in groundwater). Potter *et al.* [36] used SOLMNEQ and WATEQ to predict *in situ* leaching of uranium ore bodies. The models were not able to predict uranium concentrations very well, primarily due to the lack of consideration of kinetics and adsorption.

Minear and Rose [27] used WATEQF, MINEQL, and REDEQL2 to calculate metal speciation in coal mining spoil bank groundwater. Numerous solid phases were included in this analysis. The authors concluded that well samples were undersaturated with respect to the solid phases considered, implying that the system was not controlled by dissolution equilibrium.

Richter and Theis [38] used REDEQL2 to determine speciation and adsorption of heavy metals in fly-ash leachate, using silicon, iron, and manganese oxides as the adsorbing surfaces present. The soluble metal concentrations measured at the wells agreed favorably (within one-half log unit) with the calculated values.

Mouvet and Bourg [30] used the European model ADSORP to study adsorption and speciation of trace metals on sediment of the Meuse river; Pb, Ni, Ca, Mg, Cu and Zn were investigated. Calculated values of the adsorbed/dissolved distribution agreed well with observed values after some realistic data manipulation. This work indicates that dissolved trace metal concentration in the river is controlled by adsorption, not by a precipitation mechanism, and that the relationship between organic matter and suspended matter greatly influences the adsorption of such metals as Cu and Pb.

Finally, an application of the MEXAMS model for metal speciation and fate is being conducted for the Eight Mile River, Connecticut. The program is sponsored by the EPA and is executed by the state of Connecticut (Department of Natural Resources), under the support of the New England Interstate Water Pollution Control Commission (NEIWPCC, Boston). Model simulation results are expected by the end of 1986.

5.5.9 Example of Model Application

This example deals with the use of a model to estimate chemical speciation of trace metals in seawater. The metals originate in a wastewater treatment plant. The example is adapted from a study by Morel *et al.* [29] for Los Angeles County. It is presented in four sections:

- (1) Problem statement,
- (2) Field monitoring,

- (3) Model application, and
- (4) Discussion of results.

PROBLEM STATEMENT

The Joint Water Pollution Control Project (JWPCP) of the Los Angeles County Sanitation District discharges approximately 370 mgd of wastewater into the sea. The sewage consists of both domestic and industrial wastes containing high metal concentrations, whose effects on aquatic life are dramatic and easily measured. For example, chromium and lead are highly concentrated in both the sewage and the seawater at a ratio of C (sewage)/C (seawater) of about 4,000 and 6,000 respectively. These high values initiated a project aimed at mathematical modeling of the speciation of trace metals discharged.

The sludge from the JWPCP sewage treatment is fairly typical of that produced by primary treatment techniques. The sedimented sludge is digested anaerobically and is then centrifuged. The centrifugate is remixed with the primary effluent, contributing much of its particulate — and metal — load.

The primary sewage effluent is discharged via two submarine outfalls (a 90-inch "Y" and a 120-in. "dog leg") at a depth of 60 meters at the edge of the continental shelf. The rise of the plume as well as the dilution of sewage by seawater were well studied during the field monitoring program.

FIELD MONITORING

The sewage composition and aquatic environment were monitored at the plant, and a study of the metal concentrations in the nearby sediments was made; thus, an experimental data base was available for model application and validation.

Table 5.5-3 gives the average concentration and mass emission rates in the treated effluent of 11 metals selected for the modeling application.

MODEL APPLICATION

REDEQL, a general program for the computation of chemical equilibrium in aqueous systems [26], was selected for the modeling effort. Model selection was based on both the experience of the researchers with the particular package and the adequacy of data in the model's database.

Since the model did not account for the ligands of primary interest, a set of representative organic ligands and an absorbing surface have been added (Table 5.5-4). Addition of data to the database of a speciation model is to be expected in such modeling efforts; these data must be compiled and put into the system, with the assistance of the model developer or the agency that supports the model (e.g., the EPA).

TABLE 5.5-3
Trace Metals in JWPCP Sewage Outfall

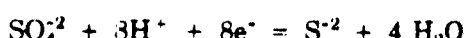
	Estimated Concentration ($\mu\text{g/l}$)			Mass Emission Rates to So. Calif. Bight (tons/yr)			JWPCP/ Total Ratio
	JWPCP ^a Sewage	So. Calif. ^b Seawater	Sewage- seawater Ratio	JWPCP ^c	Total ^d		
Fe	9900	10.0	1000	5300	20,000	0.27	
Zn	2400	10.0	250	1300	2,400	0.54	
Cr	360	0.2	4000	460	700	0.66	
Cu	560	3.0	200	300	1,000	0.30	
Pb	250	0.04	6000	140	550	0.25	
Ni	240	6.0	40	130	400	0.33	
Mn	130	2.0	70	70	350	0.20	
Cd	30	0.1	300	18	65	0.25	
Ag	20	0.3	70	11	20	0.55	
Co	10	0.2	50	5	25	0.20	
Hg	1	0.03	30	0.5	10	0.05	

- a. Data from Southern California Coastal Water Resources Project (SCCWRP) 1971 averages. Redox level (pe) not experimentally measured but was deduced to be about -3.6.
- b. Selected from SCCWRP tabulation of literature data. These data show great variability. This is particularly true for the less abundant metals, the estimates of which are probably too high.
- c. Mass emission rates obtained by multiplying column 1 by $540 \times 10^6 \text{ l/yr}$ (1971 flow).
- d. Sum of wastewater discharges, surface runoff, vessel coating, ocean dumping, rainfall, and aerial fallout as estimated by critical examination of SCCWRP data.

Source: Morel et al. [29]. (Copyright 1975, American Chemical Society. Reprinted with permission.)

The inputs to REDEQL include the analytical concentrations of trace metals found in the sewage, the analytical concentrations of major metals and ligands, and the measured pH of 7.7, as reported in Table 5.5-4 (column 1).

Model application is not a straightforward process. For example, because the redox level (pe) is not an experimentally measured quantity, the user must attempt to find a range of pe where the calculated partition of metals between the particulate and soluble phases matches the experimentally determined filterable/non-filterable fractionation. For this particular example, the pe is best described as a function of the bacterially mediated reduction of sulfate,



coupled with the oxidation of organic carbon.

Table 5.5-4, column 2, summarizes the first output (first simulation) of metal species estimated by the model for the JWPCP. To make the model more realistic, organic ligands were included. Model users selected a set of organics that represented various functional groups and complexing behaviors for the organic fraction of various wastewaters. Acetate, tartrate, glycine, salicylate, glutamate, and phthalate were added, each at an equivalent carbon concentration of 10^{-3} M. The results are presented in the third column of Table 5.5-4.

To make the model even more realistic, an adsorbing surface was added and given characteristics similar to those of metal oxides. The computations of absorption were then made according to the model of James-Healy [16]. The results are presented in the last column of Table 5.5-4.

Figure 5.5-1 represents the result of a large number of computations for various mixtures of sewage and seawater at various redox potentials. The pH imposed at each dilution was calculated from the carbonate alkalinity and total carbonate of the corresponding sewage-seawater mixture. The ionic strength was approximated by the appropriate dilution of sewage ($I = 0.01$) with seawater ($I = 0.5$). The lines in Figure 5.5-1 indicate the domain of p_e and dilution in which various insoluble forms of the trace metals are stable. (For simplicity, a detailed description of soluble speciation has been omitted from the figure.)

Figure 5.5-1 shows that, in general, the solubilization of metals is affected to a much greater extent by oxidation than by dilution. For a detailed discussion of this subject and the modeling results, the reader is referred to the original work of Morel *et al.* [29].

DISCUSSION OF RESULTS

Mathematical speciation modeling can be a useful tool if the necessary data are available. In their work, Morel *et al.* argued that "overall, an equilibrium model for sewage can be made to closely follow the existing experimental data, but such an effort is not warranted until more detailed analytical data are obtained." This statement applies to almost all water modeling studies.

For the particular example described, Morel *et al.* indicate that much insight has been gained into the factors that govern the fate of trace metals by using chemical equilibrium models. However, model applications are not always straightforward and often present difficulties that are not easily overcome.

5.5.10 Conclusions

The following conclusions can be drawn from the discussion in the previous sections:

- (1) Over a dozen computerized models are presently used for investigating metal speciation in aqueous systems. The MEXAMS, REDEQL2, WATEQ2 and MINEQL models appear to be well developed. Of these,

TABLE 5.5-4
**Metal Distribution Among Various Species In
 Three Equilibrium Models of JWPCP Sewage**

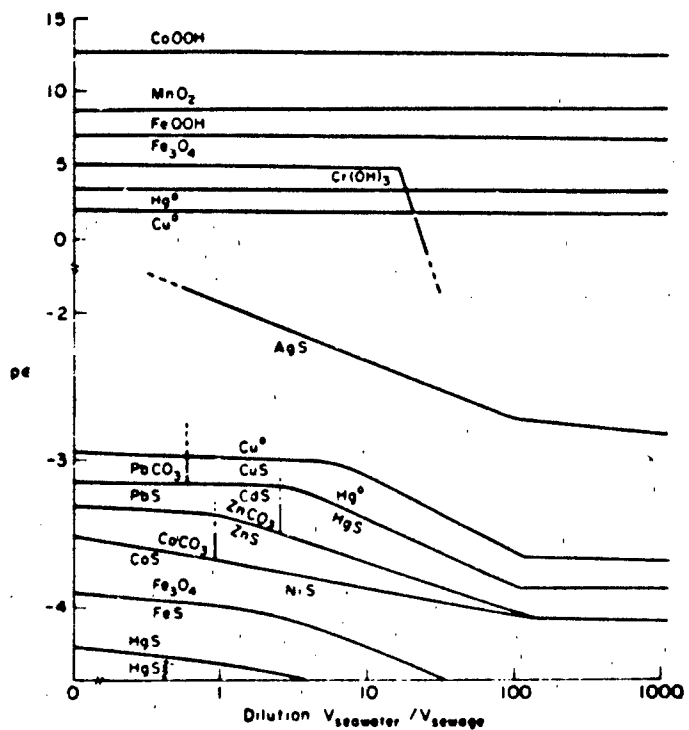
- Log Total Concn.	Inorganic Model ^a (%)	Inorganic Model with Addition of Organics ^{a,b} (%)	Inorganic Model with Addition of Organics and Adsorbing Surface ^{a,b,c} (%)
Fe, 3.7	Fe ₃ O ₄ (s), 100	Fe ₃ O ₄ (s), 100	Fe ₃ O ₄ (s), 100
Cr, 4.8	Cr(OH) ₃ (s), 97	Cr(OH) ₃ (s), 97	Cr(OH) ₃ (s), 52
	Cr(OH) ₄ ⁻ , 3	Cr(OH) ₄ ⁻ , 3	Cr(OH) ₄ ⁻ , 3
			ADS, 45
Cu, 5.0	CuS(s), 100	CuS(s), 100	CuS(s), 100
Cd, 6.5	CdS(s), 100	CdS(s), 100	CdS(s), 100
Pb, 6.0	PbS(s), 100	PbS(s), 100	PbS(s), 100
Zn, 4.5	ZnS(s), 100	ZnS(s), 99	ZnS(s), 99
Ag, 6.7	Ag ₂ S(s), 100	Ag ₂ S(s), 100	Ag ₂ S(s), 100
Hg, 8.3	HgS(s), 100	HgS(s), 100	HgS(s), 100
Ni, 5.4	NiS(s), 42	NiS(s), 22	NiS(s), 14
	Ni ⁺² , 2	Ni ⁺² , 2	Ni ⁺² , 2
	Ni(CN) ₄ ⁻² , 56	Ni(CN) ₄ ⁻² , 56	Ni(CN) ₄ ⁻² , 56
		GLY, 10	GLY, 10
		GLU, 10	GLU, 10
			ADS, 8
Co, 6.8	CoS(s), 97	CoS(s), 95	CoS(s), 93
	Co ⁺² , 2	Co ⁺² , 2	Co ⁺² , 2
		GLU, 2	GLU, 2
			ADS, 2
Mn, 5.6	Mn ⁺² , 50	Mn ⁺² , 50	Mn ⁺² , 45
	MnHCO ₃ ⁺ , 24	MnHCO ₃ ⁺ , 24	MnHCO ₃ ⁺ , 21
	MnSO ₄ ⁻ , 19	MnSO ₄ ⁻ , 19	MnSO ₄ ⁻ , 17
	MnCl ⁺ , 6	MnCl ⁺ , 6	MnCl ⁺ , 6
			ADS, 9

a. Other inputs to the model: pH = 7.7, pe = -3.6, pCa = 2.75, pMg = 3.0, pBa = 5.0, pAl = 4.5, pCO₃ = 2.0, pSO₄ = 2.3, pCl = 1.8, pF = 4.0, pNH₃ = 2.2, pPO₄ = 3.3, pCN = 5.0. Ionic strength = 0.01, T = 25°C.

b. Organic ligands added: pAcetate = 3.3, pGlycine = 3.8, pTartrate = 3.6, pGlutamate = 3.7, pSalicylate = 3.8, pPhthalate = 3.9.

c. Adsorbing surface: 10 m²·l⁻¹, constant potential. The computation is performed according to the James-Healy model which considers coulombic, solvation, and specific chemical energy interactions. The chemical energy term is essentially a fitting parameter and has been chosen arbitrarily in the model to represent high chemical affinity of the adsorbing surface for all metals (about 10 kcal/mol).

Source: Morel et al. [29]. (Copyright 1975, American Chemical Society. Reprinted with permission.)



Composition of diluting seawater:

pH = 8.2, pCa = 2.0, pMg = 1.2, pBa = 6.7, pFe = 6.8, pZn = 6.8, pCr = 8.4, pCu = 7.3, pPb = 9.7, pNi = 7.0, pMn = 7.4, pCd = 9.0, pAg = 8.5, pCo = 8.3, pHg = 9.8, pAl = 7.0, pCO₃ = 2.6, pSO₄ = 1.5, pCl = 3.6, pF = 4.2, pNH₃ = 6.0, pPO₄ = 5.7, pCN = 9.0. Ionic strength = 0.5. Redox level (pe) set at -3.6.

Source: Morel et al. [29]. (Copyright 1975, American Chemical Society.
Reprinted with permission.)

FIGURE 5.5-1 Metal Solids as a Function of Dilution and Oxidation

MEXAMS appears to have the greatest support and REDEQL2 to be the most advanced code.

- (2) The waters to be modeled should be well characterized with respect to Eh, pH, redox potential, ionic strength, concentrations of major cations and anions, concentrations of trace metals and organic ligands, and concentration and nature of suspended solids. While this is not commonly the case, enough is known about water chemistry to permit

reasonable estimates of input values for these data in many cases. However, the sensitivity of the models to each of these parameters varies, and the results of model runs using estimated water quality data may have to be interpreted with caution.

- (3) There may be a large degree of uncertainty within the model itself, with a large portion relating to uncertainty in the stability constants. Some stability constants measured in the laboratory and used in modeling of natural waters may apply only to the time period immediately following the formation of the complex and thus do not reflect long-term stability. The error or uncertainty ranges associated with measured values are seldom reported; some values may be in error by as much as an order of magnitude.
- (4) The representation of organic complexation and adsorption can be a major problem in estimating the speciation of metals. Both the concentration and nature of the organic ligands (e.g., humic and fulvic acids) and the suspended solids must be known before reasonable model parameters can be chosen. Uncertainties in the stability constants and adsorption coefficients selected can easily be an order of magnitude. Reconstituted and well waters — both low in organics and suspended solids — will be easier to model in this regard than those with higher levels.
- (5) Previous investigators have found that computer models can fairly well represent speciation of some reconstituted and well waters. However, validation has been accomplished only by measurement of the free ion (versus total metal concentration), such as Cu^{+2} ; thus, the relative importance of other species cannot be confirmed. When organic complexing has been ignored in the modeling of speciation in river waters, the results have been poor — especially when metal concentrations were low.

5.5.11 Literature Cited

1. Andrew, R.W., K.E. Biesinger and G.E. Glass, "Effects of Inorganic Complexing on the Toxicity of Copper to *Daphnia Magna*," *Water Res.*, **11**, 309-15 (1977).
2. Ball, J.W., D.K. Nordstrom and E.A. Jenne, "Additional and Revised Thermochemical Data and Computer Code for WATEQ2 — A Computerized Chemical Model for Trace and Major Element Speciation and Mineral Equilibria of Natural Waters," Water Resources Report WRI-78-116, U.S. Geological Survey (January 1980).
3. Ball, J.W., E.A. Jenne and D.K. Nordstrom, "WATEQ2 — A Computerized Chemical Model for Trace and Major Element Speciation and Mineral Equilibria of Natural Waters," in *Chemical Modeling in Aqueous Systems*, E.A. Jenne (ed.), Symposium Series No. 93, American Chemical Society, 815-35 (1979).

4. Bjerrum, N. "Ionic Association. I: Influence of Ionic Association on the Activity of Ions at Moderate Degrees of Association," *Kyl. Danske Videnskab. Math-fys. Medd.*, **7**, 1-48 (1926).
5. Dempsey, B.A. and P.C. Singer, "Role of Adsorption in Controlling the Distribution of Metals — The Great Lakes," presented at ACS, Environmental Chemistry division, Honolulu (April, 1978).
6. Felmy, A.R., D.C. Girvin and E.A. Jenne, *MINTEQ — A Computer Program for Calculating Aqueous Geochemical Equilibria*, Final Report, EPA-600/3-84-032 (1984).
7. Felmy, A.R., S.M. Brown, Y. Onishi, S.B. Yabusaki and R.S. Argo, *MEXAMS — The Metals Exposure Analysis Modeling System*, Final Report, EPA-600/3-84-031 (1985).
8. Florence, T.M. and G.E. Batley, "Chemical Speciation in Natural Waters," *CRC Crit. Rev. Anal. Chem.*, **9**, 219 (1980).
9. Fuoss, R.M., "Properties of Electrolyte Solutions," *Chem. Rev.*, **17**, 27-42 (1935).
10. Gachter, R., J.S. Davis and A. Mares, "Regulation of Copper Availability to Phytoplankton by Macromolecules in Lake Water," *Environ. Sci. Technol.*, **12**, 1416-21 (1978).
11. Giesy, J.P., Jr., L.A. Briese and G.J. Leversee, "Metal Binding Capacity of Selected Marine Surface Waters," *Environ. Geol.*, **2**, 257-68 (1978).
12. Glass, G.E., "Identification and Distribution of Inorganic Components in Water: What to Measure?" *Ann. N.Y. Acad. Sci.*, **298**, 31-46 (1977).
13. Harriss, D.K., V.R. Magnuson, D.K. Taylor and M.S. Sur, "REDEQL2: Program and Data Base Modifications," presented to the Division of Environmental Chemistry, American Chemical Society, Miami Beach, Fla. (September 1978).
14. Hem, J.D., *Study and Interpretation of the Chemical Characteristics of Natural Water*, 2nd ed., Geological Survey Water-Supply Paper 1473, U.S. Government Printing Office, Washington, D.C. (1970).
15. Hoffman, M.R. and S.J. Eisenreich, "A Chemical Equilibrium Model for the Variation of Iron and Manganese in the Hypolimnion of Lake Mendota," Paper presented before the Division of Environmental Chemistry, American Chemical Society, Miami, Fla. (September 1978).
16. James, R.O. and T.W. Healy, *J. Colloid Interface Sci.*, **40**, 42 (1972).
17. Jenne, E.A., "Chemical Modeling — Goals, Problems, Approaches, and Priorities," in *Chemical Modeling in Aqueous Systems*, E.A. Jenne (ed.), Symposium Series No. 93, American Chemical Society, Washington, D.C. (1979).
18. Khalid, R.A., R.P. Gambrell, M.G. Verloo and W.H. Patrick, Jr., "Transformations of Heavy Metals and Plant Nutrients in Dredged Sediments as Affected by Oxidation Reduction Potential and pH. Volume I: Literature Review," Contract Report D-77-4, Dredged Material Research Program, U.S. Army Engineer Waterways Experiment Station, Vicksburg, Miss. (1977).
19. Kinniburgh *et al.* (1975): cited by Perwak *et al.* [35].

20. Lawrence, J., "Semi-quantitative Determination of Fulvic Acid Tannin and Lignin in Natural Waters," *Water Res.*, **14**, 373-77 (1980).
21. Leland (1975): cited by Perwak *et al.* [35].
22. Lion, L.W. and J.O. Leckie, "Copper in Marine Microlayers: Accumulation, Speciation and Transport," in *Abstracts of the 178th National Meeting*, American Chemical Society, Division of Environmental Chemistry, Washington, D.C., 88-91 (1979).
23. Magnuson, V.R., D.K. Harriss, M.S. Sun, D.K. Taylor and G.E. Glass, "Relationships of Activities of Metal-ligand Species to Aquatic Toxicity," in *Chemical Modeling in Aqueous Systems*, E.A. Jenne (ed.), Symposium Series No. 93, American Chemical Society, Washington, D.C. (1979).
24. McCrady, J.K. and G.A. Chapman, "Determination of Copper Complexing Capacity of Natural River Water, Well Water and Artificially Reconstituted Water," *Water Res.*, **13**, 143-50 (1979).
25. McDuff, M.E. and F.M. Morel, "Description and Use of the Chemical Equilibrium Program REDEQL2," Tech. Rept. EQ-72-02, California Institute of Technology, Pasadena, Calif. (1973, updated July 1975).
26. McDuff, R.E. and F. Morel, "REDEQL, A General Program for the Computation of Chemical Equilibrium in Aqueous Systems," Tech. Rept. EQ-72-01, Keck Laboratories, California Institute of Technology, Pasadena, Calif. (1972).
27. Minear, R.A. and R.R. Rose, "Application of Various Chemical Models to the Saturation Zone of a Coal Mining Spoil Bank System," Paper presented before the Division of Environmental Chemistry, American Chemical Society, Miami, Fla. (September 1978).
28. Morel, F.M. and J.J. Morgan, "A Numerical Method for Computing Equilibria in Aqueous Chemical Systems," *Environ. Sci. Technol.*, **6**, 58-67 (1972).
29. Morel, F.M., J.C. Westall, C.R. O'Melia and J.J. Morgan, "Fate of Trace Metals in Los Angeles County Wastewater Discharge," *Environ. Sci. Technol.*, **9**, 756 (1975).
30. Mouvet, C. and A.C.M. Bourg, "Speciation of Copper, Lead, Nickel and Zinc in the Meuse River," *Water Res.*, **17**, 641-49 (1983).
31. Munro *et al.* (1976): cited by Felmy *et al.* [6].
32. Nordstrom, D.K., *et al.*, "A Comparison of Computerized Chemical Models for Equilibrium Calculations in Aqueous Systems," in *Chemical Modeling in Aqueous Systems*, E.A. Jenne (ed.), Symposium Series No. 93, American Chemical Society, Washington, D.C., 857-92 (1979).
33. Pagenkopf, G.K., "Metal-Ion Transport Mediated by Humic and Fulvic Acids," in *Organometals and Organometalloids — Occurrence and Fate in the Environment*, F.E. Brinkman and J.M. Bellama (eds.), Symposium Series No. 82, American Chemical Society, Washington, D.C. (1978).
34. Pagenkopf, G.K., "Zinc Speciation and Toxicity to Fishes," in *Toxicity to Biota of Metal Forms in Natural Water*, Proceedings of a workshop, October 7-8, 1975, Great Lakes Research Advisory Board (1976).

35. Perwak, J., B. Goodwin, W. Lyman, L. Nelken and J. Stevens, "Chemical Modeling of Metals in Water," Memorandum Report to Environmental Protection Agency, Contract No. 68-01-5959, Arthur D. Little, Inc., Cambridge, Mass. (1980).
36. Potter, R.W. II, J.M. Thompson, M.A. Clynne and V.L. Thurmond, "Equilibrium, Kinetic, and Chromatographic Controls of the Solution Composition Obtained During the *in situ* Leaching of an Uranium Ore Body," Paper presented before the Division of Environmental Chemistry, American Chemical Society, Miami, Fla. (September 1978).
37. Reilly, P.J., R.H. Wood and R.A. Robinson, "Prediction of Osmotic and Activity Coefficients in Mixed-Electrolyte Solutions," *J. Phys. Chem.*, **75**, 1305-15 (1971).
38. Richter, R.O. and T.L. Theis, "Application of Chemical Modeling Using 'REDEQL2' to the Speciation and Adsorption of Heavy Metals in Fly Ash Leachates," Paper presented before the Division of Environmental Chemistry, American Chemical Society, Miami, Fla. (September 1978).
39. Sibley and Morgan (1975): cited by Perwak *et al.* [35].
40. Truesdell, A.H. and B.F. Jones, "WATEQ, A Computer Program for Calculating Chemical Equilibria of Natural Waters," *J. Res. U.S. Geol. Surv.*, **2**, 233-48 (1974).
41. Van denBerg, C.M.G. and J.R. Kramcr, "Conditional Stability Constants for Copper Ions with Ligands in Natural Waters," in *Chemical Modeling in Aqueous Systems*, E.A. Jenne (ed.), Symposium Series No. 93, American Chemical Society, Washington, D.C. (1979).
42. Vuceta, J. and J. Morgan, "Chemical Modeling of Trace Metals in Role of Complexation and Adsorption," *Environ. Sci. Technol.*, **12**, 1302-8 (1979).
43. Westall, J.C., J.L. Zachary and F.M. Morel, "MINEQL — A Computer Program for the Calculation of Chemical Equilibrium Composition of Aqueous Systems," Tech. Note No. 18, EPA Grant R-803738, Massachusetts Institute of Technology (1976).

5.6 RADIONUCLIDE MIGRATION MODELING

This section briefly summarizes the modeling issues and approaches adopted by radionuclide transport models. These models have been developed primarily for assessing performance and risks of deep-mined nuclear waste repositories sited in salt, basalt or granite geologic media.

5.6.1 Introduction

To analyze the long-term performance of a geologic nuclear waste disposal system, separate models are needed for (a) migration of formation fluids (e.g., oxic or anoxic brines in salt media, vadose-zone pore water in tuff) and groundwater to the waste; (b) dissolution (leaching) of the nuclear wastes by the formation fluids; (c) migration of radionuclides via groundwater to the accessible environment (air, water, soil); and (d) exposure of biota to radiation. Mills and Vogt [13] discuss the use of various radiological assessment models and review the available codes. A publication of the National Research Council [14] describes the overall geologic isolation system concept and related criteria.

A number of recent reviews prepared for the Department of Energy (DOE), the Nuclear Regulatory Commission (NRC) and the U.S. Environmental Protection Agency (EPA) have focused on the radionuclide migration models. These reviews [14,15,18] contain both listings of codes and detailed discussions of their features, capabilities and modeling approaches. A synoptic overview of processes modeled, solution procedures, and other features of existing models is presented in Table 5.6-1. A directory of selected radionuclide migration computer codes is presented in section 5.6.3.

5.6.2 Principal Processes

Radionuclide migration models are one-, two-, or three-dimensional groundwater flow models that have been interfaced to geo/radio-chemistry models (subroutines). The various modeling concepts are described by Bonazountas [2].

A typical radionuclide transport model combines a source model, a groundwater flow model, and a contaminant transport (e.g., dispersion, advection, adsorption) model into a single code. For example, GETOUT [7], which has been widely used for assessing the performance of deep geologic repositories, includes each of these three models with the following assumptions:

- (1) *Source term*: constant rate of release of radionuclides into groundwater, infinite solubility (of radionuclides).
- (2) *Groundwater flow*: uniform one-dimensional flow path, steady-state fluid flow.
- (3) *Radionuclide transport*: decay chains with up to three members, axial dispersion, and sorption based on linear isotherm and instantaneous equilibrium.

TABLE 5.6-1

Synopsis of Selected Radionuclide Transport Models for Nuclear Waste Repository Performance Assessment

Model	Solution Procedure	Dimensions	Media	Process Modeled	Reference
BRINEMIG	FD	1	G	HC	1
CCC	IFDM	3	G	SF,HT,GM	4,18
CFEST	FE	2,3	—	U,HC,ST	1,4
CHAINT	FE	2	F	ST	4,18
DNET	PN	2	G,F	SF,DS	18
DPCT	FE,PT	2	G	SF,ST	18
EQ3/EQ6	—	—	—	GC	1,18
FEMWASTE	FE	2	G	ST	4,15,18
FEMWATER	FE	2	G	SF,U	4,15,18
FTRANS	FE	2	F,G,DP	ST,U	4,6,14
GETOUT	A	1	G,F	ST,PT	1,7,18
KONBRED (MOC)	FD,MC	2	G	SF,ST	4,18
LAYFLO	SA	1	G	PT,ST,GC	1
MAGNUM2D	FF	2	G,F,DP	SF,HT	4,18
MMT	PT	2	G	ST	1,8,15,18
NUTRAN	PN,N1	1,2	G,F,DP	PT,GC,DS	4,18
NWFT/DVM	PN/PT	2	G,F	SF,ST	18
PATHS	A	2	G	SF,ST	18
PHREEQE	—	—	—	GC	4,18
SEGOL	A	2,3	G	U,ST	4,15,18
SHAFT79	IFDM	3	G	SF,HT	4,18
SHALT	FE	2	G	SF,HT,ST,HC	18
SWENT	FD	3	G	SF,HT,HC	1,9
SWIFT	FD	3	G	SF,HT,ST,HC	4,18
TRACR3D	IFDM	3D	F	U,PT,ST	4,15,18
TRANSONE	FE	1	G	ST,U,SF	4,15,18
TRIPM	FE	2	G	SF,U,GC	1,15
TRUST	IFDM	3	G	SF,U,GM	4,15,18
UNSAT2	FE	2	G	SF,U	4,15,18
VS2D	FD	2	G	U,SF,ST	4,15,18
V3	FD	2	F	SF	18
WATEQ	—	—	—	GC	18

(Continued)

TABLE 5.6-1 (Continued)

Abbreviations:

A	— Analytical Solution	HT	— Heat Transport
DP	— Double Porosity Media	IFDM	— Integrated Finite Difference Method
DS	— Dissolution	MC	— Method of Characteristics
F	— Fractured Porous Media	NI	— Numerical Integration
FD	— Finite Difference	PN	— Pipe Network
FE	— Finite Element	PT	— Particle Tracker
G	— Granular Type Porous Media	SA	— Semi-Analytical
GC	— Geochemistry	SF	— Saturated Flow
GM	— Geomechanical	ST	— Solute Transport
HC	— Coupled Heat and Solute Transport	U	— Unsaturated Flow

The sophistication and capabilities of available codes vary widely. Source-term models can range in complexity from a simple specified concentration or flux boundary condition in a transport model, to the complex modeling of equilibria among various species in aqueous solution surrounding radioactive waste (e.g., PROTOCOL [11,17]). Flow models, besides dimensional capabilities, may model flow only in media that are porous or can be represented as porous, while others are capable of modeling fractured or dual-porosity media. Nuclide transport code capabilities range from those that can model only a single decaying species (e.g., CFEST, KONBRED) to those that can model decaying chains of arbitrary length (e.g., SWIFT and CHAIN). Besides decay, most transport codes consider one or more of the following solute transport processes: dispersion, diffusion, and retardation (including various adsorption processes). Special-purpose brine migration models (e.g., BRINEMIG) have been developed for the particularly impermeable domal salt repository medium, where brine inclusions slowly migrate toward the emplaced waste (thermal gradient) prior to waste dissolution.

Bedrock radionuclide models are medium-specific, because most of the flow in hard-rock (basalt and granite) geologic media is through joints or fractures. Two approaches are available for fractured flow modeling: (1) the discrete-fracture (DF) approach, which models individual fractures and treats the rock matrix as a porous medium, and (2) the dual-porosity (DP) approach, which superimposes a high-porosity medium (fractures) and a low-porosity medium (rock matrix) with a transfer function relating fluid flow between them. Typical solute transport codes for fractured media (e.g., FTRANS and TRUMP) assume saturated flow conditions and consider adsorption of radionuclides onto the rock matrix.

For a shallow tuff repository, unsaturated flow conditions would apply for modeling radionuclide transport [15]. Models developed for this purpose are FEMWASTE, TRANSONE and SEGOL [4,15].

5.6.3 Radionuclide Codes

This section considers only generalized, documented models capable of simulating advection, adsorption, decay and speciation of radionuclide chains in groundwater. Of particular interest are codes noted for their computational efficiency, user-friendliness, and validated history by a number of field tests (cf. [1] and [10]).

Table 5.6-1 provided an overview of available models. Table 5.6-2 lists widely used, well-documented radionuclide transport codes and their main features. These codes have been developed to various levels of sophistication, approximation, accuracy and flexibility; they can be used as stand-alone packages or as end-to-end codes with other models.

Model development status and confidence in model predictions are often related. Although partial validation of selected radionuclide transport models (e.g., SWENT) has been claimed and documented [9], this amounts merely to satisfactory agreement between model predictions and field observations for very specific conditions (e.g., short-term leachate migration from a landfill, or uranium-front movement in an aquifer). In most cases, such as in the random-walk 1-D multicomponent mass-transport (MMT) code, numerical code verification for a test case has been performed, but field validation has not yet been accomplished.

A number of analytical solutions to radionuclide transport equations have also been developed and are noted briefly here, in light of their value and frequent use in verifying the accuracy of numerical codes.

Lester *et al.* [12] published analytical solutions for the transport of a three-component chain and considered both impulse releases and decaying band releases. Their solutions were limited, however, by the assumptions of a constant fluid velocity in a one-dimensional flow and a single retardation factor applicable to all chain members. Nevertheless, the solutions have served as benchmarks for subsequent numerical solutions to the chain transport problem.

Extensive work on this problem has been carried out by a group at the University of California/Berkeley and Lawrence Berkeley Laboratory. This group has published a set of analytical solutions to a variety of chain transport problems (e.g., Harada *et al.* [5] and Chambre *et al.* [3]). These solutions include a variety of waste form dissolution and local transport problems, one-dimensional flow and transport, one dimensional flow with three-dimensional transport, two-dimensional flow and transport, and one-dimensional flow and transport of a single radionuclide in fractured media.

5.6.4 Model Applications

It is difficult to assess the suitability of a general-purpose code, because the applications of the code to a variety of siting assessments and contaminant flow analyses are often waste-specific, site-specific, and different in both spatial and temporal resolution. However, several well-documented, developed and maintained

TABLE 5.6-2
Selected Radionuclide Migration Models

A. Saturated Flow of Single Species

CFEST	Couples fluid energy and solute transport (CFEST): A general-purpose, three-dimensional transport code that simulates seasonal energy storage (nonisothermal) in underground confined aquifers. Can handle single-phase Darcy (laminar, transient) flows in a horizontal plane, a vertical plane, or in three dimensions. Both transient and steady-state single-species transport problems can be treated. This is an extension of the FE3DGW code.
KONBRED (GSMOC)	A one- and two-dimensional model of groundwater flow and solute transport, to compute the concentration of a dissolved chemical species in a saturated aquifer at any specified place and time. Computes changes in convective transport, hydrodynamic dispersion, and mixing from fluid sources. The groundwater flow equation is solved by a finite-difference technique and the solute transport equation by the method of characteristics. A modified version accounts for decay of a single species but does not consider formation of radioactive daughter products.

B. Saturated Flow of Multiple Species

CHAINT	A one- and two-dimensional, finite-element model for the simulation of multicomponent nuclide transport in saturated fractured or porous media. Processes modeled include advection, dispersion, diffusion, sorption, chain-decay, and mass release. Principal input required is the groundwater flow field, which can be obtained from a groundwater flow model.
GETOUT	Developed for the transport of radionuclide chains along a 1-D path. Uses analytical solutions for 1-, 2- or 3-member chains and approximate solutions for longer chains. Release may be either an impulse or a band. Assumes infinite solubility of elements and equilibrium adsorption. Model is widely applicable to steady-state problems.
LAYFLO	1-D, semianalytical model for the migration of a 3-member decay chain in a multilayered geological medium. It accounts for longitudinal dispersion, decay, sorption and desorption, in fully saturated media with steady flow.
MMT	A discrete-parcel, random-walk, 1-D Multicomponent-Mass Transport code for radionuclides in groundwater. It accounts for transport, decay, and sorption-desorption of radionuclides in a steady uniform simplified groundwater aquifer.
NUTRAN	Calculates the dose-to-man from radioactivity transported from waste repositories via groundwater pathways. Evaluates the combined effect of systems of natural and engineering barriers. The program considers leaching and dissolution of waste and calculates the migration of radionuclides from the repository as a function of time. The time-dependent concentrations of various radionuclides are calculated along the flow paths, modeled as a one-dimensional network.

(Continued)

TABLE 5.6-2 (Continued)

NWFT/DVM	The Network Flow and Transport Model/Distributed Velocity Model (NWFT/DVM) is a 1-D flow code, which simulates a flow system as a 1-D (pipe) network of segments, but also treats leach- and solubility-limited sources, and handles decay chains subject to adsorption, advection and dispersion in transport.
PATHS	A 2-D numerical model for contaminant transport. Treats both steady and transient saturated flow systems, for single-component transport in homogeneous geology. The model is based on analytical solutions for the groundwater potential. Geochemical retardation is considered, and dispersion is ignored. This is an oversimplified worst-case engineering analysis tool for releases from waste storage facilities, with no field validation to date.
SWENT	A one-, two- or three-dimensional finite difference, transient or steady-state groundwater-flow, nuclide-transport, and heat-transport model, applicable to complex geometries. Saturated flow in an isothermal or non-isothermal porous medium, as well as sorption and desorption mechanisms, can be modeled. For nuclide decay, the code considers conservation of dissolved contaminants, energy and total liquid mass. The code is fairly general and contains many options for geometry, processes, and boundary conditions. Based upon the nuclide inventory and the biosphere transport, the model can calculate the potential hazard to people from release to the biosphere.
TRIPM	A two-dimensional FE model for the simultaneous transport of water and reacting solutes through saturated and unsaturated porous media. Predicts transport and decay.

C. Codes for Unsaturated Flow Conditions

FEMWASTE	A two-dimensional finite element code for waste transport through a porous medium with varying degrees of saturation. The transport mechanisms include advection, hydrodynamic dispersion, chemical adsorption, and first-order decay. Computes the velocity flow field required for the solute transport subroutine.
FEMWATER	A two-dimensional finite element model of water flow through porous media with varying degrees of saturation. An aquifer may be modeled with anisotropic parameters. Nonlinearities such as the dependence of the hydraulic conductivity and storage on the pressure head are considered. Output includes a continuous pressure distribution and velocity field. Output is formatted for use as input to the companion code, FEMWASTE, which simulates contaminant transport in the medium.
SEGOL	A two- or three-dimensional code designed for solute transport in unsaturated flow systems. Moisture flow is based on Darcy's Law. The transport mechanisms include advection, dispersion, sorption and decay.
TRASONE	A one-dimensional finite element code for mass transport through unsaturated and saturated porous media.

(Continued)

TABLE 5.6-2 (Continued)

TRUST	An integrated finite difference algorithm for one-, two- or three-dimensional fluid flow problems in unsaturated, deformable porous media. The code uses a mixed explicit-implicit approach in setting up the matrix equations and internally calculates the time-step size. The model considers pressure-dependent density variations of water [16].
UNSAT2	A two-dimensional finite element code for flow through unsaturated porous media. Has features similar to FEMWATER and can also model axisymmetric problems. Each material may have local anisotropy, with the principal hydraulic conductivities oriented at any desired angle with respect to the coordinates.
VS2D	A two-dimensional finite difference model for flow in saturated-unsaturated media. Can handle nonlinear problems caused by infiltration into dry soils, and anisotropy and discontinuities in permeabilities and porosities.

D. Codes for Fractured Media

FTRANS	A two-dimensional finite element code for groundwater flow and single- or multiple-species radionuclide transport in fractured porous media. Fractured-flow systems may be modeled using either the dual-porosity or the discrete-fracture approach, or a combination of the two.
TRACR3D	A three-dimensional, integrated, finite-difference program for solving two-phase fluid flow problems in fractured media. Special features include one- or two-phase flow with tracers in either phase, Langmuir sorption, radioactive decay and capillary effects.

E. Coupled Flow and Thermal Codes

CCC	This code models heat and fluid flow by conduction and convection in two- or three-dimensional saturated porous media. Can also calculate one-dimensional subsidence. An integrated finite difference method is employed to solve mass-, momentum-, and energy-balance equations.
MAGNUM2D	This finite-element model can simulate groundwater flow and heat transport in fractured porous rock systems. Both dual-porosity and discrete-fracture models can be used.

F. Special-purpose Codes

BRINEMIG	One-dimensional, finite difference code for modeling intergranular brine migration to nuclear waste, and, possibly, from the waste, up the thermal gradient, through isotropic and homogeneous salt. This is a special-purpose, non-Darcian flow code limited in applicability to salt repository sites.
----------	--

Sources: Battelle [1], Curtis et al. [4], Oster [15], Thomas et al. [18].

TABLE 5.3-3
SWENT Model Validation Studies

Site Selected	Description of Problem	Variables Observed In Field and Simulated by Model with Good Agreement	Processes Validated
Canadian Air Force Base Borden Landfill, Ontario, Canada	Leachate migration from landfill	1. Piezometric surface 2. Chloride ion concentration profiles in waste region and in plume after 36 years	Fluid flow and trace component transport
Thermal Energy Storage Experiment at Mobile, Alabama	Injection, storage, and recovery of heat from a confined aquifer	Temperature profiles in the aquifer (3 dimensional) at end of each cycle, with injection period, storage period, and recovery period	Coupled fluid and heat flow
Carrizo Aquifer, Wintergarden, S.W. Texas	Uranium front movement in the aquifer	Concentrations of ^{14}C , ^{234}U and ^{238}U in the aquifer	Fluid flow and trace component transport

Source: INTERA Environmental Consultants, Inc. [9].

codes in the public domain (e.g., SWENT) have been successfully applied to analyses of injection of industrial wastes into saline aquifers, *in situ* solution mining, migration of contaminants from landfills, and saltwater intrusion in coastal regions, as well as to aquifer characterization. Table 5.6-3 summarizes the characteristics of three field-validation studies of the SWENT model; these results indicate that SWENT is generally applicable for three-dimensional radionuclide transport in multilayered aquifer systems [9].

5.6.5 Literature Cited

1. Battelle Memorial Institute, Office of Nuclear Waste Isolation, "Performance Assessment Plans and Methods for a Salt Repository Project," DOE-BMI/ONWI-545, Columbus, Ohio (August 1984).
2. Bonazountas, M., "Soil and Groundwater Fate Modeling," in *Fate of Chemicals in the Environment*, R. Swann and A. Eschenroeder (eds.), American Chemical Society, ACS Symposium Series No. 225, Washington, D.C. (1983).
3. Chambre, P.L., T.H. Pigford, A. Fujita, T. Kanki, A. Kobayashi, H. Leung, D. Ting, Y. Sato and S.J. Zavoshy, *Analytical Performance Models for Geologic Repositories*, Vols. I and II, LBL-14842, UC-70, report to the U.S. Department of Energy by the University of California, Lawrence Berkeley Laboratory (1982).
4. Curtis, R.H., R.J. Wart and E.L. Skiba, Acres American, Inc. and Teknekron Research, Inc., "A Summary of Repository Design Models," NUREG/CR-3450, prepared for U.S. Nuclear Regulatory Commission (October 1983).
5. Harada, M., P.L. Chambre, M. Foglia, K. Higashi, F. Iwamoto, D. Leung, T.H. Pigford and D. Ting, "Migration of Radionuclides through Sorbing Media. Analytical Solution — I," LBL-10500, UC-70, Draft Report to the U.S. Department of Energy, University of California, Lawrence Berkeley Laboratory (1980).
6. INTERA Environmental Consultants, Inc., "FTRANS: A Two-Dimensional Code for Simulating Fluid Flow and Transport of Radioactive Nuclides in Fractured Rock for Repository Performance Assessment," ONWI-426, prepared for Office of Nuclear Waste Isolation, Battelle Memorial Institute, Columbus, Ohio (April 1983).
7. INTERA Environmental Consultants, Inc., "GETOUT: A Computer Code for One-Dimensional Analytical Solution for Radionuclide Transport," ONWI-433, prepared for Office of Nuclear Waste Isolation, Battelle Memorial Institute, Columbus, Ohio (April 1983).
8. INTERA Environmental Consultants, Inc., "MMT: A Random-Walk One-Dimensional Multicomponent Mass Transport Code," ONWI-432, prepared for Office of Nuclear Waste Isolation, Battelle Memorial Institute, Columbus, Ohio (April 1983).
9. INTERA Environmental Consultants, Inc., "SWENT: A Three-Dimensional Finite Difference Code for the Simulation of Fluid, Energy and Solute Radionuclide Transport," ONWI-457, prepared for Office of Nuclear Waste Isolation, Battelle Memorial Institute, Columbus, Ohio (April 1983).

10. "INTRACOIN-International Nuclide Transport Code Intercomparison Study," Final Report, Level 1 (Code Verification), SKI 84:3 (September 1984).
11. Jackson, D.D., "PROTOCOL, a Numerical Simulator for the Dissolution of Inorganic Solids in Aqueous Solutions," UCRL-91631, University of California (September 1984).
12. Lester, D.H., G. Jansen and H.C. Burkholder, "Migration of Radionuclide Chains through an Adsorbing Medium," AIChE Symposium Series 71, pp. 152-202 (1975).
13. Mills, M. and D. Vogt, Teknekron Research, Inc., "A Summary of Computer Codes for Radiological Assessment," NUREG/CR-3209, prepared for U.S. Nuclear Regulatory Commission (March 1983).
14. National Research Council, Waste Isolation Systems Panel, "A Study of the Isolation System for Geologic Disposal of Radioactive Wastes," National Academy Press (1983).
15. Oster, C.A., "Review of Groundwater Flow and Transport Models in the Unsaturated Zone," NUREG/CR-2917, prepared for U.S. Nuclear Regulatory Commission (1982).
16. Pacific Northwest Laboratories, "Uranium Recovery Research Sponsored by the NRC at PNL: Quarterly Progress Reports for 1984," PNL-5015-1 through -4 (1985).
17. Pickrell, G. and D. Jackson "User's Guide to PROTOCOL, A Numerical Simulator for the Dissolution Reactions of Inorganic Solids in Aqueous Solutions," UCID-20236, University of California (October 1984).
18. Thomas, S.D., B. Ross and J.W. Mercer, GeoTrans Inc. and Teknekron Research, Inc., "A Summary of Repository Siting Models," NUREG/CR-2784, prepared for U.S. Nuclear Regulatory Commission (July 1982).

DISTRIBUTION LIST

- 16 Copies** Commander
 U.S. Army Biomedical Research and Development Laboratory
 ATTN: SGRD-UBZ-C
 Fort Detrick
 Frederick, MD 21701-5010
- 1 Copy** Commander
 U.S. Army Medical Research and Development Command
 ATTN: SGRD-RMI-S
 Fort Detrick
 Frederick, MD 21701-5012
- 2 Copies** Defense Technical Information Center (DTIC)
 ATTN: DTIC-DDA
 Cameron Station
 Alexandria, VA 22304-6145
- 8 Copies** Dr. Gary C. Thom, TS-798
 U.S. Environmental Protection Agency
 401 M Street, S.W.
 Washington, DC 20460
- 1 Copy** Commander
 U.S. Army Construction Engineering Research Laboratory
 ATTN: Dr. Jain
 P.O. Box 4005
 Champaign, IL 61520-1350
- 1 Copy** Commander
 U.S. Army Construction Engineering Research Laboratory
 ATTN: Dr. Novak
 P.O. Box 4005
 Champaign, IL 61520-1350
- 1 Copy** Commander
 U.S. Army Materiel Command
 Environmental Quality Division
 ATTN: LTC J.J. McCarthy
 5001 Eisenhower Avenue
 Alexandria, VA 22333-0001
- 2 Copies** Commander
 U.S. Army Toxic and Hazardous Materials Agency
 ATTN: AMXTH-IR
 Aberdeen Proving Ground, MD 21010-5401
- 3 Copy** Headquarters, Department of the Army
 ATTN: DAEN-RDM (Dr. Clemens Meyer)
 20 Massachusetts Avenue, N.W.
 Washington, DC 20314-1000
- 2 Copies** Commander
 U.S. Army Environmental Hygiene Agency
 ATTN: HSHB-AI-A (Library)
 Aberdeen Proving Ground, MD 21010-5422

END

8-87

OTIC